

BRITISH JOURNAL OF  
APPLIED  
PHYSICS



EDITOR

H. R. LANG

PH.D., A.R.C.S., F.INST.P.

*Secretary of The Institute of Physics*

VOLUME 4

LONDON  
THE INSTITUTE OF PHYSICS

# BRITISH JOURNAL OF APPLIED PHYSICS

ADVISORY COMMITTEE, 1952-53

## *Representing The Institute of Physics*

- C. SYKES, PH.D., D.SC., F.INST.P., F.R.S., *President*  
S. WHITEHEAD, M.A., PH.D., D.SC., M.I.E.E., F.INST.P., *Honorary Treasurer*  
B. P. DUDDING, M.B.E., PH.D., A.R.C.S., F.INST.P., *Honorary Secretary*  
T. E. ALLIBONE, PH.D., D.SC., M.I.E.E., F.INST.P., F.R.S., *Chairman and Vice-President*  
E. G. COX, D.SC., F.R.I.C., F.INST.P., *Vice-President*  
B. M. CROWTHER, M.A., PH.D., F.INST.P.  
N. L. HARRIS, B.SC., F.INST.P.  
W. J. MEREDITH, M.SC., F.INST.P.  
E. W. H. SELWYN, B.SC., A.R.C.S., F.INST.P.  
R. W. SILLARS, B.A., D.PHIL., A.M.I.E.E., F.INST.P.  
E. C. STONER, PH.D., SC.D., F.INST.P., F.R.S.

## *Representing the Institute's Branches, Groups, and the Participating Societies*

- E. M. CROOK, M.SC., PH.D., A.R.I.C., A.INST.P., *Representing the Electron Microscopy Group*  
C. CROXSON, B.SC., F.INST.P., *Representing the Industrial Radiology Group*  
A. E. DE BARR, B.SC., F.INST.P., *Representing the X-ray Analysis Group*  
E. K. FRANKL, M.A., *Representing the Stress Analysis Group*  
J. S. FORREST, M.A., D.SC., M.I.E.E., F.INST.P., *Representing the Royal Meteorological Society*  
A. G. GAYDON, PH.D., D.SC., A.R.C.S., A.INST.P., F.R.S., *Representing The Physical Society*  
P. L. KIRBY, M.SC., A.INST.P., *Representing the North Eastern Branch*  
F. LLEWELLYN JONES, M.A., D.PHIL., F.INST.P., *Representing the South Wales Branch*  
D. PARKINSON, PH.D., D.SC., F.INST.P., *Representing the Midland Branch*  
F. Y. POYNTON, M.SC., F.INST.P., *Representing the Education Group*  
J. S. RANKIN, PH.D., M.I.MECH.E., F.INST.P., *Representing the Scottish Branch*  
S. RODDA, B.SC., F.INST.P., *Representing the Electronics Group*  
R. SCHNURMANN, M.SC., DR.RET.NAT., F.INST.P., *Representing the Manchester and District Branch*  
W. S. STILES, O.B.E., PH.D., D.SC., *Representing The Physical Society*  
R. S. TEBBLE, PH.D., A.INST.P., *Representing the Yorkshire Branch*  
L. R. G. TRELOAR, PH.D., D.SC., F.INST.P., *Representing the London Branch and also the  
Faraday Society*  
E. VAN SOMEREN, B.SC., F.INST.P., *Representing the Industrial Spectroscopy Group*  
C. W. WILSON, M.SC., PH.D., F.INST.P., *Representing the British Institute of Radiology*



# INDEX TO VOLUME 4

## SUBJECT INDEX

- Analogue,  
  An electrical, to a high vacuum system 188  
  electrical, Further applications of the, to vacuum systems 350  
Analogues, electrical 193  
Analysis, spectrographic, The automatic electrical ignition of the  
  d.c. arc in 118  
Arc, d.c., The automatic electrical ignition of the, in spectrographic  
  analysis 118  
A.S.T.M. Index, Errors in the 32  
Atomizer, A photographic method of observing the approximate  
  size of liquid droplets produced by an 316
- Barium oxide, Changes in secondary and thermionic emission from,  
  during electron bombardment 56
- Books, New**  
  Adhesion and adhesives 190  
  Advanced  
    experiments in practical physics 191  
    mathematics in physics and engineering 253  
    treatise on physical chemistry, An, Vol. 3. The  
      properties of solids 126  
  Advances  
    in electronics, Vol. 4 63  
    in geophysics 191  
  Associated measurements 125  
  Automatic feedback control 125  
  Basic methods in transfer problems 94  
  Berechnung magnetischer felder 255  
  Canterbury project—New Zealand Radio Meteorological  
    Investigation 61  
  Collected works of Bernhard Riemann 383  
  Color in business, science and industry 61  
  Comets and their origin, The 286  
  Computing methods and the phase problem in X-ray crystal  
    analysis 222  
  Cosmic rays 29  
  Data for X-ray analysis, Vol. 1 351  
  Demonstrations in modern physics 30  
  Designing by photoelasticity 190  
  Detonation in condensed explosives 159  
  Dictionary of conformal representations 63  
  Elasticity in engineering 191  
  Electrical measurements and the calculation of errors involved.  
    Part II 287  
  Electric fuses. A critical review of published information 63  
  Electrodynamics 61  
  Electronic  
    analog computers 95  
    measurements 157  
  Elements of nuclear reactor theory, The 285  
  Elliptic functions, Introduction to 351  
  Essentials of microwaves 192  
  Fatigue of metals 318  
  Ferroelectricity 351  
  Ferromagnetic properties of metals and alloys 30  
  Fundamentals of thermometry 157  
  Gasdynamik 253  
  Grundlagen der elektronenoptik 287  
  Heat transfer phenomena 254  
  High speed photography 190  
  Identification of stones in glass by physical methods, The 255  
  Initiation and growth of explosions in liquids and solids, The  
    158
- Books, New (continued)**  
  Luminescence and the scintillation counter 351  
  Magnetic circuit, The 157  
  Mathematical  
    structure of the theories of viscoelasticity 319  
    theory of non-uniform gases, The, 2nd edition 223  
  Measurement of particle size in very fine powders, The 287  
  Mechanics 191  
    of the gyroscope: The dynamics of rotation 192  
  Mesons—A summary of experimental facts 190  
  Metallurgical equilibrium diagrams 29  
  Methoden und anwendungen der massenspektroskopie 319  
  Micrometeorology 286  
  Mixtures. The theory of the equilibrium properties of some  
    simple classes of mixtures, solutions and alloys 30  
  Modern  
    applied photography 255  
    mass spectrometry 157  
  Modulators and frequency changers 319  
  Molecular architecture of plant cell walls, The 95  
  Monographs for students series 157  
  Niederdruck—Stromrichterventile 222  
  Nuclear stability rules 189  
  Numerical analysis 159  
  Organisation Météorologique Internationale. Publication  
    No. 79 158  
  Oxidation of metals and alloys 253  
  Permanent magnets 317  
  Photoconductivity in the elements 94  
  Photometry, 2nd edition 223  
  Physical  
    constants of some commercial steels at elevated tempera-  
      tures 254  
    formulae 383  
    principles of thermodynamics, The 95  
    similarity and dimensional analysis 285  
  Polarized light in metallography 30  
  Practical  
    physics 62  
    radiography for industry 29  
    spectroscopy 62  
    thermometry 157  
  Principio general de la termodinamica 189  
  Proceedings of general discussion on heat transfer—London  
    1951 191  
  Progress  
    in biophysics and biophysical chemistry: Vol. 3 318  
    in metal physics, Vol. 4 286  
    in nuclear physics, Vol. 2 255  
  Progressive exercises in physics 95  
  Properties of electrical insulating materials and methods of  
    test, The 253  
  Psychological and psycho-physical studies of craftsmanship in  
    dairying 125  
  Radiations and living cells 254  
  Radio engineering 351  
  Radioisotopes in industry 317  
  Remote control by radio 159  
  Servomechanism analysis 318  
  Signal, noise and resolution in nuclear counter amplifiers  
    383  
  Small particle statistics 253  
  Soft magnetic materials used in industry 157

For Static Electrification and cognate subjects see also separate index to the supplement



Books, New (continued)

- Source book of technical literature on fractional distillation, A 30
- Spectrographic analysis of low-alloy steels 287
- Stress waves in solids 319
- Structure  
and properties of mild steel, The 62  
of metals 189  
Reports for 1949 (Vol. 12) 126
- Superconductivity, 2nd edition 223
- Television 63  
receiver design, Vol. 1, I.F. Stages 383
- Tensors in electrical machine theory 189
- Theoretical nuclear physics 158
- Theory of homogeneous turbulence, The 285
- Ultraviolet radiation 126
- University textbook of physics, A, Vol. 3. Heat 95
- Wave propagation in periodic structures 351
- Wind tunnel technique 94
- X-ray  
crystallographic technology 62  
crystallography 191
- Bridge method of measurement of the time constant of exponential decays 350
- British Standards Institution 64

- Cameras, The use of X-ray diffraction, as recording optical goniometers 88
- Carbon, radioactive, in gas counters, The measurement of 217
- Catalogue of British electrical products 31
- Cathode  
oxide-coated, Gold as a grid emission inhibitor in the presence of an 311  
spots on mercury, Current densities of free-moving 91
- Cathodes, oxide, The effects of oxygen on the electrical properties of 70
- Chronometer and watch rates, The influence of barometric pressure on 379
- Cohesive layers, The compression and bearing capacity of 20
- Colouring of diamonds by neutron and electron bombardment, The 334
- Competition, Essay 384
- Concentration, particle, The reduction in apparent, with multiple strokes of the Owens jet dust counter 316
- Conduction loss from a hot wire stretched along the axis of a vertical cylindrical tube, Ratio of convection to 204, 382
- Conductivity  
thermal, of solids and liquids, An apparatus for measuring the coefficient of 112  
thermal, problems, Papers on 320
- Conference  
International, on the science and applications of photography 256  
on applied mass spectrometry 288  
on defects in crystalline solids 352  
on electron microscopy—Bristol, September 1952, Summarized proceedings of a 1  
on ionization phenomena in discharges 96  
on static electrification 31  
on the mechanical effects of dislocations in crystals 320  
on the optical and electron-microscopical properties of textile fibres—Manchester, October 1952, Summarized proceedings of a 119  
on the physics of particle size analysis 31
- Conferences on nuclear physics and on the solid state—July 1954 320
- Control  
Electronic, of a synchronous motor 147  
techniques and instruments, Exhibition of 160

Control (continued)

- temperature, during lattice spacing measurements, A note on 189
- Convection  
and evaporation, Processes of 65  
Ratio of, to conduction loss from a hot wire stretched along the axis of a vertical cylindrical tube 204, 382
- Counter, the Owens jet dust, The reduction in apparent particle concentration with multiple strokes of 316
- Counters, The measurement of radioactive carbon in gas 217
- Counting, Scintillation, and its medical applications 353
- Creep and recovery in metals 225
- Crystallography, International Union of 352
- Crystal structures, The construction of ball-and-spoke models of 107
- Crystals  
A model for demonstrating dislocations in 144  
anisotropic, Refractive index determination for 284  
Conference on the mechanical effects of dislocations in 320  
of nickel, Production of single 342  
Refractive index determination for anisotropic 185  
single, of thallium activated alkali halides, On growing 377  
Techniques for the electron microscopy of 177
- Current densities of free-moving cathode spots on mercury 252
- Cyclotron, Harwell, Energy spectrum measurements of protons in the 175
- Data, A check on the standard observer, at 4358 Å 80
- Densities, Current, of free-moving cathode spots on mercury 91
- Detectors in photometry, Neon indicator tubes as quantitative 245
- Determination  
of the velocity of short electromagnetic waves, Proposed use of a cylindrical surface wave resonator for the 186  
Photoelastic, of stresses in a cylindrical shell 76
- Diamonds, colouring of, by neutron and electron bombardment, The 334
- Die Farbe 128
- Dielectric heating, Laboratory drying of herbage by radio-frequency 37
- Dielectrics, Propagation in waveguides filled longitudinally with two or more 39
- Diffraction, electron, Recent developments in 297
- Digital computing techniques to physics, Application of 321
- Dimensions of physical quantities, The 201
- Diode, saturated-, stability, Measurements of 114
- Discharges, Conference on ionization phenomena in 96
- Disk, The effect of centring errors on the transmission of a sector 220
- Divergence, The effect of vertical, on X-ray powder diffraction lines 92
- Droplets, liquid, produced by an atomizer, A photographic method of observing the approximate size of 316
- Drying of herbage by radio-frequency dielectric heating, Laboratory 37
- Duddell Medal, Award of the 384
- Dust counter, the Owens jet, The reduction in apparent particle concentration with multiple strokes of 316
- Education of physicists, The scientific 32
- Electrical industry, Research in the 127
- Electron  
and optical microscopes, A method of observing selected areas in 141  
bombardment, Changes in secondary and thermionic emission from barium oxide during 56  
diffraction, Recent developments in 297  
microscope for reflexion and some observations on image formation, The adaptation of an 239

For *Static Electrification* and cognate subjects see also separate index to the supplement



Electron (*continued*)

- microscope specimens, Solid bodies appearing in 338  
 microscope, The origin of specimen contamination in the 101  
 -microscopical properties of textile fibres—Manchester, October 1952, Summarized proceedings of a conference on the optical and 119  
 microscopy of crystals, Techniques for the 177  
 microscopy, Summarized proceedings of a conference on—Bristol, September 1952 1  
 Emission from barium-oxide during electron bombardment, changes in secondary and thermionic 56  
 Equations of state, The linear piezoelectric 210  
 Errors, The effect of centring, on the transmission of a sector disk 220  
 Evaporation, Processes of convection and 65  
 Exhibition  
   British Instrument Industries 31  
   Centenary, of photographs and apparatus 96  
   of control techniques and instruments 160  
   of X-ray crystallographic equipment 160  
 Fibres  
   cotton, using polarized light, Measurements of orientation in 369  
   —Manchester, October 1952, Summarized proceedings of a conference on the optical and electron-microscopical 119  
   synthetic, The chemistry and physics of 288  
 Field  
   The magnetic, along the axes of symmetry of equal semi-infinite rectangular magnetic pole-pieces 339  
   The two-dimensional magnetic or electric, above and below an infinite corrugated sheet 134  
 Fields, The magnetic, produced by uniformly magnetized ellipsoids of revolution 207  
 Fluorescence efficiencies in the Schumann region, Some relative 303  
 Frames, fixed base portal, Model to illustrate the behaviour of, in the plastic range 54  
 Frozen-stress observations, A method of correcting for initial stresses in 281  
 Gamma-ray sources, isotope, Handling equipment and safety containers for use with 268  
 Gases, Formative time lags in the electrical breakdown of 170  
 Gold as a grid emission inhibitor in the presence of an oxide-coated cathode 311  
 Goniometers, The use of X-ray diffraction cameras as recording optical 88  
 Handling equipment and safety containers for use with isotope gamma-ray sources for industrial radiography 268  
 Herbage, Laboratory drying of, by radio-frequency dielectric heating 37  
 Hot wire stretched along the axis of a vertical cylindrical tube, Ratio of convection to conduction loss from a 204  
 Ignition, The automatic electrical, of the d.c. arc in spectrographic analysis 118  
 Image formation, some observations on, The adaptation of an electron microscope for reflexion and 239  
 Impedance, The motional, of simple sources in an isotropic solid 12  
 Information theory 129, 288  
 Inhibitor, Gold as a grid emission, in the presence of an oxide-coated cathode 311  
 Institute of Physics, The 224  
   Elections to 31, 64, 127, 224, 256, 352, 384

## Ionization

- method of measuring contact potential, A modified 111  
 phenomena in discharges, Conference on 96  
 Ionizing radiations, Protection from 384  
 Isotope gamma-ray sources for industrial radiography, Handling equipment and safety containers for use with 268  
 Isotopes, radioactive, in metallurgy. The use of 326  
 Jet engine, Pressure fluctuations in a 359  
 Journal  
   of *Photographic Science, The* 288  
   of the *Audio Engineering Society* 320  
 Lattice spacing measurements, A note on temperature control during 189  
 Layers, cohesive, The compression and bearing capacity of 20  
 Lectures on various aspects of magnetism 256  
 Light  
   scattering from polydisperse systems of spherical particles, Some aspects of 344  
   scattering measurements on polydisperse systems of spherical particles 366  
 Liquid  
   droplets produced by an atomizer, A photographic method of observing the approximate size of 316  
   film, Investigation of the instability of a moving 167  
 Liquids, An apparatus for measuring the coefficient of thermal conductivity of solids and 112  
 Magnetic materials, On the temperature sensitivity of special 161  
 Magnets and magnetism—recent developments 257  
 Mercury, Current densities of free-moving cathode spots on 252  
 Metallurgy, radioactive isotopes in, The use of 326  
 Metals, Creep and recovery in 225  
 Microbalance, A vibrating reed, for susceptibility measurements in weak fields 46  
 Microscope  
   electron, The adaptation of an, for reflexion and some observations on image formation 239  
   electron, The origin of specimen contamination in the 101 specimens, electron, Solid bodies appearing in 338  
 Microscopes, electron and optical, A method of observing selected areas in 141  
 Mills, cold reduction, The stresses in the reels of 213  
 Model  
   for demonstrating dislocations in crystals, A 144  
   to illustrate the behaviour of fixed base portal frames in the plastic range 54  
 Models of crystal structures, The construction of ball-and-spoke 107  
 Moisture  
   in granular materials, The electrical measurement of 84  
   Measurement of, content by neutron counting 93  
 Motor, Electronic control of a synchronous 147  
 National Research Development Corporation, The work of the 127  
 Neon indicator tubes as quantitative detectors in photometry 245  
 Neutron counting, Measurement of moisture content by 93  
 Nickel, Production of single crystals of 342  
 Notes on the preparation of papers 32  
 Nuclear  
   physics, Conferences on, and on the solid state—July 1954 320  
   physics, Recent advances in 289  
 Orientation  
   in cotton fibres using polarized light, Measurements of 369  
   preferred, in etched metal polycrystals, A simple goniometric method for examining 29

For *Static Electrification* and cognate subjects see also separate index to the supplement



- Oxide  
barium, Changes in secondary and thermionic emission from, during electron bombardment 56  
cathodes, The effects of oxygen on the electrical properties of 70  
-coated cathode, Gold as a grid emission inhibitor in the presence of an 311  
Oxygen, The effects of, on the electrical properties of oxide cathodes 70
- Papers, Notes on the preparation of* 32
- Particle  
concentration, The reduction in apparent, with multiple strokes of the Owens jet dust counter 316  
size analysis, Conference on the physics of 31  
Particles in air current, Measurements of the speed of little 284  
Photoelastic  
determination of stresses in a cylindrical shell 76, 284  
work, An ethoxylene resin for 181  
Photography, International conference on the science and applications of 256  
Photometry, Neon indicator tubes as quantitative detectors in 245  
Photomultipliers, spectrophotometric measurements in the vacuum ultra-violet using 6  
Photoplasticity, Fundamental relations in 306  
Physicists, *The scientific education of* 32  
Piezoelectric equations of state, The linear 210  
Plastic range, Model to illustrate the behaviour of fixed base portal frames in the 54  
Pole-pieces, equal semi-infinite rectangular magnetic, The field along the axes of symmetry of 339  
Polycrystals, etched metal, A simple goniometric method for examining preferred orientation in 29  
Polymeric materials, high, Frictional and elastic properties of 260 (Vol. 3); 32  
Potential, contact, A modified ionization method of measuring 111  
*Preparation of papers, Notes on the* 32  
Pressure  
barometric, on watch and chronometer rates, The influence of 379  
fluctuations in a jet engine 359  
Prizes for original contributions in the *Journal of Scientific Instruments* 256  
Properties  
Frictional and elastic, of high polymeric materials 260 (Vol. 3); 32  
of oxide cathodes, The effects of oxygen on the electrical 70  
of textile fibres—Manchester, October 1952, Summarized proceedings of a conference on the optical and electron-microscopical 119  
of transistors, Some transient 116  
Protection, radiation, Summarized proceedings of a meeting on—London, January 1953 234  
Protons in the Harwell cyclotron, Energy spectrum measurements of 175  
Pyrometers, bichromatic, The theoretical characteristics of 374
- Radiation  
measurement, Sampling errors in, using the Moll thermopile method 273  
protection—London, January 1953, Summarized proceedings of a meeting on 234  
Radiations, ionizing, Protection from 384  
Radioactive  
carbon in gas counters, The measurement of 217  
isotopes in metallurgy, The use of 326  
Radiography, industrial, Handling equipment and safety containers for use with isotope gamma-ray sources for 268  
Reflectivity of a thermopile, A method for measuring the spectral 151  
Reflexion, The adaptation of an electron microscope for, and some observations on image formation 239
- Refractive  
index determination for anisotropic crystals 185, 284  
*Register of British manufacturers* 31  
Reports on the reliability of engineering plant 160  
*Research film* 127  
Resin, An ethoxylene, for photoelastic work 181  
Resonator, Proposed use of a cylindrical surface wave, for the determination of the velocity of short electromagnetic waves 186  
Retardations, fractional relative, On the Tardy and Sénarmont methods of measuring 138  
Rheology, Second international congress on 64  
Rotation, Some scientific applications of high-speed 97
- Safety in mines research 160  
Sensitivity, temperature, of special magnetic materials, On the 161  
Sinkage of tracked vehicles on soft ground, The 330  
Solenoids, High power, stresses and stability 50  
Solid  
bodies appearing in electron microscope specimens 338  
isotropic, The motional impedance of simple sources in an 12  
state, Conferences on nuclear physics and on the,—July 1954 320  
Solids  
An apparatus for measuring the coefficient of thermal conductivity of, and liquids 112  
crystalline, Conference on defects in 352  
Sources, isotope gamma-ray, for industrial radiography, Handling equipment and safety containers for use with 268  
Specimen contamination in the electron microscope, The origin of 101  
Spectrographic analysis, The automatic electrical ignition of the d.c. arc in 118  
Spectrometry, applied mass, Conference on 288  
Spectrophotometric measurements in the vacuum ultra-violet using photomultipliers 6  
Spectroscopy, Direct-reading emission 127  
Stability, Measurements of saturated-diode 114  
Standard observer data at 4358 Å, A check on the 80  
Static electrification, Conference on 31 *see also Supplement*  
Stresses  
in a cylindrical shell, Photoelastic determination of 76, 284  
initial, in frozen-stress observations, A method of correcting for 281  
The, in the reels of cold reduction mills 213  
Summer school  
and conference on the theory of the plastic deformation of metals 96  
in the use of electrons in the examination of metals, Cambridge 1953 160
- Tables for use in the measurement of interfacial tensions between liquids with small density differences 247  
Temperature control during lattice spacing measurements, A note on 188  
Tension in strings wrapped slantwise round cylinders, The 145  
Tensions, Tables for use in the measurement of interfacial, between liquids with small density differences 247  
Thermopile  
A method for measuring the spectral reflectivity of a 151  
method, the Moll, Sampling errors in radiation measurement using 273  
Time  
constant of exponential decays, A simple bridge method of measurement of the 350  
lags, Formative, in the electrical breakdown of gases 170  
Transistors, Some transient properties of 116  
Tubes, Neon indicator, as quantitative detectors in photometry 245

For *Static Electrification* and cognate subjects *see also* separate index to the supplement



- Ultra-violet, spectrophotometric measurements in the vacuum, using photomultipliers 6
- Vacuum
  - system, An electrical analogue to a high 188
  - systems, Further applications of the electrical analogue to 350
- Valve industry, electronic, Physics in the 262
- Valves, List of preferred 320
- Vehicles, tracked, on soft ground, The sinkage of 330
- Velocity of short electromagnetic waves, Proposed use of a cylindrical surface wave resonator for the determination of the 186
- Vibrations, transverse, of rods and reeds, A method of examining the 279
- Voltage severity, The evaluation of restriking 32
- Watch and chronometer rates, The influence of barometric pressure on 379
- Waveguides filled longitudinally with two or more dielectrics, Propagation in 39
- Waves, short electromagnetic, Proposed use of a cylindrical surface wave resonator for the determination of the velocity of 186
- Weights and measures legislation, Discussion of 64
- X-ray
  - crystallographic equipment, Exhibition of 160
  - diffraction cameras as recording optical goniometers, The use of 88
  - diffraction, Summarized proceedings of the fortieth anniversary celebrations of the discovery—London, October 1952 33
  - line breadths, The measurement of 155
  - powder diffraction lines, The effect of vertical divergence on 92
  - The British, and Radium Protection Committee 127

---

*For Static Electrification and cognate subjects see also separate index to the supplement*

---

## NAME INDEX

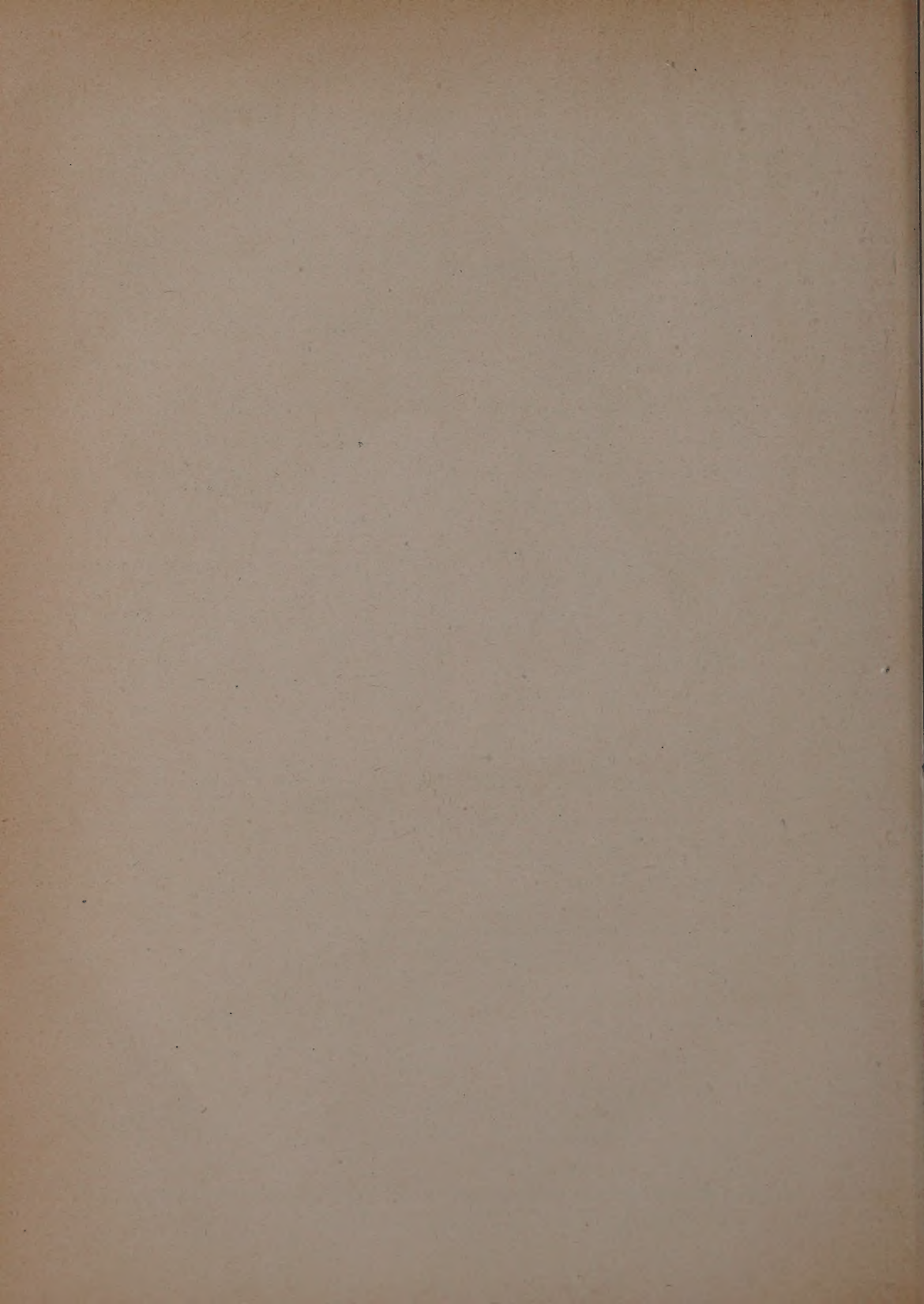
- Aitken, M. J., An electrical analogue to a high vacuum system 188  
 Alexander, L., The effect of vertical divergence on X-ray power diffraction lines 92  
 Allen, D. R., H. S. Peiser and J. R. Rait, Handling equipment and safety containers for use with isotope gamma-ray sources for industrial radiography 268  
 Anantharaman, T. R., and J. W. Christian, The measurement of X-ray line breadths 155  
 Atherton, E., and R. H. Peters, Light scattering measurements on polydisperse systems of spherical particles 366  
 Atherton, E., and R. H. Peters, Some aspects of light scattering from polydisperse systems of spherical particles 344  
 Attree, V. H., Measurements of saturated-diode stability 114  
 Axon, H. J., A. Hellawell, D. M. Poole and W. Hume-Rothery, A note on temperature control during lattice spacing measurements 189  
 Baker, B. O., Gold as a grid emission inhibitor in the presence of an oxide-coated cathode 311  
 Barlow, H. M., and A. E. Karbowiak, Proposed use of a cylindrical surface wave resonator for the determination of the velocity of short electromagnetic waves 186  
 Bassett, H. G., and J. R. Tillman, Some transient properties of transistors 116  
 Bayoumi, S. E. A., and E. K. Frankl, Fundamental relations in photoplasticity 306  
 Bechmann, R., The linear piezoelectric equations of state 210  
 Bentley, R. A., J. Cartwright and R. L. Gordon, A photographic method of observing the approximate size of liquid droplets produced by an atomizer 316  
 Berger, B., *see under* Taylor, E. D.  
 Bigg, P. H., *see under* Stone, N. W. B.  
 Bolton, J. H., and S. E. Williams, Spectrophotometric measurements in the vacuum ultra-violet using photomultipliers 6  
 Brooker, R. A., Application of digital computing techniques to physics 321  
 Bueren, H. G. van, A model for demonstrating dislocations in crystals 144  
 Bunn, C. W., Refractive index determination for anisotropic crystals 284  
 Burrell, C. M., A simple bridge method of measurement of the time constant of exponential decays 350  
 Cartwright, J., *see under* Bentley, R. A.  
 Chambers, L. G., Propagation in waveguides filled longitudinally with two or more dielectrics 39  
 Chaplin, T. K., *see under* Meyerhof, G. G.  
 Christian, J. W., *see under* T. R. Anantharaman  
 Cockcroft, J., Recent advances in nuclear physics 289  
 Cosslett, V. E., J. Nutting and R. Reed, Summarized proceedings of a conference on electron microscopy—Bristol, September 1952 1  
 Daniels, J. M., High power solenoids; stresses and stability 50  
 Davidson, P. M., Formative time lags in the electrical breakdown of gases 170  
 Davy, N., *see under* Langton, N. H.  
 Davy, N., *see under* Peake, H. J.  
 Davy, N., *see under* Snowden, W.  
 Dawson, I. M., Techniques for the electron microscopy of crystals 177  
 Dickson, J. M., and D. C. Salter, Energy spectrum measurements of protons in the Harwell cyclotron 175  
 Dillon, T. J., Neon indicator tubes as quantitative detectors in photometry 245  
 Donoghue, J. K., The reduction in apparent particle concentration with multiple strokes of the Owens jet dust counter 316  
 Drummond, D. G., Summarized proceedings of a conference on the optical and electron-microscopical properties of textile fibres—Manchester, October 1952 119  
 Dugdale, R. A., The colouring of diamonds by neutron and electron bombardment 334  
 Dunsmuir, P., A simple goniometric method for examining preferred orientation in etched metal polycrystals 29  
 Dutton, J., S. C. Haydon and F. Llewellyn Jones, Formative time lags in the electrical breakdown of gases 170  
 Eastabrook, J. N., The effect of vertical divergence on X-ray powder diffraction lines 92  
 Elliott, K. W. T., *see under* Stone, N. W. B.  
 Ennos, A. E., The origin of specimen contamination in the electron microscope 101  
 Evans, I., The sinkage of tracked vehicles on soft ground 330  
 Fairbrother, J. A. V., Ratio of convection to conduction loss from a hot wire stretched along the axis of a vertical cylindrical tube 204, 382  
 Fessler, H., and R. T. Rose, Photoelastic determination of stresses in a cylindrical shell 76, 284  
 Fox, L. L., R. C. G. Packham, P. L. Palmer and D. Whittaker, Sampling errors in radiation measurement using the Moll thermopile method 273  
 Frankl, E. K., *see under* Bayoumi, S. E. A.  
 Franks, J., On growing single crystals of thallium activated alkali halides 377  
 Froome, K. D., Current densities of free-moving cathode spots on mercury 91  
 Fürth, R., The dimensions of physical quantities 201  
 Gillham, E. J., A method for measuring the spectral reflectivity of a thermopile 151  
 Gordon, R. L., *see under* Bentley, R. A.  
 Haine, M. E., and W. Hirst, The adaptation of an electron microscope for reflexion and some observations on image formation 239  
 Harper, A. F. A., and A. J. Mortlock, The effect of centring errors on the transmission of a sector disk 220  
 Harper, W. R., A modified ionization method of measuring contact potential 111  
 Harrison, W., A check on the standard observer data at 4358 Å 80  
 Haydon, S. C., *see under* Dutton, J.  
 Heddle, T. A., On the temperature sensitivity of special magnetic materials 161  
 Hellawell, A., *see under* Axon, H. T.  
 Henson, A. F., The measurement of radioactive carbon in gas counters 217  
 Herne, H., The theoretical characteristics of bichromatic pyrometers 374  
 Hibbard, L. U., Electronic control of a synchronous motor 147  
 Hirst, W., *see under* Haine, M. E.  
 Horne, M. R., Model to illustrate the behaviour of fixed base portal frames in the plastic range 54  
 Hume-Rothery, W., *see under* Axon, H. J.

For *Static Electrification* and cognate subjects *see also* separate index to the supplement



- Jessop, H. T., and W. H. Stableford, A method of correcting for initial stresses in frozen-stress observations 281
- Jessop, H. T., On the Tardy and Sénarmont methods of measuring fractional relative retardations 138
- Karbowiak, A. E., *see under* Barlow, H. M.
- Kennedy, A. J., Creep and recovery in metals 225
- Kirby, P. L., A method of examining the transverse vibrations of rods and reeds 279
- Kobayashi, K., *see under* Yasuzumi, G.
- Langton, N. H., and N. Davy, The two-dimensional magnetic or electric field above and below an infinite corrugated sheet 134
- Liebmann, G., Electrical analogues 193
- Lincoln, B., Frictional and elastic properties of high polymeric materials 260 (Vol. 3); 32
- Lipson, H., Summarized proceedings of the fortieth anniversary celebrations of the discovery of X-ray diffraction—London, October 1952 33
- Llewellyn Jones, F., *see under* Dutton, J.
- Luscher, E., Measurements of the speed of little particles in air current 284
- Mack, C., The tension in strings wrapped slantwise round cylinders 145
- Mack, C., *see under* Donoghue, J. K.
- Mackay, A. L., Refractive index determination for anisotropic crystals 185, 284
- Marshall, T. A., An apparatus for measuring the coefficient of thermal conductivity of solids and liquids 112
- Maslen, V. W., N. E. White and S. E. Williams, Some relative fluorescence efficiencies in the Schumann region 303
- Mayneord, W. V., Scintillation counting and its medical applications 353
- McConnell, L. D., *see under* Spooner, H.
- Megaw, H. D., The construction of ball-and-spoke models of crystal structures 107
- Meredith, R., Measurements of orientation in cotton fibres using polarized light 369
- Merridew, J. N., and W. F. Raymond, Laboratory drying of herbage by radio-frequency dielectric heating 37
- Meyerhof, G. G., and T. K. Chaplin, The compression and bearing capacity of cohesive layers 20
- Millard, D. J., The electrical measurement of moisture in granular materials 84
- Mills, O. S., Tables for use in the measurement of interfacial tensions between liquids with small density differences 247
- Moon, P. B., Some scientific applications of high-speed rotation 97
- Morioka, T., *see under* Yasuzumi, G.
- Mortlock, A. J., *see under* Harper, A. F. A.
- Nankivell, J. F., A method of observing selected areas in electron and optical microscopes 141
- Nicholson, H. M., and A. Radcliffe, Pressure fluctuations in a jet engine 359
- Nobbs, J. M., The automatic electrical ignition of the d.c. arc in spectrographic analysis 118
- Nutting, J., *see under* Cosslett, V. E.
- Packham, R. C. G., *see under* Fox, L. L.
- Palmer, P. L., *see under* Fox, L. L.
- Peake, H. J., and N. Davy, The magnetic fields produced by uniformly magnetized ellipsoids of revolution 207
- Pearson, R. F., Production of single crystals of nickel 342
- Peiser, H. S., *see under* Allen, D. R.
- Peters, R. H., *see under* Atherton, E.
- Place, J. A., *see under* Sims, R. B.
- Poole, D. M., *see under* Axon, H. J.
- Pursey, H., The motional impedance of simple sources in an isotropic solid 12
- Radcliffe, A., *see under* Nicholson, H. M.
- Rait, J. R., *see under* Allen, D. R.
- Raymond, W. F., *see under* Merridew, J. N.
- Reed, R., *see under* Cosslett, V. E.
- Richardson, E. G., Processes of convection and evaporation 65
- Rose, R. T., *see under* Fessler, H.
- Rymer, T. B., Recent developments in electron diffraction 297
- Salter, D. C., *see under* Dickson, J. M.
- Sharpe, J., Measurement of moisture content by neutron counting 93
- Shepherd, A. A., The effects of oxygen on the electrical properties of oxide cathodes 70
- Shuttleworth, R., The use of radioactive isotopes in metallurgy 326
- Sims, R. B., and J. A. Place, The stresses in the reels of cold reduction mills 213
- Smith, C. G., Current densities of free-moving cathode spots on mercury 252
- Smith, E. E., Summarized proceedings of a meeting on radiation protection—London, January 1953 234
- Snowdon, W., and N. Davy, The field along the axes of symmetry of equal semi-infinite rectangular magnetic pole-pieces, 339
- Spooner, H., and L. D. McConnell, An ethoxylene resin for photo-elastic work 181
- Squire, H. B., Investigation of the instability of a moving liquid film 167
- Stableford, W. H., *see under* Jessop, H. T.
- Stanley, E., The use of X-ray diffraction cameras as recording optical goniometers 88
- Stone, N. W. B., K. W. T. Elliott and P. H. Bigg, The influence of barometric pressure on watch and chronometer rates 379
- Stops, D. W., Further applications of the electrical analogue to vacuum systems 350
- Sucksmith, W., Magnets and magnetism—recent developments 257
- Tanaka, A., *see under* Yasuzumi, G.
- Taylor, E. D., B. Berger and B. E. Western; J. A. V. Fairbrother, Ratio of convection to conduction loss from a hot wire stretched along the axis of a vertical cylindrical tube 382
- Thomson, J., Physics in the electronic valve industry 262
- Tillman, J. R., *see under* Bassett, H. G.
- v. Bertele, H., Current densities of free-moving cathode spots on mercury 91
- Western, B. E., *see under* Taylor, E. D.
- White, N. E., *see under* Maslen, V. W.
- Whittaker, D., *see under* Fox, L. L.
- Williams, S. E., *see under* Bolton, J. H.
- Williams, S. E., *see under* Maslen, V. W.
- Woods, J., and D. A. Wright, Changes in secondary and thermionic emission from barium oxide during electron bombardment 56
- Woodward, P. M., Information theory 129, 288
- Wright, D. A., *see under* Woods, J.
- Yasuzumi, G., T. Morioka, A. Tanaka and K. Kobayashi, Solid bodies appearing in electron microscope specimens 338
- Yousef, Y. L., A vibrating reed microbalance for susceptibility measurements in weak fields 46

For Static Electrification and cognate subjects *see also* separate index to the supplement





# CONTENTS OF VOLUME 4

JANUARY 1953

## CONFERENCE REPORT

- Summarized proceedings of a conference on electron microscopy—Bristol, September 1952. By V. E. COSSLETT, J. NUTTING and R. REED . . . . . 1

## ORIGINAL CONTRIBUTIONS

- Spectrophotometric measurements in the vacuum ultra-violet using photomultipliers. By J. H. BOLTON and S. E. WILLIAMS . . . . . 6  
The motional impedance of simple sources in an isotropic solid. By H. PURSEY . . . . . 12  
The compression and bearing capacity of cohesive layers. By G. G. MEYERHOF and T. K. CHAPLIN . . . . . 20  
A simple goniometric method for examining preferred orientation in etched metal polycrystals. By P. DUNSMUIR . . . . . 27

## NOTES AND NEWS

- New books . . . . . 29  
Notes and comments . . . . . 31

FEBRUARY 1953

## CONFERENCE REPORT

- Summarized proceedings of the fortieth anniversary celebrations of the discovery of X-ray diffraction—London, October 1952. By H. LIPSON . . . . . 33

## ORIGINAL CONTRIBUTIONS

- Laboratory drying of herbage by radio-frequency dielectric heating. By J. N. MERRIDEW and W. F. RAYMOND . . . . . 37  
Propagation in waveguides filled longitudinally with two or more dielectrics. By LL. G. CHAMBERS . . . . . 39  
A vibrating reed microbalance for susceptibility measurements in weak fields. By Y. L. YOUSEF . . . . . 46  
High power solenoids; stresses and stability. By J. M. DANIELS . . . . . 50  
Model to illustrate the behaviour of fixed base portal frames in the plastic range. By M. R. HORNE . . . . . 54  
Changes in secondary and thermionic emission from barium oxide during electron bombardment. By J. WOODS and D. A. WRIGHT . . . . . 56

## NOTES AND NEWS

- New books . . . . . 61  
Notes and comments . . . . . 64

MARCH 1953

## SPECIAL ARTICLE

- Processes of convection and evaporation. By E. G. RICHARDSON . . . . . 65

## ORIGINAL CONTRIBUTIONS

- The effects of oxygen on the electrical properties of oxide cathodes. By A. A. SHEPHERD . . . . . 70  
Photoelastic determination of stresses in a cylindrical shell. By H. FESSLER and R. T. ROSE . . . . . 76

PAGE

- A check on the standard observer data at 4358 Å. By W. HARRISON . . . . . 80  
The electrical measurement of moisture in granular materials. By D. J. MILLARD . . . . . 84  
The use of X-ray diffraction cameras as recording optical goniometers. By E. STANLEY . . . . . 88

## NOTES AND NEWS

### Correspondence

- Current densities of free-moving cathode spots on mercury. From K. D. FROOME; H. V. BERTELE . . . . . 91  
The effect of vertical divergence on X-ray powder diffraction lines. From L. ALEXANDER; J. N. EASTABROOK . . . . . 92  
Measurement of moisture content by neutron counting. From J. SHARPE . . . . . 93  
New books . . . . . 94  
Notes and comments . . . . . 96

APRIL 1953

## SPECIAL ARTICLE

- Some scientific applications of high-speed rotation. By P. B. MOON . . . . . 97

## ORIGINAL CONTRIBUTIONS

- The origin of specimen contamination in the electron microscope. By A. E. ENNOS . . . . . 101  
The construction of ball-and-spoke models of crystal structures. By H. D. MEGAW . . . . . 107  
A modified ionization method of measuring contact potential. By W. R. HARPER . . . . . 111  
An apparatus for measuring the coefficient of thermal conductivity of solids and liquids. By T. A. MARSHALL . . . . . 112  
Measurements of saturated-diode stability. By V. H. ATTREE . . . . . 114  
Some transient properties of transistors. By H. G. BASSETT and J. R. TILLMAN . . . . . 116  
The automatic electrical ignition of the d.c. arc in spectrographic analysis. By J. M. NOBBS . . . . . 118

## CONFERENCE REPORT

- Summarized proceedings of a conference on the optical and electron-microscopical properties of textile fibres—Manchester, October 1952. By D. G. DRUMMOND . . . . . 119

## NOTES AND NEWS

- New books . . . . . 125  
Notes and comments . . . . . 127

MAY 1953

## SPECIAL ARTICLE

- Information theory. By P. M. WOODWARD . . . . . 129

## ORIGINAL CONTRIBUTIONS

- The two-dimensional magnetic or electric field above and below an infinite corrugated sheet. By N. H. LANGTON and N. DAVY . . . . . 134

# Contents of Volume 4

	PAGE		PAGE
On the Tardy and Sénarmont methods of measuring fractional relative retardations. By H. T. JESSOP	138	The magnetic fields produced by uniformly magnetized ellipsoids of revolution. By H. J. PEAKE and N. DAVY	207
A method of observing selected areas in electron and optical microscopes. By J. F. NANKIVELL	141	The linear piezoelectric equations of state. By R. BECHMANN	210
A model for demonstrating dislocations in crystals. By H. G. VAN BUEREN	144	The stresses in the reels of cold reduction mills. By R. B. SIMS and J. A. PLACE	213
The tension in strings wrapped slantwise round cylinders. By C. MACK	145	The measurement of radioactive carbon in gas counters. By A. F. HENSON	217
Electronic control of a synchronous motor. By L. U. HIBBARD	147	The effect of centring errors on the transmission of a sector disk. By A. F. A. HARPER and A. J. MORTLOCK	220
A method for measuring the spectral reflectivity of a thermopile. By E. J. GILLHAM	151	<b>NOTES AND NEWS</b>	
The measurement of X-ray line breadths. By T. R. ANANTHARAMAN and J. W. CHRISTIAN	155	<b>New books</b>	222
<b>NOTES AND NEWS</b>		<b>Notes and comments</b>	224
<b>New books</b>	157		
<b>MONOGRAPHS FOR STUDENTS SERIES</b>		<b>AUGUST 1953</b>	
<b>Notes and comments</b>	160	<b>SPECIAL ARTICLE</b>	
		Creep and recovery in metals. By A. J. KENNEDY	225
<b>JUNE 1953</b>		<b>SPECIAL REPORT</b>	
<b>SPECIAL ARTICLE</b>		Summarized proceedings of a meeting on radiation protection—London, January 1953. By E. E. SMITH	234
On the temperature sensitivity of special magnetic materials. By T. A. HEDDLE	161	<b>ORIGINAL CONTRIBUTIONS</b>	
<b>ORIGINAL CONTRIBUTIONS</b>		The adaptation of an electron microscope for reflexion and some observations on image formation. By M. E. HAINE and W. HIRST	239
Investigation of the instability of a moving liquid film. By H. B. SQUIRE	167	Neon indicator tubes as quantitative detectors in photometry. By T. J. DILLON	245
Formative time lags in the electrical breakdown of gases. By J. DUTTON, S. C. HAYDON and F. LLEWELLYN JONES; P. M. DAVIDSON	170	Tables for use in the measurement of interfacial tensions between liquids with small density differences. By O. S. MILLS	247
Energy spectrum measurements of protons in the Harwell cyclotron. By J. M. DICKSON and D. C. SALTER	175	<b>NOTES AND NEWS</b>	
Techniques for the electron microscopy of crystals. By I. M. DAWSON	177	<b>Correspondence</b>	
An ethoxylene resin for photoelastic work. By H. SPOONER and L. D. MCCONNELL	181	Current densities of free-moving cathode spots on mercury. From C. G. SMITH	252
Refractive index determination for anisotropic crystals. By A. L. MACKAY	185	<b>New books</b>	253
Proposed use of a cylindrical surface wave resonator for the determination of the velocity of short electromagnetic waves. By H. M. BARLOW and A. E. KARBOWIAK	186	<b>Notes and comments</b>	256
<b>NOTES AND NEWS</b>			
<b>Correspondence</b>		<b>SEPTEMBER 1953</b>	
An electrical analogue to a high vacuum system. From M. J. AITKEN	188	<b>SPECIAL ARTICLES</b>	
A note on temperature control during lattice spacing measurements. From H. J. AXON, A. HELLAWELL, D. M. POOLE and W. HUME-ROTHERY	188	Magnets and magnetism—recent developments. By W. SUCKSMITH	257
<b>New books</b>	189	Physics in the electronic valve industry. By J. THOMSON	262
<b>JULY 1953</b>		<b>ORIGINAL CONTRIBUTIONS</b>	
<b>SPECIAL ARTICLE</b>		Handling equipment and safety containers for use with isotope $\gamma$ -ray sources for industrial radiography. By D. R. ALLEN, H. S. PEISER and J. R. RAIT	268
Electrical analogues. By G. LIEBMANN	193	Sampling errors in radiation measurement using the Moll thermopile method. By L. L. FOX, R. C. G. PACKHAM, P. L. PALMER and D. WHITTAKER	273
<b>SPECIAL REPORT</b>		A method of examining the transverse vibrations of rod and reeds. By P. L. KIRBY	279
The dimensions of physical quantities. By R. FÜRTH	201	A method of correcting for initial stresses in frozen-stress observations. By H. T. JESSOP and W. H. STABLEFORD	281
<b>ORIGINAL CONTRIBUTIONS</b>		<b>NOTES AND NEWS</b>	
Ratio of convection to conduction loss from a hot wire stretched along the axis of a vertical cylindrical tube. By J. A. V. FAIRBROTHER	204	<b>Correspondence</b>	
		Photoelastic determination of stresses in a cylindrical shell. From H. FESSLER and R. T. ROSE	284



# Contents of Volume 4

	PAGE		PAGE
Refractive index determination for anisotropic crystals. From C. W. BUNN; A. L. MACKAY . . . . .	284	A simple bridge method of measurement of the time constant of exponential decays. From C. M. BURRELL . . . . .	350
Measurements of the speed of little particles in air current. From E. LUSCHER . . . . .	284	New books . . . . .	351
New books . . . . .	285	Notes and comments . . . . .	352
Notes and comments . . . . .	288		

## DECEMBER 1953

OCTOBER 1953		SPECIAL ARTICLE	
SPECIAL ARTICLES		Scintillation counting and its medical applications. By W. V. MAYNEORD . . . . .	
Recent advances in nuclear physics. By J. COCKCROFT . . . . .	289		353
Recent developments in electron diffraction. By T. B. RYMER . . . . .	297	ORIGINAL CONTRIBUTIONS	
ORIGINAL CONTRIBUTIONS		Pressure fluctuations in a jet engine. By H. M. NICHOLSON and A. RADCLIFFE . . . . .	
Some relative fluorescence efficiencies in the Schumann region. By V. W. MASLEN, N. E. WHITE and S. E. WILLIAMS . . . . .	303	Light scattering measurements on polydisperse systems of spherical particles. By E. ATHERTON and R. H. PETERS . . . . .	
Fundamental relations in photoplasticity. By S. E. A. BAYOUMI and E. K. FRANKL . . . . .	306	Measurements of orientation in cotton fibres using polarized light. By R. MEREDITH . . . . .	
Gold as a grid emission inhibitor in the presence of an oxide-coated cathode. By B. O. BAKER . . . . .	311	The theoretical characteristics of bichromatic pyrometers. By H. HERNE . . . . .	
NOTES AND NEWS		On growing single crystals of thallium activated alkali halides. By J. FRANKS . . . . .	
Correspondence		The influence of barometric pressure on watch and chrono- meter rates. By N. W. B. STONE, K. W. T. ELLIOTT and P. H. BIGG . . . . .	
A photographic method of observing the approximate size of liquid droplets produced by an atomizer. From R. A. BENTLEY, J. CARTWRIGHT and R. L. GORDON . . . . .	316	NOTES AND NEWS	
The reduction in apparent particle concentration with multiple strokes of the Owens jet dust counter. From J. K. DONOGHUE and C. MACK . . . . .	316	Correspondence	
New books . . . . .	317	Ratio of convection to conduction loss from a hot wire stretched along the axis of a vertical cylindrical tube. From E. D. TAYLOR, B. BERGER and B. E. WESTERN; J. A. V. FAIRBROTHER . . . . .	
Notes and comments . . . . .	320	New books . . . . .	
		Notes and comments . . . . .	

## NOVEMBER 1953

SPECIAL ARTICLES		SUPPLEMENT No. 2	
Application of digital computing techniques to physics. By R. A. BROOKER . . . . .		STATIC ELECTRIFICATION	
The use of radioactive isotopes in metallurgy. By R. SHUTTLEWORTH . . . . .	326	CONTACT ELECTRIFICATION	
ORIGINAL CONTRIBUTIONS		Theory of contact electrification. By Professor F. A. VICK, O.B.E., Ph.D., A.M.I.E.E., F.Inst.P., University College of North Staffordshire . . . . .	
The sinkage of tracked vehicles on soft ground. By I. EVANS . . . . .	330	GENERAL PRINCIPLES	
The colouring of diamonds by neutron and electron bombardment. By R. A. DUGDALE . . . . .	334	Survey of generation and dissipation of static electricity. By P. S. H. HENRY, Ph.D., F.Inst.P., The British Cotton Industry Research Association, Manchester . . . . .	
Solid bodies appearing in electron microscope specimens. By G. YASUZUMI, T. MORIOKA, A. TANAKA and K. KOBAYASHI . . . . .	338	The electrification of fluids in motion. By W. FORDHAM COOPER, B.Sc., M.I.E.E., H.M. Electrical Inspector of Factories . . . . .	
The field along the axes of symmetry of equal semi-infinite rectangular magnetic pole-pieces. By W. SNOWDON and N. DAVY . . . . .	339	Electrification by freezing. By E. W. GILL, M.A., B.Sc., Clarendon Laboratory, University of Oxford . . . . .	
Production of single crystals of nickel. By R. F. PEARSON . . . . .	342	Liquids giving no electrification by bubbling. By W. R. HARPER, Ph.D., F.Inst.P., Imperial College of Science and Technology, London . . . . .	
Some aspects of light scattering from polydisperse systems of spherical particles. By E. ATHERTON and R. H. PETERS . . . . .	344	The dissipation of electrical charges generated by rollers. By J. A. MEDLEY, M.Sc., Wool Industries Research Association, Torridon, Leeds . . . . .	
NOTES AND NEWS		The electrostatic charging of some polymers by mercury. By J. A. MEDLEY, M.Sc., Wool Industries Research Association, Torridon, Leeds . . . . .	
Correspondence		Further applications of the electrical analogue to vacuum systems. From D. W. STOPS . . . . .	
	350		

	PAGE	HARMFUL STATIC ELECTRIFICATION	PAGE
The role of asymmetric rubbing in the generation of static electricity. By P. S. H. HENRY, Ph.D., F.Inst.P., The British Cotton Industry Research Association, Manchester	S 31	Survey of harmful static electrification. By H. W. SWANN, O.B.E., M.I.E.E., Senior Electrical Inspector, Factory Department, Ministry of Labour and National Service.	S 68
Methods of increasing the electrical conductivity of surfaces. By J. S. FORREST, M.A., D.Sc., F.Inst.P., British Electricity Authority Research Laboratories, Leatherhead	S 37	The practical estimation of electrostatic hazards. By W. FORDHAM COOPER, B.Sc., M.I.E.E., H.M. Electrical Inspector of Factories	S 71
		Electrostatic eliminators in the textile industry. By P. S. H. HENRY, Ph.D., F.Inst.P., The British Cotton Industry Research Association, Manchester	S 78
USEFUL APPLICATIONS		Static electricity on rubber-tyred vehicles. By D. BULGIN, A.I.R.I., A.Inst.P., Dunlop Research Centre, Dunlop Rubber Co. Ltd., Birmingham	S 83
The physics of electrostatic precipitation. By H. J. LOWE, B.Sc., and D. H. LUCAS, B.A., A.Inst.P., British Electricity Authority Research Laboratories, Leatherhead	S 40	Factors in the design of an operating theatre free from electrostatic risks. By D. BULGIN, A.I.R.I., A.Inst.P., Dunlop Research Centre, Dunlop Rubber Co. Ltd., Birmingham	S 87
Two electrostatic field-meters. By A. S. CROSS, M.Sc., Grad.Inst.P., Research Laboratories, Kodak Ltd., Harrow, Middlesex	S 47	Safety measures in operating theatres and the use of a radioactive thallium source to dissipate static electricity. By A. QUINTON, M.Sc., A.Inst.P., United Birmingham Hospitals, Edgbaston, Birmingham	S 92
Electrostatic coating processes. By R. TILNEY, A.M.I.Mech.E., Henry W. Peabody (Industrial) Ltd., Great Suffolk Street, London	S 51	The electrostatic ignitibility and electrification of finely powdered Hexamine. By A. G. PEACE, B.Sc., Ph.D., A.Inst.P., North Staffordshire Technical College, Stoke-on-Trent	S 94
The measurement of oxidation of coal by static electrification. By D. G. A. THOMAS, M.A., A.Inst.P., Central Research Establishment, National Coal Board, Cheltenham, Gloucestershire	S 55	The ignition of explosives by condenser discharges—effect of added circuit resistance. By G. MORRIS, Ph.D., F.Inst.P., Imperial Chemical Industries Ltd., Stevenston, Ayrshire	S 97
ELECTROSTATIC MACHINES			
Survey of electrostatic generators. By E. S. SHIRE, M.A., Cavendish Laboratory, University of Cambridge	S 56	SUBJECT INDEX TO STATIC ELECTRIFICATION	S 101
Note on the voltage stabilization of an electrostatic generator. By D. R. CHICK, M.Sc., F.Inst.P., and E. K. INALL, B.Sc., B.E., Research Laboratory, Associated Electrical Industries Ltd., Aldermaston, Berkshire	S 61	NAME INDEX TO STATIC ELECTRIFICATION	S 103
Ten years of research on electrostatics at the University of Grenoble 1942–1952. By Professor N. J. FELICI, University of Grenoble. (Translated by A. M. CASSIE, M.A., F.Inst.P.)	S 62	SUBJECT INDEX TO VOLUME 4	385
		NAME INDEX TO VOLUME 4	390



## CONFERENCE REPORT

### Summarized proceedings of a conference on electron microscopy— Bristol, September 1952

The autumn conference of the Electron Microscopy Group of The Institute of Physics was held in The H. H. Wills Physical Laboratory of The University of Bristol from 16–18 September, 1952. The papers presented and the discussion on them are summarized; they were concerned with chemical, biological and metallurgical applications of the electron microscope, the examination of surface structures by reflexion electron microscopy, instrumental techniques and instrument design. An exhibition of electron micrographs and some apparatus was an important feature of the conference.

#### CHEMICAL APPLICATIONS

DR. I. M. DAWSON (Department of Chemistry, University of Glasgow) opened the Chemical Session by reporting that his original observations of spiral growth steps on *n* paraffin crystals had been confirmed for other compounds containing both odd and even numbers of carbon atoms. In the case of two of the compounds examined, *n*-heptane  $n\text{-C}_{100}\text{H}_{202}$  and *n*-dooctacotane  $n\text{-C}_{82}\text{H}_{166}$  the rapid growth of twinned crystals was observed and this mode of growth was ascribed to the formation of an indestructible molecular step at the twin boundary. The examination of paraffin crystals which had been subjected to a sudden increase in supersaturation during growth showed numerous secondary growth centres round the edges of the (001) faces of the crystals. Under these conditions the linear edges of the growth steps assumed the irregular appearance characteristic of rapid molecular deposition on the crystal surface. The structures observed were related to the data obtained from X-ray diffraction studies. The effects of introducing carboxyl and other groupings at the end of the long chain of carbon atoms were also discussed. The preparational techniques used in this type of work were reviewed by MR. N. G. ANDERSON (of the same Department) and DR. DAWSON.

MR. J. CARTWRIGHT (Safety in Mines Research Establishment, Sheffield) described a systematic approach to particle dispersion preparation in connexion with pneumoconiosis studies. An efficient electro-mechanical grinder was used for the rapid reduction of large samples. An aerosol sampler whereby particles could be mounted directly on specimen grids and a successful spray-gun method of mounting fluid suspensions were also illustrated. MR. P. E. WRIST, MR. H. W. EMERTON (British Paper and Board Industry Research Association) and MR. P. HATFIELD (Dunlop Research Laboratories) discussed the re-suspension of dried-down latex pellets using ultrasonic radiation of 300 kc/s. With suitable contact times, the latex particles can be re-dispersed so that they are indistinguishable from those of fresh suspensions, but longer times bring about reaggregation. The shape and size variations due to intensive drying and electron bombardment were discussed by DR. V. E. COSSLETT (Cavendish Laboratory, University of Cambridge) and DR. D. G. DRUMMOND (British Cotton Industry Research Association), who stressed the role of protein and other contaminants in this connexion. PROF. P. D. RITCHIE, MR. J. W. SHARPE and MR. J. GIBB (Royal Technical College, Glasgow) outlined some physico-chemical work on particles of Madagascar quartz, natural sand and Vitreosil, which had suggested the presence of a superficial layer with a solubility in hydrofluoric acid and borate buffer solutions appreciably higher than that of the innermost regions. Comparative electron diffraction

and electron optical studies were described which confirmed this view.

#### BIOLOGICAL APPLICATIONS

The Biological Session was opened by DR. C. E. CHALLICE (National Institute for Medical Research) who described the application of thin section work to a study of spermateliosis. The production of sections from testes of rodents, and the development of spermatozoa from the spermatids, were illustrated by many beautiful slides. The localization of mitochondria round the mid-piece and the formation of a spiral, were demonstrated, whilst cross-sections of the axial filament revealed a ring of fibrils and, at the proximal end, a ring inside that. At the centre, one, and occasionally two, fibrils were observed. The cortical helix and outer membrane were also illustrated and evidence given that the latter is derived directly from that of the spermatid. This paper was received with much enthusiasm and PROF. I. MANTON (Department of Botany, University of Leeds) congratulated DR. CHALLICE on the wealth of morphological information obtained and compared the structural features of the sperm tail of the rabbit with those obtained in her plant studies. DR. V. E. COSSLETT mentioned that he also had found little evidence of structural organization in the spermatozoan heads, even after enzymic treatment, but some was occasionally observed in the head of the human organism. PROF. J. T. RANDALL (King's College, London) also remarked that the connexion between the structures revealed by the electron microscope and the actual motion of living sperms, was not at all clear.

A comprehensive review of the methods developed at the University of Geneva for the cutting of thin sections of biological tissue was given by DR. D. DANON of that University. The methods for fixing, embedding and cutting the tissue, and the handling of the sections, were described and illustrated by many fine slides. Dr. Danon regarded fixation as the most critical stage of the work and reported that buffered osmium tetroxide solution had proved the best of the many fixatives which he had tested. On the other hand, the embedding stage does not appear to involve any great difficulties and various embedding media can be used with equally satisfactory results.

MR. J. SIKORSKI (Textile Physics Laboratory, University of Leeds) discussed some aspects of the fine structure of keratin with emphasis on the problem of reconciling the particulate character of the micro-fibrils as observed in electron microscopy, with the chain-molecular structure established by X-ray diffraction studies. Experiments with Australian Merino, Cotswold and Lincoln wools, horse hair and porcupine quill, indicated that the details observed in

micrographs depend upon the technique used for preparing the specimen. The particulate appearance was associated with hydrolysis of the polypeptide chains in the neighbourhood of certain amino acid residues thus its connexion with any corpuscles from which the fibrils may have been elaborated, is still open to question. In discussion PROF. J. T. RANDALL stated that in his view the particulate nature of such structures was indistinguishable from that of the background film and hence careful control work was needed to relate its formation to specific chemical reactions.

DR. A. F. HOWATSON (Royal Beatson Memorial Hospital, Glasgow) reported on the electron microscopic appearance of extracts from both normal and tumour tissue in birds and mice. Particulate material was observed in both types of extract and by imaging single droplets—obtained by spraying methods—it was proved conclusively that such material was present in the original extract. The possibility of the particles being breakdown products of mitochondria should be taken into account when attempting to associate virus activity with a certain size of particle.

DR. J. L. FARRANT (Commonwealth Scientific and Industrial Research Organization, Melbourne) and PROF. F. FENNER (Australian National University, Canberra) stated (in a paper read by DR. C. E. CHALLICE) that the viruses of myxoma, vaccinia and fowl pox were identical in shape, size and appearance under the electron microscope. It was considered, therefore, that previous methods, based on morphological characteristics, for distinguishing between these three types, no longer apply and that alternative ones are needed.

DR. J. R. G. BRADFIELD and MR. R. C. VALENTINE (Cavendish Laboratory, University of Cambridge) described a most interesting method for the rapid assessment of bacterial viability. When cultured on a urea/agar medium, certain bacilli no longer divide but develop into long filamentous forms; any dead cells merely retain their original shape. As applied at the electron microscope level, a stainless steel specimen grid bearing a film is inoculated with a known dilution of organisms which are allowed to grow on the special medium. The cells are fixed in osmium tetroxide vapour and washed free of medium, ready for examination under the electron microscope. By counting the long filamentous forms, the viability of the original suspension can be estimated. In model experiments the agreement with other and longer methods of estimation was extremely good. Some preliminary results of determining the lethal action of X-rays on viable cells were also given.

A continuance of their studies on the bacterial cell wall was reported by DR. I. M. DAWSON and DR. H. STERN (Department of Chemistry, University of Glasgow). Electron microscopic examination of the action of cetyl trimethyl ammonium bromide on the cells of *Staph. aureus* revealed the presence of a raised equatorial structure or septum, running across the cell and forming two distinct compartments. The authors considered that septum formation of this type is a normal event during division of the cells. DR. V. E. COSSLETT remarked that in his work at Cambridge he had observed similar structures in the wall of bacteria, but he doubted whether they actually divided the cell into distinct compartments.

#### METALLURGICAL APPLICATIONS

At various times during the conference, techniques were discussed which could be applied to the study of metals; the metallurgical session, however, was concerned with results of immediate significance.

In the metallography of two-phase alloys the shape and distribution of the particles of the second phase may be readily deduced. However, when quantitative information is required on the size of the particles difficulties arise in transforming the two-dimensional representation found on an electron micrograph into the true three-dimensional picture. MR. E. D. HYAM, DR. J. NUTTING and MR. L. STIBE (Department of Metallurgy, University of Cambridge) described how, from measurements on an electron micrograph of the apparent size distribution of a dispersed phase, the true particle size distribution may be determined. Two systems were outlined, the lineal and areal, together with their corresponding advantages and disadvantages. An indication was given of the corrections to be applied for the changes produced by etching. The methods had been used in a study of tempered steels. MR. E. D. HYAM and DR. J. NUTTING, in a further paper, reported changes in ferrite grain size produced by tempering a range of carbon steels with carbon contents from 0.1–0.9% at temperatures between 500 and 700°C, and for times up to 100 h. A simple Formvar replica technique was used. The grains were outlined on the replica by films present at their boundaries. Because of the thinness of the boundary film the grains, even when large, are not clearly seen in the optical microscope. In each steel a similar pattern of behaviour was found; the grain sizes varied from 500 Å at 500°C and short times to 30 000 Å at 700°C for long times. Generally the greater the carbon content the smaller the grain size.

The structure of hard chromium electro-deposits has been widely discussed in the past; a notable advance in the subject was made in the paper by MR. C. P. BRITAIN and MR. G. C. SMITH (Department of Metallurgy, University of Cambridge). They examined, with the aid of shadowed Formvar replicas, the changes occurring during the annealing of electro-deposited chromium, and found that in the fully hardened condition the grain size was of the order 150 Å, when fully softened the grain size increased to 10 000 Å. Although they were able to show a relationship between grain size and hardness, they were not convinced that grain size alone was the controlling factor but suggested that a dispersed phase could influence both the grain size and hardness. Some evidence of such a phase had been obtained.

MR. J. W. MARTIN and MR. G. C. SMITH (Department of Metallurgy, University of Cambridge) described experiments on the development of an oxide film replica technique for general application to metals. The method depended upon the work of Price and Thomas<sup>(1)</sup> who showed how alumina or beryllia films may be formed on silver by electrolytic deposition from an aqueous solution of aluminium or beryllium salts. The authors had stripped the alumina film formed on silver or copper by immersion of the specimen in mercury. Electron diffraction examination indicated the films were of fine grain size, and electron microscopic examination showed that a faithful replica was obtained. The chief difficulties encountered were in stripping the films and in removing the contaminating mercury.

Some recent advances in emission electron microscopy were reported by MR. G. BAAS (Holland). In a series of photographs he illustrated the advancing stages of the transformation of austenite into pearlite. The growth of pearlite colonies across austenite grain boundaries was an unexpected but clearly marked feature.

While the results obtained with the electron microscope have not been as outstanding in metallurgical as in biological investigations, the papers at the conference showed that steady progress is being maintained.



An interesting review of the papers read at the recent meeting of the German Electron Microscope Society at Tübingen was given by PROF. O. SCHERZER (Technische Hochschule, Darmstadt). This meeting was attended by MR. T. MULVEY (A.E.I. Research Laboratories, Aldermaston) who has published<sup>(2)</sup> a full account of the proceedings. A review of recent Russian work was also given by DR. J. W. MENTER (Physics and Chemistry of Surfaces Laboratory, University of Cambridge) and DR. A. F. BROWN (University of Edinburgh), based on translations they had made of the proceedings of a Moscow meeting in 1950. Instrument construction appears to follow conventional lines; thus double projector lens models, small simplified versions for schools and industry, and field emission types are being produced. Metallurgical, biological and photographic applications were described and a theoretical treatment of the possibility of seeing atoms was mentioned. Microscopes working at atmospheric pressure in the column are being tested and though the early results are poor by conventional electron microscope standards, they appear capable of further development.

#### REFLEXION ELECTRON MICROSCOPY

In the Reflexion Microscopy Session, several papers dealing with the investigation of solid surfaces by means of reflected electrons were grouped together, preceded by a short contribution by DR. W. HIRST (A.E.I. Laboratories, Aldermaston) on "The evaluation of surface topography." He outlined the needs of the practical metallurgist in high resolution microscopy. They can be partly met by transmission electron microscopy, but replicas fail in at least two important respects. They cannot be taken from specimens except at room temperature and pressure, and they cannot show variations in surface relief of long period, owing to lack of contrast. The reflexion electron microscope helps in both these directions, since the specimen can be viewed whilst its temperature and other conditions are varied and because the surface is greatly foreshortened in the line of sight when inclined at an angle of a few degrees to the optic axis of the lenses; at larger angles insufficient electrons are collected to give a visible picture, except possibly in a scanning type of instrument.

PROF. C. FERT (University of Toulouse) described the reflexion electron microscope constructed in his laboratory and showed some of the first results obtained. The instrument is intended for operation up to 250 kV, in both transmission and reflexion, so that it was inconvenient to incline the electron gun by mechanical means and magnetic deflexion coils were used for varying the angle between the illumination and the specimen surface. The latter is mounted with all the desirable degrees of freedom, including rotation in azimuth. The microscope has been tested up to 100 kV, and it was found that the quality of the micrographs improved with voltage; the best resolution approaches 500 Å, with an aperture of  $5 \times 10^{-3}$ . Image clarity is improved by using a grazing angle of illumination less than that of viewing. The latter was  $4^\circ$ , so that the image suffers foreshortening in a ratio of 1 to 14 and the magnification differs correspondingly in and across the plane of incidence. PROF. FERT discussed means of correcting this distortion, either in the photographic process or in the electron optical system itself. He favoured the introduction of cylindrical lenses into the objective to produce different magnifications in the two directions concerned, and was proposing to carry out the experiment.

The factors determining resolution, contrast and image

intensity in the reflexion method were discussed in a paper by MR. M. E. HAINE, DR. W. HIRST and MR. A. E. ENNOS (A.E.I. Research Laboratories, Aldermaston). Chromatic aberration is the chief limitation on resolution owing to the large energy losses of the scattered electrons; true reflexion occurs only in those favourable cases where the Bragg conditions are satisfied. A type EM3 microscope (by Metropolitan-Vickers Electrical Co. Ltd.) was modified for reflexion by fitting a gun inclinable at angles up to  $10^\circ$  to the axis, and by measuring the lack of image sharpness, the maximum energy loss was estimated at 150 V. With the angular aperture used and from the known properties of the lens, the limiting resolution in reflexion was calculated to be about 400 Å. Micrographs approaching this definition were obtained. By using a lens of smaller chromatic error and a smaller aperture, a resolution of 40–50 Å should be possible; such an aperture would, however, reduce the illumination so much that excessive exposures would be needed. It appears that the practical limit of reflexion microscopy is around 100 Å, some ten times worse than in transmission. The contrast is determined primarily by the angle of incidence of the beam, in relation to the roughness of the surface. Micrographs were shown to illustrate the great improvement in contrast of small steps on a surface as the grazing angle was reduced to  $0.3^\circ$ . In this way imperfections on an optical flat as small as 40 Å could be made visible, as distinct from the resolution of neighbouring points, which in this experiment was some ten times worse. The exposure time, on the other hand, is determined primarily by the angle of inclination of the specimen to the optic axis of the objective. By imaging the back focal plane of the latter when the grazing angle was zero, the distribution of intensity with scattering angle was investigated. It fell less rapidly than expected, dropping to about 10% at an angle of  $10^\circ$ . An angle of  $4\text{--}10^\circ$  has been mostly used in these investigations. The same authors showed also the effect of using a small aperture in the back focal plane of the objective, in normal viewing conditions, to select Bragg reflections. Only those parts of the specimen which are favourably orientated are then clearly imaged, so that they appear bright on a normal reflexion picture of the surface.

An electron microscope specially designed for reflexion electron microscopy, as a project of the British Iron and Steel Research Association, was described by DR. V. E. COSSLETT and MR. D. JONES (Cavendish Laboratory, University of Cambridge). The electron gun can be inclined at a variable angle to the axis, to a maximum of  $10^\circ$ , and the specimen is variable in tilt as well as in position. The specimen chamber is large, allowing the introduction of a furnace, etc. In order to accommodate specimens of a size useful in metallurgical investigations, the objective lens has a long focal length (15 mm) with the focal point well outside the pole piece. An intermediate lens permits wide and continuous variation of magnification. The relative strengths and separation of the lenses are calculated to give correction of both chromatic aberration and distortion when used for electron diffraction. The instrument is designed for a maximum voltage of 90 kV and has been tested at 60 kV; the micrographs of typical metallurgical specimens show a resolution of 600–700 Å. Further improvement should be obtained by reducing the chromatic aberration of the objective and employing a smaller aperture. It was found that prolonged exposure (about 1 h) of a ruled test surface to the intense electron beam required in reflexion microscopy resulted in a visible etching or recrystallization of the metal. It seems improbable that the temperature rose high enough for thermal etching to occur,

and it may be that direct ejection of metal atoms by electron impact is the cause.

DR. J. W. MENTER (Physics and Chemistry of Surfaces Laboratory, University of Cambridge) had also modified a type EM3 instrument for reflexion operation, by inserting a metal wedge to give a fixed ( $8^\circ$ ) inclination of the gun. He had investigated a wide variety of specimens, in some cases making a direct comparison with optical methods. This showed both the great advantage of the reflexion method in displaying surface relief and the difficulties attending interpretation of a greatly foreshortened image. Expressions were given for the distortion of angular relationships, from which the true geography of a surface could be calculated when no optical comparison was available. DR. MENTER discussed also the effects arising from the deposition of contamination on the illuminated part of the surface, unavoidable unless its temperature is high. The carbonaceous layer does not form rapidly enough to obscure detail in the order of resolution so far attained by him ( $400 \text{ \AA}$ ), and is advantageous in permitting easy recognition of the area investigated when an optical comparison is subsequently made. The shadows formed behind projections on the surface also allow an estimate to be made of their height, knowing the grazing angle, from the electron micrograph or even from an optical picture. Several insulating surfaces had been examined after deposition of a layer of silver by evaporation; cleavage steps on mica and growth spirals on silicon carbide showed clearly. On a cleavage face of zinc the small relative inclination of twins was revealed by a marked difference in contrast. Some indication was also given of possible biological applications.

A different method of investigating solid surfaces with electrons was described by MR. D. MACMULLAN (Engineering Laboratory, University of Cambridge). By successive demagnification, a very fine point focus of electrons is formed at the surface to be examined, and caused to scan it in a regular pattern by deflecting fields. The scattered electrons within a cone of  $30^\circ$  are collected in an electron multiplier, the output of which is fed to a synchronously operated display tube having a long delay screen. A visible picture is thus formed, of variable contrast as well as magnification. A similar picture formed on a second tube with a smaller screen of finer grain is photographed with an exposure time of the order of 1 min. An electron spot smaller than  $500 \text{ \AA}$  has already been obtained, giving a resolution of similar order, with a beam current of  $5 \times 10^{-12} \text{ A}$ . The great advantage of the instrument, which in itself is a considerable advance over previous attempts to build a scanning microscope, is that no lenses occur after the object so that the voltage spread of the scattered beam causes no chromatic aberration; resolution is limited then only by the size of the electron spot. An ultimate resolution below  $100 \text{ \AA}$  should be attainable.

The discussion centred on the resolution obtainable and the interpretation of reflexion micrographs.

#### INSTRUMENTAL TECHNIQUES

In the session dealing with Instrumental Techniques, MR. J. CARTWRIGHT described a neat focusing magnifier and exposure aid in which, by looking into an eyepiece, a portion of the viewing screen was compared with a field of known intensity derived from a small pilot lamp. The intensity of the latter could be varied by means of apertures and these were calibrated in terms of exposure times.

MR. J. F. NANKIVELL (National Physical Laboratory) gave details for observing the same areas of a metallurgical specimen in light and electron microscopes. The specimen was placed on the stage of the light microscope and any feature

needing electron microscopic examination was marked with a circle, drawn by rotating the stage around the axis of the objective lens where a diamond point was mounted. A replica film having been made, the marking circle was easily identified in the light microscope so that by bringing a mounting grid underneath, the desired feature was mounted directly in its centre. MR. A. W. AGAR and MR. R. S. M. REVELL (Research Laboratories, Metropolitan-Vickers Electrical Co. Ltd.) described a very similar method of marking using a system of scratches of characteristic pattern. The latter was easily identified in the replica film and enabled areas of interest to be mounted in suitable positions on the supporting grid.

MR. J. W. SHARPE described the production of some new films for supporting specimens, namely, rhodium, platinum and rhodium/platinum alloy. All were easily and rapidly prepared by the sputtering technique and had good strength, smooth appearance in the electron microscope and robust handling qualities. The pure rhodium films were considered the best and had lasted up to six months without apparent deterioration.

A novel method for the production of mounting grids was explained by DR. C. E. CHALLICE and MR. C. D. SUTTON (National Institute for Medical Research). A black and white drawing of the required grid shape is carefully photographed to help produce a master negative consisting of many reduced grid images packed closely together. Copper foil,  $1/1000$  in thick, is coated with a bichromated fish glue/ammonia mixture and the image of the grids printed on to it, using the master negative and strong arc light. After development in water, the glue is baked and backed with collodion. Etching with ferric chloride removes the unexposed parts of the copper and forms the grids. Thus it is possible to produce a variety of mesh patterns for special purposes, quite quickly and in one's own laboratory.

MR. M. VENNER (Metropolitan-Vickers Electrical Co. Ltd.) using a most direct and amusing approach, gave an account of user problems which arise during the servicing of electron microscopes. Suggestions and remedies were offered.

MR. A. E. ENNOS gave a comprehensive account of object contamination in electron microscopy whereby contrast and sharpness are reduced and the specimen increases in size. The contamination has been found to be amorphous carbon, derived probably from the oil of the diffusion pump, and its build-up is continuous with time of exposure to the electron beam. Normally the rate of growth is of the order  $\frac{1}{2} \text{ \AA/sec}$ , but under less favourable conditions higher rates are possible. The contamination is greater on the bars of the specimen grid than in its centre and this was related to the observation that temperature rise reduces the rate of contamination. On the grid bars, the energy derived from beam impact is dissipated more rapidly than in the centre, so that the temperature in the latter position is higher than on the bars, thus this effect is due to temperature gradient rather than to preferential migration of contaminant along the bars. The contamination layer thicknesses for various materials used in the construction of electron microscopes were given and MR. ENNOS described how they vary with pre-treatment. In discussion various speakers mentioned that the letting in of air seems temporarily to reduce the contamination.

DR. A. F. HOWATSON described the appearance of a curious contaminant obtained from a sealed ampoule of pure water. The foreign body resembled the conventional markings placed on micrographs for magnification assessment and discussion arose as to what such a contaminant might be. DR. DANON stated that he, too, had observed similar objects but could offer no explanation for them.



## INSTRUMENT DESIGN

The details of a new electron microscope of simplified design, by Philips Electrical, Ltd., were reported by IR. A. C. VAN DORSTEN and IR. J. B. LE POOLE (Philips Laboratories). By using a new objective as described at the St. Andrews conference,<sup>(3)</sup> simplification of the voltage and current regulators is possible since the lens, of short focal length (0.8 mm at 80 kV) has a low chromatic error. The projector, with a continuously variable gap in the lens, permits a continuous range of magnification from 3000 to 15 000 times. Apart from general simplification of design, what had been most remarkable was the gain in resolution obtained and in support of this claim, IR. LE POOLE showed a hitherto unobserved particulate structure in the bacterial cell wall. In discussion speakers were at a loss to account for the increased resolution, though many suggested that the rapid exposures possible with the new instrument might account for the improvement in that mechanical and voltage instability effects were minimized.

DR. V. E. COSSLETT and MR. W. C. NIXON (Cavendish Laboratory, University of Cambridge) described the construction of a successful X-ray shadow microscope. The development of such an instrument is well worth while, since the examination of entire organisms in the living state and which are too thick for conventional microscopy, is most important for many branches of biology. The resolution already achieved is of the order of twice that of the best optical microscope, as was shown by illustrations of insect morphology. The method involves the production of a fine beam of electrons by lens demagnification and already with a beam spot size of about 1 mm, high intensities of X-ray radiation are possible. This size of spot is considered adequate and the factor at present limiting the resolution is the astigmatism of the demagnifying lens. By paying more regard to the mechanical stability of the construction some further improvement may result.

DR. D. G. DRUMMOND (British Cotton Industry Research Association) described a curious form of asymmetrical magnification which, after experiments involving rotation of the pole piece relative to the lens windings, was ascribed to a queer field distribution along the axis of the projector lens. A new pole piece constructed on the principles put forward by Liebmann was free from such asymmetry and the lens had proved most satisfactory.

PROF. O. SCHERZER (Technische Hochschule, Darmstadt) discussed the origin of spherical aberration in electron lenses and the principles underlying its correction. Theoretical considerations led to the belief that this aberration could be removed by using electrostatic correcting lenses, whereby charge was applied from a series of plates arranged round the lens axis, so that the plane of the electron beam was rotated at various stages and in a known relationship, during passage through the lens. The full treatment indicated that three such correcting lenses were needed. Slides of the actual correcting systems and the fully assembled lens were shown and Prof. Scherzer said that in spite of the large number of centration controls, actual operation of the microscope proved much easier than anticipated and the resulting gain in resolution was very satisfying.

DR. LEISEGANG (Siemens-Halske Werke A.G., Berlin) stated that astigmatism in electron lenses is a serious limiting factor to any advance in resolution and that its recognition and elimination were no easy matters. He outlined a theoretical approach to this problem, based on the shape of the cross-section of the lens caustic, which enabled him to calculate the optimum position for insertion of pieces of soft

iron in a practical lens. These iron pieces can be rotated around the optical axis to give the minimum degree of astigmatism. A resolution limit of 10 Å or better was expected and work already carried out has confirmed this. In a paper on the same topic, DR. G. D. ARCHARD (A.E.I. Laboratories, Aldermaston) mentioned that astigmatism in a lens could arise from ellipticity of bore and corrugation of the face portions, that is, from machining defects. Moreover, in the assembly of the machined parts, astigmatism (and coma also) could arise from imperfect alignment. Dr. Archard agreed with Dr. Leisegang that the theoretical treatment of this effect is not easy, but explained that the previous work of Sturrock on lens quantities enabled an approach to be made and showed how the astigmatic distances could be related to lens quantities for various bore ellipticities and face corrugations. The analysis showed that slight changes in ellipticity could produce quite large changes in the astigmatism.

DR. A. BRUAUX (A.C.E.C., Belgium) outlined a new theoretical treatment for the determination of axial field distribution in magnetic lenses which permitted the electron trajectories to be calculated numerically. PROF. C. FERT also presented an alternative approach to the same question and then described some new methods for the direct measurement of  $H_z$  and its derivatives. A small search coil mounted on a straight bar is immersed in the lens field at a particular point on the axis, the bar vibrating at a definite frequency. The a.c. voltage developed across the ends of the coil is a function of  $H_z$ , thus field determination is reduced to measurement of this voltage. By special arrangements of small coils on the vibrating bar,  $H_z'$  and  $H_z''$  can also be obtained from a knowledge of the voltage developed. Prof. Fert also described a sensitive magnetic balance in conjunction with a sensitive optical deflexion system, by means of which very slight changes in field strength could be detected at any part of the lens.

DR. G. LIEBMANN (A.E.I. Research Laboratories, Aldermaston) discussed the effect of pole piece saturation in magnetic electron lenses and investigation of lens models by his resistance-network method under conditions of high flux density showed that the effect of iron saturation in the pole piece tips is equivalent to an apparent increase in lens dimensions. Published data for unsaturated magnetic lenses can be used beyond the onset of iron saturation if this effect, and the loss of ampere turns in the iron circuit, are taken into account. A practical limit of lens operation is approached for a flux density in the iron near the gap which would make the value of  $\mu$  approximately 50. Regarding the actual design of the magnetic circuit of lenses for the electron microscope, MR. T. MULVEY stated that previous authors have obtained the axial field distribution in the lens and have then worked out the best performance for existing magnetic materials. However, in order to achieve the best performance in practice, care is needed in the design of the magnetic circuit. In a well-designed lens, the highest flux density occurs in the air gap and not in some other part of the circuit. Design curves were given which allowed a correct choice of lens dimensions to be made.

V. E. COSSLETT  
J. NUTTING  
R. REED

## REFERENCES

- (1) PRICE, L. E., and THOMAS, G. J. *J. Inst. Metals*, **65**, p. 247 (1939).
- (2) MULVEY, T. *Nature, Lond.*, **170**, p. 271 (1952).
- (3) DRUMMOND, D. G., and LIEBMANN, G. *Brit. J. Appl. Phys.*, **3**, p. 28 (1952).

# Spectrophotometric measurements in the vacuum ultra-violet using photomultipliers

By J. H. BOLTON and S. E. WILLIAMS, Department of Physics, University of Western Australia

[Paper received 11 August, 1952]

The spectrograph and light sources, namely, capillary arc and pulsed discharge, used in experiments with fluorescence sensitized photomultipliers, are described. Insufficient signal-to-noise ratio was obtained from a 931A multiplier at 1200 Å with reasonably narrow slits. A 5060 multiplier gave a good response when the spectrograph slit was 0.048 mm (0.83 Å equivalent) and photomultiplier slit 0.025 mm (0.45 Å), allowing a resolving power of about 2000 at 1200 Å. The observed profile of 1215.6 Å showed that distortion and focusing errors were too small to prevent measurement of true maximum intensities. Apiezon B oil, L grease and zinc orthosilicate on L grease were found to give the best response as fluorescing agents. Some observations were made on the effect of water vapour passing through the discharge into the spectrograph.

Until the photomultiplier tube became available, intensity measurements in the vacuum region were almost entirely made by photographic photometry. Either Schumann-type emulsions were used, and the reciprocity law assumed to hold, or a fluorescing agent was employed to convert the incident radiation to a longer wavelength for which the characteristic of the emulsion could be determined. In either case, the procedure is tedious and the errors considerable, and the volume of information of a quantitative nature so far obtained is comparatively small.

In the past few years several workers have attempted to adapt the photomultiplier for intensity measurements in the vacuum region.<sup>(1)</sup> If the device of coating its window with a fluorescing agent is adopted, the photomultiplier then becomes a detector, whose sensitivity to different wavelengths varies only with the conversion efficiency of the fluorescing agent. Since it should not be difficult to find a suitable agent whose conversion efficiency changes very little over comparatively large ranges of wavelength, heterochromatic photometry becomes possible and the technique is, indeed, simpler than in the visible region where the sensitivity of the photosurface varies considerably. Additionally, since the photomultiplier signal is available for display on a cathode-ray screen, intensity variations occurring in very short time intervals can be studied. The field of investigation thus opened is very wide.

At the time this work was started the results of Tomboulion and Pell<sup>(2)</sup> and a brief notice of the work of Tousey and his collaborators<sup>(3,4)</sup> were available. Both groups had used the 1P21 or 931A type multiplier. It had been planned to attempt to use a 931A tube before a 5060 type became available, so the first experiments were made with this tube. Although small success was achieved with the 931A, the experiments made with it are described briefly. Experiments with the 5060 tube, which were highly successful, are described in the subsequent section. A brief note of these experiments has already been published.<sup>(5)</sup>

## SPECTROGRAPH

The spectrograph follows the design of Sawyer,<sup>(6)</sup> and is a near-normal incidence type with offset slit tube, employing a grating of 1 m focal length, 14 400 grooves per in, ruled by Professor K. M. G. Siegbahn. The first order spectra are very brilliant in the visible and the ghost intensities about one

or two parts per thousand. The dispersion in the 1200 Å region is about 0.058 mm per Å. The spectrograph is shown diagrammatically in Fig. 1. The main tube is of steel and the endplates, sealed by O-rings, carry the various external controls, connexions, photomultiplier housing, etc. A 9 in length of tube between the main body and the slit is attached by cone joints and can be used for absorption measurements when desired. A stop-cock shutter, 2 in behind the slit, serves to isolate the spectrograph from the source optically,

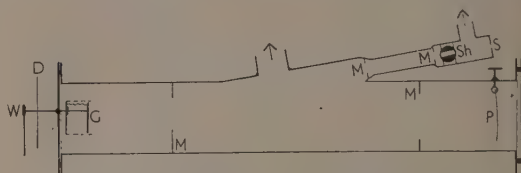


Fig. 1. Diagrammatic view of spectrograph

W, worm drive; D, graduated disk; G, grating; M, masks; P, plate; Sh, shutter; S, slit.

as well as when pumping. The slit is removed for adjustment and is set to parallelism under a microscope, which has an eyepiece graticule and a magnification about  $\times 100$ , with the aid of two eccentrically pivoted rings bearing one on each end of one slit jaw. Four masks are placed, as shown in Fig. 1, to eliminate reflected light.

For photography a plateholder is used, mounted on a hinged gate, the central image falling on the hinge axis. Focusing of the spectrum from 0–2200 Å is then arranged by swinging the gate in or out, as required. The plateholder can be moved vertically to accommodate several spectra, by rack and pinion operated through a Wilson seal. The grating mount carries the focusing control and means for moving the grating about any of three perpendicular axes. One of these, which turns the grating about a vertical axis, consists of a screwed rod moving freely in a screwed tube. When turned, the rod bears on the housing and the tube thrusts on the grating mount, extending a spring and moving the spectrum horizontally about 385 Å per turn. This control is brought out through the back plate to an 8 in disk carrying a hundred divisions. A subsidiary dial, driven off a worm, records complete revolutions of the screw.



Evacuation is from the mid-point of the body, and from between the slit and the shutter stopcock. Two mechanical pumps reduce the pressure to a value at which a three-stage diffusion pump can operate in about ten minutes. The diffusion pump completes evacuation to  $1 \mu$  or less in another ten minutes. A thermocouple gauge whose lower limit is  $1 \mu$  is used. For the region above  $1000 \text{ \AA}$ , a full-scale reading on this gauge indicates a satisfactory vacuum. When the pressure in the discharge tube is between one and two millimetres of nitrogen, which can leak into the spectrograph through a slit 5 mm long by  $0.035 \text{ mm}$  wide, the gauge shows a pressure between 5 and  $10 \mu$  in the spectrograph.

#### LIGHT SOURCES

Two types of source have been used, namely, a capillary arc either d.c. or a.c. operated, and a Lyman source involving the discharge of  $0.7 \mu\text{F}$  charged to about 12 kV through a 1.6 mm diameter capillary. The same discharge tube is used in each case. Originally, the design of Collins and Price,<sup>(7)</sup> whose tube used an internal seal as in Fig. 2(a), was followed. Failures due to localized heating by the arc discharge at the point marked *F*, prompted elimination of the seal and the use

supply to the discharge is controlled by a needle valve and the pressure is measured by an oil manometer, reading to  $0.05 \text{ mm}$  of mercury.

Blockage of the slit by sputtering and bombardment by glass particles from the discharge is minimized by a set of three diaphragms 1 by 10 mm, spaced 1 mm apart, situated about 1 cm in front of the slit. The alignment of the capillary is checked by putting a lamp at the position of the central image and viewing the slit through the hole in the rear electrode. This adjustment is facilitated by mounting the discharge tube on a support whose platform can be moved by screw controls. If the full aperture of the grating is to be used the end of the 1.6 mm capillary must be not more than 3 cm from the slit.

#### EXPERIMENTS WITH THE 931A TUBE

The 931A tube was small enough to be placed inside the spectrograph in a housing moving on rails attached to the focal curve. The housing could be moved round the focal curve by winding up a wire attached to the external control otherwise used for raising the plateholder, a very long spring being used to maintain even tension. The position of the

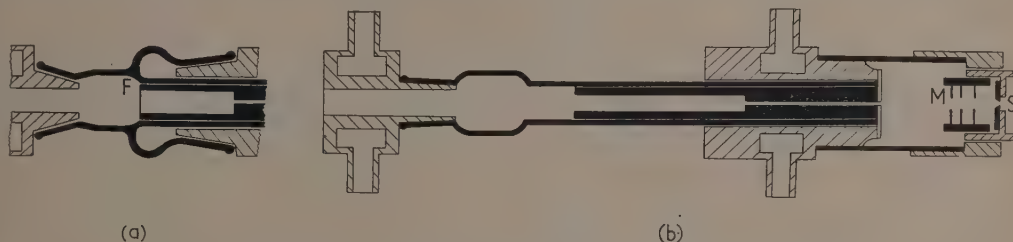


Fig. 2. (a) Discharge tube, after Collins and Price; (b) Modified discharge tube  
*M*, masks; *S*, slit.

of the tube shown in Fig. 2(b). The inter-electrode system can then be cooled by air blast. Wax seals are protected by water-cooling the aluminium electrodes.

The d.c. arc in a 1.6 mm capillary has been run at currents up to 200 mA ( $10 \text{ A per cm}^2$ ), with very satisfactory steadiness (less than 1% current variation), when care is taken to keep the tube interior clear of wax or dirt. The a.c. arc is less stable. The d.c. arc produces considerable "noise," whose spectrum extends from 1 kc/s to above 6 Mc/s and whose power is sufficient to cause severe interference by direct radiation to an ionospheric recorder some fifty yards distant. Such interference can be largely eliminated by shunting the tube with a  $0.1 \mu\text{F}$  condenser, but the intensity of wavelength  $1215.6 \text{ \AA}$  is reduced by 70%.

The pulsed discharge is operated at repetition rates up to 150 per minute by a motor-driven, short-circuiting switch consisting of a carbon rod set in a chord of a Perspex wheel and operating between similar carbon contacts. The capillary should be loosely fitted to allow movement during the shock wave caused by the passing of the current pulse.<sup>(8)</sup> This avoids shattering during warming up to full power. A good continuum extends to about  $600 \text{ \AA}$  and lines are recorded to  $360 \text{ \AA}$ . The apparent extension of the continuum from  $600 \text{ \AA}$  to near the central image is, however, spurious and due to fluorescence in the residual gas in the spectrograph occurring near the slit. The pulse is approximately exponential, falling to half in  $300 \mu\text{sec}$  with a rise-time less than  $10 \mu\text{sec}$ . Gas

931A in the spectrum was indicated by movement of a pointer on a dial outside the spectrograph, operated from the same external control.

To avoid exposing high voltage leads in the vacuum, the base of the 931A was removed, flexible leads covered by tightly-fitting polyvinyl chloride tubing were soldered to the dynode pins, and the whole covered by moulding ceresine wax on to the base. The flexible leads were taken through the endplate by attaching them to two octal metal valve bases sealed into the plate. An attempt to reduce the electrical leads into the vacuum to two, by fitting the bleeder resistance net directly to the base, was unsuccessful, as sufficient heat was developed to melt the wax. Electrical leakage, however, gave no trouble.

Fluctuations in the dark current of the 931A were larger than usual, being about  $2 \times 10^{-8}$  amps. Since signals of this order were to be looked for, a.c. excitation of the source, followed by selective amplification of the signal, was attempted so as to increase the signal-to-noise ratio.\*

A 500 c/s generator, whose frequency could be manually controlled, was used to excite the discharge with arc currents up to 400 mA in a capillary 2 mm in diameter. The photomultiplier output was passed through a pre-amplifier having a gain about  $\times 50$  and then fed to a selective audiofrequency

\* It has subsequently come to the authors' notice that a similar method was adopted by Kessler and Wolfe.<sup>(9)</sup>

amplifier modelled on the circuit described by Villard and Weaver<sup>(10)</sup> and called a "Selectoject." The advantage of this circuit is claimed to be easier adjustment of resonant frequency and degree of selectivity and higher attainable magnification factor ( $Q$ ), compared with the twin-T or Wien bridge. Battery operation was found to be necessary to obtain high selectivity and gain, as otherwise pulses from a full-wave power supply put the circuit into oscillation as tuning approached the optimum. So long as high impedance coupling was maintained at both ends of the Selectoject, it was found possible to attain a magnification factor of 75 at 1 kc/s and an overall gain through the pre-amplifier, Selectoject and a following pentode amplifier of about  $10^5$ . The signal then appeared on a voltmeter across the plate load of the pentode, a full-wave rectifier being inserted between the Selectoject and pentode stage. Alternatively, a cathode follower and galvanometer could be substituted for the voltmeter.

The spectrograph entrance slit was 0.12 mm wide and the slit before the multiplier window (exit slit) 2.0 mm wide, in the initial experiment. An area of the multiplier envelope somewhat larger than the slit was isolated by masking, and coated with Apiezon pump oil B, or grease L, or with calcium tungstate dusted on to a smear of grease. The responses were much the same, the signal-to-noise ratio varying from about 40 at 1700 Å to 2 at about 1200 Å—the noise being measured with shutter closed. After some success had been achieved in reducing electrical pick-up, some of the stronger lines or bands could be distinguished. When the exit slit was reduced to 0.25 mm the signal became too small to be useful. It is possible that a 1P21 with higher internal gain could be used effectively, but a more stable source is necessary than could be achieved with the 500 c/s supply.

The 931A output was then coupled to the plates of an oscillograph having a sensitivity of about 1 mm/V. With a 5 MΩ resistor as load in the anode of the 931A, deflexions of several centimetres were observed from the pulsed source. Several strong lines were observed, but the peak heights cannot be determined accurately by this means. Scattered light could be estimated by setting the multiplier to, say, 200 Å where no direct radiation should be present. Electrical noise was checked by closing the shutter. Signal-to-noise ratio was satisfactory and the pulse heights were reasonably constant at any given setting. Substitution of a peak-reading voltmeter should allow the pulsed source to be used with the multiplier.

#### EXPERIMENTS WITH THE 5060 TUBE

The 5060<sup>(11)</sup> is an end-window tube of considerable size and was therefore provided with a fixed housing, the grating being rotated to pass the spectrum across the exit slit. Fig. 3 shows the method of housing the 5060 tube and of controlling the variable exit slit. A large Wilson seal bears on the tube about half-way along and the end-window sits on a rubber sheet to minimize possible stress concentration on the glass. An area of the envelope surrounding the anode is coated with ceresine wax. This can be melted on with a hot-air blower to ensure that damage to the tube by overheating does not occur. It is unfortunately necessary to earth the cathode, whose contact is made on the front surface of the end-window. The anode lead is then 2 kV positive to earth and the current measuring apparatus is at the same level if d.c. sources are used. The housing is completed by a light-tight cap on the base end. The slit before the photomultiplier bears a scale in units of 0.001 in. By plotting anode current against slit scale reading, the closing point can be determined to within

0.0001 in. The dark current with 1800 V overall on the tube is about  $2 \times 10^{-8}$  A, fluctuation being unobservable. The makers' measure of the internal gain at 160 V per stage is  $7.2 \times 10^7$  A.

After some preliminary experiments with the 500 c/s arc in which the 5060 anode current variations were fed through the Selectoject and measured on the cathode follower, it was found possible to reduce the exit slit to 0.05 mm and even less. Lines were detected in the spectrum as the grating was rotated and wavelength 1215.6 Å was located. The unsteadiness of the arc current was too great, however, and a change

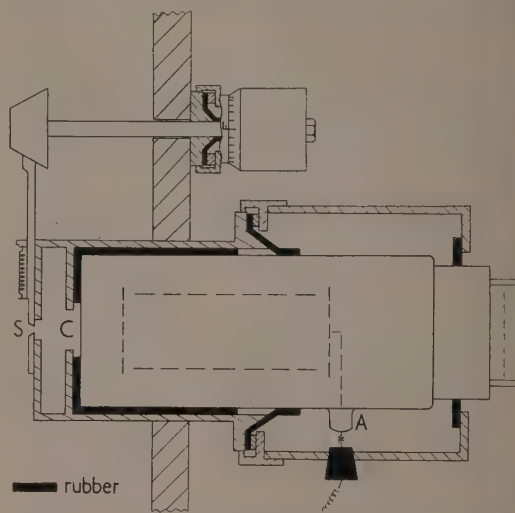


Fig. 3. Housing and variable slit for 5060 photomultiplier tube

S, slit; C, cathode; A, anode.

was made to the 40 c/s power frequency. The signal, with 450 mA of 40 c/s a.c. passing through a 5 mm capillary, was strong enough to justify reduction of the entrance slit to 0.048 mm and the exit slit to 0.025 mm, although trouble was still encountered from instability in the discharge. Finally, a change was made to a d.c. arc, the detector becoming simply a galvanometer of sensitivity 280 mm/μA and period 5 sec, connected to a universal shunt in the anode circuit and approximately critically damped.

Observations were then made by manually adjusting the grating rotating screw to obtain maximum deflexion of the galvanometer at the observed spectrum lines. The grating adjustment was always made so that the screw was thrusting the grating further round against the tension of the spring. In spite of the fact that the mechanism was originally constructed merely to set the grating in a given position for photographic observation, little evidence has been found of uneven movement of the spectrum across the slit. The position of a line maximum remains constant to within one- or two-tenths of the hundred divisions into which the control disk is divided.

Subsequently, a synchronous motor with worm reduction gear has been arranged to drive simultaneously the grating control shaft and a drum carrying a sensitized paper on which a galvanometer spot is focused. Interchangeable worms can be used to drive either or both the shafts at one revolution in



either thirteen or twenty-six minutes, representing passage of the spectrum past the exit slit at a speed of 0.5 or 0.25 Å per sec and a "dispersion" of the spectrum recorded on the photographic paper of 0.6 mm/Å, 1.2 mm/Å, or 2.5 mm/Å. The period of the galvanometer in this case is 2 sec and its sensitivity 25 mm/μA at the drum, with critical damping. The question of fidelity of response is considered in the following section. A reduction gear accurate for a movement of 385 Å per revolution of the grating screw, drives a Veeder counter which indicates the wavelength in Ångström units passing the exit slit and a rotary switch is used to put a line on the paper record every 10 Å. From 190 to 760 Å of spectrum can be recorded in a given run.

#### FOCUSING, DISPERSION AND RESOLUTION

Spectrum lines are properly focused at the photomultiplier slit only when the entrance and exit slits lie on the Rowland circle which is tangential to the grating. As rotation of the grating will rotate the Rowland circle about that end of its diameter which meets the grating normally, focusing can be correct for only one wavelength. At other wavelengths the entrance slit will be either inside or outside the Rowland circle, and a new focal curve will be formed either wholly outside or wholly inside the previous one. Focusing error will depend on the distance of this new curve from the exit slit and will, of course, vary with wavelength.

For a given instrument and wavelength at which focusing is correct, the error at any other wavelength can be calculated from formulae given in the texts.<sup>(12)</sup> For our instrument, if the reflected image is focused on the exit slit, the grating must be moved 1.2 mm in or out, to bring 1215 Å into focus, depending on whether the spectrum to right or left is used. The error which then develops in traversing 200 Å either way amounts to 0.41 mm. As the numerical aperture is about 1/20 the consequent broadening of the spectrum lines amounts to about 0.35 Å. The dispersion at the exit slit is approximately 0.058 mm/Å in the region of 1200 Å. A perfectly focused, monochromatic spectrum line on a background of constant intensity will, neglecting diffraction and distortion, form a rectangular distribution of width equal to that of the entrance slit (0.048 mm, or 0.83 Å). If this intensity distribution is analysed by the photomultiplier looking through a slit 0.025 mm wide, the photomultiplier response current should describe a symmetrical trapezium, 0.023 mm (0.4 Å) wide at the top, 0.048 mm (0.83 Å) at half-maximum intensity, and 0.073 mm (1.25 Å) wide at the base.

So long as the focusing error widens the image to a small extent compared with the width at maximum intensity, it will not affect the measurement of true maximum intensities. The focusing errors and consequent widening of the image are given for three wavelengths in the table.

Variation with wavelength of image widening due to focusing error

Rotation of spectrum from 1200 Å to red (Å)	Focusing error (mm)	Widening of image (Å)
100	0.18	0.15
200	0.41	0.35
300	1.66	1.4

Distortion by the optical system should be negligible compared with focusing error, and, of course, can be checked photographically. Natural line width, if small compared to 0.4 Å, will simply increase the apparent width by approxi-

mately its own value. If comparable with 0.4 Å it will change the theoretical trapezium in a more complicated way. Wider lines or bands will not be seriously affected. It is, therefore, an advantage not to have the entrance slit comparable with the natural line width. For photographic recording, it is essential that the width of the "line" at maximum intensity be sufficient to allow the galvanometer to attain maximum deflexion during the time maximum intensity falls on the exit slit. In the recording system now in use, with an entrance slit 0.04 mm and exit slit 0.015 mm the width of the band of maximum intensity is 0.025 mm, or 0.5 Å, which takes 2 sec to pass the exit slit. The galvanometer in use appears from measurement on experimental traces to be able to attain maximum deflexions in much less than this time.

These conditions also comply with the rough guide given by Sawyer for accurate micro-photometer recording. The width at half-intensity of 1215.6 Å was measured as  $0.95 \pm 0.05$  Å with an entrance slit 0.048 mm and exit slit 0.025 mm, compared with a theoretical width for an infinitely narrow, perfectly focused, line, 0.83 Å. In this case the grating was moved in steps, the galvanometer attaining a steady reading.

The photographic records taken with an entrance slit 0.037 mm, and "dispersion" 0.4 Å/mm yield for the same line a width at half maximum intensity of  $0.75 \pm 0.05$  Å compared with a theoretical 0.65 Å. Thermal broadening of wavelength 1215.6 could explain not more than 20% of this difference. The whole could be accounted for by a focusing error amounting to 0.12 mm. Any "lines" appearing on a record, which have a measured width at half maximum intensity less than 0.75 Å—some have occasionally been recorded—must therefore be spurious and due to sudden deflexions of the galvanometer due to leakage variation or other disturbance. The resolving power of the instrument under these conditions is then about 2000.

#### LINEARITY OF RESPONSE AND FATIGUE EFFECTS

In a region of continuous spectrum the linear response of the photomultiplier to incident intensity can be checked by varying the exit slit width. This is illustrated in Fig. 4(a), from which observations the closing point of the exit slit can also be determined. Linear response to increased intensity with the exit slit fixed could be checked by varying the entrance slit width in a region of continuous spectrum. As this test could not be made, the tube current was varied instead. Fig. 4(b) shows the results of this check.

Fatigue has been observed in a 931A tube<sup>(9)</sup> if the photocurrent is only 3 μA. Currents are maintained at this order or below. However, in observations made to determine the cause of a gradually decreasing deflexion in the case of wavelength 1215.6, for which the photocurrent was about 10 μA, fatigue was looked for and not found to be appreciable. In the normal survey of a spectrum, even currents of a few microamperes are drawn for no more than a second, during which time fatigue would be inappreciable. No effects corresponding to those described by Hillert<sup>(13)</sup> for 931A and similar tubes have been observed by the authors with the 5060 tube.

#### STRAY LIGHT

When a line spectrum, in which individual lines are well resolved, is examined, the minimum deflexion between lines can be taken as a measure of the scattered light. Measurements with the manually adjusted grating control gave the scattered light deflexion as about 20% of the average deflexion

\*\*

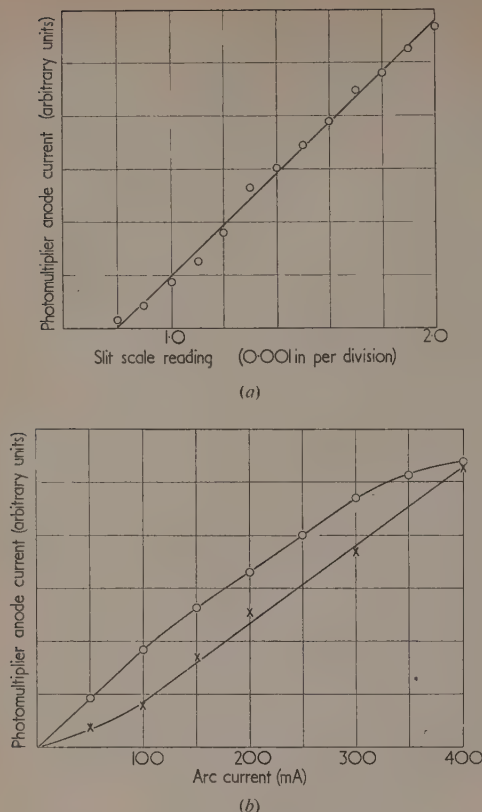


Fig. 4. Photomultiplier response curves

(a) variation with exit slit width;

(b) variation with discharge tube current.

o, d.c.; x, a.c.

for a molecular line, or  $1-2 \times 10^{-7}$  Å. Subsequent measurements on photographic records confirm this estimate. As the fluorescing agent is transparent, the effect of scattered light in these conditions comes from all frequencies in the spectrum. If the response is examined with a clean cathode window, a line spectrum is observed. The deflexions corresponding to the lines are produced presumably by fluorescence in the Pyrex window. Under these conditions, wavelengths transmitted by the Pyrex, i.e. longer than about 3000 Å, contribute a much greater part of the scattered light deflexion. The average minimum deflexion is about a third of that found when oil is on the cathode.

#### COMPARATIVE EFFICIENCY OF DIFFERENT FLUORESCING AGENTS

The results of Tombouliau and Pell and the successful use of "pump oil" by Tousey and Johnson were known to the authors before these experiments were started. As Apiezon A oil for sensitizing films in this region had been used, it was intended to use the same oil on the multiplier window. By chance, the B oil was tried first, and since, under an ultra-

violet lamp, the A oil fluoresces much less efficiently than the B, only the latter was tried. Only Apiezon L grease was tried. No visual comparisons were made with other greases.

Tombouliau and Pell found that calcium tungstate : lead and magnesium tungstate : tungsten gave the best response of a number of phosphors tried with a 1P21 multiplier. Samples of calcium tungstate and magnesium tungstate phosphors were therefore procured together with zinc orthosilicate which Tombouliau and Pell rated as much less efficient (15%). The powdered phosphors were usually dusted on to a very thin film of L grease with a powder blower to a thickness forming an almost opaque layer. Deposition from water or alcohol suspension was also tried. For various reasons consistent results could not be obtained although a number of trials were made. Normally a measure of the deflexion was obtained at four to eight chosen points (lines) in the 1100-1800 Å region with a given material on the cathode window. The multiplier was then removed and the material changed, slit widths, discharge current and pressure remaining the same. With a given material four or more runs through the spectrum showed intensities at the chosen points consistent to about 2%. However, separate runs using the same material showed apparently erratic variations up to 10% and the ratios between deflexions for grease and oil varied by a larger amount. One difficulty arose from blockage of the exit slit and obscuration of the oil or grease on the cathode by dust stirred up when air was admitted, or in the early stages of evacuation. Modification of the photomultiplier housing to allow rapid changing of the material in front of the cathode without having to break the vacuum, is being undertaken.

In general, oil and grease are about equally efficient, with a possibility that in the region of 1400 Å the efficiency of grease falls to about half that of oil. Calcium tungstate and magnesium tungstate dusted on grease were no more than half as efficient as oil, and when deposited from water or alcohol suspension, were worse still. This is most probably because the response of the 5060 photosurface lies in the blue-green region and these phosphors have a maximum in the blue. Zinc orthosilicate : manganese which Tombouliau and Pell rated at 15% of the efficiency of calcium tungstate, was found to give as good a response as oil, at least in the region 1100-1500 Å. Its maximum is in the green region.

One object of comparing the different materials was to find whether, particularly among the complex organic substances, two or more showed constant response ratios throughout the spectrum. If two or more substances show a constant response ratio, it can be safely assumed that their individual conversion efficiencies vary slowly and regularly, if at all. Since the discovery by Johnson, Watanabe and Tousey<sup>(14)</sup> that the conversion efficiency of sodium salicylate is nearly constant in the vacuum region, this substance can be used as a reference in testing others. The problems of heterochromatic photometry then become much easier.

#### SPECTRUM OF THE D.C. DISCHARGE IN HYDROGEN

In Fig. 5(a) is shown a section of the spectrum of the d.c. arc in hydrogen, plotted from two series of readings of galvanometer deflexions, taken every 0.4 Å, i.e. every one-thousandth of a revolution of the grating control, for the region 1195-1235 Å. Fig. 5(b) shows a reproduction of a photographic record of the same spectrum covering a more extensive wavelength range. The zero marks correspond to the closure of the shutter-tap. The possibility of drawing a



straight line through them is a measure of the constancy of leakage plus dark current. The width of wavelength 1215·6 at half maximum intensity in this case is 0·75 Å compared with a theoretical minimum of 0·65 Å.

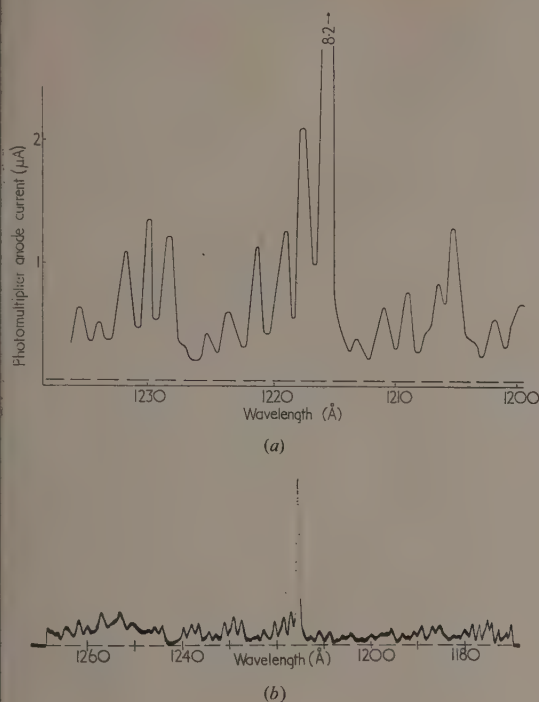


Fig. 5. Parts of the spectrum of the d.c. arc in hydrogen  
(a) photomultiplier record.  
— — — Scattered light deflexion with "clean" window.  
(b) photographic record.

#### EFFECT OF WATER VAPOUR ON THE OBSERVED INTENSITY OF WAVELENGTH 1215·6 Å

At an early stage in the experiments with the d.c. arc it was observed that for fifteen minutes or more after starting the arc, the deflexion indicating the intensity of wavelength 1215·6 Å fell from its initial value, gradually reaching an equilibrium value of a third to a half of the initial intensity. Tests were made to eliminate, as possible causes, fatigue in the multiplier, vacuum leaks or heating of the discharge. It was concluded that the intensity fell as the pressure in the spectrograph reached an equilibrium value determined by leakage through the slit and by the pumping speed. As wavelength 1215·6 Å falls within a strong water vapour absorption band,<sup>(15)</sup> the commercial hydrogen was passed over phosphorus pentoxide before it entered the discharge. The initial value was then maintained. Assuming an absorption coefficient of 400<sup>(16)</sup> the attenuation corresponds to a water vapour pressure about  $10^{-3}$  mm in the spectrograph, or, say,

5% of the total pressure. It is surprising that so much water vapour can find its way through the capillary discharge.

In a further check, observations were made on the variation of intensity of two atomic lines, wavelengths 1215·6 and 1025 Å and two molecular lines, wavelengths 1160 and 1221 Å, as the discharge pressure varied. The curves have already been published.<sup>(3)</sup> It was found that the atomic lines behave similarly though wavelength 1025 Å is unabsorbed by water vapour,<sup>(15)</sup> while wavelength 1215·6 Å is strongly absorbed, and also that the molecular lines behave similarly, though wavelength 1221 Å is strongly absorbed and wavelength 1160 Å is not. We conclude that the discharge and the spectrograph can be kept effectively free of water vapour with simple precautions. Similarly the development of an air leak was indicated from observation of the suddenly decreased intensity of molecular lines in the 1350–1550 Å region of strong oxygen absorption.

#### ACKNOWLEDGEMENTS

We wish to acknowledge the assistance of Mr. K. M. Burrows during the earlier stages of these experiments, especially in the construction of the "Selectoject." One of us (J. H. B.) is indebted to the Commonwealth Research Funds for a grant.

#### REFERENCES

- (1) PRICE, W. C. *Rep. Phys. Soc. Progr. Phys.*, **14**, p. 9 (1951).
- (2) TOMBOULIAN, D., and PELL, E. M. *J. Appl. Phys.*, **20**, p. 263 (1949).
- (3) TOUSEY, R., and JOHNSON, F. S. *J. Opt. Soc. Amer.*, **40**, p. 264 (1950).
- (4) TOUSEY, R., JOHNSON, F. S., RICHARDSON, J., and TORAN, N. *J. Opt. Soc. Amer.*, **40**, p. 264 (1950).
- (5) BOLTON, J. H., and WILLIAMS, S. E. *Nature, Lond.*, **169**, p. 325 (1952).
- (6) SAWYER, R. A. *J. Opt. Soc. Amer. and Rev. Sci. Instrum.*, **15**, p. 305 (1927).
- (7) COLLINS, G. B., and PRICE, W. C. *Rev. Sci. Instrum.*, **5**, p. 423 (1934).
- (8) ALDINGTON, J. N. *Endeavour*, **9**, p. 203 (1950).
- (9) KESSLER, K. G., and WOLFE, R. D. *J. Opt. Soc. Amer.*, **37**, p. 133 (1947).
- (10) VILLARD, O. G., and WEAVER, D. K. *Q.S.T.*, **33**, p. 11 (1949).
- (11) SOMMER, A., and TURK, W. E. *J. Sci. Instrum.*, **27**, p. 113 (1950).
- (12) SAWYER, R. A. *Experimental Spectroscopy*, p. 162 (New York, Prentice-Hall, 1944).
- (13) HILLERT, M. *Brit. J. Appl. Phys.*, **2**, p. 164 (1951).
- (14) JOHNSON, F. S., WATANABE, K., and TOUSEY, R. *J. Opt. Soc. Amer.*, **41**, p. 702 (1951).
- (15) RATHENAU, G. *Z. Phys.*, **87**, p. 32 (1933).
- (16) PRESTON, W. M. *Phys. Rev.*, **57**, p. 887 (1940).

# The motional impedance of simple sources in an isotropic solid

By H. PURSEY, B.Sc.(Eng.), National Physical Laboratory, Teddington, Middlesex.

[Paper received 11 June, 1952]

This paper analyses the motional impedance of sources of simple geometrical shapes which are either dilating or oscillating in an isotropic solid medium of infinite extent.

The equation of wave propagation in an isotropic solid is expressed in cylindrical and spherical polar co-ordinates, assuming that in the cylindrical co-ordinate case there is no motion or variation along the cylinder axis (or in other words the problem is two-dimensional), while in the case of spherical co-ordinates no motion or variation takes place around lines of latitude, the direction of oscillation being regarded as the polar axis. In the case of dilating sources the problem is further simplified, as all movement and variation takes place along radial lines, and an equation can be derived relating the particle displacement and the radial distance from the source. A solution is found which satisfies the boundary conditions on the surface of the source, and which converges to a radiated wave of the form  $e^{ik_1 r}/r$  for large values of  $r$ , where  $k_1$  is the wavelength constant for compressional waves in the surrounding medium.

In the case of oscillating sources the wave equation separates into two independent equations, one in  $\nabla \cdot \vec{u}$  and the other in  $|\nabla \times \vec{u}|$ , the latter being a scalar quantity equal in magnitude to the vector  $\nabla \times \vec{u}$ . Solutions are obtained which converge at infinity as  $e^{ik_1 r}/r$  for  $\nabla \cdot \vec{u}$  and as  $e^{ik_2 r}/r$  for  $|\nabla \times \vec{u}|$ , where  $k_1$  is as before the compressional wavelength constant and  $k_2$  the shear wavelength constant for the medium. The arbitrary constants are then adjusted to fit the boundary condition on the surface of the source. The total force on the source in the direction of motion is then calculated in each case from the generalized Hooke's law equations relating stress to strain, and hence the motional impedance is obtained by dividing force by velocity of source.

Values of motional impedance per unit source area are plotted on an Argand diagram for several values of Poissons' ratio of the surrounding medium, showing the variation of impedance with source size, the latter quantity being expressed in units of  $1/2\pi$  times the length of a compressional wave.

This work is intended as a first step towards the analysis of the more complex sources which are encountered in practice, for example, a piston source on the free surface of a semi-infinite medium.

The equation of wave-propagation in an isotropic solid is

$$c_{11}\nabla\nabla \cdot \vec{u} - c_{44}\nabla \times \nabla \times \vec{u} = \rho\partial^2\vec{u}/\partial t^2 \quad (1)$$

where  $\vec{u}$  = particle displacement,  
 $\rho$  = density of medium.

$c_{11}$  and  $c_{44}$  are respectively the longitudinal and shear elastic constants of the medium.

If the variation with time is sinusoidal and has pulsance  $\omega$ , equation (1) becomes

$$c_{11}\nabla\nabla \cdot \vec{u} - c_{44}\nabla \times \nabla \times \vec{u} + \rho\omega^2\vec{u} = 0 \quad (2)$$

It is convenient to introduce the following functions: For cylindrical co-ordinates

$$\Delta_c = \frac{1}{r} \left[ \frac{\partial}{\partial r}(ru_r) + \frac{\partial u_\phi}{\partial \phi} \right] \quad (3)$$

$$W_c = \frac{1}{r} \left[ \frac{\partial}{\partial r}(ru_\phi) - \frac{\partial u_r}{\partial \phi} \right] \quad (4)$$

For spherical co-ordinates

$$\Delta_s = \frac{1}{r^2} \frac{\partial}{\partial r}(r^2u_r) + \frac{1}{r \sin \theta} \frac{\partial}{\partial \theta}(u_\theta \sin \theta) \quad (5)$$

$$W_s = \frac{1}{r} \left[ \frac{\partial}{\partial r}(ru_\theta) - \frac{\partial u_r}{\partial \theta} \right] \quad (6)$$

For dipole sources the field is a function of two variables only,  $r$  and  $\phi$  in the cylindrical case, and  $r$  and  $\theta$  in the spherical case. For dilatational sources the fields are functions of  $r$  only.

The analysis of particular cases is now considered.

## DILATING CYLINDER

The wave equation in cylindrical co-ordinates, with no  $\phi$  or  $z$  variation, is

$$c_{11} \frac{\partial}{\partial r} \left[ \frac{1}{r} \frac{\partial}{\partial r}(ru_r) \right] + \rho\omega^2 u_r = 0 \quad (7)$$

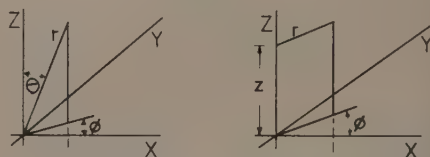


Fig. 1. (a) Spherical co-ordinate system. (b) Cylindrical co-ordinate system

The solution for a radiated wave satisfying the condition  $u_r = u_\phi$  at the surface of the source of radius  $a$  is

$$u_r = u_a H_1(k_1 r) / H_1(k_1 a) \quad (8)$$

where

$$k_1 = \omega\sqrt{\rho/c_{11}} \quad (9)$$

and

$$H_m(z) = J_m(z) + iN_m(z) \quad (10)$$

where  $J_m(z)$  is the Bessel function of order  $m$  and of the first kind and  $N_m(z)$  is the Neumann function defined by<sup>(1,2)</sup>

$$N_m(z) = \frac{1}{\sin m\pi} [J_m(z) \cos m\pi - J_{-m}(z)] \quad (11)$$

Now the total force per unit length on the surface of the source =  $-2\pi a F_r$  (12)

where  $F_r$  is the radial component of stress on the surface.



and

$$F_r = \begin{bmatrix} X_x & X_y & 0 \\ X_y & Y_y & 0 \\ 0 & 0 & Z_z \end{bmatrix} \begin{bmatrix} \cos \phi \\ \sin \phi \\ 0 \end{bmatrix} = \begin{bmatrix} X_x \cos \phi + X_y \sin \phi \\ X_y \cos \phi + Y_y \sin \phi \\ 0 \end{bmatrix} \quad (13)$$

where  $X_x$ , etc., are the components of the elastic stress tensor. Inserting the values

$$\left. \begin{aligned} X_x &= c_{11}x_x + c_{12}y_y \\ Y_y &= c_{12}x_x + c_{11}y_y \\ X_y &= c_{44}x_y \end{aligned} \right\} \quad (14)$$

where  $c_{12} = c_{11} - 2c_{44}$  and  $x_x$ , etc., are the components of strain, on changing to polar co-ordinates we find

$$F_r = c_{11} \frac{\partial u_r}{\partial r} + c_{12} \frac{u_r}{r} \quad (15)$$

Substituting from equation (8) we obtain for the force  $F$  per unit length [using equation (12)]

$$F = -2\pi a u_a \left[ k_1 c_{11} \frac{H_1'(k_1 r)}{H_1(k_1 a)} + c_{12} \frac{H_1(k_1 r)}{r H_1(k_1 a)} \right] \text{ at } r = a \quad (16)$$

$$F = -2\pi a u_a \left[ \frac{k_1 c_{11} H_0(k_1 a)}{H_1(k_1 a)} - \frac{2c_{44}}{a} \right] \quad (17)$$

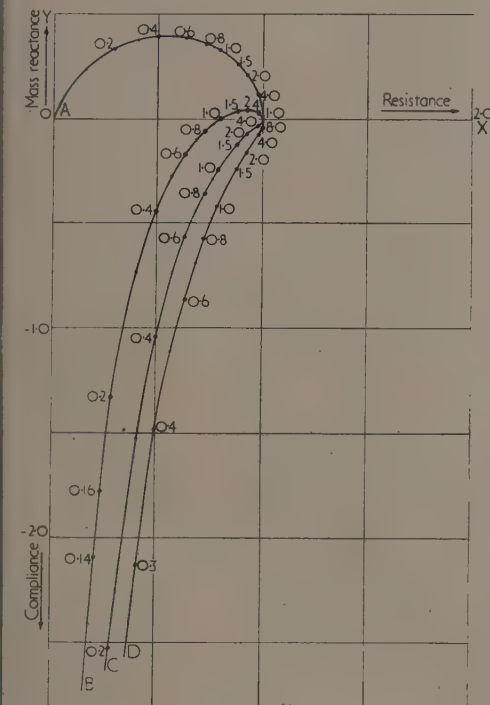


Fig. 2. Motional impedance of a dilating cylinder

$$Z_m = 2\pi a p V_L (X - iY)$$

$$X - iY = \frac{2i}{\mu^2 z} - \frac{iH_0(z)}{H_1(z)}$$

Curve A,  $\sigma = 0.5$ ; curve B,  $\sigma = 0.4$ ; curve C,  $\sigma = 0.3$ ; curve D,  $\sigma = 0.2$ . The figures given at points on the curves are the varying values of  $z$ .

from the recurrence relations for Bessel and Neumann functions. Now the motional impedance  $Z_m$  is given by the relationship

$$F = Z_m \frac{\partial u_a}{\partial t} = -i\omega u_a Z_m$$

$$\begin{aligned} \text{Therefore } Z_m &= \frac{2\pi}{i\omega} \left[ \frac{k_1 c_{11} H_0(k_1 a)}{H_1(k_1 a)} - \frac{2c_{44}}{a} \right] \\ &= 2\pi a p V_L \left[ \frac{2i}{\mu^2 z} - \frac{iH_0(z)}{H_1(z)} \right] \end{aligned} \quad (18)$$

where

$$\begin{aligned} \mu &= \sqrt{(c_{11}/c_{44})} \\ z &= k_1 a \end{aligned}$$

$V_L$  = compressional wave velocity =  $\omega/k_1 = \sqrt{(c_{11}/\rho)}$ . For small values of  $z$ ,  $Z_m$  is given approximately by the equation

$$\frac{Z_m}{2\pi a p V_L} \approx \frac{\pi z}{2} + \frac{2i}{\mu^2 z} \quad (19)$$

Values of  $Z_m/2\pi a p V_L$  have been computed for values of  $\mu$  corresponding to Poisson's ratios of 0.2, 0.3, 0.4 and 0.5, and the course of the impedance functions are shown plotted on an Argand diagram in Fig. 2. [It should be remembered that  $i$  corresponds to  $(-j)$  in engineering terminology—hence positive  $i$  means capacitive reactance.]

#### DILATING SPHERE

The wave equation in spherical co-ordinates with no  $\theta$  or  $\phi$  variation is

$$c_{11} \frac{\partial}{\partial r} \left[ \frac{1}{r^2} \frac{\partial}{\partial r} (r^2 u_r) \right] + \rho \omega^2 u_r = 0 \quad (20)$$

The solution for a radiated wave satisfying the condition  $u_r = u_a$  at the surface of the source of radius  $a$  is

$$u_r = u_a [h_1(k_1 r)/h_1(k_1 a)] \quad (21)$$

where

$$k_1 = \omega \sqrt{(\rho/c_{11})}$$

and

$$h_m(z) = j_m(z) + i n_m(z) \quad (22)$$

$j_m(z)$  is the "spherical Bessel function" of order  $m$  and of the first kind, defined by

$$j_m(z) = \sqrt{\left(\frac{\pi}{2z}\right)} J_{m+1/2}(z)$$

$n_m(z)$  is the Neumann function defined by

$$n_m(z) = \sqrt{\left(\frac{\pi}{2z}\right)} N_{m+1/2}(z)$$

Now the total force on the surface of the source

$$= -4\pi a^2 F_r \quad (23)$$

where  $F_r$  is the radial component of stress on the surface, and

$$F_r = \begin{bmatrix} X_x & X_y & X_z \\ X_y & Y_y & Y_z \\ X_z & Y_z & Z_z \end{bmatrix} \begin{bmatrix} \sin \theta \cos \phi \\ \sin \theta \sin \phi \\ \cos \theta \end{bmatrix} \quad (24)$$

Inserting the values

$$\left. \begin{aligned} X_x &= c_{11}x_x + c_{12}(y_y + z_z) \\ X_y &= c_{11}y_y + c_{12}(x_x + z_z) \\ Z_z &= c_{11}z_z + c_{12}(x_x + y_y) \\ X_y &= c_{44}x_y, Y_z = c_{44}y_z, Z_x = c_{44}z_x \end{aligned} \right\} \quad (25)$$

and changing to polar co-ordinates we find

$$F_r = c_{11} \frac{\partial u_r}{\partial r} + 2c_{12} \frac{u_r}{r} \quad (26)$$

substituting from equation (21) we obtain for the force  $F$  [using equation (23)]

$$F = -4\pi a^2 u_a \left[ k_1 c_{11} \frac{h_1'(k_1 a)}{h_1(k_1 a)} + \frac{2c_{12}}{a} \right] \quad (27)$$

at  $r = a$ .

$$= -4\pi a^2 u_a \left[ \frac{k_1 c_{11} h_0(k_1 a)}{h_1(k_1 a)} - \frac{4c_{44}}{a} \right] \quad (28)$$

from the recurrence relation for spherical Bessel and Neumann functions.

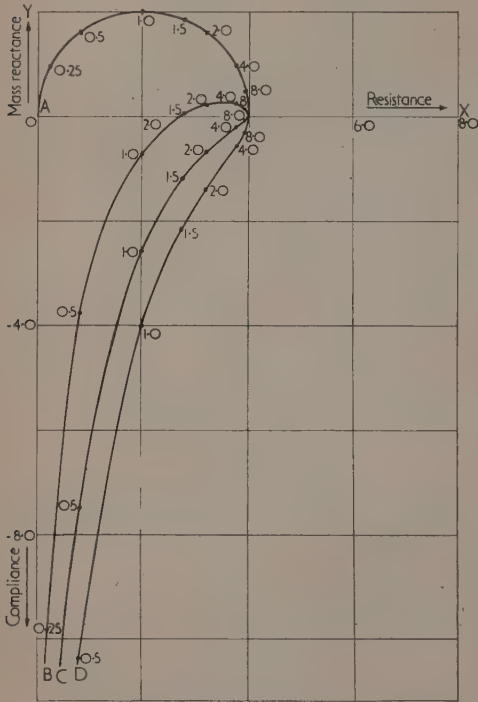


Fig. 3. Motional impedance of a dilating sphere

$$Z_m = \pi a^2 \rho V_L (X - iY)$$

$$X - iY = \frac{4z^2}{1 + z^2} + i \left( \frac{16}{\mu^2 z} - \frac{4z}{1 + z^2} \right)$$

Curve A,  $\sigma = 0.5$ ; curve B,  $\sigma = 0.4$ ; curve C,  $\sigma = 0.3$ ; curve D,  $\sigma = 0.2$ . The figures given at points on the curves are the varying values of  $z$ .

Now it may be shown<sup>(3)</sup> that

$$h_0(z) = \frac{e^{iz}}{iz}$$

and

$$h_1(z) = \left( \frac{1}{iz^2} - \frac{1}{z} \right) e^{iz}$$

Substituting these values in equation (28) we obtain

$$F = -4\pi a^2 u_a \left\{ \left[ \frac{k_1 c_{11}(k_1 a)}{1 + (k_1 a)^2} - \frac{4c_{44}}{a} \right] + i \frac{k_1 c_{11}(k_1 a)^2}{1 + (k_1 a)^2} \right\} \quad (29)$$

and  $Z_m = -F/i\omega u_a$

$$Z_m = \frac{4\pi a^2}{i\omega} \left\{ \left[ \frac{k_1 c_{11}(k_1 a)}{1 + (k_1 a)^2} - \frac{4c_{44}}{a} \right] + i \frac{k_1 c_{11}(k_1 a)^2}{1 + (k_1 a)^2} \right\} \quad (30)$$

$$Z_m = \pi a^2 V_L \left[ \frac{4z^2}{1 + z^2} + i \left( \frac{16}{\mu^2 z} - \frac{4z}{1 + z^2} \right) \right] \quad (31)$$

where  $\mu = \sqrt{c_{11}/c_{44}}$ ,  $z = k_1 a$ ,  $V_L$  = compressional wave velocity =  $\omega/k_1 = \sqrt{c_{11}/\rho}$ .

Values of  $Z_m/\pi a^2 V_L$  have been computed for values of  $\mu$  corresponding to Poisson's ratios of 0.2, 0.3, 0.4 and 0.5, and the course of the impedance functions are shown plotted on an Argand diagram in Fig. 3.

### OSCILLATING CYLINDER

The wave equation in cylindrical co-ordinates with no  $z$ -variation is

$$\left. \begin{aligned} c_{11} \frac{\partial}{\partial r} (\Delta_c) - \frac{c_{44}}{r} \frac{\partial}{\partial \phi} (W_c) + \rho \omega^2 u_r &= 0 \\ c_{11} \frac{\partial}{\partial r} (\Delta_c) + c_{44} \frac{\partial}{\partial r} (W_c) + \rho \omega^2 u_\phi &= 0 \end{aligned} \right\} \quad (32)$$

$\Delta_c$  and  $W_c$  being defined in equations (3) and (4).

From equation (32) we may derive independent wave equations in  $\Delta_c$  and  $W_c$

$$c_{11} \frac{\partial}{\partial r} \left( r \frac{\partial}{\partial r} \Delta_c \right) - \frac{c_{11}}{r} \frac{\partial^2}{\partial \phi^2} (\Delta_c) - \rho \omega^2 r \Delta_c = 0 \quad (33)$$

$$\frac{c_{44}}{r} \frac{\partial^2}{\partial \phi^2} (W_c) + c_{44} \frac{\partial}{\partial r} \left( r \frac{\partial}{\partial r} W_c \right) + \rho \omega^2 r W_c = 0 \quad (34)$$

The solutions corresponding to a radiated wave from a cylinder oscillating normal to its axis are

$$\Delta_c = A H_1(k_1 r) \cos \phi \quad (35)$$

$$W_c = B H_1(k_2 r) \sin \phi \quad (36)$$

where  $k_1 = \omega \sqrt{\rho/c_{11}}$  and  $k_2 = \omega \sqrt{\rho/c_{44}}$ .

$A$  and  $B$  are arbitrary constants.

Substituting these results in equations (32) we obtain

$$-\rho \omega^2 u_r = A c_{11} \frac{\partial}{\partial r} H_1(k_1 r) \cos \phi - B \frac{c_{44}}{r} H_1(k_2 r) \cos \phi \quad (37)$$

$$-\rho \omega^2 u_\phi = -A \frac{c_{11}}{r} H_1(k_1 r) \sin \phi - B c_{44} \frac{\partial}{\partial r} H_1(k_2 r) \sin \phi \quad (38)$$

from which

$$u_r = \left[ B' \frac{H_1(k_2 r)}{r} - A' k_1 H_0(k_1 r) - A' \frac{H_1(k_1 r)}{r} \right] \cos \phi \quad (39)$$

$$u_\phi = \left[ A' \frac{H_1(k_1 r)}{r} - B' k_2 H_0(k_2 r) + B' \frac{H_1(k_2 r)}{r} \right] \sin \phi \quad (40)$$

where  $A' = A/k_1^2$  and  $B' = B/k_2^2$ .



On the boundary surface  $r = a$  we have

$$u_r = u_0 \cos \phi$$

$$u_\phi = -u_0 \sin \phi$$

therefore

$$u_0 = B \frac{H_1(k_2 a)}{a} - A' k_1 H_0(k_1 a) + A' \frac{H_1(k_1 a)}{a} \quad (41)$$

$$-u_0 = A' \frac{H_1(k_1 a)}{a} - B' k_2 H_0(k_2 a) + B' \frac{H_1(k_2 a)}{a} \quad (42)$$

Solving these equations for  $A'$  and  $B'$ , and substituting in equations (39) and (40) we obtain

$$\frac{H_2(k_1 a) \frac{H_1(k_2 r)}{k_2 r} + H_2(k_2 a) \left[ H_0(k_1 r) - \frac{H_1(k_1 r)}{k_1 r} \right]}{H_0(k_1 a) \frac{H_1(k_2 a)}{k_2 a} + \frac{H_1(k_1 a)}{k_1 a} H_0(k_2 a) - H_0(k_1 a) H_0(k_2 a)} u_0 \cos \phi \quad (43)$$

$$\frac{-H_2(k_2 a) \frac{H_1(k_1 r)}{k_1 r} - H_2(k_1 a) \left[ H_0(k_2 r) - \frac{H_1(k_2 r)}{k_2 r} \right]}{H_0(k_1 a) \frac{H_1(k_2 a)}{k_2 a} + \frac{H_1(k_1 a)}{k_1 a} H_0(k_2 a) - H_0(k_1 a) H_0(k_2 a)} u_0 \sin \phi \quad (44)$$

Putting  $f_c(r) =$

$$\frac{H_2(k_1 a) \frac{H_1(k_2 r)}{k_2 r} + H_2(k_2 a) \left[ H_0(k_1 r) - \frac{H_1(k_1 r)}{k_1 r} \right]}{H_0(k_1 a) \frac{H_1(k_2 a)}{k_2 a} + \frac{H_1(k_1 a)}{k_1 a} H_0(k_2 a) - H_0(k_1 a) H_0(k_2 a)} u_0 \quad (45)$$

and  $g_c(r) =$

$$\frac{H_2(k_2 a) \frac{H_1(k_1 r)}{k_1 r} - H_2(k_1 a) \left[ H_0(k_2 r) - \frac{H_1(k_2 r)}{k_2 r} \right]}{H_0(k_1 a) \frac{H_1(k_2 a)}{k_2 a} + \frac{H_1(k_1 a)}{k_1 a} H_0(k_2 a) - H_0(k_1 a) H_0(k_2 a)} u_0 \quad (46)$$

$$\text{we have } u_r = f_c(r) \cos \phi \quad (47)$$

$$\text{and } u_\phi = g_c(r) \sin \phi \quad (48)$$

Now the total force on the cylinder in the direction of motion is given by

$$F = - \int_0^{2\pi} a F_X d\phi \quad (49)$$

where  $F_X$  is the component of stress in the  $x$ -direction across the boundary surface of the source

$$\text{Now } F_X = (X_X \bar{i} + X_Y \bar{j} + X_Z \bar{k}) \cdot \bar{n} \quad (50)$$

where  $\bar{i}$ ,  $\bar{j}$  and  $\bar{k}$  are unit vectors in the  $\bar{x}$ ,  $\bar{y}$  and  $\bar{z}$  directions respectively and  $\bar{n}$  is a unit vector normal to the surface of the source.

$$\text{Therefore } F_X = X_X \cos \phi + X_Y \sin \phi \quad (51)$$

Inserting the values of  $X_X$  and  $X_Y$  in terms of strain components, and changing to polar co-ordinates we find

$$F_X = c_{11} \cos \phi \left( \frac{\partial u_r}{\partial r} + \frac{u_r}{r} + \frac{1}{r} \frac{\partial u_\phi}{\partial \phi} \right) - 2c_{44} \cos \phi \left( \frac{u_r}{r} + \frac{1}{r} \frac{\partial u_\phi}{\partial \phi} \right) - c_{44} \sin \phi \left( \frac{\partial u_\phi}{\partial r} - \frac{u_\phi}{r} + \frac{1}{r} \frac{\partial u_r}{\partial \phi} \right) \quad (52)$$

taking values at  $r = a$

$$= c_{11} \cos^2 \phi \left\{ f'_c(a) + \frac{1}{a} [f_c(a) + g_c(a)] \right\} - c_{44} \left\{ g'_c(a) \sin^2 \phi + (2 \cos^2 \phi - \sin^2 \phi) \left[ \frac{f_c(a)}{a} - \frac{g_c(a)}{a} \right] \right\} \quad (53)$$

Now  $f'_c(a) = -g'_c(a)$ , since  $u_r = u_0 \cos \phi$  and  $u_\phi = -u_0 \sin \phi$  at  $r = a$ .

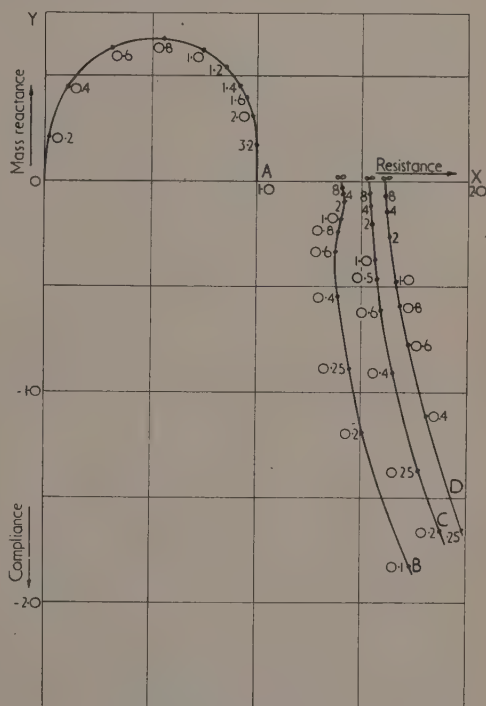
Therefore

$$F_X = c_{11} f'_c(a) \cos^2 \phi - c_{44} g'_c(a) \sin^2 \phi \quad (54)$$

Therefore

$$F = -\pi a [c_{11} f'_c(a) - c_{44} g'_c(a)] \quad (55)$$

from equations (49) and (54).



Differentiating equations (45) and (46) and substituting in equation (55) we obtain for the force per unit length on the cylinder

$$F = \pi a u_0 \left[ \frac{c_{11} k_1 H_1(k_1 a) H_2(k_2 a) + c_{44} k_2 H_2(k_1 a) H_1(k_2 a)}{H_0(k_1 a) \frac{H_1(k_2 a)}{k_2 a} + \frac{H_1(k_1 a)}{k_1 a} H_0(k_2 a) - H_0(k_1 a) H_0(k_2 a)} \right] \quad (56)$$

and

$$Z_m = -F/i\omega u_0$$

Therefore

$$Z_m = \frac{\pi a}{-i\omega} \left[ \frac{c_{11} k_1 H_1(k_1 a) H_2(k_2 a) + c_{44} k_2 H_2(k_1 a) H_1(k_2 a)}{H_0(k_1 a) \frac{H_1(k_2 a)}{k_2 a} + \frac{H_1(k_1 a)}{k_1 a} H_0(k_2 a) - H_0(k_1 a) H_0(k_2 a)} \right] \quad (57)$$

$$= \pi p a V_L \left[ \frac{i H_1(z) H_2(\mu z) + \frac{i}{\mu} H_2(z) H_1(\mu z)}{H_0(z) \frac{H_1(\mu z)}{\mu z} + \frac{H_1(z)}{z} H_0(\mu z) - H_0(z) H_0(\mu z)} \right] \quad (58)$$

Values of  $Z_m/\pi p a V_L$  have been computed for values of  $\mu$  corresponding to Poisson's ratios of 0.2, 0.3, 0.4 and 0.5, and the course of the impedance functions are shown plotted on an Argand diagram in Fig. 4. For small values of  $z$  both the real and imaginary parts of the expression in brackets (representing impedance per unit area of source) tend to  $\infty$ . However, if the expression is multiplied by  $z$  both parts now tend to zero, and values of this modified function are plotted for small values of  $z$  in Fig. 5.

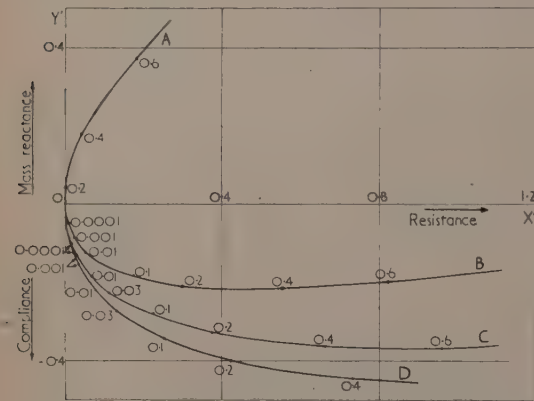


Fig. 5. Motional impedance of an oscillating cylinder for small sources

$$Z_m = \frac{\pi p V_L^2}{\omega} (X' - iY') \quad (59)$$

$$X' - iY' \simeq \frac{2\pi(1 + \mu^2) - 4i[(1 + \mu^2) \log(\lambda z) + \frac{1}{2}\mu^2 \log \mu^2]}{[(1 + \mu^2) \log(\lambda z) + \frac{1}{2}\mu^2 \log \mu^2]^2 + \frac{1}{4}\pi^2(1 + \mu^2)^2} \quad (60)$$

where  $\lambda = \frac{1}{2}e^\gamma$  and  $\gamma$  is Euler's constant ( $\simeq 0.5722$ ).

Curve A,  $\sigma = 0.5$ ; curve B,  $\sigma = 0.4$ ; curve C,  $\sigma = 0.3$ ; curve D,  $\sigma = 0.2$ . The figures given at points on the curves are the varying values of  $z$ .

For small values of  $z$ ,  $Z_m$  is given approximately by the formula

$$Z_m \simeq \pi p a V_L \left\{ \frac{2\pi(1 + \mu^2) - 4i(\log \lambda z + \mu^2 \log \lambda \mu z)}{z[(\log \lambda z + \mu^2 \log \lambda \mu z)^2 + \frac{1}{4}\pi^2(1 + \mu^2)^2]} \right\} \quad (59)$$

where  $\lambda = \frac{1}{2}e^\gamma$  and  $\gamma$  is Euler's constant ( $\simeq 0.5722$ ).

Mathematically, a liquid may be regarded as a solid with a Poisson's ratio of 0.5, corresponding to  $\mu = \infty$ .

Equation (58) then becomes

$$Z_m = \pi p a V_L \left[ \frac{i H_1(z)}{H_0(z) - H_1(z)/z} \right] \quad (60)$$

for small  $z$ ,  $Z_m \simeq \pi p a V_L (\frac{1}{2}\pi z^3 - iz)$

$$= \frac{\pi^2 \rho \omega^3 a^4}{2V_L^2} - \pi \rho \omega a^2 i \quad (61)$$

This is the well-known expression for the motional impedance of a thin wire vibrating normal to its axis in a fluid medium.<sup>(4)</sup>

#### OSCILLATING SPHERE (DIPOLE SOURCE)

The wave equation in spherical polar co-ordinates with no  $\phi$ -variation is

$$\left. \begin{aligned} c_{11} \frac{\partial}{\partial r} (\Delta_s) - \frac{c_{44}}{r \sin \theta} \frac{\partial}{\partial \theta} (W_s \sin \theta) + \rho \omega^2 u_r &= 0 \\ c_{11} \frac{\partial}{\partial \theta} (\Delta_s) + \frac{c_{44}}{r} \frac{\partial}{\partial r} (r W_s) + \rho \omega^2 u_\theta &= 0 \end{aligned} \right\} \quad (62)$$

$\Delta_s$  and  $W_s$  being defined in equations (5) and (6).

From equation (62) we may derive independent wave equations in  $\Delta_s$  and  $W_s$

$$\frac{c_{11}}{r^2} \frac{\partial}{\partial r} \left[ r^2 \frac{\partial}{\partial r} (\Delta_s) \right] + \frac{c_{11}}{r^2 \sin \theta} \frac{\partial}{\partial \theta} \left[ \sin \theta \frac{\partial}{\partial \theta} (\Delta_s) \right] + \rho \omega^2 \Delta_s = 0 \quad (63)$$

$$\frac{c_{44}}{r} \frac{\partial^2}{\partial r^2} (r W_s) + \frac{c_{44}}{r^2} \frac{\partial}{\partial \theta} \left[ \frac{1}{\sin \theta} \frac{\partial}{\partial \theta} (W_s \sin \theta) \right] + \rho \omega^2 W_s = 0 \quad (64)$$

The solutions corresponding to a radiated wave from a dipole source are

$$\Delta_s = A h_1(k_1 r) \cos \theta \quad (65)$$

$$W_s = B h_1(k_2 r) \sin \theta \quad (66)$$

where  $k_1 = \omega \sqrt{\rho/c_{11}}$  and  $k_2 = \omega \sqrt{\rho/c_{44}}$ .  $A$  and  $B$  are arbitrary constants.

As in the case of the oscillating cylinder, equations (65) and (66) are substituted in equation (62) and the resulting equation solved for  $A$  and  $B$  when  $r = a$  and  $u_r = u_0 \cos \theta$ ,  $u_\theta = -u_0 \sin \theta$  in order to satisfy the boundary conditions on the surface of the source.

We then obtain for  $u_r$  and  $u_\theta$

$$u_r = \frac{2h_2(k_1 a) \frac{h_1(k_2 r)}{k_2 r} + h_2(k_2 a) \left[ h_0(k_1 r) - \frac{2h_1(k_1 r)}{k_1 r} \right]}{h_0(k_1 a) \frac{h_1(k_2 a)}{k_2 a} + \frac{h_1(k_1 a)}{k_1 a} h_0(k_2 a) - h_0(k_1 a) h_0(k_2 a)} u_0 \cos \theta \quad (67)$$

$$u_\theta = \frac{h_2(k_2 a) \frac{h_1(k_1 r)}{k_1 r} - h_2(k_1 a) \left[ h_0(k_2 r) - \frac{h_1(k_2 r)}{k_2 r} \right]}{h_0(k_1 a) \frac{h_1(k_2 a)}{k_2 a} + \frac{h_1(k_1 a)}{k_1 a} h_0(k_2 a) - h_0(k_1 a) h_0(k_2 a)} u_0 \sin \theta \quad (68)$$



Putting

$$f_s(r) = \frac{2h_2(k_1a) \frac{h_1(k_2r)}{k_2r} + h_2(k_2a) \left[ h_0(k_1r) - \frac{2h_1(k_1r)}{k_1r} \right]}{h_0(k_1a) \frac{h_1(k_2a)}{k_2a} + 2 \frac{h_1(k_1a)}{k_1a} h_0(k_2a) - h_0(k_1a) h_0(k_2a)} u_0 \quad (69)$$

and

$$g_s(r) = \frac{h_2(k_2a) \frac{h_1(k_1r)}{k_1r} - h_2(k_1a) \left[ h_0(k_2r) - \frac{h_1(k_2r)}{k_2r} \right]}{h_0(k_1a) \frac{h_1(k_2a)}{k_2a} + 2 \frac{h_1(k_1a)}{k_1a} h_0(k_2a) - h_0(k_1a) h_0(k_2a)} u_0 \quad (70)$$

we have

$$u_r = f_s(r) \cos \theta$$

$$u_\theta = g_s(r) \sin \theta$$

Now the total force on the sphere in the direction of motion is given by

$$F = - \int_0^{2\pi} \int_0^\pi d\theta (a^2 F_z \sin \theta) \\ = - 2\pi a^2 \int_0^\pi F_z \sin \theta d\theta \quad (73)$$

where  $F_z$  is the component of stress in the  $z$ -direction across the boundary surface of the source.

$$\text{Now } F_z = (Z_x \bar{i} + Y_z \bar{j} + Z_z \bar{k}) \cdot \bar{n} \quad (74)$$

$$= Z_x \sin \theta \cos \phi + Y_z \sin \theta \sin \phi + Z_z \cos \theta \quad (75)$$

Inserting the values of  $Z_x$ ,  $Y_z$  and  $Z_z$  in terms of strain components and changing to polar co-ordinates we find

$$F_z = c_{11} \cos \theta \left( \frac{\partial u_r}{\partial r} + \frac{2u_r}{r} + \frac{1}{r} \frac{\partial u_\theta}{\partial \theta} + \frac{\cos \theta}{\sin \theta} \frac{u_\theta}{r} \right) \\ - c_{44} \left[ \frac{2 \cos \theta}{r} \frac{\partial u_\theta}{\partial \theta} + 4 \cos \theta \frac{u_r}{r} + \frac{2 \cos^2 \theta - \sin^2 \theta}{\sin \theta} \frac{u_\theta}{r} \right. \\ \left. + \sin \theta \left( \frac{\partial u_\theta}{\partial r} + \frac{1}{r} \frac{\partial u_r}{\partial \theta} \right) \right] \quad (76)$$

taking values at  $r = a$

$$= c_{11} \cos^2 \theta \left\{ f'_s(a) + \frac{2}{a} [f_s(a) + g_s(a)] \right\} \\ - c_{44} \left\{ g'_s(a) \sin^2 \theta + (4 \cos^2 \theta - \sin^2 \theta) \left[ \frac{f'_s(a) + g'_s(a)}{a} \right] \right\} \quad (77)$$

Now  $f'_s(a) = -g'_s(a)$  since  $u_r = u_0 \cos \theta$  and  $u_\theta = -u_0 \sin \theta$  at  $r = a$ .

Therefore

$$F_z = c_{11} f'_s(a) \cos^2 \theta - c_{44} g'_s(a) \sin^2 \theta \quad (78)$$

Therefore

$$F = - \frac{4}{3} \pi a^2 [c_{11} f'_s(a) - 2c_{44} g'_s(a)] \quad (79)$$

from equations (73) and (78).

VOL. 4, JANUARY 1953

Differentiating equations (69) and (70) and substituting in equation (79), we obtain for the force on the sphere

$$F = \frac{4}{3} \pi a^2 u_0 \left[ \frac{c_{11} k_1 h_1(k_1a) h_2(k_2a) - 2c_{44} k_2 h_2(k_1a) h_1(k_2a)}{h_0(k_1a) \frac{h_1(k_2a)}{k_2a} + 2 \frac{h_1(k_1a)}{k_1a} h_0(k_2a) - h_0(k_1a) h_0(k_2a)} \right] \quad (80)$$

and  $Z_m = -F/i\omega u_0$ .

Therefore

$$Z_m = - \frac{4\pi a^2}{3i\omega} \left[ \frac{c_{11} k_1 h_1(k_1a) h_2(k_2a) + 2c_{44} k_2 h_2(k_1a) h_1(k_2a)}{h_0(k_1a) \frac{h_1(k_2a)}{k_2a} + 2 \frac{h_1(k_1a)}{k_1a} h_0(k_2a) - h_0(k_1a) h_0(k_2a)} \right] \quad (81)$$

$$= \frac{4}{3} \pi \rho a^2 V_L \left[ \frac{i h_1(k_1a) h_2(k_2a) + \frac{2i}{\mu} h_2(k_1a) h_1(k_2a)}{h_0(k_1a) \frac{h_1(k_2a)}{k_2a} + 2 \frac{h_1(k_1a)}{k_1a} h_0(k_2a) - h_0(k_1a) h_0(k_2a)} \right] \quad (82)$$

$$\text{Now } h_0(z) = -\frac{ieiz}{z}, \quad h_1(z) = -\left(\frac{1}{z} + \frac{1}{z^2}\right)eiz$$

and

$$h_2(z) = \left[ -\frac{3}{z^2} + i\left(\frac{1}{z} - \frac{3}{z^3}\right) \right] eiz$$

Using these relationships, equation (82) may be transformed into an algebraic expression. After rationalizing the denominator we obtain for the motional impedance

$$Z_m = \frac{4}{3} \pi \rho a^2 V_L \left\{ \left[ \frac{z^4(\mu^4 + 2\mu^3) + 3z^2(2\mu^3 + \mu^2) + 9(2\mu^3 + 1)}{z^4\mu^4 + z^2\mu^2(4\mu - 1) + (2\mu^2 + 1)^2} \right] \right. \\ \left. + \frac{i}{z} \left[ \frac{z^4(-\mu^4 + 4\mu^3) + z^2(-2\mu^4 + 13\mu^2 - 2) + 9(2\mu^2 + 1)}{z^4\mu^4 + z^2\mu^2(4\mu - 1) + (2\mu^2 + 1)^2} \right] \right\} \quad (83)$$

Values of  $Z_m/\pi \rho a^2 V_L$  have been computed for values of  $\mu$  corresponding to Poisson's ratios of 0.2, 0.3, 0.4 and 0.5, and the course of the impedance function are shown plotted in Fig. 6.

For small values of  $z$ ,

$$Z_m \simeq \frac{4}{3} \pi \rho a^2 V_L \left[ \frac{9(2\mu^3 + 1)}{(2\mu^2 + 1)^2} + \frac{9i}{z(2\mu^2 + 1)} \right] \quad (84)$$

Thus the real part tends to a constant value, and the imaginary part to  $\infty$  as  $1/z$ .

For liquids, corresponding to  $\mu = \infty$

$$Z_m = \frac{4}{3} \pi \rho a^2 V_L \left( \frac{z^4}{z^4 + 4} - i \frac{z^3 + 2z}{z^4 + 4} \right) \quad (85)$$

For small values of  $z$

$$Z_m \simeq \frac{4}{3} \pi \rho a^2 V_L \left( \frac{1}{4} z^4 - \frac{1}{4} iz \right) \\ = \frac{\pi \rho a^6 \omega^4}{3 V_L^3} - \frac{2\pi i \rho a^3 \omega}{3} \quad (86)$$

This is the standard expression for the motional impedance of a dipole source in a fluid medium.<sup>(5)</sup>

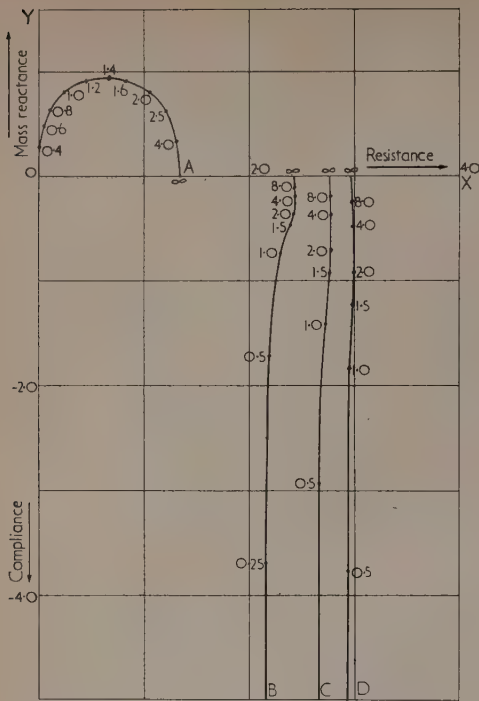


Fig. 6. Motional impedance of an oscillating sphere

$$Z_m = \pi a^2 \rho V_L (X - iY)$$

$$X - iY = \frac{4}{3} \left\{ \left[ \frac{z^4(\mu^4 + 2\mu^3) + 3z^2(\mu^3 + \mu^2) + 9(2\mu^3 + 1)}{z^4\mu^4 + z^2\mu^2(4\mu - 1) + (2\mu^2 + 1)^2} \right] + \frac{i}{z} \left[ \frac{z^4(-\mu^4 + 4\mu^3) + z^2(-2\mu^4 + 13\mu^2 - 2) + 9(2\mu^2 + 1)}{z^4\mu^4 + z^2\mu^2(4\mu - 1) + 2\mu^2 + 1)^2} \right] \right\}$$

Curve A,  $\sigma = 0.5$ ; curve B,  $\sigma = 0.4$ ; curve C,  $\sigma = 0.3$ ; curve D,  $\sigma = 0.2$ . The figures given at points on the curves are the varying values of  $z$ .

The impedance functions involved in this case are of considerable interest, and have been studied in some detail. Equation (83) may be re-written as follows:

$$\begin{aligned} \frac{Z_m}{\frac{4}{3}\pi a^2 \rho V_L} &= \left(1 + \frac{2}{\mu}\right) + \\ &+ 2\mu(\mu - 1)^2 \left[ \frac{z^2 - (\mu^2 - 1)(2\mu - 1)}{\mu^4 z^4 + \mu^2 z^2(4\mu - 1) + (1 + 2\mu^2)^2} \right] \\ &+ \frac{i}{z} \left\{ \left(\frac{4}{\mu} - 1\right) - \right. \\ &\left. 2(\mu - 1)^2 \left[ \frac{z^2(\mu^2 + 1) - (\mu - 2)(2\mu^2 + 1)}{\mu^4 z^4 + \mu^2 z^2(4\mu - 1) + (1 + 2\mu^2)^2} \right] \right\} \quad (87) \end{aligned}$$

For values of  $\mu$  between 1.5 and 2.5 (corresponding to a range of Poisson's ratio which includes the majority of

solids), the first term of the real and imaginary part predominates, and we have

$$\frac{Z_m}{\frac{4}{3}\pi a^2 \rho V_L} \simeq \left(1 + \frac{2}{\mu}\right) + \frac{i}{z} \left(\frac{4}{\mu} - 1\right) \quad (88)$$

Thus the curves of  $Z_m$  are very nearly straight lines parallel to the imaginary axis.

For fluids,  $\mu = \infty$  and  $Z_m$  is given by equation (85). This curve, in parametric form, has for its equation

$$\left. \begin{aligned} x &= z^4/(z^4 + 4) \\ -y &= (z^3 + 2z)/(z^4 + 4) \end{aligned} \right\} \quad (89)$$

Eliminating  $z$  and transferring the origin to the point  $(\frac{1}{2}, 0)$  we find

$$4x^4 + 8x^2y^2 + 4y^4 - x^2 - 2y^2 = 0 \quad (90)$$

Putting  $\alpha = x^2$  and  $\beta = y^2$  we have

$$4(\alpha + \beta)^2 = \alpha + 2\beta \quad (91)$$

which may be written

$$\left(2\alpha + 2\beta - \frac{3}{8}\right)^2 = -\frac{\alpha}{2} + \frac{\beta}{2} + \frac{9}{64} \quad (92)$$

This is the equation of a point whose distance from the line  $32\alpha - 32\beta = 9$  is equal to the square of its distance from the perpendicular line  $16\alpha + 16\beta = 3$ , i.e. a parabola whose

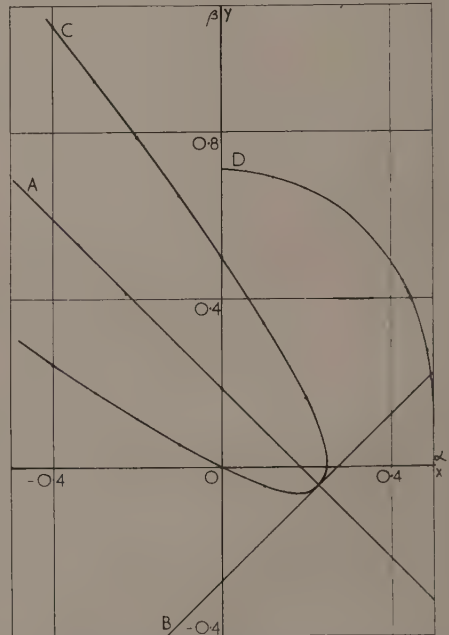


Fig. 7. Derivation of a curve representing the motional impedance of an oscillating sphere in a fluid

$$\begin{aligned} \alpha &= x^2 \\ \beta &= y^2 \end{aligned}$$

Curve A,  $16\alpha + 16\beta = 3$ ; curve B,  $32\alpha - 32\beta = 9$ ; curve C,  $4(\alpha + \beta)^2 = \alpha + 2\beta$ ; curve D,  $4x^4 + 8x^2y^2 + 4y^4 - x^2 - 2y^2 = 0$ .



axis is  $16\alpha + 16\beta = 3$  and whose tangent at the vertex is  $32\alpha - 32\beta = 9$ . The graph of  $\alpha$  against  $\beta$  is shown in Fig. 7. The arc lying in the upper right-hand quadrant [i.e. between (0, 0.5) and (0.25, 0)] represents the square of the impedance function.

On taking the square roots of  $\alpha$  and  $\beta$  over this portion, and plotting them on the same axes, we obtain a curve of somewhat similar shape to an ellipse, the lower half of which represents the motional impedance of a dipole source in a fluid medium.

The transition from the vertical lines in the upper quadrant in the solid case to the quasi-semi-ellipse in the fluid case is curious, and to show how it occurs some rough graphs have been drawn for intermediate values of  $\mu$  between 2.5 and  $\infty$ . These are shown in Fig. 8, together with the curves

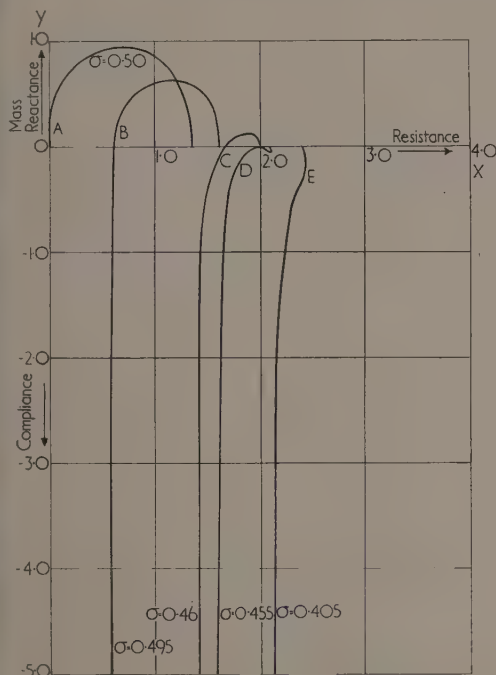


Fig. 8. Approximate curves of motional impedance of an oscillating sphere in media with Poisson's ratios between 0.4 and 0.5, showing the transition from solids to liquids

$$Z_m = \pi a^2 \rho V_L (X - iY)$$

Curve A,  $\sigma = 0.50$ ; curve B,  $\sigma = 0.495$ ; curve C,  $\sigma = 0.46$ ; curve D,  $\sigma = 0.455$ ; curve E,  $\sigma = 0.405$ .

for  $\mu = 2.5$  and  $\infty$ . Evidently the bump in the curve for  $\mu = 2.5$  becomes more pronounced as  $\mu$  increases, until at  $\mu = 3.491$  the curve touches the horizontal axis. When  $\mu = 4$  the initial portion above the real axis has disappeared, and as  $\mu$  increases further the start of the curve will move towards the point  $(1 + i0)$  and the second crossover towards the origin.

Presumably a similar transition will occur in the case of the functions for an oscillating cylinder, but as the computation is laborious and only of academic interest, it has not been thought worth while to undertake it.

As might be expected, there is a good deal of similarity between the functions for spherical and cylindrical sources, although it will be seen that the real part of the function for the oscillating sphere tends to a constant value for small sources, whereas that for the oscillating cylinder tends to infinity, although more slowly than  $1/z$ .

#### ACKNOWLEDGEMENTS

Acknowledgements are due to Mr. F. W. J. Olver for checking the calculations in the case of the spherical dipole source, and to Mr. C. W. Clenshaw for investigating the behaviour of the impedance functions of the spherical dipole for the transition region between solids and liquids; also to Mr. Clenshaw and the Mathematics Division of the National Physical Laboratory for much of the computing work. This work is part of the research programme of the National Physical Laboratory and is published with the permission of the Director.

#### REFERENCES

- (1) STRATTON, J. A. *Electromagnetic Theory*, pp. 357-8. (New York: McGraw Hill Book Co. Inc., 1941).
- (2) WATSON, G. N. *A Treatise on the Theory of Bessel Functions*, Chap. 3. (Cambridge: University Press, 1922).
- (3) MORSE, P. M. *Vibration and Sound*, pp. 316-7. (New York: McGraw Hill Book Co. Inc., 1948).
- (4) See Reference (3), p. 300.
- (5) See Reference (3), p. 319.

#### APPENDIX

##### Static field of rigid sphere in an infinite isotropic solid.

Timoshenko\* has calculated the field generated by, and displacement of, a piston when pressed into the surface of a semi-infinite isotropic solid. The solutions given in the present paper for an oscillating sphere may be used to calculate the field generated by, and force acting on, a sphere displaced in an infinite isotropic solid, by letting the functions tend to their limiting values as  $k$  tends to zero. However, considerable care is necessary in performing this operation, especially where several functions of  $k$ , each with real and imaginary parts, are multiplied together, as some of the larger terms cancel with similar terms from other products. It will be found that the following expansions are adequate for this purpose.

For small  $z$ ,  $h_0(z) \simeq 1 - i/z$

$$h_1(z) \simeq \frac{1}{2}z - i[(1/z^2) + \frac{1}{2}]$$

$$h_2(z) \simeq z^2/15 - i[(3/z^3) + (1/2z)]$$

We then find from equations (67) and (68)

$$u_r = \frac{3\mu^2(a/r) + (1 - \mu^2)(a/r)^3}{1 + 2\mu^2} u_0 \cos \theta \quad (93)$$

and

$$u_\theta = \frac{(1 - \mu^2)(a/r)^3 - 3(1 + \mu^2)(a/r)}{2(1 + 2\mu^2)} u_0 \sin \theta \quad (94)$$

Alternatively, the problem may be solved by rewriting equations (62), (63) and (64) without the terms containing  $\omega$  and solving directly for  $\Delta_s$  and  $W_s$ . It is now no longer

\* TIMOSHENKO, S. *Theory of Elasticity*, Chap. 2 (New York: McGraw Hill Book Co. Inc., 1934).

possible to find  $u_r$  and  $u_\theta$  by substitution in equation (62) since the terms containing them have vanished, but instead we must solve equations (5), and (6) substituting the solutions for  $\Delta_s$  and  $W_s$ . It is important that the various constants which appear in the final solutions should be correctly related, and for this it is necessary to substitute them in equations (5) and (6) and then back in equation (62).

For the force on the sphere, we may again use equation (79):

$$F = -\frac{4}{3}\pi a^2 [c_{11}f'(a) - 2c_{44}g'(a)]$$

From equations (93) and (94) we find

$$f'(a) = -\frac{3}{1+2\mu^2}\left(\frac{u_0}{a}\right) \quad (95)$$

$$\text{and} \quad g'(a) = \frac{3\mu^2}{1+2\mu^2}\left(\frac{u_0}{a}\right) \quad (96)$$

$$\text{Therefore} \quad F = 12\pi a u_0 \left( \frac{c_{11}}{1+2\mu^2} \right) \quad (97)$$

$$\text{Now} \quad c_{11} = E \left[ \frac{1-\sigma}{(1+\sigma)(1-2\sigma)} \right] \quad (98)$$

$$\text{and} \quad 1+2\mu^2 = \frac{5-6\sigma}{1-2\sigma} \quad (99)$$

where  $E$  is the Young's modulus and  $\sigma$  is the Poisson's ratio for the medium.

Substituting equations (98) and (99) in equation (97), we find:

$$F = 12\pi a E u_0 \left[ \frac{1-\sigma}{(1+\sigma)(5-6\sigma)} \right] \quad (100)$$

From Timoshenko can be derived:

$$F = \frac{3\pi^2 a E u_0}{2(\pi+4)(1-\sigma^2)}$$

The following table gives the ratio  $F/aEu_0$  for the various Poisson's ratios in the two cases:

Ratio  $F/aEu_0$  for various Poisson's ratios

$\sigma$	$\frac{F}{aEu_0}$ (infinite solid)	$\frac{F}{aEu_0}$ (semi-infinite solid)
0	7.54	2.07 <sub>5</sub>
0.1	7.00	2.09 <sub>5</sub>
0.2	6.62	2.16 <sub>0</sub>
0.3	6.34	2.28 <sub>0</sub>
0.4	6.22	2.47 <sub>0</sub>
0.5	6.29	2.76 <sub>5</sub>

As one would expect, the value for the infinite solid is rather greater than double that for the semi-infinite case, the additional shearing stress across the equatorial plane in the former case adding to the stiffness of the system; this effect becomes more marked as the rigidity of the surrounding medium increases (i.e. as Poisson's ratio falls).

## The compression and bearing capacity of cohesive layers\*

By G. G. MEYERHOF, Ph.D., M.Sc.(Eng.), F.G.S., A.M.I.C.E., A.M.I.Struct.E., and T. K. CHAPLIN, M.A.,  
Building Research Station, Garston, Watford, Herts.

[Paper first received 28 July and in final form 7 October, 1952]

A theoretical study of the compression of blocks and cylinders of purely cohesive material between rough plates shows that the yield pressure of the blocks and cylinders increases with the roughness of the plates and with decreasing height of the specimen. Compression tests of blocks and cylinders of Plasticine and clay between perfectly rough plates are found to be in good agreement with the theory. The above analysis has been extended to obtain an estimate of the yield pressure of footings on cohesive layers; theoretically the bearing capacity should increase with the adhesion of the material on the footing and base and with decreasing thickness of the layer. The results of some loading tests on circular and strip model footings on Plasticine layers with a perfectly rough base conform with the theory.

### 1. INTRODUCTION

It has been known for some time that the yield pressure of a uniform material is only unique if the test specimens have a certain minimum height in relation to their width. As the height of the specimens is reduced below this minimum, the yield pressure is apparently increased. A theory to explain this phenomenon can readily be developed for purely cohesive materials as indicated in the first part of this paper, which also presents additional experimental evidence. Similarly, it has been found that the yield pressure of a footing on a layer of uniform material is only unique if the layer has a certain minimum thickness in relation to the width of the loaded area. As the thickness of the layer is decreased below this minimum, the yield pressure is increased. A theoretical method for

estimating the bearing capacity of purely cohesive layers is outlined in the second part of the paper and compared with the results of loading tests on model footings. The effect of the rate of strain on the stresses in the material is outside the scope of this paper.

### 2. THEORY OF COMPRESSION

When a block of cohesive material is compressed between parallel rigid plates which are wider than the block, Prandtl<sup>(1)</sup> indicated that the stresses in it gradually change from the elastic to the plastic beginning at the edges of the block. As the load increases, the plastic zones spread to the centre of the block and then outwards until failure occurs by a relatively large compression and an outward displacement of the material. The average pressure on the block to produce such plastic deformation will be called the yield pressure of the

\* Crown copyright reserved.



block, and the corresponding zones of plastic equilibrium in the material (according to Prandtl) are shown in Fig. 1(a) for a long block which is wide compared to its height and is compressed between perfectly rough plates. In each quadrant of the block there is a central zone *ABC*, which remains in an elastic state of equilibrium and acts as part of the plate. Adjacent to these zones are a cycloidal shear zone *ACDE* and a zone of transition *DEG*; they are followed by a radial shear zone *EFG* at the edge of each plate and an outer zone *FGH*, which remains in an elastic state. For a narrow block the various shear zones coalesce as indicated in Fig. 1(b).

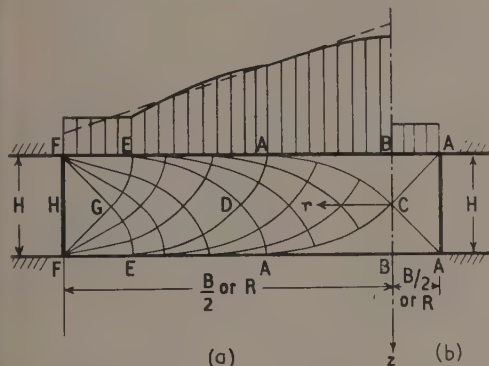


Fig. 1. Plastic zones and contact pressure for block between perfectly rough plates

(a) Wide block. (b) Narrow block.

Distribution of contact pressure:

Actual —————  
Approximate - - - - -  
Centre line . . . . .

The plastic equilibrium in the different zones can be established from the boundary conditions, starting at the free surface. For a plastic-rigid material whose shearing strength *s* is constant and independent of load, i.e.

$$s = c \quad (1)$$

where *c* = unit cohesion, Prandtl<sup>(1)</sup> has shown that at some distance from the free edges of a long block of width *B* and height *H* [Fig. 1(a)] the contact pressure on perfectly rough plates increases uniformly towards the centre; and on the simplifying assumption that the cycloidal shear zone extends throughout the block, the yield pressure is

$$p = c[(B/2H) + \pi/2] \quad (2)$$

This solution has been extended by Sokolovsky<sup>(2)</sup> to the compression of a long block by partially rough plates with an adhesion  $c_a = mc$ , where *m* is the degree of mobilization of shearing strength on the plates ( $0 \leq m \leq 1$ ). On the same assumptions as above the contact pressure increases as before and

$$p = c \left[ \frac{mB}{2H} + \frac{\sin^{-1} m}{m} + \sqrt{(1 - m^2)} \right] \quad (3)$$

The more exact shear zones near the free edges of the block lead to a greater contact pressure there, which is practically balanced by a smaller contact pressure on the central zones because of zero shearing stress above the vertical centre line of the block [Fig. 1(a)]. That the yield pressure is almost

unaffected has been shown by numerical step-by-step computations of some typical blocks between rough<sup>(2,3)</sup> and smooth<sup>(4)</sup> plates.

When a cylindrical specimen is compressed as above, plastic flow of the material occurs in both horizontal and vertical (radial) planes. Normal to the radial planes act hoop stresses, which in accordance with Coulomb-Mohr's theory of failure are assumed equal to the minor principal stresses. On that basis and the simplifying assumption that in radial planes the shear zones are identical to those in transverse planes of a corresponding long block [Fig. 1(a)], a solution of the problem is given in the Appendix. This shows that at some distance from the perimeter of a cylinder of diameter *2R* and height *H* [Fig. 1(a)] the contact pressure on the plates increases uniformly towards the centre as for a long block; on the assumption that the cycloidal shear zone extends throughout the cylinder, the yield pressure is

$$p = c \left[ \frac{2mR}{3H} + \frac{\sin^{-1} m}{m} + \sqrt{(1 - m^2)} \right] \quad (4)$$

Comparison of equations (3) and (4) indicates that the compressive strength of a thin cylinder between rough plates is up to one-third less than that of a corresponding long block. The more exact shear zones near the perimeter and centre of the cylinder would lead to a distribution of contact pressure which is similar to that indicated for a long block [Fig. 1(a)] and gives a somewhat greater yield pressure, especially for high cylinders.

If a similar pressure distribution ("stress roof") holds also for blocks of other shapes in plan, an approximate estimate of their yield pressures can readily be obtained from the average contact pressure in plan. Thus, for a rectangular block of length *L*, width *B*, and height *H*,

$$p = c \left[ \frac{mB}{2H} \left( 1 - \frac{B}{3L} \right) + \frac{\sin^{-1} m}{m} + \sqrt{(1 - m^2)} \right] \quad (5)$$

$cM_c$

where  $M_c$  is the yield pressure factor, which depends on the

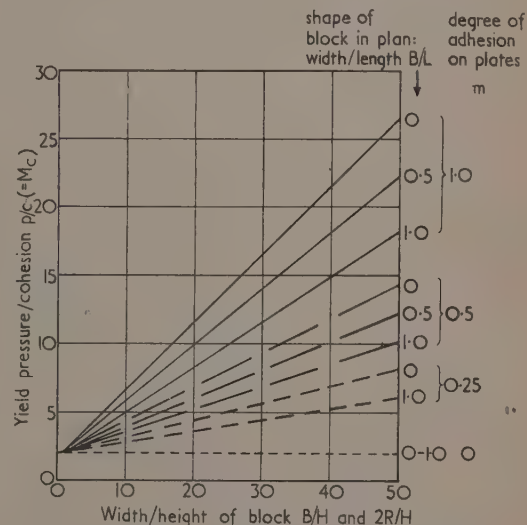


Fig. 2. Yield pressure of blocks and cylinders

Prisms and cylinders are given by  $B/L = 1.0$ .

shape of the block and the adhesion on the plates. For a long block equation (5) becomes identical with (3), and for a block of square plan (5) gives the same compressive strength as for a cylinder, equation (4).

The results of this analysis are given in Fig. 2 for blocks of various shapes and show that the yield pressure should be directly proportional to the width/height ratio  $B/H$  (or  $2R/H$ ) of the blocks and approximately also to the degree of adhesion  $m$  on the plates. For narrow blocks and high cylinders the more exact shear zones have been used in the estimates, which for  $B/H \leq 1$  give in all cases the compressive strength of the material of  $2c$ , for any  $m$ . The yield pressure of blocks between perfectly smooth plates is also  $2c$  and is independent of the ratios  $B/H$  and  $B/L$ .

### 3. COMPRESSION TESTS

Apart from some exploratory investigations<sup>(5)</sup> test results have been published<sup>(6, 7)</sup> for short cylinders of plastic materials, such as Plasticine and unvulcanized rubber, compressed in a parallel plate plastometer; similar tests have been carried out on metals.<sup>(8)</sup> No attempt was made in these tests to ensure that the plates were sufficiently rough to develop the full shearing strength of the material nor was the adhesion on the plates determined independently. The test results cannot, therefore, be analysed adequately.

The above shortcomings were avoided by Jürgenson<sup>(9)</sup> who carried out compression (squeezing) tests on thin rectangular clay samples between rough solid plates in a special box. Two of the short sides of the material were restrained so that plastic flow took place in two directions only and the conditions represented plane strain as far as possible. The shearing strength deduced from the experimental results on the basis of equation (1) agreed well with the value determined from standard compression and direct shearing tests on the clay. The same applied to similar tests on thin blocks of lead.<sup>(10)</sup>

Although the previous compression tests on rectangular blocks seemed to confirm the corresponding analysis, the tests were made on short restrained specimens so that long blocks were only simulated. Nor were any test results on short cylinders available hitherto with a known amount of adhesion on the plates. An extensive series of compression tests with full adhesion has therefore been carried out at the Building Research Station on rectangular blocks of various shapes in plan up to a long strip and on short cylinders to provide some check of the present theory. While most of this investigation was made on firm Plasticine for convenience, some additional tests were carried out on an undisturbed soft clay from a site where a large circular foundation had tilted, partly on account of plastic flow of the clay.<sup>(11)</sup> For these materials and the standard testing procedure in all experiments (see below) the effect of time on the stresses is thought to be small. Before each series of tests the Plasticine was thoroughly mixed; the samples and standard compression cylinders were prepared and tested at the same temperature to minimize temperature effects.

The experiments were carried out in a compression apparatus with a ring-type load gauge. Except in a few exploratory tests, the material was compressed between parallel rigid plates which had been roughened or covered with sand paper to ensure full mobilization of the shearing strength on the plates. Usually a load sufficient to cause appreciable plastic flow was applied; the vertical deformation was observed by a dial gauge at various time intervals until equilibrium was reached after about 15 min, which has been taken as standard

throughout the present series of tests. In a few cases the material was compressed at a constant rate of deformation of 0.06 in/min.

The specimens were rectangular Plasticine blocks of various shapes and from 1.0 to 8.5 in long, 0.3 to 1.0 in wide and 0.05 to 0.3 in high, which were compressed to final width/length ratios  $B/L$  varying from 0.1 to 1.0 and width/height ratios  $B/H$  from 5 to about 50. In addition Plasticine and clay cylinders from 1.5 to 3.0 in diameter and 0.04 to 3.2 in high were compressed to final diameter/height ratios  $2R/H$  from 0.5 to about 60. The shearing strength of the Plasticine was 12 lb/in<sup>2</sup> on the average and was obtained independently from standard compression tests on 1.5 in diameter and 3 in high cylinders tested at the same rate of deformation as that used in the main experiments. The shearing strength of the clay determined in a similar manner ranged from 3.3 to 7.6 lb/in<sup>2</sup> depending on the water content of the particular sample.

The measured yield pressure for appreciable plastic flow of the rectangular blocks is shown in Fig. 3 for the three main final shapes, i.e. strip, short rectangle and square, and the results for the cylinders are shown in Fig. 4. In spite of some scatter of the results, which for the Plasticine is probably largely due to slight temperature variations and for the clay is due to natural variability of the soil, the yield pressure is in each case found to be directly proportional to the final width/height ratio of the specimen and in agreement with the theoretical estimates for perfectly rough plates; the observed yield pressures do not depend on the initial shape of the specimen. The experimental results for a strip ( $B/L = 0.1$ ) are somewhat lower than those given by the theory for a long block, which appear, however, to be approached (Fig. 3).

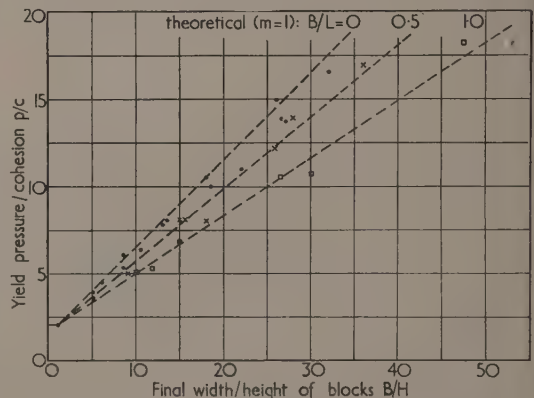


Fig. 3. Results of compression tests on rectangular blocks

Experimental results:

Average final shape:

Strip ( $B/L = 0.1$ ) ●

Rectangle ( $B/L = 0.6$ ) ×

Square ( $B/L = 1.0$ ) □

Theoretical results — — — —

The very few exploratory tests on cylinders between fairly smooth (brass) plates indicate that according to the theory only about 60% of the shearing strength of the material was mobilized along the plates (Fig. 4); this shows the importance in parallel plate plastometers of providing perfectly rough



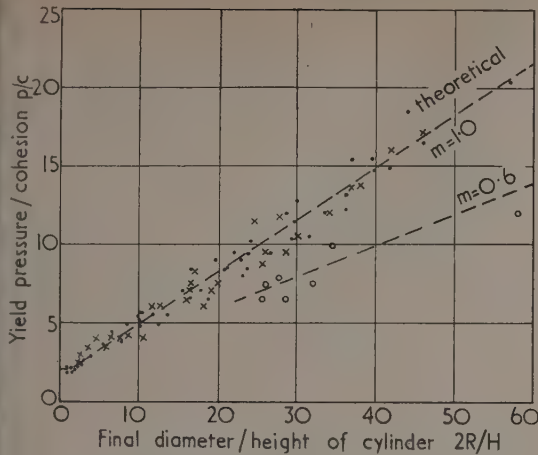


Fig. 4. Results of compression tests on cylinders

Experimental results:

Material	Plates	Symbol
Plasticine	perfectly rough	•
Plasticine	brass (smooth)	•
Soft clay	perfectly rough	×

Theoretical results

— — — — —  
 m=1.0  
 m=0.6

plates or of determining the degree of adhesion independently before the shearing strength can be deduced.

Further support for the theory is obtained from some additional tests on short cylinders compressed at a constant rate of deformation. If the shearing stress along the plates is calculated from equation (3) for various diameter/height ratios of the specimen and is plotted against the corresponding vertical strains, Fig. 5(a), it is found that these stress-strain

relations are similar to and in reasonable agreement with that of the standard compression test. The stress-strain curve of the latter test shows that for the particular material and method of testing there was very little work-hardening within the range of strains investigated.

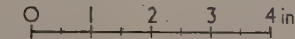
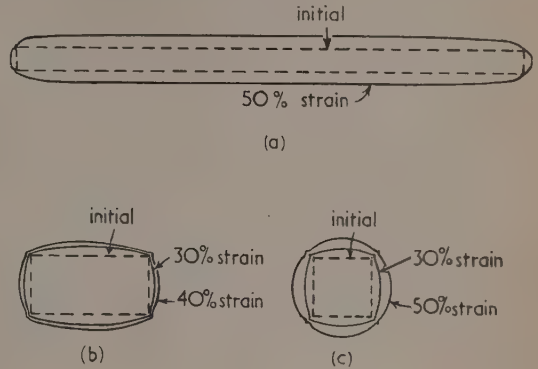


Fig. 6. Plan views of typical blocks before and after compression

(a) Strip. (b) Rectangle. (c) Square.

Examination of the specimens after compression showed that for long blocks plastic flow in plan occurred at right angles to the long centre line while the material of shorter rectangular blocks flowed also towards the short sides (Fig. 6). Square specimens exhibited practically radial flow so that for

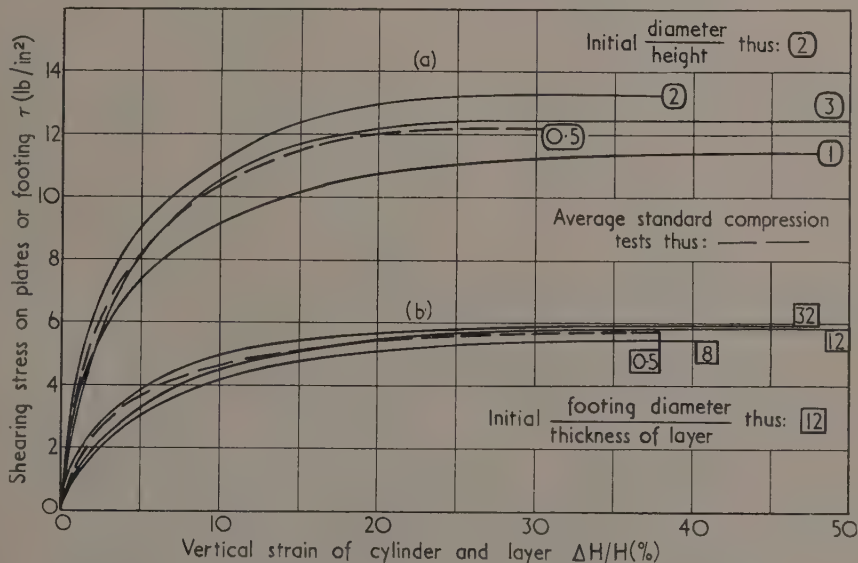


Fig. 5. Relation between shearing stress and strain of cylinders and thin layers

(a) Tests on thin cylinders. (b) Tests on circular footings on thin layers.

greater strains the specimens assumed a circular shape, and for short cylinders the flow was radial, as would be expected. In general, the material flowed to the nearest side of the specimen as assumed in the theory. The vertical sides of the specimens showed a slight barrelling due to resistance of the material along the rough plates. The initial and final volumes of the Plasticine specimens were found to be sensibly the same, but it was impossible to avoid some consolidation of the clay, especially with thin specimens. In the latter case the shearing strength of the consolidated material was used.

#### 4. THEORY OF BEARING CAPACITY

When a footing on a layer of cohesive material underlain by a rigid base stratum is loaded, the stresses in the material near the footing change from elastic to plastic, like those in the loaded block considered earlier. The material beneath the footing is displaced outwards, and outside the loaded area the movement is outwards and upwards towards the surface of the layer. The average pressure on the footing to produce appreciable plastic deformation of the material will be called the yield pressure of the footing, by analogy with the loaded block. The corresponding zones of plastic equilibrium in the material are shown in Fig. 7(a) for a shallow strip footing

extends throughout the layer immediately below the footing, the yield pressure is

$$q = c \left( \frac{B}{2H} + N_c - 1 \right) + \gamma D \quad (6)$$

from equation (2) and bearing capacity theory,<sup>(12)</sup> where  $\gamma$  = weight per unit volume of material and  $N_c$  is the bearing capacity factor for a strip footing on a layer of great thickness; this factor depends mainly on the depth of the footing and was calculated previously.<sup>(12)</sup>

Similarly, for a circular footing of diameter  $2R$  loaded as above, it may be assumed as before that the shear zones in radial planes are identical with those in transverse planes of a corresponding strip footing, Fig. 7(a). On that basis the distribution of the contact pressure is similar in both cases as the contribution from the hoop stresses is small and

$$q = c \left( \frac{2R}{3H} + N_{cr} - 1 \right) + \gamma D \quad (7)$$

where  $N_{cr}$  is the bearing capacity factor for a circular footing on a layer of great thickness.<sup>(12)</sup>

The more exact shear zones under the footing, as in the case of blocks, lead to a greater contact pressure near the edges, which is, however, only partly offset by a smaller contact

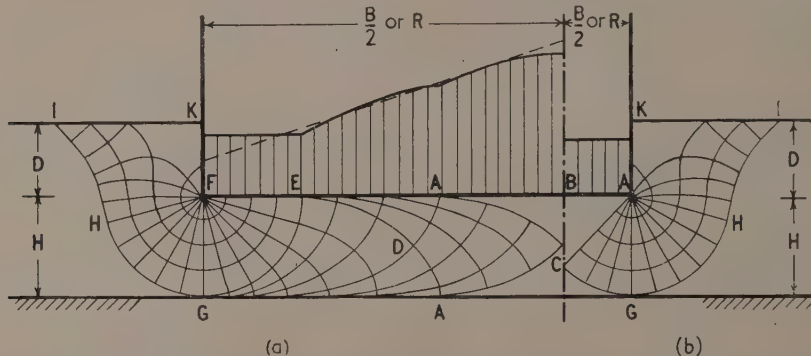


Fig. 7. Plastic zones and contact pressure for perfectly rough footing on layer with perfectly rough base

(a) Wide footing. (b) Narrow footing.

Distribution of contact pressure:

Actual —————  
Approximate - - - - -  
Centre line . . . . .

which is wide compared with the thickness of the layer, both footing and base stratum being perfectly rough. Below the footing the zones are the same as for a wide block under compression (Section 2) except near the edge of the footing where only one radial shear zone  $EFG$  occurs and extends to the base stratum. This zone is continuous with a radial shear zone  $FGH$  and followed by a mixed shear zone  $FHIK$  outside the footing where the zones are the same as for a layer of great thickness.<sup>(12)</sup> For a narrow footing the various shear zones coalesce as indicated in Fig. 7(b).

The plastic equilibrium in the zones can be established as before. At some distance from the edges of a strip footing of width  $B$  and depth  $D$  on a purely cohesive layer of thickness  $H$  (beneath the footing), Fig. 7(a), the contact pressure on a perfectly rough footing increases uniformly towards the centre as before; and on the assumption that the cycloidal shear zone

pressure on the central zones as indicated in Fig. 7(a). It is, therefore, more convenient to express the yield pressure by the relation

$$q = cN_{cq} + \gamma D \quad (8)$$

where  $N_{cq}$  is the yield pressure factor and is a function of  $M_c$  (Section 2) and  $N_c$ ; this factor depends on the depth and shape of the footing as well as the thickness of the layer.

The results of this analysis are given in Fig. 8 for strip and circular footings with a rough base and a perfectly smooth shaft; for a footing with a perfectly rough shaft the yield pressure factor  $N_{cq}$  is greater by about 0.5<sup>(12)</sup> and the skin friction on the shaft has to be added to obtain the total failing load. Fig. 8 shows that the theoretical yield pressure of a footing on a thin layer is directly proportional to the ratio of footing width/thickness of layer  $B/H$  (or  $2R/H$ ) and increases with footing depth. Beyond a depth of about three times the



thickness of the layer, the yield pressure should remain independent of depth and increase only with  $B/H$  (or  $2R/H$ ). For thick layers the more exact shear zones have been used in the estimates, which for  $B/H$  (or  $2R/H$ )  $\leq \sqrt{2}$  give the bearing capacity of a footing in a homogeneous material of great depth. This value also gives the lower limit of the yield pressure for a footing and base stratum with a trace of adhesion ( $m \approx 0$ ) and is sensibly independent of  $B/H$  (or  $2R/H$ ), Fig. 8. The yield pressure is almost directly pro-

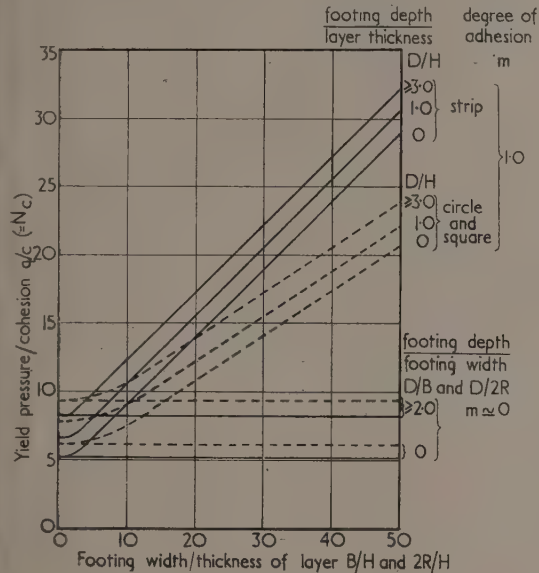


Fig. 8. Yield pressure of footings on layers

Strip footing ( $B/L = 0$ ) —————

Circular or square footing ( $B/L = 1$ ) - - - - -

portional to the degree of adhesion  $m$  (similar to Fig. 2) and can, therefore, readily be interpolated between the above limits.

It is of interest to note that for thick layers the yield pressure of a rough circular footing is up to one-fifth greater than that of a corresponding strip footing on account of the hoop stresses in the material. For thin layers, however, the yield pressure of a circular footing is up to one-third less than that of a strip footing since the hoop stresses are then relatively small and more than offset by the smaller effect of the shearing resistance on the footing and base stratum. The yield pressures of rectangular footings of length  $L$  and width  $B$  on thin layers can be estimated by interpolation between the curves for strip and circular footings (Fig. 8) in direct proportion to  $B/L$  (similar to Fig. 2), which was also found to be sufficiently accurate for thick layers.<sup>(12)</sup>

## 5. LOADING TESTS

To provide a check of the present theory for full adhesion, some loading tests were carried out on model circular and a few strip footings resting on Plasticine layers of various thicknesses. The circular footings were of 1.35 in diameter and the strip footings were 0.5 in wide by 5.0 in long, on layers from 0.1 to 3.0 in thick and supported by a rigid base; both footing and base were covered with emery paper to ensure full mobilization of the shearing strength. The experiments were carried out in a compression apparatus as before

(Section 2); the load was applied in small increments, each acting until the settlement of the footing was sensibly complete. The final ratios of footing width (or diameter) to the thickness of the layer below the footing ( $B/H$  or  $2R/H$ ) varied from 0.5 to about 60. The overall rate of deformation in the experiments was 0.1 in/min. The material used for these tests was considerably softer than for the previous series, and had a shearing strength of 5.8 lb/in<sup>2</sup>.

The experimental yield pressure of the footings for appreciable plastic flow of the material is shown in Fig. 9. For circular footings on thin layers it increases in direct proportion to the ratio of footing width/final thickness of layer, and the results are in fair agreement with the theoretical estimates for perfectly rough footings and base. The results of the limited number of tests on strip footings are consistent with the theory. All estimates were based on footings below the surface of the layer on account of the relatively great penetration required

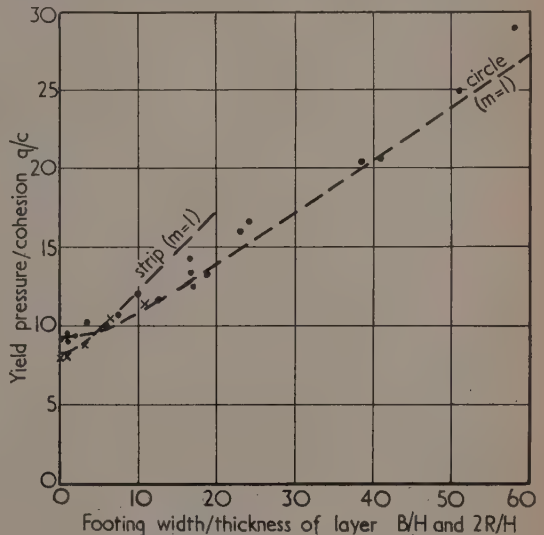


Fig. 9. Results of loading tests on footings on layers

Experimental results:

Strip footing ( $L/B = 10$ ) ×

Circular footing ●

Theoretical results ———

for mobilization of the shearing strength and the simultaneous rise of the material around the footings.

A further check of the theory is obtained from the loading tests on footings on very thin layers when the footing depth is fairly constant during the test. If the shearing stress along the footing and base is calculated from equation (7) for various ratios of footing width (or diameter) to thickness of the layer below the footing and plotted against the corresponding vertical strains in the layer, Fig. 5(b), it is found that these stress-strain relations are similar to and agree well with that of the standard compression test.

Examination of the specimens after testing showed that for thicker layers the material heaved slightly around the footing to a distance of about the width or diameter independent of the thickness of the layer. For thin layers the heave was well defined, extended around the whole footing to a distance of about twice the original thickness of the layer, and was independent of the footing width, Fig. 10. The volume of the

## ACKNOWLEDGEMENT

The work described was carried out as part of the research programme of the Building Research Board of the Department of Scientific and Industrial Research, and the paper is published by permission of the Director of Building Research.

## APPENDIX

*Compression of cylinder between partially rough plates*

On the simplifying assumptions made in Section 2 and at some distance from the perimeter of a thin cylinder of diameter  $2R$  and height  $H$  compressed between parallel rigid plates with an adhesion  $mc$ , the governing equation of equilibrium of the radial stress  $\sigma_r$ , vertical stress  $\sigma_z$  and shearing stress  $\tau$  is<sup>(5)</sup> for cylindrical co-ordinates  $(r, z)$ , Fig. 1(a)

$$\frac{\partial \sigma_r}{\partial r} + \frac{\partial \tau}{\partial z} = 0 \quad (a)$$

the plasticity yield criterion is<sup>(1)</sup>

$$\sigma_z - \sigma_r = 2\sqrt{(c^2 - \tau^2)} \quad (b)$$

and the shearing stress (as for a long block) is

$$\tau = 2mcz/H \quad (c)$$

Substituting equations (b) and (c) into equation (a) and integrating, the direct stresses are

$$\left. \begin{aligned} \sigma_r &= 2mc(R-r)/H - 2c\sqrt{[1 - (2mz/H)^2]} + A \\ \sigma_z &= 2mc(R-r)/H + A \end{aligned} \right\} \quad (d)$$

where  $A = \left[ \frac{\sin^{-1} m}{m} + \sqrt{(1 - m^2)} \right] c$

determined from the boundary condition of  $\int_0^{H/2} \sigma_r dz = 0$  for  $r = R$ .

If the cycloidal shear zone, which can be shown to satisfy equations (d), extends throughout the cylinder, the contact pressure on the plates ( $\sigma_z$  for  $z = \pm H/2$ ) increases uniformly with distance from the perimeter of the cylinder and the average value of this pressure gives the yield pressure

$$p = c \left[ \frac{2mR}{3H} + \frac{\sin^{-1} m}{m} + \sqrt{(1 - m^2)} \right] \quad (e)$$

## REFERENCES

- (1) PRANDTL, L. *Z. angew. Math. u. Mech.*, **3**, p. 401 (1923).
- (2) SOKOLOVSKY, W. W. *Theory of Plasticity*, Chap. 8 (Moscow: Acad. Sci. U.S.S.R., 1946).
- (3) HILL, R., LEE, E. H., and TUPPER, S. J. *J. Appl. Mech.*, **18**, p. 46 (1951).
- (4) GREEN, A. P. *Phil. Mag.*, **42**, p. 900 (1951).
- (5) NADAI, A. *Z. Phys.*, **30**, p. 106 (1924).
- (6) SCOTT, J. R. *Trans Instn Rubb. Ind.*, **7**, p. 169 (1931); **10**, p. 481; and **11**, p. 224 (1935).
- (7) PEEK, R. L. *J. Rheol.*, **3**, p. 345 (1932).
- (8) COOK, M., and LARKE, E. C. *J. Inst. Met.*, **71**, p. 377 (1945).
- (9) JÜRGENSON, L. *J. Boston Soc. Civ. Eng.*, **21**, p. 242 (1934).
- (10) NYE, J. F. *Ministry of Supply, A.R.D. Res. Rep.* 39/47 (1947).
- (11) MEYERHOF, G. G. *Proc. S. Wales Inst. Eng.*, **67**, p. 53 (1951).
- (12) MEYERHOF, G. G. *Géotechnique*, **2**, p. 301 (1951).

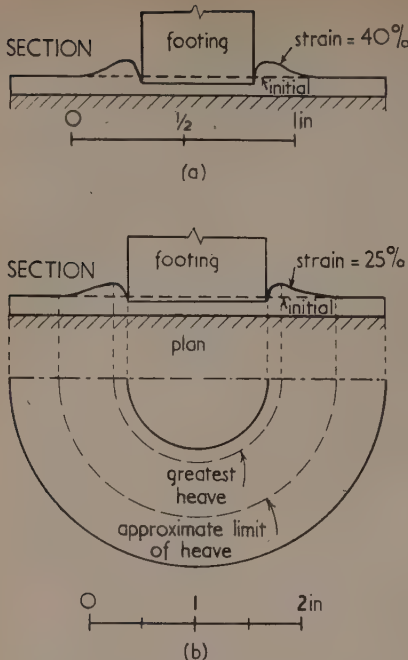


Fig. 10. Typical thin layers before and after test

(a) Strip footing. (b) Circular footing.  
Centre line — — — — —

deformed material outside the footing was found to be of the same order of magnitude as that displaced below the footing so that the deformations occurred without noticeable volume change. The above results would support the mechanism and extent of failure assumed in the theory.

## 6. CONCLUSION

The previous theory of the compression of a long block of purely cohesive material has been extended to blocks of rectangular plan and cylinders compressed between parallel rigid plates of any degree of adhesion. The theoretical results show that the yield pressure of thin blocks and cylinders should increase rapidly with the adhesion of the material on the plates and with decreasing height of the specimen. Compression tests on blocks and cylinders of Plasticine and clay between perfectly rough plates were found to be in reasonable agreement with the theoretical yield pressure and mechanism of failure. The experiments also suggest that the vertical stress-strain relations of the blocks and cylinders are the same as in the standard compression tests on the material.

The above analysis has been extended on the basis of bearing capacity theory to strip, rectangular and circular footings at any depth in a purely cohesive layer resting on a rigid base stratum. The theoretical results show that the yield pressure should increase rapidly with the adhesion of the material on the footing and base and with decreasing thickness of the layer below the footing. Loading tests on rough circular and a few strip model footings on Plasticine layers with a perfectly rough base are in fair agreement with the theoretical yield pressure and mechanism of failure. The vertical stress-strain relations of very thin layers are again similar to those of standard compression tests.



# A simple goniometric method for examining preferred orientation in etched metal polycrystals

By PAMELA DUNSMUIR, M.Sc., A.Inst.P., Research Laboratory, British Thomson-Houston Co. Ltd., Rugby

[Paper received 27 August, 1952]

A simple apparatus is described for determining the orientation of etched metal crystals. A multi-coloured source of light enables rapid assessment of preferred orientation in polycrystals to be made.

An ordinary microscope has been modified to form a kind of goniometer which has proved useful in examining the orientation of crystals in etched samples of polycrystalline metals. The goniometer consists of a microscope with a horizontal rotating stage together with an extended "semi-infinite" line source for illumination. The lack of the second circle of the standard goniometer is in effect compensated by the length of the source of light which permits illumination of the specimen at a range of angles of incidence simultaneously, instead of using the standard parallel beam. The principle of the instrument is shown diagrammatically in Fig. 1.

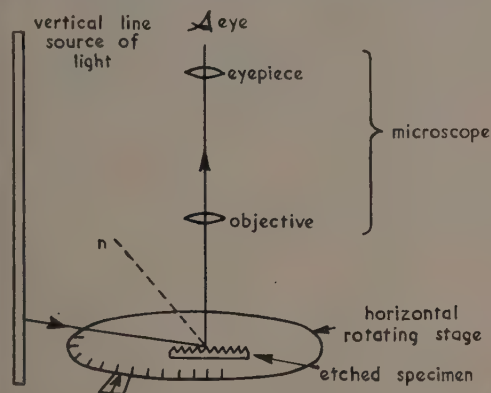


Fig. 1. Diagram showing the principle of the goniometer

The use of the instrument for determining the orientation of a given metal crystal may be understood by considering an actual example. A tungsten single crystal with a flat surface has been etched with a solution of potassium ferricyanide and potassium hydroxide, recommended by Barrett\* so as to cover the surface with exposed (110) planes. The micro-photograph of Fig. 2 shows the appearance of the surface (magnification  $\times 1500$ ). The specimen is placed on the rotating stage, which is then moved slowly through a complete revolution, and the three angles at which the crystal appears of maximum brightness are noted. When the normal to a set of reflecting facets lies in a vertical plane containing the line source, then the crystal reflects a maximum amount of light vertically into the microscope. The observed data are conveniently recorded on a stereographic projection whose centre corresponds to the plane of polish of the specimen. The angles of maximum brightness of the crystal are directly marked on the stereographic projection as radii. From the individual observations it is only known that the stereographic pole of the faces giving rise to one of the reflexions lies *somewhere* on the corresponding radius. The

three radii of Fig. 3 correspond to the possible positions of the stereographic poles of the three sets of reflecting facets. By taking a standard stereographic projection of the poles of the various (110) planes and rotating it stereographically until one pole lies on each radius, it is easy to find the orientation of the crystal. This method has some limitations for determining the orientation of single crystals. Only planes in the range between the horizontal and at  $45^\circ$  to it give observable reflexions, and it is only when at least three reflexions are observed that the orientation of the crystal can be determined completely. In the particular case of tungsten etched so as to expose (110) planes this is not a serious difficulty, since the (110) poles are only  $60^\circ$  apart, and so, for almost all possible orientations, three such poles do lie within the circle of  $45^\circ$  radius about the centre of the pole figure. (In fact, poles lying just beyond the  $45^\circ$  circle are also observed because of the finite angular width of the beam admitted to the microscope objective. They are, however, rather broad and faint.)

As a test of the accuracy of the above procedure the (110) poles were identified by X-rays and are marked on the projection in Fig. 3. It can be seen that the poles do lie on the radii to within approximately  $\pm 2^\circ$ . Figs. 4 and 5 show the stereographic projection marked with X-ray poles and radii, and also the micro-photograph ( $\times 1500$ ) corresponding to another tungsten crystal. Whereas the crystal of Figs. 2 and 3 has symmetrical reflecting facets, the crystal of Figs. 4 and 5 has reflecting facets arranged unsymmetrically with respect to the surface of the specimen.

The apparatus described has some advantages when we wish to examine polycrystalline specimens, particularly those which exhibit preferred orientation. Whereas the sharply collimated beam of a goniometer in general only allows one crystal of the polycrystalline specimen to reflect at one setting, the extended source of the present instrument enables many crystals to reflect at the same setting, and gives a vivid and, to some extent, quantitative impression of the degree of preferred orientation of the sample. For example, consider a sample of silicon-iron alloy which has been cold rolled and re-crystallized, so that most of the crystals are near the orientation [100], (110), (that is, a [100] axis is parallel to the rolling direction and a (110) plane is in the plane of the sheet). When etched with ferric sulphate to expose the (100) facets of the crystals the extended surface of most of the specimen is covered with "rooftops" formed of (100) facets at  $45^\circ$  to the surface and with the ridge or [100] axis along the rolling direction. When a specimen is rotated on the stage a majority of the crystals give rise to two maxima of brightness in a complete revolution, and these maxima are clustered near two settings  $180^\circ$  apart. In the neighbourhood of these settings a number of the crystals appear bright at the same time. The degree of preferred orientation of a specimen can be depicted semi-quantitatively by a graph of total light reflected against angular setting. It must be remembered that where (100) poles of a cubic crystal are being used to determine orientation as in this example, then

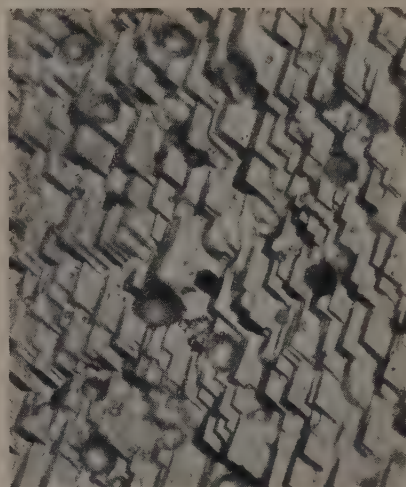
\* BARRETT. *Structure of Metals*, p. 175 (New York: McGraw-Hill Book Co. Inc., 1943).

some crystals may unfortunately be orientated so as to permit only one bright reflexion, since (100) poles are  $90^\circ$  apart and only poles near or within the  $45^\circ$  circle can reflect.

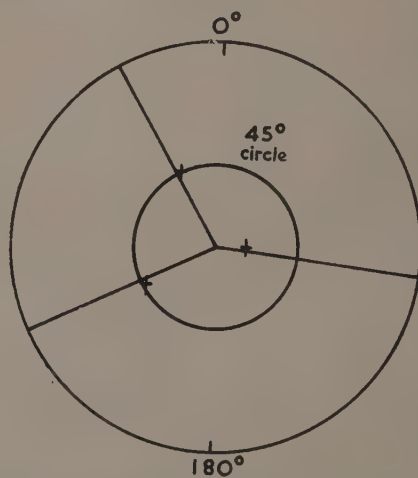
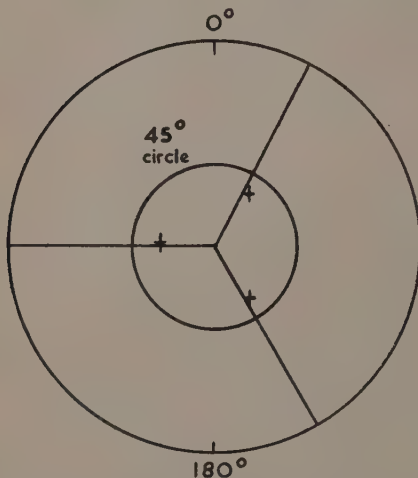
To provide more information about the orientation of the reflecting facets the following adaptation may be made.

of course, the orientation of the given crystal may be deduced when only two bright reflexions are observed.

Another scheme (suggested by Dr. C. J. Milner of this Laboratory) which has been employed is to use for the line source of light a fluorescent lamp (3 or 5 ft in length) which



Figs. 2 and 4. Microphotographs of crystallographically etched tungsten crystals of two differing orientations showing the (110) planes. (Magnification  $\times 1500$ )



Figs. 3 and 5. Pole figures corresponding to Figs. 2 and 4 respectively, on which the (110) poles as deduced by X-rays are marked. The radii [on each of which a (110) pole should lie] are found by using the apparatus of Fig. 1. The centre of each pole figure gives the normal to the plane of polish and the direction  $0-180^\circ$  is parallel to the direction of the tungsten crystal given by the long edge of the microphotograph

Suppose that a certain crystal is already placed so as to appear of maximum brightness. Then a small opaque screen can be moved up and down the line source until it cuts out the light and the given crystal appears dark. From this position of the screen one can then decide on the actual position of the stereographic pole along the corresponding radius on the stereographic projection. With this additional information,

has been coated over various parts of its length with different fluorescent powders. Thus one-third of its length may glow bright pink, one-third green, and one-third blue. From the colour of the light reflected by a given crystal the orientation may at once be deduced to within a small range. The apparatus has also been used to see whether crystals of germanium are indeed single crystals. A further application



of the apparatus may be the study of crystallographic etching. In certain cases impure or secondary colours are observed unless the etching conditions are very critically controlled. The reflexion of pure colours might be a criterion for correct crystallographic etching, where it is required for other experiments.

#### ACKNOWLEDGEMENTS

It is a pleasure to thank my colleagues Mr. J. A. James and Mr. T. J. Potter for their assistance with the examination of tungsten crystals. I also wish to thank Mr. L. J. Davies, Director of Research, British Thomson-Houston Co. Ltd., for permission to publish this paper.

## NOTES AND NEWS

### New books

**Metallurgical equilibrium diagrams.** By W. HUME-ROTHERY, F.Inst.P., F.R.S., J. W. CHRISTIAN, A.Inst.P., and W. B. PEARSON. (London: The Institute of Physics.) Pp. 311. Price 50s.

In the last thirty years there have been great advances in the science of alloy structures, and in this work the importance of metallurgical equilibrium diagrams has become increasingly apparent. This monograph gives a comprehensive and critical account of the experimental methods involved, together with full experimental details of many techniques. The authors are members of the Oxford school of metallurgists which has done much to advance the science of alloy structures and they are experienced in many of the methods described.

The monograph begins with a theoretical introduction, followed by details of general laboratory technique, and of the different methods of pyrometry. This is followed by a full description of experimental methods for the determination of the liquidus, including special chapters on high melting alloys. Similar sections deal with the determination of the solidus and solid solubility curves, and the use of X-ray methods is discussed critically. The final section deals with ternary systems from both the theoretical and experimental viewpoint.

The monograph, which contains 239 figures including many plates, is intended primarily for fourth year honours students and research students in metallurgy, but much of the subject-matter is of interest to chemists and physicists.

**Cosmic rays.** By LOUIS LEPRINCE-RINGUET. (London: Constable and Co. Ltd.) Pp. xi + 290. Price 30s.

A certain amount of the pleasure we get from reading a novel comes from the sidelights it throws on the author's character. This is usually absent in a scientific book, which is by convention limited to a factual description of some corner of nature. Leprince-Ringuet breaks this rule and manages to project himself through pages describing cloud chamber mechanisms or the intricacies of meson theory, and the book is all the better for it. His liking for adventure is manifest through such things as descriptions of manned balloon flights, of building mountain-top laboratories and of global surveys of the radiation intensity.

The book is also characteristically French. This manifests itself sometimes in the English, but more so through a constant interest in the human side of research—the qualities that make a successful investigator—the spirit of a research team (important, this, for cosmic rays where so much has been achieved by team-work)—life in a mountain-top research laboratory—and the like.

Leprince-Ringuet has attempted to bridge the gap between the frankly popular book and the advanced monograph. He is to be congratulated for attempting this difficult task which

he has successfully accomplished. The book starts by discussing the properties of particles, particularly at high energy. The main characteristics of the cosmic radiation observed at sea level are then reviewed after which the contributions of high altitude research are discussed. The evidence for the separation of the radiation into soft and hard components, and their identification with electrons and mesons is given. This leads on to meson theory and to artificial mesons. Finally the nature of the primary radiation and tentative theories of its origin are discussed.

The book is pleasantly produced and profusely illustrated by many cloud chamber photographs and nuclear emulsion photomicrographs. This translated version has been brought up to date.

The only fault the reviewer could find with it is the omission of any serious discussion of the large atmospheric showers—they have been studied much these last few years. A characteristically novel touch is the short directory of cosmic ray workers at the end—alphabetical from Alikhanian to Zhdanov.

E. P. GEORGE

**Practical radiography for industry.** By H. R. CLAUSER. (London: Chapman and Hall Ltd.) Pp. x + 301. Price 60s.

Text-books on industrial radiography which are suitable for the operating staff are still sufficiently rare to make the appearance of a new one a welcome event. This volume is the kind of book which is wanted in this field. It is of convenient length, well printed and well illustrated. Its fourteen chapters range comprehensively over the whole subject and are well balanced. The best chapters are those on practical work in radiography and in the handling of films.

Unfortunately the theoretical part, especially basic physics, is less good and there are several mis-statements other than printer's errors which call for correction in a future edition, especially since the book is intended for "those with little or no training in mathematics." On page 11, instead of talking to his readers in terms of photons, which have already been mentioned on page 8, the author asks us to count the X-rays in a beam one by one and per second as they pass through a square hole of unit area in a piece of cardboard. After this we are to calculate the intensity by multiplying this number by the energy per X-ray. What is the energy of an X-ray and why can cardboard stop X-rays which are intended to penetrate inches of steel? On page 53 we learn that as the source to film distance is increased, the difference of intensity as between the centre and the edge of a radiograph can be considerable. Moreover the increase in this distance is said to produce enlarged images on the radiograph. On page 149 we are told that a millicurie is the intensity of radiation emitted by a milligram of radium, but on page 150 we find that the amount of radon in equilibrium with one gramme of

radium is known as a curie. Again, on page 149 it is stated that a millicurie is equal to 0.0008 r per hour at one metre. All these statements are quite wrong in view of the International definition of the curie which was adopted in London in 1950 with the active support of the American delegation.

These are only a few of the errors which must be corrected if the book is really to help the non-physical, non-mathematical layman, but its price of 60s. is likely to be a serious hindrance to popularity in the Britain of today. W. E. SCHALL

**Polarized light in metallography.** Edited by G. K. T. CONN and F. J. BRADSHAW. (London: Butterworths Scientific Publications.) Pp. xi + 130. Price 21s.

The book has been prepared for the British Iron and Steel Research Association Optical Methods Sub-Committee. By implication, the preface suggests that it is a comprehensive survey of the present position of the use of polarized light in metallography. The book has to be judged against this high endeavour and, bearing in mind that the first two chapters are essentially a summary of those parts of physical optics necessary for an understanding of the use of polarized light, the editors have left themselves barely 80 pages to achieve their purpose. This is a difficult enough task made more difficult by the selection of different authors for each succeeding chapter giving, as it does, an unevenness in the writing and presentation and a certain amount of repetition. The editors have not succeeded therefore in their main aim, but they have produced a book which contains much interesting reading, some good bibliographies and an indication of how the present rule of thumb methods in use in many laboratories could be replaced by a more quantitative approach. These are minor but still worthwhile achievements. The illustrations, index and general standards of production are good and the book will be a useful addition to the library of most metallurgical laboratories. L. ROTHERHAM

**Ferromagnetic properties of metals and alloys.** By K. HOSELTZ. (London: Oxford University Press.) Pp. xi + 317. Price 40s.

In recent years there have been considerable advances in the theory of magnetic materials and in the production and utilization of more efficient forms of these materials. This work has not, until very recently, been accompanied by any equivalent increase in the number and scope of reference books. The need for such books is therefore apparent as is the necessity for an increasing specialization of their subject matter. The title of this book indicates the scope of the subject-matter treated. It is intended for post graduate and industrial research workers in physics, metallurgy and electrical engineering.

A comprehensive account is given of the present theories of the magnetization curve. The composition, treatment, and properties of a large number of both magnetically soft and hard materials are described together with the theoretical explanation for many of their properties. A small section of the book is devoted to the properties of metals and alloys in general and a large section deals with magnetic analysis, that is the application of magnetic methods to the analysis of ferromagnetic metals and alloys. This latter section is the first comprehensive account to be presented of techniques which are assuming greater importance as the uses of ferromagnetic materials increase.

The book is well produced, contains a reasonable number of figures and tables, and should prove a most useful reference book. R. MILLERSHIP

**Demonstrations in modern physics.** By M. C. NOKES. (London: William Heinemann Ltd.) Pp. viii + 134. Price 10s. 6d.

This latest book of Mr. Nokes is written for the ambitious physics master who wishes to perform some experiments in modern physics of a type not often attempted in school laboratories. The greater part of the book deals with vacuum technique applied to discharge tubes, but there are also chapters on radioactivity, Brownian movement and spectra, which deal adequately with these subjects for school work.

The book should be inspiring to most and of value to all. It gives a host of useful hints on laboratory technique. Some may think this technique beyond them, but this should not deter them from attempting many of the experiments described. There is no other book with which this may be compared, but it is hoped that others will follow. It is by performing experiments of the type described that boys acquire an inspiration for the subject which urges them to further study. W. ASHHURST

**A source book of technical literature on fractional distillation.** (London: Gulf Oil (Great Britain) Ltd.). Pp. 129.

This volume of papers originally published in scientific journals is divided into two parts. Part I is intended to cover the general theory of vapour-liquid equilibria, batch distillation and binary mixture separation, beginning with the classical paper by Lord Rayleigh in 1902. Part II is a summary of the existing literature on continuous multicomponent rectification, written by Professor W. C. Edminster. The whole book has been reproduced photographically and is an attempt to include as much as possible of the course material on which the science and practice of distillation are based in the belief that it will foster independent thought and a sound grasp of the subject. This book is available on request.

**Mixtures. The theory of the equilibrium properties of some simple classes of mixtures, solutions and alloys.** By E. A. GUGGENHEIM. (London: Oxford University Press.) Pp. x + 270. Price 42s.

This book is a welcome addition to the distinguished International Series of Monographs on Physics. It has not been the intention of the author to give a general treatment of the properties of mixtures. He has restricted himself to a statistical-thermodynamical discussion of relatively simple molecular models of solid, liquid and gaseous mixtures, and to a comparison of the results with the meagre experimental data which are available for such systems.

Some knowledge of thermodynamics and statistical mechanics is assumed, but there are two introductory chapters which give a synopsis of the formulae required later. The types of system treated include ideal mixtures, regular solutions, dilute solutions, simple crystalline binary alloys, gaseous mixtures, and solutions of molecules of different size, with and without an energy of mixing. There is also a chapter on the surfaces of ideal and of regular solutions, and one on the application of the theory to solutions of macromolecules.

Although the models reproduce the properties of only the simplest mixtures, which are themselves important enough, their study must form the basis of extensions to the wider field covered by more complex systems. The author, who has himself made important contributions to the theory, gives in this book a valuable account of the present position. All who are interested in the theory of solutions and of mixtures will wish to possess it. J. W. BELTON



## Notes and comments

### Elections to The Institute of Physics

The following elections have been made by the Board of The Institute of Physics:

*Fellows:* C. A. Coulson, F. E. Hoare.

*Associates:* W. Benson, B. Bradley, H. L. Evans, J. H. Frisby, E. R. Harrison, R. F. Hounam, W. James, H. F. T. Jarvis, G. C. Lowenthal, J. J. McNeill, J. B. Massey, H. Mykura, P. C. Newman, A. D. I. Nicol, P. Nicolson, J. R. Pattison, I. S. Quayle, R. T. D. Richards, J. Roberts, M. E. Sprinks, D. G. A. Thomas, G. H. Thorndike, M. W. H. Townsend.

Fifty-two Graduates, thirty-five Students and five Subscribers were also elected.

### Conference on static electrification

The Institute of Physics has arranged a conference on static electrification to be held at Bedford College, London, on 25–27 March, 1953. There will be an opening lecture by Professor F. A. Vick, and the other sessions will each take the form of an introductory survey, followed by specialized papers and discussion. The introductory surveys will be given by Dr. P. S. Henry (General principles of the generation and dissipation of static electricity), Dr. E. S. Shire (Electrostatic machines), and Mr. H. W. Swann (Harmful static electrification). The more specialized papers will be available as preprints to those attending the conference and the proceedings of the conference will later be published by the Institute.

Further particulars may be obtained from The Institute of Physics, 47 Belgrave Square, London, S.W.1.

### Conference on the physics of particle size analysis

There have been in recent years numerous publications relating to the development of instruments and the fundamental physics of the processes involved in measuring particle size, especially for sizes in the range of  $0.1\text{--}30\ \mu$ . Measurement of particle size distributions are made in many sciences and industries, and since it is now some five years since the last British conference on particle size analysis (organized by the Society of Chemical Industry and the Institution of Chemical Engineers) it is felt that the time is now opportune for a further exchange of views. To this end, The Institute of Physics announces that it is arranging a conference on the physics of particle size analysis to be held in the University of Nottingham from 6–9 April, 1954.

It is anticipated that the various sessions will cover not only such fundamental physical processes as the fluid dynamics and the optics of particles and systems of particles, but also accounts of other phenomena encountered in particle size analysis such as the aggregation and dispersion of particles in a fluid. Arrangements will be made also for a discussion on automatized methods of counting and sizing, to which great attention is being given at the present time. Although the conference will be primarily concerned with the physical principles of particle size analysis, the development of new instruments and their use will receive attention, particular interest being attached to the systematic comparison of different methods of particle size analysis.

The Organizing Committee is prepared to consider offers

of papers describing original work for reading and discussing at the conference. The synopsis of the proposed contribution should be sent before 3 February, 1953, to the Conference Honorary Secretary, Mr. R. L. Brown, c/o The Institute of Physics, 47 Belgrave Square, London, S.W.1. Papers will be refereed in the usual way before acceptance and will be published, with summaries of the discussion on them, as part of the *British Journal of Applied Physics*—one of the Institute's *Journals*. In order that advance proofs might be available in good time prior to the conference, it is desired that the scripts should be received by the end of October 1953.

Further details will be announced in due course.

### British Instrument Industries Exhibition

The second British Instrument Industries Exhibition will be held in the National Hall, Olympia, from 30 June to 11 July, 1953. The first exhibition was held in 1951 and it has been decided to establish these exhibitions as biennial events.

The instruments on show will cover a wide field of instrumentation in industry, medicine, research and education. In the industrial field all classes of temperature, pressure, flow and other recorders will be included. Equipment for research laboratories in pure and applied science will be well represented in addition to precision equipment in such diverse fields as metrology and photography. Complete equipment for land surveying and for navigation by air or sea will also be on show.

The exhibition should prove of value to all interested in British instruments. Further information may be obtained from the organizers, F. W. Bridges and Sons Ltd., Grand Buildings, Trafalgar Square, London, W.C.2.

### Catalogue of British electrical products

We have received the 1952–53 edition of the BEAMA catalogue which classifies the 1200 types of products of The British Electrical and Allied Manufacturers' Association (Inc.) into three groups: Power plant; Industry, transport and communications; Domestic and commercial. The 1020 pages include a catalogue index, a trade directory, a buyers' guide and a glossary in five languages, English, French, German, Portuguese and Spanish.

The catalogue is as usual very well illustrated and is published by Iliffe and Sons Ltd.

### Register of British manufacturers

We have received the 1952–53 edition of the FBI register of British manufacturers which gives information of more than 6000 members of the Federation of British Industries under six headings: Products and services; Advertisements; Addresses; Trade associations; Brands and trade names; Trade marks. In addition the 922 pages include an addenda listing the products, services and addresses of firms which have become members of the FBI since the main sections of the register closed for press, and also a list of comparatively recent publications issued by the FBI.

This twenty-fifth edition maintains the high standard of production already attained by Iliffe and Sons Ltd.



### The evaluation of restriking voltage severity

A 16-page booklet sets out interim rules for the evaluation of restriking-voltage severity which is one factor that must be considered when the short-circuit performance of a circuit-breaker is being judged. It is, however, difficult to compare the severities of circuits which produce restriking-voltage transients and which have different wave-forms. A method of overcoming this has been evolved by the Association of Short-Circuit Testing Authorities and is being considered by the International Electro-technical Commission for incorporation in the next edition of IEC Publication No. 56—"Specification for Alternating Current Circuit-Breakers." Minor modifications suggested by the IEC have been incorporated, and pending the issue of the IEC publication, a method of evaluation of restriking-voltage severity is set out in these interim rules to provide a means whereby comparisons may be made on a uniform basis during the testing of circuit-breakers in ASTA Stations.

The booklet, ASTA No. 13, is available from the Association of Short-Circuit Testing Authorities (Inc.), 36 and 38 Kingsway, London, W.C.2, price 5s. 0d.

### Errors in the A.S.T.M. Index

The A.S.T.M. Index of X-ray powder diffraction data has now been in use for about ten years and it is recognized that it contains a number of wrong identifications which are likely to lead to confusion. The X-ray Analysis Group of The Institute of Physics therefore proposes to collect information on the errors which have been observed by users of the Index and to publish as soon as possible in some suitable way a list of all those errors which seem to be substantiated. It is believed that many, if not all, of these errors have by now been noted by various workers and may in some cases have been mentioned casually in their publications, but in order to be of real use to others it is necessary

that they should all be published collectively. Accordingly, everyone who has noted such errors is asked, whether he has already published them or not, to send the details to Dr. A. J. C. Wilson, University College, Cathays Park, Cardiff.

### Notes on the preparation of papers

A revised and enlarged edition of the booklet *Notes on the preparation of contributions to the Institute's journals and other publications* is available. These notes, first issued in 1931, are intended to assist less experienced authors and to serve as a reference book for all who contribute to the Institute's publications. Apart from the special information concerning these publications the notes deal with the preparation, length and cost of publishing papers, the form of script and diagrams required, the setting out of tables and mathematics, and the correction of proofs. A short bibliography of dictionaries and books on writing is included. The appendix contains notes and examples of spellings, symbols and abbreviations, the Greek alphabet (so often unrecognizably written in scripts) and printers' marks for correcting proofs.

Copies of the booklet may be obtained from The Institute of Physics, 47 Belgrave Square, London, S.W.1, price 2s. 6d. Orders should be accompanied by remittance.

### The scientific education of physicists

The Institute of Physics has published a new report, *The scientific education of physicists*. Copies are available, price 2s., on application to the Secretary, The Institute of Physics, 47 Belgrave Square, London, S.W.1. The report includes, as appendices, factual data relating to the physics departments of all the universities and university colleges of Great Britain and Northern Ireland and of those technical colleges recognized by the Institute. The information should be of value to those studying for a degree in physics or contemplating such a course of study, as well as to others who have a close interest in the facilities for advanced training in physics.

## Journal of Scientific Instruments

### Contents of the January issue

#### ORIGINAL CONTRIBUTIONS

- An accurate wire resistance method for the measurement of pulsating pressures. By N. Gross and P. H. R. Lane.  
A continuously sensitive diffusion cloud chamber for operation at four atmospheres. By M. Snowden and A. R. Bevan.  
A simple high-speed spectrometer for the infra-red region. By D. A. H. Brown and V. Roberts.  
The experimental production of small tensile specimens by electrolytic solution (electro-turning). By M. H. Farmer and G. H. Glaysher.  
Non-linearity in a voltmeter using cathode-follower and thermocouple. By D. G. Tucker.  
A technique for cleaning hot-wires used in anemometry. By L. A. Wyatt.  
Simple and multiple gas microinjectors for adsorption studies. By J. C. P. Mignolet.  
A selective detector amplifier for 10-10 000 c/s. By G. H. Rayner.  
Temperature-stable, capacitance pressure gauges. By D. C. Pressey.

#### LABORATORY AND WORKSHOP NOTES

- A controlled fluid-feed atomizer. By J. C. Gage.  
High vacuum pipe connectors. By J. Pollard.  
An apparatus for testing switching performance of thermostats. By J. Carlebach.  
Breakdown of some plastics under pressure. By H. D. Parbrook.  
A simple device for the continuous collection of direct-writing oscillograph records. By J. Lyman and D. C. Skilling.  
An oxygen detector. By E. T. Turkdogan and L. E. Leake.

#### NEW INSTRUMENTS, MATERIALS AND TOOLS MANUFACTURERS' PUBLICATIONS

#### NEW BOOKS NOTES AND COMMENTS

## British Journal of Applied Physics

### Original contributions accepted for publication in future issues of this Journal

- Photoelastic determination of stresses in a cylindrical shell. By H. Fessler and R. T. Rose.  
The construction of ball-and-spoke models of crystal structures. By H. D. Megaw.  
A check on the standard observer data at 4358 Å. By W. Harrison.  
Changes in secondary and thermionic emission from barium oxide during electron bombardment. By J. Woods and D. A. Wright.  
The effects of oxygen on the electrical properties of oxide cathodes. By A. A. Shepherd.  
Electronic control of a synchronous motor. By L. U. Hibbard.

### Erratum

In the article "Frictional and elastic properties of high polymeric materials" by B. Lincoln, published in the August 1952 issue of this Journal, the heading of the last column in Table 1 on page 262 should read "shear strength, dyn/cm<sup>2</sup> × 10<sup>8</sup>" instead of "shear strength, dyn/cm<sup>2</sup> × 10<sup>9</sup>".

THIS JOURNAL is produced monthly by The Institute of Physics, in London. It deals with all branches of applied physics (including theory and technique). All rights reserved. Responsibility for the statements contained herein attaches only to the writers.

**EDITORIAL MATTER.** Communications concerning editorial matter should be addressed to the Editor, The Institute of Physics, 47 Belgrave Square, London, S.W.1. (Telephone: Sloane 9806.) Prospective authors are invited to prepare their scripts in accordance with the *Notes on the Preparation of Contributions*. (Price 2s. 6d. including postage.)

**REPRODUCTION.** The Institute of Physics is a signatory to The Royal Society's Fair Copying Declaration. Details may be obtained upon application from The Royal Society, London, W.1.

**ADVERTISEMENTS.** Communications concerning advertisements should be addressed to the agents, Messrs. Walter Judd Ltd., 47 Gresham Street, London, E.C.2. (Telephone: Monarch 7644.)

**SUBSCRIPTION RATES.** A new volume commences each January. The charge is £4 per volume (\$11.50 U.S.A.), including index (post paid), payable in advance. Single parts, so far as available, may be purchased at 8s. each (\$1.15 U.S.A.), post paid, cash with order. Orders should be sent to The Institute of Physics, 47 Belgrave Square, London, S.W.1, or to any bookseller.

# Summarized proceedings of the fortieth anniversary celebrations of the discovery of X-ray diffraction—London, October 1952

The autumn meeting of the X-ray Analysis Group of The Institute of Physics was held at The Royal Institution, London, on 24 and 25 October, 1952. It was designed to celebrate the fortieth anniversary of the discovery of X-ray diffraction. Addresses were given by Professor Sir Lawrence Bragg, Professor J. D. Bernal, Mrs. D. Hodgkin, and Professor G. V. Raynor. Professor von Laue and Professor J. M. Bijvoet were guests of honour. A summary of the addresses is given in this report.

X-rays were discovered in 1895. After seventeen years of intense speculation about the nature of the rays, the question was conclusively settled by a single experiment, brilliantly conceived by von Laue in Munich, and carried out under considerable difficulties by two research students, Friedrich and Knipping. This was the experiment by which it was proved that X-rays could be diffracted, a crystal acting as a diffraction grating. Probably no single experiment in the history of science has opened up so many different avenues of research, and the fortieth anniversary celebrations brought together a representative collection of the people in Great Britain whose work had evolved from this one discovery.

The occasion was particularly auspicious because of the presence of PROFESSOR VON LAUE and PROFESSOR SIR LAWRENCE BRAGG, both of whom had contributed so largely to the early development of the subject; they both spoke at the celebrations and gave vivid personal accounts of the experiences which led to the discovery and of its early applications.

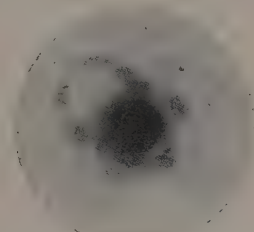
## HISTORICAL SURVEY

Sir Lawrence Bragg opened the proceedings with a fascinating description of the circumstances that led to the discovery, as he had learned it later in Munich from Laue and Ewald. In February 1912, Ewald, then a research student working under Sommerfeld, was preparing a thesis on the passage of light through crystals, treating the problem as one of scattering of light waves by atoms arranged on a lattice. Coming up against mathematical difficulties, he consulted Laue, who asked why he did not consider the much more interesting problem of the scattering of waves whose wavelength was comparable to the lattice spacing. Laue's attention was thus drawn for the first time to the concept of the crystal lattice, and he immediately thought that the periodicity might be about right to act as a diffraction grating for X-rays, if X-rays had the wavelength of about  $10^{-8}$  cm suggested by Koch and Sommerfeld.

Friedrich (a research student of Röntgen's) offered to try the experiment, but Sommerfeld was not encouraging. However, when Knipping, another research student of Röntgen's, was approached, Friedrich decided to join forces, and the necessary equipment was collected. The practical difficulties were extremely great as X-ray tubes were of a primitive type and could be run only for short periods; and several experiments were carried out before success was achieved. The crystal used was copper sulphate, and the photographic plate for detecting the diffracted beams was placed in several different positions. But it was not until Knipping suggested that the plate should be put in the path of the incident beam that diffracted beams were detected. The first successful photograph is shown in Fig. 1. The results were announced at a meeting of the Bavarian Academy of Sciences, held on 8 June, 1912, and were later published in *Naturwissenschaften*.

When a research student at Cambridge, Sir Lawrence

Bragg had had his interest in the nature of X-rays aroused by his father, Sir William H. Bragg, then Professor of Physics in the University of Leeds, who favoured the corpuscular theory because of the ionizing properties of X-rays. He soon realized that the Munich experiment proved conclusively that X-rays were waves, but he was not satisfied with Laue's explanation of the diffraction photographs. Laue had developed his now-famous equations, and had applied them to the beautifully symmetrical photographs obtained from a

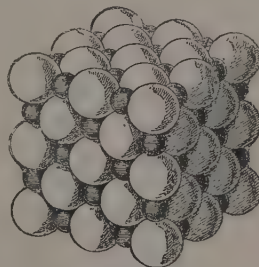


Reproduced from *Nature, Lond.*

Fig. 1. The first X-ray diffraction photograph

crystal of zinc blende, a much simpler crystal than copper sulphate; but his solution was rather complicated, necessitating the introduction of five different wavelengths, which even then did not account for all the spots which could be observed. By simple but ingenious considerations, involving the observation of the change in shape of the spots when the plate was placed at different distances from the crystal, the younger Bragg showed that the diffraction process was akin to reflexion—the most fruitful idea in the subject—and derived the law now called by his name.

This approach required that the X-rays should consist of a continuous spectrum, with wavelengths ranging from 0.2 to 0.9 Å, and on this basis all the spots on the photographs



Reproduced from *The Scientific Proceedings of The Royal Dublin Society*

Fig. 2. The first crystal structure



obtained with zinc sulphide could be accounted for, if the lattice were taken as face-centred. For this revolutionary concept, Sir Lawrence paid tribute to the ideas of Pope and Barlow, of which he heard at a students' colloquium; this was the first occasion at which he had met the concept of the space lattice, and in the next few years the suggestions of Pope and Barlow were to prove an inspiring source of new ideas for crystal structures. Pope suggested an experiment with the first crystal structure to be completely determined—that of rock salt (Fig. 2).

Sir Lawrence described vividly the difficulties under which his early work was carried out. C. T. R. Wilson was interested and suggested trying to see whether the cleavage surface of mica reflected X-rays particularly well. He tried using the cloud chamber to detect the reflected X-rays, but it was not sensitive enough. J. J. Thomson was encouraging, and he provided the X-ray tube and induction coil with which reflexion by mica was recorded on a photographic plate. But there were no workshops, and research students had to make their own apparatus. On one occasion, when the speaker had burnt out a platinum contact, the laboratory steward made him wait a month for a new one!

W. H. Bragg was more interested in the nature of X-rays. He proved by ionization methods that the diffracted rays were similar to the incident rays, and proceeded to devise the ionization spectrometer; with this he discovered the characteristic *K* and *L* radiations of a number of elements. He showed that the wavelengths were related to atomic weights, an idea later developed so successfully by Moseley in Manchester.

The ionization spectrometer proved to be a most valuable instrument, and with its use several new structures were derived including calcite and iron pyrites, both of which involved a variable parameter. Iron pyrites was interesting; the sulphur atoms obviously lay on threefold axes, but no positions would fit. It was not until a re-reading of the works of Pope and Barlow introduced the idea of non-intersecting trigonal axes that success was obtained.

Sir Lawrence drew attention to the large amount of basic work that had been carried out in the years preceding World War I. Debye's theory of the effect of heat motion on the intensity of diffraction had been checked, at least qualitatively; Darwin's papers on the fundamental theory had been published; the structures of several crystals—that of diamond excited wide interest—had been derived; and W. H. Bragg had already begun to think along the lines of Fourier theory, as presented in his Bakerian lecture to The Royal Society in 1915.

In 1918 the threads were taken up again. More complicated crystals including organic compounds and silicates were tackled, in spite of those pessimists who believed that no results involving more than two parameters could be trusted. Accurate tests of theory were carried out, chiefly by James, and new experimental methods—the oscillation photograph and the powder photograph—were devised. Sir Lawrence concluded his talk at the stage, in 1928, when the Fourier method was introduced—the method that was to prove so powerful in later work.

PROFESSOR VON LAUE then gave a brief address in German. He posed the question why, after the initial impulse, the main body of the work moved from Germany to England. It seemed, he said, that the Germans were satisfied when the general principles had been laid down, and were not interested in their exploitation. The English were more keen on the specific applications of principles and the use of physical models, and the combination of the two points of view was particularly powerful. He hoped that in future such fruitful

collaboration would be possible, not only in science, but also in politics and culture generally. In this way be believed that there would be a greater chance of harmonious relationships between the countries.

#### THE GROWTH AND SCOPE OF X-RAY CRYSTAL ANALYSIS

PROFESSOR J. D. BERNAL continued the proceedings by attempting the rather difficult task of predicting future trends in the subject. He rather ruefully admitted that most of the predictions in his previous attempt to do this, in a conference in 1947, remained as yet unfulfilled, but with post-war research again in full swing indications were now clearer.

He began by recalling his early days in The Royal Institution under W. H. Bragg; research students were expected to do a great deal for themselves, including making their own X-ray tubes from what might now be called "junk." He emphasized the great part that The Royal Institution had played in developing X-ray diffraction, and mentioned the names of people—such as Astbury, Yardley (now Lonsdale), Patterson and Robertson—whose names are now household words in the subject.

In predicting the future, Professor Bernal started by analysing the types of papers published in the first four years in *Acta Crystallographica*. Organic structures (69) appeared most frequently, but inorganic structures (57) were not far behind, and the number of papers on methods (36) was surprisingly large. This last figure was a healthy sign; it indicated a lively interest in extending the scope of present methods, so that more complicated problems would come within the range of possibility.

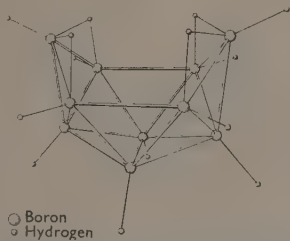
These more complicated problems, however, raised further experimental difficulties; the more complicated a crystal structure, the more extensive the data needed for its elucidation, and there was grave danger that the necessity for producing these data would limit progress. Fortunately there were signs that considerable improvements were occurring in the production and detection of X-rays; more powerful sources and more sensitive methods of measurement were being developed. Fine focus tubes, together with a general reduction in camera sizes, had speeded up exposures more than twentyfold, equivalent to a great reduction of capital cost. Photographic material was more sensitive but now had to compete with direct methods of recording such as the Geiger and scintillation counters. The principle of Sir William Bragg's ionization spectrometer was coming into its own again, and gave promise of apparatus which would be completely automatic and self-recording. Perhaps ultimately when coupled with a computer it would not even be necessary to record reflexions but to have the structure automatically computed.

Great advances might be expected in direct methods of structure determination. The Wilson statistics and Harker-Kasper inequalities (see Fig. 3) were only a first step—an extremely important first step—but we must now look for methods which made more use of structural characteristics than merely the absence of negative electron densities. The aim should be to introduce at the outset not only single atoms but pairs and even groups. It should be possible to use prominent features of molecules, such as phenyl rings; an atlas of Fourier transforms of such features was required.

There was also a surprisingly large number of papers in *Acta Crystallographica* on the study of structural imperfections from diffuse spots and streaks on X-ray photographs. It was important to realize that there was considerable difference between real and ideal crystals, and the study of



crystal structure was only a first step to a complete understanding of the crystalline state. We must also be prepared to study in more detail the "energetics" and "kinetics" of crystal formation, with the ultimate aim of finding the stable form of a compound by calculating the free energies of all possible structures.



Reproduced from *Acta Crystallographica*

Fig. 3. The first structure to be derived by means of the Harker-Kasper inequalities

Professor Bernal pointed out that there was no reason why in crystal analysis we should confine ourselves to X-ray diffraction. Information about electron densities could be supplemented by the derivation of potential gradients and nuclear positions, which are given by electron diffraction and neutron diffraction results respectively. Potentially, neutron diffraction is the most accurate method for deriving distances between atoms, since it gives the positions of the nuclei unclouded by the surrounding electrons; improvements in neutron optics should be looked for with great interest. We may even see new subjects such as meson optics!

The impact of X-ray diffraction upon chemistry had been of fundamental importance, and further results could be expected to be produced at an ever-increasing rate. Professor Bernal recalled with amusement the indignation occasioned by W. L. Bragg's first announcement that rock salt did not contain molecules of NaCl. Changes of this order of magnitude are not likely to recur, but many problems in stereochemistry still awaited solution. Stereochemistry was of particular importance, because it was likely that many chemical effects were greatly influenced by the mere geometry of the shape and fitting together of molecules.

Of particular importance was the study of proteins. The first attempt to photograph a crystalline protein was made in 1927, the first successful one in 1934, and the work has proceeded continuously since then. Some limited aspects of the structure were now known, but much more was required. Was the importance of protein molecules in living matter merely spatial? And if so, why was it necessary that there should be so many different proteins?

#### CHEMICAL PROBLEMS

Mrs. D. M. HODGKIN elaborated Professor Bernal's theme of the importance of X-ray diffraction to the chemist. She said that by the time she began to work in this field, twenty years ago, so much of fundamental importance to chemistry had already been established by X-ray analysis that she thought that there might be little left to do but verify and check what we already knew. That view had turned out to be quite wrong, and problems were arising at a far greater rate than they could be settled.

From the point of view of present chemical theory, recent highly accurate work on bond lengths and electron densities in organic compounds was of the utmost importance. The latest refinements of the structures of naphthalene and

anthracene, carried out at Leeds, bring the bond lengths, in all but one case, very close to those expected theoretically. Low temperature measurements would be necessary before we could be sure of the interpretation of the observed electron densities over chemical bonds, but already the accuracy was good enough to establish the positions of hydrogen atoms. A whole new class of chemical problem had therefore become soluble. In  $\alpha$ -pyridone, for example, the chemical structure of the molecule was proved by the direct observation of hydrogen atoms attached to nitrogen, not oxygen. And more striking still, in Cochran's projection of salicylic acid, the hydrogen atoms appear in the two different types of hydrogen bonded situation present, each singly linked to oxygen atoms in hydroxyl groups, with normal OH distances.

Crystal structure analysis was also enabling certain new rules to be introduced into stereochemistry. Thus, although the tartrate ion has a central bond about which the two parts could conceivably rotate, the tartrate ion has so far been found to have only one configuration. This configuration can be accounted in terms of the new rules, but that of oxalic acid cannot. Here there were new problems for the theoretical chemist to explore.

Perhaps the most exciting research was that connected with the stereochemistry of complex compounds. The most notable recent advances were among the terpenes and related compounds, the vitamin A precursor,  $\beta$ -ionylidene crotonic acid (Amsterdam), the first sesquiterpene, caryophyllane (Glasgow), the first triterpene (Birkbeck College, London) and the very odd molecule, lanosterol, a mixture between a terpene and a sterol (Australia).

It seems clear from these examples that present techniques allow fair possibilities of success with molecules containing about thirty atoms. One of the main tasks now was to extend this range, and Mrs. Hodgkin described briefly the attempts of her school at Oxford to determine the structure of vitamin B<sub>12</sub>. In the crystal examined, the unit cell contains 100 independent atoms—a far more difficult structure than any yet successfully solved. Fortunately, there were some features of the structure that could be established fairly easily; the molecule contained the relatively heavy atom cobalt and the sulphur atoms could be replaced by selenium; these atoms could thus be directly placed. Provisional projections from the signs given by these atoms had been calculated, but since the smallest cell dimension was 16 Å the results were not very clear.

Finally, Mrs. Hodgkin described a number of structures in which the atomic arrangements had turned out to be completely different from those expected chemically. For example, arsenobenzene had six arsenic atoms arranged in a six-membered ring, and N<sub>2</sub>O<sub>5</sub> contained NO<sub>2</sub><sup>+</sup> and NO<sub>3</sub><sup>-</sup> ions. Many of the boron compounds, such as that shown in Fig. 3, contained quite unexpected groupings of atoms, and a theoretical study of them might well lead to new chemical principles.

#### X-RAY ANALYSIS AND THE METALLIC STATE

PROFESSOR G. V. RAYNOR made a similar survey of the place of X-ray diffraction in the study of metals. By 1920, the main elements of structural metallurgy had been established; powder photographs showed that the metals were crystalline, and usually had simple structures; the effective atomic radii of most of the elements had been established; the nature of solid solutions and their difference from intermetallic compounds were reasonably well understood; and the nature of allotropic changes had been discovered. Some of the early work on allotropic changes, such as the observation by Westgren of the  $\gamma$ - $\delta$  change in iron at 1400° C, was

brilliant, and would be difficult to reproduce even with present-day apparatus.

Since 1920, however, much had been learnt of the finer details of alloy systems. The observations made by Bradley and Hume-Rothery had led to a realization of the importance of valency-electron concentrations, and the experimental observations had been beautifully confirmed by the Brillouin-zone theory as developed by Jones. Recent work has shown that the theory stands up well to the more rigorous tests imposed by the study of ternary alloys; for example, the structure  $\text{Mn}_3\text{SiAl}_2$  is pseudo-isomorphous with  $\text{Co}_2\text{Al}_3$ , although the proportion of aluminium atoms is different in the two, and this can be explained as an attempt to keep the number of electrons per unit cell the same in both structures.

In the earlier theory, the valency of each atom was assumed to be integral, ranging from zero to four; the zero value was allotted to certain transition metals which both contributed electrons from their outer shells, and absorbed electrons into their unfilled shells. A more recent theory, by Pauling, replaces these values by more complicated non-integral values, but attempts to confirm this theory by accurate measurements of electron density were not successful; the effects looked for were just at the limit of observation and further increase in accuracy might reap rich dividends.

One experimental method specifically associated with metals was the accurate measurement of lattice parameters, an accuracy approaching 0.001% being obtainable. It was these measurements which had helped to explain the nature of solid solutions, but more recently they had also given brilliant confirmation of the Brillouin-zone theory; Jones has deduced that when a high-valency metal formed alloys with a low-valency metal, there should be a small discontinuity in the slope of the curve relating lattice parameter and composition, as the added electrons overflowed into the second Brillouin zone. This had been confirmed for certain magnesium alloys. The experimental data obtained establish the number of electrons per atom at which the electronic overflow occurs, a result unattainable by the application of theory alone.

Supporting Professor Bernal, Professor Raynor mentioned the increasing importance of the study of departures from perfection in metal structures. Much information, which promised to throw light on the actual relative atomic sizes in solid solutions and the magnitudes of local lattice distortions, was being derived from studying the background of powder photographs and single-crystal photographs. Warren had made important contributions to this subject, particularly in relation to the alloys  $\text{AuCu}_3$  and  $\text{Ni}_3\text{Au}_2$ , but much more work was needed, particularly with new techniques such as neutron diffraction.

#### THE APPLICATION OF X-RAY ANALYSIS TO PROTEIN STRUCTURE

SIR LAWRENCE BRAGG wound up the celebrations by describing in detail a specific project which may well be likened to the voyage of Jason to obtain the Golden Fleece: the prize is immensely rich, but the difficulties are tremendous, and many novel and daring devices have been resorted to in an attempt to achieve success. This project, in which Perutz has played the major part, is the attempt to deduce the structure of a protein, the haemoglobin molecule.

At first sight the difficulty of the problem seems overwhelming, since the positions of 10000 atoms have to be found; but partly to compensate for this complexity, the crystals themselves have certain properties which allow some novel principles to be applied. These properties depend upon the water content of the crystals, which may amount to 50%;

firstly, this water can be caused to take up various concentrations of salt, and secondly, it can be varied in amount without any fundamental change in structure. Both these properties had been turned to account.

The variation of salt concentration enabled the general outline of the molecule to be determined. The mean electron density in the molecule is  $0.43 \text{ e}/\text{\AA}^3$ , and the electron density of water is  $0.33 \text{ e}/\text{\AA}^3$ ; by Babinet's principle, the difference between these values is responsible for the inner or low-order detail of the diffraction pattern. With a certain concentration of salt, the electron densities match, and then the inner detail disappears; the effect is similar to immersing a crystal in a solution of the same refractive index, when the external form becomes invisible. By comparing X-ray photographs of crystals with various salt concentrations, it is possible to say how much of the pattern is due to the outer form of the molecule, and how much to the detailed atomic arrangement in it, and it is then possible to determine the overall dimensions of the molecule; these turn out to be about  $65 \times 55 \times 55 \text{ \AA}$ .

The variation in amount of water in the crystals causes the unit-cell dimensions to vary, and it appears that the change is such that the molecule remains in fixed relation to the *ab* plane of the crystal. The different diffraction patterns can be interpreted as depending upon a fixed Fourier transform observed at particular points (the reciprocal-lattice points) which can be made to traverse the field. Since the essential difficulty in the determination of crystal structures is that the transform can be observed only at *fixed* points, it would appear that this process of "shrinking" the crystal has great potentialities. This is indeed so. But unfortunately the crystals change in such a way that the reciprocal lattices trace out only parallel lines in the transform, so that, although the sign relationships are clearly defined along these lines, the relationships between the separate lines are obscure. Nevertheless, the number of possibilities of sign combinations is reduced from about  $2^{1000}$  to  $2^7$ —a considerable improvement. It can thus be seen that the chance of success is by no means negligible, although the amount of work involved remains very great.

If one point emerged more clearly than any other from the celebrations, it was the interplay of one subject upon another in apparently unrelated fields. The impact of the idea of a space lattice upon von Laue and the suggestions given to W. L. Bragg by Pope and Barlow's hypothetical structures are the two most notable examples, but throughout the whole forty years of its existence the subject has been marked by the interchange of ideas between people from different countries and in different branches of science. Works such as the *International Tables for X-ray Crystallography* are a testimony to the close co-operation of the various workers in the field, and, with the formation of the International Union of Crystallography in 1948, there is every prospect of this co-operation continuing. The subject of X-ray diffraction may be expected to flourish even more vigorously in the future, and the reports of progress at the fiftieth anniversary will be eagerly awaited.

#### EXHIBITION AND DINNER

A small exhibition of historical X-ray apparatus was a feature of the celebrations. It included one of W. H. Bragg's original notebooks, some of the early correspondence on the subject between W. L. Bragg and his father and some of their original apparatus.

The anniversary dinner was attended by 140 people and was held on the evening of 24 October.

H. LIPSON



# Laboratory drying of herbage by radio-frequency dielectric heating

By J. N. MERRIDEW, M.Sc., Department of Agricultural Engineering, University of Durham, and  
W. F. RAYMOND, B.A., A.R.I.C., Grassland Research Station, Stratford-on-Avon

[Paper first received 8 August and in final form 17 October, 1952]

Losses of dry matter from herbage during hot-air drying have been reported,<sup>(1)</sup> and seem to be due to continued respiration of the herbage during the early stages of drying. These losses are reduced by more rapid drying. Preliminary tests showed that herbage can be rapidly dried by radio-frequency heating on the laboratory scale. The paper describes modifications made to a commercial radio-frequency oven to make it suitable for drying material of high moisture content. The oven will dry 300 g of herbage from 80% to 10–25% moisture content in 15 min. Comparative tests showed the radio-frequency oven to give an average dry matter yield  $\frac{1}{2}\%$  higher than that obtained by drying herbage in an efficient hot-air oven.

Radio-frequency (r.f.) heating of metals by induction heating, and of non-metals by dielectric heating, is used in industry where normal heat transfer methods are unsuitable. A description of this is given in reference books<sup>(2,3)</sup> and Maddock<sup>(4)</sup> has given the theory of dielectrics and has summarized some practical applications. This type of heating has been considered for the commercial drying of grass.

On the laboratory scale the variation in dielectric permittivity of a given material with moisture content has been used as the basis of a moisture meter<sup>(5)</sup> and is used in the N.P.L. meter.<sup>(6)</sup> No account has been found of the use of dielectric heat for laboratory drying of samples of high moisture content, though low-powered ovens of this type are supplied for the purpose by specialist firms.

The removal of moisture from fresh herbage involves a number of considerations:

- (i) Herbage is a living material, and respiration and enzymic action will continue in such material until prevented by high temperature or dehydration.
- (ii) The percentage of moisture in herbage will vary with season and stage of growth, and may have been reduced by wilting. Thus the material to be dried may vary from 40–85% initial moisture content.
- (iii) Except for surface moisture, as dew or rain, the moisture in herbage is within the cellular structure. There it may be relatively labile, as in cell-sap, or in varying degrees of physico-chemical combination.
- (iv) The moisture content and cellular structure of leaves and stems are different, and they are likely to dry at different rates.
- (v) While the initial removal of moisture from herbage occurs readily, the removal of moisture from the centre of a mass of drying herbage and from within cellular structures is more difficult. The rate of drying then depends not only on thermal conductivity and vapour pressure gradients, but also on the rate of permeation of water vapour from the centre of plant material through outer layers which have already dried.

During 1949–50 preliminary evidence was obtained<sup>(1)</sup> which suggested that during drying of fresh herbage by hot air, appreciable losses of dry matter might occur. The longer the drying time, and the lower the temperature of drying, the larger were found to be these losses. A report on their magnitude and a study of the efficiency of different drying methods will be published later. These losses are almost certainly due to continued respiration and enzymic action in

the herbage during the early stages of drying, because of slow drying of certain parts of the material due to the factors considered above.

In January 1947, the Grassland Research Station co-operated in preliminary tests on the drying of fresh herbage, using a radio-frequency generator type FA.24A, by British Thomson-Houston Co. Ltd. Although some difficulties were found, it was evident that rapid drying of herbage by r.f. heat was possible. At that date the use of expensive electronic equipment, instead of the hot-air ovens employed in the laboratory, did not seem justified. However, the evidence obtained since then on losses possible during hot-air drying encouraged further investigation into the use of r.f. heating. As considered under (v) above, where herbage is dried by hot air, water is evaporated from surface layers, and the rate of drying is dependent on the rate at which internal water will reach these surface layers. With r.f. heating the water may be heated to steam inside the cell. Because of the resulting pressure difference across the cell walls and the readier diffusion of water vapour than water, r.f. heating should allow more rapid drying than oven drying, if the use of high temperatures (and danger of chemical decomposition) is to be avoided in the latter. Such rapid drying should minimize losses of dry matter due to respiration.

This paper describes the modification of a commercial r.f. heater to make it suitable for the drying of fresh herbage.

## APPARATUS

The equipment modified was a Radyne H7/B radio-frequency oven by Radio Heaters Ltd., with an output of 1 kW at 20 Mc/s, designed for use in the plastics industry. R.f. power applied to a sample of fresh herbage contained in a polystyrene box placed between the plates gave rapid evolution of moisture. Much of this condensed on the top electrode in the form of water droplets, which in falling to the lower electrode caused overloading of the power circuit. To overcome this a current of warm air must blow through the herbage so as to remove the moisture and thus prevent condensation.

To allow this the electrode compartment has been rebuilt (Fig. 1). About 40% of the input power to the equipment is lost in heat from the oscillator, which is cooled by air drawn through the valve compartment. This air is further heated to 60° C by a small spiral element (350 W) and blown up through the perforated lower "live" electrode. It then passes through holes in the base of the polystyrene box containing the herbage sample, and out through the perforated upper



"earthed" electrode. Into the box ( $8\frac{1}{2} \times 6\frac{1}{2} \times 2\frac{1}{2}$  in) are packed 300–400 g of herbage as uniformly as possible. This is placed on the perforated lower electrode, and the top electrode lowered into it, slightly compressing the herbage. The heating circuit is switched on with the input control at zero, and the latter increased until heat is being generated inside the sample at a rate of 1 kW.

Quantities of steam immediately appear through the top electrode as water vapour is produced from the herbage. As the grass dries it absorbs less energy at any given setting of the input control. During the first 10 min of drying the setting of this control is increased to maintain the heat input at 1 kW. During the remainder of the drying period the setting is not increased, so as to avoid local overheating in a sample that has lost most of its moisture. Thus self-regulating heating takes place. After 15 min the power input drops to about 0.2 kW, and overheating of the sample seldom occurs: its moisture content varies from 10–25%.

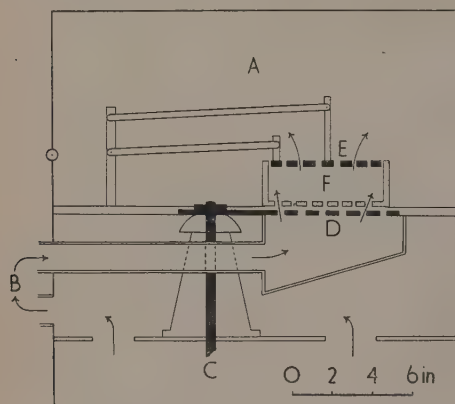


Fig. 1. Modified drying compartment of radio-frequency oven

A, drying compartment; B, blower and auxiliary heater; C, oscillator compartment; D, live electrode; E, earthed electrode; F, herbage inside drying box.

While much of the residual moisture from these samples can be removed by leaving in the low-power field, drying of material of low moisture content is relatively inefficient. Samples on which "dry matter" is required must subsequently be dried to constant weight in an oven at  $100^{\circ}\text{C}$ . This is necessary because of the arbitrary nature of "dry matter," generally defined as the constant weight of a material at  $100^{\circ}\text{C}$ . At 10% moisture content, however, respiration and enzymic action should have ceased and there should be no losses from these causes during subsequent hot-air drying of herbage. Where the sample is required only for chemical analysis, and heating at  $100^{\circ}\text{C}$  is likely to produce chemical changes (e.g. lignin<sup>(7)</sup>), the material of 10% moisture content can be ground for analysis without further drying. Changes that may occur even during the relatively low-temperature drying by r.f. heating are being studied.

Fig. 2 shows rates of loss of moisture from 300 g samples of lucerne leaf and stem in the r.f. oven, and at  $100^{\circ}\text{C}$  in a hot-air oven, Unitherm, designed by the Grassland Research Station and the Birmingham and Blackburn Engineering Co. Both leaf and stem dried much more rapidly in the r.f. oven than in the hot-air oven: in the former the leaf dried more

rapidly than the stem, while in the hot-air oven the stem dried more rapidly, due to some packing down of the succulent leaf in the drying tray.

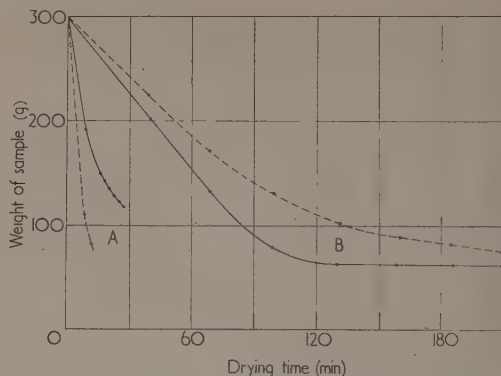


Fig. 2. Drying rates of lucerne leaf and stem using r.f. oven (A) and hot-air oven (B)

----- lucerne leaf; ——— lucerne stem

Comparative measurements of the dry matter content of twenty-five samples of herbage were made in 1951, using the r.f. oven and the Unitherm oven. The r.f. oven gave an average dry matter yield 0.5% greater than the Unitherm oven. On thirteen occasions an air-oven drying less rapidly than the Unitherm oven was used and average dry matter yields were:

Radio-frequency oven	Unitherm oven $100^{\circ}\text{C}$	Less efficient oven $90^{\circ}\text{C}$
23.94	23.87	23.62

(All samples were finally dried at  $100^{\circ}\text{C}$  to bring to standard dry matter content.)

These results confirm that the more slowly herbage is dried the greater is the loss of dry matter it suffers. While the loss of dry matter in the Unitherm oven may be minimized by careful use, it does involve heating the herbage at  $100^{\circ}\text{C}$ , which is not necessary with the r.f. oven and may be undesirable.<sup>(7)</sup> Samples dried by r.f. heat retain a remarkable brilliance of colour, and the herbage does not shrivel as much as during more prolonged oven-drying.

#### DISCUSSION

The commercial r.f. heater, modified as described here, will give very rapid low-temperature drying of herbage samples. Its throughput, however, is small and it is not at present suggested that it should replace the more efficient of the hot-air ovens used for laboratory drying. It is suggested, however, that it may be used as a "base-line," for studying possible losses of dry matter associated with other methods of drying. It may also be of value in preparing certain samples for chemical and biochemical analysis.

There is no doubt that it would be very advantageous to use a frequency higher than 20 Mc/s to obtain a more uniform heating, and reduce the danger of local overheating.<sup>(2)</sup> It is hoped later to use an r.f. power oscillator with a frequency of 70–80 Mc/s. If a larger drying capacity is required it may be practicable to design an r.f. oven with a continuous belt

assembly, similar to that used in industrial induction heating installations.

While dielectric heating can be very efficient, the capital cost of large equipments is so high that it is unlikely to be economic for commercial grass-drying. It has uses for the drying of certain biological materials which are not easily dried by hot air, or which are decomposed by high temperatures. The present paper describes only the use of dielectric heating as a laboratory method of value for the drying of herbage, and suggests that it may have special value in certain cases.

#### ACKNOWLEDGEMENTS

Our thanks are due to Mr. F. Baxendale and Mr. O. F. Gullick, of the British Thomson-Houston Co. Ltd., Rugby, for their co-operation in the earlier tests of radio-frequency drying, and to Mr. E. C. Stanley, of Radio Heaters Ltd., Wokingham, Berks, for suggestions on the use of the type H7/B oven supplied by them. To Dr. William Davies,

Director of the Grassland Research Station, and Professor Ewen McEwen, of Durham University, our appreciation is due for their encouragement given to this study of herbage drying.

#### REFERENCES

- (1) *Experiments in Progress*, No. 4, p. 57 (Grassland Research Station, 1951).
- (2) HARTSHORN, L. *Radio Frequency Heating* (London: Allen and Unwin Ltd., 1949).
- (3) BROWN, G., HOYLER, C., and BIERWIRTH, R. *Theory and Application of Radio-Frequency Heating* (New York: Van Nostrand Co. Inc., 1947).
- (4) MADDOCK, A. J. *J. Sci. Instrum.*, **23**, p. 165 (1946).
- (5) BABB, A. T. S. *Analyst*, **76**, p. 12 (1951).
- (6) HARTSHORN, L., and WILSON, W. *J. Instn Elect. Engrs*, **92**, p. 403 (1945).
- (7) MACDOUGALL, D., and DELONG, W. A. *Canad. J. Res. B*, **20**, p. 40 (1942).

## Propagation in waveguides filled longitudinally with two or more dielectrics

By LL. G. CHAMBERS, M.Sc., A.Inst.P., Military College of Science, Shrivenham

[Paper first received 1 September, and in final form 23 September, 1952]

A survey is made of all the work on inhomogeneously filled waveguides which has so far appeared. Particular attention is given to two cases of practical importance, namely the rectangular and circular waveguides.

It has been customary until recently to use only waveguides filled with air. The theory of these is well known. However, for certain purposes it has been found advisable to attempt to reduce the phase velocity of an electromagnetic wave in the guide. One way in which this may be done is partly to fill the waveguide with some suitable dielectric, the distribution of dielectric being constant over all cross-sections of the waveguide. The theoretical treatments of this problem are not well known and present, as might be expected, certain difficulties which do not arise in the case of a homogeneously filled guide. [For example, it is only when the field does not vary along the interface between the dielectrics, that it is possible for the guide to transmit a pure transverse electric (TE) mode or a pure transverse magnetic (TM) mode.<sup>(1)</sup> Unless this condition is satisfied the mode transmitted will be a mixed one and contain longitudinal components of both electric and magnetic fields.]

Because of the difficulties involved, only two basic problems appear to have been solved exactly, namely, that of a rectangular waveguide with a rectangular dielectric slab which has two of its walls in contact with two opposite walls of the tube and the other two parallel to the other two walls of the waveguide,<sup>(1, 2, 3, 4, 5, 6, 8, 14)</sup> and the problem of a cylindrical waveguide containing a coaxial cylinder of dielectric.<sup>(1, 7, 9, 12, 13, 14, 15, 16)</sup> Although the work done has been mainly concerned with the case of materials of differing dielectric constants, it is equally possible to consider materials with different permeabilities also. (In actual physical problems, however, this requirement is not likely to arise.)

The general problem of the determination of the phase velocity in an arbitrarily shaped guide with an arbitrary distribution of dielectric is almost certainly insoluble. It is

possible, however, to obtain, for pure TE and TM modes, upper and lower bounds for the propagation constants. This approximation can be made as good as we desire.<sup>(10, 11)</sup>

It may be remarked that for a guide filled in a specific manner there are only a finite number of propagating (as distinct from evanescent) modes, as in the case of a homogeneously filled guide.

#### NOTATION

Throughout this paper the rationalized M.K.S. units will be used and a time variation of  $\exp(-i\omega t)$  assumed which will in general be dropped. The axis of the guide will be assumed to be in the  $z$  direction, the walls of the guide perfectly conducting, and the contents of the waveguide perfectly lossless.

Assume the behaviour of the wave down the guide to be given in the  $z$  direction by  $\exp(ikz)$ . This factor will also in general be dropped.  $h$  is thus the propagation constant and is related to the guide wavelength  $\lambda_g$  by the relation  $h = 2\pi/\lambda_g$ . It will be found that in general this quantity appears as  $h^2$  and if  $h^2$  is positive the wave propagates, and if  $h^2$  is negative the wave is evanescent.

Assume that the electromagnetic constants of a material are  $(\epsilon, \mu)$  and  $k^2 = \omega^2\mu\epsilon$ .  $k$  is thus the propagation constant of the material and is related to the wavelength  $\lambda$  in that material by  $k = 2\pi/\lambda$ .

It will also be convenient to write

$$k^2 - h^2 = \kappa^2$$

Write the characteristic impedance of the medium as  $Z = \sqrt{(\mu/\epsilon)}$  and its characteristic admittance as  $Y = Z^{-1}$ .

FUNDAMENTAL CONCEPTS OF PROPAGATION IN  
A WAVEGUIDE

In order to appreciate the properties of waveguides which are inhomogeneously filled, it will be helpful to consider certain of the properties of propagation in an empty guide. Therefore consider a rectangular waveguide whose cross-section is defined (Fig. 1) by

$$-a < x < a, -b < y < b$$

We consider the longitudinal component of electric field  $E_z = \psi$ . Then for the fundamental mode, the field distribution is given by

$$\psi = \exp [i(hz - \omega t)] \cos (\pi x/2a)$$

where  $h^2 = k^2 - \pi^2/(2a)^2$ ,  $k$  being the propagation constant of the medium.

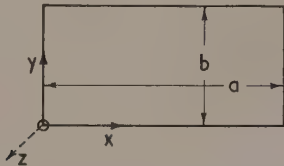


Fig. 1. Cross-section of rectangular waveguide

It is possible to consider this field as constructed in various ways which will only be considered briefly. The most usual way is to attempt to find the solution of the boundary value problem

$$\frac{\partial^2 \psi}{\partial x^2} + \frac{\partial^2 \psi}{\partial z^2} + k^2 \psi = 0$$

where  $\psi = 0$  on  $x = \pm a$ .

(For simplicity, it has been assumed that there is no variation in the  $y$  direction.) This effectively boils down to finding suitable solutions of Maxwell's equations.

An alternative way of looking at the problem is to consider the wave propagating along the  $z$  direction as composed of two plane waves

$$\begin{aligned} \psi &= \exp [ik(x \sin \alpha + z \cos \alpha)], \\ \psi &= \exp [ik(-x \sin \alpha + z \cos \alpha)] \end{aligned}$$

and finding the condition that a field composed of the combination of these is to vanish on  $x = \pm a$ .

This gives  $ka \sin \alpha = \pi/2$  and hence  $h$  from the relation  $h = k \cos \alpha$ . The wave propagating down the waveguide may thus be regarded as composed of two plane waves propagating in directions making angles  $\pm \alpha$  with the direction of the waveguide. If  $a$  is small,  $\sin \alpha > 1$  and  $\cos \alpha$  is imaginary. This case corresponds to an evanescent wave, the waveguide being too small to maintain propagation in the mode considered.

A third way of looking at the problem is to regard the region  $-b < y < b$  as a transmission line, calculate the wave impedance and propagation vector in the  $y$  direction and write down the condition for short circuiting at  $x = \pm a$ .

These three methods of looking at the problem are equivalent, although apparently different. In exactly the same way the inhomogeneously filled waveguide may be considered to be a boundary value problem, the result of the superposition of waves or a problem in transmission line theory. In fact, whichever method is used for finding the propagation constant, the same result can be obtained by using one of the other methods. It may be remarked, how-

ever, that, although this is so, the transmission line method merely gives us the propagation constant and nothing else. If we want to know the behaviour of the fields, we must proceed by attempting to subject suitable solutions of Maxwell's equations to the appropriate boundary conditions at the walls and interfaces.

## PROPAGATION IN A RECTANGULAR WAVEGUIDE

As has been indicated above, the calculation of the propagation constant may be effected in several different ways, all of which are equivalent.

Let us consider the guide indicated in Fig. 1. We may regard any mode which may be set up in the partly filled guide as a distortion of a mode which is set up in the empty guide. It is clear that the field distribution will be the same whether the guide is wholly empty or wholly full.

The method of the equivalent transmission line has been used with effect to calculate the propagation constant (or what is closely related—the guide wavelength) for the mode which is a distortion of the  $H_{10}$  mode, i.e. that mode for which  $H_z = \exp (ikz) \cos (\pi x/a)$  in the empty guide with corresponding formulae for the other field components. For the empty (or completely filled) guide  $E_x = E_z = 0$ ,  $H_y = 0$ .

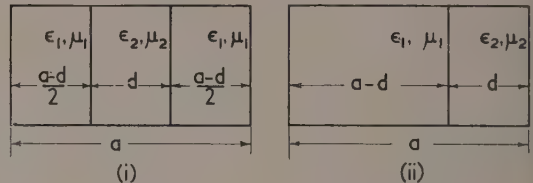


Fig. 2. Rectangular waveguides containing dielectric

Consider rectangular waveguides containing dielectric slabs as indicated in Fig. 2, the sides of the slabs being in the  $y$  direction. The corresponding transmission line circuits are given in Fig. 3. The propagation wavelength  $\lambda_g$  of the distortion of the  $H_{10}$  mode is given for case (i) by the following reasoning. The electric field is a maximum at the centre of

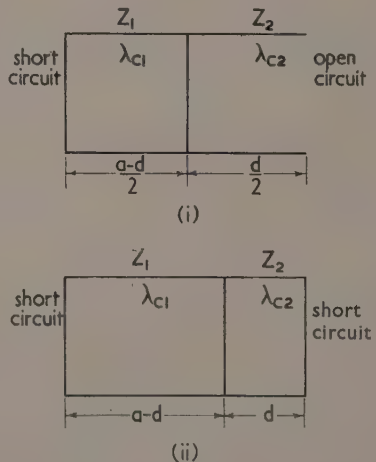


Fig. 3. Transmission line circuits corresponding to waveguides of Fig. 2



be guide. The admittance looking from the centre of the guide in the  $x$  direction must therefore be zero. The admittance at the centre is therefore

$$Y_2 \left[ \frac{Y' + iY_2 \tan(\kappa_2 d)/2}{Y_2 + iY' \tan(\kappa_2 d)/2} \right]$$

where  $Y'$  is the admittance looking to the left at the left boundary of the dielectric.

$$\text{Now } Y' = -iY_1 \cot \kappa_1(a-d)/2$$

and because the admittance at the centre of the guide is zero

$$Y' = iY_2 \tan(\kappa_2 d)/2$$

which gives the equation

$$Y_1 \cot \kappa_1(d-a)/2 + Y_2 \tan(\kappa_2 d)/2 = 0$$

Now  $\kappa_1^2 = k_1^2 - h^2$ ,  $\kappa_2^2 = k_2^2 - h^2$  and  $Y_1/Y_2 = \kappa_1/\kappa_2$ .

In case (ii), the equivalent transmission line problem is that the impedance looking to the left vanishes on the right-hand boundary and the equation for  $h_2$  turns out to be

$$Z_2 \tan \kappa_2 d + Z_1 \tan \kappa_1(a-d) = 0$$

where  $Z_1 \kappa_1 = Z_2 \kappa_2$ , or

$$\kappa_1 \tan \kappa_2 d + \kappa_2 \tan \kappa_1(a-d) = 0$$

Detailed calculations have been carried out for the case where  $\epsilon_2/\epsilon_1 = 2.45$ , and as the results are readily available, it has not been thought necessary to reproduce them.<sup>(5, 8, 14)</sup>

It is only in this particular case where the field does not vary along the interface, however, that it is possible to obtain a pure TE wave. In general this is not possible, neither is it possible to obtain a pure TM wave. It is, however, possible to split the field up into one which is characterized by the absence of  $E_x$  and one which is characterized by the absence of  $H_x$ . Such waves are called longitudinal section electric and magnetic waves and for a homogeneously filled tube reduce to those linear combinations of TE and TM waves which have a vanishing  $E_x$  and  $H_x$  respectively.

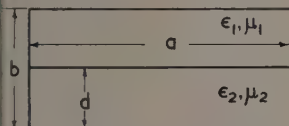


Fig. 4. Rectangular waveguide containing dielectric

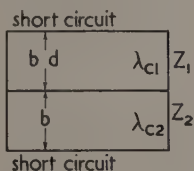


Fig. 5. Transmission line circuit corresponding to waveguide of Fig. 4

Now consider the case where the sides of the dielectric are perpendicular to the (undistorted) electric field. The set-up is given in Fig. 4 and the equivalent transmission line problem in Fig. 5.

In exactly the same way as previously we deduce the following equation for  $h^2$ :

$$Z_1 \tan \gamma_1(b-d) + Z_2 \tan \gamma_2 d = 0$$

where

$$\frac{Z_2}{Z_1} = \frac{\epsilon_1 \gamma_1}{\epsilon_2 \gamma_2}$$

where

$$\gamma_1^2 = k_1^2 - h^2 - (\pi/a)^2$$

and similarly for  $\gamma_2$ .

VOL. 4, FEBRUARY 1953

It will be seen that  $h^2$  now depends on three parameters, namely  $d/b$ ,  $b/a$ ,  $\epsilon_2/\epsilon_1$ , and the problem is rather more complicated. A few numerical results have been obtained for a case of interest, namely  $b/a = 0.45$ .<sup>(8, 14)</sup>

So far only the method of finding the propagation constant has been studied. Some very interesting results arise when the properties of the system as a whole are considered and the frequency varied.<sup>(1, 4)</sup>

Consider a wave of  $TE_{q0}$  character propagating down a waveguide wherein the dielectric constant is a function of  $x$  only. It is not difficult to see that  $E_y$  satisfies

$$\frac{d^2 \psi}{dx^2} + (\epsilon \mu \omega^2 - h^2) \psi = 0$$

where  $\psi = 0$  or  $x = 0$ ,  $x = a$ .

Let  $\epsilon_1$ ,  $\epsilon_2$  be the minimum and maximum values of  $\epsilon$  in  $0 < x < a$ . Then it may be shown that the equation for  $\psi$  possesses an infinite decreasing set of eigen values which obey the relation

$$\epsilon_1 \mu \omega^2 - (r^2 \pi^2/a^2) < h_r^2 < \epsilon_2 \mu \omega^2 - (r^2 \pi^2/a^2)$$

Now considering  $h_r^2$ , it is not difficult to see that if  $\omega^2 \epsilon_2 \mu < (\pi^2/a^2)$ ,  $h_r^2 < 0$ , and if

$$\omega^2 \epsilon_1 \mu > (\pi^2/a^2) h_1^2 > 0$$

It therefore follows that there exists in the interval

$$\frac{\pi}{a\sqrt{(\epsilon_2 \mu)}} < \omega < \frac{\pi}{a\sqrt{(\epsilon_1 \mu)}}$$

a value  $\omega_1$  of  $\omega$  for which  $h_1^2 = 0$ . Thus for  $\omega < \omega_1$ ,  $h_r^2$  and all the other eigen values are negative and it is not possible to sustain propagation.

The condition for  $n$  propagating waves are given by

$$\omega^2 > (n^2 \pi^2 / \epsilon_1 \mu a^2) \text{ sufficient}$$

$$\omega^2 > (n^2 \pi^2 / \epsilon_2 \mu a^2) \text{ necessary.}$$

It may also be shown that

$$2\omega \int_0^a \epsilon \mu \psi_r^2 dx = \frac{\partial h_r^2}{\partial \omega} \int_0^a \psi_r^2 dx$$

where  $\psi_r$  is the  $r$ th eigen function.

Indicating by  $\epsilon^{(r)}$  a suitable value of  $\epsilon$ , such that  $\epsilon_1 < \epsilon^{(r)} < \epsilon_2$ , and applying the mean value theorem

$$\begin{aligned} \epsilon^{(r)} \mu &= \frac{h_r}{\omega} \frac{\partial h_r}{\partial \omega} \\ &= \frac{1}{V_r} \frac{\partial h_r}{\partial \omega} = \frac{1}{V_r V_r'} \end{aligned}$$

where  $V_r$  is the phase velocity of waves down the guide and  $V_r'$  is the group velocity. Making use of the relation  $\epsilon_1 < \epsilon^{(r)} < \epsilon_2$  it may be shown that

$$\sqrt{\left(\frac{\epsilon_2}{\epsilon_1}\right)} \frac{1}{\sqrt{(\epsilon_1 \mu)}} > V_r' > \sqrt{\left(\frac{\epsilon_1}{\epsilon_2}\right)} \frac{1}{\sqrt{(\epsilon_2 \mu)}}$$

provided that

$$V_r > \frac{1}{\sqrt{(\epsilon_1 \mu)}}$$

In the arrangement shown in Fig. 2(i) there are certain differences which arise according as  $\epsilon_1 \mu_1$  is greater than, or less than,  $\epsilon_2 \mu_2$ . In both cases there is a frequency  $\omega$  below which the waveguide does not sustain a propagating field.

(i)  $\epsilon_2 \mu_2 > \epsilon_1 \mu_1$ . In this case there exists a frequency

$\omega_c > \omega_1$  such that  $h = k_1 = \omega_c \sqrt{(\mu_1 \epsilon_1)}$ . At this frequency the wave is, in the medium (i), of pure TEM character, only  $H_x$  and  $E_y$  existing. Now as  $\omega$  increases, the field lies more and more in the medium (ii). For  $\omega_1 < \omega < \omega_c$  the field distribution does not differ substantially from propagation in a homogeneously filled waveguide. As  $\omega \rightarrow \infty$  the propagation becomes similar to that in a slab of medium (ii) immersed in medium (i).

(ii) For  $\epsilon_2 \mu_2 < \epsilon_1 \mu_1$  also there exists a frequency  $\omega_1$  below which there is no propagation. It is also possible to find a frequency  $\omega_c$  such that the phase velocity down the tube is equal to the velocity in the less dense medium [in this case, medium (ii)]. However, it may be shown that this implies a field which is identically zero. For frequencies above this the field again tends to lie in the more dense medium [medium (i)], and as  $\omega \rightarrow \infty$  the field will behave very much in one of the slabs of medium (i) as though the other was very far removed.

### PROPAGATION IN A COAXIAL STRUCTURE

The coaxial structure which is to be considered is the one in Fig. 6. The radial co-ordinate is  $\rho$  and the angular co-ordinate is  $\phi$ . The waveguide is the region  $0 \leq \rho < a$  and material (i) occupies  $0 \leq \rho < b$ , and material (ii) occupies  $b < \rho < a$ . For the present do not assume any relationship between the electrical constants of material (i) and material (ii).

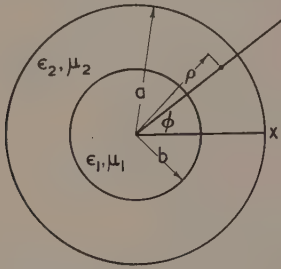


Fig. 6. Circular waveguide containing dielectric

It may be shown (the process is almost identical with that for rectangular cross-section waveguides) that it is impossible for a pure transverse electric, or pure transverse magnetic wave to exist, either evanescent or transmitted, unless there is axial symmetry. That is, the only waves of this character which can propagate are those which reduce to  $TM_{0p}$ ,  $TE_{0q}$  waves when the waveguide is filled homogeneously.<sup>(1)</sup> The propagation constant for a coaxial structure may be found in exactly the same way as it is found for rectangular waveguides.<sup>(7, 9, 12, 13, 14, 15, 16)</sup> However, for a guide of this shape, the co-ordinates which are most suitable are cylindrical polars, and the formulae which result are extremely complicated, as they involve Bessel functions. For this reason it is not proposed to reproduce them here. Calculations have been made for symmetric TM and TE modes and the results of these calculations are reproduced in Figs. 7 and 8 and the tables which have been reproduced from the original papers.<sup>(7, 9, 13)</sup>

In linear accelerators it has been found convenient to use the  $TM_{01}$  mode. In order that only one mode propagates it is necessary to know the cut-off frequency of the  $TM_{02}$  mode also. In Table 1<sup>(9)</sup> the cut-off frequencies for the  $TM_{01}$  and the  $TM_{02}$  modes are given through the values of  $k_z^2 = \omega^2 \mu \epsilon_2$  for a number of values of  $\kappa = \epsilon_1/\epsilon_2$  and  $\eta = a/b$ .

Table 1. Cut-off frequencies for  $TM_{01}$  and  $TM_{02}$  modes

$\eta = a/b$	1.5	2.0	3.0
$\kappa = \epsilon_1/\epsilon_2$	$k_2^{(1)2} b^2$	$k_2^{(2)2} b^2$	$k_2^{(1)2} b^2$
$\frac{1}{2}$	11.59	90.65	3.19
$\frac{1}{3}$	10.20	67.30	3.07
$\frac{1}{4}$	8.90	44.00	2.86
$\frac{1}{5}$	7.00	28.60	2.57
$\frac{1}{6}$	4.63	19.60	2.11
1	2.57	13.52	1.44
2	1.400	8.17	0.960
4	0.720	4.47	0.550
8	0.365	2.33	0.283
16	0.196	1.23	0.149
32	0.096	0.63	0.084
100	—	—	—

In Table 2<sup>(13)</sup> the relation is given between the value of the dielectric constant of the outer medium and the radius of the bounding conductor which is necessary to reduce the phase velocity to one-fifth of that in the inner medium when the radius of the boundary between the media is one-twentieth of the wavelength in the inner medium, i.e.  $(bk_1)/2\pi = 0.05$ .

Table 2

$(ak_1)/2\pi$	$(\epsilon_2/\epsilon_1)$
0.05064	154 000
0.05530	2 499
0.05943	774.4
0.06164	524.3
0.07187	174.4
0.08958	74.44
0.1	57.25
0.15	34.27
0.4897	25.63

Fig. 7 gives the value of  $(h^2/k_z^2)$  for the  $TM_{01}$  mode plotted against  $(k_z b)$  with  $\kappa$  and  $\eta$  as parameters. The small circles indicate the cut-off for the  $TM_{02}$  mode.

Fig. 8(a)<sup>(7)</sup> gives the cut-off frequency for the  $TM_{01}$  mode for varying values of  $(b/a)$  and  $\kappa$ . It is defined in terms of the wavelength to which it corresponds in an unbounded space composed of medium (i). Fig. 8(b) gives the cut-off frequency for the  $TM_{0p}$  type waves for varying values of  $(b/a)$  with  $\epsilon_2 = 4\epsilon_1$ . These also are determined in terms of their wavelength in medium (i).

Figs. 8(c) and 8(d) give the corresponding results for the  $TE_{01}$  type wave and  $TE_{0q}$  type waves respectively.

$j_{0p}$  and  $j'_{0q}$  are defined by

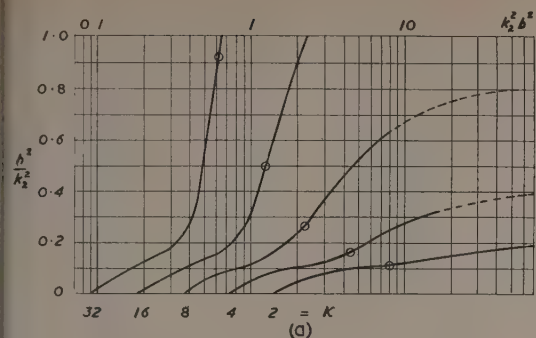
$$J_0(j_{0p}) = 0 \text{ and } J'_0(j'_{0q}) = 0$$

where  $J_0$  is the Bessel function of zero order.

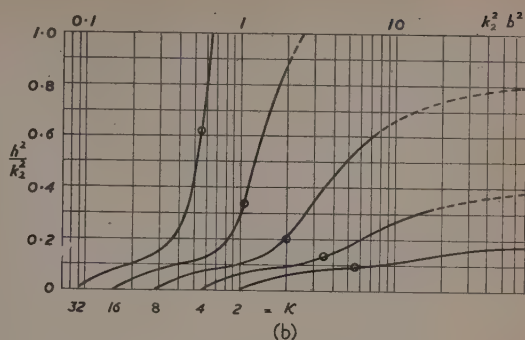
It is of interest to discuss the field configuration in such guides as the frequency varies. In the first place whatever the distribution of dielectric,  $h^2$  is a continuously increasing function of  $\omega^2$  and there exists a frequency below which waves do not propagate, but are evanescent instead. Also, as  $\omega$  becomes very large, the field tends to lie more and more in the material with the greatest value of the product  $\epsilon \mu$ . The other properties depend largely upon whether  $\epsilon_1 \mu_1 \geq \epsilon_2 \mu_2$  and it is desirable therefore for these two cases to be considered separately.

Consider first,  $\epsilon_1 \mu_1 > \epsilon_2 \mu_2$ . In this case  $0 < k_2^2 < k_1^2$ , and so after the wave becomes propagating, it would appear that as  $\omega$  increases both TM and TE waves would propagate with the velocity of light  $1/\sqrt{(\mu_2 \epsilon_2)}$  in medium (ii), for some value  $\omega_2$  of  $\omega$ . However, it may be shown exactly as in the

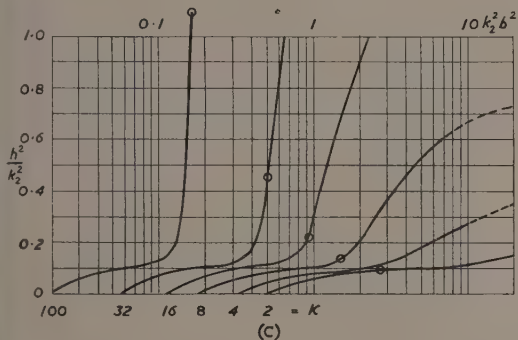
$$\eta = 1.5, K > 1$$



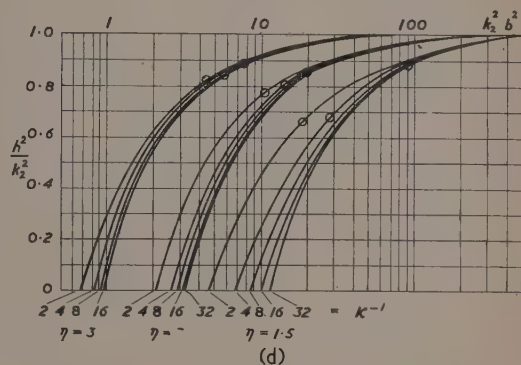
$$\eta = 2, K > 1$$



$$\eta = 3, K > 1$$



$$K < 1$$



$$K \ll 1$$

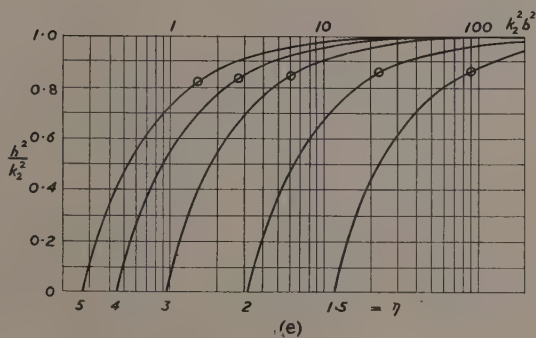


Fig. 7. Graphs giving propagation constant for  $TM_{01}$  mode in circular waveguide

case of a rectangular waveguide that the only wave with this velocity which can propagate down the guide is one of zero amplitude. For  $\omega$  less than  $\omega_2$ , the field distribution is very similar to that of an homogeneously filled waveguide. For  $\omega$  greater than  $\omega_2$  the guide behaves more as a dielectric rod than as a waveguide and when  $\omega$  becomes infinite it may be shown that the propagation constants are the same as those for a dielectric rod in free space (the problem of Hondros), and that for both TM and TE type waves the velocity of propagation is that of light in medium (ii), namely  $1/\sqrt{(\mu_1 \epsilon_1)}$ .

It may be shown that with the TM type wave for  $\omega < \omega_2$ ,  $h^2$  is an increasing function of  $a/b$  and that for  $\omega > \omega_2$   $h^2$  is a decreasing function of  $a/b$ . For TE type waves the converse

is true. If, on the other hand,  $\epsilon_2 \mu_2 > \epsilon_1 \mu_1$ , the field as  $\omega \rightarrow \infty$  tends to lie in the outer dielectric and behaves very much as though it were between a material of zero dielectric constant and permeability and a perfectly conducting wall.

Exactly similar considerations apply when, in addition, to two coaxial dielectric structures, there is an inner wall to the guide, i.e. the waveguide has walls at  $\rho = c, \rho = a, c < b < a$ . In this case the equivalent network is as indicated in Fig. 9. Because of the radial divergence factor,  $Y_{01}, Y_{02}$  are not uniform, but depend effectively on  $\rho$ . It is possible to derive an approximate expression for the guide wavelength in the principal mode which is true when the radial dimensions of the guide are small, that is if  $2\pi a \gamma_2$  and  $2\pi b \gamma_1$  are both much



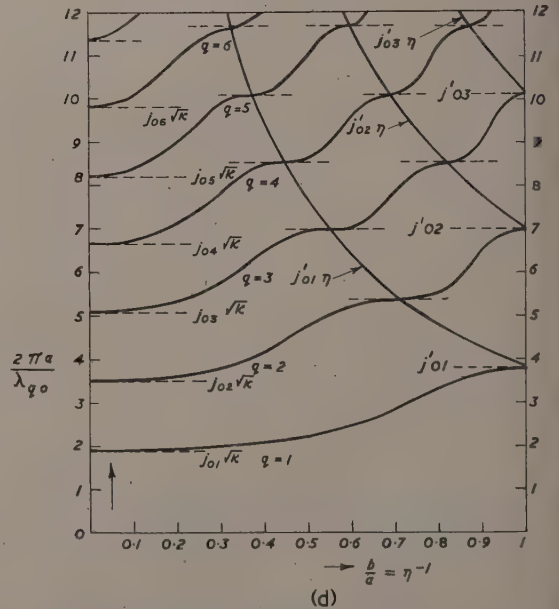
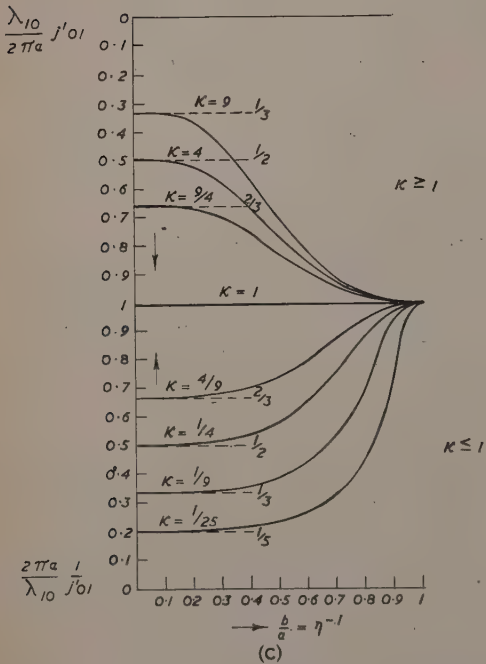
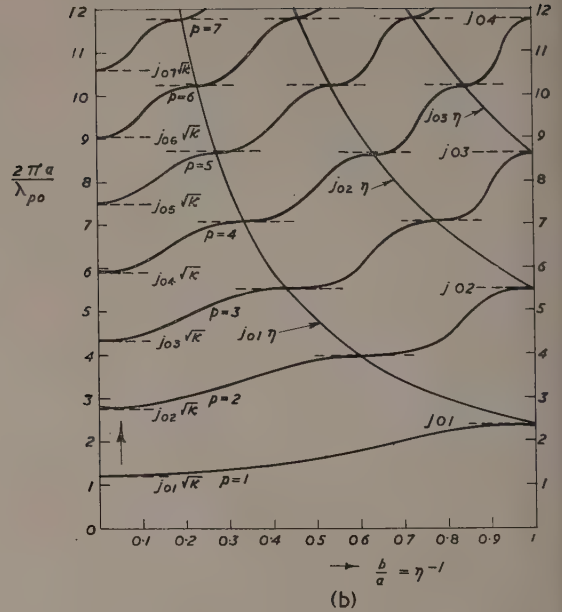
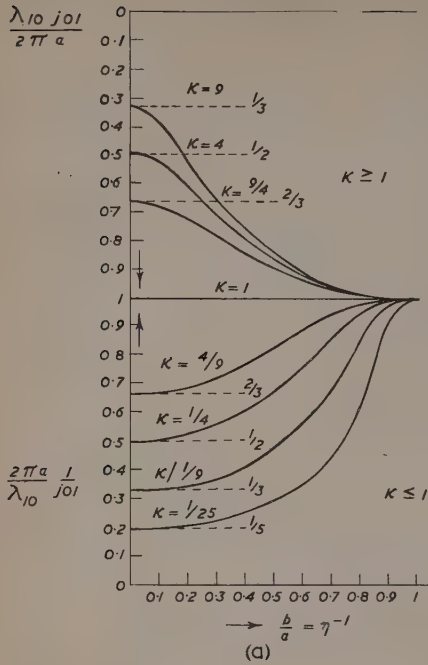


Fig. 8. Graphs giving cut-off frequencies for TE and TM modes in circular waveguide

less than unity. Under these circumstances an approximation for the guide wavelength is given by<sup>(14)</sup>

$$\left(\frac{\lambda_g}{\lambda_0}\right)^2 = \frac{(\epsilon_0/\epsilon_1) \log(b/c) + (\epsilon_0/\epsilon_2) \log(a/b)}{\log(b/c) + \log(a/b)}$$

Thus, to a first approximation the guide wavelength can be obtained by use of a weighted mean of dielectric constant. It may be noted that if we make  $c$  tend to zero, we do not reduce to the case of a guide filled merely with two dielectrics.

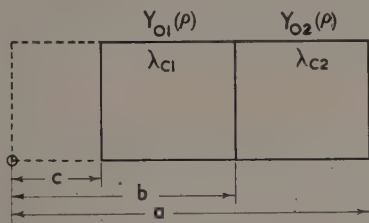


Fig. 9. Transmission line equivalent to coaxial line partly filled with dielectric

This is a well-known phenomenon, as a coaxial line with a very small inner tube behaves differently to a circular waveguide. In this case also, as the frequency increases similar phenomena occur and the field lies eventually entirely in one of the media.

#### APPROXIMATE METHODS

As has been indicated in the course of this paper, it is possible under certain circumstances to propagate a pure TE, or a pure TM mode down a waveguide of the type which we are considering. If this is the case, it is possible to obtain approximate values for the propagation constant, thereby avoiding the solution of a complicated transcendental equation. The manner in which this is done is briefly as follows<sup>(10, 11)</sup>:

If we have a homogeneously filled waveguide with an arbitrary cross-section, the propagation constant of a wave down the guide is given by

$$(k^2 - h^2) \int \psi^2 dS = \int (\nabla \psi)^2 dS$$

where  $\nabla$  is the two-dimensional gradient operator and  $\psi$  is  $E_z$  or  $H_z$  according as the wave is TM or TE.  $S$  is the guide cross-section. Supposing now that the waveguide is filled with material whose properties vary over the cross-section, this equation can be generalized to

$$\int (k^2 - h^2) \psi^2 dS = \int (\nabla \psi)^2 dS$$

where  $k^2$  is now a function of position  $\psi$  is no longer  $H_z$  or  $E_z$ , but is very closely related and satisfies the same boundary conditions on the external walls of the guide. This last equation may be re-written as

$$h^2 = \frac{\int k^2 \psi^2 dS - \int (\nabla \psi)^2 dS}{\int \psi^2 dS}$$

It has been shown that if for  $\psi$  in this last equation an approximation thereto is substituted, a good approximation to  $h^2$  is obtained. It is convenient to take as an approximation for  $\psi$  a combination of the modes for a homogeneously filled waveguide. This has the advantage that the approximate field satisfies the boundary conditions on the walls and therefore gives a fair approximation to the true field for a comparatively small number of terms.

Furthermore, the expression for  $h^2$  can be cast into a form

which is analogous to Rayleigh's principle for the calculation of frequencies of vibrating systems and thus making use of relaxation methods it is possible to obtain upper and lower bounds to  $h^2$ . By taking a sufficiently large number of terms in the approximate expression, it is possible to bracket  $h^2$  as closely as desired. However, because of the differences of dielectric constant in a material from the nominal value, an accuracy of 1% is as much as can be expected, and it is therefore sufficient to use only two or three terms in the approximate expansion. The utility of the method lies largely in avoiding the solutions of transcendental equations, the solution of the problem being obtained in effect from a Langrangian Frequency Determinant.

By using an approximation of  $n$  terms for the field distribution, a determinant of the  $n$ th order is obtained and it is possible to obtain approximate values for the propagation constants of the first  $n$  modes, of which the first is more accurate than the  $n$ th. However, as it is only the first few modes that are of interest, this inaccuracy in the  $n$ th mode is not important. If a small error is made in the assumed mode, then the approximate value for  $h^2$  differs only by second order terms from the true value. This corresponds with the physical fact that the propagation constant does not depend in detail on the field configuration.

#### CALCULATION OF LOSS

The calculation of loss in a waveguide partly filled with dielectric has been carried out with respect to the loss in the dielectric due to slight conductivities and also with respect to the loss due to the imperfect conductivity of the waveguide walls.<sup>(3, 7)</sup> These calculations are laborious and display no special features of interest, being very similar to those carried out for ordinary waveguides. For this reason, it has not been considered necessary to discuss the matter further here, and if information is desired reference should be made to the original literature.

#### REFERENCES

- (1) PINCHERLE, L. *Phys. Rev.*, **66**, p. 118 (1944).
- (2) GRAFFI, D. *Ann. Mat. Pura. App.*, **30**, p. 233 (1949).
- (3) WOODWARD, A. *Wireless Engng*, **24**, p. 192 (1947).
- (4) ABELLE, M., and GARELLI, C. M. *Atti del Congresso Internazionale per il cinquantenario della scoperta Marconiana Radio*, p. 14 (1947).
- (5) FRANK, N. H. *Radiation Laboratory Report (T9/V)*, p. 10 (1943).
- (6) MACFARLANE, G. G., and HILL, J. F. *J. Instn Elect. Engrs*, **III A**, **93**, p. 633 (1947).
- (7) BUCHOLZ, H. *Annalen der Physik*, **Lpz.**, **43**, p. 313 (1943).
- (8) MONTGOMERY, G. G., DICKE, R. M., and PURCELL, E. M. *Principles of Microwave Circuits*, pp. 385-9 (New York: McGraw-Hill Book Co. Inc., 1948).
- (9) BANOS, A., JR., SAXON, D. S., and GRUEN, H. *J. Appl. Phys.*, **22**, p. 117 (1951).
- (10) CHAMBERS, LL. G. *Brit. J. Appl. Phys.*, **3**, p. 19 (1952).
- (11) CHAMBERS, LL. G. Awaiting publication.
- (12) FRANKEL, S. *J. Appl. Phys.*, **18**, p. 650 (1947).
- (13) BRUCK, G. G., and WICHER, E. R. *J. Appl. Phys.*, **18**, p. 766 (1947).
- (14) MARCUVITZ, N. *Waveguide handbook*, pp. 387-97 (New York: McGraw-Hill Book Co. Inc., 1951).
- (15) STAEHLER, R. E. *Determination of Propagation Constants by Radial Transmission Line Theory*. M.Sc. Thesis: Polytechnic Institute of Brooklyn, 1948 [Quoted on p. 394 of reference (14).]
- (16) OLINER, A. A. *J. Appl. Phys.*, **19**, p. 109 (1948).

# A vibrating reed microbalance for susceptibility measurements in weak fields

By Y. L. YOUSEF, M.Sc., Ph.D., King's College, University of Durham, Newcastle-upon-Tyne\*

[Paper first received 18 August, and in final form 21 October, 1952]

An alternating or a modulated magnetic field of subsonic frequency exerts on a small specimen a periodic force which is communicated to a non-resonant reed, which is thereby forced to vibrate, the motion being indicated by a selective microvibration detecting arrangement. An opposing electrostatic field of the same frequency can be suitably applied to the reed so as to nullify its vibrations, and may thus give a measure of the magnetic force. A force whose amplitude is only 0.01 dyne can be readily measured to an accuracy of about 1%.

## INTRODUCTION

In a recent note,<sup>(1)</sup> the present author pointed out the possibility of determining magnetic susceptibility dynamically in a modulated field by employing the resonant vibrations of a horizontal bifilar carrying a small coil fed with an a.c., the test material being held in the field gradient of the coil. The sensitivity limit in that method is primarily set by the inevitably large mechanical noise whose dominant frequency is the same as that of the wanted signal.

The principle of the susceptibility method described below is to subject a small quantity (e.g. 0.1 g) of the material under test to an alternating magnetic field gradient. The oscillating magnetic forces thus set up are made to provoke non-resonant forced vibrations in a thin reed of phosphor-bronze, fixed at one end as a cantilever. The magnetic force may then be determined in terms of the vibration amplitude, the latter being measured on a sensitive vibration detecting arrangement, while all extraneous noise is effectively eliminated by filtering networks. Preferably, however, the measurements may be made by a null method in which the magnetic pull is opposed by a counter electrostatic pull which is just sufficient to bring the vibrating reed to rest. One of the novel features of this method is the fact that it can deal efficiently with forces whose amplitudes are as small as 0.01 dyne.

## DESCRIPTION OF THE APPARATUS

A schematic diagram of the complete arrangement is shown in Fig. 1. The vibrating reed *R* is a brass (or better, phosphor-bronze) strip  $7 \times 1.2 \times 0.01$  cm, soldered at *O* to the support *T*, and bent square at the end *X* which can be coupled to the specimen under test *S* by means of a thin glass fibre *G*. The natural frequency of flexural vibrations of the loaded reed is about 12 c/s. Situated above *R* is a plate *Q* of the same material,  $6.5 \times 1.0 \times 0.1$  cm, screwed to *T* but insulated from it by  $\frac{1}{2}$  mm of mica *M*, and meant as a capacity electrode. When *R* is set into flexural vibrations, for instance, by the magnetic forces that act on *S* as an a.c. is passed through the coil *L*, the capacity of the condenser formed by *Q* and *R* varies periodically, the variations being detected by a capacity responsive circuit *V.D.* and indicated by a valve voltmeter *W.A.* preceded by noise filters. The screw *B* (preferably insulated at tip) serves to adjust the position of *Q* and thus exercises a control of the sensitivity. The field coil *L*, which is fixed on a small levelling table (not shown) for relative adjustment with respect to *S*, has 2000 turns of insulated copper wire s.w.g. 48, wound on a brass former 0.8 cm in length and 0.6 cm in internal diameter. The average diameter of the turns is 1.1 cm. The resistance

is 650  $\Omega$  and the inductance is of the order of a few hundredths of a henry, so that the current, and in consequence the magnetic field, may be regarded as in phase with the applied voltage at the working frequency of 20 c/s. The field at the coil centre corresponding to 1 V between its ends is 7 oersteds, and the axial distribution has a flat maximum in a range of 2 mm, with a uniformity of better than 1%. The dissipation for a field of 100 oersteds is less than 0.5 W.

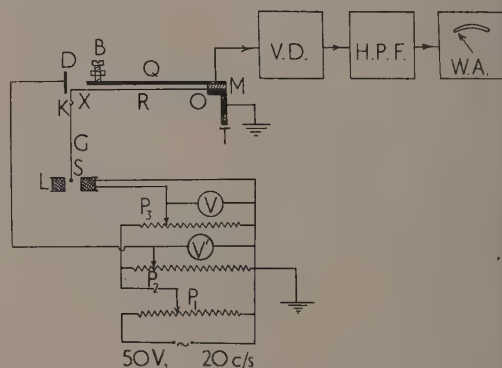


Fig. 1. The experimental arrangement

*V.D.* = vibration detector; *H.P.F.* = high-pass filter;  
*W.A.* = wave analyser

A counterbalancing vertical plate *D* is arranged parallel to *X* (at about  $\frac{1}{2}$  mm from it) so as to overlap partially its upper part. The position of *D* can be adjusted by screws (not shown). If a potential difference  $V'$  is established between *D* and *X*, then apart from the horizontal electrostatic force which does not concern us so long as *X* and *D* are adequately stiff to keep the same separation, there comes into play a vertical force proportional to  $V'^2$ , and is in fact equal to  $\gamma(bV'^2/8\pi t)$ , where *b* is the overlapped breadth, *t* the separation and  $\gamma$  a numerical constant whose value in the present arrangement is very nearly equal to 1. Although the magnitude of this pull is independent of the overlapping area within reasonable limits when *t* is small in comparison with the non-overlapping lengths of *D* and *X*, it is always wise in measurements with specimens of different masses to maintain the relative positions fixed by making the suspended mass constant with the aid of glass riders that can be hung from hook *K*.

As  $V'$  is in phase with the field voltage *V*, the electrostatic and the magnetic forces acting oppositely on the reed end can be made to counterbalance one another exactly, provided that the test material responds instantaneously to the field.

\* On study leave from Fouad I University, Cairo, Egypt.



If a polarizing magnetic field is superposed, a polarizing voltage must then also be used on the deflecting plate  $D$ . Balance in either case is secured simply by adjusting  $V'$  and/or  $V$ . If an electromagnet is employed for generating the alternating field, balance would require the use of a phase shifter. An earlier form of the vibration detector  $V.D.$  has previously been briefly described,<sup>(2)</sup> but has now been further developed to meet the requirement of microvibration detection. Basically, it is a 6 Mc/s quartz-crystal oscillator with a 10 k $\Omega$  load resistance in the cathode branch, effectively decoupled from the high-frequency paths (Fig. 2). All the components are non-microphonic, and the circuit noise is further reduced by underheating the filament and working

Here

$$H = H_0 + H_s + H_0 \sin pt$$

where  $H_0 \sin pt$  is a modulating field of pulsance  $p$ ,  $H_s$  the value of a superposed steady field acting in the direction of the alternating field, and  $H_0$  the component of the earth's field in the same direction. The assumptions that there is no field distortion or field dependence are involved.

The periodic part of  $f_m$  is

$$f = (k - k_0)v[H_0(dH_s/dz) + (H_0 + H_s)(dH_0/dz)] \sin pt - \frac{1}{2}(k - k_0)vH_0(dH_0/dz) \cos 2pt \quad (2)$$

The first term dominates when the direct field is large compared with the amplitude of the alternating field, while the second term, with pulsance  $2p$ , dominates when the steady field is relatively small. A knowledge of either component gives a measure of  $k$ . Determinations of the Curie force on a small body under the circumstances where  $H_s \gg H_0$  are particularly recommended if field dependence is to be investigated.

The technique described above is so sensitive that it was found sufficient to produce the field simply by a small air-cored coil. In this case,  $H_0 = cI_0$  and  $(dH_0/dz) = I_0(dc/dz)$ , where  $I_0$  is the amplitude of the field current and  $c$  is a constant depending on the geometry of the coil and the location of the body under test. Thus, in the absence of a polarizing field,

$$f = \frac{1}{2}(k - k_0)vI_0^2c(dc/dz) \cos 2pt \quad (3)$$

the negative sign being dropped.

The Gouy force  $F$  on a column of material of uniform cross-section  $a$  is given by

$$F = \frac{1}{2}(k - k_0)aI_0^2(c^2 - c'^2) \cos 2pt = F_0 \cos 2pt \quad (4)$$

where  $F_0 = \frac{1}{2}(k - k_0)aI_0^2(c^2 - c'^2)$ , and  $c$  and  $c'$  the values of the coil constant at the ends of the column. It should be remarked that if the material shows magnetic viscosity, i.e. time lag between the applied field and the magnetization, a phase difference will have to be introduced into the periodic terms.

Now consider the transverse vibrations of the reed caused by a harmonic force  $F_0 \cos p_1 t$  (of pulsance  $p_1 = 2p$ ) acting on a body suspended at the free end of the reed. The approximate equation of motion, assuming small viscous damping having a coefficient  $\alpha$ , is

$$M\ddot{z} + \alpha\dot{z} + \beta z = F_0 \cos p_1 t \quad (5)$$

where  $M$  is the suspended mass plus approximately 33/140 of the mass of the reed,<sup>(3)</sup> and  $\beta/M = p_0^2$ , the square of the natural undamped pulsance.

The steady state solution of equation (5) is

$$Z = F_0/[(Mp_0^2 - Mp_1^2) + \alpha^2 p_1^2]^{1/2} \cos(p_1 t - \phi) \quad (6)$$

where  $\phi$  is a phase angle introduced by the damping. The same equation holds when  $F_0$  represents the amplitude of the electrostatic force (also at a frequency  $p_1 = 2p$ ) acting at the reed end, i.e. when

$$F_0 = \gamma(bV^2/8\pi t) \quad (7)$$

If  $\alpha$  is small and  $p_1 \gg p_0$ , the amplitude  $A$  of the forced vibration is given by approximately

$$A = F_0/Mp_1^2 \quad (8)$$

Equation (8) shows that the motional amplitude increases rapidly as the frequency is reduced. When  $F_0$  is a magnetic

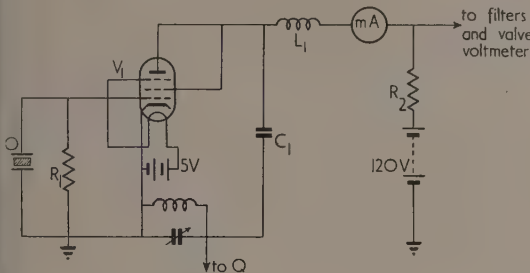


Fig. 2. The vibration detector

$R_1 = 50 \text{ k}\Omega$   $V_1 = \text{EF 37 A}$   $O = \text{quartz-crystal}$   
 $R_2 = 10 \text{ k}\Omega$   $L_1 = \text{high frequency}$   $\text{oscillator, 6 Mc/s}$   
 $C_1 = 0.0001 \mu\text{F}$   $\text{choke 1 mH}$

at a low power level. When the tuning condenser is adjusted for operation on the ascending part of the response curve (which has the form of a deep crevasse) the sensitivity for a cathode current of 2.5 mA is such that a capacity change of  $10^{-6}$  pF would give rise to a voltage change of 100  $\mu\text{V}$  on the load  $R_2$ .

The high-pass filter  $H.P.F.$  is a 3-stage T-section network, with two capacitances of 1  $\mu\text{F}$  and an inductance of 30 H in each section. It is magnetically screened and is situated at a distance from the a.c. source, the latter being a low frequency oscillator operated at 20 c/s. The mains supply frequency may be used instead, though with some sacrifice of efficiency. At the signal frequency (40 c/s) the attenuation of the filter is practically nil, whilst the attenuation at 20 c/s is 40 db, but it is estimated to be as large as 80 db at the dominant noise frequency of 12 c/s. In order to suppress still further the low frequency noise and also the noise due to possible excitation of higher modes of the reed by mechanical disturbances as well as that due to a.c. pick-up, the low-pass filter is followed by a Marconi-Ekco wave analyser  $W.A.$ , type T.F. 455, intended here as a band-pass filter and permanently set at the signal frequency. This introduces a further attenuation of the noise by about 60 db. In this way noise elimination was so effective that it was found hardly necessary to take any precautions as regards the mounting of the reed balance.

#### THEORY OF THE REED BALANCE

The vertical magnetic force  $f_m$  on a small specimen of volume  $v$  and volume susceptibility  $k$ , situated in a medium of volume susceptibility  $k_0$ , and in a region where the magnetic field is  $H$  (which may be horizontal or vertical) and the field gradient is  $dH/dz$  is given by

$$f_m = (k - k_0)vH(dH/dz) \quad (1)$$

force, it will involve the mass of the test body which itself is included in  $M$ .

With  $F_0 = 0.01$  dyne,  $M = 0.1$  g, the calculated vibration amplitude  $A$  at a frequency of 40 c/s is about  $2 \times 10^{-6}$  cm. This is approximately equivalent to an average displacement of  $0.4 \times A$  of the whole reed parallel to itself, i.e. to a displacement of about  $10^{-6}$  cm of one of the plates of the condenser  $RQ$ . It will be remembered that  $A$  stands for the deflexion at the end of the reed. The capacity change arising from that displacement is  $2 \times 10^{-4}$  pF. The vibration detector can be adjusted to give an output of  $100 \mu V$  for a capacity change of  $10^{-6}$  pF, and the output meter can definitely detect a signal of  $10 \mu V$ . Thus, even for  $M = 1$  g a displacement of  $10^{-7}$  cm can still be measured with reasonable accuracy.

Instead of measuring the magnetic force in terms of the amplitude of vibration, however, it is advisable for obvious reasons to obtain it in terms of the electrostatic force given by equation (7). When  $k_0$  is neglected, equation (3) or (4), together with Ohm's law, gives for the mass susceptibility

$$\chi \propto (V^2/mV^2) \quad (9)$$

where  $m$  is the mass of the body. The constant of proportionality is best eliminated by a standardizing substance.

Relation (9) is dependent neither on the position nor on the elasticity of the reed, nor on any property characteristic of the detecting equipment. It is convenient in practice to keep one of the voltages constant and to adjust the other for counterbalance. Once a balance is obtained, it should not be disturbed when  $V$  and  $V'$  are changed in the same proportion (just by sliding  $P_1$ ) provided that the susceptibility does not depend on field strength. This fact provides a very simple test of field dependence (see Fig. 6).

#### EXPERIMENTAL RESULTS

Expression (9) assumes that in an alternating magnetic field, the forces acting on a body are exclusively magnetic, with no electrodynamic contribution due to induced eddy currents. Generally speaking, this assumption is quite plausible at low frequencies, unless the body has a remarkably high metallic conductance. Experiments performed in a non-homogeneous field on materials of weak susceptibility and different conductances have shown that, even with copper filings, no eddy current vibrations could be detected under the present circumstances at a frequency of 20 c/s in a region where  $H(dH/dz)$  is about 40 000, although a horizontally suspended copper disk 0.2 cm thick and 0.5 cm in diameter was found to experience a force as large as 0.02 dyne. Eddy current forces are betrayed by the fact that they are nearly  $90^\circ$  out of phase with the applied field, and that they can be reduced considerably (in the vertical direction) if the magnetic field is arranged horizontally.

Numerous magnetic tests were made at room temperature ( $20^\circ C$ ) on various paramagnetic salts under different conditions as regards the mass, the sensitivity and the position of the balancing electrode. The salt was finely powdered and was contained in a micro-tube of Pyrex glass suspended from the reed as in the ordinary determinations by the column method. All the results were consistent with one another to about 2% and did not differ from the accepted values by more than 5%. The table gives typical measurements on hydrated ferric chloride, with manganese chloride as a reference substance. The last column shows that the susceptibility ratio  $\chi_1/\chi_2$  is practically constant in three different determinations.

#### Testing the vibrating reed microbalance

No.	Material	$m$ (g)	$V$ (volts)	$V'$ (volts)	$\chi_1/\chi_2$
1	Ferric chloride	0.460	24.7	30.3	0.799
	Manganese chloride	0.471	24.7	34.4	
2	Ferric chloride	0.468	28.8	38.0	0.770
	Manganese chloride	0.422	28.4	41.0	
3	Ferric chloride	0.479	26.5	33.3	0.785
	Manganese chloride	0.451	24.2	33.3	
Average value of $\chi_1/\chi_2 = 0.785$					Accepted value of $\chi_1/\chi_2 = 0.804$
Accepted value of $\chi_1/\chi_2 = 0.804$					

In Fig. 3, the relation between the field voltage  $V$  and the counterbalancing voltage  $V'$  is represented graphically for manganese chloride and for hydrated ferrous ammonium sulphate. It will be seen that the curves are straight lines passing through the origin. The observed value of  $\chi$  for manganese chloride referred to ferrous ammonium sulphate as standard ( $\chi = 32.6 \times 10^{-6}$ ) is  $102 \times 10^{-6}$  e.m.u./g. The accepted value is  $107 \times 10^{-6}$  e.m.u./g.

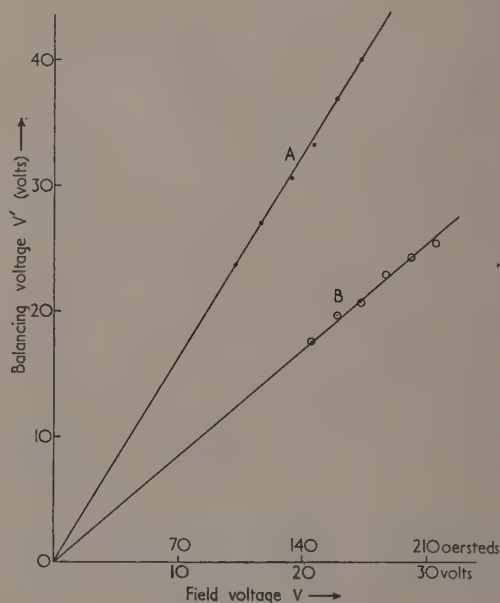


Fig. 3. Relation between  $V$  and  $V'$

A, manganese chloride, mass = 0.265 g, slope 1.64; B, ferrous ammonium sulphate, mass = 0.226 g, slope 0.856. The slopes are  $\propto (\chi m)^{1/2}$ .

Naturally a higher degree of accuracy should be expected with relative measurements on the same substance. The certainty with which the magnetic force can be counterpoised by the electrostatic force has been taken as a criterion of the accuracy of the present method. Fig. 4 shows the sharpness with which exact balance between the opposing forces can be secured in a typical case with a manganese chloride crystal (mass 100 mg) suspended in a non-homogeneous field of  $H(dH/dz) = 10^4$ . It will be realized that the balancing voltage can be measured at least to 0.2 V in 42 V, i.e. to

better than  $\frac{1}{2}\%$ . This implies an accuracy of 1% in measuring the magnetic force.

The behaviour of a material with ferromagnetic impurity is interesting. Particularly in view of the magnetic after-

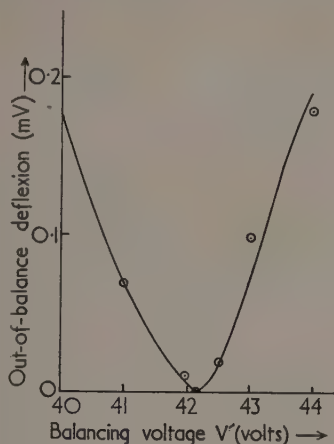


Fig. 4. Sharpness of balance

effect generally exhibited by the impurity, exact balance will not as a rule be possible without phase shifting. Fig. 5 refers to a ferrous sulphate powder injected with a 0.001 in nickel wire of mass  $10^{-5}$  g. It shows that when the electrostatic force is maintained constant while the magnetic field is varied

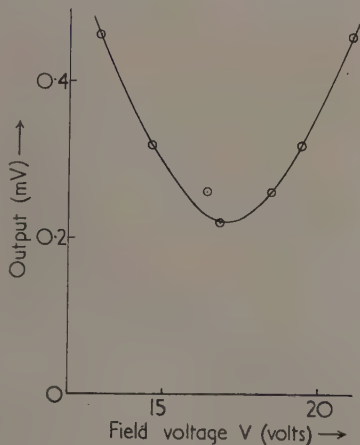


Fig. 5. Failure to secure exact balance when a ferromagnetic impurity is present

or vice versa) the vibration amplitude reaches a minimum but never vanishes completely under the counterforce. Since an amplitude corresponding to 0.01 mV output could be observed it follows that a mass of only  $5 \times 10^{-7}$  g of nickel can be detected in a field of 120 oersted, but presumably a much smaller amount would be revealed in a larger field.

In order to find out whether failure to secure balance was due to eddy currents induced in the nickel, a copper rod 1 mm in diameter and 20 mm in length was introduced into the field together with a pure sample of ferrous sulphate. No eddy current effects could be detected. Consequently, the contribution of eddy currents to the magnetic time lag of nickel must be extremely small. Again, when the magnetic force on a ferromagnetic material is balanced (at least partially)

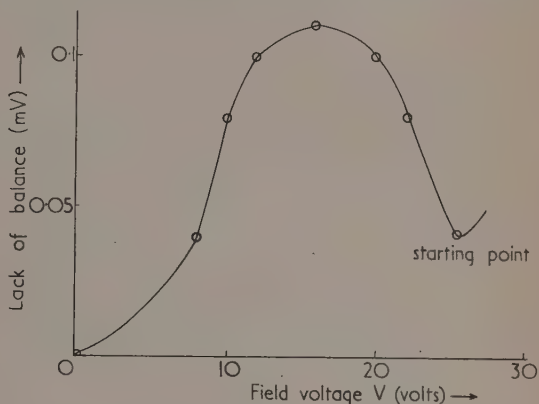


Fig. 6. Test for field dependence of a salt containing  $3 \times 10^{-6}$  g nickel

and the source supply voltage is subsequently changed so as to alter  $V$  and  $V'$  in the same proportion, the null indicator will be thrown out of balance, the deflexion showing a distinct maximum at some value of the field (Fig. 6). Such a behaviour is evidence of field dependence.

#### CONCLUSION

The present technique seems useful for determinations of small periodic forces whenever these forces can be made to produce displacements. It can thus be conveniently applied for susceptibility measurements on crystals or on small amounts of powders or liquids. Investigations of temperature dependence of susceptibility by the use of large thermostatic baths in extensive fields, as well as investigations on magnetic viscosity and eddy currents would appear possible.

#### ACKNOWLEDGEMENT

This work has been conducted with the continuous help and kind suggestions of Dr. E. G. Richardson, King's College, Newcastle-upon-Tyne. To him I wish to express my sincerest thanks.

#### REFERENCES

- (1) YOUSEF, Y. L., MIKHAIL, H., and GIRGIS, R. K. *Rev. Sci. Instrum.*, **22**, p. 342 (1951).
- (2) YOUSEF, Y. L., and SULTAN, F. *Rev. Sci. Instrum.*, **20**, p. 533 (1949).
- (3) RAYLEIGH, LORD. *Theory of Sound*, Vol. 1, p. 289 (London: Macmillan and Co. Ltd., 1944).



# High power solenoids; stresses and stability

By J. M. DANIELS, M.A., D.Phil., The Clarendon Laboratory, Oxford

[Paper received 22 September, 1952]

An exact treatment is given of the stresses in a flat coil, and account is taken of the spacing between turns by treating the windings as a homogeneous anisotropic material. The results are discussed as a guide to the stresses in thick solenoids. This is followed by a treatment of the stability of the turns of a solenoid against spontaneous deformation, using the principle of virtual work, and criteria for stability are found. It is shown that, in the absence of elastic restraining forces, the outer turns of a thick solenoid would be unstable.

It has been long known that a consideration of the stresses is important in high power solenoids producing very large fields (say 500 000 oersteds) for short periods. When we began to design water-cooled solenoids to produce fields of up to 40 000 oersteds continuously, we knew that the stresses were smaller by a factor of about 100, and ignored the problem of internal stresses. However, a mechanical breakdown occurred in one of our solenoids, and one part of the broken down coil is shown in Fig. 1. The undulating form into which the windings had been thrown led us to suspect that perhaps under certain circumstances the windings of a solenoid might be in unstable equilibrium, and might distort spontaneously into such shapes. While engaged on the problem of the stability of the windings, we considered also the problem of the internal stresses in solenoids.

It has been long known that a consideration of the stresses is important in high power solenoids producing very large fields (say 500 000 oersteds) for short periods. When we began to design water-cooled solenoids to produce fields of up to 40 000 oersteds continuously, we knew that the stresses were smaller by a factor of about 100, and ignored the problem of internal stresses. However, a mechanical breakdown occurred in one of our solenoids, and one part of the broken down coil is shown in Fig. 1. The undulating form into which the windings had been thrown led us to suspect that perhaps under certain circumstances the windings of a solenoid might be in unstable equilibrium, and might distort spontaneously into such shapes. While engaged on the problem of the stability of the windings, we considered also the problem of the internal stresses in solenoids.

The first part of this paper gives a treatment of the stresses in a solenoid on the lines indicated above. The results are presented in a form suitable for numerical computation. This is followed by an investigation of the stability of a single turn unsupported by its neighbours, but, of course, in the field of the rest of the solenoid. This treatment is reasonable in a coil where the spacing material between adjacent turns is relatively soft, and may even be applicable generally, for if two adjacent turns deform spontaneously the same way, they may offer each other no support. In any case, it is desirable to design solenoids which are, if possible, intrinsically stable (i.e. stable under the action of electromagnetic forces only).

## STRESSES IN SOLENOIDS

Let us take cylindrical polar co-ordinates ( $r, \theta, z$ ), where the  $z$ -axis is the axis of cylindrical symmetry of the solenoid. Following Cockcroft, let  $M$  be the mutual inductance of one turn with the whole of the coil ( $M$  can be obtained from tables given by Cockcroft<sup>(1)\*</sup>). Then the component of force in the  $r$  direction on an element  $dr \cdot d\theta \cdot dz$  is  $F \cdot dr \cdot d\theta \cdot dz$  where  $F = (v^2/2\pi)(\partial M/\partial r)$ ,  $v$  is the number of turns per cm<sup>2</sup> of winding space and  $i$  is the current in each turn in e.m.u.

We will now consider a two-dimensional treatment, ignoring stresses in the  $z$ -direction. This is applicable in many cases, especially to our solenoids which are built of a stack of flat coils (for details of the construction see Daniels<sup>(3)</sup>), for, since Poisson's ratio  $\sigma \approx 0.35$  for copper, and since the windings are normally in tension when carrying current, there will be a contraction in the  $z$ -thickness of the flat coils which comprise the solenoid. The nylon spacing between the turns of these flat coils does not produce any swelling in the  $z$ -direction due to radial compression. It will, in general, be very difficult to determine the effect of a  $z$ -compression of a flat coil on the other stresses existing in it, as this will depend on the exact shape and stiffness of the separators. However, the radial forces are the greatest for the central flat coil, and an exact treatment of this will act as a guide to the order of magnitude of the stresses existing in the rest of the solenoid. It will be seen that, when the insulating material is very soft,  $z$ -compression has no effect on either the radial stress or the hoop stress, in the first approximation.

A flat coil of the type used is capable of withstanding stresses  $E_{rr}$ ,  $E_{\theta\theta}$ ,  $E_{zz}$ ; but not  $E_{rz}$  nor  $E_{zr}$ , as in the first case the turns of the flat coil can slide past each other freely in the  $z$ -direction, while in the second case, the turns of consecutive

\* One printing error should be pointed out. In Table II of Cockcroft's paper, the value for  $\rho/r = 0.7$ ,  $z/r = \infty$  should read 0.26633, not 0.21633.

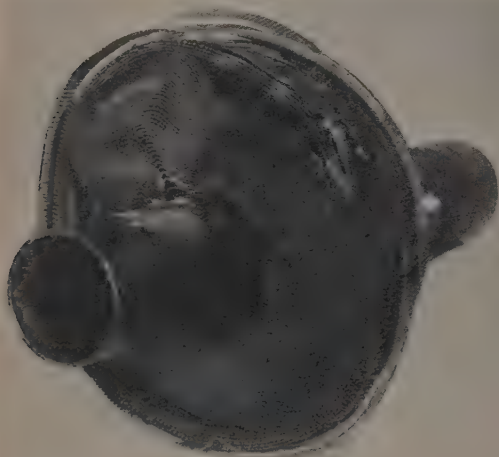


Fig. 1. Part of the windings of a high-powered solenoid distorted through the action of electromagnetic forces

The problem of determining the internal stresses in solenoids had already been treated by Cockcroft.<sup>(1)</sup> However, we decided that his treatment is not applicable to our coils, because there it is assumed that the body forces are balanced at the outer curved surface by an external pressure. This may have been true to a large extent in the solenoids which Kapitza<sup>(2)</sup> used, but it is not necessarily true for our solenoids. These can, in fact, be worked unsupported on the outside, although support is usually provided for additional safety. Cockcroft further makes the simplifying assumption that the windings of the solenoid form a homogeneous isotropic material. Our treatment considers the windings to be homo-

flat coils can also slide past each other in the  $r$ -direction without hindrance. By symmetry  $E_{\theta 0} = E_{z0} = 0$ . Define the following elastic constants:  $q_r, q_\theta = \text{Young's modulus in the } r\text{- and } \theta\text{-directions respectively for the flat coil treated as homogeneous (i.e. an average for the copper conductor and the spacing material).}$

Averaged Poisson's ratios:

$$\sigma_r = \frac{\text{fractional extension in the } \theta\text{-direction}}{\text{fractional contraction in the } r\text{-direction due to stress in the } r\text{-direction}}$$

$$\sigma_\theta = \frac{\text{fractional contraction in the } r\text{-direction}}{\text{fractional extension in the } \theta\text{-direction produced by stress in the } \theta\text{-direction}}$$

Referring to Fig. 2, consider the flat coil as a series of rings. Let  $T_n$  be the tension in the  $n$ th ring, and  $P_n$  be the pressure (force/cm) on the inside face of the  $n$ th ring. Let  $\xi_n$  be the radial displacement of the inside face of the  $n$ th ring, and

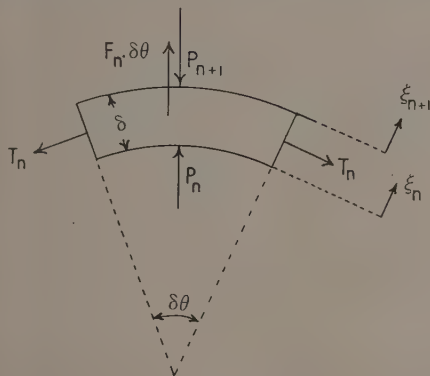


Fig. 2. Diagram illustrating the equilibrium of a portion of conductor in a high-power solenoid

Let  $r_n$  be the unstrained radius of this face. Let  $F_n \delta \theta$  be the electromagnetic "body" force on a segment  $\delta \theta$  of the  $n$ th ring, and let  $\delta$  denote  $r_{n+1} - r_n$ ; the constant unstrained thickness of each ring. Let  $\zeta$  be the thickness of the ring in the  $z$ -direction. Then for equilibrium:

$$T_n \cdot \delta \theta + (r_{n+1} P_{n+1} - r_n P_n) \delta \theta = F_n \cdot \delta \theta$$

$$\text{Now } F_n \cdot \delta \theta = F \cdot \zeta \cdot \delta \cdot \delta \theta$$

$$\text{and put } T = T_n / (\zeta \cdot \delta) \quad P = P_n / \zeta$$

$$\text{Then } T + (r_{n+1} P_{n+1} - r_n P_n) / (\zeta \cdot \delta) - F = 0$$

$$\text{or } T + (d/dr)(rP) - F = 0 \quad (1)$$

Let  $e_\theta$  be the tensile strain in the  $\theta$ -direction, and  $e_r$  be the compressive strain in the  $r$ -direction.

$$\text{Then } e_\theta = \xi_n / r \text{ and } e_r = (\xi_n - \xi_{n+1}) / \delta$$

$$\text{Thus } \xi_n / r = (1/q_\theta)(T_n / \delta) + (\sigma_r / q_r) P_n$$

$$\text{and } (\xi_n - \xi_{n+1}) / \delta = (P_n / q_\theta) + (\sigma_\theta / q_\theta)(T_n / \delta)$$

which can be written in differential form

$$\left. \begin{aligned} \xi / r &= (1/q_\theta)T + (\sigma_r / q_r)P \\ - (d\xi/dr) &= (\sigma_\theta / q_\theta)T + (1/q_\theta)P \end{aligned} \right\}$$

The condition for compatibility of stress is obtained by eliminating  $\xi$  from these two equations, and is:

$$\frac{\sigma_r}{q_r} \frac{dP}{dr} + \frac{1 + \sigma_r}{q_r} \frac{P}{r} + \frac{1}{q_\theta} \frac{dT}{dr} + \frac{1 + \sigma_\theta}{q_\theta} \frac{T}{r} = 0 \quad (2)$$

Now we know the boundary conditions for  $P$ , but not for  $T$ , hence if we eliminate  $T$  from equations (1) and (2) we get

$$r^2 \frac{d^2 P}{dr^2} + \left( 3 + \sigma_\theta - \sigma_r \frac{q_\theta}{q_r} \right) r \frac{dP}{dr} + \left[ 1 + \sigma_\theta - \frac{q_\theta}{q_r} (1 + \sigma_r) \right] P - r \frac{dF}{dr} + (1 + \sigma_\theta) F = 0 \quad (3)$$

There are two further conditions which must be satisfied. Firstly, the flat coil cannot support a tension in the  $r$ -direction for the turns would separate, therefore

$$P > 0 \quad (4)$$

Secondly, it is made up of a spiral, and not a series of rings. This spiral is kept from unwinding by the friction between adjacent turns, hence:

$$2\pi r \mu \left( 2P + \delta \frac{dP}{dr} \right) > \delta^2 \frac{dT}{dr} \quad (5)$$

where  $\mu$  is the coefficient of friction.

These, however, assume that that coil is initially unstressed, which is not always true. But by winding it tight enough these conditions can always be satisfied.

In order to solve equation (3) write  $r = e^x$ ;  $D \equiv d/dx$ ;  $F = (vi^2/2\pi)(dM/dr)$  and the equation becomes a linear one with constant coefficients. The solution is thus  $P = Ar^{m_1} + Br^{m_2} + (\text{particular integral})$ , where

$$\left. \begin{aligned} m_1 \\ m_2 \end{aligned} \right\} = - \left( 1 + \frac{1}{2}\sigma_\theta - \frac{1}{2}\sigma_r \frac{q_\theta}{q_r} \right) \pm \frac{1}{2} \sqrt{\left( \sigma_\theta - \sigma_r \frac{q_\theta}{q_r} \right)^2 + 4 \frac{q_\theta}{q_r}}$$

It is easily seen that  $m_1$  and  $m_2$  are both real, and, in the limit of an isotropic medium, they take the well-known values 0 and  $-2$ . The particular integral  $P_0$  can be expressed symbolically as

$$P_0 = \frac{vi^2}{2\pi} \cdot \frac{(D+1)^2 + \sigma_\theta(D+1)}{(D-m_1)(D-m_2)} \cdot \exp(-x)M$$

Now  $M$  is not known explicitly, but as a set of tabulated values,<sup>(1)</sup> Probably the most convenient expression for the particular integral is obtained by writing

$$P_0 = \frac{vi^2}{2\pi} \cdot \frac{D+1 + \sigma_\theta}{(D-m_1)(D-m_2)} \cdot [\exp(-x)DM]$$

Now, if we put the operator into partial fractions, and use the theorem

$$f(D) \cdot \exp(ax)V(x) = \exp(ax)f(D+a) \cdot V(x)$$

to transform this partial fraction into an integral involving  $DM$ , we can integrate by parts; and by transforming the independent variable back to  $r$ , we obtain finally the complete solution of equation (3):

$$P = Ar^{m_1} + Br^{m_2} + \frac{vi^2}{2\pi} \cdot \frac{m_1 + 1 + \sigma_\theta}{m_1 - m_2} \cdot r^{m_1} \left\{ [M\rho^{-(m_1+1)}]_{a_1}^r + (m_1 + 1) \int_{a_1}^r M\rho^{-(m_1+2)} \cdot d\rho \right\} + \frac{vi^2}{2\pi} \cdot \frac{m_2 + 1 + \sigma_\theta}{m_2 - m_1} \cdot r^{m_2} \left\{ [M\rho^{-(m_2+1)}]_{a_1}^r + (m_2 + 1) \int_{a_1}^r M\rho^{-(m_2+2)} \cdot d\rho \right\} \quad (6)$$

where  $a_1$  is the inside radius of the flat coil.

*Approximate treatment for soft spacing.* The evaluation of equation (6) is very laborious, especially when the spacing material between the copper turns is soft, i.e. when  $q$ , and  $q_0$  have very different values,  $m_1$  and  $m_2$  are large and of different sign, making the computation of  $P$  much more laborious, and also involving unnecessary labour. In this case, however, we can ignore  $P$  since the expansion of a ring under stress causes comparatively little radial force, and put  $T = F$  [equation (1)]. With nylon spacing, as used in our coils, the effective coefficient of friction for an  $(r - \theta)$  shear is large, and, as explained earlier, by winding the coil initially, moderately tight, the initial stress ( $P$ ) will prevent unwinding. Thus each turn is in equilibrium under its own body forces, and compression will not affect the magnitude of the stresses in the  $r$  and  $\theta$  directions.

From the definitions of  $F$ ,  $T$ , and  $P$ , and from Cockcroft's formulae for mutual inductance, it is seen that the stresses in similar solenoids are proportional to the square of the current density and to the square of the linear dimension. Thus, as an alternative to calculating the stresses, experiments can be made with models.

#### STABILITY AGAINST DEFORMATION

Let us consider a turn in a solenoid, of original radius  $\rho$ . Let it be slightly deformed so that its perimeter remains constant. Let  $r, \theta$  be polar co-ordinates describing this turn, and put  $r - \rho = u$ .

Then

$$ds = [du^2 + (\rho + u)^2 d\theta^2]^{\frac{1}{2}} = (\rho + u) d\theta \left[ 1 + \frac{1}{(\rho + u)^2} \left( \frac{du}{d\theta} \right)^2 \right]^{\frac{1}{2}}$$

Now, for a small deformation, we can take  $u/\rho$  and  $du/d\theta$  to be small.

Expanding the square root to the second order, we have

$$ds = \left[ \rho + u + \frac{1}{2\rho} \left( \frac{du}{d\theta} \right)^2 \right] d\theta$$

The condition that the deformed turn shall have the same perimeter as originally is that

$$\int_0^{2\pi} \left[ u + \frac{1}{2\rho} \left( \frac{du}{d\theta} \right)^2 \right] d\theta = 0 \quad (7)$$

Any displacement likely to be encountered in practice will have  $(d^2u/d\theta^2)$  finite, due to the elasticity of the copper strip, and hence satisfies Dirichlet's conditions, and can be expanded in a Fourier series

$$u = a_0 + \sum_{n=1}^{\infty} (a_n \cos n\theta + b_n \sin n\theta) \quad (8)$$

This series is uniformly convergent, and hence can be substituted in equation (7) to give, as condition for constant perimeter

$$4\rho a_0 + \sum_{n=1}^{\infty} n^2 (a_n^2 + b_n^2) = 0 \quad (9)$$

We thus see that, if  $a_n$  and  $b_n$  ( $n \geq 1$ ) are considered infinitesimals of the first order,  $a_0$  is an infinitesimal of the second order.

The condition for stability is that for any deformation (i.e. for arbitrary  $a_n$  and  $b_n$ ,  $n \neq 0$ ) the energy of the system should increase. There are two contributions to the energy of the system:

- (i) electromagnetic energy,
- (ii) elastic or strain energy.

(i) *The electromagnetic energy.* Let  $\delta\Phi$  be the increase in flux linked with the turn during deformation. Put, near the perimeter,  $H = H_0 + u(dH/d\rho) + (u^2/2)(d^2H/d\rho^2) + \dots$ , where  $H$  is the  $z$ -component of the magnetic field. Then

$$\delta\Phi = \int_{\theta=0}^{2\pi} \int_{t=0}^u \left( H_0 + t \frac{dH}{d\rho} + \dots \right) (t + \rho) \cdot dt \cdot d\theta \quad (10)$$

Using equation (9), eliminate  $a_0$  from equation (10). Also, since we are dealing with infinitesimal displacements, we can neglect all powers of the  $a$ 's and  $b$ 's except the lowest. Thus:

$$\delta\Phi = \frac{\pi}{2} H_0 \sum_1^{\infty} (1 - n^2) (a_n^2 + b_n^2) + \frac{\pi}{2} \rho \frac{dH}{d\rho} \sum_1^{\infty} (a_n^2 + b_n^2) \quad (11)$$

If the direction of  $H$  is chosen so that the field produced by the turn at its centre is positive, and if  $i$  is the current in the turn, considered always positive, the potential energy  $U$  of the system (solenoid + generator) is given by  $\delta U = -i\delta\Phi$ .

(ii) *The elastic energy.* We now consider the strain energy which must be set up in the system when deformation takes place. This is well known to be

$$\frac{1}{2} q A k^2 [\delta(1/\rho')]^2 \cdot dx$$

in the usual notation. Here  $\delta(1/\rho')$  refers to the change in curvature of the "beam" due to strain, and  $\delta x$  refers to length

along the beam. Now  $\delta\left(\frac{1}{\rho'}\right) = \frac{u + \frac{d^2u}{d\theta^2}}{\rho^2}$  as is well known and

$$u + \frac{d^2u}{d\theta^2} = a_0 + \sum_1^{\infty} a_n (1 - n^2) \cos n\theta + \sum_1^{\infty} b_n (1 - n^2) \sin n\theta$$

$$\text{Therefore } \int_0^{2\pi} \left( u + \frac{d^2u}{d\theta^2} \right)^2 d\theta = \pi \sum_1^{\infty} (1 - n^2)^2 (a_n^2 + b_n^2)$$

to the second order, whence we get for the strain energy,

$$\frac{1}{2} q A k^2 \frac{1}{\rho^3} \pi \sum_1^{\infty} (1 - n^2)^2 (a_n^2 + b_n^2) \quad (12)$$

The question arises, what is the position of the neutral axis? Now, since the elastic energy tends to restrain deformation, it is important not to over-estimate it, otherwise configurations which are unstable might erroneously be thought stable. It is, therefore, advisable to take the neutral axis to pass through the centre of gravity of the cross-section of the wire composing the turn, for by doing so, a lower bound is obtained for the strain energy. (This point, and also the effect of other stresses on the strain energy, has been the subject of much discussion in the theory of the stability of thin shells and pipes. See, for example, Bassett.<sup>(4)</sup>)

We thus have

$$\delta U = -i \frac{\pi}{2} H_0 \sum_{n=1}^{\infty} (1 - n^2) (a_n^2 + b_n^2) - i \frac{\pi}{2} \rho \frac{dH}{d\rho} \sum_{n=1}^{\infty} (a_n^2 + b_n^2) + \frac{\pi}{2} \frac{q A k^2}{\rho^3} \sum_{n=1}^{\infty} (1 - n^2)^2 (a_n^2 + b_n^2) \quad (13)$$

The condition for stability can thus be written, since  $i$  is by convention positive:

$$V = \frac{q A k^2}{i \rho^3} \sum_{n=1}^{\infty} (n^2 - 1)^2 c_n^2 + H_0 \sum_{n=1}^{\infty} (n^2 - 1) c_n^2 - \rho \frac{dH}{d\rho} \sum_{n=1}^{\infty} c_n^2 > 0 \quad (14)$$

where  $c_n^2 = a_n^2 + b_n^2$ .



Now, since the  $c_n^2$ 's are all arbitrary and positive, for stability  $V$  must be positive when all the  $c_n^2$ 's but one are zero, otherwise it is possible to choose values of the  $c_n^2$ 's for which condition (14) is not satisfied. The condition for stability is thus

$$V_n \equiv \frac{qAk^2}{ip^3}(n^2 - 1)^2 + H_p(n^2 - 1) - \rho \frac{dH}{dp} > 0 \quad (15)$$

for all integral values of  $n$ , and condition (14) becomes

$$\sum_n c_n^2 V_n > 0$$

From the equivalence of conditions (14) and (15) we can easily see that:

- no combination of modes of deformation, each separately stable, can be unstable; since all the  $c_n^2$ 's are positive;
- if any one mode is unstable, other modes which alone are stable, can occur in combination with it.

The condition for stability can be further simplified thus. Consider  $V_n$  as a function of  $(n^2 - 1)$ . Then the graph of  $V_n$  against  $(n^2 - 1)$  is a parabola, concave towards  $V_n = +\infty$ , whose intercept on the  $V_n$  axis is  $-\rho(dH/dp)$ , and whose slope there is  $H_p$ . Condition (15) is that  $V_n$  shall be positive for the values 0, 3, 8, 15, . . . of  $(n^2 - 1)$  corresponding to integral values of  $n$ . Let us now consider various cases:

(i)  $H_p$  positive. Here the curve of  $V_n$  starts with a positive slope and increases monotonically with  $(n^2 - 1)$  [see Fig. 3(a)]. The condition for stability is thus  $dH/dp < 0$ . We notice that in this case the presence of elasticity has no effect on the equilibrium, since the mode which would most easily occur is the lowest one ( $n = 1$ ), which corresponds to a uniform translation.

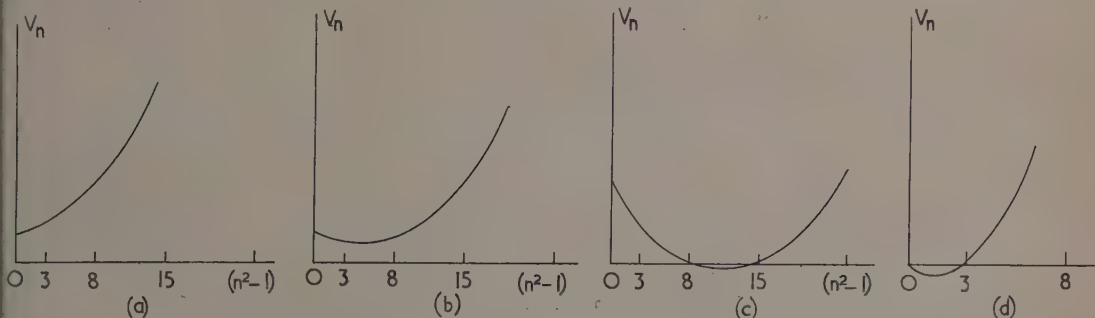


Fig. 3. Diagrams illustrating the stability of a turn against various modes of deformation

(ii)  $H_p$  negative. In this case, the graph of  $V_n$  against  $(n^2 - 1)$  has a negative slope at  $(n^2 - 1) = 0$ . The turn is certainly stable if  $V_n$  is never negative [see Fig. 3(b)], i.e.

$$H_p^2 + (4qAk^2/ip^2)(dH/dp) < 0 \quad (16)$$

This is, however, a more stringent condition than it need be, for [see Fig. 3(c)] it is possible for  $V_n$  to be negative over a range of values of  $(n^2 - 1)$ , and yet be positive for all integral values of  $n$ . An important case where condition (16) breaks down is when  $(dH/dp) = 0$  [see Fig. 3(d)]. Equation (15) can then be written

$$(qAk^2/ip^3)(n^2 - 1) + H_p > 0$$

for  $n > 1$ , since  $(n^2 - 1) > 0$  for  $n > 1$ .

The case of  $n = 1$  is one of neutral equilibrium, as is to be expected, since translation in a uniform magnetic field involves no change in potential energy. Deformation is seen to be easiest for the lowest modes, and for stability against the lowest mode ( $n = 2$ ) we have:

$$(3qAk^2/ip^3) + H_p > 0 \quad (16')$$

Cases which do not correspond to either of the two extremes (16 and 16') can be treated individually, by evaluating  $V_n$  for different values of  $n$ .

We notice that, since elasticity is responsible for the quadratic term which makes  $V_n \rightarrow \infty$  as  $(n^2 - 1) \rightarrow \infty$ , in the absence of elasticity equilibrium is unstable if  $H_p < 0$ .

The conditions for stability can now be summarized:

$$\left. \begin{array}{l} \text{either } H_p > 0; \frac{dH}{dp} < 0 \\ \text{or } H_p < 0; H_p^2 + \frac{4qAk^2}{ip^2} \cdot \frac{dH}{dp} < 0 \end{array} \right\} \quad (16a)$$

*An alternative expression.* The conditions for the stability of a turn can also be written in terms of the mutual inductance of that term with the rest of the circuit. If  $\mu_j$  is the ratio of the current in the  $j$ th part of the circuit to the current in the turn, and  $M_j$  is the mutual inductance of the turn with the  $j$ th part of the circuit, let  $M = \sum_j \mu_j M_j$ . Then the flux linking

$$\text{the turn is } iM = 2\pi \int_0^{\rho} H \cdot r \cdot dr.$$

$$\text{Therefore } H_p^2 = \frac{i}{2\pi\rho} \frac{\partial M}{\partial \rho} \quad \frac{\partial H}{\partial \rho} = \frac{i}{2\pi\rho} \left( \frac{\partial^2 M}{\partial \rho^2} - \frac{1}{\rho} \frac{\partial M}{\partial \rho} \right)$$

The conditions for stability are thus:

$$\left. \begin{array}{l} \frac{\partial M}{\partial \rho} > 0; \frac{\partial^2 M}{\partial \rho^2} - \frac{1}{\rho} \frac{\partial M}{\partial \rho} < 0 \\ \text{or } \frac{\partial M}{\partial \rho} < 0; i^2 \left( \frac{\partial M}{\partial \rho} \right)^2 + \frac{8\pi qAk^2}{\rho} \left( \frac{\partial^2 M}{\partial \rho^2} - \frac{1}{\rho} \frac{\partial M}{\partial \rho} \right) < 0 \end{array} \right\} \quad (16b)$$

*An application.* We can now show that the outer turns of a thick solenoid with rectangular section winding space are intrinsically unstable. Referring to Fig. 4, let  $AB$  be a uniformly wound single layer solenoid, and  $P$  be any point. Let  $\omega_A$  and  $\omega_B$  be the solid angles subtended at  $P$  by the end turns  $A$  and  $B$  of the solenoid. Then, as is well known, the  $z$ -component  $H$  of the field exerted at  $P$  is equal to  $ni(\omega_A - \omega_B)$ .

(The same convention about the sign of  $H$  as earlier in this section applies.) Between the planes  $\alpha$  and  $\beta$ , where  $\omega_A$  is negative and  $\omega_B$  is positive,  $H$  is certainly negative.

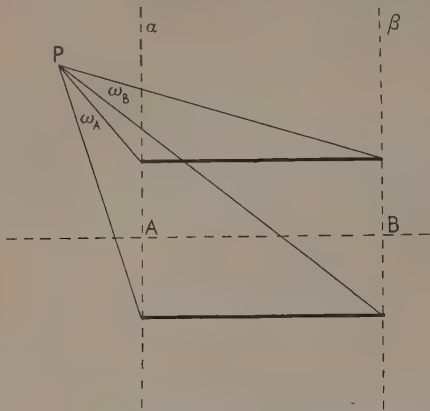


Fig. 4. Diagram illustrating the stability of turns of a solenoid

(N.B.—The windings are to be regarded as an impassable barrier; this makes  $(\omega_A - \omega_B)$  a one-valued function.)

Regarding the thick solenoid as built up of layers, it is seen

that the outside central turn of a thick solenoid is always in a region of negative  $H$ , and hence, by equation (16a), it is intrinsically unstable. The only exception to this is the case of an infinitely long solenoid where  $\omega_A$  and  $\omega_B$  are zero for all the layers. The same argument shows that all the outside turns of all finite rectangular solenoids are intrinsically unstable. Similarly, the central turns of such a solenoid are stable. When it is desired to calculate which parts of a solenoid are intrinsically unstable, and to calculate whether turns are actually unstable taking into account elastic restraining forces, numerical values are needed for  $H$ , and  $(\partial H/\partial \rho)$  [or the equivalent  $(\partial M/\partial \rho)$  and  $(\partial^2 M/\partial \rho^2) - (1/\rho)(\partial M/\partial \rho)$ ], at all points in the winding space. These numerical values have not yet been evaluated.

#### ACKNOWLEDGEMENTS

The author is indebted to the Department of Scientific and Industrial Research for a maintenance grant during the time when this work was carried out; and to Dr. N. Kurti for the interest he has shown in the work.

#### REFERENCES

- (1) COCKCROFT, J. D. *Phil. Trans.*, **A**, **227**, p. 317 (1928).
- (2) KAPITZA, P. *Proc. Roy. Soc. A*, **115**, p. 658 (1927).
- (3) DANIELS, J. M. *Proc. Phys. Soc., Lond.*, **B**, **63**, p. 1028 (1950).
- (4) BASSET, A. B. *Phil. Mag.*, **34**, p. 221 (1892).

## Model to illustrate the behaviour of fixed base portal frames in the plastic range

By M. R. HORNE, M.A., Ph.D., A.M.I.C.E., Department of Engineering, University of Cambridge

[Paper received 29 October, 1952]

The model described reproduces the modes of collapse of a fixed base steel portal frame as predicted by the plastic theory. It is composed of light alloy cubes held together by fine steel wires, the tensions in which determine the strengths of the corresponding members in the structure. Good quantitative agreement is obtained between the observed and theoretical loads necessary for collapse. It is suggested that similar models could be constructed to study the behaviour of more complicated frames.

The plastic theory of structures is receiving increasing attention as the basis of a rational design method for rigid-jointed frames of mild steel.<sup>(1,2)</sup> In applying the design process the frame is proportioned so that it would just collapse under a set of loads of magnitudes equal to the working loads multiplied by a "load factor" greater than unity. Attention is thus directed to the modes of collapse of rigid-jointed steel frames, the behaviour of which may readily be demonstrated by means of the device here described.

The relationship between bending moment and curvature for a mild steel beam takes the general form  $OAB$  (see Fig. 1). The relationship is linear up to the yield moment  $M_y$ , but the curvature increases very rapidly as the full plastic moment  $M_p$  is approached. The general behaviour at collapse of rigid-jointed frames composed of such members may be reproduced by means of models in which the relationship between bending moment and curvature has the form  $OCD$ , provided always that conditions of instability due to axial loads do not occur in the original frame. A photograph of such a model, illustrating the behaviour of a fixed base portal frame, is shown in Fig. 2. The members are composed of Duralumin cubes held together by a thin steel wire under tension. A drawing of one of the cubes within the length of a member

is shown in Fig. 3(a), and a drawing of one of the special cubes used at the corners is shown in Fig. 3(b). Each cube has two knife-edge projections on one face which fit into corresponding grooves on the near face of the adjacent cube. The wire is tensioned by means of helical springs fixed, in the

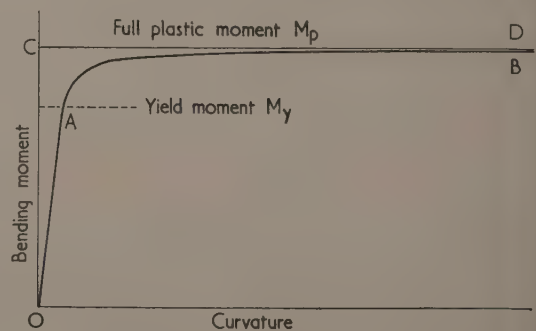


Fig. 1. Bending moment versus curvature relationship for beams according to the plastic theory

case of the beam, to one of the corners, and in the case of the vertical members, underneath the platform on which the portal frame is fixed (see Fig. 2). The cubes remain in contact until the applied bending moment is sufficient to overcome



Fig. 2. Model of portal frame, showing mode of collapse indicated in Fig. 4(b)

the tension in the steel wire, when the cubes can rotate relative to each other through an angle of some  $30^\circ$  without increasing the tension in the wire to any appreciable extent. In this way the idealized moment curvature relationship  $OC D$  (Fig. 1) is obtained.

The model shown in Fig. 2 is subjected to a vertical load applied at the centre of the beam, and a horizontal load applied at the top of one of the stanchion members. The mode of collapse of the frame depends on the ratio of these loads to each other, see Ref. (2). The three modes of collapse which can occur are shown in Fig. 4(a, b and c). The model in Fig. 2 is shown in a state of collapse according to the mode shown in Fig. 4(b), "plastic hinges" occurring at A, C, D and E. The other modes of collapse may be obtained by varying the load ratio.

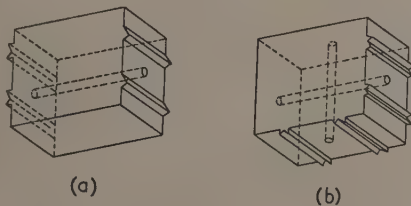


Fig. 3. Isometric views of Duralumin cubes

- (a) within the length of a member
- (b) at a corner of the frame

Fig. 5 shows the relationship for the model between the vertical and horizontal loads when these are made just large enough for collapse to occur. The effective span of the beam was 5.00 in, and the height of the portal frame 2.75 in. The beam had a "full plastic moment" of 0.35 lb in, while each stanchion had a "full plastic moment" of 0.27 lb in. The circles indicate the actual points obtained with the model, while the straight lines represent the theoretical relationship according to the plastic theory. It will be seen that the agreement is quite satisfactory.

While the calculation of modes of collapse is easy in the case of simple portal frames, it becomes more difficult for more complicated frames, and the construction of a model on the lines indicated for such a frame would very much facilitate

investigation of modes of collapse. The relative strengths of the members in a model are readily adjusted by altering the tensions of the steel wires, and hence it would be relatively easy to investigate the effect of varying the relative strengths of the members in any frame.

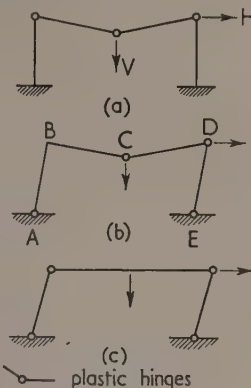


Fig. 4. Modes of collapse of a fixed base portal frame

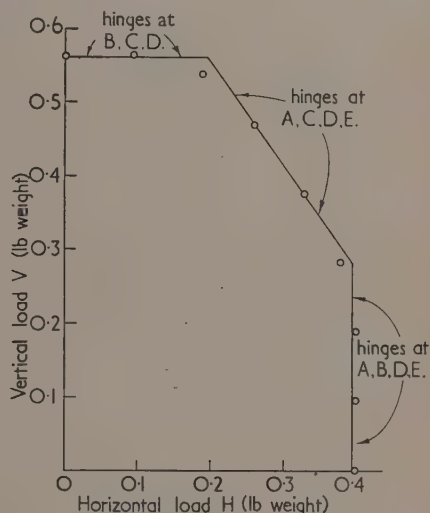


Fig. 5. Relationship between vertical and horizontal loads at collapse. Loads were increased in units of  $\frac{1}{8}$  oz (0.023 lb) until collapse occurred

○ = experimental points

#### ACKNOWLEDGEMENTS

The model here described was designed and made as part of a general investigation into the behaviour of rigid frame structures being carried out, with the support of the British Welding Research Association and the Department of Scientific and Industrial Research, at the Engineering Laboratory, University of Cambridge, under the direction of Professor J. F. Baker. The model was made in the laboratory workshops.

#### REFERENCES

- (1) BAKER, J. F. *J. Inst. Civ. Engrs*, **31**, p. 188 (1948-9).
- (2) BAKER, J. F. *J. Inst. Struct. Engrs*, **27**, p. 397 (1949-50).



# Changes in secondary and thermionic emission from barium oxide during electron bombardment\*

By J. WOODS, Ph.D., and D. A. WRIGHT, M.Sc., F.Inst.P., The M.-O. Valve Co. Ltd., at the G.E.C. Research Laboratories, Wembley, Middlesex

[Paper received 6 October, 1952]

During electron bombardment, the secondary emission from films of barium oxide changes with time in a manner which depends on the film thickness. The changes are due to a reduction process forming an excess of metal within the oxide; subsequent oxidation restores the initial behaviour. The thermionic emission from the films also varies with thickness, and increases as the tendency of the secondary emission to decay increases. Electron bombardment at room temperature lowers the thermionic emission of a thin film by increasing the oxygen concentration at the outer surface, but at temperatures above 500° C this oxygen accumulation does not occur, and the reduction process is a very effective one for activating the thermionic emission.

## 1. INTRODUCTION

In a previous paper<sup>(1)</sup> the authors have described some of the secondary emitting properties of barium oxide. The present work is a continuation of that research, and has been principally concerned with the changes in primary and secondary emission which take place during prolonged running drawing secondary emission under d.c. conditions. As before, the electrostatic deflexion valve was employed, and details of its construction and the experimental techniques used are recorded in the earlier paper.

Thin evaporated films of barium oxide have been examined, as well as coatings formed by spraying barium carbonate on to nickel targets and converting to oxide by heating in vacuum. The thin films were made either by evaporating the barium oxide from a platinum spiral, or by oxidizing an evaporated layer of barium. The secondary emission coefficient,  $\delta$ , was measured with the target and collector at potentials of 240 and 340 V respectively. The area of the film under bombardment was 1 cm<sup>2</sup>, and the current density of the primary beam was 2 mA/cm<sup>2</sup>. During continuous d.c. operation drawing secondary emission, there is always a fall in  $\delta$  after some hours running. This is due to the gradual decomposition of the oxide with the consequent formation of excess barium. In addition there are more complex short time changes which take place within 15–30 min of beginning the bombardment. It is with this aspect of the secondary emission from barium oxide that the present investigation is chiefly concerned.

## 2. FILMS FORMED BY THE EVAPORATION OF BARIUM OXIDE FROM PLATINUM

This section deals with the dependence of  $\delta$  and of the short time changes on film thickness. In several valves the evaporation was carried out at a temperature of 1200° C on to a target of pure nickel at room temperature. Under these conditions a film 10<sup>-4</sup> cm thick was deposited in 20 min. At various stages throughout the deposition, the evaporation was stopped and the secondary emission and its variation with time was noted. The curves in Fig. 1 show some typical time changes for six different film thicknesses. These measurements were made with the targets at room temperature. It will be observed that the short time effects can take three different forms: (i) a rise to a stable value, (ii) a rise to a maximum followed by a slow decay, and (iii) a straight-forward decay. Behaviour of the type (i) occurred when the colour of the film was brownish, with the first order red interference colour just beginning to appear. Type (ii) was prominent in films showing the second order red, and this

form was maintained up to thicknesses showing three complete orders of colour. After further evaporation, changes of type (ii) gave way to type (iii) and the film showed the colours red and green in particular prominence. At the greatest thickness examined, corresponding to curve *F* in Fig. 1, there were about seven or eight orders of fringes visible. It is clear that the type of short time behaviour encountered depends markedly on the thickness of the layer.

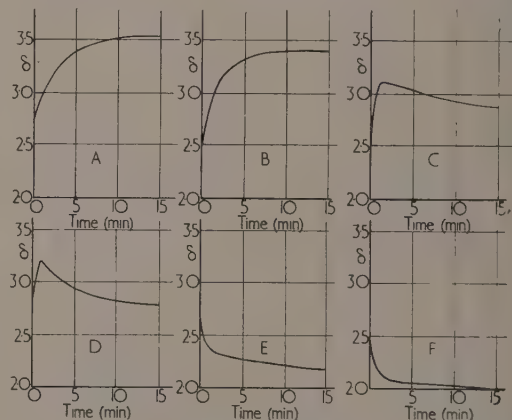


Fig. 1. Variation of  $\delta$  with time at various approximate film thicknesses

A, 10<sup>-6</sup> cm; B, 5 × 10<sup>-6</sup> cm; C, 7 × 10<sup>-6</sup> cm; D, 10<sup>-5</sup> cm; E, 5 × 10<sup>-5</sup> cm; F, 10<sup>-4</sup> cm.

Heating the thinner films at 800° C always tended to send the short time behaviour into the type of change represented to the right of it in Fig. 1. Thus after heating a film originally in a state represented by curve *A*, the subsequent behaviour was as in curve *C*. Heating the thicker films, however, after a curve such as *F* had been obtained, merely restored the initial condition so that the decay took place all over again.

In another valve the nickel substrate was held at 700° C while a film was evaporated on to it from a spiral at 1200° C. This film, which showed the beginning of the first order blue, corresponds to the thickness of films in states yielding curves such as *A* and *B*, Fig. 1. With this valve the initial value of  $\delta$  was 2.2, but drawing secondary emission at room temperature for 15 min caused  $\delta$  to increase to a value of 2.5 only. This indicates that not only the thickness, but also the conditions under which a film is formed are important in

\* Communication No. 529.

determining what changes will be observed. This was confirmed by another experiment in which a film showing seven or eight orders of interference colours was evaporated in 10 sec by heating the spiral to 1400° C.  $\delta$  (18° C) was almost constant at 2.2, but heat treatment at 1000° C introduced a tendency to decay.

### 3. OXIDIZED BARIUM FILMS AND SPRAYED COATINGS

It was shown above that the thickness of films formed by evaporation of barium oxide is a contributory factor in determining what type of short time effect is observed. Films formed by oxidizing layers of barium metal fall into this pattern quite well. Films oxidized by passing a radio frequency discharge in an atmosphere of oxygen at  $5 \times 10^{-3}$  mm of mercury were light brown in colour, indicating very thin layers. These gave short time effects of type (i). Oxidation by heating in oxygen produced films showing second order interference colours, and the short time behaviour was of type (ii). Heat treatment at 800° C of both types of film introduced or aggravated the tendency for  $\delta$  to decay. Although the time changes in secondary emission from evaporated barium oxide and oxidized barium films are similar, there is a considerable difference between their thermionic emissions. This aspect is discussed in the following section.

Sprayed coatings varying in thickness from 0.02 to 0.1 mm all yielded initial values of  $\delta$  (18° C) near 2.0, provided they had been thermionically activated. Unactivated coatings appear to have a high resistance and give values of  $\delta$  close to unity. With properly activated coatings  $\delta$  always decayed during continuous operation drawing secondary emission, and curves such as *F*, Fig. 1, resulted. The nature of the short time effects was not influenced by the base metal of the target, whether it was pure or cathode nickel.

### 4. THE EFFECT ON THERMIONIC EMISSION

In all the films and coatings examined the thermionic emission was measured at 550° C. Initially it was low, of the order of a few microamperes for films of oxidized barium and about 0.5 mA for sprayed coatings. With films of barium oxide evaporated from platinum the initial emission was higher and varied with the thickness of the layer; at the optimum thickness the emission was between 1 and 2 mA. The thin films of both kinds were activated thermionically by drawing secondary emission with  $\delta > 1$ , with the target at 550° C. During this run it was usual for  $\delta$  to increase, although a slight decay sometimes ensued after a maximum was reached. After 20 min or so the best state of activation was reached and the thermionic emission of oxidized barium was then about 0.5 mA, while the emission from sprayed coatings was 5 mA, and that of the evaporated barium oxide films was between 5 and 10 mA for all but the thinnest layers. In many cases this was the highest state of activation achieved. Sprayed coatings treated in this way were no less emissive than coatings activated by drawing space-charge limited emission with the target at 850° C.

With the films of barium oxide evaporated from platinum the effect of activation on the short time behaviour was very similar to the effect of heating at 800° C, in that activation produced a greater tendency to decay. Once the film or coating had been activated a run drawing secondary emission at 18° C with the target at 240 V depressed the thermionic emission by a large factor, no matter what type of curve  $\delta$

passed through. It will be shown in Section 7 that the decay in thermionic emission during a run at 18° C is due to the formation of a surface layer of oxygen, which of itself is not the cause of the changes in  $\delta$ . Further runs drawing secondary emission at 550° C resulted in  $\delta$  either increasing or decaying, but the thermionic emission rose at first, and in some valves continued to rise; in others it reached a maximum and thereafter decayed slowly.

The best thermionic emission obtained from the films formed by evaporation from platinum (10 mA at 550° C) was higher than from sprayed coatings of barium oxide (5 mA at 550° C) activated in the same way; though high emission from evaporated layers was only obtained if the oxide was brought down slowly with the nickel substrate at room temperature. The maximum activated thermionic emission varied with the thickness of the films. As previously stated the thermionic emission of a film as deposited was high, and this unactivated emission varied with the film thickness in exactly the same manner as the activated emission. With a thin layer in the state represented by curve *A* (Fig. 1), the activated emission was about 1 mA; at greater thicknesses, as the secondary emission time changes altered to type (ii) (curves *C* and *D*), the emission increased, and reached a maximum value of 10 to 12 mA when the thickness was sufficient to give curve *E*. At greater thicknesses the emission was reduced to 8 mA. At each thickness tested the pulsed emission at 800° C brightness temperature was determined, using 2  $\mu$ sec pulses with a repetition rate of 50 c/s. For the thinnest films the emission was 1 A/cm<sup>2</sup> at this temperature, but for films thick enough to give curves such as *E*, Fig. 1, the emission had risen to 3 A/cm<sup>2</sup>. After further evaporation, this value was reduced slightly. These values of pulsed emission were maintained constant for at least 20 min, although during this time a small amount of the oxide evaporated from the target.

In contrast with the above results it is important to note that with a film  $10^{-4}$  cm thick, which was brought down in 10 sec, the best available emission was only 0.2 mA. Similarly a thick film evaporated slowly on to a nickel target at 700° C gave low values of emission. It is clear, therefore, that the conditions under which a film is formed determine the thermionic emission available, in addition to determining the nature of the short time changes in secondary emission.

### 5. RUNS WITH $\delta = 1$

When coatings of all three kinds were run under the conditions necessary to make  $\delta = 1$ , that is with the target potential,  $V_p$ , near 30 V, and the collector potential,  $V_c$ , 100 V higher, no evidence of any change with time was forthcoming. Tests were made in the following manner. With a film known to be in a state which would yield a time change such as *A*, Fig. 1, when secondary emission was drawn with  $\delta > 1$ , the value of  $\delta$  at  $V_p = 240$  V was measured. Secondary emission with  $\delta = 1$  was drawn for half an hour with the target at room temperature. After this  $\delta$  was rechecked at the higher target potential of 240 V. No change in  $\delta$  had taken place. Further, with an unactivated target, no change in thermionic emission took place during a run with  $\delta = 1$  with the target at 550° C. When  $V_p$  was increased and secondary emission was drawn with  $\delta > 1$ , thermionic activation took place.

When  $\delta = 1$  the electric field in the oxide is zero. It seemed plausible that the time changes in thermionic and secondary emission which occur when  $\delta > 1$  are related to the electric field set up in the surface layers of the coating



under these conditions. The runs with  $\delta = 1$  were designed to test this point. At first sight the lack of change caused by bombardment with electrons with 30 eV energy suggests that there is some correlation between the time changes and the electric field. However, it is possible that electrons with 30 eV energy cause relatively few structural alterations in a coating compared with electrons with 240 eV energy, and moreover the penetration of the slower electrons will be smaller, which would confine any changes in structure to a superficial layer on the surface of the oxide.

In order to remove these doubts, a series of experiments was made in which the target potential was held at 240 V. The collector potential was reduced until no current flowed in the target circuit, at which point  $\delta = 1$ . In half an hour's run under these conditions  $\delta$  (measured before and after the run with  $V_p = 240$  V and  $V_c = 340$  V) changed just as much as if the collector potential had been at 340 V, where  $\delta$  is much greater than one. In the same way it was shown that the changes took place even when the collector was held 80 V negative with respect to the target, so that all the current flowed through the oxide in the direction opposite to the current flow when  $\delta > 1$ . The time changes in the secondary emitting properties of barium oxide are not, therefore, associated with the electric field in the coating. In a similar manner it was shown that the changes in thermionic emission which occur while drawing secondary emission with  $\delta > 1$  also take place when the coating is merely bombarded with electrons with the same energy and no secondary current is taken.

#### 6. DECAY AND RECOVERY OF THERMIONIC AND SECONDARY EMISSION

While working with films of oxidized barium giving short time effects of type (ii), curves *C* and *D*, Fig. 1, it was found that if the bombarding beam was switched off and the valve left standing idle for 20 min, after secondary emission had been drawn so that  $\delta$  had passed the maximum, the film reverted to its original state. On drawing secondary emission again the same curve was retraced. Similar results have been obtained with thin films of evaporated barium oxide. Only very slight recovery during an off period took place with sprayed coatings and thick evaporated films.

Some experiments were also made on a film of intermediate thickness while the valve was still under exhaust on the pump. First, secondary emission was drawn for 20 min so that  $\delta$  increased to a maximum value of 4.0 and then decayed slightly to 3.7. Oxygen at a pressure of  $10^{-4}$  mm of mercury was admitted for 1 min, and during this time the target was held at 400° C. Afterwards  $\delta$  had increased to a value of 3.8, but decayed on running to 3.6. Oxygen was readmitted and the target warmed as before, but this time the pressure was  $5 \times 10^{-3}$  mm of mercury. This treatment reduced the value of  $\delta$  to 3.0, but on drawing secondary emission  $\delta$  increased to maximum of 4.0 and subsequently decayed to 3.8. To make quite sure that the oxidation and not the warming at 400° C was the cause of the recovery, oxygen at a pressure of  $10^{-2}$  mm of mercury was admitted for 1 min while the target was kept at room temperature. After pumping out the gas,  $\delta$  was found to have a value near 3 and increased when secondary emission was drawn. From these experiments it is clear that the changes produced by drawing secondary emission with  $\delta > 1$  can be eradicated by oxidation. If the oxidation is insufficient, incomplete recovery takes place, but thorough oxidation restores the coating to its initial condition. This evidence establishes that

the time changes are a direct result of the accumulation of excess barium just below the surface of the oxide.

Another experiment performed on the same valve after sealing off and gettering, confirms that oxygen moves to the outer surface of the oxide when secondary emission is drawn with  $\delta > 1$ . With the film of barium oxide in its initial condition with  $\delta = 3$ , barium was evaporated on to it until  $\delta$  had fallen to 1.20. Secondary emission was drawn for 3 h and in that time  $\delta$  rose to a value of 3.5. On standing idle for 20 min  $\delta$  fell to 3.0, but increased on running again. These results show that the evaporated barium had been completely oxidized during the 3 h when secondary emission was drawn. In order to test that the oxidation took place as a result of secondary emission processes, and not because the residual vacuum in the valve was sufficient to convert all the barium to oxide, more barium was evaporated on to the film until  $\delta$  had fallen to a value of 1.4. When  $\delta$  was remeasured half an hour later it was still 1.4, whereas in the previous run when secondary emission was drawn  $\delta$  increased from 1.2 to 2.4 in the first half hour. This shows that the oxidation of the surface barium was entirely due to the secondary emission processes and not associated with the residual vacuum in the valve.

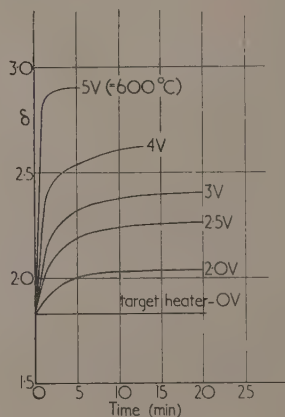


Fig. 2. Recovery of  $\delta$  (18° C) after heating at various temperatures. Before each run  $\delta$  fell from 2.90 to 1.83 while drawing secondary emission at 18° C

The effect of heating on decay and recovery rates was investigated with a film of evaporated barium oxide in a condition represented by a curve such as *E* in Fig. 1. The procedure was to heat the target at 800° C for 5 min, and to measure the value of  $\delta$  at room temperature. This heat treatment was sufficient to establish a reproducible value of  $\delta$ , near 2.8, as a starting point for each decay run. Secondary emission was drawn until  $\delta$  decayed to a value of 1.85. The recovery was observed by measuring  $\delta$  at room temperature after short periods of heating. At room temperature there was negligible recovery, but at higher temperatures there was some degree of recovery, increasing with temperature, until at 600° C recovery was complete in 2 min. These results are shown in Fig. 2. In the second series of tests the decay rate from the standard initial condition was observed as a function of temperature. The curves of Fig. 3 show that the rate of decay decreased as the temperature increased. This is to be expected in view of the results in Fig. 2.



Parallel observations were made on the thermionic emission. In the initial state ( $\delta = 2.8$ ), the primary emission at  $550^\circ\text{C}$  was 6 mA. After  $\delta$  had decayed to 1.85 in the room temperature run, the primary emission had fallen as

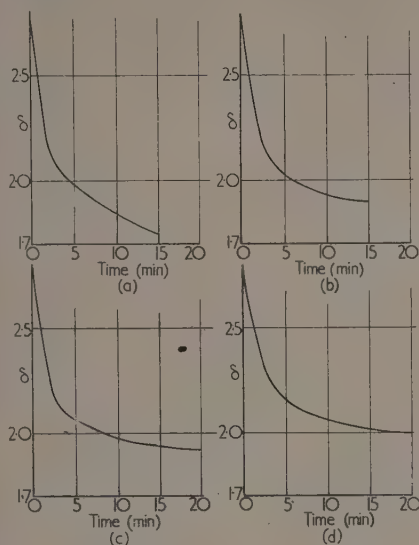


Fig. 3. Secondary emission decay of a thick film of barium oxide at several temperatures

(a) Target heater—OV; (b) IV; (c) 2 V; (d) 2.5 V.

well, to 0.15 mA. The recovery was very similar to that of  $\delta$ , i.e. it was complete at  $600^\circ\text{C}$ , and intermediate at lower temperatures; thus there is a close correlation between the two types of emission as regards decay and recovery effects.

## 7. FLUORESCENCE UNDER ELECTRON BOMBARDMENT

The films of barium oxide formed by evaporation from platinum fluoresce under bombardment by the primary beam with  $V_p = 240\text{ V}$ . In general, if the secondary emission is decaying with time, the intensity of the emitted light decays also. The luminescence is most pronounced with targets at room temperature; the intensity falls with increasing temperature until at  $600^\circ\text{C}$  no luminescence is observed. With the very thin films the emitted light is light blue in colour, at increasing thicknesses a reddish-yellow tinge is apparent, but at the greatest thicknesses of the oxide layer the colour is almost purple. With a thick layer, after  $\delta$  has decayed, and with it the fluorescence, the intensity can be restored, together with  $\delta$ , by flashing the target at  $800^\circ\text{C}$ . The whole cycle of decay and recovery of luminescence and  $\delta$  can be repeated many times.

## 8. THE EFFECT OF SURFACE BARIUM

In general, if a monatomic layer of material such as barium is deposited on a metallic surface, the work function is lowered and there are large changes in thermionic and photoemission. Treloar<sup>(2)</sup> showed that there is some increase in secondary emission, though the effect is small for a given change of work function compared with that on thermionic emission. The effect of a layer of barium on the surface of

barium oxide has not previously been established in detail. In either case it is to be expected that as the thickness increases, the deposition of barium will establish the bulk properties of barium. This will happen at about 4 atomic layers for thermionic emission and at a greater thickness for secondary emission.

On evaporating barium on to a pure nickel target,  $\delta$  rose to a maximum and finally decreased to the value for barium (0.85), as in curve 1, Fig. 4. This corresponds with Treloar's results. On evaporating barium on to an oxidized layer of barium or a sprayed coating, previously flashed at  $1000^\circ\text{C}$  to drive off any excess barium,  $\delta$  decreased continuously with no suggestion whatever of a maximum. Typical results for a sprayed coating are shown in curve 2, Fig. 4. (The details of the further experiments described in this section all refer to one particular sprayed coating, although the results are typical of both sprayed coatings and oxidized barium films.) Following heat treatment at  $1000^\circ\text{C}$  to drive off the first deposition of barium, the experiment was repeated and the thermionic emission at  $550^\circ\text{C}$  was measured. This time there was a definite maximum as curve 3, Fig. 4, illustrates. The thermionic emission increased by a factor of 10, which corresponds with a decrease in work function of about 0.15 eV. It seems reasonable that this small increase would have a negligible effect on  $\delta$ , while the increasing concentration of barium will itself lead to a decrease in  $\delta$ .

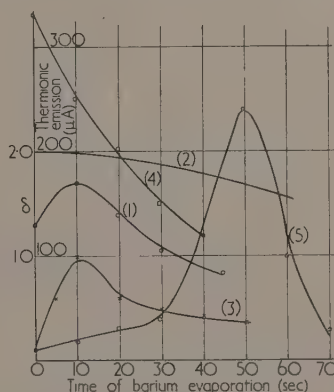


Fig. 4. Effect of thin layers of barium on a sprayed coating

(1)  $\delta$  for barium on nickel; (2)  $\delta$  for barium on barium oxide; (3) thermionic emission, barium on barium oxide after  $1000^\circ\text{C}$  flash; (4) thermionic emission, barium on barium oxide after soaking in barium; (5) thermionic emission, barium on barium oxide after drawing secondary emission.

After the second test, following the deposition of surface barium to a total thickness of 4 mono-layers, the target was heated at  $550^\circ\text{C}$  for 5 min, with the object of diffusing the barium into the oxide. This raised the primary emission from 35 to  $330\text{ }\mu\text{A}$ , higher than during the deposition. When further barium was deposited on the oxide in this condition, the primary emission decreased as in curve 4, Fig. 4. There was now no maximum, indicating that surface barium remained present following the diffusion process, as is to be expected. Heating again at  $550^\circ\text{C}$  raised the emission to  $280\text{ }\mu\text{A}$ , i.e. similar to the previous value and the best encountered.

With this state as the starting point, secondary emission was drawn at room temperature for 15 min. During this

time  $\delta$  fell slightly, and the primary emission was reduced to  $15 \mu\text{A}$ . Following the decay, barium was evaporated on to the surface. The effect on primary emission is shown in curve 5, Fig. 4, where it is seen that there is a rise to a maximum as in the first test. Evidently the decay had been associated with a decrease in the concentration of surface barium. This result indicates that during the secondary emission decay process, barium moves inwards from the oxide surface, or oxygen moves outwards to it, or the two processes occur together.

The experiment was continued by heating again at  $550^\circ\text{C}$ , and restoring the primary emission to  $310 \mu\text{A}$ . Secondary emission was drawn, causing  $\delta$  to fall from 1.9 to 1.5. Barium was deposited on the surface and had little effect on the value of  $\delta$ . The deposition of barium thus had little effect on  $\delta$ , even when the surface had been modified by drawing secondary emission at  $18^\circ\text{C}$ . This shows that the decay in  $\delta$  during room temperature operation is not due directly to the accumulation of surface oxygen. The change in  $\delta$  is caused by the production of excess barium inside the coating, as demonstrated by the effect of oxidation described in Section 6.

### 9. SUMMARY AND CONCLUSIONS

These experiments show that the changes in secondary emission are due to the formation of excess barium in the oxide, in the region penetrated by the incident electron beam. The excess barium is destroyed and the secondary emission restored if oxygen is admitted. If the bombardment is carried out at room temperature, there is a decrease in the barium-oxygen ratio at the outer surface, and probably an actual accumulation of oxygen there, which lowers the thermionic emission. During bombardment at temperatures above  $450^\circ\text{C}$ , however, this relative increase in oxygen concentration at the surface does not occur, and the thermionic emission is increased to the highest value obtainable by any means. The oxygen formed in the decomposition process is either evaporated at this higher temperature, or there is a rapid reversal of barium and oxygen at the surface, maintaining a high emission.

With the thin films near  $10^{-6}\text{ cm}$ , the secondary emission first rises during bombardment, and then remains stable over periods of  $\frac{1}{2}$ –2 h. Thicker films give rise to a flat maximum, and a slow decay; the initial value is a little higher than with the very thin films. When the thickness approaches  $10^{-5}\text{ cm}$ , the initial value is lower, and there is a decay immediately on bombardment. As thickness increases further, the initial value continues to fall slowly, and the decay effects remain similar. The thermionic emission has an initial value which increases with thickness up to about  $10^{-5}\text{ cm}$ , and then falls a little and becomes constant. The highest state of activation gives an emission about three times as large as the initial value at all thicknesses.

With films of thickness  $10^{-5}\text{ cm}$  or greater, after a decay in secondary and primary emission has occurred while bombarding at room temperature, the values are stable at room temperature. Heating to  $600^\circ\text{C}$  restores the initial values in a few minutes, while intermediate temperature gives a partial restoration. There is evidently a diffusion process which is effective at  $600^\circ\text{C}$  in redistributing the excess barium, but at room temperature the diffusion rate is negligible with these films. This is not true, however, with thinner films. The recovery rate at any temperature is more rapid the thinner the film; with films of thickness  $10^{-6}\text{ cm}$ , recovery to the initial values occurs within 15 min at room temperature in the best attainable vacuum.

These results show that the diffusion rate decreases as thickness increases, until  $10^{-5}\text{ cm}$  is reached. Now the excess barium is produced in the surface layers penetrated by the primary beam, so that the lower the rate at which barium can diffuse away from these layers, the faster will be the changes in secondary emission coefficient. Thus the observed variation of diffusion rate with thickness, as indicated by the recovery processes, is consistent with the observed variation in the rate of change of secondary emission. The variation in diffusion rate must cause at least part, and perhaps all, of the variation in the rate of change of secondary emission.

As the thickness increases, up to  $10^{-5}\text{ cm}$ , it appears that the initial concentration of free barium increases. This is indicated both by the increase in thermionic emission, and by the variation of the initial value of the secondary emission. Thus it is possible that the diffusion rate is inversely dependent on the concentration of excess barium already present, and that this is the parameter whose increase with thickness influences all the observed features of the changes in secondary emission. On the other hand there may be some other structural differences, in addition to the increasing free barium concentration, which tend to lower diffusion rates as thickness increases. It is hoped to obtain information on this point by electron diffraction studies.

The interpretation of the changes in secondary emission as due to increasing barium concentration requires that at high concentration,  $\delta$  falls as concentration rises. This is to be expected as soon as coagulation of the excess barium occurs to form colloidal particles, since the secondary emission of barium metal is only 0.8; moreover, colloidal particles will act as traps for secondaries liberated in the surrounding oxide. At low concentration, it is reasonable to suppose that there can be an increase in  $\delta$  with concentration, due to (a) the rising conductivity of the coating, making easier the replacement of emitted secondaries, (b) secondary emission from the free barium atoms, and (c) if the free barium is present in the form of negative ion vacancies, their gradual occupation by electrons might lower the trapping probability of internal secondaries at the vacancies (this cannot be taken for granted, however, since there is a considerable probability of trapping a second electron). If any of these factors are operative there will be a maximum in  $\delta$  as concentration rises, as observed.

In view of the recovery of  $\delta$  on exposure to oxygen, the residual oxygen pressure must influence the rate of change of  $\delta$  during bombardment. It seemed possible that the increased rate of change with thickness might be due to a continuous fall in residual pressure during evaporation of barium oxide. This point has been checked by giving much more rigorous outgassing treatments than normal, to all the tube components, and then, before evaporating on to the target, volatilizing a quantity of barium oxide on to the surroundings equivalent to 200 atomic layers on the target. This gave the same variation of rate of change with thickness as in the normal procedure, thus, although oxygen pressure is important, its variation is not the cause of the variation of behaviour with thickness.

The changes in  $\delta$  and in thermionic emission during bombardment with 240 V electrons are independent of the magnitude and even the direction of the potential gradient in the coating, so that the ion flow is not the cause of the decomposition process. This must be attributed directly to the electron bombardment. The subject of decomposition under electron bombardment is under further investigation, and will, it is hoped, be dealt with in a later publication.

In order to obtain stability of secondary emission, the conclusions are that it is desirable to have (a) a high diffusion rate, attained either by control of structure or by raising the temperature sufficiently, (b) a residual oxygen pressure sufficient to oxidize the excess metal as formed in the oxide, and (c) a compound where the bond is not wholly ionic; the structure is required to be stable after an electron transition has occurred in the lattice as a result of electron bombardment, and this will be then more readily achieved the more the bond is of the co-valent type.

#### ACKNOWLEDGEMENTS

In conclusion, the authors desire to tender their acknowledgements to the M.-O. Valve Co. Ltd., on whose behalf the work described in this publication was carried out.

#### REFERENCES

- (1) WOODS, J., and WRIGHT, D. A. *Brit. J. Appl. Phys.*, **3**, p. 323 (1952).
- (2) TRELOAR, L. R. G. *Proc. Phys. Soc., Lond.*, **49**, p. 392 (1937).

## NOTES AND NEWS

### New books

**Electrodynamics.** By A. SOMMERFELD. (New York: Academic Press Inc.) Pp. xiii + 371. Price \$6.80.

This book is the third of a series which forms the printed version of a course of lectures on theoretical physics. The author is a master both in research and in its lively exposition. We can therefore assume authenticity and significance and only consider the author's selection and the standard he intends for his readers and hearers. His method is to examine at some length and establish the basic principles and equations. The theory is then developed into its most important branches as far as the principles and mathematical relations on which detailed solutions of particular problems can be founded. A few well-known problems are solved in illustration where the mathematical detail is simple enough not to distract attention from principles for too long. The scope is the theory of the electromagnetic field on a macroscopic scale, that is, excluding phenomena of the close propinquity of atoms or of detailed atomic structure which cannot be replaced by a continuum. Part I gives the electromagnetic equations in the Maxwellian form. The treatment is based on the concept of the field from which can be deduced charges, currents and potentials. Part II covers the application of Maxwell's equations to the most important macroscopic phenomena, the electrostatic field, charges, the dielectric field, the analogous magnetic phenomena, stationary currents, distributed currents and rapidly varying currents leading to electromagnetic waves in wires, wave-guides and free space. Part III is entitled "Theory of relativity and electron theory." In fact it covers the special theory of relativity applied to electromagnetism, based on the invariance of Maxwell's equations, so that relativistic kinematics are not given independence. The author follows Minkowski as far as possible. Part IV extends the theory to moving media, forces and radiation with its reactions, ending with a brief outline of the nature of the general theory of relativity.

One might criticize the author for ignoring or barely mentioning alternative methods of development which are as likely ultimately to prove correct as those he selects. On the other hand, his selection is probably the easiest to follow and leads quickly to those results which are of practical importance or current interest. His account is so lively and clear and illuminates so many branches of physics, that a more comparative treatment would have diminished its readability. It is a most attractive and stimulating book.

S. WHITEHEAD

**Color in business, science and industry.** By D. B. JUDD. (London: Chapman and Hall Ltd.; New York: J. Wiley and Sons, Inc.) Pp. ix + 401. Price 52s.

Whatever the merits—and they are by no means inconsiderable—of this book as a contribution to applied physics, there can be no doubt of its illuminating testimony to American public psychology. For, as the preface remarks, "The colors of consumer goods profoundly influence consumer acceptance." And, thus, the technique of colour science has gone from strength to strength. Actually, a very sound basis is laid by starting with the human eye as receptor, and the impact of colour sensation upon it. Then follows a sufficient but somewhat over-simplified treatment of the necessary instrumentation, reinforced by a wealth of diagrams and charts, including one in colour from the Munsell book.

There are copious references and—a welcome feature—tables of absorption/scattering ratios, and hyperbolic cotangents. All this does not amount to anything very original, but colour laboratories will be well advised to have Dr. Judd's volume near at hand.

F. I. G. RAWLINS

**Canterbury project—New Zealand Radio Meteorological Investigation.** (3 volumes.) (Wellington, New Zealand: Department of Scientific and Industrial Research.) Pp. xi + 858, 283, 187.

Experiments on anomalous radio wave propagation were made in the United Kingdom throughout the 1939–45 war and in U.S.A. from 1943–46, but only limited success was obtained in correlating field strength with the refractive index profile along the path. A joint long-term investigation was made by the Departments of Scientific and Industrial Research of the United Kingdom and New Zealand during the period September 1946–December 1947. Vol. I contains details of the meteorological and radio equipment and the experimental technique employed together with details of the sites used. Typical weather situations at Canterbury were used and for each occasion the modification in the structure of air temperature, humidity and refractive index along a track out to sea is described, and the meteorological and radio data discussed. All the observations are tabulated. Vol. II contains graphs for ninety sets of observations of all meteorological data comprising land and ship soundings to obtain wind, potential temperature and specific humidity together with charts of the synoptic situation. Vol. III contains graphs of radio-wave propagation for each occasion. The results



obtained were analysed jointly by New Zealand staff under R. S. Unwin and by G. G. Macfarlane and others of the Telecommunication Research Establishment (Ministry of Supply). The meteorological conditions and refractive index structure are summarized in two tables and the conclusions drawn are considered to be largely qualitative even for this area across the Canterbury Plain and out to sea. This comprehensive report has however provided much information of great value.

R. S. READ

[A few copies are available on loan from the Central Radio Bureau, First Avenue House, High Holborn, London, W.C.1.]

**Practical spectroscopy.** By T. A. CUTTING. (London: W. Heinemann Ltd.) Pp. viii + 220. Price 10s. 6d.

This book has the same title as a major textbook published in the U.S.A. which covers the subject much more completely; it may be that this author used the title first, but this British edition does not state the date of the original American edition. A few of the errors in the earlier edition have been corrected, and the list of U.S. apparatus dealers has been replaced by a list of British dealers; also the list of elements has been brought up to date in one part of the book, but not throughout.

"Popular spectroscopy" would be a better name for this book, which is suitable for mineralogists or geologists who are neither physicists nor chemists. If trained in physics, they would be put off by the absence of any mathematical formulae, by a diagram to illustrate series in line spectra captioned "Hydrogen atoms" and by a naïve attitude towards electricity. Chemists will be amused by the odd pieces of information about each element, unless shocked by a statement such as "Hydrofluoric acid has many of the properties of the element and is about as toxic"!

Useful features of the book are its straightforward approach to the problem of building a spectroscope for oneself; the instructions are clear enough for the reviewer to have followed them in making a simple spectroscope in his own basement. There is also helpful information about the recognition of lines in the visual spectrum, and about the arc spectra of certain minerals. The author omits descriptions of ordinary spectroscopes, skipping from the home-made one to a brief description of a quantumeter. Analytical spectroscopists should beware of this book, which compensates for its lack of precise information with a certain charm, so that one goes on reading it to the end.

E. VAN SOMEREN

**Practical physics.** By W. LLOWARCH. (London: Longmans, Green and Co. Ltd.) Pp. xii + 266. Price 12s. 6d.

This volume is strongly recommended for, in addition to covering the ground of sixth form and first year university physics experiments, it has additional attractive features. The apparatus demanded is mostly simple and can often be "home-made"; the questions included are designed to make the student think about the work he has done; simple electronic apparatus is introduced at an early stage, for example, to enliven practical sound; and some new experiments, not found in the older texts, are introduced.

The simple line drawings used are clear except in one or two cases, e.g. Fig. 68 illustrating Fresnel's biprism might not be understood.

The "fiction" of the magnetic pole, associated with  $4\pi m$  lines of force, is preserved in introducing practical magnetism. Though this goes against some recent theoretical texts, yet it is a wise introductory method.

J. YARWOOD

**The structure and properties of mild steel.** By C. A. EDWARDS. (London: J. Garnet Miller Ltd.) Pp. 222. Price 20s.

So far as the reviewer is aware, this is the first published monograph on mild steel. Hitherto, the available literature has been widely dispersed in the transactions and proceedings of various technical and scientific societies, but here we have a concise summary of the information and views which have been put forward through the years. In writing this book the author, who is one of the world's leading authorities on the subject, has had in mind the student and the practical man who is called upon to use mild steel. The work is presented simply and, at least in the opening chapters, technical terms have been avoided as far as possible.

The earlier chapters deal briefly with steel-making, micro-structure and constituents, the effect of heat treatment and cold work. Consideration is given to the effect of various elements, present in very small quantities, but which may exert a considerable influence in mild steel, which otherwise is virtually pure iron. For example, the presence of 0.10% nickel, which in a structural steel would be disregarded, leads, it is stated, to certain difficulties in the manufacture of tin plate.

The later chapters dealing respectively with age-hardening, strain age-hardening, quench age-hardening, cold-rolling and pickling, are based on papers previously presented by the author to the Iron and Steel Institute and in these the reviewer finds a slight change in style. For instance, in the earlier chapters the processes of normalizing and annealing are very fully described and defined whilst in the later chapters such terms as "skin pass" are used without any explanation.

Although primarily intended for students, this will form a most valuable work of reference. It is, however, unfortunate that the quality of the paper in particular, and to some extent the reproductions, should fall so far below the high standard of the text.

A. K. OSBORNE

**X-ray crystallographic technology.** By A. GUINIER. (London: Hilger and Watts Ltd.) Pp. xiii + 330. Price 55s.

The original French edition of this book, published in 1945, was acclaimed as an invaluable handbook of X-ray crystallography, and this revised English text has gone far towards remedying the few points which were previously criticized. The title is no longer ambiguous, and indicates clearly that the contents are primarily intended, not for those who solve atomic structures, but for those who use X-ray methods as an important but auxiliary research tool. The amount of theoretical treatment given (partly in appendices) is, however, such that all students of the subject will benefit, and the book has the great merit of explaining many small points, not usually mentioned in text books, which may puzzle the beginner.

More than half of the book is concerned with experimental methods and their applications, the latter being described in general terms and illustrated by an admirable choice of examples. A fair assessment is given of the difficulties and limitations associated with X-ray methods.

The usefulness of the text has been much enhanced by the addition of a subject index and of a combined name and bibliography index, but it must be admitted that in some respects the book has not been improved by translation. The treatment of Bravais lattices does not differentiate clearly between lattice type and atomic structure, and another long-standing confusion has been perpetuated by applying both of the terms "structure factor" and "structure amplitude" to

the same expression. The literal translation "crystal base," meaning the arrangement of atoms within the unit cell, reads commendably briefly, but "crystals with base" does sound a little odd, and there are other examples which are perhaps even more misleading.

These defects are, however, outweighed by the merits of the book, which can therefore be recommended with confidence to all who use X-ray diffraction methods.

A. M. B. DOUGLAS

**Dictionary of conformal representations.** By H. KOBER. (New York: Dover Publications Inc.) Pp. xvi + 208. Price \$3.95.

If one complex variable is an analytic function of another, and each is represented in an Argand diagram, so that, for example, the point  $z = x + iy$  is plotted as  $(x, y)$ , then obviously a curve in the plane of the first variable corresponds to a different curve in the plane of the second variable. In particular, by suitable choice of the functional relationship, a given curve in the first case may correspond to a circle or straight line in the other. The advantages of this procedure in devising map projections, and in solving flow problems, where flow lines and equipotentials can be transformed into networks of mutually perpendicular lines, are obvious. The difficulty is usually to find the function that effects this.

The present dictionary, prepared in the (British) Admiralty during the war, shows the transformations which can be effected by a great number of different functions, taken in turn. The ideal dictionary for this work would perhaps be arranged the other way, that is to show how a given curve could be transformed to a straight line, but meanwhile, this will be of great value to workers in such fields as electricity, hydrodynamics, aerodynamics and heat flow. It is reproduced from typescript, and is copiously illustrated with graphs.

J. H. AWBERY

**Advances in electronics. Vol. 4.** Edited by L. MARTON. (New York: Academic Press Inc.) Pp. x + 344. Price \$7.80.

The several articles in this volume of *Advances in electronics* can be divided into three groups, each article being an authoritative survey in its own particular field, well supplied with references, with the exception of that on *Electronic digital computers* by C. V. L. Smith; although from this broad title one would have expected a dissertation on such devices, in fact only two American machines are described and the article, good though it is in its limited way, does not really fit into the pattern that it is believed these volumes are intended to cover.

On the other hand, though in one group specific types of instrument are described, these have a wide appeal and represent the results of much widespread research and development. It is particularly opportune to study *The scintillation counter* by G. A. Morton and *The magnetic airborne detector* by W. E. Fromm; the former is a valuable tool in nuclear research for the detection of high energy radiations whilst the latter, after its war-time development for submarine detection, bids fair to becoming of great use in geophysical prospecting.

The second group comprises *Modulation of continuous-wave magnetrons* by J. S. Donal and *Multichannel radio telemetering* by M. G. Pawley and W. E. Triest; the modulation of large continuous powers is a requirement for communication purposes at very high frequencies, whilst the transmission of quantities of information over short periods

of time is a necessity in recording data in many applications, e.g. high-altitude rockets.

Theoretical aspects are treated in the third group in two well-written articles; *Electron scattering in solids* by H. S. W. Massey, and *Fluctuation phenomena* by A. van der Ziel.

A. J. MADDOCK

**Electric fuses. A critical review of published information.** By Dipl. Ing. H. LÄPPLE. (London: Butterworths Scientific Publications.) Pp. viii + 173. Price 25s.

This critical review, published for the Electrical Research Association, was prepared by the Chief Engineer of the Fuse Gear Department of Siemens Schuckertwerke, Berlin, who visited this country under the Darwin scheme especially to do this work. The book, which reviews practically all important available literature, comprises seven chapters as follows: Introduction; The circuit-breaking process; Breaking-capacity; Deterioration of fuse-elements owing to corona effects; Time/current characteristics; Ratings, rules, requirements and standards; and Special fields of application for fuses.

The information is presented in an interesting way by a commercial fuse-gear engineer with a profound appreciation of the practical problems, and the comments, which appear frequently throughout the text, are enlightening and constructive.

The last ninety pages are devoted to a useful bibliography of 267 references, each reference being followed by a short summary. The book will interest not only fuse-gear engineers, but also those concerned generally with the problem of protection. Its appeal to the student might be increased if it were more liberally illustrated.

H. W. BAXTER

**Television.** By F. KERKHOF and W. WERNER. (London: Cleaver Hume Press Ltd.) Pp. xv + 434. Price 50s.

The qualified radio engineer who wishes to become familiar with the principles of modern television receiver design will have difficulty in finding a suitable book on the subject. *Television* will fulfil his need admirably. One of the Philips Technical Library series, it was written as a result of a course of lectures given to engineers training for development work in television technique.

The subject matter begins with a general review of television and proceeds, via the normal path of principles of electronic scanning and pick-up tubes, to detailed descriptions of standard signals, synchronizing signal separators, pulse and waveform generators, time bases and e.h.t. supplies. About one-third of the book is devoted to wide-band amplifiers, and there are chapters on transmission lines, aerials and, as might be expected, on the design of a projection system. Circuits and descriptions of two typical receivers are given, and there is a short chapter on modern colour systems. An extensive bibliography is included.

The book is a translation, and occasionally reads rather oddly; as, for example, "The time signals . . . are the line-synchronizing pulses, also referred to as line sync pulses, owing to their pulse-like character"; but the few lapses will not cause the reader any inconvenience. The mathematical treatment, in rationalized M.K.S. units throughout, is in small print and according to the authors may be omitted if necessary. The whole work is of an excellent standard and will probably be very welcome to many engineers who have specialized in some sections of television development, in addition to those just beginning work in this field.

R. D. NIXON



## Notes and comments

### Elections to The Instituté of Physics

The following elections have been made by the Board of The Institute of Physics:

*Fellows:* G. N. Bhattacharya, D. D. Lindsay, C. W. Miller, G. R. Richards, E. Robinson.

*Associates:* J. A. Balchin, A. H. Bedford, F. Blaha, A. F. Blanchard, E. J. Burton, W. W. H. Clarke, J. K. Claxton, R. L. Durant, A. N. Gent, A. M. Grant, J. A. Greenacre, K. D. Hall, E. H. Hirsch, H. E. Hogwood, G. Hulse, R. Ingham, F. Jackson, D. Jones, P. E. Knapp, B. E. Knight, A. Lempicki, W. M. Morley, J. W. Noakes, J. L. Olsen, M. E. Peplow, M. B. Pinder, L. J. R. Postle, M. H. Roberts, C. B. Sharma, D. I. Smith.

Fifty-nine Graduates, thirty-one Students and four Subscribers were also elected.

### Discussion of proposed weights and measures legislation

In October 1948 the President of the Board of Trade appointed a committee "to review the existing weights and measures legislation containing provisions affecting Weights and Measures and the administration thereof, and to make recommendations for bringing these into line with present-day requirements." The Report of this committee was completed on 13 December, 1950, published on 15 May, 1951 (Cmd. 8219, price 4s. 8d. post paid), and was summarized in the September 1951 issue of this *Journal*.

The President of the Board of Trade has now arranged for consultations of the recommendations of the committee to take place with trade associations, local authorities and other interests concerned; and comments are invited on any of the committee's recommendations. Persons or organizations intending to submit comments are requested to give the Board of Trade notice of their intention to do so and indicate the recommendations on which they propose to comment. All correspondence should be addressed to the Controller, Standards Department, Board of Trade, 26 Chapter Street, London, S.W.1.

### British Standards Institution

The British Standards Institution has announced that at the end of next summer it will change its address from No. 24 Victoria Street, London, S.W.1, to No. 2 Park Street, London, W.1. The new accommodation will be called British Standards House, and since it is a single, self-contained office block it will enable the staff and facilities to be concentrated under one roof and thus contribute to more efficient operation of the Institute's services.

Although the new premises have a floor space not substantially greater than the combined floor space of the several premises at present occupied, there will be accommodation for the nearly 4000 committee meetings which the B.S.I. convenes in the course of a year.

### Second international congress on rheology

The British Society of Rheology, supported by the Joint Commission on Rheology of the International Council of Scientific Unions, is arranging the Second international congress on rheology, to be held at St. Hilda's College, Oxford, from 26-31 July, 1953. The congress will cover the whole field of the study of the deformation and flow of matter, except such specialized subjects as have come to be regarded as branches of applied mechanics, e.g. the classical theory of elasticity or aerodynamics. The programme will include a presidential address, a number of invited lectures, and a discussion on the international organization of rheology. As stated in the October 1952 issue of this *Journal* (p. 336) the organizing secretary is Dr. G. W. Scott Blair, The University, Reading, Berkshire.

An exhibition of commercially available rheological testing apparatus will also be arranged, further details of which may be obtained from the exhibition secretary, Mr. E. B. Atkinson, c/o B.X. Plastics Limited, Research Station, Lawford Place, Manningtree, Essex.

## British Journal of Applied Physics

### Original contributions accepted for publication in future issues of this Journal

A method of observing selected areas in electron and optical microscopes. By J. F. Nankivell.  
Electronic control of a synchronous motor. By L. U. Hibbard.  
An apparatus for measuring the coefficient of thermal conductivity of solids and liquids. By T. A. Marshall.  
Techniques for the electron microscopy of crystals. By I. M. Dawson.  
Measurements of saturated-diode stability. By V. H. Attree.  
Apparatus for the automatic electrical ignition of the d.c. arc in spectrographic analysis. By J. M. Nobbs.  
The origin of specimen contamination in the electron microscope. By A. E. Ennos.  
The two-dimensional magnetic or electric field above and below an infinite corrugated sheet. By N. H. Langton and D. Davy.

## Journal of Scientific Instruments

### Contents of the February issue

#### ORIGINAL CONTRIBUTIONS

Design of a high-resolution electron diffraction camera. By J. M. Cowley and A. L. G. Rees.  
Intense drying of gases with potassium metal. By E. R. Harrison.  
A moving coil galvanometer of extreme sensitivity. By K. Copeland, A. C. Downing and A. V. Hill.  
The Brownian fluctuations of a coupled galvanometer system. By A. V. Hill.  
A wide range temperature controller using a resistance element. By S. J. Borgard.  
The power factor and capacitance of mica capacitors at low frequencies. By P. R. Bray.  
An optical system and thermopile amplifier for double-beam recording of infra-red spectra. By J. L. Hales.

#### LABORATORY AND WORKSHOP NOTES

Insulated electrical leads into pressure vessels. By H. D. Parbrook.  
A contact bush for use in lead castles with type M6 Geiger-Müller tubes. By L. W. Blow.  
A positive action vacuum valve. By A. H. Morton and P. M. Jeffery.  
A modification to the hot-wire thermal precipitator. By J. K. Donoghue and D. G. Drummond.

#### CORRESPONDENCE

The temperature coefficient of the e.m.f. of Kalium cells. From M. W. Jervis.  
Measurement of small voltages and currents at high potentials. From C. H. Hertz.  
A versatile X-ray camera for low-angle diffraction studies. From J. B. Fineman.

#### MANUFACTURERS' PUBLICATIONS NEW INSTRUMENTS, MATERIALS AND TOOLS NOTES AND COMMENTS

THIS JOURNAL is produced monthly by The Institute of Physics, in London. It deals with all branches of applied physics (including theory and technique). All rights reserved. Responsibility for the statements contained therein attaches only to the writers.

**EDITORIAL MATTER.** Communications concerning editorial matter should be addressed to the Editor, The Institute of Physics, 47 Belgrave Square, London, S.W.1. (Telephone: Slone 9806.) Prospective authors are invited to prepare their scripts in accordance with the *Notes on the Preparation of Contributions*. (Price 2s. 6d. including postage.)

**REPRODUCTION.** The Institute of Physics is a signatory to The Royal Society's Fair Copying Declaration. Details may be obtained upon application from The Royal Society, London, W.1.

**ADVERTISEMENTS.** Communications concerning advertisements should be addressed to the agents, Messrs. Walter Judd Ltd., 47 Gresham Street, London, E.C.2. (Telephone: Monarch 7644.)

**SUBSCRIPTION RATES.** A new volume commences each January. The charge is £4 per volume (\$11.50 U.S.A.), including index (post paid), payable in advance. Single parts, so far as available, may be purchased at 8s. each (£1.15 U.S.A.), post paid, cash with order. Orders should be sent to The Institute of Physics, 47 Belgrave Square, London, S.W.1, or to any bookseller.



## Processes of convection and evaporation\*

By E. G. RICHARDSON, B.A., Ph.D., D.Sc., F.Inst.P., King's College, Newcastle-upon-Tyne

The use of non-dimensional parameters to express the results of heat transfer experiments and analogies with other problems in fluid mechanics are discussed. Applications of fundamental processes in convection are instanced in the thermal precipitator and hot wire anemometer. As examples of processes involving convectational evaporation the liquid drop and the wetted plate exposed to the wind and the application of such laboratory experiments in large-scale industrial plants and in meteorology are discussed.

The scientist who has even a general acquaintance with fluid dynamics cannot have failed to realize the importance in the study of convection and evaporation of the parameters, Reynolds number, Froude number and (latterly) of Mach number—parameters which having no dimensions describe the scale of a flow phenomenon and allow one to relate experiments done on a model scale with those performed at full scale. Whereas these three will suffice for most experiments in conventional aero- or hydro-dynamics, when one has, in addition, to cope with convection or evaporation they do not cover all the possible variables that may be involved in an experiment. In fact, the subjects that are treated in this article fairly bristle with non-dimensional quantities, though I shall endeavour to limit those I introduce to the essential. When a parameter has reached a certain numerical value, determined by experiment, a change in the type of flow takes place. The existence of these "magic" numbers, as of all magic numbers, is, of course, a confession of weakness, weakness in our knowledge of the fundamental processes involved and of the means of solving the mathematical equations. It is, however, not to be supposed that the contriving of parameters amounts to mere juggling with dimensions, for they all must be based on some knowledge of the underlying physical processes.

Experiments on heat transfer are simplified by the introduction of a fortunate analogy, that between the heat loss from a body and the loss of concentration by diffusion of a diffusible material applied to its surface. In both of these transfer operations we are usually concerned with a rate of loss of heat or material which is so great compared with that due to pure conduction or molecular diffusion that the direct contribution of these factors to the process may be neglected. Nevertheless, the coefficient of thermal conductivity  $k$  or rather that of thermal diffusivity  $\kappa$  (i.e. the conductivity divided by the specific heat per unit volume) is a factor in every convection process, since it is the fundamental physical property of the fluid involved, which takes the place of the coefficient of kinematic viscosity ( $\nu$ ) in constant temperature flow.

## NATURAL CONVECTION

So we shall relate the loss of heat from a body to two parameters, one the usual Reynolds number of the flow and the other the Prandtl number ( $\nu/\kappa$ ) which characterizes the fluid. If as in a number of gases  $\kappa = \nu$ , we need the Reynolds number only. From the heat loss from a body characterized by the linear dimension  $d$  at a not too large excess of tem-

perature  $\theta$  over its surroundings we can construct two non-dimensional quantities. If natural convection is taking place local differences in weight of portions of fluid, hence  $g$ , must come in and the coefficient of expansion  $\beta$ . From these Grashof constructed a dimensionless parameter  $Gr = d^3 g \beta \theta / \nu^2$ . In forced convection or diffusion where the velocity  $U$  must intervene a simpler form

$$Pe = Ud/\kappa$$

(Péclet number) suffices. To express the heat loss  $H$  per unit area per sec itself in non-dimensional form it is usual to employ the Nusselt number

$$Nu = Hd/k\theta.$$

Then the results of a series of heat transfer or diffusion experiments should be capable, when plotted in this form against Grashof or Péclet number for free or forced convection respectively, of reduction to a single line (if several fluids are used in the series allowance must of course be made for the respective relationship between  $\kappa$  and  $\nu$  in the different fluids).

When the flow over the solid is sufficiently fast for the critical value at which turbulence supervenes to be exceeded we may use the "boundary layer" concept of Prandtl,<sup>(1)</sup> i.e. we can estimate the thickness  $\delta$  of the thin layer in which the temperature falls from that of the solid to that of the general fluid and express the ratio of this to the width of the body as a dimensionless distance  $\delta/d$  in function of  $Gr$  or  $Pe$  as the case may be.

In natural convection it appears that  $\delta/d$  is proportional to  $Gr^{-1/4}$ ; in forced convection, authorities differ, making it depend on various powers of  $Pe$  between 0.5 and 0.8. One of the causes for the discrepancy is the uncertainty in the value to be ascribed to  $k$ . Thermal conductivity (and viscosity) vary with temperature and one is obliged to assign to them a mean value throughout the boundary layer.

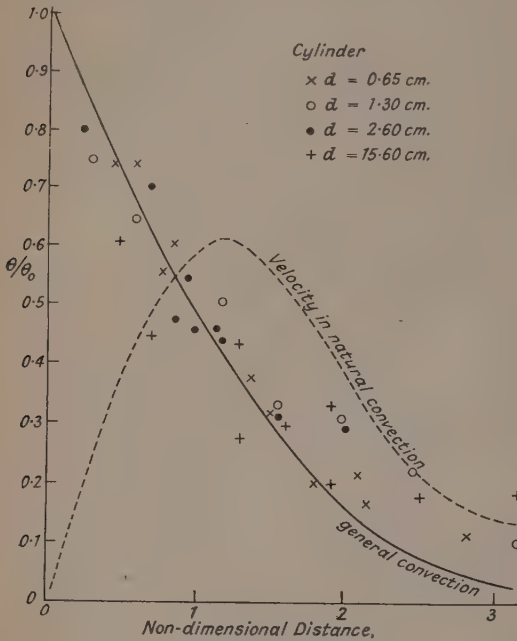
The author<sup>(2)</sup> has measured the temperature along a median horizontal plane in the vicinity of electrically heated cylinders in natural convection in air and his temperature results are grouped on Fig. 1 in the form  $\theta/\theta_0$ ,  $\theta_0$  being the temperature of the cylinder surface, against  $\delta/d$ . The velocity distribution is also plotted on the same basis.

These changes in boundary layer thickness are of course accompanied by changes in the temperature wake corresponding to those well known in the case of sphere or cylinder. To demonstrate the analogy between convection and diffusion we illustrate two stages in the regime of flow past a sphere.

Fig. 2(a) is of a drop of liquid titanium chloride which, falling through air at a speed of about 10 cm/sec liberates smoke which diffuses into the wake to form the well-known

\* Based on a lecture given to the Scottish Branch of The Institute of Physics on 9 December (in Glasgow) and on 10 December, 1952 in Edinburgh.

stationary eddies, pertinent to flow at a low Reynolds number. Fig. 2(b) is a *Schlieren* photograph due to E. Schmidt<sup>(3)</sup> of the quasi-turbulent heat wake in the rear of a sphere (shown in outline by broken line) of diameter 2 in. in natural convection where the fluid is optically "troubled" by the fluctuations in density set up.



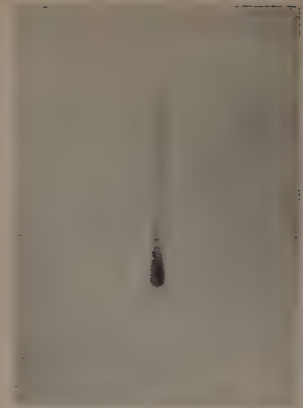
Reproduced from the *Philosophical Magazine*

Fig. 1. Temperature and velocity distribution in the median plane through a heated cylinder in natural convection

Two interesting sidelights on this natural convection problem may here be mentioned.

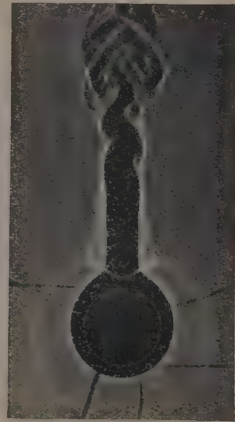
Although it appears to lead to no industrial application and would in any case be a very inefficient process it is possible to derive a lifting force on a hot cylinder from the currents and density differences set up near it. This the author<sup>(2)</sup> has investigated with hollow cylinders of glazed Vitreosil (carrying internal heating coils) and supported on the arm of a force balance inside a vertical wind-tunnel. The lifting force due to natural convection is found to vary as the  $\frac{3}{4}$ th power of the excess temperature and the square root of the radius. When the tunnel wind was turned on the drag of the hot cylinder was found to be less than that of the cold (at any rate, up to Reynolds numbers of about 3000). This effect is presumably due to the hot boundary layer having a greater kinematic viscosity, whereby the layer is "lubricated" and thereby the transition to turbulence delayed, a matter of moment in supersonic aircraft, where a wing may be warmed by friction at its high speed of translation through the air.

In a hollow cylinder or sphere there is of course an additional force due to buoyancy, which aeronauts such as the Montgolfier brothers in earlier times exploited in the fire-balloon. Such a "lift" much outweighs that due to isothermal currents of the same magnitude. (It is probably true



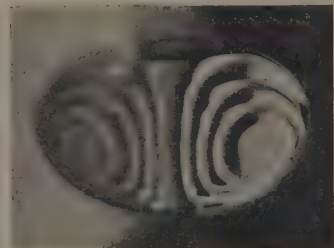
Reproduced from *Science Progress*

(a) Falling drop of smoke-producing liquid (Author).



Reproduced from *Forschung. a.d. Gebiet des Ingenieurwesens*

(b) Schlieren photograph of natural convective flow from heated sphere (E. Schmidt).



Reproduced from the *Proceedings of the Physical Society*

(c) Circulations set up in large falling drop of liquid (K. E. Spells).

Fig. 2. Types of convective flow

to say that Archimedes' principle does not apply to such a case, but it is a nice exercise to examine the "why not!")

The other application is of industrial importance, though the householder would probably regard it rather as a nuisance. It is well known that solid particles are driven out of a convection boundary layer into cooler regions—hence the black stains on the walls above radiators or panel-heaters in a room—leaving the so-called "dust-free space" surrounding the sources of heat. In the "thermal precipitator," much used now for sampling mine dust, an electrically heated wire spans the space between two nearby and parallel vertical plates (shown in section in Fig. 3). If the thickness of the hot

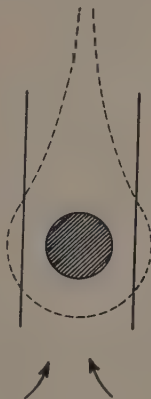


Fig. 3. Dust-free space of wire in vertical tube

boundary layer in the median plane—indicated roughly in Fig. 1 by the distance in which the temperature falls to one-tenth that of the wire—exceeds the separation of wire and plate, all the dust sucked in from the coal face is caught by the plates, which may then be removed for counting and sizing of particles.<sup>(4, 5)</sup>

#### FORCED CONVECTION

In forced convection there is likewise a temperature boundary layer, specified by Péclet number, which replaces the isothermal velocity boundary layer, characterized by Reynolds number. After allowing for the higher mean coefficient of kinematic viscosity in the former, due to the variation of density with temperature, the two layers may be considered continuous. This means that in this case momentum and heat are transported at the same rate. In other cases, for example, that of a jet of hot air debouching into a cold atmosphere, it has been claimed by comparison of the temperature and velocity profiles that matter and heat are transported at a slightly higher rate than momentum.<sup>(6)</sup> This may be explained by saying that momentum transport gets up advancing pressure gradients which act as a barrier to its further transport but do not stop heat passing through.

For the thin plate, the boundary layer thickens from the leading edge so that  $\delta$  is proportional to  $y\sqrt{(U/x)}$  where  $x$  is the distance along and  $y$  distance perpendicular to the plate. This is a theoretical prediction due to Blasius and Pohlhausen,<sup>(8)</sup> valid over a considerable range of Reynolds (or Péclet) number. A similar relation holds for the hot

cylinder from which King<sup>(9)</sup> derived the calibration curve for the hot-wire anemometer, namely

$$\frac{Hd}{k\theta} = 1 + \left(\frac{\pi U d}{2\kappa}\right)^{1/2}$$

or

$$Nu = 1 + \sqrt{(\pi/2) \cdot (Re \cdot Pr)^{1/2}}$$

The heat loss from a ferromagnetic sphere in forced convection in a tube has been measured by Kramers,<sup>(10)</sup> the heat being supplied from outside the tube by electromagnetic induction. His results fit an equation:

$$Nu = 2 + 0.66 \cdot Re^{0.5} Pr^{0.31}$$

plus a small correction for low Reynolds numbers. The fluids used were air, water and oil.

All the instances of convection that we have quoted so far are ones in which a steady state is implied, but there is one unsteady case at least which has such importance that it should be mentioned, i.e. that in which a thin electrically heated wire is used to measure quasi-periodic or turbulent flow. Solving the equations for heat loss from a cylinder with retention of a term in  $\partial\theta/\partial t$  one finds a solution involving a "thermal inertia" factor. This explains why, in a regime involving a fluctuating flow, the wire responds with only a fraction of that change of temperature proper to an infinitely slow variation of velocity. This inertia factor is rather like the time factor of an electric circuit containing resistance and capacitance and this thought gives the clue to the method of correction to be adopted, i.e. to put an additional electrical delay in the circuit, which further delays the fluctuation of resistance experienced by the hot wire, until the phase lag comes full circle. This adjustment must of course be dependent on frequency, but it is possible in the amplifier to make the response independent of frequency over a considerable range and—to this extent—make the hot-wire measure the local intensity of turbulence in the stream where the wire is exposed.

#### DIFFUSION AND EVAPORATION

The equivalence of diffusion of heat and matter in a turbulent field leads to two methods of studying such a field of flow, in a gross method as opposed to the rather tedious point-to-point investigation which the hot-wire demands. In this technique a spot or a line source, depending on whether the flow is believed to be three or two-dimensional, is set up in which heat,<sup>(11)</sup> smoke,<sup>(12)</sup> or a dye<sup>(13)</sup> is let out into a stream and the temperature or concentration determined at a limited number of points. In such a fashion the author has studied the diffusion of turbulence in the vicinity of a plate immersed edgewise in a water channel which it completely spanned. The source was a line of dye (potassium permanganate) along the leading edge, but initially pasted over with a water-solvent glue, to enable a steady flow to be set up before diffusion of the dye commenced. The concentration at various localities  $(x, y)$  over the plate was measured by a traversing pencil of light athwart the channel falling on a photocell.

It should be obvious from what has gone before that we can transpose problems in heat loss and diffusion into the corresponding problems in evaporation, with the added complication that the latter process requires the provision of latent heat. The difference of vapour pressure at the free surface—usually taken at its saturation value—and that further away will form the potential gradient. One would



rightly guess natural evaporation to be an intractable subject of investigation, but forced evaporation lends itself fairly readily to comparison of theory with experiment.

Mostly the subject of researches of this type has been the "wet plate," in the form of a sheet of liquid-impregnated blotting paper laid out in a wind-tunnel, or a sphere or cylinder covered with impregnated paper with initially dry air aspirated over the paper, subsequently removed and reweighed after a suitable time-interval.<sup>(14,15)</sup> When turbulence is fully developed the rate of evaporation is found to be proportional to  $U^{0.8}$  which result can be assimilated to a one-seventh power law of variation of velocity with distance from the solid.<sup>(16)</sup> Such inconsistencies as are observed in practical experiments are mostly to be ascribed to transitory flow; laminar flow at the leading edge, gradually leading to turbulence and the consequent variations in velocity profile in this transition regime.

(In all these cases we are assuming that the turbulent diffusion or "eddy viscosity" coefficients are large enough to swamp the corresponding molecular coefficients.)

#### EVAPORATION OF LIQUID DROPS

Though the evaporation from plane surfaces on a large scale has of course meteorological implications, a more important case is that of the liquid drop evaporating into a gas stream. This has applications not only in meteorology to the fall of raindrops, but industrially in cooling towers for dissipating heat from hot water spray; conversely in spray-drying where a solution to be dried is "atomised" into a fine spray and shot at high speed into hot gas; thirdly, in fuel-oil injection as a spray into a cylinder.

The author has carried out experiments which refer particularly to the first and last of these applications. The drop and the gas were, however, initially at the same temperature.

At the time when these experiments were commenced in 1943, data were required for military purposes on the rate of evaporation of drops falling freely over a 100 ft or so in still air. For this purpose the pagoda in Kew Gardens, London, was opportune, having had holes cut in every storey so that a small drop of liquid could be released from a microburette at the top and its time of fall to the bottom (110 ft) measured as well as its size on release and in fall. Fig. 2(a) is in fact a photograph of such a drop of smoke-producing liquid taken a few feet below the release point.

For the evaporation loss of a drop of diameter  $d$  of liquid of molecular weight  $M$  in still air, the expression deduced by Langmuir, i.e.  $2\pi d(MDp/R\theta)$  holds,  $D$  being the diffusivity and  $R$  the gas constant.

If we may assimilate the expression in brackets to the thermal conductivity  $k$  and the evaporation to the heat loss coefficient per unit temperature excess  $H/\theta$ , we derive for the sphere in still air  $Nu = 2$ . When the drop is in relative motion with respect to the gas a term for convective evaporation must be added. Frössling<sup>(19)</sup> put this in a form which may be compared with that of Kramers, already quoted, for the heat loss from a sphere in forced convection, thus:

$$Nu = 2 + 0.55 \cdot Re^{1/2} Pr^{1/3}$$

In the Kew experiments, values for  $Nu$  as a function of  $Re$ , deduced from the time of fall and change of size *en route*, indicated that the Frössling theoretical rates were too low, particularly for liquids having a high rate of evaporation.

In more recent experiments drops have been supported on fine wire rings about 1 mm diameter enclosing fine thermo-

couples mounted in a small wind-tunnel (Fig. 4). Knowing the latent heat of the liquid in the drop, it is then possible to measure the rate of evaporation from the fall of temperature in the drop while a steady wind blows upon it (cf. Fig. 5).

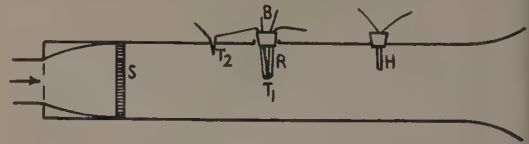


Fig. 4. Wind-tunnel and supported drop for evaporation experiments

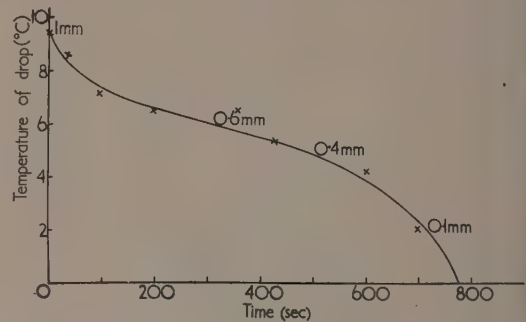


Fig. 5. Fall of temperature and decrease of diameter of a drop in forced evaporation

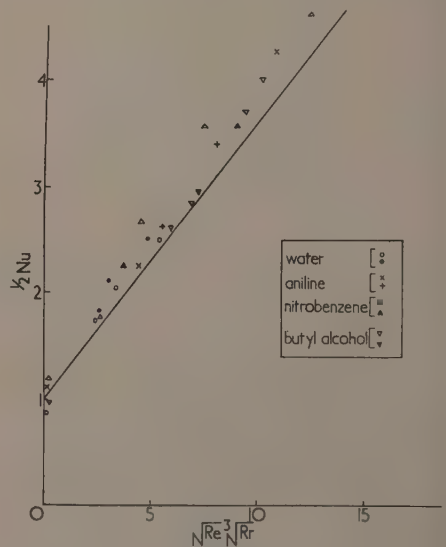


Fig. 6. Evaporation experimental results plotted non-dimensionally

By introducing gauzes at the entry of the tube, a controlled form of turbulence was introduced into the air and measured by hot-wires employed in the way already referred to. Again, values somewhat in excess of Frössling's values were obtained, especially at the higher intensities of turbulence. The general

form of Frössling's expression was, however, confirmed (see Fig. 6).

Of course, during evaporation the drop cools; rapidly, after it has passed a critical small radius. The steep fall of temperature at the start (Fig. 5) is possibly due to the rotations set up in a large drop, slowing down as the drop gets smaller. The circulation currents in large falling drops have been illustrated by Spells,<sup>(18)</sup> who injected dyes for this purpose (Fig. 2c). Such simultaneous measurements of size and temperature give information on the formation of hail and the cooling of drops in spray coolers.

Although these drops were initially at the temperature of the surrounding fluid, experiments such as these have relevance to many fuel injection and spray drying problems when the drop is initially at a higher temperature, as already remarked, and permit what might at first sight seem a complex process of heat transfer to be expressed in a comparatively simple formulae. These formulae can be replaced by nomograms of Nusselt, Prandtl and Reynolds numbers, for the convenience of the engineer.

#### ATMOSPHERIC CONVECTION AND EVAPORATION

In concluding this account something should be said of the relation of these processes to large-scale movements in the atmosphere. The agricultural applications of large-scale evaporation have already been thoroughly treated in an article by Penman,<sup>(19)</sup> and will not be further discussed here, but the atmosphere is a vast laboratory in which processes of mass, heat and water vapour transfer may be studied in relation to our puny experiments in turbulent flow in wind-tunnels. Most of these movements have been correlated with the well-established empirical law of Sutton<sup>(20)</sup> based on the idea that these entities are transported by a vertical mixing of eddies in accordance with which the mean wind varies with height  $z$ , thus  $U = U_0(z/z_0)^{n/(2-n)}$ . The exponent  $n$  must be interposed from the results of experiment and is of order 0.2 to 0.25 depending on prevailing meteorological conditions.

There is one important difference in the mechanism of heat and momentum transport in the atmosphere, as Priestley and Swinbank<sup>(21)</sup> point out. Hot air is buoyant and tends to carry energy up with it. This acts as a "free-convection" correction on the forced convection due to turbulent winds and may result in an upward transport of energy in a region where the gradient of mean temperature is negative.

Both Swinbank<sup>(22)</sup> and the writer<sup>(23)</sup> have measured the temperature and wind fluctuations at a fixed point near the ground. The former has also measured vapour pressure fluctuations.

Fig. 7 shows, as an example of the author's measurements, simultaneous fluctuations of velocity (as variations of hot-

wire resistance) and of temperature (as modulations of a 1000 c/s a.c. carrier wave in a circuit containing a thermistor). These cathode ray oscillographs records were obtained 6 ft above the level of a grassy field.

What is wanted for these experiments is a value of the mean and r.m.s. fluctuation in the mass transport of air, i.e. of  $\bar{\rho w}$  where  $\rho$  is the instantaneous density and  $w$  the vertical component of velocity at the instant and site of the instrument, to which the heat transport per unit area is related by the expression  $c\bar{\rho w}(T_0 + T_1)$ , wherein  $c$  is the specific heat,  $T_0$  the mean and  $T_1$  the amplitude of fluctuation of temperature. In both the investigations mentioned, the required products were obtained by combinations of thermocouples and hot-wires and rather intricate circuitry.

So far, however, these investigations have not passed beyond the instrumental stage. Reports are merely of "try-outs" in typical sites. The problem of convection and evaporation in the atmosphere itself in whole or in part has scarcely been tackled experimentally and obviously entails a major co-operative research by many meteorological stations.

#### REFERENCES

- (1) PRANDTL, L. *Proc. Maths. Congress* (Heidelberg: 1904).
- (2) RICHARDSON, E. G. *Phil. Mag.*, **23**, p. 681 (1937).
- (3) SCHMIDT, E. *Forsch. a.d. Geb. d. Ingenieurwes.*, **3**, p. 181 (1932).
- (4) WATSON, H. H. *Trans Farad. Soc.*, **32**, p. 1073 (1936).
- (5) PARANJPE, M. K. *Proc. Ind. Acad. Sci.*, **4a**, p. 423 (1936).
- (6) HINZE, J. O., and VAN DER HEGGE ZIJNEN. *App. Sci. Res.*, **A**, **1**, p. 435 (1949).
- (7) BLASIUS, H. *Z. angew. Math. u. Phys.*, **56**, p. 4 (1908).
- (8) POHLHAUSEN, F. *Z. angew. Math. u. Mech.*, **1**, p. 115 (1921).
- (9) KING, L. V. *Phil. Trans.*, **A**, **214**, p. 373 (1914).
- (10) KRAMERS, H. *Physica*, **12**, p. 61 (1946).
- (11) SCHUBAUER, G. B. *National Advisory Committee for Aeronautics Report*, No. 524 (1935).
- (12) ROBERTS, O. F. T. *Proc. Roy. Soc. A*, **104**, p. 640 (1923).
- (13) RICHARDSON, E. G. *Proc. Phys. Soc., Lond.*, **49**, p. 484 (1937).
- (14) PASQUILL, F. *Proc. Roy. Soc. A*, **182**, p. 75 (1943).
- (15) DAVIES, D. R., and WALTERS, T. S. *Quart. J. Mech. Appl. Math.*, **4**, p. 466 (1951); *Proc. Phys. Soc., Lond.*, **65B**, p. 640 (1952).
- (16) POWELL, R. W. *Trans Instn Chem. Engrs*, **13**, p. 36 (1940).
- (17) FRÖSSLING, N. *Beit. zu. Geophysik.*, **52**, p. 170 (1938).
- (18) SPELLS, K. E. *Proc. Phys. Soc., Lond.*, **65B**, p. 541 (1952).
- (19) PENMAN, H. L. *Brit. J. Appl. Phys.*, **2**, p. 145 (1951).
- (20) SUTTON, O. G. *Proc. Roy. Soc. A*, **135**, p. 143 (1932); **A**, **146**, p. 701 (1934).
- (21) PRIESTLEY, C. H. B., and SWINBANK, W. C. *Proc. Roy. Soc. A*, **189**, p. 543 (1947).
- (22) SWINBANK, W. C. *J. Met.*, **8**, p. 135 (1951).
- (23) RICHARDSON, E. G. *Proc. Roy. Soc. A*, **203**, p. 149 (1950).

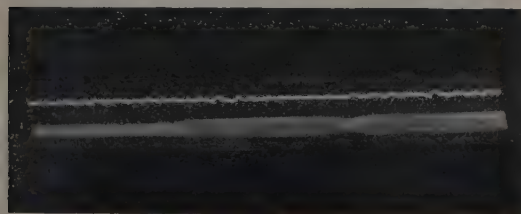


Fig. 7. Simultaneous records of atmospheric fluctuations of velocity (above) and temperature (below)

# The effects of oxygen on the electrical properties of oxide cathodes

By A. A. SHEPHERD, M.Sc., Ph.D., A.Inst.P., Physics Department, University College of North Staffordshire

[Paper first received 22 October, and in final form 23 November, 1952]

The mechanism of reduction of electron emission from oxide-coated cathodes by oxygen, and the recovery process after oxygen poisoning, have been studied using mass spectrometer techniques, showing that the formation of singly charged oxygen ions in the cathode coating plays a major part in the recovery process.

Further studies employing diodes having a helical probe embedded in the cathode coating provided information on the reduction of coating conductivity by oxygen, the results being explicable on the basis of the Loosjes and Vink theory of conduction, which postulates two conduction processes in the cathode, one predominating below, the other above 700° K.

The results obtained in both series of experiments are discussed, and a mechanism is proposed to account for the observed phenomena on the poisoning of emission and conductivity of cathode coatings by oxygen.

## 1. INTRODUCTION

Although the phenomenon of reduction of electron emission from oxide cathodes by oxygen has been known for some time, the exact mechanism of this poisoning has not been determined. Metson<sup>(1)</sup> has demonstrated the reversibility of poisoning by oxygen, and his results imply that a likely mechanism for recovery of emission after poisoning is the outward diffusion of negative oxygen ions from the oxide cathode coating.

In §2 experiments are described in which a mass spectrometer with an oxide cathode source was used to attempt to detect any change in negative oxygen ion emission from the cathode on poisoning.

In order to determine more details of the poisoning process, further experiments (described in §3) were carried out, using low voltage diodes with a probe embedded in the cathode coating. This enabled the effect of oxygen on both emission and coating conductivity to be studied.

## 2. OXYGEN ION EMISSION

**Apparatus.** The type of mass spectrometer tube used was developed for general measurements of negative ion emission from oxide cathodes, and covers a range of mass numbers up to 50. It is designed with a view to maintaining the best possible vacuum conditions, and dispenses with auxiliary focusing electrodes, employing a small electron gun of simple construction for the ion source, in which all parts can be efficiently eddy-current heated. The principle of magnetic focusing of the ions is used, making for simplicity of construction, and a cathode modulator section which is easily interchangeable without loss of alignment is incorporated.

The tube is shown in Fig. 1. A gun system is used to produce the electron and ion beams, and also contains an oxygen-producing filament for poisoning experiments. The parts employed are commercially used in magnetic cathode-ray tubes and were supplied by Ferranti Ltd. The anode is a closed nickel cylinder with an aperture at each end, which is clamped to an inner glass tube on the spectrometer envelope. Behind the anode, four projecting ceramic rods allow the modulator-cathode section to slide on to them, giving correct alignment when this section is replaced. The cathode carries a nickel-tungsten thermocouple for temperature measurement. Between anode and modulator is mounted an alumina-coated tungsten wire coated with barium peroxide, which,

when heated, evolves oxygen at an easily controllable rate. The tube envelope is flattened in the spectrometer plane at the section where deflexion of the ions takes place, and is here coated internally with colloidal graphite to prevent bulb charges on the inner walls.

The collecting head consists of a flat nickel plate maintained at anode potential by a spring clip to the graphite coating, a

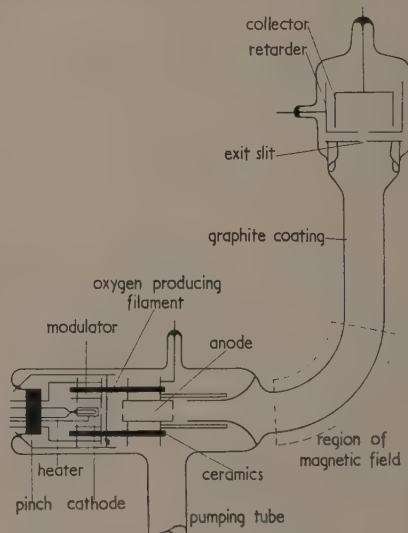


Fig. 1. The mass spectrometer tube

retarder electrode, and a beam collector. The collector slit, 1 mm wide, is arranged to be collinear with the cathode and the centre of curvature of the deflector section of the spectrometer, so that ions leaving the cathode are refocused at the slit. The collecting Faraday cylinder is screened from the anode by the retarder electrode, which carries a 2 mm slit, and care is taken to ensure a long electrical leakage path between collector and retarder leads.

The anode voltage of the spectrometer is supplied from a bank of h.t. batteries, and is normally kept fixed at about



1 kV. The modulator-cathode voltage is continuously variable from  $-20$  V to  $+20$  V and the retarder-cathode voltage is continuously variable from  $-75$  V to  $+75$  V.

The ion currents flowing to the collector are measured by an electrometer valve circuit using a type BM2 electrometer tetrode with a grid resistor of  $10^{10} \Omega$ ; currents are recorded by a galvanometer, the overall sensitivity of the circuit being about  $2 \times 10^{-12}$  A/cm deflexion.

The system of recording ion currents is to keep the h.t. voltage constant, and vary the magnetic field which is produced by an electromagnet having a maximum field strength in the region of 2500 oersted. The magnet is standardized at a fixed point on the hysteresis cycle and the ion beams swept past the collector in turn by varying the magnet current by means of a motor-driven rheostat.

*Oxygen ion emission during recovery from poisoning.* A mass spectrometer tube of the type described was constructed, with a mixed (barium-strontium) oxide cathode as source. The tube was pumped out, and baked for four hours at  $400^\circ\text{C}$ , and all electrodes were heated to a bright red heat to facilitate outgassing. The cathode was then broken down and activated in the usual way, and when activation was complete, the tube was isolated by a tap immediately below the baked section of the system. A getter was then fired, when the pressure remained at about  $10^{-7}$  mm of mercury.

The mass spectrum was comparable to those previously obtained in similar tubes.<sup>(2)</sup> The mass numbers of the ions were determined by calibrating the spectrometer, using the  $\text{Cl}_{35}^-$  and  $\text{Cl}_{37}^-$  peaks as standards, since these always occurred and were easily recognizable. The ions found for the first cathode were  $\text{Cl}_{35}^-$ ,  $\text{Cl}_{37}^-$ , an ion of mass number 43,  $\text{CNO}_{42}^-$ ,  $\text{Al}_{27}^-$  and  $\text{O}_{16}^-$ . No trace of  $\text{O}_{32}^-$  was found.

Energy distribution measurements were then made on the oxygen ions by the retarding potential method. Before these experiments were made, the cathode had been left cold for several days, and on running it again, a considerable increase in the  $\text{O}_{16}^-$  ion intensity was noted, although the pressure in the tube had not altered, nor had any other ion intensities.

The retarding potential curve obtained for  $\text{O}_{16}^-$  is shown in Fig. 2. This is typical of all cathodes examined. It would appear that all the oxygen ions emitted possess excess energy, since no decrease in intensity takes place until the retarding voltage is less than 2 V positive of the cathode, which corresponds to the effective potential of the coating surface. Two factors contribute to this effective potential:

(a) Voltage drop in the coating, which is estimated from the electron emission and the conductivity measurements of the same coating material described later.

(b) Contact potential difference between the retarder electrode and cathode. In this case, the current voltage characteristics for electron emission at low temperatures indicated a contact potential difference of 0.6 V.

Combination of these two factors indicated an effective potential of the coating surface in the region of 2 V. Hence it may be assumed that the entire oxygen flux is provided by the sputtering off of a surface layer of oxygen by positive ion bombardment since this is the only reasonable explanation of the possession of excess energies. The increase in oxygen ion flux after standing cold for some time may be due to the accumulation of such a surface oxygen layer.

The experiments to determine the results of oxygen poisoning of such cathodes were carried out as follows.

Before poisoning experiments were commenced the emission characteristics of the cathode were taken at low temperatures ( $567$ – $689^\circ\text{K}$ ) to enable a Richardson plot to be drawn. Although the method of Richardson plots is

not a satisfactory one for the absolute determination of work functions, comparison of Richardson lines before poisoning and after recovery gives an indication of whether the cathode surface has suffered a permanent change as a result of a series of poisoning attacks.

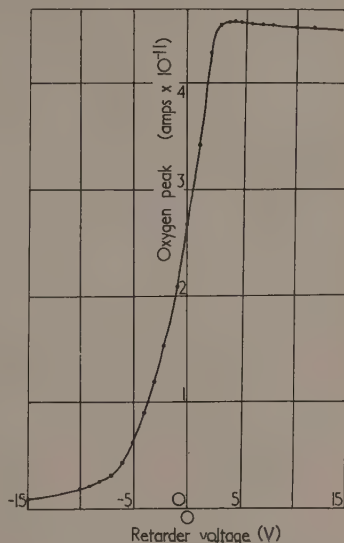


Fig. 2. A typical retarding potential curve for the ion  $\text{O}_{16}^-$

In a typical experiment, the work function of the cathode before commencing poisoning was  $1.10$  eV as determined by Richardson plot, the modulator-cathode contact potential being  $0.8$  V. Oxygen was then released in the spectrometer until the electron emission was reduced to  $\frac{1}{10}$ th of its original value, when the oxygen flow was cut off and the variation of both the electron emission and  $\text{O}_{16}^-$  emission with time were subsequently recorded.

The results of one such experiment, at a cathode temperature of  $1200^\circ\text{K}$  with modulator  $10$  V positive of cathode, are shown in Fig. 3. The emission current was reduced by the

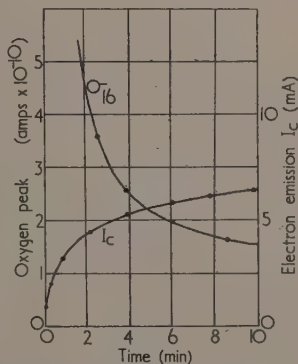


Fig. 3. Showing the variation in electron emission and  $\text{O}_{16}^-$  ion emission during recovery from poisoning at  $1200^\circ\text{K}$

presence of oxygen from 8.5 mA to 0.85 mA and the oxygen ion current, measured soon after recovery had commenced, had increased by a factor of 3, gradually falling to its original value as recovery was completed. The oxygen pressure in the tube during poisoning reached a maximum of  $3 \times 10^{-5}$  mm of mercury. Very similar results were obtained for cathode temperatures of 1100° K and 1000° K, but a marked increase in sensitivity to poisoning was noted at the lower temperatures; at 1100° K, the oxygen pressure needed to reduce emission to  $\frac{1}{3}$ th of its original value was  $5 \times 10^{-6}$  mm of mercury, while during poisoning at 1000° K the pressure did not rise above  $10^{-6}$  mm of mercury. This would appear to indicate that the mechanism of poisoning is due in some degree to an increase in surface work function caused by adsorption of the gas on the cathode crystal surfaces, since this would take place with increasing ease at lower temperatures.

After the cathode had been running for 100 h, the emission measurements at low temperatures were repeated, with the following results:

Mean modulator-cathode contact potential 0.72 V.

Work function from Richardson plot,  $\phi = 1.08$  eV.

The decrease in contact potential difference after 100 h is probably due to the evaporation of cathode material on to the modulator. The value of  $\phi$  shows no significant change (within the limits of experimental error) which shows that

cathode in the mass spectrometer to determine the effect of varying potential gradients in the coating on  $O_{16}^-$  ion emission during recovery, since Metson<sup>(1)</sup> suggested that increasing potential gradients in the coating would result in more rapid ejection of oxygen ions. Three sets of recovery characteristics were plotted at a temperature of 1200° K, the initial currents being 2, 5.3 and 7 mA. These currents were chosen from the "saturation" range of the current voltage characteristic, in order to avoid space charge effects. In each case the emission current was reduced to 10% of its initial value by releasing oxygen in the tube, and the emission current and  $O_{16}^-$  peak height were measured continuously from the time the oxygen flow was discontinued. The characteristics are shown in Fig. 4. In each characteristic it will be seen that two regions exist, the initial varying recovery rate and one of almost constant recovery rate during the subsequent period. During this second period the recovery rate depends on the potential gradient in the coating during recovery, as may be seen from the fact that the rate successively increases from Fig. 4(a) to Fig. 4(c). In Fig. 4(a) it will be seen that the initial rate of decrease in  $O_{16}^-$  peak height is lower than that in Figs. 4(b) and 4(c). Although this would appear to indicate a lower rate of ejection of ions from the coating, the evidence is by no means conclusive since an unknown contribution to all the  $O_{16}^-$  curves of Fig. 4 exists due to ions formed in front of the cathode surface (see later).

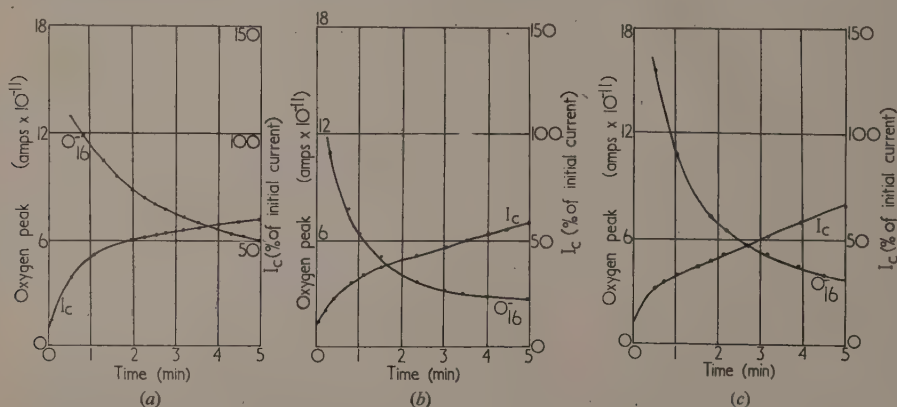


Fig. 4. Emission current and  $O_{16}^-$  ion emission during recovery from poisoning: (a) Initial current 2.0 mA, (b) Initial current 5.3 mA, (c) Initial current 7.0 mA

no permanent change has taken place in the cathode as a result of several oxygen poisoning attacks. It seems, therefore, that as long as the oxygen produced during poisoning is absorbed by the getter, complete recovery of emission after poisoning can take place a large number of times.

During the life of this cathode a further ion peak developed, with a mass number 32. This was identified as  $O_{32}^-$ , its intensity being about  $\frac{1}{3}$ rd that of the  $O_{16}^-$  peak. In previous experiments performed by the author,<sup>(2)</sup>  $O_{32}^-$  was found as in this case, only after prolonged running of the cathode. Its retarding potential distribution indicated that a large proportion of the  $O_{32}^-$  ions emitted possessed excess energies, pointing to a similar method of formation as for  $O_{16}^-$ ; no explanation of the tendency to form  $O_{32}^-$  ions after continued running of the cathode can, however, be given.

**Effects of potential gradient in the coating on cathode recovery.** A series of poisoning experiments was made on a

**Effects of cathode temperature on recovery.** The effect of cathode temperature on the recovery process is shown in Fig. 5 in which emission recovery at temperatures of 1200, 1138, and 1060° K are plotted on a percentage basis, along with the corresponding oxygen ion current densities during recovery. The initial emission current densities at the three temperatures were 230, 190 and 148 mA/cm<sup>2</sup> respectively, but comparison with Fig. 4 shows that the diversity in rates of emission recovery and  $O_{16}^-$  evolution at the three temperatures is far greater than can be accounted for by the variation in emission density alone. Hence it may be concluded that the temperature of the cathode coating has a considerable influence on the rate of ejection of occluded oxygen, this rate increasing rapidly with increasing temperature. The results also confirmed the increased sensitivity to oxygen poisoning at low temperatures.

**Origin of  $O_{16}^-$  ions formed during recovery.** The experiments

previously described gave little information on the precise origin of the  $O_{16}^-$  ions formed during recovery, although it seemed likely that the adsorption of oxygen on cathode crystal surfaces and its subsequent release in ionized form played a large part. Further experiments were therefore carried out to find the energy distribution, and hence the

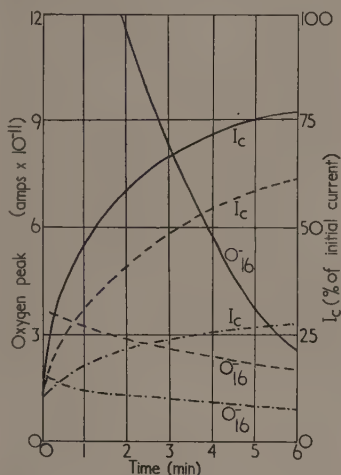


Fig. 5. Showing recovery characteristics of a cathode at temperatures of 1200, 1138 and 1060° K

— 1200° K. --- 1138° K. - · - 1060° K.

precise origin of the  $O_{16}^-$  ions emitted during each stage of recovery. For this purpose it was necessary to make several energy distribution measurements on the  $O_{16}^-$  peak during a recovery period. This necessitated making a retarding potential run in a short time; a.c. measurements employing an oscilloscope were impracticable on account of the high time-constant of the ion recording circuit. A mechanical method was therefore devised enabling the retarding voltage to be varied from +15 V to -15 V in 30 sec. In this way, by setting the spectrometer to receive the  $O_{16}^-$  ion peak, and varying the retarder voltage mechanically while plotting the  $O_{16}^-$  peak height, a retarding potential plot could be made in 0 sec.

The method of investigating the  $O_{16}^-$  energy distribution during recovery periods was as follows:

(a) After poisoning the cathode, the spectrometer was set to receive the  $O_{16}^-$  peak with the retarding electrode 15 V positive of the cathode ( $V_R = +15$  V). Retarding potential measurements were taken by the mechanical method at min intervals after emission recovery had commenced.

(b) From the maximum values of  $O_{16}^-$  ion current occurring in these curves, a normal plot was constructed showing the time variation of  $O_{16}^-$  during the 10 min after recovery had commenced.

(c) From this graph the retarding potential plots obtained in (a) were corrected for the time decay of the  $O_{16}^-$  peak occurring in the 30 sec taken to record; hence a series of curves was obtained representing the instantaneous energy distributions of  $O_{16}^-$  at 2 min intervals during recovery.

A typical set of retarding potential curves for  $O_{16}^-$  during recovery from poisoning at a temperature of 1200° K is shown in Fig. 6; these are plotted on a percentage basis to facilitate comparison.

The following points will be noticed:

(i) Curve 5, taken 10 h after recovery started, shows a complete return to normal conditions, well over 90% of the oxygen ions possessing excess energies attributable to the surface layer effect previously described.

(ii) In Curve 1, taken only 2 min after recovery began, a far smaller proportion of the ions possess excess energies; although the voltage drop in the coating could not be directly determined, subsequent conductivity measurements showed that at the temperatures used, poisoning of the emission to 10% of its initial value was accompanied by a similar reduction in coating conductivity. This increased resistance of the coating resulted in the voltage drop across the coating remaining almost constant. Also, the analogous form of the conductivity and emission curves referred to in §3 indicated that little variation in the voltage drop across the coating occurred during recovery. In this particular case, the estimated voltage drop from these considerations was in the region 2.5–3.0 V during recovery. Thus the part of the curve to the right of an ordinate at 3.0 V may be taken to represent ions formed in front of the cathode without excess energies. The percentage of ions formed by such a process decreases progressively in Curves 1 to 5.

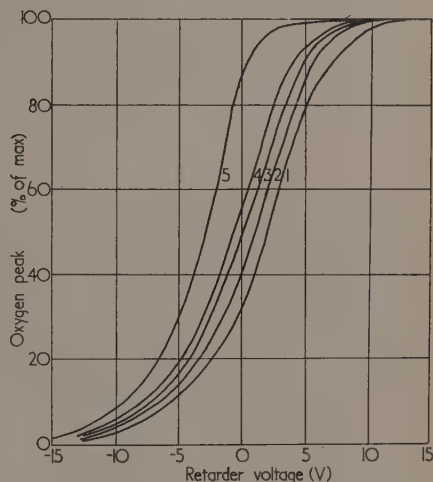


Fig. 6. Retarding potential curves for  $O_{16}^-$  during recovery from poisoning:

(1) After 2 min, (2) After 4 min, (3) After 6 min, (4) After 10 min, (5) After 10 h.

(iii) In Curve 5, which represents normal running conditions, only a very small decrease in intensity takes place in the region 0 to +3.0 V. The considerable decrease in intensity occurring in this region for Curves 1 to 4 indicates that a different source of ions exists during the recovery period, apart from the surface oxygen layer. These curves, combined with the fact that high potential gradients in the coating favour recovery, points to formation of oxygen ions in the coating itself.

The results may thus be summarized as follows:

Three sources of oxygen ions exist.

(i) The surface layer of oxygen, from which negative ions are normally formed by positive bombardment. These ions are characterized by the possession of excess energies.

\*\*\*



(ii) The interior of the coating. Ions are formed in this region during recovery periods, from oxygen which has diffused into coating during poisoning.

(iii) The space in front of the cathode, which supplies an appreciable proportion of the ion beam only in the initial stages of recovery.

### 3. THE EFFECT OF POISONING ON COATING CONDUCTIVITY

This section describes a series of experiments on the effect of oxygen on the conductivity of cathode coating; tubes having a spiral probe embedded in the coating were used. The experiments gave further information on the mechanism of the poisoning effect as well as furnishing details of the conduction processes occurring in the cathode under various conditions.

**Apparatus.** The tubes employed for conductivity measurements in connexion with oxygen poisoning were cylindrical diodes of the type shown in Fig. 7. An "O" nickel cathode with a barium-strontium oxide coating was normally employed, and a spiral probe wire was embedded in the coating to enable conductivity measurements between the cathode core and the spiral to be made. An oxygen producing filament was incorporated consisting of a wire coated with barium peroxide as in the mass spectrometer experiments.

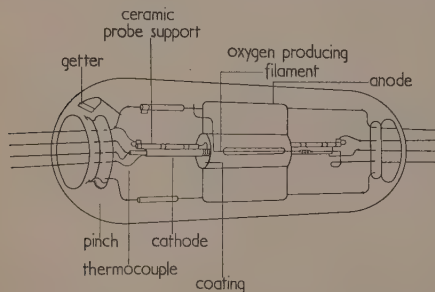


Fig. 7. Diode used for conductivity measurements

The cathode temperature was measured by means of a tungsten-nickel thermocouple.

When activating the cathodes of such tubes, care was taken to break down the coating slowly to avoid cracking by rapid evolution of carbon dioxide, since the coatings containing probe wires were up to  $100\ \mu$  thick. All cathodes were aged for 20 or 30 h, drawing emission currents of about  $100\ \text{mA/cm}^2$ , before experiments were started.

**Conductivity measurements.** Measurements of cathode coating conductivity were made over a wide temperature range, usually between  $350^\circ\text{K}$  and  $1000^\circ\text{K}$ , some twelve current-voltage characteristics being plotted in this range. At each temperature a complete characteristic was plotted, applying voltages up to 100 mV between probe and cathode in both directions, and recording the resulting conduction current. For all tubes studied, such characteristics were always linear, no trace of rectification being observed.

A typical set of results for the variation of conductivity with temperature is given in Fig. 8 in which  $\log 1/R$  is plotted against the reciprocal of temperature in the usual way,  $R$  being the coating resistance. The shape of this curve is very similar to that found by Loosjes and Vink,<sup>(3)</sup> consisting of

two linear portions with a break at  $700^\circ\text{K}$ . All tubes used showed a transition temperature very close to  $700^\circ\text{K}$ . This suggests the existence of two conductivity mechanisms in parallel, the resistance of the coating  $R$  being given by an expression of the type

$$1/R = A \exp(-Q_1/kT) + B \exp(-Q_2/kT)$$

where  $k$  is the Boltzmann constant.

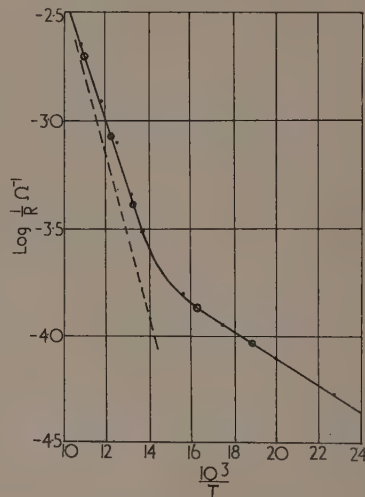


Fig. 8. Showing the variation of coating conductivity with temperature

--- corrected line at high temperatures.  
● poisoning experiments made at these points.

The apparent values of  $Q_1$  and  $Q_2$  from the slopes of the two sections are  $0.12\ \text{eV}$  (low temperature section) and  $0.60\ \text{eV}$  (high temperature section). After correction for the effect of the low temperature conduction mechanism, the true activation energy for the high temperature section was found to be  $0.75\ \text{eV}$ . Loosjes and Vink, using a similar method, found close correspondence between the high temperature activation energy and the work function of the cathode, taking this as evidence for a crystal-to-crystal emission process in the coating to provide electron transport at high temperatures. In all the present experiments, however, the high temperature activation energy was smaller than the work function as determined from Richardson plots (in this particular case the work function was  $0.90\ \text{eV}$ ). This would appear to indicate some difference between the high temperature conduction process and the normal emission process. It seems likely that the cause is located at the outer surface of the coating, and may be the surface oxygen film.

**Poisoning experiments.** The effect of oxygen absorption by the cathode on the conductivity in both regions was subsequently studied in conjunction with emission poisoning measurements. The method used was as follows:

The cathode temperature was set, and the value of saturated emission current determined. The conductivity was then measured over a small range of the current-voltage characteristic including the zero current point, with the anode floating. The emission current was reduced (usually to 10% of its initial value) by releasing oxygen, and, after cut-off of the gas

low, both emission and conductivity were recorded during the subsequent period.

Poisoning attacks were made at the temperatures indicated on Fig. 8 for this particular tube. The results are shown in the following table.

Temperature (° K)	530	615	760	820	916
% conductivity after poisoning	67	67	44	20	12

In each case the emission was poisoned to 10% of its initial value.

At the lower temperatures the emission recovery after poisoning was very slow; and the conductivity remained almost constant; at the higher temperatures similar emission recovery curves to that of Fig. 3 were found, and in the high temperature region the conductivity recovered in an analogous manner to the emission. Increasing potential gradients in the coating favoured both emission and conductivity recovery in the high temperature region. These results are typical of several cathodes on which the experiments were carried out; in all cases the conductivity at low temperatures was affected only slightly by the introduction of sufficient oxygen to reduce the emission to 10% of its original value, while at high temperatures the conductivity was reduced in the same way as the emission.

#### 4. CONCLUSIONS

Although many measurements of the variation of conductivity with temperature in alkaline earth oxides have been made, nearly all such experiments were carried out above 800° K. The work of Loosjes and Vink was the first to demonstrate that two parallel conduction mechanisms exist in oxide cathodes, the resultant conductivity at any temperature being determined by the mechanism with highest conductivity. Such an assumption can be shown to explain the observed characteristic curves over a wide temperature range. The results obtained using probe-type tubes are in striking agreement with those obtained by a different method by Loosjes and Vink, and lend themselves to an explanation of this type.

Loosjes and Vink assumed the two conduction processes to be:

(i) A current flow through crystals and crystal contacts predominating at low temperatures.

(ii) Conduction through the electron space charge in crystal interstices, predominating at high temperatures.

The fact that the reduction in low temperature conductivity by oxygen in the coating is slight points to such a low temperature conduction process, since the presence of oxygen in the crystal pores would not be expected to affect conduction through the crystals themselves. The adsorption of oxygen on interior crystal surfaces would be expected to reduce the crystal-to-crystal emission by raising the work function at crystal surfaces, and the large decrease in conductivity observed on admitting oxygen to the coating at temperatures well above 700° K can therefore be explained on the basis of the Loosjes and Vink model. The fact that the work function as determined from Richardson plots was invariably higher than the high temperature activation energy indicates a difference in the surface conditions between the interior crystals and the coating boundary which was not implied by Loosjes and Vink, and may be explicable in terms of the

surface oxygen layer shown to exist in the mass spectrometer experiments.

Metson's results showed the reversibility of oxygen poisoning; and also, that the observed recovery characteristics could be explained if it were assumed that ionized oxygen was released from the coating during recovery. The experiments reported in the present paper show directly that increased oxygen ion emission does in fact occur during recovery, and show also that most of this oxygen originates within the body of the coating; it may therefore be concluded that either:

(a) The oxygen is adsorbed on interior crystal surfaces as well as the outer coating surface, causing an increase in work function of the crystals; or

(b) The oxygen actually enters the crystals, reducing the activity by occupation of vacant electronegative lattice sites.

Herrmann and Wagener,<sup>(4)</sup> in discussing the results of Herrmann and Kreig,<sup>(5)</sup> have estimated the amount of oxygen adsorbed on the cathode during a poisoning experiment at 1000° K, and conclude that  $10^{17}$  oxygen atoms were taken up by the cathode, compared with a total number of impurity centres of  $10^{16}$ . From this result, and from the fact that reactivation may be repeated many times, it is concluded that all the poisoning oxygen ions cannot be bound by a certain fraction of the excess barium in the cathode. The experiments reported here agree with this conclusion, and suggest the main cause of poisoning of emission and conductivity at high temperatures to be cause (a) above.

It has been shown, however, that a slight poisoning of conductivity occurs at low temperatures, and this may be due to a process of type (b) in which oxygen diffuses into vacant lattice sites near crystal surfaces. Since, at low temperatures, the reduction in conductivity is slight, the limitation of emission due to oxygen would be expected to be due to adsorbed oxygen on the outer coating surface.

In conclusion, it may be said that the experiments performed with both the mass spectrometer and probe-type tubes give results explicable by the Loosjes-Vink conduction mechanism, although the discrepancy always found between the work function of the cathode and the high temperature activation energy cannot be explained on the basis of this model alone.

#### ACKNOWLEDGEMENTS

The experimental work described above was carried out in the Physics Department of Manchester University.

Acknowledgements are due to Professor P. M. S. Blackett for laboratory facilities, and to Professor F. A. Vick for much helpful discussion and advice.

#### REFERENCES

- (1) METSON, G. H. *Nature, Lond.*, **164**, p. 540 (1949).
- (2) GRATTIDGE, W., and SHEPHERD, A. A. *Proc. Phys. Soc., Lond.* In the press, (1953).
- (3) LOOSJES, R., and VINK, H. J. *Philips Res. Rep.*, **4**, p. 449 (1949).
- (4) HERRMANN, G., and WAGENER, S. *The Oxide-coated Cathode*, Vol. II (London: Chapman and Hall Ltd., 1951).
- (5) HERRMANN, G., and KRIEG, O. *Ann. Phys.*, **4**, p. 441 (1949).

# Photoelastic determination of stresses in a cylindrical shell

By H. FESSLER, B.Sc.(Eng.), and R. T. ROSE, B.Sc., University of Nottingham

[Paper first received 23 July, 1952, and in final form 27 October, 1952]

The frozen stress photoelastic technique is used to determine the surface stresses and deformations of a cylinder with flat disk head (2.7 in bore, 0.380 in wall thickness) under internal pressure. The material used was Marco Resin SB.26.C; the technique of casting, machining, freezing and slicing of the models is described. The observed stresses and deformations are compared with values calculated from an analysis by Watts and Burrows<sup>(1)</sup> and found to be in fair agreement except near the juncture of head and shell.

The majority of design formulae for pressure vessels are based on the membrane theory which neglects bending and shear stresses. Love's exact analysis of symmetrical shells has been used by Watts and Burrows<sup>(1)</sup> to establish a matrix solution of the stresses and deformations of the semi-infinite cylinder with different shapes of heads. This analytical approach is limited to comparatively simple geometrical shapes and, to be able to deal with actual pressure vessel problems, it was decided to investigate the suitability of the frozen stress photoelastic method for this type of problem. A simple shape, for which an analytical solution is possible, was chosen in order to compare the photoelastic results with the analytical ones.

## PHOTOELASTIC ANALYSIS

The frozen stress technique, first used by Oppel<sup>(2)</sup> and developed mainly by Kuske<sup>(3)</sup> and Hetenyi,<sup>(4)</sup> relies on the ability of certain photoelastic materials to maintain an internal stress system after the removal of the external forces.

The diphasic theory, due to Houwink,<sup>(5)</sup> provides a convenient explanation of this phenomenon. It supposes the material to consist of two phases, a primary one which remains elastic at all temperatures and a secondary one which offers viscous resistance to deformation. At an elevated temperature the viscosity of the latter is so small that only the primary phase resists deformation. If the material is allowed to cool under the action of the external forces the secondary phase sets around the deformed primary phase and, on removal of the external forces, the viscous resistance of the secondary phase maintains the deformations. Thus deformations and stresses have been fixed or "frozen" into the material. Because these phases are supposed to exist on a molecular scale, a model, into which stresses have been frozen, may be cut into convenient slices without releasing the stresses or deformations. This was demonstrated by Hetenyi. For the purposes of the present and similar investigations, it may be assumed that the optical behaviour or the birefringence occurs in a manner similar to the strain.

This diphasic nature of certain materials makes three-dimensional photoelastic investigations possible. A model of the component to be investigated is made, loaded at an elevated temperature and allowed to cool under the load. After removal of the load, slices are cut out of the model and analysed in the polariscope in the same way as in the usual two-dimensional photoelastic investigations. The interference fringes which appear in a slice at the point considered are proportional to the mean difference of the principal stresses in the plane of the slice. To obtain useful information, certain limitations must be imposed. The slice must be so thin that the principal stresses parallel to its faces do not change appreciably in magnitude or direction through the thickness. Furthermore, in general the plane of the slice will not be a principal plane of stress so that the fringe order gives

a measure of the secondary principal stresses, which are usually only of very limited interest.

In the case of cylindrical shells subjected to internal pressure, the problem is simplified because every plane which contains the axis of the cylinder is a plane of symmetry and, therefore, a principal plane of stress. The individual principal stresses at the surfaces are easily determined from the fringe pattern. The surfaces are free boundaries which cannot sustain any shear stresses and one principal stress must be perpendicular to the free boundary (it is equal to the hydrostatic pressure on the surface). It follows that, at the surfaces, the principal stresses are radial, parallel to the axis and tangential to circular sections.

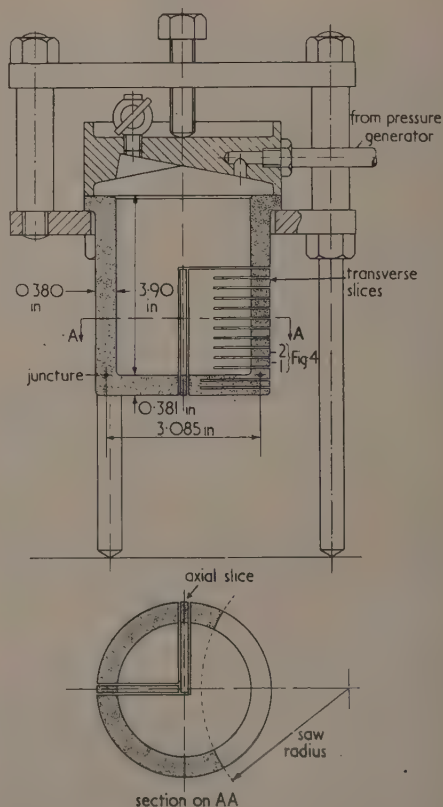


Fig. 1. Model in position in pressure loading device, showing also the position of the slices cut after freezing



In the cylinder, the fringe orders at the edges of transverse and axial slices, as shown in Fig. 1, will therefore be proportional to the circumferential and axial stresses respectively at the outer surface. At the inner surface the fringe order will be proportional to the difference between the above stresses and the (known) hydrostatic pressure. The radial stresses in the head are determined from the axial slices in the same way. The circumferential stresses in the head were obtained from transverse slices taken at the inside and outside surfaces of the head. The fringe orders obtained from these thin thick slices are therefore (unlike all other values) not the actual surface stresses, but the mean stresses through the thickness of the slices. The resulting error was tolerated to reduce the number of slices to be cut. The circumferential stresses were then calculated from these fringe orders by subtraction of the previously determined radial stresses.

#### MATERIAL

Catalin, Fosterite and Marco Resin are materials which exhibit the frozen stress phenomenon and are available in thicknesses of more than  $1\frac{1}{2}$  in. Catalin<sup>(6)</sup> shows such severe edge effects and recovery (disappearance of the frozen birefringence after unloading) that, in the writers' opinion, it can hardly be considered for a quantitative investigation. Fosterite,<sup>(7)</sup> an American material specially invented for frozen stress photoelasticity, is very expensive and difficult to obtain in this country. For these reasons Marco Resin was used.

Marco Resin SB.26.C<sup>(8)</sup> by Scott Bader and Co. Ltd. consists of a viscous resin which is mixed with a monomeric modifier to reduce its viscosity. If small quantities of catalyst and an accelerator are added, the mixture, a liquid of low (machine oil) viscosity, will polymerize into a solid at room temperature and atmospheric pressure. The possibility of casting any shape in the laboratory is a considerable advantage, but the heat liberated in the polymerization must be dissipated to prevent too rapid solidification. For castings of appreciable mass, such as the cylinders used in this investigation, this heat may be conveniently absorbed in a cooling bath.

The composition used was (by weight) 100 parts of resin, 7 parts of monomer, 0.5 parts of catalyst and 0.5 parts of accelerator. When this mixture was poured into a cast iron mould with a wooden core it gelled in 20 h if kept between 12 and 25° C. As soon as the castings were sufficiently rigid they were removed from the mould and allowed to harden in a bath containing paraffin oil. The absence of restraint at this stage prevented the fixing of initial stresses in the casting. The paraffin oil absorbed the heat liberated and prevented contact of the casting with air. The thickness of the walls of the casting was  $\frac{5}{8}$  in which allowed  $\frac{1}{8}$  in to be machined off very surface. It seems possible that the boundaries may affect the polymerization and the properties of the material in their vicinity. This, as well as the large contraction of the casting, makes complete machining desirable.

A tensile specimen cut from one of the cylinders showed the material to have an effective material fringe value of 7. (The effective material fringe value is the load in pounds, applied when hot, divided by the original cross-sectional area, multiplied by the relative retardation in fringes per inch thickness, using green mercury vapour light of 5460 Å wavelength.) The effective modulus determined in the same test was 2900 lb/in<sup>2</sup>. A compression test on a  $\frac{1}{2}$  in cube, loaded between platens of the same material to eliminate the effect of end restraint, showed Poisson's ratio to be 0.50.

This value was used in the evaluation of the matrices for the theoretical results. The material showed no appreciable rind effect (edge stresses caused by loss or gain of moisture during the "stress freezing") and it would appear that the only weakness of Marco Resin as a frozen stress material is the mottle or streaky appearance of the fringes, as may be seen on Fig. 3.

#### THE MODEL

At least fourteen days after mixing, when the casting was considered to be hard, it was machined on a lathe, using ordinary tools and speeds. Marco Resin is easily machined and a good surface finish can be obtained without difficulty. The finished dimensions are shown on Fig. 1. Before loading, the profile was checked with a dial gauge and the usual measuring equipment. The model was loaded as shown in Fig. 1 inside a hot air oven. The hydrostatic pressure was applied by a dead-weight loading device from outside the oven, using cylinder oil as the pressure fluid. The oven was heated by a water jacket to 99° C; the temperature and a pressure of 7.4 lb/in<sup>2</sup> (0.0025 of the elastic modulus) were maintained for one hour, after which the whole apparatus

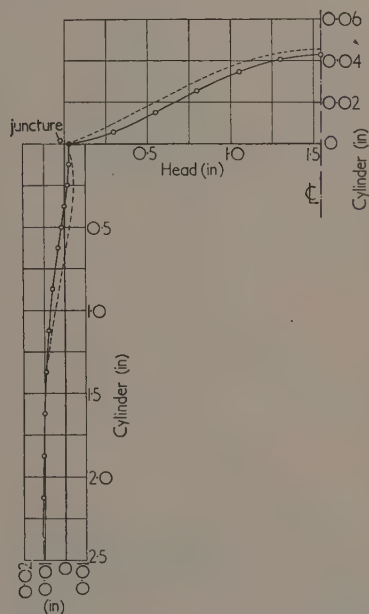


Fig. 2. Axial deformation of head and radial deformation of cylinder outside surfaces, relative to the juncture of head and cylinder. Dotted curves show calculated values

was allowed to cool slowly. Below 40° C some leakage of oil occurred between the cylinder flange and the blank, presumably due to the thermal contraction of the former. The profile of the unloaded model was measured and the radial deformation of the cylinder and the axial deformation of the head were determined. These are shown in Fig. 2.

To obtain accurate slices, the model was mounted on an angle plate on the cross side of a small lathe used as a milling machine. The model could be rotated about its own axis and moved vertically on the angle plate; the angle plate could be

moved across and along the lathe bed by the usual lathe mechanism. These three orthogonal movements were effected by micrometer headed screws so that they could be determined accurately to 0.001 in. This arrangement combined with the use of a thin milling cutter (6 in diameter,  $\frac{3}{8}$  in wide), rotating in place of the "work," ensured that all slices were of constant thickness and located accurately. Although the slitting saw produced a good finish, the faces of the slices were rubbed on metallurgical emery paper to improve their transparency. The thickness of the slices was 0.150 in.

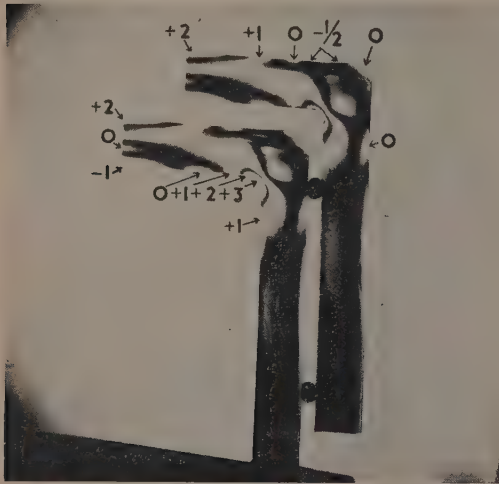


Fig. 3. Fringe pattern in two axial slices (light field polariscope). The figures refer to the fringe orders. Positive signs denote tensile stress differences in the axial plane, tangential to the surfaces of the model

Fig. 3 shows the fringe pattern for two axial slices, illustrating symmetry of loading by their similarity. The streaky effect in the vertical parts is usually denoted as mottle. As

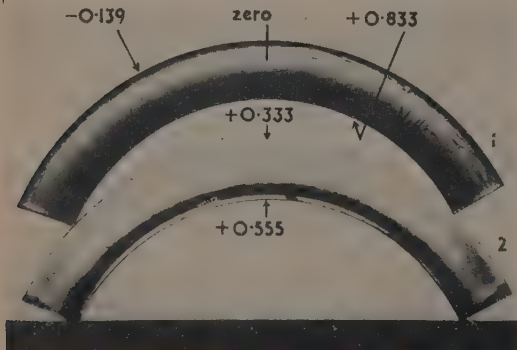


Fig. 4. Fringe pattern in transverse slices (light field polariscope). See Fig. 1 for their positions in model. The figures are the fractional fringe orders. Positive signs denote tensile stress difference in transverse planes, tangential to the surfaces of the model

the photograph was taken in a "light field" circular polariscope, the light areas indicate integral fringe orders. Fig. 4, also photographed in a light field, shows the fringe pattern in two transverse slices cut at different distances from the cylinder head. The fringe orders along the edges of the slices were determined by the Tardy method of compensation.<sup>(9)</sup> This consists of rotating the analyser of the crossed circular polariscope until extinction occurs at the point considered. If the direction of one principal stress at that point has been aligned with the polarizer, the angle turned through, expressed as a fraction of a semi-revolution, is the fractional fringe order at the point. This method of measurement is simple, accurate and requires no special equipment. For transverse slices of the cylinder in which no zero fringe appeared (compare slice 2 in Fig. 4) the integral fringe order was determined with a beam compensator. Using the material fringe value obtained in the tensile tests, the measured fringe orders were converted into differences of principal stresses. From these the surface stresses were obtained as explained in the section on photoelastic analysis.

## RESULTS

The axial stress in the cylinder, radial stress in the head and circumferential stresses in the cylinder and head are shown in Figs. 5 to 8 by the unbroken lines. The dotted curves were obtained by calculations based on an analysis by

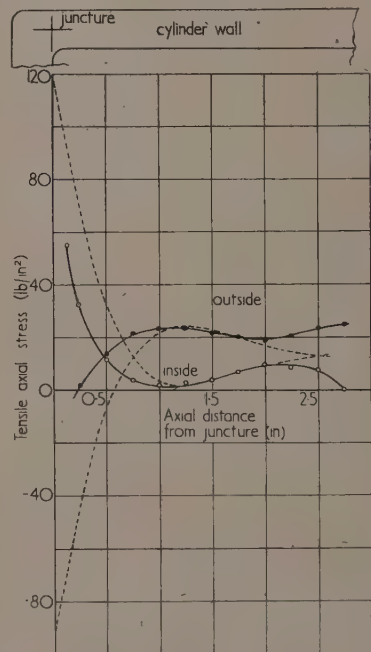


Fig. 5. Axial stress on inside and outside surface of cylinder. Dotted curves show calculated values

Watts and Burrows.<sup>(1)</sup> Watts and Burrows established the equations of equilibrium for cylindrical shells with different closed ends and obtained, in matrix form, solutions to these equations which satisfied the boundary conditions of the shells. To obtain their solutions they had to ignore all

external forces except the hydrostatic pressure; to assume that the cylinders are sufficiently long for the closure at the far end not to affect the stresses near the head; and to ignore all stress concentrations at the juncture of head to shell. They also assumed that the diameter of the head was equal to the mean diameter of the cylinder, and that the head was

must necessarily cause divergence of the stresses and deformations from those calculated from classical elasticity which assumes infinitesimally small deformations. This is evident in Fig. 2.

Another possible source of differences is the small mean diameter/wall thickness ratio of the model. This was 8.15

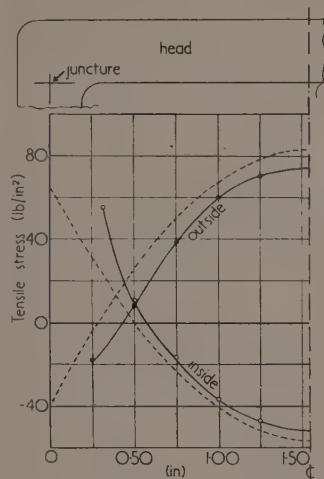


Fig. 6. Radial stress on inside and outside surface of head. Dotted curves show calculated values

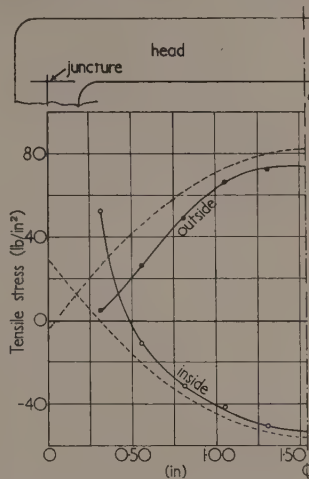


Fig. 8. Circumferential stress on inside and outside of head. Dotted curves show calculated values

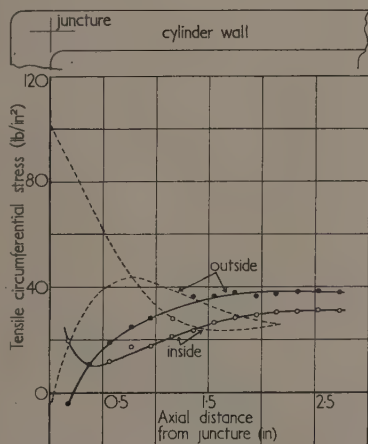


Fig. 7. Circumferential stress on inside and outside surface of cylinder. Dotted curves show calculated values

connected to the cylinder only along the circumference of one of its faces.

In an actual model the connexion between head and shell must extend over a finite area and stress concentrations at the juncture cannot be avoided. These factors are deemed to be the main cause of the divergence of the calculated from the experimental curves. It will be noted that fairly good agreement exists, except near the juncture. The large deformations necessary for frozen stress photoelastic analysis

and although Watts and Burrows suggest that their analysis is applicable to ratios as low as 5, an analysis based on a "thin" shell theory cannot be expected to fit perfectly in the transition range to "thick" shells.

The graphs indicate that, excepting in the vicinity of the juncture, the photoelastic stresses are lower than the calculated ones. Excluding the circumferential stresses in the cylinder, the theoretical assumptions may be assumed to account for the differences between the curves.

#### ACKNOWLEDGEMENTS

The authors wish to express their thanks to Professor J. A. Pope, Head of the Department of Mechanical Engineering at Nottingham University, who provided all necessary facilities for this work.

#### REFERENCES

- (1) WATTS, G. W., and BURROWS, W. R. *Trans. Amer. Soc. Mech. Engrs.*, **71**, pp. 55-73 (1949).
- (2) OPPEL, G. *Forschung a. d. Gebiete d. Ingenieurwesens*, **7**, pp. 240-8 (1936).
- (3) KUSKE, A. *Forschung a. d. Gebiete d. Ingenieurwesens*, **9**, pp. 139-49 (1938).
- (4) HETENYI, M. *J. Appl. Phys.*, **10**, pp. 295-300 (1939).
- (5) HOUWINK, R. *Elasticity, Plasticity and Structure of Matter* (London: Cambridge University Press, 1937).
- (6) FISHER, W. A. F. *Proc. Instn Mech. Engrs*, **158**, pp. 230-5 (1947).
- (7) LEVEN, M. M. *Proc. Soc. Exp. Stress Analysis*, **6**, No. 1, pp. 19-28 (1948).
- (8) SUGARMAN, B., MOXLEY, G. O., and MARSHALL, I. A. *Brit. J. Appl. Phys.*, **3**, p. 233 (1952).
- (9) TARDY, H. L. *Rev. Opt. (Théor. Instrum.)*, **8**, p. 59 (1929).



# A check on the standard observer data at 4358 Å

By W. HARRISON, B.Sc., Siemens Lamp Research Laboratory, Preston

[Paper first received 27 October, and in final form 17 November, 1952]

It has been suggested that the C.I.E. standard observer data for colorimetry may be seriously in error below 4600 Å. In this paper it is shown that the fluorescent lamp can be of particular value in checking the data at 4358 Å since fluorescent lamps and standard illuminants can form "metameric pairs" with different spectral distributions in the blue-violet and principally at 4358 Å. The check is made by visual comparison of the "metameric pair" and correlating the chromaticity so obtained for the fluorescent lamp with that obtained by computation from the spectral distribution. Measurements on warm white and daylight fluorescent lamps gave reasonable correlation with the C.I.E. data but not with the Wald-Gibson-Tyndall average data.

The chromaticity of a colour stimulus, whether it be from a light source or light reflected from a material, can be determined in two different ways. The full spectral energy distribution may be first measured and the distribution coefficients of the standard observer data (the  $\bar{x}$ ,  $\bar{y}$ ,  $\bar{z}$  values of the C.I.E. system) applied to give  $E_{\lambda}\bar{x}_{\lambda}$ ,  $E_{\lambda}\bar{y}_{\lambda}$ ,  $E_{\lambda}\bar{z}_{\lambda}$  wavelength by wavelength. Summation to  $\sum E_{\lambda}\bar{x}_{\lambda}$ ,  $\sum E_{\lambda}\bar{y}_{\lambda}$ ,  $\sum E_{\lambda}\bar{z}_{\lambda}$  and reduction to a unit equation gives the chromaticity co-ordinates ( $x$ ,  $y$ ,  $z$  values) of the stimulus. This method is, of course, a purely physical measurement involving only the particular data employed apart from the spectral distribution measurement. Secondly a visual match may be made in a tri-chromatic colorimeter and the readings of the matching stimuli converted to the  $x$ ,  $y$ ,  $z$  values. This method involves both the observer making the visual match and the data for the matching stimuli.

A system of colorimetry which in all cases gave good correlation between the two methods would be satisfactory but failure in even one instance, if definitely attributable to the observer data, would indicate that the particular data was not completely satisfactory. During recent years it has been suggested from the U.S.A.<sup>(1,2)</sup> that there appear to be inconsistencies in the C.I.E. data below 4600 Å which sometimes lead to errors when chromaticity is computed from the

spectral energy distribution. For example the computed values of chromaticity co-ordinates for two near-white pigments which have different reflexion curves in the blue-violet region may come out identical but the eye see a difference when a visual comparison is made, or *vice versa*.

The C.I.E. standard observer data adopted in 1931 was based on the colour mixture data of Wright and Guild, linked with the 1924 standard observer data for photometry, i.e. curve for the spectral sensitivity of the average eye or relative spectral luminosity. This curve became the distribution curve for the  $Y$  stimulus ( $\bar{y}$  values) with the  $X$  and  $Z$  distribution curves, proportional to it as shown in Fig. 1. It is suggested that any errors below 4600 Å are primarily due to errors in the 1924 data which are insignificant in the photometry of near-white light sources. It may be seen from Fig. 1 that the  $\bar{y}$  values below 4600 Å are very small but the  $\bar{x}$  values and particularly the  $\bar{z}$  values are large, therefore an error in these could lead to significant errors when chromaticity co-ordinates are computed from spectral energy measurements. Such errors will, however, only arise when the energy distributions being compared are different in the blue-violet region of the spectrum.

The term "metameric pair" has been applied to two materials which have the same overall colour but different spectral reflexion curves, and such materials are useful in the checking of any observer data by correlation of the physical and visual measurements.

## SUITABILITY OF THE FLUORESCENT LAMP FOR CHECKING DISTRIBUTION COEFFICIENTS

The spectrum of the fluorescent lamp comprises a continuum due to the fluorescence of the phosphor plus the mercury line spectrum in which the 4358 Å line is prominent. Particularly in the case of a lamp colour such as the warm white which is commercially available, and usually made with calcium halophosphate phosphor, the continuum is relatively weak at the violet end and about 60% of the  $Z$  co-ordinate is due to the mercury line. In the case of standard illuminant  $A$ , however, only about 20% of the  $Z$  co-ordinate is due to radiation below 4400 Å, thus although the two colours are roughly in the same chromaticity region they are quite different in spectral distribution at the blue-violet end of the spectrum. Extending the term "metameric pair" to illuminants, the standard illuminant  $A$  and a warm-white fluorescent lamp of the same chromaticity would form a "metameric pair" *par excellence* owing to the wide difference in spectral distribution.

The standard warm-white fluorescent lamp is slightly different in chromaticity from illuminant  $A$  but can be matched by a mixture of illuminant  $A$  and illuminant  $C$  with sometimes a very small addition or subtraction of green.

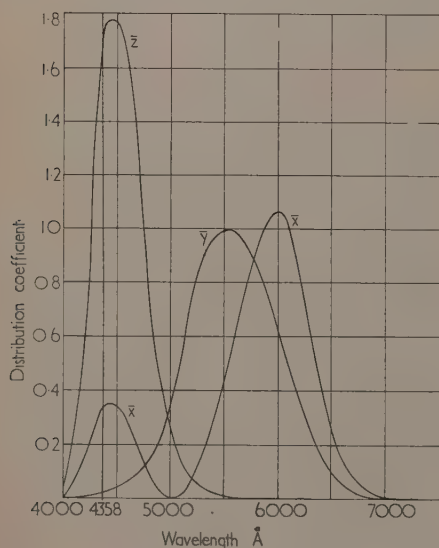


Fig. 1. Distribution curves for  $X$ ,  $Y$ ,  $Z$

Any error in the  $\bar{z}$  value at 4358 Å arising from error in the standard observer data should therefore be revealed when a comparison is made of the chromaticity of a warm-white fluorescent lamp as computed from the spectral distribution with that obtained by direct visual colorimetry in which the standard illuminants  $A$  and  $C$  provide the matching stimuli of the colorimeter. The same argument, to a lesser degree, also applies for the daylight fluorescent lamp.

It is interesting to note that in the measurement of the chromaticity of fluorescent lamps both the physical and visual methods have been employed by a number of workers<sup>(3)</sup> but no serious discrepancies have been reported. This appears to give a qualified confirmation that there is no serious error in the 4358 Å data.

However, in the suggestions from the U.S.A. for the modification of the C.I.E. data, based on other evidence, it is stated that the  $\bar{y}$  value and hence the  $\bar{x}$  and  $\bar{z}$  values for 4358 Å ought to be 2.4 times that of the present data, with other correction factors at wavelengths from 3800 Å as shown in Table 1.

Table 1. Comparison of relative spectral luminosity values of Wald-Gibson-Tyndall and C.I.E.

Wavelength Å	Wald-Gibson-Tyndall average	C.I.E.	Ratio W.G.T. C.I.E.
3800	0.0004	—	—
3900	0.0014	0.0001	14.0
4000	0.0040	0.0004	10.0
4100	0.0100	0.0012	8.3
4200	0.0200	0.0040	5.0
4300	0.0320	0.0116	2.75
4400	0.0430	0.0230	1.87
4500	0.0510	0.0380	1.34
4600	0.0680	0.0600	1.13
> 4600	as C.I.E.	—	1.00

A comparison of chromaticity co-ordinates obtained by direct colorimetry and by computation from the spectral distribution data has been made on warm-white and daylight fluorescent lamps as described below. The lamps are the 5 ft 80 W size.

#### METHOD OF MAKING THE VISUAL MEASUREMENTS

The direct visual measurement was made on a tri-chromatic colorimeter designed especially for the measurement of fluorescent lamps.<sup>(4)</sup> A sketch of the instrument is shown in Fig. 2. It comprises a box divided horizontally into two sections, the partition also dividing the flashed opal window. Fluorescent lamps can be carried in either section and the amount of light reaching the window is regulated by Paxolin sleeves which slide along the lamps. Alternatively, as was the case in the present work and as is shown in the sketch, the top half of the window can be illuminated by incandescent lamps placed at appropriate distances behind apertures in the back of the box with any required filters placed across the apertures. The mixing of the light from the two or three lamps in one section of the box is achieved on the diffusing surface of the window. The amounts of the matching stimuli are measured by placing a selenium photocell against the window and switching on each lamp in turn. The photocell is colour corrected by means of a Weston Viscor filter. The particular combination of photocell and filter has been selected by photometric tests on calibrated fluorescent and discharge

lamps against incandescent standards and found to read the luminance of near-white and coloured fluorescent lamps within the limits of experimental error (approximately 1% on near-whites). This photocell/filter combination will be referred to as the standard photocell, a second photocell and filter combination prepared by the British Scientific Instrument Research Association<sup>(5)</sup> has been used as a check. Measurements of the matching stimuli are thus in terms of luminance or  $Y$  value, and the transformation from photocell readings to  $X Y Z$  co-ordinates is simple, as may be seen from the measurements recorded later. The measurements were made by four observers of approximately normal colour sensitivity,  $WH$  and  $IE$  believed to be slightly red sensitive and  $RF$  and  $RR$  slightly blue-green sensitive. The window was viewed from sufficient distance to give a  $2^\circ$  field of view.

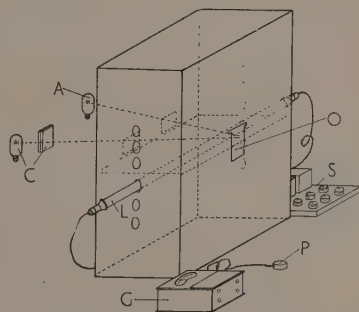


Fig. 2. Visual colorimeter showing matching of warm-white fluorescent lamp by mixture of standard illuminants

$A$ , standard illuminant  $A$ ;  $C$ , standard illuminant  $C$ ;  $G$ , galvanometer;  $L$ , warm-white fluorescent lamp;  $O$ , flashed opal window;  $P$ , photocell with filter;  $S$ , fluorescent lamp control panel.

The warm-white fluorescent lamp was matched with a mixture of illuminant  $A$  and illuminant  $C$  and the daylight fluorescent lamp was matched with a mixture of illuminant  $B$  and an incandescent lamp at  $2500^\circ \text{K}$ . In some cases a small amount of green fluorescent was added to one side or the other. The chromaticity co-ordinates for the green fluorescent lamp are  $x = 0.224$ ,  $y = 0.603$ ,  $z = 0.173$ .

#### Matching warm-white fluorescent lamp.

Observer	Photocell	Mixture
$WH$	Standard	100 parts $A + 21.2$ parts $C$
$IE$	Standard	100 parts $A + 21.2$ parts $C$
$RF$	Standard	100 parts $A + 21.2$ parts $C -$ 4.2 parts green fluorescent
$RR$	Standard	100 parts $A + 21.2$ parts $C -$ 4.2 parts green fluorescent
$WH$	B.S.I.R.A.	100 parts $A + 23$ parts $C$
$IE$	B.S.I.R.A.	100 parts $A + 23$ parts $C$
$RF$	B.S.I.R.A.	100 parts $A + 23$ parts $C -$ 4.9 parts green fluorescent*
$RR$	B.S.I.R.A.	100 parts $A + 23$ parts $C -$ 4.9 parts green fluorescent

#### Calculation of chromaticity co-ordinates.

The following shows the calculation for the mixture of 100 parts by luminance of  $A$  and 21.2 parts by luminance of  $C$ .

	<i>x</i>	<i>y</i>	<i>z</i>
100 <i>A</i> . Put down chromaticity co-ordinates	0.448	0.407	0.145
21.2 <i>C</i> . <i>Y</i> is 21.2% of 0.407 and <i>X</i> and <i>Z</i> follow from the chromaticity of <i>C</i>	0.084	0.086	0.102
Sum	0.532	0.493	0.247
Reduce to a unit equation	0.418	0.388	0.194

The following are the chromaticity co-ordinates from the above mixtures.

Observer	Standard photocell			B.S.I.R. photocell		
	<i>x</i>	<i>y</i>	<i>z</i>	<i>x</i>	<i>y</i>	<i>z</i>
WH	0.418	0.388	0.194	0.416	0.387	0.197
IE	0.418	0.388	0.194	0.416	0.387	0.197
RF	0.423	0.382	0.195	0.422	0.380	0.198
RR	0.423	0.382	0.195	0.422	0.380	0.198
Average	0.421	0.385	0.194	0.419	0.384	0.197

#### Matching daylight fluorescent lamp.

Observer	Photocell	Mixture
WH	Standard	100 parts <i>B</i> + 12.2 parts 2500° K filament lamp + 3.9 parts green
IE	Standard	100 parts <i>B</i> + 12.2 parts 2500° K filament lamp + 3.9 parts green
RF	Standard	100 parts <i>B</i> + 14.2 parts 2500° K filament lamp
RR	Standard	100 parts <i>B</i> + 14.2 parts 2500° K filament lamp
WH	B.S.I.R.A.	100 parts <i>B</i> + 15.7 parts 2500° K filament lamp + 6.6 parts green
IE	B.S.I.R.A.	100 parts <i>B</i> + 15.7 parts 2500° K filament lamp + 2.4 parts green
RF	B.S.I.R.A.	100 parts <i>B</i> + 15.7 parts 2500° K filament lamp
RR	B.S.I.R.A.	100 parts <i>B</i> + 13.7 parts 2500° K filament lamp.

Table 2. Factors for obtaining  $\Sigma E_{\lambda} \bar{x}_{\lambda}$  and  $\Sigma E_{\lambda} \bar{z}_{\lambda}$  for spectral bands from spectral band luminance data

(The luminance is multiplied by the factor shown.)

Spectral band No.	Wavelength <i>A</i>	Equal energy		Illuminant A		Warm-white fluorescent		Daylight fluorescent	
		$\Sigma E_{\lambda} \bar{x}_{\lambda}$	$\Sigma E_{\lambda} \bar{z}_{\lambda}$	$\Sigma E_{\lambda} \bar{x}_{\lambda}$	$\Sigma E_{\lambda} \bar{z}_{\lambda}$	$\Sigma E_{\lambda} \bar{x}_{\lambda}$	$\Sigma E_{\lambda} \bar{z}_{\lambda}$	$\Sigma E_{\lambda} \bar{x}_{\lambda}$	$\Sigma E_{\lambda} \bar{z}_{\lambda}$
1	3800-4200	36.0	177.0	35.0	167.0	35.0	167.0	35.0	168.0
2	4200-4400	22.0	109.0	21.3	105.0	19.0	95.0	19.0	95.0
3	4400-4600	8.4	44.5	8.2	43.5	8.2	43.6	8.25	44.0
4	4600-5100	0.46	3.63	0.36	3.0	0.45	3.6	0.46	3.75
5	5100-5600	0.29	0.05	0.31	0.046	0.38	0.03	0.32	0.04
6	5600-6100	1.157	0.002	1.19	0.002	1.14	0.002	1.16	0.002
7	6100-6600	2.34	—	2.35	—	2.28	—	2.28	—
8	6600-7600	2.7	—	2.7	—	2.8	—	2.75	—

The following are the chromaticity co-ordinates from the above mixtures.

Observer	Standard photocell			B.S.I.R.A. A photocell		
	<i>x</i>	<i>y</i>	<i>z</i>	<i>x</i>	<i>y</i>	<i>z</i>
WH	0.358	0.363	0.279	0.359	0.367	0.274
IE	0.358	0.363	0.279	0.362	0.362	0.276
RF	0.362	0.358	0.280	0.364	0.359	0.277
RR	0.362	0.358	0.280	0.361	0.359	0.280
Average	0.360	0.361	0.279	0.361	0.362	0.277

#### CHROMATICITY FROM THE SPECTRAL DISTRIBUTION

Basically the method is to obtain the spectral energy distribution in 50 Å or 100 Å steps and apply the distribution coefficients of the observer data (standard or modified as the case may be).

It is, however, the practice to make measurements of the spectral distribution of fluorescent lamps by the method of abridged spectrophotometry in which the percentage luminance in eight wavebands is measured, and it was felt that there might be some advantage if the eight-band measurements could be used instead of the full spectral energy curve. The advantages are: (i) An instrument specially designed for the eight-band measurement can be used. (ii) Since the bands are wide a relatively wide entrance slit can be used giving increased light pick-up. Also the mercury lines fall well inside the bands and do not need to be measured separately.

The luminance values for the bands are the  $\bar{y}$  values ( $\Sigma E_{\lambda} \bar{y}_{\lambda}$ ) and to obtain the  $\bar{x}$  and  $\bar{z}$  values for the bands multiplying factors have to be applied. These multiplying factors will in most cases be different for different illuminants owing to the different slope of the energy curve in a relatively wide waveband of 200 Å or 500 Å. Multiplying factors have been worked out for equal energy, illuminant A, warm-white fluorescent and daylight fluorescent, and are given in Table 2.

These factors have been obtained from the full energy distribution measurements previously made on similar type warm-white and daylight fluorescent lamps, and in the case of equal energy and illuminant A from the published data.  $E_{\lambda} \bar{x}_{\lambda}$ ,  $E_{\lambda} \bar{y}_{\lambda}$  and  $E_{\lambda} \bar{z}_{\lambda}$  curves were plotted for each and divided up into the eight bands.

It may be seen that the factors for illuminants as far different in spectral distribution as equal energy, illuminant A and the fluorescent lamps are similar, thus it is felt that the factors obtained on one warm-white fluorescent lamp can, with confidence, be applied to another warm-white fluorescent lamp employing the same kind of phosphor. The factors

having been obtained, once and for all, the chromaticity of a lamp can readily be derived from the eight-band data. This, incidentally, forms a useful method of measurement of the chromaticity of a fluorescent lamp.

*Measurement of warm-white fluorescent lamp and computation of chromaticity co-ordinates.* The following shows the application of the warm-white factors to the spectral band luminance data for the lamp previously measured visually. The *Y* values are the measured luminance values.



# A check on the standard observer data at 4358 Å

Spectral band No.	x	y	z
1	0.35	0.010	1.76
2	5.4	0.285	27.0
3	1.52	0.185	8.05
4	1.26	2.8	10.1
5	12.1	31.9	0.96
6	61.5	53.9	0.11
7	24.2	10.6	—
8	0.76	0.27	—
Sum	107.13	99.95	47.89

Chromaticity co-ordinates	x	y	z
	0.420	0.392	0.188

Measurement of daylight fluorescent lamp and computation of chromaticity co-ordinates. The following shows the application of the daylight fluorescent factors to the spectral and luminance data (Y column) for the lamp previously measured visually.

Spectral band No.	x	y	z
1	0.60	0.017	2.86
2	6.95	0.365	34.7
3	3.0	0.365	15.95
4	2.59	5.75	20.7
5	14.6	38.5	1.15
6	52.9	46.3	0.09
7	19.4	8.5	—
8	0.64	0.23	—
Sum	100.68	100.03	75.45

Chromaticity co-ordinates	x	y	z
	0.365	0.362	0.273

## EFFECT OF APPLYING WALD-GIBSON-TYNDALL DATA

The effect of applying the Wald-Gibson-Tyndall data to the energy distribution of standard illuminant A is shown in Table 3.

Table 3. Computation of the chromaticity of illuminant A with Wald-Gibson-Tyndall data

Wavelength Å	$E_A \bar{x}$	$E_A \bar{y}$	$E_B \bar{z}$
3800	0.0200	0.0005	0.0960
3900	0.0650	0.0014	0.0219
4000	0.1930	0.0050	0.9160
4100	0.5700	0.0157	2.7200
4200	1.3330	0.0400	6.4050
4300	1.7850	0.0730	8.7000
4400	1.7300	0.1140	8.6800
4500	1.3850	0.1565	7.3000
4600	1.1530	0.2370	6.6300
700-7700	105.863	99.5756	14.7479
Sum	114.097	100.2187	56.2168

Chromaticity co-ordinates	x	y	z
	0.422	0.370	0.208

Comparison with the standard tables<sup>(7)</sup> shows how largely  $E_A \bar{z}$  is affected by the Wald-Gibson-Tyndall modification.

The chromaticity co-ordinates for the other standard illuminants and the 2500° K full radiator are modified to the following by using the Wald-Gibson-Tyndall data.

	x	y	z
Illuminant B	0.309	0.277	0.414
Illuminant C	0.273	0.235	0.492
2500° K radiator	0.457	0.388	0.155
Green fluorescent	0.210	0.468	0.322

Applying these values to the visual measurements gives the following values of chromaticity co-ordinates for the fluorescent lamps.

	x	y	z
warm white	0.387	0.335	0.278
daylight	0.321	0.288	0.391

In the measurements where the green fluorescent is used the amount is so small that any uncertainty in its chromaticity with W-G-T data can only introduce a negligible error in the chromaticity co-ordinates of the warm white or daylight.

Applying the Wald-Gibson-Tyndall average data to the spectral band measurements by multiplying Band No. 1 by 9 and Band No. 2 by 2.4 gives the following computed chromaticities.

	x	y	z
warm white	0.371	0.317	0.312
daylight	0.317	0.276	0.407

## SUMMARY OF MEASUREMENTS

Table 4 gives a summary of the chromaticities obtained and indicates the degree of correlation obtained.

It will be seen that the correlation is much better with the C.I.E. data than with the Wald-Gibson-Tyndall data.

## CONCLUSIONS

The correlation which has been obtained between visual measurements and computed values of chromaticity co-ordinates on warm-white and daylight fluorescent lamps is satisfactory when the C.I.E. data is employed but is not satisfactory with the Wald-Gibson-Tyndall data.

Whilst the inconsistencies reported from the U.S.A. obviously require to be resolved, any modification of the C.I.E. data should give as good correlation on fluorescent lamp measurements as the present C.I.E. data. The fluorescent lamp should be of value in assessing the merits of any proposed modification to the blue-violet end of the spectrum.

The measurements reported in this paper have indicated no appreciable error in the standard observer data at 4358 Å but do not check the data at lower wavelengths.

## ACKNOWLEDGEMENT

Thanks are due to Dr. J. N. Aldington, Managing Director of Siemens Electric Lamps and Supplies Limited, for permission to publish this paper.

Table 4. Comparison of chromaticities obtained with C.I.E. and Wald-Gibson-Tyndall data

	Chromaticities with C.I.E. data						Difference spectral bands from visual		
	Visual			From spectral bands			x	y	z
	x	y	z	x	y	z			
warm white	0.421	0.385	0.194	0.420	0.392	0.188	-0.001	+0.007	-0.006
daylight	0.360	0.361	0.279	0.365	0.362	0.273	+0.005	+0.001	-0.006
	Chromaticities with Wald-Gibson-Tyndall data								
	x	y	z	x	y	z			
warm white	0.387	0.335	0.278	0.371	0.317	0.312	-0.016	-0.018	+0.034
daylight	0.321	0.288	0.391	0.317	0.276	0.407	-0.004	-0.012	+0.016

## REFERENCES

- (1) JACOBSON, A. E. *J. Opt. Soc. Amer.*, **38**, p. 442 (1948).
- (2) JUDD, D. B. Comparison of direct colorimetry of titanium pigments with their indirect colorimetry based on spectro-photometry and a standard observer. C.I.E. Meeting (1948).
- (3) HENDERSON, S. T., and HALSTEAD, M. B. *Brit. J. Appl. Phys.*, **3**, p. 255 (1952).
- (4) HARRISON, W. *Siemens Engineering Bulletin*, No. 231 (1947).
- (5) HARDING, H. G. W. *J. Sci. Instrum.*, **27**, p. 132 (1950).
- (6) HARRISON, W. *Light and Ltg.*, **45**, No. 4 (1952).
- (7) WRIGHT, W. D. *The Measurement of Colour*, p. 214 (London: Adam Hilger Ltd., 1944).

## The electrical measurement of moisture in granular materials

By D. J. MILLARD, B.Sc., Ph.D., National Coal Board, Central Research Establishment, Stoke Orchard, Cheltenham

[Paper first received 17 September, 1952, and in final form 24 October, 1952]

A study has been made of the electrical properties of wet granular materials. Variations of conductance and capacitance with moisture content are given for a capacitor containing samples of coal, sand, gravel, soil and glass beads. The effects of material packing on these variables have also been studied. The use of these data in designing an electrical moisture meter has been considered, and the performance of such a meter, used with a specially designed "fringe field" capacitor to monitor the moisture content of a stream of coal leaving a drying tower, is described.

Many moisture meters have been developed commercially for use with materials ranging from wheat to fabrics, and an exhaustive survey of the work that has been done in this field has been prepared by the British Coal Utilisation Research Association Laboratories.<sup>(1)</sup> Unfortunately, for reasons set out below, none of the available devices are directly applicable to the needs of the coal industry, where it may be necessary to control a continuous process plant handling fine coal containing up to 15% by weight of moisture free on the surface of the coal. The instrument described in this paper was developed to meet this need, and has proved satisfactory, not

only for use with coal, but also for measuring the moisture content of sands, soil, gravel, and other such particulate materials.

### ELECTRICAL PROPERTIES OF WET GRANULAR MATERIALS

The electrical properties of wet granular materials were studied by packing samples of the various materials listed in Table 1 between the plates of a parallel plate capacitor (plates 4.8 × 6.3 cm; spacing 1.2 cm), measuring the conductance, capacitance and loss angle of the capacitor with an

Table 1. Details of the materials supplied

Material	Source	Description	Size range of particles
Coals			
(i) Penallta Cobbles	Penallta Colliery, N.C.B., S.W. Division	Steam coal 6.34% ash 19% volatiles	- 10 + 30 B.S.S. sieve size
(ii) Great Mountain Anthracite	Great Mountain Colliery, N.C.B., S.W. Division	Anthracite 2.89% ash 5.3% volatiles	- 10 + 30 B.S.S. sieve size
(iii) Park Plodder	Ince Moss Colliery, N.C.B., N.W. Division	Coking coal 13.85% ash 32.2% volatile	- 10 + 30 B.S.S. sieve size
(iv) Phurnacite blend	Sampled from Phurnacite plant	Blended Welsh steam coals	- 10 + 30 B.S.S. sieve size
Sand		Builders' sand	- $\frac{1}{16}$ in
Gravel		Cotswold stone	- $\frac{1}{8}$ in + 18
Soil	Stoke Orchard, Cheltenham, Gloucester	builders' gravel	B.S.S. sieve size
Glass beads		Clay soil	- $\frac{1}{16}$ in - 1.5 mm + 0.5 mm

c. bridge circuit and then comparing the observed variables with the moisture contents of the samples as determined by loss of weight on drying in an air oven at 105° C. Preliminary experiments with a Marconi Universal 1000 c/s bridge showed that for coal, once free water was present on the surface of the particles, the conductance was so high (of the order of  $3 \times 10^{-4}$  mhos) that dielectric effects were virtually unobservable. Observed capacitances were due to polarized layers on the measuring electrodes (compare work on soils by Smith-Rose<sup>(2, 3, 4)</sup>).

To enable dielectric effects to be observed more readily, further experiments were then carried out using a 20 Mc/s bridge circuit. The choice of frequency for this bridge was governed by the previously observed conductance of the coal specimens. It was decided that the operating frequency should be such that the susceptance of the capacitor should be equal to or greater than its conductance. The dielectric constant of a water-coal mixture was assumed to be of the order of 6, then the observed values of conductance required a working frequency of 4 Mc/s or higher. To allow an adequate safety factor in the event of underestimation, 20 Mc/s was chosen as a suitable frequency for all further experiments.

Before carrying out extensive investigations at 20 Mc/s it was necessary to devise a standard technique for packing specimens into the test capacitor. In doing so some interesting observations were made as to the effects of particle packing on the electrical properties of wet granular materials. The test capacitor was loosely filled with a sample of coal. Its capacitance and conductance were determined with a 20 Mc/s bridge. The d.c. conductance was also measured. The sample was then compressed with a plunger and the readings repeated for various degrees of compression of the coal. The result of a typical experiment is shown in Table 2. In all cases the high frequency conductance is larger than the d.c. conductance.<sup>(2)</sup> This may be attributed to the fact that at high frequencies individual water droplets are able to absorb energy directly, irrespective of the connexion between droplets. It will also be seen that the fractional changes in capacitance and conductance with packing differ greatly, relatively large conductance changes being due to the fact that the conductance depends on "bridges" between the moisture films on adjacent coal particles, and these bridges are greatly affected by the closeness of packing of the coal.

Table 2. Effects of packing on the electrical properties of a wet coal sample

Material: Phurnacite blend coal, 6.5% water

State of specimen	Conductance in mhos $\times 10^{-4}$ 20 Mc/s		Capacitance pF
Loose	3.41	8.40	13.59
States of increasing compression	3.76	8.62	13.68
	4.13	9.52	13.98
	4.46	10.00	14.00
Tightly compressed (two-thirds of original volume)	4.72	10.20	14.00
Ratio of final to original values	1.38 : 1	1.21 : 1	1.03 : 1

Once a standard packing technique (the compression of a sample to a state of maximum conductivity) was available, a study was made of a number of coals, glass beads, sand, soil and gravel. The capacitance and conductance of the test capacitor were determined for various samples and correlated

with the moisture content of the samples. Fig. 1 shows plots of capacitance *versus* moisture and Fig. 2 conductance *versus* moisture for the various materials. As might be expected, these curves show a substantially linear relationship between the observed variable and moisture content. However, for both sets of curves, the slopes differ for different materials.

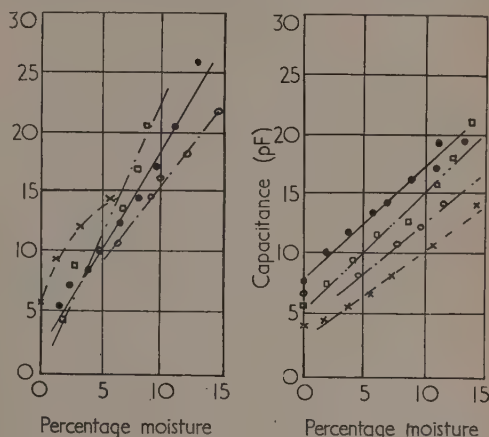


Fig. 1. Capacitance *versus* moisture content for four coals, glass beads, sand, soil and gravel

× Park Plodder Coal  
□ Sand  
○ Soil  
● Gravel  
× Penallta Cobbles Coal  
□ Great Mountain Anthracite  
○ Glass Beads  
● Phurnacite Blend Coal

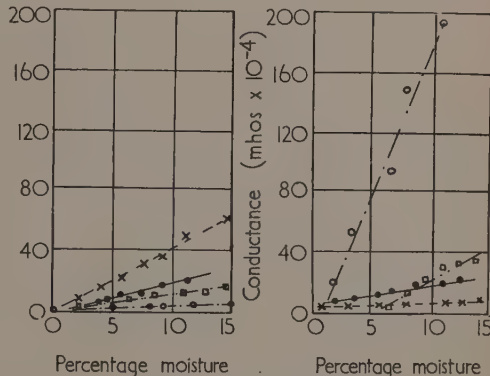


Fig. 2. Conductance *versus* moisture content for four coals, glass beads, sand, soil and gravel

× Sand  
□ Great Mountain Anthracite  
○ Glass Beads  
● Gravel  
× Penallta Cobbles Coal  
□ Soil  
○ Park Plodder Coal  
● Phurnacite Blend Coal

For the capacitance *versus* moisture curves this may be attributed to a particle shape factor dependent on the material being studied. It has been shown by Wiener<sup>(5)</sup> that the dielectric constant of a mixture depends on the pattern of the components and must lie between calculable limits which correspond to the material being in the form of laminae either parallel (maximum limit) or perpendicular (minimum limit) to the applied field. Thus a particle shape factor is to be



expected. The limiting slopes of the capacitance *versus* moisture curves have been calculated and it is seen, Table 3, that except for the case of sand all observed values do lie between these limits.

Table 3. *Slopes of capacitance versus moisture curves taken in range 10–15% free moisture*

Substance	Slope in pF per percentage moisture
Great Mountain Anthracite	1.40
Penallta Cobbles	1.04
Park Plodder	1.68 range 0–5% moisture
Phurnacite blend	0.96
Glass beads	0.60
Soil	0.70
Gravel	1.70 range 5–10% moisture
Sand	1.78 range 5–10% moisture

Estimated permissible range of slopes, calculated according to Wiener on the assumption that materials contain 30% by volume of air; 0.12 to 1.170 pF per percentage moisture.

In the case of the conductance *versus* moisture curves there is a much greater range of observed slopes. Here, any particle shape factor is of minor importance, the differing slopes being principally due to the different amount of water-soluble impurities in the specimens. This was confirmed by a series of subsidiary experiments on water that had been used to wash samples to extract these impurities.

#### DESIGN OF A MEASURING INSTRUMENT

It will be seen from the results of the above experiments that when a capacitor is filled with a given sample of wet granular material the observed conductance is influenced by the packing of the material and impurities in the water to a much greater extent than is the observed capacitance. Further evidence on this point is provided by Drake, Pierce and Daw<sup>(6)</sup> who showed that on increasing the concentration of a solution of potassium chloride from 0 to 1/70 normal, the conductance increased by a factor of 200 without any perceptible change in dielectric constant.

Thus it is preferable that an electrical moisture meter for use with the materials tested should be a capacitance measuring rather than a conductance or loss angle measuring device, the latter being discarded on the grounds that it, too, would contain all the disadvantages inherent in a conductance measurement. The problem is reduced, then, to the construction of a directly indicating capacitance measuring device, the behaviour of which must not be influenced by conductance in the capacitors to be measured. Most of the commercially available capacitance measuring electrical moisture meters are unsuitable for use with the materials under consideration since they would be influenced by conductance.

Following the experience gained in the initial stages of this work, the measuring device chosen was a 27.12 Mc/s bridge circuit in which a test capacitor was compared directly with a standard capacitor. It was arranged for the bridge to be balanced when the test capacitor was empty, capacitance changes being observed as the out-of-balance signal of the bridge. Thus, the moisture content of material placed in the test capacitor was directly indicated by the reading of a suitably connected valve voltmeter.

The choice of a frequency was governed by the need to compromise between the conflicting requirements of making

conductance effects negligible and of avoiding both excessive constructional difficulties and increased conductances which are found at frequencies above about 20 Mc/s.<sup>(2)</sup> The first of these requirements indicates a high working frequency, the latter two a low working frequency. This compromise is best met by using a frequency of the order of 20 to 30 Mc/s. The actual value, 27.12 Mc/s, was chosen since it is the centre of a band allocated by international agreement for the use of industrial and scientific equipment.

Using this bridge, measurements were made on samples of coal, sand, gravel, soil and glass beads containing up to 15%

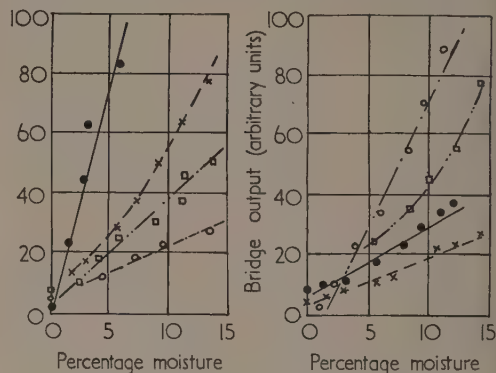


Fig. 3. Output from 27 Mc/s bridge *versus* moisture content for four coals, glass beads, sand, soil and gravel

× Gravel  
□ Great Mountain Anthracite  
○ Glass Beads  
● Park Plodder Coal  
× Penallta Cobbles Coal  
□ Soil  
○ Sand  
● Phurnacite Blend Coal

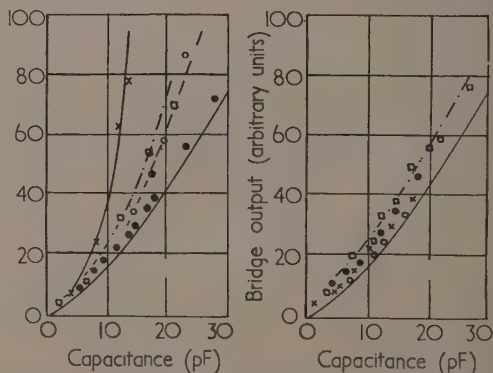


Fig. 4. Comparison of plots of bridge output *versus* capacitance curves for a pure capacitance and for a capacitor containing samples of materials used

× Park Plodder Coal  
□ Sand  
○ Soil  
● Phurnacite Blend Coal  
× Gravel  
□ Great Mountain Anthracite  
× Penallta Cobbles Coal  
● Glass Beads

by weight of water, the samples being packed between the plates of the capacitor previously described. The results of these experiments are shown in Fig. 3. It is seen that there is a usable, and in most cases a linear, relationship between moisture content and the observed variable. It is important

to check how far this relationship depends solely upon capacitance effects and how far it is influenced by conductance. It can be shown that, for small changes, the off balance voltage of a bridge is proportional to  $C(1 + G^2/C^2\omega^2)^{1/2}$  where  $C$  and  $G$  are the out-of-balance capacitance and conductance respectively and  $\omega$  is the angular frequency of measurement. Thus, comparing a graph of  $V$  versus  $C$  for a series of readings taken on any material with a calibration plot of  $V$  versus  $C$  for a standard capacitor will show at once if the bridge output is being influenced by conductance, since conductance effects will cause the line of the test plot to rise above the calibration line. This has been done for the various materials tested (Fig. 4) and the results show that the bridge output was free of undesirable effects in all cases except that of Park Plodder coal. In this case readings were as much as 30% higher than would be expected for a pure capacitance measurement and so changes in conductance due to variations other than in moisture content would affect the instrument reading for this material. The general expression for the effect of this influence can be shown to be

$$\frac{\Delta V}{V} = \frac{1}{1 + G/C\omega} \cdot \frac{\Delta G}{G}$$

where  $\Delta V$  is the variation in reading and  $\Delta G$  is the conductance change producing that variation and  $G$ ,  $C$  and  $\omega$  are as previously defined.

#### THE DESIGN OF A SAMPLING CAPACITOR AND THE TESTING OF THE APPARATUS UNDER INDUSTRIAL CONDITIONS

The sampling capacitor in which material to be studied is packed for measurement must, in practice, be varied to suit each individual use of the instrument. The capacitor described below was designed for use at the National Coal Board's Phurnacite plant at Aberaman. At this plant the instrument is required to monitor the moisture content of coal leaving a drying tower. This coal may be expected to contain up to 1% by weight of water. It falls from the tower on to a rotating feed table and is scraped from the table on to a screw conveyor by a fixed plough blade mounted above the table. The rate of feed of coal is about 20 tons an hour and its size is  $\frac{1}{2}$  in, but at this point in the plant the coal stream may contain foreign bodies much larger than  $\frac{1}{2}$  in. Thus, it was necessary to design a sample capacitor that would neither block this stream nor itself become blocked. Following Heinrich<sup>(7)</sup> and Hearle and Jones,<sup>(8)</sup> it was decided to use a "fringe field" capacitor. This type of capacitor employs flat electrodes placed side by side, the material to be tested passing over the plates and altering the fringe field between them. It has the advantage that the material to be studied flows over a surface and not between plates, thus the flow cannot readily be obstructed. The form of the capacitor finally chosen consisted of two foil strips  $10 \times \frac{1}{2}$  in ( $25 \times 1.3$  cm) connected together ("live" electrode) mounted in a  $11 \times 1\frac{1}{2}$  in ( $27.5 \times 3.8$  cm) window in a steel frame ("earthy" electrode). This particular geometrical pattern was chosen after studying the field patterns of various capacitors by means of two-dimensional models mounted on an electrolytic sheet. The apparatus was temporarily installed at the Phurnacite plant, the sampling capacitor being mounted on the plough blade clearing the feed table. The angle between the capacitor face and the plough blade was adjusted until coal flowed continuously over the face and did not block or form stationary shadows. When so mounted it was found that even for

low rates of coal feed there was always enough material passing to cover adequately the face of the capacitor. The instrument was calibrated under these conditions and it was found that all spot readings taken lay within  $\pm 0.4\%$  moisture of the average calibration line. Unfortunately, due to the gain control being too far advanced, during these field trials, it was not possible to calibrate the apparatus for coal containing more than 3.5% of water.

#### DISCUSSION OF POSSIBLE IMPROVEMENTS

The apparatus described above has been found satisfactory for measuring the moisture content of various granular materials containing up to 15% moisture, but with Park Plodder coal, the instrument was influenced by undesirable conductivity effects.

There are two possible ways of preventing conductivity influencing the meter readings which can be seen on consideration of Maxwell's equations, in which conductivity in a dielectric is allowed for by replacing the dielectric constant  $\epsilon$  by the complex quantity  $\epsilon' = \epsilon(1 - j4\pi\sigma/\omega)$  where  $\sigma$  is the conductivity and  $\omega$  the angular frequency. To produce a measurement independent of  $\sigma$  one must either make the imaginary term negligible (i.e. increase  $\omega$ ) or separate the real and imaginary terms (i.e. use some phase sensitive device). A simple change of measuring technique at a given frequency cannot in itself effect any great improvement in the conductivity characteristics of a capacitance measuring instrument. For the instrument under consideration, however, it was decided that the advantages to be gained either by increasing the frequency to 100 Mc/s—that at which conductance effects would be negligible even for the most highly conducting material encountered—or by introducing a phase sensitive detector, would be outweighed by the increase in complexity of the apparatus.

#### ACKNOWLEDGEMENTS

The author wishes to express his thanks to Mr. D. G. A. Thomas for help with the electronics, and to Fielden (Electronics) Ltd. for co-operation in the supply of industrial electronic equipment. The equipment is covered by British Provisional Patent No. 25350/51, and is being produced by Fielden (Electronics) Ltd. in a form suitable for general industrial use. The author also wishes to express his thanks to the National Coal Board for permission to publish this article. The views expressed in it are those of the author and not necessarily those of the Board.

#### REFERENCES

- (1) BADZIOCH, S., and CORNFORD, G. B. *Mon. Bull. Brit. Coal. Util. Res. Ass.*, **16**, p. 97 (1952).
- (2) SMITH-ROSE, R. L. *J. Inst. Elect. Engrs*, **75**, p. 221 (1934).
- (3) SMITH-ROSE, R. L. *Proc. Phys. Soc.*, **47**, p. 923 (1935).
- (4) SMITH-ROSE, R. L. *Proc. Roy. Soc. Lond. (A)*, **143**, p. 135 (1933).
- (5) WEINER, O. *Akad. Wiss. Leipzig*, **1912**, p. 509; *Leipzig Ber.*, **61**, p. 113 (1910); **62**, p. 256 (1910).
- (6) DRAKE, PIERCE and DAW. *Phys. Rev.*, **35**, p. 613 (1930).
- (7) HEINRICH, F. A. German Patent No. 708,389 (1941).
- (8) HEARLE, J. S., and JONES, E. H. *J. Text. Inst. Manchr.*, **40**, p. 311 (1949).

# The use of X-ray diffraction cameras as recording optical goniometers

By E. STANLEY, B.Sc., Ph.D., A.Inst.P.,\* Viriamu Jones Laboratory, University College, Cardiff

[Paper first received 18 September, and in final form 22 October, 1952]

A method is described for the rough goniometry of small crystals using X-ray diffraction cameras. Visible light is used instead of X-rays and a photographic record of the external reflexions is obtained by either the rotating-crystal or the Weissenberg technique. Each type of photograph is discussed in detail and examples are given showing how the goniometric data for all the faces may be rapidly determined with the aid of existing charts. The method requires crystals with linear dimensions not exceeding 1 or 2 mm and will reveal faces less than  $0.01 \text{ mm}^2$ . Practical details are given of the modifications of technique that are necessary and the precautions to be taken.

The idea of making a photographic record of the reflexions of a collimated beam of light by the faces of a crystal under examination is not new. A number of methods have been proposed in the past, but they do not seem to have been used at all extensively. Schwartzmann<sup>(1,2)</sup> used an ordinary camera to record the reflected light beams.<sup>3</sup> The geometry of the directions of the reflected beams, the way in which the intensities vary with direction and the occurrence of internal reflexions have been dealt with by Rosch,<sup>(3-7)</sup> who also proposed the use of "back-reflexion" and cylindrical-film cameras for recording the reflexions. A moving-film method for optical goniometry was suggested by Herlinger.<sup>(8)</sup> The purpose of this paper is to indicate the way in which standard X-ray cameras, with little modification, can be used for rough optical goniometry and orientation studies.

## GENERAL PRINCIPLES

If a small single crystal is mounted in the usual way on an X-ray goniometer and a suitable light source substituted for the X-ray target, a photograph can be obtained on which are recorded the reflexions from those faces of the crystal which are in a position to reflect. The crystals used in these methods are small (usually less than 1 mm in cross-section) and it is not necessary to make any correction for the fact that the faces are not all in the same position with respect to the beam and the axis of rotation. If the crystal is rotated continuously about the axis during the exposure, the reflexions appear on the film as a series of  $\rho$ -lines, each line corresponding to the inclination  $\rho$  of the face normal of the corresponding face to the axis of rotation. Under suitable conditions the values of  $\rho$  can be determined to within about  $1^\circ$ . The strength and sharpness of the lines indicate the importance and perfection of the faces to which the reflexions correspond. Using a stationary-film camera, it is possible to obtain a complete description of the crystal in its orientation with respect to the goniometer arcs from three separate rotation photographs taken as described below. If a moving-film camera of the Weissenberg type is used a single photograph, with an oscillation of more than  $180^\circ$ , is sufficient for the complete description of the crystal.

## ROTATION PHOTOGRAPHS AND THEIR INTERPRETATION

A rotation photograph using a light source is shown in Fig. 1. The  $\rho$ -lines formed by the light beams reflected by

the external faces can be seen as continuous lines. The values of  $\rho$  for the faces of the crystal can be obtained from measurements made directly on the film, or with the aid of a  $\rho$ -line chart (see, for example, Henry, Lipson and Wooster<sup>(9)</sup>). If the crystal is transparent there occur, in addition, a number of single or multiple internal reflexions. Some reflexions of this type appear in Fig. 1. They can usually be distinguished

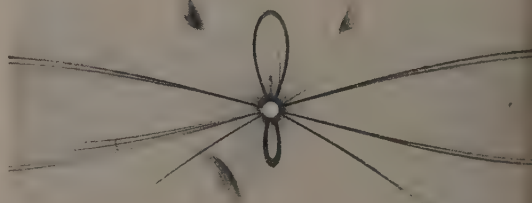


Fig. 1. Rotation photograph of a transparent crystal using a light source. Photograph shows continuous streaks due to external reflexions, and discontinuous, diffuse streaks due to internal reflexions

Crystal of cinchonidine hydrochloride (about  $0.5 \times 0.5 \times 0.3 \text{ mm}$ ) in an arbitrarily tilted setting).

from the external reflexions because they are broad (owing to the optical dispersion), they are discontinuous (owing to the critical angle of reflexion), and they do not, in general, follow the  $\rho$ -lines. A stationary-crystal photograph is much more difficult to interpret because of these internal reflexions, and has not been found to be of any use.

A single rotation photograph is not directly very informative, but when used in conjunction with an indexed X-ray rotation photograph taken with the same crystal in the same orientation, it should be possible to index the principal faces of the crystal. If two further photographs are taken using the same crystal in different, relatively known, orientations, it is possible to carry out all the measurements normally required for a complete description of the crystal.

The stereogram of the first photograph about the axis of rotation is a set of concentric circles of angular radius  $\rho$

\* Now at the University of Southern California, Los Angeles, U.S.A.



about the centre of the primitive. The crystal is then displaced through a known angle  $\alpha$  about one of the goniometer arcs and a second photograph obtained. The stereogram of the second, in the same orientation as the first, is a set of circles (no longer concentric on the stereogram) about an axis inclined at an angle  $\alpha$  to the axis of the original stereogram. The two sets of circles intersect, in general, in two points. The crystal is restored to its original orientation and then displaced through a known angle  $\beta$  about the other goniometer arc (perpendicular to the first arc), a third photograph taken, and the corresponding stereogram constructed. Three sets of intersecting circles are obtained in this way, and those points common to three circles, one from each set, correspond to the poles of the crystal in the original orientation. Fig. 2 shows this construction for a single pole. In

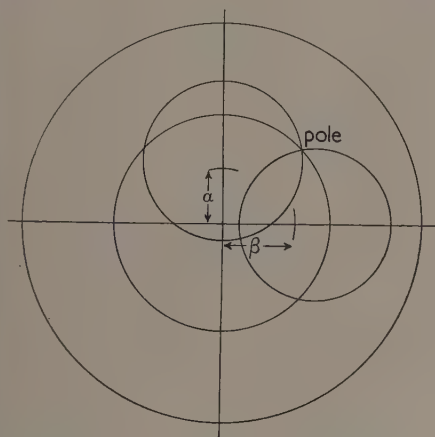


Fig. 2. Stereographic construction leading to the location of a single pole

this way the complete stereogram of the crystal can be constructed in the original orientation with respect to the goniometer arcs. Any ambiguities remaining can be resolved by taking further photographs with the crystal displaced through angles  $\alpha'$ ,  $\beta'$ , etc. If the original axis of rotation has been arbitrarily chosen, the final stereogram can be manipulated by standard methods to give a more convenient orientation.

By applying this method to a crystal of cinchonidine hydrochloride the probable crystal class, 222, was inferred and the axial ratios determined as 1.00 : 1 : 0.81. These measurements are in reasonable agreement with those of Roth<sup>(10)</sup> using standard optical methods (0.9601 : 1 : 0.7855) and the X-ray measurements of Griffiths<sup>(11)</sup> (0.96 : 1 : 0.80).

#### WEISSENBERG PHOTOGRAPHS AND THEIR INTERPRETATION

If the Weissenberg technique is used, only a single photograph, taken with the layer-line screen removed from the camera, is necessary for the complete description. Such photographs contain sufficient information to enable the stereogram about the axis of rotation to be drawn directly from measurements made on the photographs. The principal features of the photographs are: (a)  $90^\circ$   $\rho$ -lines appear as

straight lines whose inclination depends on the constants of the camera, and all other values of  $\rho$  give rise to lines of a characteristic shape depending only on  $\rho$  and the camera constants; (b) the positions of the  $\rho$ -lines depend only on the angle  $\omega$  which the crystal-face normals make with the plane containing the direction of the incident beam and the axis of rotation; (c) faces in any zone whose axis is perpendicular to the axis of rotation give rise to a set of  $\rho$ -lines which all

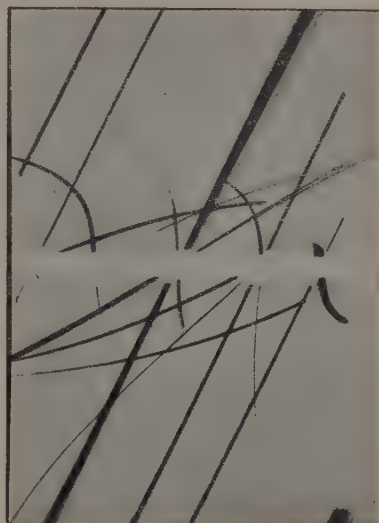


Fig. 3. Weissenberg photograph of an opaque crystal using a light source. The crystal of potassium permanganate ( $0.3 \times 0.3 \times 0.3$  mm) was rotated about a principal zone axis

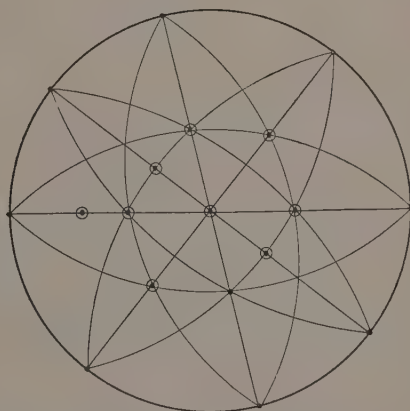


Fig. 4. Stereogram constructed from the information in the Weissenberg photograph (Fig. 3). The two groups of end facets are indicated in the usual way. The terminating faces normal to the zone axis are included although not indicated in Fig. 3. They were inferred from photographs of the mis-set crystal and were visible under the microscope

intersect the centre line of the film at the same point. For interpretation it is convenient to use a special chart\* which has been prepared by Wooster and Wooster<sup>(12)</sup> for the interpretation of photographs taken with X-rays. From the two angles  $\rho$  and  $\omega$  (measured from an arbitrary origin) the complete stereogram of the crystal can be constructed. Transparent crystals give rise to additional, internal, reflexions which again are usually distinguishable from the external reflexions. Fig. 3 is a typical Weissenberg photograph of an opaque crystal (potassium permanganate), oscillated about a principal zone axis, which shows the main features listed above. Fig. 4 is the stereogram derived from the photograph (Fig. 3), and from it the probable crystal class, *mmm*, was inferred and the axial ratios of 0.83 : 1 : 1.28 were obtained. These figures compare reasonably well with those obtained by Mooney<sup>(13)</sup> from X-ray measurements, 0.773 : 1 : 1.23. Although the Weissenberg camera is the only moving-film camera which has been used so far, there seems to be no reason why other moving film cameras could not be used for the same purpose.

## PRACTICAL DETAILS

The most important practical consideration is the elimination of unwanted light. A considerable amount of scatter occurs inside the collimator, but can be reduced either by blackening with a matt black paint or by smoking. The glass fibre, on which the crystal is mounted, and the adhesive can also cause a great deal of unwanted scatter. The glass fibre can be smoked to reduce this and the amount of adhesive used should be the very minimum necessary. All extraneous light should be excluded from the inside of the camera. The light source itself can be a coiled filament lamp of the type used in galvanometer lamps, and optical collimation is optional. Ordinary X-ray film is quite satisfactory; galvanometer recording paper has also proved useful although considerably slower. Comparatively short exposures are required. With X-ray film (Ilford Industrial A), and a 12 V, 24 W tungsten-filament lamp (not optically collimated) as the source, a single rotation of duration  $1\frac{1}{2}$  min was more than sufficient to record all the reflexions. The internal reflexions from strongly coloured crystals are very weak and are often not recorded. With lightly coloured crystals the intensity of the internal reflexions could perhaps be reduced by suitably filtering the light incident on the crystal, provided that the remaining light were sufficiently actinic. The crystals should be completely enveloped by the beam, but if needle-like crystals are being investigated this is often impossible. In that event the needle should be attached half-way along one of its prism faces to an inclined glass fibre, care being taken to keep both ends of that face free from adhesive. It is then mounted for rotation about its needle axis. In this way both groups of terminating facets and portions of the prism faces may be introduced into the light beam by a translation along the rotation axis. Two separate exposures are then taken (on the same or on two different films), one for each

end of the crystal. It seems possible to record reflexions from very small faces ( $\approx 10^{-3}$  mm<sup>2</sup>) which would be difficult to locate by ordinary methods.

The methods described are not very accurate, and the results which can be obtained do not compare with those obtainable from the standard optical methods, but the determination of the axial ratios and the interaxial angles by the present methods is of the same order of accuracy as the measurements made from X-ray photographs using charts. The convenience of the methods, however, recommends them. At the most it is only necessary to adjust the crystal about one zone axis. The stationary-film method may have some applications to orientation studies. The Weissenberg method is much more convenient for optical goniometry; it can indicate the symmetry of the crystal and provide approximate values for the axial ratios and the interaxial angles with considerably less labour than a single-circle goniometer. As a supplementary method for preliminary optical examination the methods are likely to be most useful.

## ACKNOWLEDGEMENTS

I am indebted to the Department of Scientific and Industrial Research for the award of a maintenance grant during the tenure of which the methods were devised, and to Dr. A. J. C. Wilson for the use of equipment purchased with a Royal Society Grant.

## REFERENCES

- (1) SCHWARTZMANN, M. *Neues Jahrbuch für Mineralogie, etc.*, **II**, p. 4 (1900).
- (2) SCHWARTZMANN, M. *Neues Jahrbuch für Mineralogie, etc.*, **I**, p. 9 (1901).
- (3) ROSCH, S. *Berichte der math.-phys. Klasse der sächsischen Akademie der Wissenschaften*, **39** (6), p. 89 (1925).
- (4) ROSCH, S. *Beiträge zur Krystallographie und Mineralogie III*, No. 1, p. 105 (1926).
- (5) ROSCH, S. *Abhandlungen der math.-phys. Klasse der sächsischen Akademie der Wissenschaften*, **39**, No. 6 (1926).
- (6) ROSCH, S. *Z. Krist.*, **65**, p. 46 (1927).
- (7) ROSCH, S. *Z. Krist.*, **65**, p. 28 (1927).
- (8) HERLINGER, E. *Z. Krist.*, **66**, p. 282 (1928).
- (9) HENRY, N. F. M., LIPSON, H., and WOOSTER, W. A. *The Interpretation of X-Ray Diffraction Photographs*. (London: Macmillan and Sons, 1951.)
- (10) GROTH, P. *Chemische Krystallographie*. Vol. 5, p. 921. (Leipzig: W. Engelmann, 1919.)
- (11) GRIFFITHS, P. J. F. *Acta Cryst.*, **5**, p. 290 (1952).
- (12) WOOSTER, N., and WOOSTER, W. A. *Phil. Mag.*, **37**, p. 262 (1946).
- (13) MOONEY, R. C. L. *Phys. Rev.*, **37**, p. 1306 (1931).

\* Available from The Institute of Physics, 47 Belgrave Square, London, S.W.1, price 1s. 6d. for twenty copies on bleached transparent paper. Please quote reference PC.17.

## Correspondence

## Current densities of free-moving cathode spots on mercury

In a recent paper in this *Journal* H. v. Bertele<sup>(1)</sup> attempts to prove that the emission current density from the cathode "spot" of a vacuum mercury arc varies as the inverse logarithm of the time elapsed since the striking of the arc. A more careful assessment of the experimental evidence suggests that this conclusion is incorrect.

Bertele uses but three measurements of current density; that of Güntherschulze<sup>(2)</sup> reporting emission densities of 4000 A/cm<sup>2</sup> for well-established arcs; that of Cobine and Gallagher<sup>(3)</sup> reporting densities of about  $2 \times 10^5$  A/cm<sup>2</sup> for arcs which have been in existence for times of the order of a millisecond; and that of the writer<sup>(4)</sup> reporting densities of up to  $10^7$  A/cm<sup>2</sup>, which Bertele tacitly implies in Fig. 1 of his paper were observed over the time interval of from 1 to 10  $\mu$ sec from the start of the arc.

No reliance can be placed upon the first of these measurements. Güntherschulze never observed the true cathode emitting area at all. He made moving-film observations in a time interval of about  $10^{-2}$  sec, and this combination of a long exposure time and a moving-film would obliterate the nature and size of the real current-emitting areas.

When the writer<sup>(5)</sup> first noticed that the 4000 A/cm<sup>2</sup> value for the emission current density was wildly in error he stated that the bright, erratically-moving spot which one sees upon the cathode is actually a relatively slow-moving envelope containing several minute emitting areas each carrying a current of the order of 1 A. When the arc current exceeds 5-30 A two or more such groups are formed, and so on for increasing currents. These tiny areas are much faster moving than their containing envelope, and microsecond exposures through a microscope are needed to arrest their motion and reveal their minuteness. The apparent size of these areas is quite independent of the time from the start of the arc, being observed the same for transient arcs of a few microseconds duration or for normal d.c. arcs one-two hundredths of a second after the start. The division of these small areas into groups has no special significance and is a rather slower process, taking perhaps a millisecond. If the emission is erroneously thought to proceed from the whole envelope of such groups, then Güntherschulze's value of current density can be approximately obtained.

At this time<sup>(5,6)</sup> the writer estimated the emission current density as "at least"  $10^5$  A/cm<sup>2</sup>, but he is now of the opinion that the current density is always between  $2 \times 10^6$  and  $10^7$  A/cm<sup>2</sup> as stated on p. 812 of ref. (4), and for the reasons given there.

The emitting areas are so small and rapidly moving that very refined apparatus<sup>(7,8)</sup> is required if they are to be observed at all properly. In order that a magnified image can be obtained, small arc discharge tubes are essential. Yet these tubes must carry currents of up to hundreds of amperes if the cathode "spot" is to be thoroughly investigated. Hence the writer's predominant use of transient discharges.

The results of Cobine and Gallagher are in agreement with those of the writer, provided the correct interpretation is placed upon the former. Cobine and Gallagher took photomicrographs of the track of the cathode emitting area when made to move rapidly and unidirectionally by placing the

discharge tube in a magnetic field. The camera shutter was left open for the whole of the time taken for the area to move across the field of the microscope objective. In order to estimate current density they assumed that the true "spot" was circular, of diameter equal to the width of the track photographed. The writer's high speed photographs<sup>(4)</sup> show that this assumption is not justified, and that the emitting area (when in a magnetic field) consists of a linked, or partly linked, chain of the tiny spots already mentioned extending in a serrated line at right-angles to its direction of motion. Once this difference in technique is noted, Cobine and Gallagher's results are not at variance with the writer's.

Bertele finds support for his conclusions in the theory of Smith.<sup>(9)</sup> Smith subsequently published an *erratum*<sup>(10)</sup> stating that one of the constants he had used in his calculations was in error by no less than five orders of magnitude, thus rendering his theory of low emission current densities untenable.

This letter is published by permission of the Director of the National Physical Laboratory.

Metrology Division,  
National Physical Laboratory,  
Teddington, Middlesex.

K. D. FROOME

## REFERENCES

- (1) BERTELE, H. v. *Brit. J. Appl. Phys.*, **3**, p. 358 (1952).
- (2) GÜNTHERSCHULZE, A. *Z. Phys.*, **11**, p. 74 (1922).
- (3) COBINE, J. D., and GALLAGHER, C. J. *Phys. Rev.*, **74**, p. 1524 (1948).
- (4) FROOME, K. D. *Proc. Phys. Soc., Lond.*, **62**, p. 805 (1949).
- (5) FROOME, K. D. *Nature, Lond.*, **167**, p. 446 (1946).
- (6) FROOME, K. D. *Proc. Phys. Soc., Lond.*, **60**, p. 424 (1948).
- (7) FROOME, K. D. *J. Sci. Instrum.*, **25**, p. 371 (1948).
- (8) FROOME, K. D. *Phot. J.*, **92B**, p. 158 (1952).
- (9) SMITH, C. G. *Phys. Rev.*, **62**, p. 48 (1942).
- (10) SMITH, C. G. *Phys. Rev.*, **64**, p. 40 (1943).

The chief aim of my paper was to define those values of current density in spot emission which are instrumental in determining the thermal behaviour of the system. The conclusion reached was that it is correct to use the old values for the calculation of the thermal fields of free moving spots. This conclusion was based on the results of investigations of the surface appearance of pool cathodes under steady state conditions (see ref. (5) in the original paper). By using a highspeed cine-camera the occurrence of a limited number of concentrated emission areas was established, which are distributed over the pool surface and have emission intensities lying within narrow limits. It is the energy liberated within these well-defined areas which has to account for the thermal fields developed as a result of the heat flow through the cathode pool.

The occurrence of these (well-defined) emission groups, which develop from minute units in milliseconds, agrees with Froome's statement; he refers to them as "divisions," although a better term would be "aggregations."

The average behaviour of these patch-like emission areas on the mercury surface is characterized by expansion and random extinction as described in my paper.

No explanation has as yet been given for the existence and



the peculiarities of these "emission patches," as they will be referred to in the following, and it might therefore still be worth while to consider C. G. Smith's basic concept as the underlying mechanism, since the Thomson heat need not enter the picture. According to this, a distinct inflow of electrons into the metal takes place as a result of the thermal velocities which they acquired in the cathode fall zone above the spot. In the top layer of the metal preferential electron collisions take place with the electron gas which must increase the energy of the latter without disturbing the metal lattice itself. In fact, it can be shown experimentally that if a sufficiently low heat transfer resistance is provided directly at the emission zone, any mass transference from the spot area may be suppressed and even a mass inflow from the vapour may be produced. This may be regarded as definite proof of the existence of a spot-metal temperature as low as that of the vapour saturation and of the irrelevance of this temperature for the emission itself. However, if this is so, then the heat flowing in the pool from the spot area could not have originated above the spot but must have been transformed within the metal lattice. Moreover, if the metal matrix is irrelevant for the emission, the transference of energy must have occurred by particles of size far below the ion-size, i.e. by electrons as suggested by Smith.

Froome's observation of minute and highly concentrated emission units which carry low currents, forms an important contribution to the knowledge of the obscure emission phenomena which occur at the cathode spots. However, as yet there is no evidence which would suggest that these units are the only sources of spot emission. There seems to be no doubt that they represent the initiation of new emission centres both at the beginning of a discharge as well as at each formation of a new group. The latter, however, is more probable when the current increases, provided steady distribution of emission has not yet been reached, i.e. under conditions which obviously still prevailed during the 5 msec observations mentioned by Froome. The writer believes that besides the minute emission units discovered by Froome, parallel emission with lower current density occurs. This belief was not only formed from a study of the steady-state records, mentioned above. It seems to be supported by the appearance of the emission, when attached to low temperature anchors. This consists eventually both of minute and very bright emission centres as well as extended homogeneous areas, which are not so bright.

Froome's interpretation of the results of Cobine and Gallagher does not appear to be in complete agreement with the pictures he published in his paper. Fig. 7(a), for instance, of the 1949 paper rather gives the impression of a coherent area for the bulk emission surrounded by a few scattered spot individuals. Moreover, it must be borne in mind, that the case illustrated, being both a transient pulse and occurring in a superimposed magnetic field, is different from that envisaged by the writer, i.e. a steady state of free moving spot emission.

Besides the micro-structure of the patches, the formation of the patches and their existence as well, as perhaps their life cycle have to be considered as characteristic features of free spot emission. The facts that the emission intensity is restricted to close current limits and that both random speed and extinction follow definite distribution functions, all seem to give to the patches the character of a physical entity.

I welcome Dr. Froome's comments for their clarification of the essential difference between minute emission units and emission patches. They also throw light on the different conditions of operation to which spot emission is subjected

in discharges. Although extensive practical applications have been made of cathode spot emission, the phenomena involved still lack a satisfactory explanation. Such an explanation will be possible only by novel methods of investigation such as, for example, Froome's refined Kerr-cell technique.

Purley,  
Surrey.

H. V. BERTELE

### The effect of vertical divergence on X-ray powder diffraction lines

I was happy to see the improved treatment of this topic published recently in this *Journal* by Eastabrook.<sup>(1)</sup> However, the latter conveys the impression that my earlier published results for the X-ray spectrometer<sup>(2, 3)</sup> are quite in error, whereas actually my equation (3)–(24) (equation 24 of reference 3) for the limiting line displacement in the region  $2\theta = 0$  to  $90^\circ$  due to finite sample height is simply a more approximate expression of the aberration than Eastabrook's equation (13a). Furthermore, my equation (3)–(26) for the line profile due to sample height

$$I(\epsilon) = \epsilon^{-1} \quad (1)$$

is identical with his equation (15a)

$$I(\epsilon) = (2\epsilon \cot \theta)^{-1} \quad (2)$$

when the constant coefficients are neglected, including his factor  $\cot \theta$ , which is virtually invariant over the small angular range  $\epsilon = 0$  to  $\epsilon_{\max}$ . Hence, except for a small difference in the limiting angle,  $\epsilon_{\max}$  [see Fig. 3 of ref. (1)], our vertical divergence profiles are identical at small Bragg angles where this effect is consequential. At larger angles this aberration is too small to be experimentally observable.

In my first paper on this subject<sup>(2)</sup> an attempt was made to illustrate in a semi-quantitative manner how third-dimensional properties of the ideally two-dimensional focusing geometry of an X-ray spectrometer lead to asymmetry in the low-angle region. A formula (2)–(4), intended for the angular range  $2\theta = 0 - 90^\circ$ , was developed on the basis of circular diffraction haloes. A factor  $\cos 2\theta$  was incorporated to allow for the fact that, as Eastabrook points out, the receiving slit in an actual spectrometer intercepts the diffraction cones in sections other than circular. In ref. (3) this formula for the limiting displacement from the ideal angle,  $2\theta$ , was simplified by taking into account only the dominant effect of sample height, which yielded equation (3)–(24):

$$\epsilon_{\max} = -(\beta^2/8)(1 + \cos 2\theta)^2 \cot 2\theta \quad (3)$$

where  $\beta$  is the overall vertical divergence angle. Noting that in the present notation Eastabrook's  $\epsilon$  is equal to  $-\epsilon/2$  and  $p/R$  is equivalent to  $\beta/2$ , we are to compare equation (3) above with his equation (13a) in the form

$$\epsilon_{\max} = -(\beta^2/4) \cot \theta. \quad (4)$$

In Fig. 1 these two functions are compared in the range of  $2\theta$  from 0 to  $90^\circ$ . It is seen that the more exact equation (4) does not give significantly different results in the low-angle region where the vertical divergence effect is great enough to visibly distort the diffraction profiles. At higher angles the difference between the two functions admittedly becomes great in a relative sense, but here the magnitude of the effect is so small in relation to the other instrumental factors affecting the line profile that it cannot be detected experimentally.

I have recently employed an analytical method to synthesize vertical divergence profiles for spectrometers with Soller slits and obtained curves very similar to those given by Eastbrook

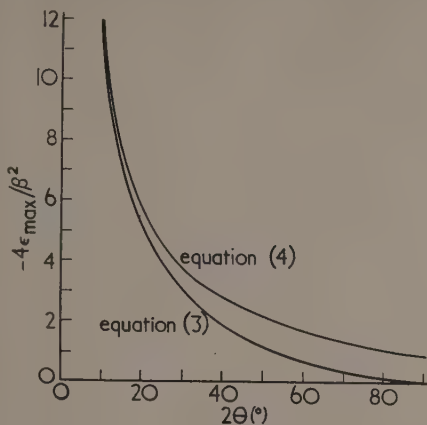


Fig. 1. Comparison of equations (3) and (4)

[see Fig. 4 of ref. (1)]. The same study also embraces an improved convolution treatment of the generation of spectrometer line profiles from the joint action of the several important geometrical factors.<sup>(4)</sup> Fig. 2 shows the excellent

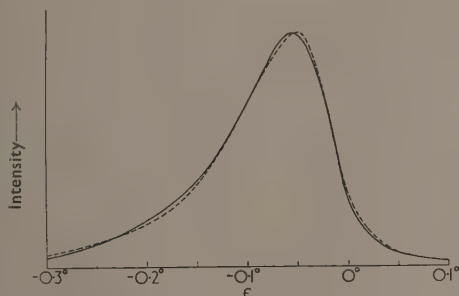


Fig. 2. Comparison of theoretical and observed profiles

agreement obtained between the theoretical and observed profiles under conditions involving considerable distortion due to vertical divergence [ $2\theta = 24^\circ$ ,  $\beta = 2.2^\circ$  (Soller slits),  $\mu = 34$ ].

Mellon Institute,  
4400 Fifth Avenue,  
Pittsburgh 13, Pennsylvania.

LEROY ALEXANDER

#### REFERENCES

- (1) EASTBROOK, J. N. *Brit. J. Appl. Phys.*, **3**, p. 349 (1952).
- (2) ALEXANDER, L. *J. Appl. Phys.*, **19**, p. 1068 (1948).
- (3) ALEXANDER, L. *J. Appl. Phys.*, **21**, p. 126 (1950).
- (4) Material presented before the American Crystallographic Association at its meeting at Tamiment, Pennsylvania, 20 June, 1952. To be submitted for publication elsewhere.

I agree that the line profiles given by Alexander and myself for specimen-height broadening differ only in the normalizing factor  $2 \cot \theta$  and the value of the limiting displacement  $\epsilon_{max}$ .

At low angles our values of  $\epsilon_{max}$  are not very different, but his expression, equation (3), is misleading in the back-reflexion region. It gives  $\epsilon_{max}$  a large positive value, whereas equation (4) shows it to be small and negative.

University College,  
Cardiff, Wales.

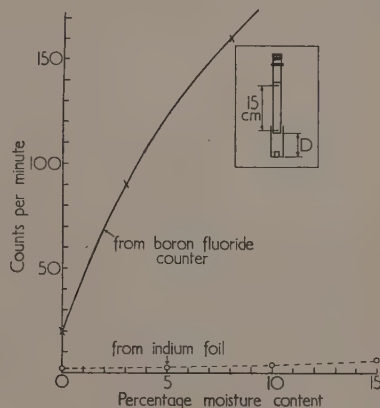
J. N. EASTBROOK

#### Measurement of moisture content by neutron counting

A fast neutron source embedded in a hydrogenous medium will be surrounded by a zone of thermal neutrons which have been slowed down by neutron-proton (np) scattering in the material. The thermal neutron density at a given point will be a function of the distance from the source and the hydrogen content of the medium. Spinks, Lane and Torchinsky have published a method\* of measuring the moisture content of soils by observing the  $\beta$ -ray activity induced in an indium foil by thermal neutrons produced as described. In their apparatus, a 250 mc radium-beryllium source was mounted below a paraffin wax cylinder, the top of which was shielded by cadmium; indium foil was mounted above this. The whole device was embedded in the soil under investigation and exposed for five minutes. The foil was then assayed by a  $\beta$ -ray counter.

The advantage of this method is that a simple portable equipment may be used for the  $\beta$ -ray assay. The disadvantage lies in the comparative insensitivity and long time required for a measurement unless a large source is used. The latter objection may be overcome by using a proportional counter filled with boron fluoride gas in place of the foil. Under these conditions there is no advantage in using the cadmium shielded paraffin wax plug between source and detector (indeed, there is a positive disadvantage), and the experiments described below were carried out to determine the optimum position of a source with regard to the counter.

The inset on the figure shows the mounting arrangement. A 2 mc radium-beryllium source emitting approximately



Measurement of moisture content by neutron counting\*  
Inset: Boron fluoride counter and source

$2 \times 10^4$  n/sec was supported in an aluminium tube at a variable distance  $D$  below a boron fluoride counter of A.E.R.E. type 15BE40. This is a tube of 15 cm active length

\* SPINKS, J. W. T., LANE, D. A., and TORCHINSKY, B. B. *Canad. J. Techn.*, **29**, p. 371 (1951).

and 2.2 cm internal diameter filled with 96%  $\text{B}^{10}\text{F}_3$  to a pressure of 40 cm of mercury, and giving about 4500 counts/sec in a thermal neutron density of  $0.01 \text{ n/cm}^3$  (corresponding to a flux of  $2200 \text{ n per cm}^2/\text{sec}$ ).

The full curve of the figure shows the results obtained with the source at its optimum position of 5 cm below the counter when the assembly was immersed (source downwards) in a drum of sand so that the source was 25 cm below the surface. The diameter of the drum was 30 cm and the total depth of sand was 45 cm. Three fillings of sand were used, containing 0% ( $< 0.2\%$ ), 3% and 8% by weight of water.

Variation of the source to base-of-counter distance,  $D$  altered the value of the count rate for dry sand much more than it altered the reading for sand containing 8% by weight of water. The ratio of these readings is given in the table.

$D(\text{cm})$	—8	3	5	10
Count rate 8% water	3.5	5	8	6
Count rate dry sand				

It will be noted that the best discrimination was obtained at 5 cm. (The counter and source mounted in air, away from scattering objects, gave a background of less than  $0.25 \text{ c/min.}$ )

Plotted on the figure is the curve (dotted) given by Spinks and others, reduced to the count rate of 5 min exposure to a 2 mc radium-beryllium source. The considerable gain in sensitivity and discrimination obtainable by the use of a boron fluoride counter will be noted.

The equipment used in the above tests was laboratory apparatus, including an amplifier for the proportional counter, and so could not compete in portability with the use of a foil and Geiger-Müller tube. However, highly portable neutron survey instruments employing boron fluoride counters are now becoming available commercially (A.E.R.E. type 1262A) and there seems every likelihood that these could be modified to make the neutron counter method suitable for field use.

The assistance of J. Morgan and M. Awcock is acknowledged. The work was done at the request of Dr. Whiffen of the Road Research Laboratory, Harmondsworth, and this letter is published by permission of the Director of the Atomic Energy Research Establishment.

Atomic Energy Research Establishment,  
Harwell, Berkshire.

J. SHARPE

## New books

**Basic methods in transfer problems.** By V. KOURGANOFF. (London: Oxford University Press). Pp. xv + 281. Price 35s.

When a beam of neutrons enters a block of graphite it is scattered. After a sufficient number of separate deflexions a stationary distribution both in velocity and density is achieved. An almost identical problem arises in the envelope of a hot star, where instead of neutrons we are dealing with radiation. It is not difficult to set up a description of this process. It takes the form of an integro-differential equation, or a pair of coupled equations. The study of these equations, and the best methods for discovering approximate solutions, owes much to the late E. A. Milne and A. S. Eddington. Among living writers there are Professors Chandrasekhar and Kourganoff. Chandrasekhar has written a large book on radiative transfer, in which most of the distinct astrophysical applications are discussed. The present book, most ably translated and extended by Dr. Busbridge, is concerned more with the methods themselves than with the physical applications that give rise to the problems. The treatment is exceedingly thorough, and in places the mathematics is seen to possess considerable beauty and elegance. At no stage, however, does it become difficult or tedious. This account is clearly going to become the standard one for those whose interests lie in understanding the techniques already used in the fields of neutron scattering and radiation, and probably applicable in other fields as well.

C. A. COULSON

**Photoconductivity in the elements.** By T. S. MOSS. (London: Butterworths Scientific Publications Ltd.) Pp. x + 263. Price 50s.

In recent years there has been considerable industrial interest in the properties of photoconducting and semiconducting materials. The author has collected in this volume a very useful summary of our present theoretical and experimental knowledge of photoconductivity and phenomena allied to it in the elements.

Part I, comprising rather less than one-third of the book,

is devoted to a theoretical introduction to the subject under ten headings. These include the optical properties of materials, Hall effect, theory of photoresponse, temperature dependence and activation energy, threshold wavelength and refractive index.

The remainder of the book, Part II, lists twelve non-metallic elements from boron to iodine under each of which the relevant experimental information, which is now considerable, is collected. Though this method of recording the results leads inevitably to some repetition in phraseology, it has the advantage that all the known data for a given element are concentrated within a few pages. This is particularly useful to those readers who wish to use it as a work of reference. Indeed it may be recommended as such.

A. M. TYNDALL

**Wind tunnel technique.** By R. C. PANKHURST and D. W. HOLDER. (London: Sir Isaac Pitman and Sons Ltd.) Pp. xviii + 702. Price 57s. 6d.

Aeronautical engineering, it has been said, is ordinary engineering made more difficult; it might be added that it would be impossible without the aid of the wind tunnel, that invaluable tool of the research worker and designer. This book is to the reviewer's knowledge the first written by British authors wholly devoted to the subject of wind tunnels. Wind tunnels have developed rapidly in size and complexity with the science they serve, and it might have seemed that no text-book could for long avoid being out of date. Nevertheless, this book is most timely and should readily attain the status of a near classic serving both as a text-book and reference book for many years to come.

The authors have covered the field of low and high speed tunnels and their testing techniques with admirable clarity and thoroughness. Their scope can be gauged from the fact that there are chapters on wind tunnel design, fluid motion visualization, fluid velocity measurement, balances, pressure distribution and total head explorations, manometers, interference effects, reduction of observations, and the



measurement of boundary layer characteristics, turbulence, stability and flutter derivatives, propeller characteristics, ground effects, and other problems. There is also a chapter on experimental analogies, e.g. the electric tank, and one on models and rigging. There are four valuable appendices in which many useful aerodynamic functions, data, conversion factors and other information are collected. Each chapter ends with a comprehensive list of references. Where the context has required it the relevant theory has been presented clearly and concisely.

Further editions will no doubt provide more details on the latest preoccupations of the experimental aerodynamicist, viz. shock tubes, hypersonic flow and the flow of rarified gases, and perhaps the excellent plates will be supplemented by photographs of typical tunnels both ancient and modern. These are, however, small points; this book can be wholeheartedly commended to all concerned with fluid motion and its measurement.

A. D. YOUNG

**The molecular architecture of plant cell walls.** By R. D. PRESTON. (London: Chapman and Hall Ltd.) Pp. xii + 211. Price 36s.

Every physicist who is thinking of applying his talents and special training to the problems of biology should make a point of reading this book, for it is essentially the personal record of one who early chose such a path and opened it up to such good account that he is now an acknowledged leader in plant biophysics. Preston has concentrated chiefly on the structure of the plant cell wall by optical methods and X-ray diffraction, and more recently by electron microscopy too, and he here brings together his many contributions in various journals and presents a unified picture which has the particularly valuable character these days of appealing just as intelligibly and equally strongly to biologists and physicists alike. We thank him warmly for it—and especially those of us who want to see eliminated all spurious repulsive forces between biology and the rest—and wish him further success in developing a most fascinating theme.

W. T. ASTBURY

**Electronic analog computers.** By G. A. KORN and T. M. KORN. (London: McGraw-Hill Publishing Co. Ltd.) Pp. xv + 378. Price 59s. 6d.

The development of the electronic analogue computer occurred largely in connexion with radar during the war, as a specialized technique mainly directed towards the elucidation of servo behaviour. Such computers use elements from several branches of electrical engineering. The central core is electronic circuit technique with particular emphasis on feedback methods, but much use is made of the devices developed for data transmission and instrument servo-mechanism. The book gives an adequate description of accepted techniques of computation by these methods, and of the necessary preliminary considerations leading to the synthesis of suitable circuits, but it does not deal with the large class of computers that are more appropriately called "simulators" in that they are designed to retain the closest possible identity with the physical system under consideration, and so provide a physical insight into a device that may be too complicated, or non-linear for exact analysis. Such simulators also found great utility as "trainers." Electrolytic tank methods do not lie within the scope of the book.

The book may be criticized on the grounds that the treatment of stability of feedback amplifiers is totally inadequate and to some extent inaccurate (Nyquist is never mentioned),

and for what it contains it is rather lengthy. It is also unfortunate that the references in the text appear to be exclusively to American sources despite the fact that the first uses and many of the techniques originated in Great Britain.

F. C. WILLIAMS

**The physical principles of thermodynamics.** By R. A. SMITH. (London: Chapman and Hall Ltd.) Pp. xiii + 280. Price 30s.

This useful little book will find many appreciative readers, not only among those interested in theoretical and experimental physics but also among applied physicists whose work touches the subject of thermodynamics. It is a well-known shortcoming of many otherwise excellent books on classical thermodynamics that they plunge directly into the mathematical argument without first explaining the underlying physical principles. Mr. Smith introduces each of his chapters with a short account of these principles which will greatly help the reader to gain a real understanding of the subject. The book follows the classical thermodynamic treatment and considers the main applications to physical and chemical phenomena, including chemical reactions and low temperatures. References might have been given in some places to other works, for example, the classical paper of Carathéodory. The examples at the ends of the chapters although valuable are mostly of a mathematical nature which is perhaps unavoidable. The treatment of the subject is thoroughly sound and the book is well written.

The author excludes any account of kinetic theory or of statistical methods. He also omits any consideration of cycles other than Carnot and some readers will find it strange to see a book on thermodynamics with scarcely a single temperature-entropy chart, but the author claims that these and other considerations so familiar to engineering students are not in fact essential to a book for the students of physics. Nevertheless, applied thermodynamicists may perhaps regret that the author was not able to extend his treatment a little towards such applications as steam cycles and flowing fluids.

O. A. SAUNDERS

**A university textbook of physics. Vol. 3. Heat.** By J. H. AWBERRY. (London: Charles Griffin and Co. Ltd.) Pp. x + 439. Price 36s.

This book is described as the eleventh edition and a largely rewritten version of Poynting and Thomson's *Textbook of heat*. It keeps closely to the form of the original work, with the exception of the short additional chapter on statistical mechanics and quantum theory. One feels that Mr. Awbery has, quite understandably, been handicapped by his respect for the authors of a book which is a classic of nearly half a century ago. Viewed as a university textbook, it contains much that is now covered effectively in school courses and the elementary books provided for them. Any student reading it will, however, benefit from the philosophical approach to the subject which was a characteristic of the original volume and which has been retained in the new version.

T. L. IBBS

**Progressive exercises in physics.** By O. WILSON, B.Sc. (London: William Heinemann Ltd.) Pp. 60. Price 2s. 6d.

This sixty-page, paper-covered book contains over 900 examples (together with answers) from all branches of physics found in syllabuses up to the ordinary level standard in the General Certificate of Education. The figures are chosen so that mathematical work is reduced to a minimum.

## Notes and comments

### Centenary exhibition of photographs and apparatus

From 16 February to 28 March, 1953, an exhibition of photographs from The Royal Photographic Society's permanent collection and of photographic apparatus collected by the Society and the Science Museum, London, will be shown in the Science Museum, Exhibition Road, London, S.W.7, by permission of the Director. During the same period a further selection of photographs from the Society's permanent collection will be shown in the Society's house at 16 Princes Gate, S.W.7 (five minutes walk from the Science Museum). The total number of prints on view will be 415.

The exhibition has been arranged to commemorate the centenary of The Royal Photographic Society and contains many relics of great interest and value. The apparatus which is being shown includes early and modern cameras of all types and sizes; lenses; experimental apparatus used by Hurter and Driffeld, Friese Greene, Muybridge, and other pioneers.

The exhibition in the Science Museum will be open from 10 a.m. to 6 p.m., from Monday to Saturday, and from 2.30 p.m. to 6 p.m. on Sunday. The exhibition in the Society's house will be open from 9.30 a.m. to 5.30 p.m. from Monday to Friday, and from 9.30 a.m. to 5 p.m. on Saturday. Admission to both exhibitions is free.

### Conference on ionization phenomena in discharges

The Clarendon Laboratory, Oxford, in co-operation with The Institute of Physics, The Physical Society and the British Electrical and Allied Industries Research Association will be holding a conference on "Ionization phenomena in discharges" from 18-23 July, 1953. The main subjects to be discussed are: the mechanisms of glow discharges, sparks

and arcs, electrodeless discharges, Geiger counters, photo-ionization processes and ionization by electron collision in gases. There will also be a session reserved for questions of general interest.

Further particulars may be obtained from the Conference Secretary, Dr. G. Francis, A.Inst.P., Clarendon Laboratory, Oxford (Telephone: Oxford 57359).

### Summer school and conference on the theory of the plastic deformation of metals

The H. H. Wills Physical Laboratory and the Department of Adult Education of the University of Bristol, in co-operation with The Institute of Physics, will be conducting a short summer school followed by a conference on "The theory of the plastic deformation of metals, with special reference to creep and to fatigue" from 13-16 July, 1953, in Bristol. The provisional programme of the course which will precede the conference includes lectures by Professor N. F. Mott, Dr. A. J. Forty and Dr. F. C. Frank. The course is similar in conception to those held in the University of Bristol on this and similar subjects; it is intended mainly for research students at universities and for members of the staffs of government and industrial laboratories. The particular aims are to see to what extent the observed phenomena can be explained in terms of present theories, and to guide future work.

The fee for the summer school, which will be on 13 and 14 July, is 30s.; but there will be no fee for the conference. Further particulars and forms of application, to be returned before 31 May, can be obtained from either the Director of the Department of Adult Education, The University, Bristol 8, or the Secretary of The Institute of Physics, 47 Belgrave Square, London, S.W.1.

## Journal of Scientific Instruments

### Contents of the March issue

#### ORIGINAL CONTRIBUTIONS

##### Papers

- The examination and calibration of Soleil compensators. By H. G. Jerrard.  
An adjustable slit for a vacuum spectrograph. By M. T. Christensen.  
A high-frequency reciprocating drill. By E. A. Neppiras.  
A laboratory plant for making liquid air from liquid oxygen. By A. J. Croft.  
A camera for texture mapping by X-ray diffraction. By C. J. Milner and J. A. James.  
A silica micro-balance; its construction and manipulation, and the theory of its action. By R. S. Bradley.  
Two methods of measuring the degree of straightness of a microscope stage. By R. M. Tennent.  
An electrometer valve voltmeter of wide range. By A. W. Brewer.  
An electrical manometer for gas pressures up to 40 mm of mercury. By F. H. Reynolds.

##### Laboratory and workshop notes

- Glass bursting stoppers. By E. R. Harrison.  
The use of silicone rubber gaskets for high vacuum work. By R. F. Gale and C. F. Machin.  
Adjustable mount using differential screws. By J. A. Macinante.  
Location of white light fringes in the Michelson interferometer. By P. G. Guest and W. M. Simmons.  
A versatile laboratory scale atomizer for use at reduced pressures. By V. E. Henny and H. A. Cheetham.

#### NOTES AND NEWS

##### Correspondence

- Sliding lens compensators. From D. H. Rank; H. Asher.  
Note on pen friction with vertical drum recording instruments. From R. H. Eldridge.

##### New books

New instruments, materials and tools

##### Notes and comments

## British Journal of Applied Physics

### Original contributions accepted for publication in future issues of this Journal

- A modified ionization method of measuring contact potential. By W. R. Harper. The tension in strings wrapped slantwise round cylinders. By C. Mack.  
The measurement of X-ray line breadths. By T. R. Anantharaman and J. W. Christian.  
Some transient properties of transistors. By H. G. Bassett and J. R. Tillman.  
The measurement of radioactive carbon in gas counters. By A. F. Henson.  
On the Tardy and Sénarmont methods of measuring fractional relative retardations. By H. T. Jessop.  
A method for measuring the spectral reflectivity of a thermopile. By E. J. Gillham.  
An ethylene resin for photoelastic work. By H. Spooner and L. D. McConnell.  
Investigation of the instability of a moving liquid film. By H. B. Squire.

THIS JOURNAL is produced monthly by The Institute of Physics, in London. It deals with all branches of applied physics (including theory and technique). All rights reserved. Responsibility for the statements contained herein attaches only to the writers.

**EDITORIAL MATTER.** Communications concerning editorial matter should be addressed to the Editor, The Institute of Physics, 47 Belgrave Square, London, S.W.1. (Telephone: Sloane 9806.) Prospective authors are invited to prepare their scripts in accordance with the *Notes on the preparation of contributions*. (Price 2s. 6d. including postage.)

**REPRODUCTION.** The Institute of Physics is a signatory to The Royal Society's Fair Copying Declaration. Details may be obtained upon application from The Royal Society, London, W.1.

**ADVERTISEMENTS.** Communications concerning advertisements should be addressed to the agents, Messrs. Walter Judd Ltd., 47 Gresham Street, London, E.C.2. (Telephone: Monarch 7644.)

**SUBSCRIPTION RATES.** A new volume commences each January. The charge is £4 per volume (\$11.50 U.S.A.), including index (post paid), payable in advance. Single parts, so far as available, may be purchased at 8s. each (\$1.15 U.S.A.), post paid, cash with order. Orders should be sent to The Institute of Physics, 47 Belgrave Square, London, S.W.1, or to any Bookseller.



## Some scientific applications of high speed-rotation\*

By Professor P. B. MOON, F.Inst.P., F.R.S., The University of Birmingham

A general account is given of scientific uses of rotary apparatus, including high-speed shutters for neutrons, Doppler effect measurements with gamma-rays and work with molecular beams. Classical applications are briefly mentioned, and the principles of rotor design are discussed.

It is sometimes useful to bring together diverse applications of a single technique, and it is proposed to do this for scientific applications of high-speed rotation, with particular reference to some recent developments.

The classical examples are to be found in measurements of the velocity of light, from Fizeau's toothed wheel and Foucault's rotating mirror to the extensive series of experiments of Michelson and his school. The centrifuge, used for technical purposes for many years and superbly developed by Svedberg and his collaborators<sup>(1)</sup> as a scientific instrument, is another familiar application, typical uses being the determination of molecular weights and the separation of isotopes. The so-called molecular pump, the advantages of which have not been fully appreciated outside Sweden, depends like the Svedberg centrifuge upon the achievement of speeds comparable with those of the molecules that are to be dealt with. Then there are rotary shutters of various types. Fizeau's wheel has already been mentioned, but rotary shutters for molecules and for neutrons must not be forgotten, and examples will be mentioned later.

Another category is the search for effects of a fundamental nature that might be associated with high speeds or with high angular momentum. One may recall Lodge's attempt<sup>(2)</sup> to "drag" the ether by rotating disks, and the possibility (see Blackett<sup>(3)</sup>) of testing the hypothesis that a magnetic moment is possessed by any body having angular momentum.

It is well known that the greatest angular velocity  $\omega$  that a body of given shape and material can withstand without bursting is inversely proportional to its linear dimensions; the linear velocity attainable is independent of the size of the rotor. If  $r$  is a characteristic dimension of the rotor,  $\omega r = f\sqrt{s/\rho}$  where  $s$  is the breaking stress of the material,  $\rho$  its density and  $f$  a shape function.

In many applications a high linear speed is the essential requirement, and rotational motion is used simply because the moving parts come quickly round for use again. From the rule just mentioned, it follows that for these applications the size is basically unimportant. In the rotating-mirror class, high angular velocity seems at first sight to be the requirement but, since the optical resolution is limited by the width of the mirror, linear speed is again the fundamental need. In centrifuges, one may either want high radial acceleration to get high force per unit mass (in which case a small rotor is preferable), or high linear velocity of the outer wall of the rotating vessel, to get the maximum degree of separation when equilibrium is reached. In the obvious notation, the ratio of peripheral to central concentration for molecules of mass  $m$  is  $\exp(m\omega^2 r^2/2KT)$ , so for two types of molecule we have

$$\left(\frac{C_1}{C_2}\right)_r = \left(\frac{C_1}{C_2}\right)_0 \exp\left(\frac{(m_1 - m_2)\omega^2 r^2}{2KT}\right)$$

For a search for magnetic effects of rotation, supposing a sphere of density  $\rho$  and radius  $r$  to rotate with angular velocity  $\omega$ , we have an angular momentum and hence a presumed magnetic moment proportional to  $\rho r^5 \omega$ . Since the magnetic field has to be measured outside the sphere, and the field due to a dipole falls off as the inverse cube of the distance, the hope of generating a detectable field depends upon obtaining a high value of  $\rho \omega r^2$  or [since the maximum value of  $\omega r$  is proportional to  $\sqrt{s/\rho}$ ] a high value of  $r\sqrt{s/\rho}$ . This calls for a large rotor of strong, heavy material, and is in contrast to other applications which depend on a high ratio of strength to density.

Other factors may often outweigh these theoretical criteria; for example, it is no use making a "high-g" apparatus so small that it cannot hold a reasonable load of the material on which the high acceleration is required to act, and, as Blackett has said, one would not try to detect the magnetic effect with a rotor so large that it could not either be started and stopped or moved to and from the magnetometer in a short enough time for drift of the magnetometer's zero to be unimportant. There are, however, occasions when practice follows theory pretty closely, and it is instructive to consider what is the best shape of a rotor for attaining the highest practicable linear velocity at the periphery.

The ideal shape is independent of the material and of the size, and the criterion for finding it was given in words of one syllable by the Deacon in O. W. Holmes's verses:<sup>(4)</sup>

"Fur," said the Deacon, "t's mighty plain  
That the weakes' place mus' stan' the strain;  
'n the way t' fix it, uz I maintain,  
Is only jest  
T' make that place uz strong uz the rest."

In physicists' language, unless the forces set up by rotation stress all parts of the rotor equally, some parts are unnecessarily heavy and by transferring material from them to the more highly stressed parts we shall raise the breaking speed of the rotor.

Consider, for example, a thin rod spinning about an axis perpendicular to its length. It is easy to show that the criterion of equal stress requires that the cross-section of the rod shall decrease exponentially with the square of the distance from the axis, i.e.

$$A = A_0 e^{-Kr^2} \quad (1)$$

and the limiting angular velocity, when all parts of the rod are at the breaking-stress  $S$ , is  $\sqrt{2KS/\rho}$ . If this Gauss-error-curve-shaped rod is arbitrarily cut off at a distance  $r_m$  from the centre, where the cross-section is  $A_m$  and is much less than  $A_0$ , the stress will be appreciably relieved only quite near the ends and the limiting linear velocity of the tips ( $v_m$ ) will be  $r_m \sqrt{2KS/\rho}$ . Using equation (1) we find

$$v_m = [(2S/\rho) \log_e (A_0/A_m)]^{1/2} \quad (2)$$

A rod of steel, with  $S = 100$  tons/in<sup>2</sup>,  $\rho = 8$  and  $A_0/A_m = 100$

\* Based on a lecture given to the South Wales Branch of The Institute of Physics on 27 April, 1951.



should break at a tip-speed of about  $1.3 \times 10^5$  cm/sec, or about four times the speed of sound in air.

I shall mention some experiments for which rotors of something like this shape are suitable, but for many purposes a disk-like rotor is more appropriate. Once again, the disk should be thin at the edge and the ideal profile is that of the Gauss error-function. Making the same approximations as for the rod, one calculates a limiting speed of  $[(2S/\rho) \log_e(t_0/t_m)]$  where  $t_0$  and  $t_m$  are the central and peripheral thicknesses. Although the disk has the advantage of the "tyre strength" of the concentric rings into which it may be imagined to be divided, it can be tapered in one dimension only, and for a given ratio of central to peripheral thickness it will withstand a speed  $\sqrt{2}$  times less than does a rod.

If the material of the rotor is not too brittle, it may flow at places of highest stress, which (so far as circumferential stresses are concerned) will be relieved at the expense of other less highly-stressed regions. This measure of self-adjustment is absent from rod-type rotors, where local flow simply reduces the cross-section and increases the local stress.

The lightening of the material towards the edge or tip need not be achieved only by reducing the external dimensions; internal cavities may be provided and for some applications are indeed necessary. As soon as such cavities are introduced, the problems of design cease to have simple solutions, but the guiding principle of uniform stress remains. In theory, some advantage would be gained by making the central parts of the rotor of a material that is strong if unavoidably dense, and the outer parts of a lighter if less strong substance; steel for the centre and Duralumin for the edge, for example. The theoretical advantage is not great and is offset by the practical difficulty of making a strong enough joint.

The problem of providing a suitable axis of rotation for a high speed rotor is at first sight formidable. Not only is the rate of revolution very great (typically of the order of 100 000 r.p.m.), but unless the rotor is dynamically balanced to very high accuracy the forces on the bearings can be large. The centrifugal force due to 1 mg moving at 1 km/sec in a circle of radius 10 cm is  $10^6$  dynes or about the weight of 1 kg.

Friction, wear and still more the rapidly alternating nature of the force between the rotor and its housing raise serious problems, for mechanical resonances may be encountered as the rotor accelerates. There are two ways round this difficulty, the hard and the comparatively easy. The hard way is to balance the rotor with extreme precision and to provide accurate and rigidly-supported bearings. The easy way is to make the rotor self-balancing, either by hanging it vertically on a flexible shaft or by some device internal to the rotor. The shaft will have its own flexural resonances but, apart from the one at very low frequency in which the rotor moves as a conical pendulum, they are not strongly coupled to the rotor which is nearly at a node. Those resonances which are excited build up comparatively slowly and if the acceleration is rapid can usually be passed through without difficulty.

There are many methods of driving rotors, and most of them can be applied either directly to the rotor or to a separate driving unit on the same shaft. Svedberg, the pioneer of the ultra centrifuge, used precisely-balanced horizontal-shaft machines driven by oil turbines and cooled by hydrogen gas. The hydrogen, having a molecular velocity higher than that of any part of the rotor, forms an effective coolant, and Svedberg's centrifuges run in the gas at a pressure of a few centimetres of mercury.

Henriot and Huguenard<sup>(5)</sup> drove rotors of fluted conical

form by gas-jets impinging obliquely on them from holes in a surrounding cup; the rotor was not only driven but lifted and stabilized by the gas-flow round it. Beams and his collaborators<sup>(6,7,8)</sup> at the University of Virginia developed this by hanging a separate rotor from the cone by a thin wire which passed through an oil-sealed gland in the base of the cup into a vacuum chamber; later, they used an a.c. induction motor as the driving agent, employing gas-flow to support the weight of the system. This was followed<sup>(9)</sup> by a most elegant system of levitating a steel rotor in mid-vacuum by the automatically-controlled current in a solenoid above it; there is then no physical connexion to the rotor, which is virtually frictionless and is driven either by the eddy-current action of a rotating magnetic field, by a suitably-commutated electric field between vanes on the rotor and surrounding metal quadrants, or—as a final *tour de force*—by the radiation pressure of a beam of light shining tangentially on one side of the rotor.

Using the levitation technique and the electromagnetic drive, Beams and his collaborators<sup>(10)</sup> have spun small spheres of exceptionally strong steel to peripheral speeds exceeding a kilometre per second, with radial accelerations of over  $4 \times 10^8$  g. A spot of paint on the surface of such a sphere is subject to an extremely strong radial force which can be calculated if the thickness and density of the layer is known. This has been used in America for measuring the strength of adherence of the paint.

A rotor designed, as it must be, for mechanical strength and not for efficiency as an induction motor will inevitably waste some power which will appear as heat; that being so, a small loss of power to ordinary friction is comparatively unobjectionable and it is possible, as Colwell and Hall<sup>(11)</sup> showed, to reach high speeds with a metal rotor running as a peg-top on a glass surface in a vacuum chamber. Difficulties of stability were encountered that were stated to require high symmetry of construction.

During the last few years, a method has been used in the University of Birmingham<sup>(12)</sup> that is nearly as simple as that of Colwell and Hall and nearly as effective as that of Beams. The rotor, which is a doubly-tapered steel rod because the applications require very high peripheral speed, has in its base a small ball of hardened steel that runs on a glass plate. About 90% of the weight of the rotor is taken by an electromagnet above it (outside the vacuum chamber). If the rotor wanders from its normal position beneath the magnet, the magnet draws it back; however, the rotor tends to overshoot and to oscillate, sometimes uncontrollably, about its correct position. This is remedied by suspending the magnet by a short thread so that it can move as a conical pendulum: oil damping is applied to this motion and the damping is effectively transferred to the rotor which now runs safely up to the limit of speed set by its mechanical strength, or by the driving arrangements. With a rotor about 6 in long driven by a rotating magnetic field derived from a pair of 2500 c/s alternators mechanically coupled so as to be in quadrature, peripheral speeds up to about  $1.1 \times 10^5$  cm/sec have been obtained, and these speeds could be increased somewhat by the use of stronger steel in place of the 75-ton material that is now used as a compromise between strength and machinability. The rate of rotation is easily measured by allowing the rotor tips to interrupt a beam of light falling on a photocell.

Examples of the rotor are shown in Fig. 1. They are designed for high tip speed and not for carrying appreciable loads, and their principal use has been for the production of high-speed beams of heavy atoms and molecules. For this

urpose it is sufficient to run the rotor in gas at a pressure, say,  $10^{-3}$  mm of mercury; the fast-moving tip sweeps up the molecules and throws them off again. If the molecules stick and re-evaporate rather than bounce, they will leave with the velocity of the rotor plus their comparatively small thermal velocities, and will therefore give a roughly energetic spray moving approximately in the plane of rotation. On the other hand, the molecules rebound elastically from the metal, they will go in a wide range of directions with velocities approximately twice that of the moving surface. In either case a narrow beam can be selected by a suitable aperture in the wall of the enclosing vessel.

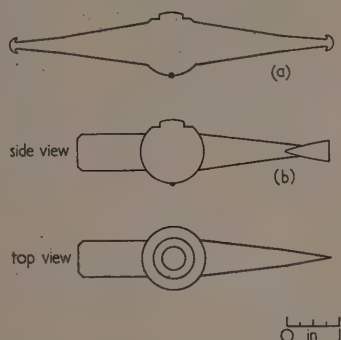


Fig. 1. Examples of high-speed rotors  
(a) "Mushroom" tipped; (b) single ended.

We have at present only slight evidence (which will be mentioned later in this article) for any bouncing and shall ignore it for present purposes. Let us assume, therefore, that molecules leave the tip with speeds of  $10^5$  cm/sec.

In addition to their high speed, which for a mercury atom corresponds to an energy of about 1 eV or a temperature of the order of  $10^4$ ° C, these beams have high intensity. When moving at  $10^5$  cm/sec in mercury vapour at a pressure of  $10^{-6}$  atmosphere, a square centimetre of the rotor tip sweeps up about a milligram of gas per second which carries off power at the rate of about half a watt and momentum at the rate of  $100$  g cm sec $^{-1}$  per second. Though only a small action of the stream will be left after collimation by a small aperture, the intensity at a given degree of collimation compares favourably with what can be got at lower velocities from molecular-beam sources.

The power is enough to be measured by the rise in temperature of a thermocouple or a resistance-thermometer element struck by the stream of high-speed molecules, while the momentum will give good deflexions of a vane suspended on a torsion fibre.

The total number of molecules swept up and the velocity given to each are both roughly proportional to the tip speed, while the solid angle of divergence of the beam is inversely proportional to the square of that speed; so the flux of kinetic energy through small collimating apertures aligned tangentially to the tip's path should vary as the fourth power of the rotor's speed. Some unpublished experiments by Mr. T. H. Bull show a much smaller variation with speed for mercury atoms directed upon a platinum wire used as a resistance-thermometer. The obvious conclusion is that the atoms have an increasing chance of bouncing off the metal as the speed of impact increases, but it has yet to be proved that the effect is not due to a change in thermal emissivity produced by the bombardment.

Furthermore, the beam passing through an aperture to a not-too-distant detector will be of an intermittent nature and will lend itself to time-of-flight measurements. The pulses are sharper than might be expected, for a reason that may be seen from the left-hand part of Fig. 2 which shows by full and broken lines the paths of two molecules leaving the

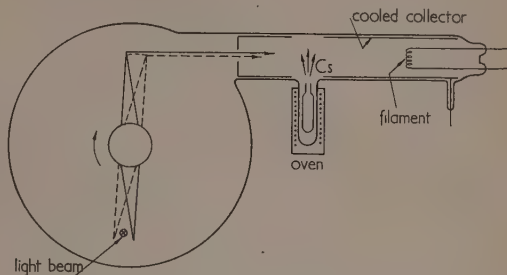


Fig. 2. Apparatus for measuring the time-of-flight of atomic beams

tip of the rotor at different times. The full and broken paths are of very nearly the same length and are traversed at very nearly the same speed, the only difference being that one molecule is carried round an arc on the tip of the rotor while the other is travelling freely on a straight line with a velocity that is greater by the thermal contribution—perhaps 20%. An example of such pulses as seen on the screen of an oscilloscope is shown in Fig. 3 which was obtained by my colleagues Dr. Marshall and Mr. Bull,<sup>(13)</sup> not by sweeping up molecules from the gas but by evaporating them from the rotor. A rotor was made with mushroom-like cavities at the tips (Fig. 1a) into which a few milligrams of potassium metal were pressed. The rotor, having been placed quickly into the apparatus which was evacuated before too much of the

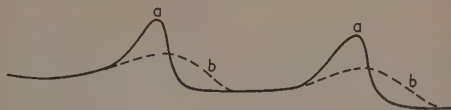


Fig. 3. Pulses of potassium ions as seen on the oscilloscope (Ref. 13)

Curve a: pulses reaching the hot filament; Curve b: pulses obtained when the temperature of the filament is lowered.

potassium had oxidized, was run up to a tip speed of about  $6 \times 10^4$  cm/sec. Owing to eddy-current heating, the rotor was now warm, but not hot enough for the potassium to evaporate at a suitable rate; the correct temperature was easily obtained by repeated reversals of the direction of the rotating field, so that further heating occurred without any large change of speed. The beam of potassium atoms selected by an aperture then fell upon a hot tungsten filament surrounded by a negatively-charged cylinder to which  $K^+$  ions were drawn. Curve a (Fig. 3) shows the pulses of ions which, if the ionization takes place in a negligible time, should faithfully represent the pulses of atoms reaching the hot filament.

As the temperature of the filament is reduced, the potassium remains on the tungsten for an observable time and the ion pulses are lengthened (curve b, Fig. 3). In this way the mean life of potassium on tungsten at 1460° K was found



to be about  $3 \times 10^{-5}$  sec. This lifetime had previously been measured only at much lower temperatures where it was a tenth of a second or longer. A somewhat different method of measuring "sitting times" with an interrupted beam has been reported by Marple and Levinstein,<sup>(14)</sup> who used a rotating shutter<sup>(15)</sup> to interrupt a molecular beam emerging from an oven.

If, at some point on its path, a bunch of fast molecules crosses a relatively slow-moving stream of other molecules, some of the latter will be projected forwards by molecular collisions and will reach a distant detector at a time depending upon the relative masses and upon whether the collisions are elastic. Using the apparatus indicated in Fig. 2, Mr. Bull has studied collisions between mercury atoms and caesium atoms, and between carbon tetrachloride molecules and caesium atoms, at speeds up to nearly  $10^5$  cm/sec, corresponding to temperatures of 3000° K or thereabouts.

The rotor may be "single-ended" (Fig. 1*b*), firing one pulse per revolution, or "double-ended" as shown in Fig. 2; in either case the tip is shaped rather like the blade of a screw-driver, providing a greater working area while still conforming closely to the ideal Gaussian variation of cross-section with distance from the axis of rotation. The rotor runs in the vapour of the substance under investigation, at a pressure between  $10^{-3}$  and  $10^{-4}$  mm; when in the "shooting position" it interrupts a beam of light passing to a photocell, and so provides a signal of the instant at which the bunch of molecules leaves the tip. The arrival of the bunch at a point some 20 cm distant is detected by the ionization current passing between a hot tungsten filament and a surrounding positively-charged cylinder. If now the caesium jet is turned on, with an intensity such that single collisions are reasonably frequent but multiple collisions rare, pulses of projected caesium atoms may be observed by reversing the voltage between filament and cylinder and making use of the thermal ionization of caesium on hot tungsten. All three sets of pulses may be amplified by the same amplifier and displayed in turn on an oscilloscope synchronized to the frequency of the rotor. From the relative positions of the pulses and the path-lengths involved, the mean speed of the "knocked-on" caesium atoms may be found. As would be expected for atoms at these speeds (which are insufficient to excite the electron shells), the mercury-caesium collisions are found to be elastic. The collisions between carbon tetrachloride molecules and caesium atoms are mainly inelastic, doubtless owing to the transformation of translational energy to molecular rotation and vibration, but there is some evidence for the chemical reaction



the CsCl molecules being detected by dissociation and ionization on the hot filament. The possibility of studying in detail the collisions of neutral atoms and molecules is an interesting one, particularly because the energy-range involved lies between those conveniently obtainable from ovens and from neutralization of positive-ion beams. The technique is, however, at present rather crude and requires much development before its possibilities can be realized.

In the field of nuclear physics, the rotating condensers used for frequency-modulation in synchrocyclotrons present some interesting and difficult problems of design. The classic application of rotational technique in nuclear research is, however, the use of rotating shutters for neutrons. These were first used by Dunning and others<sup>(16)</sup> in the form of sector disks of cadmium, which is highly opaque to very slow neutrons. In recent years the technique has been

developed at the University of Chicago, the form of the rotors being changed to allow greater thicknesses of absorbing material and to permit faster neutrons to be interrupted. A "sandwich" type of shutter,<sup>(17)</sup> composed of alternate layers of cadmium and aluminium and enclosed in a strong steel shell, is shown diagrammatically in Fig. 4. Rotated as indicated, it passes two short pulses of neutrons in each revolution. A more recent type<sup>(18)</sup> employs a slotted shaft of steel rotating in front of a similar and coaxial fixed one,

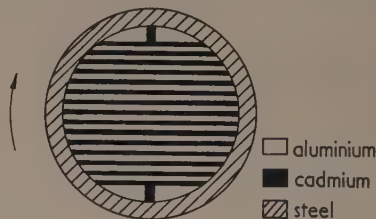


Fig. 4. "Sandwich" type of shutter for passing short pulses of neutrons (Ref. 17)

the principle being reminiscent of Fizeau, though the design is very different because a considerable thickness of steel is required to stop neutrons. The cylindrical rotor is 16 in. long and the slots, running parallel to its length, are about  $\frac{1}{8}$  mm wide. It is driven mechanically, being supported by double-row ball bearings at each end, and runs at a peripheral speed of  $2 \times 10^4$  cm/sec.

A quite different application<sup>(19)</sup> depends upon carrying strong radioactive sources of low mass on the tips of high-speed rotors. A few milligrams of gold, after irradiation in one of the Harwell piles, may contain tens of millicuries of  $^{198}\text{Au}$  which decays radioactively to an excited state of the nucleus  $^{198}\text{Hg}$ . This state decays to the ground state with an extremely short half-life, emitting a gamma-ray with a quantum energy of about 0.41 MeV. These gamma-rays have not quite enough energy to excite resonance in the ground-state  $^{198}\text{Hg}$  nuclei that constitute 10% of normal mercury, because nearly an electron-volt is lost to nuclear recoil and the nuclear resonance is much narrower than 1 eV. By moving the source at high speed towards the mercury, the necessary energy may be restored by virtue of the Doppler effect, and the gamma-rays are then strongly scattered by the  $^{198}\text{Hg}$  nuclei—a phenomenon analogous with the well-known resonance fluorescence of atoms irradiated by their "own" radiation. There are complications due to the Doppler effect of thermal motions in source and scatterer, but it has been possible to observe the process, to estimate the intrinsic width of the nuclear resonance (about  $10^{-3}$  eV) and hence to deduce the lifetime of the excited state, which comes out between  $10^{-10}$  and  $10^{-11}$  sec. An interesting feature of the method is that the shorter the lifetime the more easily is it measured.

Although this article is concerned with purely scientific applications of rotation, it must not be forgotten that high-speed techniques are much used in industry. Airscrews and turbine blades spring to mind at once, but electric motors and generators are made to run at armature speeds such that the strengths of the materials are of prime importance. Johnson and Holder<sup>(20)</sup> list several large generators with safe peripheral speeds approaching 0.2 km/sec. Turbine exhaust blades now reach tip speeds of 0.5 km/sec, and they are not only subject to lateral forces but also to very high temperatures



and to corrosive action, so the designers have had to overcome difficulties well beyond those encountered in the scientific applications mentioned here.

# REFERENCES

- (1) SVEDBERG, T., and PEDERSEN, K. O. *The Ultracentrifuge*. (London: Oxford University Press, 1940).
- (2) LODGE, O. J. *Phil. Trans Roy. Soc. A*, **189**, p. 149 (1897).
- (3) BLACKETT, P. M. S. *Phil. Trans Roy. Soc. A*, **245**, p. 309 (1952).
- (4) HOLMES, O. W. *Atlantic Monthly*, **2**, p. 496 (1858).
- (5) HENRIOT, E., and HUGUENARD, E. *C.R. Acad. Sci., Paris*, **180**, p. 1389 (1925).
- (6) BEAMS, J. W., and PICKLES, E. B. *Rev. Sci. Instrum.*, **6**, p. 299 (1935).
- (7) BEAMS, J. W. *Rev. Mod. Phys.*, **10**, p. 245 (1938).
- (8) BEAMS, J. W. *Rep. Phys. Soc. Progr. Phys.*, **8**, p. 31 (1941).
- (9) MACHATTIE, L. E. *Rev. Sci. Instrum.*, **12**, p. 429 (1941).

- (10) BEAMS, J. W., and YOUNG, J. L. *Phys. Rev.*, **71**, p. 131 (1947).
- (11) COLWELL, R. C., and HALL, N. I. *Rev. Sci. Instrum.*, **6**, p. 238 (1935).
- (12) MARSHALL, D. G., MOON, P. B., ROBINSON, J. E. S., and STRINGER, J. T. *J. Sci. Instrum.*, **25**, p. 348 (1948).
- (13) MARSHALL, D. G., and BULL, T. H. *Nature, Lond.*, **167**, p. 478 (1951).
- (14) MARPLE, D. T. F., and LEVINSTEIN, H. *Phys. Rev.*, **79**, p. 223 (1950).
- (15) KOFSKY, I. L., and LEVINSTEIN, H. *Phys. Rev.*, **74**, p. 500 (1948).
- (16) DUNNING, J. R., PEGRAM, G. B., FINK, G. A., and MITCHELL, D. P. *Phys. Rev.*, **48**, p. 704 (1935).
- (17) FERMI, E., MARSHALL, J., and MARSHALL, L. *Phys. Rev.*, **72**, p. 193 (1947).
- (18) SELOVE, W. *Rev. Sci. Instrum.*, **23**, p. 350 (1952).
- (19) MOON, P. B. *Proc. Phys. Soc. Lond. A*, **64**, p. 76 (1951).
- (20) JOHNSON, E. M., and HOLDER, C. P. *J. Instn. Elect. Engrs*, **95**, p. 757 (1948).

## ORIGINAL CONTRIBUTIONS

### The origin of specimen contamination in the electron microscope\*

By A. E. ENNOS, M.Sc., A.Inst.P., Research Laboratory, Associated Electrical Industries Ltd., Aldermaston Court, Aldermaston, Berkshire

[Paper first received 12 January and in final form 21 January, 1953]

Electron beam contamination has been studied in simple vacuum systems to determine how it originates and methods by which it may be prevented. It is concluded that the contamination is formed by the interaction of the electrons with organic molecules adsorbed on the bombarded surfaces, the molecules being replenished from the vapour phase. Contamination may be prevented by heating the bombarded surface or surrounding it with an efficient cold trap.

When a beam of electrons, or other charged particles, is directed upon a surface in a continually-pumped vacuum system, a contaminating deposit is formed wherever the beam strikes the surface. For example, the edges of beam-limiting apertures become coated with a brownish-black deposit which may charge up and deflect the beam, owing to the poor conducting nature of the contamination. Discharge tubes become discoloured with the deposition of contamination; and the targets of certain types of demountable soft X-ray tubes collect a deposit which may alter the characteristics of the radiation emitted. Similarly, targets used to study nuclear reactions, when bombarded by a stream of high-speed ions, can become poisoned with contamination which will then give its own characteristic scattering.

Whereas the effects mentioned above take place relatively slowly, and normally do not cause serious trouble if periodic cleaning of the affected parts is carried out, contamination can be of much greater consequence in electron-optical instruments where the specimen to be examined is irradiated by electrons. For example, in electron diffraction studies of surface structure, the overgrowth of contamination may cause the diffraction pattern to be reduced in contrast, or even

totally obscured. In electron microscopy, the contamination growth may be viewed directly, either as the building up of a shell round individual particles, or as the gradual thickening of support films, leading to loss of contrast and masking of fine detail. Fig. 1 shows the growth of contamination round crystals of zinc oxide smoke. The photographs were taken at five-minute intervals, at an electron optical magnification of  $\times 18\,000$ .

Since contamination growth takes place as soon as the specimen is irradiated, some effect will have taken place before a photograph is secured. This constitutes a practical difficulty in the achievement of very high resolution since any increase in instrumental resolution may be offset by the contamination effect. In the electron diffraction microscope<sup>(1)</sup> it is particularly troublesome. Contamination is also the main factor limiting the use of the electron microanalyser,<sup>(2)</sup> in which a fine electron probe of high current density irradiates part of the specimen to be examined. Build-up of a contamination deposit virtually masks any effect due to the original material of the specimen.

Specimen contamination in the electron microscope was first reported by König<sup>(3)</sup> and by Watson<sup>(4)</sup> in the course of particle size determinations on carbon black. These particles gradually increased in size, the growth rate being higher for those nearer to the meshes of the grid than for those further away. Cosslett<sup>(5)</sup> showed similar growths on crystals of

\* A shortened version of this paper was read before the Electron Microscopy Group of The Institute of Physics at the Group's conference in Bristol in September 1952.

metallic oxide smokes, whereas Burton, Sennet and Ellis,<sup>(6)</sup> and Kinder<sup>(7)</sup> reported the formation of a contamination "skin" surrounding crystal specimens, which remained as a hollow transparent envelope after the crystals had been partially or completely evaporated by heating in the beam. Hillier<sup>(8)</sup> showed that the contamination material was amorphous and structureless and that carbon was the main constituent. He found that freezing-out the oil vapour of the diffusion pump or surrounding the specimen with a liquid air trap did not reduce contamination to a marked degree. A subsequent electron diffraction study of the contamination by König<sup>(9)</sup> indicated that it consisted essentially of carbon in the form of flat six-membered rings, randomly oriented as in a powder. However, the presence of small proportions of other elements cannot be ruled out.

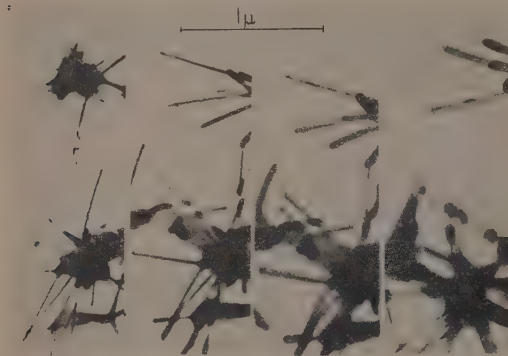


Fig. 1. Zinc oxide smoke crystals contaminating in the electron beam

Various theories have been put forward to account for the formation of the contamination. Watson<sup>(4)</sup> suggested that the electron beam forms ion clusters in the residual oil vapour atmosphere of the vacuum system, the ions being deposited on the specimen near an electrically-conducting surface. However, calculation of the rate of formation of ions at the pressure existing within the vacuum system gives a value of contamination rate several orders smaller than the observed rate. Furthermore, contamination is only found on those parts directly irradiated by the electron beam. Cosslett's<sup>(5)</sup> suggestion that the contamination may arise from adsorbed material being ejected from the mesh wires by electron bombardment fails to explain the contamination found in the centre of support films; moreover, the granular deposits formed by the ejection of material under electron bombardment<sup>(6)</sup> are not observed.

In a recent study of the contamination effect, Ellis<sup>(10)</sup> suggests that specimen contamination is due to polymerization by the electron beam of organic molecules which migrate along the specimen supports. According to Ellis, the sources of these molecules are patches of organic contamination on the walls of the instrument which have remained after cleaning, although a contribution from organic vapours condensing on the walls is considered possible. While some of the experiments described by Ellis support his views, others are inconclusive or even inconsistent with the migration theory.

An alternative source of contamination which appears to be more probable is from the organic vapours known to exist in the vacuum atmosphere. These will partially condense on

the internal walls of the apparatus as an adsorbed film. As molecules of the film are effectively removed by interaction with the electron beam, fresh ones will take their place from the vapour.

The present investigation was undertaken to obtain clear-cut experimental results from which a more satisfactory picture of the mechanism and origin of the specimen contamination might be derived. It is hoped to treat the sources of contaminants quantitatively in a further paper.

#### CONTAMINATION RATE IN THE ELECTRON MICROSCOPE

Initial experiments were made on the rate of build-up of contamination round zinc oxide smoke crystals in the electron microscope. These showed, in agreement with Watson, that the growth was linear with time and that contamination continued to grow indefinitely. In general, the absolute rate of contamination varied widely from specimen to specimen, although there was always a higher rate of growth for areas close to mesh wires of the grid. Measurements of contamination rate made on the same crystal under conditions of constant current density showed no significant dependence on the accelerating voltage of the electrons in the range of 40–75 kV normally employed. Similar measurements on the contamination rate as a function of current density showed that for small current densities the relationship was linear, with a falling off of the rate for more intense bombardments, as shown in Fig. 2.

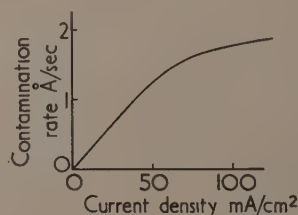


Fig. 2. Variation of contamination rate with current density

Rates of growth of up to 3 Å/sec have been observed for the highest electron beam intensity obtainable in the electron microscope.

#### INVESTIGATIONS IN A SIMPLIFIED VACUUM SYSTEM

The variable nature of the contamination rate from specimen to specimen indicates that a number of factors may be operative, e.g. the temperature of the specimen is one factor that may vary, and whose value is difficult to assess accurately. Further experiments were thus designed to investigate independently the influence of the various factors upon which contamination in the electron microscope may depend. These were carried out in simple demountable systems containing an electron source and a surface to be bombarded.

A simple three-electrode gun constructed of brass was mounted inside the bell-jar of a standard evaporation plant evacuated by an oil diffusion pump to a pressure of  $10^{-5}$  mm of mercury (see Fig. 3). The gun was arranged to send a beam of electrons on to a suitably placed target, a shutter between gun and target being operated magnetically from outside the

vacuum system. To avoid undue heating of the target, which introduces an additional factor influencing contamination, an electron accelerating potential of 2 kV was employed, instead of the 50 kV employed in the electron microscope. On running the beam for some time (10 min) at a current density of 0.5 mA/cm<sup>2</sup>, a light brown stain was observed on the surface of the target. The appearance of the stain was

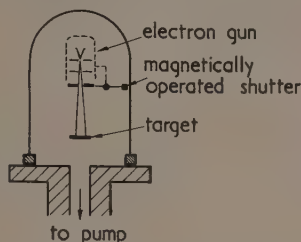


Fig. 3. Simplified vacuum system for investigation of contamination

unaffected by the nature of the surface material, e.g. both metals and glass surfaces became contaminated. Further bombardment of the surface produced a dark brown-black deposit, as had been noted by Stewart.<sup>(11)</sup> Very light contamination on glass or polished metal surfaces, invisible to the eye, could be detected by differential breath figures shown on breathing on the target (subsequent measurement has shown these to be less than 50 Å thick).

It was first verified that this brown stain deposit was similar to the contamination produced in the electron microscope. Specimens of zinc oxide smoke crystals supported on a standard microscope grid were laid on the target and bombarded in the beam until stained brown. Upon subsequent examination in the electron microscope, they exhibited contamination indistinguishable from that produced in the microscope itself. Contamination deposits were also detached from metal surfaces by dissolving away the metal, and the resulting films (forming a replica of the surface) were found to have a similar amorphous structure and thermal resistance to the electron beam, when viewed in the electron microscope, as the normal electron microscope contamination. (Fig. 4 shows a typical "contamination" replica of an etched stainless steel surface formed by electron bombardment.)

It is reasonable to suppose, then, that conditions influencing the formation of contamination caused by the 2 kV electron beam will have similar effects when electrons of higher energy are used. As discussed later, it is most probable that the electron energy losses causing the chemical changes which take place are of the order of a few volts only, and in this respect it is interesting to note that similar contamination deposits were obtained during these experiments with electron energies of down to 80 V, the lower limit of satisfactory operation of the electron gun in use.

In order to check that the rate of build up of contamination using the 2 kV gun was not greatly different from that observed in the electron microscope at similar current densities, the thickness of the deposits formed on a glass target were measured, using the multiple beam interference technique due to Tolansky.<sup>(12)</sup> For low intensity bombardment, contamination rates measured in the electron microscope agreed with these thickness measurements to well within an order of magnitude in all cases. This confirms that the accelerating voltage has a relatively small effect in influencing the formation of contamination. The specimen

current density normally employed in the electron microscope for photographing at  $\times 10000$  is of the order of 5 mA/cm<sup>2</sup>, i.e. ten times that employed in the low-voltage gun used in these experiments.



Fig. 4. "Contamination" replica of etched stainless steel surface

#### TEMPERATURE DEPENDENCE OF CONTAMINATION

Qualitative tests were carried out to determine the effect of surface temperature on the contamination rate. A polished stainless steel disk was first cleaned chemically, followed by running a spark discharge over its surface to remove any remaining grease films. It was then mounted on a heater in the bell jar, a thermocouple being used to measure the temperature. By moving the magnetically operated shutter, which was pierced by an aperture, separate areas of the specimen could be bombarded in turn without breaking the vacuum. By giving each area a standard bombardment of 2 coulombs/cm<sup>2</sup> at constant beam intensity, the effect of surface temperature was found. Warming the surface reduced the contamination markedly. When the contamination rate was such that a medium brown stain was observed at room temperature, raising the temperature to 100° C produced an almost invisible deposit for the same degree of bombardment. Complete elimination of contamination (when no differential breath figures could be detected) was only obtained, however, when the surface temperature was raised to about 250° C. A similar comparison experiment with the target cooled showed an initial increase in the contamination rate with drop in surface temperature. When the target temperature was lowered sufficiently (to about -50° C) appreciable condensation of oil vapour took place. The impinging electron beam then formed a white substance instead of the normal brown contamination.

Fig. 5 gives a qualitative picture of the relationship between contamination rate and surface temperature for the region in which condensation of pump oil does not take place.

As a result of his experiments in the electron microscope,



Ellis suggested that specimen temperature may affect contamination. A previously warmed specimen holder inserted into his instrument did not at first contaminate, yet on cooling, the normal contamination was restored. He gives no exact data on the degree of dependence of contamination on temperature, but suggests that temperature differences in a specimen may account for differential contamination over its area.

In the light of these experiments on temperature dependence, it is possible to interpret many of the contamination effects in the electron microscope. For example, the relative falling-off of contamination rate with increase in beam intensity can be explained by the increased absorption of energy and consequent rise in temperature of the specimen. Preferential contamination near to a mesh wire is due to the difference in temperature between the centre and periphery of a mesh opening. Von Borries<sup>(13)</sup> has calculated the temperature distribution in a collodion support film under normal operating conditions and concludes that, at the centre, the temperature may be in the region of 200° C. For unsupported specimens, e.g. smoke crystals, the temperature will depend largely on the degree of contact between individual particles, and may rise very rapidly if this is poor. The temperature of the copper grid meshes normally used, on the other hand, will not rise more than a few degrees above the ambient temperature. If stainless steel grids are used, however, the wires may attain a temperature of 50° C or more due to their poor thermal conductivity. This will account for the reduced contamination reported by Ellis in using these grids, confirmed by the author's measurements.

#### THE MECHANISM OF CONTAMINATION

The work of Hillier<sup>(8)</sup> and of König,<sup>(9)</sup> previously cited, has shown that the contamination deposit has an amorphous structure and is of a carbonaceous nature. This suggests that the source material is organic in nature, and that contamination is formed by the reaction of the electron beam with the organic molecules on the specimen. In a vacuum system evacuated by an oil diffusion pump, the residual gases will consist largely of oil vapour at the saturated vapour pressure of the pump oil, but Blears<sup>(14)</sup> has shown that similar systems fitted with a liquid air trap, or pumped by a mercury diffusion pump, also contain a high proportion of hydrocarbon vapour in their atmosphere. These hydrocarbons persist for many hours after pumping even when the system is baked at 100° C. The source of these organic vapours will not be treated in detail here, but in general they may be said to come from oil, grease, gasket material, etc., in the system. The conversion of these organic substances to form the contamination deposit must take place on the surface of the specimen and not in the vapour for reasons already put forward. On the specimen surface, there may exist an adsorbed hydrocarbon layer which effectively enhances the concentration of molecules.

The bombarding electrons cause ionization and dissociation of the molecules they strike by the knocking out of the bonding electrons. The subsequent de-ionization and recombination of the molecules may then lead to the formation of stable chemical compounds with formation energies much greater than those possible by thermal excitation. Harkins<sup>(15)</sup> has shown spectroscopically that the high velocity electrons in an electric discharge passed through hydrocarbon vapours causes free radicals to be formed, the radicals rapidly recombining to form polymer compounds similar in nature to the contamination compounds under discussion here. It

therefore seems possible that free radicals may also be formed on the surface as a result of electron bombardment.

Whatever electron mechanism causes the formation of contamination, the original organic molecules are effectively "fixed" by the electron beam. The electron energies necessary to bring about the chemical reactions are relatively small in comparison with the beam energies employed (e.g. the critical potentials of the hydrocarbons methane and benzene are 14.4 V and 9.6 V respectively), which would explain why there is no great dependence of contamination on the electron energy.

The actual contamination compound formed is extremely resistant to chemical solvents and is most probably a hydrocarbon polymer of the type obtained when a gaseous discharge is passed through hydrocarbon gases. These compounds have been extensively studied by König and Helwig<sup>(16)</sup> and others.<sup>(15,17)</sup> Subsequent bombardment may produce partial or total carbonization of the polymer compounds.

The contamination process is continuous with time for so long as the electron beam is operative, so that an equilibrium condition must be set up between the rate of conversion of hydrocarbon molecules to contamination on the surface, and the net rate of supply of fresh molecules from outside. It has been established that no build-up of hydrocarbon takes place on the surface in the absence of the electron beam (a built-up layer would be directly visible in the microscope) so that if any hydrocarbon is present on the surface, it must result from an equilibrium between molecules arriving on the surface and those leaving it. Since the surface concentration under normal temperature conditions must therefore be low, it can be inferred that the hydrocarbon molecules are approaching the target area at a high rate but stay in that area only a very short time. At these low surface concentrations, the contamination rate will be directly proportional to the surface concentration of molecules and to the current density. It must be remembered, however, that at high current densities there may be a conversion of sufficient molecules to contamination, bringing about their effective removal, to be comparable with the rate of supply of the molecules. In this case, the effective concentration of molecules on the surface is reduced, leading to a relative falling off of contamination rate with current density.

#### REPLENISHMENT OF THE HYDROCARBON FILM

There are two possible ways in which the hydrocarbon film on the surface of the bombarded region may be replenished. These are (i) the migration of molecules over the surfaces surrounding the irradiated region (as suggested by Ellis); (ii) the arrival of molecules by condensation from the surrounding vapour. It is important, from a practical point of view, to decide which of these two mechanisms is responsible, since if migration alone is the mechanism of replenishment, the contamination could be reduced by cooling the specimen supports sufficiently to prevent the migration. If vapour is the source, however, an efficient cold trap surrounding the bombarded region should suffice to prevent contamination. These two possibilities will be examined in detail in relation to the temperature dependence of contamination.

(a) *Migration theory.* Assuming that adsorbed molecules on the surface are free to migrate over it and cross to the bombarded area, one can predict the effect of varying surface temperature on contamination. Although little is known about surface migration of hydrocarbon molecules, it is reasonable to suppose that at low concentration of molecules,

they will behave like a two-dimensional gas, whose equation of state will be

$$\pi A = RT \quad (1)$$

where  $\pi$  is the surface pressure and  $A$  the surface area per gram-molecule. On varying the temperature  $T$  of the bombarded area, the surface pressure  $\pi$  will remain constant throughout the instrument, which means that the surface area per gram-molecule  $A$  will change. Thus, in the absence of electron bombardment, the surface concentration  $\delta$  (which is inversely proportional to  $A$ ) will depend on temperature as

$$\delta \propto 1/T \quad (2)$$

This indicates that the contamination rate, which is proportional to  $\delta$ , will decrease with increase of temperature, as is observed experimentally. However, this argument does not take into account the removal of molecules by fixation with the electron beam.

Consider a circular area of target which is being bombarded by electrons. As molecules are fixed by the electron beam, fresh ones must cross the boundary between the bombarded and unbombarded regions to replace them, and the supply rate will depend on the mobility of the migrating molecules. According to the theory of Lennard-Jones<sup>(18)</sup> the rate of migration of each molecule is dependent upon the temperature  $T$  by a relation of the type

$$\nu \propto e^{-B/T} \quad (3)$$

where  $B$  is a constant.

At low temperatures, this factor will bring about a considerable reduction in the supply, and thus to the contamination rate. Such a reduction is not in fact observed.

(b) *Condensation theory.* According to current theories of adsorption<sup>(19)</sup> the surface of a solid in contact with a gas or vapour has a layer of gas molecules adsorbed on the surface. The concentration of these molecules, which are in dynamic equilibrium with the vapour, is dependent upon the pressure of the vapour, the temperature of the surface and the binding or activation energy of the vapour molecules on the surface. At very high temperatures, no vapour molecules can exist for a significant time on the surface but, as the temperature is lowered, the average time for which a molecule can stay on it increases, with consequent increase in surface concentration. The degree of adsorption will be directly proportional to the pressure of the vapour (which governs the rate of arrival of molecules on the surface) since for the low vapour pressures which exist in a normal kinetic vacuum system, it is reasonable to assume that the surface concentration of vapour molecules never exceeds one monolayer except under conditions of very low surface temperature. The fraction of the surface area covered with molecules will then be given by a formula due to Langmuir,<sup>(20)</sup>

$$\theta = \frac{\alpha_0 \nu}{\nu + \mu_0 e^{-Q/RT}} \quad (4)$$

where  $\alpha_0$  is the accommodation coefficient (a constant, approximately equal to 1),  $\nu$  is the rate of arrival of molecules from the vapour on to the surface (proportional to the pressure of the vapour),  $Q$  the activation energy necessary to evaporate 1 gram-molecule of the condensate and  $T$  the absolute temperature.  $\mu_0$  is a constant.

The decrease in surface concentration with rise in temperature, plotted from the above formula, will give a curve similar in shape to Fig. 5. The condensation theory can thus account for the temperature dependence of contamination, assuming that the contamination rate is proportional to the surface concentration. Further, the rate of supply of vapour

molecules is not restricted by the surface temperature of the specimen as it was in the case of migration, for kinetic theory shows that the mass of vapour at pressure  $p$  mm of mercury striking each square centimetre of surface in one second is given by

$$G = 5.83 \times 10^{-2} p \sqrt{M/T} \text{ grams} \quad (5)$$

where  $M$  is the molecular weight and  $T$  the absolute temperature of the vapour molecules in the system. It must be remembered that the temperature of the small area of surface

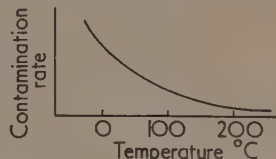


Fig. 5. Qualitative relation between contamination rate and temperature

under consideration may be widely different from the average temperature of the vapour (which is at normal ambient temperature).

Inserting values of vapour pressure of  $10^{-5}$  mm of mercury and molecular weight 350 for the oil vapour present in a normal demountable vacuum system, one obtains

$$G = 6 \times 10^{-7} \text{ g. sec. cm}^{-2}$$

Assuming now that this vapour is all converted into contamination, of unit density, the maximum possible rate of growth of the layer will then be  $60 \text{ \AA/sec}$ . In the electron microscope, growth rates of up to  $3 \text{ \AA/sec}$  have been observed, while Ellis<sup>(10)</sup> has reported rates of up to  $60 \text{ \AA/sec}$  using an electron probe.

Ellis considers that this rate of contamination is too high to be accounted for by oil pump vapour (which he estimates to be at the pressure of  $10^{-7}$  mm of mercury). However, there are many other sources of hydrocarbon molecules besides the vacuum pump oil. For instance, Blears<sup>(14)</sup> has shown that partial pressures of up to  $10^{-5}$  mm of mercury or more of hydrocarbons persist for at least 25 min after pumping down a metal vacuum system, and this is supported by the author's experiments on the contamination properties of various gasket materials, etc.

It thus appears that contamination can be accounted for by the arrival of organic molecules from the vapour rather than by migration on to the surface under bombardment. However, the possibility exists that both mechanisms are operative simultaneously to some degree, and so further experiments were carried out to investigate this.

#### EXPERIMENTS ON SURFACE FILM REPLENISHMENT

To confirm that contamination results from the arrival of hydrocarbon molecules from the vapour, the following experiments were carried out.

(a) The stainless steel target was cleaned as before and mounted inside a long, narrow glass liquid air trap of the design shown in Fig. 6. It was supported by a  $1/16$  in. diameter steel rod, attached at the other end to the electron gun, so as not to touch the walls of the trap. Electrons from the 2 kV gun were directed on to the target and, by means of the magnetically operated shutter, two equal electron bombardments were given to adjacent areas of the target, the first with the trap not cooled, the second with it containing liquid air. While the normal brown deposit was obtained for the first



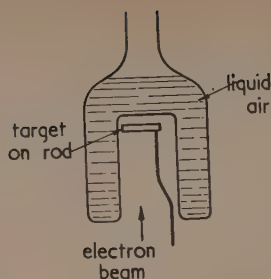


Fig. 6. Design of liquid air trap

bombardment, only very slight contamination (detected by breathing on the target) was evident for the second run.

Now the liquid air trap will prevent all condensable vapours from reaching the surface of the target except those molecules which pass straight through the open end of the trap and strike the target without first colliding with the trap wall. The very small contamination observed when the liquid air trap was in operation could be accounted for by the finite aperture. From the dimensions of the trap, a reduction of contamination of between ten and twenty times would be expected. Migration of organic molecules would not be prevented but might be slowed down by a drop in temperature of the target and supports caused by radiation exchange. A thermocouple attached to the target showed this temperature drop to be negligible, however. It appears then that very little contamination by migration of molecules takes place.

(b) The target in the second instance consisted of a clean glass microscope cover-slip, suspended by fine tungsten wires from two thicker tungsten wires which could be heated electrically (see Fig. 7). Hydrocarbon molecules which might

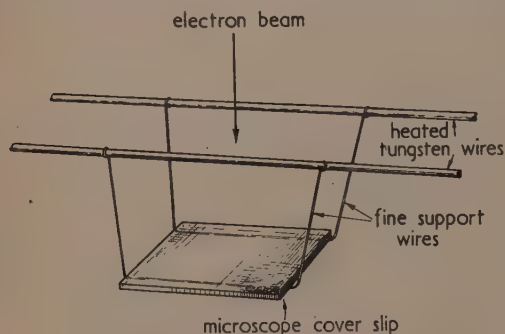


Fig. 7. Target consisting of glass microscope cover slip

otherwise migrate over the hot wires would be either carbonized or evaporated off. Contamination formed on the target to the same extent whether or not the tungsten wires were heated, provided the target did not become heated by radiation (the support wires were made long to prevent this). On depositing gold on the glass by evaporation (and thus creating a fresh surface) further contamination still appeared on electron bombardment. This experiment again indicates that surface migration, if existing at all, plays a very small part in the contamination process.

#### CONCLUSIONS

The experimental and other considerations described show that contamination in the electron microscope is produced by

interaction of the electron beam with organic molecules on the surface of the specimen. It has been shown that these molecules are derived from the residual organic vapours which are always present in a continuously-pumped demountable vacuum system, and that most of these molecules arrive on the surface direct from the vapour, and not by migration, as had previously been suggested (by Ellis).

While the presence of these vapours, many of which are derived from the metal walls, gaskets, etc., of the instrument is unavoidable in principle, it is possible to reduce their effect by heating the specimen, so preventing condensation of the vapours on the surface. This has been successfully carried out in practice, although in the case of the electron microscope, various technical difficulties in keeping the specimen thermally stable at high temperatures have to be dealt with. (Prevention of contamination on the targets used to study nuclear reactions has also been carried out successfully by heating the targets.)

Alternatively, a cold trap surrounding the specimen will also prevent contamination, providing that the apertures necessary for introducing the specimen and allowing the beam to pass through are small. A cold trap surrounding the specimen in an electron diffraction camera has, in fact, been found to be completely efficient in preventing its contamination. However, such a method of preventing contamination would meet considerable design difficulties in electron microscopes.

Reduction of the hydrocarbon vapour pressure throughout a demountable system, which would reduce contamination, presents a number of practical difficulties. It is hoped to discuss these in a further paper dealing with the source materials from which contamination is formed.

#### ACKNOWLEDGEMENTS

The author wishes to thank Dr. T. E. Allibone, the Director of this Laboratory, for permission to publish this paper.

#### REFERENCES

- HAINE, M. E., and MULVEY, T. *J. Opt. Soc. Amer.*, **42**, p. 763 (1952).
- HILLIER, J. *J. Appl. Phys.*, **15**, p. 663 (1944).
- KÖNIG, H. *Naturwiss.*, **35**, p. 261 (1948).
- WATSON, J. H. L. *J. Appl. Phys.*, **18**, p. 153 (1947).
- COSSLETT, V. E. *J. Appl. Phys.*, **18**, p. 844 (1947).
- BURTON, E. F., SENNET, R. S., and ELLIS, S. G. *Nature, Lond.*, **160**, p. 565 (1947).
- KINDER, E. *Naturwiss.*, **34**, p. 23 (1947).
- HILLIER, J. *J. Appl. Phys.*, **19**, p. 226 (1948).
- KÖNIG, H. *Z. Phys.*, **129**, p. 483 (1951).
- ELLIS, S. G. Paper read to Amer. E.M. Soc., Washington (November 1951).
- STEWART, R. L. *Phys. Rev.*, **45**, p. 488 (1934).
- TOLANSKY, S. *Multiple Beam Interferometry of Surfaces and Films* (London: Oxford University Press, 1948).
- VON BORRIES, B. *Optik*, **3**, p. 321 (1948).
- BLEARS, J. *J. Sci. Instrum.*, Supplement No. 1, *Vacuum Physics*, p. 36 (1951).
- HARKINS, W. D. *Trans Faraday Soc.*, **30**, p. 221 (1934).
- KÖNIG, H., and HELWIG, G. *Z. Phys.*, **129**, p. 491 (1951).
- LINDER, E. G., and DAVIES, A. P. *J. Phys. Chem.*, **35**, p. 3649 (1931).
- LENNARD-JONES, J. E. *Trans Faraday Soc.*, **28**, p. 333 (1932).
- e.g. BRUNAUER, S. *The Adsorption of Gases and Vapours* (Princeton University Press, 1943).
- LANGMUIR, I. *J. Amer. Chem. Soc.*, **40**, p. 1361 (1918).



# The construction of ball-and-spoke models of crystal structures

By HELEN D. MEGAW, M.A., Ph.D., F.Inst.P., Crystallographic Laboratory, Cavendish Laboratory, University of Cambridge

[Paper received 22 October, 1952]

Suggestions are made for simplifying the calculations required in the construction of models, and for rendering the models more easily reproducible. The requirements are (a) a drilling schedule in which angular co-ordinates are calculated with reference to directions fixed in space, and are recorded in an agreed notation applicable to any two-circle jig; (b) a "key diagram," a projection showing all included atoms marked with their heights and "code-numbers"; (c) a note referring to the original paper from which the data are taken. It may often be possible to add written instructions for assembling. Full instructions for a model of  $\text{KH}_2\text{PO}_4$  are given as an example.

Ball-and-spoke models have been much used by crystallographers to display in three dimensions the environment and bonding of the atoms in a structure; in such a model, relationships may often be seen which are far from obvious in projections or perspective diagrams. A model may thus be needed by the original worker in the course of determining a structure, and also by later workers who are concerned with further investigations of its properties or its relations to other substances. Though models can be bought commercially, the necessity of "home-made" models still remains. The type of model considered here is that showing only positions of atomic centres and bonds, and not sizes or packing. The construction of packing models has been described by Buerger and Butler<sup>(1)</sup>; the atom-centre-and-bond model is simpler to make, and for many purposes is more useful.

For structures of the degree of complexity which are studied nowadays, the construction of a model is inevitably laborious and fairly costly. The situation is made worse, however, by the lack of any approach to systematization, so that each new model has to be thought out *ab initio*, and the calculations and planning which have gone into it are largely lost if a repetition is subsequently wanted by another laboratory. It is the purpose of this paper to show how this situation could be improved without loss of flexibility in design. It is based on experience of co-operation with the Cambridge University Engineering Laboratory in the construction of a number of different models. Throughout, the recommendations<sup>(2)</sup> of the Crystal Structure Model Panel of the X-ray Analysis Group of The Institute of Physics have been assumed as a starting point.

The work of making a model may be divided into four steps.

(1) *Design.* This involves decisions on such points as the number of atoms to be included, the bonds to be shown by spokes, and the representation of the outline of the unit cell. The recommendations of the Structure Model Panel<sup>(2)</sup> are chiefly concerned with this stage.

(2) *Calculation.* From the known atomic co-ordinates, it is necessary to calculate the angles made by the bonds with certain fixed directions, and translate them into a drilling schedule. Bond lengths must also be calculated.

(3) *Preparation of balls and spokes.* If the drilling schedule is given in terms of the drilling jig to be used, this step can be handed over to the workshop to be carried out as a routine process.

(4) *Assembly.* The spokes must be fitted into the balls, and the whole rigidly put together. It may or may not be mounted on a base.

The problem considered here is that of stage (2)—the calculation and preparation of drilling schedules which will be universally intelligible and can be followed by any workshop without continual supervision by the designer. If such

schedules could be devised, it might be possible to ask the X-ray Analysis Group of The Institute of Physics to keep a central file of them, available for loan. It would be desirable to go further and include written instructions for assembly of the models. Some suggestions about this are made later, but it cannot be standardized as easily, and its omission does not spoil the usefulness of the rest.

## CALCULATIONS AND DRILLING SCHEDULES

The systematization of drilling schedules is not hard to achieve for a laboratory using a particular type of jig. The two-circle jig in use in the Cambridge University Engineering Laboratory was designed by Dr. R. C. Evans as a simplification of one described by Buerger;<sup>(3)</sup> a photograph of it is shown in Fig. 1. With such an instrument the most natural

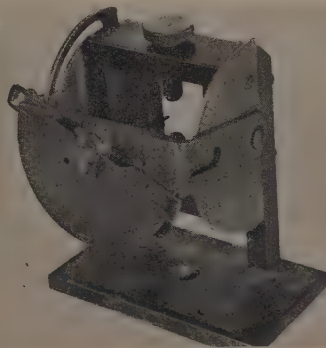


Fig. 1. Photograph of Cambridge jig

way of defining directions is by use of two angular co-ordinates,  $\rho$  and  $\phi$ , related to latitude and longitude respectively, the origin of co-ordinates and direction of reading depending on the particular instrument. It is an obvious step forward to define them in a more general way, which could be translated by the user into terms of any two-circle jig. Experience suggests that this standardization would be worth while in making the work of one laboratory freely available to another.

For this purpose, the angle  $\rho$  is defined as the *co-latitude measured from the north pole*, running from  $0^\circ$  to  $180^\circ$ ; and the angle  $\phi$  as the *longitude measured continuously westwards* (i.e. clockwise from above), running from  $0^\circ$  to  $360^\circ$ .

It is necessary to choose one direction (which may be called the pilot direction) as the north pole, and one great

circle through this as the  $0^\circ$  meridian. These directions may be chosen independently for every separate ball; but much simplification can be achieved if they are kept constant with respect to the completed model. It is suggested that in the standard form the pilot direction should be vertical and the  $0^\circ$  meridian run from left to right (starting from the pilot direction). These directions (or others in a known relation to them) *must be marked on each ball at the time of drilling*, as they show its orientation in the finished structure.

The easiest method of determining angles is from a projection of the structure on the horizontal plane, drawn to a scale which may most conveniently be that of the model, and with the heights of atoms in Ångström units above an arbitrary zero marked on it. It is desirable that this projection should show all the atoms to be inserted in the model; if appropriately labelled, it can then serve as the key to the drilling schedule. (If a single projection has so many superimposed atoms as to be confusing, a series of projections of successive layers of the structure should be used instead; upward or downward slope of bonds can be indicated by using a line which broadens towards its upper end, or arrows always pointing upwards.)

Each atom is considered in turn. The bonds to be represented as spokes are drawn from it to its neighbours, and the angle  $\phi$  for each line is measured clockwise from a fixed left-to-right line. The projected length of the bond is measured; if this is  $b$  and the difference in heights is  $h$  (reckoned positive if the central atom is the lower), then  $\tan \rho = b/h$ . All values of  $\rho$  and  $\phi$  for the atom are tabulated. It is convenient to make a sketch stereogram showing the directions of the neighbours marked with the bond lengths.

The atom is given a "code number" for subsequent reference, and this is marked on the key diagram and attached to the appropriate  $\phi$ ,  $\rho$  table. The "code number" is not identical with the crystallographic symbol, because crystallographically-equivalent atoms will in general be differently oriented with respect to the reference directions; the balls having extra holes to carry the outlines of the unit cell may also need to be labelled separately. Balls on the outside of the model will not need their full complement of holes, but it is generally less trouble to drill them all than to distinguish the separate cases. Exceptions to this rule are those outer balls with only a single neighbour; single-hole balls are easily drilled, and do not need to be marked with reference directions, as the balls are added when the structure is otherwise complete.

In a complicated structure it is useful to engrave on the balls the symbol given by the author to the corresponding atoms in the paper describing the structure. It has been found a very great help to the user to have this identifying mark.

#### SPECIFICATION OF BONDS

Bond lengths have generally been recorded in the paper describing a new structure; if not, they are easily calculated from the key diagram. In the specification, they should be given as centre-to-centre distances—i.e. the actual bond length on the chosen scale. Corrections giving the cut length of spoke, which depend on the ball diameter and drilling depth, can easily be made by the workshop to suit its own circumstances. Slotted distance pieces placed over the bonding spokes ensure correct length when an assembly is being made.

Cell outlines, or spokes used to give mechanical rigidity to a model, may be distinguished from bonds by covering them with coloured sleeving. Unusual types of bond may be

emphasized by different colours. For example, weak bonds or contacts regarded as doubtful bonds, may be covered with black; hydrogen bonds may be covered with white. A small white ball may be threaded on a spoke to represent the hydrogen atom of a hydrogen bond. Ordinary bonds are left uncovered.

#### FURTHER INSTRUCTIONS

Numbers of atoms of each kind, and bonds of each kind are counted on the key diagram. Colours for the balls are selected in accordance with the accepted code.<sup>(2)</sup>

The set of drilling schedules, details of spokes, key diagram or diagrams, and a reference to the paper from which the crystallographic data are taken, together make up the information which would be needed by any later worker. The importance of this reference to the source of the data needs to be emphasized. If photographs of the completed models are available, prints in which the balls have been coloured according to code are a useful addition to the file of instructions.

In practice, it has been found possible to go beyond this, and devise written instructions, based on the key diagram, for the assembly of most models attempted. An example is *afwillite*,  $\text{Ca}_3(\text{SiO}_3\text{OH})_2\text{H}_2\text{O}$ , which is monoclinic and contains over 100 balls. The existence of reference lines on each ball, running always in the same direction, was a vital factor in achieving this. Each structure, however, will have its own individual problems at this stage.

It is desirable that the label on the completed structure should give, besides its name and formula, the author and date of the paper from which the data for the structure are taken. This can be of great help to the user.

#### ADAPTATION FOR USE WITH PARTICULAR JIGS

It is believed that the standard drilling schedule can be adapted easily, and in a routine way, to the technique of any particular jig. The details of its application to the Cambridge instrument are given as illustration.

In this, a pilot hole must be drilled in the pilot direction, on which the ball is mounted for further drilling. The scale of  $\rho$  reads from  $0$  to  $180^\circ$ ; the scale of  $\phi$  also reads from  $0$  to  $180^\circ$ , but the pointer indicating the setting has two ends marked *A* and *B*, the latter to the right in Fig. 1. If ( $\rho_0$ ,  $\phi_0$ ) are the standard co-ordinates, it would be necessary to give the practical co-ordinates as ( $\rho$ ,  $\phi$ ), where

$$\begin{cases} \rho_0 = \rho \\ \phi_0 = \phi_A \text{ (if } \phi_0 < 180^\circ) \\ \phi_0 - 180^\circ = \phi_B \text{ (if } \phi_0 > 180^\circ). \end{cases}$$

The co-ordinates are given in Table 1(b) for a ball drilled with tetrahedral holes, the cubic direction [001] being the pilot direction and (100) the meridian plane. Co-ordinates in standard form for the same set of holes are given in Table 1(a).

Table 1. Angular co-ordinates for tetrahedral holes

	(a) standard notation		(b) Cambridge jig	
	$\rho$	$\phi$	$\rho$	$\phi$
111	$54\frac{1}{2}$	45	$54\frac{1}{2}$	45A
$\bar{1}\bar{1}\bar{1}$	$125\frac{1}{2}$	135	$125\frac{1}{2}$	135A
$\bar{1}\bar{1}1$	$54\frac{1}{2}$	225	$54\frac{1}{2}$	45B
$\bar{1}\bar{1}\bar{1}$	$125\frac{1}{2}$	315	$125\frac{1}{2}$	135B

The appearance of unused pilot holes at the top of each atom may be thought unsightly. It would be preferable to have them below, where they do not show. This can be done by drawing the stereograms of atomic environments viewed from above as usual, but measuring  $\rho$  from the south pole, and  $\phi$  anticlockwise. The instructions for assembly must then specify that the pilot hole is to point downwards. The guide for assembling is in this case a scribed horizontal line starting from the point on the ball diametrically opposite the pilot hole.

It is not possible to drill holes at less than  $30^\circ$  to the pilot hole. If these are needed, an auxiliary pilot hole has to be used, and there is more danger of splitting the ball on assembly.

#### EXAMPLE

To illustrate the method, instructions for making a model of  $\text{KH}_2\text{PO}_4$  are given in detail.

The crystallographic information needed is as follows<sup>(4)</sup>: space group  $I\bar{4}2d$  (tetragonal body-centred),

$$a = 7.43 \text{ \AA}, c = 6.97 \text{ \AA}.$$

formula-units per cell.

Atomic co-ordinates as follows:

$$4P: 000, \frac{1}{2}0\frac{1}{2}, \frac{1}{2}\frac{1}{2}0, 0\frac{1}{2}\frac{1}{2}$$

$$4K: 00\frac{1}{2}, \frac{1}{2}0\frac{1}{2}, \frac{1}{2}\frac{1}{2}0, 0\frac{1}{2}\frac{1}{2}$$

$$16O: xyz; \bar{x}\bar{y}z; \bar{y}x\bar{z}; y\bar{x}\bar{z}$$

and similar points round each P;

$$x = 0.080, y = 0.144, z = 0.139.$$

A larger unit cell, with axes rotated through  $45^\circ$ , is sometimes used; it was decided to mark this on the base of the

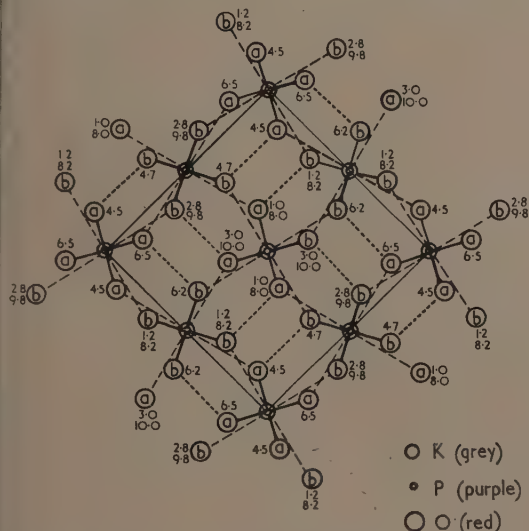


Fig. 2. Projection of unit cell of  $\text{KH}_2\text{PO}_4$ , to serve as key diagram for model

Thick lines, P-O bonds superposed on K-O.

Dashed lines, K-O.

Dotted lines, O-H-O.

Heights of O atoms given in Angstrom units above an arbitrary zero (base of model); heights of K and P omitted for clarity.  $a$  and  $b$  refer to code-numbers

model, and mount the smaller cell within it, outlined with spokes. The projection of the smaller cell in this orientation (with origin at the centre of the square) is shown in Fig. 2, its relation to the larger cell in Fig. 3. The reference on the label of the model is to the work of Frazer and Pepinsky<sup>(5)</sup> who use the larger cell; the axes in Fig. 3 are marked accordingly.

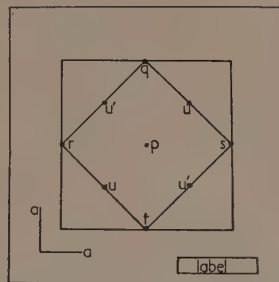


Fig. 3. Arrangement of model on baseboard

There are three kinds of bonds in the structure, P-O, K-O, and O-H-O. The first are normal strong bonds, which must obviously be represented by spokes. The third, the hydrogen bonds, are an interesting feature of this structure; they need to be emphasized, and a ball sliding on them to represent the hydrogen atom is an effective way of doing so. Regarding the second, recent work by Frazer and Pepinsky<sup>(5)</sup> has called attention to the importance of the K-O distances, and therefore it is desirable to insert spokes here, but as the bonds are fairly weak they may be covered in black. With such a network of bonds, there will be no need for non-bonding supports in the final model, but to simplify the assembly temporary vertical spokes are used.

Once these decisions are taken, a routine set of calculations leads to the following drilling schedule, for which Fig. 2 is the key diagram.

#### DRILLING SCHEDULE

Co-ordinates  $\rho$ ,  $\phi$  given in terms of Cambridge jig. Standard co-ordinates are:

$$\rho_0 = \rho$$

$$\phi_0 = \phi_A \text{ or } \phi_B + 180^\circ$$

Balls  $\frac{1}{8}$  in. diameter.

Colours: P, purple; K, grey; O, red.

For each ball, drill pilot hole in jig at 0, 0A; then set at 90, 90B, and scribe a horizontal line from pilot hole towards left. (In assembling, pilot hole will be vertical, and scribed line run towards right.) Then proceed to drill as follows:

Code Pa		Code Pb	
No. off = 6		No. off = 4	
0	0A	0	0A
128	74A	52	16A
52	164A	128	106A
128	74B	52	16B
52	164B	128	106B



Code Kp	No. off = 1	Code Ku	No. off = 4
0	0A	0	0A
26	74A	154	16A
154	164A	26	106A
26	74B	154	16B
154	164B	26	106B
106	57½A	74	32½A
74	147½A	106	122½A
106	57½B	74	32½B
74	147½B	106	122½B

Code Kq	90	45A	in addition to holes of Kp. No. off, 2 of each.
	90	135A	
Code Kr	90	45A	
	90	135B	
Code Ks	90	135A	
	90	45B	
Code Kt	90	45B	
	90	135B	

Drill pilot hole right through all P and K balls.

Code Oa <sub>1</sub>	Code Oa <sub>2</sub>	Code Oa <sub>3</sub>	Code Oa <sub>4</sub>
No. off = 6	No. off = 6	No. off = 6	No. off = 6
0	0A	0	0A
74	122½A	154	74A
94½	45B	52	74A
128	154B	106	32½B
26	154B	85½	135B
		52	74B

Code Ob <sub>1</sub>	Code Ob <sub>2</sub>	Code Ob <sub>3</sub>	Code Ob <sub>4</sub>
No. off = 6	No. off = 6	No. off = 6	No. off = 6
0	0A	0	0A
52	106A	26	16A
154	106A	128	16A
85½	45B	94½	135A
106	147½B	74	57½B
		94½	135B

Code Oc.

No. off = 28.

Pilot hole only.

Spokes (centre-to-centre length)

PO 1.56 in., No. off 52.

KO, KO' 2.80 in., No. off 32, sleeved in black.

OO' 2.53 in., No. off 16. On these, thread a white ball ¼ in. diameter with a sliding fit.

Outline, 9 in. clear of board, No. off 4 permanent } (vertical)  
5 temporary }

7.44 in. (centre-to-centre), No. off 8 (horizontal).

#### ASSEMBLY

Mount 9 vertical spokes in temporary board, as Fig. 3. (Those at *qrst* will remain in finished structure.)

For all balls, keep pilot hole vertical and scribed line to the right.

On each Pa, put Oa<sub>1</sub> Oa<sub>2</sub> Oa<sub>3</sub> Oa<sub>4</sub>.

On each Pb, put Ob<sub>1</sub> Ob<sub>2</sub> Ob<sub>3</sub> Ob<sub>4</sub>.

using 1.57 in. spokes. (There is only one way which satisfies the reference lines.)

The holes in K's are of two kinds, ordinary and extra. The extra are for the cell outline; the ordinary all take 2.80 in. spokes.

At height 2 in. above board, put *Kqrst* on the appropriate verticals. Join with 4 horizontal spokes to outline square.

At height 5.5 in. above board, put 4 Pa's on the same verticals.

At height 9 in., put *Kqrst* on the same verticals, and join with horizontal spokes.

On central vertical *p*, put Pa at 2 in., Kp at 5.5 in., Pa at 9 in.

On verticals at *u*, put 2 Ku's at 3.75 in., 2 Pb's at 7.25 in.

On verticals at *u'*, put 2 Pb's at 3.75 in., 2 Ku's at 7.25 in.

The structure should now join up, bonds from K fitting into holes in O. Place the remaining 8 Ob's at the junctions of two K spokes. (There is only one way which satisfies the reference lines.) Insert O-H-O' bonds into the empty holes so that they run nearly horizontal and parallel to the cell outline. Add Oc to all empty spokes.

Remove the temporary verticals at *p*, *u*, *u'*. Mount on a permanent base, 18 in. square, marked as shown in Fig. 3a. Label to read:

Potassium dihydrogen phosphate, KH<sub>2</sub>PO<sub>4</sub>.

West, 1930.

(Axes and origin, Frazer and Pepinsky, 1952.)

(Scale, 1 in. : 1 Å.)

#### SUMMARY AND CONCLUSION

It should be emphasized that there is nothing new in principle in the methods of model construction outlined above. What is believed to be new is the attempt to reduce them to a routine, so that instructions can be written down which may be followed by those without previous knowledge or specialized skill. The features which enable this to be done are:

(1) Tabulation of all angular co-ordinates in a form independent of the particular jig to be used.

(2) Reference of all angular co-ordinates to two constant directions in the completed model.

(3) The marking of these directions on the balls at the time of drilling.

(4) Use of a key diagram showing the code-numbers of the balls.

If the amount of individual attention that must be given to the models can be reduced in this way it should reduce their effective cost, and increase their availability whether as prototype models or as duplicate copies.

#### ACKNOWLEDGEMENT

The author wishes to express thanks to Mr. J. H. Brooks and Mr. A. Barker for advice and collaboration in the search for improved methods of construction of models.

#### REFERENCES

- (1) BUEGER, M. J., and BUTLER, R. D. *Amer. Min.*, **21**, p. 150 (1936).
- (2) Report of the Crystal Structure Model Panel. *J. Sci. Instrum.*, **24**, p. 249 (1947).
- (3) BUEGER, M. J. *Rev. Sci. Instrum.*, **6**, p. 412 (1935).
- (4) WEST, J. Z. *Krist.*, **74**, p. 306 (1930).
- (5) FRAZER, B. C., and PEPINSKY, R. *Phys. Rev.*, **85**, p. 479 (1952).

# A modified ionization method of measuring contact potential

By W. R. HARPER, Ph.D., F.Inst.P., Imperial College of Science and Technology, London

[Paper first received 16 December, 1952, and in final form 31 January, 1953]

The use of an insulated probe is described, for the case in which the relevant electrodes cannot themselves be used for the measurement.

Experimental methods available for the measurement of the contact potential between two metals have been fully discussed in recent summaries,<sup>(1,2,3)</sup> but if the metals take the form of two electrodes in an apparatus designed for some other purpose, additional difficulties may arise which make these methods unsuitable. The variability of contact potentials may nevertheless make it important to measure the required value *in situ*. In appropriate circumstances, an example of which occurred in the author's work on the generation of static charges, a modification of the ionization method can be used. This new method will be briefly described.

In the author's apparatus, the contact potential between a  $\frac{1}{2}$  in. metal sphere supported by fine wires inside metal screening, and the screening, had to be determined. The relevant capacitance could not be varied, and the presence of air excluded electronic methods. The ionization method in its usual form was unsuitable because of inadequate insulation and excessive capacitance of the parts. The apparatus is shown schematically in Fig. 1, the required contact potential  $V_{AB}$  being that between the sphere *A* and the screening *B*.

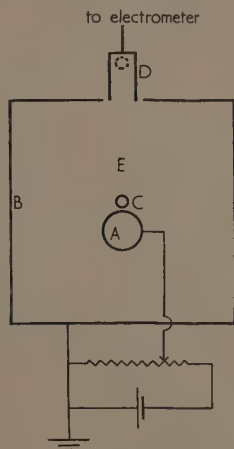


Fig. 1. Apparatus for modified ionization method of measuring contact potential

A potentiometer was provided to compensate  $V_{AB}$ , the fact that this had been done being indicated by the absence of ionization current in the neighbourhood of *A* when the air between *A* and *B* was heavily ionized using a gamma-ray source (of about 100 mc  $^{192}\text{Ir}$ ). The presence of ionization current was detected by inserting an insulated probe at *C*, leaving it to acquire its equilibrium charge, and measuring this charge by transferring the probe to a Faraday cylinder *D*. It happened conveniently that a mechanism for doing this was already available in the form of a 5/32 in silica ball supported by fine silica fibres. The probe actually used was therefore an insulator, but this is not necessary. The procedure was to plot equilibrium charge against potentiometer setting, as in Fig. 2. The intercept on the voltage axis could be determined accurately by taking a few readings on either side, confining them to the limited range in which the curve is linear.

Neglecting, for the moment, the thermal agitation of the ions, the charge on the probe attains its equilibrium value when the field in its neighbourhood is zero. When, in addition, the probe is uncharged, it makes no contribution to this field, in which case  $V_{AB}$  must have been compensated. The argument holds even if the probe is conducting and has its own contact potential. The finite size of the probe compli-

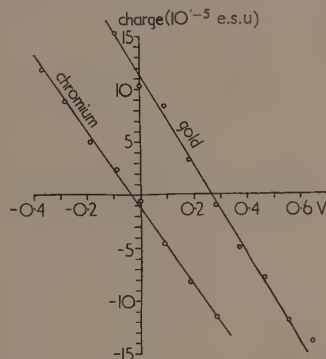


Fig. 2. Relation between equilibrium charge and potentiometer setting. The intercepts are at minus the contact potential for chromium/brass and gold/brass

cates the argument, but will clearly not affect the conclusion that the intercept is  $-V_{AB}$ . Any departure from this, due to a difference in the diffusion coefficients of positive and negative ions, will be a fraction of the energy of thermal agitation of a single ion, that is, a fraction of about 1/25 V, and this is negligible.

The best position for the probe appeared to be just not touching the metal sphere, and the gamma-rays were directed at *E* (Fig. 1) above it, so as to give a rain of ions on the probe. A minute's irradiation was sufficient for the equilibrium charge to become established. The sensitivity obtained under these conditions is seen from Fig. 2, which gives the results for chromium and gold spheres in a brass screening. The error of measurement, as far as the potentiometer is concerned, does not exceed 1/50 V, but an additional small error is caused by the differential diffusion rates of the positive and negative ions. The contact potential between the two spheres may be obtained as a difference, with a correspondingly greater error.

## REFERENCES

- (1) BOURION, R. *J. de Phys.*, **12**, p. 930 (1951).
- (2) PATAI, I. F., and POMERANTZ, M. A. *J. Franklin Inst.*, **252**, p. 239 (1951).
- (3) NEUERT, H. *Arch. Tech. Messen*, No. 189 (Ref. V 3313-2), T. 107 (1951).

# An apparatus for measuring the coefficient of thermal conductivity of solids and liquids

By T. A. MARSHALL, B.Sc., Grad.Inst.P.,\* W. T. Henley's Telegraph Works Co. Ltd., Research Laboratories, Gravesend

[Paper received 24 November, 1952]

A flat plate type of apparatus for measuring the coefficient of thermal conductivity of solids and liquids is described. Values which have been obtained for the coefficients of several typical cable dielectric materials over their working temperature range are given.

The temperature rise of electrical apparatus in operation is largely determined by the thermal conductivity of the insulating materials employed in its construction. A survey of the literature revealed only a few values of the coefficients of thermal conductivity of dielectric materials, and little about the manner in which they varied with temperature. It is the purpose of this paper to describe apparatus which has been constructed to measure the thermal conductivity of solid and liquid dielectrics over their operating temperature range and to give the results of measurements which have been made on insulating materials commonly used in the manufacture of electric cables and wires.

## TYPE OF APPARATUS

As the apparatus had to be suitable for testing both solids and liquids, it was decided that the Hercus and Laby modification<sup>(1)</sup> of Lees' disk apparatus<sup>(2)</sup> would be the most suitable type to use. The basic components of the apparatus are shown diagrammatically in Fig. 1, from which it will be seen to consist of a heated plate, screened by a guard cap maintained at the same temperature, so that all the heat generated in the "hot" plate is dissipated downwards through the sample to a "cold" plate which is maintained at a lower

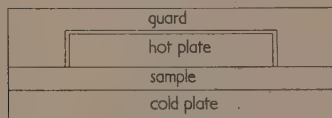


Fig. 1. Basic components of thermal conductivity apparatus

temperature. When the temperature  $T_1$  of the hot plate and guard are equal and constant, and the cold plate temperature  $T_2$  is also constant, the coefficient of thermal conductivity  $K$  of the sample material may be calculated from the equation:

$$K = Qd/(T_1 - T_2)$$

where  $Q$  is the rate at which heat is lost from the hot plate which has an area  $A$  in contact with a sample of thickness  $d$ .

Using C.G.S. units for the calculation, values of the thermal conductivity are obtained in units of calorie cm/cm<sup>2</sup> sec °C or, if the recommendations of The Royal Society<sup>(3)</sup> are followed, in joules cm/cm<sup>2</sup> sec °C (1 cal<sub>15°</sub> = 4.1855 j). Should the thermal resistivity,  $G$ , be required, it can be calculated in °C/W/cm cube from

$$G = 1/4 \cdot 1855 K$$

when  $K$  is in cal cm/cm<sup>2</sup> sec °C.

## DESCRIPTION OF THE APPARATUS

A cross-sectional drawing of the apparatus is given in Fig. 2. The apparatus is mounted on a water-cooled tank

$A$  which provides a constant temperature heat sink for the cold plate  $B$  which rests upon it, and thus reduces the time taken for the apparatus to reach thermal equilibrium and facilitates the maintenance of equilibrium. By removing the cork sheet  $C$ , which is normally under the cold plate to

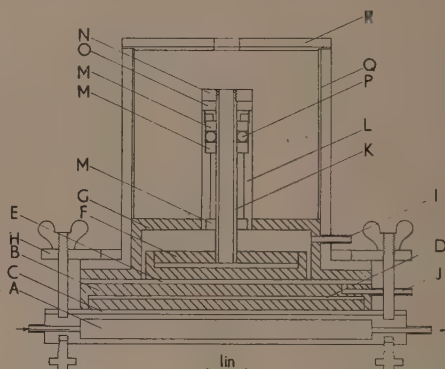


Fig. 2. Diametral section through thermal conductivity apparatus

reduce its heat loss to the base, measurements can be made down to an average sample temperature of 15° C so that with the designed maximum temperature of 150° C experiments can be made over the working range of most dielectrics.

The cold plate is constructed from two copper disks, one of which has a recess in one side in which a heater and the other disk are clamped. The heater  $D$  which is used to raise the cold plate temperature when the variation of thermal conductivity with temperature is being studied, consists of Nichrome tape closely wound on a mica disk  $\frac{1}{2}$  in. smaller in diameter than the cold plate and insulated from it by mica disks. The use of the minimum of insulation around the heater ensures a rapid response to changes in heater power, whilst the evenly distributed construction and the  $\frac{3}{8}$  in. of copper surrounding it ensures that the surface of the cold plate is at uniform temperature. This has been proved in practice by the readings of eight copper-constantan thermocouples which are located approximately 0.02 in. below various points of the surface in contact with the sample.

A solid sample  $E$  is placed directly on the cold plate and the hot plate  $F$  and the guard  $G$  are clamped on it by a ring  $H$  attached to the top of the guard ring to ensure good thermal contact between the surfaces. To test a liquid a rubber ring is first clamped at the circumference of the sample space to define the thickness and area of the liquid sample. This space is then evacuated through the tube  $I$  and the sample is drawn in under vacuum through the pipe  $J$  after being degassed in the apparatus shown in Fig. 3. The test liquid is heated, placed in the heated funnel and drawn through the sintered glass filter by a vacuum so that it loses

\* Now at A. Gallenkamp and Co. Ltd.



most of its dissolved gas before it falls into the graduated vessel where the remainder is removed before the liquid is admitted to the sample space.

The hot plate and its heater are constructed in a similar manner to the cold plate. The leads from its heater and the thermojunctions which are placed under all the surfaces, pass from the centre of the top of the hot plate through a

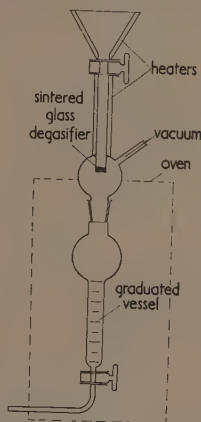


Fig. 3. Oil degasifier and measuring vessel

thin-walled tube of K monel, by H. Wiggin and Co. Ltd. (K). This metal was chosen as its low thermal conductivity reduces any tendency for heat transfer along it to the guide tube L fitted to the copper inner guard cap G, and for the same reason the smallest gauge thermocouple leads consistent with durability were used. Small Mycalex rings M are fitted in the guide tube to fix the hot plate on the same axis as the guard cap, and a nut N threaded on the hot plate lead tube and working on the top of the guide tube via a Mycalex washer O allows the vertical position of the hot plate to be adjusted so that its lower surface is flush with the guard ring surface. An O-ring seal p between the two upper Mycalex guides completes the sealing of the sample space. The guide assembly is enclosed by an insulated brass cylinder Q and a removable lid R, which are wound with Nichrome tape at the same density as the rest of the outer surfaces of the guard to form an oven to maintain it, and the copper inner guard, at the same temperature as the hot plate. The thermocouple and heater leads from the hot plate and guard are brought out through the hole in the centre of the lid.

The whole apparatus is provided with a cover to minimize the effects of draughts on the guard temperature.

#### AUXILIARY APPARATUS AND SERVICES

All heaters in the apparatus are tapped so that either a mains supply or storage batteries can be used as a source of power, but up to the present it has been found that the d.c. main, with potential divider voltage control gear, has been sufficiently stable to be used on all heaters. A voltmeter and selector switch are mounted in the apparatus base to allow the various voltages to be measured when adjusting test conditions, and a potential divider in parallel with the hot plate heater and a small resistance in series with it allow the voltage and current to be measured accurately with a potentiometer when hot plate power measurements are required.

During preliminary trials of the apparatus it was found that a considerable saving in time could be made if a two-channel

recorder was connected so that both the cold plate temperature and the difference in the temperatures of the hot plate and guard were recorded. In this way the state of equilibrium of the apparatus, and thus the time at which measurements could be usefully started, could then be seen at a glance.

#### EXPERIMENTAL

The results of measurements which have been made of the coefficients of thermal conductivity of polythene, polyvinylchloride, rubber, oil impregnated paper and impregnating oil, over their working temperature ranges are shown in Fig. 4. These results were obtained from samples approxi-

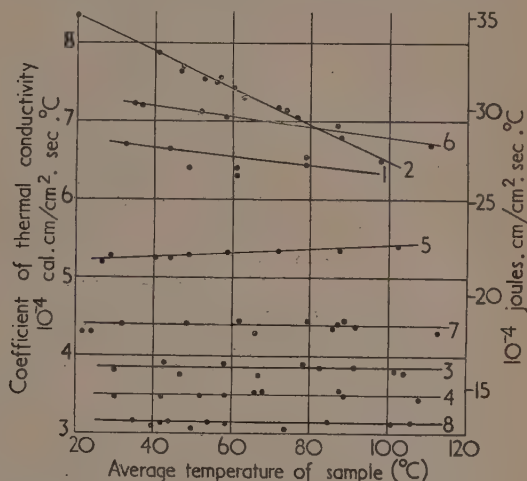


Fig. 4. The temperature variation of the coefficient of thermal conductivity of some dielectric materials

- Curve 1. Polythene—dry surfaces.
- Curve 2. Polythene—glycerine on surfaces.
- Curve 3. Polyvinylchloride mix—low plasticizer content.
- Curve 4. Polyvinylchloride mix—high plasticizer content.
- Curve 5. Rubber—typical dielectric mix.
- Curve 6. Rubber designed for high conductivity.
- Curve 7. Oil impregnated paper.
- Curve 8. Impregnating oil for Curve 7.

mately 0.05 in. thick which were placed under a slight pressure, estimated at 2 lb/in<sup>2</sup>.

A literature search revealed only a few isolated values<sup>(4, 5, 6)</sup> of the thermal conductivity of polythene and so the tests recorded as Curves 1 and 2 on Fig. 4 were carried out. Initially, tests were made without any special precautions being taken to ensure good thermal contact between the sample and the plates, and the variable results shown by Curve 1 were obtained. Subsequent tests with the polythene surfaces coated with a high thermal conductivity liquid, glycerine, reduced the scatter and produced the results shown by Curve No. 2, thus illustrating the importance of eliminating low thermal conductivity air films in both experimental work and practical applications.

Measurements on polyvinylchloride<sup>(7)</sup> with low and high plasticizer contents (di-octyl-phthalate) are shown in Curves 3 and 4, Fig. 4.

The results for rubber are given on Curves 5 and 6. Curve 5 is for a typical dielectric mix and Curve 6 for a special mix designed to have a high thermal conductivity. The curves illustrate the manner in which products may be improved by the proper selection of constituents.

Curve No. 7 shows the results of measurements on oil-impregnated cable paper. To prevent the inclusion of air or oil pockets between the paper sheets making up the samples, these were vacuum dried and impregnated with oil from the degasifier whilst in position in the sample space in the manner described above for introducing liquid samples. An oil-proof rubber ring was used around the circumference of the sample to form a vacuum seal during the drying and impregnating period and to define the thickness of the sample during the measurements. Curve No. 8 shows the thermal conductivity of the oil used to impregnate the samples, measured over the same temperature range. In connexion with this test, it is of interest to note that, in common with previous investigators,<sup>(8,9)</sup> it was found necessary to reduce the sample thickness to 0.05 in. or less in order to completely eliminate convection effects, in spite of the source of heat being at the top of the sample, and the guarding arrangements.

#### ACKNOWLEDGEMENTS

The author wishes to record his thanks to Mr. W. C. Barry, Manager of the Research Laboratories, to Mr. S. E. Goodall,

Chief Engineer of W. T. Henley's Telegraph Works Co. Ltd., and to the company for permission to publish this paper. He also thanks Dr. E. Griffiths for advice on the design of the apparatus, and acknowledges the help of Mr. G. Brett who constructed the apparatus, and Dr. B. Salvage for his advice on the preparation of this paper.

#### REFERENCES

- (1) HERCUS and LABY. *Proc. Roy. Soc. A*, **95**, p. 190 (1919).
- (2) LEES. *Phil. Trans.*, **191**, p. 399 (1898).
- (3) *The Unit of Heat*, issued by The Royal Society (1950).
- (4) MILDNER. *J. Instn. Elect. Engrs*, **93**, Part III, p. 296 (1946).
- (5) MYERS. *Modern Plastics*, **21**, p. 103 (August, 1944).
- (6) I.C.I. Publication on "Alkathene" brand of polythene (1951).
- (7) SIMONDS, ELLIS and BIGELOW. *Handbook of Plastics*, p. 40. (London: Chapman and Hall Ltd., 1943).
- (8) BATES. *Industr. Engng Chem., Industr. Ed.*, **25**, p. 431 (1938).
- (9) KAYE and HIGGINS. *Proc. Roy. Soc. A*, **117**, p. 459 (1928).

## Measurements of saturated-diode stability

By V. H. ATTREE, B.Sc.(Eng.), Fluid Motion Laboratory, University of Manchester

[Paper received 17 December, 1952]

Results are given of 1000 h stability tests on Mazda 29C1 saturated diodes run at emission currents of 5 mA and 0.5 mA. The filament current, for a given emission, shows smaller variations than the voltage, and results at 0.5 mA are much better than at 5 mA. At 0.5 mA the filament current is constant to 1 part in 500 over 1000 h. Results for a single Ferranti GRD6 diode are also presented.

The anode current of a tungsten-filament diode, run under saturated conditions, depends critically on the filament temperature so that the diode may be used as an r.m.s. reference-level device. Typical circuit applications are in regulators on a.c. generators<sup>(1-5)</sup> in a.c. stabilizers<sup>(6-10)</sup> and for measurement circuits.<sup>(11, 12)</sup> The filament temperature of the diode is high (2000–2400° K) and the characteristics are therefore very little affected by changes in ambient temperature. Other r.m.s. devices, such as heater-type thermojunctions and thermistors, do not have this property as they run at relatively low temperatures.

Although the performance of gaseous-discharge reference-voltage tubes has been adequately investigated,<sup>(13)</sup> there is very little published information on the long-term stability of saturated-diodes. In a recent paper,<sup>(12)</sup> the author gave some figures for a circuit using the Mazda 29C1 (by Edison Swan Electric Co.). For test periods of 24 h the change in the filament voltage required to maintain an emission of 2.5 mA was approximately 0.1%. The present note describes some measurements made on four 29C1 diodes over a test period of 1000 h. The results of similar measurements made on a GRD6 diode (by Ferranti Ltd.) are also reported. The rate of evaporation from a tungsten filament increases rapidly with temperature,<sup>(14)</sup> and it would be expected that the drift of the diode characteristics would be greatly reduced by running at a lower temperature. However, the emission is enhanced by impurities in the wire and by surface contamination, so that a reduced temperature does not necessarily give much improvement in the stability. In order to determine

the effect of temperature on stability, two of the 29C1 diodes were run at an emission of 5 mA (about 2340° K) and two at 0.5 mA (about 2140° K). For ideal tungsten filaments this decrease of operating temperature reduces the evaporation by a factor of twenty.<sup>(14)</sup> As will be seen from the results given below, the improvement in stability cannot be stated exactly, because the drift obtained at 0.5 mA emission is very small, but it is certainly better than ten times.

#### METHOD OF TEST

The diodes were run from a 250 VA saturable transformer with a 6 V secondary winding. The filament of each diode had a coarse and a fine control resistance, a current shunt and a voltage-divider. A 50 V stabilized power-unit was used for the anode supply, and the emission current was read on a sub-standard milliammeter which could be switched into each of the four anode circuits in turn. The milliammeter could be read to 1 part in 1000 which corresponds to a change in filament current of less than 1 part in 10000. The filament current was adjusted to give the nominal emission which was maintained to within approximately 5%. As the emission currents for the two pairs of diodes are in the ratio of 10 : 1 (5 mA and 0.5 mA) it is unnecessary to control the conditions more closely. The actual measurements were made by switching over to an automobile battery and adjusting the filaments to give exactly the required emission. The filament current and voltage were obtained from potentiometer readings. Individual readings, taken over intervals of a few

minutes, agreed to 1 part in 5000. The shunt and voltage-divider resistances were checked both before and after the 1000 h test.

#### TESTS ON THE 29C1 DIODES

The results of the measurements on the Mazda 29C1 diodes are shown in Fig. 1. The diodes were put on test without any preliminary ageing. During the first 200 h the filament voltage increased by 1.0% (at 5 mA) and 0.3% (at 0.5 mA). The filament voltage subsequently increased at a fairly

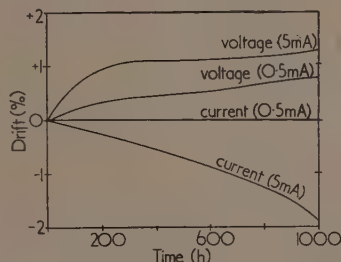


Fig. 1. Drift of filament input with a constant emission of 5.0 mA and 0.5 mA for 29C1 diode

uniform rate until, at the end of the 1000 h period, the voltage had changed by 1.3% (at 5 mA) and 0.8% (at 0.5 mA). From the time of switch-on, the filament current, for 5 mA emission, decreased uniformly until at 1000 h it was 1.9% smaller than the initial value. The filament current for 0.5 mA emission remained substantially constant for the full duration of the test. Short-term changes in the characteristics (not shown in Fig. 1) are conveniently specified by considering the maximum and r.m.s. values of the differences between readings taken at 24 h intervals. At 0.5 mA the largest single variation is 0.19% and the r.m.s. value of the 24 h variation, taken over the whole test, is 0.09%. Direct measurement of the cathode temperature of diodes is often difficult or impossible and it is useful to note that the emission-efficiency forms a guide to the operating temperature. With the 29C1, the efficiencies for 5 and 0.5 mA emission are 1.4 and 0.2 mA/W respectively.

The general shape of the characteristics shown in Fig. 1 may be explained by considering the manner in which the cathode evaporates. The diameter of the uniform-temperature zone at the centre of the filament gradually gets smaller, due to evaporation of the tungsten, while the regions near the cooling junctions remain substantially unchanged. The reduction in diameter at the centre results in a gradual increase in the total filament-resistance and, therefore, in the voltage required to obtain a certain filament current. Now, if the filament current is maintained exactly constant, the power dissipation per unit length of the filament, and hence the temperature, will increase with time, due to the increased filament resistance. The thermionic emission depends both on the temperature and the surface area of the filament, but the effect of the increase in temperature is much greater than the effect of the corresponding reduction in area so that when the filament is run at constant-current the emission increases with time. In the present tests the emission is maintained constant and one would therefore expect the filament voltage to increase and the filament current to fall. It is important to note that all pure-metal filaments will behave in this way, providing the operating temperature and dimensions of the filament are such that there is a reasonably

long uniform-temperature zone at the centre. Deviations from the expected behaviour can only be due to subsidiary effects, such as slight impurity in the emitter or deterioration of the vacuum.

#### TESTS ON THE GRD6 DIODE

The Ferranti GRD6 is an experimental coaxial guard-ring diode intended for student demonstrations of Richardson's law. No special precautions are taken in its construction and it is likely that the diode would be improved by the provision of multiple filament-pins (as on the 29C1) and by a reduction in the anode temperature. However, the coaxial construction has the advantage that the filament has only two cooling junctions, instead of five junctions as for the double-V filament. The GRD6 was run at an emission of 5 mA on the central anode; this corresponds to a total emission, anode plus guard-rings, of nearly 10 mA and an emission efficiency of 1.0 mA/W. In order to determine whether the guard-rings improved the stability, potentiometer readings on the filament were taken for an anode current of 5 mA and also for a total emission of 10 mA. There is very little difference between the two sets of readings, plotted on a percentage basis, and only the filament variations for a constant anode-current are shown in Fig. 2. The filament

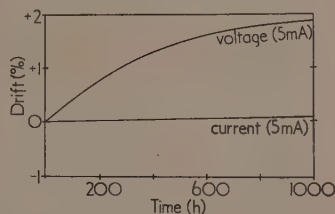


Fig. 2. Drift of filament input with a constant emission of 5.0 mA for GRD6 diode

voltage increased by approximately 2% over 1000 h; the filament current also increased, but in this case by only 0.15%. The reason for the increase in filament current is not known but it is encouraging to see that, as for the 29C1, the filament current is much more constant than the filament voltage.

#### CONCLUSION

The long-term stability of the Mazda 29C1 saturated diode may be improved by running at an emission current of 0.5 mA, instead of 2-3 mA as in circuits previously described.<sup>(10,12)</sup> For both the Mazda 29C1 and the Ferranti GRD6 the change of filament current with time is much smaller than the change of filament voltage. Thus, long-term stability may also be improved by inserting a large resistance in series with the filament. As shown previously,<sup>(12)</sup> added resistance in the filament circuit increases the sensitivity of the diode. The drift of the filament current for the GRD6 is considerably smaller than the drift for the 29C1 run at approximately the same emission efficiency (1 mA/W). The reason for this may be that the GRD6 has a single straight filament, with only two cooling junctions, whereas the 29C1 has two filament loops with a total of five cooling junctions.

#### REFERENCES

- (1) VERMAN, L. C., and RICHARDS, L. A. *Rev. Sci. Instrum.*, **1**, p. 581 (1930).
- (2) GULLIKSEN, F. H. *Elect. Engng, N.Y.*, **53**, p. 877 (1934).



- (3) DROBISH, A. E. U.S. Patent No. 2008 855 (1935).
- (4) PHILPOTT, R. U.S. Patent No. 2066 943 (1937).
- (5) WOLFF, I. U.S. Patent No. 2149 080 (1939).
- (6) STÖLLER, H. M., and POWER, J. R. *J. Amer. Inst. Elect. Engrs*, **48**, p. 110 (1929).
- (7) HELTERLINE, L. *Electronics*, **20**, p. 96 (June 1947).
- (8) SORESENSEN, E. M. U.S. Patent No. 2455 143 (1948).
- (9) MURRAY, D. M., and KUSTERS, N. L. *Trans Amer. Inst. Elect. Engrs*, **70** (Pt II) p. 1741 (1951).
- (10) RICHARDS, J. C. S. *J. Sci. Instrum.*, **28**, p. 333 (1951).
- (11) BARLOW, H. E. M. *J. Instn Elect. Engrs*, **77**, p. 612 (1935).
- (12) ATTREE, V. H. *J. Sci. Instrum.*, **29**, p. 226 (1952).
- (13) BENSON, F. A. *J. Sci. Instrum.*, **28**, p. 339 (1951) [see also correspondence with G. GRIMSDALL, *J. Sci. Instrum.*, **29**, p. 301 (1952)].
- (14) JONES, H. A., and LANGMUIR, I. *Gen. Elect. Rev.*, **30**, p. 310 (1927).

## Some transient properties of transistors

By H. G. BASSETT, B.Sc., A.M.I.E.E., and J. R. TILLMAN, Ph.D., A.R.C.S., Post Office Engineering Research Station, London

[Paper first received 28 January, and in final form 12 February, 1953]

The build-up and decay of the collector current of point-contact transistors, in response to a rectangular pulse of emitter current, take place roughly exponentially with time, after a delay of the order of a tenth of a microsecond during which there is negligible response. If the collector current is saturated, or if the collector voltage, instead of being steadily applied, is pulsed on, during or after the pulse of emitter current, effects due to delayed carriers are strikingly noted.

### 1. INTRODUCTION

The operating time of conventional switching circuits using thermionic valves depends on properties of the valves as well as on other circuit parameters. Thus it will rarely be less than several times the ratio,  $C/g$ , of the sum of the input and output capacitances of the valve to its mutual conductance; modern h.f. pentodes have effective values of  $C/g$  as small as perhaps  $3 \times 10^{-9}$  sec, enabling multivibrators to switch in about  $20 \times 10^{-9}$  sec, by comparison with which the transit times of the valves of  $1 \times 10^{-9}$  sec or less are small.

The introduction of germanium transistors to electronic switching brings new factors to the determination of operating time and circuit performance. Bardeen and Brattain<sup>(1)</sup> have shown that transistor action depends on the passage of minority carriers, injected by the emitter, to the collector where they give rise to a collector current,  $I_c$ , which, in point contact transistors, usually exceeds the emitter current  $I_e$ . The minority carriers (holes if the germanium is *n*-type) travel from the emitter to the collector only slowly, however, and by paths of different lengths so that the resulting collector current lags behind the emitter current, different parts of it by different times. Carriers injected while little or no bias is applied to the collector may remain in the bulk germanium without recombination for long periods (e.g. several microseconds); Meacham and Michaels<sup>(2)</sup> have already reported some interesting effects so resulting, both in transistors and diodes.

An investigation of some of the transient properties of transistors, suggested by this theory of their action, has accordingly been started—primarily as a step towards the correct prediction of the performance of high-speed switching and pulse circuits.

### 2. THE TRANSIENT RESPONSE OF TRANSISTORS WITH STEADY COLLECTOR BIAS

Fig. 1 shows the waveform of the collector current of a typical British point-contact transistor, when a rectangular pulse of current is applied to the emitter at time  $t_0$ , the collector potential,  $V_c$ , being maintained at a steady negative value. After a delay  $t_d$  (overlooked apparently by Meacham

and Michaels) the collector current rises approximately exponentially with a time constant  $t_r$ . Upon cessation of the emitter current, the collector current falls in a similar way after a similar delay. For a small batch of transistors  $t_d$  ranged from 0.07 to 0.25  $\mu$ sec,\* and  $t_r$  from 0.09 to 0.5  $\mu$ sec, with a rough correlation between  $t_d$  and  $t_r$ . The transient behaviour is qualitatively explained by the processes described

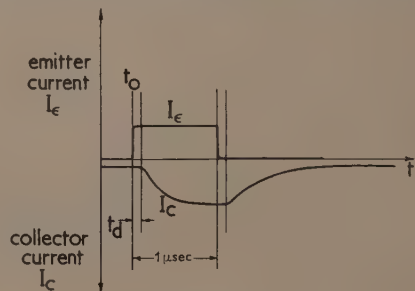


Fig. 1. Showing the transient response of a point-contact transistor

in Section 1 and implies a fall of gain at high frequencies. Measurements of gain-frequency response show good agreement with transient behaviour.

A similar test has been applied to a few *n-p-n* junction transistors. Again there is an initial delay in the onset of significant collector current, but the rise of collector current is no longer as closely exponential. The waveform of the collector current is qualitatively consistent with the theory of Shockley and others<sup>(3)</sup> that the minority carriers traverse the base layer of a junction transistor primarily under the influence of diffusion, and not of any drift field. Junction transistors made so far have had collector-base and emitter-base capacitances of the order of 10 pF (varying with collector voltage and emitter current) giving the input and output circuits time constants which may set important speed

\*  $t_d$  is less, however, when there is standing emitter current.

limitations; the circuit conditions will decide whether the capacitances or the transit phenomena set the more important limitation.

### 3. TRANSIENT EFFECTS DUE TO DELAYED CARRIERS IN POINT CONTACT TRANSISTORS

The operating conditions of a point contact transistor with a resistive load are illustrated in Fig. 2. If the emitter current,  $I_e$ , is made zero, the collector is said to be at collector current

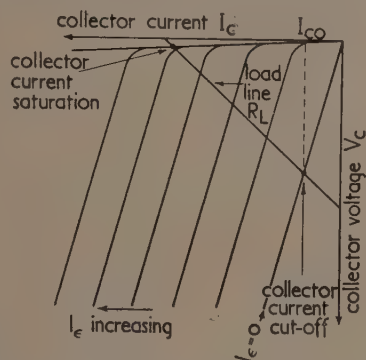


Fig. 2. The operating conditions of a point-contact transistor with a resistive load ( $R_L$ )

cutoff (sometimes called collector voltage saturation), though in fact some residual collector current ( $I_{co}$ ) flows. As  $I_e$  is increased,  $I_c$  first rises steadily, but later collector current saturation occurs, accompanied by low collector impedance (of the order of a few hundred ohms). The situation is similar to that in a pentode with a resistive anode load when the anode current  $I_a$  has been made so large that the anode potential,  $V_a$ , has fallen below the knee of the  $I_a$ ,  $V_a$  curves.

At collector current saturation (sometimes termed collector voltage cutoff) very many minority carriers are present in the body of the germanium, so that if  $I_e$  is suddenly returned to zero, collector current (in excess of  $I_{co}$ ) may continue to flow for as long as a few microseconds. Fig. 3 shows



Fig. 3. An effect of collector current saturation in a point-contact transistor

a typical waveform of the collector current under the conditions of Fig. 2, saturation having been reached during the pulse.

The slow recovery (sometimes called turnoff) after collector current saturation may restrict the use of the saturation region in high-speed switching circuits.

An allied effect, thought to be due also to delayed carriers, can be observed if a pulse of current is applied to the emitter while the collector is unbiased. If the collector is later biased by a pulse of voltage, collector current flows immediately; its amplitude is greater than that obtained under steady collector bias, but, as would be expected, decreases as the delay between the emitter and collector pulses is increased. Thus Fig. 4, derived from oscillograms, compares (a) a superposition of waveforms observed for a range of delays between

emitter and collector pulses with (b) the waveform obtained for steady collector bias. The waveforms were derived from the base current and therefore display both emitter and collector currents (only that portion of the collector current in excess of  $I_{co}$  is in fact shown). Delayed carriers can be

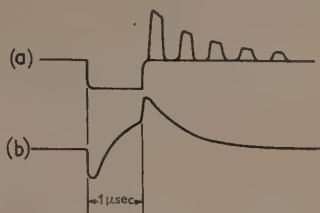


Fig. 4. Base current waveforms

- (a) For a pulse of emitter current followed by a pulse of collector voltage (composite waveform).
- (b) For a pulse of emitter current with steady collector bias.

readily observed as long as  $4 \mu\text{sec}$  after the cessation of the emitter current.

Fig. 5 was obtained in the same way as was Fig. 4, except that the collector was pulsed during the emitter pulse. The current available at the collector first rises very rapidly and then approximately exponentially; the envelope of the pulses

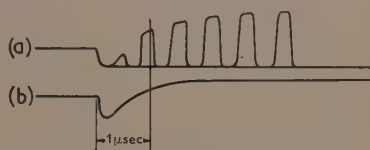


Fig. 5. Base current waveforms

- (a) For a step of emitter current followed by a pulse of collector voltage (composite waveform).
- (b) For a step of emitter current with steady collector bias.

of  $I_c$  resembles the waveform of the collector current obtained with steady collector bias, particularly during the first  $0.5 \mu\text{sec}$ . The waveforms suggest that diffusion, rather than drift due to a field set up by the collector voltage, dominated the movement of the carriers in the point contact transistors under the test conditions yielding Fig. 5. Ryder and Kircher,<sup>(4)</sup> however, have found that the frequency response of some of their point contact transistors varies markedly with collector potential, suggesting the predominance of drift. Further work on the variation of  $t_r$  (see Section 2) with change of  $V_c$  has suggested that diffusion predominates at low potentials and drift at high potentials (e.g. above 10 V) in the units tested.

### ACKNOWLEDGEMENT

Acknowledgement is made to the Engineer-in-Chief of the General Post Office for permission to make use of the information contained in the paper.

### REFERENCES

- (1) BARDEEN, J., and BRATTAIN, W. H. *Phys. Rev.*, **75**, p. 1208 (1949).
- (2) MEACHAM, L. A., and MICHAELS, S. E. *Phys. Rev.*, **78**, p. 175 (1950).
- (3) SHOCKLEY, W., SPARKS, M., and TEAL, G. K. *Phys. Rev.*, **83**, p. 151 (1951).
- (4) RYDER, R. M., and KIRCHER, R. J. *Bell System Tech. J.*, **28**, p. 367 (1949).

# The automatic electrical ignition of the d.c. arc in spectrographic analysis

By J. M. NOBBS, M.Sc., A.A.C.I.,\* The British Non-Ferrous Metals Research Association, London, N.W.1

[Paper received 9 January, 1953]

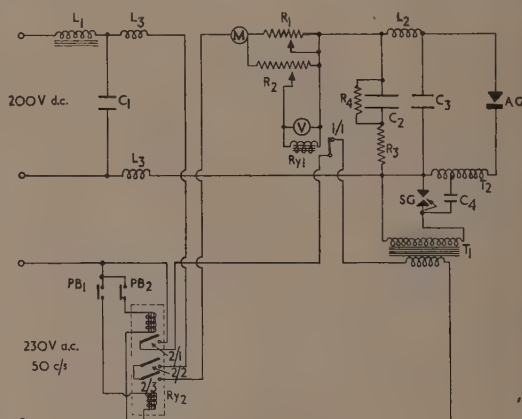
In spectrographic analysis the striking of a d.c. arc between electrodes of the material under test is usually performed mechanically; in this paper apparatus is described which besides igniting the arc electrically by means of a high-frequency trigger spark re-ignites it automatically should it be accidentally extinguished or the arc current drop below a predetermined value during the period of exposure.

The normal method of striking a d.c. arc in spectrographic analysis is to close the circuit momentarily by bringing the sample electrodes together, or, when one sample electrode contains non-conducting or damp material, by bringing up a third electrode. Both methods are time-consuming and difficulty is sometimes experienced with the latter in striking and maintaining the arc. The apparatus described below, besides igniting the arc by means of a high-frequency discharge, re-ignites it automatically, should it be extinguished or the current fall below a predetermined value. High-frequency ignition of the arc has been used extensively and is incorporated in most of the newer types of source unit. It consists simply of a high-voltage triggering spark introduced into the d.c. circuit by means of an inductively coupled condensed spark.

The apparatus which is described here incorporates the high-frequency generating circuit devised by Sinclair.† This circuit is simpler and more reliable in performance than circuits using Tesla-coil coupling. The circuit diagram is shown in the figure. Operation of the start button  $PB_1$  of relay  $Ry_2$  closes the d.c. circuit through contacts 2/2 and 2/3 and supplies power to the transformer  $T_1$  through contact 2/1. A triggering spark then passes across the analytical gap rendering it conducting and an arc develops. The arc current develops a voltage across resistance  $R_2$  which energizes the relay  $Ry_1$  and opens the contact 1/1; the triggering spark is thus stopped when an arc has been established.  $R_2$  can be adjusted so that contact 1/1 automatically closes when the arc current drops below a predetermined value, as when the arc wanders, or in the extreme case when it is extinguished. In this way an arc is maintained until terminated by operation of the stop button  $PB_2$  or the relay  $Ry_2$ .

When using the d.c. supply from a rectifier with a simple triggering circuit the high inductance of the rectifier filter choke prevented the arc from igniting, since the direct current did not build up sufficiently rapidly to maintain an arc during the time in which the high-frequency discharge took place. It was necessary to add a condenser  $C_2$  to the d.c. arc circuit which discharged through the resistance  $R_3$ , inductance  $L_2$  and the analytical gap to maintain the conductivity of the gap in the period between the high-frequency pulse and the main arc discharge. This difficulty was also experienced with a d.c. supply from a motor generator set, but to a lesser extent since the inductance in the supply circuit was much

lower and the voltage higher (260 V). It was found that satisfactory ignition could be obtained with  $C_2$  at  $4\ \mu\text{F}$ ,  $R_3$  at  $50\ \Omega$  and  $L_2$  removed.



Circuit diagram of automatic d.c. arc igniter

- |   |   |
|---|---|
| $R_1 = 17\ \Omega$ , 10 A (arc current control resistance)              | $T_1$ = high-voltage transformer, 3 kV  |
| $R_2 = 210\ \Omega$ , 1 A (relay control)                               | $T_2$ = high-frequency transformer (12 turns, 14 s.w.g. wire on 10 in. square former, primary tapping at 2 turns) |
| $R_3 = 60\ \Omega$ , 1 A  |   |
| $R_4 = 10\ \text{k}\Omega$ (condenser discharge)                        | $PB_1$ = push-button start  |
| $C_1 = 0.002\ \mu\text{F}$ , 400 V (h.f. filter)                        | $PB_2$ = push-button stop   |
| $C_2 = 96\ \mu\text{F}$ , 400 V   | $Ry_1$ = d.c. relay, 12 V, 1 pole   |
| $C_3 = 0.002\ \mu\text{F}$ , 10 kV (h.f. bypass)                        | $Ry_2$ = a.c. relay, 230 V, 3 pole  |
| $C_4 = 0.002\ \mu\text{F}$ , 10 kV (spark condenser)                    | $AG$ = analytical gap   |
| $L_1 = 0.5\ \text{H}$ (rectifier filter choke)                          | $SG$ = spark gap  |
| $L_2 = 5\ \text{mH}$ air-cored  | $M$ = d.c. ammeter 0–10 A   |
| $L_3$ = h.f. filter (15 turns, 16 s.w.g. wire on 1 in. diameter former) | $V$ = d.c. voltmeter 0–12 V   |

The apparatus has been used successfully with both metal and graphite electrodes. With the latter it has been particularly useful for the excitation of damp and non-conducting samples and metal globules; one drawback is that the trigger is apt to scatter powdered samples when loosely packed.

## ACKNOWLEDGEMENTS

The author is indebted to the Director and Council of The British Non-Ferrous Metals Research Association and the Senior Representative, Department of Supply, Australia, for permission to publish this paper.

\* Seconded from the Defence Research Laboratories, Australia.

† SINCLAIR, D. A. *J. Opt. Soc. Amer.*, 38 (6), p. 547 (1948).



# Summarized proceedings of a conference on the optical and electron-microscopical properties of textile fibres— Manchester, October 1952

The Manchester and District Branch of The Institute of Physics held a one-day conference on 29 October, 1952, on "The optical and electron-microscopical properties of textile fibres." Eight papers were read and discussed in two sessions: one on electron-optical topics and the other on ordinary optical topics. The papers and discussion are summarized in this article.

## ELECTRON MICROSCOPY

PROF. W. T. ASTBURY (University of Leeds) opened by remarking on the somewhat disappointingly small contribution made so far by the electron microscope to studies of textile fibres in the technological field, and proceeded, characteristically, to stretch his terms of reference to include all fibrous materials whether of textile importance or not. He drew attention to the difficulties now being encountered, in the field of fundamental molecular structure of fibres, in reconciling the evidence from electron microscopy with the tidy picture which had previously been built up, from evidence of various kinds, including that of X-ray diffraction, of a system of crystalline "micelles" of fairly well-defined size which merge into amorphous intercrystalline regions.

In the electron microscope all fibrous materials, whatever their chemical nature, and whether they are of biological or synthetic origin, show microfibrils which have much the same lateral dimensions, of the order of  $250 \text{ \AA} \pm 50\%$ . These are of remarkably uniform thickness but their internal structures are unknown and the question is what limits them to such a narrow range of sizes. Can they be, in fact, strings of uniformly sized corpuscles? Are they of uniform crystalline structure throughout, and if so how does the amorphous material come into the picture? The answers may not be the same for all materials since, though collagen does not exist as strings of particles, *actin* definitely does, and "corpuscular fibrils" may be more common than has previously been suspected. It was remarkable how cautious subsequent speakers in the conference were in the use of terms such as "crystalline," "amorphous," "orientation" and so on.

The next two papers were delivered by foreign guests, PROF. NILS GRALÉN (Swedish Institute of Textile Research) and DR. K. MÜHLETHALER (Pflanzenphysiologisches Institut, Zürich) respectively, and were concerned less with these ultimate units than with the histological structures of whole fibres. Prof. Gralén added force to Prof. Astbury's opening comment by saying that the electron microscope had had a difficult start in the textile field and had perhaps fallen into some disrepute—he had himself been warned against buying such an instrument for his work—but he then exhibited some beautiful pictures, taken by himself and his collaborators, of the membranous epicuticle and other features of the wool fibre, which showed that this prejudice can no longer be justified.

The epicuticle of wool is a thin membrane covering the outside of the fibre. It is resistant chemically, except to alkali, and may be released from the fibre by treatment with sodium sulphide or with aqueous halogens (as in the Allwörden reaction), or by digestion with phenol followed by trypsin. This last reaction allows of a close control of the stage to which digestion has been taken and has enabled another layer to be detected, between the epicuticle and the

scales, to which the name exocuticle has been given (Fig. 1). This is streaky in appearance in the electron microscope and readily distinguishable from the epicuticle.

The epicuticle has a thickness of about  $100 \text{ \AA}$  and appears to be continuous over the whole fibre rather than over individual scales (Fig. 2), though it does show certain stringlike features, which Prof. Gralén likened to butt-welded joints in the membrane, roughly parallel to, but not coincident with, the positions of the underlying scale edges. Longitudinal streaks seen in favourable preparations of the epicuticle (Fig. 3) do not cross these "strings" though they do run past features of another type, also parallel to the scale edges, which have the appearance of bars of elastic ribbon attached to the epicuticle. It is hoped that the interpretation of these observations will be aided by a technique for the examination of the same field or view after successive stages of chemical or digestive treatments; this is made possible by the use of silicon monoxide supporting films which are inert to the reagents used, though the proportion of specimens which survive the necessary series of operations without mechanical damage is less than could be desired.

The epicuticle is not a feature peculiar to the wool fibre but has also been shown by Prof. Gralén and Dr. Lagermalm on horse hair, feathers and human skin. In some feathers the epicuticle shows collapsed, cusped bags from which protein has evidently been digested by the trypsin treatment; it is suggested that these may be associated with water repellency.

DR. MÜHLETHALER's material was cellulosic rather than protein in nature, being derived from plant cell walls, and he has examined cut sections as well as chemically released membranes. It is of interest to note that, in answer to later questions, Dr. Mühlethaler stated that he always uses glass knives for sectioning, which are prepared by breaking a half inch thick glass plate, after scratching it with a diamond, and have an angle of  $45^\circ$  to  $60^\circ$ ; each knife is used for up to 70 cuts giving sections from  $0.2$  to  $0.1 \mu$  thick. He prefers a polymerized methyl methacrylate for embedding and uses thermal expansion to advance the specimen between cuts.

In the pictures which he showed of cut sections, the lamellar nature of the cell walls was clearly shown (Fig. 4), as well as an abrupt shift of fibril direction between one lamella and the next. The primary cell wall is stated to be a "two dimensional tangle" of randomly arranged cellulose fibrils and consists of only one lamella of such fibrils embedded in a matrix which is probably pectin.

In primitive cells such as those of algae, the lamellae of secondary cellulose are clearly separated by layers of pectin, but this is almost absent from the fibre cells of higher plants where the lamellae are so closely packed that they are difficult to distinguish and the secondary wall appears to have the same density throughout.



Fig. 1. Wool epicuticle with adhering exocuticle. (Specimen prepared by treatment with ethanol, water and  $\text{NaHSO}_5$  at  $75^\circ\text{C}$ , followed by digestion with trypsin.) Similar streakiness in the exocuticle is observed after other methods of preparation (N. Gralén)

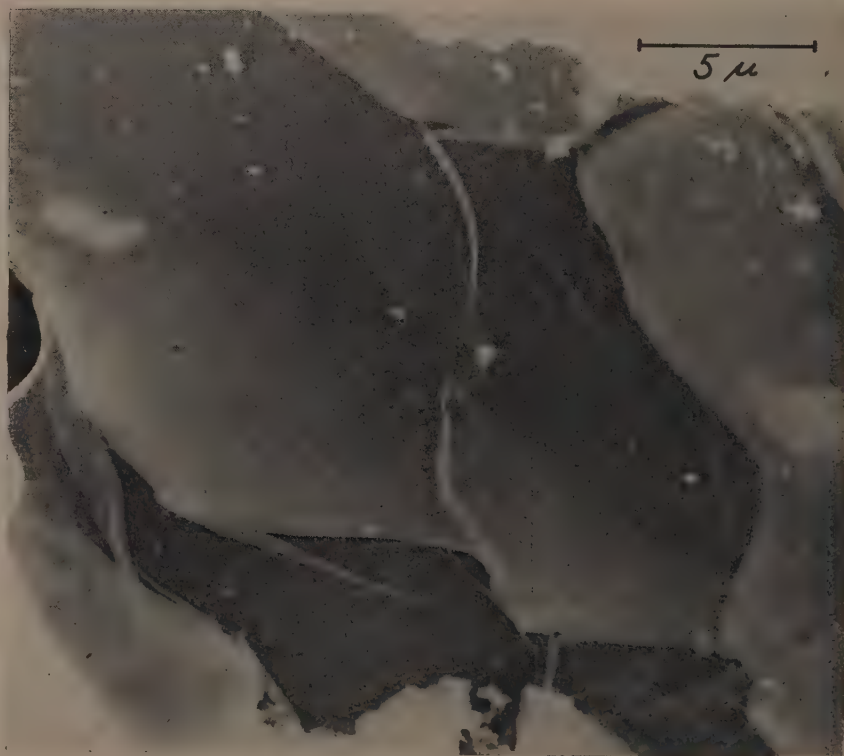


Fig. 2. Sheet of wool epicuticle with adhering exocuticle. (Specimen prepared by phenol-trypsin method.) The epicuticle extends over several scales as is shown by the fine streakiness running uninterruptedly over the scale edges, one of which ends abruptly in the middle of the sheet. "Strings" and "bars" are also visible, some of the bars lying so close to the scale edges as to give the impression of doubling of the edges (N. Gralén)

The study of the course of development of cell walls is facilitated by the fact that the alga *Valonia ventricosa* can be grown in a laboratory culture, and material in all stages of development is readily available. In *Valonia* the wall of the developing spore has at first the character of a liquid, but within a few hours shows solid cellulose strands in a slimy matrix. This first layer cannot expand sufficiently with the growing cell, however, and tears so that fragments of the initial layer are to be found superposed as thicker patches

from one cell to the next. The structure of the pits themselves is very variable; some are completely open while others are partially closed by a loose network of fibrils and many are ultimately closed completely by the secondary wall. All Dr. Mühlethaler's pictures were taken during a stay in Dr. Wyckoff's laboratory at the National Institute of Health, Bethesda, U.S.A.

The paper by MR. J. AMES (Imperial Chemical Industries Ltd.) described the cutting of thin sections for electron

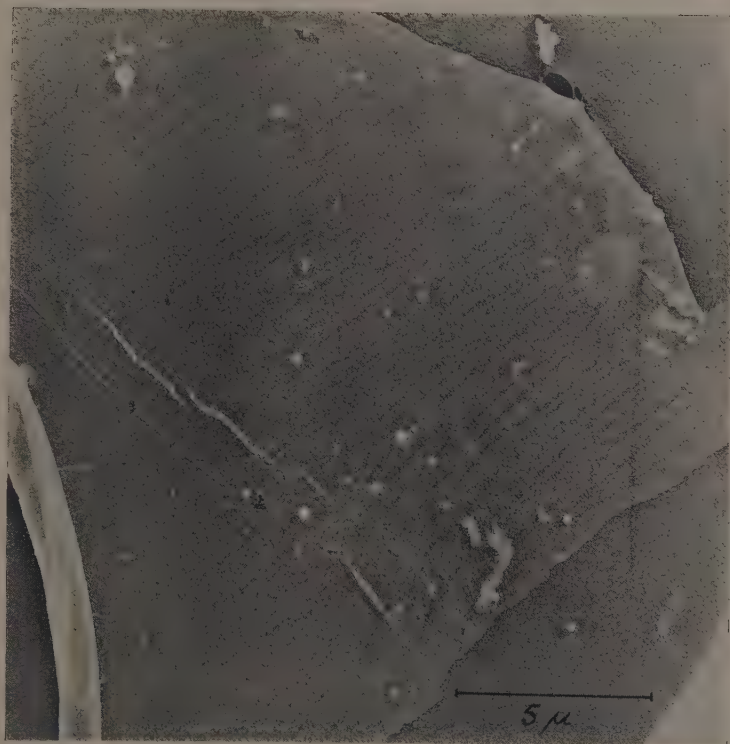


Fig. 3. Epicuticle of wool. (Specimen prepared by phenol trypsin method.) Shows the fine streakiness of the epicuticle and also "strings" and remnants of "bars." Holes are located along the "strings" and in another place the sheet has folded along a "string" (N. Gralén)

on the later layers. The primary wall finally forms a dense reticular network.

The secondary cellulose is then laid down in sheets of parallel fibrils which, in successive layers, are oriented at about  $120^\circ$  to those immediately below them, so that in the fourth and seventh lamellae the fibrils tend to be parallel to those in the first, and so on (Fig. 5).

In higher plants the cell walls of most types of tissue are generally similar in structure to that of *Valonia*, though parenchymatic, phloem, and xylem cells, for instance, are distinguishable by differences in detail. The triple nature of the wall separating two cells—two primary cell walls and the amorphous middle lamella—can be clearly seen in cut sections of plant tissues, as can the pits which perforate these membranes and the protoplasmic strands which pass through

microscopy by taking advantage of a microtome defect. A rocking microtome modified to give a specimen feed of  $0.2 \mu$  between cuts was found to produce sections much thicker than expected. This was attributed to frictional effects resulting from wear on the inclined plane bearing surfaces, and when the specimen feed mechanism was disengaged these residual effects alone were found to advance the block sufficiently to give sections transparent to a 50 kV electron beam. Mr. Ames uses ester wax as the embedding medium in preference to a paraffin beeswax mixture, but finds it desirable to leave the prepared block at least 24 hours before attempting to cut it. Fibres are simply held in the wax and not fully impregnated by it.

The work was illustrated by slides of sections of wool fibres and regenerated ground-nut protein fibres. In some of



the sections of wool which had had a chlorine treatment, the epicuticle, exocuticle and endocuticle could be distinctly seen as three separate layers, while in the whitened variety of

## OPTICAL METHODS

The evening session was introduced by Mr. J. M. PRESTON (Manchester College of Technology) in a paper which, happily, included a great deal more of original work than one might expect in an introductory review.

There is certainly no need to be apologetic about the contribution of optical microscopy to our knowledge of textile fibres and Mr. Preston showed that the optical microscope does not merely aid identification of fibres by their morphology but also tells us a great deal about their internal structures from refractive index measurements, photometry, interferometry and other special techniques; the geometrical shapes of fibres and their small lateral dimensions lead, however, to difficulties in observation and measurement with the optical microscope which are only overcome by the exercise of much ingenuity (in parenthesis one might add that these same factors are possibly even more troublesome to the electron microscopist).

The old micellar theory was based on Naegeli's microscopical observations of optical anisotropy which had to be reconciled with observations of swelling behaviour. Much more refined qualitative and quantitative work has been carried out since Naegeli's time and it has been found possible to derive an orientation factor from observations of double refraction in fibres. This orientation factor takes account of both the crystalline and non-crystalline cellulose and usually indicates a lower degree of orientation than that derived from X-ray diffraction measurements, which only refer to the fully crystalline regions.

Another anisotropic property of dyed fibrous structures is the dichroism which is observed in the absorption of polarized light. This can lead to estimates of orientation which are sometimes in agreement with those obtained from double refraction measurements but which sometimes require a more complex interpretation which needs further investigation.

The fluorescence of dyed fibres often shows a degree of polarization which reveals orientation in much the same way as does dichroism, and the orientation factors derived from the two effects bear the same significance. Measurements of polarized fluorescence have some experimental advantages over measurements of dichroism and are perhaps more directly interpretable.

Mr. Preston then suggested that dichroism in absorption would certainly give the true orientation of the cellulose if the dye could be dispensed with and the infra-red absorption of the cellulose itself examined in polarized light. In a later paper Dr. A. ELLIOTT (Courtaulds Ltd.) described a technique for making just this kind of measurement.

When measuring refractive indices in cross-sections of rayon fibres by the Becke line method, Mr. Preston has observed a line at the inner as well as the outer boundary of the surface "skin" of the fibre. This has been followed up by making the measurements in polarized light and it appears that the molecules at the inner boundary may lie tangentially rather than radially in relation to the periphery of the transverse fibre section. This kind of effect has also been shown by the dichroism in sections of viscose rayon which had been dyed with chlorazol sky blue FF and then partially stripped in pyridine to leave the skin dyed and the core clear (Fig. 6). This method indicates that where the skin is sharply folded round the re-entrant cusps, *A*, in the cross-section the orientation is tangential, whereas over the main surfaces of the lobes, *B*, where the curvature—and so the tangential strain—is much less, the orientation is radial.

This complexity of the cross-sectional structure of viscose



Fig. 4. Cross-section through cell wall of *Dictyosphaeria*, showing successive lamellae with different orientations (K. Mühlethaler)

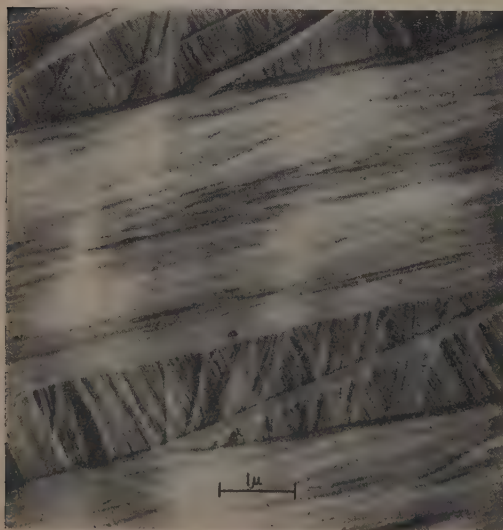


Fig. 5. Surface view of cell wall of mature vesicle of *Valonia ventricosa*. Showing three successive lamellae at approximately  $120^\circ$  to each other (K. Mühlethaler)

ground-nut protein fibre the whitening was shown to be due to holes or bubbles in the core of the fibre, which was surrounded by an annular bubble-free region and finally by a denser peripheral layer.

rayon fibres is also shown up in phase contrast observations in polarized light.

Methods for the observation of infra-red dichroism of polypeptides were described by DR. A. ELLIOTT. These have been made possible by the development of an efficient polarizing device for the near infra-red region, consisting of a pile of plates of selenium, or of silver chloride, set at an appropriate angle; the transmitted beam is polarized and the efficiency is about 44% (maximum efficiency possible is 50%). A mirror system is used to focus the radiation onto the specimen, and the specimen onto a spectrometer slit. So far, Dr. Elliott has been content with the modest magnification of five diameters in the image on the slit since greater magnification results in failure to fill the spectrometer aperture, and a consequent loss in intensity.

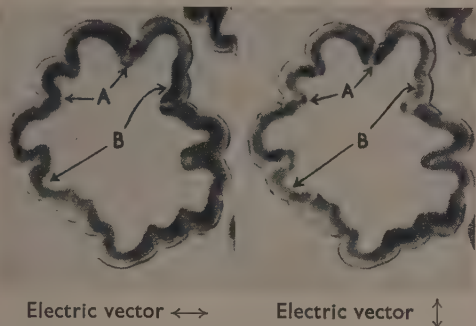


Fig. 6. Orientation in the skin of a viscose rayon fibre, shown by dichroic effects in cross-sections dyed with chlorazol sky blue FF and partially stripped with pyridine to clear the core.

The orientation over the tips of the cusps (A) is tangential and over the smaller curvatures of the lobe surfaces (B) it tends to be radial.

(J. M. Preston and G. D. Joshi)

Results of great interest were described in which the orientations of certain chemical bonds such as N-H or C=O have been deduced from the dichroism at the appropriate infra-red frequencies and are found to show opposite effects according to whether the oriented polypeptide chains are folded or extended. The work has been mainly on thin oriented films rather than on fibres since the fundamental bands are too strong for convenient measurement in anything but a very thin layer. This leads to acute experimental difficulty when fibres themselves are to be examined, but this can be partially overcome by working with overtone bands, which are much less intense than the fundamentals. Some results on silk fibres and hair have been obtained in this way.

The kind of dichroism obtained with natural hair is similar to that observed in folded synthetic polypeptides. Stretched hair, on the other hand, gives dichroism of opposite character, and resembles silk, which has the extended form of polypeptide chain. These results are in qualitative agreement with Astbury's interpretation of his  $\alpha$ - and  $\beta$ -keratin X-ray diffraction diagrams. The infra-red spectra show, however, that neither natural hair nor steam-stretched hair are homogeneous—the former contains some extended chains and the latter some which are folded. Since these components do not appear in the X-ray diagrams, it is inferred that they

are amorphous. In these materials there is no doubt that crystalline and amorphous regions exist.

Dr. Elliott referred a question on dichroic measurements in the ultra-violet region to DR. J. C. WARD (Courtauld's Ltd.), who stated that some work was proceeding in this field. Initial determinations of the direction of transition moments in chromophoric groups have been made by studying thin crystals, and show that, in the case of the benzene absorption at 2600 Å, substitution by saturated side chains (e.g. dibenzyl) has no effect on the direction of the transition moment, which lies in the plane of the ring; on the other hand a substituent containing *p*-electrons which can conjugate with the aromatic sextet (e.g. acetanilide) causes the transition moment to be localized at right-angles to the axis of substitution. Studies of the 2100 Å band of the amide group in diketopiperazine and N acetyl glycine crystals, and in nylon fibres have shown that the transition moment in this case must lie very near to the direction of the CN bond.

A paper by MR. R. MEREDITH (British Cotton Industry Research Association, and now of the Manchester College of Technology) dealt with the measurement of orientation in cotton by optical methods using polarized light. Because of the variable shape and small size of a cotton fibre the standard methods of determining birefringence were unsatisfactory, and the Becke line method was used to measure the principal refractive indices independently and obtain the birefringence by difference. This method gives the refractive index at the edge of the specimen, that is at the surface layers in the case of a fibre. There was some discussion, later, on the question of the depth into the fibre to which such measurements refer; the answer seems to be that the primary cell wall of cotton is too thin (below the optical resolution limit) to affect the results and that the indices measured are those of the outer layers of the secondary cellulose. This conclusion is in accord with Mr. Meredith's observation of correlations between his mean optical orientation factors for different varieties of cotton, and the mean tensile strengths and Young's moduli of their fibres; these mechanical properties depend on the secondary cellulose and hardly at all on the primary wall. It would nevertheless be of interest to compare Mr. Meredith's figures with refractive index measurements made on cotton by the methods described by Dr. Faust in the next paper.

The orientation deduced from refractive index measurements is largely a function of the spiral angle of the "pit-spiral fibrils" and, since this also controls the development of convolutions in the cotton fibre after the opening of the boll, one is not surprised to find an inverse correlation between the mean optical orientation factor and the mean convolution angle from one variety of cotton to another; the more the fibrils are inclined away from the axial direction the lower is the longitudinal refractive index and the greater is the number of convolutions developed per unit length. This effect is observed for individual fibres within one variety of cotton, as well as in the mean figures for different varieties, though the fineness and maturity of the fibre observed must then be taken into account. These latter two quantities were examined independently, in fibres taken all from one sample of cotton, and though the longitudinal refractive index showed some inverse correlation with the perimeter of the fibre ("fineness") it was very little affected by the degree of secondary thickening ("maturity"). This result also suggests that the refractive indices obtained from Becke line measurements refer only to the outer, or first formed, layers of secondary cellulose.

DR. R. C. FAUST (British Rayon Research Association)



described interferometric methods of measuring refractive indices in small transparent solid bodies of awkward shapes. In his first method the object is immersed in a liquid of approximately the same refractive index, between highly reflecting (85% reflexion) flat surfaces arranged as a parallel plate interferometer with a small gap. This system is illuminated by white light, and an image of the object, and adjacent parts of liquid-filled field, is focused onto the slit of a spectrometer. Bright fringes occur in the spectrum at wavelengths  $\lambda_n$  which satisfy the relation

$$(n - \Omega_n)\lambda_n = 2(\mu_n)_l(t_g - t) + 2(\mu_n)_s t$$

[where  $(\mu_n)_l$  and  $(\mu_n)_s$  are refractive indices of liquid and solid respectively at the  $n$ th order fringe;  $t_g$  is the interferometer gap thickness, and  $t$  the thickness of the solid.  $\Omega_n$  is a term taking account of phase changes at the reflexions].

In regions where the interferometer gap contains liquid only,  $t = 0$  and  $\lambda_n$  is determined by quantities which are all constant so that each fringe is monochromatic and straight. Similarly if solid and liquid are both present in the optical path the gap is still optically homogeneous at the wavelength at which the dispersion curves for the two media intersect, and if a fringe happens to coincide with this wavelength it will be straight and undistorted. In general no fringe will coincide exactly with this wavelength but the nearest fringes at each side of it will be distorted in opposite senses, where they cross over the position of the solid object, and a short interpolation will suffice to find the true wavelength at which the refractive indices of solid and liquid are equal. The experiment is repeated with several liquid mixtures of different refractive indices (and known dispersion curves) and a dispersion curve for the solid is thus built up. The results are quite independent of the geometrical form of the solid though it is presumed to be optically homogeneous.

The method will give the mean refractive index through the depth of a non-homogeneous body, at any point of its projected area, but can only be used to find the separate refractive indices of different zones in certain geometrically simple cases. In a fibre consisting of a cylindrical "core" surrounded by a "skin" of uniform thickness, for instance, it may be adapted to determine the refractive indices separately for skin and core.

The method breaks down if the body to be examined is thicker than about 0.1 mm because then the fringes are so crowded that they merge into a continuous spectrum. In such a case an interferometer with a wedge-shaped, instead of a parallel, gap may be used. The fibre is laid in the gap with its axis at right-angles to the line of intersection of the plates, and is surrounded by liquid of suitable refractive index. Monochromatic illumination is used (mercury green line), and a microscope is focused on the interference fringes which, being contours of constant optical thickness, are straight and parallel to the wedge apex except where the fibre crosses them. In general, the presence of the fibre alters the optical path length in the gap and so the fringes are displaced, by an amount proportional to  $(\mu_l - \mu_s)t$ , towards or away from the apex of the wedge according as  $\mu_s$  is greater or less than  $\mu_l$ . At points where  $\mu_s = \mu_l$ , of course, there is no displacement, and the fringe crosses the line it would follow in the absence of the fibre. (Fig. 7.)

The refractive index of the liquid is known, or can be measured, and so the mean refractive index through the solid at these points is determined. Another set of points could be found with a liquid of different refractive index but, if the temperature coefficient of refractive index of the solid can be neglected in comparison with that of the liquid, a simpler method is to vary the temperature of the system through 2 or 3° C, when a continuous series of readings of points of

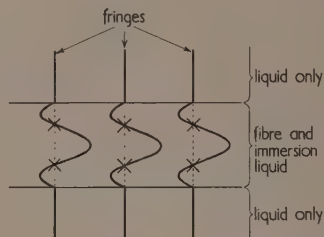


Fig. 7. Fringes traversing a fibre in a wedge-shaped interferometer gap. Each cross indicates a point where

$$\mu_{\text{liquid}} = \mu_{\text{solid}} \text{ (mean) (R. C. Faust)}$$

zero displacement can be made. An internal calibration of the changing refractive indices of the liquid is provided by inserting a cylindrical fibre of known diameter (for example, a drawn glass fibre) alongside the specimen in the gap, the change in fringe displacement along the centre line of the calibrating fibre being then proportional to the change in refractive index according to the formula:

$$(\mu_1 - \mu_2) = (a_2 - a_1)\lambda/2st$$

where  $a_1, a_2$  are fringe displacements at temperatures  $\theta_1$  and  $\theta_2$  respectively,

$\mu_1, \mu_2$  are refractive indices of liquid at temperatures  $\theta_1$  and  $\theta_2$  respectively,

$t$  is the diameter of the calibrating fibre,

$\lambda$  the wavelength of the illuminating light

and  $s$  the fringe separation measured along the wedge.

The refractive index of the liquid at room temperature ( $\mu_1$ ) is measured separately with an Abbé refractometer.

With a birefringent specimen, such as a fibre, the fringes observed in these methods are doubled; they may be clearly differentiated by using polarized light, however, and information thus obtained on the variations of orientation and packing of the molecules from point to point in the fibre.

DR. F. C. TOY (Director of the British Cotton Industry Research Association and a Past-President of The Institute of Physics) presided over the Conference and expressed his thanks to all those who had taken part, and particularly to MR. A. G. THOMPSON (Tootal Broadhurst Lee Co.) who had acted as Organizing Secretary and to those firms who had given financial support to the Conference.

D. G. DRUMMOND



## New books

**Psychological and psycho-physical studies of craftsmanship in dairying.** By R. HARPER. (London: Cambridge University Press.) Pp. xii + 63. Price 9s. 6d.

This monograph is divided into four chapters. The first outlines the problems of judgment encountered in processing and assessments of quality in the dairy industry. The second discusses the basic concepts of psycho-rheology, i.e. the relation between subjective judgments and objectively measurable properties. The third and main chapter contains a detailed critical account of Dr. Harper's painstaking investigations in this field, in which, in particular, extensive judgments of "firmness" are subjected to statistical analysis. The final chapter summarizes the results and the tentative conclusions to be drawn from them.

On account of the detailed and critical form of presentation this work will be of particular value to those engaged in psycho-physical research. For the same reason, its appeal to the general physicist is likely to be extremely limited.

L. R. G. TRELOAR

**Associated measurements.** By M. H. QUENOUILLE, M.A. (London: Butterworth's Scientific Publications Ltd.) Pp. x + 242. Price 35s.

In the preface the author calls attention to the fact that the application of statistical methods to research problems has expanded greatly over the last fifty years, and appears to justify the production of this excellent book on the grounds that methods adapted to the study of association between quantitative measurements have had much less attention than other branches of applied statistics.

The application of statistical methods to the varied problems of the manufacturing industries is less than thirty years old and was not practised at all ten years ago by a large majority of those who now consider them essential tools for investigations of diverse kinds.

It is also a marked characteristic of industrial problems that the study of associations between data often proves extremely valuable, so that this book will attract the attention of those industrialists who during recent years have learnt to value the techniques so well suited to the presentation and study of data exhibiting variability.

Industrial workers responsible for maintaining the technical qualities of a product, the economic efficiency of production, the planning of manufacturing programmes or the problems associated with accidents, sickness and other sources of lost time will find the first of the four parts into which the book is divided of great interest. Not only will they find the graphical procedures, so clearly described in the first part, time saving and often of sufficient accuracy but familiarity with their use will greatly assist them to comprehend the numerical methods dealt with in the second part.

All readers are recommended to make acquaintance with some sections of the third and fourth parts, even though they may postpone close study of much in these parts; for example, the comments on the taking and scrutiny of the observations and the planning of the investigations. What economies would be made in much research and industrial investigation work if the first paragraph of 9.3, p. 143, was printed in

large letters and hung in laboratories and other places where people so often neglect the important precept there enunciated! It reads:

"The analysis of any large-scale investigation needs to be considered before starting the investigation, not only because it is often possible to devise quick and appropriate methods of tabulation and presentation if the analysis can be planned in advance, but also because a consideration of the form that the analysis may take will often suggest modifications in the methods of collection of data."

A feature of the book is the use of the same data in the first and second parts in order to create confidence in the graphical methods as a first if not final examination of data.

It would have been useful to follow the same procedure and to use the data of the example described on page 25 for fitting a curvilinear regression to a set of nine observations when describing the orthogonal polynomial method of fitting a curvilinear regression to data where the independent variable is spaced at equal intervals. (The use of "dependent" in the text is apparently a mistake, p. 97.)

All the examples have not been checked, nor have the tables, but a slip has been noticed in Table XII, p. 237, in the last line where  $n = 9$ , the middle value should read + 28 instead of + 7.

It is notoriously difficult to decide in what order statistical techniques should be presented—the author has achieved considerable success by the plan adopted. The restriction in the number of significant figures given in the tables of the Appendix emphasizes the practical outlook which characterizes this excellent book.

B. P. DUDDING

**Automatic feedback control.** By W. R. AHRENDT and J. F. TAPLIN. (London: McGraw-Hill Publishing Co. Ltd.) Pp. xiv + 412. Price 64s.

Just as, some ten years ago, electronic valve techniques became essential for almost all types of physical measurement, so now servo-mechanisms and automatic control systems are becoming similarly ubiquitous. And this relatively new branch of applied science is likely to become important not only in the technological field but in other spheres of human activity too. Whether or not the ultimate repercussions of this development will extend as far as some of the writers of science fiction have imagined, its potentialities, as outlined for instance by Wiener in his works on "cybernetics," are almost certainly great enough to justify the amount of effort now being expended in this field. But the advantages to be gained today from the application of automatic control are so great that demand for a knowledge of the subject must increase rapidly and will focus attention on such textbooks as have yet been published.

This book sets out to supply, in a manner which can readily be understood by the non-specialist, a concise account of the whole subject. About one-half of the book is devoted to the theory of control systems of various kinds and, although the more mathematically inclined may not approve of the rather rule-of-thumb approach to the Laplace transform and the other mathematical devices required, it cannot be denied that the method adopted allows a comprehensive theoretical account to be followed by the less erudite reader. Another

difficulty which faces the beginner in any subject is that of symbols. The authors have tried to use a consistent set and have, on the whole, succeeded in their aim, but so many symbols are involved that it is not easy to keep track of all their meanings. There is an excellent chapter on non-linearities and discontinuities where the usual theoretical treatments break down. Here some attempt is made to apply the theory to these cases and the problems and difficulties involved are clearly stated.

The remainder of the book contains discussions of some of the more usual types of automatic control systems and components. There is also a large number of problems covering the whole field of the subject, many of these being of the type which are met with in the design of feedback systems. This section is likely to be particularly helpful to all students of the subject.

Altogether this is a book on a new and complicated subject written from an eminently practical standpoint and which, in the reviewer's opinion, more than makes up in sound common sense what it does not attempt in mathematical rigour. Printing and presentation are of the usual high standard associated with the publishers.

A. E. DE BARR

**Structure Reports for 1949 (Vol. 12).** General editor: A. J. C. WILSON. (Holland N.V. A. Oosthoek's Uitgevers Mij.) Pp. 478. Price 45 Dutch florins (post free).

*Structure Reports* is an international undertaking sponsored by the International Union of Crystallography, and this volume (12) is the second to be published. The aim of the editors is to collect together information on all work on crystal structure determination, and to report on this work so fully that, in general, no reference need be made to the original papers. In this aim, which is being so admirably fulfilled, the *Reports* follow in the tradition of *Strukturbericht*, whose seven volumes cover structural work published from 1913 to 1939. Volume 11 of *Structure Reports*, published in 1951, covers 1947-48, while volumes 8, 9 and 10 will cover the years 1940-46.

The *Reports* are divided into three sections, Metals, Inorganic, and Organic compounds, and subject and formula indexes are provided for the two latter sections. Direct reference can easily be made to the Metals section where the arrangement is strictly alphabetical. A combined author index for all three sections is included. It is inevitable that some of the work reported in this volume should already be superseded, but in several cases the editors have met this difficulty by inserting brief comments on work published as late as 1951.

It may confidently be predicted that *Structure Reports* will be very widely used, since these unusually thorough abstracts provide an invaluable reference book for workers in all the many scientific fields in which X-ray diffraction methods are applied.

AUDREY M. B. DOUGLAS

**An advanced treatise on physical chemistry. Vol. 3. The properties of solids.** By J. R. PARTINGTON. (London: Longmans, Green and Co. Ltd.) Pp. ix + 639. Price 70s.

Approximately ten per cent of this volume is taken up with tables of literature abbreviations, lists of symbols and the index. A further ten per cent consists of mathematical appendices—vectors, tensors, the complex variable and the calculus of variations. In the remaining 550 pages of text, the author deals in a comprehensive and exceedingly

well-balanced manner with the physical chemistry of solids. Upwards of 15000 references to the literature, both historical and recent (of which about one-third are German), are incorporated and the text is furnished with a bibliography for each topic.

Special attention has been devoted to crystal lattices and space groups, isomorphism, elastic properties, tensile strength, hardness, density, surface tension and viscometry as well as to the properties of solids in their association with heat reactions. The quantum theory of specific heat is also included.

Professor Partington's thorough and systematic method of treatment, exemplified in the two earlier volumes, is again evident in this text. When completed, the series will provide a monumental work unrivalled in any language.

While not essentially a practical text, the book contains many descriptions of apparatus and of experimental technique. In addition, valuable tables and data have been collected. This is a necessary work for every science library. Not only will it be extremely valuable to the physical chemist, but also to workers in very many other fields.

JOSEPH REILLY

**Ultraviolet radiation.** By L. R. KOLLER. (London: Chapman and Hall Ltd.) Pp. ix + 270. Price 52s.

The subject-matter of this book is divided into chapters on arcs, incandescent sources, solar radiation, transmission, reflexion, applications and finally on radiation detectors. Its scope is thus identical with Luckiesh's *Ultraviolet Radiation* published some thirty years ago, although there is little more in common than the title. Practically the whole of the information given in the new book is the result of investigations made during the past twenty-five years.

Dr. Koller has produced a readable text packed with useful quantitative data, much of which is of permanent value for reference purposes, for example the values of transmission and reflexion coefficients of specified materials, solar radiation characteristics, photo-cathode sensitivities and the like. It is a great convenience to have these collected together in one book. The descriptions and characteristics of various radiation sources are also useful, but are of somewhat less general interest since the types dealt with are restricted to those of American manufacture.

Literature references to original source material appear adequate but somewhat more generous reference to other textbooks would be an advantage; Ellis and Wells' *The Chemical Action of Ultraviolet-Rays* receives cursory mention but no proper reference, whilst Radley and Grant's *Fluorescence Analysis in Ultraviolet Light* is not mentioned at all. This latter subject is, in fact, dismissed in one brief paragraph.

There are a few fairly obvious errors. The rod used to "pipe" radiation is incorrectly described as a tube in Fig. 15 of Chapter 6. Also in Fig. 5(b) of Chapter 1 the wavelengths of the lines of the mercury spectrum have some unfamiliar values. Reference to figures and tables could be unambiguous if there were a single numerical sequence throughout the book instead of a fresh set in each chapter.

This book deserves strong recommendation and should be useful to workers in many diverse fields. Reading between the lines of Dr. Koller's preface, it is to be hoped that physicists, chemists, biologists and medical men who intend to make use of the ultraviolet region of the spectrum will make a careful study of the book before presenting their requirements to the radiation specialist or lamp manufacturer.

B. S. COOPER



## Notes and comments

### Elections to The Institute of Physics

The following elections have been made by the Board of The Institute of Physics:

*Fellows:* H. Cole, I. Evans, J. E. Houldin, W. J. Oosterkamp, S. K. Runcorn, C. C. Voddan.

*Associates:* J. G. Brown, R. C. T. Buchan, R. W. Burns, R. H. B. Buteux, H. E. Carrington, F. A. Chappell, N. D. Clarence, M. E. Clarkson, S. W. R. Cox, A. Crook, R. G. Dorman, W. H. Fry, B. A. Garland, P. Gay, A. P. Green, P. C. S. Hayfield, H. Hubbard, R. H. Jones, T. D. Jones, G. M. Leak, J. S. Mackelvie, D. G. Marshall, W. M. T. Mason, W. D. Matthews, C. D. Mee, A. J. Milne, D. A. Morris, A. J. Mortlock, W. A. Runciman, G. E. Sharp, D. L. Simms, F. Sumner, C. G. Wilson, P. E. Wrist, R. G. Wylie.

Forty-six Graduates, thirty-two Students and six Subscribers were also elected.

### Direct-reading emission spectroscopy

The Industrial Spectroscopy Group of The Institute of Physics has formed a panel of members interested in direct-reading equipment for spectrochemical analysis. These devices combine spectrographs with electronic equipment in such a way that the intensities of characteristic spectral lines give a direct reading of the percentage of the elements present in the specimen. The object of the panel is to organize meetings which would serve the interests of users and potential users of this equipment. The first meeting arranged by the panel took place in the Institute's House on 26 March last when Dr. A. C. Menzies introduced the subject. Mr. A. L. Pendrey and Mr. R. T. Staples followed with accounts of their experiences in this type of work and there followed a general discussion. Readers who would like notices of the meetings on this subject are invited to join the Group, particulars of which may be obtained from the Secretary, The Institute of Physics, 47 Belgrave Square, London, S.W.1.

### Research Film

We have received the first issue of a new bulletin entitled *Research Film* which has been distributed free to certain libraries and members of the Research Film Section of the International Scientific Film Association (I.S.F.A.). This bulletin will be issued at regular intervals by the Committee of the Research Film Section and its aim is to cater for all those interested in the film as a tool in scientific research and it carries articles in English, French and German. The first issue has 36 pages ( $8\frac{1}{2} \times 5\frac{1}{2}$  in.) and contains a semi-technical article on micro-cinematography by J. Frederic (Liège); six essays and reports by A. Policard and A. Collet (Paris), A. Pijper (Pretoria), L. Bull (Paris), J. Frederic (Liège), G. Bekow (Göttingen) and A. Pijper (Pretoria). In addition it contains the first items in a bibliography of references to information already published on the use of the film in research. Copies of papers referred to in the bibliography will be made available. The Joint Editors, Dr. G. Wolf, Institut für Film und Bild, Abt: Hochschule und Forschung, Göttingen and M. Jean Dragesco, Collège de France, Laboratoire d'Embryogénée Comparée, Paris, are to be congratulated upon the high standard of presentation attained in this first issue.

### The work of the National Research Development Corporation

The report and statement of accounts for the year ending 30 June, 1952, of the National Research Development Corporation has recently been issued by H.M. Stationery Office. In this, the third report of the Corporation, some indication is given of the extent and type of work which is now being carried out. During the year under review 1027 inventions were communicated to the Corporation; about half from Government sources and 445 patent rights in inventions were assigned to it, 414 of them from Government sources. The total holding of British and foreign patents and patent applications is given as 1736 and the total number of licence agreements to which the Corporation is a party is given as 199. Among the projects selected for development "in the public interest" are electronic digital computers, hydrocarbon synthesis, the manufacture of diffraction gratings, a photogrammetric plotting instrument, and a small microscope originally invented to facilitate delicate operations within the ear cavity and subsequently adapted for accurate determinations of the sex of chickens. The income of the Corporation during the year was £25 676 and its expenditure £83 556; it may borrow up to £5 million from the Board of Trade.

### Research in the electrical industry

We have received a paper-bound volume containing the papers read at the 1952 British Electrical Power Convention and the discussion on them. They were: "A survey of research in the electrical industry," by Sir Arthur Fleming; "Co-operative research in the electrical industry," by Dr. S. Whitehead; "Research in the electricity supply industry," by Dr. J. S. Forrest; "The nature of research in the electrical manufacturing industry," by Dr. K. J. R. Wilkinson; "Researches into some problems associated with steam generation," by Mr. W. F. Simonson; "Some aspects of research in the cable making industry," by Mr. E. L. Davey; "The influence of research on the electric lamp industry," by Dr. J. N. Aldington.

In summarizing the convention Dr. Dunsheath said that what stood out was the tremendous value which was available to the electrical industry, for the picking up, through research and that as Dr. Whitehead said: "Individuals or teams carry out research, not committees or organizations. Co-operation in research therefore concerns, not its detailed conduct, but the arrangements which, on the one hand, encourage persons and groups jointly to provide for and control research, and, on the other hand, encourage the interchange of opinions and results between the workers and others interested."

### The British X-ray and Radium Protection Committee

With new statutory developments the existence of the British X-ray and Radium Protection Committee, which has done such wonderful work in the past thirty years, has been ended. The final meeting of the Committee was held in September, 1952, and we felt that the passing of this voluntary committee through which Great Britain set a pattern for the world should be recorded in this *Journal*. We therefore invited Professor Sidney Russ, who was one of its honorary secretaries and, for many years, the representative of The Institute of Physics on the Committee, to write a valedictory which we print below.

"The hazards of X-ray and radium work were only recognized gradually; in fact for many years X-rays were used in



diagnostic work as though they were harmless. About the year 1921 there was a disturbing series of deaths among medical and lay radiologists, so a small group of people got together under the chairmanship of Sir Humphrey Rolleston and tried to frame some rules which would, if followed, help to prevent further casualties.

"The first memorandum of recommendations was produced in 1923 and it was welcomed by all classes of radiological workers and indeed it formed the basis for similar recommendations in most countries of the world and for subsequent international codes.

"It may be difficult for those accustomed to operating a modern diagnostic set to realize working conditions in 1921; the X-ray tube was usually contained in some sort of box which was neither ray nor light-proof, the high tension leads were hooked on to naked overhead wires giving a copious corona discharge and it was often possible to light up a fluorescent screen anywhere in the room by the scattered radiation that was all too abundant. These were the conditions which had somehow to be rectified by 'persuasion' as there was no statutory authority behind our recommendations.

"The Committee continued its work for over thirty years; it had no official sanction, it had no money (our Chairman paid the expenses of the first Report) it had no permanent headquarters but it was convinced that its reports were meeting a need. No less than six editions appeared, the last one being in 1951; the several editions were not mere reprints for they showed year by year a tightening up of the safeguards to health that were thought necessary as the scope of radiological work extended. The expenses of publication were now largely borne by the Medical Research Council and the British Institute of Radiology.

"Shortly after the end of the war the Medical Research Council formed a new committee on the Medical and Biological Applications of Nuclear Physics; one of its sub-committees, the Tolerance Doses Panel, produced a large series of papers dealing with data on which protective measures could be based, whether in the domain of medicine, research or industry. Further, after the passing of the Radioactive Substances Act about the same period, a Statutory Committee came into being with the duty of seeing that the recommendations of the Act were brought into practice.

"My first colleague as Co-Honorary Secretary was Dr. Stanley Melville who was a victim of malignant changes set up by X-rays; he was succeeded by Dr. Harrison Orton who suffered similarly and paid the same penalty after years of suffering. The fact that these men sat round the committee table left no doubt in our minds about the need for protection against the hazard of ionizing radiations." SIDNEY RUSS

### Die Farbe

A new journal on colour, *Die Farbe*, has been received from Germany. The publishers are Verlag für Angewandte Wissenschaften, G.m.b.H., Wiesbaden, and the editor M. Richter. The purpose of the journal is the publication of

papers on the different aspects of colour science. The foreword contains a list of subjects which outline the scope of the journal. This list contains colour vision and its testing, colour matching, light and colour, evaluation of fastness, colour photography, television and reproduction, colour psychology and colour conditioning, colour standardization work and colour nomenclature and terminology. It is intended to publish also reviews and news about events, persons and organizations concerned with colour problems. The abstract at the beginning of each article is published in both German and English. The subscription is D.M.46,80 for six parts which form one volume.

## Journal of Scientific Instruments

### Contents of the April issue

#### ORIGINAL CONTRIBUTIONS

##### Papers

- Apparatus used in the development of optical-diffraction methods for the solution of problems in X-ray analysis. By W. Hughes and C. A. Taylor.
- A photoelectric densitometer. By O. L. Goble.
- Combined Pirani and ionization gauge circuit. By G. von Dardel.
- The "screening" of neutral particles in high voltage ion accelerator tubes. By K. Firth and D. R. Chick.
- A demountable flash-discharge tube for production of the Lyman continuum. By W. R. S. Garton.
- A portable oximeter with provision for continuous recording. By F. D. Stott.
- Peak-noise characteristics of some glow-discharge tubes. By H. Bache and F. A. Benson.
- An apparatus for the photometric study of flash-initiated reactions. By F. W. Trowse.
- A simple quartz infra-red spectrometer for the determination of absorbed water in some polymers. By E. R. S. Jones.
- A saturable-core reference source for use with magnetic amplifiers. By A. G. Milnes and T. V. Vernon.

#### Laboratory and workshop notes

- A centre stable electronic relay. By R. Bailey.
- Wavelength and slit-dive mechanisms for an infra-red spectrometer. By J. D. S. Goulden.
- A semi-micro manipulator for crystal mounting. By A. L. Mackay.
- Multi-bore glass sleeves for insulation. By L. Elsort.
- Making of biprisms. By A. O. Mathai.
- A simple timing device. By R. H. Cook and R. D. Keynes.
- Uranium shadowing for electron microscopy. By K. Little and C. S. Lees.

#### NOTES AND NEWS

##### Correspondence

- The design of thermocouple transformers for infra-red chopped beam systems. From J. A. Sirs; T. S. Robinson.

#### New instruments, materials and tools

##### Notes and comments

## British Journal of Applied Physics

### Original contributions accepted for publication in future issues of this Journal

- The stresses in the reels of cold reduction mills. By R. B. Sims and J. A. Place.
- Energy spectrum measurements of protons in the Harwell cyclotron. By J. M. Dickson and D. C. Salter.
- Refractive index determination for anisotropic crystals. By A. L. Mackay.
- The adaptation of an electron microscope for reflexion and some observations on image formation. By M. E. Haine and W. Hirst.
- Ratio of convection to conduction loss from a hot wire stretched along the axis of a vertical cylindrical tube. By J. A. V. Fairbrother.
- The magnetic fields produced by uniformly magnetized ellipsoids or revolution. By H. J. Peake and N. Davy.
- Neon indicator tubes as quantitative detectors in photometry. By T. J. Dillon.
- Proposed use of a cylindrical surface wave resonator for the determination of the velocity of short electromagnetic waves. By H. M. Barlow and A. E. Karbowiak.
- The effect of charging errors on the transmission of a sector disk. By A. F. A. Harper and A. J. Mortlock.

THIS JOURNAL is produced monthly by The Institute of Physics, in London. It deals with all branches of applied physics (including theory and technique). All rights reserved. Responsibility for the statements contained herein attaches only to the writers.

**EDITORIAL MATTER.** Communications concerning editorial matter should be addressed to the Editor, The Institute of Physics, 47 Belgrave Square, London, S.W.1. (Telephone: Sloane 9806.) Prospective authors are invited to prepare their scripts in accordance with the *Notes on the preparation of contributions*. (Price 2s. 6d. including postage.)

**REPRODUCTION.** The Institute of Physics is a signatory to The Royal Society's Fair Copying Declaration. Details may be obtained upon application from The Royal Society, London, W.1.

**ADVERTISEMENTS.** Communications concerning advertisements should be addressed to the agents, Messrs. Walter Judd Ltd., 47 Gresham Street, London, E.C.2. (Telephone: Monarch 7644.)

**SUBSCRIPTION RATES.** A new volume commences each January. The charge is £4 per volume (\$11.50 U.S.A.), including index (post paid), payable in advance. Single parts, so far as available, may be purchased at 8s. each (\$1.15 U.S.A.), post paid, cash with order. Orders should be sent to The Institute of Physics, 47 Belgrave Square, London, S.W.1, or to any bookseller.

## Information theory\*

By P. M. WOODWARD, B.A., Telecommunications Research Establishment, Ministry of Supply

This paper is not intended as an original contribution to information theory; its purpose is to introduce the early work of R. V. L. Hartley and the newer statistical theory developed by C. E. Shannon to readers unfamiliar with the subject. With the problem of storing information as a model, the information capacity of a physical system may be defined as the logarithm of the number of its distinguishable states. The information content of a message is then defined as the minimum capacity required to store it. These two definitions make it possible to appraise scientifically the efficiency of any storage system or communication channel; it is shown that the efficient use of a communication channel entails coding apparatus to match the statistical properties of the source to those which maximize the (macroscopic) entropy of the channel.

## 1. INTRODUCTION

In 1927 a remarkable paper was presented to the International Congress of Telegraphy and Telephony by R. V. L. Hartley<sup>(1)</sup> of the Bell Telephone Laboratories. Hartley's object was to "set up a quantitative measure whereby the capacities of various systems to transmit information may be compared." Today it hardly seems necessary to justify such an aim, except simply to say that no completely scientific analysis of a communication problem is possible unless there exists a proper scientific measure of the stuff with which communication deals, namely, *information*. By themselves, quantities such as energy, bandwidths or noise-levels do not go deep enough. Hartley was the first to realize this, and took the first step towards formulating a precise mathematical theory of information.

Theoretical physicists, familiar with information theory, may find it surprising that it was not until 1927 that any attempt to measure communicated information was made, for all the mathematical apparatus was already in existence under a different guise, in the subject of statistical mechanics. The expression which is now used in communication theory to describe initial uncertainty, or missing information prior to receiving a communication, is mathematically identical with that for entropy in statistical mechanics. However, even Hartley was apparently unaware of the connexion, and it is only in recent years that it has been fully exploited.

After Hartley's contribution, and apart from an elegant analysis of communication signals by D. Gabor<sup>(2)</sup> in 1946, the subject received little attention in the literature until 1948, when Shannon's major work<sup>(3)</sup> appeared. The precise origins of this modern formulation of information theory are a little obscure, but it would appear that Shannon and Norbert Wiener<sup>(4)</sup> were the first to see the importance of the relationship between information and entropy. The detailed mathematical treatment of the subject along these lines is due to Shannon, though Tuller's work<sup>(5)</sup> should not pass unnoticed. Quite independently, Tuller had been following up the original paper by Hartley and had applied Hartley's measure of information to the problem of the "noisy communication channel," obtaining an approximate formula for its information-handling capacity which is similar to the one which has been obtained by Shannon in a more rigorous manner. Since 1948 a large number of papers have appeared, but in the author's opinion the fundamental theory has not been advanced to any significant extent, and it is difficult to

select further references which do not deal with specialized aspects of the subject. However, there are two complete accounts in the form of reports, those of R. M. Fano<sup>(6)</sup> and A. E. Laemmel.<sup>(7)</sup> The elementary introduction by W. Weaver<sup>(8)</sup> should also be mentioned, and a short history of the subject by E. C. Cherry.<sup>(9)</sup> Further, there is an interesting geometrical interpretation of the theory of the noisy communication channel in another paper by Shannon.<sup>(10)</sup>

In the present treatment, only a very brief and elementary introduction is given, first to Hartley's work and then to Shannon's, with particular emphasis on the statistical aspects of the theory. The subject is largely based on statistics, and cannot be understood apart from that context. A very little mathematics is included, for the purpose of indicating methods rather than obtaining actual results.

## 2. HARTLEY'S MEASURE OF CAPACITY

Hartley formulated his problem in terms of communication, but the theory can be applied equally well to the static problem of information storage. Mathematically it makes no difference, and the static problem is simpler to discuss.

The essential feature of a storage system is that it shall admit of a number of *distinguishable states*. For example, a sheet of paper stores information because there are a large number of distinguishable ways of filling it with symbols. A bank of two-state levers can similarly be set up in a large number of different ways so as to store information according to some pre-arranged code. If two storage systems, possibly of quite different types, each possess the same total number of distinguishable states, they are precisely equivalent from an information-theoretical point of view, because each state of the one system can be made to tally with a state of the other. In other words, a transfer-code can be set up. For example, the "capacity" of a knob with thirty-two click-positions is precisely the same as the capacity of five two-position levers, which also admit of thirty-two distinguishable states. Either system could be used to store (or remember) a letter of the alphabet, with six states to spare. In practice, of course, other properties of a store have also to be considered. The engineer will demand that the various states shall not be liable to spontaneous changes, but shall be stable. He may also require that old information shall be easily erased, and so on. However, these are essentially matters of practical detail. The *capacity* of a store depends only on the number  $n$  of its distinguishable states. This suggests that we might define capacity by the number  $n$ , but it will be found that a logarithmic measure is more convenient. Thus, if one

\* Based on a lecture given before the Electronics Group of The Institute of Physics on 11 November, 1952.



sheet of paper can be filled in  $n$  ways, two can be filled in  $n^2$  altogether. By adopting Hartley's definition

$$C = \log n \quad (1)$$

the capacity of two sheets becomes double that of one. The logarithmic definition is the only one which enables us to add separate capacities to obtain a total capacity—an obviously convenient property.

At least for explanatory purposes, it has become customary in information theory to use logarithms to the base 2. Capacity is then equal to the equivalent number of binary storage units. For example, the knob with thirty-two discrete positions will hold five binary digits, and its capacity is five bits. There is, of course, no magic in the binary terminology; it is used purely for convenience. Ordinary natural logarithms can be used instead and the associated natural unit of capacity is rather more than a bit.

The idea that a sheet of paper offers  $\log_2 26$  bits of storage space per letter of the alphabet may seem to imply that a page which has been filled with 5000 letters does actually contain  $5000 \log_2 26$  bits of information. This is not so, and Hartley was evidently aware that the actual information content of a store is not necessarily the same thing as its capacity. In fact he makes it plain that he is deliberately omitting "psychological factors" and confining himself strictly to a quantity which is characteristic of the physical system and not a function of the way in which the system is used. In Shannon's theory this restriction is removed, and actual information content is defined mathematically. It turns out that Hartley's "psychological factors" are of a purely statistical nature and can most fruitfully be taken into account in the mathematical theory. Indeed, it is here that the whole interest of the subject now lies.

### 3. SHANNON'S MEASURE OF INFORMATION

We might define the information content of a message as the minimum capacity required for storage. For simplicity, consider a two-state message such as the reply to some question which only admits of yes or no. If I ask the question, "Are you right-handed?" there are two possible message-states, and I shall be able to store the reply in a binary store of capacity one bit. It is tempting to say immediately that the message contains one bit of information, for by itself it cannot be stored any more efficiently. In fact, the message may contain less than one bit, as we shall shortly see.

Suppose that 128 people are questioned, and 128 binary messages have therefore to be stored. (It is assumed, of course, that we are interested in preserving the correct order of the replies, so that the left- or right-handedness of each individual can be reconstructed.) The naïve procedure would be to set aside one binary store for each reply. But there is a more economical method. The question "Are you right-handed?" expects the answer yes, and of the 128 messages, there will be only one or two no-states. Rather than store a sequence such as

YYYYYYYNNYYYYYYYYYYYYYYYYYYYYYYYYYYY (2)

it would obviously be more economical to store the positions of the no's. If we are using a set of binary storage units, we should have to code the numbers

$$9, 25, \text{etc.} \quad (3)$$

into binary digits. Seven binary digits will describe any

location from 1 to 128 in the sequence (2), and allotting a group of seven digits for each no, we could store 0001001 to represent 9 in the scale of two, and 0011001 to represent 25. Thus, instead of (2) we should store the sequence

$$00010010011001 \dots \quad (4)$$

it being understood that the decoding must proceed in blocks of seven. It is easy to see that, provided the no's occur only seldom, considerable compression will result, and the average storage space required per message will be less than one bit. Even now, the storage units are being used wastefully. It would have been even more economical in the long run to code the differences between the numbers in the sequence (3) though to do so without using commas in addition to the symbols 0 and 1 would require a little ingenuity. (Commas, naturally, would count as additional symbols and could only be retained in a system employing three-state storage units.) However, without striving for perfection in this example, it will be seen that economy of storage space has been effected by applying two inter-related principles,

- (i) constructing a code which takes advantage of prior expectations, and
- (ii) collecting a large number of messages, and coding them as a whole.

If the prior probabilities of the message states were altered, a good code would become a bad one. Obviously in the example, if yes were the infrequent state, it would be better to store yes-locations than no-locations. In other words, the best possible code will depend on the relative prior probabilities of the different message-states, and it follows that the true information content of a message depends on these probabilities.

We are now faced with the interesting mathematical problem of calculating the minimum storage capacity required for a set of messages, when the probabilities of the different states are assumed to be known in advance. It is not an easy problem for those unacquainted with statistical technique, but the method of solution will be briefly indicated. Let us suppose, for simplicity, that each message has only two states, yes and no, and that there are  $N$  messages. Then the expectation is that there will be  $Np$  yes's and  $Nq$  no's, where  $p$  and  $q$  are the probabilities of yes and no, and  $p + q = 1$ . The difficult step in the proof is to justify the assumption that there will be *exactly*  $Np$  yes's and  $Nq$  no's. Naturally, there will be statistical fluctuations about these numbers, but it can be proved that if they are completely ignored, the final answer is wrong by an amount which becomes more and more negligible as  $N$  is increased. The proof of this will be omitted, though mathematically it is an essential step. The method of solving the problem is now to calculate the total number of storage states needed to allow for all the possible ways in which  $Np$  yes's and  $Nq$  no's can occur. The logarithm of this number, divided by  $N$ , then gives the average information content of one message. The actual calculation proceeds as follows.

The total number of ways of arranging  $Np$  yes's and  $Nq$  no's is given by

$$m = \frac{N!}{(Np)!(Nq)!} \quad (5)$$

or in logarithmic form,

$$\frac{\log m}{N} = \frac{\log N!}{N} - \frac{p \log (Np!)}{Np} - \frac{q \log (Nq!)}{Nq} \quad (6)$$



If the factorials are of large enough numbers, which is ensured by taking  $N$  sufficiently large, we can use Stirling's formula

$$\frac{\log x!}{x} \simeq \log(x/e) \quad (7)$$

Substituting Stirling's formula (7) into equation (6), we obtain

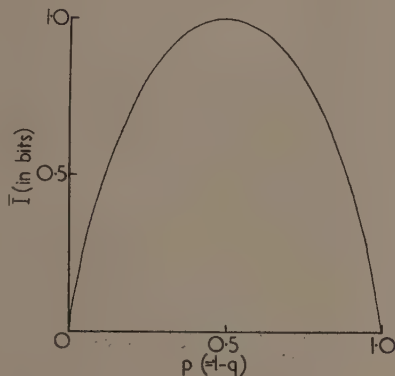
$$\frac{\log m}{N} \simeq \log(N/e) - p \log(Np/e) - q \log(Nq/e) \quad (8)$$

Remembering that  $p + q = 1$ , we can readily simplify this expression and write, finally,

$$\bar{I} = \lim_{N \rightarrow \infty} \frac{\log m}{N} = -p \log p - q \log q \quad (9)$$

This is the answer we have been seeking: it is the average quantity of information in a two-state message in terms of the probabilities of the states. Once again, the units are bits if the logarithms are taken to the base two.

The formula (9) repays examination. In the first place, it is really only a function of one variable, since  $q = 1 - p$ , and can be plotted against  $p$  alone, as shown in the figure.



Observe that it is a maximum when  $p = q = \frac{1}{2}$ , when  $\bar{I} = 1$  bit. This we might have expected, because a two-state message can always be stored in a two-state store, and its average information content cannot, therefore, exceed one bit. But notice also that there is no information when either  $p$  or  $q$  is unity. Again, the result is intuitive. If a question is certain to yield the reply yes, no information is obtained when the reply yes is actually given. Only one storage state is needed, and the capacity by Hartley's formula is zero. Here, surely, is a most elegant mathematical explanation of Hartley's "psychological factors"? And basically, no assumptions or postulates have been introduced beyond those required to set up Hartley's original definition.

Care has been taken to speak only of the *average* information content of a message. This is because the method of deriving  $\bar{I}$  has been to consider an ensemble of  $N$  messages and finally to divide by  $N$ . In this ensemble, *both* message-states occur, in proportion to their probabilities. The expression for  $\bar{I}$  must therefore be an average over both states, as is immediately evident from the actual formula (9). The obvious inference is that the quantity of information in the state of probability  $p$  is  $-\log p$  and in the other  $-\log q$ . Thus, omitting the averaging sign, we may write

$$I = -\log p \quad (10)$$

where  $p$  is the prior probability of the particular state in question. It can now be seen that the frequent reply "yes" in the example with which we began contains less than one bit of information, but that the infrequent reply "no" contains *more* than one bit. In the average (9) yes predominates and the average information, or expectation of gain, is less than one bit per message.

The general formula upon which Shannon's theory is based is

$$I = -\sum p_i \log p_i \quad (11)$$

Here there is no assumption that each message has only two states. The states are distinguished by the suffix  $i$ , and there may be any number  $n$  of them,  $p_i$  being the probability of the  $i$ th state. This expression is a maximum, for given  $n$ , when all the  $p_i$  are equal, and it is zero whenever one of the  $p_i$  is equal to unity, the rest then being zero (since probabilities have to add up to unity). When all  $p_i$  are equal, it is very easily seen that  $\bar{I}$  is equal to  $\log n$ , so by comparison with Hartley's formula (1), we have

$$C = \quad (12)$$

This means that storage is efficient only when all the storage states have equal probabilities of being used. If the probabilities are unequal, the content is less than the capacity.

We may summarize by saying that Shannon's formula (11) gives the minimum number of binary digits into which a message can, on the average, be converted in a reversible manner.

#### 4. CODING FOR EFFICIENT STORAGE

In order to store efficiently a set of independent messages whose states have unequal prior probabilities, a code must be devised which will equalize the probabilities with which the storage states are used. It is evident in the example given at the beginning of Section 3, that the two states of each symbol in sequence (4) occur more equally than the original message-states in sequence (2). Shannon has given a very simple example of an *ideal* code which illustrates this point to perfection. It is as follows:

Message-state	A	B	C	D
Prior probability	$\frac{1}{2}$	$\frac{1}{4}$	$\frac{1}{8}$	$\frac{1}{8}$
Information (bits)	1	2	3	3
Code	0	10	110	111

(13)

There are four message-states, having the probabilities shown in the table. A typical sequence of messages might be

$$DAABACBA \quad (14)$$

and this sequence would be encoded into binary digits thus:

$$11100100110100 \quad (15)$$

It will be noticed that the original sequence is too perfect, because the frequencies of occurrence of the symbols exactly reproduce the given probabilities. They would tend to do this only in a much longer sequence. However, the coded sequence is made up of equal numbers of 0's and 1's, and is exactly typical of a very long sequence. There are, on the average, fourteen binary digits for eight messages, or 1.75 bits per message, in strict accordance with equation (11). Further, each coded message *state* occupies a storage capacity given precisely by equation (10). And finally, it will be found (perhaps surprisingly) that the code is completely reversible even though the original messages are coded into

sequences of varying length. There is no ambiguity in decoding.

Lest the whole magic of this example be lost, Shannon has pointed out that the coded sequence (15) can, if desired, be divided off into *pairs* of digits, and each pair (having four states) coded again into a letter *A, B, C* or *D*. The result is that the original sequence of eight symbols ends up as a sequence of only seven symbols from the same alphabet, yet no information has been destroyed. It has merely been expressed more concisely.

The above example was specially chosen by Shannon because it comes out exactly. In general, with arbitrary message probabilities, ideal coding can be approached only by a laborious process of cataloguing long sequences of messages. The general procedure is implicit in the derivation of the formula for information content, outlined in Section 3. One takes a sequence of messages so long that the law of averages comes strongly into play. This means that of all the possible sequences, quite a small fraction account for most of the probability, whilst the remainder have altogether a very small probability. The highly probable set can then be coded concisely, and the improbable set can be coded at greater length without appreciably increasing the average capacity required.

#### 5. THE CAPACITY OF A COMMUNICATION CHANNEL

The obvious difference between storage and communication is that the capacity of a communication channel must be measured as a *rate* of transferring information, in bits per second, but this occasions no more difficulty than converting, say, an energy argument into a power one. The real and important difference between a simple storage problem and a communication problem is that communication is generally subject to constraints or "accessory conditions" which have to be taken into account when calculating the capacity. (Actually, a storage system may well be subject to constraints also. If so, the same more general treatment must be applied to storage.) Hartley's formula, in fact, may not be directly applicable.

Let us consider what happens in a communication channel in the course of one second—assuming, for convenience, an infinite velocity of propagation of the signals. A large number of different waveforms can pass down the channel; for example, a piece of speech waveform, a bar of music modulating a carrier, pulses of various amplitudes—any wave shape, in fact, which does not violate the physical constraints of the system, such as its limited bandwidth or signal power. If it were possible to count the number *n* of permissible "states" which can occur at the receiver in one second, and if each interval of a second were independent of the rest, then  $\log_2 n$  would be the capacity in bits per second, by Hartley's formula. However, it may not always be possible to treat each second independently. For instance, suppose that there is a mean power limitation and no peak power limitation, even though strictly this is impracticable. Then we should have to limit the states we were permitted to count, but the limitation could not be applied to each interval individually. It would only apply "in the large." Shannon removes this difficulty by defining capacity in a more general way, as

$$C = \lim_{T \rightarrow \infty} \frac{\log n(T)}{T} \quad (16)$$

The units are bits per second, provided the logarithm is to the base 2. The evaluation of *C* for a given system directly

from equation (16) would be difficult, but fortunately there is a short cut based on the results already obtained in Section 3.

Although information content has been tentatively defined as the minimum capacity required for storage, there is now no reason why equation (11) should not be taken as the fundamental definition of the theory, and capacity defined as its maximum possible value. Thus the capacity of a communication channel may be calculated by considering the states *i* in a one-second interval, and maximizing equation (11) subject to the necessary constraints. As an illustration of this mathematical technique, suppose that associated with each state *i* there is some quantity *E<sub>i</sub>*, which might in fact be the *energy* of the *i*th waveform. And suppose that the average energy has to be constrained to have some given value *E*, say. Then we have to maximize

$$I = - \sum p_i \log p_i \quad (17)$$

subject to the accessory conditions

$$\sum p_i = 1, \sum p_i E_i = E \quad (18)$$

This is a standard problem in the calculus of variations (well known in statistical mechanics) and the technique is to maximize, with the "undetermined multipliers"  $\lambda$  and  $\mu$ , the expression

$$\Sigma(-p_i \log p_i + \lambda p_i + \mu p_i E_i) \quad (19)$$

by differentiating with respect to all the *p<sub>i</sub>*'s and equating the result to zero. This gives

$$-\log p_i - 1 + \lambda + \mu E_i = 0 \quad (20)$$

or by changing the arbitrary constants

$$p_i = A e^{-BE_i} \quad (21)$$

The constants *A* and *B* are finally determined by making the *p<sub>i</sub>* satisfy the two conditions (18).

The expression (21) shows with what probabilities, or relative frequencies, the different states can be used so as to maximize the average quantity of information communicated in one second, and yet to ensure that the average value of *E<sub>i</sub>* is fixed at some pre-arranged value *E*. If *E* represents energy, this constraint is simply a mean power limitation. A bandwidth limitation can also be taken into account quite easily by considering time-intervals not of one second duration but related to the reciprocal of the bandwidth. It is then possible to describe a waveform *i* in each interval in terms of one single sample amplitude. One may notice that if energy is proportional to the square of amplitude, equation (21) implies a Gaussian choice of amplitude. Finally, having enumerated all the possible waveforms, and calculated their optimum probabilities taking constraints into account, one substitutes the probabilities back into equation (11) to obtain the capacity.

The above calculation will not be carried to a practical conclusion: it is merely intended to illustrate the way in which a channel capacity may be evaluated. It does not explain how noise is taken into account, and to do so would take us too deeply into the theory. It is clear that noise will decide how close together the possible states can be taken without becoming indistinguishable at the receiver, but for a precise treatment, the reader must be referred to Shannon's paper.<sup>(3)</sup>

#### 6. STATISTICAL MATCHING

We have seen that a simple storage system is efficient only when all the storage states have equal probabilities of being

used. A communication system differs in that it may not be possible to use all the different signals with equal probabilities without violating the physical constraints of the system. As has been shown in the previous section, these constraints can, in principle, be taken into account and an optimum set of generally *unequal* probabilities calculated. The problem of coding now becomes more complex. The original message-states have themselves a distribution or probabilities, and these will not, in general, tally with the optimum set. The messages must therefore be coded, not simply to equalize the probabilities of using each of the states of the physical system, but to make them correspond to an optimum distribution. Efficient use of a communication system can therefore be said to result from the *statistical matching* of the message-source to the communication channel.

An excellent example of inefficient matching is afforded by the ordinary (uncompressed) speech channel. The capacity calculated from Shannon's formula (reference 3, theorem 17) is very much greater than the estimated rate at which information is communicated, and the reason is not hard to find. A channel such as is ordinarily used to transmit speech, is inherently capable of communicating a multitude of waveforms which do not correspond to speech at all. In order to utilize the channel efficiently—that is, to pass information at the maximum possible rate—all these neglected waveforms would have to be used with certain probabilities. When speech exclusively is transmitted, these other possible waveforms are not used at all. Statistically, the source is not matched to the channel. This implies that further constraints could be applied to the channel without in any way reducing the fidelity of speech transmission, yet reducing the channel capacity. Capacity, of course, is easily reduced, either by using less signal power (compared with a fixed noise power) or by using a narrower band of the frequency spectrum (*ibid.*) and still it should be possible to transmit speech with the same quality as before. However, merely to reduce the channel capacity does not solve the matching problem, in fact it only makes it more acute. From a practical point of view, the problem of matching speech, with its complicated statistics, to a communication channel of minimal capacity, is a formidable one, and is still far from being completely solved. Television presents a similar problem.

## 7. CONCLUSION

Whenever a new technique or a new theory is evolved there is some adverse criticism; it may be said of information theory that it is merely an amusement for the mathematician and that the communication engineer has been intuitively aware of all its conclusions for a long time. Even if this were true, which is very doubtful, the subject has, in the author's opinion, a profound significance.

In the first place, it provides a precise language for the description of physical systems which handle information where before there was only intuition. The existence of a precise language always tends to clarify thought, and acts as a stimulus to further research. And in the second place, the relation between communication theory and statistical mechanics contributes to the general understanding of *both* these branches of physics.<sup>(11)</sup> Few things in science are more exciting than the sudden realization that two apparently disconnected phenomena can both be expressed in terms of

a single idea. It has already been remarked that Shannon's definition of information content is the very same expression, apart from a factor of Boltzmann's constant, as is used for entropy in physics, and a few further remarks on this matter might not be out of place.

Entropy is a measure of *disorder* or "*missing information*" concerning the state of a physical system, and the apparent contradiction in the face of mathematical identity with *positive* information has caused some unnecessary confusion. This is due entirely to the fact that Shannon's formula, measures a *posteriori* information in terms of *a priori* probabilities, as has been pointed out by D. K. C. MacDonald. The states of a storage system have been described by probabilities  $p_i$  which imply that we do not know precisely what state the system is in. If we want to find out we "*read*" the store, probabilities become certainties, and information is gained. The amount of our gain is measured by our uncertainty in the first place, and it is this uncertainty which entropy is supposed to describe. There is, however, this difference: the probabilities which enter into the calculation of entropy refer to quantum states whereas in communication theory they refer to macroscopic states or even to non-equilibrium conditions which the physicist might hesitate to describe as "*states*" at all. As a question of physics, it is not yet clear whether this difference is anything more than a trivial one, concerning the zero of entropy.

## ACKNOWLEDGEMENT

The author acknowledges the permission of the Chief Scientist, Ministry of Supply, to publish this paper.

## REFERENCES

- (1) HARTLEY, R. V. L. *Bell Sys. Tech. J.*, **7**, p. 535 (1928).
- (2) GABOR, D. J. *Instn Elect. Engrs, Pt. III*, **93**, p. 429 (1946).
- (3) SHANNON, C. E. *Bell Sys. Tech. J.*, **27**, p. 379 and 623 (1948). Also in book form: SHANNON, C. E., and WEAVER, W. *The Mathematical theory of communication* (Urbana: University of Illinois Press, 1949).
- (4) WIENER, N. *Cybernetics* (New York: John Wiley and Sons Inc., 1948).
- (5) TULLER, W. G. *Proc. Inst. Radio Engrs*, **37**, p. 468 (1949).
- (6) FANO, R. M. Massachusetts Institute of Technology, Research Laboratory of Electronics, *Technical Reports* 65 (1949) and 149 (1950).
- (7) LAEMMEL, A. E. Polytechnic Institute of Brooklyn, Microwave Research Institute, *Report R-208-49*, P15-152 (1949).
- (8) WEAVER, W. *Recent contributions to the mathematical theory of communication* appearing in ref. (3) above.
- (9) CHERRY, E. C. *Proc. Instn Elect. Engrs, Pt. III*, **98**, p. 383 (1951).
- (10) SHANNON, C. E. *Proc. Inst. Radio Engrs*, **37**, p. 10 (1949).
- (11) BRILLOUIN, L. *J. Appl. Phys.*, **22**, p. 334 (1951).



# The two-dimensional magnetic or electric field above and below an infinite corrugated sheet

By N. H. LANGTON, Ph.D., A.Inst.P., and N. DAVY, D.Sc., The University of Nottingham

[Paper first received 12 November, 1952, and in final form 19 January, 1953]

The field is investigated above and below the surface of an infinite corrugated sheet. The sheet may be regarded as a magnetized ferromagnetic body, or a charged electrical conductor. The corrugations are parallel, semi-circular cylinders. The method involves the use of conformal transformations and elliptic integrals. Tables and graphs of the field strength at important points are given.

The field inside a semi-infinite slot terminated by a semi-circular cylinder has already been investigated by the authors.<sup>(1)</sup> From this solution, and that for a similar slot differing only in that the end is convex upwards as in Fig. 1, the problem of a corrugated sheet can be solved. Figs. 2

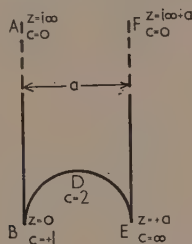


Fig. 1. The semi-infinite slot (z-plane)

and 3 show the two-dimensional systems to be investigated. The corrugations PQBDE are cross-sections of semi-circular cylinders whose generators are perpendicular to the plane of the diagrams. In both cases the whole field consists of repetitions of the field in the cell ABDEF, so that it is sufficient to investigate a conductor whose cross-section is

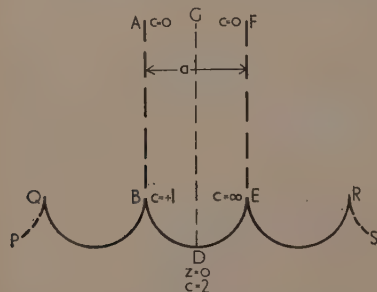


Fig. 2. The corrugated sheet (z-plane)

BDE, the lines BA and EF representing lines of force. The solution for the cell ABDEF of Fig. 2 has already been obtained,<sup>(1)</sup> but that for the cell ABDEF of Fig. 3 must first be obtained before the corrugated sheet problem can be completely solved.

Fig. 1 represents a cross-section of a semi-infinite slot in a magnetized but not saturated ferromagnetic body, or else a cavity in a charged electrical conductor. The parallel sides AB and EF terminate at infinity, and BDE is a semi-circle of radius  $a/2$ . The face of the slot is an equipotential. The perimeter ABDEF is drawn in the  $z$ -plane, and must be transformed into the real axis of a  $c$ -plane, not shown, so that the interior of ABDEF becomes the upper half of the  $c$ -plane. The geometrical transformation that performs this gives  $z$  as a function of two solutions of the hypergeometric equation, the independent variable being  $c = k^2$ , where  $k$  is the elliptic modular function. In the resulting bilinear transformation  $z$  is expressed as a function of  $c$  and the elliptic integrals  $K$  and  $K'$ .

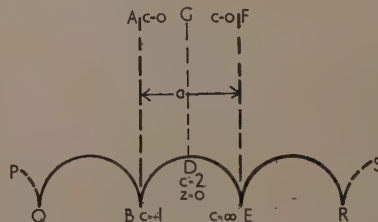


Fig. 3. The corrugated sheet (z-plane)

An electric or magnetic transformation is then required which links the geometric transformation with the physical properties of the system. For details of this transformation reference should be made to the previous paper quoted above.<sup>(1)</sup>

## THE TRANSFORMATIONS

(a) *The geometrical transformation.* This transformation is obtained by Nehari,<sup>(2)</sup> who shows that the equation

$$z = ia.K'/K \quad (1)$$

transforms the edge ABDEF of the curvilinear triangle into the real axis of the  $c$ -plane so that the internal area corresponds to the upper half of the  $c$ -plane. Table 1 gives the calculated values of  $z/a$  and the corresponding values of  $c$ .

(b) *The magnetic or electric transformation.* Let  $W = U + i.V$ , where  $U$  is the stream function and  $V$  the potential at any point in the  $z$ -plane. The  $W$ -plane is shown in Fig. 4 and the line ABDEF which has an equation  $W = U + i.V_0$  must be made to correspond to the edge of the conductor

thus raising it to a potential of  $+V_0$ . The required electrical transformation is

$$dW = -A \cdot dc/c^2 \quad (2)$$

as explained in the first reference. With this transformation the lines of force in the  $z$ -plane all terminate at the point at infinity which therefore has a potential of  $-\infty$ .

Table 1. The geometrical transformation

$c = 0.0$	0.0301	0.1170	0.2500	0.4100
$z/a = i \cdot \infty$	1.99i	1.546i	1.232i	1.083i
$c = 0.8830$	0.9700	0.9924	0.9952	0.9988
$z/a = 0.647i$	0.501i	0.410i	0.397i	0.331i
$c = 1.000$	1.030	1.334	1.703	2.000
$z/a = 0.000$	$\begin{Bmatrix} 0.202 + \\ 0.401i \end{Bmatrix}$	$\begin{Bmatrix} 0.378 + \\ 0.485i \end{Bmatrix}$	$\begin{Bmatrix} 0.460 + \\ 0.498i \end{Bmatrix}$	$\begin{Bmatrix} 0.500 + \\ 0.500i \end{Bmatrix}$



Fig. 4.  $W$ -plane.  $ABDEF$  is an infinitely long horizontal straight line having the equation  $W = U + iV_0$ . Points below  $ABDEF$  correspond to internal points of the slot of Fig. 1

#### THE FIELD STRENGTH

The magnetic or electric intensity at any point in the  $z$ -plane is given by

$$F = |dW/dz| = |dW/dc \cdot dc/dk \cdot dk/dz| \quad (3)$$

Hence, from equation (2) and the facts that  $dc/dk = 2k$ , and  $dz/dk = ia\pi/2c'kK^2$ , we obtain

$$F = (4A/\pi a) \cdot |c' \cdot K^2/c| \quad (4)$$

for moduli less than unity, where  $A$  is a real constant. Hence at the corners  $A$  or  $F$ , where  $c = 0$ ,  $c' = 1$  and  $K = \infty$  we have  $F = 0$ . At the corner  $B$ ,  $c' = 0$ ,  $c = 1$  and  $K = \infty$  which gives  $F = 0$  when we take the limit. Finally, at the corner  $E$ ,  $c = \infty$ ,  $c' = -\infty$  and the equation for  $F$  becomes

$$F = (4A/\pi a) \cdot |ic' \cdot (k \cdot K + ik \cdot K')^2| \quad (5)$$

for moduli greater than unity. Hence  $F = 0$  at the point  $E$ . Numerical values of  $F$  are calculated for points along the edge  $ABDEF$  of the conductor and also along the centre line  $DG$ . From  $A$  to  $B$ ,  $c$  is real and less than unity so that calculation is straightforward, but from  $B$  to  $D$ ,  $c$  is greater than unity so that equation (5) must be used. Along  $DG$ ,  $c$  is complex, and a special method, now to be described, must be used to find the values of  $F$ . If we write  $c_2 = (2 - c)/c$ , then when  $c = 2$ ,  $c_2 = 0$  and thus the point  $D$  is made the origin of a new  $c_2$ -plane. Thus symmetry with respect to  $c_2$  is introduced and  $DG$  corresponds to the negative imaginary axis of the  $c_2$ -plane. Along  $DG$  therefore, any point will correspond to  $c_2 = -i \cdot \alpha$ , where  $\alpha$  is real and positive. Also, writing  $\alpha = \sin x/(1 + \cos x)$  so that  $c_2 = -i \cdot \tan(x/2)$  we obtain  $c = 1 + \exp(ix)$ . Values of  $K$  for various values of  $x$  and  $\alpha$  can be found from the tables of Cambi,<sup>(3)</sup> whose Table 4 gives the variation of  $F$  along  $DG$ .

#### Results for conductor of Fig. 1

(1) *Field strength  $F$  along the edge  $AB$ .* The field strength  $F$  (e.s.u. or e.m.u. according to whether the problem is an electrical or magnetic one) is expressed as a multiple of the constant  $4A/\pi a$  so that  $F \cdot (\pi a/4A)$  is tabulated. The distance

$z$  of the points concerned is measured along  $AB$  from  $B$  in terms of  $a$ , the width of the conductor.

Table 2. Field strength along  $AB$ . (See also Fig. 5.)

$z/a = 0.000$	0.331i	0.377i	0.410i	0.501i	0.578i
$F \cdot (\pi a/4A) = 0.000$	0.023	0.0877	0.1183	0.308	0.550
$z/a = 0.647i$	0.708i	0.924i	1.083i	1.278i	
$F \cdot (\pi a/4A) = 0.833$	1.551	2.64	4.58	8.526	

(2) *Field strength along the edge  $BD$ .* The distances of the points concerned are measured from  $B$  along the real axis of  $z$ , that is, a point on the curved portion  $BD$  is located by the real part of its complex co-ordinate. The modulus  $c$  is real and greater than unity except at the corner  $B$  where  $c = 1$ .

Table 3. Field strength along  $BD$ . (See also Fig. 5.)

$z/a = 0.0989$	0.127	0.146	0.202
$F \cdot (\pi a/4A) = 0.0299$	0.0954	0.133	0.366
$z/a = 0.378$	0.460	0.5000	
$F \cdot (\pi a/4A) = 1.405$	1.69	1.719	

(3) *Field strength along the centre line  $DG$ .* The distance of the points concerned is measured along  $DG$  from  $D$  in terms of  $a$ . The modulus  $c$  is complex except for the point  $D$  itself, where  $c = +2$ .

Table 4. (See also Fig. 5)

$z/a = 0.000$	0.015i	0.038i	0.060i
$F \cdot (\pi a/4A) = 1.719$	1.68	1.66	1.61
$c = 2.000$	$\begin{Bmatrix} 1.9877 \\ +0.1564i \end{Bmatrix}$	$\begin{Bmatrix} 1.951 \\ +0.309i \end{Bmatrix}$	$\begin{Bmatrix} 1.890 \\ +0.458i \end{Bmatrix}$
$z/a = 0.077i$	0.084i	0.123i	0.145i
$F \cdot (\pi a/4A) = 1.59$	1.60	1.624	1.658
$c = \begin{Bmatrix} 1.808 \\ +0.5878i \end{Bmatrix}$	$\begin{Bmatrix} 1.707 \\ +0.707i \end{Bmatrix}$	$\begin{Bmatrix} 1.588 \\ +0.810i \end{Bmatrix}$	$\begin{Bmatrix} 1.454 \\ +0.890i \end{Bmatrix}$
$z/a = 0.175i$	0.200i	0.236i	0.270i
$F \cdot (\pi a/4A) = 1.714$	1.793	1.89	2.022
$c = \begin{Bmatrix} 1.309 \\ +0.951i \end{Bmatrix}$	$\begin{Bmatrix} 1.156 \\ +0.9877i \end{Bmatrix}$	$\begin{Bmatrix} 1.000 \\ +1.000i \end{Bmatrix}$	$\begin{Bmatrix} 0.843 \\ +0.987 \end{Bmatrix}$
$z/a = 0.352i$	0.433i	0.768i	
$F \cdot (\pi a/4A) = 2.45$	2.80	11.12	
$c = \begin{Bmatrix} 0.5458 \\ +0.890i \end{Bmatrix}$	$\begin{Bmatrix} 0.4122 \\ +0.809i \end{Bmatrix}$	$\begin{Bmatrix} 0.0488 \\ +0.3090i \end{Bmatrix}$	

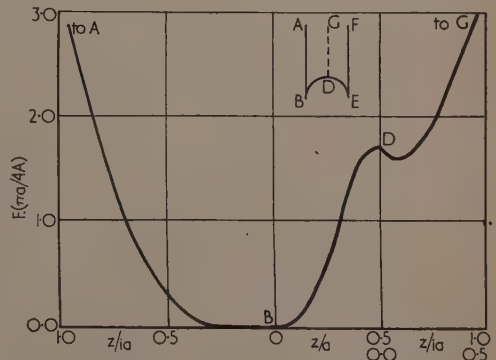


Fig. 5. Variation of field strength  $F$

These results when plotted give the graph of Fig. 5. The variation of  $F$  along the sides  $AB$  and  $BD$  are what would be expected. An interesting point, however, is the presence of a minimum in  $F$  along the axis  $DG$  at a distance of about  $0.077ia$  from  $D$ .

#### THE CORRUGATED SHEET OF FIG. 2

We are now in a position to investigate the field of the corrugated sheet. The field above the sheet, that is, above the concave side, as indicated in Fig. 2, will be obtained first. We need consider only the field within the cell  $ABDEF$  of Fig. 2. This cell consists of a semi-circular conductor  $BDE$  at a potential of  $+V_0$  volts and two parallel lines of force  $BA$  and  $EF$  terminating at infinity. The perimeter  $ABDEF$  and the enclosed area must be transformed so that the edge  $ABDEF$  becomes the real axis of the  $c$ -plane and the area becomes the upper half of this plane. Taking  $D$  as the origin of the  $z$ -plane, the required transformation has been shown to be <sup>(1)</sup>

$$z = ia \cdot (K' - E')/E + a \cdot (1 - i)/2 \quad (6)$$

The  $c$ -plane is shown in Fig. 6, where the portion  $BDE$  corresponds to the conductor.

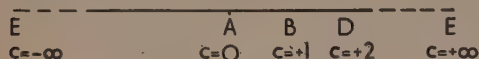


Fig. 6. The  $c$ -plane

The electrical transformation. In the  $W$ -plane (see Fig. 4) the line  $ABDEF$  which has the equation  $W = U + i \cdot V_0$  must be made to correspond to the portion  $BDE$  of the  $c$ -plane. Thus the values of  $c$  at its ends must be  $c = \infty$  and  $c = +1$ . The transformation is obtained using the Schwarz-Christoffel equation, the angles at the corners of the figure in the  $W$ -plane being all right angles. Thus the required electrical transformation is

$$dW = B \cdot dc / [c\sqrt{c-1}] \quad (7)$$

This equation can be integrated by putting  $c = \sec^2 \phi$ , hence

$$W = 2B \cdot \cos^{-1}(1/k) + B_1 \quad (8)$$

where  $B$  and  $B_1$  are constants. When  $c = 1$  then  $W = i \cdot V_0$  so that  $B_1 = i \cdot V_0$ . To evaluate  $B$ , we suppose that the charge on the portion  $BD$  of the conductor per unit depth is  $q$ . Then  $q = (W_2 - W_1)/4\pi$ , where  $W_2$  is the value of  $W$  at the corner  $B$  and  $W_1$  that at the point  $D$ . Hence

$$B = 8q \quad (9)$$

Thus  $B$  is four times the total charge on the end  $BDE$ .

#### THE FIELD STRENGTH

If  $F$  is the electrical intensity at any point in the  $z$ -plane then

$$F = |(dW/dc) \cdot (dc/dz)|$$

It has been shown that  $dc/dz = -4cE^2/ia\pi$ . Hence

$$F = (4B/\pi a)|E^2/k'| \quad (10)$$

At the point  $B$ ,  $c = 1$  so that  $F = \infty$ . At the point  $E$ ,  $c = \infty$  and it can be shown that the limiting value of  $E/k'$  when  $c$  approaches  $\infty$  is  $i \cdot \infty$ . Thus  $F = \infty$  at the point  $E$ .

At the points  $A$  and  $F$ ,  $c = 0$  and  $E = \pi/2$ , hence  $F = 4\pi q/a$ . These values of  $F$  are satisfactory. For a flat plate,  $F = 4\pi q/a$  for a length  $a$ , which is the same as the above value for  $F$  at a great distance from the corrugations. This fact verifies the correctness of equation (10).

#### Results for conductor of Fig. 2

(1) Field strength  $F$  along the line  $BA$ . The field strength  $F$  (e.s.u. or e.m.u.) is expressed as a multiple of  $(\pi a/4B)$  and the positions of the points along  $BA$  are measured in terms of  $a$  from the point  $B$ . These distances are called  $s_1$ .

Table 5. Field strength along  $BA$ . (See also Fig. 7)

$s_1/a = 0.000i$	0.025i	0.085i	0.176i	0.301i
$s_2/a = 1.571i$	1.596i	1.656i	1.747i	1.872i
$F.(\pi a/4B) = \infty$	6.235	3.663	2.932	2.648
$s_1/a = 0.376i$	0.666i	1.09i	$\infty i$	
$s_2/a = 1.947i$	2.237i	2.661i	$\infty i$	
$F.(\pi a/4B) = 2.582$	2.488	2.476	2.465	

The distances  $s_2/a$  are measured from the point  $D$  for ease of plotting and are obtained by adding  $1.571i$  to  $s_1/a$ .

(2) Field strength along  $BD$ . The modulus  $c$  varies between 1.000 and 2.000 along  $BD$ . The points concerned are located by their horizontal distances from the point  $D$ , that is, the values of  $F.(\pi a/4B)$  are tabulated against the real part of  $z/a$ .

Table 6. Field strength along  $BD$ . (See also Fig. 7)

$z/a = 0.000$	0.067	0.121	0.223
$F.(\pi a/4B) = 0.719$	0.822	0.896	1.138
$z/a = 0.388$	0.477	0.500	
$F.(\pi a/4B) = 2.315$	5.32	$\infty$	

(3) Field strength along the axis of symmetry  $DG$ . The origin of the  $c$ -plane is altered as explained above using the transformation  $c = 2/(1 + c_2)$  so that the line  $DG$  becomes

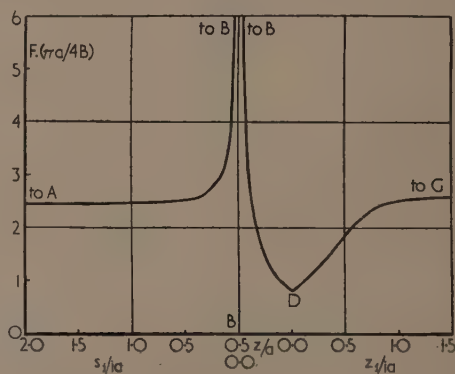


Fig. 7. Variation of field strength  $F$

the negative imaginary axis of the  $c_2$ -plane. Any point along  $DG$  corresponds to  $c_2 = -i \cdot \alpha$  and hence to complex  $c$  as shown below. The points are located by their distances from  $D$  in terms of  $i \cdot a$ .



Table 7. Field strength along DG. (See also Fig. 7)

$c =$	2.000	$\begin{Bmatrix} 1.9877 \\ +0.1564i \end{Bmatrix}$	$\begin{Bmatrix} 1.951 \\ +0.309i \end{Bmatrix}$
$z/a =$	0.000	0.076i	0.151i
$F.(\pi a/4B) =$	0.718	0.845	0.971
$c =$	$\begin{Bmatrix} 1.890 \\ +0.458i \end{Bmatrix}$	$\begin{Bmatrix} 1.808 \\ +0.5878i \end{Bmatrix}$	$\begin{Bmatrix} 1.588 \\ +0.810i \end{Bmatrix}$
$z/a =$	0.207i	0.252i	0.361i
$F.(\pi a/4B) =$	1.097	1.128	1.469
$c =$	$\begin{Bmatrix} 1.309 \\ +0.951i \end{Bmatrix}$	$\begin{Bmatrix} 1.000 \\ +1.000i \end{Bmatrix}$	$\begin{Bmatrix} 0.5458 \\ +0.890i \end{Bmatrix}$
$z/a =$	0.451i	0.542i	0.688i
$F.(\pi a/4B) =$	1.706	1.899	2.196

These results are plotted in Fig. 7. Here it can be seen that  $F$  becomes infinite at the corner  $B$ , and has a minimum at the point  $D$ , as expected. As we approach  $A$  or  $G$  the value of  $F$  approaches  $2.196(4B/\pi a)$ .

THE CORRUGATED SHEET OF FIG. 3

The field below the corrugations, that is, above the convex side as shown in Fig. 3, will now be investigated. As in the previous problem, we need only consider the field inside the cell  $ABDEF$  consisting of a semi-circular conductor  $BDE$  at a potential  $+V_0$  e.s.u. and diameter  $a$ , and the two infinite parallel lines of force  $AB$  and  $EF$ . To transform  $ABDEF$  into the real axis of the  $c$ -plane we use the transformation of the problem of Fig. 1 with the origin in the  $z$ -plane moved to the point  $D$ . Thus the geometrical transformation is

$$z = ia \cdot K'/K - a(1 + i)/2 \quad (11)$$

The electrical transformation is the same as in the last problem, so that the expression for the electrical intensity at any point in the  $z$ -plane is

$$F = (4B/\pi a) \cdot |k' \cdot K^2| \quad (12)$$

where  $B$  is a constant equal to four times the charge on the curved end  $BDE$  per unit depth, as before. At the points  $A, G$  and  $F, c = 0, k' = 1$  and  $K = -\pi/2$ , so that  $F = B\pi/a$ . At the point  $B, c = 1, k' = 0$  and  $K = \infty$ , which give  $F = 0$ . At the point  $E, c = \infty, k' = -\infty$  and by using the expressions for when the elliptic modulus is greater than unity we obtain  $F = 0$  at  $E$ . Thus the values for  $F$  at the corners are satisfactory. At the point  $D$  where  $c = 2$  we obtain  $F = 0.786 \cdot (4B/\pi a)$ . For a flat plate,  $F = 4\pi q/a$ , which is the same as that given by equation (12) at the points  $A, G$  or  $F$ . As will be seen later,  $F$  is approximately equal to  $4\pi q/a$  at a distance of about  $0.5a$  from the surface, so that the effect of the corrugations disappears quite rapidly.

Results for conductor of Fig. 3

(1) *Field strength along BA.* Along  $BA$  the modulus  $c$  varies from 0 to unity at  $B$ , so we have to evaluate equation (12) for these values. The intensity  $F$  is expressed in terms of  $(4B/\pi a)$  and the points are located by their distances from  $B$  in terms of  $a$ . These distances are called  $s_1$ , so that  $s_1/a$  is tabulated.

Table 8. Field strength along BA. (See also Fig. 8)

$s_1/a = \infty$	1.99	1.742	1.278	0.923	0.780
$F.(\pi a/4B) =$	2.470	2.468	2.466	2.460	2.408
$s_1/a = 0.503$	0.411	0.289	0.262	0.000	
$F.(\pi a/4B) =$	1.726	1.280	0.517	0.327	0.000

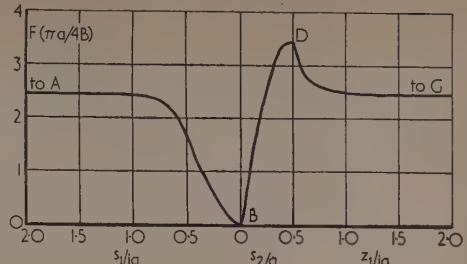


Fig. 8. Variation of field strength  $F$

(2) *Field strength along BD.* Along  $BD$  the modulus varies from unity at  $B$  to 2.000 at the point  $D$ . Equation (12) must therefore be rewritten for moduli greater than unity and it then becomes  $F = (4B/\pi a) \cdot |ik'K^2/k|$ . The position of any point along  $BD$  is given by the real part of its complex co-ordinate. This distance is called  $s_2$  so that  $s_2/a$  is tabulated, the distances being measured from the point  $B$ .

Table 9. Field strength along BD. (See also Fig. 8)

$c =$	1.000	1.002	1.005	1.030
$s_2/a =$	0.000	0.099	0.127	0.146
$F.(\pi a/4B) =$	0.000	0.864	1.392	1.528
$c =$	1.133	1.334	1.703	2.000
$s_2/a =$	0.202	0.295	0.460	0.500
$F.(\pi a/4B) =$	2.13	2.62	3.41	3.438

(3) *The field strength along the centre line DG.* Along  $DG$  the modulus is complex so that the transformation  $c = 2/(1 + c_2)$  is performed. The position of any point along  $DG$  is measured by its distance from  $D$  in terms of  $ia$ , this distance being called  $z_1$ .

Table 10. Field strength along DG. (See also Fig. 8)

$z_1/ia =$	0.000	0.015	0.038	0.060
$F.(\pi a/4B) =$	3.44	3.32	3.21	3.12
$c =$	2.000	$\begin{Bmatrix} 1.9877 \\ +0.1564i \end{Bmatrix}$	$\begin{Bmatrix} 1.951 \\ +0.3090i \end{Bmatrix}$	$\begin{Bmatrix} 1.890 \\ +0.458i \end{Bmatrix}$
$z_1/ia =$	0.077	0.084	0.123	0.145
$F.(\pi a/4B) =$	3.04	2.95	2.88	2.83
$c =$	$\begin{Bmatrix} 1.808 \\ +0.5878i \end{Bmatrix}$	$\begin{Bmatrix} 1.707 \\ +0.707i \end{Bmatrix}$	$\begin{Bmatrix} 1.588 \\ +0.810i \end{Bmatrix}$	$\begin{Bmatrix} 1.454 \\ +0.890i \end{Bmatrix}$
$z_1/ia =$	0.175	0.200	0.236	0.270
$F.(\pi a/4B) =$	2.77	2.71	2.66	2.60
$c =$	$\begin{Bmatrix} 1.309 \\ +0.951i \end{Bmatrix}$	$\begin{Bmatrix} 1.1564 \\ +0.9877i \end{Bmatrix}$	$\begin{Bmatrix} 1.000 \\ +1.000i \end{Bmatrix}$	$\begin{Bmatrix} 0.8434 \\ +0.9877i \end{Bmatrix}$
$z_1/ia =$	0.352	0.433	0.768	$\infty$
$F.(\pi a/4B) =$	2.56	2.53	2.48	2.47
$c =$	$\begin{Bmatrix} 0.5458 \\ +0.890i \end{Bmatrix}$	$\begin{Bmatrix} 0.4122 \\ +0.809i \end{Bmatrix}$	$\begin{Bmatrix} 0.0488 \\ +0.309i \end{Bmatrix}$	0.000

#### REFERENCES

- (1) DAVY, N., and LANGTON, N. H. *Brit. J. Appl. Phys.*, **3**, pp. 156-8 (1952).
- (2) NEHARI, Z. *Conformal Mapping*, p. 318 (New York: McGraw-Hill Book Co. Inc., 1952).
- (3) CAMBI, E. *J. Math. Phys.*, **26**, p. 234 (1948).

# On the Tardy and Sénarmont methods of measuring fractional relative retardations

By H. T. JESSOP, M.Sc., F.Inst.P., University College, London

[Paper received 23 January, 1953]

An investigation into the errors in measurements by the Tardy and Sénarmont methods shows: (i) that the errors due to inaccurate quarter-wave plates are less in the Sénarmont method than in the Tardy, (ii) that errors due to inaccurate setting of the polaroids are of the same order in both methods, and (iii) that in general the error in the final setting of the analyser is the only one which need be considered. A full account is given of the less well-known Sénarmont method.

For most photoelastic observations the Tardy and Sénarmont methods have superseded the old compensator method of measurement, since they require no apparatus additional to the standard photoelastic bench, are more convenient in operation and are generally capable of greater accuracy.

Of the two methods, the Tardy is by far the better known and the more generally used, probably because of a mistaken idea that any errors in the two quarter-wave plates employed in this method could be made to oppose each other and so reduce the total error in the readings. It can be shown, however, that this is not the case, and that, whatever be the relative magnitudes and signs of the errors in the two plates, the errors they produce in Tardy readings are always greater than those in Sénarmont readings.

## ANALYSIS OF THE SÉNARMONT METHOD

In this method the polarizer and analyser are set "crossed" with their vibration axes at  $45^\circ$  to the axes of principal stress at the point under observation in the model. Thus the plane polarized vibration  $\vec{OP}$  [Fig. 1(a)] is resolved on entering the

model into two vibrations  $\vec{OX}, \vec{OY}$  of equal amplitude and initially in phase. If  $Ox$  is the "fast" axis in the model, the vibration  $Ox$  will gain on  $Oy$  by some phase-angle,  $\phi$ , during the passage of the waves through the model, so that

on emergence  $\vec{OX}$  will lead  $\vec{OY}$  by an angle  $\phi$ , giving the equivalent elliptic vibration  $KLK'L'$ , described in the direction indicated by the arrows. The light now passes through the quarter-wave plate whose axes  $Oq, Oq'$  are at  $45^\circ$  to  $Ox$  and  $Oy$  (that is parallel to the principal axes of  $KLK'L'$ ). On entering this plate the elliptic vibration is

resolved into the two vibrations  $\vec{OQ}$ ,  $\vec{OQ'}$  [Fig. 1(b)], where  $\vec{OQ}$  leads  $\vec{OQ'}$  by a phase-angle  $\pi/2$ . In traversing the quarter-wave plate this lead is either reduced to zero or increased to  $\pi$  according as  $Oq'$  or  $Oq$  is the fast axis of the plate. Thus the elliptic vibration is converted to a linear vibration,  $\vec{OP'}$  or  $\vec{OP''}$ . In either case the analyser, whose vibration axis was initially normal to  $Oq$ , must be turned through an angle of magnitude  $\theta$  (or  $\pi - \theta$ ) to produce extinction.

In Fig. 1(a) it is seen from considerations of symmetry that the time of describing the arc  $KT$  of the ellipse is equal to that of describing  $TL$ , and that, therefore,  $X\hat{O}M = M\hat{O}R = \frac{1}{2}\phi$ . Also comparing the triangles  $QOP'$  in Fig. 1(b) and  $NOM$  in Fig. 1(a), we see that

$$OQ = OT = \sqrt{2}ON$$

and

$$OP' \doteq OP = \sqrt{2}OX = \sqrt{2}OM$$

Therefore the triangles are similar and  $\theta = \frac{1}{2}\phi$ .

The effect of an error in the quarter-wave plate will be to

produce a narrow elliptical vibration, such as is indicated by the broken line in Fig. 1(b), instead of a linear vibration. In this case, when measuring a relative retardation, the analyser will be turned to the position which gives minimum intensity of transmitted light; i.e. with its vibration direction perpendicular to the major axis of the narrow ellipse, and in general this axis will not coincide with  $OP'$ . The magnitude of the resulting error in measurement of  $\phi$  is, however, not easily calculated from the geometry of the figure, but is best obtained from an algebraic analysis.

Let the vibration from the polarizer be represented by

$$u = \sqrt{2a} \cos nt$$

in direction  $\vec{Op}$  [Fig. 1(a)].

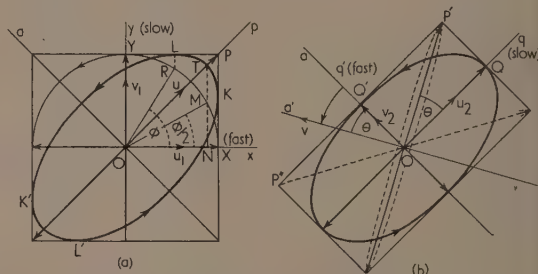


Fig. 1. Vector diagrams in the plane of the wave-front for the Sénarmont method, showing (a) plane polarized vibrations converted to elliptical vibrations by a relative retardation  $\phi$  radians in the model, (b) the elliptical vibrations converted to plane polarized vibrations by a relative retardation  $\frac{1}{2}\pi$  in the quarter-wave plate

On entering the model in which the axes of principal stress,  $Ox$  and  $Oy$ , are at  $45^\circ$  to  $Op$ , we shall have two vibrations,

$u_1 = a \cos nt$  along  $Ox$ , and  $v_1 = a \cos nt$  along  $Oy$ .

Emerging from the model, if the  $u_1$  vibration has gained a phase angle  $\phi$ , we shall have

$$u'_1 = a \cos (nt + \phi), \quad v'_1 = a \cos nt$$

(neglecting phase changes common to the two waves).

Entering the quarter-wave plate these are resolved into  $u_2 = (u_1' + v_1')/\sqrt{2}$ , and  $v_2 = (v_1' - u_1')/\sqrt{2}$  in the directions of the quarter-wave plate axes as indicated in Fig. 1(b).

These give

$$u_2 = a/\sqrt{2}[\cos(nt + \phi) + \cos nt] = \sqrt{2}a \cos \frac{1}{2}\phi \cos(nt + \frac{1}{2}\phi)$$

$$v_2 = a/\sqrt{2}[\cos nt - \cos (nt + \phi)] = \sqrt{2}a \sin \frac{1}{2}\phi \sin (nt + \frac{1}{2}\phi)$$

If the error in the quarter-wave plate is  $\epsilon$  radians, so that the relative retardation produced in the waves passing through it is  $(\pi/2 + \epsilon)$ , we shall have emerging from the plate,  $Oq'$  being the fast axis,

$$u'_2 = \sqrt{2a} \cos \frac{1}{2}\phi \cos (nt + \frac{1}{2}\phi) \\ v'_2 = \sqrt{2a} \sin \frac{1}{2}\phi \cos (nt + \frac{1}{2}\phi + \epsilon)$$

If the analyser be now rotated through an angle  $\theta$  from its initial position, the vibration passing through it will be

$$v = v'_2 \cos \theta - u'_2 \sin \theta \\ = \sqrt{2a} \sin \frac{1}{2}\phi \cos \theta \cos (nt + \frac{1}{2}\phi + \epsilon) \\ - \sqrt{2a} \cos \frac{1}{2}\phi \sin \theta \cos (nt + \frac{1}{2}\phi) \\ = \sqrt{2}[(a \cos \epsilon \sin \frac{1}{2}\phi \cos \theta - \cos \frac{1}{2}\phi \sin \theta) \\ \cos (nt + \frac{1}{2}\phi) - \sin \epsilon \sin \frac{1}{2}\phi \cos \theta \sin (nt + \frac{1}{2}\phi)]$$

The square of the amplitude of this is

$$A^2 = \sin^2 \frac{1}{2}\phi \cos^2 \theta + \cos^2 \frac{1}{2}\phi \sin^2 \theta - \frac{1}{2} \cos \epsilon \sin \phi \sin 2\theta$$

The amplitude will be a maximum or minimum when

$$\partial(A^2)/\partial\theta = 0$$

i.e. when

$$-\sin^2 \frac{1}{2}\phi \sin 2\theta + \cos^2 \frac{1}{2}\phi \sin 2\theta - \cos \epsilon \sin \phi \cos 2\theta = 0$$

that is when

$$\tan 2\theta = \tan \phi \cos \epsilon \\ \simeq \tan \phi (1 - \frac{1}{2}\epsilon^2)$$

The error in  $\tan 2\theta$  is then  $-\frac{1}{2}\epsilon^2 \tan \phi$ , and the error in  $2\theta$  is given by

$$\Delta(2\theta) = \Delta(\tan 2\theta) \cos^2 2\theta \simeq -\frac{1}{2}\epsilon^2 \tan \phi \cos^2 \phi \\ |\Delta(2\theta)| \simeq \frac{1}{2}\epsilon^2 \sin 2\phi \quad (1)$$

#### THE TARDY METHOD

The principle of the Tardy method is the same as that of the Sénarmont, but in this case the light entering the model is, in the ideal case, circularly polarized by passage through the first quarter-wave plate. The geometrical analysis is a little longer than that for the Sénarmont method, but follows similar lines. The operation of the second quarter-wave plate is precisely the same as before, and it is easily shown that, in this case also, the relation  $\theta = \frac{1}{2}\phi$ , holds if both quarter-wave plates are free from error. The assessment of the effect of errors in the plates is again best done by an algebraic analysis of the vibrations.

Such an analysis has already been made for the Tardy method. Mindlin<sup>(1)</sup> worked out the effect of quarter-wave plate errors in a "crossed" circular polariscope, and Hickson<sup>(2)</sup> deduced from his results an expression for the rotation of the analyser in a Tardy measurement in the form

$$\tan 2\theta = \sin \phi / (\tan \epsilon_1 \sin \epsilon_2 + \cos \epsilon_2 \cos \phi) \quad (2)$$

where  $\theta$  is the rotation of the analyser,  $\phi$  the fractional relative retardation in the model,  $\epsilon_1$  and  $\epsilon_2$  the errors in the first and second quarter-wave plates respectively.

This is not in a convenient form for assessing the error of the observation, but if we invert the expression for  $\tan 2\theta$  and apply the method used in obtaining equation (1) we find

$$\cot 2\theta = \cot \phi \cos \epsilon_2 + \tan \epsilon_1 \sin \epsilon_2 \operatorname{cosec} \phi \\ \simeq \cot \phi (1 - \frac{1}{2}\epsilon_2^2) + \epsilon_1 \epsilon_2 \operatorname{cosec} \phi$$

Thus  $\Delta(\cot 2\theta) \simeq \epsilon_1 \epsilon_2 \operatorname{cosec} \phi - \frac{1}{2}\epsilon_2^2 \cot \phi$

and  $|\Delta(2\theta)| \simeq \epsilon_1 \epsilon_2 \sin \phi - \frac{1}{2}\epsilon_2^2 \sin 2\phi \quad (3)$

#### COMPARISON OF ERRORS

The relation between the errors of the two methods is best appreciated by a study of a graph of the errors plotted against  $\phi$ . Fig. 2 shows the errors on the assumption that  $\epsilon_1$  and  $\epsilon_2$  are of the same magnitude  $\epsilon$ . The maximum error in the Tardy reading is more than four times that in the Sénarmont, and this ratio will be increased if  $\epsilon_1$  is greater than  $\epsilon_2$ . Now

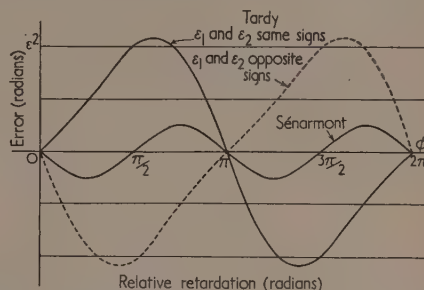


Fig. 2. Graphs of errors in the measurement of relative retardations by the Tardy and Sénarmont methods. The errors  $\epsilon_1$  and  $\epsilon_2$  in the quarter-wave plates are here assumed equal

it is always possible to put the more accurate of a pair of quarter-wave plates at the analyser, and if this is done there will be no value of  $\phi$  for which the error in the Tardy method is less than that in the Sénarmont, while the maximum errors will be in a ratio greater than four to one. It may, however, be noted from equation (3) that if the error  $\epsilon_2$  in the second quarter-wave plate is very small, a considerable error in the first plate may be present with negligible effect even on the Tardy readings.

In equations (1) and (3) above the errors all appear in radians. If  $\delta$  is the quarter-wave plate error in wavelengths,  $\epsilon = 2\pi\delta$ , and the reading errors in wavelengths for the two methods will be

$$2\pi\delta_1\delta_2 \sin \phi - \frac{1}{2}\pi\delta_2^2 \sin 2\phi, \text{ and } \frac{1}{2}\pi\delta_2^2 \sin 2\phi$$

respectively. The graph of Fig. 3 shows the maximum error obtained in Sénarmont readings for an error  $\delta$  wavelengths in the second quarter-wave plate.

Measurements were recently carried out by the author on ten quarter-wave plates (five of diameter 6 in and five of 4 in), all described by the suppliers as of good accuracy. In

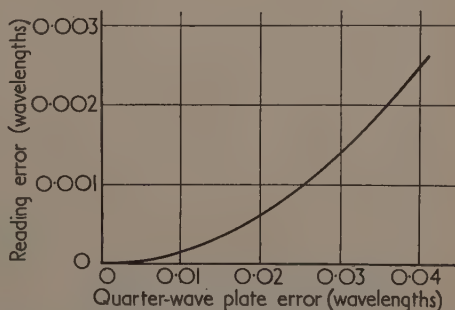


Fig. 3. Graph of the maximum error in readings by the Sénarmont method due to an error  $\delta$  wavelengths in the quarter-wave plate



one of these the error was 0.035 wavelengths, the errors in the other nine ranged from 0.00 to 0.025 wavelengths (all to the nearest 0.005). Even with the most inaccurate of these the maximum error in Sénarmont measurements will be only 0.002 wavelengths, and it is very doubtful whether the conditions of any practical stress-exploration would justify account being taken of such an error.

The error of the first quarter-wave plate of a polariscope may be measured by the Sénarmont method, using the second plate in the normal way. The best method of measuring the error in the second plate will depend upon the construction of the polariscope. We may (a) interchange the two quarter-wave plates, (b) insert another quarter-wave plate between the second plate and the analyser, or (c) reverse the direction of the light path through the polariscope. In each case the Sénarmont method of measurement is used.

#### OTHER ERRORS

Assuming that the graduations of the polaroids and quarter-wave plates are accurate to at least  $0.2^\circ$ , the only other sources of error in Sénarmont or Tardy readings are (i) the initial setting of the polaroids to give the isoclinic through the point under observation, and (ii) the final setting of the analyser to the extinction position. An error in the latter setting leads to a direct error in the value of  $\theta$ , and the probable error from this source in any given measurement may be estimated by repeating the setting a number of times. The effect of an error in the initial isoclinic setting is not, however, immediately obvious.

If, in the Sénarmont method, an error  $\delta$  radians is made in the isoclinic setting, then after turning the polaroids through a further  $45^\circ$ , the polarizer will be inclined to one of the principal stresses in the model, say the  $x$  stress, at an angle  $\tan^{-1}(1 + \delta/1 - \delta)$ . The vibration will then be resolved into two components whose amplitudes will be in the ratio  $1 - \delta : 1 + \delta$ . Let these vibrations be

$$u_1 = (1 - \delta) \cos nt \text{ along } OX, \text{ and } v_1 = (1 + \delta) \cos nt \text{ along } Oy.$$

Emerging from the model we shall have

$$u'_1 = (1 - \delta) \cos(nt + \phi), \quad v'_1 = (1 + \delta) \cos nt$$

Entering the quarter-wave plate these give

$$u_2 = 1/\sqrt{2}[(1 - \delta)^2 \cos(nt + \phi) + (1 + \delta)^2 \cos nt] \text{ along } Oq$$

$$v_2 = 1/\sqrt{2}[(1 - \delta)^2 \cos nt - (1 + \delta)^2 \cos(nt + \phi)] \text{ along } Oq'$$

These emerge from the quarter-wave plate as

$$u'_2 = (1 - \delta)^2 \cos(nt + \phi) + (1 + \delta)^2 \cos nt$$

$$v'_2 = (1 - \delta)^2 \sin(nt + \phi) - (1 + \delta)^2 \sin nt$$

(omitting the  $1/\sqrt{2}$  and the common phase change).

The vibration passing the analyser when it has been turned through an angle  $\theta$  from the crossed position will be

$$\begin{aligned} a &= v'_2 \cos \theta - u'_2 \sin \theta \\ &= \cos \theta \sin(nt + \phi) - \cos \theta \sin nt \\ &\quad - (1 - 2\delta) \sin \theta \cos(nt + \phi) - (1 + 2\delta) \sin \theta \cos nt \end{aligned}$$

(neglecting second order terms in  $\delta$ ).

$$\begin{aligned} &= [\cos \theta \cos \phi - \cos \theta + (1 - 2\delta) \sin \theta \sin \phi] \sin nt \\ &\quad + [\cos \theta \sin \phi - (1 - 2\delta) \sin \theta \cos \phi \\ &\quad - (1 + 2\delta) \sin \theta] \cos nt \end{aligned}$$

The square of the amplitude reduces to

$$A^2 = 2 - 2 \cos 2\theta \cos \phi - 2 \sin 2\theta \sin \phi$$

This is independent of  $\delta$ , and is a minimum when  $\tan 2\theta = \tan \phi$ .

Thus to the first order of the small error  $\delta$  the readings are not affected by errors in setting the polaroids to the initial "isoclinic" position. A similar analysis applied to the Tardy method shows that the same result will follow in this method also.

If second order terms are retained in these analyses, the reading error appears in each method in terms of  $\frac{1}{2}\delta^2$ . Thus if the initial isoclinic setting were in error by as much as two or three degrees, the error in the final reading would still be negligible. Thus with a properly adjusted polariscope and reasonably good quarter-wave plates the only error which need be considered in the most refined measurements is the error in the final setting of the analyser.

#### PRACTICAL CONSIDERATIONS

The sequence of operations in using the Sénarmont method is as follows:

- (i) Rotate crossed polaroids to the position which gives extinction of light at the point under observation.
- (ii) Rotate crossed polaroids through a further  $45^\circ$  and note analyser reading.
- (iii) Insert the analyser quarter-wave plate with its vibration axes parallel to the axes of polarizer and analyser.
- (iv) Rotate the analyser to restore extinction at the point.

The operation of this method is as simple and as rapid as that of the Tardy, the further rotation of the polaroids in (ii) replacing the insertion and adjustment of the polarizer quarter-wave plate, and there would appear to be no respect in which the Tardy method has any advantage.

One point which must be considered is the direction of rotation of the analyser which will give the reading  $\theta = \frac{1}{2}\phi$ . The determination of this from the theory would necessitate consideration of the directions of the "fast" and "slow" axes in both model and quarter-wave plate in relation to the vibration direction of the polarizer. This might be somewhat confusing in view of the differences in the sign of the stress-optical effect in different materials and in some cases in the same material for the frozen-stress and stress under direct loading. There is, however, a simple practical means of determining the direction of rotation, which is quite dependable provided that attention is paid to one consideration. It must be borne in mind that while using these methods the fringe-pattern is significant only at points in the model at which the principal stresses are correctly oriented with respect to the polarizer, that is at points on the isoclinic line passing through the point under observation. At other points in the field the fringes may move in an erratic manner, and will, in general, change in intensity as the analyser is rotated. The position of the isoclinic should be noted when the polaroids are first turned to extinction, and subsequent observations of the movement of fringes must be confined to the path of this isoclinic.

The direction of rotation of the analyser which leads to the relation  $\theta = \frac{1}{2}\phi$  is that which causes the extinction fringe to move along the trace of the isoclinic in the direction of increasing fringe-order. The angle of rotation in the opposite direction will, of course, be  $(\pi - \frac{1}{2}\phi)$ . Both settings should be made in any measurement, for it will frequently be found

## REFERENCES

- (1) MINDLIN, R. D. *J. Opt. Soc. Amer.*, **27**, p. 289 (1937).  
(2) HICKSON, V. H. *Brit. J. Appl. Phys.*, **3**, p. 176 (1952).

[Paper received 22 September, 1952]

A technique enabling systematic observations of metallurgical features in the electron microscope is outlined. Such features of interest are suitably marked; and wet stripped plastic replicas are prepared in the normal manner. A simple apparatus, briefly described, allows one to position these replicas on electron microscope specimen grids as desired. This permits direct comparison of electron and photo micrographs of any surface detail. In addition, changes in surface detail or of a given feature in depth may be followed.

by many workers. Some preliminary experiments, from which this method was subsequently developed at the National Physical Laboratories, were carried out with Dr. R. I. Garrod at the Chemical and Physical Research Laboratories, Melbourne.

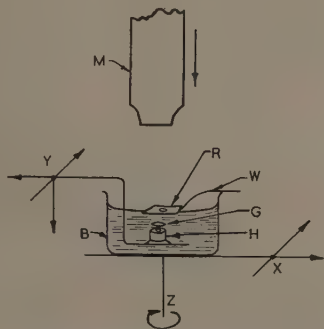


Fig. 1. Schematic arrangement of apparatus for positioning replica  $R$  on grid  $G$

A number of investigators have used fine reference scratches on the surface to identify particular areas. However, such a method suffers from the disadvantage that the area itself may be obscured by the specimen grid. Recently, Hyam and Nutting<sup>†</sup> have reported a more elaborate method of positioning the grid over the selected area. This entails dry-stripping of the replica whereas the method to be described herein is primarily designed for the wet-stripping technique advocated

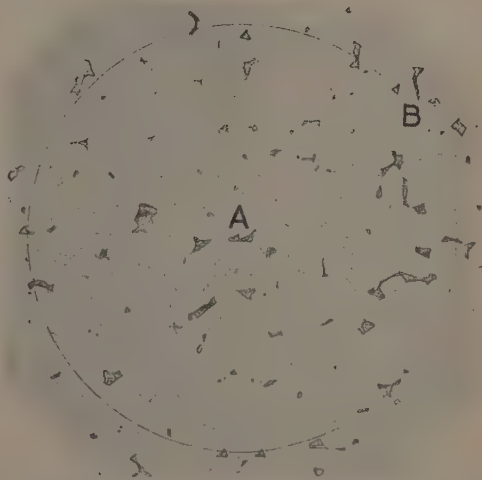
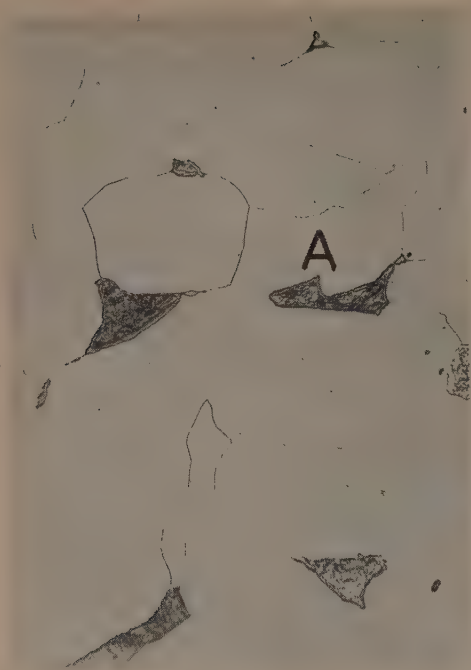


Fig. 2. Optical micrograph showing scribed circle around feature of interest *A*. Magnification  $\times 30$

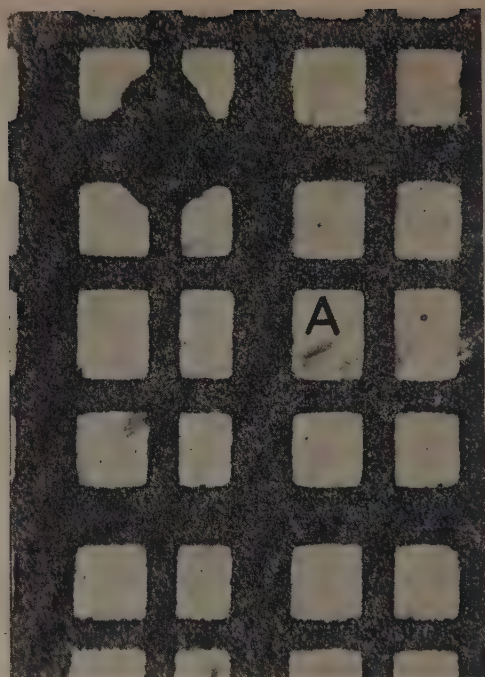
The technique is as follows: The specimen, suitably polished and etched, is mounted in a Bergsman micro-hardness tester. This apparatus bolts on to the platform of a metallurgical projection microscope and is essentially a beam balanced about a horizontal axis. Viewing the specimen with a high power objective (4 mm), the area of interest is brought to the centre of the field of view. The objective is replaced by a Vickers hardness diamond, offset from the optical axis by

\* Now at Cavendish Laboratory, Cambridge.

† HYAM, E. D., and NUTTING, J. *Brit. J. Appl. Phys.*, 3, p. 173 (1952).



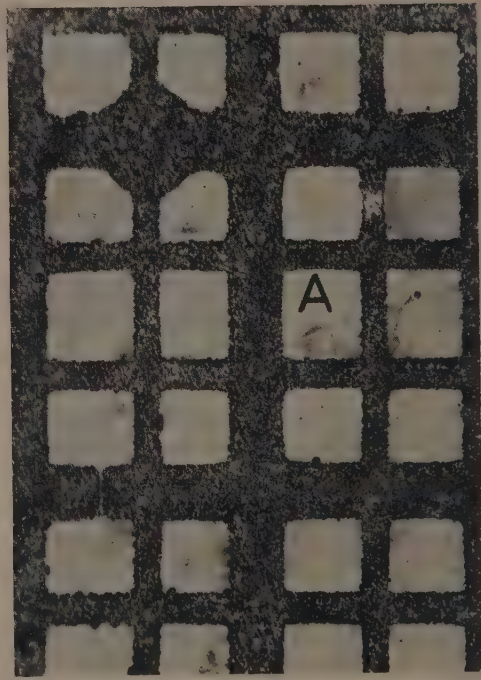
(a)



(b)



(c)



(d)

Fig. 3. (a) Optical micrograph showing feature of interest *A*. Magnification  $\times 150$ . (b), (c), (d) Optical micrographs showing three successive Formvar replicas of feature of interest *A*. Magnification  $\times 150$



1 mm. The microscope table is lowered until the diamond is in contact with the specimen and then rotated about the optical axis, so that the diamond scribes a circle on the surface. A suitable width of ruling, which is determined by the load on the diamond point, is about  $3\ \mu$ .

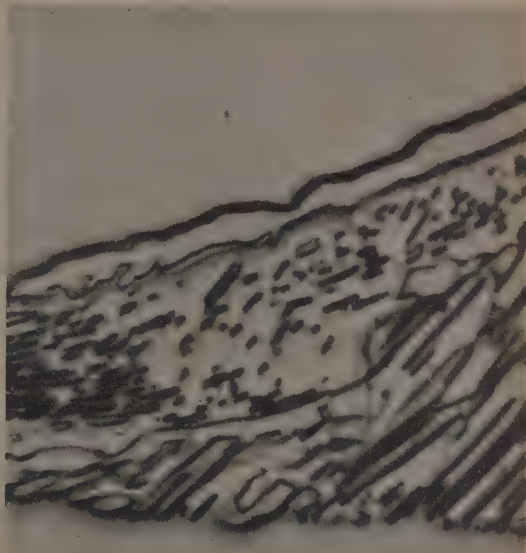
A replica of the surface is next prepared. Throughout this work it was found most satisfactory to use a Formvar replica ( $\frac{1}{2}\%$  Formvar in chloroform) backed by a film of 2% nitrocellulose in iso-propyl-acetate. An important property of this composite film is that considerable surface detail can be seen under the optical microscope with vertical illumination

dripping from a burette. After drying, the Formvar replica is ready for examination in the electron microscope. This method, with some modification, is also suitable if shadowing of the replica is desired.

The application of the method is illustrated by the following micrographs of a pure iron-carbon alloy (0.044% C). Fig. 2 is an optical micrograph ( $\times 30$ ) showing the scribed circle around a chosen area of interest *A*, in this case a particular region of pearlite. The gap, *B*, in the circle defines the orientation and position of the micrographs with respect to the specimen. Fig. 3(a) shows the same feature, under an



(a)



(b)

Fig. 4. (a) Electron micrograph of area of interest. Magnification  $\times 2500$ . (Unshadowed Formvar replica taken at an initial magnification of  $\times 1100$ ). (b) Optical micrograph of area of interest. Magnification  $\times 2500$

when the stripped film is floating on water. This greatly assists correct placing of the replica on the specimen grid.

Referring to Fig. 1, the replica *R* floating in the beaker *B* has one edge resting on a wire *W* which maintains the replica in a fixed position relative to the beaker. The beaker is moved by the translational motions *X* until the feature of interest on the replica is visible in the centre of the field of view of the optical microscope *M*. The scribed circle helps to locate this feature. An overall magnification of about  $\times 100$  is suitable for the microscope. The electron microscope grid *G* carried on a hollow pedestal *H* is moved by the three translational motions *Y* until its centre is just below the centre of the circle on the replica. Final adjustment of the movements *X* and *Z* are made to bring the feature of interest into a suitable grid square and to orient it with respect to the grid bars. This latter operation is desirable if several features are to be studied in a series of replicas from the same specimen. The pedestal and grid are now raised to lift the replica from the surface of the water. The slight suction down the hollow pedestal tends to hold the replica in position. The film on the grid, still supported on the pedestal, is dried and then softened with amyl acetate vapour. After about half an hour, the nitro-cellulose backing film is dissolved with amyl acetate

optical magnification of  $\times 150$ . Figs 3 (b, c and d) also at a magnification of  $\times 150$ , show three replicas ready for examination in the electron microscope. These replicas, prepared from three successive strippings, clearly indicate the precision of the method. The letter *A* denotes the same pearlitic region in each case. Finally Fig. 4 shows electron and optical micrographs of this region at a magnification of  $\times 2500$ .

In conclusion, it must be pointed out that the accuracy of the method relies in no way on precision machining of the components of the positioning apparatus, and in fact, these may be of any simple and convenient design.

#### ACKNOWLEDGEMENTS

The author wishes to acknowledge his indebtedness to Mr. J. Trotter for advice and helpful discussion. He also acknowledges that he is a scientific officer of the Chemical and Physical Laboratories, Melbourne, on attachment to the N.P.L. The work described above has been carried out as part of the general research programme of the National Physical Laboratory, and this paper is published by permission of the Director of the Laboratory.

# A model for demonstrating dislocations in crystals

By DR. H. G. VAN BUEREN, Philips Research Laboratories, N. V. Philips' Gloeilampenfabrieken, Eindhoven Netherlands

[Paper received 30 September, 1952]

A simple dynamic model, in which the interatomic forces are simulated partially by magnetic forces and partially by the elastic forces exerted by small springs, is described. With it the movement of edge and screw dislocations through a crystal lattice can easily be demonstrated.

In order to demonstrate the occurrence and behaviour of dislocations, several mechanical or semi-mechanical models have been described in literature. One of these is the bubble raft of Bragg and Nye,\* with which it is possible to demonstrate the behaviour of edge dislocations in one atomic plane. Another model is that due to W. Renninger and described by Kochendörfer,† which by means of a system of magnets can show a cross-section through a moving edge dislocation. A very illustrative model is that of Bilby,‡ which, however, is a static one.

The model to be described can demonstrate the behaviour of edge as well as of screw dislocations. By means of it, it should be possible to study the influence of other lattice faults on dislocations, the interaction between two dis-

The symmetry of the system of magnets and pendulums corresponds in this model to the simple cubic structure. It is, of course, possible to imitate (two-dimensionally) the close packed structure as well. One extra row of magnets, with no corresponding row of pendulums, has been added.

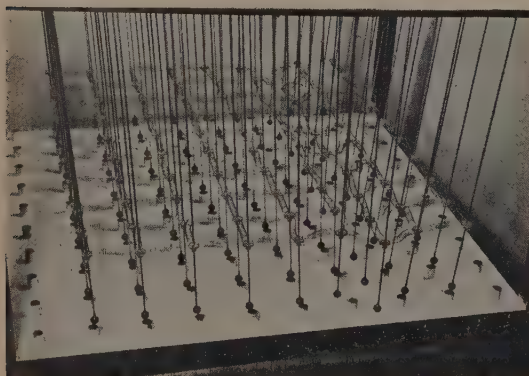


Fig. 1. Model showing positive edge dislocation moving from the right to the left

locations, and the influence of crystal structure, although it must be borne in mind that the behaviour of the model need not necessarily be exactly analogous to the behaviour of dislocations in an actual crystal. The model is not so much meant for study as for instruction.

The model is shown in the figures. It consists of a system of pendulums, suspended from a brass rack that can be moved by hand from the left to the right and back. In the "unstressed" position the pendulums all hang exactly above small bar magnets which are mounted in a bottom baseboard. The pendulums carry small iron spheres that are attracted by the magnets. They are elastically coupled among each other by means of small helical springs, which are unstrained if the rack is in an unstressed position. The distance between the magnets is 4 cm and the vertical distance between the spheres and magnets is 1 mm.

\* BRAGG, W. L., and NYE, J. F. *J. Sci. Instrum.*, **19**, p. 148 (1942); *Proc. Roy. Soc. A*, **190**, p. 474 (1947).

† KOCHENDÖRFER, A. *Plastische Eigenschaften von Kristallen und metallischen Werkstoffen*, p. 67 (Berlin: Springer, 1941).

‡ BILBY, B. A. *J. Inst. Metals*, **76**, p. 613 (1950).

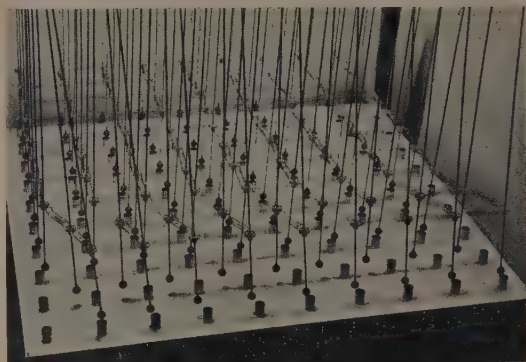


Fig. 2. Screw dislocation; the slip direction is to the right

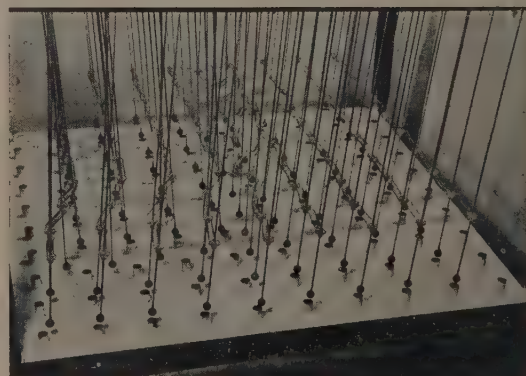


Fig. 3. Combination of edge and screw dislocations: where the edge ends, the screw begins. By moving the rack to the right the edge part runs to the right, the screw part to the front

The plane of the magnets corresponds to one atomic layer in the crystal, and the plane formed by the pendulum spheres to the layer just above it. In the bottom plane, the "atoms" are rigidly mounted—which is not, of course, in agreement with the situation in a real crystal. The behaviour of the system is probably not appreciably influenced by this lack of analogy, whereas the simplicity is very much enhanced.

Fig. 1 shows how, by moving the rack by hand from its



normal position to the left, a positive edge dislocation suddenly appears; it moves very quickly from the right to the left through the lattice to the other side of the "crystal." In Fig. 2 a moving screw dislocation is shown. This dislocation was formed by moving the rack from the normal position obtained in the former experiment, again slightly to the right.

The occurrence of either edge or screw dislocations is largely a matter of chance. In our model, screw dislocations are more easily formed than edge ones, probably because the rack is usually moved somewhat askew over the lattice. The motion of the dislocations is fairly rapid and, after their formation, requires only a very small additional strain.

Fig. 3 shows part of a dislocation ring, consisting of an edge dislocation and a screw dislocation. Such a ring is occasionally formed.

With this model it is easily possible to follow the behaviour of a dislocation when it meets an "impurity" which can be introduced by replacing one magnet by a stronger or weaker one. The effect of stress on a locked dislocation can also be imitated.

This model can be easily constructed, since the strength of the magnets and the springs can be varied between quite large limits without any appreciable effect on the behaviour, except on the speed of motion of the dislocations.

## The tension in strings wrapped slantwise round cylinders

By C. MACK, M.A., British Cotton Industry Research Association, Shirley Institute, Manchester

[Paper first received 9 December, 1952, and in final form 23 January, 1953]

The relations between the tension, normal reaction, coefficient of friction and certain angles involved, are found for a string wrapped slantwise round a cylinder: (i) when moving along a stationary path, friction thus being tangential to this path, and (ii) moving parallel to the cylinder axis, the relative configuration of the string remaining unchanged so that friction is parallel to the axis. In both cases the cylinder is of general cross-section. For certain cross-sections (e.g. circles) it is possible to obtain formulae completely specifying the curves adopted by the string.

### 1. INTRODUCTION

In many applications strings or ropes are wound round various objects and the resulting variation of tension is of considerable practical importance. The formula governing the tension in a string wrapped transversely round a circular cylinder is well known, being

$$T = T_0 \exp(-\mu\theta) \quad (1)$$

where  $\theta$  is the angle between the tangents to the string at the two points whose tensions are  $T$  and  $T_0$ . The string is assumed to be moving, or just about to move, so that the ratio of friction to normal reaction is equal to the coefficient of friction which is assumed to be constant. The generalization of equation (1) to the three-dimensional case of a string wrapped slantwise about a cylinder has not, as far as the author is aware, been given before. In practice, an intuitive value is taken for  $\theta$ : often the angle between the tangents at the two points considered or the angle between the lines formed by projecting these tangents on to a plane. Very serious inaccuracies may arise in this way as may be seen in § 2 of this paper, which compares the accurate with the intuitive formulae.

The formulae developed in this paper are quite simple and though it is true that not many objects are exact cylinders, even of general cross-section, there are many for which a cylinder is a good approximation. We might consider, for example, a torus (or anchor-ring). Here, if the cross-sectional diameter is small compared with the ring diameter, that portion on which the string rubs is quite well approximated by a cylinder. It is also true that exact formulae can be obtained for strings passing over a torus, but they are complicated and difficult to handle.

### 2. STRING MOVING UNIFORMLY ALONG A STATIONARY PATH

**Basic differential equations.** To start with, suppose the string lies on a general surface  $G$ , say; let  $(l, m, n)$  be the direction cosines of the normal to  $G$  at a point  $P \equiv (x, y, z)$

on the path of the string. Suppose  $s$  to be the length of the path measured from some point on it. The tangent to the path at  $P$  then has the direction cosines  $(dx/ds, dy/ds, dz/ds)$ . Now the friction at  $P$  acts along this tangent since the string moves along this path. Thus, if  $T$  is the tension at  $P$ , the forces per unit length on the string at  $P$  are:

(i) the tension, which vectorially is

$$\left[ \frac{d}{ds} \left( T \frac{dx}{ds} \right), \frac{d}{ds} \left( T \frac{dy}{ds} \right), \frac{d}{ds} \left( T \frac{dz}{ds} \right) \right]$$

(ii) the normal force  $N$ , which vectorially is  $N(l, m, n)$ ;

(iii) the friction  $\mu N$ , which vectorially is  $\mu N \left( \frac{dx}{ds}, \frac{dy}{ds}, \frac{dz}{ds} \right)$

(iv) gravity, air resistance, etc.

We shall neglect the forces in (iv) and also shall assume that acceleration forces (e.g. centrifugal, Coriolis) are negligible. The forces (i), (ii) and (iii) are then in equilibrium; hence

$$\frac{d}{ds} \left( T \frac{dx}{ds} \right) + \mu N \frac{dx}{ds} + Nl = 0; \quad \frac{d}{ds} \left( T \frac{dy}{ds} \right) + \mu N \frac{dy}{ds} + Nm = 0;$$

$$\frac{d}{ds} \left( T \frac{dz}{ds} \right) + \mu N \frac{dz}{ds} + Nn = 0 \quad (2)$$

In addition there are two identities to be satisfied, namely

$$\left( \frac{dx}{ds} \right)^2 + \left( \frac{dy}{ds} \right)^2 + \left( \frac{dz}{ds} \right)^2 = 1; \quad \frac{dx}{ds} + m \frac{dy}{ds} + n \frac{dz}{ds} = 0 \quad (3)$$

the latter result expressing the fact that normal and tangent are perpendicular. The first part of equation (3) is automatically satisfied by taking

$$dx/ds = \sin \zeta \cos \psi; \quad dy/ds = \sin \zeta \sin \psi; \quad dz/ds = \cos \zeta \quad (4)$$

Multiplication of the three parts of equation (2) by  $dx/ds$ ,  $dy/ds$ ,  $dz/ds$ , respectively shows that

$$dT/ds + \mu N = 0 \quad (5)$$

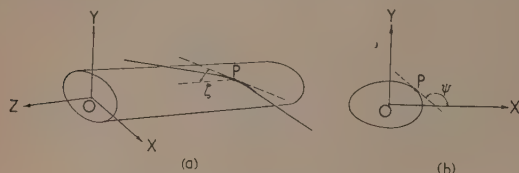
This is a result to be expected on physical grounds since the



friction is always tangential. Substitution from equation (5) in equation (1) yields the results:

$$\frac{d^2x}{ds^2}l = \frac{d^2y}{ds^2}m \quad \frac{d^2z}{ds^2}n = \frac{dT}{ds}(\mu T) \quad (6)$$

The foregoing results hold for a string lying on a general surface. We shall henceforth confine our attention to cylinders and, in such cases, if  $OZ$  is taken to be the cylinder axis the angle  $\zeta$  of equation (4) is the angle made by the tangent at  $P$  with  $OZ$ , while  $\psi$  is the angle made by the tangent to the cross-section at  $P$  with  $OX$  (see the figure).



(a) String passing slantwise over a cylinder

(b) Cylinder cross-section

Furthermore, any normal to the cylinder is parallel to the plane  $OXY$ ; in fact, from the figure we see that

$$l = \sin \psi; m = -\cos \psi; n = 0 \quad (7)$$

Relations between tension, normal force, coefficient of friction,  $\zeta$  and  $\psi$ . We shall prove that:

- (i)  $\zeta$  is constant everywhere on the string;
- (ii)  $T = T_0 \exp [-\mu(\psi - \psi_0) \sin \zeta]$ ; and
- (iii)  $N = (T \sin^2 \zeta) / \rho$  where  $\rho$  is the radius of curvature to the cross-section perpendicular to  $OZ$ .

*Proofs.* Since  $n = 0$  equation (6) shows that

$$d^2z/ds^2 = 0$$

and hence

$$dz/ds \equiv \cos \zeta = \text{constant} \quad (8)$$

Result (i) is thus proved. Now equations (4) and (7) show that

$$\begin{aligned} l \frac{d^2x}{ds^2} + m \frac{d^2y}{ds^2} &= \sin \zeta \left( -\sin^2 \psi \frac{d\psi}{ds} - \cos^2 \psi \frac{d\psi}{ds} \right) \\ &= -\sin \zeta \frac{d\psi}{ds} \end{aligned} \quad (9)$$

and, from equations (6) and (7), we find that

$$l \frac{d^2x}{ds^2} + m \frac{d^2y}{ds^2} = \frac{l^2 + m^2}{\mu T} \cdot \frac{dT}{ds} = \frac{1}{\mu T} \cdot \frac{dT}{ds} \quad (10)$$

By equating these last two results and integrating we prove (ii) provided  $T = T_0$  when  $\psi = \psi_0$ .

If, as a point moves a distance  $s$  along the path, its projection on the plane  $OXY$  moves a distance  $s'$  along the perimeter of the cross-section then, by definition of  $\zeta$ ,

$$ds'/ds = \sin \zeta \quad (11)$$

Further, as  $\rho$  is the radius of curvature of the cross-section at  $P$ , we see that

$$ds'/d\psi \equiv \rho = \sin \zeta (ds/d\psi) \quad (12)$$

Substitution from equations (9), (10) and (12) in equation (5) then proves (iii).

It is worth noting that  $N$  is positive if  $\rho$  is positive and

hence the results proved hold only if the cross-section is convex over the region involved. At any concave region the string will leave the cylinder and meet it again in a convex region.

*Comparison with  $T = T_0 \exp (-\mu\theta)$ .* Here we shall take  $\theta$  as the angle between the tangents at the two points where the tensions are  $T$  and  $T_0$ .

If  $l_1, m_1, n_1$  and  $l_2, m_2, n_2$  are the direction cosines of two lines at an angle  $\alpha$  it is known that

$$\cos \alpha = l_1 l_2 + m_1 m_2 + n_1 n_2 \quad (13)$$

Applying this result and using equation (4), we find that

$$\cos \theta = \sin^2 \zeta (\cos \psi \cos \psi_0 + \sin \psi \sin \psi_0) + \cos^2 \zeta$$

Hence

$$\begin{aligned} 2 \sin^2(\theta/2) &\equiv 1 - \cos \theta = \sin^2 \zeta [1 - \cos(\psi - \psi_0)] \\ &= 2 \sin^2 \zeta \sin^2[(\psi - \psi_0)/2] \end{aligned}$$

$$\text{and thus} \quad \sin(\theta/2) = \sin \zeta \sin[(\psi - \psi_0)/2] \quad (14)$$

Starting with  $\theta = 0$  when  $\psi = \psi_0$  and letting  $\psi$  increase we can show in fact that

$$(\psi - \psi_0) \sin \zeta - \theta \geq 0$$

that is, there is actually a greater difference between  $T$  and  $T_0$  [comparing (b) § 2 with equation (1)] than our "intuitive" value of  $\theta$  would indicate. The proof is as follows. Since, by differentiating equation (14)

$$\cos \frac{\theta}{2} = \sin \zeta \cos \left( \frac{\psi - \psi_0}{2} \right) \frac{d\psi}{d\theta}$$

$$\begin{aligned} \frac{d}{d\theta} [(\psi - \psi_0) \sin \zeta - \theta] &= \sin \zeta \frac{d\psi}{d\theta} - 1 \\ &= \frac{\cos(\theta/2)}{\cos[(\psi - \psi_0)/2]} - 1 \geq 0 \end{aligned}$$

as equation (14) shows that  $\theta/2 \leq (\psi - \psi_0)/2$ . In fact when  $\zeta = 50.6^\circ$  and  $\psi - \psi_0 = \pi$ , then  $(\psi - \psi_0) \sin \zeta - \theta = 0.66$  radians.

It can be seen that, if  $\theta$  is treated as varying continuously with  $\psi$ ,  $\theta$  increases with  $\psi - \psi_0$  until  $\psi - \psi_0$  reaches  $\pi$  when  $\sin(\theta/2)$  reaches its maximum value of  $\sin \zeta$ . Thereafter, as  $\psi$  increases,  $\sin(\theta/2)$  decreases. What should happen to  $\theta$  is not at all clear. Obviously when  $\psi - \psi_0 = 2\pi$  the string has wound completely round the cylinder and it might be reasonable to take  $\theta = 2\pi$ . But then  $(\psi - \psi_0) \sin \zeta = 2\pi \sin \zeta$ . Hence, if  $\zeta$  is small, the use of  $\theta$  can lead to gross errors, the difference between  $T$  and  $T_0$  being greatly exaggerated.

*Equations of the string path for cylinders of various cross-section.* The previous results hold whatever the shape of the cylinder cross-sections. In obtaining the actual paths adopted by the strings it is necessary to specify the cross-sections more precisely. Our first result is still general, however, for from equation (8) we see that whatever the cross-section,

$$z - z_0 = (s - s_0) \cos \zeta \quad (15)$$

For a circular cylinder  $\rho$  is constant and equation (12) shows that

$$s - s_0 = \rho(\psi - \psi_0) / \sin \zeta \quad (16)$$

which is the equation of a helix.

In general, if the intrinsic equation<sup>(1)</sup> (i.e. the relation between  $s'$  and  $\psi$ ) of the curve of cross-section is known,

equations (11) and (15) show that the relation between  $z$  and  $\psi$  can be found. Examples of such curves with their Cartesian or polar equations are:

- (i) the catenary  $s' = c \tan \psi$ ;  $y = c \cosh(x/c)$ ;  $\tan \psi = \sinh(x/c)$ ;
- (ii) the cycloid  $s' = 4a \sin \psi$ ;  $x = a(t + \sin t)$ ;  $y = a(t - \cos t)$ ;  $\psi = t/2$ ;
- (iii) the equiangular spiral  $s' = (a/\cos \alpha) \exp[(\psi - \alpha) \cot^{-1} \alpha] - \text{constant}$ ;  
 $r = a \exp(\theta \cot \alpha)$ ;  $\psi = \theta + \alpha$ ;
- (iv) the ellipse, best expressed in parametric form,  $x = a \cos \phi$ ;  $y = b \sin \phi$ ;  $s' = \int [a^2 - (a^2 - b^2) \cos^2 \phi]^{1/2} d\phi$  which can be evaluated as an elliptic integral<sup>(2)</sup>;  
 $\tan \psi = -(b \cot \phi)/a$ .

Thus, given  $\psi$ , the co-ordinates  $x$ ,  $y$ ,  $z$  of the corresponding point can be found in each example.

### 3. STRING MOVING AS A WHOLE PARALLEL TO THE CYLINDER AXIS

**Basic differential equations.** We assume here that the string is not moving along its path but that the path as a whole is moving. Alternatively we can regard the string as absolutely stationary but the cylinder to be moving along its axis. Friction is now entirely in the direction  $OZ$  and, since  $n = 0$ , the basic differential equations (see § 2) now become

$$\begin{aligned} \frac{d}{ds} \left( T \frac{dx}{ds} \right) + Nl = 0(a); \quad \frac{d}{ds} \left( T \frac{dy}{ds} \right) + Nm = 0(b); \\ \frac{d}{ds} \left( T \frac{dz}{ds} \right) + \mu N = 0(c) \end{aligned} \quad (17)$$

*Relations between tension, normal reaction, coefficient of friction,  $\zeta$  and  $\psi$ .* We shall show that

- (i)  $T \sin \zeta = \text{constant} = K$ , say;
- (ii)  $\mu(\psi - \psi_0) = \cot \zeta - \cot \zeta_0$ ; and
- (iii)  $N = (T \sin^2 \zeta)/\rho$ .

**Proofs.** Substitution from equations (4) and (7) in equations (17a) and (b) shows that

$$\frac{d}{ds} (T \sin \zeta) = 0; \quad T \sin \zeta \frac{d\psi}{ds} = N \quad (18)$$

The first equation proves (i). From (i), equations (18) and (17b) we find that

$$\frac{d}{ds} (K \cot \zeta) = \mu K \frac{d\psi}{ds} \quad (19)$$

and (ii) follows by integration. Substitution from equation (12) in the second part of equation (18) proves (iii).

**Equations of the string path.** Now equation (12) holds even if  $\zeta$  is not a constant; thus, from equation (19),

$$\frac{dz}{d\psi} = \frac{dz}{ds} \cdot \frac{ds}{d\psi} = \frac{\rho \cos \zeta}{\sin \zeta} = \rho(L + \mu\psi) \quad (20)$$

where  $L = \cot \zeta_0 - \mu\psi_0 = \text{constant}$ . For a circular cylinder  $\rho$  is a constant and hence

$$z - z_0 = \rho [L(\psi - \psi_0) + \frac{1}{2}\mu(\psi^2 - \psi_0^2)] \quad (21)$$

Hence, more generally, if  $\rho$  is given in terms of  $\psi$ , and  $\rho d\psi$  and  $\rho\psi d\psi$  can be integrated,  $z$  can be obtained explicitly in terms of  $\psi$ . For the cross-sections given in § 2,  $x$ ,  $y$ ,  $z$  can be found in terms of  $\psi$  and thus the string path can be completely specified.

#### REFERENCES

- (1) EDWARDS, J. *Differential Calculus*, p. 272 (London: Macmillan and Co. Ltd., 1929).
- (2) EDWARDS, J. *Integral Calculus*, Vol I, p. 367 (London: Macmillan and Co. Ltd., 1930).

## Electronic control of a synchronous motor

By L. U. HIBBARD, B.Sc., M.E., Ph.D., Department of Physics, University of Birmingham

[Paper received 18 November, 1952]

A means is described by which a synchronous motor, started on 230 V, 50 c/s mains, can be transferred to an oscillator-driven amplifier. The oscillator can be synchronized to an arbitrary frequency signal within the range 50 c/s  $\pm$  20%.

A master and slave system is described in which a geared-down load driven by the motor is synchronized with and locked to a slowly rotating master unit. No power is taken from the master.

In connexion with the design of the radio frequency system of the Birmingham Proton Synchrotron\* it is necessary for two separate motor-driven equipments to be maintained in exact phase with respect to one another. One, the master, rotates at about 1 r.p.s. and can vary in speed by several per cent about the mean. The other, the slave, must follow it faithfully with a time accuracy of a few milliseconds. It should be capable of being started up, accurately phased and then locked to the master, in a short space of time. It is also necessary for an automatic indication of loss of synchronism to be given, as the units are some distance apart in separate rooms.

The equipment described here fulfils all these requirements. It is considered that the details will be of general interest, as the synchronizing of two such units is a not uncommon problem. The use of Selsyn-type motors is precluded since the master operates at slow speed and can provide no power,

whereas the slave requires up to  $\frac{1}{8}$  h.p. for its operation. The method used is to drive the slave with a  $\frac{1}{8}$  h.p. single-phase synchronous motor followed by a triple-reduction gear train. Power for the motor is provided by an oscillator-driven amplifier which is synchronized to a signal derived from the master. This signal is produced by means of light impulses reflected on to a photocell from a sequence of mirrors on the master. The choice of a mirror system was dictated by other requirements involved in the control and operation of the master. The details will not be discussed here as they are not essential to the general problem of motor phasing and control. The motor used requires a starting current of 9 A at 230 V, which would necessitate a very much larger power amplifier than is needed for safe running. The method that has been adopted is shown in Fig. 1. The motor  $M$  is started with the 230 V 50 c/s mains and then transferred to the oscillator-driven amplifier  $PA$ . The oscillator  $O$  is locked to the mains before the transfer is made. The locking signal

\* HIBBARD, L. U. *Nucleonics*, 7, No. 4, p. 30 (1950).

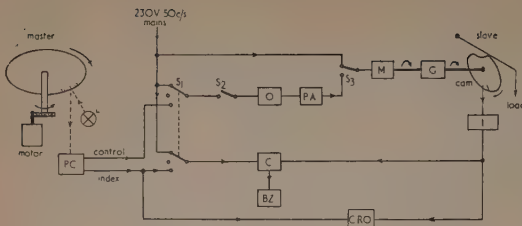


Fig. 1. Block schematic of master and slave system

*L*, lamp; *PC*, photocell units; *O*, oscillator; *PA*, power amplifier; *M*, slave motor; *G*, reduction gearing; *I*, slave index unit; *C*, coincidence unit; *BZ*, buzzer; *S*<sub>1</sub>, synchronizing signal selector; *S*<sub>2</sub>, oscillator locking switch (or relay); *S*<sub>3</sub>, motor power selector; *CRO*, cathode-ray index comparator.

is then removed and the free-running frequency adjusted manually until the two rotating systems have the required correspondence. When this is achieved the oscillator is locked to the signal derived from the master. The addition or removal of the locking signals is done without introducing frequency, phase or amplitude discontinuities which could cause the motor to drop out of synchronism.

Indication of the correspondence between the two rotating systems is given by comparison on a cathode-ray oscilloscope of two index-signals, one per cycle of rotation from each system. Either is made to trigger a cathode-ray sweep upon which the other is viewed. This signal is made to move along the time base by manual control of the oscillator frequency until it reaches the start. When the two index-signals overlap, a coincidence circuit *C* is operated and closes a relay which stops a buzzer *BZ* and permits the master locking-signal to be fed to the oscillator. If the index signals cease to overlap on any cycle of rotation the buzzer is started again, thereby warning the operator of loss of synchronism.

The above mixture of manual and automatic control is a compromise which enables the operations to be carried out quickly and simply. The phasing could be done entirely automatically and the oscilloscope eliminated if the rate of drift of one system relative to the other were made so small that the index signals could not jump past each other during one revolution. With the slow speeds involved and the high accuracy of phasing required this would take an objectionably long time. It would, however, be quite feasible following an initial manual speed-up, using a rough aural or visual indication of index separation. The use of a cathode-ray oscilloscope as described above is, however, the quickest and

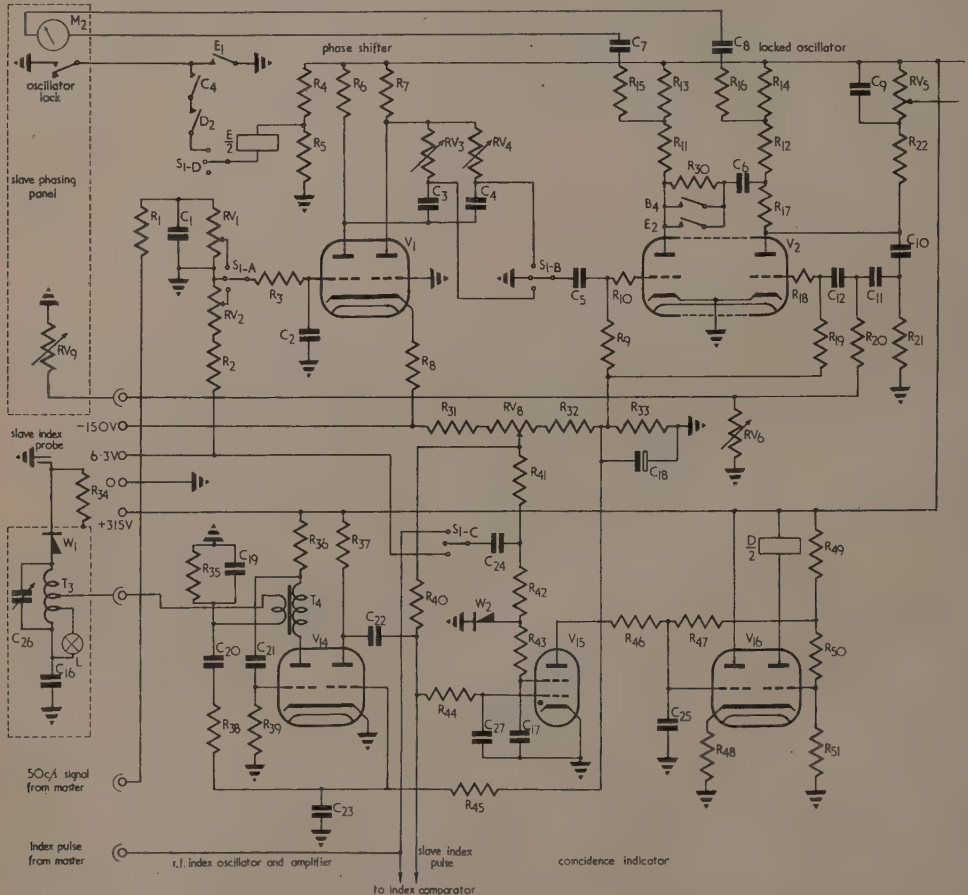


Fig. 2. Circuit of oscillator driven amplifier and coincidence detector



most satisfactory method since an accidental overshoot is quickly detected and corrected.

In addition to the phasing operations described above, there is an important ambiguity which must be resolved every time the system is started up. This arises because the synchronous motor can start in either of two phases with respect to the applied a.c. voltage. In the equipment to be described this ambiguity is resolved by first using the index coincidence circuit *C* to observe coincidence between the slave index pulse and the positive half cycle of the applied a.c. voltage. If coincidence does not occur, as indicated by the stopping of the buzzer, the motor is stopped and restarted repeatedly by the operator until coincidence is achieved.

#### GENERAL DESCRIPTION

The complete circuit of the synchronized oscillator, amplifier and coincidence unit is shown in Fig. 2. Valves  $V_4$  to  $V_{13}$  are Mazda type 12E1 beam tetrodes. These form a parallel push-pull power amplifier with a power capability of over 400 W. This valve type was adopted because it particularly suited a 220-0-220 V d.c. mains supply that was available and by this means the usual difficulty of screen supply regulation was avoided. The valves are biased near cut-off and the full power is obtained without grid current. The cathodes are at -220 V d.c. with respect to ground but with transformer coupling in and out this is of no consequence.

The screens operate at ground potential, a relay in series protecting against overload or anode supply failure.

Valve  $V_3$  is a pentode shunt-coupled to the drive transformer in such a way that only the screen current passes through the primary. A measure of current feedback is given by  $R_{27}$  in the cathode. In addition to this an overall voltage-feedback is applied from the output transformer secondary to the grid of  $V_3$  via the feedback control  $RV_7$ . The principal function of this feedback is to lower the output impedance and damp out any hunting of the synchronous motor. Without it the motor cannot be operated stably for any length of time. A secondary function of the feedback is to improve the output waveform. This was necessary in some degree to offset the large amount of 300 c/s ripple on the d.c. mains. The degree of harmonic and unwanted ripple cancellation is limited by  $C_{14}$  which was found to be necessary to prevent instability.

The double triode  $V_2$  is the oscillator and synchronizing signal amplifier. The right-hand half is a CR phase-shift oscillator and the left-hand half amplifies the selected control signal. In order that the signal can be applied to the oscillator without causing any discontinuity of frequency, phase or amplitude, it is necessary that it should be exactly equal in all these respects to the signal naturally occurring at the point of the oscillator circuit to which it is applied. So that the two signals can be compared before connexion is

made, a meter  $M_2$  is connected between suitable tapping points in the anode circuits of the two valve halves. When this meter indicates zero beat and the phasing is such that the deflexion is very nearly zero, it is permissible to apply the locking signal by closing relay contacts  $E_2$  or  $B_4$ .

Condenser  $C_6$  is required in order to prevent the injection of transients due to differences in d.c. level on the two sides of  $V_2$ . The resistor  $R_{30}$  allows the d.c. potentials on  $C_6$  to adjust themselves. It also allows a weak synchronizing signal to leak to the oscillator. This is very helpful, as will be explained later under "Operation."

Valve  $V_1$  is a cathode-coupled phase splitter which feeds

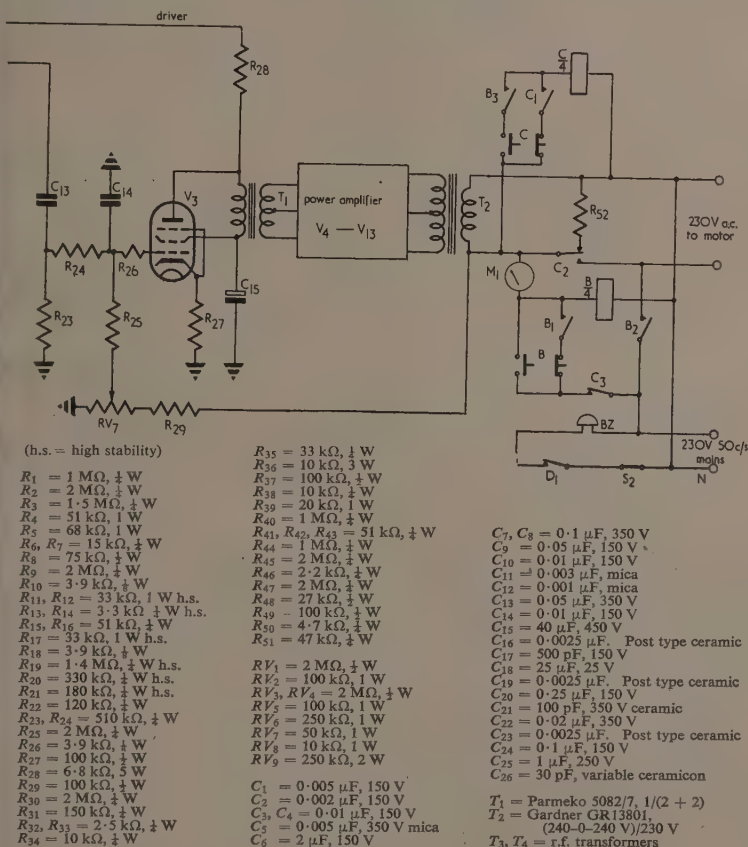


Fig. 2 (continued)

balanced inputs to the two phase-shifters  $RV_3$ ,  $C_3$ , and  $RV_4$ ,  $C_4$ . Ganged switches  $S_{1-A}$  and  $S_{1-B}$  choose the source of synchronizing signal. A phase shifter is needed for the mains input in order to compensate for phase shift throughout the unit. Another is needed for the input derived from the master unit in order to allow fine adjustment of the phasing of the slave system with respect to the master. The components  $R_1$ ,  $C_1$  and  $R_3$ ,  $C_2$  were inserted in order to reduce the harmonic content of the synchronizing signals. The signal from the master unit is a square wave and in order to obtain an intelligible waveform from the phase shifter it is essential to purify it to this extent.

#### COINCIDENCE UNIT

The index signals from the master and slave equipments are fed to the two grids of a 2D21 thyatron  $V_{15}$ . When the signals overlap the thyatron strikes and discharges  $C_{25}$ . This cuts off the left-hand side of  $V_{16}$  and renders the right-hand side conducting thereby closing relay  $D/2$ . One contact of  $D/2$  disconnects a buzzer  $BZ$  indicating that coincidence has been achieved. The other makes it possible for relay  $E/2$  to be closed in order to lock the oscillator frequency. Condenser  $C_{25}$  recharges through  $R_{47}$  and, unless discharged again by the thyatron  $V_{15}$ , it will release relay  $D/2$ , operating the buzzer and giving warning of loss of synchronism. The recharge time constant is proportioned to give warning if one coincidence is missed.

#### INDEX GENERATOR

The requirement of millisecond accuracy for the index pulses makes the use of a mechanical system undesirable. In addition the choice of electronic methods, in the case of the slave, was severely limited by a requirement that this equipment should operate on top of the synchrotron magnet in a region of strong varying magnetic field. The system to be described uses the variation of capacitance between two probes to modulate an r.f. signal. The fixed probe consists of a  $\frac{1}{2}$  in length of one of the wire leads of a germanium diode. The rotating probe is a piece of earthed metal plate placed so that its edge passes parallel to and distant about 0.010 in from the wire.

The left-hand half of  $V_{14}$  oscillates continuously at 25 Mc/s. Its output is fed via a coaxial line to a tuned auto-transformer  $T_3$  which develops about 20 V at the germanium diode  $W_1$ . Rectified current through  $W_1$  finds its return path via the coaxial line and develops a steady voltage across  $R_{35}$ . The magnitude of this depends on the r.f. impedance presented to the probe side of the germanium diode. With the probe arrangement described a variation of capacitance of 0.02 pF or more can be obtained as the probes pass and, provided care is taken to keep stray capacitance to a minimum, this gives rise to a modulation of the voltage across  $R_{35}$  by 0.5 V or more. This signal is amplified by the right-hand side of  $V_{14}$  and applied to a grid of the coincidence valve  $V_{15}$ . The effective width of the index is adjusted by varying the bias on  $V_{15}$ . A width of 5 msec has proved most suitable.

#### OPERATION

The relays  $B/4$  and  $C/4$  effect the change over from mains to amplifier operation of the motor. They are interlocked with each other and with relay  $E/2$  so that it is impossible to do any damage by wrong switching. The starting-up procedure is as follows. Relay  $B/4$  is closed by pushing its start button  $B$ . This applies the 230 V mains to the motor

and starts it. In general it will be in either of two phases with respect to the mains voltage and it is necessary to stop and start it until the right phase relationship is achieved. To do this, buzzer  $BZ$  is made to operate by closing its series switch  $S_2$ . Then switch  $S_1$  is moved to the position in which  $S_{1-C}$  feeds a mains frequency voltage to the grid of the coincidence valve  $V_{15}$ . The index probe is positioned so that its signal always coincides with a crest of the voltage applied to the motor. If the motor starts with the index overlapping the positive crest the coincidence relay  $D/2$  will be closed and the buzzer will stop. The procedure for phasing the motor with respect to the voltage on its terminals is thus to stop and restart until the buzzer ceases.

With relay  $B/4$  closed and  $S_1$  as above, the relay contact  $B_4$  causes the oscillator to be locked to the mains frequency. Under these conditions, with  $C/4$  unexcited, the power amplifier operates and delivers its full power to a resistor  $R_{52}$ . The meter  $M_1$  is connected between the amplifier output and the mains and reads the difference voltage, which will be zero if the motor phasing and amplitude are correctly adjusted. In general, with the phase shifter  $RV_3$ ,  $C_3$  correctly set, this will be so, provided that the natural oscillator-frequency is identical with the mains frequency. To achieve this condition the oscillator frequency control  $RV_5$  on the remote phasing panel is set to the middle of its range, and the frequency control  $RV_6$  adjusted until  $M_1$  reads zero or a minimum close to zero. When this is so, transfer to amplifier operation is achieved by closing  $C/4$  with its start button  $C$ . This switches the amplifier output from the resistive load  $R_{52}$  to the motor, and opens  $B/4$ , removing the mains supply. There is thus no period when the motor is without power.

The release of  $B/4$  opens  $B_4$  and leaves the oscillator synchronized very lightly via  $R_{30}$ . If  $S_1$  is now made to select the control signal from the master, this weak synchronizing signal will, in general, not lock the oscillator but, within a limited range of the frequency controls  $RV_6$  and  $RV_9$ , it will take over and, within this range, the controls merely function as phase shifters. In general it is a very simple matter, by watching meter  $M_2$ , to operate  $RV_9$  and achieve zero beat and zero phase difference or to slip a cycle in either direction. With the aid of an additional indication, cathode-ray tube or otherwise, of the separation between the two index pulses, it is a very simple matter to run them close together in a few seconds, stop and then slip one cycle at a time until coincidence is established as determined by the coincidence thyatron  $V_{15}$  and indicated by the buzzer. When this condition is achieved, it is possible to press the "oscillator-lock" button on the remote phasing panel and close relay  $E/2$ , putting the full lock signal on the oscillator.

In general it is not necessary to interlock  $E/2$  as extensively as is shown in the circuit. This was done here because additional contacts on the relay were required to interlock further equipment which should not be operated unless the slave equipment is phased and locked with the master. A remote phasing panel was necessary because of the physical separation between the rest of the equipment and the cathode-ray tube used for index comparison.

#### ACKNOWLEDGEMENTS

The work described in this paper has been carried out as part of the programme for building the Birmingham Proton Synchrotron which is financed principally by the Department of Scientific and Industrial Research. The author is indebted to the Walter and Eliza Hall Trust and to the Australian National University for fellowships during the tenure of which the work was carried out.

# A method for measuring the spectral reflectivity of a thermopile

By E. J. GILLHAM, M.A., National Physical Laboratory, Teddington, Middlesex

[Paper received 26 January, 1953]

A method of measuring the reflectivity of a thermopile is described in which the reflected radiation is refocused back on to the thermopile by means of a spherical mirror. A specially constructed thermopile, incorporating an electrical heating element, was used, so that the contribution of thermal radiation to the apparent reflectivity could be determined. The spectral reflectivity of this thermopile has been measured in the wavelength range extending from the visible to  $13\ \mu$ , and the relative sensitivity values so obtained used to establish accurate standards for the measurement of monochromatic radiation in this region. Various sources of error are discussed, in particular the effect of the thermal resistance of the thermopile black on the apparent reflectivity and on the thermopile sensitivity.

The establishment of standards for the measurement of radiant energy in the infra-red, visible and ultra-violet regions of the spectrum involves at some stage the use of a radiometer whose absorption factor, for the type of radiation in question, is known with the required accuracy. The absorption factor of the absolute radiometer used at the National Physical Laboratory, the Guild drift radiometer,<sup>(1)</sup> is determined readily only in the visible and near infra-red regions of the spectrum. The measurement of radiation of other wavelengths is therefore based on relative measurements made with the Callendar radiometer,<sup>(2)</sup> an instrument in which the receiving element is of the black-body type, and which therefore has constant sensitivity over the whole spectral range.

The Callendar radiometer, although adequate for the measurement of total radiation from sources at various temperatures, is not adapted for use with monochromatic radiation owing to its low sensitivity and sluggish response, and to the fact that its receiving area is not of a suitable size or shape to utilize fully the radiation from the exit slit of a monochromator. For spectral measurements in the visible and ultra-violet, thermopiles may be used with sufficient accuracy, since in this region of the spectrum the variation of thermopile absorptivity with wavelength is usually small, and may if necessary be determined from reflectivity measurements carried out by conventional methods. In the infra-red, however, little information has been available on the spectral reflectivity of the thermopiles employed as substandards. In order to eliminate this uncertainty, of the order of a few per cent, in the scale of intensity for monochromatic radiation maintained at the Laboratory, it was decided to construct a suitable thermopile, and to develop a method for measuring its spectral reflectivity in the infra-red.

## DESCRIPTION OF THERMOPILE

The receiving area of the thermopile would preferably have been similar in size and shape to the exit slits of the monochromators in use at the Laboratory, that is to say, about 10 mm high and perhaps  $\frac{1}{2}$  mm wide; actually, however, it was restricted in height to about 5 mm by the limitations of the optical system used in the reflectivity measurements. Since the radiant intensity at the exit slit of a monochromator is often not uniform, it was desirable that the sensitivity of the thermopile should vary as little as possible from point to point of the receiving area. In order to avoid the difficulties entailed by the use of a transparent window, the thermopile was operated in air, and compensated so as to reduce the disturbances produced by atmospheric pressure fluctuations.

Since reflectivity measurements were to be made as far

into the infra-red as possible, the detector used for measuring the reflected radiation had to be of a kind which would necessarily respond not only to the radiation reflected from the thermopile but also to that emitted by it when heated by the incident radiation. The proportion of incident energy emitted as thermal radiation could have been estimated from the apparent reflectivity values obtained when using visible radiation, for which the true reflectivity may be readily determined by other means, but it was decided, however, to measure it directly by heating the thermopile electrically in such a way as to reproduce as closely as possible the temperature distribution produced by exposure to radiation. It was concluded that a suitable thermopile could most easily be constructed by depositing the thermojunctions and electrical heating element on to a mica substrate by means of a vacuum evaporation process. The final form of instrument is shown in Fig. 1.

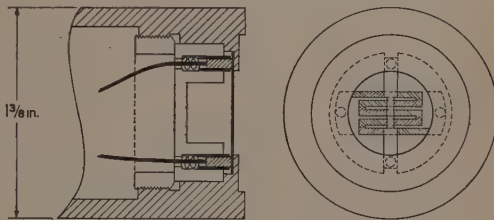


Fig. 1. Side and front views of thermopile.

The receiving part of the thermopile is the rectangular area 5 mm high and 1 mm wide in the centre of a thin circular disk of mica approximately 2 cm in diameter and 0.01 mm thick. The heating element, which consists of a thin layer of gold deposited on the front surface of the mica, extends over the same area and has a total resistance of about 20  $\Omega$ . It is provided with somewhat thicker gold electrodes 2 mm in width which extend from the top and bottom of the element to within about 1 mm from the edge of the disk. These electrodes are connected to spring-loaded contacts pressing against the rear surface of the mica disk by means of two strips of gold foil folded round the edge.

The thermo-element, comprising ten antimony-bismuth junctions connected in series, is deposited on the rear surface of the disk in the form of alternate strips of antimony and bismuth, each 1 mm wide. The five hot junctions occupy a rectangular area in the centre 7 mm high and 1 mm wide, and thus extend beyond the receiving area on the front of the mica by 1 mm at each end; the cold junctions are disposed



on either side of the receiving area at a distance from it of about 5 mm. Connexions are brought out by strips of bismuth terminating near the edge of the disk in gold electrodes to which connexion is made by means of two more spring-loaded plungers. The antimony deposit is about  $1\ \mu$  thick, and the bismuth deposit about  $2\ \mu$ , the total resistance of the thermopile being approximately  $30\ \Omega$ . The front surface of the mica was blackened over a central area 7 mm high and 2 mm wide, and also over the two areas of similar size and shape which overlay the cold junctions of the thermopile; the rest of the surface was left clear.

The sensitivity of the thermopile to radiation filling the whole of the receiving area was  $0.32\ \text{V/W}$ , and the time constant of the instrument was approximately 2 sec. Better values would have been obtained with a thinner mica substrate but the advantage gained would have been outweighed by the difficulty of handling a more fragile disk, particularly in the preliminary experimental work which involved the deposition and removal of several different blacking materials. The sensitivity was greatest at the centre of the receiving area and fell to about 85% of the maximum value at the upper and lower ends; the variation of sensitivity across the width of the receiving area was less than 5%. The exactness with which the electrical heating of the thermopile reproduced the temperature distribution resulting from exposure to radiation was indicated by the fact that the sensitivity to electrical heating differed from the sensitivity to radiation by less than 2%.

#### APPARATUS FOR MEASURING REFLECTIVITY

The measurement of the reflectivity of a surface is facilitated by the use of a hemispherical mirror to collect the reflected radiation and focus it on to a small and sensitive detector. For measuring the reflectivity of a thermopile, a second detector is unnecessary since the thermopile itself may be used to measure the reflected radiation; this may be done by tilting the mirror so that the focused beam of reflected radiation is alternately directed on to and off the thermopile, and its intensity thus measured as the difference in the intensity of the radiation received by the thermopile in the two cases. This procedure requires a stable source of radiation, but it was not found difficult to provide this in practice, and the method had the advantage of minimizing the optical aberrations and so permitting the use of a smaller mirror than would otherwise have been necessary. This method was therefore adopted.

Fig. 2 shows a diagram of the apparatus. A mirror in the form of a complete hemisphere was not available and one with a slightly smaller collecting power was therefore used. It was made of glass, with the reflecting surface aluminized, and had a radius of curvature of 3.5 cm and a diameter, at its periphery, of about 6.4 cm; the half-angle subtended by the periphery at the centre of curvature was thus about  $65^\circ$ . The receiving area of the thermopile was situated at the centre of curvature of the mirror and uniformly irradiated with the desired radiation by means of a focused beam passing through a hole, 8 mm in diameter, cut in the centre of the mirror. The frame holding the mirror was pivoted about a horizontal axis passing through the pole of the mirror, and could be tilted upwards against a stop by means of a cord so that the image of the receiving area of the thermopile formed by reflected radiation fell, not on the receiving area itself, but on the blackened diaphragm surrounding it. A circular stop of 6 mm diameter placed immediately to the right of the hole in the mirror ensured that the beam of

incident radiation passed through the hole well clear of the sides, and was not affected by the tilting. The mirror and thermopile were enclosed in a rectangular box with removable top and sides, and the cord attached to the mirror was actuated from outside the box by means of a spring-loaded plunger passing through the rear wall.

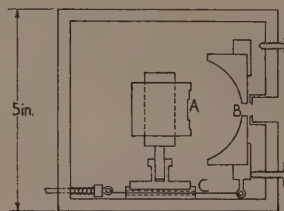


Fig. 2. Side view of reflectivity apparatus

A, receiving area of thermopile; B, axis of mirror tilt; C, cord for tilting mirror.

To set up the apparatus the sides of the box were removed and a small plane mirror mounted in front of the thermopile in a position which enabled the surface of the thermopile to be viewed from the side without obscuring the incident beam. The thermopile was placed a little to one side of the axis of the spherical mirror and a thin line of light about 5 mm high thrown on to the uncoated mica surface next to the blackened receiving area, in a position such that the image of it formed by the mirror fell to one side of it, again on the uncoated mica where it was clearly visible. The thermopile was then moved along the axis of the mirror until the line and its image were of equal size and the line then shifted slightly so as to bring it into coincidence with its image. This procedure served to locate the centre of curvature of the mirror, and it was then only necessary to bring the centre of the thermopile receiving area into this position by moving the thermopile at right angles to the mirror axis.

#### METHOD OF MEASUREMENT

The procedure to be described later in this section yields a value for the proportional increase  $\alpha_r$  in thermopile response which results when the thermopile is exposed to radiation of constant intensity and the mirror moved from the tilted position to the normal one. Measurement of the corresponding increase  $\alpha_e$  in the response to electrical heating enables a correction to be made for the thermal radiation emitted by the thermopile. The relation between  $\alpha_r$ ,  $\alpha_e$  and the thermopile reflectivity  $\rho$  may be derived in the following manner.

The proportion  $I$  of the primary incident radiation absorbed by the thermopile with the mirror tilted upwards is by definition equal to  $1 - \rho$ . When the mirror is in its normal position, a fraction  $k$  of the radiation reflected from the thermopile is returned to the thermopile by the mirror,  $k$  depending on the reflectivity of the mirror surface for approximately normal incidence and also, since the mirror is not a complete hemisphere, on its angular aperture and on the angular distribution of the reflected radiation. Since the radiation returned to the thermopile has an angular distribution different from that of the primary beam, the proportion of it absorbed will be determined by a new reflexion factor  $\rho'$ . Similarly in evaluating the radiation absorbed by the thermopile after undergoing further inter-reflexions between

thermopile and mirror, it is necessary, in the most general case, to take account of further changes in angular distribution by introducing at each stage new values for  $\rho$  and  $k$ . The total fraction of the incident radiation absorbed by the thermopile with the mirror in the normal position is thus given by an expression of the form

$$I' = 1 - \rho + \rho k(1 - \rho') + \rho k \rho' k'(1 - \rho'') + \dots$$

Fortunately the reflectivity of a thermopile black is usually small and not greatly dependent on angle of incidence, so that the difference between the dashed and un-dashed quantities in the above equation may be neglected, and we have

$$I'/I = 1/(1 - \rho k)$$

The change in radiative heat loss which results when the mirror is moved from the tilted position to the normal one is equivalent to a change in the sensitivity of the thermopile from a value  $S$  to a value  $S'$  where  $S'/S = 1 + \alpha_e$ , so that

$$1 + \alpha_e = (1 + \alpha_e)(I'/I)$$

whence

$$\rho k = (\alpha_e - \alpha_e)/(1 + \alpha_e) \quad (1)$$

In practice, the change in the thermopile response resulting from the change in position of the mirror was measured both with the thermopile exposed to the radiation and with the radiation cut off by a shutter, the true change being taken as the difference between the two values so obtained. The response of the thermopile to the radiation was measured with the mirror in the tilted position using the same shutter to obtain the necessary zero readings. In making these measurements, the e.m.f. generated by the thermopile was measured with a potentiometer, a galvanometer amplifier being used as the null detector. The quantity  $\alpha_e$ , which was determined in the same way, had a magnitude of about 0.06.

The reflectivity of the mirror surface, which enters into the factor  $k$ , was measured by removing the mirror from the box and placing it so that the rays diverging from the focus of a convergent beam were reflected from the mirror and refocused at a point slightly to one side. A plane mirror, similar in size to the blackened area of the thermopile, was mounted so that it could be turned about a vertical axis into a position where it reflected out to the side either the incident beam or the beam reflected from the mirror, the geometry of the system being arranged so that in each case the emergent beam issued from the same image point in the same direction. The emergent radiation was then focused on to the thermopile. The incident beam of radiation was not convergent enough to allow more than a part of the mirror surface to be irradiated, but measurements made with visible radiation showed that the reflectivity did not vary much from point to point of the surface, and it was concluded that in other regions of the spectrum a single measurement would give the mean reflectivity of the mirror with sufficient accuracy.

The geometrical factor entering into  $k$  was evaluated on the assumption that the radiation reflected from the thermopile had an angular distribution in accordance with Lambert's law; this assumption led to a value for the collecting power of the mirror of approximately 0.8.

#### ACCURACY OF REFLECTIVITY MEASUREMENTS

Before any detailed spectral measurements of thermopile reflectivity were made, a number of tests were carried out,

VOL. 4, MAY 1953

mainly with visible radiation, in order to check the performance of the apparatus and the accuracy of the method.

A measurement made with the receiving surface of the thermopile coated with a matt white paint of about 75% reflectivity, gave a value for the reflectivity which was in error by less than 5%. The assumptions made in deriving equation (1) may not be valid for so highly reflecting a surface, but the result indicated that the alignment of the apparatus and the optical quality of the mirror were satisfactory. When, however, the thermopile was coated with a smoked carbon black, the measured reflectivity for visible radiation came out too high, the observed value being 2.9% and the true value 2.1%. It was at first thought that the discrepancy might be due to stray light from the illumination system falling outside the blackened area of the thermopile on to the highly reflecting part of the mica where there was still some residual sensitivity. The stray light was, however, too weak for this effect to be appreciable, and a reflectivity measurement made with the whole of the mica surface blackened was also in error by a similar amount.

The method used to compensate for the thermal radiation emitted by the thermopile may be expected to fail if the temperature distribution resulting from exposure to radiation differs from that produced by electrical heating, as it will, for example, if the intensity of the incident radiation is not uniform over the receiving area. Actually, local variations of intensity much greater than those normally encountered were found to have little effect on the results. There is, however, another kind of difference between the temperature distributions produced by the two types of heating; if there is appreciable thermal resistance between the front and rear surfaces of the layer of black with which the thermopile is coated, a temperature gradient will be established across the layer which will be of different sign for the two types of heating, and the thermal radiation emitted on exposure to radiation will be in excess of the expected amount. The existence of an effect of this kind, which was first noted by Coblenz<sup>(3)</sup> in carrying out reflectivity measurements of a similar type using a non-selective detector, was demonstrated by depositing on the original carbon-black layer a second coat of about the same thickness. The fact that the difference between the true and measured values of reflectivity was approximately doubled by this procedure, indicated that the thermal resistance of the black was sufficient to account for the greater part, if not all, of the original discrepancy.

If the thermal resistance between the electrical heating strip and the region in which radiation is absorbed were independent of the wavelength of the radiation, the difference between the true and measured reflectivities would be constant, and the relative values obtained at different wavelengths for the absorptivity, and hence sensitivity, of the thermopile would only be in error by a second-order amount. The radiation penetrates the black, however, to an appreciable depth which is dependent on wavelength. The effective thermal resistance is therefore less than the total resistance of the black and is likewise dependent on wavelength. It follows that the error in measured absorptivity is not constant throughout the spectrum.

So far as this investigation was concerned, however, the object of chief interest was the accuracy, not of the measured reflectivity values themselves, but of the values for relative sensitivity based on these values. It has so far been assumed that the two are equivalent, i.e., that the sensitivity of the thermopile at different wavelengths is accurately proportional to the absorptivity of the black. When, however, there exists a wavelength-dependent thermal resistance between the



region in which radiation is absorbed and the sensitive element of the thermopile, this is no longer the case, since the magnitude of the thermal resistance will affect the rate of heat loss from the front surface of the black. Variations in thermal resistance will thus affect not only the measured absorptivity but also the true sensitivity of the thermopile.

In order to assess the overall effect of thermal resistance variations on the accuracy of the measured values for relative sensitivity, let us consider the case where the black has constant reflectivity over the spectrum. Let us assume, further, that at a particular wavelength the depth of penetration of the radiation decreases. The effective thermal resistance will increase and with it the temperature of the front surface of the black. This increase in surface temperature will, as already indicated, lead to a high value for the measured reflectivity and hence to a low value for the derived absorptivity and relative sensitivity. On the other hand it will also lead to an increase in the rate of heat loss from the surface, and hence to a lower value for the actual sensitivity.

It is clear that these two effects combine to make the error in the measured sensitivity less than the error in the measured absorptivity. In the particular case in which the loss of heat from the front surface of the black is by radiation alone, this compensation of errors is complete. This may be seen from the fact that the reflectivity measurements serve in effect to measure the proportion of the incident radiation which is lost from the front surface of the black both by direct reflexion and by the emission of thermal radiation. If these are the only means by which heat is lost from the surface, the relative sensitivity values obtained from the measured reflectivities will be correct no matter how widely the effective thermal resistance varies.

With an air-operated thermopile, heat is lost from the front surface of the black by air conduction and convection as well as by radiation. The compensation of errors is then not complete, the decrease in actual sensitivity due to an increase in thermal resistance exceeding the decrease predicted from the measured reflectivity. If the change in the thermal resistance  $R$  of the black is  $\delta R$ , it may be shown that in this case the fractional error in the measured sensitivity is approximately  $(R/R_0)(\delta R/R)$  where  $R_0$  is the thermal resistance representing the heat losses at the front surface of the black by air conduction and convection alone.

The value of  $R_0$  may from general experience be taken as  $2000^\circ \text{C per W per cm}^2$ . The value of  $R$  for a particular black may be derived from the difference between the true and observed values of reflectivity for visible radiation by making the reasonable assumption that the depth of penetration for visible radiation is negligible, and that the black is sufficiently opaque for the thermal radiation from it to depend only on its surface temperature. The difference between the apparent reflectivity  $\rho'$  and the true reflectivity  $\rho$  is then given by

$$\rho' - \rho = 4\sigma T^3 \epsilon (1 - \rho) R$$

where  $\sigma$  is the total radiation constant,  $T$  the absolute temperature,  $\epsilon$  the emissivity of the black and  $R$  its thermal resistance per unit area. Assuming  $\rho$  to be small and  $\epsilon$  equal to unity, we have approximately

$$R = 1500(\rho' - \rho)^\circ \text{C per W per cm}^2$$

The factor  $\delta R/R$  is equal to the change in depth of penetration expressed as a fraction of the total thickness of the black. If, in its passage into the black, the radiation is attenuated according to an exponential law, the fractional depth of penetration will be approximately equal to  $1/\log(1/T)$  where  $T$  is the transmission factor of the black for a single

passage of radiation. It was confirmed experimentally that the value of  $T$  for the black used in the final spectral measurements was less than 1% over the whole spectral range, so that the fractional depth of penetration, and hence the maximum possible value of  $\delta R/R$ , nowhere exceeded  $1/4$ . Since the value of  $\rho' - \rho$  for this black was found to be  $0.012$ , corresponding to a thermal resistance of  $18^\circ \text{C per W per cm}^2$ , it follows that the maximum possible error in measured sensitivity due to variations in the depth of penetration of the radiation, was about two parts per thousand.

The only other errors in the reflectivity measurements likely to be significant are those which may result from the use of an incomplete hemisphere to collect the reflected radiation. If, for example, there is appreciable semi-specular reflexion, the proportion of radiation which escapes through the hole in the mirror will exceed that predicted by Lambert's law. Specular reflexion may, however, be easily detected by measuring the reflectivity with the thermopile surface inclined to the incident beam at an angle sufficient to divert any specular component away from the entrance hole. This procedure was carried out at a number of wavelengths, and in no case was any significant increase in reflexion factor observed.

Although it is improbable that significant deviations from Lambert's law will occur unaccompanied by specular reflexion, it was decided to measure the reflectivity of the thermopile in the long-wavelength region of the spectrum, where possible effects of this kind are likely to be most evident, and to check the result by comparing the sensitivity of the thermopile with that of the Callendar radiometer. This was done using the total radiation emitted by a black-body source operated at a temperature of about  $200^\circ \text{C}$ . The values obtained by the two methods for the sensitivity of the thermopile, relative to the sensitivity to visible radiation, agreed to within two parts per thousand.

#### MEASUREMENTS AND CONCLUSIONS

Spectral reflectivity measurements were carried out over the range  $0.4$  to  $13 \mu$ , using a prism monochromator with mirror optics fitted with a quartz prism for wavelengths less than about  $3 \mu$ , and with a rocksalt prism for longer wavelengths. The source of radiation for the short-wavelength region was a tungsten lamp, and for the long-wavelength region a Nernst filament.

For the purpose for which the measurements were made, i.e. the establishment of a scale of radiation intensity, it was sufficient that the black used for coating the thermopile should have reasonably high absorptivity at all wavelengths, and that its thermal resistance should not be excessive. A sample of optical black lacquer MFB manufactured by Thos. Parsons Ltd., was found to give good results when applied to the thermopile by spraying. The reflexion factor of this paint over the spectral range investigated is shown in Fig. 3.

At wavelengths less than  $5 \mu$  the precision of a single reflectivity measurement, taking about 3 min to make, was one or two parts per thousand in absorptivity. At longer wavelengths, where less radiant energy was available, the precision was limited by atmospheric pressure disturbances which, on a blustery day, produced fluctuations in thermopile output amounting to as much as fifty times thermal noise. On a calm day, however, the fluctuations were often no more than five times thermal noise; in these circumstances the r.m.s. error in absorptivity for a single measurement carried out at  $13 \mu$  with a spectral bandwidth of  $0.2 \mu$  was



about  $\frac{1}{2}\%$ . The precision was sufficient to enable the spectral sensitivity of the thermopile to be measured over the spectral range  $0.4$  to  $13\ \mu$  with a spectral bandwidth varying from  $0.02\ \mu$  at the shorter wavelength to  $0.2\ \mu$  at the longer one.

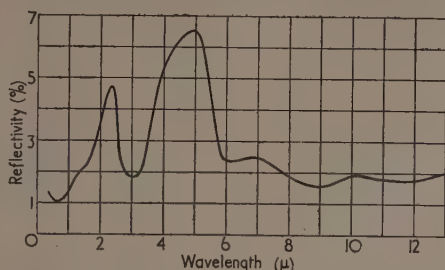


Fig. 3. Reflectivity of black

It was concluded that the overall accuracy of the results was about  $\pm 1/4\%$ .

If the measurements are to be extended to longer wavelengths, it will be necessary, in order to obtain the necessary precision, to seal the box which encloses the thermopile by

fitting a window over the entrance hole. The effect of radiation scattered by the window may be eliminated by blacking the entire surface of the thermopile. It should then be possible to approach the limit of precision set by thermal noise, which, with a source and monochromator of normal efficiency and a spectral bandwidth of  $0.2\ \mu$ , is, for a single measurement, of the order of  $0.1\%$  at a wavelength of  $13\ \mu$ , and  $1\%$  at a wavelength of  $25\ \mu$ . The corresponding figures for measurements made with the Callendar radiometer, which has a sensitivity of  $0.07\ \text{V/W}$  and a resistance of  $4\ \Omega$ , are about four times as great under the most favourable conditions of illumination.

#### ACKNOWLEDGEMENTS

The work described above has been carried out as part of the research programme of the National Physical Laboratory, and this paper is published by permission of the Director of the Laboratory.

#### REFERENCES

- (1) GUILD, J. *Proc. Roy. Soc. A*, **161**, p. 1 (1937).
- (2) CALLENDAR, H. L. *Proc. Phys. Soc., Lond.*, **23**, p. 1 (1910).
- (3) COBLENTZ, W. W. *Bull. Bur. Stand.*, **9**, p. 283 (1913).

## The measurement of X-ray line breadths

By T. R. ANANTHARAMAN, M.A., M.Sc., and J. W. CHRISTIAN, M.A., D.Phil., A.Inst.P., Inorganic Chemistry Laboratory, South Parks Road, Oxford

[Paper received 5 February, 1953]

Simple analytical methods for finding the position of the  $\alpha_1$  peak and the integral breadth of the  $\alpha_1$  component of a composite Debye-Scherrer powder line are described. The expressions are exact for symmetrical lines, and sufficiently accurate for very broad asymmetrical lines. The problem of correct location of the background level is also considered.

Many methods have been suggested for determining the position of the  $\alpha_1$  peak and the integral breadth of the  $\alpha_1$  component from the photometer record of an unresolved Debye-Scherrer line. The graphical method described by Rachinger,<sup>(1)</sup> and further discussed by Pease,<sup>(2)</sup> involves no assumptions about line shape, and appears to be very satisfactory, provided the beginning and end of the composite line can be located accurately. Unfortunately this is often impossible and, in addition, the method becomes tedious when dealing with very broad lines, and with low-angle lines with small doublet separations. In this paper we describe an analytical procedure based on the same principle.

We use the following notation:

$d$  = separation of the  $\alpha_1$  and  $\alpha_2$  components.

$I_p$  = peak intensity of the  $\alpha_1$  component.

$I_1$  = intensity of the composite line at the position of the  $\alpha_1$  peak.

$I_2, I_3 \dots I_n$  = intensities of the composite line at distances  $d, 2d \dots (n-1)d$  from  $I_1$  towards the low angle end.

$I'_1$  = intensity of the composite line at the position of the  $\alpha_2$  peak.

$I'_2, I'_3 \dots I'_n$  = intensities of the composite line at distances  $d, 2d \dots (n-1)d$  from  $I'_1$  towards the high angle end.

$i_1, i_2 \dots i_n$  = intensities of the composite line at distances  $d, 2d \dots nd$  from the low angle end of the line.

$i'_1, i'_2 \dots i'_n$  = intensities of the composite line at distances  $d, 2d \dots nd$  from the high angle end of the line.

For convenience we assume throughout that  $I(\alpha_1) = 2I(\alpha_2)$ , but the method is equally applicable to the more general case where  $I(\alpha_1) = a \cdot I(\alpha_2)$ , and  $a$  is known.

If each component is symmetrical about its peak intensity, and the ends of the line can be clearly distinguished,  $I_1$  and  $I'_1$  can readily be located. For example, to find  $I_1$ , we mark off a distance  $d$  from the high angle end of the line and  $I_1$  is then the intensity at the mid-point of the remainder. It is readily seen that  $I_p = \frac{2}{3}(I_1 - I'_1)$ , and the integral breadth

$$B = A/(2I_1 - I'_1) \quad (1)$$

where  $A$  is the total area under the line.

When the positions of the ends of the line are uncertain,

$I_1$  and  $I'_1$  can be correctly located by also measuring  $I_2$  and  $I'_2$ . For symmetrical lines it follows that:

$$I_1 + 2I_2 = 2I'_1 + I'_2 \quad (2)$$

If the first chosen positions of  $I_1$  and  $I'_1$  do not satisfy equation (2), slightly different positions should be taken, until satisfactory agreement is found by trial and error. This procedure is less laborious than it sounds, and in practice two or three trials suffice. The relation is unaffected by a uniform loss of intensity due to insufficient photometering, or wrong location of the background level, but in such cases the integral breadth obtained from equation (1) will be inaccurate, as both  $A$  and  $(2I_1 - I'_1)$  will be slightly smaller than the true values.

Equations (1) and (2) are valid only for symmetrical lines. Any marked asymmetry will be revealed when the values of  $I_1$ ,  $I_2$ ,  $I'_1$  and  $I'_2$  in their first locations are tested by equation (2). With slight asymmetry it may be possible to satisfy equation (2) accidentally, but this may be avoided by use of the equation:

$$I_n + 2I_{n+1} = 2I'_n + I'_{n+1} \quad (3)$$

which is valid for all values of  $n$  (including non-integral values), if the lines are symmetrical. After locating  $I_1$  and  $I'_1$  by equation (2), we take  $I_n$  and  $I'_n$  at any convenient equal distance from  $I_1$  and  $I'_1$  respectively. In practice, it is best to take  $I_n \simeq \frac{1}{2}I_1$ , and equation (3) then gives a reliable test for asymmetry.

For asymmetrical lines, Rachinger's graphical method is probably the most reliable, but we have found the following procedure very useful. We may write

$$I_1 = I_p + kI_p/2$$

$$I'_1 = (k + \delta)I_p + I_p/2$$

where  $\delta$  expresses the asymmetry. Similarly

$$I_2 = kI_p + jI_p/2$$

$$I'_2 = (j + \delta')I_p + (k + \delta)I_p/2$$

where  $\delta'$  is another asymmetry factor. For a very broad line, when  $I_1$ ,  $I_2$ ,  $I'_1$  and  $I'_2$  are nearly equal, we may take as a first approximation  $\delta' = 2\delta$ . The above equations then have the solution:

$$I_p = \frac{(32I_1 + 4I'_2) - (10I'_1 + 8I_2)}{27} \quad (4)$$

If we locate  $I_1$  at various points within a distance  $d$  from the peak of the composite line towards the low angle end, we can calculate corresponding values of  $I_p$  which are nearly constant when we approach the correct location of  $I_1$ . An analysis of equation (4) shows that the maximum value of  $I_p$  corresponds to the correct location.

Equation (4) is valid also for symmetrical lines, as may be seen by substitution from equation (2). The following procedure thus allows any very broad line to be accurately analysed.

- (i) Using equation (4), calculate  $I_p$  for various possible positions of  $I_1$ . The maximum value of  $I_p$  corresponds to the correct position.

- (ii) Use equation (3) to check whether or not the line profile is symmetrical about  $I_p$ . This is often important in deciding the cause of line-broadening.  
(iii) If the intensity lost by insufficient range of photometering is negligible, the integral breadth is given by  $B = 2A/3I_p$ .

If there is doubt about whether the background level has been taken too high, the intensities  $i_1$ ,  $i_2$ , etc., should be measured. For symmetrical lines we have

$$2i'_2 - i_2 = i_1 + i'_1 \quad (5a)$$

$$= 2i_1 - i'_1 \quad (5b)$$

Equation (5a) is valid only if there is no loss in intensity, whereas equation (5b) is unaffected by constant loss of intensity, provided  $i_1$ ,  $i_2$ ,  $i'_1$  and  $i'_2$  are correctly positioned. In practice, the positions will be wrong if intensity is lost, and both equations will show the line is not ended correctly. The background level may then be adjusted by trial and error until equation (5) is satisfied.

Equation (5) is satisfactory for only slightly broadened lines where  $i_1$ ,  $i_2$ , etc., are measurably different. With such lines, however, there is little difficulty in determining the limits by inspection of the photometer trace. For broad lines we use the equation:

$$2i_n + i_{n+1} = 2i'_{n+1} + i'_n \quad (6)$$

where  $n$  may have any suitable integral or non-integral value, provided  $i_{n+1}$  is on the low angle side of  $I_1$ . By adjusting the background level and testing equation (6) with a number of different values for  $n$ , we can arrive at the correct line profile and integral breadth. The corrections are very tedious and seem to be justified only when very high accuracy is required.

A general correction of the background level for asymmetrical lines seems to be impossible. With very broad lines, it may often be valid to approximate the tails of the intensity curves by straight lines, and this leads to the equation:

$$2i_n + i_{n+1} = p(2i'_{n+1} + i'_n) \quad (7)$$

where the asymmetry factor,  $p$ , is constant. Equation (7) can also be used, in principle, for trial and error location of the background level. In practice, the values of  $p$  will not be constant but will increase or decrease slowly.

We have applied the above methods to measurements of line breadths in powder patterns of hexagonal cobalt containing stacking errors caused by transformation and by cold-work. The results show that the position of the  $\alpha_1$  peak can always be found by equation (4), but with broad lines the adjustment of the background level is very difficult. The tails of broad lines often extend so far that lines which appear to the eye to be well separated interfere appreciably with each other.

#### ACKNOWLEDGEMENT

We should like to thank Dr. W. Hume-Rothery for laboratory facilities, and for his interest in this work.

#### REFERENCES

- (1) RACHINGER, W. A. *J. Sci. Instrum.*, **25**, p. 254 (1948).  
(2) PEASE, R. S. *J. Sci. Instrum.*, **25**, p. 353 (1948).

# New books

## MONOGRAPHS FOR STUDENTS SERIES

*The Institute of Physics announces the publication this month of the following four monographs. They commence a new series which is intended for general reading by students such as those in the first two years of a degree course or those reading for Higher National Certificates. Members of The Institute of Physics may obtain copies for their personal use at reduced prices in accordance with the terms which have already been sent to them.*

**Fundamentals of thermometry.** By J. A. HALL, B.Sc., D.I.C., A.R.C.S., F.Inst.P. (London: The Institute of Physics.) 48 pages, 13 figures. Price 5s.

The aim of this monograph is to give students and others who are concerned with the practical measurement of temperature a sufficient knowledge of the temperature scales on which their measurements are based. Attention has therefore been concentrated on the International Temperature Scale rather than on the thermodynamic scale; that is to say, on the practical rather than the theoretical scale.

This treatment leads to a discussion of the instruments (resistance thermometer, thermocouple and optical pyrometer) which are used in the realization of the scale and of the methods by which they are calibrated at the freezing and boiling points on which the scale is based. A chapter on the use of the mercury thermometer as a working standard of temperature is also included.

**Practical thermometry.** By J. A. HALL, B.Sc., D.I.C., A.R.C.S., F.Inst.P. (London: The Institute of Physics.) 51 pages, 8 figures, 4 tables. Price 5s.

This monograph is a companion volume to *Fundamentals of thermometry* in this series and is again intended for students and others who are concerned with the practical measurement of temperature.

The same instruments which have already been discussed as the means for the realization of the International Temperature Scale may be used for the routine measurement of temperature, but for industrial purposes modified forms may be necessary in order to secure greater robustness and greater convenience, usually at the expense of some loss of precision. These modifications are considered in the present monograph, which also deals with other useful types of instrument and the methods of calibration which can most conveniently be employed.

**Modern mass spectrometry.** By G. P. BARNARD, B.Sc., Ph.D., A.M.I.E.E., F.Inst.P. (London: The Institute of Physics.) Pp. 326. Price 50s.

This latest addition to the Physics in Industry series collects together and discusses the existing state of knowledge of the theory, design, techniques of operation and applications of the mass spectrometer.

The author is in charge of the mass spectrometry work at the National Physical Laboratory and thus is in a unique position to discuss the design and errors of these new instruments and their uses. Moreover, he has been assisted not only by other specialists at the N.P.L., but also by several in the universities and in industry, who are using the methods of mass spectrometry for particular purposes.

The monograph opens with an introductory chapter which includes the general theory of the instrument. This is followed by chapters on ion sources, vacuum techniques and gas-flow problems cognate to mass spectrometry, on the collection and measurement of ion beams and the associated electronic devices. Some existing research and industrial instruments are next described and then five chapters (115 pages) are devoted to applications in physics, chemistry and engineering, to hydrocarbon analysis, to studies of molecular structure and chemical kinetics, to applications of isotopic tracer techniques to biochemistry and to isotopic studies in geology and nuclear chemistry.

The monograph contains 153 figures in addition to a list of some 400 references and an appendix which refers to 30 reviews published since 1940 on mass spectrometry. A

**Soft magnetic materials used in industry.** By A. E. DE BARR, B.Sc., F.Inst.P. (London: The Institute of Physics.) 62 pages, 35 figures, 1 table. Price 5s.

Throughout this monograph the emphasis has been placed on the physical basis of magnetic properties and the aim has been to try to account, in terms of a physical theory of ferromagnetism, for the particular properties of each of the modern soft magnetic materials with which the monograph deals.

Some knowledge of elementary magnetostatics and electromagnetism has been assumed but, for convenience, many of the relevant concepts are reintroduced in Chapter 1. An introductory account of the domain theory of ferromagnetism is given in Chapter 2.

**The magnetic circuit.** (Powder cores, ferrites, permanent magnet materials and miscellaneous magnetic materials.) By A. E. DE BARR, B.Sc., F.Inst.P. (London: The Institute of Physics.) 62 pages, 19 figures, 11 tables. Price 5s.

In this companion volume to *Soft magnetic materials used in industry*, an account is given of the manner in which the properties of a magnetic material are affected by the way in which it is built up into a magnetic circuit, and this is followed by descriptions of the properties of those materials (powder cores and permanent magnet materials) which are most influenced in this way. To complete the survey of magnetic materials there are chapters on ferrites and some miscellaneous magnetic materials. Thus this monograph covers, as well as the magnetically hard materials, others which, although they may be regarded as magnetically soft, are of industrial importance mainly for quite different reasons.

second appendix, which gives hints on the location of equipment maintenance and staff required, will be useful where these instruments are to be installed.

**Electronic measurements.** By F. E. TERMAN and J. M. PETTIT. (London: McGraw-Hill Publishing Co. Ltd.) Pp. xiii + 707. Price 72s. 6d.

The preface to this book states that it succeeds Terman's *Measurements in radio engineering*, that much of it has been re-written and many new sections added so that it is now almost twice as long as the original. There is some doubt in one's mind of the scope of the book derived from its title alone; it is only after a study of the contents that it becomes apparent that measurements by electronic means—such as the measurement of length, mass, time, temperature, flow, etc.—are not in its purview though the title might well suggest these. Rather are the authors concerned with measurements upon electronic devices themselves and in electronic devices are included radio, radar and television equipment. To this end they discuss voltmeters and ammeters, bridges, etc., since they are used to determine the performance of these electronic devices, such as power output, voltage characteristic and the like. Because oscillators, waveform generators, modulation monitors, etc., are required to make measurements these are described also.

There is a considerable volume of useful material dealt with so that any one item is necessarily only discussed briefly, but the text is well backed up by numerous references for those requiring more detailed information. The book is



certainly valuable as a reference source and should find its greatest use with practising engineers. One is rather more doubtful about its value for a university course, for which the authors also intend it; too much has been compressed into it to make it easily digestible for this purpose.

A. J. MADDOCK

**The initiation and growth of explosions in liquids and solids.**

By F. P. BOWDEN and A. D. YOFFE. (London: Cambridge University Press.) Pp. xiii + 104. Price 22s. 0d.

Until an explosive has fulfilled its destiny and exploded it is a potential source of danger. Its violent energy may be unexpectedly released by various means including friction and impact. The book is essentially a description of a series of experiments to elucidate the basic causes of such explosions.

An account is given showing how the trapping of air bubbles in liquid explosives makes them sensitive to very gentle impacts. (When Dr. Bowden drew attention to this important phenomenon some years ago it had immediate effect in the safety precautions of the explosives industry.) Experiments are described to show that a similar process is partly responsible for the sensitivity of solid explosives.

The final chapter is concerned with the growth of weak explosions into powerful detonations.

The book is easily readable and well illustrated. It is a pity that little reference is made to pre-war work.

C. A. MEEK

**Organisation Météorologique Internationale. Publication No.**

79. (Geneva: World Meteorological Organization.) Pp. 95. Price Sw. fr. 2.-.

The Aerological Commission of the International Meteorological Organization appointed a sub-commission under the chairmanship of Professor P. A. Sheppard to provide (i) values of physical functions and constants used in meteorology, and (ii) definitions and specifications of water vapour in the atmosphere. The aim of the report was to provide values acceptable with particular reference to synoptic practice and the thermodynamics of the atmosphere. The guiding principles in the choice of magnitudes of physical quantities were to obtain consistency with (a) the results of modern laboratory techniques and physical theory, (b) thermodynamic logic, (c) theoretical and practical requirements of meteorology, (d) the choice of magnitudes of physical quantities adopted in recent years by physicists and engineers, in particular with those recommended by (i) Birge (1941), (ii) the Working Sub-committee of the International Joint Committee on Psychrometric Data. It is stated that further proposals are required regarding additional physical quantities used in various applications of meteorological theories and principles, e.g. radiation and turbulence. In the section on specifications of water vapour no attempt is made to specify the liquid water or ice content of air. At the conference of Directors of Meteorological Services, Washington 1947, the recommendations of the sub-commission were not accepted entirely and the resolutions adopted at the conference are also quoted. For example the sub-commission states the need for an extensive and thorough experimental determination of the saturated vapour pressures over super-cooled water, experimental data for temperatures below  $-15.3^{\circ}\text{C}$  not being at present available. The Smithsonian Meteorological Tables (1951) are based on the 1947 resolutions of the Washington conference. The publication is a valuable one in that it is based on sound principles and it gives indications where further experimental work is required.

R. S. READ

**Theoretical nuclear physics.** By J. M. BLATT and V. F.

WEISSKOPF. (London: Chapman and Hall Ltd.)

Pp. xiv + 864. Price 100s.

It takes considerable courage to write, at this time, a book on nuclear theory. While much has been achieved in this field there remain many loose ends. Theoretical methods have proved themselves sufficiently to confirm the general principles, but it is yet too early to present the subject deductively, without the aid of semi-empirical arguments. At the same time the state has been reached where all empirical facts should be discussed to see how they fit in with theoretical concepts, rather than, as might have been reasonable even a few years ago, single out only those few relationships that lend themselves to a complete theoretical treatment.

Blatt and Weisskopf have made a gallant effort to give a fair presentation of the subject. They have not tried to oversimplify, or to put on the kind of gloss that impresses the superficial reader but presents obstacles to the student who really wants to learn where the difficulties are.

The selection of material and the method of presentation must in a subject of this kind be very largely a matter of individual taste and it is probably unavoidable that the reviewer should disagree in places with the authors' choice. It seems to me that in many places the text could have been shortened and made easier to follow if some of the verbal explanations had been replaced by a more quantitative reasoning. For example, the theory of nuclear reactions, to which the senior author has made very important contributions, is treated successively on three levels, a general descriptive account, a comparison of the results with experiments, and a formal mathematical theory. This division might, in principle, be very useful, but it has the danger of leading to repetition and also of leaving the reader somewhat puzzled about the relations between the results obtained at the different levels. I would have preferred to see the simple descriptive treatment made simpler still and to see more cross-references between intuitive statements and the formal reasoning by which they can be justified.

It is a pity that only very little space could be found for the nuclear shell model, which occupies only 19 pages out of a total of over 800; probably the reason is that the plans for the book were too far advanced by the time the shell model had established itself firmly as a tool for the study of the nucleus. This is the price one has to pay for obtaining a book on a rapidly developing subject. It is a little surprising to see the model due to Feenberg regarded as practically equivalent to that of Mayer and Jensen (p. 767). One would have liked also to see the discussion of the shell model linked more closely with Section VII (iii) on the independent particle model. For example, on page 290, it is stressed that a pair of like nucleons, which do not contribute to the spin of the ground state, may yet influence its magnetic moment, yet on page 772 the fact that a configuration with a single proton and an even number of neutrons in an incomplete shell does not give the one-particle value for the magnetic moment appears as a difficulty.

Like anybody concerned with a field as complex as nuclear theory the authors have their clear likes and dislikes. To the latter belongs the concept of isotopic spin, which is described for the sake of completeness, but without enthusiasm. In fact, the relation between this concept and the charge independence of nuclear forces is not mentioned and this leads to the surprising claim (equation 5.34) that by a suitable choice of coefficients the charge-independent expression (5.31)

can be made to yield the evidently charged-dependent result of the "charged theory."

However, this list of criticisms should not be allowed to obscure the merits of the book, which contains a wealth of useful information and explanation, particularly in the theory of nuclear reactions and in the discussion of multipole moments, to stress only two of the strongest parts of the book. There is an extensive and useful list of references, more complete and less parochial than might be gathered from the warning in the preface that there might be references missing "especially to papers which appeared in journals other than the *Physical Review*."

While the authors rightly are not afraid of using mathematics where it is of advantage, they have placed suitable danger signs on the sections that might be troublesome to readers with a dislike for mathematical symbols and (as far as this can be judged by a mathematically trained reviewer) the demands made on the knowledge of the reader are not exacting, though the statement in the preface that one term's work on wave mechanics might be sufficient as a preparation, implies a very high opinion of the ability of the average student.

R. E. PEIERLS

**Numerical analysis.** By D. R. HARTREE. (London: Oxford University Press.) Pp. xiv + 287. Price 30s.

This is a book about numerical methods for those who wish to use them. It is based on a course of lectures on numerical analysis which the author has given in the University of Cambridge for several years. Those who have had the privilege of attending lectures by Professor Hartree will find here the clear and lucid exposition to which they are accustomed.

The book has throughout a practical approach. It meets the needs of the reader who wants to know how best to carry out an extensive calculation, such as the solution of a large number of simultaneous algebraic equations, with a reasonable chance of getting the right answer or of detecting a mistake if he makes one. The main topics discussed are: the tools of numerical work, including calculating machines and mathematical tables, and how to use them; evaluation of formulae; finite differences; interpolation; integration and differentiation; integration of ordinary differential equations; simultaneous linear algebraic equations and matrices; non-linear algebraic equations; functions of two or more variables, including the solution of partial differential equations; miscellaneous processes such as the summation of slowly convergent series and the smoothing of a set of function values. Southwell's relaxation process is discussed with reference to the solution of simultaneous algebraic equations and of partial differential equations of the elliptic type. In the reviewer's opinion it would have been more in keeping with the character of the rest of the book to have omitted the final chapter on the organization of calculations for an automatic machine. In each section the formulae underlying the method are derived as briefly as possible and the numerical procedure is described in detail. Usually there is a worked example to show the best method of arranging the calculation and of including routine checking procedures for the detection and elimination of errors. Finally the worked example is discussed critically in footnotes that reveal very clearly the author's wide experience of this subject. There are forty-one examples for the reader to attempt.

The author says in his preface that the book is not meant

so much for the specialist in numerical analysis as for the general reader who wishes to apply numerical methods to his own problems. In this aim he has undoubtedly succeeded and the book is to be strongly recommended.

J. CRANK

**Remote control by radio.** By A. H. BRUINSMA. (Holland: Philips Technical Library; London: Cleaver Hume Press Ltd.) Pp. viii + 96. Price 8s. 6d.

This book is not, as one might suppose from the title, a general survey of radio control methods, but a detailed description of the two radio controlled model boats which were demonstrated at the 1952 Radio Exhibition. Their development must have been an enjoyable occupation.

Thirty pages of the book are devoted to valve characteristics, and in view of its general "publicity" nature and the fact that the cover so readily parts company with the pages, the price is high.

R. D. NIXON

**Detonation in condensed explosives.** By J. TAYLOR. (London: Oxford University Press.) Pp. xi + 196. Price 25s.

Dr. Taylor explains in his preface that this monograph, although prepared to his plan and under his guidance, should be regarded as a concerted effort of the research workers of The Nobel Laboratories of Imperial Chemical Industries Ltd., many of whose hitherto unpublished results have been drawn upon in its preparation. Nearly all commercial explosives are mixtures, in the not very distant past compounded by trial and error to attain the desired characteristics, and therefore certainly not ideal starting material for fundamental investigations; nevertheless notable contributions to our understanding of the principles underlying detonation processes have come from Dr. Taylor and his colleagues in recent years and this review of the present state of the subject from such an authoritative source will be welcomed by industrial and academic scientists alike.

The blast is tempered to the latter by introductory chapters on the nature and use of high explosives and the measurement of detonation velocity; chapters on equations of state, thermochemistry, and the hydrodynamic theory of detonation follow. The hydrodynamic theory enables the detonation velocity in gaseous explosives to be calculated with considerable accuracy; perhaps the most remarkable example of this is the prediction, verified by experiment, that the addition of helium, a chemically inert material, increases the detonation velocity. The chief difficulty encountered in the application of the theory to the detonation of condensed explosives lies in choosing a suitable equation of state for the products, and further difficulties arise when some of these are solid. Nevertheless, as two of the main chapters in the book show, the theory has been extended with considerable success to condensed explosives in so far as the calculation of detonation velocity is concerned, although it is doubtful if calculations of maximum temperatures are yet reliable.

Later chapters deal with the variation of detonation velocity with cartridge diameter, with the nature of the reaction zone, and with the puzzling phenomenon of two detonation velocities, high and low, with a discontinuity between them, which occurs chiefly in nitroglycerine explosives. The book contains a wealth of experimental data to support the theoretical discussions and gives many practical examples of explosive calculations worked out in detail.

E. G. COX



## Notes and comments

### Exhibition of X-ray crystallographic equipment

The X-ray Analysis Group of The Institute of Physics will hold its autumn conference in London on 20 and 21 November, 1953, and an exhibition of X-ray diffraction equipment will be arranged. Offers of exhibits are invited under two headings: (i) apparatus commercially available in this country, and (ii) examples of recent developments in X-ray crystallographic equipment that have been made in universities and other research centres in this country. Examples of the kind of exhibit envisaged are: X-ray tubes, diffraction cameras of all types, microbeam techniques, counters and counter-spectrometers for diffraction work, any aids to interpretation, monochromators, microdensitometers, travelling microscopes, X-ray films and photographic accessories, and spectrometers for fluorescent analysis. Owing to the limited space available a selection will have to be made from the offers submitted.

Offers of exhibits giving details of approximate bench and floor space required and of any services needed should be submitted before 1 September, 1953, to the Conference Secretary, Mr. H. J. Goldschmidt, F.Inst.P., c/o The Institute of Physics, 47 Belgrave Square, London, S.W.1.

### Summer school in the use of electrons in the examination of metals, Cambridge 1953

A summer school consisting of lectures, demonstrations and practical classes in the use of electrons in the examination of metals will be held in the Cavendish and Goldsmiths' Laboratory at Cambridge during the period 20-31 July, 1953. A detailed syllabus and form of application for admission may be obtained from G. F. Hickson, M.A., Secretary of the Board of Extra-Mural Studies, Stuart House, Cambridge, to whom the completed application form should be returned not later than 30 May.

### Exhibition of control techniques and instruments

The Norwegian Industries Development Association is sponsoring an exhibition entitled "Automation, servo-mechanisms, instrumentation" to be held in Norway from 10-20 June, 1953. The exhibition will cover measuring and control techniques and associated instruments and apparatus. In connexion with the exhibition a study conference is being planned. Further details may be obtained from Studieselskapet for Norsk Industri, Munkedamsvn, 53B, Oslo.

### Safety in mines research

The 30th Annual Report on Safety in Mines Research, which has just been published by H.M. Stationery Office, records some interesting work in applied physics. This includes the use of  $\gamma$ -rays, ultrasonics, and magnetic ink methods of flaw detection in equipment, and investigations on the static electricity charges resulting from the flow of compressed air. Work on dust control has included the consideration of equipment for automatically counting and

sizing dust particles collected on a microscope slide. X-ray diffraction analysis techniques have been developed further for the rapid quantitative determination of the mineral constituents of dusts. Apparatus for the measurement of X-ray line intensities using Geiger-Müller counters is being constructed and a photographic method using magnesium oxide as internal standard is in use. Electron microscopy and diffraction techniques have been studied for measuring concentrations and size distributions of airborne dusts with a modified stationary internal precipitator.

### Reports on the reliability of engineering plant

We have received a copy of Volume 1 of a new series of technical reports prepared by the British Engine Boiler and Electrical Insurance Co. Ltd. of Manchester. These reports are based on the experience gained by the Company in inspecting failures in different types of power plants. This new series of reports replaces the annual reports published until 1938 and it is intended to publish each volume at intervals determined largely by the availability of suitable material. It is anticipated that the average interval will be about two years.

Volume 1 has 212 pages and contains thirty illustrated reports which cover such items as: Failure of rotating shafts due to repairs by welding; Turbine blade failure; Structural deterioration of a steel chain subjected to high temperature; Excess current protection of electric motor circuits; Explosion of an air vessel; Multiple cracking of case-hardened pins; Some sources of error in quasi-static and impact notched-bar testing. Copies are available from British Engine Boiler and Electrical Insurance Co. Ltd., 80 Lombard Street, London, E.C.3. Price 12s. 6d.

## Journal of Scientific Instruments

### Contents of the May issue

- SPECIAL ARTICLE  
Instruments for measuring plasticity in the rubber industry. By J. R. Scott.
- ORIGINAL CONTRIBUTIONS  
Papers  
The design and operation of a precision Geiger-Müller counter X-ray diffraction spectrometer. By R. A. Coyle, K. F. Hale and C. Wainwright.  
Electromagnetic vibration pick-ups with simple seismic suspension. By J. A. Macinante.  
An instrument for measuring small forces. By R. Gibson, J. Ingham and L. J. Postle.  
A recording microdensitometer applicable to biological problems. By P. M. B. Walker.  
An oximeter for continuous absolute estimation of oxygen saturation. By W. Paul.  
A direct-reading standing-wave indicator. By A. C. Grace and J. A. Lane.
- Laboratory and workshop notes  
Glass leak and control valves. By E. R. Harrison.  
An electrically operated all metal capillary vacuum valve for adjustable gas flow. By G. W. Green.  
A technique for mixing radioactive solutions. By K. W. Bagnall and G. L. Miles.  
A compact refluxing head for a large fractionating column. By J. S. George.
- NOTES AND NEWS  
New instruments, materials and tools  
New books  
Notes and comments

THIS JOURNAL is produced monthly by The Institute of Physics, in London. It deals with all branches of applied physics (including theory and technique). All rights reserved. Responsibility for the statements contained therein attaches only to the writers.

EDITORIAL MATTER. Communications concerning editorial matter should be addressed to the Editor, The Institute of Physics, 47 Belgrave Square, London, S.W.1. (Telephone: Sloane 9806.) Prospective authors are invited to prepare their scripts in accordance with the *Notes on the preparation of contributions*. (Price 2s. 6d. including postage.)

REPRODUCTION. The Institute of Physics is a signatory to The Royal Society's Fair Copying Declaration. Details may be obtained upon application from The Royal Society, London, W.1.

ADVERTISEMENTS. Communications concerning advertisements should be addressed to the agents, Messrs. Walter Judd Ltd., 47 Gresham Street, London, E.C.2. (Telephone: Monarch 7644.)

SUBSCRIPTION RATES. A new volume commences each January. The charge is £4 per volume (\$11.50 U.S.A.), including index (post paid), payable in advance. Single parts, so far as available, may be purchased at 8s. each (\$1.15 U.S.A.), post paid, cash with order. Orders should be sent to The Institute of Physics, 47 Belgrave Square, London, S.W.1, or to any bookseller.



# On the temperature sensitivity of special magnetic materials

By T. A. HEDDLE, B.Sc., A.Inst.P., British Scientific Instrument Research Association, Chislehurst, Kent

A description is given, in survey form, of magnetic materials which are sensitive to temperature in the range  $-60$  to  $+120^{\circ}\text{C}$ . Applications of these materials to temperature detecting and compensating devices are also considered.

The common ferromagnetic elements, iron, nickel and cobalt, have different intensities of saturation magnetization and different Curie temperatures (approximately: iron,  $770^{\circ}\text{C}$ ; nickel,  $350^{\circ}\text{C}$ ; cobalt,  $1120^{\circ}\text{C}$ ), but the graphs of Fig. 1,<sup>(1, 2)</sup> showing the temperature dependence of the saturation magnetization of these metals, display a fundamental similarity. In Fig. 1 the abscissae give temperature as a proportion of the Curie temperature of the particular metal on the absolute scale, and the ordinates give intensity of saturation magnetization as a proportion of the intensity at  $0^{\circ}\text{K}$ . The theoretical curve, derived from the theories of Langevin, Weiss and Heisenberg, agrees well, over much of its range, with the characteristics of these elements and of some alloys also.<sup>(2, 3, 4)</sup>

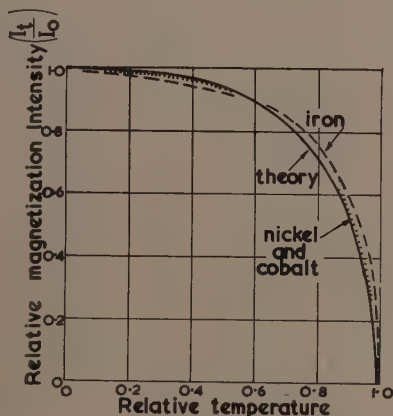


Fig. 1. Temperature dependence of saturation magnetization

It will be seen from Fig. 1 that the maximum sensitivity to an increment of temperature occurs just below the Curie point, so that, when high sensitivity is desired near room temperature, a material with a Curie point also near room temperature is required. Materials which are valued on account of their high temperature-sensitivity are known as thermomagnetic materials. They are basically alloys of one of the ferromagnetic elements with a less magnetic, or non-magnetic, secondary metal in solid solution.

## REDUCTION OF THE CURIE POINT BY ALLOYING

Figs. 2 and 3 show the Curie temperatures and saturation values of specific magnetization (magnetic moment per gram) of binary alloys of nickel,<sup>(1, 2, 5)</sup> and similar results have been

obtained for binary alloys of iron.<sup>(1, 2, 6)</sup> In general, a small proportion of the less magnetic constituent reduces the magnetization and the Curie temperature.

Some exceptions to the above generalization should be noted. Firstly, the anomalous increase of saturation magnetization due to the addition of manganese to nickel, see Fig. 3, is explained by the theory of interchange forces which give rise to the Weiss molecular field. Manganese is not ferromagnetic on its own, but may become so when its atoms are suitably dispersed in a matrix of some other material, as in the Heusler alloys.<sup>(1)</sup>

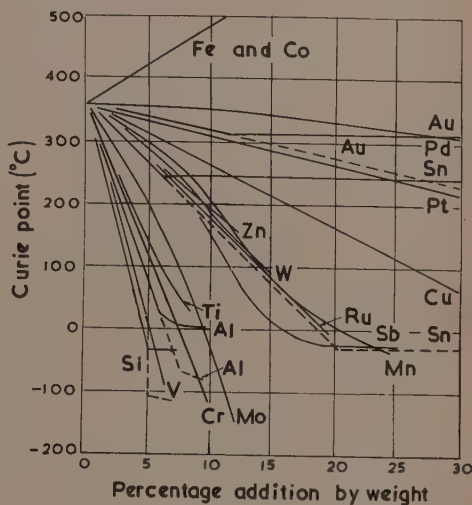


Fig. 2. Curie points of nickel alloys

Secondly, some of the continuous lines of Fig. 2 become horizontal at a point representing the normal limit of solid solubility of the minor metal in nickel. Nevertheless a super-saturated solid solution can be obtained in some alloys by quenching the material from the annealing temperature, the resulting Curie points being shown by the broken lines. These may also become horizontal, showing a limit to the super-saturation.

Finally, it must be noted that the curves of Fig. 2 cannot be extrapolated reliably. In particular, the Curie temperatures of binary iron-nickel alloys, after rising above those of pure nickel, eventually fall below it, reaching room temperatures at about 70% iron. Alloys of such composition are important commercially, because of their temperature sensitivity near room temperature, and are described in the following sections.

## THERMOMAGNETIC MATERIALS

There are two main types of thermomagnetic materials in commercial production, namely, alloys with approximate compositions of 70% iron-30% nickel and of 70% nickel-30% copper. The Curie points and intensities of saturation magnetization of pure nickel-copper alloys are shown in Figs. 2 and 3, but those of iron-nickel alloys<sup>(1, 2, 7, 8, 9)</sup> are

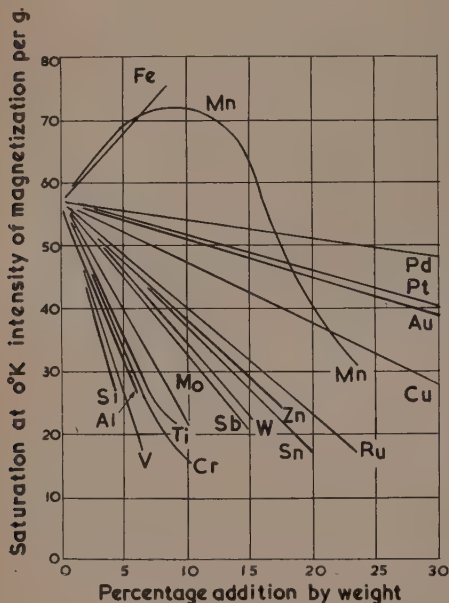


Fig. 3. Saturation magnetization of nickel alloys

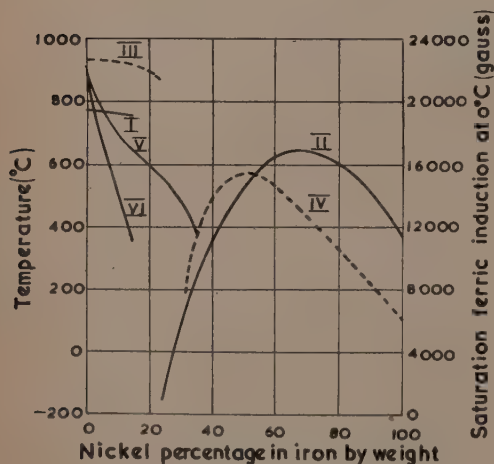


Fig. 4. Iron-nickel alloys

I. Curie points of  $\alpha$ -phase; II. Curie points of  $\gamma$ -phase; III. Saturation magnetization of  $\alpha$ -phase; IV. Saturation magnetization of  $\gamma$ -phase; V. Boundary (temperature) of single  $\gamma$ -phase in equilibrium; VI. Boundary (temperature) of single  $\alpha$ -phase in equilibrium.

shown in Fig. 4 since they exhibit a feature which is discussed later.

Typical temperature-induction characteristics of several commercial materials, at constant field strength, are shown in Fig. 5, where it is seen that the iron-nickel alloys have a greater temperature sensitivity than the nickel-copper alloys. All four curves show Curie points which are not sharply defined, each characteristic having an extended foot. This is a common feature, in some degree, of the pure elements as well as of many alloys.<sup>(5, 10)</sup> Consequently a convention must be adopted in stating the temperature of the Curie point. Most often the temperature is taken from the point of intersection of the steepest tangent to the curve with the temperature axis. Thus the curves of Fig. 5 are said to show Curie points at approximately 10, 35, 50 and 65°C respectively. It would be a mistake, of course, to consider these temperatures as the exact upper limits of the respective ferromagnetic ranges.

The effect of small changes in the proportion of the constituents is mainly to move the characteristic along the temperature axis, giving a higher or lower Curie point, as shown for the three iron-nickel alloys of Fig. 5. In both

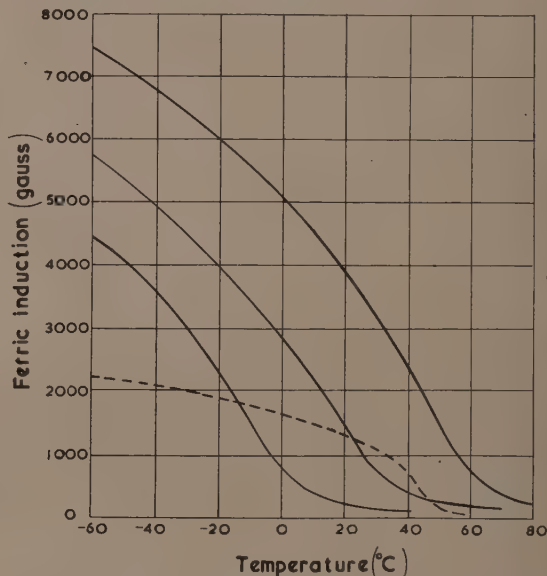


Fig. 5. Typical thermomagnetic characteristics with field strength of 100 oersteds

— iron-nickel alloys  
- - - - - nickel-copper alloy

iron-nickel and nickel-copper alloys around these proportions the Curie point rises with increase of nickel content.

The type of curve shown in Fig. 5 shows an approximately linear fall of induction with rising temperature over a limited range. A numerical estimate of the temperature range, within which a certain approximation to linearity is obtained, can be made, as in Fig. 6, by drawing two curves (broken lines) alongside the characteristic at appropriate ordinate distances, say  $\pm 200$  G; these curves then form an envelope enclosing all points lying within a range of  $\pm 200$  G from the characteristic. The common tangent to the envelope curves

is then drawn, cutting these curves again at points  $P_1$  and  $P_2$ . These points give the temperature limits,  $T_1$  and  $T_2$ , between which the actual characteristic approximates to the straight line of the tangent within the limits of  $\pm 200$  G. The gradient and "Curie point" as indicated by this tangent (not quite the same as that determined by the convention mentioned previously) are also useful in judging the material.

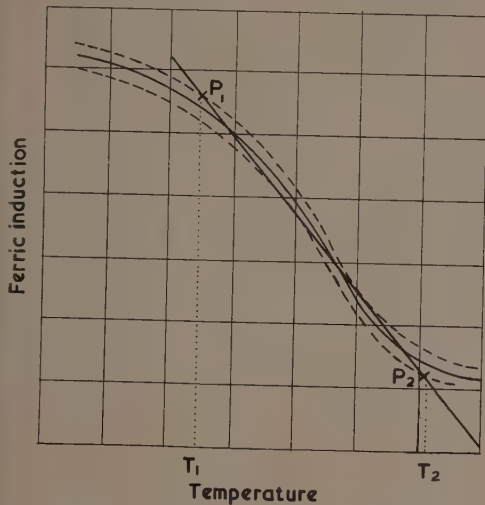


Fig. 6. Estimation of range of approximate linearity

It is shown in Fig. 7 that the range of approximate linearity is greatest at the higher field strengths, where the magnetization approaches saturation. At low field strengths, however, the variation of magnetization with temperature may be of a very different type from that so far considered. At low field strengths, the permeability often increases with rising temperature and reaches a sharp peak before falling steeply at the Curie point.<sup>(3, 11, 12)</sup> The field strength should therefore be stated when stating the range or sensitivity of the material, unless it may fairly be assumed that these refer to a state of quasi-saturation.

#### HETEROGENEITY

The fall of induction near the Curie temperature of a homogeneous material is too abrupt for some applications which are discussed later. The requirements are more nearly met by a gradual slope of the characteristic, as in the lower curve of Fig. 8 which is typical of a heterogeneous material in which the composition is not constant throughout, but varies within a small range. The characteristic is then the resultant of a number of individual characteristics, each corresponding with the composition of a particular part. This heterogeneous structure may be obtained in some alloys by suitable cold working and heat treatment of a uniform solid solution.<sup>(2, 5)</sup> A small addition of molybdenum or

copper has also been used to improve the linearity of characteristic of an iron-nickel alloy.<sup>(2)</sup> This effect of heterogeneous structure can be illustrated by an arrangement, which improves the linearity over a wide temperature range.<sup>(13, 14)</sup> If strips of two materials with different Curie points are used in parallel to carry magnetic flux, the mean flux density at any temperature is a simple numerical average depending upon

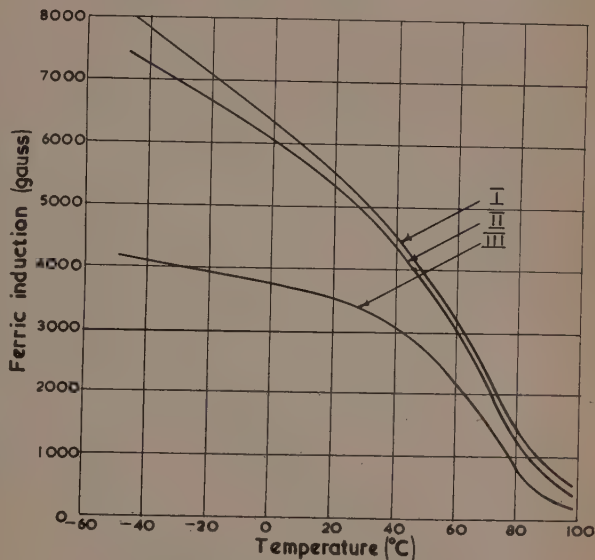


Fig. 7. Effect of field strength upon typical characteristic

I. Field strength 100 oersteds; II. Field strength 50 oersteds; III. Field strength 10 oersteds.

the density in, and the cross-section of each strip. Fig. 9 shows such a resultant characteristic for two suitable materials of equal cross-sections. It is seen that the approximation to linearity is much improved in a temperature range of at least  $170^\circ\text{C}$ .

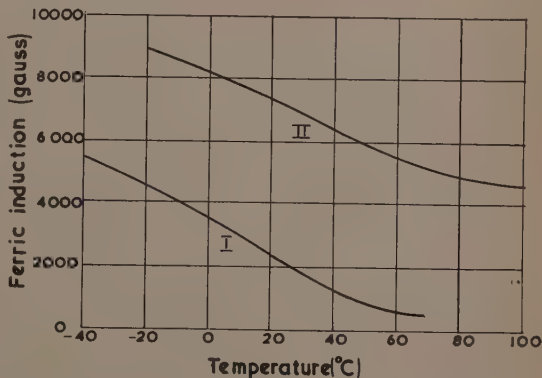


Fig. 8. Change of characteristic due to chilling, with field strength of 100 oersteds

I. Original condition; II. After chilling to  $-90^\circ\text{C}$ .



It is reported that excellent linearity is obtained with only one piece of material if this is made by sintering together the powders of two or more alloys.<sup>(15,16)</sup> The alloys may be made by normal melting and casting, and are chosen so that one has a Curie point at the upper limit of the required temperature range and the others at lower temperatures. They are then pulverized and mixed in certain proportions.

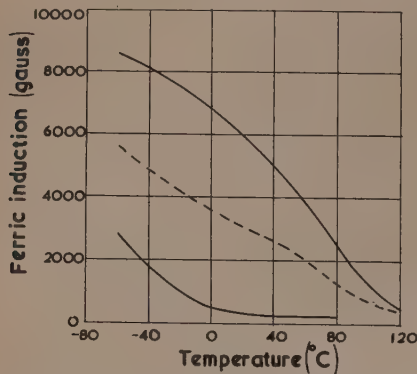


Fig. 9. Characteristic of parallel pair of materials with field strength of 100 oersteds

----- pair of materials;  
—— individual materials

The mixture is sintered at a temperature high enough to yield a solid compact, but upper limits of time and temperature of sintering are set by the need to avoid excessive diffusion or segregation of the constituents. Some diffusion seems desirable in order to obtain a more continuous range of compositions. The choice of the initial alloys and the proportions in which they are mixed seems largely a matter of trial and error.

#### IRREVERSIBILITY

An important requirement in most applications of thermomagnetic materials is that any change of magnetization due to a temperature change must be reversed when the temperature change is reversed. Unfortunately some iron-nickel alloys show severe temperature hysteresis which seriously limits their usefulness at low temperatures.

This hysteresis is associated with changes of crystal lattice structure and is explained by reference to Fig. 4. Pure iron-nickel alloys with nickel content below about 35% exist in either, or both, of two forms depending upon the temperature and history of temperature changes.<sup>(1,2,8,9)</sup> At temperatures just above those shown by curve V of Fig. 4 these alloys are in the  $\gamma$ -state with a face-centred cubic lattice, while below curve VI the  $\gamma$ -state is unstable and the lattice exists in the body-centred cubic  $\alpha$ -state. In the intermediate region between curves V and VI a mixture of  $\alpha$ - and  $\gamma$ -phases may exist, the compositions and proportions of the phases depending on the history of temperature changes. In this region there is a tendency for the compositions and proportion of the phases to change to a state of equilibrium at each temperature, but, particularly at the lower temperatures, the rate at which equilibrium is attained is very slow. However, in the single-phase regions, above curve V and below curve VI, the appropriate lattice is formed instantly even at very low temperatures.

Thus, if an alloy having a nickel content of 30% is quenched in water from 800° C, the material passes quickly from the single  $\gamma$ -phase region into the lower part of the two-phase region. (The boundaries in this part of the diagram are not accurately known.)<sup>(1,9)</sup> Such quenching cools this material through the higher temperatures of the two-phase region without allowing time for appreciable phase segregation, and leaves it, still in the  $\gamma$ -state, at a temperature where the rate of change toward equilibrium is negligible. If the temperature is lowered still further, the change to  $\alpha$ -state occurs suddenly at some temperature near the extension of curve VI of the equilibrium diagram. This  $\alpha$ -state then persists when the material returns to room temperature, and changes again to the  $\gamma$ -state only if the temperature is raised to a value near, or above, curve V.

Since the  $\alpha$ - and  $\gamma$ -states have different magnetic properties, changes from one to the other affect the induction-temperature characteristic of a material. Thus, if a 30% alloy in the  $\alpha$ -state is heated, it changes to the  $\gamma$ -state at a point which is below the Curie temperature of the  $\alpha$ -phase but above that of the  $\gamma$ -phase. Hence the change is from a magnetic  $\alpha$ -state to a non-magnetic  $\gamma$ -state. This change of magnetization resembles the change at a Curie temperature, but a true Curie point is essentially reversible and not associated with a lattice change. Thus the Curie point of pure iron at about 770° C does not denote a change of lattice, as supposed at one time. A change of structure does not occur until about 910° C, when the lattice changes from body-centred to face-centred cubic.

Fig. 8 shows the change in the temperature-induction characteristic due to lattice changes in a particular iron-nickel alloy. In the initial condition of the material, the ferric induction at constant field strength is reversible with temperature change in the range  $-50$  to  $+70$ ° C and follows the lower curve of the figure with a Curie point at about 60° C. If, however, the material is chilled progressively below  $-50$ ° C, a new temperature characteristic results for each stage of the chilling procedure; curve II of Fig. 8 is the final result of chilling to  $-90$ ° C. This characteristic is reversible in the temperature range  $-90$  to  $+100$ ° C, although only the higher temperature end is shown in this figure.

In the original condition, the material of Fig. 8 is in a heterogeneous  $\gamma$ -state, the composition varying within a small range of values such that the resultant characteristic has a gradual slope, as previously pointed out. The effect of chilling progressively below  $-50$ ° C is to convert to the  $\alpha$ -state first those parts with most iron and then those with less. At each step of temperature between  $-50$  and  $-90$ ° C the magnetization quickly reaches a steady value, but even at  $-90$ ° C the full change to  $\alpha$ -state does not occur. On returning to higher temperatures both phases persist and contribute to the magnetization. As before, the  $\gamma$ -phase is near its Curie point and is therefore temperature sensitive, but the  $\alpha$ -phase has a much higher Curie temperature and therefore has relatively constant magnetization. Hence the new characteristic, the upper curve of Fig. 8, shows the drop in magnetization of the  $\gamma$ -phase with increasing temperature superimposed on the relatively constant magnetization of the  $\alpha$ -phase.

The presence of a small amount of carbon or chromium in these iron-nickel alloys has the effect of depressing the transformation temperature and thus increases the temperature range in which the material is reversible in the  $\gamma$ -state.<sup>(17)</sup> Such additions are particularly necessary in materials designed to have a low Curie point, otherwise an attempt to produce such a material by considerably reducing

the nickel content results in one which, even before chilling below room temperature, is predominantly in the  $\alpha$ -state with a consequently high Curie point.

#### COMMERCIAL MATERIALS

The most important commercial materials are basically 70/30 iron-nickel alloys,<sup>(14,17,18,19,20)</sup> They are produced under various trade names: Mutemp (Richard Thomas and Baldwins Ltd.), R.2799 (Telegraph Construction and Maintenance Co. Ltd.), N.I.F.E. 30 (Edgar Allen and Co. Ltd.), in this country; Compensator Alloy (Simonds Saw and Steel Co.), Temperature Compensator Alloy N.30 (Carpenter Steel Co.) in the U.S.A.; Thermoperm (F. Krupps) in Germany; N.M.H.G. (Acieries d'Imphy) in France; Varioperm (Vimetal S.A.) in Switzerland; Shunt Steel (Japan Special Steel Co.) in Japan.

Most of these materials are reversible to temperatures as low as  $-75^{\circ}\text{C}$ , and the vast majority, including all British materials, have Curie points at approximately  $60^{\circ}\text{C}$ , this giving useful temperature sensitivity throughout the ordinary range of ambient temperatures. Some of the foreign materials are available in a number of varieties having different Curie points, some as low as  $10^{\circ}\text{C}$ .

The proportion of nickel is most important since a change from 30.0 to 29.75% results in a drop in Curie temperature of approximately  $10^{\circ}\text{C}$ . Some manganese is added to improve the malleability, although it affects the Curie point also. Silicon and cobalt are common impurities which must be controlled carefully for reproducibility of results.<sup>(17)</sup> As already pointed out, the presence of carbon or chromium is important.

The other important commercial materials are basically 70/30 nickel-copper alloys,<sup>(21, 22, 23)</sup> and are produced in this country under the trade name of JAE Metal (Henry Wiggin and Co. Ltd.), and in the U.S.A. under the names of Calmaloy (General Electric Co.) and Westinghouse Alloy (Westinghouse Electric Co.). These materials have a smaller temperature range of sensitivity than the iron-nickel alloys, but do not show any irreversibility. They may also include small percentages of other constituents such as iron.<sup>(23)</sup>

Various nickel-copper base alloys are produced commercially for uses other than magnetic purposes, e.g. Monel Metal (Henry Wiggin and Co. Ltd.). These may have low Curie points, some below room temperature when the material is normally non-magnetic, but the compositions are not controlled with sufficient accuracy to yield consistent magnetic properties.<sup>(24, 25)</sup>

Silicon-manganese-nickel alloys, with silicon content up to about 4%, e.g. materials with trade names W5, W6, W7 (Henry Wiggin and Co. Ltd.), are made for sparking plug electrodes. Such an alloy, containing 4% silicon and various impurities, may have a Curie temperature at about  $25^{\circ}\text{C}$ , but again the commercial product is not controlled with a view to consistent magnetic properties. Pure nickel-silicon alloys have higher Curie points than these commercial alloys.<sup>(26)</sup> Similarly, various nickel-chromium base alloys such as Nichrome (British Driver-Harris Co. Ltd.) are manufactured for electrical conductors, etc., but may have low Curie points, some below room temperature.

The common high permeability alloys of the nickel-iron series, e.g. Mumetal and Radiometal (Telegraph Construction and Maintenance Co. Ltd.), and the Permalloys (Standard Telephones and Cables Ltd.) have low temperature sensitivity at room temperature.<sup>(27, 28)</sup> This is to be expected in view

of their high nickel contents, in the region of 45 to 80%, and of their consequently high Curie points, but the presence of other constituents in addition to the nickel and iron, complicates their interpretation along these lines.

Finally, mention should be made of the ferrite materials which are sintered complex metallic oxides. Some of these have low Curie points and therefore considerable temperature sensitivity.<sup>(1, 29, 30)</sup>

#### APPLICATIONS OF THERMOMAGNETIC MATERIALS

The applications of thermomagnetic materials may be divided into two groups. The first group comprises electromagnetic devices that are intended to respond to temperature variations, and the second comprises electromagnetic instruments or apparatus that require compensation for temperature errors.

In the first group, an elementary device is a thermostatic relay or fire alarm in which a thermomagnetic armature is held by a permanent magnet. An increase in temperature weakens the attraction between the armature and magnet and, when a certain temperature is reached, the armature is released. Alternatively the thermomagnetic material may be stationary and the permanent magnet pivoted so as to swing away when released. One such arrangement uses a nickel armature operating at about  $350^{\circ}\text{C}$  with an on/off differential of about  $5^{\circ}\text{C}$ .<sup>(31)</sup>

A choke or transformer, made with thermomagnetic material as part, or all, of the core, responds slowly to ambient temperature change in a manner depending upon the particular arrangement of the thermomagnetic and ordinary magnetic parts.<sup>(3, 4)</sup> A thermomagnetic choke tuned with a capacitor resonates to a frequency depending upon the temperature and, with reference to a given frequency, may be said to have a "resonant temperature." If the self-heating of a choke, due to the current flowing in its winding, is sufficient to raise the temperature of the core to its Curie temperature, the voltage-current characteristic takes the form of a hysteresis loop.

A type of induction furnace, having a muffle of thermomagnetic material in the field of an alternating-current solenoid, is thermostatic at a temperature depending upon the Curie point of the muffle.<sup>(32)</sup> The eddy currents induced in the charge and in the muffle depend upon the permeability of the latter, so that their strength drops as the temperature approaches the Curie point.

Several designs of thermometer incorporating thermomagnetic material have been suggested.<sup>(22)</sup> One arrangement utilizes a pivoted thermomagnetic vane in the field of a permanent magnet, set so that the magnetic torque on the vane is opposed to the control of a spring. The equilibrium position is then dependent upon temperature.

Finally, in the first group, are a motor and generator that are of interest but up to the present have not apparently been used in practice. The motor may be made by pivoting a thermomagnetic rotor in the field of a permanent magnet. Heating part of the rotor near the magnet poles then upsets the balance of magnetic forces and results in a torque on the rotor. Continuous rotation of several hundred r.p.m. can be obtained but the torque is very low.<sup>(33, 34)</sup> In the generator, a low-frequency alternating-current may be produced by alternately heating and cooling a stationary armature in a constant magnetic field, but again, the efficiency is very low.<sup>(35)</sup>

The second group of applications, where temperature

compensation is desired, consumes by far the greater quantity of thermomagnetic materials produced, and the most important of these applications, in quantity, is the temperature compensation of induction watt-hour meters.<sup>(18, 22, 36, 37)</sup> Here a thermomagnetic shunt on the permanent magnet brake gives a breaking torque varying with temperature, and provides compensation for the resistance changes of the electrical circuits, particularly those of the rotating disk.

A similar application is made in drag-disk or drag-cup tachometers as used in cars and locomotives, and more particularly in aircraft where high accuracy of working over a wide temperature range is required. In a drag-cup tachometer a spinning permanent magnet induces currents in a cup which therefore tends to rotate with the magnet against the action of a control spring. Temperature errors, due mainly to variation in the cup resistance, may be considerably reduced by shunting part of the magnetic flux through thermomagnetic material.<sup>(3, 13, 17, 38, 39)</sup> As the temperature rises the shunt becomes less effective and the main flux increases, so maintaining the strength of the induced currents.

A further application is made in the temperature compensation of powder cores of inductors used in crystal filters.<sup>(40)</sup> A small proportion of a temperature sensitive alloy is incorporated in the powder used in making the core.

Other applications<sup>(3, 17)</sup> include the temperature compensation of moving-coil millivoltmeters. Here, again, a thermomagnetic shunt on the permanent magnet causes the magnetic field in the gap to vary with temperature, to offset the change in resistance and spring elasticity.

Interest in these thermomagnetic materials depends mainly on the applications to watt-hour meters and aircraft tachometers. The former maintains a steady demand for the materials already being produced with Curie points around 60° C. The latter leads to an increasing demand for a single material, or a parallel pair, with a characteristic of wider temperature range of good approximation to linearity.

#### ACKNOWLEDGEMENTS

The author wishes to thank those individuals and firms who have contributed information and material for testing. He also wishes to thank Dr. A. J. Maddock for continued interest in the subject and the Director and Council of the British Scientific Instrument Research Association for permission to publish this article.

#### REFERENCES

- (1) BOZORTH, R. M. *Ferromagnetism* (New York: D. Van Nostrand Co. Inc., 1951).
- (2) HOSELTZ, K. *Ferromagnetic Properties of Metals and Alloys* (Oxford: Clarendon Press, 1952).
- (3) SHAW, J. *Prod. Engng*, **19**, p. 158 (1948).
- (4) JACKSON, L. R., and RUSSELL, H. W. *Instruments*, **11**, p. 280 (1938).
- (5) MARIAN, V. *Ann. Phys., Paris*, **7**, p. 459 (1937).
- (6) FALLOT, M. *Ann. Phys., Paris*, **6**, p. 305 (1936).
- (7) YENSEN, T. D. *Trans Amer. Inst. Elect. Engrs*, **39**, p. 791 (1920).
- (8) MARSH, J. S. *The Alloys of Iron and Nickel*, **1** (New York: McGraw-Hill Book Co. Inc., 1938).
- (9) HOSELTZ, K., and SUCKSMITH, W. *Proc. Roy. Soc. A*, **181**, p. 303 (1943).
- (10) GERLACH, W. *Z. Elektrochem*, **45**, p. 151 (1939).
- (11) MORRIS, D. K. *Phil. Mag.*, **44**, p. 213 (1897).
- (12) ZAIMOVSKY, A. S. *J. Phys., Moscow*, **4**, p. 569 (1941).
- (13) BALLARD, R. G. *Elect. Engng, N.Y.*, **61**, p. 366 (1942).
- (14) YENSEN, T. D. *Metals Handbook*, p. 587 (Am. Soc. Met., 1948).
- (15) SCHRAEDER, H., and FAHLENBRACH, H. *Z. Ver. Dtsch. Ing.* [VDI], **91**, p. 485 (1949).
- (16) STABLEIN, F. German Patent No. 743249 (1943).
- (17) HINDLEY, W. N. *B.I.O.S. Report*, Final No. 1259 (1946).
- (18) COLONNA-CECCALDI, J. *Rev. Gén. Elect.*, **42**, p. 35 (1937).
- (19) VIMETAL LTD. *Microtecnic*, **5**, p. 24 (1951).
- (20) NISHINA, T. *Japan Nick. Rev.*, **7**, p. 45 (1939).
- (21) MOND NICKEL CO. LTD. *The Magnetic Properties of the Nickel-Iron Alloys* (1949).
- (22) KINNARD, I. F., and FAUS, H. T. *J. Amer. Inst. Elec. Engrs*, **44**, p. 275 (1925).
- (23) KINNARD, I. F., and FAUS, H. T. *J. Amer. Inst. Elec. Engrs*, **49**, p. 343 (1930).
- (24) WILLIAMS, S. R. *Magnetic Phenomena*, p. 154 (New York: McGraw-Hill Book Co. Inc., 1931).
- (25) BURROWS, C. W. *Elect. World, N.Y.*, **78**, p. 115 (1921).
- (26) E. N. SKINNER. *Metals Handbook*, p. 1233 (Am. Soc. Met., 1948).
- (27) SOWTER, G. A. V. *Proc. Instn Elect. Engrs*, Pt II, **98**, p. 714 (1951).
- (28) BUCKLEY, S. E. *Steels in Modern Industry*, p. 388 (Iliffe and Sons Ltd., 1951).
- (29) SNOEK, J. L. *New Developments in Ferromagnetic Materials* (London: Elsevier Publishing Co. Ltd., 1947).
- (30) POLDER, D. *Proc. Instn Elect. Engrs*, Pt II, **97**, p. 246 (1950).
- (31) *Engineering, Lond.*, **169**, p. 161 (1950).
- (32) PERRIN, R., and SORREL, V. *Rev. Metall.*, **28**, p. 448 (1931).
- (33) *Nature, Lond.*, **37**, p. 33 (1887).
- (34) *Nature, Lond.*, **19**, p. 397 (1879).
- (35) BRILLOUIN, L., and ISKENDERIAN, H. P. *Elect. Commun.*, **25**, p. 300 (1948).
- (36) PERRIGO, A. E. B. *Electricity Supply Meters*, p. 224 (Chapman and Hall Ltd., 1947).
- (37) KINNARD, I. F. *Elect. Engng, N.Y.*, **67**, p. 627 (1948).
- (38) RICHTER, B. *Arch. Tech. Messen.*, **186**, p. T75 (1951).
- (39) MOSS, E. B. *Trans Soc. Instrum. Tech.*, **3**, p. 143 (1951).
- (40) LEGG, V. E. *Bell Syst. Tech. J.*, **18**, p. 438 (1939).



# Investigation of the instability of a moving liquid film

By H. B. SQUIRE, M.A., Imperial College, London

[Paper received 23 January, 1953]

The stability of a thin layer of liquid moving in still air is studied theoretically with the object of throwing light on the break-up of films during atomization. It is found that instability occurs if  $W = T/\rho_1 U^2 h < 1$  and that the wavelength for maximum growth factor, for  $W \ll 1$ , is

$$\lambda = (4\pi T/\rho_2 U^2)$$

where  $\rho_1$  is the liquid density,  $\rho_2$  is the air density,  $U$  is the film velocity,  $2h$  is the film thickness and  $T$  is the surface tension of the liquid. Comparison with experimental data shows fair agreement with the observed wavelengths.

## 1. INTRODUCTION

Moving films of liquid occur in atomizers in certain conditions of operation. Such films also occur on seaplane hulls as the blister which is flung forward and sideways and which gives rise to the spray. These films break-up into drops and although the break-up into drops cannot be followed completely, there is evidence<sup>(1,2)</sup> to show that it often occurs through the formation of transverse waves (lines of crests normal to the direction of motion) which grow until a break in the film occurs. The present investigation deals with the growth of the waves through an instability but does not explain the final formation of the drops. It is thought to be worth recording as it seems to describe correctly the initial stages of the collapse of the film and to indicate which are the principal parameters concerned.

The investigation given below treats the film as two-dimensional and of constant thickness. It is not practicable to investigate the stability of a conical film of variable thickness and it is considered that most of the important features are included in the two-dimensional problem.

### List of symbols

$2h$	thickness of film
$U$	velocity of liquid
$\rho_1$	density of liquid
$\rho_2$	density of air
$T$	surface tension of liquid
$x$	distance measured along film
$y$	distance measured normal to film
$\eta$	displacement of surface of film
$t$	time
$\lambda = 2\pi/k$	wavelength of oscillations
$\sigma = \sigma_r + i\sigma_i$	growth factor of oscillations
$\sigma_r/k$	wave velocity
$\phi_1$	velocity potential of motion in liquid
$\phi_2$	velocity potential of motion in air
$r = \rho_2/\rho_1$	density ratio
$W = T/\rho_1 U^2 h$	Weber number

## 2. INVESTIGATION OF STABILITY

The investigation of stability is a straightforward application of classical methods given by Lamb.<sup>(3)</sup> Consider a two-dimensional film of liquid of density  $\rho_1$ , surface tension  $T$ , and thickness  $2h$  moving with velocity  $U$  through air of density  $\rho_2$ , the air being at rest [Fig. 1(a)]. As the film is moving freely the only effect of gravity will be to produce some curvature of the film and this will be ignored.

Because the system is symmetrical about the central plane of the film the oscillations of the film can be divided into

symmetric and antisymmetric modes. For the former the middle plane is undisturbed and for the latter the displacements of corresponding points on the free surfaces are equal in magnitude and in the same direction [Fig. 1(b)]. An investigation of the symmetrical disturbances by the same procedure as the one below showed that long waves of this type are unstable. The degree of instability was, however, found to be very much less than for the antisymmetrical disturbances, which will only be considered in this paper. It

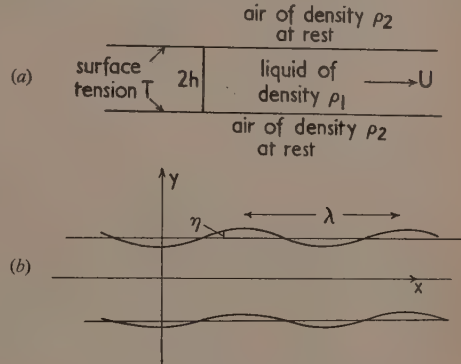


Fig. 1. Antisymmetrical oscillations

may also be noted that the same results could be obtained by treating the film as a membrane, but there is little additional complication in allowing for the finite thickness.

## 3. ANALYSIS OF ANTISYMMETRICAL OSCILLATIONS

Let  $\eta = \exp ikx - \sigma t$  be the displacement of both boundary surfaces of the film in the positive direction of the  $y$ -axis [Fig. 1(b)]. In this formula  $x$  is measured in the direction of motion from an origin in the median plane of the film,  $t$  is the time,  $k$  is related to the wavelength  $\lambda$  of the oscillation by the equation  $k = 2\pi/\lambda$ , the complex quantity  $\sigma$  determines the wave-velocity and damping of the waves, and  $a$  is a constant. Let  $\phi = -Ux + \phi_1$  be the velocity potential of the motion in the liquid layer where  $\phi_1$  is the disturbance potential and let  $\phi_2$  be the velocity potential of the air above the film.\* Then the kinematic boundary conditions are<sup>(3)</sup>

$$\frac{\partial \eta}{\partial t} + U \frac{\partial \eta}{\partial x} = - \frac{\partial \phi_1}{\partial y} \frac{\partial \eta}{\partial t} = - \frac{\partial \phi_2}{\partial y}$$

\* The sign of the velocity potential will be taken to be the same as in ref. (3).

which are to be satisfied, to a sufficient approximation, at  $y = \pm h$ , the undisturbed surface of separation between liquid and air.

Suitable expressions for  $\phi_1$  and  $\phi_2$  corresponding to anti-symmetric oscillations which satisfy Laplace's equation and the above conditions are found by inspection to be

$$\phi_1 = ia \left( \frac{\sigma}{k} - U \right) \frac{\sinh ky}{\cosh kh} \exp i(kx - \sigma t)$$

$$\phi_2 = -ia \frac{\sigma}{k} \exp[-k(y-h)] \exp i(kx - \sigma t)$$

where  $\phi_2$  refers to the upper region  $y > h$  and  $y$  is replaced by  $-y$  in the lower region  $y < -h$ .

The pressure in the liquid near the surface is greater by  $T/R$  than the pressure just outside the liquid, where  $T$  is the surface tension and  $R$  is the radius of curvature of the surface. Hence<sup>(3)</sup>

$$\rho_1 \left( \frac{\partial \phi_1}{\partial t} + U \frac{\partial \phi_1}{\partial x} \right) - \rho_2 \frac{\partial \phi_2}{\partial t} = -T \frac{\partial^2 \eta}{\partial x^2}$$

since  $1/R = -(\partial^2 \eta / \partial x^2)$  approximately. This equation is to be satisfied at the surface  $y = h$ .

Substituting for  $\phi_1$ ,  $\phi_2$  and  $\eta$  we obtain

$$\rho_1 \left( \frac{\sigma}{k} - U \right)^2 \tanh kh + \rho_2 \left( \frac{\sigma}{k} \right)^2 = Tk$$

and the solution of this equation is

$$\frac{\sigma}{kU} = \frac{1 \pm \left( \frac{\rho_2}{\rho_1} \coth kh \right)^{\frac{1}{2}} \left[ -1 + \frac{Tk}{\rho_2 U^2} \left( 1 + \frac{\rho_2}{\rho_1} \coth kh \right) \right]^{\frac{1}{2}}}{1 + \frac{\rho_2}{\rho_1} \coth kh} \quad (1)$$

Unstable waves will only occur if the term in square brackets is negative. It will appear from the analysis below that one of the necessary conditions for instability is  $T/\rho_1 U^2 h < 1$ . We shall for the moment assume that instability is present and hence that  $\sigma$  is complex. We therefore put  $\sigma = \sigma_r + i\sigma_i$ , so that  $\sigma_r$  determines the wave velocity and  $\sigma_i$  the damping coefficient, and obtain

$$\sigma_r/kU = 1/(1 + r \coth kh)$$

$$\frac{h\sigma_i}{U} = \frac{kh(r \coth kh)^{\frac{1}{2}} [1 - W(kh \coth kh + kh/r)]^{\frac{1}{2}}}{1 + r \coth kh} \quad (2)$$

where we have also put

$$r = \rho_2/\rho_1, \quad W = T/\rho_1 U^2 h$$

The Weber number  $W$  is a measure of the ratio of the forces due to surface tension to the forces due to inertia.

We are interested in the waves which grow most rapidly for a film of liquid in air. For such films the density ratio  $r = \rho_2/\rho_1$  is small of order  $10^{-3}$ . In addition it can also be shown that the wavelengths of the unstable waves are large compared with the film thickness and hence that  $kh$  is less than 0.25 (say). Then equation (2) gives

$$\frac{h\sigma_i}{U} = \frac{(kh)^{\frac{1}{2}} [r(1-W) - Wkh]^{\frac{1}{2}}}{1 + r/kh}$$

It can be seen from this expression that  $W$  must be less than unity for  $\sigma_i$  to be real and the film unstable. For the important range of  $W$  below 0.1,  $r/kh$  is much less than unity

and hence the denominator is a slowly varying function of  $kh$ . It follows then that the maximum value of  $\sigma_i$  occurs for

$$kh = \frac{r}{2} \left( \frac{1-W}{W} \right) \simeq \frac{r}{2W} \quad (3)$$

and has the value

$$\frac{h\sigma_i}{U} = \frac{r(1-W)^2}{2W^{\frac{1}{2}}(1+W)} \simeq \frac{r}{2W^{\frac{1}{2}}} \quad (4)$$

The final expressions (3) and (4) are only valid for  $W \ll 1$ .

The significance of expression (3) can best be appreciated for  $W \ll 1$  by substituting the expressions for  $r$  and  $W$  so that we obtain

$$kh \simeq (\rho_2 U^2 h / 2T)$$

Hence the wavelength  $\lambda$  for maximum instability is given by

$$\lambda = 2\pi/k \simeq 4\pi T / \rho_2 U^2$$

and the corresponding growth factor is given by

$$\sigma_i \lambda / U \simeq 2\pi W^{\frac{1}{2}} = 2\pi \sqrt{(T/\rho_1 U^2 h)}$$

Thus the wavelength of the most unstable waves is, for  $W \ll 1$ , proportional to the surface tension of the liquid and inversely proportional to the density of the ambient air and to the fuel pressure (which is proportional to  $U^2$ ).

As an example we may take:

$$\begin{aligned} h &= 4 \times 10^{-4} \text{ cm} & U &= 2 \times 10^3 \text{ cm/sec} \\ \rho_1 &= 1 & \rho_2 &= 10^{-3} \text{ g/c.c.} \\ T &= 40 \text{ dynes/cm} \end{aligned}$$

Hence  $r = 10^{-3}$ ,  $W = 0.025$  and the corresponding values of  $kh$  and  $\sigma_i$  for maximum instability are

$$kh = 0.02$$

$$h\sigma_i/U = 3.16 \times 10^{-3}$$

Thus the wavelength  $\lambda$  of the most unstable oscillations is

$$\lambda = 2\pi/k = 0.13 \text{ cm}$$

and the rate of growth factor is  $\sigma_i \lambda / U = 1.0$ . This value of  $\sigma_i$  indicates that the waves increase in amplitude by  $e^{1.0} = 2.7$  in the time in which the film moves one wavelength (0.13 cm).

#### 4. COMPARISON WITH EXPERIMENT

Photographs of liquid films are given in ref. (1) for a range of fuel pressures and ambient air pressures, and one set of photographs from this report is reproduced in Fig. 2. A comparison has been made between the data of ref. (1), together with supplementary photographs supplied by National Gas Turbine Establishment (N.G.T.E.), and the above theory. The results of this comparison between measured and calculated wavelengths are given in the table and it will be seen that the calculated values are of the same order as the measured values. It has, however, been assumed in the calculations that the loss of head in the nozzle is equal to one half the fuel pressure, but there are few data on nozzle losses and in addition the loss of head may vary with fuel pressure, so there is some uncertainty in the comparison.

The break-up of films by wave formation is also shown in the photographs of ref. (2), but the information available was not sufficient to enable a comparison with the theory to be made.

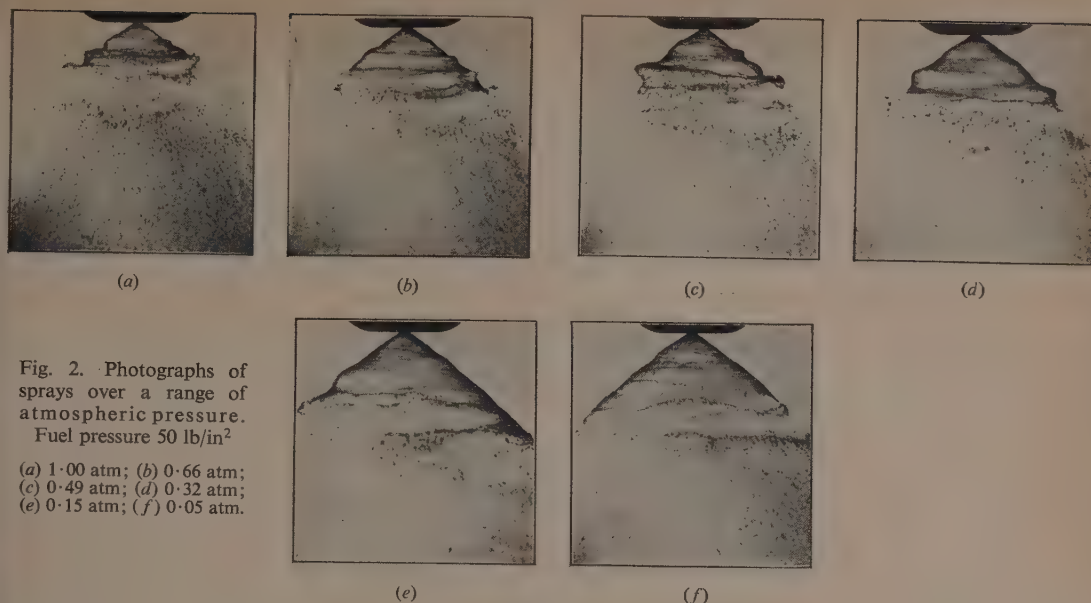


Fig. 2. Photographs of sprays over a range of atmospheric pressure.

Fuel pressure 50 lb/in<sup>2</sup>

(a) 1.00 atm; (b) 0.66 atm;  
(c) 0.49 atm; (d) 0.32 atm;  
(e) 0.15 atm; (f) 0.05 atm.

Comparison of measured and calculated wavelengths for oscillations of liquid film of pool burning oil

(Data from ref. (1) and from supplementary photographs supplied by N.G.T.E.)

Ambient pressure (atm.)	Wavelength (cm)		Calculated growth factor $\sigma\lambda/U$	Density ratio $r \times 10^3$	$W = \frac{T}{\rho_1 U^2 h}$
	measured	calculated			
Fuel pressure 20 lb/in <sup>2</sup>					
1.00	0.18	0.15	1.07	1.53	0.028
0.83	0.16	0.19	1.07	1.27	0.028
0.66	0.17	0.23	1.13	1.01	0.032
0.49	0.22	0.32	1.13	0.75	0.032
Fuel pressure 30 lb/in <sup>2</sup>					
1.00	0.13	0.10	0.83	1.53	0.017
0.83	0.14	0.12	0.83	1.27	0.017
0.66	0.20	0.16	0.93	1.01	0.022
0.49	0.22	0.21	0.93	0.75	0.022
0.32	0.25	0.33	1.01	0.48	0.026
Fuel pressure 50 lb/in <sup>2</sup>					
1.00	0.125	0.06	0.60	1.53	0.0091
0.83	0.14	0.07	0.60	1.27	0.0091
0.66	0.17	0.09	0.64	1.01	0.0104
0.49	0.18	0.13	0.68	0.75	0.0117
0.32	0.22	0.20	0.71	0.48	0.0130
0.15	0.30	0.41	0.75	0.23	0.0143

Nozzle flow = 0.85 gal/h at 100 lb/in<sup>2</sup>.

Surface tension  $T = 26$  dynes/cm.

Density of liquid  $\rho_1 = 0.8$  g/c.c.

Film velocity determined on assumption that losses in atomizer are equal to one half the fuel pressure.

## 5. DISCUSSION OF FILM INSTABILITY AND RUPTURE

The comparison in Section 4 between theoretical and experimental values of the length of the waves which grow most rapidly is near enough to indicate that the theory given above is satisfactory in describing the features of the waves which are observed. However, the theory does not give any indication of how rupture of the film takes place. An examination of the photographs given in ref. (1) indicates that rupture occurs through the generation of waves of large amplitude in cases where the air density is not too low and when the fuel pressure is fairly high. Waves of large amplitude develop as a consequence of the instability and are then subjected to larger air forces than are provided by the theory of small amplitude waves.

However, if either the ambient pressure or the fuel pressure is low the breakdown of the film does not appear to be related to instability of wave-motion. Thus the above stability investigation is only one aspect of the breakdown of a film into drops. It may also be noted that the instability of the film would probably be greatly increased by providing a different air velocity on the two sides of the film.

## ACKNOWLEDGEMENTS

This investigation was suggested by a discussion with Dr. Dixon and Mr. Russell of the Government Chemist's Department. Acknowledgement is also made to the N.G.T.E. for providing photographs and for permitting the reproduction of Fig. 2, and to Mr. Radcliffe of N.G.T.E. for information.

## REFERENCES

- (1) COLBOURN and HEATH. *Swirl Atomizer Sprays in Partial Vacuum*. Unpublished memorandum (N.G.T.E., 1950).
- (2) SIMONS and GOFFE. *Photographs of Sprays from Pressure Jets*. Aeronautical Research Council R. and M. 2343 (1950).
- (3) LAMB. *Hydrodynamics*. 5th Ed. Chapter 9 (London: Cambridge University Press, 1932).



# Formative time lags in the electrical breakdown of gases

By J. DUTTON, B.Sc., Ph.D., A.Inst.P., S. C. HAYDON, M.A., Ph.D., A.Inst.P., and F. LLEWELLYN JONES, M.A., D.Phil., F.Inst.P.,  
University College of Swansea

With a mathematical appendix by P. M. DAVIDSON, B.A., Ph.D.

[Paper first received 9 February, 1953, and in final form 20 March, 1953]

The time rate of growth of ionization currents in a gas in a uniform electric field greater than that corresponding to the static sparking potential is investigated theoretically. This theoretical analysis is then applied to the breakdown of a gas at high values of the parameter  $pd$ . It is shown that the same primary and secondary ionization processes which lead to a growth of pre-breakdown currents in agreement with experiment, and to the calculation of static sparking potentials in agreement with those measured, also lead to a rapid decrease of the formative time lag with increasing overvoltage. The introduction of some other quite different process to account for the short formative time lag is unnecessary. The present theoretical investigation, together with previous experimental and theoretical studies, therefore, lay the basis of a comprehensive view of the electrical breakdown of gases covering a wide range of parameters. Curves showing the dependence of the formative time lag on overvoltage, calculated by means of the above analysis, are given; these curves may be used to elucidate the various secondary ionization processes operative in the breakdown mechanism.

## MECHANISM OF BREAKDOWN

The small steady ionization currents established in gases at a pressure  $p$  by potentials  $V$  insufficient to cause a spark are known as pre-breakdown currents. Experiments have shown that in a uniform field  $E$ , and for constant values of the parameter  $E/p$ , the development of the pre-breakdown current is in accord with Townsend's formula

$$I = I_0 \exp \alpha d / [1 - (\omega/\alpha)(\exp \alpha d - 1)] \quad (1)$$

where  $I_0$  is the constant externally generated cathode current,  $d$  is the distance between the electrodes,  $\alpha$  may be identified with the primary ionization coefficient, and  $\omega/\alpha$  a generalized secondary ionization coefficient consisting approximately of a linear sum of coefficients representing separately the action of photons  $\delta$ , positive ions  $\gamma$  or metastable atoms  $\epsilon$ , at the cathode; or of positive ions  $\beta$  or photons  $\eta$  (under certain conditions),<sup>(1)</sup> in the gas. For example, when only the first two agencies are present, then

$$\omega/\alpha = \gamma + \delta/\alpha.$$

It is evident that the growth of current curve cannot itself specify the contributions of the individual effects to the linear sum, but further information can be obtained from the form of the curve expressing  $\omega/\alpha$  as a function of  $E/p$ ; this method of elucidating the processes operative in breakdown has been used for hydrogen in the lower ranges of the product  $pd$ .<sup>(2,3)</sup>

As is seen from equation (1) the condition that a steady current can be self-maintained, with  $I_0$  zero, is expressed by the vanishing of the denominator:

$$1 - (\omega/\alpha)(\exp \alpha d - 1) = 0 \quad (2)$$

and the potential which gives this condition is conveniently called the static sparking potential  $V_s$ .

Until recently it was often stated that equation (1), though valid for uniform fields at low values of  $pd$  ( $< 150 \text{ cm} \times \text{mm}$  of mercury),<sup>(4,5)</sup> was not applicable at high values of  $pd$  ( $\sim 760 \text{ cm} \times \text{mm}$  of mercury), especially in the range of  $V$  approaching  $V_s$ , and that the criterion of equation (2) should be replaced by one of a different nature, which, it was suggested, caused the occurrence of the spark.<sup>(6,7,8)</sup> It has recently been shown experimentally, however,<sup>(9,10,11)</sup> that the supposed failure of equation (1) does not in fact occur with  $pd \sim 760 \text{ cm} \times \text{mm}$  of mercury. The general ionization

processes which lead to equation (1) in uniform fields appear therefore to be the controlling processes of the breakdown mechanism over the whole pressure range.

From this it follows that when  $V$  attains the value  $V_s$ , an instantaneous generation of electrons will develop into the steady self-maintained current, described above, with  $I_0$  zero; if, on the other hand,  $I_0$  is finite, the current will increase progressively with time, but not at an increasing rate.

When  $V > V_s$ ,

$$V - V_s = \Delta V \quad (3)$$

will be called the overvoltage. The purpose of this present paper is to investigate the time rate of development of ionization currents for various overvoltages, on the basis of those same secondary ionization processes which are known to be operative under steady state conditions giving rise to equation (1), the ionization coefficients being continuous functions of  $V$ .

## INCREASE OF CURRENT UNDER NON-STEADY STATE CONDITIONS

In the non-steady state with  $V > V_s$ , the Townsend primary coefficient  $\alpha$ , being a function of  $V/pd$ , will exceed the value obtaining at the static sparking potential; consequently, the generation of electrons by both primary and secondary processes will occur at a higher rate and it is important to investigate quantitatively the rate of growth of current which then occurs.

This time rate of development of the current in the gas will depend on the particular secondary processes which are operative. For instance, the times required in the development of the secondary ionization mechanisms involving photoelectric action at the cathode depend on the mobilities of electrons only (the transit time of the photons being negligible), and such ionization effects will become apparent more rapidly than those resulting from the incidence of positive ions on the cathode, because of the lower mobilities of positive ions. For such reasons, measurement of the time interval elapsing between the appearance of an initiatory electron in the gap and the attainment of a given value of current in the gap should help to distinguish between the various possible secondary ionization processes. This time interval is known as the formative time lag  $T_f$ , and in practice is defined as the time elapsing from the appearance of an initiatory electron

in the gap to the commencement of the potential fall across the gap produced by the current increase.

Although it can readily be seen that in all cases increasing  $\Delta V$  will decrease  $T_f$ , it is, however, not immediately obvious how the shape of the curve expressing the formative time lag in terms of the overvoltage depends on the particular secondary processes. No rigorous theoretical analysis of this dependence has been published for high values of the parameter  $pd$ . Such an analysis requires consideration of the temporal growth of ionization currents, and for this purpose the following assumptions will be made. Firstly, the positive ion ionization of gas molecules is neglected, because under conditions of uniform field at high values of the parameter  $pd$  it is probable that the contribution to the total ionization due to this process is small. Secondly, photo-ionization of the gas is neglected, because a recent quantitative investigation of this effect has shown that even in a mixed gas such as air in the conditions here considered, this process will be insignificant in comparison with the effects of photon action at the cathode.<sup>(1)</sup>

For these reasons the only electron generation in the bulk of the gas is assumed to be due to single electron-atom collisions, the  $\alpha$  process. With these assumptions the continuity equations (4) and (5) below relating the electron current  $I_-$ , the positive ion current  $I_+$ , the electron and ion drift velocities  $v_-$  and  $v_+$ , the Townsend primary coefficient  $\alpha$  of ionization by electron collision, and the time  $t$ , may be applied to the growth of an ionization current with time between electrodes in a uniform field when  $V > V_s$ .

$$\partial(I_-/v_-)/\partial t = -\partial I_-/\partial x + \alpha I_- \quad (4)$$

and

$$\partial(I_+/v_+)/\partial t = \partial I_+/\partial x + \alpha I_- \quad (5)$$

The boundary conditions necessary for the solution of these equations are obtained by considering the initial space charge distribution at time  $t = 0$ , and by assuming that the electron generation at the cathode ( $x = 0$ ) is due to the incidence of positive ions and photons produced in the electron avalanche and of photons from a constant external source of radiation.

An approximate solution of the continuity equations with approximate boundary conditions has been given by Bartholomeyczyk<sup>(12)</sup> and by Gugelberg,<sup>(13)</sup> but for the purposes of completeness an accurate solution is given by Davidson in the Appendix to this paper.

When the absorption coefficient  $\mu$  of the relevant photons in the gas is small compared with  $\alpha$ , the secondary ionization process of photoelectric action at the cathode leads to an expression for the growth of pre-breakdown currents given by equation (1). Since equation (1) is confirmed by experiment it follows that if photoelectric action is entirely responsible for the secondary ionization, the absorption coefficient  $\mu$  can be neglected. Again, for the purposes of the present analysis a sufficiently accurate approximation to the boundary condition that there is no current in the gas at  $t = 0$  (i.e. before the application of the pulse of voltage) can be obtained by putting  $C = -I_0/P$  in equation (5) of the Appendix. These simplifying assumptions give a solution for  $I_-(o, t)$  of the form

$$I_-(o, t) = I_0(1 - \exp \lambda t)/[1 - (\gamma + \delta/\alpha)(\exp \alpha d - 1)] \quad (6)$$

By calculating the value of  $\lambda$  from equation (4) of the Appendix, and inserting this value in equation (6) above, it is possible to obtain a value of the current from the cathode at any time  $t$  with any overvoltage  $\Delta V$ .

Equation (6) shows that the time taken for the current in

the gap to increase to any given value is dependent on the value of  $I_0$ , so that it is now necessary to consider what values of this current must be considered in this analysis. In any discussion of spark breakdown one is normally concerned with cold cathode conditions in which the initiatory electrons are produced fortuitously, e.g. by natural processes in the gap. To eliminate statistical time lag an initial current  $I_0$  of the order  $10^{-12}$  A is required, and in the present analysis values of  $I_0$  of this order will be considered.

In order to proceed further with this analysis, it is necessary to consider what particular current  $I_-(x, t)$  in the gap shall be taken to indicate, in practice, that the gap has broken down. Now the establishment of a clearly visible discharge, for example, provides definite experimental evidence that complete breakdown of the gap has occurred, so that the mean current density necessary for the visual detection of the discharge might well be taken to indicate breakdown. Since this current density is not known, it is therefore necessary to choose a practical convenient criterion for completed breakdown in terms of the current rather than in terms of the current density. Schade,<sup>(14)</sup> working at low values of  $pd$  and using a similar criterion, found satisfactory agreement between observed and theoretical values of the formative time lag. At values of  $pd \sim 760$  cm  $\times$  mm of mercury clearly visible discharges have been observed with currents as low as a few microamperes, so that if values of the currents at the cathode ( $I_-(o, t)$  in the range  $10^{-5}$ – $10^{-7}$  A are considered as convenient indications of completed breakdown, it is reasonable to assume that this covers a large number of cases of practical interest.

Assuming, then, these values of the current  $I_-(o, t)$  calculations of the formative time lag can now be made for various values of the overvoltage  $\Delta V$ , on the basis of the operation of various secondary ionization processes ranging from the one extreme case in which the secondary cathode emission is due only to the incidence of positive ions, to the other extreme case in which this emission is photoelectric. (Some preliminary results of these calculations were communicated to the Physical Society Spring Meeting at Swansea 1951 on "Some Aspects of Discharge Physics"<sup>(15)</sup> and later to Section A of the British Association for the Advancement of Science<sup>(16)</sup> at Belfast 1952.)

## NUMERICAL SOLUTIONS

There were strong indications from the measurements of the growth of pre-breakdown ionization currents<sup>(9,10,11)</sup> that the secondary processes operative were those involving the action at the cathode of photons and positive ions. It was in order to examine the influence of these same secondary processes on the temporal growth of ionization currents under non-steady state conditions, discussed above, that the present analysis was undertaken. The results will be applied to the typical case of a 1 cm gap at a pressure of 760 mm of mercury.

In order to determine the time taken for a current  $I_-(o, t)$  to increase to a critical value discussed above, the following procedure was adopted:

(i) The values of the total secondary coefficient  $(\omega/\alpha)$  were calculated from the static sparking potential  $V_s$  and the known values<sup>(17)</sup> of  $\alpha$  at this value of  $E/p$  ( $V_s/pd$  was taken here as  $41.6$  V/cm  $\times$  mm of mercury).

(ii) Various values of  $\delta/\alpha$  and  $\delta$  were chosen satisfying the equation

$$\omega/\alpha = (\delta/\alpha) + \gamma$$

(iii) A particular value of  $\Delta V$  was taken, and the corresponding value of  $\alpha$  found; then assuming that  $\omega/\alpha$  does not vary with overvoltage (which is approximately true for small overvoltages of the order of 2%) and assuming mean values for the electron<sup>(18)</sup> and positive ion<sup>(19-22)</sup> drift velocities equal to  $1.3 \times 10^7$  and  $0.5 \times 10^5$  cm/sec respectively,  $\lambda$  was calculated from equation (4) of the Appendix.

(iv) The value of  $\lambda$  thus determined was inserted in equation (6), and the time taken for the current  $I_-(o, t)$  to increase to the critical value chosen was calculated.

As shown above, no definite value can be assigned to the critical current  $I_-(o, t)$ ; thus, for the present analysis to be as complete as possible, various values of both  $I_-(o, t)$  and of the ratio

$$(\delta/\alpha)/(\omega/\alpha) = \delta/\omega \quad (7)$$

will be considered: this ratio represents the contribution of electrons liberated at the cathode by photon action to the total secondary ionization. The results of the complete analysis are shown in Figs. (1) and (2) as graphs of formative time lag against percentage overvoltage, where  $100 \Delta V/V_s$  defines the percentage overvoltage.

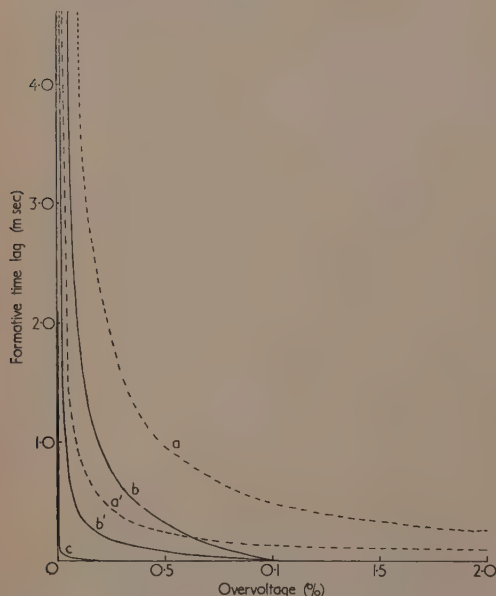


Fig. 1. Theoretical curve showing the variation of the formative time lag, with percentage overvoltage for various values of  $\delta/\omega$  and  $I_-(o, t)$

	$\delta/\omega$	$I_-(o, t)$
a	0	$10^{-1}$ A
a'	0	$10^{-9}$ A
b	0.5	$10^{-1}$ A
b'	0.5	$10^{-9}$ A
c	1.0	$10^{-1}$ A

The dependence of the shape of the formative time lag  $T_f$  against percentage overvoltage curve on the value of  $I_-(o, t)$  is illustrated in Fig. 1, where the graphs are plotted for the three cases when  $\delta/\omega = 1, 0.5$  and 0 respectively. It should be noted that because the value of  $I_-(o, t)$  given by equation (6) depends on the value assumed for the initial photoelectric current  $I_0$ , the curves plotted in Fig. 1 show also the dependence

of the formative time lag against percentage overvoltage curve on the value of this initial current when the critical current  $I_-(o, t)$  is taken to be constant. It can be seen that the dependence of the value of  $T_f$  on  $I_0$  is more marked the smaller is  $\delta/\omega$  (i.e. the greater the contribution of electrons liberated at the cathode by positive ions to the total secondary

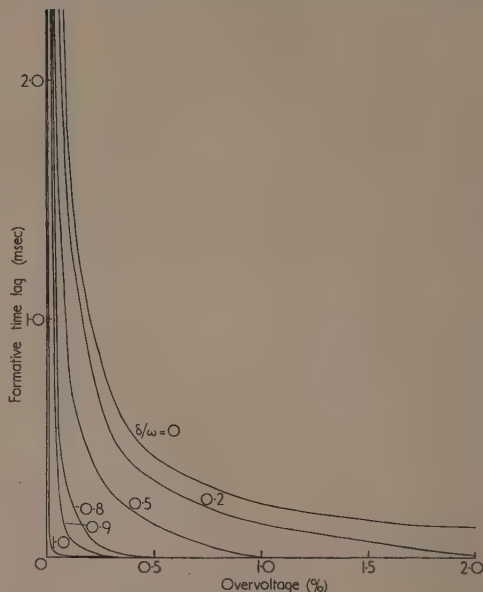


Fig. 2. Theoretical curve showing the variation of the formative time lag with percentage overvoltage for a value of  $I_-(o, t) = 10^{-7}$  A and various values of the ratio  $\delta/\omega$

ionization), and the smaller is the overvoltage. When the error involved in any experimental investigation is known, curves such as those shown in Fig. 1 will determine the order of magnitude of the change necessary in  $I_0$  to give observable variations in the formative time lag.

Fig. 2 shows the dependence of the formative time lag against percentage overvoltage curve on the value of the ratio  $\delta/\omega$  over the complete range of values of  $\delta/\omega$  from 0 to 1, when the critical current  $I_-(o, t)$  is assumed to be  $10^{-7}$  A. It can be seen that the values of the formative time lag show a greater dependence on the value of  $\delta/\omega$  at the lower rather than at the higher overvoltages. It is also interesting to note that for values of  $\delta/\omega$  greater than 0.5, the time lag at 2% overvoltage is always less than about  $10^{-6}$  sec. This result is significant in that it shows that the particular cathode secondary processes assumed here can lead to short formative time lags for low overvoltages, of the order of 2%. This will be discussed further below.

It is clear also that experimental determination of the variation of formative time lag with overvoltage can yield information concerning the nature of the secondary ionization processes operative, because the shape of the time lag against overvoltage curve depends markedly on the ratio  $\delta/\omega$ . The present analysis requires a knowledge of the various factors: electronic and ionic mobilities and the coefficients  $\alpha$  and  $\omega/\alpha$ , so that the application of the analysis to the determination of  $\delta/\omega$  from any particular measurements of time lag, necessitates



a knowledge of all those factors under the particular conditions of gas purity and electrodes in which the time lags are measured. No such complete set of determinations for exactly the same conditions have been published; nevertheless, it is of interest to compare the results of the present analysis with published observations on the basis of the available experimental data, and this will be done in the next section.

## APPLICATIONS

Theoretical curves based on equation (6) for a number of different values of  $I_-(o, t)$  in the range from  $10^{-9}$ – $10^{-1}$  A, and for the particular case when the secondary cathode emission is only photoelectric, i.e.  $\delta/\omega = 1$ , are plotted in Fig. 3, together with experimental data given by Fisher and

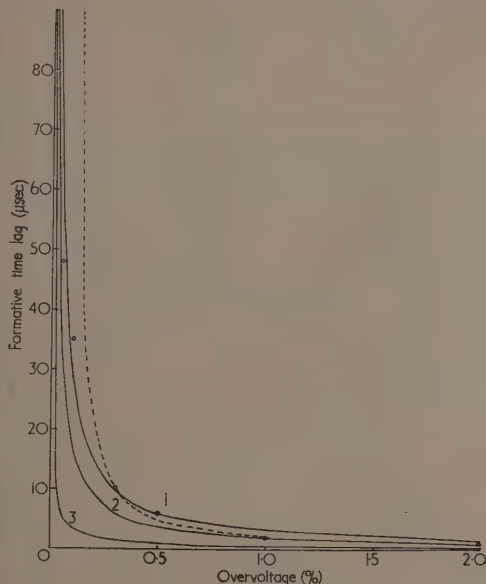


Fig. 3. Comparison of the theoretical curves of a formative time lag against percentage overvoltage (assuming various values for  $I_-(o, t)$  and  $\delta/\omega$ ) with the measurements of Fisher and Bederson<sup>(23)</sup>

	$\delta/\omega$	$I_-(o, t)$
1	1.0	$10^6$ A
2	1.0	$10^{-1}$ A
3	1.0	$10^{-9}$ A
---	0.9	$10^{-1}$ A

○ = measured values of Fisher and Bederson.

Bederson.<sup>(23)</sup> It can be seen that the theoretical curves are of the same general form as that given by the experimental points, but that the agreement is not exact. For this particular case, the experimental curve always lies above the theoretical curve for all the reasonable values of critical current  $I_-(o, t)$  which have been considered. Better agreement, but still not perfect, can be obtained, however, by taking the value of  $I_-(o, t)$  as  $10^6$  A. Although too great a significance should not be attached to the actual value of  $I_-(o, t)$  necessary to give approximate agreement between theory and experiment (because of the assumptions concerning the mobilities and the coefficients  $\alpha$  and  $\omega/\alpha$  discussed above), this value  $10^6$  A still seems unreasonably large.

It is therefore necessary to consider whether a different proportion of photoelectric emission to the total emission, i.e. of the ratio  $\delta/\omega$ , can give better agreement when more reasonable values of  $I_-(o, t)$  are assumed. A curve showing the variation of the formative time lag with percentage overvoltage for the case when  $\delta/\omega = 0.9$ , and for a value of the critical current  $I_-(o, t) = 0.1$  A, is also shown in Fig. 3. It can be seen that, although good agreement is obtained for percentage overvoltages  $\geq 0.3$ , the calculated time lags at the lower percentage overvoltages are very much longer than those measured. It can be seen from Figs. 1 and 2, however, that this discrepancy at the low percentage overvoltage can be reduced considerably by only slight adjustment of the values of  $\delta/\omega$  and  $I_-(o, t)$  assumed, and that slight adjustment will not appreciably affect the time lags at the larger overvoltages. In this way it is possible to obtain fair agreement between the theoretical analysis and the experimental results with more reasonable values of the critical current  $I_-(o, t)$ .

It would thus appear from the application of the above analysis to these experimental results that the secondary mechanism operative in the particular case examined by Fisher and Bederson was the liberation of electrons from the cathode predominantly by the incidence of photons, but that there was also some emission due to the incidence of positive ions.

## DISCUSSION

The following conclusions can be drawn from the results of the present analysis given in Figs. 1, 2 and 3.

(i) The same primary and secondary ionization processes which give rise to the observed growth of pre-breakdown current given by equation (1) lead, under non-steady state conditions ( $V > V_b$ ), to a rapid decrease of the formative time lag with increasing overvoltage.

(ii) The particular values of the time lags obtained depend on the precise nature of these secondary ionization processes; time lags as low as  $10^{-6}$  sec can be obtained with an overvoltage as low as 2% when the significant secondary process is photoelectric emission from the cathode.

The significance of these results lies in the fact that the development of a spark in low times of this order, first observed experimentally by Rogowski,<sup>(24)</sup> has been widely regarded<sup>(7)</sup> as inconsistent with a breakdown mechanism dependent on primary and secondary ionization processes of the Townsend type in accordance with equation (1). The present analysis shows, on the contrary, that these short time lags are consistent with a theory of breakdown dependent on processes of the Townsend type, because these same processes are themselves sufficient to produce the rapid breakdown observed experimentally for low overvoltages. A similar conclusion has now been expressed by Kachickas and Fisher,<sup>(25)</sup> following their very recent measurements of the formative time lags in nitrogen.

The present theoretical investigations indicate how a careful analysis of measured variations of time lag with overvoltage is able to augment the knowledge already obtained by other methods concerning the relative importance of the several possible secondary ionization processes.

## APPENDIX

THE GROWTH OF IONIZATION CURRENTS IN A UNIFORM FIELD  $E(>E_3)$ 

By P. M. DAVIDSON, B.A., Ph.D.

Two infinite parallel plates are considered at a separation  $d$ , the cathode (at  $x = 0$ ) being exposed to a constant external

illumination. At time zero the potential difference of the plates is suddenly increased, and then maintained constant. It is desired to calculate the conditions at any later time (so long as the effects of space charge remain unimportant).

An approximate solution of this problem has already been given by Bartholomeyczzyk,<sup>(12)</sup> who, from a consideration of the differential equations

$$(\partial I_-/\partial t)/v_- = -\partial I_-/\partial x + \alpha I_- \quad (1a)$$

$$(\partial I_+/\partial t)/v_+ = \partial I_+/\partial x + \alpha I_+ \quad (1b)$$

and boundary conditions

$$I_-(0, t) = \gamma I_+(0, t) + \delta \int_0^d I_- e^{-\mu x} dx \quad (2a)$$

$$I_+(d, t) = 0 \quad (2b)$$

employs, for calculating current amplification, an expression

$$I_-(x, t) e^{-\alpha x} = C \exp [\lambda(t - x/v_-)] \quad (3)$$

in which  $C$  is a constant and  $\lambda$  is given a real value satisfying  $F(d) = 0$ , where

$$F(x) = 1 - (\gamma\alpha/\phi)(e^{\phi x} - 1) - (\delta/\psi)(e^{\psi x} - 1) \quad (4)$$

$$\phi = \alpha - (\lambda/v_-), \quad \psi = \alpha - \mu - (\lambda/v_-)$$

$$\text{and } (1/v) = (1/v_-) + (1/v_+)$$

Bartholomeyczzyk's expression (3) for  $I_-$ , together with an accompanying expression for  $I_+$ , satisfy the differential equations (1) and the boundary conditions (2), and are of fundamental importance in the problem. They are not, however, an accurate solution of it, since they do not reduce at  $t = 0$  to the charge distributions actually present at that time; moreover, the boundary condition (2a) omits an additive constant, say  $I_0$ , due to the external illumination. (Gugelburg<sup>(13)</sup> has noted one of these defects—the omission of the constant in the boundary condition—but has not proposed a valid way of correcting for its effects.) It is thus difficult to estimate to what extent the simple expression (3) will approximate to the true solution, or what value should be assigned to the constant  $C$  in order to give the best agreement with the true solution.

Before proceeding to the exact solution, it should be noted that Bartholomeyczzyk's formula can be altered so as to satisfy equations (1) and the corrected boundary conditions (but still not the correct initial conditions) by the following procedure. If  $\lambda$  is given Bartholomeyczzyk's value, and, if

$$P = 1 - \gamma(e^{\alpha d} - 1) - [\delta/(\alpha - \mu)](e^{(\alpha - \mu)d} - 1)$$

then a short calculation shows that an expression

$$I_-(x, t)e^{-\alpha x} = (I_0/P) + C \exp [\lambda(t - x/v_-)] \quad (5)$$

with an accompanying expression for  $I_+$  satisfy equations (1) and the corrected boundary conditions. The constant  $C$  may be given a value which gives rough agreement with the initial conditions; for example, of the initial value of  $I_-(0, t)$  is  $c$ , the solution can be made to have that initial value of  $I_-(0, t)$  by taking  $C$  as  $c - I_0/P$ .

To see how much inaccuracy still remains, a solution must be found which not only satisfies equations (1) and the correct boundary conditions, but also satisfies the initial conditions completely, that is, gives a prescribed initial distribution of positive and negative charge in the whole range  $x = 0$  to  $d$ . The nature of this exact solution may be simply stated. The equation  $F(d) = 0$  has, in addition to the real root, an infinite number of complex roots; the last term in equation (5) must be replaced by a summation containing these various  $\lambda$ 's and

with  $C$ 's determined by the initial conditions. The mathematical problem is of little interest, and it will be sufficient to state the final expressions obtained for  $I_-$  and  $I_+$  (the latter being of importance for estimating when the effects of space charge cease to be unimportant).

It is convenient to think of the expression for, say,  $I_-(x, t)$  as consisting of two parts: (i) the value which it would have if the initial charge distribution had been absent; and (ii) the value which it would have if the constant generation  $I_0$  had been absent. The quantity  $I_-(x, t)$  which will be present in the experiment is the sum of the two parts. The same remarks apply to  $I_+(x, t)$ .

In the part (ii),  $I_-(x, t)$  and  $I_+(x, t)$  are conveniently calculated from the initial distribution, say  $\rho_- = f_-(x)$  and  $\rho_+ = f_+(x)$ , by means of four  $g$ 's (Green's functions), of which, for example,  $g_-(x, x_1)$  is the  $I_-(x, t)$  due to the presence at time zero of unit positive quantity in the region of  $x = x_1$ . Thus the required  $I_-(x, t)$  of part (ii) is

$$\int_0^d [g_- f_-(x_1) + g_+ f_+(x_1)] dx_1$$

and a corresponding expression gives  $I_+(x, t)$ .

At  $t$ 's less than  $x/v_-$  the values of  $g_-$  and  $g_+$ , and also of the  $I_-$  and  $I_+$  of part (i), are of a simple nature, readily seen on visualizing the motion. [For example,  $g_-$  is zero in this range of time if  $x < x_1$ . If  $x > x_1$  there is a sudden pulse at  $t = (x - x_1)/v_-$ , conveying a quantity  $\exp \alpha(x - x_1)$ .] At all later times the series expressions given below for these quantities are valid. Similarly the values of  $g_+$  and  $g_-$  are readily seen at times up to  $(x_1/v_+) + (x/v_-)$  after which the series are to be used.

The series expressions are:

Part (i).

$$I_-/I_0 = e^{\alpha x}/P + \Sigma Q$$

$$I_+/I_0 = (e^{\alpha d} - e^{\alpha x})/P + \Sigma RQ$$

where  $Q = (\lambda d)^{-1} \exp \{[\alpha - (\lambda/v_-)]x + \lambda t\}$

$$R = (\alpha/\phi)[e^{\phi(d-x)} - 1]$$

$$D = (\gamma\alpha/\phi^2 v)[1 - (1 - \phi d)e^{\phi d} + (\delta/\psi^2 v_-)[1 - (1 - \psi d)e^{\psi d}]$$

Part (ii).

$$g_- = \Sigma G_- \quad g_+ = \Sigma R G_-$$

$$g_+ = \Sigma G_+ \quad g_- = \Sigma R G_+$$

$$G_- = \lambda Q F(x_1) \exp \{[(\lambda/v_-) - \alpha]x_1\}$$

$$G_+ = \gamma \lambda Q \exp [-\lambda x_1/v_+]$$

#### REFERENCES

- (1) DUTTON, J., HAYDON, S. C., LLEWELLYN JONES, F. and DAVIDSON, P. M. *Proc. Roy. Soc. A.* To be published. 1953.
- (2) LLEWELLYN JONES, F., and DAVIES, D. E. *Proc. Phys. Soc., Lond., B*, **54**, p. 397 (1951).
- (3) LLEWELLYN JONES, F., and DAVIES, D. E. *Proc. Phys. Soc., Lond., B*, **54**, p. 519 (1951).
- (4) TOWNSEND, J. S. *Phil. Mag.*, **45**, p. 444 (1923).
- (5) TOWNSEND, J. S., and MCCALLUM, S. P. *Phil. Mag.*, **6**, p. 857 (1928); **17**, p. 678 (1934).
- (6) LOEB, L. B. *Fundamental processes of electrical discharges in gases*, p. 407 (Ref. 62) (New York: John Wiley and Sons Inc., 1939).
- (7) LOEB, L. B., and MEEK, J. M. *The mechanism of the electric spark* (Stanford: The University Press, 1941).

- (8) LOEB, L. B. *Phys. Rev.*, **81**, p. 287 (1951).
- (9) LLEWELLYN JONES, F., and PARKER, A. B. *Nature, Lond.*, **165**, p. 960 (1950).
- (10) LLEWELLYN JONES, F., and PARKER, A. B. *Proc. Roy. Soc. A*, **213**, p. 185 (1952).
- (11) DUTTON, J., HAYDON, S. C., and LLEWELLYN JONES, F. *Proc. Roy. Soc. A*, **213**, p. 203 (1952).
- (12) BARTHOLOMEYCZYK, W. *Z. Phys.*, **116**, p. 235 (1940).
- (13) VON GUGELBURG, H. L. *Helv. Phys. Acta*, **20**, pp. 250 and 307 (1947).
- (14) SCHADE, R. *Z. Phys.*, **104**, p. 487 (1937).
- (15) Report on the Physical Society Spring Meeting, 1951, *Nature, Lond.*, **168**, p. 140 (1951).
- (16) Report on the British Association meeting at Belfast, 1952, *Nature, Lond.*, **170**, p. 601 (1952).
- (17) SANDERS, F. G. *Phys. Rev.*, **44**, p. 667 (1932).
- (18) HEALEY, R. H., and REED, J. W. *The behaviour of slow electrons in gases* (Sydney: Amalgamated Wireless (Australasia) Ltd., 1941).
- (19) TYNDALL, A. M., and GRINDLEY, G. C. *Proc. Roy. Soc. A*, **110**, p. 341 (1936).
- (20) VARNEY, R. N. *Phys. Rev.*, **42**, p. 547 (1932).
- (21) BRADBURY, N. E. *Phys. Rev.*, **40**, pp. 508 and 524 (1932).
- (22) LOEB, L. B. *F. Franklin Inst.*, **196**, pp. 537 and 771 (1923).
- (23) FISHER, L. H., and BEDERSON, B. *Phys. Rev.*, **81**, p. 109 (1951).
- (24) ROGOWSKI, W. *Arch. Elektrotech.*, **20**, p. 99 (1928).
- (25) KACHICKAS, G. A., and FISHER, L. H. *Phys. Rev.*, **88**, p. 878 (1952).

## Energy spectrum measurements of protons in the Harwell cyclotron

By J. M. DICKSON, B.Sc., and D. C. SALTER, B.Sc., Atomic Energy Research Establishment, Harwell, Berks.

[Paper received 19 February, 1953]

The proton spectrum of the Harwell cyclotron has been measured by a method which uses the cyclotron magnet as a momentum analyser. For a maximum energy of 174 MeV, the width of the spectrum at half height was of the order of 10 MeV. Random variations of the spectrum shape were observed which were thought to depend on the ion source. A systematic variation of spectrum width with radio-frequency accelerating voltage was found.

The energy of an ion in the beam striking a cyclotron target is a function of the radius of curvature of the ion orbit. Generally the centre of curvature of the orbit is not a fixed point situated at (or near) the geometrical centre of the cyclotron magnet, but is a point which describes a small circle as the ion executes radial oscillations, at a frequency of  $(1-n)^{1/2}$  times the radio frequency of the dee voltage.<sup>(1)</sup> Here  $n = -(r/H)(\delta H/\delta r)$ , and  $H$  is the magnetic field at radius  $r$ . An ion will strike the target only when its centre of curvature is approaching the same azimuth as the target, since the increase of energy per revolution is small. The radius of curvature of the ion orbit is, therefore, very nearly the difference between the radius of the target and the amplitude of radial oscillation. Since the ions in the beam possess various amplitudes of radial oscillation from zero upwards, then the beam striking a target will contain ions of various radii of curvature and hence of various energies.

### ENERGY SPECTRUM MEASUREMENT

If the ion beam in the cyclotron is scattered by a thin target, then the ions of each energy will be focused together again after describing an arc of  $180^\circ$  in the magnetic field. By measuring the variation with radial position of the number of scattered ions arriving at some detecting device placed radially in the cyclotron, at  $180^\circ$  from the target, the distribution of radii of curvature of the ions can be determined. The ion paths from the target to the detectors are not in a constant magnetic field, but the error involved in the calculation of the energy of the ions by assuming a value of the field appropriate to the radius of curvature is small enough to be neglected.

This method of spectrum measurement was used by Bloembergen and van Heerden<sup>(2)</sup> to measure the internal proton spectrum in the Harvard cyclotron. The targets used were

beryllium and tungsten and the detectors of the scattered protons were photographic plates. In the measurements of spectra in the 110 in. Harwell cyclotron only a tungsten target was used and the detector was a linear array of rectangular carbon plates each of which was  $\frac{1}{2} \times \frac{3}{4} \times \frac{1}{8}$  in. The carbon-11 positron activity produced in these detectors by the protons was measured by counting annihilation  $\gamma$ -rays, using a Geiger counter in a standard geometry. The counting rates were corrected for decay of the carbon-11 and for variation of the  $^{12}\text{C}(p, pn)^{11}\text{C}$  cross-section with proton energy.<sup>(3)</sup> The tungsten target was 0.005 in thick (0.246 g/cm<sup>2</sup>) and the energy loss of 165 MeV protons in traversing the target once was about 1 MeV.

The aperture of the cyclotron was reduced to 1 in. by inserting two copper bars, each 9 in. long by 2 in. high by 1 in. thick, above and below the median plane of the beam and extending from the target radius to a radius less than that of the lowest energy detector. The aperture at the tips of the bars was reduced to  $\frac{1}{2}$  in. so that the beam was prevented from striking any other part of the bars. Without this precaution, there was a possibility that some protons from the beam might be scattered by one of the bars and subsequently focused on to the detectors after traversing  $360^\circ$  of arc. The detectors were located on the lower bar and were about  $1\frac{1}{2}$  in. below the median plane. The number of traversals of the tungsten target was calculated to be 1.2.<sup>(4)</sup> A first order correction for this multiple traversal effect was made by reducing the observed intensity for energy  $E$  by 0.2 times the corrected intensity for energy  $(E+1)$  MeV.

### RESULTS

Fig. 1 shows a typical energy spectrum before and after correction for multiple traversals of the target. The width at



half height remained unchanged by this correction, but the peak in most spectra moved about 0.5 MeV towards the high energy end of the spectrum. The spectrum of Fig. 1 was the mean of six runs spread out over a period of  $2\frac{1}{2}$  hours, during which time the ion source arc was maintained in its normal operating condition. All other conditions were maintained constant during each of the 10 min irradiations. Variation in the number of protons per MeV from run to run for any energy in this set of six runs was less than  $\pm 2$  with the maximum of each run normalized to 100.

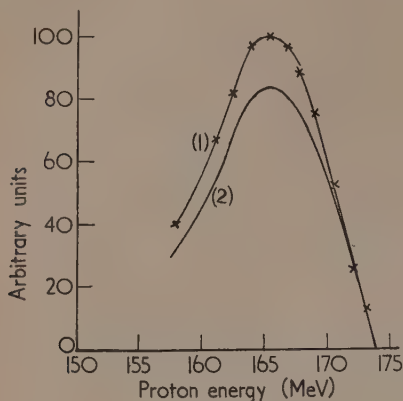


Fig. 1. Proton spectrum at 48.5 in. radius in the Harwell cyclotron, (1) as measured with a tungsten scatterer with 1.2 multiple traversals, and (2) after correction for multiple traversals

Day-to-day variations in the shape of the spectrum could not be fully explained, but the most likely source of variation was the ion source. During a set of eight runs the ion source operating conditions were changed after run four by increasing the hydrogen supply; all other conditions were as in the previous set of measurements. The width of the spectrum at half amplitude for the average curves of the two sets (1 to 4) and (5 to 8) were 12.3 MeV and 11.5 MeV and the displacement of the peak from the maximum energy was 8.5 MeV and 9.4 MeV respectively. The variation within each set was less than  $\pm 0.25$  MeV in width and displacement. The corresponding values for the spectrum of Fig. 1 were 11.7 MeV and 8.8 MeV, whereas on another occasion with similar conditions they were 12.4 MeV and 9.7 MeV. No rational explanation of this variation was discovered.

Four runs at 121 MeV maximum energy gave identical curves, which had a width of 11.75 MeV and a peak at (121–6.5) MeV. When the distribution of amplitudes of radial oscillation were compared for maximum energies of 121 MeV and 174 MeV it was observed that the most probable amplitude of radial oscillation increased with energy from 1.25 to 1.5 in. The energy resolution was approximately the same for the two spectra.

A quite definite and reproducible variation of spectrum shape with dee voltage was observed. The dee voltage was measured as the peak r.f. voltage on the dee averaged over the complete f.m. cycle; the voltage increased by a factor of two during the beam accelerating period. The dee voltages used were 7.9, 9.0, 9.9, 7.0, 7.9, 9.0, 9.9, 7.0 and 8.5 kV, in that order. The repeated runs agreed very closely and were averaged. Fig. 2 shows the relation between (A) the

dee voltage and spectrum width, and (B) the dee voltage and the energy at the peak of the spectrum (maximum energy = 174 MeV). The spectrum width extrapolated linearly to zero dee voltage was about 7 MeV. It has not yet been possible

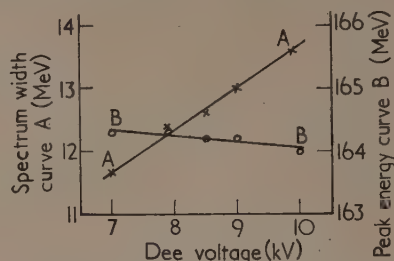


Fig. 2. Variation with dee voltage of (A) the width of the proton spectrum and (B) the energy of the peak of the proton spectrum. Maximum energy of the protons = 174 MeV

to arrive at a logical explanation of this phenomenon, but it seems likely that the asymmetrical nature of the r.f. electric field near the ion source should have some influence on the radial oscillations.

#### DISCUSSION

The spectrum of the protons striking an internal target in a cyclotron is normally much wider than in Fig. 1 due to multiple traversals of the target. The spectrum of Fig. 1 gives the energy of the protons at the start of their first traversal of the target. A fraction of these protons will continue to rotate in the cyclotron with reduced energy, due to energy loss in the target, and will precess until a second traversal of the target occurs. The process can be repeated several times with ever-decreasing energy and numbers of protons. It is obvious that the resulting effective proton spectrum is very wide. All cyclotron experiments using the internal proton beam are affected by this wide spectrum and it must always be taken into account when interpreting the results of such experiments. For example, much of the width of the neutron spectrum of various targets as measured with the Harwell cyclotron<sup>(5)</sup> is due to the proton spectrum. The effective internal proton spectrum depends on the target material and is much wider for light elements than for heavy elements.

#### ACKNOWLEDGEMENTS

The authors wish to thank the cyclotron operating crew for their co-operation during this experiment. This paper is published by permission of the Director, Atomic Energy Research Establishment, Harwell.

#### REFERENCES

- (1) RICHARDSON, J. R., WRIGHT, B. T., LOFGREN, E. J., and PETERS, B. *Phys. Rev.*, **73**, p. 424 (1948).
- (2) BLOEMBERGEN, N., and VAN HEERDEN, P. J. *Phys. Rev.*, **83**, p. 561 (1951).
- (3) AAMODT, R. L., PETERSON, V., and PHILIPS, R. *Phys. Rev.*, **88**, p. 739 (1952).
- (4) CASSELS, J. M., DICKSON, J. M., and HOWLETT, J. *Proc. Phys. Soc. Lond. B.*, **64**, p. 590 (1951).
- (5) CASSELS, J. M., RANDLE, T. C., PICKAVANCE, T. G., and TAYLOR, A. E. *Phil. Mag.*, **42**, p. 215 (1951); *Phil. Mag.*, **44**, p. 425 (1953).

# Techniques for the electron microscopy of crystals

By I. M. DAWSON, B.Sc., Ph.D., Chemistry Department, University of Glasgow

[Paper received 22 December, 1952]

New electron microscopy techniques and modifications of existing techniques are described and discussed with reference to the examination of crystals. Methods of preparation of crystals, replica techniques and shadowcasting are fully examined. Crystals of a suitable size for examination in the electron microscope can be grown by the evaporation of saturated solutions of concentration 0.2–0.5%. The importance of obtaining crystal surfaces uncontaminated by amorphous material is discussed and a technique for freeze-drying protein crystals in such a way as to minimize this surface contamination is described. By a modification of standard replica procedures for electron microscopy replicas of organic crystals can be prepared on the microscope specimen mount without intermediate manipulation. This *in situ* replica technique has considerable advantages in studying the details of crystal surface structure. This method can be used to detect molecular steps of 12–15 Å height on crystal faces.

When the electron microscope first became available for structural studies its resolving power, although greatly superior to that of the light microscope, was still much inferior to that given by X-ray diffraction studies of crystalline solids. The tendency, therefore, in the original structural work with the electron microscope, was to use the instrument primarily for the study of those materials which, being lacking in crystallinity, did not lend themselves to study by X-ray diffraction methods. Into this category came most biological materials and those microcrystalline systems, such as the inorganic colloids and the natural and synthetic fibres, which could not be examined by single-crystal X-ray diffraction techniques. But now, in spite of the fact that the resolving power of the electron microscope is still some fifty times less than that obtainable by X-ray diffraction methods, there are a number of problems in the study of ordered crystalline structures which can best be answered by microscopy rather than by diffraction. These problems are, briefly, those in which we are interested in a non-periodic property the effect of which is not usually apparent in the statistical data available from single-crystal diffraction studies.

In diffraction studies, when optimum use is made of the data obtained, a map can be made of the electron-density distribution for the unit of pattern in the crystal structure and from it bond lengths and bond angles can be calculated for the component atoms in the crystal and the packing arrangement of the molecules determined. The results thus obtained are a statistical mean of the packing conditions prevailing throughout the whole volume of the crystal, and represent the mean values of some millions of molecules. It is therefore not possible by this method to get information of the precise arrangement of molecules at faces, edges and around lattice faults, in all of which positions the molecular arrangements play an important role in both growth and mechanical strength of the crystal. The application of electron microscopy to the study of these non-periodic structures in crystals has only just begun, but it is already beginning to give important information on growth phenomena.

In multiple-beam interferometry, as developed by Tolansky<sup>(1)</sup> in crystal-growth studies with the light microscope, it is possible to detect and measure molecular step heights down to 30 Å, but it is not possible to resolve molecular terraces and islands which are less than 3000 Å in diameter. It is obvious, therefore, that the method of electron microscopy in which the resolving power in the case of shadowcast specimens is equal in all three dimensions is much less liable to misinterpretation than a method which gives resolution in one dimension some one hundred times better than in the other two. This, of course, does not mean

that light optical methods do not have their applications in work of this kind but would suggest, rather, two complementary methods of tackling the problem, the electron microscopical methods giving the maximum of useful information on the structural details of crystal architecture and the light optical methods supplying the information on the dynamic aspects of growth phenomena. The electron microscope should provide the information which will relate the monomolecular growth steps of organic crystals to the multimolecular steps of minerals, of such inorganic crystals as beryl, cadmium iodide and silicon carbide studied by Griffin,<sup>(2)</sup> Forty<sup>(3)</sup> and Verma,<sup>(4)</sup> and of the metals gold, zinc and magnesium studied by Amelinckx<sup>(5)</sup> and Forty.<sup>(6)</sup> The light optical methods have the advantage of permitting serial pictures of growing crystals and migrating dislocations. Both microscopical methods used in conjunction should provide the link between dynamic theories of crystal growth and the basic molecular structure as determined by X-ray diffraction methods.

## THE PREPARATION OF CRYSTALS

In preparing crystalline materials for electron microscopy using either direct or replica methods there are two prime requirements to be borne in mind. Firstly, it is always essential to obtain a molecularly clean crystal surface. Secondly, the crystals themselves must be as thin as possible.

The first of these conditions is sometimes difficult to satisfy when, on the final evaporation of the solvent, an amorphous deposit is left on the surface of the crystal. With organic crystals, a suitable choice of solvent should obviate any difficulty. In practice, in this field, it has been found that a solubility range for a saturated solution of 0.2–0.5% by weight is desirable. Higher values of solubility usually produce crystals which are too large. At the relatively slow rate of evaporation of most common solvents there is little danger of surface contamination of the crystals by amorphous deposit. Where it is not possible to find a simple solvent which will give a saturated solution of the right concentration, then mixed solvents (e.g. alcohol-benzene or water-alcohol) may be used provided always that on evaporation at room temperature there is a decrease in the solubility of the solute due to the preferential evaporation of one of the components of the solvent pair. An alternative to mixed solvents is control of the temperature so that a satisfactory deposition takes place.

In the case of protein crystals the main difficulty is usually that of contamination by amorphous material. There is also the considerable risk of contamination of the final preparation with inorganic crystals from the buffers used to dissolve the protein and to obviate this contamination crystallization



of proteins should be from water if possible. The contamination by amorphous material is, however, more difficult to overcome. The rate of crystallization of all proteins is relatively so much slower than that of other crystalline materials that the final evaporation of even a minute amount of solution surrounding the crystal leaves it covered by an amorphous protein layer. For proteins which are soluble in water, it is possible to overcome the trouble by freeze-drying the protein preparation prior to replica preparation by the Wyckoff<sup>(7)</sup> pseudo-replica technique. The method of freeze-drying can best be described by reference to the study of  $\beta$ -lactoglobulin, Dawson.<sup>(8)</sup> Here a drop of the mother liquors from a solution of the protein containing suitable microcrystals was spread on a clean glass slide and the microcrystals allowed to settle on the glass surface. On rapid freezing of the slide by placing it on top of a liquid-air cooled metal block it was found that freezing took place from the bottom layer upwards; and so the protein microcrystals which had settled on the glass surface were first frozen to the surface and the protein in solution was driven upwards by an advancing front of ice until finally this concentrated protein solution froze in a layer on top of the preparation. After careful vacuum drying of the preparation at  $-30^{\circ}\text{C}$  it was found that the amorphous layer peeled off as a loose thin sheet.

The second condition for satisfactory preparation of crystals, namely that the crystals themselves should be as thin as possible, is essential to minimize overheating in direct examination and to reduce the damage of edge-tearing in replicas.

#### REPLICA TECHNIQUES

Replica techniques are invariably necessary where the crystals are too thick or too unstable for direct examination in the microscope. On the basis of thickness alone it is usually difficult to obtain satisfactory pictures of hydrocarbon crystals of thickness in excess of 2000 Å in normal commercial electron microscopes operating in the region 80–100 kV. For inorganic materials or where the crystals are composed of atoms of greater scattering power (i.e. higher atomic weight), this figure would be further reduced. It can be seen, therefore, that except in special instances which are fortunately fairly important ones from the structural point of view replicas of some kind or another are necessary.

Wyckoff's early work on protein crystals showed the valuable results which could be obtained by the pseudo-replica technique in this instance. The method is now a well-established technique in biological investigations of various types and has been fully described by Wyckoff.<sup>(7)</sup> The method is as follows. The material is deposited on a clean glass slide, allowed to dry and this deposited layer is shadowcast in the usual way: on top of this shadowcast layer there is formed a thin organic film by evaporation of a very dilute solution of either Collodion or Formvar and on careful immersion of the slide in water the film with the adhering shadowcast layer and possibly the topmost layer of the material being replicated, floats off and can be collected on specimen mounts, dried and examined in the electron microscope. The solvent used for the dilute plastic solution is usually amyl acetate for nitrocellulose (Collodion) or ethylene dichloride for polyvinyl formal (Formvar). Both these solvents have some solvent action on a large proportion of organic crystals and thus the replica is completely destroyed at the stage of film formation. This method which has proved most satisfactory for protein and water soluble systems thus becomes impossible for a large number of

organic crystals and to overcome this difficulty a number of classical replica techniques have been used in the past for the study of crystal topography. Since most metallurgical replicas have the serious disadvantage of low resolving power a method involving some form of atomic replica has usually been preferred as instanced in the work of Ames, Cottrell and Sampson,<sup>(9)</sup> where a thick shadowcast layer was evaporated on to the surface of macroscopic crystals and collected without further support after dissolving the crystal itself in some suitable solvent. Variations of this method described by Drummond (Ref. 10, p. 57) involve two step evaporation processes with shadowcasting metal and supporting backing material such as silica or silicon monoxide.

These techniques have their limitations for detailed studies of the surface structure of crystals in that they require the use of macroscopic crystals. If, for example, we take for study a crystal face of area  $1\text{ mm}^2$  then at the reasonable magnification of 40 000 diameters it would be necessary to examine and photograph an area of  $16\text{ m}^2$ , which rather formidable task is a recurrent one in the examination of a representative group of faces. This is possibly the reason for the slow development of the use of the electron microscope in chemical microscopy. However, fortunately the difficulties are not insuperable since it is possible so to modify the silicon monoxide replica technique as to permit the examination of small crystals without intermediate handling. The method is very simple. The crystals themselves are grown on normally prepared microscope specimen mounts (Formvar or Collodion), are shadowcast in the usual way and then have a layer of silicon monoxide (Barcote) evaporated normally on top, to a thickness of approximately 100 Å. The quadruple layer specimen consisting of supporting film, crystal, shadowcast layer and silicon monoxide layer is then treated with an appropriate solvent to remove both supporting film and crystal. For this some type of distillation technique similar to that described by Barnes, Burton and Scott,<sup>(11)</sup> for polystyrene silica replicas can be used. It is frequently necessary to use two solvents in succession, for example, ethylene dichloride to remove the supporting film and water to remove the crystals themselves. In the small number of compounds for which the only suitable solvent is also a strong solvent for Collodion or Formvar it is possible to utilize as a primary support a thin evaporated aluminium or similar metal film.

Another satisfactory method is to use a modification of the carbon replica technique developed by König.<sup>(12)</sup> In this method specimens are exposed to a gas discharge in an atmosphere of benzene at a pressure of 0.1 mm of mercury. Under the conditions operating in the gas discharge the benzene is decomposed and forms on the surface of the specimen a highly insoluble solid layer which appears to follow the molecular contours of the crystal very closely. The supporting film and crystal can then be dissolved out with suitable solvents. This particular technique has one advantage over the others described above in that shadowcasting can be carried out before or after replication so that it is possible to examine crystals on which all shadowcasting metals show extreme mobility and a tendency to aggregate. Unfortunately, however, in practice it is difficult to obtain replicas of satisfactory thickness and mechanical strength and the silicon monoxide technique, where possible, is to be preferred for that reason.

#### SHADOWCASTING

Theory was that materials of melting point below  $200^{\circ}\text{C}$  would melt if subjected to electron microscopy and this



happens with specimens which are so thick that they absorb at least 50% of the energy of the electron beam. From the numerous examples cited in the literature illustrations of this point can be gained from the decomposition of polystyrene

and recent work on the *n*-paraffins, Dawson and Vand,<sup>(16)</sup> and Dawson,<sup>(17)</sup> has shown that organic compounds of melting point around 60° C can be examined successfully. Indeed, in some instances, it is possible to show that a

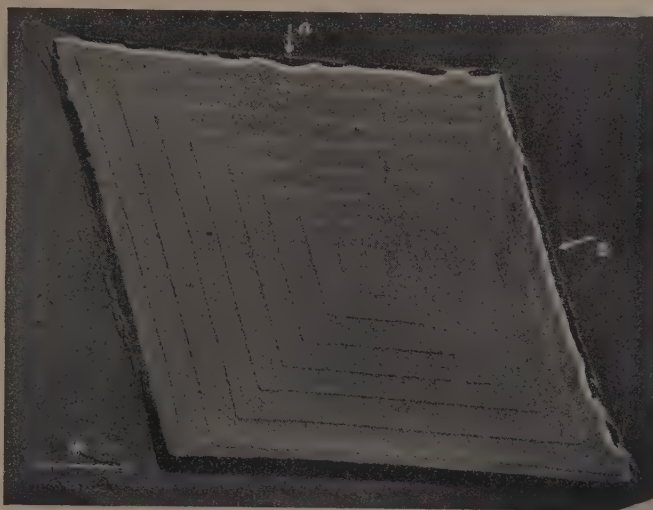


Fig. 1. Electron micrograph of a single crystal of the paraffin *n*-hexatriacontane showing the melting effect of the shadowing metal, in this instance palladium, on edges *A* and *B*



Fig. 2. Electron micrograph of a single crystal of the paraffin *n*-hexatriacontane. This gold-shadowcast specimen has been overheated in the electron microscope and the gross granulation of the shadowcasting metal on the crystal surface and on adjacent paraffin monolayers is clearly seen

latex, Scott,<sup>(13)</sup> and the volatilization of inorganic halides, Burton, Sennet and Ellis.<sup>(14)</sup> However, if the specimens are made thin enough there need be no serious risk of overheating in the electron beam as can be seen from the early examination of rhombic sulphur crystals by von Ardenne,<sup>(15)</sup>

specimen has been partially melted not in the electron microscope but in shadowcasting. Fig. 1 is a micrograph of a single crystal of *n*-hexatriacontane in which some degree of melting can be detected in the regions *A* and *B* on the vertical faces which, being almost normal to the electron beam,

receive most metal. It is obvious that with the previously described *in situ* techniques developed to the point where it is possible to overcome completely the difficulties of the exposure of the crystals themselves to the electron beam it is the question of the effect of the shadowcasting metal on crystals of low melting point that is of paramount importance. It is possible to overcome this difficulty to some extent by using the polymerization technique developed by König,<sup>(12)</sup> as already described in the section on replica techniques, since König replicas can be shadowcast after the support and crystal have been dissolved away. The method is not an ideal one, however, since, if faithful reproduction of the original crystal face is to be obtained, the gas discharge should have no effect on the surface layer of the crystal and in dissolving away both the supporting film and the crystal, solution should be complete with no residual pockets of

shadowcasting unit, condensing on the surface of the specimen. That a chemical factor is involved in metal granulation is also suggested by the well-known fact that coherent films are formed by chromium on oxide containing surfaces, Drummond (Ref. 10, p. 103), and by the high mobility of the chemically unreactive metal gold. It should be possible therefore to choose a metal for shadowcasting which for chemical reasons has minimum mobility on the surface under study. Palladium has been found satisfactory for most hydrocarbon crystals as would be expected from its ability to combine with hydrogen and its frequent use as a catalyst in reactions involving hydrogen. Recently it has been found that by using an equal amount of palladium and nickel for shadowcasting hydrocarbon specimens a striking improvement in the quality of the result can be obtained. I am indebted to Mr. D. H. Watson for Fig. 3 illustrating the



Fig. 3. Electron micrograph of a single crystal of the paraffin *n*-hexatriacontane showing the improved surface quality with nickel-palladium shadowing. The magnification is four times that of Fig. 2

undissolved material in corners and on the edges of the replica. These two conditions are rather difficult to achieve in practice.

Experience has shown that the best results are obtained either by direct examination of shadowcast specimens if the crystals can be made thin enough to justify employing this or by the Wyckoff replica method or the modified silicon monoxide replica method. The melting effect of the shadowcasting metal can be reduced considerably by ensuring that metal evaporation takes place slowly during shadowcasting and by cutting down the amount of radiant heat from the filament which falls directly on the specimen.

The granulation of the shadowcasting layer which sometimes takes place on examination of specimens in the electron microscope is now a well-known effect and Fig. 2 shows the extreme mobility of gold on hydrocarbon crystals. This effect was first strikingly shown by Mandle<sup>(18)</sup> in the examination of tobacco-mosaic virus, and recent work by Williams<sup>(19)</sup> on the same specimen has shown that the granulation which takes place is not solely due to the heating effect of the electron beam but is also much accelerated by traces of oil, in this instance from the diffusion pump system of the

improvement obtained in the case of *n*-hexatriacontane specimens. This result is in agreement with the observation first made by Le Poole<sup>(20)</sup> that alloys should granulate less readily than pure metals.

#### CONCLUSIONS

By one or other of the direct or *in situ* replica methods outlined above it is generally possible to examine all crystals which are too thick for direct study in the electron microscope. The only exceptions are those crystals which are of such high vapour pressure that on exposure to even the moderately low pressures of the König<sup>(12)</sup> replica method they evaporate to such an extent as to make a detailed study worthless. The use of some form of low temperature support for the specimen in these instances can minimize the effect, but it is frequently necessary to revert to plastic replica methods, Drummond (Ref. 10, p. 58) which give much less detailed information on structure.

The essential limits in the study of crystal structure with the electron microscope are then, firstly, the resolving power of the instrument itself, and, secondly, that limitation inherent in specimen techniques of which the most serious difficulty

is the degree of aggregation of the shadowcast layer used to give surface contrast in the crystals examined. As a result of both these limitations step heights down only to 10–15 Å may be resolved, and intermolecular distances on a flat crystal face of 50 Å separation can be recognized in globular molecules under favourable packing conditions. It is thus at present impossible to study details of crystal growth and crystal deformation at the molecular level in crystals in general so that one must choose for study those crystals composed of molecules which have at least one parameter of size greater than the limit of resolution of the technique.

#### ACKNOWLEDGEMENT

This work has been carried out while the author was holding an I.C.I. Research Fellowship.

#### REFERENCES

- (1) TOLANSKY, S. *Multiple Beam Interferometry* (Oxford: Clarendon Press, 1948).
- (2) GRIFFIN, L. J. *Phil. Mag.*, **42**, p. 775 (1951); **42**, p. 1337 (1951).
- (3) FORTY, A. J. *Phil. Mag.*, **42**, p. 670 (1951); **43**, p. 377 (1952).
- (4) VERMA, A. R. *Nature, Lond.*, **167**, p. 939 (1951); *Phil. Mag.*, **42**, p. 1005 (1951); **43**, p. 441 (1952); *Z. Elektrochem.*, **56**, p. 268 (1952).
- (5) AMELINCKX, S. *Phil. Mag.*, **43**, p. 562 (1952).

- (6) FORTY, A. J. *Phil. Mag.*, **43**, p. 481 (1952).
- (7) WYCKOFF, R. W. G. *Electron Microscopy*, p. 72 (New York: Interscience Publishers, Inc., 1949).
- (8) DAWSON, I. M. *Nature, Lond.*, **168**, p. 241 (1951).
- (9) AMES, J., COTTRELL, T. L., and SAMPSON, A. M. D. *Trans Faraday Soc.*, **46**, p. 938 (1950).
- (10) DRUMMOND, D. G. (Ed.). *The Practice of Electron Microscopy* (London: Royal Microscopical Society, 1950).
- (11) BARNES, R. B., BURTON, C. J., and SCOTT, R. C. *J. Appl. Phys.*, **16**, p. 731 (1945).
- (12) KÖNIG, H., cited by Liebman, G., in *Nature, Lond.*, **168**, p. 70 (1951).
- (13) SCOTT, G. D. *J. Appl. Phys.*, **20**, p. 417 (1949).
- (14) BURTON, E. F., SENNET, R. S., and ELLIS, S. G. *Nature, Lond.*, **160**, p. 565 (1947).
- (15) VON ARDENNE, M. *Kolloidschr.*, **111**, p. 22 (1949).
- (16) DAWSON, I. M., and VAND, V. *Nature, Lond.*, **167**, p. 476 (1951); *Proc. Roy. Soc., A* **206**, p. 555 (1951).
- (17) DAWSON, I. M. *Proc. Roy. Soc., A* **214**, p. 72 (1952).
- (18) MANDLE, R. J. *Proc. Soc. Exp. Biol., N.Y.*, **64**, p. 362 (1947).
- (19) WILLIAMS, R. C. *Biochim. biophys. Acta*, **8**, p. 227 (1952).
- (20) LE POOLE, J. B., unpublished observation cited by Wyckoff, R. W. G., in *Electron Microscopy*, p. 93 (New York: Interscience Publishers Inc., 1949).

## An ethoxylene resin for photoelastic work

By H. SPOONER, B.Sc., A.Inst.P., and L. D. MCCONNELL, G.I.Mech.E., Research Laboratory, Rolls-Royce Ltd., Derby

[Paper received 9 February, 1953]

The comparatively late development of photoelasticity as a practical technique can be directly attributed to the absence of suitable materials. A new material, commercially available, is described which, it is believed, removes most of the present restrictions on the method in this country. The material, Araldite casting resin type B, has a higher figure of merit than any other presently in use for three-dimensional analysis. It can be readily cast into large sizes, and it has admirable bonding properties. The more important properties of the material are briefly described and the opportunities it gives for increased precision in photoelastic work are discussed. Some typical examples of its use are described and the major defects of the material, namely mottle and the development of time-edge stress, are discussed.

The progress of photoelasticity as a practical means of stress analysis has been closely allied with the development of suitable photoelastic materials. The principles of the subject are now 137 years old, dating back to the discovery (by Brewster in 1816) of the birefringence of glass under strain, yet it is only during the last twenty years that the method has found large application to industrial problems.

This comparatively late development of photoelasticity as a practical technique can be directly attributed to the absence of suitable materials. The development of celluloid in the early years of this century coincided with the growth of the London school, under the late Professor Coker, and later the introduction of the glyptal resin BT. 61–893 by the Bakelite Corporation of America saw a large development and considerable application of the method in that country. Until the introduction of Fosterite by the Westinghouse Corporation,<sup>(1)</sup> however, there was still a severe limitation on the size of model that could be used for three-dimensional frozen stress work. This material started a new era in photoelasticity in the United States, but there was still no really satisfactory material available in this country which could

be cast into large sizes and used with success in frozen stress work. The present paper describes a material, already briefly reported in France,<sup>(2)</sup> which has been used with success by the authors' firm for two years in the solution of three-dimensional problems, and which has many of the characteristics desirable in such a material. The material is an ethoxylene resin marketed by Aero Research Ltd. under the name of Araldite type B casting resin. It is a hot setting resin used with hardener 901; the resin is supplied as a yellow-brown solid and the hardener as a white powder. The makers' instructions for casting are as follows.

The resin is first heated to 120–140° C at which temperature it is a fairly mobile liquid; 25–30 parts by weight of hardener 901 are then added to 100 parts by weight of the resin, and mixed thoroughly. This mixture has a usable life of 1–1½ h at a temperature of 120° C; it may, however, be cast at temperatures up to 160° C but with considerable loss of life. For a large number of castings steel moulds are recommended, but if only one or two castings are required plaster of Paris, or thin sheet aluminium, may be used. The recommended mould release agent is DC7 silicone grease, supplied



by Midland Silicones Ltd. A range of curing times for temperatures varying from 100 to 200°C is listed; at 160°C the recommended time is 5–7 h.

The authors have followed this procedure using 30 parts by weight of hardener to 100 parts by weight of resin and casting the resulting mix at 130°C. An investigation of the effect of the curing time on the material has shown that there is no significant change in the properties at 135°C for curing periods as widely different as 2 h at 160°C and 70 h at 135°C. Within this range the material fringe value  $f$  can be expressed as  $1.39 \pm 0.05$  lb/in fringe. The Young's modulus  $E$  of the material shows considerable scatter and values have been obtained ranging from 1700 lb/in<sup>2</sup> to 2200 lb/in<sup>2</sup>. The correlation between the modulus and the curing time is small and, if it exists, has been masked by the scatter in the

the lower temperature is now always used. Using the values quoted on the figures, the figure of merit of the material, defined by Leven<sup>(1)</sup> as  $E/f$ , is 1380 fringes/in. On the basis of this criterion the material is considerably superior to either BT. 61–893 or Fosterite which have figures of 325 and 505 fringes/in respectively. The ultimate tensile strength of the material is not accurately known but it is believed to be at least 280 lb/in<sup>2</sup> for a 1 h time of loading, and, since the fringe order-stress curve is linear up to this point, it is possible to develop as many as 200 fringes/in before fracture.

This material opens up the possibility of increased precision in photoelastic determinations in either of two ways.<sup>(3)</sup> In the first place there is virtually no limit to the size of the material that can be cast and, consequently, large scale models can be used, which means that a very large number of slices may be taken from a frozen stress specimen. This is often useful in plotting the distribution of stress through the thickness of a model if steep gradients are to be accurately estimated. On the other hand, if the load-stress relationship is non-linear, it is necessary to work in the model with strains of the same order as those experienced in the prototype. The high figure of merit of Araldite allows this condition to be approached more nearly than does any other material presently in use. A stress of 40 t/in<sup>2</sup>, which frequently occurs locally in an alloy steel part, would result in rather more than 4.0 fringes/in. in an Araldite model loaded to the same strain, and, if a photometer such as that described by Brown and Hickson<sup>(4)</sup> is used to give accurate determination of fractional fringe orders, the analysis of such a model is quite a reasonable proposition. The authors have regularly worked to a strain of five times that in the prototype, whereas, with BT. 61–893, this factor was of the order of twenty. In one case, a model has been successfully analysed using actual prototype strains.

The linearity of Figs. 1 and 2 demonstrates that both the optical and mechanical creep are small, and, if they exist, are less than the experimental error involved in the determinations. The presence of creep is a serious limitation in similar materials. In particular, Araldite type D, which is a cold-setting material, also supplied by Aero Research Ltd., shows pronounced optical and mechanical creep when tested at 90°C after curing for 1 h at 100°C.

Araldite type B resin is also suitable for use at room temperature, and it can readily be cast into large sheets 0.250 in thick. At this temperature it has a material fringe value of 59 lb/in fringe, and a Young's modulus of  $4.2 \times 10^5$  lb/in<sup>2</sup>. It has recently found useful application in simulating, in conjunction with BT. 61–893, a blade and disk in dissimilar materials, Fig. 4.

Some of the ways in which the material has found application in frozen stress work are now briefly described. From blocks cast roughly to size, models have been machined by conventional methods using the care normally needed with photoelastic specimens. No adverse effects have been noted during critical examination after turning, milling, boring, slotting and grinding, despite the increased material sensitivity. Three recently tested models are of particular interest in that they serve to illustrate the material in the widening scope of photoelasticity as an engineering tool.

The first is a model of the first stage rotor wheel for an axial flow compressor which was fully machined from a flat cylinder 16½ in diameter, and 2½ in thick with an integrally cast hub, 6 in diameter by 3½ in thick. During machining the hub was unfortunately damaged. A repair was effected by casting a further block to the hub dimensions, providing a taper seating on old and new pieces, and bonding together

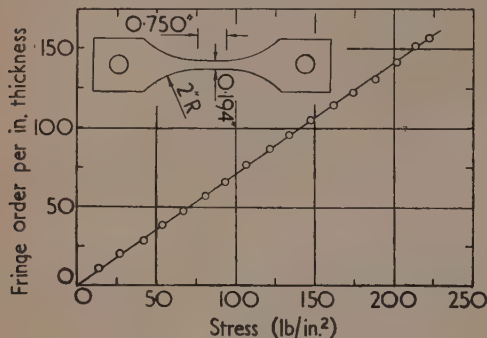


Fig. 1. Stress-optic relationship at 150°C

Load increments at 15-min intervals; every third point shown.  
 $f = 1.41$  lb/in fringe.  
 $\lambda = 5893 \text{ Å}$

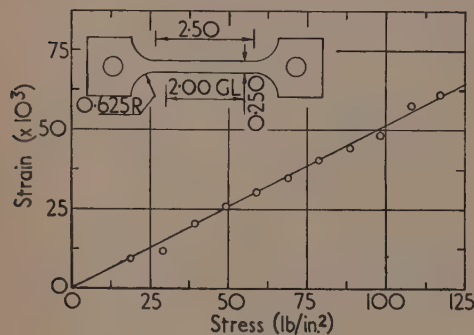


Fig. 2. Stress-strain relationship at 135°C

Load increments at 10-min intervals; all points shown.  
 $E = 1950 \text{ lb/in}^2$

results from different batches of material. The average value from a number of determinations is 1950 lb/in<sup>2</sup> and this is the figure used by the authors. Most of the work has been carried out using material cured for 2 h at 160°C and Figs. 1 and 2 show respectively the material fringe value and the Young's modulus obtained for this material. It will be noticed that Fig. 1 refers to 150°C and Fig. 2 to 135°C. The authors have found, however, that there is no significant change in properties for temperatures within this range, and

with the same material. The resulting joint is barely noticeable in the frozen stress sections and does not disturb the course of the isochromatics.

The second model is a full-size representation of a hollow shaft perforated by a series of holes. The finished piece is shown in Fig. 3. In order to reduce casting stresses and to conserve material, the model was cast as a hollow cylinder

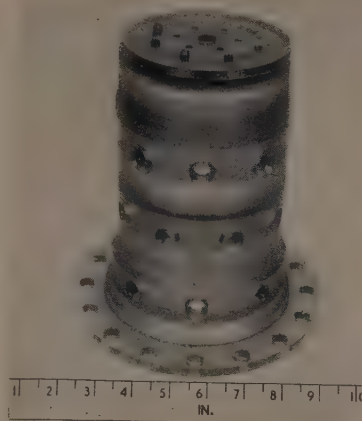


Fig. 3. Model of hollow shaft with holes

with an end flange. Casting dimensions were: flange 8 in diameter, cylinder  $5\frac{1}{2}$  in outer diameter, wall thickness  $1\frac{1}{2}$  in, length 9 in. Preliminary to the main casting, a core was cast in Araldite and cooled to room temperature as soon as gelling took place. Core and mould were then coated with DC, 7 mould release agent, and the main casting poured. By this procedure, the casting and core were cured simultaneously; differential shrinkage between the two parts was almost entirely eliminated, and a casting thus produced which was almost completely free of residual stress.

A third model represented an aluminium bronze compressor blade in a steel disk where the components have a modular ratio of 18 : 30. Using a BT, 61-893 blade in an Araldite disk, the modular ratio of 1200 : 1950 approached almost exactly that of the prototype.

Most photoelastic materials used to date have undesirable features and Araldite is no exception. The material, as obtained, is intended as a basic thermosetting plastic, consequently inclusions of dirt and other extraneous matter are likely to be present in small quantities. These inclusions may be troublesome in a photoelastic model. Passing the hardener through a 100-mesh sieve has improved but not eliminated the trouble. Streaks and mottle on a large scale similar to that found in certain other plastics, e.g. Marco SB, 26 C,<sup>(5)</sup> were noticed in some early casts, but more attention to the mixing of resin and hardener resulted in uniform castings.

A secondary mottle is present in Araldite, and is worthy of a fuller description. It was early noticed that the material possessed a small scale mottle uniformly distributed throughout, which in the unstressed state has a random orientation. On loading a specimen, this mottle takes up a regular configuration and is prominent only where the isochromatics are diffuse. As the fringe gradient increases the effect is barely discernible. Closer examination of the phenomenon shows

that it is composed of small variations of approximately  $\pm 1/10$  fringe about a mean value, and oriented in the directions of the isostatics. The effect is noticeable in the typical fringe pattern, Fig. 4, and in Fig. 5, where the stress

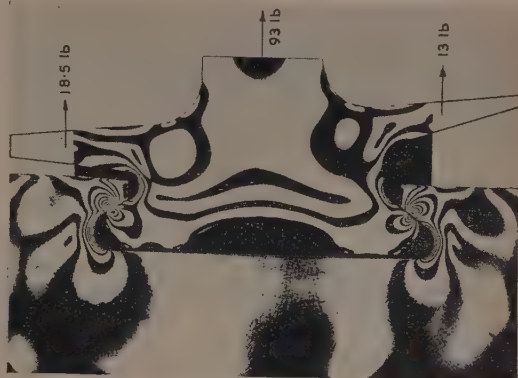


Fig. 4. Fringe pattern in composite model. Blade (upper) in BT, 61-893 and disk (lower) in Araldite

trajectories for the particular case have been plotted by conventional methods from the isoclinics for comparison. Casts made with an alternative hardener, namely maleic anhydride, also show this "isostatic effect." It is suggested<sup>(6)</sup> that the effect is due to the inclusion of a number of randomly distributed fibrous elements, possibly excess hardener, which exhibit different stress-optic coefficients along and across the fibre in much the same way as do many crystals. Thus on a minute scale the fibres are anisotropic, but, in the aggregate, the material displays the isotropy required for photoelastic analysis.

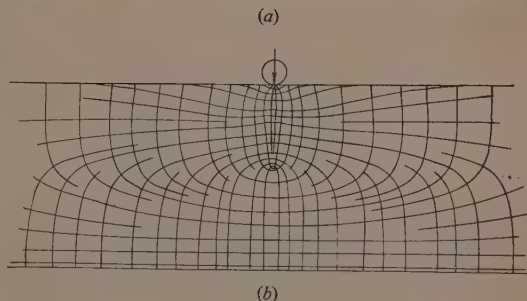
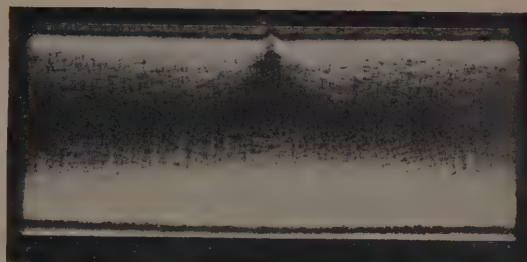
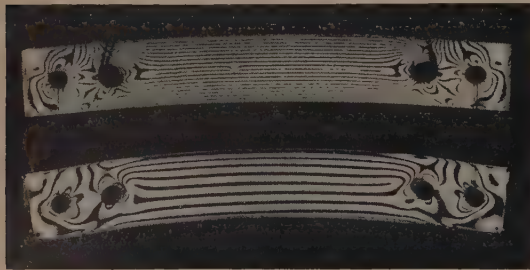


Fig. 5. (a) "Isostatic mottle"; (b) Isostatics drawn from isoclinics for centrally loaded beam



Araldite suffers from time-edge stresses although not to such a marked extent as, for instance, BT. 61-893. Fig. 6(a) shows two beams, the upper Araldite and the lower BT. 61-893, of similar dimensions subjected to the same bending moment. The photograph was taken two days after freezing so that some time-edge stress was already present. Fig. 6(b)



(a)



(b)

Fig. 6. Comparison of beams in bending. Araldite (upper) and BT. 61-893 (lower) subject to same bending moment. (a) Two days after freezing, and (b) twenty months after freezing

Beam  $1 \times \frac{1}{2} \times 4\frac{1}{2}$  in centres. Bending moment 2.52 lb in

shows the same two beams after twenty months together in a closed cabinet. The distortion of the pattern is immediately apparent. During the interval the Araldite acquired 3 fringes of time-edge stress on the tensile and 2 fringes on the compressive surface while the BT. 61-893 had  $9\frac{1}{2}$  and 8 fringes respectively. Thus Araldite is some  $2\frac{1}{2}$  times better than the traditional material in terms of unwanted fringes, and this, coupled with the increased material sensitivity, reduces the change as a percentage of the observed pattern, for a given model load, to about 12% of that for BT. 61-893. The stress distributions for the two beams are shown in Fig. 7. Nevertheless, time-edge effect is still a serious disadvantage and models must be analysed within a short while of machining or freezing. The rate of development of time-edge stress appears to vary slightly between batches of material and no explanation is apparent. Fortunately, the material shows negligible rind effect during either the curing or freezing cycles.

No mention has so far been made of the use of Araldite in the scattered light method. Preliminary investigations have shown that the resin contains too much extraneous material dispersed throughout to make the method feasible until the resin can be cleaned. The impurities lead to specular reflexions which completely mask the true scattering. A

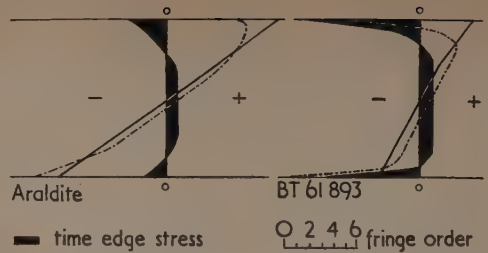


Fig. 7. Time-edge stress in Araldite and BT. 61-893. Curves showing stress distribution in beams of Fig. 6 together with time-edge stress resulting from the twenty months exposure

— initial distribution; - - - distribution after twenty months.

number of methods of both cleaning and decolorizing the material are being investigated and, if these are successful, Araldite should prove a very useful "scattered light material." The effect of curing time on its scattering powers have not yet been investigated, but presumably a prolonged cure at a relatively low temperature would be most effective. The remarkable bonding properties of Araldite make it an admirable material for two further variations of the standard photoelastic technique. In the first place it can be cast directly on to a polished metal surface and used as a stress sensitive layer. Secondly, it can be cast between two pieces of insensitive material, for example Perspex, to make a composite model, as used in the familiar "sandwich" technique.<sup>(7)</sup> Some time ago, the authors experimented with a Duralumin strip bearing a cast-on layer of Araldite 0.040 in thick. It was found that at room temperature approximately  $2\frac{1}{2}$  fringes could be developed before the limit of proportionality of Dural was approached, corresponding to a strain of 0.0035 in/in, and subsequently, after increasing the load beyond this limit, unloading, and reloading, a plot of load against fringe order yielded a satisfactory stress-strain curve of the Dural.

There seems little doubt that the outstanding properties of Araldite, namely its high figure of merit, its ability to be cast in large sizes, and its excellent bonding properties, are sufficient to justify further work in the development of this material; in particular, to obtaining the material in a considerably cleaner form.

#### ACKNOWLEDGEMENT

The authors wish to thank the Directors of Rolls-Royce Ltd. for permission to publish this paper.

#### REFERENCES

- (1) LEVEN, M. M. *Proc. Soc. Exp. Stress Analysis*, 6, No. 1, p. 19 (1948).
- (2) BALLE, M., and MALLET, G. *C.R. Acad. Sci., Paris*, 233, No. 16, p. 846 (1951).
- (3) HEYWOOD, R. B. *Designing by Photoelasticity*, p. 145 (London: Chapman and Hall, 1952).
- (4) BROWN, A. F. C., and HICKSON, V. M. *Brit. J. Appl. Phys.*, 1, p. 39 (1950).
- (5) SUGARMAN, B., MOXLEY, G. O., and MARSHALL, I. A. *Brit. J. Appl. Phys.*, 3, p. 233 (1952).
- (6) HICKSON, V. M. Private communication.
- (7) LAMBLE, J. H., and BAYOUMI, S. E. A. *Proc. Instn Mech. Engrs* paper presented on 20 March, 1953—to be published.



# Refractive index determination for anisotropic crystals

By A. L. MACKAY, M.A., Ph.D., A.Inst.P., Birkbeck College, University of London

[Paper received 20 February, 1953]

Ambronn's method, matching the refractive indices of immersion liquid and crystal by rotating the plane of polarization of the incident light relative to the crystal, has been simplified by the use of a nomogram which also enables refractive index to be related to direction in the indicatrix without calculation.

The method described here was in fact developed independently for measuring refractive indices of anisotropic crystals quickly and with reasonable accuracy, but is not claimed to be new as it was described first by Ambronn,\* but after mention by Johannsen† it seems to have disappeared from current textbooks.

The single (temperature) variation method is generally recommended for the final small adjustment of the refractive index of the immersion liquid to that of the crystal for a particular vibration-direction. If only a few determinations are required the outlay of time and equipment is often prohibitive. The method which follows is designed to give accurate values of the two principal indices of the section of the indicatrix being studied at a particular moment. A diagram (Fig. 1) represents this section. The two indices  $n_1$

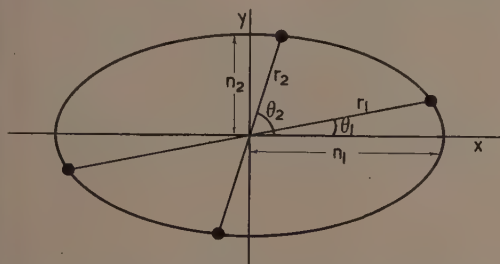


Fig. 1. Section of indicatrix showing variation of refractive index  $r$  with vibration direction  $\theta$

and  $n_2$  are to be measured and the corresponding vibration directions can be found from the extinction positions. Suppose that first an immersion liquid of refractive index  $r_1$ , between  $n_1$  and  $n_2$  is used. By rotating the plane of polarization of the incident light with respect to the crystal, a position can be found in which the index of the liquid is matched exactly by that of the crystal, employing the Becke-line or other test. From the microscope scale, the angle  $\theta_1$  between the greater index  $n_1$  and the vibration direction which has an index  $r_1$  can be read. Suppose further that this procedure is repeated with another liquid of refractive index  $r_2$ ; then the two points obtained are, together with the extinction directions, sufficient to define the whole ellipse.

The equation for the ellipse is

$$\frac{x^2}{n_1^2} + \frac{y^2}{n_2^2} = 1$$

Let  $r^2 = x^2 + y^2$ ,  $x = r \cos \theta$ , and  $y = r \sin \theta$ .

Hence

$$\frac{\cos^2 \theta}{n_1^2} + \frac{\sin^2 \theta}{n_2^2} = \frac{1}{r^2}$$

and

$$\left(\frac{1}{n_1^2} - \frac{1}{n_2^2}\right) \cos^2 \theta + \frac{1}{n_2^2} = \frac{1}{r^2}$$

This relationship can best be represented by a diagram (Fig. 2) in which  $1/r^2$  is plotted vertically and  $\cos^2 \theta$  horizontally. With such axial scales the variation of refractive index with angle appears as a straight line.

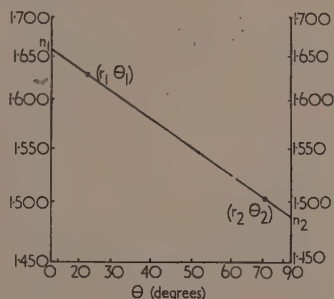


Fig. 2. Nomogram representing variation of refractive index (ordinate) with vibration direction (abscissa)

When a straight line is drawn through the two points obtained experimentally, the principal indices can be read directly by extrapolation. Considering that the accuracy of observing the equality of refractive index is as great as in the

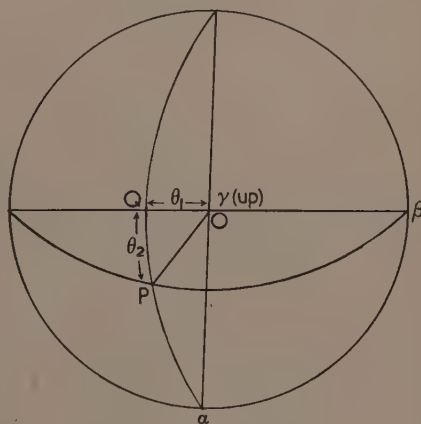


Fig. 3. Stereogram showing the stages in calculating the radius of a triaxial ellipsoid in any known direction

\* AMBRONN, H. *Ber. Akad. Gesell. Wiss. Leipzig*, 45, p. 316 (1893).

† JOHANNSEN, A. *Manual of petrographic methods*, p. 253 (New York: McGraw-Hill Book Co. Inc., 1914).

temperature-variation method, it is apparent from Fig. 2 that the probable errors in  $n_1$  and  $n_2$  need not be more than twice the errors of the individual points if the angular distance between the latter is adequate.

As a corollary, if one of the indices is already known the second can be found directly with one immersion.

From the position of observed points in the diagram, it can be at once seen whether an additional immersion is required to attain the necessary accuracy in  $n_1$  and  $n_2$  and if so, what is the optimum value of the refractive index of the liquid which should be used.

The nomogram (Fig. 2) can also be employed more generally for relating refractive index and orientation in any section of the triaxial indicatrix. Suppose it is required to find the

refractive index  $n_p$  in the vibration direction  $OP$  (see stereogram Fig. 3) which is related to the principal planes of the indicatrix by the angles  $\theta_1$  and  $\theta_2$ . Then, marking  $\gamma$  and  $\beta$  on the nomogram, the index corresponding to an angle  $\theta_1$  from  $\gamma$  is read off. This index is transferred to the left refractive index scale and  $\alpha$  to the other refractive index scale.  $n_p$  is read off as being the index at an angle  $\theta_2$  from  $n_Q$ . Similar problems and their inverses can also be solved. The optic axial angle can be calculated by drawing a line between  $\alpha$  and  $\gamma$  and reading the angular distance corresponding to  $\beta$ . If  $2V$  has been measured directly, a knowledge of its value can be used to provide a relationship between the indices, reducing the number of independent refractive index determinations necessary.

## Proposed use of a cylindrical surface wave resonator for the determination of the velocity of short electromagnetic waves

By PROFESSOR H. M. BARLOW, B.Sc.(Eng.), and A. E. KARBOWIAK, Ph.D., M.I.E.E., University College, London

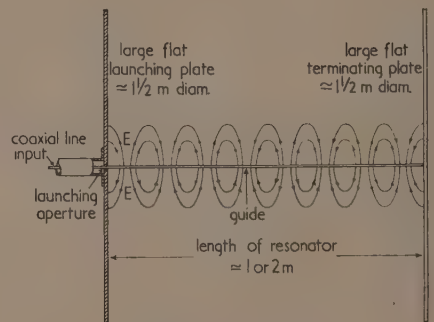
[Paper received 29 January, 1953]

It is proposed to set up a surface wave resonator consisting of a length of smooth bare wire acting as the guide and short-circuited at both ends by large flat conducting plates mounted at right angles with the guide. Energy would be supplied to the resonator at a frequency between 1000 and 40 000 Mc/s using either a coaxial or loop coupling and a similar device would be employed for the detector. From a knowledge of the guide wavelength, the frequency and the radial propagation coefficient of the wave in the air surrounding the guide, the corresponding T.E.M. wave velocity can be determined and thence  $c$  deduced for vacuum conditions. Attention is drawn to certain helpful features of the method but no attempt is made to assess its ultimate accuracy in comparison with other techniques whose value has been established for this purpose.

In recent years a number of measurements have been made of the velocity of electromagnetic waves and the results up to the beginning of 1952 are summarized in a paper by Froome.<sup>(1)</sup> As Essen<sup>(2)</sup> has emphasized, the position cannot be regarded with any complacency and a higher degree of accuracy is required to establish beyond any reasonable doubt the value of  $c$  to the nearest kilometre per second. There are indications that the method of measurement may have some influence on the precise value obtained even though every care is taken to eliminate any recognizable disturbances. It is important, therefore, that all possible avenues leading to an accurate determination of  $c$  should be explored. Only in that way can the various factors creating uncertainty about the final result be assessed.

It is the object of this paper to call attention to a possible method of measurement which has not yet, so far as we are aware, been applied to the present purpose. In doing so no attempt will be made to offer detailed comments on the merits of the scheme in comparison with others already used, because that can only be done by those who have an intimate knowledge and experience of work of this kind.

plates mounted at right angles with the guide. Energy would be supplied to the resonator at a frequency between 1000 and 40 000 Mc/s using either a coaxial or a loop coupling and a similar device would be employed for the detector. An instrument of this kind has been used by the authors for the



Surface wave resonator

### APPLICATION OF THE CYLINDRICAL SURFACE WAVE RESONATOR

It is proposed to set up a surface wave resonator (see figure) consisting of a length of smooth bare wire acting as the guide and short-circuited at both ends by large flat conducting

reverse process of determining the reactance of different guide surfaces from a knowledge of the corresponding phase velocity and the present suggestion arose out of that work.<sup>(3)</sup> The resonator might be set up with its axis either horizontal or vertical, whichever arrangement affords the higher accuracy

of alignment. It seems likely that heavy silvering on a sheet of plate glass at each termination would provide a good reflecting surface and be sufficiently flat to meet the permissible tolerances. Should it be found that nylon threads could be used to support a horizontal guide at intervals along its length without significant disturbance of the field then this arrangement with vertical terminating plates would probably prove the more convenient. The length of the resonator would then only be limited by the space available.

#### CALCULATIONS FOR THE WAVE VELOCITY

It is easy to show<sup>(4)</sup> that for a cylindrical surface wave the phase velocity  $v_p$  along the guide is given by:

$$v_p = \frac{2\omega^2}{\sqrt{\left[\left(b_2^2 - a_2^2 - \frac{\omega^2}{v^2}\right)^2 + (2a_2b_2)^2\right] - \left(b_2^2 - a_2^2 - \frac{\omega^2}{v^2}\right)^2}} \quad (1)$$

where  $u_2 = a_2 - jb_2$  = radial propagation coefficient in the air surrounding the guide;  $v = 1/\sqrt{(\mu_2 K_2)}$  = T.E.M. wave velocity in the air (having permeability  $\mu_2$  and permittivity  $K_2$ ) outside the guide, and  $\omega = 2\pi f$ .

When  $\omega^2/v^2 \gg (b_2^2 - a_2^2)$ , equation (1) reduces to:

$$\frac{v}{v_p} = \frac{v}{f\lambda_g} \simeq \left\{1 - \frac{1}{2} \left[ \frac{v^2}{\omega^2} (b_2^2 - a_2^2) + \frac{v^4}{\omega^4} a_2^2 b_2^2 \right] \right\} = [1 - \frac{1}{2}\delta] \quad (2)$$

and it is possible that under the conditions of the experiment proposed, equation (2) may be sufficiently accurate.

With a knowledge of  $\lambda_g$ ,  $f$  and  $u_2$  the T.E.M. wave velocity  $v$  in air can be determined and thence  $c$  deduced for vacuum conditions. The wavelength  $\lambda_g$  along the guide can be measured to a high degree of accuracy since the resonator can be at least one or two metres long and therefore would include a large number of wavelengths. The frequency  $f$  can be ascertained using the technique employed by Essen to an accuracy of 1 part in  $10^8$ . Subject to certain approximations, the validity of which must be checked in the present application,  $u_2$  can be determined from the analysis given by Sommerfeld<sup>(5)</sup> and Goubau<sup>(6)</sup> as follows:

(i) Calculate

$$|\eta| = 1.584K_2S\sqrt{(\omega^3\mu_1/\sigma_1)} \quad (3)$$

where  $S$  = radius of the guide;  $\mu_1$  = permeability of the guide;  $\sigma_1$  = conductivity of the guide.

(ii) Derive  $|\xi|$  from the relation

$$|\eta| = -|\xi| \log_e |\xi| \quad (4)$$

(iii) Calculate

$$\psi = -\frac{\pi}{4} \left( 1 - \frac{1}{\log_e |\xi| + 1} \right) \quad (5)$$

(iv) Find

$$ju_2 = b_2 + ja_2 = 1.12|\xi|^{\frac{1}{2}} e^{j(\psi + \pi)/2} \quad (6)$$

It is important to observe that for a smooth bare copper wire guide a small error in  $S$  or in  $\sigma_1$  does not significantly affect the value obtained for  $v$ .

Thus in the case of an 18 s.w.g. copper wire at a frequency of 9370 Mc/s a 1% error in the diameter of the wire results in about 0.8% error in  $\delta$  and since  $\delta$  is less than  $10^{-4}$  the

consequential error in  $v$  is only about 4 parts in  $10^7$ . Similarly a 10% error in  $\sigma_1$  leads to an error in  $v$  of less than 3 parts in  $10^6$ .

#### SPECIAL FEATURES OF THE SURFACE WAVE RESONATOR FOR VELOCITY MEASUREMENTS

The use of the cavity resonator technique for the determination of  $c$  has been established by Essen<sup>(2)</sup> and the precision and limitations of the method are well known. The length of the corresponding surface wave resonator will in general be greater and therefore it will include a larger number of wavelengths. Moreover, a series of resonant frequencies at close intervals, and a hundred or more in number, can be conveniently employed for the measurement. Along the axis of the resonator, the guide, which might for example consist of silver wire, can be made to close dimensional tolerances with a carefully finished surface, possibly electrolytically polished. Attention has already been drawn to the comparatively small effect on the wave velocity of variations in the diameter and conductivity of the wire. The terminating plates at the ends of the resonator should each be not less than about 4 ft diameter in order to prevent errors arising from diffraction of the wave at the edges. Arrangements for the mechanical alignment of these plates and for preventing them from buckling would clearly be a matter of some difficulty.

The phase velocity of waves guided along an interface, as in the case of a resonator, may depend to some extent on the purity of the wave mode employed. To avoid contamination of the surface wave mode, the energy lost in the end plates of the resonator, in the guide, and in the detector coupling must be reduced to a minimum, thus ensuring that the standing wave inside the resonator is as perfect as possible and eliminating any slight radiation from the launching device. The influence of such factors as temperature, humidity, air pressure, etc., on the velocity of the waves would have to be ascertained accurately.

#### ACKNOWLEDGEMENTS

The authors wish to acknowledge their thanks to Dr. R. L. Smith-Rose whose encouragement of the development of the surface wave resonator technique as an instrument of measurement led to the formulation of this proposal and to Dr. A. L. Cullen for helpful discussions upon it.

#### REFERENCES

- (1) FROOME, K. D. *Proc. Roy. Soc. A.*, **213**, p. 123 (1952).
- (2) ESSEN, L. *Nature, Lond.*, **165**, p. 821 (1950); *Proc. Roy. Soc. A.*, **204**, p. 260 (1950).
- See also: ESSEN, L., and FROOME, K. D. *Nature, Lond.*, **167**, p. 512 (1951); *Proc. Phys. Soc. B.*, **64**, p. 862 (1951).
- (3) BARLOW, H. M., and KARBOWIAK, A. E. *Proc. Instn Elect. Engrs*, Pt III (1953). To be published.
- (4) BARLOW, H. M., and CULLEN, A. L. *Proc. Instn Elect. Engrs*, Pt III (1953). To be published.
- (5) SOMMERFELD, A. *Ann. der Phys. und Chemie*, **67**, p. 233 (1899).
- (6) GOUBAU, G. *J. Appl. Phys.*, **21**, p. 1119 (1950).



## Correspondence

## An electrical analogue to a high vacuum system

In a complex vacuum system where there are several pumping lines in parallel, or, where, as in synchrotrons and betatrons, the vacuum chamber is a toroidal tube of low pumping speed, the calculation of the effect on the pressure of altering various parts of the pumping system (e.g. speed or number of pumps, length of pumping lines) is rather tedious. So too is the estimation of the whereabouts of a leak from observed pressure gauge readings on the system. An electrical analogue can be used to obtain the required answers very quickly by simple voltage measurements.

The analogue is only applicable when the pressure is small enough for the mean free path to be larger than the dimensions of the system; the rate of mass flow through a tube is then given by,

$$Q = S(p_1 - p_2) \quad (1)$$

where  $S$  is the speed of the tube and depends only on its dimensions,  $p_1$  and  $p_2$  are the pressures at either end of the tube.

Similarly for a diffusion pump of speed  $S_0$ , at the throat of which the pressure is  $p_0$ , the rate of mass flow through the pump is,

$$Q = S_0 p_0 \quad (2)$$

Both equations (1) and (2) are analogous to Ohm's law, so that an electrical analogue can be constructed in which voltage corresponds to pressure, current to mass flow, and resistance

measure the pressures on the five gauges on the vacuum system. The probe leak on the analogue is then connected on to various points of the electrical network until one is found for which the ratios of the voltages at the points corresponding to the gauges is the same as the ratios of the actual gauge readings.

The permanent leak into the system is due to diffusion of air through the eight neoprene sleeves (see figure) which join the eight sectors of the orbit tube together and the residual pressure due to this leak for various different pumping arrangements is found by connecting eight equal current sources (not shown) to the points corresponding to the sleeves; the electrical circuit is then altered to correspond to the various arrangements and the voltages observed in each case. Pressure due to evolution of vapour (e.g. from the gun heater) which is condensed on the cold trap, can be dealt with by closing the three switches shown, connecting on the probe leak at the point corresponding to the gun heater and proceeding as before.

The analogue has been in use for the past year and has been found invaluable, particularly in the localization of leaks. There are fifteen places around the orbit tube at which leaks may occur and, by use of the analogue, suspicion can in a few minutes be centred on one of these places. With this localization procedure a straightforward method of leak finding (a jet of coal gas or butane in conjunction with a normal ionization gauge) has been found quite adequate.

Clarendon Laboratory,  
Oxford.

M. J. AITKEN

## A note on temperature control during lattice spacing measurements

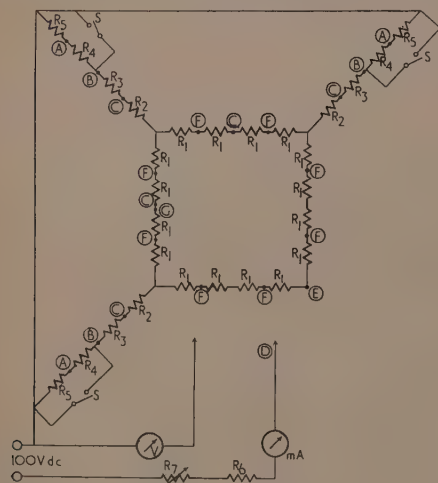
The accurate measurement of lattice spacings requires a precise knowledge of the temperature of the specimen during the X-ray exposure. In many laboratories 19 cm Debye-Scherrer cameras are used, and the temperature is measured by a thermometer placed outside the camera case. The errors introduced by this method have not been discussed previously, and the present note shows that unless a suitable technique is used the errors may be 1 to 3° C.

Experiments were made on two 19 cm Unicam cameras, of which one was of the original design (Oxford), and the other (Manchester) incorporated a built-in motor for rotating the specimen. Thermometers and thermocouples were placed inside the camera case to measure the temperature of the air inside the camera, and, with specimens thermally insulated from the frame of the camera, this may be taken as the true specimen temperature.

The following sources of error have been noted:

(i) With the room temperature maintained constant, the built-in motor heated the camera at the rate of 1–2° C per hour; the built-in motor was therefore removed.

(ii) The ideal method is to load the camera in the X-ray room if this can be darkened, since considerable temperature differences may arise between the X-ray room and a separate dark-room. Such temperature differences may be very persistent. In one instance where the temperature difference between the two rooms was 6° C the discrepancy between the true specimen temperature and that measured by a thermometer placed on the camera case was 3° C after 15 min and



Electrical analogue

$R_1 = 90 \Omega$   
 $R_2 = 170 \Omega$   
 $R_3 = 95 \Omega$   
 $R_4 = 65 \Omega$   
 $R_5 = 850 \Omega$   
 $R_6 = 25 \text{ k}\Omega$   
 $R_7 = 100 \text{ k}\Omega$

$V$  = voltmeter (f.s.d. 2½ V)

$mA$  = milliammeter (f.s.d. 4 mA)

$S$  = switches

$A$ , pump throat  $B$ , cold trap

$C$ , gauge  $D$ , probe leak  $E$ , electron gun

$F$ , neoprene sleeves  $G$ , target

to the reciprocal of speed. The figure shows the analogue constructed for the vacuum system of the Oxford 140-MeV synchrotron.

The procedure for finding the locality of a leak is first to

1° C after 1 hour. If a separate dark-room must be used the camera should be loaded as rapidly as possible and the camera left on the X-ray set for some time before the exposure is commenced. The temperature should then be measured by a thermocouple or thermometer placed inside the camera and as near to the specimen as possible.

(iii) Errors of up to 2° C may arise from thermal radiation or irregular draughts falling on the camera case. This may be avoided by enclosing the camera within a light cardboard box and the temperature of the specimen may then be controlled to  $\pm 0.2^\circ$  C by altering the ventilation of the room.

(iv) In the absence of the above effects the camera may heat up during an exposure and since heat flows inwards an error of up to 0.5° C may arise between the camera case and the specimen.

With many metals an error of 1° C corresponds to an error in the lattice spacing of 1 part in 40 000 so that errors arising from the use of an *external* thermometer may be serious.

Department of Metallurgy,  
University of Manchester.

H. J. AXON  
A. HELLAWELL

Inorganic Chemistry Laboratory,  
Oxford.

D. M. POOLE  
W. HUME-ROTHERY

## New books

**Nuclear stability rules.** By N. FEATHER. (London: Cambridge University Press.) Pp. ix + 162. Price 20s.

This is essentially a book of clues to a partially solved puzzle: why are stable nuclei formed by particular combinations of protons and neutrons?

In addition to well-known general features such as the high neutron-proton ratio of heavy nuclei and the instability of nuclei containing odd numbers of both protons and neutrons, the book deals with detailed regularities and anomalies, some known for many years and others discovered by recent workers, including Professor Feather himself.

Much of the monograph is about quantitative questions of nuclear instability: what rules can be discovered about the rates of transformation of unstable nuclei? Here, again, broad features are well known but the author records new and detailed regularities, including some of his own finding. Though "shell structure" is deliberately soft pedalled, the monograph is well up to date and is closely packed with information, much of it in graphical form. Many gaps in our knowledge are pointed out, and hints for possible new discoveries are freely given.

In the words of a reviewer of an earlier work in this series, "Ce n'est-pas un oeuvre de vulgarisation." P. B. MOON

**Principio general de la termodinamica.** By Ing. Eduardo A. Quinterno. (Buenos Aires: Centro Estudiantes de Ingenieria.) Pp. 139.

This little book on thermodynamics is evidently intended for engineers; at least, the applications of most interest to chemists receive little or no notice. Yet the engineers to whom it would appeal must have a more academic outlook than would most engineering students in this country, and perhaps correspond more closely to our notions of students of physics.

After a page or two on general notions of energy, in which Einstein's equation,  $E = mc^2$ , plays a dominant rôle, the author takes up the theory of probability, as required for a statistical basis to thermodynamics. This part is rather elementary, but is written very clearly indeed. It must certainly be conceded that it takes topical examples, for the decay chains of the xenon and strontium formed in the neutron-induced fission of a  $^{235}\text{U}$  nucleus are included.

The subsequent development is normal, logical and clear. There are useful folding charts at the end, giving the main formulae for reference.

J. H. AWBERY

**Tensors in electrical machine theory.** By W. J. GIBBS. (London: Chapman and Hall Ltd.) Pp. xii + 238. Price 30s.

In 1932 Gabriel Kron in America applied tensor calculus for

the first time to the analysis of electrical machines, and since then many publications on this subject have appeared, mainly in America.

The book under review is the first one to be published in England on this subject, of which it covers a very substantial part. Approximately half of the book is devoted to the more elementary concepts of tensor and matrix theories which are developed slowly and in great detail. The second half of the book deals with the more advanced parts of the theory. It contains a brief account of differential geometry, which is followed by the application of tensors to analytical dynamics. This then leads naturally to the analysis of electrical machines, which are treated as combined electrical and dynamical systems.

Although the subject-matter ranges from elementary to very advanced topics, the transition is gradual and the presentation is always clear and lucid. The book is written mainly for electrical engineering students, but large sections of it should also be of value to students of physics.

H. TROPPER

**Structure of metals.** 2nd edition. By CHARLES S. BARRETT. (London: McGraw-Hill Publishing Company Ltd.) Pp. 661. Price 72s. 6d.

The first edition of *Structure of metals* was published in 1943, and it soon became recognized as an authoritative and unique textbook. In the nine years that have elapsed since 1943, however, there has been a great deal of progress and development in all branches of metallurgy, and not least in those crystallographic and physical spheres with which the book was chiefly concerned. Consequently, many of us who have always kept Professor Barrett's earlier edition handy on our shelves, have ventured to hope that, in spite of the obvious magnitude of the task, revision would eventually be undertaken.

In this new edition it is not too much to say that all reasonable expectations have been realized. The general plan of the earlier edition has been maintained, but there are now 661 pages compared with the original 567. It is a tribute to the original text that, in the first few chapters, which deal so concisely with the fundamentals of crystal structure and the techniques of X-ray diffraction, relatively few changes have been necessary. Some new matter on counter spectrometer methods, which had hardly commenced in 1943, is a little sketchy, but this is understandable in a book that embraces such a wide field.

It is when we come to the later chapters, from perhaps Chapter 11 onwards, which discuss the significance of crystal structure in physical metallurgy, that we find the most extensive revisions and additions. Chapter 16, for example, is now entitled "Dislocation theory" instead of "Theories of slip," and has been largely rewritten to take



account of the current theories of Frank and others. The chapters on X-ray line-broadening by cold-worked metals, on preferred orientation textures, and on age-hardening and transformations, are also considerably revised and expanded to include discussion of research investigations published as recently as the early part of 1952.

The book can be confidently recommended to all those with an interest in physical metallurgy. Moreover, it is no exaggeration to claim that crystallographers themselves will derive much of value from reading the pages describing the practice of their subject.

H. P. ROOKSBY

**Mesons—A summary of experimental facts.** By A. M. THORNDIKE. (London: McGraw-Hill Publishing Co. Ltd.) Pp. viii + 242. Price 47s.

This book is an introduction to the study of meson physics. It is descriptive, non-mathematical and limited to experimental results. Recently there has been a rapid development in our knowledge of the properties of mesons; but there has been no review of the remarkable results obtained, since that by Professor Powell (*Rep. Phys. Soc. Progr. Phys.*, 1950). Dr. Thorndike's summary covers the data available up to the end of 1951. The detailed list of references, given at the end of each chapter, will appeal to many physicists working in these fields. Only well established results are discussed in detail, other investigations in progress being merely touched upon. This is natural, when writing on a subject which is still in a state of flux. Dr. Thorndike has taken pains to give credit, where due, to all the earlier investigators. The production of the book attains the usual excellent standard of McGraw-Hill publications, though the price may put it beyond the reach of many in this country who would otherwise profit by reading it.

M. G. K. MENON

**High speed photography.** By G. A. JONES, M.A., A.R.I.C., F.R.P.S. (London: Chapman and Hall Ltd.) Pp. xvi + 311. Price 42s.

The author states as his aim that this book should "summarize the fundamentals, the current practice, and the scope of high speed photography in all its various aspects." This is a formidable objective in a rapidly expanding subject, although the summarized work in this field is at present covered only in the French text by Naslin and one other English work. There is also the series of five symposia collections by the American Society of Motion Picture and Television Engineers. Mr. Jones has made a serious and most readable effort to classify and interpret this wide field of diverse investigation. The book is written with matters presented in a clear historical perspective.

Particularly interesting are the parts dealing with the earlier pioneers in the field. The most important recent developments such as the Miller cameras and the Sultanoff multiple-aperture focal-plane scanning instrument are clearly described. The bibliography of some 470 references is composed about equally of those concerning techniques and those concerning applications, and the references are made more valuable to the reader by the quoting of titles of all papers.

When describing the principles of various systems, it would have been helpful to have more line diagrams. For instance, the pictures of commercial apparatus (e.g. Figs. 32-35, 40, 51, 60, 61 or 71) could be omitted in exchange for diagrams of other optical compensators, the Zeiss cameras, or further details of the different Schlieren systems in common use. The resolution figures given (page 81) seem abnormally high.

These are, however, minor criticisms. This book is to be welcomed particularly because it is written from direct

practical experience by a worker who has made considerable contributions to the intelligent use of the methods in industrial problems.

W. DERYCK CHESTERMAN

**Designing by photoelasticity.** By R. B. HEYWOOD. (London: Chapman and Hall Ltd.) Pp. xvi + 414. Price 65s.

Dr. Heywood has drawn on his extensive experience of the use of photoelastic methods as applied to problems of engineering design to write a book addressed to both engineers and photoelasticians.

The first 150 pages are devoted to an elementary discussion of the fundamental optics involved in photoelasticity together with chapters dealing with model materials, the preparation of models, the transfer of information from model to prototype, and "frozen stress" techniques.

The remainder of the book deals with the results obtained from both theoretical considerations and photoelastic analysis in investigations of the stress concentrations arising round notches and holes, in screw threads, nuts and bolts, and also with some examples of the improvements effected in engineering components by the reduction of stress concentrations without paying the price of increases in weight.

Photoelasticians may wish to quarrel with some of the statements made in Part I of this book; engineers, who have a sound grasp of the background of the subjects dealt with, will find here collected together a great deal of useful information about stress concentration factors which has not hitherto been available in as convenient a form.

Last, but not least, Dr. Heywood has included an extensive bibliography of 826 items in his book.

E. K. FRANKL

**Adhesion and adhesives.** By N. A. DE BRUYNE and R. HOUWINK. (London: Cleaver-Hume Press Ltd.) Pp. xv + 517. Price 70s.

The very scattered literature on adhesives and adhesion ensures a welcome for any book attempting to collect the information together, both from those making adhesives and from those using them. The present volume has the advantage of being edited by two of the principal contributors to knowledge in this field. Within the limits of the knowledge available, the volume is authoritative and, on the whole, well written.

The introductory chapters are concerned with the theory of adhesion and of molecular forces, dealt with by R. Houwink and by A. J. Staverman, followed by the rheology of adhesives, by J. Hoekstra and C. P. Fritzius, and with a final chapter on stress distribution in joints by C. Mylonas and N. A. de Bruyne. These chapters illustrate the very uneven development of the subject. Physico-chemical theory has at present little of value to say concerning adhesion, and the unsatisfactory character of the two chapters dealing with this side, reflects the state of the subject rather than faulty presentation. Rheological aspects are being rapidly developed and the chapter on them must be regarded rather as an introduction and a progress report. The chapter on stress distribution, on the other hand, gives a very clear account of a field in which important contributions have been made recently, not least by the authors themselves.

Chapters follow on animal glues, vegetable adhesives, synthetic resins, asphaltic bitumen, inorganic adhesives and cements, rubbery adhesives, and adhesion in soldered joints. Each of these is written by a specialist in the subject, their usefulness varying both in accord with the information available, and with the viewpoint of the author. The book concludes with a valuable chapter on physical testing.

A. G. WARD



**Mechanics.** By A. SOMMERFELD. (New York: Academic Press Inc.) Pp. xiv + 289. Price \$6.50.

Professor Ewald in the foreword to this book explains that "Sommerfeld was over seventy, and retired after forty years of academic teaching, when he committed his lectures to paper." One of his general lecture-courses on theoretical physics which he gave regularly for thirty-two years at Munich is comprised in this volume on mechanics. By all accounts a great lecturer, some of the inspiration of his lectures is inevitably lost in this printed version and more still, one suspects, in this translation. Nevertheless, many readers will find his treatment of the subject interesting and suggestive, and in various ways different from the normal English texts.

This book sets forth, with suitable applications, the mechanics which should be included in University courses for physicists. There is a good account of the basis of the dynamics of a particle, followed by a chapter on the mechanics of systems and a useful chapter on oscillations. The mechanics of rigid bodies in three dimensions is discussed rather generally with some account of Euler's equations and their application to the precession of tops. (There is a supplement on the mechanics of billiards, for "the beautiful game of billiards opens up a rich field for applications of the dynamics of rigid bodies.")

There are three later chapters devoted to generalized mechanics, including Lagrange's equations, the principle of least action and Hamilton's equations, culminating as we would expect in the Hamilton-Jacobi method applied in atomic physics.

There are no exercises such as usually adorn English books on the subject, but in keeping with the use of "exercise-classes" in the continental system of University education a collection of problems is given at the end of this book along with hints for their solution.

J. TOPPING

**Proceedings of general discussion on heat transfer—London, 1951.** (London: The Institution of Mechanical Engineers.) Pp. xiv + 496. Price 45s.

This important volume contains the proceedings of a conference for a general discussion on heat transfer arranged jointly by The Institution of Mechanical Engineers and the American Society of Mechanical Engineers in co-operation with a large number of kindred societies in Britain, the British Commonwealth, and Europe, including The Institute of Physics. The conference was held in London on 11 to 13 September, 1951, and was continued at Atlantic City, New Jersey, U.S.A., on 26 to 28 November, 1951. Ninety-three papers were presented, dealing with developments in the mechanism of transference of heat and in the design of apparatus relating thereto, and the subject-matter for consideration was divided into five main group headings covering the field of discussion, as follows:

- (1) heat transfer with change of state;
- (2) heat transfer between fluids and surfaces;
- (3) conduction in solids and fluids;
- (4) radiation, instrumentation, measurement techniques and analogies;
- (5) special problems such as heat transfer in turbine blade cooling, in liquid metals, in gas turbines, in piston engines, in the mercury boiler, etc.

This volume is a comprehensive and up-to-date treatise on the developments in the subject, which have taken place during the past ten years. Clearly, it is one of those standard works which will be needed by the many pure and applied physicists who are concerned, one way or another, with the

transfer of heat or who require the most recent data about the thermal properties of materials used in industry.

H. R. LANG

**X-ray crystallography.** 5th edition. By R. W. JAMES. (London: Methuen and Co. Ltd.) Pp. x + 101. Price 7s. 6d.

This little book, first published in 1930, provides a brief general account of the basic principles of X-ray crystallography, and is distinguished by the clarity and simplicity of exposition for which the author has always been noted. In the new (fifth) edition the text has been modified slightly in a number of places, in order to take account of new developments, and to reflect changes of emphasis inevitable in the period of rapid growth of a science which could be described in 1930 as "still in its infancy." In addition, a whole new chapter on Fourier methods, determination of phases, and so forth, replaces a few short paragraphs of the previous editions and provides an admirable brief survey of many of the most significant of recent developments in interpretative methods.

The new edition can be recommended without reservation.

W. H. TAYLOR

**Advanced experiments in practical physics.** 2nd edition. By J. E. CALTHROP, M.A., M.Sc. Revised by J. A. PRYDE, B.Sc., Ph.D. (London: William Heinemann Ltd.) Pp. xvi + 142. Price 10s. 6d.

The first edition of this book appeared in 1938. Though it seems to have been somewhat overshadowed by much larger volumes, it has undoubtedly proved to be a work which has assisted greatly those who have had to design courses in advanced physics. The fifty-five experiments described are well selected and particularly suitable for the student at General Degree level who is proceeding to the B.Sc. Special Physics examination. The revision includes some new experiments, particularly in electricity and magnetism, radioactivity and some electronics. It is a pity that the author recommends grease and sealing wax for making demountable vacuum joints; modern, inexpensive neoprene gaskets are much preferable. Again the amplifier of Fig. 159 has a distressingly old-fashioned look.

Many useful references are given in the text, and twenty additional problems suggested. It is very good value for money.

J. YARWOOD

**Elasticity in engineering.** By E. E. SECHLER. (London: Chapman and Hall Ltd.) Pp. ix + 419. Price 68s.

This book is unlikely to appeal to any but the practising structural engineer. It does indeed contain all the essential matter of the theory of elasticity, and the basic theorems are presented fully if a little tediously; yet it seems that this is but a necessary chore to be completed before the author exercises his loving art on rather complicated, and perhaps in some cases, rather peculiar structures. The classic stresses in a twisted rod of rectangular section thus find themselves sandwiched between such upstarts as a self-avoided airplane elevator (mercifully not in a wave state) and a palpable D-nose structure. The book is certainly too structural for the physicist.

H. L. COX

**Advances in geophysics.** By H. E. LANDSBERG. (New York: Academic Press Inc.) Pp. xi + 362. Price \$7.80.

In the foreword to this first volume of a proposed series, it is stated that activity in all branches of geophysics has increased by several orders of magnitude since the start of

World War II. The series is to satisfy a need for readily accessible and critical reviews of progress for the purpose of stocktaking and the possible cross-fertilization between different fields. The present volume covers a number of geophysical topics, each section written by an expert in his field. The topics of the first two sections are of interest to workers in all branches since they treat the automatic processing of geophysical data and the application of new developments in statistical methods to the assessment of observations. The remaining six articles are more specialized. Three deal with problems of the atmosphere embracing its circulation, observations on meteors to determine conditions in the upper atmosphere and unsolved problems of the upper atmosphere. Under the title Estuarine Hydrology are discussed the circulation, the salinity and tidal flushing for different types of estuary. The volume concludes with a description of the initiation of a world-wide gravity network by use of modern gravity meters and the applications and limitations of the airborne magnetometer for the study of structural geology. J. MCG. BRUCKSHAW

**Essentials of microwaves.** By R. B. MUCHMORE. (London: Chapman and Hall Ltd.) Pp. vi + 236. Price 36s.

This book represents an attempt to explain microwave phenomena, apparatus and measurements without recourse to the mathematical descriptions which normally make microwaves an "advanced" subject. This is clearly a task of heroic proportions, but the reviewer feels that it is on the whole successful. It is certainly a worthwhile effort, in that

there are and will be more people who need to work with microwaves apparatus than can be trained at the advanced level. It is indeed not impossible that people who grasp the basic physical principles will work better than those who are adrift in a sea of mathematics.

There are inevitably a few passages which one feels might have been improved (e.g. the second paragraph on p. 88, and the reference to thermocouples at the foot of p. 220), but the verbal explanation of physical principles is generally done well. An account is given of the basic laws, the properties of waveguides, resonators and antennas, the several types of tube for generating and amplifying microwave signals, the applications to radar, microwave measurements and the use of microwaves for physical research. The standard of production is good, though this is perhaps to be expected at 36s. The price will probably be considered high by those who would benefit most from reading this book.

D. A. WRIGHT

**Mechanics of the gyroscope: The dynamics of rotation.** 2nd edition. By R. F. DEIMEL, D.Eng. (New York: Dover Publications Inc.) Pp. xii + 192. Price \$3.25; Paper bound cheap edition, \$1.60.

This book was first published in 1929 and except for a new frontispiece and correction of errata, the text is the same as the first edition. It is primarily an elementary general treatment of the dynamics of rotation by the Professor of Mechanical Engineering of Stevens Institute of Technology.

## Journal of Scientific Instruments

### Contents of the June issue

#### ORIGINAL CONTRIBUTIONS Papers

- A thermoelectric method of comparing intensities of ultrasonic fields in liquids. By R. B. J. Pinner.
- High resistance bridge for conductivity measurements. By M. Unz.
- An automatic analogue computer for the solution of mine ventilation networks. By D. R. Scott and R. F. Hudson.
- The production of water spray of uniform drop size by a battery of hypodermic needles. By D. J. Rasbash.
- Variations in the characteristics of some corona-stabilizer tubes. By F. A. Benson and J. P. Smith.
- The construction of radiation thermocouples using semi-conducting thermoelectric materials. By D. A. H. Brown, R. P. Chasmar and P. B. Fellgett.
- The application of lead selenide photoconductive cells to infra-red spectroscopy. By V. Roberts and A. S. Young.
- A precision back-reflexion microbeam X-ray camera with provision for pre-selecting the irradiated area. By R. W. Cahn.
- Apparatus for the measurement of ionic conductance of solid salts. By P. W. M. Jacobs.
- A float type airflow meter for use on beds of agricultural grains. By W. F. Williamson and J. McCloy.

#### Laboratory and workshop notes

- A large unwelded vacuum gate valve. By S. Asao and K. Muramatsu.
- A simple test for anisotropic materials. By R. W. Powell.
- Making thin films of polythene. By G. C. Reid.

#### NOTES AND NEWS

##### Correspondence

- A method for obtaining long exposures at high altitudes using rubber balloons. From V. D. Hopper and A. R. W. Wilson.
- A photomechanical wave analyser for Fourier analysis of transient waveforms. From J. Darbyshire and M. J. Tucker.
- The effective radius of curvature of knife edges. From A. L. Rawlings; G. F. Hodsmar and F. A. Chappell.

British Instrument Industries Exhibition—A preview

Notes and comments

## British Journal of Applied Physics

### Original contributions accepted for publication in future issues of this Journal

- The linear piezoelectric equations of state. By R. Bechmann.
- Production of single crystals of nickel. By R. F. Pearson.
- A method of correcting for initial stresses in frozen-stress observations. By H. T. Jessop and W. H. Stadford.
- Solid bodies appearing in electron microscope specimens. By G. Yasuzumi.
- The sinkage of tracked vehicles on soft ground. By I. Evans.
- On growing single crystals of thallium activated alkali halides. By J. Franks.
- Tables for use in the measurement of interfacial tensions between liquids with small density differences. By O. S. Mills.
- Light scattering measurements on polydisperse systems of spherical particles. By E. Atherton and R. H. Peters.
- Some aspects of light scattering from polydisperse systems of spherical particles. By E. Atherton and R. H. Peters.
- Gold as a grid emission inhibitor in the presence of an oxide-coated cathode. By B. O. Baker.
- Pressure fluctuations in a jet engine. By H. M. Nicholson and A. Radcliffe.
- The reduction in apparent particle concentration with multiple strokes of the Owens jet dust counter. By J. K. Donoghue and C. Mack.
- Some relative fluorescence efficiencies in the Schumann region. By W. Maslen, N. E. White and S. E. Williams.
- The colouring of diamonds by neutron and electron bombardment. By R. A. Dugdale.
- The field along the axes of symmetry of equal semi-infinite rectangular magnetic pole-pieces. By W. Snowdon and N. Davy.
- Measurements of orientation in cotton fibres using polarized light. By R. Meredith.
- Fundamental relations in photoplasticity. By S. E. A. Bayoumi and E. K. Frankl.
- Sampling errors in radiation measurement using the Moll thermopile method. By L. L. Fox, R. C. G. Packham, P. L. Palmer and D. Whittaker.

THIS JOURNAL is produced monthly by The Institute of Physics, in London. It deals with all branches of applied physics (including theory and technique). All rights reserved. Responsibility for the statements contained herein attaches only to the writers.

**EDITORIAL MATTER.** Communications concerning editorial matter should be addressed to the Editor, The Institute of Physics, 47 Belgrave Square, London, S.W.1. (Telephone: Sloane 9806.) Prospective authors are invited to prepare their scripts in accordance with the *Notes on the preparation of contributions*. (Price 2s. 6d. including postage.)

**REPRODUCTION.** The Institute of Physics is a signatory to The Royal Society's Fair Copying Declaration. Details may be obtained upon application from The Royal Society, London, W.1.

**ADVERTISEMENTS.** Communications concerning advertisements should be addressed to the agents, Messrs. Walter Judd Ltd., 47 Gresham Street, London, E.C.2. (Telephone: Monarch 1644.)

**SUBSCRIPTION RATES.** A new volume commences each January. The charge is £4 per volume (\$11.50 U.S.A.), including index (post paid), payable in advance. Single parts, so far as available, may be purchased at 8s. each (\$1.15 U.S.A.), post paid, cash with order. Orders should be sent to The Institute of Physics, 47 Belgrave Square, London, S.W.1, or to any bookseller.



# Electrical analogues\*

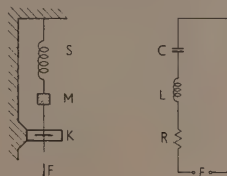
By G. LIEBMANN, D.Phil., F.Inst.P., Research Laboratory, Associated Electrical Industries Ltd., Aldermaston, Berkshire

The idea of the analogue representation of physical problems is discussed. The principles and operating techniques of the conducting paper, the electrolytic tank, the resistance-network, and networks using resistive and reactive components are described and illustrated by a number of applications from various fields of physics and engineering. A table is given summarizing the advantages and disadvantages of the various types of analogue.

## ANALOGIES IN PHYSICS AND ANALOGUES

An analogy is often used to explain an unfamiliar or difficult matter in terms of a better known or a simpler case. In particular, if two different physical phenomena *A* and *B* are described by the same mathematical formalism, *quantitative* conclusions can be drawn about the phenomenon *A* by studying the phenomenon *B*. For instance, the vibration of a weight suspended from a spring can be investigated by studying the analogous system of an inductance-capacitance circuit (Fig. 1). It is seen from the equations which describe

Fig. 1. Mechanical system and analogous electrical system



$$\text{Mechanical: } F = M \frac{d^2x}{dt^2} + K \frac{dx}{dt} + Sx \text{ or}$$

$$F = M \frac{dv}{dt} + Kv + S \int v dt \left\{ \begin{array}{l} M \simeq L, K \simeq R, S \simeq \frac{1}{C} \end{array} \right.$$

$$\text{Electrical: } E = L \frac{di}{dt} + R_1 i + \frac{1}{C} \int i dt$$

these two phenomena that if "mechanical stiffness" is equated to the reciprocal of "electrical capacitance," "mass" to "inductance," and "friction" to "resistance," then "velocity" corresponds to "electric current" and "mechanical force" to "e.m.f." In practice, it is often much easier to investigate the electrical system, e.g. it is much simpler to use an adjustable capacitor than to make a spring of adjustable stiffness, etc. An apparatus designed to solve in a systematic manner certain problems arising in physics or engineering by analogy, as just defined, is called an *analogue*.

All analogues have one characteristic in common, which distinguishes the solution of problems found with their help from that obtainable, e.g. by numerical analysis. In an analogue, the magnitudes to be determined in the solution of the problem always appear as physical magnitudes, e.g. as voltages or currents. There is, therefore, always a limit to the accuracy with which a solution can be written down. The errors are due to errors in the measurements and to the tolerances in the setting-up of the analogue. Often, there is an additional error due to the analogue not being perfect. These errors may be as large as, say, 10% in some cases, and as small as 1 part in 10000 or even less in others. But they are unavoidable and cannot be reduced below a certain level given by the type and often by the physical dimensions of the analogue apparatus.

There are numerous types of analogues. Many of these, particularly some of the analogue computers, are of a highly specialized kind, designed for a specific purpose. The further discussion in this paper will be confined to electrical analogue apparatus designed to solve *boundary value problems*, under static or transient conditions. The solution of such problems, often described mathematically by partial differential equations, is of great practical importance.

When constructing such analogues, two distinct approaches can be used, one based on the *field analogy*, and one based on the idea of the "equivalent circuit," although it will be seen later that this distinction is not always a sharp one, as elsewhere in electromagnetism. For example, the electrical circuit shown in the right half of Fig. 1 can be considered as the "equivalent circuit" of the mechanical system on the left. A more complicated mechanical system may be represented as a combination of a number of springs, masses, dashpots, levers, etc.; then an "equivalent circuit" may be set up which will be a network of interconnected capacitors, inductors, resistors and transformers, with a few suitably placed sources of e.m.f. This is a type of analogue discussed by Kron<sup>(1)</sup> and in part realized by the CAL-TECH-Computer,<sup>†(2)</sup> which will be referred to later. The characteristic feature of this approach is the representation of the original (mechanical) system by a mechanical system with a finite number of parameters, each of which then has a direct analogue counterpart in the equivalent electrical system. It is fairly obvious that even a moderately large number of parameters in the original system may lead to great complexity of its electrical analogue. This approach is, therefore, most useful in the study of the *dynamic* characteristics of systems which can be described by relatively few parameters.

The other approach is based on the fact that many problems in physics or engineering are described mathematically by an equation of the type

$$\left. \begin{aligned} \nabla^2 U &= 0 \\ \nabla^2 U &= f(x, y, z) \\ \nabla^2 U &= -\left(\frac{2\pi}{\lambda}\right)^2 U \\ \nabla^2 U &= \frac{1}{\kappa} \frac{\partial U}{\partial t} \end{aligned} \right\} \quad (1)$$

where the independent variables *x*, *y*, *z* are continuously variable and  $\nabla^2$  represents the Laplacian operator

$$\frac{\partial^2}{\partial x^2} + \frac{\partial^2}{\partial y^2} + \frac{\partial^2}{\partial z^2}$$

Take, for example,  $\nabla^2 U = 0$ , or more generally

$$\text{div}(pF) = -\text{div}(p \text{ grad } U) = 0 \quad (2)$$

with

$$F = -\text{grad } U \quad (3)$$

\* Based on a lecture given before the Electronics Group of The Institute of Physics on 14 October, 1952.

† California Institute of Technology Electric Analogue Computer.



This equation describes the electrostatic field between electrodes, the magnetic field near magnets, the flow of current in a conducting solid or liquid, the mass flow of gases or liquids, or the flow of heat under steady state conditions.

Now consider electric current flowing through a conducting medium. By Ohm's law:

$J = \sigma E$ , where  $J$  is the current density,  $E = -\text{grad } \phi$  the field strength in the conducting medium, and  $\sigma$  its electrical conductivity.

From the law of conservation of current

$$\text{div } J = \text{div } (\sigma E) = 0 \quad (4)$$

one sees that if one puts

$$\sigma = \alpha \rho \text{ and } E = \beta F$$

there is a mathematically complete identity of the two sets of equations (2) and (4),  $\alpha$  and  $\beta$  being scaling constants. Hence, the pattern of flux tubes of current flow, and of the orthogonal equipotential surfaces in the conducting medium, describes at the same time the field distribution arising in many other problems. This coincidence is, of course, not fortuitous. It just expresses the principle of conservation of mass, or of energy.

#### CONDUCTING PAPER TECHNIQUE

Consider now a fairly simple case, that of a field distribution in a homogeneous medium, depending only on the two co-ordinates  $x$  and  $y$ . Such field distributions are very common in practice; for example, the electrostatic field distribution in a radio valve, or the mass flow past a long cylinder or an aerofoil belong in this class, as do many field problems which can be solved by rigorous mathematical analysis.

Then 
$$\frac{\partial^2 U}{\partial x^2} + \frac{\partial^2 U}{\partial y^2} = 0 \quad (5)$$

Obviously, such field distributions can be investigated by using a conducting sheet to which electrodes representing the desired shape of the boundaries are attached. This technique is very old; indeed, the first known experimental field plot was published by Kirchhoff<sup>(3)</sup> in 1845 (Fig. 2). The

Fig. 2. Kirchhoff's field plot

(Reproduced from *Annalen der Physik und Chemie*, Leipzig, 1845.)



disc used by Kirchhoff was a thin sheet of copper; the equipotential lines were sought out with two copper wires, using the deflexion of a compass needle due to the current as a balance indication. However, this very easy looking technique was not applied much in the next 100 years; in practice, difficulties arose from lack of uniformity of resistance of the conducting metal sheet and from contact troubles, and a few cases only have become known where this method was employed. Very recently, several authors<sup>(4)</sup> showed that a type of *conducting paper* sold commercially for use in teleprinters\* is particularly suitable for field mapping. The resistance is of the order of 1000–5000  $\Omega$ /unit square, varying from roll to roll and depending to some extent on the relative

humidity. The electrodes of the model may be painted directly on the paper with conducting silver paint† and the equipotential plot is directly drawn on the paper. There are no polarization effects, so either a.c. or d.c. may be used. The field plotting process is therefore extremely simple. All that is needed is a low voltage battery, a calibrated potentiometer and a galvanometer. The equipotential lines, corresponding to the potentiometer setting, are then traced with a probe. The author's colleague, Mr. F. J. Miranda, uses the tip of a ball pen as a probe, drawing in the equipotential lines straight away as he goes along. Fig. 3 shows one of his field



(By courtesy of Mr. F. J. Miranda.)

Fig. 3. Map of equipotential lines between accelerating electrodes of high voltage discharge tube obtained by conducting paper method

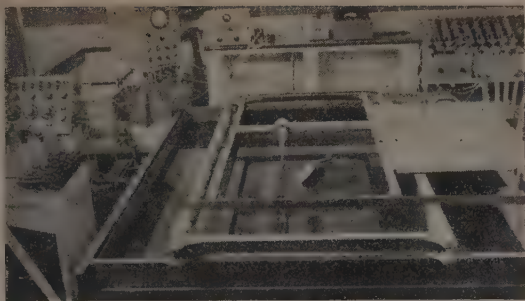
plots taken by this method during an investigation into the design of the discharge tube of a 4 MV van de Graaff generator. There is only one small difficulty, the resistance of the paper is not quite isotropic; the ratio of specific resistance in the two principal directions, perpendicular to each other, varies slightly from specimen to specimen, between about 1.10 and 1.15. This can, however, be taken into account by distorting the scale of the investigated model in the ratio of  $\sigma_x/\sigma_y$ , if the principal directions of conductivity are made into the  $x$ - and  $y$ -axes respectively. Another small point is that one has to be very careful not to crease the paper before or during taking the plot as this would cause local changes in resistance. An accuracy of the order of 2% can be expected. Local differences in the parameter  $p$  [equation (2)] can be simulated within limits by increasing the local resistance by perforating the paper or by decreasing its resistance by painting with a graphite solution.<sup>(5)</sup> That even untreated writing paper may be used for equipotential plotting if a measuring circuit of extremely high impedance is employed, has just been shown by Murray and Holloway.<sup>(6)</sup>

#### ELECTROLYTIC TANKS

Another analogue which has been more widely used is the *electrolytic tank*. Instead of a sheet of conducting paper, one uses a large basin filled with a weak electrolyte, say tap water. A model of the system under investigation is immersed in the tank. The exploration of the field distribution is then carried out with a thin wire probe dipped into the electrolyte. A typical electrolytic tank for field plotting is shown in Fig. 4.<sup>(7)</sup> However, while with some care one can avoid the anisotropy of the resistance of the electrolyte, there are

\* "Teledeltos" paper, grade "L" by Standard Telephone and Cables Ltd.

† e.g. Conducting paint, Grade EM50, by Metallurgical Products Ltd.



(Reproduced from the *Journal of the Royal Aeronautical Society*.)

Fig. 4. Typical electrolytic plotting tank

several factors which make the measuring technique more difficult. First of all, it is necessary to supply the tank from an a.c. voltage source of a frequency of about 1000 c/s as a polarization layer forms on the surfaces of the electrodes immersed in the electrolyte. This layer is equivalent to the insertion of an unwanted capacitance-resistance combination as shown in Fig. 5. This leads to the appearance of a

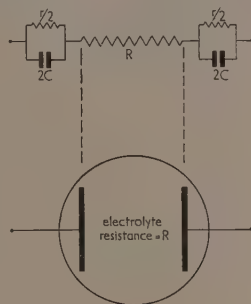


Fig. 5. Electrical circuit equivalent of electrolytic tank

quadrature component, upsetting the balance condition, and to an additional resistance, which is equivalent in its effect to a displacement of the electrodes; these effects can be reduced to a sufficient degree by graphiting of the electrodes. Next, the positioning of the electrodes of the model and of the exploring probe must be carried out with precision, a higher precision than is often realized. Finally, great care must be taken with the actual measurements, partly owing to the remaining quadrature components and partly owing to the high probe impedance. While it is easy to get an accuracy of, say, 5%, one has to be careful if one wishes to get an error of about 1%. Still greater accuracy, down to about 0.1% to 0.2%, has been reached by several authors<sup>(8,9)</sup> through great attention to every detail of the apparatus and

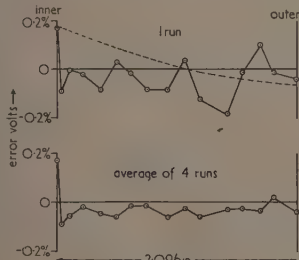


Fig. 6. Experimental errors in cylindrical test tank

(By courtesy of Mr. P. A. Einstein.)

particularly the measuring equipment. A typical result, obtained by Mr. P. A. Einstein during a study of the best obtainable accuracy, is shown in Fig. 6. However, in most practical problems one will do well to get an accuracy of the order of 0.5%.

For all its limitations, the electrolytic tank has proved a very useful tool, and has been employed in many fields, e.g. the study of air flow around aerofoils<sup>(7)</sup> and through turbine cascades,<sup>(8,10)</sup> and in problems of fluid flow.<sup>(11,12)</sup>

Rewriting equation (2):

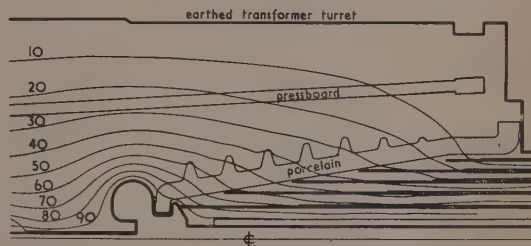
$$\operatorname{div} (p \operatorname{grad} U) = \operatorname{div} (\sigma \operatorname{grad} \phi) \\ = \frac{\partial}{\partial x} \left( \sigma \frac{\partial \phi}{\partial x} \right) + \frac{\partial}{\partial y} \left( \sigma \frac{\partial \phi}{\partial y} \right) = 0 \quad (6)$$

one sees that a locally different value of the scalar constant  $p$  can be represented by changing the local value of the conductance  $\sigma$ . As  $\sigma = \text{const.} \times t$ , where  $t$  is the depth of the electrolyte, an easy way to represent different values of  $p$  is to make  $t$  a function of  $x$  and  $y$ .<sup>(13)</sup> For example, if in an electric field problem, a value  $\epsilon$  of permittivity has to be represented, and the depth of electrolyte is  $t_0$  for the space corresponding to air, its depth will be  $t = \epsilon t_0$  for the space taken up by the dielectric. Details of the technique required are given in a recent paper by McDonald.<sup>(14)</sup>

If  $t \propto r$ , equation (6) takes the form:

$$\frac{\partial}{\partial r} \left( r \frac{\partial \phi}{\partial r} \right) + r \frac{\partial^2 \phi}{\partial z^2} = 0 \quad (7)$$

which is the Laplace equation in cylindrical co-ordinates. Hence, a tank with inclined insulating bottom can solve problems of rotational symmetry.<sup>(13,15)</sup> This has been extensively used, e.g. in electron optics.<sup>(16)</sup> Rotationally symmetrical problems involving cylindrical layers of different permittivity  $\epsilon$  can be similarly investigated by making  $t \propto \epsilon r$ . The solution of such a problem is illustrated by Fig. 7, which



(By courtesy of Mr. D. McDonald and of the British Thomson-Houston Co. Ltd.)

Fig. 7. Potential distribution around oil end of a conventional high voltage transformer bushing. The equipotentials are expressed as a percentage of the applied voltage

shows the field distribution at the oil end of a high voltage transformer bushing, as measured in the electrolytic tank.

In the last few years, several interesting applications have been based on the fact that *plane vortex flow* can be represented by feeding currents into the tank at the vortices.<sup>(12,13,17)</sup> In this way, circulation in fluid flow or gas flow can be studied. This principle has been further developed by Malavard<sup>(7)</sup> and his school, who designed a complete "wing calculator" with which the wing lift can be determined for various aerofoil designs, angles of attack, etc. Electrical engineers have used the method for solving certain vector problems, e.g. the design of shaped betatron



(By courtesy of Dr. K. J. R. Wilkinson and of the British Thomson-Houston Co. Ltd.)

Fig. 8. Wax model of betatron magnet in electrolytic tank, showing current feeding probes

magnets<sup>(18)</sup> (Fig. 8) and for finding experimentally the poles and zeros of complex functions, as required in advanced electrical circuit theory.<sup>(19)</sup>

#### RESISTANCE NETWORK ANALOGUES

Now consider that the electrolyte of the tank be divided up into a great but finite number of cells, and that the resistance of each cell is then replaced by its "lumped" resistance. The result is a network of interconnected resistances as shown by Fig. 9 which is called a "resistance-net-

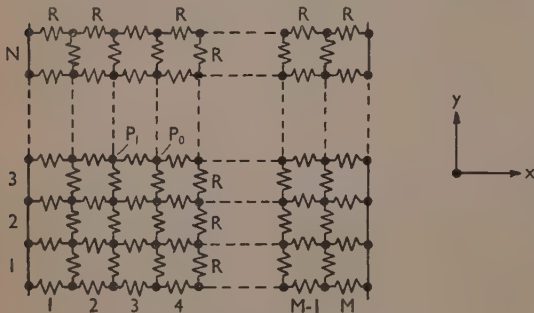


Fig. 9. Resistance-network

work analogue."<sup>(1, 20-22)</sup> All previous considerations regarding the representation of varying permittivity, of rotationally symmetrical cases, of vortex flow in a plane, etc., then apply,<sup>(22)</sup> but important advantages are gained by this "lumping" of the resistance. First of all, any change in  $\sigma$ , which had to be effected by changing the depth of the tank, can be much more easily achieved by changing the local value of the resistances and a very much wider range of  $\sigma$  can be covered. Second, practically all the measuring difficulties inherent in the electrolytic tank method are eliminated; there is no polarization, and the impedance of the network and of the probe connexion is low. Third, accuracy is inherently very high. The reason for this is that if one makes a network of several thousand components, there is a statistical cancellation of errors.<sup>(22)</sup> For instance, if one uses resistances of 1% tolerance, one can expect accuracies of the order of a few parts in 10000. Fourth, one can set up a problem very

quickly and accurately just by running a few wires along the network studs. Fifth, the resistance-network lends itself to the solution of a greater variety of problems<sup>(23, 24)</sup> as will be discussed below.

An earlier type of resistance-network was described and illustrated in a previous paper.<sup>(22)</sup> Since then a precision resistance-network, using 0.1% tolerance wire-wound resistors, has been constructed. This network is used with a specially made high precision potentiometer bridge, to take advantage of its high intrinsic accuracy; tests have shown that in "favourable" problems (i.e. models of large dimensions with straight boundaries and no high local potential gradients) accuracies of the order of 1 part in 30000 can be obtained without difficulty. The reasons for constructing such a precision network were that it still maintains a relatively high accuracy even when only small-scale models are used, as is sometimes necessary, and that in problems containing an axis of symmetry (e.g. rotationally symmetrical problems, as in electron optics), measurement of the potential distribution along this axis only is needed to know the potential everywhere, e.g. the potential  $\phi(r, z)$  at the point  $(r, z)$  is given by the series

$$\phi(r, z) = \phi(0, z) - \frac{r^2}{4}\phi''(0, z) + \frac{r^4}{64}\phi''''(0, z) \mp \dots$$

However, the potential distribution along the axis of symmetry must then be measurable with high accuracy, to counteract the loss of accuracy in the numerical differentiation of the measured potential values.

Against the great advantages of the resistance-network analogue must be set some disadvantages, stemming from the division of the model into discrete "cells," although these disadvantages are not serious if the network is large enough. For example, it is possible to represent curved boundaries by local modifications of the resistance values.<sup>(21, 22, 26)</sup>

Errors due to the finite distances of the mesh points can be greatly reduced by an easily applied extrapolation method,<sup>(22, 25)</sup> and it is possible to obtain potential measurements within a mesh square by using a small clip-on potentiometer bridge, which gives a "weighted" electrically interpolated value within the mesh.<sup>(22)</sup> This last method is particularly useful if it is desired to obtain an equipotential plot on the resistance-network, i.e. the loci of prescribed values of potential in the model. Fig. 10 shows the lines of

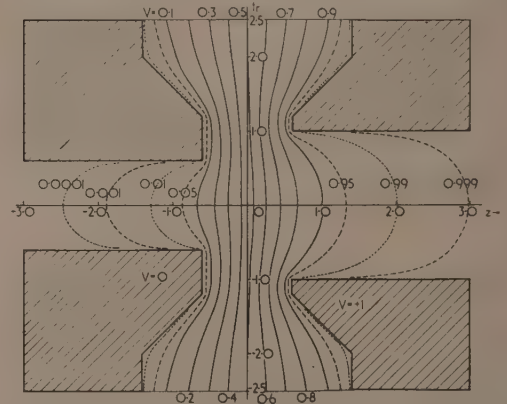


Fig. 10. Lines of equal magnetic potential in magnetic electron lens as obtained with the resistance-network analogue. (Relative units of voltage and distance)



equal magnetic potential in a magnetic electron lens which were obtained in this way. It should be noted that the position of the equipotential lines can be ascertained with far greater accuracy than would have been possible in the electrolytic tank, e.g. while the position of the 0.01 equipotential line would already be difficult in the electrolytic tank, this can be very accurately located in the resistance-network analogue, and even the 0.0001 equipotential line can still be found with fair accuracy.

The resistance-network analogue has also been used to plot the magnetic flux distribution within iron. It has even been possible to take account of the local increase of flux density near corners and the resulting iron saturation effects. This is illustrated by Fig. 11 which shows the flux distribution

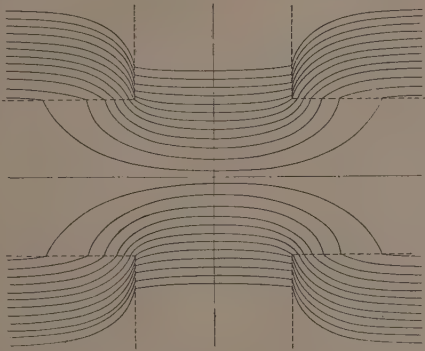


Fig. 11. Flux distribution in pole pieces of magnetic electron lens at incipient iron saturation (measured with the resistance-network analogue)

in a magnetic electron lens at incipient iron saturation. The technique employed<sup>(27)</sup> is this: first a uniform flux density within the iron is assumed, and the resistance values are adjusted, for the space taken up by the iron, to the value corresponding to the permeability  $\mu$  of the iron at the chosen flux density. A first field plot is then taken, and from the measured flux densities (or field strengths) new values of  $\mu$ , and hence new network resistance values are determined, etc. This procedure can be reduced to two iteration steps only by combining it with extrapolation. When applied to fluid flow problems, it would be equivalent to Taylor and Sharman's<sup>(12)</sup> electrolytic tank with adjustable depth, used in the study of the flow of compressible fluids; however, the resistance-network adjustments are carried out more easily and more quickly, and can cover a much wider range.

Local adjustments of resistance values in the network to satisfy problems described by equation (6), are also often required in heat conduction problems where the different thermal conductivities of a composite body can be represented in this manner. Such a problem is illustrated by Fig. 12, which shows the temperature distribution in a composite blast furnace hearth. (The physical data underlying the resistance-network solution of this problem were supplied by Mr. Daws of the British Iron and Steel Research Association.) Several other applications of the resistance-network to heat flow problems under steady-state conditions have been made, but recently the method was extended to the solution of heat flow problems under transient conditions.<sup>(28)</sup> The underlying principle is illustrated by Fig. 13. The resistances  $R_x$  form the network model of the spatial features of the problem. At each network node, current is fed in

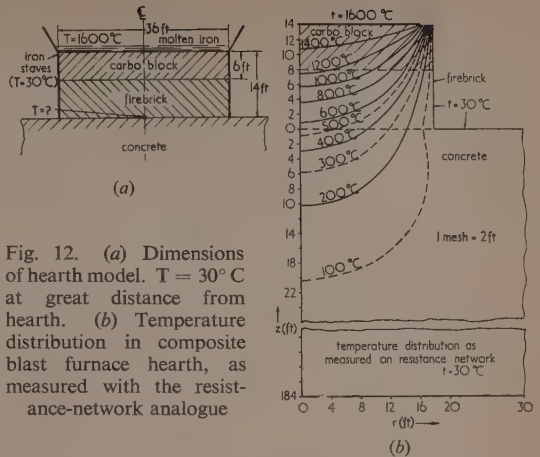


Fig. 12. (a) Dimensions of hearth model.  $T = 30^\circ\text{C}$  at great distance from hearth. (b) Temperature distribution in composite blast furnace hearth, as measured with the resistance-network analogue

from the potentiometer  $P$  through a series resistance  $R_i = \kappa \Delta t R_x / (\Delta x)^2$ ,  $\kappa$  being the thermal diffusivity,  $\Delta t$  the time interval in which the solution is worked and  $\Delta x$  the (real) distance between the network nodes. One can show that if the potentiometer voltages  $V_n$  represent the temperature distribution in the network model at the time  $n\Delta t$ , the voltages at the network nodes give the temperature distribution  $V_{n+1}$  at the time  $(n+1)\Delta t$ . The problem is solved by repeatedly resetting the potentiometer  $P$ . An advantage

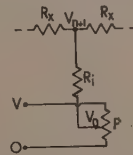


Fig. 13. Principle of resistance-network method for solving transient heat flow problems

of this method is that it is easy to adjust the resistances  $R_x$  and  $R_i$  during the progress of the work, so that account can be taken of thermal properties which are functions of the temperature, or heat input or heat loss conditions which are functions of the time. An application to an engineering problem, the temperature distribution in the flange of a steam turbine casing at a certain time during the running-up period to the full load condition, is shown in Fig. 14. (The physical data underlying the resistance-network solution of

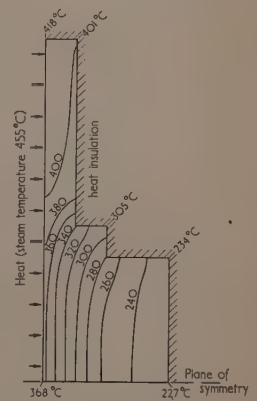
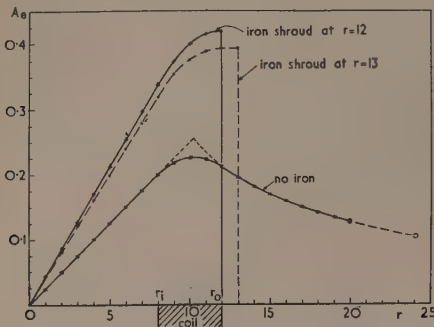


Fig. 14. Temperature distribution in model of flange of steam turbine casing, 15 minutes from application of load (initial temperature  $205^\circ\text{C}$ , steam temperature  $455^\circ\text{C}$ , heat transfer coefficient rising linearly with time)

this problem were supplied by Mr. Tapsell of Metropolitan-Vickers Electrical Co. Ltd.)

While an  $x$ - $y$  network (equal value resistances) can deal with plane vortex flow in a similar way as the electrolytic tank, one can go one step further by setting up a modified resistance network which can deal with vortex flow in rotationally symmetrical systems,<sup>(24)</sup> e.g. the vector potential distribution due to a long cylindrical coil (Fig. 15).



(Reproduced from the *Philosophical Magazine*.)

Fig. 15. Radial vector potential distribution inside and outside very long coil, without and with iron shroud, as obtained with the resistance-network analogue.  $A_0$  and  $r$  in relative units

One of the greatest advantages of the resistance-network method is that it can deal with much more complicated problems than the electrolytic tank. Any problem described by an equation of the type

$$\text{div} (p \text{ grad } U) = f(x, y, z, U, k) \quad (8)$$

$k$  being a previously unknown "eigen value" parameter, can be solved with the help of an iteration method.<sup>(23)</sup> First it can easily be shown that  $f$  can be represented by the current  $I$  flowing into the resistance-network at the corresponding network junction, if

$$I = -fh^2/R_N \quad (9)$$

where  $h$  is the distance between mesh junctions, and  $R_N$  the local value of the resistances in the network. The process of solving the equation is then first to assume any suitable distribution of  $f=f_0$  and feed in the required currents at the mesh nodes. This gives a first solution  $U_0$  and a first value  $k_0$ . These values are used in  $f$  to determine a better approximation  $f_1$ . The fed-in currents are then adjusted accordingly, a next better solution  $U_1$  and  $k_1$  being obtained, etc. This process has been found to converge rapidly to a "self-consistent" final solution because the voltages  $f$ , being

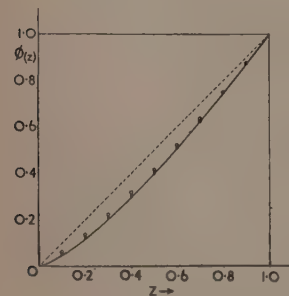


Fig. 16. Potential distribution in plane diode under space charge conditions, as measured with the resistance-network analogue

— — — = Laplacian solution;  
○ = first approximation;  
× = second approximation;  
— = exact.

(Reproduced from *Nature*.)

averaged by the network, are always much more accurate than the fed-in currents  $I$ . As an example, consider the space charge flow in a plane-parallel diode; the equation can be written as  $\nabla^2\phi = C/\sqrt{\phi}$ . Fig. 16 shows the good convergence.

Another application of this iteration method is to the wave equation

$$\nabla^2 U + k^2 U = 0 \quad (10)$$

where  $k = 2\pi/\lambda$ . This method has been applied to determine the cut-off frequencies of waveguides and the resonance frequencies of cavity resonators, and their electric and magnetic field distributions.<sup>(26)</sup> A typical result, the field distribution in a ridge waveguide, is shown in Fig. 17.

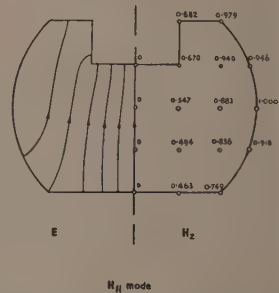


Fig. 17. Electromagnetic field distribution in ridge-waveguide for  $H_{11}$  mode, as obtained with the resistance-network analogue

(Reproduced from the *Proceedings of the Institution of Electrical Engineers*.)

Recently, the method was further improved by the use of a multipoint display unit, designed by the author's colleague, Mr. R. Bailey, which displays simultaneously on a cathode-ray oscilloscope screen an error signal for each of 25 network points. The error signals, corresponding to the "residuals" of the relaxation technique, are a measure of the degree to which equation (10) is satisfied. The iteration process for the solution of the wave equation can then be carried out in a very simple manner, by adjusting the fed-in currents until all error signals have been reduced to negligibly small values. It is thus possible to establish the solution of a 25 point waveguide problem to about 0.2% accuracy in less than 15 min,\* once the network has been set up. Of course, the complete numerical evaluation of the electric and magnetic field components takes somewhat longer. Another method of solving vibration problems with resistance networks by an iteration method has been described by Swenson and Higgins.<sup>(29)</sup> These authors synthesize negative resistances by subsidiary resistance-networks containing voltage sources which are cyclically adjusted, until the solution is "self-consistent."

#### COMPLEX IMPEDANCE-NETWORK ANALOGUES

An apparatus which may be considered a "resistance"-network analogue comprising "positive" and "negative" resistances, although it was originally developed by Kron<sup>(1)</sup> and Spangenberg<sup>(30)</sup> from the "equivalent circuit" idea, is the *inductance-capacitance network* for the solution of waveguide and cavity resonator problems at Stanford University. Fig. 18 shows the network arrangement. The model of the resonator is set up on the network in a similar way as on a resistance-network, and the frequency of the exciting a.c. voltage is adjusted until resonance occurs. The measurements require some care to avoid spurious oscillations. Also, the "equivalent circuit" concept does not give a very obvious correlation between the field data measured on the analogue and those of the real problem.

\* A demonstration of this was given during the lecture.

However, the "equivalent circuit" concept furnishes an immediate and direct analogy between the physical problem and the resistance-capacitance analogue for the solution of transient heat flow problems.<sup>(31)</sup> In this apparatus thermal conductivity is represented by electrical conductance, and heat capacity by electrical capacitance, as shown in Fig. 19.

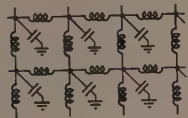


Fig. 18. Capacitance-inductance-network for solving waveguide and resonator problems

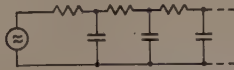


Fig. 19. Resistance-capacitance-network for solving transient heat flow problems

Fig. 20 is a photograph of the control desk of Dr. Paschkis's analogue at Columbia University. Of course, it is not always necessary to use elaborate equipment, as shown in Fig. 20; in practice one may often be satisfied with a fairly rough approximation obtainable with few components,<sup>(32)</sup> parti-



(By courtesy of Dr. V. Paschkis and of Columbia University.)

Fig. 20. Control and measuring desk of Dr. Paschkis's heat flow analogue



(By courtesy of Professor G. D. McCann.)

Fig. 21. Photograph of part of the CAL-TECH computer

cularly as in many cases the thermal constants of the materials are not accurately known. A simulation of a change of conditions during the period of the measurement is not easy to carry out, although an analogue of this type, employing non-ohmic resistances, has recently been developed.<sup>(33)</sup>

Finally, Fig. 21 shows a photograph of the CAL-TECH Analogue Computer, probably the most versatile of its kind. So-called "network analysers" have been used to investigate transients in power transmission lines and complete grid systems. There are several of these in the U.S.A., and one

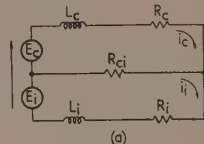
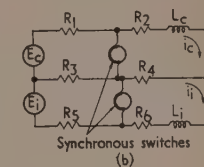
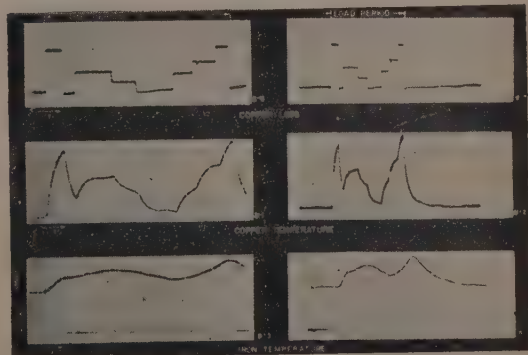


Fig. 22. Equivalent circuit for heat flow in electric motor under various load conditions



(Reproduced from the Transactions of the American Society of Mechanical Engineers.)

has been in operation for several years in this country.<sup>(34)</sup> The CAL-TECH Computer<sup>(2)</sup> is a direct descendant of the network analyser. It consists of a great number of resistors, capacitors, inductors, transformers, generators, switches, amplifiers and attenuators, as well as special function generators, which can be connected in any desired combination through bus bars leading to distributor panels. The analogue for the solution of a particular problem is then made up as required using either the field concept or the equivalent circuit principle, as may be most appropriate to the problem under consideration. This apparatus is therefore particularly useful in the study of transient conditions in complicated systems. For instance, it has been used recently to investigate the conditions leading to flutter of aeroplane wings. Figs. 22 and 23 give a typical, although small-scale, example of the use of this analogue. Fig. 22 shows the equivalent circuit for the heat flow in an electric motor under various load conditions and Fig. 23 the temperature rise in the copper



(Reproduced from the Transactions of the American Society of Mechanical Engineers.)

Fig. 23. Temperature rise in the copper and iron of an electric motor during a variable load cycle, as obtained on the CAL-TECH computer



and iron during a variable load cycle, as found by the analogue method.

## COMPARISON OF ANALOGUES

The survey of electrical analogues, which has been given in this paper, shows that it is often possible to solve a problem by any one of several analogue methods, each having its particular advantages and disadvantages. The main characteristics of the various analogues are summarized in the table.

## Comparison of electrical analogues

Type of analogue	Advantages	Disadvantages
Conducting paper	Cheap equipment, easy technique; applicable to complicated geometries	Limited accuracy; scale distortion. 2-dimensional only
Electrolytic tank	Applicable to complicated geometries	Difficult measuring technique; limited accuracy
Resistance-network	High accuracy; easy technique. Applicable to mathematically more complicated problems	Cumbersome when applied to complicated geometries
RC and LC networks	Apply to transient conditions	Limited accuracy. Specialized applications only. Require simple geometries
CAL-TECH computer	Applies to complex problems of great variety	Expensive equipment. Limited accuracy. Requires simple geometries

The literature references given below are those which have been used as a background for this article; numerous other papers, partly dealing with the question of the design of electrical analogues and partly dealing with their application in several fields of physics and engineering, had to be omitted. In conclusion, it may be noted that the development of new electrical analogues continues and that one can expect a widening application of analogue methods in the future.

## ACKNOWLEDGEMENTS

The author wishes to express his gratitude to all those who helped him with information or the loan of photographs, or permission to reproduce figures from unpublished or published work. He is also indebted to Dr. T. E. Allibone, the Director of the A.E.I. Research Laboratory, for permission to publish this article.

## REFERENCES

- (1) KRON, G. *Elect. Engng, N.Y.*, **67**, p. 672 (1948).
- (2) CRINER, H. E., McCANN, G. D., and WARREN, P. E. *Trans. Amer. Soc. Mech. Engrs*, **67**, p. A-135 (1945).
- (3) McCANN, G. D., and WILTS, C. H. *J. Appl. Mech.*, **16**, p. 247 (1949).
- (4) McCANN, G. D., WILTS, C. H., and LOCANTHI, B. N. *Proc. Inst. Radio Engrs*, **37**, p. 954 (1949).
- (5) KIRCHHOFF, G. *Ann. Phys., Lpz.*, **64**, p. 497 (1845); *Collected Papers, Lpz.*, 1882, p. 56.
- (6) CLAUSNITZER, W., and HEUMANN, H. *Z. angew. Phys.*, **2**, p. 443 (Nov. 1950).
- (7) MILNER, C. J. *B.T.H. Res. Rep.*, L4021 (Feb. 1951).
- (8) MALAVARD, L. *Rech. Aéronaut.*, No. 20 (March 1951).
- (9) KAYAN, C. F. *Trans. Amer. Soc. Mech. Engrs*, **67**, p. 713 (1945);
- (10) MIRANDA, F. J. *Proc. Instn Elect. Engrs*, **100**, Pt. II, p. 178 (1953).
- (11) MURRAY, C. T., and HOLLWAY, D. L. *J. Appl. Phys.*, **24**, p. 110 (1953).
- (12) MALAVARD, L. *J. Roy. Aero. Soc.*, **51**, p. 739 (1947).
- (13) DE HALLER, P. *Sulzer Tech. Rev.*, No. 3/4, p. 11 (1947).
- (14) DADDA, L. *Energia Elett.*, **26**, p. 469 (1949).
- (15) EINSTEIN, P. A. *Brit. J. Appl. Phys.*, **2**, p. 49 (1951).
- (16) SANDER, K. F., and YATES, J. G. *Proc. Instn Elect. Engrs*, **100**, Pt. II, p. 167 (1953).
- (17) MALAVARD, L., SIESTRUNCK, R., and GERMAIN, P. *Rech. Aéronaut.*, No. 4 (1948).
- (18) RELF, E. F. *Phil. Mag.*, **48**, p. 535 (1924).
- (19) PÉREZ, J., and MALAVARD, L. *Assoc. Techn. Maritime et Aéronautique*, No. 762 (1938).
- (20) TAYLOR, G. I., and SHARMAN, C. F. *Proc. Roy. Soc. A*, **121**, p. 194 (1928).
- (21) PÉREZ, J., and MALAVARD, L. *Bull. Soc. Franç. Élect.*, **8**, p. 715 (1938).
- (22) McDONALD, D. *Proc. Instn Elect. Engrs*, **100**, Pt. II, p. 145 (1953).
- (23) BOWMAN-MANIFOLD, M., and NICOLL, F. A. *Nature (Lond.)*, **142**, p. 39 (1938).
- (24) ERTAUD, A. *L'Optique Electronique*, p. 105. Ed. L. de Broglie (Paris: Rev. d'Optique, 1946).
- (25) LIEBMANN, G. *Advances in Electronics*, **2**, p. 102 (1950).
- (26) PEIERLS, R. E. *Nature (Lond.)*, **158**, p. 831 (1946).
- (27) WILKINSON, K. J. R. *BT-H Activ.*, **23**, No. 4, p. 3 (1952).
- (28) BOOTHROYD, A. R., CHERRY, E. C., and MAKAR, R. *Proc. Instn Elect. Engrs*, **96**, Pt. I, p. 163 (1949).
- (29) GUTENMACHER, L. *Comptes Rendus (Doklady), Acad. Sci. U.R.S.S.*, **27**, p. 198 (1940).
- (30) HOGAN, T. K. *J. Instn Engrs, Aust.*, **15**, p. 89 (1943).
- (31) DE PACKH, D. C. *Rev. Sci. Instrum.*, **18**, p. 798 (1947).
- (32) REDSHAW, S. C. *Brit. J. Appl. Phys.*, **2**, p. 291 (1951).
- (33) PERSICO, E. *Nuovo Cimento*, **9**, p. 74 (1952).
- (34) REDSHAW, S. C. *Proc. Instn Mech. Engrs*, **159**, p. 25 (1948).
- (35) LIEBMANN, G. *Brit. J. Appl. Phys.*, **1**, p. 92 (1950).
- (36) LIEBMANN, G. *Nature (Lond.)*, **164**, p. 149 (1949).
- (37) LIEBMANN, G. *Phil. Mag.*, **41**, p. 1143 (1950).
- (38) CULVER, R. *Brit. J. Appl. Phys.*, **3**, p. 376 (1952).
- (39) LIEBMANN, G. *Proc. Instn Elect. Engrs*, **99**, Pt. IV, p. 260 (1952).
- (40) LIEBMANN, G. *Proc. Phys. Soc. (Lond.) B*, **66**, p. 448, (1953).
- (41) LIEBMANN, G. *Proc. General Discuss. Heat Transfer, Lond.*, 1951, p. 300. Details to be published elsewhere.
- (42) SWENSON, G. W., and HIGGINS, T. J. *J. Appl. Phys.*, **23**, p. 126 (1952).
- (43) SPANGENBERG, K., WALTERS, G., and SCHOTT, F. *Proc. Instn Radio Engrs*, **37**, pp. 724 and 866 (1949).
- (44) BEUKEN, C. L. *Economisch Technisch Tijdschrift*, No. 1, (Netherlands: Maastricht, 1937).
- (45) PASCHKIS, V., and BAKER, H. D. *Trans. Amer. Soc. Mech. Engrs*, **64**, p. 105 (1942).
- (46) WILLIAMS, J. C. *Brit. J. Appl. Phys.*, **3**, 197 (1952).
- (47) LAWSON, D. I., and MCGUIRE, J. H. To be published in *Proc. Instn Mech. Engrs*.
- (48) LYON, G. *Proc. Instn Elect. Engrs*, **97**, Pt. II, p. 697 (1950).

## The dimensions of physical quantities

The Education Group of The Institute of Physics arranged a discussion on dimensions which took place at the Institute's house on 18 March, 1953. The principal speakers were Dr. R. Fürth, Professor G. F. Nicholson and Mr. E. W. H. Selwyn and a summary of their addresses and of the subsequent discussion is given in this report.

The notion of "dimensions" of physical quantities and the method of "dimensional analysis" are widely used in the teaching of physics in schools and universities. They are, at the same time, the subject of a great deal of controversy in scientific literature. The Education Group of The Institute of Physics felt therefore that a discussion on dimensions from various points of view would serve a useful purpose. The discussion was opened by short exposés by three principal speakers: Dr. R. FÜRTH (Birkbeck College, University of London), PROFESSOR G. F. NICHOLSON (Royal Naval College, Greenwich), and Mr. E. W. H. SELWYN (Kodak Ltd.).

Dr. Fürth gave a brief outline on the fundamental meaning of dimension in physics as taken over from geometry. The mathematical representation of a physical law can always be taken to be an equation of the form

$$f(x, y, z, \dots) = 0 \quad (1)$$

where the variables  $x, y, z, \dots$  represent certain physical quantities. The equation connects the numerical values of these variables in a specified way. From the purely mathematical point of view there is no reason why the form of the function  $f$  should be restricted in any way; as it can always be approximated by a finite sequence of arithmetical operations like addition and multiplication, any such sequence of operations is *a priori* admissible. But from the physical point of view it is important to realize how the numerical values  $x, y, z, \dots$  are obtained. They are always either numbers, directly read off the scales of measuring instruments, or indirectly computed from such readings by some defined mathematical operation. The combined operation consisting of the physical operation of measurements by means of specific methods and specified instruments and the mathematical operation of manipulating the readings defines in fact the physical quantity whose numerical values are represented by the variable  $x$ . It is clear, therefore, that an equation of the form (1) will represent a law of physics only if additional information is supplied in the form of detailed procedure as to how to "measure" the values  $x, y, z, \dots$  of the variables which it connects. This procedure is to a great extent arbitrary, and if it is changed the mathematical form of the physical law is also changed. In particular we may change the scales of the measuring instruments by multiplying all the figures on each scale by certain constants; this is called a "change of units." The numerical values of the variables  $x, y, z, \dots$  will, in general, be altered by a change of units, and the sentence "each physical quantity has a certain dimension" is meant to indicate that its values are affected by changes of units in a different way; we call a quantity "dimensionless" if its value is not affected by a change of units.

The term "dimension" is taken from geometry, and in order to understand its meaning in physics one has first to analyse its meaning in geometry. It is usually said that a

length has one dimension, an area two dimensions, and a volume three dimensions, because one instinctively feels that an area has infinitely more points in it than a line of finite length, and a volume infinitely more points in it than, say, its surface. But this can easily be proved to be wrong. For example, a unique one-to-one relationship can be set up between the points in the interior of a square and those on one of its sides. A mathematically precise definition of the dimension of a manifold of points is the following: A manifold is said to be  $n$ -dimensional if each of its members is defined by a set of  $n$  numbers. But this definition has no direct bearing on the practical problem of measuring lengths, areas and volumes. Lengths are measured, to the nearest integer, by a measuring rod whose length is arbitrarily chosen as the unit of length, and similarly an area is measured, again to the nearest integer, by an arbitrarily chosen "unit square." *A priori* there is no necessity of linking up the "unit length" and the "unit area" at all. If, however, we postulate a rational relationship between these two units, e.g. by giving the unit square sides of unit length, it appears at once that by a change of the unit of length to  $s$ -times its value the unit of area becomes  $s^2$ -times larger when  $s$  is an integer. It is not obvious that this also holds for non-integers, and even less so for irrational numbers  $s$ . But assuming the general validity of the statement we may now call the exponent 2 the dimension of an area and write the result of this consideration in the abbreviated form of a "dimensional equation"

$$[\text{area}] = [\text{length}]^2 \quad (2)$$

But it has to be kept in mind that this equation is *not* a mathematical equation of the form (1) but only a symbolic abbreviation of the prescription as to how to convert the numerical value of an area when the unit of length is changed. The same consideration, of course, applies to volumes which are said to have the dimension of the cube of a length, and it is easily seen that the sine or cosine of an angle is dimensionless as its numerical value is unaffected by a change of the unit of length.

A geometrical law concerning lengths, areas, volumes, angles, etc., must evidently also have the form of equation (1), and one must demand that this relation be independent of the units if it is to be a general law. Suppose  $f$  to have the form of a sum

$$f(x, y, z, \dots) = f_1(x, y, z, \dots) + f_2(x, y, z, \dots) + \dots \quad (3)$$

It is immediately clear that equation (1) will not be affected by a change of units only if  $f_1, f_2, \dots$  are each changed by the same conversion factor  $a$ , or in mathematical language, if the functions  $f_1, f_2, \dots$  are covariant with respect to a change of units. Clearly this will be the case if  $f_1, f_2, \dots$  have the same dimensions. Thus in order to obtain a universally valid geometrical relationship all additive terms in an equation

must have the same dimension. Combining equations (1) and (3) and dividing the whole equation by one of the terms, say  $f_1$ , one obtains

$$\frac{f_2}{f_1} + \frac{f_3}{f_1} + \dots = 1 \quad (4)$$

$$\text{or } \phi_2(x, y, z, \dots) + \phi_3(x, y, z, \dots) + \dots = 1 \quad (5)$$

The terms in equation (5) are all dimensionless, i.e. they are *invariant* with respect to a change of unit, and equation (5) is an invariant relationship between  $x, y, z, \dots$

Similar considerations can now be applied to physical laws connecting physical quantities. *A priori* each physical quantity could be defined operationally by a separate measuring process, so that each quantity would be defined completely independently of all the others. But in a rational procedure one will naturally try to reduce the number of independent operational definitions to a minimum and define all other quantities in terms of these. We then have a finite small number of *fundamental units* in terms of which all other units can be expressed. Again one has to demand that all additive terms in an equation expressing a physical law be co-variant with respect to a change of fundamental units. A *dimensional formula* for a physical quantity like that for velocity

$$[v] = [l][t]^{-1} \quad (6)$$

is just an abbreviated symbolic form for the definition of this quantity in terms of the fundamental ones and a prescription for the evaluation of the "conversion factor" by which the numerical values of the quantity are to be multiplied when the fundamental units are changed. There is, of course, no objection against the appearance of fractions in the exponents of dimensional formulae, and there is, in fact, no *a priori* reason why a dimensional formula should have an algebraic form at all. Again dimensionless physical quantities can be defined, like strain or "reduced temperatures," and physical laws can be written in *invariant* form. The number of fundamental physical quantities must, in the nature of the problem, to a certain extent remain conventional, and the controversy about the virtues of the various systems of units cannot be resolved by fundamental considerations.

There is universal agreement that the number of fundamental quantities in the field of dynamics is three, and the system of units based on those of length, time, and mass is generally accepted for scientific purposes. The usual procedure is to extend this system in one or the other direction so as to make it applicable to other fields of physics. However, from the didactic point of view, it might be preferable under certain circumstances to proceed in a different way. It was the purpose of Professor Nicholson's talk to show how in the teaching of electromagnetism to students of electrical engineering an independent system of three purely electromagnetic fundamental quantities and corresponding units could be employed.

To begin with, the notion of *uniform* fields is introduced which effectively reduces the three spatial dimensions to one and permits so-called "rationalized" units to be used, avoiding the appearance of factors  $4\pi$  in some of the basic equations. The subject is built up around the three circuit parameters "capacitance"  $C$ , "inductance"  $L$ , and "resistance"  $R$  or "conductance"  $G$ . These are used as fundamental quantities, as most of the new engineering student's early work will be concerned with circuits. It is important that he should obtain an early grasp of their behaviour. Knowledge of the principal laws of dynamics is, of course, assumed, and

mechanical analogy is used throughout as a guide in building up the subject.

*Electrostatics* is based on the observation of charge separation between two parallel plates, which leads to the notion of uniform electric field and "electric flux." The fact that energy is stored in this process leads, in analogy, to *elastostatics* to the notion of capacitance. The expression for the capacitance of a parallel plate capacitor of area  $A$  and plate distance  $d$

$$C = \kappa A/d \quad (7)$$

is then easily found. Capacitance is seen to be analogous to mechanical "compliance."

The laws of *current electricity* are based on observations of "current flux" between parallel plates. Ohm's law is derived empirically and the notion of conductance introduced in analogy to hydrodynamics. The expression

$$G = \sigma A/d \quad (8)$$

for the conductance of two parallel plate electrodes is deduced and the analogy between electric resistance and viscous friction of fluids is drawn.

Mechanical analogy further suggests the search for an electric analogue to mass. The fundamental *electromagnetic* observation is that a constant potential difference is required to maintain a constant rate of change of current in a circuit with vanishingly small resistance. The notion of electric *inertia* is based on the fact that energy is thus stored in the circuit, and the analogy between the expression for mechanical kinetic energy and the corresponding expression for the circuit energy leads to the introduction of inductance. The inductance of a parallel plate "inductor" is found to be

$$L = \mu A/d \quad (9)$$

The laws of *magnetism* ought to be derived from those of electrostatics by applying relativity theory. But as this would hardly be practicable at this stage they are instead introduced on the basis of the preceding considerations by "inventing" magnetic flux in analogy to electric flux and using Faraday's law of electromagnetic induction. This is more satisfactory than the customary historic procedure which starts from observations on forces between magnets.

In his summary the speaker suggested that the method may make it easier for the engineering student to link his early applied work with fundamental principles. He also suggested that the method was essentially an "honest" one.

Mr. Selwyn in his talk put the main emphasis on the method of dimensional analysis and the difficulties it provides for the teacher and the student. He followed mainly the argument expounded in his recent article on the method of dimensions in this *Journal*.<sup>\*</sup> He started with giving some amusing examples, one of which was the derivation of a formula for the period of practice  $T$  required before a golf player of mass  $m$  can swipe the ball a distance  $l$ . As the acceleration of gravity  $g$  is also clearly relevant one may expect a formula of the type

$$T = m^a l^b g^c \quad (10)$$

or in dimensional form

$$[T] = [M]^a [L]^b [T]^{-2c}$$

from which follows  $a = 0$ ,  $-2c = 1$ ,  $b = 1/2$ , so that equation (10) becomes

$$T = \text{const.} \sqrt{(l/g)} \quad (10')$$

\* SELWYN, E. W. H. *Brit. J. Appl. Phys.*, 3, p. 209 (1952).



Examples like this and more serious ones to be found in textbooks make it difficult for the student to realize to what extent he may legitimately use the method of dimensions to get a definite answer to a problem. Physics is concerned with the variation of quantities, and to measure variations one must have units to build up magnitudes of the same sort by adding units together. It happens that the units which are most commonly used are those of mass, length, and time, but this is only because they appeared first in the study of physics. There are other "respectable" units like the ampere, the standard candle, and the unit of optical density.

It is always possible to define variables  $\pi_1, \pi_2, \dots$  each of which has the form of a product of powers of the fundamental variables  $x, y, z, \dots$ :

$$\pi_s = x^{a_s} y^{b_s} z^{c_s} \dots \quad (11)$$

such that the  $\pi_s$  are independent of the units or invariant with respect to a change of units; they are thus "dimensionless" quantities. Any physical law can then be expressed in the invariant form

$$F(\pi_1, \pi_2, \dots) = 1 \quad (12)$$

If a problem involves  $m$  essential variables which depend on  $n$  units altogether the number of dimensionless variables  $\pi_s$  which can be formed is  $m - n$ . Dimensional analysis is concerned with finding the essential variables involved in a phenomenon and sorting them out into groups, independent of variation in the units. Whether it is then possible to express the law governing the phenomenon in an invariant form of the type (12) is not *a priori* certain and must be tested by experiment.

A well-known example is the flow of liquid through a pipe. The variables here are: the mean velocity of flow  $v$ , the pipe diameter  $d$ , the density of the liquid  $\rho$ , its viscosity  $\eta$ , and the pressure gradient  $\Delta P/l$ ; i.e.  $m = 5$ . The units in which they can be expressed are  $L, M, T$ , i.e.  $n = 3$ . Thus two dimensionless variables  $\pi_1$  and  $\pi_2$  can be formed, for example

$$\pi_1 = \frac{vd\rho}{\eta}, \pi_2 = \left(\frac{\Delta P}{l}\right) \frac{d^3\rho}{\eta^2} \quad (13)$$

It can indeed be proved by experiment that if  $\pi_2$  is plotted against  $\pi_1$  all the points (except those within a certain small region) are situated on one and the same graph.

A lively discussion followed these talks, the main points of which may be briefly summarized.

DR. J. TOPPING (The Polytechnic, Regent Street) pointed out that in dimensional analysis one has to distinguish between the physical and the mathematical parts. The physical part consists in selecting the essential parameters. The student must be made to realize that the number of variables which may possibly influence a certain phenomenon is usually very large, although most of them may turn out to be non-essential. This can be very clearly seen in the example of the golf ball mentioned by Mr. Selwyn. Restricting the number of variables to, say, three already constitutes a physical hypothesis. This point was also stressed by Dr. Fürth who remarked that one can never be sure whether a particular phenomenon may not depend explicitly on some atomic parameter.

DR. STOPS (Northampton Polytechnic) doubted the statement that a dimensionless quantity was unaffected by a change of units. It is certainly true if the scales used are linear, but the change-over from one non-linear scale to another must in general alter the values of the ratios of two measurements of the same quantity which are dimensionless. To this Dr. Fürth remarked that the definition of the scale of the measuring instrument is an essential part of the operational definition of the physical quantity which is being measured. If this scale is changed the quantity has, strictly speaking, no longer the same dimension. A change of unit, with respect to which a dimensionless quantity is invariant, does not presuppose a "linear" scale; it only means that all numbers on the scale are multiplied by one and the same factor.

DR. A. BLOCH (Research Laboratories, General Electric Co. Ltd., Wembley) pointed out the importance of the formulation of physical laws in the form of relations between dimensionless quantities for the engineer as this enables him to construct models of the phenomenon in question on a convenient scale.

MR. F. Y. POYNTON (Northampton Polytechnic) drew attention to the article on dimensions and units by J. Wallot\* in which a chapter is devoted to a discussion on the meaning of equations between physical magnitudes as distinct from ordinary mathematical equations between numbers.

R. FÜRTH

\* WALLOT, J. *Handbuch der Physik*, Vol. 2 (Berlin: Springer, 1926).

# Ratio of convection to conduction loss from a hot wire stretched along the axis of a vertical cylindrical tube

By Professor J. A. V. FAIRBROTHER, Ph.D., F.Inst.P., University of Natal, Pietermaritzburg, South Africa

[Paper first received 28 May, 1952, and in final form 25 February, 1953]

The ratio of the axial heat loss by convection to the radial heat loss by conduction for a wire mounted on the axis of a vertical tube is calculated for two cases: (a) when the tube is open at both ends to allow unrestricted circulation, and (b) when the tube is closed at both ends.

The calculations are based on the assumption that the axial flow is not so large as to cause the form of the radial temperature drop to depart appreciably from the logarithmic and that the system is sufficiently long for end effects to be negligible. The elementary calculations made possible by these simplifying assumptions show that for a radius of wire of 0.05 cm and of the cylinder 0.25 cm, the axial heat loss for the closed case is about 7.5 times smaller than for the open case. For a 10 cm long tube with temperature drop between the wire and the surrounding tube of 1° C, the calculation for water shows that the axial heat loss is 2.5% of the radial heat loss for the open case and 0.3% for the closed case. For air under the same conditions the axial heat loss is 0.02% of the radial for the open case and 0.003% for the closed case.

## LIST OF SYMBOLS

$S$  = radius of wire  
 $R$  = radius of cylinder  
 $\rho$  = density of fluid at radius  $r$   
 $\rho_0$  = density of fluid at radius  $R$   
 $K$  = thermal conductivity  
 $\eta$  = viscosity  
 $C_p$  = specific heat  
 $g$  = acceleration due to gravity  
 $\alpha$  = temperature coefficient of change of density  
 $\theta$  = temperature drop between  $R$  and  $r$   
 $\Theta$  = temperature drop between  $R$  and  $S$   
 $Q$  = heat loss, axial or radial, open or closed case, according to suffix  
 $T$  = radius of zero velocity  
 $v$  = velocity  
 $L$  = length of tube

As simple a way as any of measuring the thermal conductivity of a liquid or gas is to stretch a wire along the axis of a tube immersed in the substance to be studied and to measure the temperature drop across the annular gap for a known power dissipation in the wire. Unfortunately, however, the temperature gradient gives rise to convection currents which carry heat away from the wire and in practice it is necessary to arrange for the convection loss to be negligible or to correct for it. The calculation of the loss of heat from a wire by convection is in general a formidable problem though the case of a wire mounted on the axis of a vertical tube with open or closed ends, immersed in the fluid to be studied, and considered sufficiently long for end effects to be negligible, is amenable to elementary treatment provided it be assumed that the radial temperature drop is still approximately given by the formula which applies when convection effects are absent. This is equivalent to assuming that the heat transported axially is small compared with that transported radially and is the condition aimed at in making an experiment.

## "OPEN" CASE

Consider the equilibrium of a ring of liquid or gas (Fig. 1) of unit length, radius  $r$  and thickness  $\Delta r$ , between the wire of radius  $S$  and the cylinder of radius  $R$ . This ring will be in equilibrium, that is, moving with steady velocity, when the vertical force brought about by the difference in its density  $\rho$

and that of the liquid at the outer wall  $\rho_0$  is equal and opposite to the net viscous force, namely when

$$\frac{d}{dr} \left( 2\pi r \eta \frac{dv}{dr} \right) \Delta r = 2\pi r (\rho - \rho_0) g \Delta r \quad (1)$$

$$\text{and since} \quad \rho = \rho_0 (1 + \alpha \theta) \quad (2)$$

$$\text{and} \quad \theta = \frac{Q_r}{2\pi K L} \log \frac{R}{r} \quad (\text{approximately}) \quad (3)$$

$$\text{we can write} \quad \frac{d^2 v}{dr^2} + \frac{1}{r} \frac{dv}{dr} - A \log \frac{R}{r} = 0 \quad (4)$$

$$\text{where} \quad A = \frac{g \rho_0 \alpha Q_r}{2\pi \eta K L}$$

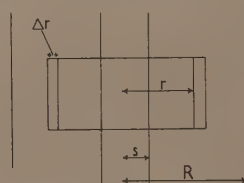


Fig. 1

The solution of this equation, bearing in mind that  $v = 0$  when  $r = R$  and  $S$  is

$$v = \frac{A}{4} \left[ \delta \log \frac{R}{r} + (r^2 - S^2) \log \frac{R}{r} + r^2 - R^2 \right] \\ = \frac{A}{4} f_1 \text{ say, where } \delta = \frac{R^2 - S^2}{\log(R/S)} \quad (5)$$

The heat transported axially per second is thus

$$Q_a = \int_S^R \rho C_p \theta v 2\pi r dr \\ = Q_r \frac{\Theta}{L} \frac{\rho_0^2 \alpha C_p g}{4\eta K} \frac{1}{\log(R/S)} \int_S^R f_1 r \log \frac{R}{r} dr \quad (6)$$

$$\text{therefore} \quad \frac{Q_a}{Q_r} = \frac{\Theta}{L} \beta \gamma \left[ f_1 \right]_S^R \quad (7)$$

$$\text{where} \quad \beta = \frac{\rho_0^2 \alpha C_p g}{4\eta K} \quad \text{and} \quad \gamma = \frac{1}{\log(R/S)}$$

The indefinite and definite forms of  $\mathcal{F}_1$  are given at the end of this paper. When  $S = 0.05$  cm and  $R = 0.25$  cm,  $\gamma = 0.62$  and  $[\mathcal{F}_1]_S^R = -1.15 \times 10^{-4}$ . For water, data gleaned from the Chemical Rubber Publishing Company's *Handbook of Physics* gives a value for  $\beta$  of  $3.5 \times 10^3$  so that

$$\frac{Q_a}{Q_r} = (-2.5 \times 10^{-1}) \frac{\Theta}{L} \quad (8)$$

(The negative sign is associated with temperature and density gradient and is not otherwise significant.) The axial loss in the case of water might therefore be expected to be as much as 2.5% of the radial loss for a temperature difference of  $1^\circ$  C and a tube length of 10 cm.

For air, using data from the same source,  $\beta = 30$  so that

$$\frac{Q_a}{Q_r} = (-2.2 \times 10^{-3}) \frac{\Theta}{L} \quad (9)$$

and the axial heat loss in this case, when the temperature drop is  $1^\circ$  C and tube length 10 cm, can be expected to be of the order of 0.02% of the radial.

The ratio for other parameters and fluids can be obtained by inserting appropriate values in the formulae.

#### "CLOSED" CASE

Since in this case there is no loss of fluid from the system a pressure difference must be built up between top and bottom sufficient to drive back a volume of fluid equal to that produced by the density difference ("open" case). If the return flow is assumed to take place under Poiseuille conditions its equation of motion is

$$\frac{d}{dr} \left( 2\pi r \eta \frac{dv}{dr} \right) \Delta r = \frac{p}{L} 2\pi r \Delta r \quad (10)$$

(where  $p$  is the pressure difference) the solution of which is

$$v = \frac{B}{4} \left( r^2 - R^2 + \delta \log \frac{R}{r} \right) = \frac{B}{4} f_2 \quad (11)$$

where  $B = \frac{p}{L\eta}$  and  $\delta = \frac{R^2 - S^2}{\log(R/S)}$  as before.

Functions  $f_1$  and  $f_2$  are plotted against  $r$  in Fig. 2 and from them the shapes of the functions  $f_1 \times r$  and  $f_2 \times r$ ,

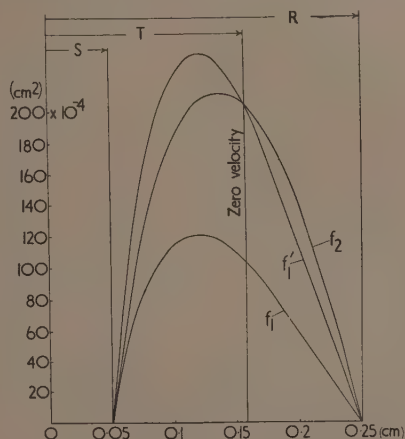


Fig. 2

representing the volume flow, are plotted in Fig. 3, the scale of  $f_1 \times r$  having been multiplied by the factor 1.98 to make the area under it equal to that under  $f_2 \times r$ . At  $r = 0.16$  cm =  $T$ , say, the volume flow, and hence the velocity,

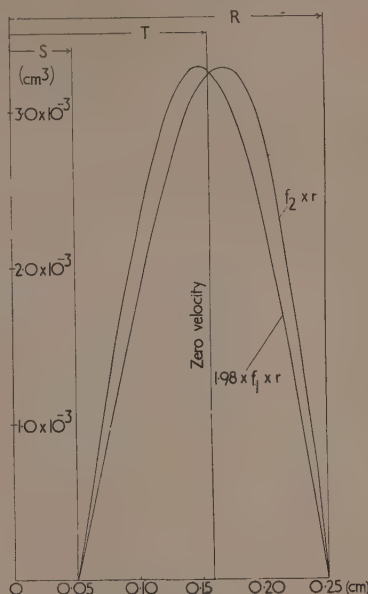


Fig. 3

is zero, and it is here assumed that the heat lost from the wire by axial flow is that transported by the liquid flowing upwards inside this radius and delivered to the outer annulus after reversal at the ends. The shape of the resultant volume flow curve is shown in Fig. 4 and is the difference of the two curves in Fig. 3. The shape of the resultant velocity flow curve is also shown in Fig. 4 and is the difference of  $f_1'$  and  $f_2'$  in Fig. 2,  $f_1'$  having been obtained from  $f_1$  by scaling the latter up to intersect  $f_2$  at  $r = 0.16$  cm =  $T$ .

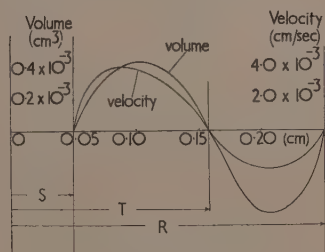


Fig. 4

The axial heat flow between  $S$  and  $T$  associated with  $f_1$ , only is

$$\int_S^T 2\pi p C_p \theta r dr \frac{A}{4} f_1 = 2\pi p C_p \Theta \frac{A}{4} \int_S^T f_1 r \log \frac{R}{r} dr \quad (12)$$

$$= 2\pi p C_p \Theta \frac{A}{4} \left[ \mathcal{F}_1 \right]_S^T \quad (13)$$



and that associated with the return flow is

$$\int_S^T 2\pi\rho C_p \theta v r dr = 2\pi\rho C_p \Theta \gamma \frac{B}{4} \int_S^T f_2 r \log \frac{R}{r} dr \quad (14)$$

$$= 2\pi\rho C_p \Theta \gamma \frac{B}{4} \left[ \mathcal{J}_2 \right]_S^T \quad (15)$$

so that the net loss due to axial flow is

$$Q_a = 2\pi\rho C_p \frac{\Theta}{\log(R/S)} \left( \frac{A}{4} \left[ \mathcal{J}_1 \right]_S^T - \frac{B}{4} \left[ \mathcal{J}_2 \right]_S^T \right) \quad (16)$$

Since the return flow is equal to the upward flow

$$2\pi \frac{B}{4} \int_S^R f_2 r dr = 2\pi \frac{A}{4} \int_S^R f_1 r dr \quad (17)$$

$$\text{or} \quad B \left[ \mathcal{J}_3 \right]_S^R = A \left[ \mathcal{J}_4 \right]_S^R \quad (18)$$

and

$$Q_a (\text{closed}) = 2\pi\rho C_p \Theta \gamma \frac{A}{4} \left\{ \left[ \mathcal{J}_1 \right]_S^T - \frac{\left[ \mathcal{J}_2 \right]_S^T \left[ \mathcal{J}_4 \right]_S^R}{\left[ \mathcal{J}_3 \right]_S^R} \right\} \quad (19)$$

$$\text{and} \quad \frac{Q_a}{Q_r} (\text{closed}) = \frac{\Theta}{L} \beta \gamma \left\{ \left[ \mathcal{J}_1 \right]_S^T - \frac{\left[ \mathcal{J}_2 \right]_S^T \left[ \mathcal{J}_4 \right]_S^R}{\left[ \mathcal{J}_3 \right]_S^R} \right\} \quad (20)$$

The indefinite and definite forms of the integrals  $\mathcal{J}_1, \mathcal{J}_2, \mathcal{J}_3, \mathcal{J}_4$ , together with their numerical values for  $S = 0.05$  cm,  $T = 0.16$  cm, and  $R = 0.25$  cm are given at the end. For these values of the radii, and dividing equation (7) by equation (20)

$$\frac{Q_a (\text{open})}{Q_a (\text{closed})} = \frac{\left[ \mathcal{J}_1 \right]_S^R \left[ \mathcal{J}_3 \right]_S^R}{\left[ \mathcal{J}_1 \right]_S^T \left[ \mathcal{J}_3 \right]_S^R - \left[ \mathcal{J}_2 \right]_S^T \left[ \mathcal{J}_4 \right]_S^R} \quad (21)$$

$$= 7.5 \quad (22)$$

It is of interest to note that the axial flow of heat in the open case effectively decreases the thermal conductivity (since it is not delivered to the surrounding cylinder) whereas the axial flow in the closed case produces an effective increase.

#### ACKNOWLEDGEMENT

I wish to thank Dr. G. Bateman for her kindness in checking the integrals.

#### APPENDIX

The integrals evaluated for  $S = 0.05$  cm,  $R = 0.25$  cm, and  $T = 0.16$  cm

$$\begin{aligned} \mathcal{J}_1 &= \left[ \frac{\delta r^2}{2} + \frac{r^4}{4} - \frac{S^2 r^2}{2} \right] \log^2 \frac{R}{r} + \left[ \frac{\delta r^2}{2} + \frac{3}{8} r^4 - \frac{r^2}{2} (R^2 + S^2) \right] \log \frac{R}{r} + \left[ \frac{\delta r^2}{4} + \frac{3}{32} r^4 - \frac{r^2}{4} (R^2 + S^2) \right] \\ \left[ \mathcal{J}_1 \right]_S^R &= \frac{S^4}{4} \log^2 \frac{R}{S} + \frac{5}{8} S^4 \log \frac{R}{S} - \frac{(R^2 - S^2)(5R^2 + 21S^2)}{32} + \frac{(R^2 - S^2)^2}{4 \log(R/S)} \\ &= -1.15 \times 10^{-4} \\ \left[ \mathcal{J}_1 \right]_S^T &= \mathcal{J}_1 (\text{with } r = T) - \frac{(R^2 - S^2)S^2}{4 \log(R/S)} - \frac{S^2}{32} (8R^2 - 21S^2) + \frac{5}{8} S^4 \log \frac{R}{S} + \frac{S^4}{4} \log^2 \frac{R}{S} \\ &= -0.914 \times 10^{-4} \\ \mathcal{J}_2 &= \delta \left[ \frac{r^2}{2} \log^2 \frac{R}{r} + \frac{r^2}{2} \log \frac{R}{r} + \frac{r^2}{4} \right] - R^2 \left[ \frac{r^2}{2} \log \frac{R}{r} + \frac{r^2}{4} \right] + \frac{r^4}{4} \log \frac{R}{r} + \frac{r^4}{16} \\ \left[ \mathcal{J}_2 \right]_S^T &= \delta \left[ \frac{T^2}{2} \log^2 \frac{R}{T} + \frac{T^2}{2} \log \frac{R}{T} + \frac{T^2 - S^2}{4} \right] - \frac{T^2}{4} (2R^2 - T^2) \log \frac{R}{T} + \frac{S^4}{4} \log \frac{R}{S} - \frac{R^2}{4} (S^2 + T^2) + \frac{7S^4 + T^4}{16} \\ &= -1.534 \times 10^{-4} \\ \mathcal{J}_3 &= \frac{r^4}{4} - \frac{S^2 r^2}{2} - \delta \left[ \frac{r^2}{2} \log \frac{r}{S} - \frac{r^2}{4} \right] \\ \left[ \mathcal{J}_3 \right]_S^R &= \frac{(R^2 - S^2)^2}{4 \log(R/S)} - \frac{R^4 - S^4}{4} \\ &= -4.16 \times 10^{-4} \\ \mathcal{J}_4 &= \left[ \frac{\delta r^2}{2} + \frac{r^4}{4} - \frac{r^2 S^2}{2} \right] \log \frac{R}{r} + \frac{\delta r^2}{4} - \frac{R^2 r^2}{2} - \frac{S^2 r^2}{4} + \frac{5}{16} r^4 \\ \left[ \mathcal{J}_4 \right]_S^R &= \frac{(R^2 - S^2)^2}{4 \log(R/S)} + \frac{S^4}{4} \log \frac{R}{S} - \frac{(R^2 - S^2)(3R^2 + 7S^2)}{16} \\ &= -2.07 \times 10^{-4} \end{aligned}$$

# The magnetic fields produced by uniformly magnetized ellipsoids of revolution

By H. J. PEAKE, M.A., M.Sc., and N. DAVY, D.Sc., The University, Nottingham

[Paper received 16 February, 1953]

Expressions are obtained for the field produced by a uniformly magnetized ellipsoid of revolution with a given intensity of magnetization at external points on its axes of symmetry. The formulae are stated in a form suitable for arithmetical calculation. Tables and graphs are provided.

Various experimenters measuring the magnetic fields produced by uniformly magnetized ellipsoids of ferromagnetic material have found the need for theoretical values of such fields for purposes of comparison with experiment.<sup>(1, 2)</sup> Values of the fields at external points on the axes of symmetry of ellipsoids of revolution would seem to be particularly useful in this connexion.

## METHOD

The method employed is due to Poisson.<sup>(3)</sup> Consider the ellipsoid  $x^2/a^2 + y^2/b^2 + z^2/c^2 = 1$ , possessing a uniform volume density  $m$  of positive magnetic charge. Since gravitational and magnetic attraction both enjoy the inverse-square law, Ivory's theorem concerning the attraction of a homogeneous solid ellipsoid at an external point<sup>(4)</sup> may be applied to the problem under consideration. Consequently, if,

$$A = 2\pi abc \int_0^\infty du / [(a^2 + u)^3(b^2 + u)(c^2 + u)]^{\frac{1}{2}}$$

and similar expressions for  $B$  and  $C$ , the field  $F_1$  at an external point  $P$ , co-ordinates  $(x_1, y_1, z_1)$  is given by

$$F_1 = (mabc/a_1b_1c_1)(A_1x_1, B_1y_1, C_1z_1)$$

where  $a_1, b_1, c_1$ , are the semi-axes of the confocal ellipsoid which passes through  $P$ , and  $A_1, B_1, C_1$  are the same functions of  $a_1, b_1, c_1$ , as  $A, B, C$  are of  $a, b, c$ . Similarly, the field  $F_2$  produced at  $P$  by an equal ellipsoid, centre at  $(-k, 0, 0)$ , and axes parallel to the first, possessing a uniform volume density  $-m$ , is given by,

$$F_2 = -(mabc/a_2b_2c_2)[A_2(x_1 + k), B_2y_1, C_2z_1]$$

where  $a_2, b_2, c_2, A_2, B_2, C_2$ , are defined with reference to the confocal ellipsoid centre  $(-k, 0, 0)$ , through  $P$ . By superposition, the field produced by a uniformly magnetized ellipsoid at  $P$  is the limit of  $F_1 + F_2$  as  $k \rightarrow 0$ , subject to the condition that  $mk$  remains constant, equal to  $I$  say, the intensity of magnetization in the positive direction of  $OX$ .

## PROLATE SPHEROID

The field produced by a uniformly magnetized prolate spheroid at external points on its axes. In this case,  $a > b = c$ . If  $e$  is the eccentricity of the generating ellipse,  $a^2e^2 = a^2 - b^2 = a_1^2 - b_1^2 = a_1^2e_1^2$ ,  $B = C$ .

Points on the equatorial plane at a distance  $z_1$  from the centre.

$P$  has co-ordinates  $(0, 0, z_1)$ ,  $b_1 = z_1$ ,  $a_1^2 = a^2e^2 + z_1^2$ .

Since  $k^2/a_2^2 + z_1^2/b_2^2 = 1$ , and  $k^2$  may be neglected,  $z_1 = b_2$ . Consequently,  $A_1 = A_2$  and  $B_1 = B_2 = C_1 = C_2$ , giving

$$F = -(mab^2/a_1b_1^2)(A_1k, 0, 0) \quad (1)$$

It can be shown that

$$A_1 = 4\pi b_1^2 \left( \frac{1}{2} \ln \frac{1 + e_1}{1 - e_1} - e_1 \right) / a_1^2 e_1^3$$

On substituting  $ae$  and  $ae/(a^2e^2 + z_1^2)^{\frac{1}{2}}$  for  $a_1e_1$  and  $e_1$  respectively, and  $I$  for  $mk$ , we obtain

$$F = -4\pi I(1 - e^2)/e^3 \left[ \frac{-ae}{(a^2e^2 + z_1^2)^{\frac{1}{2}}} + \frac{1}{2} \ln \frac{(z_1^2 + a^2e^2)^{\frac{1}{2}} + ae}{(z_1^2 + a^2e^2)^{\frac{1}{2}} - ae} \right] \quad (2)$$

parallel to  $OX$ , the direction of magnetization.

Points on the magnetic axis at a distance  $x_1$  from the centre.

$P$  has co-ordinates  $(x_1, 0, 0)$ ,  $a_2 = x_1 + k$ ,  $a_1 = x_1$ , so that  $b_2^2 = a_2^2 - a^2e^2 = (x_1 + k)^2 - a^2e^2$  and  $e_2 = ae/(x_1 + k)$ . Consequently,

$$A_2/a_2b_2^2 = (4\pi/a_2^3e_2^2) \left[ \left( \frac{1}{2e_2} \right) \ln \left( \frac{1 + e_2}{1 - e_2} \right) - 1 \right] \\ = (4\pi/a^2e^2) \left[ (\frac{1}{2}ae) \ln \left( \frac{x_1 + k + ae}{x_1 + k - ae} \right) - 1/(x_1 + k) \right]$$

Now

$$F_1 + F_2 = mab^2[x_1A_1/a_1b_1^2 - (x_1 + k)A_2/a_2b_2^2, 0, 0] \quad (3) \\ = 2\pi ma(1 - e^2)/e^2 \left\{ \left( \frac{x_1}{ae} \right) \ln \left( \frac{x_1 + ae}{x_1 - ae} \right) \right. \\ \left. - [(x_1 + k)/ae] \ln \left( \frac{x_1 + ae + k}{x_1 - ae + k} \right) \right\}$$

parallel to  $OX$ .

Since  $k/(x_1 - ae) < 1$ , ( $k$  is small), we may replace the logarithm in the expression

$$(x_1 + k)/ae \{ \ln [1 + k/(x_1 + ae)] - \ln [1 + k/(x_1 - ae)] \}$$

by the appropriate power series, giving  $-2kx_1/(x_1^2 - a^2e^2) + O(k^2)$ .

Whence,

$$F = 4\pi I(1 - e^2)/e^3 \left\{ aex_1/(x_1^2 - a^2e^2) \right. \\ \left. - \frac{1}{2} \ln [(x_1 + ae)/(x_1 - ae)] \right\} \quad (4)$$

parallel to the direction of magnetization.

## OBLATE SPHEROID

The field produced by a uniformly magnetized oblate spheroid at external points on its axes.

In this case,  $a < b = c$ ,  $b^2e^2 = b^2 - a^2$ , etc.,

$$A = 4\pi/e^2 \left\{ 1 - [(1 - e^2)^{\frac{1}{2}}/e] \tan^{-1} [e/(1 - e^2)^{\frac{1}{2}}] \right\}$$

Points on the equatorial plane.

$$b_1 = z_1, a_1^2 = z_1^2 - b^2 e^2, e_1 = be/z_1$$

Using equation (1) which is still applicable, we have

$$F = 4\pi I(1 - e^2)^{3/2} [\sin^{-1}(be/z_1) - be/(z_1^2 - b^2 e^2)^{1/2}] \quad (5)$$

parallel to the direction of magnetization.

Points on the magnetic axis.

$$a_2 = x_1 + k, b_2 e_2 = be$$

so that

$$A_2/a_2 b_2^2 = 4\pi/a_2 b^2 e^2 [1 - (a_2/be) \tan^{-1}(be/a_2)]$$

$$\begin{aligned} F_1 + F_2 &= 4\pi ma/e^2 \left\{ [(x_1 + k)/be] \tan^{-1} [be/(x_1 + k)] \right. \\ &\quad \left. - (x_1/be) \tan^{-1}(be/x_1) \right\} \\ &= 4\pi ma/e^2 \left\{ (k/be) \tan^{-1}(be/x_1) \right. \\ &\quad \left. - [(x_1 + k)/be] \tan^{-1} [kbe/(x_1^2 + b^2 e^2 + x_1 k)] \right\} \end{aligned}$$

parallel to  $OX$ .

Since  $kbe/(x_1^2 + b^2 e^2 + x_1 k) < 1$  we may replace the second inverse function by a power series. After some reduction the second term becomes  $kx_1/(x_1^2 + b^2 e^2) + O(k^2)$ . Whence,

$$F = 4\pi I(1 - e^2)^{3/2} [\tan^{-1}(be/x_1) - bex_1/(x_1^2 + b^2 e^2)] \quad (6)$$

parallel to the direction of magnetization.

#### SPHERE

By considering the value of  $F$  when  $e \rightarrow 0$ , the field produced by a uniformly magnetized sphere may be deduced. It can be shown that formulae (2), (5) and (4), (6) reduce to

$$F = -\frac{4}{3}\pi Ia^3/z_1^3 \text{ and } 2\frac{4}{3}\pi Ia^3/x_1^3$$

respectively. Both forces are parallel to the direction of magnetization. These are well-known results.

#### CALCULATION OF THE FIELD STRENGTH

To facilitate calculation the variable  $\theta$  defined below is introduced and the eccentricity  $e$  replaced by the appropriate expression involving the semi-axes  $a$  and  $b$ . The formulae become:

##### (i) Prolate spheroid

Points on equatorial plane  $\theta = z_1/ae > 0$ .

$$F = -4\pi Iab^2/(a^2 - b^2)^{3/2} \left[ \frac{1}{2} \ln \frac{(1 + \theta^2)^{1/2} + 1}{(1 + \theta^2)^{1/2} - 1} - 1/(1 + \theta^2)^{1/2} \right] \quad (7)$$

Points on magnetic axis  $\theta = x_1/ae > 1$ .

$$F = 4\pi Iab^2/(a^2 - b^2)^{3/2} \left[ \theta/(\theta^2 - 1) - \frac{1}{2} \ln \frac{\theta + 1}{\theta - 1} \right] \quad (8)$$

##### Prolate spheroid

Table 1. Points on equatorial plane. Formula (7)

$\theta$	0.2	0.4	0.6	0.8	1.0	1.2	1.4	1.6	1.8	2.0	3.0
$10^2 \Phi$	133.19	71.857	42.630	26.672	17.427	11.843	8.3092	6.0145	4.4700	3.3998	1.1222
$\theta$	4	5	6	7	8	9	10	15	20	25	30
$10^4 \Phi$	49.308	25.740	15.055	9.5429	6.4178	4.5222	3.3036	0.98997	0.4157	0.2130	0.1233

##### (ii) Oblate spheroid

Points on equatorial plane  $\theta = z_1/be > 1$

$$F = -4\pi Iab^2/(b^2 - a^2)^{3/2} [1/(\theta^2 - 1)^{1/2} - \sin^{-1}(1/\theta)] \quad (9)$$

Points on magnetic axis  $\theta = x_1/be > 0$ .

$$F = 4\pi Iab^2/(b^2 - a^2)^{3/2} [\cot^{-1} \theta - \theta/(\theta^2 + 1)] \quad (10)$$

$F$  being parallel to the direction of magnetization in each case.

Denote  $F(a^2 \sim b^2)^{3/2}/4\pi Iab^2$  by  $\Phi$

The values of  $\Phi$  for given values of  $\theta$  tabulated below were obtained by means of seven-figure tables and the appropriate power series for  $\theta > 7$ .

Since  $\theta$  and  $\Phi$  are proportional to  $x_1$  (or  $z_1$ ), and the force  $F$  respectively, the graphs indicate the form of  $F(x_1)$ , or  $F(z_1)$ .

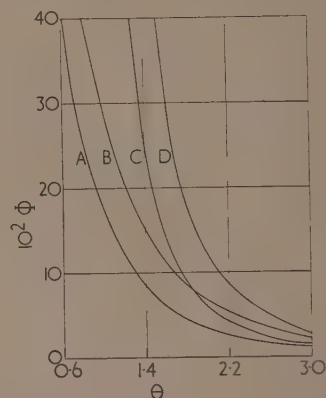


Fig. 1. Graph of  $10^2 \Phi/\theta$  for  $0.6 < \theta < 3.0$

A, prolate, equatorial plane; B, oblate, magnetic axis; C, oblate, equatorial plane; D, prolate, magnetic axis.

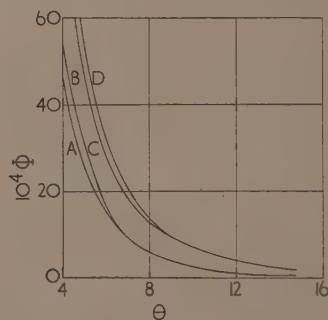


Fig. 2. Graph of  $10^4 \Phi/\theta$  for  $4 < \theta < 16$



## Prolate spheroid (continued)

Table 2. Points on magnetic axis. Formula (8)

$\theta$	1.2	1.4	1.6	1.8	2.0	2.2	2.4	2.6	2.8	3.0	4.0
$10^2\Phi$	152.83	56.245	29.247	17.719	11.736	8.2502	6.0550	4.5924	3.5750	2.8426	1.1254
$\theta$	5	6	7	8	9	10	15	20	25	30	35
$10^4\Phi$	56.01	31.93	19.92	13.27	9.282	6.748	1.986	0.8358	0.4275	0.2472	0.2335

## Oblate spheroid

Table 3. Points on equatorial plane. Formula (9)

$\theta$	1.2	1.4	1.6	1.8	2.0	2.2	2.4	2.6	2.8	3.0	4.0
$10^2\Phi$	52.245	22.502	12.551	7.9122	5.3751	3.8449	2.8574	2.1875	1.8607	1.3717	0.5519
$\theta$	5	6	7	8	9	10	15	20	25	30	35
$10^4\Phi$	27.68	15.83	9.9000	6.6033	4.6238	3.3636	0.9916	0.4169	0.2136	0.1236	0.0778

Table 4. Points on magnetic axis. Formula (10)

$\theta$	0.2	0.4	0.6	0.8	1.0	1.2	1.4	1.6	1.8	2.0	3.0
$10^2\Phi$	118.11	84.546	58.920	40.825	28.540	20.294	14.728	10.916	8.257	6.365	2.175
$\theta$	4	5	6	7	8	9	10	15	20	25	30
$10^4\Phi$	96.85	50.88	29.86	18.97	12.78	9.011	6.588	1.961	0.8308	0.4255	0.2466

FORMULAE FOR  $\Phi$  WHEN  $\theta$  IS LARGE

Convenient power series for  $\Phi$  are as follows:

## (i) Prolate spheroid

Equatorial plane

$$\Phi = -(\frac{1}{3}t^3 + \frac{1}{5}t^5 + \frac{1}{7}t^7 + \dots) \text{ where } t^2 = 1/(1 + \theta^2)$$

Magnetic axis

$$\Phi = 2(\frac{1}{3}t^3 + \frac{2}{5}t^5 + \frac{3}{7}t^7 + \dots) \text{ where } t = 1/\theta$$

## (ii) Oblate spheroid

Equatorial plane

$$\Phi = -(\frac{1}{3}t^3 - \frac{1}{5}t^5 + \frac{1}{7}t^7 - \dots) \text{ where } t^2 = 1/(\theta^2 - 1)$$

Magnetic axis

$$\Phi = 2(\frac{1}{3}t^3 - \frac{2}{5}t^5 + \frac{3}{7}t^7 - \dots) \text{ where } t = 1/\theta$$

It is found that provided  $\theta \geq 20$ , the first term in the series gives  $10^4\Phi$  correct to the three significant figures. Conse-

quently the following formulae give  $10^4\Phi$  correct to three significant figures when  $\theta \geq 20$ .

## Prolate spheroid

$$\text{Equatorial plane } \Phi = -\frac{1}{3}(\theta^2 + 1)^{3/2} \quad \theta = z_1/ae$$

$$\text{Magnetic axis } \Phi = \frac{2}{3}\theta^3 \quad \theta = x_1/ae$$

## Oblate spheroid

$$\text{Equatorial plane } \Phi = -\frac{1}{3}(\theta^2 - 1)^{3/2} \quad \theta = z_1/be$$

$$\text{Magnetic axis } \Phi = \frac{2}{3}\theta^3 \quad \theta = x_1/be$$

## REFERENCES

- (1) STREET, R., WOOLLEY, J. C., and SMITH, P. B. *Proc. Phys. Soc., Lond. B*, **65**, p. 679 (1952).
- (2) TEBBLE, R. S., WOOD, J. E., and FLORENTIN, J. J. *Proc. Phys. Soc., Lond. B*, **65**, p. 858 (1952).
- (3) POISSON, S. D. *Journal de l'Ecole Polytechnique*, **13**, (1835).
- (4) IVORY, J. *Phil. Trans. Roy. Soc. A*, I, p. 345 (1809).

# The linear piezoelectric equations of state

By R. BECHMANN, Ph.D., Post Office Research Station, Dollis Hill, London

[Paper received 4 February, 1953]

The different forms of the linear piezoelectric equations of state obtained from the various combinations of the two elastic (stress, strain) with the three electric quantities (field, displacement and polarization) are given in a table. In order to show the similarities of the various piezoelectric constants more clearly, the three groups of piezoelectric moduli (piezoelectric stress constants) usually expressed as  $e, h, a$  are denoted respectively by  $e^E, e^D, e^P$  and the piezoelectric coefficients (piezoelectric strain constants)  $d, g, b$  are expressed by  $d^E, d^D, d^P$ . The superscripts refer to the electric quantity,  $E, D$  or  $P$ , held constant for the direct piezoelectric effect or to the applied electric quantity for the converse effect.

The phenomenological theory of piezoelectricity is based on thermodynamic principles and the fundamental physical properties of crystals can be described by equations of state.<sup>(1-4)</sup> The equations of state are usually derived from thermodynamic potentials which are a necessary consequence of the principle of conservation of energy, but they can also be obtained directly from this principle. Recently Haskins and Hickman<sup>(5)</sup> have derived the linear piezoelectric equations of state by the latter method and have tabulated these equations.

The elastic properties are expressed in terms of the relationships between the second-order symmetric tensors of stress  $T_\lambda$  and strain  $S_\lambda$ . The electric properties are expressed by the relationships between the vectors of the electric field  $E_l$ , the electric displacement  $D_l$  or the polarization  $P_l$ . The thermal properties are described by the scalars of temperature  $\theta$  and entropy  $\sigma$ . In the notation used here (see ref. 4) subscripts numbered from 1 to 6 will be represented by Greek letters, indicating a second-order tensor and those numbered from 1 to 3, by Roman letters indicating a vector. In thermodynamics a distinction is made between intensive parameters,  $i$ , and extensive parameters,  $e$ . Intensive parameters are generalized forces, and extensive parameters are generalized displacements, related to the unit volume of the body. Generalized forces are stress, electric field, temperature; and the corresponding generalized displacements are, respectively, strain, electric displacement or polarization, change of entropy. Constants defined by  $\partial i/\partial e$  are called moduli and those by  $\partial e/\partial i$  are coefficients.

The piezoelectric effect is described by relationships between

the second-order tensors and the vectors, the thermoelastic effect by the relations between tensors and scalars and the pyroelectric effect by relations between the vectors and scalars.

For the present purpose, in all relationships, one of the thermal scalars is taken as constant and only the elastic and electric properties are considered; thermal phenomena are ignored. All the constants discussed here will be either adiabatic (at constant entropy) or isothermal (at constant temperature) dependent on which thermal conditions are assumed. Quadratic and higher-order terms in the equations of state will be neglected. The fundamental linear piezoelectric equations for any piezoelectric crystal can be given in twelve different forms, dependent on which of the two elastic or three electric quantities are taken as independent variables and which taken as dependent variables. Each form consists of a set of nine equations, comprising a group of six elastic equations (corresponding to  $\lambda = 1 \dots 6$ ) together with three electric equations taken from either of two alternative groups of electric equations (corresponding to  $l = 1$  to 3). In addition there is, for each set, a thermal equation giving the change in temperature or in entropy, as a function of the corresponding independent variable for constant entropy or constant temperature respectively. In all cases these thermal equations are omitted here.

In Table 1 each of the six rows represents one group of elastic equations together with their appropriate alternative groups of electric equations shown in columns (a) and (b), respectively, making twelve sets in all. In the most general case of a crystal of the triclinic hemihedral class with no

Table 1. Linear piezoelectric equations of state

$$\delta_{lm} \begin{cases} = 1 \text{ for equal indices } (l = m) \\ = 0 \text{ for different indices } (l \neq m) \end{cases}$$

	Elastic equations (converse piezoelectric effect)	Electric equations (direct piezoelectric effect)	
		a	b
1	$T_\lambda = \Sigma c_{\lambda\mu}^E S_\mu - \Sigma e_{\lambda m}^E E_m$	$D_l = 4\pi \Sigma e_{l\mu}^E S_\mu + \Sigma \epsilon_{lm}^S E_m$	$P_l = \Sigma e_{l\mu}^E S_\mu + \Sigma \chi_{lm}^S E_m$
2	$T_\lambda = \Sigma c_{\lambda\mu}^D S_\mu - \frac{1}{4\pi} \Sigma e_{m\lambda}^D D_m$	$E_l = - \Sigma e_{l\mu}^D S_\mu + \Sigma \beta_{lm}^S D_m$	$P_l = \frac{1}{4\pi} \Sigma e_{l\mu}^D S_\mu + \frac{1}{4\pi} \Sigma (\delta_{lm} - \beta_{lm}^S) D_m$
3	$T_\lambda = \Sigma c_{\lambda\mu}^P S_\mu - \Sigma e_{m\lambda}^P P_m$	$E_l = - \Sigma e_{l\mu}^P S_\mu + \Sigma \chi_{lm}^S P_m$	$D_l = - \Sigma e_{l\mu}^P S_\mu + \Sigma (\chi_{lm}^S + 4\pi \delta_{lm}) P_m$
4	$S_\lambda = \Sigma s_{\lambda\mu}^E T_\mu + \Sigma d_{\lambda m}^E E_m$	$D_l = 4\pi \Sigma d_{l\mu}^E T_\mu + \Sigma \epsilon_{lm}^T E_m$	$P_l = \Sigma d_{l\mu}^E T_\mu + \Sigma \eta_{lm}^T E_m$
5	$S_\lambda = \Sigma s_{\lambda\mu}^D T_\mu + \frac{1}{4\pi} \Sigma d_{m\lambda}^D D_m$	$E_l = - \Sigma d_{l\mu}^D T_\mu + \Sigma \beta_{lm}^T D_m$	$P_l = \frac{1}{4\pi} \Sigma d_{l\mu}^D T_\mu + \frac{1}{4\pi} \Sigma (\delta_{lm} - \beta_{lm}^T) D_m$
6	$S_\lambda = \Sigma s_{\lambda\mu}^P T_\mu + \Sigma d_{m\lambda}^P P_m$	$E_l = - \Sigma d_{l\mu}^P T_\mu + \Sigma \chi_{lm}^T P_m$	$D_l = \Sigma d_{l\mu}^P T_\mu + \Sigma (\chi_{lm}^T + 4\pi \delta_{lm}) P_m$

Table 2. Elastic, electric quantities and constants and their dimensions

Term	Definition	Symbol	Dimensions			C.G.S. units	Rationalized M.K.S. units	Conversion factor Rationalized M.K.S./C.G.S.	Order in C.G.S. units	
			cm	g	sec					
Elastic quantity	Stress	$T_{\lambda}$	-1	1	-2	dyne $cm^{-2}$	$Nm^{-2}$	$10^{-1}$		
	Strain	$S_{\lambda}$	—	—	—	$cm\ cm^{-1}$	$m\ m^{-1}$	1		
Electric quantity	Field	$E_l$	$-\frac{1}{2}$	$\frac{1}{2}$	-1		volt. $m^{-1}$	$3 \cdot 10^4$		
	Displacement	$D_l$	$-\frac{1}{2}$	$\frac{1}{2}$	-1		coulomb. $m^{-2}$	$\frac{1}{12\pi} \cdot 10^{-5}$		
	Polarization	$P_l$	$-\frac{1}{2}$	$\frac{1}{2}$	-1		coulomb. $m^{-2}$	$\frac{1}{3} \cdot 10^{-5}$		
Elastic constants	Elastic modulus, el. stiffness	$\frac{\partial T_{\lambda}}{\partial S_{\mu}}$	$c_{\lambda\mu}$	-1	1	-2	dyne $cm^{-2}$	$Nm^{-2}$	$10^{-1}$	$10^{10}$
	Elastic coefficient, el. compliance	$\frac{\partial S_{\lambda}}{\partial T_{\mu}}$	$s_{\lambda\mu}$	1	-1	2	$cm^2\ dyne^{-1}$	$m^2N^{-1}$	10	$10^{-13}$
Electric constants	Dielectric impermeability	$\frac{\partial E_l}{\partial D_m}$	$\beta_{lm}$	0	0	0		$mF^{-1}$	$36 \cdot \pi \cdot 10^9$	
	Reciprocal susceptibility	$\frac{\partial E_l}{\partial P_m}$	$\chi_{lm}$	0	0	0			$\frac{1}{4\pi}$	
	Dielectric permit- tivity (Dielectric constant)	$\frac{\partial D_l}{\partial E_m}$	$\epsilon_{lm}$	0	0	0		$Fm^{-1}$	$\frac{1}{36\pi} \cdot 10^{-9}$	
	Dielectric susceptibility	$\frac{\partial P_l}{\partial E_m}$	$\eta_{lm}$	0	0	0			$4\pi$	
Piezo- electric constants	Piezoelectric modulus, p.e. stress coefficient	$e_{l\mu} = -\frac{\partial T_{\mu}}{\partial E_l}^S = \frac{1}{4\pi} \frac{\partial D_l}{\partial S_{\mu}}^E = \frac{\partial P_l}{\partial S_{\mu}}^E$	$e_{l\mu}^E$	$-\frac{1}{2}$	$\frac{1}{2}$	-1	dyne.e.s.u. $^{-1}$ (e.s.u. $cm^{-2}$ )	$Nm^{-1}V^{-1}, Cm^{-2}$	$\frac{1}{3} \cdot 10^{-5}$	$10^4$
		$h_{l\mu} = -4\pi \frac{\partial T_{\mu}}{\partial D_l}^S = -\frac{\partial E_l}{\partial S_{\mu}}^D = 4\pi \frac{\partial P_l}{\partial S_{\mu}}^D$	$e_{l\mu}^D$	$-\frac{1}{2}$	$\frac{1}{2}$	-1	dyne.e.s.u. $^{-1}$ (e.s.u. $cm^{-2}$ )	$NC^{-1}, Vm^{-1}, [Cm^{-2}]$	$3 \cdot 10^4$	$10^4$
		$a_{l\mu} = -\frac{\partial T_{\mu}}{\partial P_l}^S = -\frac{\partial E_l}{\partial S_{\mu}}^P = -\frac{\partial D_l}{\partial S_{\mu}}^P$	$e_{l\mu}^P$	$-\frac{1}{2}$	$\frac{1}{2}$	-1	dyne.e.s.u. $^{-1}$ (e.s.u. $cm^{-2}$ )	$NC^{-1}, Vm^{-1}, [Cm^{-2}]$	$3 \cdot 10^4$	$10^4$
	Piezoelectric coefficient, p.e. strain coefficient	$d_{l\mu} = \frac{\partial S_{\mu}}{\partial E_l}^T = \frac{1}{4\pi} \frac{\partial D_l}{\partial T_{\mu}}^E = \frac{\partial P_l}{\partial T_{\mu}}^E$	$d_{l\mu}^E$	$\frac{1}{2}$	$-\frac{1}{2}$	1	$cm^2\ e.s.u.^{-1}$ (e.s.u. $dyne^{-1}$ )	$mV^{-1}, CN^{-1}$	$\frac{1}{3} \cdot 10^{-4}$	$10^{-8}$
		$g_{l\mu} = 4\pi \frac{\partial S_{\mu}}{\partial D_l}^T = -\frac{\partial E_l}{\partial T_{\mu}}^D = 4\pi \frac{\partial P_l}{\partial T_{\mu}}^D$	$d_{l\mu}^D$	$\frac{1}{2}$	$-\frac{1}{2}$	1	$cm^2\ e.s.u.^{-1}$ (e.s.u. $dyne^{-1}$ )	$m^2C^{-1}, VmN^{-1}, [CN^{-1}]$	$3 \cdot 10^5$	$10^{-8}$
		$b_{l\mu} = \frac{\partial S_{\mu}}{\partial P_l}^T = -\frac{\partial E_l}{\partial T_{\mu}}^P = -\frac{\partial D_l}{\partial T_{\mu}}^P$	$d_{l\mu}^P$	$\frac{1}{2}$	$-\frac{1}{2}$	1	$cm^2\ e.s.u.^{-1}$ (e.s.u. $dyne^{-1}$ )	$m^2C^{-1}, VmN^{-1}, [CN^{-1}]$	$3 \cdot 10^5$	$10^{-8}$



symmetry, the dependent variables are related to the independent by twenty-one elastic, eighteen piezoelectric and six dielectric constants. The number of constants reduces with increasing crystal symmetry.

Using the usual notation, the superscripts  $E$ ,  $D$ ,  $P$  in the elastic constants and  $T$ ,  $S$  in the dielectric constants in Table 1 designate the boundary conditions and refer to quantities kept constant. For example,  $s^E$  are the isagrig elastic coefficients when the electric field is constant or zero. In order to show the similarities of the various piezoelectric constants more clearly, the three groups of piezoelectric moduli (piezoelectric stress constants) usually expressed as  $e_{l\mu}$ ,  $h_{l\mu}$ ,  $a_{l\mu}$  are denoted here respectively by  $e_{l\mu}^E$ ,  $e_{l\mu}^D$ ,  $e_{l\mu}^P$  and the piezoelectric

are homogeneous while the electric variables are inhomogeneous and in all cases are extensive parameters. When the sets of equations are mixed the definitions of moduli and coefficients given above do not necessarily hold, but the piezoelectric stress constants are always moduli and the piezoelectric strain constants always coefficients.

The elastic and electric quantities and all the constants as partial derivatives of these quantities are listed in Table 2, together with their dimensions and their units in the C.G.S. and rationalized M.K.S. system. The constants in the first half of each set are moduli and those in the second half are coefficients. The relationships between the different moduli and coefficients are given in Table 3. This table gives a further

Table 3. Relations between crystal constants

$$\delta_{lm}, \delta_{\lambda\mu} \begin{cases} = 1 \text{ for equal indices} \\ = 0 \text{ for different indices} \end{cases}$$

$$\Sigma s_{\lambda\tau}^{\dagger} c_{l\tau}^{\dagger} = \delta_{\lambda\mu}; \Sigma \beta_{lt}^* \epsilon_{mt}^* = \delta_{lm}; \Sigma \chi_{lt}^* \eta_{mt}^* = \delta_{lm} \\ (\dagger = E, D \text{ or } P; * = S \text{ or } T)$$

$$e_{m\lambda}^{\dagger} = \Sigma d_{m\tau}^{\dagger} c_{l\tau}^{\dagger}$$

$$d_{m\lambda}^{\dagger} = \Sigma e_{m\tau}^{\dagger} c_{l\tau}^{\dagger}$$

$$e_{m\lambda}^E = \frac{1}{4\pi} \Sigma \epsilon_{lm}^S e_{l\lambda}^D = \Sigma \eta_{lm}^S e_{l\lambda}^P$$

$$d_{m\lambda}^E = \frac{1}{4\pi} \Sigma \epsilon_{lm}^T d_{l\lambda}^D = \Sigma \eta_{lm}^T d_{l\lambda}^P$$

$$e_{m\lambda}^D = 4\pi \Sigma \beta_{lm}^S e_{l\lambda}^E = \Sigma (\delta_{lm} - \beta_{lm}^S) e_{l\lambda}^P$$

$$d_{m\lambda}^D = 4\pi \Sigma \beta_{lm}^T d_{l\lambda}^E = \Sigma (\delta_{lm} - \beta_{lm}^T) d_{l\lambda}^P$$

$$e_{m\lambda}^P = \Sigma \chi_{lm}^S e_{l\lambda}^E = \Sigma \left( \frac{1}{4\pi} \chi_{lm}^T + \delta_{lm} \right) e_{l\lambda}^D$$

$$d_{m\lambda}^P = \Sigma \chi_{lm}^T d_{l\lambda}^E = \Sigma \left( \frac{1}{4\pi} \chi_{lm}^S + \delta_{lm} \right) d_{l\lambda}^D$$

$$c_{\lambda\mu}^D - c_{\lambda\mu}^E = \Sigma e_{l\lambda}^D e_{l\mu}^E$$

$$s_{\lambda\mu}^D - s_{\lambda\mu}^E = - \Sigma d_{l\lambda}^D d_{l\mu}^E$$

$$c_{\lambda\mu}^P - c_{\lambda\mu}^E = \Sigma e_{l\lambda}^P e_{l\mu}^E$$

$$s_{\lambda\mu}^P - s_{\lambda\mu}^E = - \Sigma d_{l\lambda}^P d_{l\mu}^E$$

$$c_{\lambda\mu}^P - c_{\lambda\mu}^D = \frac{1}{4\pi} \Sigma e_{l\lambda}^P e_{l\mu}^D$$

$$s_{\lambda\mu}^P - s_{\lambda\mu}^D = - \frac{1}{4\pi} \Sigma d_{l\lambda}^P d_{l\mu}^D$$

$$\beta_{lm}^S - \beta_{lm}^T = \frac{1}{4\pi} \Sigma e_{l\tau}^D d_{m\tau}^D = \frac{1}{4\pi} \Sigma e_{m\tau}^D d_{l\tau}^D$$

$$\epsilon_{lm}^S - \epsilon_{lm}^T = - 4\pi \Sigma e_{l\tau}^E d_{m\tau}^E = - 4\pi \Sigma e_{m\tau}^E d_{l\tau}^E$$

$$\chi_{lm}^S - \chi_{lm}^T = \Sigma e_{l\tau}^P d_{m\tau}^P = \Sigma e_{m\tau}^P d_{l\tau}^P$$

$$\eta_{lm}^S - \eta_{lm}^T = - \Sigma e_{l\tau}^E d_{m\tau}^E = - \Sigma e_{m\tau}^E d_{l\tau}^E$$

coefficients (piezoelectric strain constants)  $d_{l\mu}$ ,  $g_{l\mu}$ ,  $b_{l\mu}$  are denoted by  $d_{l\mu}^E$ ,  $d_{l\mu}^D$ ,  $d_{l\mu}^P$ . In these cases, owing to the alternative definitions for the piezoelectric constants, the superscripts  $E$ ,  $D$ ,  $P$  indicate respectively that the electric field, displacement or polarization are held constant for the direct piezoelectric effect but, for the converse effect, although the values of these constants are identical with those for constant field, etc., they are actually defined as stress and strain constants for an applied electric field, etc.

A set of linear equations is called homogeneous if its independent variables are extensive and its dependent variables intensive or *vice versa*. When the independent and dependent variables are each a mixture of intensive and extensive parameters, the sets of equations are called mixed. In the following sentence, "equations (1a), (1b), etc.," mean the appropriate equation in the first column of Table 1 combined with the corresponding equation (a) or (b) in this line. Equations (2a), (3a), (4a), (4b) in Table 1 are homogeneous, equations (1a), (1b), (5a), (6a) are mixed but individually the elastic and electric variables are homogeneous. Equations (2b), (3b), (5b), (6b) are also mixed and the elastic variables

illustration of the advantages of the notation for the piezoelectric moduli and coefficients introduced in the above equations.

#### ACKNOWLEDGEMENT

Acknowledgement is made to the Engineer-in-Chief of the General Post Office for permission to make use of the information contained in this paper.

#### REFERENCES

- (1) CADY, W. G. *Piezoelectricity* (New York: McGraw-Hill Publishing Co. Inc., 1946).
- (2) MASON, W. P. *Bell Syst. Tech. J.*, **26**, p. 80 (1947).
- (3) MASON, W. P. *Piezoelectric Crystals and their Application to Ultrasonics* (New York: D. van Nostrand Inc., 1950).
- (4) I.R.E. Standards on piezoelectric crystals, *Proc. Instn Radio Engrs*, **37**, p. 1378 (1949).
- (5) HASKINS, J. F., and HICKMAN, J. S. *J. Acoust. Soc. Amer.*, **22**, p. 584 (1950).

# The stresses in the reels of cold reduction mills

By R. B. SIMS, B.Sc., A.M.I.Mech.E., A.Inst.P.,\* and J. A. PLACE, B.Sc., A.Inst.P.,† Rolling Mill Laboratories, The British Iron and Steel Research Association, London, W.1

[Paper received 23 January, 1953]

An investigation into the stress distribution in the reels of a cold reduction mill is described. The results indicated that the distribution is nearly axially symmetrical, and it was concluded that Inglis's theory of wire winding might be adapted to give a reasonable approximation of the stresses over the surface of a reel drum in the form of a thick-walled tube. This has been confirmed by the direct measurement of tangential stress in the lap of a coil next to the reel.

In the cold rolling of metals in the form of thin wide strip, it is usual to pay off the coiled material from a reel on one side of the mill, and re-coil it under a heavy tension on a second reel after its passage through the rolls. The arrangement of the reels in a modern mill is shown in Fig. 1. As the material builds up it exerts an increasing radial stress on the reel drum, which occasionally causes bending and fracture of the components. One of the difficulties in designing reels for a given duty arises from the fact that there is no established

and the displacement of the laps relative to each other was measured with a travelling microscope as the applied tension was varied. The results are given in Table 1. The coil was re-formed to an outer radius of 8 in. at a tension of 0.96 t, and a line scribed across the laps as before. The coil was then increased in radius to 9 in. No relative movement between the inner laps was observed when the position of the line was checked by the travelling microscope.

Table 1. Relative displacement of coil laps under tension

Test No.	Lap No.	Tension (tons) increasing				Tension decreasing		
		0.96	1.60	2.24	3.09	2.24	1.60	0.96
		Displacement of scribed line (mm)						
1	1	0	0.31	0.62	0.79	0.78	0.75	0.63
	2	0	0.04	0.09	0.09	0.08	0.08	0.09
	3	0	0	0	0	0	0	0
2	1	0	0.32	0.58	0.89	0.84	0.78	0.68
	2	0	0	0	0.07	0.05	0.08	0.09
	3	0	0	0	0	0	0	0

These experiments indicate that there is no relative movement of the inner laps of the coil as the tension on the strip is varied, or when they are overlaid by additional laps under tension. It seems reasonable to assume that the stress distribution within the coil approaches axial symmetry, although it is obvious from the field of force external to the coil and reel that the distribution cannot be exactly symmetrical. The stresses due to external forces are small, however, compared with those due to the applied tension.

An estimation may be made of the coefficient of friction,  $\mu$ , between the laps of the coil from the results in Table 1. It may be shown that when the thickness of the strip ( $h$ ) is small and the radius of curvature of the laps ( $r$ ) is such that  $2r \gg \mu h$ , the tension change in the strip approximates to the simple relationship

$$t = t_0 \exp [-\mu \theta]$$

where  $t_0$  is the applied tension stress,  $t$  is the stress at the point with co-ordinates  $r, \theta$  and  $\theta = 0$  when the strip is tangential to the coil. The strain displacement in the first lap is then

$$\xi = \int_0^{2\pi} \frac{rt_0}{E} \exp(\mu\theta) d\theta = \frac{rt_0}{\mu E} [1 - \exp(-2\pi\mu)]$$

and the coefficient of friction has been calculated in Table 2 from the change in strain displacement with increasing tension, assuming the changes are negligible in the second lap.

Equation (1) cannot be applied to the change in strain displacement when the applied tension is reduced, since the sign of the frictional forces between the laps of the coil cannot be determined accurately. It will be noticed, however, from



Fig. 1. Reel of a modern wide strip mill

method of calculating the stress distribution in the reels and coils. In the present investigation, stress has been measured in a coil wound on a simplified design of reel drum and compared with the theoretical value in an attempt to determine the reliability of methods for calculating the reel loading. [The experiments were carried out on the mill of the British Iron and Steel Research Association.]

## PRELIMINARY EXPERIMENTS

A coil of prestrained mild steel 0.050 in. thick and 3.50 in. wide was formed on the reel of the mill under a constant tension of 0.96 ton. The inner coil radius was 5 in. and the outer radius 9 in. A line was scribed radially on one side of the coil close to the point where the strip was tangential to it,

\* Now at Davy and United Engineering Co. Ltd.

† Now at British Nylon Spinners Ltd.

the results in Table 1, that the observed movement between the laps of coil is much less on unloading, and indicates a much higher coefficient of friction.

Table 2. Coefficient of function between laps of coil

Test No.	Lap No.	Change in tension from 0.96 ton (tons)			
		0	+0.64	+1.28	+2.13
Change in strain displacement (in.)					
1	1	0	0.0120	0.0120	0.0093
2	1	0	0.0124	0.0115	0.0110
Coefficient of rubbing friction					
1	1	—	0.08	0.08	0.16
2	1	—	0.07	0.10	0.13

#### EQUATIONS TO THE DISTRIBUTION OF STRESS WITHIN THE COIL

The general solution in polar co-ordinates to an axially symmetrical distribution of stress in one plane for a tube is

$$\begin{aligned}\sigma_r &= +A/r^2 + 2c \\ \sigma_\theta &= -A/r^2 + 2c\end{aligned}\quad (2)$$

where  $\sigma_r$  and  $\sigma_\theta$  are the radial and tangential stresses respectively, with  $A$  and  $C$  as constants determined by the boundary conditions. Compressive stresses are written with a positive sign. These equations may be applied to the present problem by assuming that the reel and coil behave as a homogeneous tube. The stresses in the laps of the coil may then be found by superimposing the tensile stress in the strip on the stresses in the composite tube. This assumption was made by C. E. Inglis\* in his theory of the wire-winding of guns, and from his solution it may be shown that at any radius  $r_3$  in the coil shown in Fig. 2, the radial stress  $S_r$  and the tangential stress  $S_\theta$  are given by the relationships

$$S_r = \frac{t_0}{2}(1 - w_b^2) \ln \left( \frac{w_a^2 - w_b^2}{1 - w_b^2} \right) \quad (3)$$

$$S_\theta = -\frac{t_0}{2} \left[ 2 - (1 + w_b^2) \ln \left( \frac{w_a^2 - w_b^2}{1 - w_b^2} \right) \right] \quad (4)$$

where  $t_0$  is the applied tensile stress,  $w_a = r_2/r_3$  and  $w_b = r_1/r_3$ . In practice,  $r_3$  is made the inner radius of the coil and then

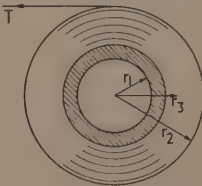


Fig. 2. Assumed geometry of simplified reel

$w_b$  is the ratio of the inner and outer radii of the reel drum and  $w_a$  is the ratio of coil build-up. The value of  $S_r$  calculated from equation (3) is then the radial stress on the surface of the reel. Solutions of equations (3) and (4) are given in Figs. 3 and 4.

\* These equations were given to the authors in a private communication from C. E. Inglis. They have been published by J. Case in his book *Strength of Materials*, p. 454 (Arnold, 1938).

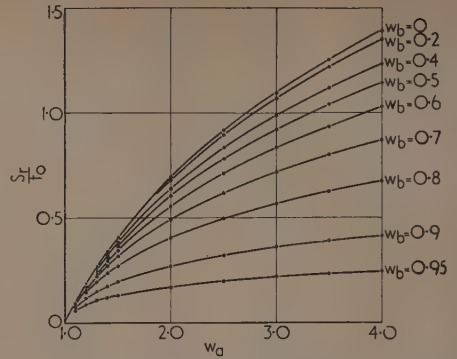


Fig. 3. Radial stress versus coil build-up for various values of reel wall thickness

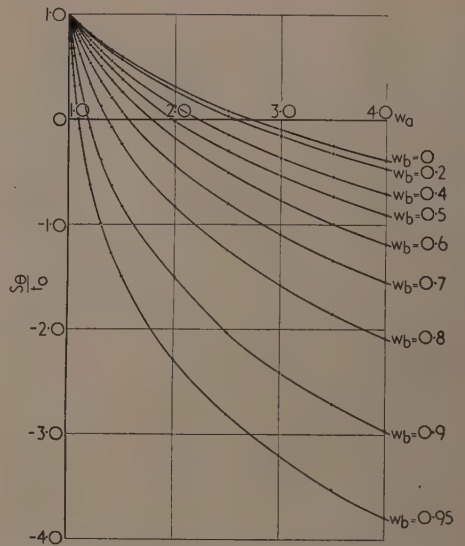


Fig. 4. Tangential stress on reel versus coil build-up for various values of reel wall thickness

#### EXPERIMENTAL MEASUREMENT OF THE TANGENTIAL STRESS IN A COIL

The validity of these equations was demonstrated by a direct measurement of the tangential stress,  $S_\theta$ . A coil of strain hardened 1.3% carbon steel strip 3 in. wide, 0.018 in. thick and 500 ft in length was used for the experiment. Its thickness and yield strength were chosen so that only elastic deformation occurred on bending to a radius of curvature of 5 in. under the tensions used in the experiments. Eight electric resistance strain (e.r.s.) gauges were bonded to the material at 75 in. from the end of the strip attached to the reel of the mill. Four of these gauges were bonded to the upper surface and four to the lower surface, and of each four, two were arranged longitudinally and two transversely. The eight gauges were wired to form a Wheatstone bridge as shown in Fig. 5. To prevent damage to the gauges when the strip was taken up on the coiler drum the lap containing the bridge



was sandwiched between two strips of 0.063 in. thick copper on which were apertures coinciding with the gauge areas. The gauges and copper shields are illustrated in Fig. 6. The positioning of the shields was quite critical, and an experiment

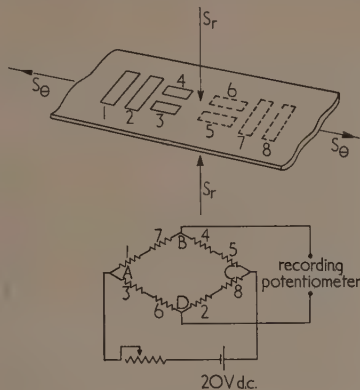


Fig. 5. Arrangement of strain gauge bridge to measure  $S_\theta$



Fig. 6. Strain gauge bridge with shields in position

was abandoned if the apertures in either shield did not locate correctly.

The construction of the simplified reel drum is shown in Fig. 7. The end of the strip was entered in the slot and packing pieces inserted to close the gap and make the outer wall of the drum effectively a hollow cylinder. A maximum tension force of 1.4 t was available from the electric drive of the mill and this was measured to within  $\pm 2\%$  by a torque sensitive network of e.r.s. gauges bonded to the driving shaft of the reel. As the coil radius increased it was measured by a follower and rheostat arranged to divide the output (torque) of the e.r.s. network by the coil radius, and so indicate directly the tension in the strip.

An experiment was begun by lubricating the strip with oleic acid and setting the automatic controls of the mill to the desired tension. The coil was built up continuously on the reel with the output of the e.r.s. gauge bridge on the strip

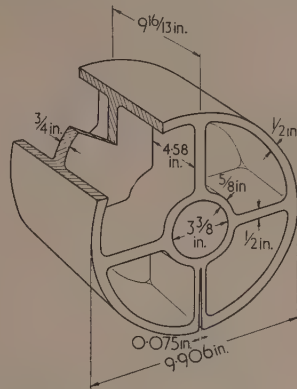


Fig. 7. Section of simplified reel used for experiments

indicated on a recording potentiometer, until the bridge became short-circuited. This occurred quite suddenly due to the penetration, under the heavy radial stresses, of the laps of the coil through the apertures in the shields. The e.r.s. gauges forming the network on the strip were matched in resistance and almost insensitive to lateral strains. With the arrangement adopted, the bridge is compensated fully for temperature and for the bending of the strip. It will now be shown that it is also insensitive to the radial stress.

If  $V_{AB}$  and  $V_{AD}$  are the p.d.'s between the points  $AB$  and  $AD$  of the network shown in Fig. 5 and  $V_N$  is the applied p.d. then

$$V_{AB} = V_N \left( \frac{2R + \Delta R_1 + \Delta R_7}{4R + \Delta R_1 + \Delta R_4 + \Delta R_5 + \Delta R_7} \right)$$

$$V_{AD} = V_N \left( \frac{2R + \Delta R_3 + \Delta R_6}{4R + \Delta R_2 + \Delta R_3 + \Delta R_6 + \Delta R_8} \right)$$

where  $\Delta R_1 \dots \Delta R_8$  are the changes in resistances of gauges 1 to 8, each of resistance  $R$ . The p.d. across the terminals  $BD$  is

$$V_{BD} = V_N (\Delta R_3 + \Delta R_6 - \Delta R_1 - \Delta R_7) / 4R$$

since the changes in the resistances are small and may be neglected in the numerator with an error of less than 0.1%. If  $E$  is the modulus of elasticity and  $\lambda$  Poisson's ratio for the strip material,  $\epsilon_1$  denotes strain due to  $S_0$  and  $\epsilon_2$  strain due to  $S_r$  and  $\nu$  is the gauge factor, then

$$\Delta R_1 / R = \Delta R_7 / R = \nu \lambda (\epsilon_2 - \epsilon_1)$$

$$\Delta R_3 / R = \Delta R_6 / R = \nu (\epsilon_1 - \lambda \epsilon_2)$$

and

$$V_{BD} = (V_N \nu S_0 / 2E) (1 + \lambda)$$

and the bridge output is insensitive to the radial stress. The output of the bridge is linear, and a calibration is shown in Fig. 8.

## RESULTS

It has been mentioned that the position of the copper shields over the e.r.s. gauge network was critical and a reliable reading of  $S_0$  from the bridge output could not be

obtained until the first  $2\frac{1}{2}$  laps had been formed and the shields properly adjusted. This value is denoted by  $S'_0$  and in Fig. 9 the experimental results are shown for a number of

The scatter in the experimental results, although relatively large, is not unreasonable in view of the experimental difficulties involved in working with heavily stressed insulation and with e.r.s. gauges at large strains.

## DISCUSSION

The value of  $S_0/S'_0$  at any value of coil build-up on the reel is independent of the applied tension stress. A mean line through the results corresponds to a value of  $w_b = 0.91$  whilst the actual value for the outer shell of the reel is 0.9. It may be concluded, therefore, that the assumptions made in Inglis's theory are reasonable and the stress on the reel drum may be calculated from equation (3). It is of interest to note that the struts inside the drum have little influence on the value of  $w_b$ . It might be assumed that since the struts are intended to stiffen the outer shell, they would reduce the effective value of  $w_b$ . This effect was observed only when the reel was a close fit on its shaft; so that during an experiment the radial stress exerted by the strip caused the bearing to grip the shaft. In the experiments described above a clearance of 0.030 in. was machined between the shaft and bearing to avoid random errors from this cause.

These experiments have been made with a drum which is effectively a thin-walled tube. Modern designs for reels are far removed from this simple shape, particularly the types in which the diameter may be decreased to facilitate the removal of the coil. Until experiments can be made with reels of contemporary design, it is suggested that mill engineers should stress their components using limiting values of the radial stress  $S_r$  at the surface of the drum calculated for reel drums in the form of thick tubes in which the stresses can be shown to be greater and less than the actual design. In this connexion it is of interest to note that as the thickness of the reel drum is decreased (i.e.  $w_b$  approaches 1) the value of  $S_r$  also decreases so that the loading on the mechanism within the drum is lessened. At the same time the stress  $S_0$  becomes compressive for quite small values of the build-up ratio, and may lead to kinking of the laps within a coil of thin material when it is ejected from the reel.

Finally it should be mentioned that the experiments described in this paper took no account of the thermal contraction of the coil of strip. In high-speed strip mills, the coil is wound on to the reel when at a temperature between 100 and 250° C, and when the rolling takes several minutes to complete the contraction of the coil on to the colder drum may be appreciable. The magnitude of this contraction and the resulting stress can only be assessed after a study of the proposed duty of the mill and the delays which may occur in rolling, but it is suggested that the effect, which has not received close attention hitherto, may be of considerable magnitude.

## ACKNOWLEDGEMENTS

This paper is published with the permission of the Director and Council of the British Iron and Steel Research Association. The authors acknowledge with thanks the gift of the coil of high carbon steel from Samuel Fox and Co., Ltd., Sheffield, and the assistance of their colleagues at the Rolling Mill Laboratories in carrying out the experiments.

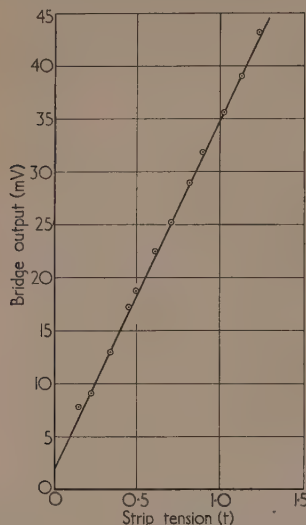


Fig. 8. Calibration of strain gauge bridge measuring  $S_0$

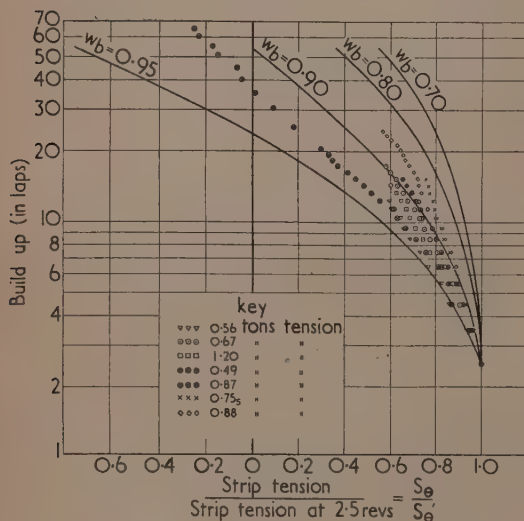


Fig. 9. Measured values of  $S_0$  as a function of build up

experiments as the ratio  $S_0/S'_0$ , thus avoiding calibration errors. The solution of equation (4) is also given in Fig. 9 in terms of  $S_0/S'_0$  versus build up of coil.

# The measurement of radioactive carbon in gas counters

By A. F. HENSON, M.Sc., F.Inst.P., Imperial Chemical Industries Ltd., Butterwick Research Laboratories,  
The Frythe, Welwyn, Herts

[Paper received 3 February, 1953]

An a.c. coupled quench circuit is used to quench counters containing non-self-quenching carbon dioxide-carbon disulphide mixtures for the measurement of radioactive carbon as carbon dioxide. The counters operate reliably at quite high counting rates and continuous discharges do not occur. Plateaux 200 V or more long with slopes of about 2 to 4% per 100 V are obtained. Accurate corrections for resolving time loss can be made for counting rates up to at least 15 000 counts/min.

The method of measurement of the activity of radioactive carbon,  $C^{14}$ , by means of gaseous samples is well known<sup>(1,2)</sup> but not widely used. The carbon in the material to be assayed is converted to carbon dioxide which is then transferred into a suitable Geiger counter together with a small amount of carbon disulphide vapour. The method has several advantages over the use of solid samples: the efficiency is high; "geometry" is fixed; self-absorption in the sample does not occur; sample preparation is simple, and after preparation there is no possibility of exchange with atmospheric carbon dioxide. The carbon dioxide-carbon disulphide mixture is not self-quenching, so that an external quenching unit of some kind is required. The most commonly used quenching circuit is that due to Neher and Harper,<sup>(3)</sup> which gives very good plateaux with carbon dioxide-carbon disulphide counters. Its main disadvantage is that its resolving time is long (of the order of 2 or 3 msec) and resolving time loss becomes appreciable at quite low counting rates. Correction for this loss can be made if the resolving time is known accurately, but with the Neher-Harper circuit this time is not constant. After quenching, the potential of the counter anode recovers exponentially, and the anode is therefore at an intermediate potential between threshold and full operating potential for an appreciable length of time. A discharge initiated while the potential is thus recovering will produce an abnormally small pulse in the counter, and as the length of the quench pulse varies with the size of the initial pulse, this small pulse will be followed by an abnormally short resolving time. The higher the counting rate the more probable is the occurrence of a count while the anode potential is recovering from a previous count: therefore the effective resolving time will decrease with increasing counting rate. The resolving time also varies with the height of the anode potential above threshold and with the grid bias on the quenching valve. For accurate work with this circuit counting rates must be restricted to less than about 4000 counts/min, a restriction which is rather troublesome. In this laboratory a commercially available quenching unit has been used, which, with slight modification, has proved very satisfactory for this purpose, permitting relatively high counting rates with accurate correction for resolving time.

A desirable quench circuit would rapidly lower the anode potential below the threshold of the counter, hold it there for a fixed period, then rapidly restore it to its operating value, so that it is at an intermediate value for an infinitesimal time; i.e. it would apply a negative square pulse of known length to the counter anode. A circuit which almost fulfils the requirements has been devised by Cooke-Yarborough and others.<sup>(4)</sup> It is intended for the improvement of the characteristics of self-quenching counters and provides a negative square quenching pulse of some 200 V amplitude, and of a predetermined length which is independent of the valve

characteristics and of size of input pulse. The circuit is commercially available (Probe Unit Type 1014 in the A.E.R.E. range of instruments for radioactivity measurements) and has the advantage of being made to work in conjunction with, and draw its power supplies from the scaling units in the same range of instruments. Its chief disadvantage for this work appeared to be that it is coupled to the counter anode through a condenser, and if for any reason the counter went into smooth discharge the circuit would be unable to quench it. The alternative of d.c. coupling has the disadvantage that the whole circuit must operate at the high voltage of the counter anode, in which case power supplies are difficult; alternatively the counter must be operated with the cathode at high negative potential, which is inconvenient because of the difficulties of mounting and insulating the counter and decoupling and shielding the cathode from stray pick-up. Such a d.c. coupled square pulse quench unit has been used by Mann and Parkinson.<sup>(5)</sup> The a.c. coupled Type 1014 would be expected to quench a non-self-quenching counter satisfactorily except when a discharge occurred within a few microseconds after the end of a quench pulse. At this time the voltage on the counter has risen above threshold but the circuit has not recovered its normal sensitivity and cannot be triggered. If the counter then went into a smooth discharge it would not be quenched. Cooke-Yarborough<sup>(6)</sup> suggests the use of an auxiliary "flip-flop" circuit with a period slightly longer than the period following a quench pulse during which the circuit is insensitive. This auxiliary circuit is triggered by every pulse from the counter and generates a pulse, say, 10  $\mu$ sec later which triggers the quench circuit if it has not already been triggered. However such a device does not seem to be necessary with carbon dioxide-carbon disulphide counters. Consideration of the mechanism of the Geiger discharge indicates the probability that the continuous discharge will not be really smooth, but is more likely to consist of a continuous series of individual discharges each giving a small voltage pulse. The Type 1014 unit, having an input sensitivity of about 0.2 V, apparently responds to these pulses, and a counter which goes into continuous discharge during the insensitive period is quenched as soon as the circuit recovers. A first trial showed that the unit did operate to give a short plateau with a carbon dioxide-carbon disulphide filled counter. With the applied voltage higher than the end of the plateau the counter went into continuous discharge, but the individual discharges were sufficient to trigger the quenching unit, which then continued to operate at a high rate.

## THE BEHAVIOUR OF COUNTERS WITH AN A.C. COUPLED QUENCHING UNIT

An investigation has been carried out to find the conditions for reliable counting of radioactive carbon dioxide with this



equipment. The constructional details of the standard counters used are as follows: the cathode is a polished graphite\* layer on the inside of the glass envelope, length 11.5 cm, diameter 1.9 cm. A backing layer of silver such as used by Brown and Miller<sup>(1)</sup> is not necessary. The anode is a molybdenum wire 0.05 mm diameter, effective length 10 cm defined at the ends by 2 mm diameter glass sheaths. It is found that a coating of graphite, connected to the cathode, on the outside of those parts of the glass walls which are not coated internally improves the stability of the tubes, presumably by inhibiting the building up of static charges on the internal exposed glass surfaces. The counters are fitted with a tap, a B10 cone for attachment to the filling line, and a small side tube into which the carbon dioxide and carbon disulphide are condensed when filling. The volumes of the counters are about 40 ml, of which the sensitive volume is estimated to be about 75%. A few other counters of different cathode diameters and volumes have also been used.

In an attempt to improve the results with the Type 1014 probe the effects of increasing the quench pulse height and length were tried. The pulse height was increased by increasing the anode supply voltage of the quenching valve. (Valve  $V_2$  in the circuit diagram in the paper by Cooke-Yarborough and others.<sup>(4)</sup>) An increase in this voltage of 120 V increased the pulse height by 100 V and the plateau length by about 50 V. This feature has therefore been retained. It is conveniently effected by disconnecting the resistor  $R_5$  from the + h.t. line and returning it *via* the spare lead in the 6-core connecting cable to a socket on the back of the scaling unit. A 120 V dry battery is then connected between this socket and the + h.t. socket. The drain on the battery is small, and it may be left permanently connected. It should be replaced when its voltage drops below 110 V.

A 56 pF condenser was connected in parallel with the variable condenser  $C_3$  permitting the generation of longer pulses than is possible with the unmodified probe unit. The results of a series of experiments with fillings covering a range of pressures of carbon dioxide from 2 cm to 60 cm of mercury and activities giving counting rates up to 15000 counts/min can be summarized as follows. For a given counter, with a given filling pressure and activity, a quench time that is too short produces a plateau which is very poor or non-existent. As the quench time is increased there is a fairly sudden improvement when a minimum quench time is reached. Increase in quench time beyond this minimum does not further improve the plateau to any great extent. Three counters, with cathode diameters of 1.35 cm, 1.9 cm and 3.3 cm, each filled with 17.5 cm pressure of carbon dioxide and 2 cm pressure of carbon disulphide had minimum quench times of 150  $\mu$ sec, 500  $\mu$ sec and 1250  $\mu$ sec respectively, for a counting rate of about 3000 counts/min. These times are, very approximately, directly proportional to the squares of the cathode diameters, which is what would be expected if this minimum quench time represents the time taken for the ion sheath to move out to the cathode. The variation of minimum quench time with carbon dioxide pressure (carbon disulphide pressure constant) is not rapid. For example, with a standard counter at a counting rate of about 3000 counts/min, it varied from 450  $\mu$ sec at 10 cm pressure of carbon dioxide to 650  $\mu$ sec at 46 cm pressure. This variation is probably comparable with the variation in the mobility of the carbon disulphide positive ions in the mixture. However, the simple view that the minimum quench time is equal to, or slightly larger than the transit time of the ions

requires some modification in view of the fact that at higher counting rates a longer quench time is found to be necessary. This effect is more marked with high pressures of carbon dioxide in the counter. The point has not been pursued. It is possible that the charge transfer from carbon dioxide to carbon disulphide ions is not complete and there is still a small probability of the production of negative carbon dioxide ions at the cathode.

For routine use the quenching pulse characteristics have been standardized at a height of 320 V and duration of 1500  $\mu$ sec. With the standard counter under these conditions plateau lengths of at least 200 V are normally obtainable with active fillings giving (corrected) counting rates up to 15000 counts/min and at carbon dioxide pressures up to 60 cm. As a precaution, however, at high counting rates the carbon dioxide pressure is usually restricted to less than 30 cm. The slopes of the plateaux are about 2 to 4% per 100 V. The quench time is long but the design of the circuit is such that the time remains constant over long periods and is independent of counting rate and size of pulse from the Geiger tube. It is therefore possible to make accurate correction for resolving time. The resolving time was measured with a calibrated double pulse generator. Correction is made using the expression

$$N = n/(1 - nt)$$

where  $N$  is the counting rate corrected for resolving time losses,  $n$  is the observed rate and  $t$  the resolving time. The accuracy of the correction is illustrated by the results obtained during the intercomparison of nineteen counters. Measured amounts of active carbon dioxide were introduced into the counters, the counting rate determined, corrected for resolving time and background, and the activity of the gas in terms of counts/min  $\times$  millimole carbon dioxide calculated. The corrected counting rates covered the range up to 9000 counts/min. The number of "counts" recorded in each case was approximately 40000 and the number of determinations per counter varied between 3 and 6 (average 4.2). The coefficient of variation was calculated for the values for each counter, and found to vary from 0.2% to 1.3% for the nineteen counters, with an average value of 0.8%. The correction has been shown to be accurate up to corrected rates of 15000 counts/min (observed rate approximately 11000 counts/min). When higher rates than this are expected a known fraction of the sample is taken. This can be done easily and accurately in a suitable set of calibrated volumes on the filling line. Thus when assaying material of high specific activity (approximately  $3 \times 10^7$  counts/min  $\times$  mg) samples of about 1 mg were weighed and oxidized to carbon dioxide. This was diluted with inactive carbon dioxide and a known fraction taken twice in succession, the final fraction being about  $10^{-4}$  of the original. In this way four determinations were made and had a coefficient of variation of 1%.

The counters will continue to operate satisfactorily at higher observed rates than 11000 counts/min, but there is evidence that the rate tends to be a little higher than it should, possibly due to the occurrence of spurious counts. On numerous occasions samples giving corrected rates up to 26000 counts/min have been used (approximately 16000 counts/min observed). Subsequent determinations of known fractions have shown these values to be up to 5% high. The highest rate which has been observed is 26900 counts/min, which gives approximately 82000 counts/min when corrected. Subsequent determinations with smaller samples showed this value to be about 16% too high. The plateau at this high rate was at least 60 V long; its full length was not investigated.

\* Acheson Colloids Ltd. Product 660B.

In the absence of a calibrated double pulse generator an alternative and possibly preferable method of measuring the resolving time would be to make up a supply of carbon dioxide of suitable specific activity, fill accurately measured amounts into a counter and observe the counting rates. These rates should then be plotted against amount of active carbon dioxide. Substitution of the co-ordinates of suitable pairs of points on the curve (restricted to rates below 11 000 counts/min) in the expression

$$m = k[n/(1 - nt) - b]$$

will enable  $t$  to be calculated. ( $m$  is the amount of carbon dioxide in convenient units such as millimoles,  $b$  is the measured background counting rate of the counter and  $k$  is a constant.) This method might permit more accurate corrections to rates higher than 11 000 counts/min if the experimental calibrations were extended into this range. Using the value of  $t$  the points on the curve in the lower, reliable range can be corrected for resolving time loss, and a straight line drawn (the line of initial slope of the curve) showing the relation between amount of carbon dioxide and corrected counting rate. The correction to be applied to high rates could then be determined graphically by noting the difference between the experimentally determined curve and the straight line at a value of  $m$  corresponding to the observed counting rate. The correction is thus experimentally determined, and includes the effects of spurious counts and would be accurate providing the ratio of spurious counts to true counts is constant at a given observed counting rate.

Experiment has shown that for a given amount of active carbon dioxide in the counter, the observed counting rate is independent of the total pressure of carbon dioxide. The addition of inactive carbon dioxide does not alter the rate, but merely raises the operating voltage. The highest pressure of carbon dioxide which can be accommodated in a standard counter without raising the operating voltage above the 4 kV maximum of the high voltage supply in use is about 60 cm. This pressure corresponds to a filling of about 1.3 millimoles of carbon dioxide. The pressure of carbon disulphide vapour may also be varied over a range at least from 0.5 cm to 4 cm without affecting the performance of the counter. 2 cm pressure is normally used in all fillings. A slightly modified version of the mercury cut-off described by Honig<sup>(7)</sup> has been found useful for controlling the carbon disulphide vapour.

#### ROUTINE USE OF THE METHOD

This method of gas counting has now been in routine use for the measurement of radioactive carbon in biological samples for more than a year, during which time it has proved very satisfactory. Samples of animal tissue, excreta, etc., weighing from a few milligrams up to 160 mg have been used. They are oxidized by a method based on that due to Van Slyke and others<sup>(8)</sup> (to be described elsewhere) and the resulting carbon dioxide transferred, without measurement, to a counter together with the requisite amount of carbon disulphide vapour. After allowing half an hour for the contents of the counter to warm to room temperature and to mix thoroughly, the counter characteristics are rapidly determined to find the start of the plateau and to ensure that it is at least 100 V long. The voltage on the counter is then set to 60 V above the start of the plateau and counts recorded for sufficient time to give the required statistical accuracy. An alternative procedure would be to add sufficient inactive carbon dioxide to bring each filling to a standard pressure which would mean that all counting could be done at the

same counter voltage. However, more time would be taken in measuring both the active and inactive carbon dioxide than in determining the plateau for each filling. In this connexion mention may be made of brief experiments with alcohol vapour instead of carbon disulphide as the charge transfer gas in the fillings.<sup>(9)</sup> Alcohol is easier to handle in the vacuum system than carbon disulphide, but such fillings give an extremely slow rise to the plateau, an effect which would be very troublesome with the present method since many readings would be required to find the start of the plateau. Such a filling would probably be satisfactory with the method using a standard pressure of carbon dioxide. The present method has the additional advantage that the nature of the plateau is a good indication of the behaviour of the counter: contamination with air or other undesirable materials causes a slow rise to a plateau of high slope.

The background counting rates of the counters in a 3 cm thick lead shield, when filled with inactive carbon dioxide, are mostly between 30 and 40 counts/min. "Memory" effects due to adsorption are not normally troublesome and it is sufficient to determine the background rate of each tube, say, once every two weeks. Sometimes, however, after a highly active filling has been measured the background rate is raised by as much as 10 or 20 counts/min. A remedy for this is to evacuate the tube and bake it at 250 to 300° C for an hour (making suitable provision to protect the tap grease from the heat). At more infrequent intervals it is useful to bake the whole tube, open to air (after removing the grease from the tap), at 300° C for an hour. This is an even more effective means of reducing unusually high backgrounds to normal. It also removes the finely divided mercury and its compounds which are inevitably introduced into the tubes when condensing fillings with liquid nitrogen. It is probable that this material is mainly responsible for adsorption and "memory" effects. When measuring very low activity material greater precautions are taken. Each filling is allowed to stand at least 2 hours before measurement; the counter background is determined before each sample measurement; and both background and sample are counted for 40 min. Under these conditions, with the present equipment, the limit of detectability of sample activity is 3 counts/min.

An illustration of the reliability of this method of measurement of radioactive carbon is provided by the recovery of administered radioactivity in animal experiments. A known amount of active material is injected intraperitoneally into a rat, and the excreta collected until the animal is killed. After dissection, the various organs, the remaining carcass and the excreta are separately homogenized and assayed for radioactivity. On every occasion when there has been no known loss of (highly active) urine the total activity recovered represents 95 to 99% of the administered dose.

#### REFERENCES

- (1) BROWN and MILLER. *Rev. Sci. Instrum.*, **18**, p. 496 (1947).
- (2) EIDINOFF. *Anal. Chem.*, **22**, p. 529 (1950).
- (3) NEHER and HARPER. *Phys. Rev.*, **49**, p. 940 (1936).
- (4) COOKE-YARBOROUGH, FLORIDA and DAVEY. *J. Sci. Instrum.*, **26**, p. 124 (1949).
- (5) MANN and PARKINSON. *Rev. Sci. Instrum.*, **20**, p. 41 (1949).
- (6) COOKE-YARBOROUGH. *Nucleonics*, **6**, 2, p. 86 (1950).
- (7) HONIG. *Rev. Sci. Instrum.*, **21**, p. 1024 (1950).
- (8) VAN SLYKE, STEELE and PLAZIN. *J. Biol. Chem.*, **192**, p. 769 (1951).
- (9) LABEYRIE. *J. Phys. Radium*, **12**, p. 146 (1951).



# The effect of centring errors on the transmission of a sector disk

By A. F. A. HARPER, M.Sc., F.Inst.P., and A. J. MORTLOCK, M.Sc., A.Inst.P., Division of Physics, National Standards Laboratory, Commonwealth Scientific and Industrial Research Organization, Sydney, Australia

[Paper received 10 February, 1953]

Formulae are given for the transmission of rotating sector disks for which the edges of the sectors are not radial with respect to the centre of rotation of the disk. The cases considered include single-aperture disks for beams of various cross-sectional forms and multi-aperture disks for which the edges of the sectors are centred on the same and different points. The formulae indicate how errors due to lack of correct centring can be minimized by suitable construction of the disk.

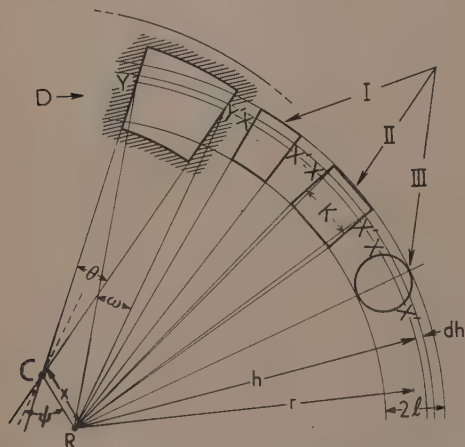
It is concluded that the errors likely to arise in practice will be negligible for all except single-aperture disks, and disks the apertures of which are not symmetrically placed about a common centre, or for the most precise work. Where significant the errors can be estimated with sufficient accuracy from the approximate formulae given. These conclusions have been confirmed by experimental test.

A rotating disk with one or more sector apertures is commonly used in photometry and in optical pyrometry as an achromatic filter of accurately known transmission. One important application is in the establishment and maintenance of the International Temperature Scale in the optical pyrometry range.

The purpose of this note is to discuss some of the errors which may arise from the construction, measurement and use of sector disks and to indicate the conditions in which the errors may be reduced or eliminated.

## TRANSMISSION OF A SINGLE-APERTURE DISK

In the figure is shown a single aperture, the edges of which, assumed to be straight, meet at an angle  $\theta$  at a point  $C$ , distant  $x$  from the centre  $R$  about which the disk is rotated. The line  $CR$  makes an angle  $\psi$  with the bisector of  $\theta$  through  $C$ . In the discussion which follows,  $\theta/2\pi$  will be termed the nominal transmission of the disk.



Geometrical relationship of sector disk aperture,  $D$ , and interrupted light beams.  $C$ , convergence point;  $R$ , rotational centre. The three basic light beam shapes are: I. sector; II. rectangular; III. circular

The actual transmission in the case postulated will depend not only on the parameters  $\theta$ ,  $x$  and  $\psi$ , but also on the form

of the cross-section of the beam of radiation interrupted by the disk. If the intensity of the beam is uniform across its section, the transmission  $A$  is given in all cases by

$$A = \int_{r-l}^{r+l} \frac{\omega}{2\pi} (\text{arc } XX') dh \int_{r-l}^{r+l} (\text{arc } XX') dh \quad (1)$$

where the arc  $XX'$  is the arc of radius  $h$  and centre  $R$  intercepted by the beam of radiation,  $\omega$  is the angle subtended at  $R$  by the arc  $YY'$  of radius  $h$  intercepted by the aperture, and  $2l$  and  $r$  are respectively the radial width of the beam and the distance of its centre from  $R$ . For beams of simple cross-section, and when  $l$  and  $x$  are each small compared with  $r$ , the transmission is given to a sufficient degree of approximation by

$$A = \frac{\theta}{2\pi} - \frac{x}{\pi r} \left( 1 + \frac{\alpha l^2 - \beta K^2}{r^2} \right) \sin \frac{\theta}{2} \cos \psi \quad (2)$$

where  $K$  is the circumferential width of the beam, and  $\alpha$  and  $\beta$  are constants, the values of which depend on the beam shape and are as follows:

Cross section of beam	$\alpha$	$\beta$
Rectangular	1/3	1/16
Sector	0	0
Circular	1/8	0

In the exact solution for  $A$  the next term in  $x$  is one of  $(x/r)^3$  multiplied by a factor which is small compared to unity. Alternatively, equation (2) may be expressed in the form

$$A = \frac{\theta}{2\pi} - \frac{y' + y''}{2\pi r} \left( 1 + \frac{\alpha l^2 - \beta K^2}{r^2} \right) \quad (3)$$

where  $y'$  and  $y''$  are the perpendicular distances from  $R$  to the lines defining the aperture edges,  $y$  being taken as positive when  $R$  and the aperture are on opposite sides of the edge.

For most purposes the term  $(\alpha l^2 - \beta K^2)/r^2$  may be neglected and this, in fact, will be done in the subsequent discussion.

Equation (2) shows that when  $\psi = \pi/2$  or  $3\pi/2$  the error in the nominal transmission is zero, and for  $\psi = 0$  or  $\pi$ , the error is a maximum, its fractional value being then

$$\left| \frac{\Delta A_{\max}}{A} \right| = \frac{2x}{\theta r} \sin \frac{\theta}{2}$$



If  $y''$  is put equal to zero, equation (3) gives the error caused by the misalignment of a single aperture edge with respect to the centre of rotation.

The transmission of a disk, as determined by angular measurements of the aperture with a divided circle, the centre of rotation of which is  $R$ , is equal to its actual transmission for rotation about this same point as centre. (For exact equality each of the individual angular measurements, the mean of which is taken, would need to be weighted in proportion to the amount of light contained in the beam at the particular radius to which the measurement pertains.) It is convenient to imagine a sector, the edges of which are directed through the point  $R$ , and which is of such an angle as to correspond to the transmission appropriate to rotation about  $R$ . It can be shown that, if the disk is now rotated about a centre other than  $R$ , say  $R'$ , the transmission obtained by the application of equations (2) or (3) to the imagined sector and that obtained by the application of these equations to the actual sector are the same, to the first order. The formulae may therefore serve as a basis for assessing the errors arising from lack of coincidence of any two of the convergence point  $C$ , the centre of angular measurement and the centre of rotation. In practice, the parameters  $x$  and  $\psi$  or the parameters  $y$  will not usually be known precisely, but estimates of the maximum errors may be made from estimates of these quantities, for single or for multi-aperture disks.

#### TRANSMISSION OF MULTI-APERTURE DISKS

If more than one aperture is used, then the departure of the transmission from its nominal value  $\sum \theta/2\pi$ , where  $n$  is the number of apertures, is given generally by

$$\Delta A = -\frac{1}{2\pi r} \sum_{i=1}^{i=n} (y'_i + y''_i) \quad (4)$$

If the angular apertures are equal and the edges have a common convergence point, the error is given by

$$\Delta A = -\frac{x}{\pi r} \sin \frac{\theta}{2} \sum_{i=1}^{i=n} \cos \psi_i \quad (5)$$

It follows immediately that a sufficient condition for zero error in this case is that the apertures be uniformly spaced around the disk with respect to the convergence point. An obvious corollary of this result, of application to the construction of a disk having an even number of apertures, is that if care is taken to ensure collinearity of the diametrically opposite sector edges then there will be no error due to lack of coincidence of the convergence point (or points), the centre about which the aperture angles are measured and the actual centre of rotation of the disk. In other words the physical transmission of the disk will equal the measured transmission independent of the relative disposition of these three points.

#### THE EFFECT OF SECTOR DISK ERRORS IN OPTICAL PYROMETRY

If the transmission of the sector disk be in error by  $\Delta A$ , then the resulting error  $\Delta T_2$  in a temperature  $T_2$ , determined

relative to a known lower temperature  $T_1$  by means of an optical pyrometer and the disk, will be given to a close approximation by:

$$\Delta T_2 = -\frac{\lambda T_2^2}{C_2} \frac{\Delta A}{A} \quad (6)$$

where  $\lambda$  is the wavelength of the radiation in terms of which the measurement was made and  $C_2$  is Planck's second radiation constant ( $1.438 \text{ cm-degrees}$ ). For  $\lambda = 0.65 \times 10^{-5} \text{ cm}$ , the errors in the calculated temperatures due to a 1% error in the transmission of a disk at temperature 1000, 2000 and 3000° K are respectively 0.5, 1.8 and 4.0° K. An error of this magnitude could arise in the case of a single-aperture disk in which the edges met at a point distant 0.16 cm from the centre of rotation, the axis of the light beam being 15 cm from the centre of the disk.

If a double-aperture disk had been used and the corresponding edges arranged to be collinear, the errors would be quite negligible. If one aperture were now imagined to be rotated relative to the other through an angle of 0.05 radian, the maximum relative error in the transmission would be only 0.025%. Small departures from exact equality of aperture angle lead to errors of a similar order of magnitude; for a disk having apertures of 0.10 and 0.12 radian the maximum error would be 0.1%.

The above considerations show that for a reasonably well-made sector disk, which has been accurately measured, the centring errors will be significant only for work of the highest precision. For accurate work the advantage of using disks with an even number of apertures, corresponding edges of which can be made collinear with one another, is evident.

It should be noted that, in order to be able to apply the formulae given above to disks the apertures of which have irregular edges, it is sufficiently accurate to take the latter as being defined by mean lines on the basis of area. From the fact that no significant correction is necessary for beam shape it follows that non-uniformity of radiant intensity within the beam is also unimportant.

#### EXPERIMENTAL TEST

An experimental test of the main theoretical conclusions was made by one of the authors (A.J.M.) using an optical pyrometer sighted through a two-aperture sector disk on to a source operating at a fixed temperature. This disk could be rotated off-centre by a known amount either in the line of the apertures or perpendicular to that line. Tests were made with both apertures open and one covered.

It was found that the variation in apparent brightness was, in all cases, consistent with the formulae given.

#### ACKNOWLEDGEMENTS

The authors wish to express their thanks to Dr. G. H. Briggs who made a number of helpful suggestions relevant to the work, and to Miss M. Briggs for her assistance in the experimental test.

## New books

**Computing methods and the phase problem in X-ray crystal analysis.** By R. PEPINSKY. (Pennsylvania: State College.) Pp. 390. Price \$7.50.

The inherent difficulty in determining crystal structures can be stated in physical terms as follows. X-rays have a wavelength small enough, and can be diffracted through angles which are large enough, to satisfy the conditions for the resolution of atoms. There is, however, no way of causing the scattered X-rays to interfere to form an image of the diffracting object. Therefore we must record the diffraction pattern itself and try to reconstitute from it the required image. But in recording the diffraction pattern some vital information is lost—the relative phases of the diffracted rays. The problem of finding this lost information is known as the “phase problem.”

The present book is a report of a conference, held at Pennsylvania State College in April, 1950, at which various approaches to the solution of the problem were discussed by representatives from some of the leading laboratories in Europe and America; and since computational processes are intimately bound up with the problem, these also formed a large part of the discussion. In fact, the conference was occasioned, and its location decided, by the completion of the most ambitious computational project yet devised—the Pepinsky machine, which presents a complete two-dimensional Fourier synthesis instantaneously on the screen of a cathode-ray tube. About one third of the book is devoted to this instrument, and since this is the most detailed description so far published, the book is important for this alone.

The rest of the book contains papers by over twenty different contributors, and in the short space of this review it would be invidious to single out particular ones for mention. But the general scope can be described by dividing the papers into three groups—methods of computation, contributions to basic theory, and contributions to the art of deriving crystal structures.

In the first group are papers on punched-card machines, digital computers, optical-analogue methods, and certain new mechanical devices. Some of these are not published elsewhere.

This is also true of some of the theoretical papers, which form a group more complete than the other two, but at the same time less satisfying. It is more complete because in it are included some which present solutions to the phase problem; it is less satisfying because these solutions indicate that, even with existing computers, there seems to be little chance in practice of being able to carry out the necessary calculations. Nevertheless, it is valuable to have these papers collected together.

The papers on practical devices are perhaps the most immediately useful and invigorating. Several unpublished procedures are described, and the contributors have not been afraid to put forward new and imperfectly developed ideas, in the hope that they may germinate elsewhere.

Thus, on the whole, the publication of this book has been very much worth while. It is, however, a pity that it has been over two years in appearing, since certain subjects have, in the meantime, rather lost their topicality. Moreover, although one appreciates the immense work which has gone into the production of the book, an index would have made it still more useful. The covers, also, are unlikely to stand up to the

hard usage the book is likely to receive. These minor criticisms, however, should not be taken as diminishing the thanks which the crystallographic world owes to Professor Pepinsky for his part in calling the conference and in producing this report of it. H. LIPSON

**Niederdruck-Stromrichterventile.** By H. VON BERTELE. (Berlin: Springer-Verlag.) Pp. xii + 239. Price 66s. 6d.

The translation of the full title of this book is *Low pressure rectifier valves. An attempt to explain how mechanism and performance depend on their construction*. The author is an engineer of long standing experience who himself has made various contributions to this field. The book is largely an introduction to the subject and deals mainly with mercury pool rectifiers. It contains a section on the special requirements of the rectifier circuits, another on the mechanism of rectification and the physical principles involved; the methods of producing the initial ionization for starting and maintaining the discharge and its control are also discussed and another chapter is devoted to the construction and technical data of glass and metal rectifiers and their performance.

In reading the book one has the feeling that our knowledge of the processes in rectifiers is so scanty that it is really surprising that so much can be technically achieved with so little understanding of the underlying physics. There is for example the role of the cathode which is still an unsolved problem; the distribution of vapour density within the vessel and associated thermodynamic problems; de-ionization and backfire are other problems about which little is known.

The book provides a good general summary of published results though preference is given to data and publications from two continental firms in whose laboratories the author worked; a large number of illustrations showing the construction of rectifiers and subsidiary equipment are also given. There is an extensive treatment of the cooling of the various parts of the discharge. Finally the author makes a strong appeal for more fundamental research into rectification and conversion particularly for super-grid voltages, and for a study of the vacuum problems.

After the praise the criticism. An unusually large number of errors were noticed which we hope were not due to the proof readers! Here are some instances: the Maxwellian distribution (p. 33) should read  $\exp(-v^2/\omega^2)$ ; the symbols in the barometric equation 15 (p. 38) are wrongly defined and the units in 16 (p. 51) and 23 (p. 55) are wrong. In Poiseuille's equation (p. 177) the factor  $\pi$  is missing but makes an unwelcome appearance in the following equation. Other misprints are in the three equations on p. 163. Furthermore, effects whose origin is doubtful (p. 81), are treated as if they would be well established, others known for a long time are attributed to authors who happen to write about it. For example, the fact that the cathode spot on mercury extinguishes when suppressed for about  $10^{-8}$  sec was first published by W. Burstyn in 1924. The mean free electronic path in mercury vapour is not even approximately  $4\sqrt{2}$  times the gas kinetic one, neither at high nor at low energy. Practical and electrostatic units are often muddled (p. 56).

The involved style, even for one who is fluent in the language, makes the reading difficult. Nevertheless, this book will certainly be studied by electrical engineers as well as by

all those applied physicists who wish to learn more about the intricacies of this technical development.

A. VON ENGEL

**Superconductivity, 2nd edition.** By D. SHOENBERG. (London: Cambridge University Press.) Pp. x + 256. Price 30s.

When the second edition of a book is found to have grown to nearly three times its original size with a corresponding increase in price, one instinctively asks whether such a drastic change was necessary. In the case of Dr. Shoenberg's *Superconductivity* which has recently exchanged the modest grey paper cover of the Cambridge Physical Tracts for the handsome red binding of the Cambridge Monographs on Physics, the answer is emphatically "Yes." To say this is not to belittle the merits of the first edition; the growth of the subject and the more ambitious scope of the Monographs have combined to make such a large increase in the size of the book imperative.

The chapters describing the fundamental phenomena and the magnetic and thermodynamic properties of superconductors cover roughly the same ground as the corresponding chapters of the first edition, but they have been brought up to date and enlarged by the inclusion of topics previously omitted (e.g. thermal conductivity). The chapters on the structure of the intermediate state and on penetration effects have been rewritten and provide an excellent account of this important phase in the study of superconductivity. The chapter on theoretical aspects contains a lucid and full exposition of the Londons' phenomenological theory and its applications and also gives a short description of fundamental theories including the recent ones by Fröhlich and by Bardeen. The essential physical data of superconductors are assembled in an appendix and the book ends with a representative, if not comprehensive, bibliography.

Dr. Shoenberg's mastery of his subject, his wise and critical selection from the vast material and his faculty for clear exposition enabled him to achieve his self-imposed task of writing a book which could serve both as a general account and as a reference manual. There is no doubt that this monograph will be a trusted and indispensable companion to all interested in the fascinating phenomena of superconductivity.

N. KURTI

**The mathematical theory of non-uniform gases. 2nd edition.**

By S. CHAPMAN and T. G. COWLING. (London: Cambridge University Press.) Pp. xxiii + 431. Price 60s. (Notes added in 1951 can be obtained separately; pp. 392-431, price 5s.)

This book is a comprehensive treatment of the calculation of the transport of momentum, heat and molecular species in gases by kinetic theory, that is, by making various classical assumptions as to the properties of the molecules composing the gas. To assume that the molecules are rigid spheres is inadequate, and it is necessary to treat them as having forces between them which are more complex functions of distance. On the other hand the actual character of the molecule inside the closest distance that they can approach need not be specified so that the model can omit complexities of structure which must be postulated to explain total heat phenomena and interactions of the molecules with radiant energy. Even the asymmetry of polyatomic molecules can be largely neglected because the consequences of asymmetry almost disappear when averaged over a very large number of encounters.

The first ten chapters develop the various formulae for viscosity, thermal conductivity and diffusivity for models

based on the smooth rigid elastic spherical molecule, molecules repelling each other with a force  $K/r^v$ , attracting spheres, spheres attracting and repelling with different power laws, and rough elastic spheres. The next three chapters compare these formulae with experimental results or rather with the experimentally determined changes of the properties with temperature or concentration and the ratios between them because there is always at least one parameter (e.g. the radius of the sphere) which can be adjusted to fit at one value.

Corrections to the theories for the cases of very low and very high densities are dealt with but the latter cannot be extended to thermal conductivity of liquids. Then the classical treatment of fields of force is replaced by the quantum theory and this gives a greatly improved agreement with the observed values for the viscosity of hydrogen and helium at very low temperatures. The final chapter deals with movement of ions in gases.

This new edition of the book (the first edition came out in 1939) has been reprinted by offset-litho with slight corrections to the text, while a separate booklet contains notes extending the treatment for the viscosity of gases on the combined attractive-repulsive model for volume viscosity on the rough spherical model, for self-diffusion and thermodiffusion, and giving a new table of values for the thermal diffusion factor.

The book is a classic and must provide the most convenient survey for anyone who wants to see the very elegant development of simple theories to explain transport phenomena in gases.

M. W. THRING

**Photometry. 2nd edition.** By J. W. T. WALSH, O.B.E., M.A., D.Sc., M.I.E.E. (London: Constable and Co, Ltd.) Pp. xxiv + 544. Price 63s.

When this book was first published in 1926 it rapidly established itself as the standard work on photometry. Earlier books on this subject had never dealt fully with the physical laws on which the science of photometric apparatus design is based, nor adequately discussed the properties of the eye which must be appreciated if the results of measurements are to have practical interpretation of value.

The incidence of a second world war no doubt postponed a revision of this excellent book but it has thereby gained because of the rapidity with which photoelectric photometers and colorimeters have been developed under the stimulus of the commercial advances in the production of light-giving sources. These developments have been so rapid that the only criticism that could be sustained is that they have not been treated as fully as they deserve. The earnest student and the practising illuminating engineer will be driven to original literature, some of which finds a place in the very adequate list of references.

The word "photometry" suggests to most people a relatively small subject in a narrow field of utility, but the author has rightly expanded the book to cover the manifold and ever growing engineering activities by which human beings utilize the rapid advances in the production of light for their entertainment and comfort, as well as for increasing their efficiency during their hours of work.

The presentation of the book maintains the high standard adopted in the first edition but, of course, the price is quite high.

It may be of interest to consider whether in revising books of this quality that some of the older matter should be omitted in order to deal more adequately with modern developments without further addition to the cost.

B. P. DUDGING



## The Institute of Physics

At the Annual General Meeting of The Institute of Physics, held on 29 May, 1953, Dr. C. Sykes (Managing Director, Thos. Firth and John Brown Ltd., Sheffield) was re-elected President. Prof. F. A. Vick was elected a Vice-President, Dr. S. Whitehead was re-elected Honorary Treasurer and Dr. B. P. Dudding was re-elected Honorary Secretary. The two new ordinary members of the Board elected were Mr. A. T. Pickles and Dr. P. S. H. Henry. Prof. A. M. Tyndall was elected to Honorary Fellowship, the highest honour which the Institute can bestow. Prof. Tyndall was Professor of Physics in the University of Bristol for many years and is known for his distinguished fundamental work on the mobility of ions and for his services to science and education. He is a Founder Fellow of the Institute and a Past President.

The Report for 1952 which was adopted at the meeting states that 251 new members (i.e. not previously members of any grade) were elected to grades for which approved academic qualifications in physics are demanded; this was the highest since the foundation of the Institute. 651 applications for membership (all grades) were considered during 1952 and the total membership at the end of the year was 4347. Six technical colleges which had applied for recognition or for an extension of recognition were inspected.

The Institute's Graduateship examination was held for the first time; there were 24 candidates. A report entitled *The Scientific Education of Physicists* published during the year is a guide to the facilities available in this country for professional education and training in physics. There was a large increase in the interest shown in National Certificates in Applied Physics; 137 candidates took the Ordinary and 33 the Higher Certificate papers.

About half the work of the Institute is now devoted to its publications, the receipts from which were £28 000 in 1952, including advertisement revenue, and the Report records the plans for the publication of a new series entitled *Mono-graphs for Students*. These cost 5s. each and are intended for general reading by students such as those in the first two years of a degree course in science or engineering, or those reading for Higher National Certificates. (The first four have just been published, see p. 157.) Among the books published during the year were two more volumes in the "Physics in Industry" series (*Industrial Magnetic Testing*, by Prof. N. F. Astbury, and *Metallurgical Equilibrium Diagrams*, by Dr. W. Hume-Rothery, Mr. J. W. Christian and Mr. W. B. Pearson), the Deputy Secretary's *Physics as a Career* and a *Memorandum on Gamma-ray Sources for Radiography* prepared by the Industrial Radiology Group.

Professional and other matters referred to in the Report include a proposed increase in life insurance premium on account of supposed "occupational hazard" as a research physicist, the delay in obtaining visas for certain countries, the supply and demand for physicists, salary statistics, deferment from military service, civil defence, and statutory regulations concerning protection from radiation hazards.

The Report includes a brief account of the Fourth Industrial Physics Conference and Exhibition which was held in Glasgow in June 1952, the object of which was "to promote the application of physics to industry by bringing to the attention of industrial executive engineers and scientists recent developments in applied physics."

The Institute's sixteen local Branches and specialist subject Groups were again very active and held many meetings, including some short specialist conferences and exhibitions. Mention can only be made here of a few. The Australian Branch held a four-day Conference in Melbourne on microscopy, the Manchester Branch was responsible for a Conference on textile physics, the Scottish Branch ran a course of lectures on semiconductors, the Education Group held a Conference on "School and university examinations in physics," the X-ray Analysis Group held a two-day Conference to celebrate the 40th anniversary of the discovery of X-ray diffraction and the Industrial Spectroscopy Group was responsible for the Third International Spectroscopy Colloquium which many foreign scientists attended.

## Elections to The Institute of Physics

The following elections have been made by the Board of The Institute of Physics:

*Fellows:* C. R. Barber, J. W. Broadhurst, R. M. Chaudhri, A. W. Gillies, J. C. Guthrie, M. E. Haine, S. Holmes, H. F. Nitka, J. E. Stanworth.

*Associates:* N. L. Allen, A. J. Bird, J. Blackie, J. Brodrie, G. F. Butler, G. J. Camfield, W. F. Campbell, V. G. Cattrell, K. W. Cunningham, L. W. Davies, W. Fulop, R. J. Hamilton, R. A. Horsley, C. G. McCue, J. Middlehurst, G. E. Owen, P. A. Peckover, A. Rae, N. Ramanathan, F. Rhoden, J. A. Roberts, S. Temple, D. Wilkinson, B. T. M. Willis.

Twenty-six Graduates, eighteen Students and four Subscribers were also elected.

## Journal of Scientific Instruments

### Contents of the July issue

- SPECIAL ARTICLE  
The Physical Society's Exhibition—London 1953. By E. J. Harris.
- ORIGINAL CONTRIBUTIONS  
Papers  
On the preparation of plane diffraction grating replicas from helical rulings. By G. D. Dew.  
An electromagnetic torque-meter for use in viscometry. By C. A. R. Pearce.  
The construction of small solenoids for the production of intense magnetic fields. By W. R. Myers.  
A simple diaphragm micromanometer. By D. B. Cook and C. J. Danby.  
An instrument for the measurement of the density of aqueous ionic solutions. By C. F. McCourt.  
An X-ray camera for measuring preferred orientation in wires. By A. L. Mackay.  
A wide band high-power radio-frequency transformer. By L. U. Hibbard, W. Raudorf and L. Riddiford.  
An overload device for X-ray sets. By R. G. Ackland.
- Laboratory and workshop notes  
A simple agitation device for highly radioactive volumetric flasks. By L. E. Preuss.  
Simple scintillation crystal growing technique. By W. A. Little.  
A simple repetitive timing circuit for scaling units. By J. C. Jones.  
An expansion head for thin section cutting. By A. F. Howatson and P. R. Price.

NOTES AND NEWS  
New instruments, materials and tools  
Notes and comments

THIS JOURNAL is produced monthly by The Institute of Physics, in London. It deals with all branches of applied physics (including theory and technique). All rights reserved. Responsibility for the statements contained herein attaches only to the writers.

EDITORIAL MATTER. Communications concerning editorial matter should be addressed to the Editor, The Institute of Physics, 47 Belgrave Square, London, S.W.1. (Telephone: Sloane 9806.) Prospective authors are invited to prepare their scripts in accordance with the *Notes on the preparation of contributions*. (Price 2s. 6d. including postage.)

REPRODUCTION. The Institute of Physics is a signatory to The Royal Society's Fair Copying Declaration. Details may be obtained upon application from The Royal Society, London, W.1.

ADVERTISEMENTS. Communications concerning advertisements should be addressed to the agents, Messrs. Walter Judd Ltd., 47 Gresham Street, London, E.C.2. (Telephone: Monarch 7644.)

SUBSCRIPTION RATES. A new volume commences each January. The charge is £4 per volume (\$11.50 U.S.A.), including index (post paid), payable in advance. Single parts, so far as available, may be purchased at 8s. each (\$1.15 U.S.A.), post paid, cash with order. Orders should be sent to The Institute of Physics, 47 Belgrave Square, London, S.W.1, or to any bookseller.

# Creep and recovery in metals

By A. J. KENNEDY, Ph.D., A.M.I.E.E., A.Inst.P., Davy Faraday Research Laboratory,  
The Royal Institution, London

A review is made of the experimental evidence available on the nature of the creep and recovery mechanisms in single crystal and polycrystalline metals. This leads to consideration of the character of creep when periods of recovery, under reduced stress, are interposed, and it is shown that such conditions have an important effect on the behaviour of structures and machines, particularly at high stresses and temperatures.

This article traces the progress of two lines of physical inquiry and their convergence in the essentially modern technological problem of creep-resistant materials and structures. The general background information available on the physical nature of the processes of creep and recovery cannot possibly be treated comprehensively, but some general review of this is necessary, even if the major controversial issues are left unargued. These may be traced more fully through the fairly extensive references.

## THE PROGRESS OF CREEP STUDIES

The interpretation of creep phenomena, and their expression in terms of physical forces, is a comparatively modern study. Structural details, on a macroscopic scale, were certainly known by 1886,<sup>(1)</sup> and the observation of such a fundamental phenomenon as the appearance of slip-lines in mineral crystals goes back at least to 1867;<sup>(2)</sup> their observation in metals dating from 1899.<sup>(3)</sup> The basic lattice-structure facts, however, were not known until Bragg,<sup>(4)</sup> in his classic work, developed X-ray methods of analysis. No sooner had the essentially crystalline nature of metals been established in this way, than the development of crystal growing techniques<sup>(5)</sup> and the consequent examination of single crystal properties, made some modification essential. Basically, unworked crystals were far softer than predicted by calculations based on the forces of cohesion existing in a regular atomic lattice. The mechanical properties of such crystals were clearly crystallographic in origin,<sup>(6)</sup> and it was natural to seek an explanation for their character in terms of a revised crystalline matrix. Bragg,<sup>(7)</sup> indeed, had already noted that the large angular spread of X-ray reflexions suggested a mosaic lattice consisting of blocks of slightly differing orientation, implying some imperfection at the block boundaries. Imperfections in a crystal lattice, and their behaviour under stress, were introduced into the theory by Masing and Polanyi<sup>(8)</sup> and by Dehlinger,<sup>(9)</sup> and with distinguished and diverse contributions by Orowan,<sup>(10)</sup> Polanyi,<sup>(11)</sup> Taylor,<sup>(12)</sup> Burgers,<sup>(13)</sup> Mott<sup>(14,15,112)</sup> Nabarro<sup>(15,16)</sup> Frank<sup>(17,18)</sup> and Read<sup>(18,19)</sup> amongst others, the study of dislocations (a word apparently due to Love<sup>(20)</sup>) has now emerged as the most fruitful and influential force in modern solid state physics. A considerable examination of the theory and application of the mathematical methods has been made by Nabarro.<sup>(21)</sup>

The examination of the behaviour of crystals free from the influences of neighbours in an aggregate constitutes one major field of inquiry. A brief survey of the range of these investigations reveals how detailed is the information that is now to hand. Using X-rays, disorientations can be detected in crystals as grown,<sup>(22)</sup> and the progress of polygonization, or clock formation, with strain and heat treatment, followed.<sup>(23)</sup> Non-homogeneity of deformation may be very marked,<sup>(24)</sup>

and possibly, for small deformations, only a minor part of the total strain may be concentrated in the slip packets.<sup>(25)</sup> The fine structure of slip bands is revealed by electron microscope and X-ray studies. Wide bands, widely spaced, characterize deformation at slow rates, and at high rates only, apparently, is the slip band composed of many narrow lamellae.<sup>(26)</sup> The thickness of the lamellae is about 200 Å in aluminium, with lamellae displacement of about 2000 Å; the displacement is not a simple translation but involves rotation as well.<sup>(27)</sup> Critical shear stresses can be measured<sup>(6,28)</sup> and dislocation theories compared.<sup>(29)</sup> The influence of surface conditions<sup>(30)</sup> suggests that the presence of very thin surface films exercises a profound effect on the movement of dislocations. Further, considerable superficial structural changes can occur under cold work; a surface layer, a few  $\mu$  thick, can exist over the undisturbed parent crystal.<sup>(31)</sup> Surface effects also greatly influence the internal friction.<sup>(32)</sup> At low temperatures, in very pure metals, so-called easy glide may be possible by a mechanism hindered by increasing temperature,<sup>(33)</sup> which is distinctly different from the usual type of temperature dependence observed in deformation properties.

The structure of kink-bands,<sup>(34)</sup> deformation-bands,<sup>(35)</sup> and twin-bands<sup>(36)</sup> has been studied in detail<sup>(37)</sup> and related with fair success to dislocation theory. Such mechanical properties are closely linked with the mechanisms of crystal growth;<sup>(38)</sup> the appearance of sub-structures in crystals depending markedly upon the growth rate and temperature.<sup>(39)</sup> Rotational slip of one plane over another can theoretically<sup>(21,40)</sup> create a mosaic of regions of perfect crystallinity bounded by screw dislocations: such a structure has been detected in a variety of crystals.<sup>(40)</sup> Quite large mosaic structures have also been noted in synthetic corundum.<sup>(41)</sup> Sub-crystal structures consisting of blocks of different orientation are fairly readily revealed by etching.<sup>(42)</sup> Impurities can give rise to a sharp yield point,<sup>(43)</sup> with strain aging treatment, and yield point experiments<sup>(44)</sup> on iron crystals, containing carbon, taken in conjunction with Cottrell's concept of dislocations bound by carbon atmospheres<sup>(45)</sup> have clarified considerably this aspect of crystal deformation. The theory is supported by calculation of the relevant activation energy.<sup>(46)</sup> In very thin crystals slip may occur along shorter slip paths,<sup>(47)</sup> rather than in the crystallographic slip direction. The production of discontinuous asterisms in X-ray Laue patterns can be traced to a form of recrystallization in a bent crystal under which dislocations diffuse into arrays between the mosaic blocks.<sup>(48)</sup> A number of experiments on the creep behaviour of crystals<sup>(49,106)</sup> all support a general law of the form

$$\epsilon = \beta t^p \quad (1)$$

where  $\epsilon$  is creep strain,  $t$  time under stress, and  $\beta$  and  $p$



constants, with  $p$  taking a large range of fractional values from about 0.2 to 0.7. Dislocation treatments of the creep phenomena have been proposed,<sup>(15,50)</sup> and certain observations concerning the related phenomena of work-hardening, such as those on slip-band formation, can now be successfully reconciled with dislocation ideas,<sup>(14,51)</sup> where the basic processes are taken to be dislocation generation from sources, the hardening of sources, and the interlocking of dislocations themselves.

A parallel inquiry on the nature of the processes of slip at the boundaries of crystals has been made possible by the development of techniques for the growth of bi-crystals. The boundary appears to have a lower melting point than the crystalline material,<sup>(52)</sup> and measurements on diffusion<sup>(53)</sup> and boundary direction<sup>(54)</sup> show a dependence on the relative orientation of the neighbour crystals. The mechanical properties of the boundary when subjected to simple shear, at various temperatures, have been established<sup>(55)</sup> and they may be summarized by saying that the boundary behaviour is approximately viscous (as distinct from the parabolic flow behaviour of the crystals themselves), but that some hardening occurs, though this may be due to secondary effects.<sup>(56)</sup> Both the amorphous region theory and the abrupt lattice transition theory must be rejected, according to Kê,<sup>(57)</sup> for a chain of disordered groups of atoms, slip occurring by a shear process involving units of a few atoms only. A very small amount of impurity blocks low-stress boundary flow altogether. On the other hand, dislocation models of the boundary can account for intercrystalline slip, and provide a theory for dislocation generation: quantitative agreement is also claimed.<sup>(58)</sup>

These two main classes of phenomena, the crystalline and the intercrystalline, appear together in polycrystalline aggregates. Clearly the limitations imposed by neighbours must further complicate the types of deformation observed in the more simple cases. The fine-structure of slip-bands has again been studied.<sup>(59)</sup> The formation of new bands involves greater work-hardening than progressive slip in the old bands. Grains certainly break down, on deformation, into some form of sub-structure,<sup>(60)</sup> and considerable work on the nature and the formation of sub-structures, and their role in the creep processes, has been carried out by Wood;<sup>(61)</sup> essentially, it has been shown that at high temperatures and low deformation rates it is the relative movements of the sub-units, or cells, which is the dominant mechanism, rather than slip and break-down into sub-microscopic crystallites. These processes have been examined in different types of alloys<sup>(62)</sup> and there is some basis for their direct relation to the polygonization and dislocation mechanisms already observed in single crystals.<sup>(63)</sup> The surface, as in single crystal work, plays a large part in controlling the deformation processes.<sup>(64)</sup> Certainly the surface crystals deform more readily than the internal ones.<sup>(65)</sup> It is also known that the elastic and plastic properties of very fine wires ( $\approx 10^{-4}$  cm diameter) are very close to those of a perfect crystal.<sup>(66)</sup>

The use of X-ray micro-beam techniques enables the size of the crystal particles within the grains of a polycrystal, after deformation, to be established.<sup>(67)</sup> The fact that a limiting particle size exists agrees with other work;<sup>(68)</sup> the dislocation concentration within the particle boundaries being estimated to be as high as  $10^{10}/\text{cm}^2$ . Different views are held as to whether the appearance of mosaic phenomena in creep are fundamentally causes or effects. The breakdown indeed has been suggested to be an entirely secondary effect.<sup>(69)</sup> In contrast with the work which substantiates the large contribution to the crystal strain by deformation outside

the slip bands, certain X-ray work appears to re-establish the predominance of the slip process even at fairly slow rates,<sup>(70)</sup> but inhomogeneity, even within a particular grain, is a striking feature of the process. Quite large-scale inhomogeneities can clearly be produced under the simplest deformation systems.<sup>(71)</sup>

The foregoing sets out some of the features of crystalline deformation. The problem of creep-resistance is usually formulated, however, not in the qualitative terms of these phenomena, but in terms of measurements made on the strain-time properties of metals subjected to constant stress. The compilation of such data has developed, since 1940, into a major industrial activity. Creep testing, on the lines now commonly adopted, was established by Andrade<sup>(72)</sup> to whom is due the basic division of the creep strain into a transient and a permanent component. These processes correspond in character to the types of deformation exhibited, respectively, by crystalline blocks, and by the boundaries between blocks, whether these be granular or sub-granular. To the foregoing review of crystal properties we must add the evidence that the density decreases with deformation,<sup>(73)</sup> that actual rifts may occur in the lattice,<sup>(74)</sup> and that the grain boundaries may have a more spacious structure than usually supposed.<sup>(75)</sup> Such facts must modify even further the supposed deformation mechanisms (structurally reviewed by Cook and Richards<sup>(76)</sup>) of slip, twinning, cell-movement, boundary-flow, recrystallization and grain growth, all of which, for some range of conditions, contribute to the creep process. Work-hardening thus has two origins, granular and inter-granular, and at least some of the main properties of flow and fatigue, such as the differing behaviour of cubic and hexagonal metals, can be explained on this basis.<sup>(77)</sup>

The fact that the creep curve can be reduced to two components is now widely recognized,<sup>(78)</sup> as is the existence of a transient power law similar to that noted in single crystals.<sup>(79)</sup> There is some dissension on the most generally applicable equation, and other forms have been proposed,<sup>(80)</sup> but the evidence provided by a range of solids, metallic and non-metallic,<sup>(81)</sup> is overwhelmingly in favour of a simple power law, and in a great many cases<sup>(82)</sup> the power is very near to Andrade's one-third.<sup>(72)</sup>

Recently, a number of equations have been introduced derived by rheological methods. These set out to embrace and to express, within the terms of a comprehensive equation, all the empirical creep phenomena. This represents an approach which is quite opposite from that pursued by physical argument, which must start from some physical structure, but the method may indeed uncover generalities which the closer observations of physics have left unrecognized.<sup>(83)</sup>

The two-mechanism nature of creep provides the basis for two works on the subject, that of Rotherham<sup>(84)</sup> and that of Sully<sup>(85)</sup> to which reference must be made for the full development of the thesis. It must suffice to say that the results of a range of experiments, including work on electrical resistance,<sup>(86)</sup> pre-straining,<sup>(87)</sup> pure shear,<sup>(88)</sup> size-effect<sup>(64)</sup> and intermittent stressing,<sup>(89)</sup> can all be broadly reconciled with the two-mechanism model.

Detailed reconciliation of quantitative creep measurements, on a complex aggregate, with individual deformation mechanisms may never be achieved, but some statistical generalization based on simple concepts of crystalline order and disorder<sup>(82)</sup> may explain the fundamental nature of the parabolic creep law, and possibly provide a basis for more certain creep prediction and design.



## THE PROGRESS OF RECOVERY STUDIES

The term *recovery* has been applied loosely to any process, or processes, by which some measured property of a material, subjected to an initial treatment, returns with time towards its original value. The property in question may be, for instance, electrical resistivity,<sup>(90)</sup> hardness,<sup>(91)</sup> thermoelectric force<sup>(92)</sup> or density,<sup>(93)</sup> or even strain (creep recovery)<sup>(94)</sup> or stress relaxation.<sup>(95)</sup> In this discussion it will be taken to imply the softening with time of the metal which occurs after cold-working, during which no detectable structural changes take place. This definition is almost certainly completely arbitrary, as more sensitive techniques merely shift the threshold of detectability.<sup>(96)</sup> However, it is useful to use the term in this sense, and to reserve *recrystallization* for the processes of nucleation and growth of new grains in the matrix.<sup>(97)</sup> The full separation and definition of the changes that can occur during heat treatment is by no means accomplished, and the application of the existing terms, as has been pointed out by Thorley,<sup>(98)</sup> is inconsistent. The process of polygonization must now be included as an operative mechanism, and the contemporary attitude towards the whole problem of distinguishing structural changes may best be judged from the articles of Cahn<sup>(99)</sup> and Guinier and Tennevin.<sup>(100)</sup>

The recovery-recrystallization process is strongly temperature dependent, and a characteristic curve, shown in Fig. 1, is obtained by plotting the quantity under measurement

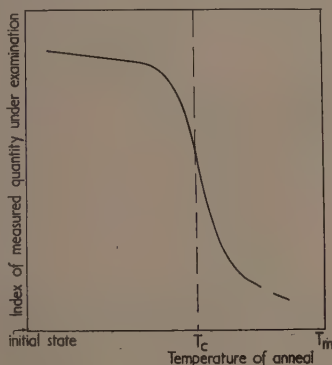


Fig. 1. Typical isochronal annealing curve, showing the rapid change near some critical temperature  $T_c$ .  $T_m$  is the melting point

against temperature of anneal for fixed anneal times. Beilby,<sup>(101)</sup> as early as 1907, obtained such a curve for copper, using as an index a quantity called "mechanical stability," which he defined as the stress required to produce a permanent deformation of 1%. Bailey<sup>(102)</sup> proposes  $t = t_0 e^{-b\theta}$  as the significant equation, relating the time ( $t$ ) for recovery at  $\theta^\circ$  absolute to the time ( $t_0$ ) for the same amount of recovery at zero temperature,  $b$  being a constant. This has support from X-ray line broadening changes.<sup>(91,103)</sup> The separation of individual components in the total softening process has always been a contentious question, but Thorley's success in demonstrating the simultaneous operation of two activation energies, from hardness measurements, that for recovery and that for recrystallization, gives support to his conclusion that both occur simultaneously throughout the whole of the anneal. The actual energies are very nearly the same. Tensile strength measurements<sup>(104)</sup> also give the same activation energy for

recovery and recrystallization. Thorley's work, and that on thermoelectrical forces<sup>(92)</sup> also supports the process as a single-stage one. Two processes, with different activation energies, are needed to explain the low-temperature electrical resistivity measurements on copper,<sup>(105,90)</sup> and on gold and silver,<sup>(90)</sup> one possibly associated with the diffusion of single vacant lattice sites, and the other with clusters of vacant lattice sites. As it is likely that these are created at dislocation generators (possibly of the Frank-Read<sup>(18)</sup> type) then it becomes clear that the processes of recovery need not involve any destruction or large-scale re-organization of generators, but merely the diffusion towards such generators of the vacancies created. It is understandable, on this model, why single crystals when subjected to an interrupted creep test can exhibit almost identical creep curves on reloading;<sup>(106)</sup> the identity of the metal is retained in the pattern of generators.

A two-stage process is favoured by Owen and Liu<sup>(107)</sup> from X-ray work on aluminium. It is suggested that the first stage is controlled by the internal strain energy, and the second by thermal energy; the processes of recovery and recrystallization being distinct, but dependent. A two-stage process is also supported by interrupted creep test work on single crystal<sup>(106)</sup> and polycrystalline metals.<sup>(89)</sup> Nor has it been possible to represent the annealing processes in platinum (as detected by electrical quantities) by a single-valued activation energy process.<sup>(108)</sup> It is also suggested by Varley<sup>(104)</sup> that recovery must proceed to a certain stage before recrystallization can occur, and that stopping the anneal at a selected time restricts the process to one of recovery only. This, then, is also a two-stage picture. An "incubation period" for nucleus formation to begin has been examined as a function of the test parameters<sup>(109)</sup> and the existence of some such period has been proposed elsewhere.<sup>(126)</sup> As far as recovery is concerned, some threshold value of the strain, required for the process to commence, has been put forward by Cottrell<sup>(110)</sup> in a review (1940) of the physical changes brought about by the process. The recovery mechanisms, viewed as dislocation problems, have been treated by Burgers<sup>(111)</sup> and by Mott.<sup>(112)</sup>

The two general questions which arise in these recovery studies have not yet been resolved convincingly. These are: (i) is the complete process a single-stage one; and (ii) are recovery and recrystallization basically the same mechanisms on different scales? It must at least be accepted that the activation energies for the processes are very nearly the same. It may be that much of the contradiction is due to the existence of thermal hardening<sup>(113)</sup> which can occur anomalously in apparently identical crystals,<sup>(106)</sup> and is certainly a consideration in polycrystalline materials as well.

## THE RELATION BETWEEN CREEP AND RECOVERY

The hypothesis has been advanced that creep is due to the thermal softening of a material plastically defined by a stress-strain relationship. Thus creep proceeds at a constant rate such that a running balance is achieved between the dual mechanisms of strain-hardening and thermal softening. Not only is it necessary to modify this simple treatment to take account of the transient stage, but even during the steady-state stage of creep the physical properties of the material do not remain a constant. Again, in the majority of cases, no exact linearity in the creep curve is observed at all. Increased sensitivity of measurement usually reveals some curvature—a result which is in accord with the formulation of creep as the sum of a parabolic and a linear component.

The fact that a set of creep curves, for a particular metal, over a fairly wide range of stress and temperature conditions,

obeys an equation of the form  $\epsilon = \beta t^p$ , with  $\beta$  a function of the conditions, but with  $p$  a constant, suggests that the applied conditions are varying the *rate* at which the hardening mechanism proceeds, without changing its basic character. This would imply that the creep rate should be a function of strain only, if the stress  $\sigma$  and the temperature  $T$  were constant, and we are thus led to the concept of a mechanical equation of state, as discussed by Ludwik,<sup>(114)</sup> Hollomon<sup>(115)</sup> and Orowan.<sup>(116)</sup> This equation which we may write as  $\dot{\epsilon} = f(\epsilon, \sigma, T)$ , does not universally hold, although it may be approached at low temperatures.<sup>(117)</sup> Referring now to Fig. 2: the creep curves of a metal under stresses  $\sigma_1$  and  $\sigma_2$ , for the same temperature  $T$ , are marked as *A* and *B*. Suppose

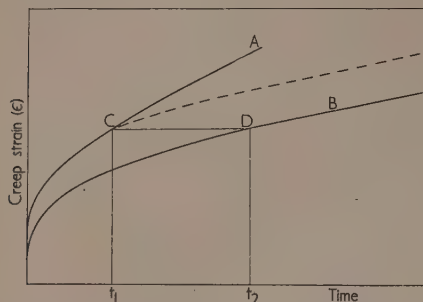


Fig. 2. *A* and *B* are creep curves at stresses  $\sigma_1$  and  $\sigma_2$  for the same test temperature. Changing the stress from  $\sigma_1$  to  $\sigma_2$  at the point *C* does not result in the dotted creep curve parallel to *B*

creep occurs under  $\sigma_1$  up to the point *C*, when it is reduced to  $\sigma_2$ . If the strain alone were the significant quantity then creep should now proceed along the dotted line, parallel to the *B* curve. No such behaviour is observed. Although, then, transient creep is characterized by a simple, fairly universal function, the coefficient ( $\beta$ ) cannot be taken to represent a single physical mechanism, although it can, of course, be taken as an index of the magnitude of the transient creep which results from the competing mechanisms of hardening and softening.

This being so, does the discrepancy arise because of the difference in the creep times involved in the test? In one case (point *C*) the creep time along *A* is  $t_1$ , in the other (point *D*), the time along *B* is  $t_2$ . If, then, the creep state of the material

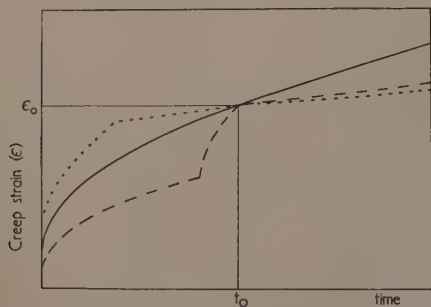


Fig. 3. Demonstrating the behaviour of lead wires, of different creep histories up to the point  $(\epsilon_0, t_0)$ , when extended under the same stress from  $t_0$  onwards

can be defined as a *point* in the  $\epsilon$ -time plane (as distinct from a line such as *CD*), then, by whatever path in the plane we reach the specified point (say  $\epsilon_0, t_0$ ), the creep curves for times  $> t_0$ , under some given stress, must coincide. This hypothesis may easily be tested and results are shown in Fig. 3. The point  $\epsilon = 5.0\%$ ,  $t = 20$  min, lies on the creep curve of lead under a stress ( $\sigma_0$ ) of 220 kg/cm<sup>2</sup> at 22° C. This point is now attained by various paths, the stress then being set at  $\sigma_0$ . All paths, whatever their nature relative to the continuous ( $\sigma_0$ ) creep curve, give rise to greater hardening than that under a continuous stress of  $\sigma_0$ . In other words, if a material is to be extended to a point  $(\epsilon_0, t_0)$ , at a constant temperature, then it would appear that the least work-hardening (or the greatest recovery) is achieved by extending it along the continuous creep curve on which  $(\epsilon_0, t_0)$  lies. Thus a principle of least action appears to operate, in which the creep curve may be defined as the creep path, from  $(0, 0)$  to  $(\epsilon_0, t_0)$  of least work-hardening. This is not wholly true, however; the exceptions have important consequences and these will be considered later.

What, then, is the influence of interposing a period of changed stress during a creep test? Orowan<sup>(116)</sup> reports testing the recovery theory of creep by reducing the creep stress by a small amount: creep should cease altogether until thermal softening reduces the yield stress to the value of the new applied stress, when creep recommences. No such behaviour was observed, the creep rate merely being reduced. This is in contrast with other results<sup>(117)</sup> in which the creep of lead ceased altogether when the stress was reduced by about 2.5%, but later recommenced and increased transiently to a new, lower, steady value. This accords with the nucleation concepts of slip in crystalline solids.<sup>(118)</sup> A set of results (from the author's unpublished work), shown in Fig. 4,

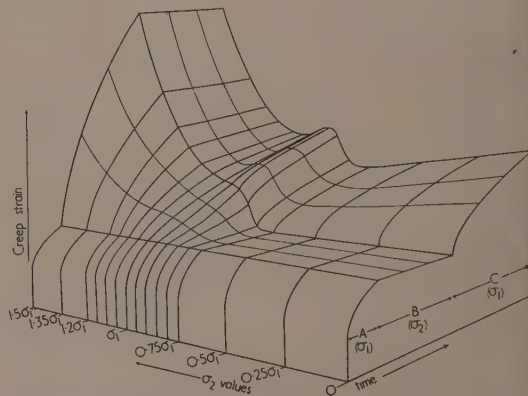


Fig. 4. The type of result obtained when the stress in a creep test at constant temperature is changed from  $\sigma_1$  to  $\sigma_2$  for some fixed period (*B*)

confirms the existence of a period of zero creep provided the value of the stress reduction is suitably chosen. Fig. 4 shows the effect of changing the stress, for a period of 20 min, during a creep test on lead, and then restoring the stress to its original value. In general, the creep curves in the third section, *C*, tend towards the curve of continuous creep under the stress  $\sigma_1$ , but in detail the behaviour is much more complex than this, notably near the case where  $\sigma_1 = \sigma_2$ . The distinctive features are that (i) a greater creep strain is eventually achieved for  $\sigma_2 = 0.95\sigma_1$  than for  $\sigma_1 = \sigma_2$ ; (ii) a slightly

ss creep strain is achieved for  $\sigma_2 = 1.05\sigma_1$  than for  $\sigma_1 = \sigma_2$ , and (iii) a minimum is exhibited at  $\sigma_2 = 0.75\sigma_1$ . This last case is also the maximum value of  $\sigma_2$  for which no creep occurs during stage B. Lowering  $\sigma_2$  below this increases the amount of recovery that occurs during stage B, and hence leads to a greater creep strain on reloading (stage C). It is clear, then, that we are faced with a very complex behaviour, and that a material can be less work-hardened, when taken to the point represented by some chosen  $\epsilon$  and  $t$  values, by creep extensions along paths other than that of continuous, constant, stress.

It is common practice to use as the effective stress, in any practical case, the average stress computed from the known stress variation. This is obviously fallacious if the transient creep coefficient ( $\beta$ ) is not a linear function of the stress over the stress-range encountered. Even if we restrict the stress-variation to such a linear region, however (say <5% variation about a mean), no simple averaging is valid. In Fig. 5,

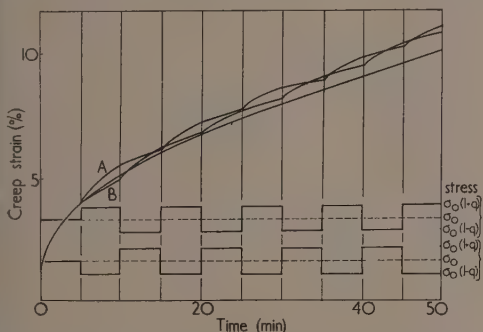


Fig. 5. Creep under a constant stress  $\sigma_0$  compared with creep under stresses varying about a mean of  $\sigma_0$ . The material is pure lead,  $\sigma_0 = 280 \text{ kg/cm}^2$ ,  $q = 0.01$ , and the test temperature is  $22^\circ \text{C}$

results are shown of experiments on lead in which creep under a constant stress  $\sigma_0$  is compared with creep under a square-wave stress alternating about a mean of  $\sigma_0$ . The  $\sigma$ -variation is restricted to the region of linearity between  $\beta$  and  $\sigma$ . All tests commence by a five-minute load at  $\sigma_0$ . The stress is then varied cyclically, in periods of 10 min, as shown, between  $\sigma_0(1+q)$  and  $\sigma_0(1-q)$ . Tests were made for the case where the stress is first increased, and also for the case where it is first decreased. It will be seen that in both cases the actual creep strain after five cycles is distinctly greater than that under constant stress. This is in agreement with the phenomena exhibited in Fig. 4.

The next major question is that of the dependence of recovery on temperature. If the stress is removed for a fixed period and the material allowed to anneal, how does the character of the creep curve on reloading depend on the temperature of the anneal? These experiments are of the standard recovery type, but the observations are here made on creep properties instead of hardness, tensile strength, and the like.

The type of result obtained is shown in Fig. 6. Probably the most striking feature is the very small difference in the results, for lead, for annealing temperatures from  $-180$  to  $20^\circ \text{C}$ . Above  $20^\circ \text{C}$  the change becomes very rapid, the phenomena being fairly critical in this region, as has been observed with other properties. As a basis for the inter-

pretation of these results, some index of the amount of recovery softening must be extracted from the curves. A formulation of the effect of a period of recovery on the creep characteristics has already been developed<sup>(89)</sup> and some brief indication of the method must be given here.

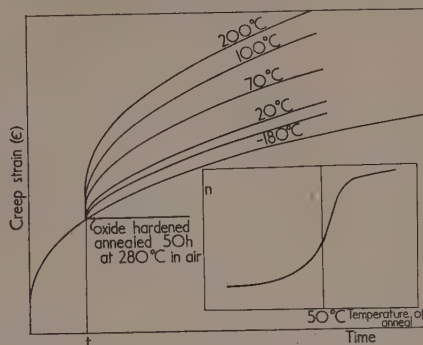


Fig. 6. The effect on the creep of pure lead at  $22^\circ \text{C}$  of a fixed period of anneal (30 min) at different temperatures, as marked. The fractions  $n$ , deduced as described, lie on a curve similar to that shown in the inset. The stress is  $280 \text{ kg/cm}^2$ , and  $t = 5 \text{ min}$

It can be shown that if the creep curve is represented by an equation of the form  $\epsilon = \alpha + \beta t^p + \kappa t$ , then the curve after annealing can be satisfied by assuming a fraction  $n$  of the material to have recovered in full its original  $\beta$ -flow properties, the fraction  $(1-n)$  continuing to behave as if no period of anneal had occurred.  $\alpha$ ,  $\beta$  and  $\kappa$  are constants. Thus, if the stress is removed, for some period, after a previous creep time  $\tau$ , the subsequent transient creep curve is given by the sum of two components:

- (1)  $\beta[\tau^p + (1-n)(t^p - \tau^p)]$
- (2)  $\beta n[t - \tau]^p$  (a new transient)

and

where  $t$  is the time under stress. If  $\kappa$  is finite, the  $\kappa$ -flow is simply added to this to give the total strain.

This suffices to deal with the single-interruption annealing experiments described, and we may deduce the  $n$ -values corresponding to any particular temperature and plot them as in Fig. 6. It is possible, further, to study the behaviour of  $n$  with time of anneal,<sup>(89)</sup> and to derive an activation energy for the recovery process, at least over a limited range of results. Whilst a significant correlation of these results with other measurements has not yet been achieved, the value of the activation energy so obtained fits in reasonably with other work. It may be added here that prolonged annealing of lead at high temperatures leads to a considerably hardened material which shows no creep at all under the test stress (see Fig. 6). A light etch completely restores the full creep properties, so that a thin film of oxide exerts a very large influence on the mechanical behaviour of the material, and may be an influence, to a lesser extent, for shorter anneal times. Recent single-crystal work<sup>(123)</sup> suggests that such results are due to simple load-sharing between a strong film and a weaker bulk material: this is not universally accepted.<sup>(124)</sup>

The major practical problem to which all the foregoing is related is that of creep under regular repetitive stress pulses. The recovery analysis already proposed above becomes very unwieldy as the number of cycles increases. Approximations have been developed to deal with such cases,<sup>(89)</sup> and these lead



to the prediction of certain important properties which agree very well with the experimental facts.

An expression can be derived by the analysis for the ratio,  $\chi$ , after  $m$  cycles, of the creep strain  $(\epsilon - \alpha)$  of a metal under intermittent stress, to the creep strain  $(\epsilon - \alpha)$  under the same continuous stress:  $\alpha$  is here the instantaneous strain on loading. If  $m^p \gg 1$ , and  $r = \tau/(\tau + R)$ ,  $\tau$  being the load time per cycle, and  $R$  the recovery time per cycle, we have

$$\chi = \left[ \frac{C}{1 + A \left( \frac{r}{1-r} \right)^p} + 1 \right] r^p \quad (2)$$

where  $C$  is a constant, but a function of  $p$  (for  $p = \frac{1}{3}$ ,  $C = 2.845$ ), and  $A$  is the constant characterizing the recovery behaviour of the material. It is related to the fraction  $n$  by the equation

$$\frac{1}{n} = 1 + A \left( \frac{r}{1-r} \right)^p \quad (3)$$

The behaviour of  $\chi$  for different  $A$ -values has already been worked out, and compared with the behaviour of metals.<sup>(89,119)</sup> Fig. 7 shows the type of result obtained. Fig. 7(a) demonstrates the behaviour of a metal subjected to stress cycles of constant frequency, but of differing wave-forms ( $r$ -values).

Fig. 7(b) shows the  $\chi$ -values, plotted for the case  $m = 12$ , where the extension  $(\epsilon - \alpha)$  under continuous creep is taken as unity. Experiment confirms the theoretical prediction that  $\chi$ -values  $> 1$  can occur. It is also noteworthy that equation (2) takes no account of frequency once  $m^p \gg 1$ , and provided  $r$  is unchanged. There is, then, no frequency effect in the accepted sense, but only an  $m$ -effect. (An important exception occurs when the time of recovery becomes very large. Reference must be made to the original work for discussion of this.) As  $m$  increases, the  $\chi$ -variation rapidly levels out towards an asymptote at 1.17. This is confirmed by the experimental results, plotted in Fig. 8(a) and (b), of tests in which  $r$  is maintained constant, but the frequency varied.

Periods of recovery interposed during a creep test can, then, lead to a greater strain than under continuous stress for the same total time; a result also obtained experimentally by Foley,<sup>(125)</sup> and in agreement with the observations plotted in Fig. 4. As the  $\beta$ -against-stress curves are not linear, but of a sigmoid character, then stresses alternating about the threshold creep value can lead to very nearly square stress pulses, and hence this type of stressing may occur quite widely in practice.

Another significant indication of the character of the recovery processes in polycrystalline materials is provided by

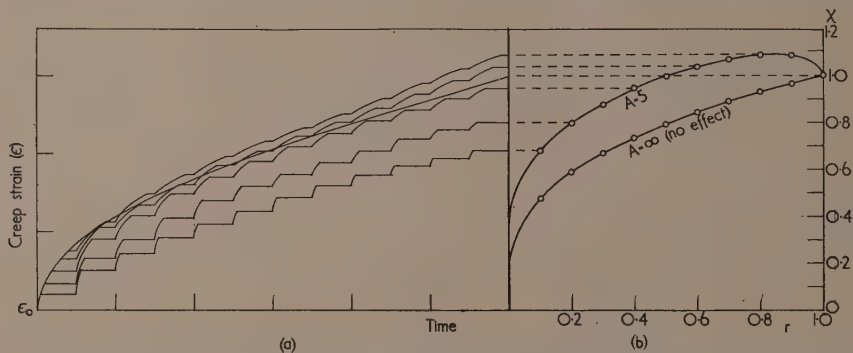


Fig. 7. (a) The behaviour of a material, with a recovery constant  $A = 5$  and  $p = \frac{1}{3}$ , over 12 cycles of stress, for differing  $r$ -values. (b) The  $\chi$ -values compared with those for a material which shows no recovery on unloading ( $A = \infty$ )

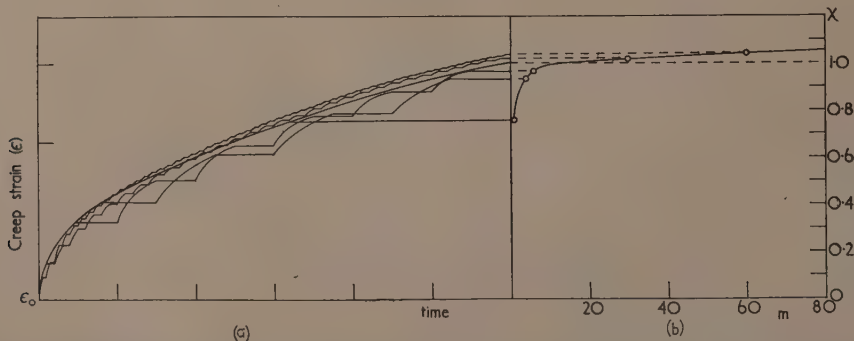


Fig. 8. (a) The behaviour of a material, with a recovery constant  $A = 5$  and  $p = \frac{1}{3}$ , at different stress-cycle frequencies, with  $r$  constant at 0.5. (b) The ratio  $\chi$ , after some chosen time  $t$ , plotted against  $m$ , the number of cycles completed during the time  $t$

comparison of single-crystal results. Slifkin and Kauzmann<sup>(106)</sup> have shown that the creep properties of zinc single crystals are recovered almost instantaneously on unloading at room temperature. There is no doubt that the interaction between grains not only impedes the creep processes, but also impedes the processes of recovery. Consequently we are led to the suggestion that, in general, a small grain size material may be more creep resistant, particularly under intermittent stressing. This is in contrast with the usual proposition, supported by experiment<sup>(120)</sup> that a small grain size is less desirable because of the increased permanent creep component, which varies approximately linearly with the total grain boundary area. These two considerations act in opposition, and some compromise is required in practical design.

In general, then, experiment shows the very great effect exerted by boundary conditions, and the close relation which exists between recovery properties and grain boundary mobility. Hirst<sup>(121)</sup> has shown, in work on five-crystal specimens of lead, that deformation of the crystal lattice takes place most rapidly at the crystal boundary, and that the manner of deformation for small crystals is not the same as for large ones. It is clear that recovery of this distortion must be strongly boundary dependent. Release of the internal stresses may also be achieved by recrystallization, a process which can certainly occur simultaneously with recovery. Experiments, by the author, on a very pure lead recrystallizing during creep under an intermittent stress give results in distinct contrast to those obtained with a lead that does not recrystallize. In the latter case, the effect of an interruption decreases with increase in the creep time prior to the interruption.<sup>(89)</sup> For a recrystallizing material there is an initial decrease in the effect and then, as recrystallization starts, a steady increase which continues approximately in step with the increasing grain size. The observations are consistent with the general statement that recovery increases with grain size, but more experiment is required before the exact role played by recrystallization in this process can be separated out.

#### APPLICATIONS IN APPLIED PHYSICS AND ENGINEERING

The above survey has attempted to cover the fundamental knowledge that is to hand on the nature of deformation processes in crystalline solids, and, in particular, the behaviour of such solids under complex stress conditions where recovery exerts an important influence. The consideration of these properties has increased in importance with the development of machines operating at high stresses and temperatures. The main approach to creep problems, however, has continued to be based on those continuous stress creep characteristics which have proved adequate for previous engineering design. As the test conditions become more rigorous, this ceases to be a valid basis, and account must be taken of the true stress history. For example, in gas turbines, the rotor blades are stressed at high temperatures during running periods, and are then allowed to recover at a lower temperature over cycles as long, possibly, as days. The windings in alternators are similarly stressed in a discontinuous manner.<sup>(122)</sup> Much high-pressure equipment is subjected to daily cycles of stress where industrial processes are closed down at night, and a variety of architectural structures similarly undergo a very obvious daily cycle of stress and temperature. Because of the wide application of the parabolic creep law it is note-

worthy that the considerations outlined here may also be relevant to the study of the behaviour of a wide variety of non-metallic materials. The effect also appears, at a higher frequency, in machine members subjected to vibration, where the combined effects of intermittent creep and fatigue may be extremely complex. It is, indeed, in this field of engineering, where creep and fatigue are both important, that the foregoing studies may find their most fruitful application.

#### REFERENCES

- (1) SORBY, H. C. *J. Iron Steel Inst.*, p. 140 (1886); p. 255 (1887).
- (2) REUSCH, E. *Ann. Phys. [Leipzig]*, **132**, p. 441 (1867).
- (3) EWING, J. A., and ROSENHAIN, W. *Phil. Trans.*, **193**, p. 353 (1900).
- (4) BRAGG, W. H. *Proc. Cambridge Phil. Soc.*, **17**, p. 43 (1913); *Nature [London]*, **90**, p. 410 (1912).
- (5) CZOCHRAŁSKI, J. *Z. Phys. Chem.*, **92**, p. 219 (1918).  
CARPENTER, H. C. H., and ELAM, C. F. *Proc. Roy. Soc. A*, **100**, p. 329 (1921).  
GOMPERZ, E. *Z. Phys.*, **8**, p. 184 (1922).  
KOREF, F. *Z. Elektrotech.*, **28**, p. 511 (1922).  
VAN ARKEL, A. E. *Physica*, **2**, p. 56 (1922).  
BRIDGMAN, P. W. *Proc. Amer. Acad. Arts Sci.*, **60**, p. 305 (1924).  
TAMMANN, G. *Lehrbuch der Metallographie* (Leipzig, 1923).
- (6) SCHUBNIKOW, I., and OBRIMOW, L. *Z. Phys.*, **25**, p. 31 (1924).
- (7) SCHMID, E. *Proc. Int. Congress App. Mech., Delft*, p. 342 (Delft: J. Waltman, Jr., 1924).
- (8) BRAGG, W. L., JAMES, R. W., and BOSANQUET, C. H. *Phil. Mag.*, **42**, p. 1 (1921).
- (9) MASING, G., and POLANYI, M. *Ergeb. exact. Naturwiss.*, **2**, p. 177 (1923).
- (10) DEHLINGER, U. *Ann. Phys. [Leipzig]*, **5**, 2, p. 749 (1929).
- (11) OROWAN, E. *Z. Phys.*, **89**, p. 654 (1934).
- (12) POLANYI, M. *Z. Phys.*, **89**, p. 660 (1934).
- (13) TAYLOR, G. I. *Proc. Roy. Soc. A*, **145**, p. 362 (1934).
- (14) BURGERS, J. M. *Proc. Acad. Sci. Amst.*, **42**, p. 293 (1939).
- (15) MOTT, N. F. *Phil. Mag.*, **43**, p. 1151 (1952).
- (16) MOTT, N. F., and NABARRO, F. R. N. *Report of a Conference on the Strength of Solids* (London: Physical Society, 1948).
- (17) NABARRO, F. R. N. *Proc. Phys. Soc.*, **59**, p. 256 (1947); *Phil. Mag.*, **42**, pp. 213, 1224 (1950).
- (18) FRANK, F. C. *Report of a Conference on the Strength of Solids*, p. 46 (London: Physical Society, 1948); *Proc. Phys. Soc. [London]*, **A**, **62**, pp. 131, 202 (1949); *Phil. Mag.*, **42**, p. 809 (1951); *Advances in Phys.*, **1**, p. 91 (1952).
- (19) FRANK, F. C., and READ, W. T. *Phys. Rev.*, **79**, p. 722 (1950).
- (20) READ, W. T., and SHOCKLEY, W. *Phys. Rev.*, **78**, p. 275 (1950).
- (21) LOVE, A. E. H. *The Mathematical Theory of Elasticity* (London: Cambridge University Press, 1927).
- (22) NABARRO, F. R. N. *Advances in Phys.*, **1**, p. 271 (1952).
- (23) LAMBOT, H., and VASSAMILLET, L. *C.R. Acad. Sci. [Paris]*, **235**, p. 1136 (1952).
- (24) LAMBOT, H., and VASSAMILLET, L. *C.R. Acad. Sci. [Paris]*, **235**, p. 1232 (1952).
- (25) RYBALKO, F. P., and YAKUTOVICH, M. V. *J. Tech. Phys., USSR*, **18**, p. 915 (1948).

- (25) KURNOSOV, K. G., TRONINA, N. M., and YAKUTOVICH, M. V. *J. Tech. Phys., USSR*, **18**, p. 197 (1948).
- (26) NISHIMURA, H., and TAKAMURA, J. *Mem. Fac. Engng, Kyoto Univ.*, **13**, p. 1 (1951).
- (27) HEIDENREICH, R. D., and SHOCKLEY, W. *Report of a Conference on the Strength of Solids*, p. 57. (London: Physical Society, 1948).
- (28) ELAM, C. F. *Distortion of Metal Crystals*, p. 26 (London: Oxford University Press, 1935).
- (29) SMOLUCHOWSKY, R. *Phys. Rev.*, **86**, p. 787 (1952).
- (30) ANDRADE, E. N. DA C., and RANDALL, R. F. Y. *Nature [London]*, **162**, p. 890 (1948).  
ANDRADE, E. N. DA C., RANDALL, R. F. Y., and MAKIN, M. J. *Proc. Phys. Soc. [London]*, **B**, **63**, p. 990 (1950).  
HARPER, S., and COTTRELL, A. H. *Proc. Phys. Soc. [London]*, **B**, **63**, p. 331 (1950).  
PHILLIPS, D. J., and THOMPSON, N. *Proc. Phys. Soc. [London]*, **B**, **63**, p. 839 (1950).  
MENTER, J. W., and HALL, E. O. *Nature [London]*, **165**, p. 611 (1950).  
GILMAN, J. J., and READ, T. A. *J. Inst. Metals*, **4**, p. 875 (1952).
- (31) KRANET, W., and RAETHER, H. *Ann. Phys. [Leipzig]*, **43**, p. 520 (1943).
- (32) WERT, C. A. *J. Appl. Phys.*, **20**, p. 29 (1949).
- (33) ANDRADE, E. N. DA C., and HENDERSON, C. *Phil. Trans.*, **244**, p. 177 (1951).
- (34) FRANK, F. C., and STROH, A. N. *Proc. Phys. Soc. [London]*, **B**, **65**, p. 811 (1952).
- (35) BARRETT, C. S. *Cold Working of Metals* (Cleveland: American Society for Metals, 1949).  
BARRETT, C. S. *Trans. Amer. Inst. Min. Metall. Engrs*, **135**, p. 296 (1939).  
PFEIL, L. B. *J. Iron Steel Inst.*, **15**, p. 319 (1926).
- (36) CLARK, R., and CRAIG, G. B. *Progress in Metal Physics*, **3**, p. 115 (London: Butterworth and Co. Ltd., 1952).
- (37) HOLDEN, J. *Phil. Mag.*, **43**, p. 976 (1952).
- (38) BURTON, W. K., and CABRERA, N. *Disc. Faraday Soc.*, No. 5, pp. 33, 40 (1949).
- (39) RUTTER, J. W., and CHALMERS, B. *Canad. J. Phys.*, **31**, p. 15 (1953).
- (40) WILMAN, H. *Nature [London]*, **165**, p. 321 (1950); *Proc. Phys. Soc. [London]*, **A**, **64**, p. 329 (1951).
- (41) IKORNIKOVA, N. YU. *Dokl. Akad. Nauk, SSSR*, **81**, p. 403 (1951).
- (42) LACOMBE, P. *Report of a Conference on the Strength of Solids*, p. 91 (London: Physical Society, 1948).
- (43) WAIN, H. L., and COTTRELL, A. H. *Proc. Phys. Soc. [London]*, **A**, **63**, p. 339 (1950).  
EDWARDS, C. A., PHILLIPS, D. L., and LIU, Y. H. *J. Iron Steel Inst.*, **147**, p. 145 (1943).
- (44) EDWARDS, C. A., PHILLIPS, D. L., and LIU, Y. H. *J. Iron Steel Inst.*, **149**, p. 199 (1940).  
SNOEK, J. L. *Physica*, **8**, p. 734 (1941).  
LOW, R. J., and GENSAMER, M. *Trans. Amer. Inst. Min. Metall. Engrs*, **158**, p. 207 (1944).
- (45) COTTRELL, A. H. *Report of a Conference on the Strength of Solids*, p. 30 (London: Physical Society, 1948).
- (46) NABARRO, F. R. N. *Report of a Conference on the Strength of Solids*, p. 38 (London: Physical Society, 1948).
- (47) WU, T. L., and SMOLUCHOWSKI, R. *Phys. Rev.*, **78**, p. 468 (1950).
- (48) CAHN, R. W. *J. Inst. Metals*, **17**, p. 121 (1949).
- (49) COTTRELL, A. H., and AYTEKIN, V. *J. Inst. Metals*, **77**, p. 389 (1950).  
WEINBERG, E. H. *J. Appl. Phys.*, **23**, p. 1277 (1952).  
THOMPSON, D. O. *J. Appl. Phys.*, **23**, p. 1277 (1952).  
TYNDALL, E. P. T. *J. Appl. Phys.*, **21**, p. 939 (1950).  
SWIFT, I. H., and TYNDALL, E. P. T. *Phys. Rev.*, **61**, p. 359 (1942).
- (50) KOCHENDORFER, A. *Naturwissenschaften*, **39**, p. 187 (1952).
- (51) KOEHLER, J. S. *Phys. Rev.*, **86**, p. 52 (1952).  
SEITZ, F. *Advances in Phys.*, **1**, p. 43 (1952).  
FISHER, J. C., HART, E. W., and PRY, R. H. *Phys. Rev.*, **87**, p. 958 (1952).  
COTTRELL, A. H. *Phil. Mag.*, **43**, p. 645 (1952).
- (52) CHALMERS, B. *Proc. Roy. Soc., A*, **175**, p. 100 (1940).  
PUMPHREY, W. I., and LYONS, J. V. *Nature [London]*, **163**, p. 960 (1949).
- (53) ACHTER, M. R., and SMOLUCHOWSKI, R. *Phys. Rev.*, **83**, p. 163 (1951).
- (54) CHALMERS, B. *Proc. Roy. Soc., A*, **196**, p. 64 (1949).
- (55) KING, R., CAHN, R. W., and CHALMERS, B. *Nature [London]*, **161**, p. 682 (1948).
- (56) PUTTICK, K. E., and KING, R. *J. Inst. Metals*, **80**, p. 537 (1952).
- (57) KÊ, T.-S. *J. Appl. Phys.*, **20**, p. 274 (1949).
- (58) READ, W. T., and SHOCKLEY, W. *Phys. Rev.*, **78**, p. 275 (1950).
- (59) BROWN, A. F. *Nature [London]*, **163**, p. 961 (1949); *J. Inst. Metals*, **80**, p. 115 (1951).
- (60) RAMSEY, J. A. *Nature [London]*, **166**, p. 867 (1950).
- (61) WOOD, W. A. *Proc. Phys. Soc. [London]*, **52**, p. 110 (1940).  
WOOD, W. A., and RACHINGER, W. A. *J. Inst. Metals*, **75**, p. 237 (1949).  
WILMS, G. R., and WOOD, W. A. *J. Inst. Metals*, **75**, p. 693 (1949).  
WOOD, W. A., and SCRUTTON, R. F. *J. Inst. Metals*, **77**, p. 423 (1950).  
WOOD, W. A., WILMS, G. R., and RACHINGER, W. A. *J. Inst. Metals*, **79**, p. 159 (1951).  
GARROD, R. I., SUITER, J. W., and WOOD, W. A. *Phil. Mag.*, **43**, p. 677 (1952).
- (62) GREENOUGH, G. B., BATEMAN, C. M., and SMITH, E. M. *J. Inst. Metals*, **80**, p. 545 (1952).
- (63) GREENOUGH, G. B., and SMITH, E. M. *J. Inst. Metals*, **77**, p. 435 (1950).
- (64) BROWN, A. F. *Advances in Phys.*, **1**, p. 427 (1952).
- (65) ANDRADE, E. N. DA C., and KENNEDY, A. J. *Proc. Phys. Soc. [London]*, **B**, **64**, p. 363 (1951).  
VITOVEC, F., and SLIBAR, A. *Schweiz. Arch. Angew. Wiss. Tech.*, **16**, p. 76 (1950).
- (66) HERRING, C., and GALT, J. K. *Phys. Rev.*, **85**, p. 1060 (1952).
- (67) HIRSCH, P. B., and KELLAR, J. N. *Acta Cryst.*, **5**, p. 162 (1952).  
HIRSCH, P. B. *Acta Cryst.*, **5**, p. 168 (1952).  
HIRSCH, P. B. *Acta Cryst.*, **5**, p. 172 (1952).
- (68) WOOD, W. A., and RACHINGER, W. A. *J. Inst. Metals*, **75**, p. 571 (1949).
- (69) ROTHERHAM, L., and LARKE, L. W. *Research*, **3**, p. 434 (1950).



- (70) CALNAN, E. A., and BURNS, B. D. *J. Inst. Metals*, **77**, p. 445 (1950).
- (71) BOAS, W. *Helv. Phys. Acta*, **23**, p. 159 (1950).
- (72) ANDRADE, E. N. DA C. *Proc. Roy. Soc. A*, **84**, p. 1 (1910).  
ANDRADE, E. N. DA C. *Proc. Roy. Soc. A*, **90**, p. 329 (1914).
- (73) ALKINS, W. E. *J. Inst. Metals*, **8**, p. 381 (1920).  
O'NEILL, H. *J. Iron Steel Inst.*, **109**, p. 93 (1924).
- (74) SMITH, D. P. *J. Appl. Phys.*, **20**, p. 1186 (1949).
- (75) SNOEK, J. L. *Phil. Mag.*, **41**, p. 1188 (1950).
- (76) COOK, M., and RICHARDS, T. L. *J. Inst. Metals*, **78**, p. 463 (1951).
- (77) CRUSSARD, C. *Rev. Metall.*, **43**, p. 307 (1946).
- (78) ANDRADE, E. N. DA C. *J. Iron Steel Inst.*, **171**, p. 217 (1952).  
JENKINS, W. D., and DIGGES, T. G. *J. Res. Nat. Bur. Stand.*, **45**, p. 153 (1950).  
ALEXANDER, B. H., DAWSON, M. H., and KING, H. P. *J. Appl. Phys.*, **22**, p. 439 (1951).  
CARREKER, R. P. *J. Appl. Phys.*, **21**, p. 1289 (1950).  
WYATT, O. H. *Nature [London]*, **167**, p. 866 (1951).  
JENKINS, W. D. *J. Res. Nat. Bur. Stand.*, **46**, p. 310 (1951).  
MACK, C. *J. Appl. Phys.*, **17**, p. 1093 (1946).
- (79) HAZLETT, T. H., and PARKER, E. R. *Trans. Amer. Inst. Min. Metall. Engrs*, **5**, p. 318 (1953).
- (80) HASIGUTI, R. R., and OWADANO, T. *Nature [London]*, **168**, p. 706 (1951).  
MCVETTY, P. G. *Mech. Engng*, **56**, p. 169 (1934); **162**, p. 363 (1934).  
SMITH, C. L. *Proc. Phys. Soc. [London]*, **61**, p. 201 (1948).
- (81) BRAUN, M. L. *Physics*, **4**, p. 92 (1933).  
DILLON, J. H., and PRETTYMAN, I. B. *J. Appl. Phys.*, **16**, p. 159 (1945).  
EVERETT, F. L. *Physics*, **4**, p. 120 (1933).  
FILON, L. N. G., and JESSOP, H. T. *Phil. Trans., A*, **223**, p. 89 (1923).  
GLANVILLE, W. H. *Struct. Engng*, **11**, pp. 54, 143 (1933).  
MCHENRY, D. *Proc. American Society for Testing Materials*, **43**, p. 1069 (1943).  
SAAL, R. N. J., and LABOUT, J. W. A. *J. Phys. Chem.*, **44**, p. 149 (1940).  
STEINBERGER, R. L. *Text. Res. J.*, **6**, p. 325 (1936).
- (82) KENNEDY, A. J. *J. Mech. Phys. Solids*, **1**, p. 172 (1953).
- (83) GRAHAM, A. *Research*, **6**, p. 92 (1953).
- (84) ROTHERHAM, L. *The Creep of Metals* (London: Institute of Physics, London, 1951).
- (85) SULLY, A. H. *Metallic Creep* (London: Butterworth and Co. Ltd., 1949).
- (86) ANDRADE, E. N. DA C., and CHALMERS, B. *Proc. Roy. Soc. A*, **138**, p. 348 (1932).
- (87) KENNEDY, A. J. *Proc. Phys. Soc. [London]*, **B**, **62**, p. 501 (1949).
- (88) ANDRADE, E. N. DA C., and JOLLIFFE, K. H. *Proc. Roy. Soc. A*, **213**, p. 3 (1952).
- (89) KENNEDY, A. J. *Proc. Roy. Soc. A*, **213**, p. 492 (1952).
- (90) TAMMANN, G. *Z. Metallkunde*, **30**, p. 41 (1938).  
MANINTVELD, J. A. *Nature [London]*, **169**, p. 623 (1952).  
DRUYVESTYEN, M. J., and MANINTVELD, J. A. *Nature [London]*, **168**, p. 868 (1951).
- (91) WILSON, J. E., and THOMASSEN, L. *Trans. American Society for Metals*, **22**, p. 769 (1934).
- (92) BRINDLEY, G. W. *Report of a Conference on the Strength of Solids*, p. 95 (London: Physical Society, 1948).
- (93) LEA, F. C., COLLINS, V. A., and REEVE, E. A. F. *J. Inst. Metals*, **29**, p. 217 (1923).
- (94) CHALMERS, B. *J. Inst. Metals*, **61**, p. 103 (1937).  
HENDERSON, C. *Proc. Roy. Soc., A*, **206**, p. 72 (1951).
- (95) TROUTON, F. T., and RANKINE, A. O. *Phil. Mag.*, **8**, p. 538 (1904).
- (96) GUINIER, A., and TENNEVIN, J. *C.R. Acad. Sci. [Paris]*, **226**, p. 1530 (1948).
- (97) COOK, M., and RICHARDS, T. L. *J. Inst. Metals*, **73**, p. 1 (1947).
- (98) THORLEY, N. *J. Inst. Metals*, **77**, p. 141 (1950).
- (99) CAHN, R. W. *Progress in Metal Physics*, Vol. 2, p. 151 (London: Butterworth and Co. Ltd., 1950).
- (100) GUINIER, A., and TENNEVIN, J. *Progress in Metal Physics*, Vol. 2, p. 177 (London: Butterworth and Co. Ltd., 1950).
- (101) BEILBY, G. T. *Proc. Roy. Soc. A*, **79**, p. 463 (1907).
- (102) BAILEY, R. W. *J. Inst. Metals*, **35**, p. 27 (1926).
- (103) WILSON, J. E., and THOMASSEN, L. *Phys. Rev.*, **46**, p. 337 (1934).
- (104) VARLEY, P. C. *J. Inst. Metals*, **75**, p. 185 (1948).
- (105) EGGLESTON, R. R. *J. Appl. Phys.*, **23**, p. 1400 (1952).
- (106) SLIFKIN, L., and KAUFMANN, W. *J. Appl. Phys.*, **23**, p. 746 (1952).
- (107) OWEN, E. A., and LIU, Y. H. *Proc. Phys. Soc. [London]*, **B**, **64**, p. 386 (1951).
- (108) CORRUCINI, R. J. *J. Res. Nat. Bur. Stand.*, **47**, p. 94 (1951).
- (109) YOKOBORI, T. *J. Phys. Soc., Japan*, **6**, p. 404 (1951).
- (110) COTTRELL, A. H. *J. Inst. Metals*, **66**, p. 163 (1940).
- (111) BURGERS, W. A. *Physica*, **15**, p. 92 (1949); *Proc. K. Ned. Akad. Wet.*, **50**, p. 452 (1947).
- (112) MOTT, N. F. *Proc. Phys. Soc. [London]*, **B**, **64**, p. 729 (1951).
- (113) OROWAN, E. *Z. Phys.*, **89**, p. 634 (1934).
- (114) LUDWIG, P. *Elemente der technologischen Mechanik* (Berlin: J. Springer, 1909).
- (115) HOLLOMON, J. H. *American Institute of Mining and Metallurgical Engineers. Tech. Pub. No. 2034* (1946).
- (116) OROWAN, E. *J. West Scot. Iron Steel Inst.* (1947).
- (117) HOLLOMON, J. H. *Cold working of metals*, p. 148 (Cleveland: American Society for Metals, 1949).
- (118) LESCHEN, J. G., CARREKER, R. P., and HOLLOMON, J. H. *Metals Tech.*, **15** (Publication No. 2476) (1948).
- (119) KENNEDY, A. J. *Proc. 2nd International Conference on Rheology, Oxford* (London: Butterworth and Co. Ltd., 1953); *Nature [London]*, **171**, p. 927 (1953).
- (120) MCKEOWN, J. *J. Inst. Metals*, **60**, p. 201 (1937).
- (121) HIRST, H. *Aust. Inst. Min. Met.*, **118**, p. 101 (1940); **120**, p. 761 (1940); **120**, p. 777 (1940); **121**, p. 11 (1941).
- (122) BENSON, N. D., MCKEOWN, J., and MENDS, D. N. *J. Inst. Metals*, **80**, p. 131 (1951).
- (123) COFFIN, F. C., and WEIMAN, A. L. *J. Appl. Phys.*, **24**, p. 282 (1953).
- (124) SWEETLAND, E. D., and PARKER, E. R. *J. Appl. Mech.*, **20**, p. 30 (1953).
- (125) FOLEY, F. B. *Metal Progr.*, **51**, p. 951 (1947).
- (126) BURGHOF, H. L., and MATHEWSON, C. H. *Trans. Amer. Min. Metall. Engrs*, **143**, p. 45 (1941).  
GENSAMER, M., and MEHL, R. F. *Trans. Amer. Min. Metall. Engrs*, **131**, p. 372 (1938).

## Summarized proceedings of a meeting on radiation protection— London, January 1953

A joint meeting of the Industrial Radiology Group of The Institute of Physics and the Hospital Physicists' Association was held at The Royal Institution, London, on 16 and 17 January, 1953. The papers presented and the discussion on them are summarized; they were concerned with radiation protection, medical and industrial aspects of the subject and methods of personnel monitoring.

### MEDICAL AND INDUSTRIAL ASPECTS OF RADIATION PROTECTION

The first session was opened by the chairman, Dr. C. SYKES, President of The Institute of Physics, who emphasized the importance of the subject under discussion, having particular regard to the rapid expansion that has occurred in the application of radiology to industry. In this field it is necessary to employ all types of labour, and these are inevitably brought into contact with the radiological work. In these circumstances it is essential that simple and easily administered codes of practice should be prepared without delay. These codes should aim at making industrial radiology as foolproof as possible.

The first paper was presented by Dr. J. F. LOUTIT (Director of Medical Research Council, Radiobiological Research Unit, Atomic Energy Research Establishment, Harwell) who took as his title "Medical, Biological and Haematological Aspects of Radiation Protection." He described the factors which need to be considered in deciding maximum permissible doses and gave details of the injuries which result from excessive exposure to ionizing radiations.

He pointed out that the International Commission on Radiological Protection in its last report (1950)<sup>(1)</sup> had revised the tolerance figure for X- and  $\gamma$ -rays, had added some new figures for various other forms of ionizing radiation and had generally extended the scope of its recommendations. The new figures were based very largely on evidence presented by the British delegation, led by Sir Ernest Rock Carlŕing. This delegation, drawn from members of the M.R.C. Protection Committee, had considered the extensive medical and biological data available. In this context, by medical is meant information derived from human subjects, largely from the field of occupational medicine and by biological information resulting from planned experiment in the laboratory, either on animals or on plants and lower forms of life. As disorders of the blood frequently result from radiation damage, the haematological aspects bulk largely in both the medical and biological sides. In weighing the evidence, by far the greatest account was placed on that derived from the human sources.

In assessing the effects of X- and  $\gamma$ -radiation, the delegation took note of the following factors:

(a) *Superficial injury.* There was medical evidence from the early radiation workers. Acute overexposure resulted in severe skin burns. Chronic overexposure led to "radiodermatitis," an atrophy of the skin, and in some cases to cancerous transformation.

(b) *General effects on the body, particularly blood and blood-forming organs, e.g. the production of anaemia and leukaemia.* Overexposure, both acute and chronic, has caused, in extreme cases in man and animals, destruction of the haemopoietic tissues in the bone marrow and lymphatic system, causing death from aplastic anaemia: in the less severe instances there has been impairment of health resulting from the inadequacy

of the circulating elements of the blood, red cells or white cells or both. Occasionally, instead of depression of cellular activity, stimulation of an abnormal type (leukaemia) occurs. This, if not a true malignancy, is very akin to it.

(c) *The induction of malignant tumours.* Here again, both in man and in animals, it is well established that malignant changes can be induced by penetrating radiation, not only in blood-forming tissues but in other deep-seated tissues.

(d) *Other deleterious effects, including cataract, obesity, impaired fertility and reduction of life span.* This heading embraces a number of effects that have been reliably recorded in experimental animals under appropriate conditions. For some of these, there is good evidence of their occurrence in man.

(e) *Genetic effects.* The evidence is wholly biological. In many forms of life, from the mouse down to bacteria, it can be shown that "mutation" can be readily induced by radiation, and the great majority of these mutations lead to a lowered resistance to the perils of existence. The risk in this form of damage is not to the individual but to future generations.

As long as industry is concerned only with X-rays, or with sealed radioactive materials emitting  $\beta$ - or  $\gamma$ -radiation, adequate protection should always be attainable by the use of appropriate amounts of screening. A far more difficult problem is involved when radioactive materials are used in an "open" condition and are thus liable to be ingested or inhaled. This state of affairs exists now in many experimental laboratories and in a few industries. Industry in the past has provided medical evidence of the hazards, and the biological laboratory is providing confirmation. The calculated tolerance concentrations are derived chiefly from the following medical evidence.

(a) The miners of the Schneeberg in Saxony and Joachimsthal in Bohemia died very largely from cancer of the lung. This is now generally attributed to the continued inhalation of radon, produced in the radium-bearing ores in these mines, and present in a concentration of about  $10^{-9}$  curie per litre of air.

(b) The luminizing industry in the U.S.A. had an unfortunate medical record after the First World War. In that country it was the practice of the girl operatives to point the brushes with their lips. The traces of radioactive paint thus swallowed, and also probably inhaled as dust, produced anaemias and bone disorders, both of which were often fatal. An ultimately lethal dose of retained radium may be as low as one microgramme. From figures such as these it is easy to see that protective precautions with open sources of the wide variety of radioactive substances now available must be both elaborate and expensive.

The second paper was given by Mr. W. BINKS (Director of the National Radiological Protection Organization) and was entitled "General Review of Radiological Protection Problems." He pointed out that the main difference between



most occupational hazards and radiation hazards is that the effects of the latter are delayed—sometimes for years. Accordingly, the approach to protection problems, which arise both from the multiplicity of the applications of X-rays and radioactive isotopes and from the growing numbers of persons involved, must be based not upon the evidence of the few cases of injury appearing at the moment, but upon the knowledge of the ill effects which will ensue if reasonable and practicable precautions are not taken. The aim of radiation protection authorities should be to guide users of ionizing radiations to an appreciation that, by taking certain simple measures, injuries can be avoided and that there is no justification either for fear on the one hand or carelessness on the other.

The effects produced in living tissues by electromagnetic radiations (X- and  $\gamma$ -rays) and by corpuscular radiations ( $\alpha$ -rays,  $\beta$ -rays, electrons, neutrons, protons, etc.) are related to the ionization which such radiations produce. It is thus current practice to express, in terms of the ionization unit of dose (the röntgen), the maximum exposures to various types of radiation which may be received without injury. The International Commission on Radiological Protection recommended, in 1950,<sup>(1)</sup> certain permissible exposure levels both for external irradiation of the body and for internal irradiation due to inhaled or ingested radioactive substances. The basic figure which is believed to be appropriate for X- and  $\gamma$ -rays is 0.3 röntgen per week at the critical tissue. For other ionizing radiations, allowance has to be made for biological efficiencies relative to X- or  $\gamma$ -rays. Thus, in the case of  $\alpha$ -particles, for like quantities of absorbed energy per gramme of tissue, the biological effect is about twenty times that produced by X-rays. A factor of ten applies in the case of protons and fast neutrons.

In the case of external radiation, adequate protection can sometimes be achieved by distance alone but, in general, a combination of screening and distance is necessary. Mr. Binks showed that, on the basis of available experimental data and of our knowledge of the fundamental physical processes of radiation absorption, it is possible to calculate the protection required for different qualities and quantities of radiation. The importance of scattered, as well as of direct, radiation was stressed. The greater the energy of the radiation emitted by the source, the thicker is the protective shield required and the more important is the part played by multiple scattering. Examples were given which showed that, in some cases, the amount of scattered radiation generated in a shield is many times greater than the direct radiation transmitted through the shield.

As regards the permissible amounts of radioactive materials which may be taken into the body, there is the clinical evidence of the effects of radium, mentioned by Dr. Loutit. This provides a basis for calculating the amount of other bone-seeking substances which, after making allowance for their different energy emissions and for their relative biological efficiencies, would produce the same rate of energy absorption in tissue as the permissible quantity of radium (0.1 microcurie). For substances which are not bone-seeking, the equivalent energy absorption is taken to be 0.3 r per week. Starting from the value for the maximum permissible level of any radioactive material in the body, the maximum concentration in the atmosphere or in drinking water can be calculated from a knowledge of (1) the fraction which is retained in the body, (2) the rate of elimination from the body, and (3) radioactive decay. Values for eleven materials were given in the 1950 Recommendations<sup>(1)</sup> and since then, as a result of the efforts of American and British workers, the number has been raised to about eighty.

In working with radioisotopes, the aim should be to keep the deposition as low as possible by adequate ventilation and by enforcing strict personal care and cleanliness.

The necessity for radiation monitoring and periodic blood and general medical examinations was then stressed. This might be questioned on the grounds that the protection afforded by shields or by ventilation could be assessed once and for all. There are, however, many operations which involve exposure under conditions in which full protection is impracticable, for example, in handling radioisotopes or in adjusting specimens or patients under X-ray tubes which are provided with shutters and are continuously excited. Furthermore, one must safeguard against the development of defects in protective equipment.

Finally, reference was made to recent developments in this country to co-ordinate, through a central radiological protection organization, which Mr. Binks had been invited to direct, the efforts of the various authorities who have assumed responsibility for guiding radiological workers in protection problems. Advances in radiological techniques call for simultaneous advances in our codes of practice and in their implementation. The assessment of maximum permissible levels, based upon clinical and laboratory evidence supplied by hospital research groups and by radiobiological research units, is undertaken by the Medical Research Council's Committee on Protection against Ionizing Radiations. These levels form the basis upon which codes of practice or regulations can be evolved by the Ministries responsible. It is envisaged that the new central organization will assist all in ensuring implementation of the codes, by advising on plans of radiological departments and by providing monitoring services for both external and internal radiation.

Having received these two reviews covering the basic medical and physical factors and the organization set up to deal with protection problems in this country, the meeting then turned to practical protection problems in industry. The first speaker on this topic was Dr. H. HARRIS (Babcock and Wilcox Ltd.) who said that radiology must be regarded as merely another tool in the factory. It should not be necessary for the safe running of an X-ray set to have a deep knowledge of the physics of the subject, nor of the medical and biological effects of the radiation. Some principles and some data are all that are required. The type of literature in which these may be found is often not easily accessible to the factory manager and in many cases such information as can be disentangled is rather incredible and unpractical. The data are almost entirely concerned with protection from the direct beam, which in industrial work is generally sufficiently attenuated in the specimen under examination. Protection from scattered radiation is the prime necessity and although this is less exacting than the direct beam, very few data are so far available. In these circumstances the use of personnel monitoring techniques provides an invaluable check. Dr. Harris concluded by asking that care should be taken that any regulations to be introduced would not make industrial radiology more cumbersome than is really necessary.

The next speaker was Mr. K. L. GOODALL (H.M. Inspector of Factories, Engineering and Chemical Branch) who explained the inspection and monitoring work of H.M. Factory Inspectorate in the protection of factory workers against radiation hazards, mentioning the free blood count service run by his Department.

The Factory Department had some time ago drafted a set of regulations to cover the industrial use of X- and  $\gamma$ -rays (as a supplement to the Luminizing Regulations which have been in force for ten years) and Mr. Goodall explained the



various reasons why these draft regulations have not yet been given statutory force. He was convinced that they would eventually be made law, but inspections and the Department's study of the results of thousands of blood counts indicated that, at present, industrial conditions in this field are extremely satisfactory and that most firms are doing voluntarily nearly all they could be required to do by regulation. A Departmental pamphlet has been prepared and would be issued shortly on "The Industrial use of Ionizing Radiations," giving guidance on the hazards and necessary precautions which should be taken in radiography, fluoroscopy and crystallography, and in the use of radioactive materials for static elimination, thickness gauging and tracer work.

Mr. Goodall then gave a brief account of some of the lessons he had learned from his own inspections of luminizing and radiology departments. Of all industrial radiation workers, the radium luminizers, using unsealed sources, still cause most concern and work closest to the safety limits. With  $\gamma$ -ray radiography, almost complete protection is at least possible, but the use of personal dosimeters is not yet as widespread as it should be. He had observed a tendency to overload protective containers, of which more should be commercially available for  $^{60}\text{Co}$  and  $^{182}\text{Ta}$  sources of activity greater than 0.5 curie. A more widespread use should be made of distinguishing orange markings for all containers housing industrial radioactive materials. He also advocated a greater use of portable lead screens and of lead diaphragms or cones with the high-voltage mobile X-ray sets used in open workshops.

In conclusion, Mr. Goodall said that the Factory Inspectorate could do much to ensure that proper protective facilities are provided, but good supervision coupled with the training of the workers is vital if these facilities are to be properly maintained and used.

The use of radioactive isotopes for industrial radiography was then discussed by Dr. J. S. BLAIR (Stewarts and Lloyds Ltd.). He said that his firm had been using these materials in considerable strengths for the past three years and the secret of satisfactory protection was rigid discipline. This involves the constant checking of the intensity of local radiation by means of dose-rate monitors, and then providing the personnel, who should be skilled, with electrometer dosimeters to be carried on the wrist. Thereafter, the keeping of records of dose, monthly blood counts, etc., would ensure satisfactory control.

A brief description, illustrated by slides, of the methods used by his firm was then given, the various types of containers, and the methods of handling and storing the isotopes being shown.

Dr. Blair considered that the estimation of health from blood counts is unsatisfactory, as by the time damage has been revealed, it is probably too late to do much about it. He thought that earlier medical evidence might be obtained by studying the finger-print pattern, although overdosage should have been evident already from the data provided by the personal dosimeters.

The next speaker was Commander P. CHANDLER (Inspectorate of Naval Ordnance) who said that it was necessary for him to use relatively unskilled people as radiographers and a very strict discipline backed by elaborate safety devices was required to ensure their safety. As a check on exposure to radiation, he preferred ion chambers or pocket electrometers to film monitoring, in view of the delay before the results of the latter technique are known. He was of the opinion that, at the general level of dose received, members of the general medical profession were frequently too dogmatic in ascribing

blood count anomalies in workers as being due to the effects of overexposure to radiation.

Mr. SCHALL (Solus-Schall Ltd.), Chairman of the Industrial Radiology Group of the Institute of Physics, brought the first session to a close by stating that the views expressed had amply confirmed the contentions of the Group Committee. It was evident that the good firm, or the large firm, took reasonable precautions, but the practice of radiology has spread to many small organizations, having fewer facilities and less skilled personnel. For the benefit of these firms and their workpeople protection regulations appear to be necessary and it is important that these regulations should be in a form that is intelligible to all.

#### PERSONNEL MONITORING

The second session was opened by the Chairman, Dr. L. H. S. CLARK, President of the Hospital Physicists' Association, who presented a paper entitled "Some Radiation Protection Measurements by Diverse Means." He began by giving an account of the film monitoring service which he and Mr. D. E. A. Jones inaugurated at Lambeth Hospital in 1936. Specially packed dental films were worn for a week in lead cassettes which screened a part of the film from X-rays. The dose received by each film was assessed by subjecting the previously unexposed portion to known quantities of X-rays of a similar quality. Results published in 1943<sup>(2)</sup> on approximately 2000 films worn in four different hospitals showed that 90% received less than 0.2 r per day (the tolerance dose then recommended). On 1 July, 1943, the scheme was extended to cover all London County Council hospitals. Every quarter the workers wore two films, each for a few days. By this means some idea was obtained of the doses of radiation being received in the X-ray diagnostic departments of 38 hospitals. When films showing densities greater than normal were returned, a protection survey was carried out at the hospital concerned. By May 1945, 1754 more films had been issued and of those returned, 98% indicated doses of less than 1 r per week. These films served as a check on the efficiency of the X-ray protection in the hospitals and of the methods of the workers. Unfortunately, the workers were not being tested all the time they were on duty. S. R. Pelc found that the slower films, Kodak and Ilford Line Film could be worn continuously for 3 months. Films of this slow type were adopted in 1945 and have been used in this service ever since. The results indicate a progressive lowering of the general level of irradiation, suggesting that the film service has exercised a cautionary influence on the X-ray staff.

Smaller finger films have been developed by T. M. Robb and R. E. Ellis<sup>(3)</sup> to measure the radiation received by the fingers during manipulations with radium. These films can be strapped to the finger and are mounted so that they will withstand scrubbing in hot water before a surgical operation. It has been found that standard X-ray film is satisfactory for doses of  $\gamma$ -radiation up to 4 r.

Ionization measurements have been made at Lambeth Hospital by W. E. Liversage of the amount of radiation received by workers in the radium department. M.R.C. protection chambers, type BD. 11, were used and the results of measurements made daily over a period of 9 months are given in Table 1.

Inconsistent results are sometimes obtained with the chambers and D. K. Bewley has made a number of experiments at Hammersmith Hospital to determine the cause. Members of the Physics Department have carried four chambers for two periods of a week, two in close-fitting plastic tubes and two loose in a cardboard box, the chambers and carriers being

interchanged for the second week. The results obtained indicate that when the chambers rattle about, there is a greater risk of inconsistent readings than when they are fixed in tubes.

Table 1.  $\gamma$ -ray protection measurements at Lambeth Hospital, March to November 1952 (9 months)

Personnel	Radium working weeks	Total dose in röntgens	Average weekly dose in mr	Maximum weekly dose in mr	Maximum daily dose in mr
Radium radio-therapist	34	2.9	85	180	115
Radium theatre anaesthetist	36	0.8	22	43	34
Radium custodian-physicist	37	4.6	125	260	123
Superintendent radiographer	36	0.9	25	62	35
Radium nurse, radiotherapy department	23	3.0	130	267	85
Radium theatre nurse	34	2.9	85	214	106

A fluorescent method is being developed by D. K. Bewley for use during screening operations in X-ray diagnostic departments, or wherever X-rays are used in a darkened room. For this purpose, small disks of Levy-West mark 48 fluorescent screen are used enclosed in Perspex cases made up like buttons. It is hoped to develop self-luminous buttons to serve as standards of comparison. Preliminary measurements have shown that when irradiated at 5 to 10 mr/h, the fluorescent buttons are just visible to a fully dark-adapted observer.

Whilst many of the early X-ray workers suffered crippling injury, there were others who suffered no damage. Dr. Clark expressed the opinion that the difference was due to the influence which the British X-ray and Radium Protection Committee had had on the mode of thought in radiology. He himself had been fortunate, during his early years as a hospital physicist, in working under the direction of an Honorary Secretary of that Committee, and despite the absence of personal monitoring devices, safe working conditions were achieved. By the foresight of the original members of the Protection Committee, we have witnessed an excellent example of preventive medicine, the value of which will grow as the story of radiology unfolds to the benefit of mankind.

The second speaker was Dr. G. SPIEGLER (Royal Cancer Hospital). His main subject was the determination of the quality of radiation, and hence the dose, from the density contrast between a filter-covered part of a monitoring film and a filter-free part. In recent experiments it has been established that this contrast, whilst being a unique criterion of the quality up to about 300 kV, may become ambiguous with higher energies.

He reported that he had frequently found contrasts on films exposed to  $\gamma$ -rays from radium and radioactive isotopes which are not accounted for by absorption in the 1.5 mm brass front filter used on the cassettes at the Royal Cancer Hospital. If these contrasts are taken as indicators of the incident radiation, a 250–300 kV radiation might be “diagnosed,” when actually  $^{24}\text{Na}$  or radium  $\gamma$ -radiation may have been used.

The ratio of the densities in the window and filter-covered parts, when plotted against energy, goes through a flat minimum at about 0.4 MeV. When the bulk of the secondary particles responsible for the high contrasts is removed, the density ratio approaches the true low value governed by the absorption of the incident  $\gamma$ -rays. This can be achieved by

placing 1 mm of lead over the window of the cassette, as such a filter absorbs many more  $\beta$ -particles than it emits.

The three years' experience gained from the film protection service at the Royal Cancer Hospital has shown that most films coming from the Radium Department and the Isotope Laboratories indicate a density contrast of about 1.4 : 1. However, on films worn by persons who stand behind thick lead screens to prepare radium applicators, the contrast is within a few per cent of unity.

Higher contrasts than 1.4 : 1 are obtained with  $\beta$ -ray emitters such as  $^{32}\text{P}$ . With a mixture of exposures involving primary  $\beta$ - and  $\gamma$ -rays, a satisfactory estimate of the respective doses can be arrived at as follows: (a) the  $\gamma$ -ray dose is determined as usual from the blackening under the metal filter; (b) on multiplying the  $\gamma$ -ray dose by 1.4, the average value of  $\gamma$ -ray dose plus secondary  $\beta$ -ray dose at the window is obtained; (c) by subtracting this value from the total dose appearing in the window, the primary  $\beta$ -ray dose is obtained. A mixture of diagnostic radiation or soft scattered radiation from conventional therapy beams and  $\gamma$ -radiation can be dealt with in the same way.

The third paper was entitled “Pocket Ionization Chambers,” and was presented by Dr. E. D. DYSON (Atomic Energy Research Establishment). He opened by detailing the requirements of monitoring chambers, namely, adequate sensitivity, reliability and freedom from quality dependence, comparing them with film badges in these respects. Two types of pocket ionization chamber instruments have been developed for personnel monitoring, the condenser chamber, e.g. M.R.C. type BD.11, and the direct reading quartz-fibre electroscop, e.g. A.E.R.E. type 1183A. Condenser chambers require a special electrometer to measure their charge, such as Baldwin-Farmer electrometers, types RB and MF. Direct reading electroscopes require a voltage source for charging purposes, and various types were described.

Design requirements and typical operating characteristics of these pocket instruments were detailed, and comparisons with American instruments were given. The type BD.11 condenser chambers have a voltage sensitivity of about 600 V/r. Their natural leakage is less than 1% in 24 hours. The air-wall material used gives energy independence to within  $\pm 10\%$  for radiation energies between 100 keV and 2 MeV. Type 1183A quartz-fibre electroscopes measure up to 500 mr with a natural leakage rate up to 2% in 24 hours. Energy dependence is within  $\pm 15\%$  down to about 90 keV X-rays.

Dr. Dyson concluded by outlining the organization of personnel monitoring and record keeping at A.E.R.E.

The final paper of the session was given by Mr. E. E. SMITH (National Physical Laboratory). It dealt with the N.P.L. Film Dosage Service and gave details of its origin, the methods used and the results obtained during the ten years of its existence. The service for medical workers commenced in November 1942, at the request of the Ministry of Health, and that for Industrial and Research workers in April 1943, at the request of the Ministry of Labour and National Service. Films were chosen as the medium of test as the use of ionization chambers was considered to present too many difficulties. The chief disadvantage of films lies in the considerable quality dependence exhibited, whereby sensitivity varies over a range of some 15 to 1. This difficulty is partially overcome by issuing a card with each film which, when completed and returned, gives details of the range of qualities involved, so that a maximum figure for the dose can be assessed. In some circumstances the margin of uncertainty may be considerable, but in most cases, e.g. that of diagnostic



radiographers, the result is unlikely to be in error by more than a factor of two. The value given in the report is always the worst interpretation, considering the range of qualities involved, and thus the results are always stated as "less than" the figure given. If the film tests reveal unsatisfactory conditions, an inspection is arranged in order that the causes may be discovered and remedies suggested. Two types of film are used at the present time, PM1 for radiations above 500 keV and PM3 for those below. Each PM1 film is half covered with 1 mm lead in order to eliminate  $\beta$ -radiation, and to provide an additional basis of assessment in cases where radiations of mixed qualities are involved.

The policy has been to keep the methods as simple as possible and not to introduce elaborate devices for the more accurate assessment of dose. The accumulation of returned films is processed under reasonably standard conditions in three batches every week. Standard films, which have been given known doses at two or more qualities, are developed with each batch. The blackenings of the test films are then assessed in terms of dose with the aid of the standard films and the details given on the record cards, and reports are issued. The inclusive fee at the outset was fixed at 2s. per film and, by virtue of the numbers involved and the simplicity of the methods, this still obtains to-day.

The number of films issued reached a peak of over 5000 per month in 1948 when the Atomic Energy Establishments were included in the scheme. Subsequently, as these Establishments took over their own work, the figure fell but, apart from this, the general trend over the years has been a steady rise. The present level, despite the introduction, in 1951, of a fortnightly, instead of a weekly, period of test, is about 2500 industrial and 600 medical films per month. The total number issued since the service began is about 150 000.

In an analysis of the results obtained, which is reproduced in Table 2, it is shown that a marked improvement has taken

Table 2. Analysis of results of N.P.L. radiation monitoring tests

Dose received (in r per week) (Report values)	Percentage of workers in radiation group			
	Medical Up to 1950	1951-52	Industrial and Research Up to 1950	1951-52
Less than 0.05	53.0	66.4	67.7	71.7
0.05 to 0.1	18.6	16.0	15.2	12.8
0.1 to 0.2	12.6	10.7	7.3	8.0
0.2 to 0.3	6.5	3.4	2.3	4.5
0.3 to 0.4	2.8	1.3	1.4	1.2
0.4 to 0.5	1.3	1.2	1.1	0.9
Greater than 0.5	5.2	1.0	5.0	0.9

place since the commencement of the service. This is due, in part, to the clearing up of bad cases, but the fact that people, in general, are now more protection conscious than before cannot be ignored.

The discussion was opened by Mr. PIERCEY (English Electric Co. Ltd.) who said that the avoidance of radiation was the most satisfactory principle to adopt. Personnel monitoring should be used only to obtain a measure of the efficiency of shielding, and laboratories should be made safe before work started in them. The speaker expressed surprise at the way in which stray radiation seemed to be accepted as normal in hospital work.

Mr. LOATES (G. A. Harvey and Co. Ltd.) expressed agreement with the previous speaker. He considered that all apparatus should be inherently safe and that this should be made the responsibility of the manufacturer. He suggested that all industrial radiology laboratories should be inspected by an independent body before being occupied.

Mr. W. BINKS, in reply, said that there is no fundamental difference between industrial and medical protection problems. In both cases it is occasionally necessary to receive higher doses than the specified maximum permissible value. Manufacturers can only make equipment safe under average conditions; careless operation, or a particular technique, could defeat all attempts to provide protection. He drew attention to the necessity for accurate absorption data, particularly in the case of the very high voltage X-ray equipment installed in some industrial establishments for the examination of articles of considerable size. This type of work involves buildings of large dimensions, where the provision of unnecessary protection adds considerably to the cost. In these cases there must be protection but not over-protection.

Mr. G. S. INNES (St. Bartholomew's Hospital) pointed out that a knowledge of the quality of the radiation was essential for the estimation of the dose. He questioned some of the 50 kV results quoted by Dr. Dyson for pocket dosimeters. Dr. DYSON, in reply, gave some calibration figures which showed that the multiplying factor was varying rapidly in the region in question. The factors were 1.15, 0.92, 0.84, 0.82 and 0.88 for 55, 90, 110, 150 and 195 kV (constant voltage) X-rays, respectively.

Mr. G. SYKE (Baldwin Instrument Co. Ltd.) referred to the fact that the use of thickness gauges and static eliminators involved different risks from those occurring with sealed sources in industrial radiology. Very lightly screened  $\beta$ -ray sources are employed in these instruments and thorough protection is required if hazards are to be avoided. Mr. P. TOTHILL (Mount Vernon Hospital) said that Dr. Spiegler had over-simplified the problem of dose assessment with films, as he had considered the case of only two different qualities of radiation. Frequently, three or more qualities are involved, and the accurate assessment of the dose is a most difficult matter. He then asked for information regarding the value for the maximum permissible dose which is applicable to film monitoring tests, 0.3 r in free air or 0.5 r with backscatter.

Dr. SPIEGLER agreed that he had, in the interests of brevity, over-simplified the problem. He thought that some measure of the energy of the radiation could be obtained by the methods to which he had referred in his paper. He thought that 0.3 r per week was applicable to film badges in cassettes which largely eliminate backscatter. Mr. E. E. SMITH emphasized that the N.P.L. film service dealt with external establishments and the basis of the dose assessment was the information provided on the record card, which frequently was very meagre. In the circumstances, high accuracy or elaborate procedures were not possible. If, in the case of highly mixed radiations, there was a possibility of over-exposure, separate films might be issued for each particular type of work. As regards the value taken for the maximum permissible dose, metal cassettes are not employed in the N.P.L. scheme, hence the films record backscatter, and in these circumstances 0.5 r per week is applicable.

The meeting was then terminated by Dr. CLARK who expressed the thanks of the Hospital Physicists' Association to the Industrial Radiology Group of The Institute of Physics for co-operation in arranging the meeting.

E. E. SMITH

#### REFERENCES

- (1) Recommendations of the International Commission on Radiological Protection. *Brit. J. Radiol.*, **24**, p. 46 (1951).
- (2) CLARK, L. H., and JONES, D. E. A. *Brit. J. Radiol.*, **16**, p. 166 (1943).
- (3) ROBB, T. M., and ELLIS, R. E. *Brit. J. Radiol.*, **25**, p. 100 (1952).



# The adaptation of an electron microscope for reflexion and some observations on image formation\*

By M. E. HAINE, M.Sc., A.Inst.P., and W. HIRST, Ph.D., F.Inst.P., Research Laboratory, Associated Electrical Industries Ltd., Aldermaston, Berkshire

[Paper first received 3 February and in final form 27 February, 1953]

Designs are described of modified mechanical stage arrangements to allow the type E.M.3 electron microscope (by the Metropolitan-Vickers Electrical Co. Ltd.) to be used for the glancing angle "reflexion" technique.

The theoretical limit of resolution is discussed. For the experimental conditions used, a resolution of about 400 Å would be expected. The actual resolution obtained agrees with this figure.

The surfaces of solids opaque to electrons may be imaged directly by bombarding the surface with an electron beam and focusing the scattered electrons. Ruska<sup>(2)</sup> first attempted to do this using an angle of 90° between the incident and scattered beams. The resolution was poor, about 20 to 30  $\mu$ , but later von Borries and Janzen,<sup>(3)</sup> by reducing the angle of deviation of the beam to 8°, achieved a resolution of a few hundred Ångström units. However, the use of an oblique angle of viewing led to distortion and the direct method of surface examination soon became superseded by the replica method which does not have this disadvantage. Recently interest in the direct method has been revived in several laboratories in this country and in France and Russia. Its compensating advantages are: (1) direct observation permitting the study of surface changes whilst they are occurring; (2) the convenience of the method for the examination of the surface profile, particularly when the slopes of the surface asperities or hollows are small; (3) the appearance it gives of the surface when viewed and illuminated at angles comparable with those used in electron diffraction, thus providing information which should facilitate the interpretation of electron diffraction patterns.

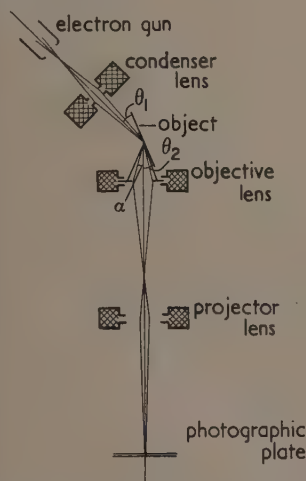


Fig. 1. Schematic representation of reflexion electron microscope system

The method strictly comprises a dark field technique and the image is formed by electrons scattered by atomic nuclei

\* Based on a paper (one of four on the subject) presented to a Conference of the Electron Microscope Group of The Institute of Physics held in Bristol in September, 1952. The papers were largely complementary and a summary of them was published in the January, 1953, issue of this *Journal*. One paper has been published in full elsewhere.<sup>(1)</sup>

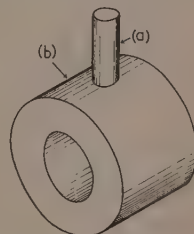
in or just below the surface of the solid being examined. Fig. 1 shows schematically the arrangement used:  $\theta_1$  is the incident glancing angle,  $\theta_2$  the viewing angle and  $\alpha$  is the semi-angular aperture (as defined by the aperture stop) of the scattered beam entering the objective lens. In this paper the direct method of surface examination is described as a "reflexion" method, but it should be understood that this conventional terminology is misleading; the formation of the image by scattered electrons leads to a dependence of the resolving power, the image intensity, and the image contrast upon  $\theta_1$ ,  $\theta_2$  and  $\alpha$  in a manner different from that to be expected were the image formed by specular electron reflexion. This paper describes modifications to a standard commercial electron microscope to enable it to be used as a reflexion instrument and discusses the mechanism of image formation in some detail.

## DESIGN OF THE REFLEXION ADAPTOR

The electron microscope was a standard type E.M.3 electron microscope<sup>(4)</sup> by Metropolitan-Vickers Electrical Co. Ltd. The adaptor was designed to take specimens whose wear characteristics were being studied in a pin and ring type apparatus; the types of specimen are illustrated in Fig. 2.

Fig. 2. Pin and ring type wear specimens

- (a) Flat ended  $\frac{1}{8}$  in. diameter pin, loaded against ring.
- (b) Ring  $\frac{1}{8}$  in. diameter.



The holders for the  $\frac{1}{8}$  in. diameter pins may be used as a mount for flat specimens and by minor modifications other shapes of specimen might easily be used.

The modification to the microscope is fairly simple and is achieved by replacing the existing mechanical stage by one of two alternative stages designed to hold the two standard types of wear specimen. The ring can be mounted in one holder to observe its periphery with the beam perpendicular to the ring axis or in the other to observe the periphery with the beam axis parallel to the ring axis. The end of the pin can be observed in the second of these holders. The two holders are shown (in plan and elevation) in Fig. 3.

Fig. 3a shows the arrangement for observing the test ring with the electron beam perpendicular to the ring axis. The block (1) is the main stage, movable in two perpendicular directions by the normal stage drives (2) with a spring return (3). (The standard transmission arrangement for the stage

drives has been described elsewhere.<sup>(4)</sup> The stage is held down against the top of the lens by two leaf springs (4) which can be swivelled about the screws (5) when removing the stage. The ring specimen (6) fits on to a horizontal mandril (7) attached to the stage block with its axis parallel to one stage drive. The mandril and hence the ring can be rotated through a small angle by a lever (8) driven by a crank (9) attached to

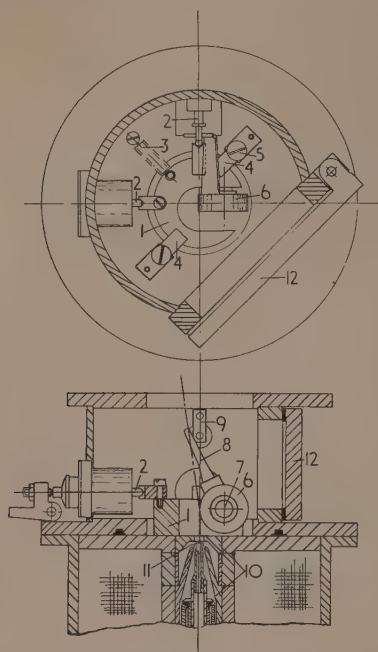


Fig. 3(a). Mechanical stage for ring specimen (observation perpendicular to ring axis)

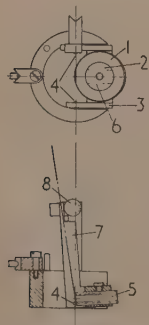


Fig. 3(b). Mechanical stage for ring (observation parallel to axis), pin, or similar specimens

a shaft leading out of the object chamber to a control knob. This shaft is fitted in place of the normal stereo-control in the standard instrument. Thus searching of the object is carried out by one stage drive and the tilt control. The other stage drive is used to adjust the position of the object with respect to the imaging axis. The rather crude rotation arrangement for one search co-ordinate would be a disadvantage in normal microscopy but, in observing continuous surfaces over which a very fair degree of structure uniformity exists, it represents no serious hindrance. The objective lens pole

pieces (10) and the centrable aperture (11) are also shown in Fig. 3a.

Fig. 3b shows the arrangement for observing the end of the pin or the ring with the electron beam parallel to its axis. The ring (1) (shown in the plan only) is mounted on a vertical mandril (2) attached to a stirrup (3) which is pivoted on pins (4) giving a tilt centred on the point of intersection of the beam and the object. The pin specimen (5) (in the elevation) can be mounted in a diametrical hole (6) in the mandril. The tilting stirrup is controlled through an attached lever (7) bearing against a cam (8) which is operated by the rotation of the control previously mentioned. This control is used to vary the angle between the object and the beam. Searching is only possible in one direction unless the focus is altered at the same time as the second traversing control. This, in fact, can be done quite easily.

The operation of the adapted object stages is quite simple. The normal transmission stage can be removed and either of the reflexion stages fitted in a few minutes through the object chamber door (12) in Fig. 3a.

The normal electron gun alining mechanism fitted to the type E.M.3 instrument only allows a tilt of a little over 2° from the instrument axis. To obtain greater angles for the present work a 6° tapered block was at first fitted between gun and object chamber. This was later replaced by a modified alining mechanism similar to the standard one but allowing a continuous tilt up to 12°.

An objective aperture is an essential feature in the reflexion technique. The standard adjustable aperture holder fitted to the instrument was used with a 75  $\mu$  aperture.

#### RESOLVING POWER

The resolving power obtained in the reflexion microscope falls short of that obtained in the transmission instrument by about an order of magnitude. The principal cause is the relatively large energy spread in the scattered electron beam and the chromatic aberration of the imaging lens.

In the transmission instrument, the object is normally thin and the object support can be made sufficiently thin to keep the energy loss to a few tens of electron volts at the most. In the reflexion instrument, on the other hand, the effective object thickness is determined not by the amount of scattering material in the object but by the distance travelled in the object by the electrons which are scattered into the objective lens aperture. Such electrons must be scattered through a total angle of  $(\theta_1 + \theta_2)$  ( $\sim 6^\circ$ – $10^\circ$ ). The fraction of the illuminating beam which will be singly scattered through this angle is small compared with that multiply scattered. Multiple scattering theory in its present form can only be applied to this problem in a very approximate manner, but it suggests that, on the average, electrons must travel several hundred Ångström units in a metal (e.g. iron) to account for the measured fraction scattered through an angle of 8°. In penetrating such a distance, a spread of energy loss of several hundred electron volts will result.

An approximate measurement was made of the energy spread by imaging a straight edge illuminated with the scattered electrons and measuring the defocusing produced at the edge of the image field by the chromatic difference in magnification. The measurement gave a spread of half value between 100 and 200 V. A value of 100 V has been given by Kushnir and others<sup>(5)</sup> who also evaluated the resulting resolving power  $d$  from the well-known expression

$$d = C_c \frac{\delta V}{V} \quad (1)$$

where  $C_c$  is the chromatic aberration constant of the objective lens, and is very nearly equal to the focal length except for very strong lenses,  $\alpha$  is the objective semi-angular aperture and  $\delta V/V$  is the fractional spread in electron energy. Kushnir and others put in values of  $C_c$  ( $K_0$  in their paper) = 0.7 cm,  $\alpha = 0.005$  and  $\delta V/V = 1/800$  giving  $d = 430 \text{ \AA}$ . These values are very close to those used in the apparatus described earlier. The resolution obtained agrees reasonably with the figure just given.

This resolution need not be regarded as the final limit even for an energy spread of 1/800. Improvement should be possible either by reduction of  $C_c$  or  $\alpha$ . On reducing  $\alpha$ , a limit would ultimately be reached where diffraction overrides the effect of chromatic aberration. Hence a minimum resolution will be obtained at some optimum aperture angle. Simple calculation shows the optimum aperture angle to be given when:

$$\alpha = [0.5\lambda/C_c(dV/V)]^{1/2} \quad (2)$$

The minimum resolution is then given by:

$$d_{min} = (C_c \lambda dV/V)^{1/2} \quad (3)$$

The minimum value of  $C_c$  has been given by Liebmann<sup>(6)</sup> as about 0.07 cm. With an energy spread of 1/800 and  $\lambda = 0.05 \text{ \AA}$ , the optimum angle is then  $1.7 \times 10^{-3}$  and minimum resolution 21  $\text{\AA}$ .

The use of so short a focal length lens severely restricts the space available for the object, calls for an extremely small physical limiting aperture ( $\sim 2.5 \mu$ ) and, since the object must now lie in the magnetic field of the lens, magnetic specimens could not be used.

Using the more reasonable value of  $C_c$  (and hence focal length) of 0.7 cm, the optimum aperture now becomes  $5.4 \times 10^{-4}$  and the resolution 66  $\text{\AA}$ . The physical aperture is now about 7  $\mu$ . Practical difficulty now arises because of loss of intensity which falls off as the fourth power of the resolution if the magnification is kept in inverse proportion to the resolution. (An aperture angle reduction of  $n$  times reduces the image intensity by  $n^2$  and gives a gain in resolution of  $n$ . If, to distinguish these details on the photographic plate, the magnification has then to be increased  $n$  times, the total diminution in intensity becomes  $n^4$ .) The intensity of the reflected image is already less than a transmission image by an order of magnitude owing to the low probability of any electron being scattered into the aperture. A typical exposure in the present apparatus lasts for 2 sec at a magnification of  $\times 1500$  with critical condenser focus.

It is also probable that contamination of the solid surface in the electron beam might tend to restrict resolution when using the very long exposures necessary when the image intensity is low. Contamination can be greatly reduced by heating the specimen to about 200° C as has been found by Ennos.<sup>(7)</sup> The effect of contamination is easily seen on a reflexion specimen as the illuminated area rapidly becomes covered with a brown-black deposit. An interesting secondary effect of this contamination is mentioned below in the section on contrast.

Scherzer<sup>(8)</sup> has described a method of correcting chromatic aberration by the use of a non-axially symmetric lens system comprising two crossed cylindrical lenses with special corrector elements. The use of such a system might open up new possibilities for the reflexion technique.

Ultimate resolution will of course be limited by spherical aberration, and it is possible that a higher limit might be set by the effects of penetration of electrons into the object.

## FIELD OF VIEW

The field of view which lies within the depth of focus in the reflexion system is severely limited in the direction along the plane of incidence due to the obliquity of the object.

The extent  $D$  over which the resolution is within a factor of two of the best value is given by:

$$D = \frac{d \times \theta_2}{\alpha}$$

where  $d$  is the on focus resolution and  $\alpha$  the semi-angular aperture as before.

Thus, it can be said that the number of resolved object points  $n$  in this direction is equal to  $\theta_2/\alpha$ .

From equation (1)

$$\alpha = d/C_c(\delta V/V)$$

and putting  $C_c = 0.7 \text{ cm}$ ,  $\delta V/V = 1/800$  and  $\theta_2 = 4^\circ \simeq 0.07$  gives  $n = 6300/d$  ( $d$  in Angström units).

The table shows the resulting field of view in terms of the number of resolved object points in focus and its actual value on the image for a magnification sufficient to make the resolved distance equal 0.2 mm.

Field of view			
$d$ $\text{\AA}$	$n$	Magnification	$D$ mm
1000	6.3	2000	1.26
500	12.6	4000	2.52
250	25.2	8000	5.04
50	126	40000	25.2

The extent of this limitation is at once apparent.

## CONTRAST

Shadows will arise when either hills or valleys are present provided their sides slope sufficiently steeply. For a hill with vertical sides, the height  $h$  is related to the length  $l$  of the shadow in the image by the expression

$$l/h = m_{\perp} \frac{\sin(\theta_1 + \theta_2)}{\sin \theta_1}$$

$m_{\perp}$  denotes the magnification in a direction perpendicular to the plane of incidence. Kushnir and others<sup>(5)</sup> and Menter<sup>(1)</sup> give an incorrect expression for the ratio  $l/h$ .

Consider the types of surface detail shown in Fig. 4. In each diagram a parallel electron beam enters from the left, the "reflected" beam being observed through the electron optical system away to the right. Each incident ray is given a corresponding scattered ray on the initial assumption that the scattering intensity is independent of angle. Under these conditions, the intensity distribution obtained at the right of each diagram corresponds to that which the eye will finally see. It will be noted that detail (b) would not be seen, but details (a), (c), (d) and (e) would all give shadows. Details (a), (c) and (e) throw similar shadows and are indistinguishable; (d), a relatively narrow groove would, however, be distinguishable because the shadow length does not change when the angle of the incident beam is altered. It is unlikely that many details will actually have perfectly sharp edges and more probable models are shown at (f) and (g).

Rounded hills and valleys both give shadows, but they can be differentiated in a single photograph because bright areas appear where the direction of viewing becomes nearly tangential to the surface. The bright regions come before the peak of a hill and after the trough of a valley. This effect is



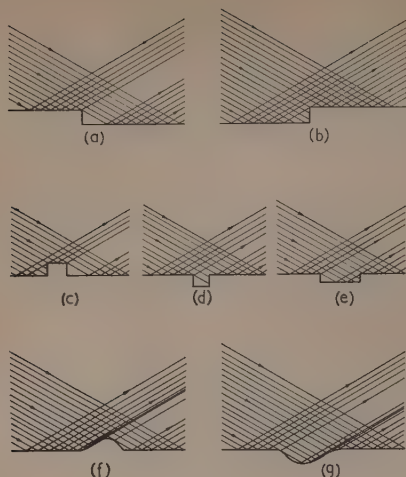


Fig. 4. Illustrating shadow contrast formation

somewhat, but not significantly, altered by the variation of intensity of scattering with  $\theta_1$  and  $\theta_2$  which is described in the following paragraphs. The bright bands are easily visible in Fig. 6b.

In addition to the shadowing effect there will be variations in intensity over the illuminated parts of the object. These will depend on a number of factors such as the variation of scattering with constitution of the object and with local surface orientation. Suppose a local area of the surface is oriented at an angle of  $\theta_1$  to the illuminating beam and  $\theta_2$  to the instrument axis. If the scattering probability is independent of the angle of scatter ( $\theta_1 + \theta_2$ ), the image intensity will be proportional to  $\theta_1$  ( $\theta_1$  and  $\theta_2$  small), since an increase in  $\theta_1$  gives a higher illuminating current density at the object surface, and inversely proportional to  $\theta_2$  since viewing the surface more obliquely will give a higher projected current density. Thus, the image intensity  $I \propto \theta_1/\theta_2$ . The intensity also will depend upon some function of  $\theta_1$  and  $\theta_2$ — $f(\theta_1, \theta_2)$ —determined by the variation of scattering intensity with angle, so that

$$I = (\theta_1/\theta_2)f(\theta_1, \theta_2)$$

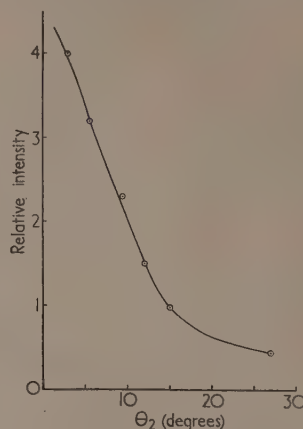
The approximate form of the function  $f(\theta_1, \theta_2)$  was investigated experimentally. The total variation of intensity with  $\theta_1$  was determined simply by varying the electron gun tilt and observing the intensity on the fluorescent screen of the image of a flat optically polished specimen. No significant change in intensity took place for a variation of  $\theta_1$  from almost zero to  $12^\circ$ . Thus, over this range, the function  $f(\theta_1, \theta_2)$  varies with  $\theta_1$  as  $1/\theta_1$ .

The dependence of intensity on  $\theta_2$  was found by using the instrument in the diffraction condition (the use of the instrument for diffraction is described later). The resulting distribution across the screen now varies as the intensity of scattering with angle ( $\theta_2$ ) in the object space.

Fig. 5 shows the intensity distribution obtained by measurement of the distribution of density of the photographic plate (the plate characteristic is known). The determination gives a valid result only if the surface used in the experiments is itself perfectly flat. An optically polished steel surface was used (see below) and a portion chosen which gave no shadows until the incident glancing angle was reduced below  $0.3^\circ$ .

This provides an estimate of the departure of the surface from flatness.

The observed dependence of scattering intensity on  $\theta_1$  and  $\theta_2$  is somewhat unexpected; the relative independence on  $\theta_1$  means that the obliquity effect is just cancelled by the variation of scattering with angle. The intensity is therefore mainly

Fig. 5. Experimentally determined distribution of electron scattering with  $\theta_2$ 

affected by variations in  $\theta_2$ , increasing as  $\theta_2$  diminishes. It will be noted that the intensity still becomes relatively great when  $\theta_2$  tends to zero so that the earlier argument for distinguishing between hills and valleys is unaffected.

#### THE APPEARANCE OF POLISHED SURFACES

Fig. 6 shows photographs of polished surfaces taken in the modified microscope. The material was mild steel and the specimen had been optically polished. (The polishing was carried out by Mr. J. Dyson of this laboratory.) The angle of viewing ( $\theta_2$ ) was kept constant at  $6^\circ$  and the photographs show the effect of altering  $\theta_1$  from  $3^\circ$  to  $1/3^\circ$  and  $1/6^\circ$ . The angle of  $3^\circ$  was used at first and it was found extremely difficult to focus the image; this was eventually done by traversing the specimen until the details *A* and *B* were observed and these then served as objects on which to focus; such detail was difficult to find and is therefore not typical of the polished surface. The increase in the details visible when the illuminating angle is reduced from  $3^\circ$  to  $1/3^\circ$  demonstrates that the slopes of the asperities on the surface are mostly small; the ridge *C*, for example, is from 1 to  $2\mu$  in width and from 50 to  $100\text{ \AA}$  in height (calculated from the shadow length and the shadowing angle). The details *A* and *B* represent grooves because the shadow length does not change appreciably with the angle of illumination (e.g. Fig. 4d). It will be noted that the edge of the groove towards the direction of viewing appears bright in Fig. 6b as predicted by the theoretical argument above. On Fig. 6b it can also be seen that the groove *A* is only sufficiently deep to shadow along part of its length and as the groove shallows and the angle of inclination of the sides lessens, the intensity contrast is reduced also. The striking changes in intensity which are produced by small variations in the inclination of the surface are demonstrated by the intensity variations in the image of the groove *A*, immediately to the left-hand end of the shadow; since shadowing results when the slope exceeds  $\theta_1$ , the

illuminating angle ( $1/3^\circ$ ), the total change in slope across the groove presumably does not exceed  $2/3^\circ$ .<sup>1</sup> On reducing the illuminating angle still further to  $1/6^\circ$ , the detail shows up with even higher contrast. The increase in intensity of the raised details on the upper edge of the groove suggests that when  $\theta_1$  becomes very small, the intensity of the scattered beam also becomes dependent upon  $\theta_1$ .

supposed to fall along  $AB$ . A layer of contamination then builds up (represented in Fig. 7a by the shaded area) and later the incident electrons fall along  $A'B'$ . To a first-order approximation, the appearance of the image is unchanged. If the incident glancing angle is then reduced, the contamination continues to build up, but there is no marked falsification in the appearance of the image (Fig. 7b). An increase in the

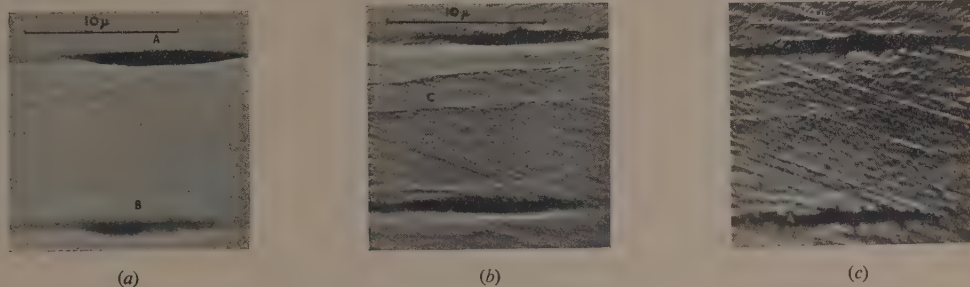


Fig. 6. Reflexion electron micrograms of optically polished steel surface, for three different values of  $\theta_1$ , (a)  $\theta_1 = 3^\circ$ , (b)  $\theta_1 = 1/3^\circ$ , and (c)  $\theta_1 = 1/6^\circ$

These pictures of the polished surface illustrate an advantage of the reflexion technique over the replica method. They make it clear that a suitable choice of illuminating angle or angles is essential if optimum information about the surface topography is to be obtained. Whilst smaller shadowing angles could no doubt be employed when using the replica method with metallic shadowing, the advantage of the reflexion method is that the image can be observed whilst the illuminating angle is being varied. It is then an easy matter to find which angles are the most suitable to use to bring out the details of interest.

#### CONTAMINATION

If several illuminating angles are employed, the part of the surface under examination becomes exposed to the electron beam for a relatively long time and the effect of carbonaceous contamination upon the appearance of the image has to be considered. Consider the surface detail illustrated in Fig. 7. On the initially clean surface, the incident electrons may be

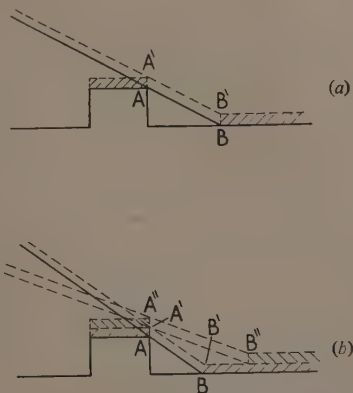


Fig. 7. Illustrating the effect of surface contamination on the shadow contrast

glancing angle, however, reduces the shadow length and the end of the shadow then falls upon an uncontaminated part of the surface. The height of the detail being shadowed has, however, been increased by the film of contamination and the detail will, therefore, appear unduly prominent. If a series of illuminating angles are to be used, the glancing angle should therefore initially be large and thereafter be reduced. The effect on the appearance of the image is shown in Fig. 8. This specimen is mechanically polished mild steel; it was initially illuminated at a very small angle (Fig. 8a) and afterwards at a much larger angle (Fig. 8b). The shape

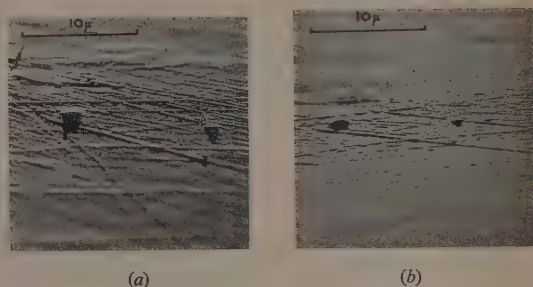


Fig. 8. Reflexion electron micrograms of mechanically polished mild steel surface. (a)  $\theta_1$  small, and (b)  $\theta_1$  subsequently increased about twice

of the earlier longer shadow of the detail  $A$  is clearly seen. It can also be seen in the original photograph that there is less detail within the original shadow than immediately outside the shadow. The small detail in the photograph has, therefore, been "developed" by the contamination. Confirmation is provided by Fig. 9 which shows a consecutive series of photographs using glancing incident angles of  $3^\circ$ ,  $1/3^\circ$  and then again  $3^\circ$ ; the development of detail after the reduction in glancing angle is apparent. These carbon shadows or "ghosts" have been mentioned by Menter.<sup>(1)</sup> It is of interest that the carbonaceous deposit acts as a resist to etching. If the surface is etched after observation, the

uncontaminated regions which were within the electron beam shadow are etched out and are subsequently visible in the optical microscope. In this way, scratches or hollows only a few tens of Ångström units deep can be made quite visible in a normal optical microscope.

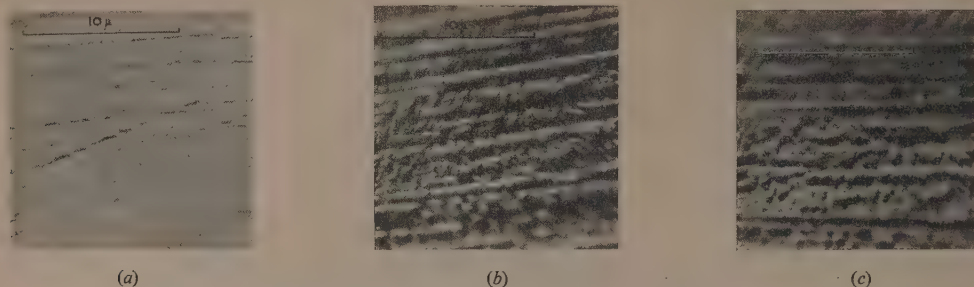


Fig. 9. Reflexion electron micrograms showing development of contrast by carbon contamination  
(a)  $\theta_1 = 3^\circ$ , (b)  $\theta_1$  reduced to  $0.3^\circ$ , and (c)  $\theta_1$  increased again to  $3^\circ$ .

#### REFLEXION ELECTRON DIFFRACTION

The type E.M.3 instrument may be used for obtaining the electron diffraction patterns of transmission specimens. The method has been fully described elsewhere.<sup>(4)</sup> In essence, the object is illuminated with a coherent (near parallel) beam and the diffraction pattern produced in the back focus of the objective lens is imaged with a magnification of about  $\times 200$  on the final viewing screen or photographic plate. The objective aperture is removed or raised into a plane near the object to allow the diffracted beams to go through. The same procedure allows diffraction patterns to be obtained by reflexion in the modified arrangement described. Fig. 10 shows a diffraction pattern from an electrolytically oxidized copper specimen; the pattern is of cupric oxide.

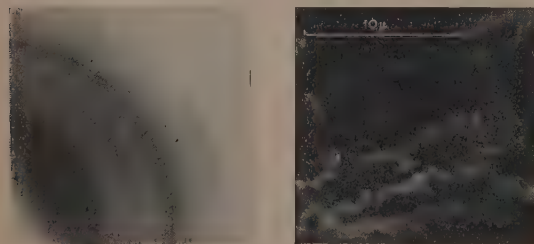


Fig. 10. Reflexion electron diffraction pattern from an electrolytically oxidized copper specimen

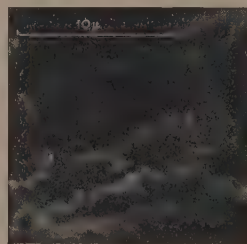


Fig. 11. Reflexion electron microgram showing bright images of Bragg oriented crystals superimposed on normal reflexion image

A further possibility is to insert the objective aperture and then to arrange the electron gun tilt so that one of the Bragg diffracted beams passes through the aperture. If the lenses are then adjusted for reflexion microscopy, a brilliant image of the particular crystals giving the diffracted beams will be superposed on the normal image produced by the multiply scattered electrons. Fig. 11 shows such an image for the copper oxide surface already mentioned.

It is felt that much might be learnt about the mechanism of electron diffraction by this method of surface examination.

The figure clearly indicates that only small crystals at the top edge on the surface contribute to electron diffraction. The inference is that electrons which have penetrated more than a few hundred Ångström units no longer have sufficient coherence to produce interference effects.

#### CONCLUSIONS

It is fairly simple to modify a standard commercial electron microscope to give "reflexion" photographs with a resolution of a few hundred Ångström units. To obtain higher resolution, several rather severe practical difficulties have to be overcome.

Apart from shadowing, contrast also arises because the scattering intensity depends on the illuminating and viewing angles so that the brightness of any part of the surface depends on the local inclination. Other effects such as those due to electron penetration probably play some small part also. The method is better regarded as a means of obtaining a series of surface profiles in depth than of obtaining a plan of the surface detail.

The method also promises to be useful when used in conjunction with electron diffraction and by showing which parts of the surface contribute to the diffracted beams should facilitate the interpretation of the patterns and provide a better understanding of the limitations in the electron diffraction method.

#### ACKNOWLEDGEMENTS

The authors wish to acknowledge the co-operation of Mr. A. E. Ennos in some of the experimental work, and to thank Dr. T. E. Allibone for permission to publish the paper.

#### REFERENCES

- (1) MENTER, J. W. *J. Inst. Metals*, **81**, p. 163 (1952).
- (2) RUSKA, E. *Z. Phys.*, **83**, p. 492 (1933).
- (3) VON BORRIES, B., and JANZEN, S. Z. *Verein. Dtsch. Ingen. (VDI)*, **85**, p. 207 (1941).
- (4) HAINE, M. E., PAGE, R. S., and GARFITT, R. G. *J. Appl. Phys.*, **21**, p. 173 (1952).
- (5) KUSHNIR, YU. M., BIBERMAN, L. M., and LEVKIN, N. P. *Bull. Acad. Sci., U.R.S.S. Fer. Phys.*, **15**, p. 306 (1951).
- (6) LIEBMANN, G. *Proc. Phys. Soc. [London]*, B, **65**, p. 188 (1951).
- (7) ENNOS, A. E. *Brit. J. Appl. Phys.*, **4**, p. 101 (1953).
- (8) SCHERZER, O. *Optik*, **2**, p. 114 (1947).



# Neon indicator tubes as quantitative detectors in photometry

By T. J. DILLON, M.Sc., F.Inst.P., Queen Elizabeth College, University of London

[Paper first received 23 February, and in final form 12 March, 1953]

The photosensitive properties of certain types of neon indicator tubes in relaxation oscillator circuits have been investigated and used in a frequency light meter. Illumination is measured in terms of change of frequency caused by the alteration in the striking potential on irradiation. The experimental results are in accord with the theory and illuminations range from 50 to  $10^4$  f.c. Sample calibration curves at low and high levels of illumination are given for a number of tubes.

In a recent paper<sup>(1)</sup> the writer showed that if a light sensitive neon-argon indicator tube is used as a relaxation oscillator, the alteration in striking potential produced by irradiation from an external source causes a change of frequency of the oscillations. It was claimed that tubes of certain types could be used as quantitative detectors in photometry over a small range of illuminations. The work has since been extended to cover a large range and the frequency change of the oscillations has been used for direct measurement of illuminations of more than  $10^4$  f.c. There is a critical value of the illumination when the irradiation is sufficient to stop the intermittency of the discharge. This has already been shown to occur when the frequency becomes infinite.

Allowance has to be made for the fatigue and hysteresis effects as well as for the initial current drift but, as the tubes are used in the transition region corresponding to the negative resistance part of the volt-ampere characteristic, the currents are small and there is little danger of overloading. The photosensitive properties of discharge tubes containing neon or a neon-argon mixture are examples of the positive Joshi effect.<sup>(2)</sup> They were observed by Benson<sup>(3)</sup> in his study of the characteristics in the normal and the abnormal regions and Titterton<sup>(4)</sup> showed that indicator tubes are unsuitable for use in precision circuits unless they are carefully controlled. In spite of these peculiarities it is found that the tubes selected for these photometric experiments are satisfactory, especially if they are calibrated frequently, or if comparative rather than absolute determinations are undertaken.

In early experiments on the conventional "glow lamp" type of neon tube the photosensitivity was present, but the effect was too small to be put to practical use without amplification. Subsequently tubes were found that exhibited the photosensitive properties to a far greater degree. The electrodes in both the pure neon and neon-argon filled tubes of this type had a thin barium caesium coating. In addition to increasing the photosensitivity the coating decreases the striking potential so that, even for the tubes without the argon, the striking potential is considerably less than for pure neon. The tubes are used in a simple relaxation oscillation circuit. Telephones must be included and, using an oscillator or tuning-forks, the tubes can be calibrated in terms of change of frequency for known foot-candle illumination. With small circuit components a compact portable "frequency-lightmeter" approximately  $6 \times 3 \times 3$  in<sup>3</sup>, can be assembled at low cost.

## THEORETICAL BASIS

The relation between the frequency  $n$  and the striking voltage  $V_B$  of a tube in a relaxation oscillation circuit is given by

$$1/n = RC \ln x, \text{ where } x = (E - V_A)/(E - V_B) \quad (1)$$

$RC$  is the time constant and  $E$  and  $V_A$  are the circuit battery voltage and extinction voltage respectively.

Suppose that an alteration in the striking voltage from  $V_B$  to  $V_{B'}$  for a given irradiation is the operative cause of the

change in frequency from  $n$  to  $n'$  and that the extinction voltage does not alter appreciably. Then in a circuit with a given time constant  $RC$

$$n'/n = \ln x / \ln x', \text{ where } x' = (E - V_A)/(E - V_{B'}) \quad (2)$$

Alternatively, in order to keep the tube oscillating at the fundamental frequency  $n$ , under a given irradiation the time constant  $RC$  could be increased to a value  $R'C'$  and from equation (1)

$$R'C'/RC = \ln x / \ln x' \quad (3)$$

Observations using different tubes when oscillating over ranges from 100 to 500 c/s and using condensers of capacities from 0.002 to 0.02  $\mu$ F gave results which were in good agreement with the above theory. It therefore appeared that the irradiated tubes conform to the principles of simple relaxation oscillators and justifies the use of the parameters concerned as a quantitative measure of illumination.

As the change of frequency,  $(n' - n)$ , was used throughout these experiments as the basis for measurement, the relevant relationship can be expressed as

$$(n' - n) = \frac{1}{RC} \left( \frac{1}{\ln x'} - \frac{1}{\ln x} \right) \quad (4)$$

$$\text{and therefore } (n' - n) \propto \left( \frac{1}{\log x'} - K \right) \quad (5)$$

where  $K$  is a constant.

Curve I of Fig. 1 shows  $(n' - n)$  plotted against  $1/\log x'$  for one of the tubes and an approximately linear relationship

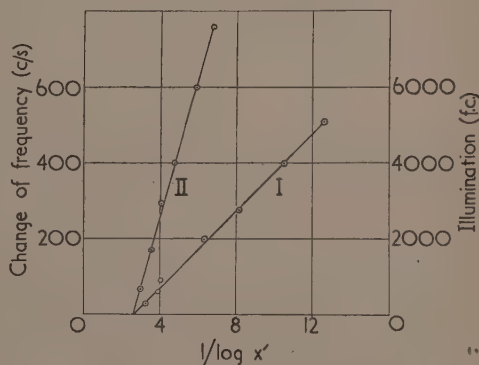


Fig. 1. Variation of change of frequency (curve I), and foot candle illumination (curve II) with  $1/\log x'$

holds up to a value of 12 for  $1/\log x'$ , which corresponds to a lowering of the striking potential of over 20 V. The illumination for each position of the tube was found by an independent method and in curve II the foot-candle illumination is plotted against  $1/\log x'$ . It is seen that, for the tube

under investigation,  $(n' - n)$  is proportional to the illumination up to 5000 f.c. Above this value there was non-linearity and the tube showed signs of fatigue and instability. From the value of  $K$ , taken from the graph, the normal striking potential for the tube was found and this was in agreement with the value determined from experiments on the normal flashing characteristics.

#### APPARATUS AND METHOD OF CALIBRATION

The tubes were the L7A and L10 types of neon indicator by Siemens Electric Lamps and Supplies Ltd. The former contained pure neon and the latter 99.5% neon and 0.5% argon. With the gas at a pressure of approximately 10 mm of mercury the normal striking potential was about 90 V. For the initial investigations the circuit included a sensitive balanced galvanometer and low resistance telephones or loud-speaker. The frequency of the oscillations was found by tuning to an oscillator. A calibrated double beam cathode-ray oscillograph, placed across the tube electrodes, showed the difference between the striking potential  $V_B$  and the extinction potential  $V_A$ , and measurements or photographic records of the charge-discharge traces provided an alternative method of frequency determination.

The photometric apparatus used with the lower wattage tungsten filament lamps of known luminous output was as described in a previous paper.<sup>(5)</sup> The neon indicator tube replaced the photovoltaic cell in the black box photometer. The lamp and tube were arranged so that the light from the lamp fell normally on the cathode through the top of the tube, and suitable screens limited the size of the source. When the heating effect of sources of high intensity such as projector lamps was considerable, the photometric methods were modified by using darkened alleys open at both ends for housing the tubes. The illumination at various distances from the lamp filament was found by calculation, or by substituting for the tube a previously calibrated photovoltaic cell, and f.c.-distance curves plotted for various sources. Neutral filters of known transmission factor were used with high wattage projector lamps. A tube was then moved through the same distance range in front of the lamp and the change of frequency recorded. An example is given in Fig. 2 of a  $(n' - n)$ -f.c. calibration graph obtained in this way. The tube was tuned to a fundamental of 400 c/s and was irradiated

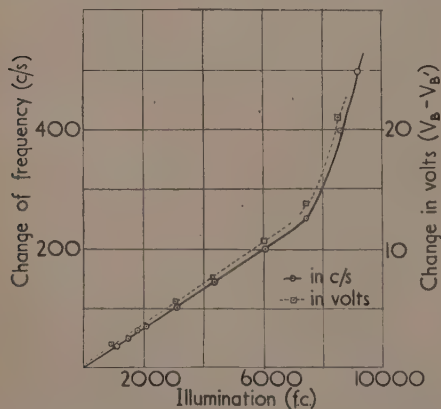


Fig. 2. Change of frequency and decrease in striking potential plotted against foot-candle illumination

by a 500 W lamp. At the same time measurements were made of the  $(V_B - V_A)$  trace on the cathode-ray oscilloscope, and, from these, the corresponding decreases in striking potential  $(V_B - V_A)$  were estimated. These are plotted on a comparable scale on the same graph to show the similarity in the shapes of the curves.

#### USE OF TUBES IN FOOT-CANDLE DETERMINATIONS

In the previous paper<sup>(1)</sup> low illuminations up to 300 f.c. were considered and, in addition to frequency change, measurements were also made of the change of mean current through the tubes. Calibration graphs for a selection of tubes are given in Fig. 3. It will be seen that the tubes vary

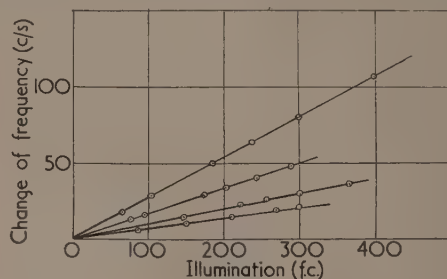


Fig. 3. Calibration graphs. (Low illuminations)

in sensitivity and this is expected on account of the differences in the volt-ampere characteristics and in the striking potentials. For use with sources of high intensity tubes of low sensitivity were selected, and tests were carried out to determine the range, for each tube, for which the frequency change was proportional to illumination. Three calibration curves are given in Fig. 4. Curves I and II are for the same tube, but

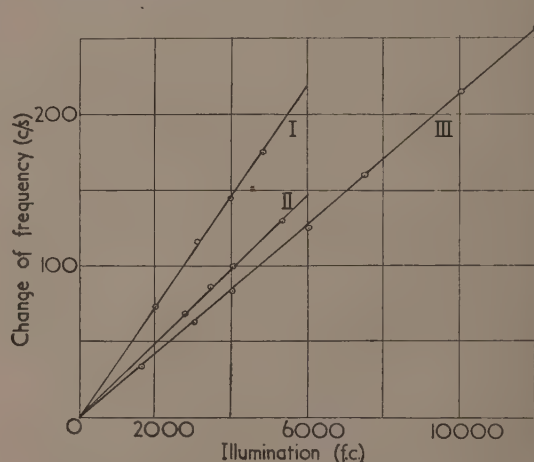


Fig. 4. Calibration graphs. (High illuminations)

with fundamentals set at 400 and 256 c/s respectively. For curve I an oscillator was used for tuning and for curve II a series of tuning-forks. A quick method of calibration is illustrated in curve III where a tube was tuned to 256 c/s with a tuning-fork and was then placed at such a distance from

the lamp that the frequency had gone up by a recognizable interval. Knowing the illumination at that distance from the lamp, the slope of the graph was found. This method was used successfully in the foot-candle determinations corresponding to other changes of frequency. Attempts were made to find the illumination which just stopped the oscillations and this appeared to be at about  $1.1 \times 10^4$  f.c. and corresponded to a decrease in the striking potential equal to the normal potential drop across the electrodes. Illuminations of this order are produced at a distance of approximately 4 in. from a 1000 W projector lamp. During the summer months the midday sun was used for irradiating the tubes and cathode-ray oscilloscope photographic records of ( $V_B - V_A$ ) and frequency traces gave reasonable assessments of the illuminations up to this critical value.

#### CONCLUSION

Although no high degree of accuracy can be claimed for these tubes as photometric detectors there are advantages in this method of using the Joshi effect especially for the comparison of illuminations and of the intensity of lamps of widely different luminous outputs in terms of change of frequency. If an oscillator or an oscillograph is not available, anyone who has a musical ear can, with the help of a tuning-fork, compare illuminations or mean candle power of two sources in terms of the intervals of the scale or the common chord. Fluctuations, not apparent to the eye, in the light from a discharge tube can also be detected in the frequency

change and work is in progress on the application of this method to the study of light variation from sources of this type.

The illuminations used in these experiments ranged from 100 to  $10^4$  f.c. which is far greater than would normally be attempted with the usual type of photocell. Frequent calibrations are necessary for absolute determinations but, if a preliminary reading is taken at a given distance from a standard lamp, a "change of frequency-foot candle" sensitivity value for a tube can be determined which will be maintained for many hours if the tube is not fatigued or overheated.

#### ACKNOWLEDGEMENTS

The author wishes to express thanks to members of the Research Laboratory of Siemens Electric Lamps and Supplies Ltd. for kindly providing information about different types of lamps supplied by their firm and to her colleague, Dr. U. Andrewes, for helpful suggestions.

#### REFERENCES

- (1) DILLON, T. J. *Proc. Phys. Soc. [London]*, **B**, **65**, p. 236 (1952).
- (2) ARNIKAR, H. J. *J. Phys. Chem.*, **56**, p. 457 (1952).
- (3) BENSON, F. A. *Elect. Engng*, **24**, p. 456 (1952).
- (4) TITERTON, E. W. *J. Sci. Instrum.*, **26**, p. 33 (1949).
- (5) ANDREWES, U., and DILLON, T. J. *Amer. J. Phys.*, **19**, p. 514 (1951).

## Tables for use in the measurement of interfacial tensions between liquids with small density differences

By O. S. MILLS, B.Sc., Department of Chemistry, University of Sheffield

[Paper first received 15 December, 1952, and in final form 10 April, 1953]

In order that the pendant drop method for the determination of interfacial tensions can be applied to systems with small density differences, extensions have been made to tables published by Fordham. These extensions are also useful when the interfacial tension is large or where the drop size is small, that is as the drop tends to become spherical. As a result, the combined tables are some two and a half times as extensive as before. The choice of measurements as suggested by Andreas and others has been shown to be satisfactory.

The method of using pendant drops for interfacial tension determinations is an important practical technique since it permits the continuous study of adsorption changes with time at a liquid/liquid interface without any mechanical interference such as occurs with the ring, maximum bubble pressure and similar methods, whilst it is independent of the contact angles between the liquids and the support. The method, though fundamental, was not made absolute until recently. In the original work of Andreas, Hauser and Tucker<sup>(1)</sup> the profile of a drop, pendant from a circular tip, was photographed at a suitable magnification and from the negative were estimated two parameters relating size and shape to interfacial tension. This they accomplished by measuring the maximum diameter of the meridional section,  $d_m$ , and the diameter,  $d_v$ , at a distance, measured vertically from the vertex, equal to the maximum diameter. The ratio of these two diameters,  $d_v/d_m$ , designated  $S$  by Andreas and others, gives an estimate of the shape parameter and is implicitly related to a second factor  $1/H$ . A simple equation

then relates interfacial tension,  $\gamma$ , maximum diameter,  $d_m$ , density difference,  $\Delta$ , with  $1/H$ , namely

$$\gamma = 1/Hg\Delta d_m^2$$

$g$  being the acceleration due to gravity.

Whilst these authors realized that the differential equation to the profile could be solved numerically, as indeed Bashforth and Adams<sup>(2)</sup> had done for certain values of the shape parameter, they did not believe that the integrations could be carried out to a sufficient degree of accuracy and so they constructed, from experimental data for water, a table of  $S$  versus  $1/H$ . Later Fordham<sup>(3)</sup> performed further integrations and, with the relevant values obtained by Bashforth and Adams, constructed a similar table without recourse to calibration. These tables give the values of  $1/H$  varying from 0.94 to 0.30 corresponding to  $S$  values of 0.66 to 1.00.

Fordham's table covers a wide range of application, especially for liquid/air surfaces, but occasion arises when values of  $S$  less than 0.66 are required, i.e. as the shape



becomes more spherical. Although in some cases it is possible to work with larger drops a practical limit is set to their size, and here extensions to the table are desirable. Accordingly, in this paper such an extension has been completed which more than doubles the range of the tables. Further, it will be apparent that the choice of the two measurements to be made on the drop section will be arbitrary so long as one estimates size and the other shape. In particular the choice that the distance from the vertex to the chosen plane be equal to the equatorial diameter is completely arbitrary. This latter choice of distance has been studied statistically to determine which distance will afford the best conditions for the accurate estimation of the diameter ratio and hence  $1/H$ .

#### THE CHOICE OF DROP MEASUREMENTS

The equation to the drop profile is a second-order non-linear differential equation of  $z$ ,  $x$  (see Fig. 1) and two parameters  $b$  and  $\beta$  defining size and shape respectively, so that selected values of  $z$ ,  $b$  and  $\beta$  give a single numerically valued solution for  $x$ .

$$b \frac{d^2 z}{dx^2} + \left[ 1 + \left( \frac{dz}{dx} \right)^2 \right] \frac{1}{x/b} \frac{dz}{dx} = \left( 2 + \frac{\beta z}{b} \right) \left[ 1 + \left( \frac{dx}{dz} \right)^2 \right]^{3/2} \quad (1)$$

According to Andreas and others, the size of the drop may be estimated by  $d_e$  and its shape by  $d_s$  and  $d_e$ , whence we may define  $x$  as a function of  $z$ ,  $d_e$  and  $d_s$ , i.e.  $x = f(z, d_e, d_s)$ , whose form is such that by substituting the requisite values of these three variables,  $x$  is completely defined.

The drop could also be identified by  $d_e$  and  $w$ , where  $w$  is the abscissa at  $z = \theta d_e$ , in which  $\theta$  is arbitrary and put equal to unity by Andreas and others, and is given by the relation  $w = f(\theta d_e, d_e, d_s)$ . Then the ratio of the radius of this selected plane to that of the equatorial plane is a function of  $d_e$ ,  $w$  and  $\theta$ , being related to the function  $f$  by the values of the parameters is equation (1). Now, whilst any practically reasonable value of  $\theta$  would serve to estimate  $b$  and  $\beta$  and hence  $1/H$ , there will be a certain selected value which will estimate them with less variance than any other. The results of a statistical inquiry on these lines indicate that there is no greatly preferred value of  $\theta$ .

In reaching this conclusion, errors in measurement were allowed for in  $d_e$ , laying off the distance from the vertex  $\theta d_e$  and in  $d_s$ , these errors being assumed independent and of equal variance. Then the variance of  $S$  is given by the expectation of  $(\bar{S} - S)^2$ , where  $\bar{S}$  is the true value of the ratio and  $\bar{S}$  all calculated ratios involving errors. The necessary equations were solved numerically to yield values of  $E(\bar{S} - S)^2/\sigma^2$ , where  $\sigma$  is the common standard deviation, at various  $\theta$  values.

#### Values of $E(\bar{S} - S)^2/\sigma^2$

	$\beta = -0.225$	$\beta = -0.325$	$\beta = -0.425$
$\theta = 0.7$	2.25	2.18	2.11
$\theta = 0.9$	2.68	2.46	2.18
$\theta = 1.0$	2.99	2.92	2.11
$\theta = 1.1$		2.49	1.91

The major contribution to  $E_{max}$  is caused by the slope at the point of intersection of the chosen plane and the surface, the error being a maximum at the plane of inflexion. This

error will increase as  $\beta$  decreases numerically and  $E$  thus increases in this direction. The choice of Andreas, Hauser and Tucker in taking  $\theta = 1$  is thus satisfactory.

#### EXTENSIONS OF FORDHAM'S TABLE TO SMALLER VALUES OF $S$

With reference to Fig. 2, taking origin at the vertex, with abscissa  $0_x$  and ordinate  $0_z$ , then at any point  $(x, z)$  on the surface of the section we may define  $\phi$  as the angle of inclination between the normal and the axis of revolution  $0_z$ ,  $\rho$  the radius of curvature of the meridional section taking into account its sign, and  $b$  the radius of curvature at the vertex.

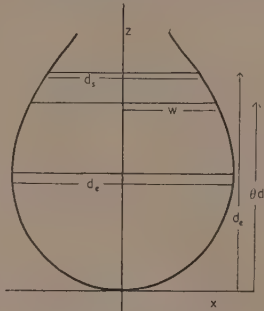


Fig. 1. Alternative estimates of shape

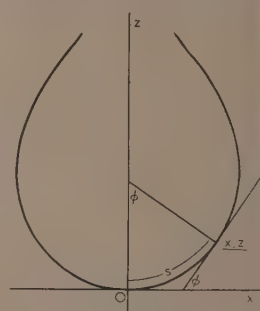


Fig. 2. Meridional section.  
 $\beta = -0.275$

Then the equation to the meridional section of a drop of fluid bounded by surfaces of revolution meeting the vertical axis of revolution at right angles is

$$\frac{1}{(\rho/b)} + \frac{\sin \phi}{(x/b)} = 2 - \frac{g\Delta b^2}{\gamma} \left( \frac{z}{b} \right) = 2 + \beta \left( \frac{z}{b} \right) \quad (2)$$

in which  $\beta = -g\Delta b^2/\gamma$  is dimensionally a pure number. On replacing  $1/\rho$  and  $\sin \phi$  in terms of the slope, equation (1) results.

It follows that

$$\gamma = -\frac{g\Delta b^2}{\beta} = \frac{1}{H} g\Delta d_e^2 \quad (3)$$

in which

$$\frac{1}{H} = \frac{1}{\beta(d_e/b)^2} = \frac{1}{4\beta(x_e/b)^2} \quad (4)$$

Values of  $S$  and  $1/H$  for  $\beta = -0.2500$  to  $-0.6000$  were calculated by Fordham. Further values have been calculated between  $\beta = -0.1000$  and  $-0.2250$  during the present work.

#### CALCULATIONS

Full details of the method of calculation can be found in Fordham's paper, but are summarized here.

By taking  $b$  as unit of length,  $z/b$ ,  $x/b$  and  $s/b$  are dimensionless and for abbreviation written  $z$ ,  $x$  and  $s$ ,  $s$  being the arcual distance from the origin to the point  $(x, z)$ . The equations to be integrated then are the identities for a curve

$$d\phi/ds = 1/\rho \quad (5)$$

$$dx/ds = \cos \phi \quad (6)$$

$$dz/ds = \sin \phi \quad (7)$$

together with the particular equation (2) written

$$\frac{1}{\rho} + \frac{\sin \phi}{x} = 2 + \beta z$$

i.e.  $\frac{d\phi}{ds} + \frac{\sin \phi}{x} = 2 + \beta z$

for each value of  $\beta$ , with initial values  $s = x = z = \phi = 0$ ,  $1/\rho = 1$ .

- (i) Integrate equations by the method of Bashforth and Adams, using  $s$  as the independent variable, i.e. estimate following  $d\phi/ds$  from previous known values, integrate  $d\phi/ds$  to give  $\phi$ ,  $dx/ds$  to give  $x$  and  $dz/ds$  to give  $z$ , then compute a better estimate of  $d\phi/ds$  from equation (2). Integration is carried out as far as  $s/b = 3.0$ , using an interval of 0.1. Using an interval of half this size does not significantly alter the solution.
- (ii) For each value of  $\beta$ , find the maximum value of  $x$ , ( $x_e$ ). This can be checked by verifying that the corresponding value of  $\phi$  is  $\pi/2$ , that  $dx/ds = 0$  and that  $dz/ds = 1.0$ . Difference the values of  $x_e$  as a further check.
- (iii) For each value of  $\beta$ , find the value of  $x$  corresponding to  $z = 2x_e$ . This will be  $x_s$ , the radius of the selected plane. These values should difference satisfactorily.
- (iv) From the difference tables in (ii) and (iii) above, estimate  $x_e$  and  $x_s$  at intervals of  $\beta$  of 0.0125.
- (v) Form  $S$  and  $1/H$  for each  $\beta$ . These values must also difference satisfactorily.
- (vi) Find values of  $1/H$  corresponding to equal intervals of  $S$  (by 0.01) by a six-point Lagrange formula. Using an eight-point formula does not significantly alter these values.
- (vii) Subtabulate  $1/H$  against  $S$  at intervals of 0.001. Between  $S = 0.49$  and 0.63 a system due to Comrie based on Everett's formula was used. Between 0.46 and 0.49 it was necessary to use a Newton forward difference formula.

#### COMPARISON AND DISCUSSION OF THE SOLUTIONS

When the values of  $x_s$  and  $x_e$  were differenced for  $\beta = -0.1000(0.025)0.6000$ , a smooth join was observed between Fordham's values and those from the present solutions. However, whilst  $1/H$  differenced smoothly  $S$  did not. This was attributed to an error in  $S$  at  $\beta = -0.2500$ . The differences are rendered smooth if  $S$  is put equal to 0.66779 instead of 0.66781. Fordham's values of  $x_s$  and  $x_e$  themselves lead to this corrected figure, as do extrapolations from the present work. The corrected value was thus used in the present subtabulations and hence a comparison between Fordham's table and Table 3 shows slight disagreement in the region  $S = 0.66$  to 0.67, but the values converge rapidly.

The integrations were performed on a mechanical figure calculating machine and all product totals checked by repetition. Sines and cosines were obtained to nine figures at each value of  $s$  from *Tables of circular and hyperbolic sines and cosines*,<sup>(4)</sup> the values being checked for mutual agreement. As seven figures were retained during integrations and differences beyond the fifth taken into account, and as the six complete solutions all checked with one another, it appears improbable that any errors greater than rounding off errors should occur in the final table of  $1/H$  against  $S$ .

The two sets of solutions therefore agree in general, the inconsistency at the join being attributed to an error in  $S$  at  $\beta = -0.2500$ .

Table 1. Computed meridional sections

$\beta = -0.2250$			
$s/b$	$\phi$	$x/b$	$z/b$
0.0	0.000 000 00	0.000 000 00	0.000 000 00
0.1	0.099 971 89	0.099 833 47	0.004 995 13
0.2	0.199 775 38	0.198 671 12	0.019 922 33
0.3	0.299 243 52	0.295 533 68	0.044 608 39
0.4	0.398 212 13	0.389 474 49	0.078 769 24
0.5	0.496 521 11	0.479 594 47	0.122 016 65
0.6	0.594 015 53	0.565 055 58	0.173 867 20
0.7	0.690 546 58	0.645 092 47	0.233 753 20
0.8	0.785 972 23	0.719 021 93	0.301 035 06
0.9	0.880 157 66	0.786 250 11	0.375 014 66
1.0	0.972 975 33	0.846 277 31	0.454 949 37
1.1	1.064 304 71	0.898 700 55	0.540 066 08
1.2	1.154 031 66	0.943 213 88	0.629 575 05
1.3	1.242 047 27	0.979 606 87	0.722 683 03
1.4	1.328 246 29	1.007 761 28	0.818 605 60
1.5	1.412 524 85	1.027 646 48	0.916 578 36
1.6	1.494 777 57	1.039 313 71	1.015 867 02
1.7	1.574 893 60	1.042 889 77	1.115 776 30
1.8	1.652 751 60	1.038 570 21	1.215 657 68
1.9	1.728 213 08	1.026 612 54	1.314 916 28
2.0	1.801 113 40	1.007 329 63	1.413 016 95
2.1	1.871 249 98	0.981 083 73	1.509 490 02
2.2	1.938 365 58	0.948 281 38	1.603 937 11
2.3	2.002 125 33	0.909 369 59	1.696 037 51
2.4	2.062 083 36	0.864 833 92	1.785 556 10
2.5	2.117 633 83	0.815 199 14	1.872 353 66
2.6	2.167 936 96	0.761 033 92	1.956 401 37
2.7	2.211 804 3	0.702 961 7	2.037 801 7
2.8	2.247 516 0	0.641 682 2	2.116 819 1
2.9	2.272 522 2	0.578 010 8	2.193 925 7
3.0	2.282 946 3	0.512 951 6	2.269 868 1

$$x_e/b = 1.042 900 39$$

$$\beta = -0.2000$$

$s/b$	$\phi$	$x/b$	$z/b$
0.0	0.000 000 00	0.000 000 00	0.000 000 00
0.1	0.099 975 01	0.099 833 47	0.004 995 21
0.2	0.199 800 33	0.198 670 92	0.019 923 57
0.3	0.299 327 51	0.295 532 19	0.044 614 52
0.4	0.398 410 52	0.389 468 27	0.078 788 09
0.5	0.496 906 87	0.479 575 77	0.122 061 14
0.6	0.594 678 56	0.565 009 91	0.173 955 68
0.7	0.691 592 91	0.644 995 90	0.233 909 13
0.8	0.787 523 15	0.718 838 36	0.301 285 87
0.9	0.882 348 79	0.785 928 54	0.375 389 96
1.0	0.975 955 66	0.845 749 53	0.455 478 34
1.1	1.068 235 72	0.897 879 12	0.540 774 36
1.2	1.159 086 43	0.941 990 82	0.630 481 00
1.3	1.248 409 71	0.977 852 82	0.723 793 75
1.4	1.336 110 51	1.005 325 50	0.819 912 66
1.5	1.422 094 63	1.024 357 39	0.918 053 51
1.6	1.506 265 98	1.034 980 24	1.017 458 00
1.7	1.588 522 79	1.037 303 16	1.117 402 82
1.8	1.668 752 66	1.031 506 43	1.217 207 80
1.9	1.746 825 87	1.017 835 02	1.316 243 22

Table 1 (continued)

$s/b$	$\phi$	$x/b$	$z/b$
2.0	1.822 586 43	0.996 592 32	1.413 936 44
2.1	1.895 839 61	0.968 134 28	1.509 778 33
2.2	1.966 334 51	0.932 864 29	1.603 329 85
2.3	2.033 738 93	0.891 229 22	1.694 229 43
2.4	2.097 602 21	0.843 717 22	1.782 202 22
2.5	2.157 298 8	0.790 858 0	1.867 072 3
2.6	2.211 939 9	0.733 227 3	1.948 780 4
2.7	2.260 229 5	0.671 457 7	2.027 409 7
2.8	2.300 222 8	0.606 261 5	2.103 226 1
2.9	2.328 903 2	0.538 475 8	2.176 740 8
3.0	2.341 413 1	0.469 151 8	2.248 810 4

$$x_e/b = 1.037 496 14$$

$$\beta = -0.1750$$

$s/b$	$\phi$	$x/b$	$z/b$
0.0	0.000 000 00	0.000 000 00	0.000 000 00
0.1	0.099 978 13	0.099 833 46	0.004 995 29
0.2	0.199 825 28	0.198 670 72	0.019 924 80
0.3	0.299 411 52	0.295 530 69	0.044 620 64
0.4	0.398 608 98	0.389 462 04	0.078 806 94
0.5	0.497 292 83	0.479 557 05	0.122 105 64
0.6	0.595 342 06	0.564 964 18	0.174 044 19
0.7	0.692 640 25	0.644 899 18	0.234 065 09
0.8	0.789 076 00	0.718 654 40	0.301 536 71
0.9	0.884 543 30	0.785 606 17	0.375 765 19
1.0	0.978 941 58	0.845 220 18	0.456 006 99
1.1	1.072 175 50	0.897 054 92	0.541 481 65
1.2	1.164 154 37	0.940 763 11	0.631 384 63
1.3	1.254 791 30	0.976 091 48	0.724 899 67
1.4	1.344 001 77	1.002 878 83	0.821 210 66
1.5	1.431 701 72	1.021 052 86	0.919 512 73
1.6	1.517 804 94	1.030 625 82	1.019 022 43
1.7	1.602 219 45	1.031 689 42	1.118 987 08
1.8	1.684 842 81	1.024 409 07	1.218 693 20
1.9	1.765 555 51	1.009 017 96	1.317 474 19
2.0	1.844 212 10	0.985 811 05	1.414 717 62
2.1	1.920 628 49	0.955 139 41	1.509 872 15
2.2	1.994 563 98	0.917 405 08	1.602 454 90
2.3	2.065 694 49	0.873 056 99	1.692 059 76
2.4	2.133 572 22	0.822 588 34	1.778 367 78
2.5	2.197 562 2	0.766 536 4	1.861 161 3
2.6	2.256 738 8	0.705 486 4	1.940 344 5
2.7	2.309 711 4	0.640 081 9	2.015 974 6
2.8	2.354 312 0	0.571 048 3	2.088 312 0
2.9	2.387 011 4	0.499 242 3	2.157 903 6
3.0	2.401 757 6	0.425 758 4	2.225 726 3

$$x_e/b = 1.032 278 81$$

$$\beta = -0.1500$$

$s/b$	$\phi$	$x/b$	$z/b$
0.0	0.000 000 00	0.000 000 00	0.000 000 00
0.1	0.099 981 26	0.099 833 45	0.004 995 37
0.2	0.199 850 24	0.198 670 52	0.019 926 03
0.3	0.299 495 54	0.295 529 19	0.044 626 76
0.4	0.398 807 50	0.389 455 81	0.078 825 80

Table 1 (continued)

$s/b$	$\phi$	$x/b$	$z/b$
0.5	0.497 678 98	0.479 538 31	0.122 150 15
0.6	0.596 006 05	0.564 918 39	0.174 132 72
0.7	0.693 688 60	0.644 802 30	0.234 221 09
0.8	0.790 630 78	0.718 470 07	0.301 787 57
0.9	0.886 741 21	0.785 282 99	0.376 140 37
1.0	0.981 933 10	0.844 689 28	0.456 535 30
1.1	1.076 124 05	0.896 227 93	0.542 187 94
1.2	1.169 235 51	0.939 530 76	0.632 285 90
1.3	1.261 192 06	0.974 322 84	0.726 000 71
1.4	1.351 920 10	1.000 421 31	0.822 499 48
1.5	1.441 346 19	1.017 732 95	0.920 955 79
1.6	1.529 394 53	1.026 250 64	1.020 559 95
1.7	1.615 983 77	1.026 048 90	1.120 528 51
1.8	1.701 022 44	1.017 278 82	1.220 112 95
1.9	1.784 402 75	1.000 162 59	1.318 607 84
2.0	1.865 991 88	0.974 987 94	1.415 358 49
2.1	1.945 619 52	0.942 102 59	1.509 768 62
2.2	2.023 059 58	0.901 909 27	1.601 308 27
2.3	2.098 002 71	0.854 861 34	1.689 522 85
2.4	2.170 013 37	0.801 459 85	1.774 044 79
2.5	2.238 460 6	0.742 252 7	1.854 609 1
2.6	2.302 401 1	0.677 837 2	1.931 076 3
2.7	2.350 371 6	0.608 870 1	2.003 469 2
2.8	2.409 999 2	0.536 090 0	2.072 033 1
2.9	2.447 214 6	0.460 370 0	2.137 342 4
3.0	2.464 532 2	0.382 840 7	2.200 500 4

$$x_e/b = 1.027 234 49$$

$$\beta = -0.1250$$

$s/b$	$\phi$	$x/b$	$z/b$
0.0	0.000 000 00	0.000 000 00	0.000 000 00
0.1	0.099 984 38	0.099 833 45	0.004 995 45
0.2	0.199 875 19	0.198 670 32	0.019 927 26
0.3	0.299 579 58	0.295 527 70	0.044 632 88
0.4	0.399 006 09	0.389 449 57	0.078 844 66
0.5	0.498 065 33	0.479 519 55	0.122 194 67
0.6	0.596 670 51	0.564 872 54	0.174 221 27
0.7	0.694 737 97	0.644 705 26	0.234 377 12
0.8	0.792 187 48	0.718 285 36	0.302 038 47
0.9	0.888 942 51	0.784 959 00	0.376 515 48
1.0	0.984 930 23	0.844 156 81	0.457 063 25
1.1	1.080 081 38	0.895 398 15	0.542 893 22
1.2	1.174 329 85	0.938 293 77	0.633 184 77
1.3	1.267 611 99	0.972 546 92	0.727 096 82
1.4	1.359 865 53	0.997 952 95	0.823 778 99
1.5	1.451 028 05	1.014 397 74	0.922 382 47
1.6	1.541 034 82	1.021 854 86	1.022 070 19
1.7	1.629 815 89	1.020 381 97	1.122 026 50
1.8	1.717 291 88	1.010 116 38	1.221 466 14
1.9	1.803 368 31	0.991 270 20	1.319 642 76
2.0	1.887 927 32	0.964 125 16	1.415 857 05
2.1	1.970 815 77	0.929 027 42	1.509 464 87
2.2	2.051 827 38	0.886 382 53	1.599 885 80
2.3	2.130 675 24	0.836 651 00	1.686 612 92
2.4	2.206 947 89	0.780 344 80	1.769 225 05



Table 1 (continued)

$s/b$	$\phi$	$x/b$	$z/b$
2.5	2.2800361	0.7180257	1.8474035
2.6	2.3490051	0.6503068	1.9209575
2.7	2.4123569	0.5778600	1.9898641
2.8	2.4675578	0.5014376	2.0543394
2.9	2.5100105	0.4219240	2.1149701
3.0	2.5305600	0.3404733	2.1729818

$$x_e/b = 1.02235093$$

$$\beta = -0.1000$$

$s/b$	$\phi$	$x/b$	$z/b$
0.0	0.00000000	0.00000000	0.00000000
0.1	0.09998750	0.09983344	0.00499552
0.2	0.19990015	0.19867013	0.01992849
0.3	0.29966363	0.29552620	0.04463901
0.4	0.39920474	0.38944333	0.07886352
0.5	0.49845187	0.47950078	0.12223921
0.6	0.59733545	0.56482664	0.17430985
0.7	0.69578835	0.64460806	0.23453319
0.8	0.79374612	0.71810026	0.30228938
0.9	0.89114720	0.78463420	0.37689053
1.0	0.98793295	0.84362277	0.45759087
1.1	1.08404749	0.89456558	0.54359746
1.2	1.17943741	0.93705213	0.63408123
1.3	1.27405113	0.97076371	0.72818793
1.4	1.36783808	0.99547380	0.82504909
1.5	1.46074736	1.01104731	0.92379257
1.6	1.55272591	1.01743867	1.02355279
1.7	1.64371599	1.01468900	1.12348047
1.8	1.73365151	1.00292248	1.22275187
1.9	1.82245297	0.98234209	1.32057762

Table 1 (continued)

$s/b$	$\phi$	$x/b$	$z/b$
2.0	1.91002003	0.95322499	1.41621133
2.1	1.99622055	0.91591760	1.50895812
2.2	2.08087395	0.87083074	1.59818370
2.3	2.16372496	0.81843499	1.68332456
2.4	2.24440060	0.75925674	1.76390068
2.5	2.3223365	0.6938755	1.8395329
2.6	2.3966431	0.6229237	1.9099690
2.7	2.4658458	0.5470921	1.9751270
2.8	2.5273366	0.4671468	2.0351736
2.9	2.5760816	0.3839778	2.0906795
3.0	2.6010990	0.2987422	2.1429701

$$x_e/b = 1.01761723$$

Table 2.- Derived factors for pendant drops

$-\beta$	$x_e/b$	$1/H$	$x_e/b$	$S$
0.1000	1.01761723	2.414188	0.467060	0.458974
0.1125	1.01996599	2.136073	0.490883	0.481274
0.1250	1.02235093	1.913507	0.513407	0.502182
0.1375	1.02477332	1.731337	0.534861	0.521931
0.1500	1.02723449	1.579463	0.555422	0.540697
0.1625	1.02973582	1.450892	0.575230	0.558619
0.1750	1.03227881	1.340627	0.594395	0.575809
0.1875	1.03486502	1.245006	0.613011	0.592359
0.2000	1.03749614	1.161280	0.631154	0.608344
0.2125	1.04017397	1.087349	0.648890	0.623828
0.2250	1.04290039	1.021579	0.666274	0.638867
0.2375	1.045676	0.962680	0.683354	0.653505
0.2500	1.048502	0.909625	0.700175	0.667786
	(1.04850)	0.90963	0.70018	0.66781)

Table 3. Table of  $1/H$  at intervals of 0.001 in  $S$

$S$	$0$	$1$	$2$	$3$	$4$	$5$	$6$	$7$	$8$	$9$	$0$
0.46	2.40035	38696	37367	36048	34739	33440	32150	30871	29600	28340	27089
0.47	2.27089	25847	24614	23390	22176	20970	19774	18586	17407	16234	15075
0.48	2.15075	13921	12777	11640	10512	09391	08279	07175	06079	04991	03911
0.49	2.03911	02838	01773	00716	99666	98624	97589	96561	95541	94528	93522
0.50	1.93522	92523	91531	90546	89568	88596	87632	86674	85723	84779	83841
0.51	1.83841	82909	81984	81065	80153	79247	78347	77453	76565	75684	74808
0.52	1.74808	73938	73074	72216	71364	70518	69677	68842	68012	67188	66370
0.53	1.66370	65556	64749	63946	63150	62358	61571	60790	60014	59243	58477
0.54	1.58477	57716	56960	56209	55463	54721	53985	53253	52526	51804	51086
0.55	1.51086	50373	49665	48961	48262	47567	46876	46190	45509	44831	44158
0.56	1.44158	43490	42825	42165	41508	40856	40208	39564	38924	38289	37657
0.57	1.37657	37029	36405	35784	35168	34555	33947	33342	32740	32143	31549
0.58	1.31549	30959	30372	29789	29209	28633	28061	27492	26926	26364	25805
0.59	1.25805	25250	24698	24149	23604	23061	22523	21987	21454	20925	20399
0.60	1.20399	19876	19356	18839	18325	17814	17306	16802	16300	15801	15305
0.61	1.15305	14812	14322	13834	13350	12868	12389	11913	11440	10969	10501
0.62	1.10501	10036	09574	09114	08657	08202	07750	07300	06854	06409	05967
0.63	1.05967	05528	05091	04657	04225	03796	03369	02944	02522	02102	01685
0.64	1.01685	01269	00857	00446	00038	99632	99228	98826	98427	98030	97635
0.65	0.97635	97242	96852	96463	96077	95693	95311	94931	94553	94177	93803
0.66	0.93803	93432	93062	92694	92329	91965	91603	91244	90886	90530	90176

Second differences are not negligible when interpolating values of  $S$  less than 0.57.

## ACKNOWLEDGEMENTS

Thanks are due to the Department of Mathematics for the loan of calculating machines and tables, and to Mr. I. F. Scott for his varied advice during the numerical work.

## REFERENCES

- (1) ANDREAS, J. M., HAUSER, E. A., and TUCKER, W. B. *J. Phys. Chem.*, **42**, p. 1001 (1938).

- (2) BASHFORTH, F., and ADAMS, J. C. *An attempt to test the theories of capillary action* (Cambridge: University Press, 1883).
- (3) FORDHAM, S. *Proc. Roy. Soc. A*, **194**, p. 1 (1948).
- (4) FLETCHER, MILLER and ROSENHEAD. *Tables of circular and hyperbolic sines and cosines* (New York: W.P.A., 1940).

## NOTES AND NEWS

## Correspondence

## Current densities of free-moving cathode spots on mercury

In the correspondence<sup>(1)</sup> on a contribution by H. v. Bertele<sup>(2)</sup> the question is raised whether spot emission on free mercury surfaces occurs only at individual spots of very high current density, as Dr. Froome assumes, or whether there are also extended emission areas of lower current density as Dr. Bertele indicates.

In this connexion I would like to describe an unpublished experiment carried out in 1951 which gives evidence for emission occurring exclusively in extended areas with very low current density. The discharge system consisted of a disk-shaped glass envelope *e* (see Fig. 1) situated between the

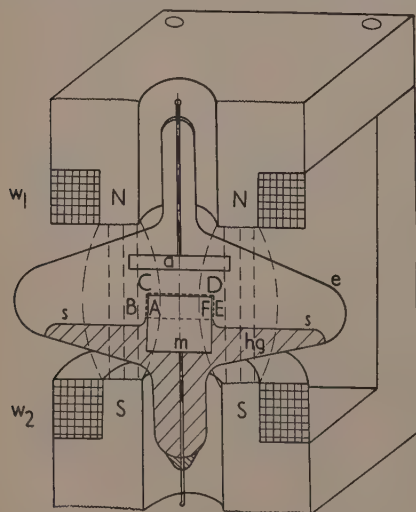


Fig. 1. Experimental arrangement

*a*, molybdenum anode; *e*, glass envelope; *s*, free mercury surface; *hg*, mercury filling; *m*, molybdenum cylinder of 12 mm diameter; *w*<sub>1</sub>, *w*<sub>2</sub>, armature coils.

poles *N* and *S* of an electromagnet with the windings *w*<sub>1</sub> and *w*<sub>2</sub>, having a molybdenum cylinder *m* protruding from the free mercury surface *s*, and an anode *a*. After careful degassing and applying a weak magnetic field it is possible to clean the surface of the molybdenum and to get it completely wetted by mercury. When increasing the magnetic field, the anchored spot, originally concentrated in the known way along the wetting line *A-F*, jumps over to the top of the molybdenum cylinder and begins to spread out. At relatively low fields (see Fig. 2) it forms a more or less continuous

cover on top of the molybdenum cylinder and may spread a little way over the rim. At higher magnetic fields, however, it spreads evenly over the whole top surface *C-D* and yields a symmetrical, cylinder-shaped discharge to the anode *a*. Finally, at still higher magnetic fields the emission seems to concentrate on a multitude of places while still spreading uniformly over the surface, making the discharge appear like a rainfall. All these phenomena are reproducible and may be observed for hours.

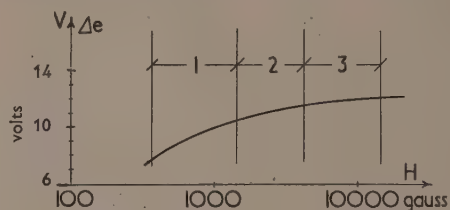


Fig. 2. Arc drop and spreading performance of anchored spot emission as function of the vertical magnetic field *H*

Range (1) emission extends across top from *B* to *E*; Range (2) emission covers only top between *C* and *D*; Range (3) emission spreads over top between *C* and *D*, yet tends to yield a multitude of small concentrated centres.

The total current of the discharge in the experiments described did not exceed 6 A yielding a current density in the range of approximately 10 A/cm<sup>2</sup>. Furthermore, observations of the current density of spots racing round at the level *A-F* yielded values of the order of about 150 A/cm. In this case, the vertical spot width was measured with a microscope, and its length by accurately timing the passages by a highly resolving probe.

Hence there seems little doubt that the current density does not represent a basic feature of spot emission, as external operating conditions influence it by many orders of magnitude. The preponderance of emission concentrated on many very small spots in Froome's observations is understandable as due to the restriction to a particular specialized case amongst very many possibilities.

A real understanding of the mechanism underlying spot emission cannot be realized before the actual significance of current density is understood.

Raytheon Mfg. Co.,  
Newton, Mass., U.S.A.

CHARLES G. SMITH

- (1) FROOME, K. D.; BERTELE, H. v. *Brit. J. Appl. Phys.*, **4**, p. 91 (1953).
- (2) BERTELE, H. v. *Brit. J. Appl. Phys.*, **3**, p. 358 (1952).

## New books

**Oxidation of metals and alloys.** By O. KUBASCHEWSKI, Dr.Phil.habil., and B. E. HOPKINS, M.Sc.(London: Butterworths Scientific Publications, Ltd.) Pp. xv + 239. Price 35s.

Metallic materials are being increasingly used at high temperatures and the problems of oxidation are receiving corresponding attention. This book is an excellent detailed account of the more theoretical aspects of the subject. The section on "Basic information" reviews the various physical factors influencing oxidation, e.g. diffusion, electrical conductivity, etc. The tables of properties are very useful, but there are some gaps which could be filled and some melting- and boiling-points are out of date. The second section discusses the techniques for studying the phenomena and examining oxidation products; the third deals with the various theories proposed to explain the mechanism of oxidation and, although it may need revising in view of the progress being made, is most useful.

The fourth section deals with experimental results and the behaviour of metals in practice and is perhaps the least satisfactory part for users of metals as distinct from the academic research worker. More attention could well have been given to the problems of the protection of metals and the effect of solid phases on oxidation: both are important current problems that are not yet readily available in the literature. The bibliography is excellent (549 references) and up to date to 1952.

G. T. HARRIS

**Advanced mathematics in physics and engineering.** By ARTHUR BRONWELL. (London: McGraw-Hill Book Co. Ltd.) Pp. xvi + 475. Price 51s.

Faraday is said to have boasted that he had once in his life performed a mathematical operation—when he turned the handle of Babbage's calculating machine. For those less endowed with physical perception and who have more frequently to pay court to the Queen of the Sciences, this book provides very efficiently the short refresher courses which are so often necessary on these occasions. Indeed it forms a very useful reference book, for not only is the field it covers very wide, but each chapter is succeeded by a list of references, mostly to other texts but occasionally to original papers. This is typical of its outlook, and the book should form a satisfactory accompaniment to courses on physics or engineering. To this end, each chapter is followed by a series of problems, and as a cunning incentive to broader investigation the student is informed that some of the problems appear as developments in the texts to which reference is made at the end of the chapter.

After laying a mathematical foundation with chapters on complex numbers, infinite series, Fourier series and two very good ones on differential equations and the series solution thereof, there are treatments of mechanical vibration and electrical oscillation with lumped and distributed elements, and a thorough treatment of Lagrange's equation. The emphasis throughout is on dynamic rather than static problems, and there are chapters on the solutions of the wave equation, heat flow, dynamics of fluids and electromagnetic theory. Finally there is a good and advanced chapter on complex variable theory, and a detailed treatment of Laplace transforms. In face of this very comprehensive treatment it is perhaps ungracious to ask for more, but the writer would like to have seen a chapter on statistical methods. The

number and magnitude of the errors at times committed from the lack of what one might call statistical awareness is sometimes surprising. Unfortunately the book's price will put it beyond the reach of many students.

C. E. R. BRUCE

**Gasdynamik.** By K. OSWATITSCH. (Vienna: Springer-Verlag.) Pp. xii + 456. Price 133s.

Jets push passengers across the Atlantic in a time that would have been insufficient for Columbus to travel from Italy to Spain. Before they can do it, some back-room boys somewhere have done immense amounts of calculation on air flow and air resistance, not only for calculating the behaviour of the aircraft, but to study the flow of gas in the engine itself.

Here is a text-book that brings together a great deal of the theory on which they must rely. It is a straight development of the hydrodynamics that the Cambridge mathematicians used to study rather more than fifty years ago, but is in fact almost all the result of work carried out since the outbreak of the second world war. Perhaps the most striking feature is the fact that this new and advanced work requires such relatively elementary mathematics, in contrast to some of the other subjects which are almost equally recent.

The book opens with a chapter on thermodynamics, and then proceeds to the different cases of fluid flow, most often with reference to speeds near or above that of sound. The exposition is invariably clear, and every help is given to the student, even to the provision of a table of integrals, in which we are given, separately, the integral of  $1/(1+t^2)$  as  $\arctan t$ , and the value between 0 and  $\infty$  as  $\pi/2$  (though the limits of integration have been omitted).

J. H. AWBERY

**The properties of electrical insulating materials and methods of test.** (London: National Physical Laboratory.) Pp. 16. Price 1s. 3d.

The purpose of this booklet appears to be to emphasize one of the functions performed by the National Physical Laboratory, namely, testing in accordance with British Standard Specifications requirements. This service is already well known to designers and manufacturers, as are the details of the specifications on which it is based, and they do not require the very elementary definitions of properties and methods of test that form the bulk of this text. It is therefore difficult to visualize any purpose for the booklet other than that of an introduction of the subject to junior students, for which it is well suited, if brief.

FREDERICK M. BRUCE

**Small particle statistics.** By G. HERDAN, M.Sc., Ph.D., LL.D., and M. L. SMITH, Ph.D., F.R.I.C. (Holland: Elsevier Publishing Co.) Pp. xxiii + 520. Price 70s.

According to the preface, this book sets out to put the statistics of particles (sieve and sub-sieve) upon a basis entitling this subject to recognition "in its own right." It is not inappropriate therefore that some four-fifths of this massive volume should be devoted to statistical matters as such (but excluding particle dynamics), leaving about one-fifth for the discussion, by Dr. M. L. Smith, of experimental techniques.

The general plan is as follows. Firstly, we have the determination of the fineness of solids, and secondly, the technological importance of this factor. Then comes a section dealing with the attainment of a specified fineness and homogeneity of a substance, leading up to a review of the



principles of statistics of coarse disperse systems. At this point there is a break, after which questions of experimental design and errors are considered. An author index and a subject index bring the work to a close.

What is not altogether easy to grasp is exactly why the book should have been written. The crux of the whole problem, for the moment at any rate, is not how to treat (statistically) the findings of research workers who have to deal with particles falling within a certain size-range, but how to advance our knowledge of the highly complex physical events with which, in this field, we are inevitably confronted. This latter aspect the book seems scarcely calculated to enlighten.

F. I. G. RAWLINS

**Radiations and living cells.** By F. G. SPEAR, M.D., M.A., D.M.R.E. (London: Chapman and Hall Ltd.) Pp. xii + 222. Price 18s.

Before the development of atomic energy the physicists concerned with the biological effects of high energy radiations had been chiefly those relatively few hospital physicists whose daily work was intimately related to the radiotherapy of malignant disease. Since then, however, the number of interested physicists has increased considerably; but they have been very much handicapped by the lack of accurate and critical summaries of existing data, to say nothing of their lack of basic biological knowledge. Dr. Spear has done a most useful service to these physicists by making available in a readily understandable form the information contained in this excellent little book which is another of the *Frontiers of Science Series*. All physicists interested in the biological effects of radiations should possess a copy.

Since Dr. Lea's book *Actions of radiations on living cells* appeared in 1946 and set out so beautifully the successes of the target theory, there has been a regrettable (but natural) tendency for physicists to regard this as the whole story—yet Lea himself repeatedly emphasized the limitations of the theory. Dr. Spear's book should help to correct this tendency and it is most fitting that he works in the same laboratory as did the late Dr. Lea.

It is difficult to especially praise one section in a book which is wholly excellent, but the reviewer found that Chapter VI, on Irradiation of the blood and of the Circulatory system was a most exciting voyage of discovery.

Very few errors seem to have escaped the author's eye except perhaps the spelling of "phosphorus" for "phosphorus" on p. 150 and Fig. 57 seems to be wrongly orientated. On p. 195 there seems to be some confusion between ionizing particles and ionization as the causative agent of the biological effect discussed, but these are insignificant defects.

The reviewer believes that it is desirable for more physicists to participate in radiobiological research than do at present, and in respect of this he would quote from Dr. Spear's book: "The most important considerations are that the experimenter shall be familiar with the material chosen for experiment, be able to distinguish with certainty the changes produced by radiation and those unconnected with it, and should have ability to judge to what extent the results may have application to, or a bearing on, other kinds of biological tissue exposed to similar doses of radiation under comparable conditions." This means essentially that "radiological problems are much better attacked by physicist and biologist working in harmonious collaboration . . . an achievement which in the past has been too seldom realized." Can it be achieved more frequently in the future?

Although quite small, this book sets out signposts to

avenues yet to be explored. Let us hope that it encourages more of the new Elizabethans to join in the exploration.

C. W. WILSON

**Heat transfer phenomena.** By R. C. L. BOSWORTH, Ph.D. (Cantab.), D.Sc.(Adel.), F.Inst.P., F.A.C.I. (Sydney: Associated General Publications Pty. Ltd.; London: Pergamon Press Ltd.) Pp. xii + 211. Price 42s.

This monograph arose out of the opening review paper prepared for a Conference of the Australian Branch of The Institute of Physics, in 1948. It has the double aim of showing the different processes of heat transfer as varieties of a single process, and of reviewing the laws in each of the fields of technical interest, and collating the constants which enter into the theoretical formulae.

It is much more successful in the second aim than the first. True, it groups convection, radiation and conduction as transfer processes, but the mean free path for the carriers of radiation is so much greater than that for the carriers of conduction or convection that the laws are naturally of different form. As a reference book for the methods of calculating transfer by each of the processes, and for good values of the constants, it is, however, a most valuable compendium. There are, for good measure, chapters on heat transfer in boiling and condensation, and on the use of the equivalent electrical circuit. This is, today, probably of less general value than numerical methods of calculation, such as the several modifications of the relaxation method, but for those who prefer a physical method this book contains a good survey.

J. H. AWBERY

**Physical constants of some commercial steels at elevated temperatures.** (London: Butterworths Scientific Publications Ltd., for the British Iron and Steel Research Association.) Pp. x + 38. Price 21s.

This book contains a reissue, in more convenient form, of the results of measurements of specific heat, expansion, electrical resistance, thermal conductivity and density of twenty-two typical steels taken from two papers by the National Physical Laboratory. Additional tables give the mean coefficient of expansion over 50° intervals and thermal diffusivity. Some information on thermal and electrical conductivities is given for a further thirteen steels. A uniform temperature interval has been used in all tables and this should facilitate reference. However, some loss of detail occurs which may be important in the case of the specific heat at the magnetic change point and through the transformation range. The value of the tables would have been increased by a more critical review of the data. One is inclined to wonder to what extent the differences in specific heat between the various carbon steels are significant, apart from in the transformation range.

The introduction anticipates that these tables will be of use to engineers. A word of caution would have been desirable for this class of reader as the properties were determined for one condition only. In other conditions they may differ appreciably from the values given. Furthermore, all measurements were made on heating and should be used with considerable caution during cooling after heating into the austenitic range, particularly for low alloy steels.

Finally, there are one or two unexplained differences between certain results in these tables and the original N.P.L. data. For example the expansion temperature curves for steel 6 and 8 (0.9 and 1.22% carbon) differ from those given in Fig. 164 of the first N.P.L. report. Further, steel 13 (3.5%

nickel-chrome-molybdenum) has a minimum in the expansion temperature curve at 800° C in the book under review and at 750° C in the N.P.L. paper. A. BARKER

**Progress in nuclear physics, Vol. 2.** Edited by O. R. FRISCH, O.B.E., F.R.S. (London: Pergamon Press, Ltd.) Pp. viii + 295. Price 63s.

This volume is beautifully produced and has appeared with a commendably short delay after the writing of the articles; in both these respects it is superior to Volume 1. The subject matter also seems more satisfying, perhaps because a more uniform standard has been preserved over all the articles. Unfortunately the price has been increased, but this is a longer work and publishing costs have evidently continued to rise.

The value of authoritative review articles of this standard, particularly to specialists in nearby fields, is well established; much of a scattered, unwieldy mass of information is again sifted and summarized by active workers in the individual fields. There are now eight articles, on the electron optics of magnetic  $\beta$ -spectrometers (N. F. Verster); nuclear paramagnetic resonance (R. V. Pound); materials for scintillation counters (G. F. J. Garlick); neutron-proton interaction (G. L. Squires); fission (W. J. Whitehouse); low-lying excited states of light nuclei (W. E. Burcham); the nuclear shell model (B. H. Flowers); and ionization by fast particles (T. E. Cranshaw). With Volume I as a basis, it has been possible to shift the main emphasis away from techniques and towards experiments and theory. Only two articles in Volume 1 is superseded, except for slight overlapping in the treatment of  $\beta$ -ray spectrometers; there are now so many virtue specialized fields of nuclear physics that it seems likely that most topics will be treated at fairly long intervals.

It would be unfair to select any article for special comment in a short review. All are well written and well provided with references, and Professor Frisch's good influence as Editor is much in evidence. This series should grow into a most valuable work of reference as further volumes are added, and the timing of the choice of topics has so far been such that the inevitable decline in value of the articles should be comparatively slow. T. G. PICKAVANCE

**Berechnung magnetischer felder.** By F. OLENDORFF. (Vienna: Springer-Verlag.) Pp. x + 432. Price 112s.

The rigorous calculation of magnetic fields in electro-magnetic machines and apparatus involves naturally the use of fairly advanced mathematics. In this book numerous problems of potential theory are solved with elegance and the boundary conditions of complicated shapes are introduced by skilful simplification.

The book is mainly concerned with electrical power engineering apparatus, but some problems more usually confronting the physicist are also treated in considerable detail. Amongst these one might mention the earth's magnetic field, the bar magnet, the inductance of a diode with cylindrical electrodes and the a.c. and d.c. lifting magnet. Fields in large air gaps of electromagnets are unfortunately not included.

The physicist may conclude that the severely mathematical approach of the book is sometimes confusing in the absence of adequate textual explanations. Numerous line drawings offer a valuable contribution to the subject-matter but emphasis is generally confined to mathematical expressions

whose meaning has often to be discovered by extensive back-reading to understand the significance of symbols and of the notation used.

On the whole one feels that this is an excellent book which is specifically intended to help the electrical engineer in many design problems, but its value to the physicist will probably be rather limited.

The book is very well produced and clearly printed and the index is concise and adequate. K. HOSELTZ

**Modern applied photography.** By G. A. JONES. (London: Temple Press Ltd.) Pp. vi + 162. Price 9s. 6d.

This is an excellent little book. The author has performed a feat of compression which few others would have been competent to attempt and in which none other, perhaps, could have succeeded so well. The very diversity of the uses to which photography is now put, in the laboratory and in everyday affairs, creates a risk that any such survey might easily become a mere catalogue, devoid of readability. This risk has been on the whole successfully avoided by skilful organization of the material and by discussion of some examples in fair detail. Even so, the book is likely to require close reading by the reader possessing a "general knowledge of elementary photographic principles," to whom it is addressed. It carries an adequate index, but might have been improved for such a reader by more direct correlation between the text and the well-chosen half-tone illustrations.

L. V. CHILTON

**The identification of stones in glass by physical methods.**

By H. E. TAYLOR, M.A., A.Inst.P., and D. K. HILL, B.Sc. (Sheffield: The Glass Delegacy of The University of Sheffield.) Pp. 70. Price 42s.

This little book in the series of monographs on glass technology should be in every laboratory connected with the manufacture of glass and, by sponsoring its publication, the Glass Delegacy has rendered a service to the industry.

The identification of stones in glass with a view to deciding their origin and methods of prevention is such a highly specialized branch of glass and refractories technology that it is frequently neglected. The authors therefore deserve to be congratulated on producing so condensed an account of the subject that it should serve as a manual for laboratory use and reference. The chapter describing simple visual tests as an aid to identification of stones in glass should be invaluable to many glass technologists.

The five chapters deal respectively with: I. The origins of stones. II. Identification by simple visual tests. III. The use of the petrological microscope. IV. Characteristic features of materials found in stones. V. The X-ray diffraction technique. But the book is rendered more valuable by the inclusion of three appendices giving, in a form convenient for easy reference, crystallographic data for materials found in stones, a list of possible sources of materials found in stones, 64 photo-micrographs of inclusions found in specimens of glass and an excellent index.

The work is an extension of that begun in this country by Holland and Preston; it could have been improved by inclusion of illustrations from other sources and by the expansion of some sections. However, it was probably the authors' intention to produce a manual which should find everyday use in glass works and in this they have undoubtedly succeeded. J. H. PARTRIDGE



## Notes and comments

### Elections to The Institute of Physics

The following elections have been made by the Board of The Institute of Physics:

*Fellows:* P. R. Bardell, J. E. Caffyn, D. R. Chick, A. W. Ireland, K. H. Kreuchen, H. Messel, R. Taylor, D. Walker.  
*Associates:* D. C. Bisset, G. F. Claringbull, J. W. Cole, P. Davis, W. J. Duffin, A. J. Dyer, M. P. Gupta, M. G. Harwood, R. M. Hinde, B. G. Knowles, D. R. McCall, T. A. Margerison, K. J. Marsh, P. M. Martin, W. C. Nixon, K. C. Randle, S. Salkauskas, M. G. Smith, M. C. J. Todd, E. V. Vernon, J. Woods, J. Zussman.

Thirteen Graduates, nine Students and five Subscribers were also elected.

### Lectures on various aspects of magnetism

The first of a new series of lectures inaugurated by the Permanent Magnet Association was delivered on 22 April last by Professor W. Sucksmith, in Sheffield before a distinguished audience of some 200 people representing the metallurgical and electrical industries. He traced the remarkable developments that have taken place in the theory of magnetism and its practical applications during the last fifty years. Starting from the classical work of Ewing and Weiss he touched on the developments which took place up to the 1930's and then spoke of the parallel advances in theory and practice in the last 25 years. These, he said, had resulted in a forty-fold increase in the energy of permanent magnets and a thousand-fold increase in the permeability of soft magnetic materials. The lecture is to be published shortly in full in this *Journal*.

Mr. Spencer Levick, the Chairman of the Association, presided over a dinner which followed the lecture and he and others paid tribute to the team spirit pervading the Permanent Magnet Association. Not only did it perform the functions of a trade association, but it also owned its own central research laboratories and maintained an information service.

### International conference on the science and applications of photography

The Royal Photographic Society has arranged an international conference on the science and applications of photography which is to be held in London from 19 to 25 September, 1953. The papers to be presented have been classified into the following sections: Photographic science; Kinematography and colour photography; Technique and applications of photography; Photomechanical processes; and History, literature and training in photography.

The fee for the conference is £1 1s. 0d. for members of the Society and lecturers, and £2 2s. 0d. for non-members. One set of preprints of the papers read in any one section will be presented to each person attending the conference. Sets of preprints of the papers read in any other section will be obtainable for 5s. for each section.

Further information may be obtained from The Secretary,

The Royal Photographic Society, 16 Princes Gate, London, S.W.7.

### Prizes for original contributions in the Journal of Scientific Instruments

The Board of The Institute of Physics has awarded Bowen Prizes of fifteen guineas each to the following for their papers published in the *Journal of Scientific Instruments*.

Mr. G. T. Wright, B.Sc., of the University of Birmingham, for his paper *A single-channel pulse-height discriminator of high speed and stability* (p. 157, May 1952).

Mr. G. D. Dew, of the National Physical Laboratory, Teddington, Middlesex, for his paper *On the preservation of groove-form in replicas of diffraction gratings* (p. 277, September 1952).

Mr. H. Aspden, B.Sc., of Trinity College, Cambridge, for his paper *A method of measuring the magnetic permeability of rod specimens* (p. 371, November 1952).

These prizes are awarded to authors who are not more than 35 years of age whose papers are judged to be the best in respect of originality, scientific value, practical utility to instrument makers and users, and presentation, including the standard of presentation of the manuscript. Money for them is provided by the Scientific Instrument Manufacturers' Association of Great Britain Ltd. from the Bowen Trust Fund established by the late Mr. William Bowen.

## Journal of Scientific Instruments

### Contents of the August issue

#### ORIGINAL CONTRIBUTIONS

- Papers*  
A simple low-frequency double-flash stroboscope. By J. E. Caffyn and R. M. Underwood.  
A vacuum microbalance for measuring sorption in dielectrics. By A. G. Day.  
Some automatic devices for use on tidal models. By M. J. Wilkie.  
The measurement of low concentrations of hydrogen in nitrogen. By A. H. Turnbull and M. F. A. Harrison.  
A direct-reading microdensitometer. By R. I. Tait and F. C. Chalklin.  
Sorption and desorption of gas in the cold-cathode ionization gauge. By J. H. Lusk.  
An apparatus for the ultra-violet spectroscopy of solutions at low temperatures. By R. Passerini and I. G. Ross.  
The optical projection of the profile of an article at a given cross-section. By G. F. Morton and V. E. Gough.  
Measurement of X-ray intensities on integrated Weissenberg photographs. By D. W. Smits and E. H. Wiebenga.  
A sensitive differential wattmeter. By L. M. Clarebrough, M. E. Hargreaves, D. Michell and G. W. West.  
An optical goniometer for the examination of long metal single crystals. By A. J. Goss.  
Scintillation counters using liquid luminescent media for absolute standardization and radioactive assay. By E. H. Belcher.  
Laboratory and workshop notes  
A null-detector for power frequency bridges. By J. S. T. Looms.  
A pneumatic conveyor for BEPO irradiation cans. By G. Shepherd and R. West.  
The reproduction of an evaporated highly reflecting film of desired reflectivity. By E. V. Vernon.

#### NOTES AND NEWS

- Correspondence*  
Measurement of force required to pull through a 1 in. diameter Wilson vacuum seal. From D. McLean and M. H. Farmer.  
Improvements in fine wire thermocouples. From C. H. W. Slater.  
A low-torque multi-way flexible connecting tape. From D. L. Turner.  
Insulated electrical leads into pressure vessels. From P. H. R. Lane.

#### New instruments, materials and tools

#### Notes and comments

THIS JOURNAL is produced monthly by The Institute of Physics, in London. It deals with all branches of applied physics (including theory and technique). All rights reserved. Responsibility for the statements contained herein attaches only to the writers.

**EDITORIAL MATTER.** Communications concerning editorial matter should be addressed to the Editor, The Institute of Physics, 47 Belgrave Square, London, S.W.1. (Telephone: Sloane 9806.) Prospective authors are invited to prepare their scripts in accordance with the *Notes on the preparation of contributions*. (Price 2s. 6d. including postage.)

**REPRODUCTION.** The Institute of Physics is a signatory to The Royal Society's Fair Copying Declaration. Details may be obtained upon application from The Royal Society, London, W.1.

**ADVERTISEMENTS.** Communications concerning advertisements should be addressed to the agents, Messrs. Walter Judd Ltd., 47 Gresham Street, London, E.C.2. (Telephone: Monarch 7644.)

**SUBSCRIPTION RATES.** A new volume commences each January. The charge is £4 per volume (\$11.50 U.S.A.), including index (post paid), payable in advance. Single parts, so far as available, may be purchased at 8s. each (\$1.15 U.S.A.), post paid, cash with order. Orders should be sent to The Institute of Physics, 47 Belgrave Square, London, S.W.1, or to any bookseller.



# Magnets and magnetism—recent developments\*

By PROF. W. SUCKSMITH, D.Sc., F.Inst.P., F.R.S., University of Sheffield

An account is given of the present state of the subject of ferromagnetism, with particular application to ferromagnetic materials. Brief reference is made to the state of development at the beginning of the century and the significant phenomena and principles discovered since then are discussed. Particular attention is directed to the explanation of the magnetization curves of "hard" and "soft" ferromagnetics. The report deals also with the recently discovered ferromagnetic oxides, a new type of magnetic material offering wide possibilities for future investigation and application.

Progress in both the theory and practice of magnetism during the last decades has been so remarkable that the subject calls for little justification, and the following account is an attempt to present an outline of this progress.

With this in mind, it is necessary to summarize the development of the subject of magnets and magnetism in the early part of this century since much of this has its bearing upon recent work. At that time Ewing presented an adequate survey of the subject in his *Magnetic Induction in Iron and other Metals*, a book constituting a notable landmark in magnetism. Of theory there was little. Some support was given to the concept of Weber's elementary magnets, each molecule being regarded as a magnet, subject to a frictional force which maintains it in its established orientation. This was adequate in explaining the approach to saturation but was unsatisfactory in so far as residual magnetization was concerned, and Clerk Maxwell's suggestion that the molecule had more than one position of equilibrium was a shrewd foretaste of things to come. Ewing further saw that the constraints upon the orientations could arise from the magnetic forces due to neighbouring molecules, and showed both by models and by calculation how such forces could account for the shape of magnetization curves and also the major and minor hysteresis loops. The remarkable agreement seemed at the time full of promise.

With regard to the materials available perhaps this is best illustrated by means of examples taken from the literature of the time. "Annealed soft wrought iron" appeared to be the most highly permeable material, the initial permeability being a few hundreds. Speaking of the hard magnetic materials Ewing says "Other constituents than carbon affect the magnetic quality very greatly, such as chromium and in particular tungsten. In soft iron, as we have seen, the coercive force is about 2 or even less. In chrome steel, hardened by quenching in oil, it is 40, and in tungsten steel it may even exceed 50."

In other words, there was no quantitative theory, but only qualitative views, whilst the materials were few enough not to make life too complicated for the manufacturer, for Low Moor iron on the one hand and Vickers or Jessops' tool steel on the other would supply most magnetic demands.

The first important influence of modern concepts on the theory of magnetism came from Paul Langevin in 1905, who used statistical theory to explain the variation of paramagnetic susceptibility with temperature. He assumed that each molecule had a definite magnetic moment whose orientation was influenced by the applied field and at the same time disturbed by thermal agitation. There is the magnetic energy, which we can write  $\mu H$ , warring with the thermal energy  $kT$ . This theory explained the pioneer experimental

work ten years before of Pierre Curie, who had discovered that the feeble magnetization of the paramagnetics decreased as the temperature increased. But this revealing explanation of paramagnetic phenomena only deepened the cloud which obscured the origin of ferromagnetism. The slow approach to saturation of paramagnetics, needing millions of oersteds at room temperature contrasted sharply with the similar approach in tens of oersteds for the ferromagnetics. Two years later, in 1907, Pierre Weiss was responsible for the two hypotheses which were to have far-reaching effects and the complete significance of which is not even now fully appreciated. The approach to saturation is brought about by the rotation of these domains as a whole, instead of the rotation of the elementary magnet, supposed at the time to be the molecule or atom. To the applied field  $H$  is added the Weiss intermolecular field  $NI$  whose magnitude is some millions, such that any field which we can produce in the laboratory is negligible in comparison. It is therefore necessary to adopt Weiss's second postulate—that small regions or "domains" are magnetized to saturation even when the specimen as a whole has zero magnetization, a state of affairs in which these domains are orientated at random. It transpired later that Weiss's concepts were supported by a wealth of experimental data, most of it subsequent to the theory, and some of it only in the last few years. No clue as to the origin of this assumed intermolecular field was available. The maximum value of the Weiss constant  $N$  which could be justified on theoretical grounds was only  $4\pi/3$ , the field arising from the polarizing effect of neighbouring elementary magnets. Values demanded by the Weiss theory of some thousands for  $N$  defied explanation completely and the *ad hoc* nature of this hypothesis remained for many years. After Weiss propounded his concepts, there emerged a protracted period marked by the consolidation of the theory, and the gradual filling in of experimental detail. In order properly to appreciate the position one must remember that the Weiss domains had never been seen, whilst the magnitude of the magnetic moment  $\mu$  we have referred to above was quite unknown. Whilst physicists had some ideas about the atomic structure of solids, there was little firm evidence. A few years had to elapse before the Braggs discovered the first atomic arrangements in solids by means of X-ray diffraction.

It was not until 1919 that Barkhausen discovered the effect to be known later by his name. If a secondary coil of some thousands of turns surrounding a ferromagnetic wire is connected to a loudspeaker through an amplifier, there are heard a succession of noises when the magnetizing field is changed continuously. He correctly interpreted the phenomenon as demonstrating the discontinuities of the magnetization progress. These were found to be most marked on the steep part of the magnetization curve and were almost absent elsewhere. Extension of the experiments to heavily quenched

\* Based on a lecture given in Sheffield on 22 April, 1953, under the auspices of the Permanent Magnet Association.

steels on the one hand and single crystals of iron on the other showed that the number of Barkhausen clicks varied very little and thus shows that the domain cannot be identified with the grain size. On the assumption that each discontinuity was caused by the rotation of a single domain, counting of the clicks showed the size of the average domain to be about a hundredth of a millimetre across. At about the same time Bitter,<sup>(1)</sup> by putting a suspension of colloidal iron on a polished surface of iron, observed a fine pattern which was thought to mark domain boundaries, thus providing experimental proof of the phenomenon. Meanwhile the last remaining support for the original Weber-Ewing theory was removed by Mahajani. The concept of the spinning electron had attached a precise magnitude to the magnetic moment  $\mu$ , previously mentioned. The unit of magnetic moment is directly related to the unit of angular momentum by the simple relation  $\mu = (1/2mc)(h/2\pi)$ , and so quantitative check becomes easy since all the other constants are known within reasonable limits. The magnitude of the coercivity was found to be around 5000 oersteds for the perfect lattice, whereas we know it should be at least 100 000 times less. On the other hand, the initial permeability according to the model is unity, and this should be about 100 000 times bigger. There are other faults but it is easy to see that Ewing's model is for a paramagnetic, rather than for a ferromagnetic as he had thought.

Ewing had discovered many years before that many ferromagnetic materials are sensitive to the application of stress. If these stresses are below the elastic limit, they may cause an increase or decrease in permeability. It is highly significant that substances which increase in permeability under tension also increase in length when magnetized, this change in length being known as the magnetostriction. Thus a nickel-iron alloy containing 68% nickel has a positive magnetostriction, i.e. increases its length on magnetization. It may increase its permeability no less than 30-fold under tension (see Figs. 1 and 2), whilst conversely pure nickel, with negative

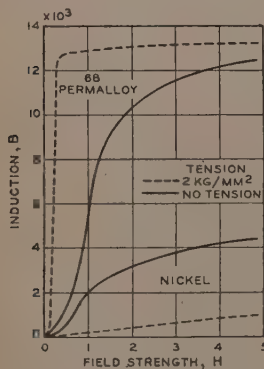
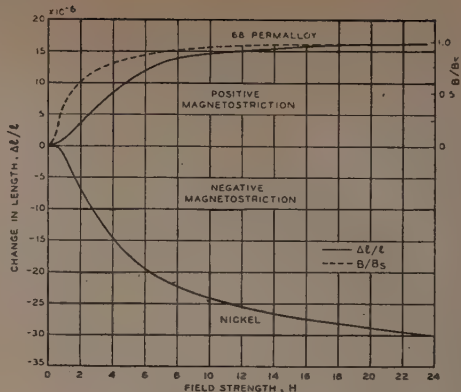


Fig. 1. Effect of tension on magnetization of 68 Permalloy and nickel is in opposite directions. Tension is held constant while field is increased from zero. [Bozorth.]

(Reproduced from Review of Modern Physics)

magnetostriction, becomes less magnetizable under tension. In the alloys somewhere between 68% and 100% nickel we may therefore look for zero magnetostriction. In this way low values of the magnetostriction can confidently be associated with high permeability, and it is in this region that the academic prototypes of Mumetal and Permalloy lie.

The discovery of the strain method of producing single crystals of aluminium by Carpenter and Elam in 1921 had been followed by the application of the method to iron by Edwards and Pfeil shortly afterwards. Very early it was discovered that along certain directions in the crystal it was

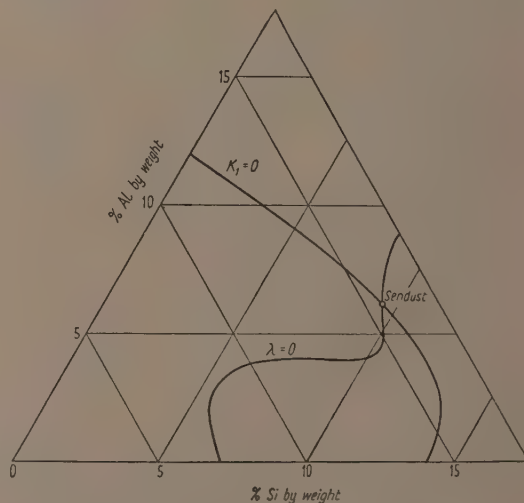


(Reproduced from Review of Modern Physics)

Fig. 2. Application of field causes increase in length of 68 Permalloy (positive magnetostriction) and a decrease in nickel (negative magnetostriction). Compare with reciprocal effect of Fig. 1. [Bozorth.]

easy to magnetize the material. These directions of "easy magnetization"—the cube edge in iron (6 directions), the cube diagonal in nickel (8 directions), and the perpendicular to the hexagonal plane in cobalt (2 directions)—were to prove of paramount importance in explaining the magnetization curve. It is important to realize that the cubic crystals iron and nickel, as well as other alloys of similar structure, become isotropic at about 500 oersteds, whilst the hexagonal structure of cobalt has a corresponding value of not less than 14 000 oersteds. It should be noted further that cobalt, with only parallel and antiparallel directions of easy magnetization, possesses the advantage of a relative simplicity important for theoretical tests.

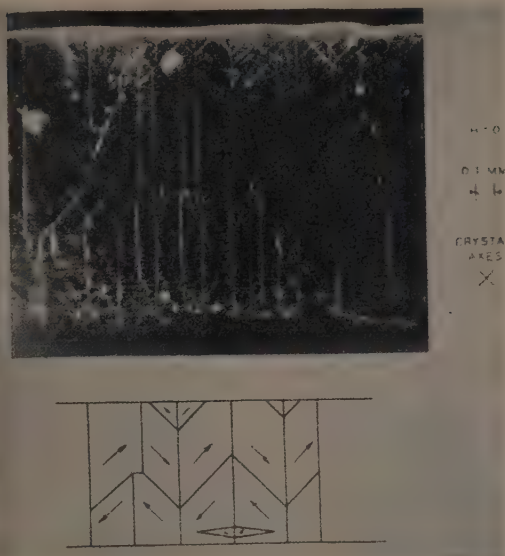
Thus we can see that both low magnetostriction and ease



(Reproduced by courtesy of Oxford University Press)

Fig. 3. Explanation of the high permeability of Sendust. Lines of zero crystal energy and zero magnetostriction for Fe-Si-Al alloys. [Hoselitz.]

of magnetization are conducive to high permeability. Fig. 3, quoted by Hoselitz<sup>(2)</sup> from Went and Snoek's<sup>(3)</sup> data, shows

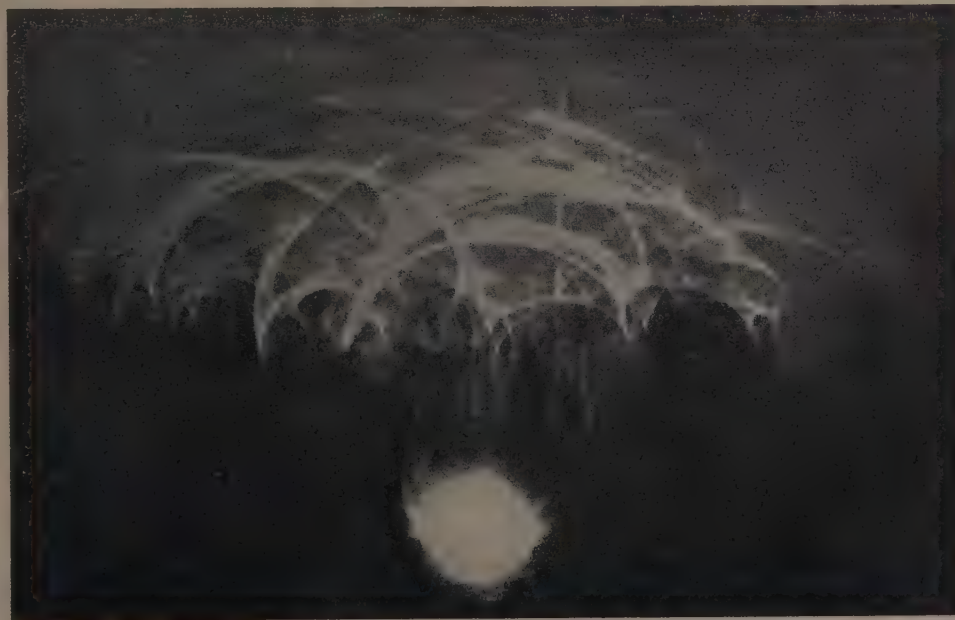


(Reproduced from Physica)

Fig. 4. Powder pattern of iron crystal containing 3.8% silicon. Interpretation of pattern is shown schematically in lower part of figure. [Bozorth.]

the lines of minimum value of these two factors in the ternary iron-silicon-aluminium system. Where they cross is the high permeability alloy Sendust. To these criteria must be added perfection of the lattice. It is well known that foreign atoms, particularly if of a different size from the parent matrix, cause distortion extending over many atom diameters, and obstruct the free rotation of the elementary magnets. Many such likely atoms, e.g. carbon, phosphorus, sulphur, can be effectually removed by appropriate heat treatment in hydrogen, and this technique gives a most valuable improvement to the ease of magnetization. The very marked improvements in "soft" materials which have taken place in recent years owe their high permeabilities chiefly to these causes, and values of 100 000 and above in isotropic materials are available. The limit, where still higher permeabilities can have little or no practical use, appears to be well within sight, since practical considerations prevent the application of these high values. Effective permeabilities as high as those quoted can only be achieved under the most exacting closed-circuit conditions, so that design rather than material must become increasingly important.

But whilst the domain theory progressed, there is no doubt that the Bitter patterns, which might well be expected to provide satisfactory confirmation of the theories, were quite incapable of even qualitative explanation of the different stages in the magnetization curve, and it was not until the technique of electrolytic polishing, originally introduced by Elmore<sup>(4)</sup> at the Bell Telephone Laboratories, revealed the fact that the true domain patterns were vastly different from those obtained earlier on polished surfaces. Not only that, but the patterns proved a remarkable tribute to the theory of Néel, who had forecast patterns which were remarkably similar to those which are obtained by the Elmore technique. The now familiar "tree" pattern (Figs. 4 and 6a) undoubtedly



(Reproduced from Review of Modern Physics)

Fig. 5. Results obtained in scattering of electrons from the hexagonal face of a cobalt single crystal. [Germer; Kittel.]  
VOL. 4, SEPTEMBER 1953



gives us a true picture of the domain boundaries. Experimental verification of these views has been provided. One remarkable, though simple, test for finding the direction of magnetization in a domain has been devised in the scratch technique. Thus if a very fine scratch is perpendicular to the direction of magnetization in a particular domain, the lines of force leak out into the air and attract the colloid, but if the scratch lies along the magnetization direction there is no such

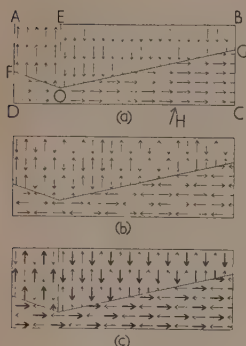


Fig. 6. (a) Domain pattern in a ferromagnetic. (b) Possible domains in an antiferromagnetic. (c) Possible domains in a ferrimagnetic.

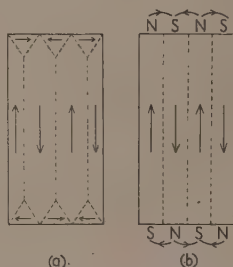


Fig. 7. (a) Domain arrangement of an unmagnetized cubic crystal such as iron, in which the directions of easy magnetization lie along the cube edges. Note the closed flux circuits in the metal. (b) Domain arrangement in a hexagonal crystal such as cobalt with only two easy directions of magnetization. Note the emergence of the lines of force in the surroundings.

leakage and the scratch is almost invisible. Thus the direction of magnetization in a domain can easily be found. An even more convincing experiment has been carried out. A beam of electrons is fired at grazing incidence to the surface of a ferromagnetic crystal. In an iron crystal suitably cut there are four directions of easy magnetization for the closed flux circuits (Fig. 7); but with cobalt there are only the two directions so that the flux must of necessity leak out into the air, thus producing a deflexion of the electron beam, which is recorded on a photographic plate. This phenomenon therefore occurs only for cobalt crystals and Fig. 5 shows the effect. By this and other evidence the domain picture is firmly established and confirmed.

We are now in a position to form a picture of the magnetization curve. At the lowest fields, at the "toe" of the magnetization curve, in the so-called Rayleigh region, reversible boundary displacements take place. Here the more favourably disposed domains, i.e. those with a component of magnetization parallel to the applied field, grow in size at the expense of those less favourably placed. Thus in Fig. 6(a) if the field  $H$  is applied in the direction shown, a domain such as  $AEOF$  would grow at the expense of others, e.g. by movement of the domain wall  $EO$  to the right. This stage gradually gives place to the irreversible region, i.e. the steepest part of the magnetization curve, where discontinuous changes of the directions of magnetization from one easy direction of magnetization to another which has a greater component along the field, i.e. the direction of magnetization in  $EBGO$  would turn discontinuously through  $180^\circ$ . This

means that the domain wall  $EO$  disappears. Similarly the magnetization in  $FOGCD$  turns discontinuously through  $90^\circ$  leaving the whole as one domain with the magnetization directed along  $DA$ . The third stage beyond the "knee" of the magnetization curve is marked by gradual rotation of the elementary magnets, where, in the high fields approaching saturation, these are constrained gradually to leave the easy directions and to align themselves with the now powerful magnetizing field.

So far, however, we have not considered the hysteresis loop. It is quite evident that the perfect unstrained arrangement of the atomic lattice together with minimum crystal anisotropy and magnetostriction gives the ideal conditions for no hysteresis, we must therefore seek the opposite state of affairs for our permanent magnet material, i.e. high magnetostriction, evidence of high internal stress and high anisotropy.

The magnet steels of Ewing's day had been improved to a marked degree by the introduction of the cobalt steels by Honda and Saito<sup>(5)</sup> in Japan whereby the coercive forces produced rose gradually to a value around 250 oersteds. Here the causes of the high coercivity are most probably due to a combination of anisotropy and the internal strain arising from magnetostriction.

But a new type of magnet materials was to be developed in Japan by Mishima, a pupil of Honda, in the early 1930's. The prototype alloy  $Fe_2NiAl$  with appropriate heat treatment gave an isotropic alloy of coercivity greater than 400, whilst empirical additions secured considerable improvement on this figure. At this stage Bradley and Taylor<sup>(6)</sup> showed by X-ray diffraction experiments that in the transition region between the single and two-phase states, the iron atoms would be held apart under conditions of great stress, which it was suggested was responsible for the high coercivity. Many developments, with changes in composition by the empirical addition of cobalt, copper, etc., effected considerable improvement in the permanent magnet properties, both in coercivity as well as remanence. On the theoretical side, however, it became increasingly clear that the internal stresses necessary were sufficiently near to the tensile limits of the material as to cast some doubts upon the validity of this explanation, and that other factors were, at least in part, operative. It was not until after the war that a more satisfactory theoretical explanation came almost simultaneously from Stoner and Wohlfarth<sup>(7)</sup> in this country and Néel<sup>(8)</sup> in France, who considered a material consisting of isolated magnetic particles in a non-magnetic matrix. These authors showed that the dominant controlling factors were the size and shape of the particles. The theory only applies when the particles are single domains, i.e. not more than  $0.01$  mm across, whilst the shape is all important. Isotropic spherical particles, i.e. those possessing no easy direction of magnetization, will exhibit no coercivity whatever, nor will oblate spheroids. On the other hand, the suitably oriented prolate ellipsoids can develop great coercivity which increases with departure from spherical shape. Experiments on powders, etc., have supplied overwhelming proof for the existence of hysteresis arising from this new cause, though the most recent work indicates that a combination of crystal and shape anisotropy are probably the most likely causes of hysteresis in the dispersion type of magnet material. We see now that to the two previously named causes of hysteresis is added a third, and all three can be attributed to some form of anisotropy, strain, crystal, and lastly shape anisotropy.

Maximum values of the coercive force for the three ferromagnetic metals due to the three causes are given in the table,

and for the cubic crystals, iron and nickel, obviously shape anisotropy is the likeliest cause of the highest values of the coercivity. We see also from the table that the high crystal anisotropy such as is present in cobalt can be a very important contribution towards the coercivity. This is to some extent a reflexion of the fact that this substance has only one easy direction of magnetization and if cubic crystals could have their directions of easiest magnetization reduced in number, then further improvement might result.

*Maximum possible coercive forces of small particles due to different causes*

	Anisotropy 2K/I <sub>s</sub>	Shape 2π/l <sub>s</sub>	Internal strain 3γ <sub>2</sub> /I <sub>s</sub>
Iron	400	11 000	600
Cobalt	6000	9000	600
Nickel	200	3000	4000

$I_s$  = Intensity of magnetization at saturation

$K$  = Anisotropy constant

$\lambda$  = Coefficient of magnetostriction

$T$  = Strain taken as 200 kg/mm<sup>2</sup>

In this general framework can be fitted the work of Oliver and Shelden<sup>(9)</sup> in 1938, who made a significant development by cooling a sample of (isotropic) Alnico in a strong magnetic field and improved the permanent magnet properties in the field direction at the expense of reduction in the perpendicular directions. The improvement, though small, was significant, and it was not long before improvements of considerable magnitude were made. The explanation lies in the increase in anisotropy in the field direction, whereby this easy direction of magnetization is made still easier. This technique is paralleled in "soft" magnetic materials. Even higher permeabilities than those stated above can be achieved by appropriate heat treatment in a magnetic field. Thus, the maximum permeability of 65 Permalloy (65% nickel-iron) is increased about 50-fold if a field of 10 oersteds is applied during cooling.

Yet another step forward in the anisotropic magnet alloys was made by Hoselitz and McCaig<sup>(10)</sup> in 1949. These investigators showed that if columnar crystals could be produced with a cube axis directed along the same direction as the magnetic field applied during cooling, then a still further improvement over equi-axed crystals was attainable. Here again is the anisotropy concentrated in the appropriate direction for increased efficiency.

The latest development is marked by the introduction of not only a new type of material, but also a new principle appears. As far back as 1933 in Japan, Kato and Takei<sup>(11)</sup> prepared magnets of sintered ferromagnetic oxides. The general formula is  $MO \cdot Fe_2O_3$ , where M in this case represents a mixture of cobalt and iron. The coercivity was adequate, 500 oersteds, but the low remanence,  $B_r$  less than 3000, was not sufficiently attractive in spite of the low density. Nothing further emerged for many years, and it was only after the war that it became generally known that during the German occupation the Dutch<sup>(12)</sup> had been developing this type of material to an extensive degree. These new ferrites, in contrast to the Japanese material, have very low coercivities and rank as "soft" magnetic materials, comparable with pure iron, silicon-iron, etc. Unlike these materials, however, they resemble non-metals in that their electrical resistivity, ranging from  $10^2$  to  $10^5 \Omega \cdot \text{cm}$ , is very high compared with the average ferromagnetic alloy ( $10^{-5}$  for most metals), so that additional fields of application come into consideration, for example, in alternating current work, where at ordinary frequencies

the reduction of eddy current losses is only achieved by laminating, or at higher frequencies by the use of powdered cores. The possible frequency range of application extends to the television and radar range of very high frequencies, where such materials can be used as high permeability cores in transformers, loading materials for coaxial cables, for travelling wave tubes and microwave lenses.

The theoretical interpretation of these new properties is full of interest, since they are now known to be a quite new series of ferromagnetic material. The beginning goes back to the 1930's when Néel<sup>(13)</sup> was seeking an explanation of the weakly magnetic materials whose paramagnetism is approximately independent of temperature. In spite of the apparent remoteness of these substances, there is, as will shortly be evident, a close resemblance to the ferrites. A few domains of an ordinary ferromagnetic substance can be represented as in Fig. 6(a). All the elementary magnets are exactly alike in magnitude  $\mu$ . If now we reverse the direction of alternate magnets the domain magnetization becomes zero in the unmagnetized state—instead of being magnetized to saturation as in the ferromagnetic. Such a substance will respond differently according to whether the magnetic field is applied along or at right angles to the line of magnets. In other words, it will exhibit features quite different from the ferromagnetics we have been considering. These implied properties have received overwhelming experimental proof of varying kinds, and these substances, of which some 30 or 40 have been discovered already, are named "antiferromagnetics." An excellent account of this work has been given by Street.<sup>(14)</sup> For example, the magnetic susceptibility increases gradually with temperature, until at some particular temperature the antiparallel arrangement breaks down. This critical temperature has now become to be known as the Néel temperature, a just recognition of the substantial contributions of this French physicist to this branch of magnetism. Above this temperature the antiferromagnetic becomes a normal paramagnetic, and the susceptibility now decreases with further increasing temperature.

If now instead of there being one type of elementary magnet, we have two,  $\mu_1$  and  $\mu_2$ , whose magnitudes are different, then we have what Néel calls a "ferrimagnetic" of which many ferrites are typical examples, the net magnetization will be proportional to  $(\mu_1 - \mu_2)$  instead of  $\mu$  as hitherto; Fig. 6(c) indicates the possible domain structure of such a substance, the heavy arrows indicating the larger magnetic moment. The ferrimagnetics resemble ferromagnetics in that the variation with temperature of the spontaneous magnetization—the magnetization of the domain—is not unlike the ferromagnetic as is also its paramagnetic behaviour above the Curie temperature. On the other hand, it does not possess conduction electrons, such conductivity as it might possess being a consequence of slight departure from the exact stoichiometry of the ionic lattice. This absence of conductivity offers the possible advantage that magnetic phenomena are free from complications introduced by the presence of conduction electrons.

The X-ray structure, taken in conjunction with the experimental data available, reveals an extensive field for possible exploration. The lattice is complicated, but based on the oxygen atoms, with the two kinds of metal ion occupying only one-quarter of the available interstices. The trivalent iron is invariably one kind, but the other can be not only divalent iron, cobalt, nickel, manganese or copper, but also a mixture of two or more, including also magnesium and zinc. The most strongly magnetic yet available is the manganese ferrite which, one must note, contains neither of the two



increasingly scarce constituents, cobalt and nickel. Some ferrites are non-magnetic, for example, those of cadmium or zinc, but their utility lies in that they possess the property of improving some of the magnetic ferrites.

The last word in this final chapter of progress falls into this field and is the introduction of a substance of similar, though not identical, type to the above. This is the material  $\text{BaO} \cdot 6\text{Fe}_2\text{O}_3$  announced above a year ago by Went<sup>(15)</sup> and others in Holland. This is claimed to be a pure ceramic, its electrical resistance being so much higher than the ferrites that it can be regarded as an electrical insulator. In sharp distinction from the ferrites, it is a permanent magnet material, with an average permeability of about 1, whilst the coercivity depends sharply upon the individual crystal size, having a maximum of around 1500 oersteds at room temperature when the individual particles are about  $1\ \mu$  in diameter. In this grade of material, the coercivity rises with increasing temperature and a maximum value of 4700 oersteds is reached. The bulk material is extremely difficult to magnetize and the coercivity is still increasing, though slowly, with a magnetizing field greater than 25000 oersteds. Experiments carried out make it clear that of the three possible causes for the high coercivity, shape and stress anisotropy make only negligible contributions, whilst the crystalline anisotropy, similar to cobalt, gives a maximum possible value for the coercive force of 16000 oersteds (cf. the table)—easily large enough to account for the high value claimed. Still further improvement can be produced by orienting the fine crystals to parallelism in a magnetic field such that an energy value of  $(BH)_{\text{max}}$  equal to 3 millions has been reached.<sup>(16)</sup> That this substance is not so isolated case is shown by the fact that barium can be replaced by strontium without loss of the magnetic properties. The scope for further investigations seems great. Not only are there the extensions to other single or mixed metallic radicles, but also the variables of crystal size, long and short distance order, etc., to be more fully investigated, as well as the possibility of substitution of one or more of the oxygen atoms by another element.

It is evident that highly significant developments have taken place in magnetism which will have far-reaching effects. The new ferrimagnetics, or uncompensated antiferromagnetics, have great possibilities, particularly in their application to the

control of the various physical properties required to meet specific demands. The rapid experimental developments of the last two decades have not only been phenomenal, but also give little indication of any slackening. In so far as the metallic conductors are concerned, both "soft" and "hard" magnetic materials appear to lie within sight of a stage of development where further increases in the relevant qualities are only achieved under exacting laboratory conditions. The practical application is becoming more and more limited by commercial expediency such that increasing attention needs to be directed to design rather than to new alloys. On the other hand, the full theoretical interpretation of this new discovery at present leaves much to be desired, for these new types of magnetic materials call for a recasting of our conceptions of the origin of the intermolecular field.

#### REFERENCES

- (1) BITTER. *Phys. Rev.*, **41**, p. 507 (1932).
- (2) HOSELTZ. *Ferromagnetic Properties of Metals and Alloys* (London: Oxford University Press, 1952).
- (3) WENT and SNOEK. [See Ref. (12), pp. 19–20.]
- (4) ELMORE. *Phys. Rev.*, **53**, p. 757 (1938).
- (5) HONDA and SAITO. *Sci. Rep. Tôhoku*, **9**, p. 417 (1920).
- (6) BRADLEY and TAYLOR. *Proc. Phys. Soc. [London] A*, **166**, p. 353 (1938).
- (7) STONER and WOHLFARTH. *Trans Roy. Soc. A*, **240**, p. 599 (1948).
- (8) NÉEL. *C.R. Acad. Sci., Paris*, **24**, p. 1488 (1947); *J. Phys. Radium*, **5**, p. 265 (1944).
- (9) OLIVER and SHEDDEN. *Nature [London]*, **42**, p. 163 (1938).
- (10) HOSELTZ and MCCAIG. *Proc. Phys. Soc. [London] B*, **62**, p. 163 (1949).
- (11) KATO and TAKEI. *J. Inst. Elect. Engrs Japan*, **53**, p. 408 (1933).
- (12) SNOEK. *New Developments in Ferromagnetic Materials* (Amsterdam: Elsevier Publishing Co. Ltd., 1947).
- (13) NÉEL. *Ann. Phys. [Paris]*, **5**, p. 232 (1936).
- (14) STREET. *Sci. Progr.*, **154**, p. 258 (1951).
- (15) WENT, RATHENAU, GORTER and VAN OOSTERHOUT. *Philips Tech. Rev.*, **13**, p. 194 (1952).
- (16) RATHENAU. *Rev. Mod. Phys.*, **25**, p. 297 (1953).

## Physics in the electronic valve industry

By J. THOMSON, M.A., D.Sc., F.Inst.P., M.I.E.E., Royal Naval Scientific Service, London, S.W.1

This article shows the importance of physics in the development and production of thermionic valves, cathode-ray and flash tubes, photocells, transistors, crystal diodes and similar devices; some examples of this work are cited. The author expresses the view that the problems encountered in development and production require as much basic research for their solution as do the problems encountered in the pre-development stage to which reference is also made.

The products referred to in this article are those mentioned in the abstract above and are produced by the industry which will be referred to as "the valve industry." Much of the work in developing these devices and in manufacturing them must be classed as engineering. In effect this means that a fairly complete specification is available to guide the scientist with regard to his materials, their fabrication and their assembly. The physicists' share in this development comprises that part of the work where specifications cannot be written in detail and where it is necessary to use fundamental science for guidance. It follows that in one sense all physics

in the valve industry is research, but this research may stand alone as in the earlier stages, or may be associated with valve design or manufacture. It is proposed, therefore, to divide this article under the headings of Research, Development and Production. The use of these categories emphasizes the ubiquity of physical problems and demonstrates the flow from the general investigation to the particular application. The contribution made by physical science at the production end of the industry is not less than at the inception of the project, but it is a different kind of contribution.

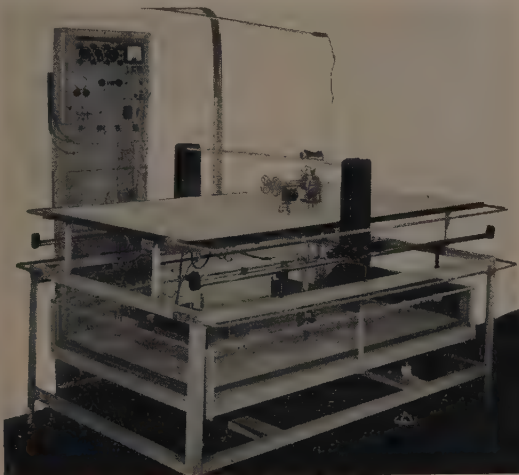


## RESEARCH

Pure research in many branches of physics is of importance in the design of valves and allied devices, but investigations under the following three headings are of fundamental interest and have a multitude of applications:

- (a) the interaction of electron streams with electromagnetic fields,
- (b) the electronic emission from solids and liquids,
- (c) the mechanism of electric conduction in gases, vapours and crystals.

(a) *The interaction of electron streams with electromagnetic fields.* A valve performs its function of modifying currents and voltages by virtue of the interaction of its electrons with the electromagnetic fields induced in it. It is this interaction which makes the valve the "active" component in electronic apparatus: in the jargon of the radio engineer the valve is a "non-linear circuit element." The detailed techniques for the investigations under this heading are many. There are several mathematical methods, depending upon approximations, and in simple cases these are known to be successful, but the field for future investigation is large. In the absence of space-charge the mathematical approach is elegant and convincing,<sup>(1)</sup> but where space-charge is present this procedure is at the moment lame. More work is required to establish a useful "drill." Pseudo-mathematical techniques, involving the use of electrolytic tanks and computers, are rather more successful,<sup>(2)</sup> but there is room for improvement and for new ideas. Purely experimental methods, ranging from modified tank investigations to a planned series of measurements on actual valve structures, are at present as successful as any. Fig. 1 gives a general view of



(Reproduced by courtesy of the Research Laboratories of the General Electric Co. Ltd.)

Fig. 1. An electrolytic tank used for the design of electron optical systems

an apparatus which has been built to allow measurements to be made rapidly on diverse electrode arrangements. The tank itself can be rotated about a horizontal axis to give a wedge-shaped volume of electrolyte, and the probe is so linked to the drawing board that electron trajectories can be traced automatically.

In a valve where the time of transit of the electron is of no importance, the physical problem is to determine how externally applied electromagnetic fields modify the electron space-charge. This is the problem in the triode, beam tetrode and pentode, where these valves are used at frequencies less than a few hundred megacycles per second. In valves where transit-time is important, the problem involves in addition changes in the space-charge during the passage of the electrons through the valve, these changes being due to the electron inertia. This extended problem is typical of the investigations of klystrons, magnetrons and travelling-wave tubes at frequencies above a few hundred megacycles per second. In either case current densities may range from a few milliamperes per square centimetre to many amperes per square centimetre, so that the self-repulsion of the electrons may be a matter of great importance. The whole of the science of electron optics is of vital interest to the valve physicist. The problems encountered in electron microscopes are, however, quite different from those which confront the valve designer. The fact that adequate solutions to many of the valve problems have still to be found should act as a challenge.

(b) *The electronic emission from solids and liquids.* Electronic emission has been studied intensively for several decades. The situation regarding thermionics has recently been described by Wright,<sup>(3)</sup> and his paper shows that from the valve designer's standpoint we have a long way to go. No existing thermionic cathode can be regarded as more than a rough compromise between the conflicting claims of emission and longevity, and in many cases the self-destruction of the hot cathode is not acceptable to the designer. The opportunities for objective fundamental research are considerable: we probably know enough now to make a serious attempt to obtain a good cathode.

If we have a long way to go on thermionic emission, we have even further to travel on photoelectric and secondary emission, while the possibilities of auto-electronic emission have not even been realized. The valve designer is, or should be, catholic in his choice, but his need for a source of electrons which while emitting will not destroy either itself or its environment is a very real one. He is concerned with currents up to hundreds of amperes, and he wishes to draw this current for thousands of hours without the emission or absorption of any kind of matter. The problem is a big one but its solution is possible.

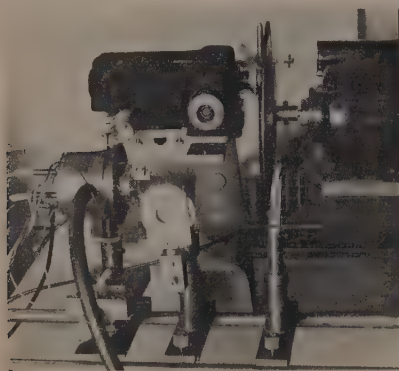
(c) *The mechanism of electric conduction in gases, vapours and crystals.* There can be few more "unsatisfactory" subjects for research than the gaseous electric discharge. Although our understanding of the mechanism is gradually improving,<sup>(4)</sup> the literature of the subject is strewn with abortive explanations of phenomena. Yet various properties of the discharge are in common use in both hot and cold cathode valves. Much remains to be done in this field, and some of the work can only be tackled properly in a valve laboratory which possesses the necessary facilities for purification both of metal parts and of filling gases. As Dr. J. Taylor wrote a long time ago, the essence of discharge tube work is "a refined and meticulous technique." One reason for the lack of progress in the subject has been the lack of such refinement. In recent years attention has been focused on plasmas and on high frequency discharges. Both exhibit intriguing phenomena. The importance of the plasma to the valve industry is two-fold. There is an immediate possible application to low voltage switching, since the plasma can by its very nature be radically altered by a change of potential of a fraction of a volt at an electrode immersed in it. The more

long range applications centre around the feasibility of causing electrons to move relative to their matrix of positive ions. One can imagine many interesting effects in a suitably controlled discharge.

The high frequency discharge, where the amplitude of oscillation of the electron is small compared with the distance between electrodes, is another subject which may yield dividends. It has already found applications in duplexers for centimetric radar and communication. The high frequency excitation of a plasma may offer a new gamut of electronic devices.

Conduction in crystals has now become a major preoccupation of the valve industry, since the relative success of the transistor in imitating the action of the thermionic valve at low frequencies gives a promise of better things to come. This branch of solid physics has assumed an importance equal to that of electron conduction in a vacuum. The popular material is germanium on which much of the fundamental work has been done, but the known disadvantages of this substance have encouraged research in other directions. Silicon and the binary compounds of groups three and five in the periodic table are among the more promising crystals under investigation. A new jargon has been invented to cope with the new ideas, and novel concepts of the purity of crystals have emerged. Germanium single crystals are now being grown as a matter of routine having a total impurity content of only a few parts in  $10^8$ .

Fig. 2 shows a laboratory arrangement for the measurement of the diffusion distance of minority carriers in germanium,



(Reproduced by courtesy of the A.E.I. Research Laboratory)

Fig. 2. The measurement of diffusion distance of carriers in germanium

using infra-red excitation. The light beam is interrupted regularly by a pierced disk driven by the motor shown on the right of the figure. The light then passes through the spectrometer which acts as a monochromator and is focused on the specimen of germanium by the mirror shown towards the bottom of the photograph. The infra-red energy creates carriers where it falls and these carriers diffuse through the specimen. The electrical signal produced by the moving charges is taken off by a probe and amplified. From the geometry of the arrangement and the variation of the signal the diffusion distance can be estimated. An infra-red detector measures the input energy.

It is unusual to find a field of physical research where important discoveries can be made at any time; for example,

the likelihood of making a major advance in conduction through a vacuum is small. Semi-conductor research is, however, such a field, where the chemist and physicist working together are exploring entirely new territory.

#### DEVELOPMENT

A great disservice is done to industrial development by ignoring or neglecting the contribution which physics has to make to the detailed design of electronic devices. Most physicists who have been engaged at one time or another on research and development agree that the problems are more difficult and the work more exacting in the development stage. This is probably not so well known as it should be, since the difficult task is usually preferred by the good man, and there is a tendency for physicists to choose fundamental research rather than development work. In a short article it is impossible to do much more than mention some of the design questions where the answer lies in physical science.

*Materials.* First, there is a class of problem characterized by the use and test of new materials. Some of this work is more appropriately done in a materials laboratory, but much of it is the direct concern of the valve designer and must be under his eye. The chemist and the physicist work on materials in the closest collaboration. The improvement of valves and the demand for new types continually require the development of new dielectrics and alloys. Each new material must possess certain properties and these properties may be mutually exclusive. For example, valve parts cannot usually be ferromagnetic; it should be possible to heat them in a suitable atmosphere to a temperature above  $1200^\circ \text{K}$ ; some parts have to be sealed to glass or some other dielectric; they are usually required in sheet or in wire form; the heat conductivity of certain parts should be high; the high frequency resistance should in some cases be low; in all cases the behaviour of the parts in the presence and absence of gases is important.

Nowadays, valve envelopes and insulating sleeves are made of a variety of glasses and ceramics. In early days almost all valves were made of lead glass, but now hard glasses are used extensively and in some cases a glass having a very low dielectric loss is necessary. In most cases the loss is a fairly rapidly varying function of temperature and since the glass may operate at a high temperature this is important. Going a step further, certain parts of valve envelopes are now made of ceramic. This is becoming more common. It may be necessary to use a low-loss ceramic; the material will certainly need to be non-porous. Insulators within the envelope are the subject of much study. Good though it may be, mica possesses some disadvantages and other materials are constantly being sought.

Curious effects are found in glass ends to cathode-ray tubes working at high voltages. The formation of "colour centres" in the glass, due probably to impurities, determines in some cases the life of the tube. Much work remains to be done if the use of high voltage tubes is to be exploited.

Indeed, the future of certain special valves and cathode-ray tubes depends as much on the materials used in their construction as it does on their electrical characteristics.

*Seals.* Another way in which physics contributes to valve manufacture is in the development of new methods and materials for sealing metal to metal, metal to glass and metal to ceramic. This is another combined operation with the chemist and physicist playing complementary parts. Many years ago valve manufacturers adopted certain standard methods of connecting things together. For example, nickel



was almost universally used for valve parts, and welded joints were the rule. When a wire had to be taken through a lead glass pinch, copper-covered nickel-iron (Dumet) was used. In modern valves we find copper, tungsten, tantalum, steel, molybdenum and certain alloys. The envelope may be of hard glass with various metal seals, or it may be in part a ceramic sealed to a copper body by the use of titanium hydride or some other agent. New flux materials are required and every new process is subject to the conditions that joints must be vacuum-tight and all parts must be able to withstand violent changes of temperature. Research in metallurgy is the background to all this, but the physical problems attendant upon the applications of the new materials to valves are many and difficult.

**Electrical design.** Turning to the electrical design, special development problems arise from the general investigations considered in the section on research. It is only possible to choose a few important examples. One of the most interesting physical problems in valve manufacture is how to couple a stream of electrons to a circuit. In the case of conventional valves, where the inductances and resistances of the leads may be neglected, the investigation takes the form of designing cathodes, grids and anodes for optimum performance. Fortunately, it is possible in many cases to investigate each electrode separately. The "optimum design" for a triode grid is an elegant problem, particularly if the current density is large; the design of a beam tetrode for 100 W output at frequencies up to 200 Mc/s with a space current of the order of 100 mA is a complicated exercise in electron optics.

The detailed application of the laws of electron optics to specific valve structures is another never-ending task for the valve designer. It would probably surprise many academic physicists to know how much detailed analysis goes into the design of the electrodes and magnetic coils for a television viewing tube to obtain a picture which is free from distortions. Moreover, electron optical methods are now being applied in greater measure to the construction of conventional valves. A good example of this is the beam tetrode already mentioned and commonly used for power amplification. The electrode system in this valve is designed to produce a high electron density just short of the anode without the use of a decelerating electrode. The device is one of the most elegant practical examples of the intelligent use of electron optics.<sup>(5)</sup>

It is when we come to valves for very high frequencies (above 300 Mc/s, let us say) that the most interesting problems relating to coupling an electron beam to a circuit arise. The classic example is the modulation imposed upon an initially uniform beam of electrons traversing the space between the ends of two open coaxial cylinders which are maintained at different potentials. Practical problems are much more complex and modern methods of solution are a combination of mathematical and experimental techniques. An example of a difficult problem of this kind is the determination of the interaction between an electron beam and a helix in a travelling wave tube.<sup>(6)</sup>

The behaviour of a space distribution of electrons in crossed electric and magnetic fields determines the action of a magnetron. From the research aspect the magnetron problem has not yet been solved.<sup>(7)</sup> Indeed, all workers in the fundamental field say that the mechanism of the more complex magnetrons used commercially is not understood. Nevertheless satisfactory valves are made and used; progress has been continuous since 1939 and valves giving a peak power output of 10 MW have been made in this country. The physical problem, therefore, until a satisfactory quantitative theory has been evolved, is to interpret previous results

and to employ these empirically with a cautious use of a qualitative picture of the behaviour of the electron cloud.

Other space-charge problems are not so difficult. By the use of one or other of the techniques mentioned in the section in this article on Research, it is often possible for the physicist to design a valve on paper without much experimental work. This is the case with many klystrons which are more amenable than magnetrons to theoretical treatment.

**Emission.** Fundamental investigations of emission are succeeded by the development of specific cathodes for particular types of valve. In general terms the physics of tungsten, thoriated tungsten and oxide-coated emitters is applied to cathodes for transmitting valves, rectifiers and receiving valves. Problems of heat concentration and heat dissipation are constantly encountered in this work. But it is once more in valves for use at very high frequencies that the greatest interest centres, for it is in such valves that the problems are most difficult, and solutions, when they become available, can often be applied with good effect at lower frequencies. The flat cathode of a disk-seal triode for use at 1000 Mc/s is



(Reproduced by courtesy of the Research Laboratories of Mullard Ltd.)

Fig. 3. Photographs of the growth and decay of the discharge in a flash tube; exposure  $10^{-7}$  sec. (a)  $1\mu\text{sec}$  after triggering; (b)  $1\mu\text{sec}$  later; (c)  $35\mu\text{sec}$  after triggering; (d)  $60\mu\text{sec}$  after triggering



situated some four-thousandths of an inch from the grid. This degree of proximity demands that the surface of the cathode should be very nearly plane and that the cathode and the grid should be very parallel. New cathode materials are required for this type of work: interest at the moment centres on emitters which can be machined with accuracy. It is worth while calling attention at this point to the different kinds of physical problems associated with a single element of valve development. For example, the fundamental problems of emission from a treated metal or semi-conducting mixture are concerned with the states of the "free" electrons and the potential barriers in the material. These are research problems in the narrowest sense of the word. If, however, some-one has a "bright idea" and a new material is found to have possibilities as an emitter, the fundamental physical action may not be understood and yet the valve physicist may be able, in due course, to define exactly how to make a good cathode. To do so he has to engage in a major investigation of a semi-empirical nature<sup>(8)</sup> to determine (a) the composition of the material to give the best performance and the allowable tolerances, and (b) the conditions under which emission can be obtained. Under (b) he would have to examine in detail the permissible schedule for activation as well as the permissible limits for operation. Such an investigation, although it cannot be called fundamental, is in the field of physics and is, from a practical point of view, of great importance. As an example of how electronic tubes may themselves be applied in development of other devices, reference may be made to the photographs (Fig. 3) of the discharge in a flash tube taken by means of an image converter camera. When one remembers the difficulties which used to be associated with this type of photography, the new techniques are obviously worth while.

*Gas.* Another most interesting field for investigation of great practical importance is the migration of residual gas ions and molecules in a valve envelope. It is in problems of this kind that the physicist realizes his lack of knowledge and the inadequacy of his physical tools. It is sometimes necessary to estimate gas pressures of the order of  $10^{-11}$  mm of mercury and apparatus for doing this has been developed, but the valve physicist is constantly made aware of the fact that even at such low pressures there are on the average  $10^{10}$  molecules in each cubic centimetre of his so-called "vacuum" device. Recently there has been an increasing demand for more reliable valves. With the advent of electronic control reliable valves have become a simple necessity. In the examination of how to make a valve more reliable, physicists have encountered many difficult problems due to the residual gas in the envelope. This is particularly true of valves which have to operate over a long period—say 10 000 h—for in certain cases it has been well established that the life of the device is determined almost entirely by the number of gaseous or vapour molecules present at one time or another. The use of radio-active tracers has been very effective in this field for one of the most difficult problems in valve development was to know where constituent materials went inside the envelope during operation.

*Vacuum pumps.* Another important subject in which development is active is the design of good pumps capable of operating efficiently under the arduous conditions imposed by the valve manufacturer. It has been shown recently (and the results will soon be published) that for certain pumping operations it is useless to attempt to use an oil as the fluid, and, of course, mercury has much too high a vapour pressure. Experiments are being made with a new pumping fluid having a vapour pressure less than  $10^{-11}$  mm of mercury

at room temperatures. This, associated with recent work on the physical form of the pump itself, has opened up new horizons in vacuum practice.

*Gas phenomena.* When we come to valves which are deliberately filled with gas and which make use of ionization phenomena, such as the thyatron or the transmit-receive switch, the physics of the electric discharge finds many applications. In all cases there are gaps in our theoretical knowledge, but these gaps do not prevent useful devices from being made. Academic physics, by which is meant the interpretation of simple, basic phenomena, forms a satisfactory starting point for development. Complex data, such as the life-time of specific ions in particular gas mixtures, have to be determined by patient thoughtful investigations. To illustrate the practical difficulties the case of the hydrogen thyatron may be cited. As most physicists are aware, the first gas switches or thyatrons used mercury vapour. One primary objection to mercury is that the atom is too massive, causing the device to be sluggish in action. The hydrogen thyatron, more recently proposed, uses ions of much smaller inertia, but a new difficulty is encountered. Hydrogen "cleans up" as the valve is used, leaving finally a small fraction of the desired gas pressure. Physicists have made and are making serious attempts to replenish the hydrogen supply in the valve, but although success has been almost achieved for certain valves handling low powers, the problem is not by any means solved.

An interesting example of a combination of physics and chemistry is illustrated by Fig. 4. This is an apparatus for



(Reproduced by courtesy of the Valve Laboratories of Standard Telephones and Cables Ltd.)

Fig. 4. Oxygen estimation by use of a thermistor

estimating the mass of a trace of oxygen in a given mass of hydrogen. The method adopted is to measure the temperature rise when the gas under test passes through a vessel containing a catalyst, and uses a sensitive thermistor to detect the change of temperature. The photograph shows a test set which can be readily calibrated and used in the development laboratory.

#### PRODUCTION

Enough has been said in the previous paragraphs to indicate that the tasks confronting the valve physicist in the

development laboratory are many and various. Corresponding problems arise in the factory where valves are being made in large numbers.

Physics is a basic science which interprets (or should interpret) the phenomena within its province in terms of a small number of general "laws." It does not admit the existence of "black magic" and the first duty of the production physicist is to investigate all cases of "magic" with the purpose of understanding them. There is talk of "green fingers" even at the present day among valve makers! Investigation proves that designers with "green fingers" make good use of well-known chemical and physical principles, albeit they may do so without conscious cerebration. All processes used in production should be the result of or the cause of scientific investigation: if a process is not thoroughly understood in the scientific sense, it is liable to "go wrong" at an inconvenient moment, resulting in considerable waste of effort.

To avoid misapprehension it should be stated here that where sound engineering methods are applicable to valve manufacture the foregoing never applies, but even the most confident production engineer would admit that there are many problems arising in his work where there is no engineering practice to guide him.

Probably the most important function of the physics laboratory in production is to determine rapidly and accurately the properties of materials. For example, a routine check by means of the optical or mass spectrograph on the constituents of the residual gas in a valve or cathode-ray tube envelope is of great value. The physics laboratory associated with valve production should be equipped with the best and most modern tools. Radio-active tracers can be used with effect in investigating the migration of ions and molecules; the electron microscope is essential for the rapid examination of surfaces; while a good electrical measurements section can often pick up a mistake before much harm is done. The more use is made of physical investigation during production, the more certain the process becomes. Guess-work and chance are largely eliminated.



(Reproduced by courtesy of the Research Laboratory of the British Thomson-Houston Co. Ltd.)

Fig. 5. A radiograph of the segments of a magnetron

A good example of the intelligent use of physical principles to obtain detailed information on a finished valve is furnished by the pinhole radiography of magnetrons.<sup>(9)</sup> The magnetron during operation gives rise to X-radiation where electrons strike the anode. A pin-hole X-ray photograph of the anode therefore gives a picture of the intensity of the emitted radiation in relation to its source. This in turn shows where the electrons are striking the anode segments and brings to light any asymmetries which may exist; Fig. 5 is such a pin-hole photograph and the method of examination was

developed in the Research Laboratory of the British Thomson-Houston Co. Ltd.

The physics laboratory associated with production may well be combined with the laboratory concerned with development, but the two functions are entirely separate. The development unit may investigate new materials as such: the production unit investigates materials already in use for control purposes.

One of the most important materials in use is the gas in the valve or cathode-ray tube, however little there may be of it. A remarkable mass spectrograph has been specifically designed for the examination of the residual gases in electronic devices, and it works at a gas pressure of the order of  $10^{-6}$  mm of mercury.

Another important use of physics in production is in the testing of the finished product. In some cases this is a difficult and expensive item which can only be simplified and cheapened by the exercise of physical ingenuity. Such work calls for a particular kind of inventiveness which can be very satisfying. As might be expected, the objects are (a) to reduce to a minimum the parameters which must be measured and (b) to design test gear which can be operated by semi-skilled or unskilled labour. Many interesting discoveries in electronics have been made as a consequence of attempting to develop test equipment, while the absence of adequate testing facilities has been responsible for many disappointments in the past.

Transistors have reached a stage of development where the devices made in the laboratory or by semi-production methods are reasonably satisfactory, within a limited category of applications. Leaving aside their disabilities which were referred to in an earlier section, the production problem is a difficult one. So-called "point-contact" transistors have two metallic probes in contact with the crystal and a few thousandths of an inch apart. This is difficult to achieve by ordinary factory methods and present practice causes the price of the finished article to be high. The modern "junction" transistor has a layer of one type of germanium sandwiched between two layers of another type. The middle layer is only a few thousandths of an inch thick, and this is again difficult to achieve. It will be seen, therefore, that leaving aside the operational difficulties, the success of the transistor or of any other crystal valve will depend largely upon the development of a manufacturing technique. Certainly, if crystal valves are to compete in price with thermionic valves, some interesting physical and chemical discoveries will have to be made.

#### REFERENCES

- (1) SPANGENBERG. *Vacuum Tubes*, p. 82 et seq. (New York: McGraw Hill Book Co. Inc., 1948).
- (2) LIEBMANN. *Brit. J. Appl. Phys.*, 1, p. 92 (1950).
- (3) WRIGHT. *J. Instn Elect. Engrs*, Part III (May 1953).
- (4) LOEB. *Fundamental Processes of Electrical Discharge in Gases* (New York: John Wiley and Sons, Inc., 1939).
- (5) See Ref. (1), p. 245.
- (6) PIERCE. *Traveling Wave Tubes* (New York: D. Van Nostrand Co. Inc., 1950).
- (7) COLLINS. *Micro-Wave Magnetrons*, Radiation Laboratory Series, Vol. 6 (New York: McGraw Hill Book Co. Inc., 1948).
- (8) For example, BRUCHE and MAHL. *Z. Tech. Phys.*, p. 623 (1935).
- (9) DUNSMUIR. "Pinhole Radiography of Magnetrons," *BT-H Res. Lab. Publ.* 229.



# Handling equipment and safety containers for use with isotope $\gamma$ -ray sources for industrial radiography

By D. R. ALLEN, A.Met., A.I.M., H. S. PEISER, M.A., A.R.I.C., F.Inst.P., and J. R. RAIT, D.Sc., A.R.T.C., F.I.M.,  
Hadfields Ltd., Sheffield

[Paper received 2 March, 1953]

The safe use of active  $\gamma$ -ray isotope sources for radiography in non-destructive testing laboratories requires efficient containing and handling equipment. The design and construction of a complete set of such tools is described. These comprise (a) source adaptor, plug and container with trolley for safe storage; (b) source-transfer equipment, adjustable rods, stands with quick-release clamps and spider supports for remote handling; and (c) special sighting cones and jigs, used prior to positioning the source for exposure, to avoid unnecessary handling.

During recent years the authors have been responsible for building up a modern radiographic laboratory for the examination of a large variety of alloy steel castings. Apart from diverse X-ray equipment the department employs a number of radio-isotope sources of activity up to 1 c. At the time when these were introduced, safe handling equipment could not be readily bought commercially. The authors therefore have preferred to design and manufacture their own handling equipment which is described here in the hope that it may be of help to other workers in this field. Most of the apparatus has been in use for over two years with apparent success, the average dose rate received by members of the staff being less than 1/50th of the maximum permissible one.<sup>(1)</sup>

## SAFE STORAGE EQUIPMENT

### Containers

The purpose of the container, or "bomb" as it is sometimes called, is to provide safe storage for the isotope  $\gamma$ -ray source during its "idle-life," i.e. when it is not in use for radiographic exposures. At the same time it is desirable, but not always necessary, that the container should be capable of being transported so that the source can be used for "site" radiography.

Before considering the design and manufacture of the containers, the meaning of the term "safe container" will be discussed. The medical authorities in this country seem to be agreed that the maximum permissible dose to which a person may be continuously exposed, without suffering any ill effect, is 500 milliröntgens (mr) per working week. Therefore the container should provide sufficient protection so that even in the most adverse, practical working conditions the dose received is small compared with the maximum permissible one because those handling these containers are usually also called upon to handle open sources, involving some unavoidable exposure (see below).

In Fig. 1 the absorption data, obtained from the Harwell catalogue,<sup>(2)</sup> for iridium<sup>192</sup>, tantalum<sup>182</sup> and cobalt<sup>60</sup> has been plotted. It will be noted that the radiation rate is given at the surface of the container and not, as in the catalogue,<sup>3</sup> at 1 m distance from the source. This latter mode of giving radiation rates may give rise to misunderstanding since people can approach much nearer than 1 m to the container. For example, 1 in. of lead shielding a 1 c iridium  $\gamma$ -source cuts down the radiation rate, at 1 m range, to 6 mr/h. This at first sight appears to be quite safe. Calculation shows, however, that the radiation rate at the container's surface is approximately 10 000 mr/h, so that for a hand held in contact with the surface the maximum permissible weekly dose would be exceeded in 3 min.

All three graphs shown in Fig. 1 commence at a radiation rate of 1000 mr/h at the surface, a figure the authors consider to be a reasonably safe radiation level, for it is unlikely that any person will be in contact with the surface for any length

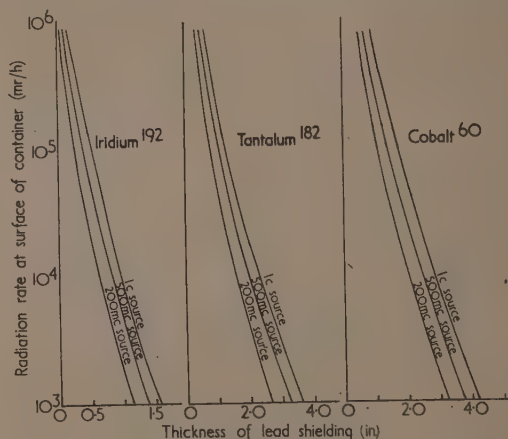


Fig. 1.  $\gamma$ -ray absorption data

of time. This will certainly be so if suitable laboratory working rules are framed and rigidly adhered to. Two further points must, however, be considered before the final choice of the thickness of shielding for any one type of source is made.

(i) *The characteristic radiation factor.* Other things being equal, the more penetrating the  $\gamma$ -rays given off by a source the more detrimental is the effect on the human body.<sup>(3)</sup> Thus a container for iridium<sup>192</sup> having a surface radiation rate of 1000 mr/h would be safer than a cobalt<sup>60</sup> container having the same surface radiation rate. The more penetrating the radiation of a given source, therefore, the lower should be the surface radiation rate of the container. Owing to difficulties of handling the heavier containers necessary for the more penetrating radiations, the tendency is unfortunately the reverse, that is to lower the standards of safety for these sources.

(ii) *The container size factor.* The decrease in radiation rate on receding from the container obeys to a first approximation the inverse square law, the distances being measured from the source and not from the surface. Therefore the larger the container the smaller is the radiation decrement on receding from the container by a given distance (Fig. 2). This factor



adds further to the characteristic radiation factor in making it advisable to increase the shielding provided for the more penetrating radiations over and above that which would appear adequate from the absorption data (Fig. 1).

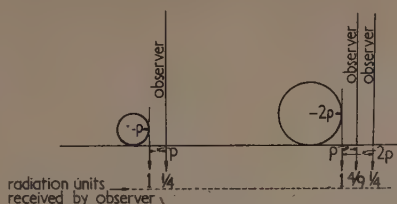


Fig. 2. Effect of container size

The material decided upon by the authors for use as the shielding medium is a lead alloy containing 2% of antimony, since this alloy is somewhat "stiffer" than pure lead, is readily available, machines quite well and is quite easily cast. For a dense material other than lead, the required protection thicknesses can be calculated from the lead thickness values (these thicknesses are inversely proportional to the density of the material). The moulds for casting the lead alloy have been made by ramming sand around suitably dimensioned patterns.

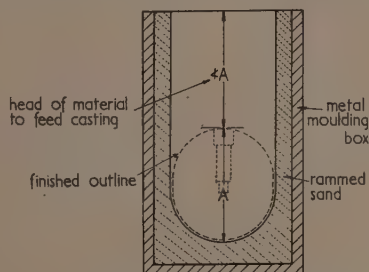


Fig. 3. Mould for casting lead containers

They were conveniently to hand as standard "atmospheric head" patterns used in the foundry. When making the pattern, attention should be paid to its design, so that it can easily be withdrawn from the mould. Allowance should also be made to accommodate contraction of the lead on cooling. Fig. 3 shows a typical mould from which it will be noted that

the overall depth is at least twice that finally required in the container. This is to provide an adequate "head" of material to ensure that the part of the casting, from which the container will be machined, is completely sound. Machining, furthermore, is done from the head end to ensure that boring is carried out along the axis of any remaining centre-line shrinkage. Prior to casting the mould is carefully dried.

As a guide to design Fig. 4(a) and (b) shows the final shape of the lead containers (for iridium, tantalum and cobalt sources) and the mode of mounting to some type of frame

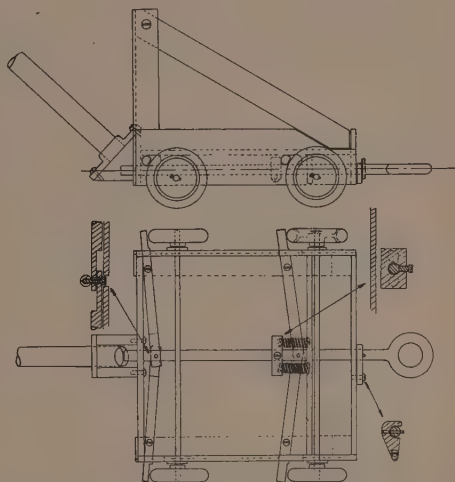


Fig. 5. Carriage for transport of lead containers

which can be transported. The small container, for a 500 mc iridium  $\gamma$ -source, weighs only approximately 10 lb. It is equipped with a single handle, which is plastic-covered to reduce secondary  $\beta$ -emission from the metal core. The larger type bombs for 500 mc of tantalum and a 1 c of cobalt weigh approximately 160 and 250 lb respectively. It has facilities for carrying with two handles. These handles, made from standard gaspipe, ensure that the two persons lifting the containers maintain an adequate safe distance from the more penetrating radiation. Rubber (cycle handbar) grips again ensure a low level of  $\beta$ -exposure to the hands.

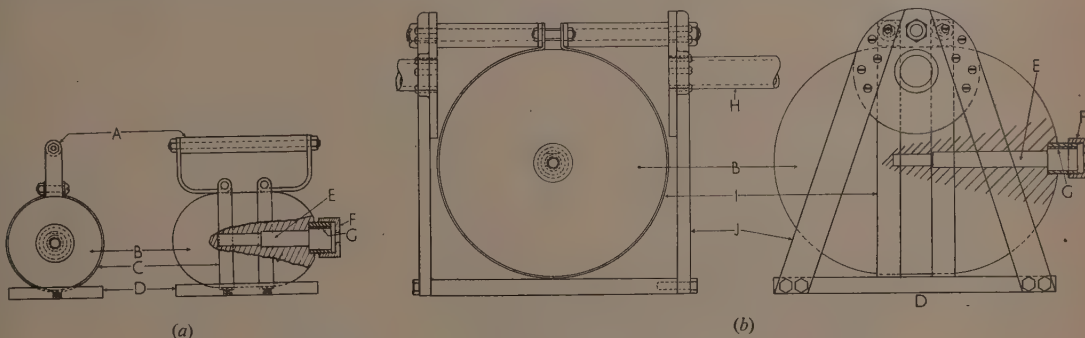


Fig. 4. Gamma-ray source containers for (a) iridium, (b) tantalum or cobalt.

(Dimensions are dependent on source strength)

A, plastic handle; B, lead body; C, brass straps; D, base plate; E, plug chamber; F, plug retaining cap; G, key; H, carrying handle; I, steel straps; J, steel supports.

To move the containers a long distance a small four-wheeled carriage (Fig. 5) has been designed, which uses one of the lifting handles as a shaft. Special features of the carriage include the spring-loaded brakes, which can be locked in the "off" position by a small catch for movement on the level. For moving on a slope, however, the carriage is held by a rope passed through an eye bolt. As long as the tension is maintained for uphill or downhill movement the brakes are in the "off" position, but as soon as the tension slackens the brakes are automatically applied.

#### Isotope adaptor

The  $\gamma$ -ray sources are supplied by the Atomic Energy Research Establishment, Harwell, in holders of a standard design, as shown in Fig. 6. An adaptor must therefore be

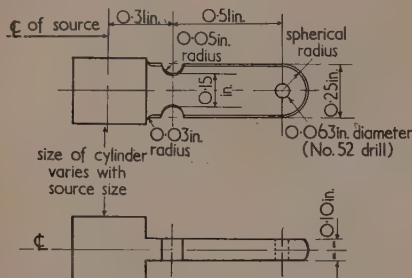


Fig. 6. A.E.R.E. standard source holder

designed which holds the tongue-end of these holders rigidly without, on the one hand, depleting the lead protection of the container or, on the other hand, necessitating the recommended protection to be placed at a greater distance from the source, because the weight of "bomb" of given lead thickness increases rapidly with diameter. One design of adaptor is tentatively suggested by A.E.R.E. It is, however, not as shock-proof nor as simple to manufacture as the one suggested here.

This latter adaptor (Fig. 7) is manufactured from free-cutting stainless steel, because earlier experience has shown

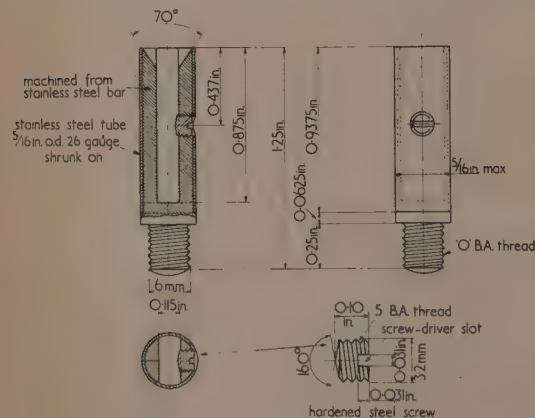


Fig. 7. Adaptor for source holder

that there is a hazard due to corrosion at the contact between the "Birmabright" tongue of the A.E.R.E. source and brass adaptors first tried (possibly due to some soldering flux

remaining). Corrosion may make it difficult to remove the source for reactivation. It will be seen that this adaptor does not reduce the final lead protection of the containers by any appreciable amount and yet provides a rigid mounting to the lead plug, for all positions of the source.

#### Lead plug

The lead plug (Fig. 8) to which the adaptor is screwed, provides part of the protection whilst the  $\gamma$ -ray source is

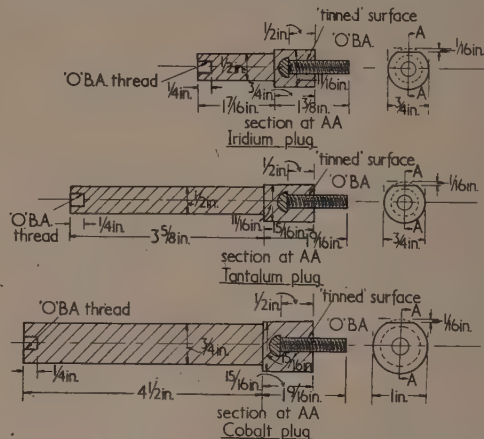


Fig. 8. Lead plugs for holding adaptor with  $\gamma$ -ray sources and for insertion in containers

housed in the container and also a cone of protection approximately 2 ft diameter at 6 ft behind the source after withdrawal. Thus the hands and part of the body of an operator handling an open source are fairly well protected. The former are generally the parts of the body most liable to irradiation and the nearest to the source when setting up for an exposure.

The material used is again a lead alloy containing 2% of antimony, the plug being cast as a cylinder (Fig. 9) with

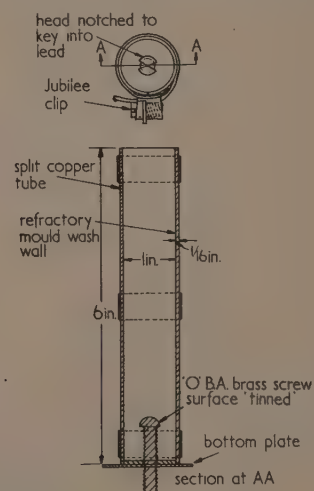


Fig. 9. Mould for casting lead plugs

sufficient excess to ensure that the piece used is sound. Some trouble has been experienced in the earlier stages of development with the screwed brass end to which the handling rods are attached. At one time this was simply a fully threaded brass screw, of which a length of  $\frac{1}{4}$  in. was soldered into the end of the lead plug. This gave very short life because of failure at the soldered joint. The whole end has been redesigned as shown in Fig. 9, the lead is cast around the brass screw, the end of which is notched and "tinned" prior to casting.

To overcome the lead to lead bearing surfaces when inserting or withdrawing the lead plug, experience has shown that it is advantageous to nickel "flash" the lead plug. This can be done quite adequately in a glass or porcelain bath of Watts solution:

250 g/l.	$\text{NiSO}_4 \cdot 7\text{H}_2\text{O}$
37.5 g/l.	$\text{NiCl}_2 \cdot 6\text{H}_2\text{O}$
25 g/l.	$\text{H}_3\text{BO}_3$
2 g/l.	$\text{NaF}$

with a current density of approximately 5 A/1000  $\text{cm}^2$ . Before plating, the lead plug should be prepared in the following way: (i) degrease thoroughly in trichlorethylene; (ii) wash in hot water to remove all traces of trichlorethylene; (iii) anodic etch—5 to 30 sec in a bath of 2½%  $\text{H}_3\text{PO}_4$  solution with 3 V across the cell.

The nickel plate so deposited has good adhesion with the lead and provides a hard wearing surface.

#### SAFE HANDLING EQUIPMENT

##### Handling rods

To maintain the required safe distance during the handling of an open source a series of light but rigid Duralumin rods [Fig. 10(a)] have been made. The lengths are such that it is possible to have rods varying from 2 ft to 16 ft in 2-ft steps.

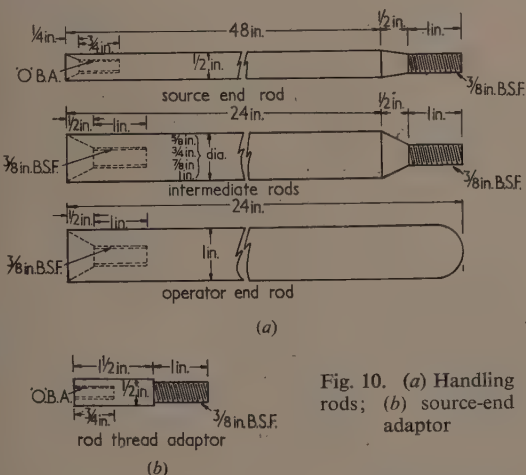


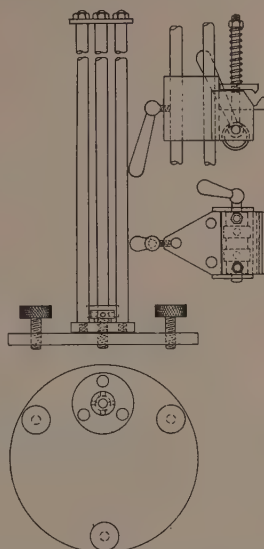
Fig. 10. (a) Handling rods; (b) source-end adaptor

When using the greater lengths in a horizontal position it becomes necessary to make up the lengths with the larger diameter rods to increase the rigidity and minimize the "sag" at the source end of the rod. To enable the rods to be attached to the 0 B.A. thread of the lead plug a number of thread adaptors have been made to fix to the source end of the large diameter rods [Fig. 10(b)].

##### Source stand

Speed of setting the open source into any desired position decreases the amount of exposure received by the operator. The isotope container is placed conveniently near the place of exposure. With the source stand (Fig. 11) a proficient

Fig. 11. Source stand



operator can reduce the handling time to a matter of 5 sec or less. Essentially the source stand is a quick-action clamp which can be raised, lowered or rotated to any desired position.

The quick-action clamp is opened by a lever-operated cam acting against a spring-loaded top plate. The handling rods are placed in the vee-groove. A simple anti-clockwise movement of the lever then releases the top plate and secures the rod in position. The height of the rod in the clamp can be adjusted up to a maximum of 5 ft above the floor or fixed support by releasing the lever-operated screw and sliding the clamp to the desired position, which can be read off from a scale on one of the vertical slide-rods. Three levelling screws are provided in the base plate to enable the stand to be used on an uneven surface. A rotational movement about the vertical and a clamping mechanism for it are also provided.

##### Sighting cones and cassette angulation jigs

As an aid to accurate setting up of castings and cassettes a number of brass cones (Fig. 12) have been made. These

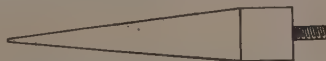


Fig. 12. Sighting cone. (Dimensions are dependent on plug size; i.e. on source strength)

cones, one for each type of  $\gamma$ -source, correspond both in length and weight to the lead plug-adaptor assembly so that the tip of the cones can be used as indication of the point of the source of radiation for measuring distances and angulations. The "sag" of the handling rods is by this means automatically allowed for.

The azimuth of the cassettes themselves when placed on the floor under small castings can be changed and adjusted to the correct distance from the source to provide the required



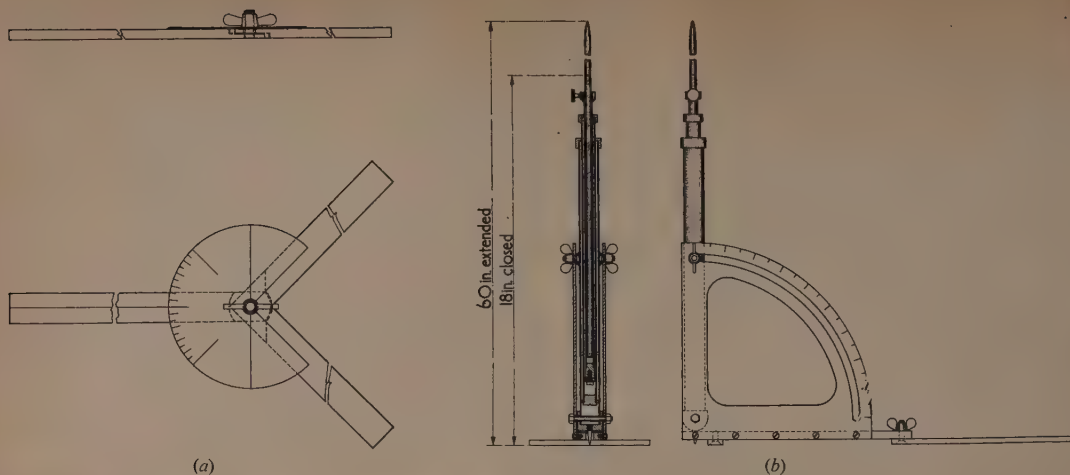


Fig. 13. Angulation jigs for (a) azimuth adjustment of cassette; (b) beam direction adjustment in vertical plane



(Reproduced from Foundry Trade Journal)

Fig. 13(c). Angulation jigs for automatic positioning of castings

beam angulation by means of the jigs shown in Figs. 13(a) and (b). These are especially useful and time saving whenever a number of castings require the same radiographic view. The desired view is first obtained by trial exposures. Once this is established the source position relative to the cassette is marked off by the two jigs. The "settings" so obtained are used for all subsequent castings requiring the same view.

If the number of castings to be examined is large and the views required standardized, it may prove economical to prepare wooden jigs which position the casting relative to a fixed source. Such a jig assembly is shown in Fig. 13(c) in which there are twenty stations for the castings angulated for three different views. No manufacturing details need be given because this type of jig will vary in construction according to the casting shape and the required radiographic views.

*Spider support for exposures in cylindrical specimens, etc.*

Where accurate aligning is necessary, as in cylindrical objects or in large cavities inside specimens, further in inaccessible spaces, or when very long handling rods must be

used for highly active sources, the spider support (Fig. 14), made of Duralumin, overcomes difficulties of supporting the front end of the rod. The length of the two legs can be adjusted by means of appropriate extension pieces. This spider is most useful for the radiography of circumferential welds, simplifying the centring of the  $\gamma$ -source. Finally, two such spiders can be used for supporting the rod in a vertical position.

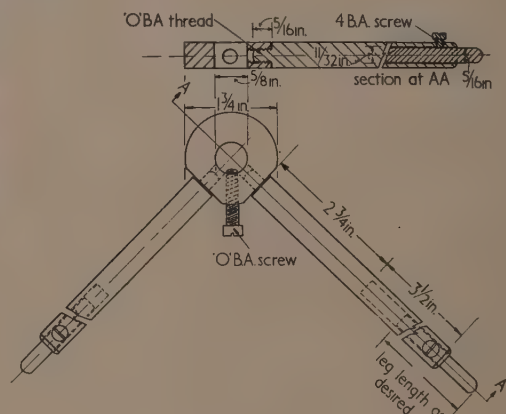


Fig. 14. Spider support for handling rods

#### *Isotope transfer equipment*

When an isotope  $\gamma$ -ray source is spent it is necessary to remove it from the adaptor and replace it with a reactivated source. This transfer takes longer than is considered safe with an open source in view of the relatively short source-operator distances necessary for loosening and later tightening the grub-screw on the adaptor even when using a long-handled screwdriver. The operation is made safe by using a lead shield as transfer jig (Fig. 15). The source, while still attached to its plug and handling rod, is placed into this shield. It is now surrounded by approximately 2 in. of lead, yet the grub-screw is accessible to be loosened, using a long-handled screwdriver. With the grub-screw loosened the lead plug and

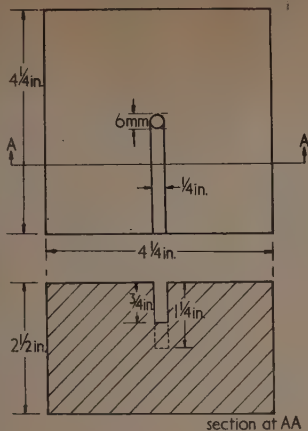


Fig. 15. Source transfer jig in lead

The long-handled screwdriver, used for loosening and tightening the grub-screw of the adaptor, is approximately 2 ft 3 in. long, 1 ft of which is a  $\frac{1}{2}$ -in. diameter ebonite handle. The tongs, for transferring the  $\gamma$ -ray source, should preferably have flat-ended pincers to give a good grip on the small  $\gamma$ -ray source.

#### ACKNOWLEDGEMENTS

During the early stages of this work Mr. J. Rhodes made most valuable contributions which are gratefully acknowledged. The authors express their thanks to various colleagues who manufactured most of the equipment, and to Mr. E. W. Colbeck, Metallurgical Director, Messrs. Hadfields Ltd., Sheffield, for permission to publish this paper.

#### REFERENCES

- (1) *Introductory Manual on the Control of Health Hazards from Radioactive Materials* (Issue No. 2, 1949). Prepared for the Medical Research Council by the Ministry of Supply. (Obtainable free of charge from the National Physical Laboratory, Teddington, Middlesex.)
- (2) *Catalogue No. 2 of Radioactive Materials and Stable Isotopes* (A.E.R.E., Harwell, and R.C.C., Amersham). Ministry of Supply (1950) with amendments (1952).
- (3) ELLIS, F. *Brit. J. Radiology*, 23, p. 28 (1950).

## Sampling errors in radiation measurement using the Moll thermopile method

By L. L. FOX, B.Sc., F.Inst.P., R. C. G. PACKHAM, B.Sc., A.R.C.S., P. L. PALMER, B.Sc., and D. WHITTAKER, B.Sc., A. Inst.P., Fuel Research Station, London, S.E.10

[Paper first received 21 November, 1952, and in final form 6 May, 1953.]

The determination of the radiant heat output from solid-fuel fires requires that the radiation be measured at a number of sampling points on the surface of a hemisphere surrounding the front of the fire. For routine work the number of sampling positions must be kept to the minimum consistent with a reasonable degree of accuracy. This paper describes experiments to compare the measurements given by various sampling arrangements with that given by the "standard" sampling arrangement of 21 Russell latitudes–27 Russell longitudes.

The results indicate that it is possible to reduce the number of sampling positions to 5 Russell latitudes–5 Russell longitudes and still retain a sampling accuracy of the order of 1%.

### 1. INTRODUCTION

When considering the performance of a domestic heating appliance it is often required to know its radiant heat output. Under test-bench<sup>(1)</sup> conditions this is interpreted to mean the determination, at regular intervals throughout a test period, of the total radiant flux (sometimes called "total radiation") through some simple surface whose boundary encircles the appliance in the plane of the "front" of the appliance. In practice, and for convenience, the radiation is measured over the surface of a hemisphere by thermopiles mounted tangentially on a semicircular arc. This arc is pivoted about a vertical diameter in the plane of the "front" of the appliance, its centre of curvature being at what is considered to be the centre of radiation of the fire. With such an arrangement the arc may be made to sweep out the whole hemisphere surrounding the appliance. Ideally the total radiation would be determined by measuring the normal component of radiation at every point on this hemispherical surface. As this is impracticable, the total radiation must be estimated from measurements of the normal components of radiation at certain carefully selected sampling positions.

When only one thermopile is available for the determination of the radiant heat output from a solid-fuel appliance,

readings with this thermopile, when in one sampling position, are taken at regular time intervals throughout the test period. To be able to calculate, from these single-point readings, values of total (hemispherical) radiation it is necessary to make frequent determinations of the "distribution factor" which relates the total radiation from the fire to the single-point reading. To do this, the thermopile has to be placed in turn in the selected sampling positions on the surface of the hemisphere. In general when a single thermopile has been used at the Fuel Research Station the sampling positions have been what may be termed the "(7–9) Russell<sup>(2)</sup> positions," i.e. the thermopile was placed on the radiometer arc in each of the 7 Russell latitudes in turn and, with the thermopile in each such position, the radiometer arc was placed successively in each of nine equiangular positions of longitude (see Appendix 1). In this paper, equiangular positions of longitude are referred to as Russell longitudes. The time to take a set of readings, in which the thermopile occupied in turn each of the 63 sampling positions, was about 8 min. As, during these 8 min, the intensity of the radiation from the appliance had, in general, changed, it was necessary to apply a small correction to each of the 63 readings.

If the latitude sampling is achieved by having a number of

thermopiles attached to a single radiometer arc, the value of the total radiation can be found during one traverse of the arc in which it is placed, in turn, in the various longitude sampling positions. This single traverse takes about 1 min and is equivalent to taking, say, a 63-position sample of the radiation from the appliance. Whether only one thermopile is used or a multiple thermopile system is employed, it is clearly necessary to ensure that the sampling positions are such that a true estimate of total radiation results. Sampling problems similar to these have arisen in the past. Before the advent of the globe photometer, a good deal of work was done on the determination of the spherical candle power of light sources using numerical integration methods such as those discussed by Buckley<sup>(3)</sup> and others. More recently, Bennett and Hartley<sup>(4)</sup> and Morpurgo and Silver<sup>(5)</sup> have discussed the sampling of the radiation from gas fires. The present paper deals with experiments on the sampling of the radiation from a solid-fuel open fire. All the experiments consisted in the measurement, at intervals, of the total radiation from an open fire under conditions generally similar to those of a "high radiation output test"<sup>(6)</sup> of the type used in official tests on open fires. The appliance used was a 16-in. improved type of open fire included in the Coal Utilisation Council List of "Recommended Domestic Solid Fuel Appliances." An open fire was chosen because it gives a high intensity of radiation and because there is a large variation in the spatial distribution of its radiation.

The standard of measurement of total radiation was taken to be the radiation measured by using 21 thermopiles in Russell latitudes on a radiometer arc which was itself placed, in turn, in the 27 Russell longitudes—the (21–27) Russell arrangement (see Appendix 2).

## 2. TYPE OF THERMOPILE USED

In the work of testing solid-fuel appliances it is necessary that the thermopile used shall have the following characteristics:

- it shall obey the Lambert cosine law of radiation;
- it shall have a linear response with variation of intensity incident upon it;
- it shall be non-selective in its response to radiation of various wavelengths.

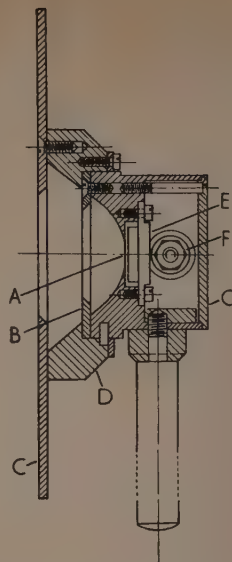
In fact, thermopiles do not fulfil these conditions perfectly, but the type of Moll thermopile in use at the Fuel Research Station was developed specially for this kind of work and experience in its use has shown that its characteristics approximate very closely to the ideal. The housing of the thermopile was designed according to principles laid down by the Fuel Research Station and the National Physical Laboratory. A sectional drawing of the thermopile is shown in Fig. 1 which, by permission of the Cambridge Instrument Co., Ltd., is based on their Drawing No. 333–1.

## 3. ADJUSTMENT OF MOLL THERMOPILES FOR RESPONSE AND RESISTANCE

In the methods of numerical integration investigated, it is necessary that equal weight be given to the radiation at each sampling point. However, the sensitivities of the thermopiles available were spread over a range extending 14% on either side of the mean, and, since in the tests it was the combined outputs of numbers of thermopiles in series which was recorded, any weighting of the individual outputs by calculation was impossible. It was thus essential to make the effective sensitivities of the thermopiles identical and this was

Fig. 1. Sectional drawing of Moll thermopile

- A, thermopile elements;  
B, inner screen;  
C, front screen;  
D, thermopile housing;  
E, cold junction support;  
F, terminal;  
G, inspection cover.



accomplished by placing a suitable resistance in parallel with each thermopile. It was also found convenient, in the interests of their interchangeability in the various circuit arrangements, to make up the resistances of all the shunted thermopiles to a common value by the addition to each of a suitable series resistance.

Let  $M$  be the resistance of a thermopile,

$e$  be its e.m.f. (open circuit) when exposed to radiation of unit intensity,

$r$  be the resistance placed in parallel with  $M$ ,

$s$  be the resistance placed in series with the shunted thermopile.

The value of  $r$  was chosen to make  $er/(r + M) = E$ , where  $E$  was a constant which was less than the lowest value of  $e$  in the group. The value of  $s$  was chosen to make  $s + [rM/(r + M)] = P$ , where  $P$  was a constant which was greater than the highest value of  $rM/(r + M)$  in the group of shunted thermopiles. It may be shown that a thermopile modified in the way described will behave in any circuit arrangement as a generator having internal resistance  $P$  and producing an e.m.f.  $E$  when exposed to radiation of unit intensity.

## 4. DETERMINATION OF THE SENSITIVITIES AND THE RESISTANCES OF THE THERMOPILES

The sensitivities of the thermopiles were determined by comparison with a sub-standard thermopile calibrated at the National Physical Laboratory. The source used was an electric heater operating at a temperature of about 1650° F. The sensitivity was measured with the thermopiles exposed to the same intensity (about 400 B.Th.U. per ft<sup>2</sup> per h) because this type of thermopile exhibits a slight variation of sensitivity with intensity.

The resistances were determined potentiometrically, after the thermopiles had attained thermal equilibrium in a vacuum flask. When the additional resistances had been fitted to the thermopiles their sensitivities all lay within a range of  $\pm 0.4\%$  of the mean value.



## 5. SETTING UP THE FIRST RADIOMETER ARC

The open fire was installed in a two-piece refractory fire-back, conforming dimensionally to B.S. 1251, under a 24-ft brick chimney having a 9 in.  $\times$  9 in. flue. The fireplace recess behind the fireback was filled in with builder's rubble, and the fireplace surround was of brick. A semicircular radiometer arc of radius 3 ft was pivoted vertically in front of the appliance, with its centre of curvature at the mid-point of the top of the firefront. Twenty-one Moll thermopile holders, each carrying a thermopile, were then placed on the radiometer arc in such a way that the centres of the receiving elements of the thermopiles occupied the 21 Russell-latitude positions. These 21 positions incidentally incorporated the 3 Russell-latitude and the 7 Russell-latitude positions. The galvanometer could be connected either across all 21 thermopiles in series or across the thermopiles in the 7 Russell-latitude positions,

and low-temperature coke. It will be seen that if the (21-27) Russell arrangement is taken as correct:

- the radiation measured by the (7-9) Russell arrangement is, on the average, about 1.5% too high; and
- of this 1.5%, about 1.2 units are due to using 7 latitude sampling positions, while the remaining 0.3 unit is due to using 9 longitude sampling positions.

## 7. EFFECT OF USING VARIOUS LONGITUDE SAMPLING POSITIONS

Throughout this series of tests 21 thermopiles were used in the 21 Russell latitudes and the object was to find the effect on measured total radiation of varying the longitude sampling positions. Since it had already been discovered that the difference between 9 Russell longitudes and 27 Russell

Table 1. Effect on measured total radiation of sampling with the (21-27), the (7-9), and the (21-9) Russell arrangements

Percentage difference in measured total radiation

State of fire	$\frac{R_{7,9}-R_{21,27}}{R_{21,27}} \times 100 (\%)$		$\frac{R_{7,9}-R_{21,9}}{R_{21,9}} \times 100 (\%)$		$\frac{R_{21,9}-R_{21,27}}{R_{21,27}} \times 100 (\%)$	
	Gas coke (21.10.49)	Low-temperature coke (20.10.49)	Gas coke (21.10.49)	Low-temperature coke (20.10.49)	Gas coke (21.10.49)	Low-temperature coke (20.10.49)
Rising fire	+1.1	—	+0.9	—	+0.2	—
Approaching peak	+1.1	—	+0.8	—	+0.3	—
Just past peak	+1.7	+1.8	+1.2	+1.5	+0.5	+0.2
Falling fire	+1.6	+1.3	+1.1	+1.1	+0.5	+0.2
Low fire	+1.4	+1.5	+1.2	+1.3	+0.2	+0.2
Refuel	+1.1	+1.2	+1.0	+1.2	+0.1	0.0
Rising fire	+1.2	+2.5	+1.0	+2.6	+0.2	-0.2
Approaching peak	+1.0	+1.8	+1.0	+1.4	-0.1	+0.4
Just past peak	+1.4	+1.5	+1.2	+1.2	+0.3	+0.3
Falling fire	+1.5	—	+1.3	—	+0.2	—
Low fire	+1.7	+1.3	+1.2	+1.3	+0.5	0.0
Average of the percentage difference values	—	+1.6	—	+1.2	—	+0.4
	+1.7	+1.2	+1.3	+0.9	+0.4	+0.4

connected in series. The circuit resistances were such that, with the arc in any one position, the ratio of the radiation measured by the 7-thermopile circuit to that measured at the same instant by the 21-thermopile circuit was given by the ratio of the two galvanometer deflexions. A pointer attached to the radiometer arc traversed a semicircular azimuth scale.

## 6. PRELIMINARY EXPERIMENT

The aim of the first experiment was to compare the (7-9) Russell arrangement with the (21-27) Russell arrangement at various times throughout the period of a test of the type referred to in the Introduction. Readings were taken of the total output of the 21 thermopiles with the radiometer arc in each of the 27 Russell-longitude positions and of the total output of the 7 thermopiles with the arc in each of the 9 Russell-longitude positions. Since the 9 Russell longitudes are included in the 27 Russell longitudes the results enabled two other comparisons to be made: that between the (7-9) and the (21-9) Russell arrangements, and that between the (21-9) and the (21-27) Russell arrangements.

Table 1 shows the results obtained in tests using gas coke

longitudes was only about 0.3%, it was decided to compare other longitude sampling arrangements against the 9 Russell longitudes, as time would thereby be saved. The sampling arrangements investigated were the 7, 5 and 3 Russell longitudes and the 9-, 7-, 5- and 3-fold longitudes calculated according to the usual form of Tchebycheff's method for numerical integration (see Appendix III). Several times throughout each test, the readings in the two sets of positions being compared were taken as the arc made a single traverse in front of the fire.

Low-temperature coke was used for the tests. The difference between the mean reading given by the (21-9) Russell sampling arrangement and the mean reading given by the sampling arrangement being investigated was then calculated as a percentage of the former. Table 2 summarizes all the results obtained in the various comparisons. From the figures given in the bottom row of this table it will be seen that with 7 and 5 Russell longitudes, the measured total radiation differs by an average of 0.3% from that given by the 27 Russell longitudes. The corresponding differences for 3 Russell longitudes is about 5%. When using the Tchebycheff longitudes, the measured values of total radiation given by the 9 and 7 longitudes are both within 0.3% of that given by the

Table 2. *Effect on measured total radiation of using various longitude sampling positions. (Throughout the experiment 21 thermopiles were used in the 21 Russell latitudes)*

(Fuel: Low-temperature coke)

State of fire	Percentage difference in measured total radiation compared with the (21-9) Russell arrangement							
	27 Russell (20.10.49)	7 Russell (16.12.49)	5 Russell (16.12.49)	3 Russell (16.12.49)	9 Tchebycheff (12.12.49)	7 Tchebycheff (12.12.49)	5 Tchebycheff (12.12.49)	3 Tchebycheff (12.12.49)
Rising fire	—	-0.2	-0.8	+5.6	+0.4	-0.6	-2.1	-1.2
Approaching peak	-0.2	+0.2	-0.2	+4.8	-0.3	-0.4	-1.5	-2.5
Just past peak	-0.2	-0.2	-0.4	+4.6	—	—	—	—
Falling fire	-0.2	+0.4	-0.1	+4.9	-0.4	-0.5	-2.2	-1.6
Low fire	0.0	-0.2	-0.9	+5.8	0.0	-0.5	-2.1	-0.6
Very low fire	—	0.0	-1.0	+4.9	—	—	—	—
<i>Refuel</i>								
Rising fire	+0.2	+0.2	-0.7	+3.0	-0.4	-0.7	-1.6	-1.6
Approaching peak	-0.4	—	—	—	—	—	—	—
Just past peak	-0.3	+0.5	-0.6	+4.1	0.0	-0.5	-1.4	-2.2
Falling fire	0.0	0.0	-0.7	+4.6	—	—	—	—
Low fire	-0.4	+0.1	+0.6	+2.7	-0.7	-0.4	-1.5	-1.4
Very low fire	-0.4	0.0	-0.8	+5.4	-0.6	-0.4	-2.0	-0.9
Average of the percentage difference values	-0.2	+0.1	-0.5	+4.6	-0.3	-0.5	-1.8	-1.5

27 Russell longitudes; the measured values of total radiation with the 5 and 3 Tchebycheff longitudes differ by about 1.5% from the same standard. It would appear that the longitude sampling arrangement which keeps within 0.5% of the standard for the smallest number of positions is that of the 5 Russell longitudes.

#### 8. EFFECT OF USING VARIOUS LATITUDE SAMPLING POSITIONS

Since it was not possible, on one radiometer arc, to locate thermopiles in all the required latitude sampling positions, it was necessary for this comparison to pivot a second arc, of radius equal to that of the original arc, on the same axis and having the same centre as the original arc. The construction of the second arc was such that the two arcs, if required, could be positioned very close to each other. Fig. 2 shows the two arcs in position. Throughout the comparisons, 9 Russell longitudes were used and the various latitude sampling arrangements were all compared with 21 Russell latitudes. As in the preliminary experiment (Section 6), the total circuit resistances were proportional to the number of

thermopiles in use on the arc, so that with each one of the various latitude sampling arrangements the total radiation was proportional to the sum of the galvanometer deflexions obtained in one traverse.

The first sampling arrangement investigated was that of 5 Russell latitudes. To obtain comparisons, alternate readings were taken with each of the two arcs in the 9 longitude positions. As before, readings were taken at intervals throughout a test. The second sampling arrangement was that of 5 latitudes calculated according to a special case of Tchebycheff's method (see Appendix III). The third sampling arrangement was that of 3 Russell latitudes, which were obtained from the 21 latitudes on the original arc by suitable wiring and switching. Tests were performed using both gas coke and low-temperature coke. Table 3 summarizes all the results obtained in the various latitude comparisons. It will be noted that the totals with 7, with 5 and with 3 Russell latitudes are all within 1.5% of that with 21 Russell latitudes, while the total with the 5 Tchebycheff latitudes is within 1% of the same standard.

#### 9. COMPARISON OF COMBINED LATITUDE AND LONGITUDE SAMPLING ARRANGEMENTS

This final series of experiments was designed to compare the measured total radiation given by various combined latitude and longitude sampling arrangements with that given by the sub-standard arrangement (21 Russell latitudes—9 Russell longitudes). Readings were taken at intervals throughout a test.

The first sampling arrangement investigated was that of 5 Russell latitudes—5 Russell longitudes. The percentage by which this (5-5) Russell sampling arrangement differed from the (21-9) sub-standard arrangement was calculated. Table 4 gives a summary of the results obtained. It will be noted that on an average the total radiation measured with the (5-5) Russell sampling arrangement is less than 1% greater than that measured with the (21-9) sub-standard arrangement. In Section 6 it was shown that the (7-9) Russell sampling arrangement gave results 1.2% greater than did the (21-9) sub-standard arrangement.



Fig. 2. Photograph of fire showing the two radiometer arcs pivoted about the same axis

Table 3. The effect on measured total radiation of using various latitude sampling positions  
(In each test the arc was placed, in turn, in the 9 Russell longitudes)

Percentage difference in measured total radiation compared with the (21-9) Russell arrangement

State of fire	7 Russell		5 Russell		3 Russell	5 Tchebycheff	
	Gas coke (21.10.49)	Low-temperature coke (20.10.49)	Gas coke (11.1.50)	Low-temperature coke (16.1.50)	Gas coke (21.12.49)	Gas coke (21.12.49)	Low-temperature coke (19.12.49)
Rising fire	+0.9	—	+0.8	+2.2	+2.3	0.0	+0.4
Approaching peak	+0.8	—	+0.7	—	+1.8	+0.6	—
Just past peak	+1.2	+1.5	+0.9	—	+1.4	+0.8	+1.3
Falling fire	+1.1	+1.1	+1.1	+2.3	+0.9	+1.2	+1.1
Low fire	+1.2	+1.3	+1.0	+2.6	+0.8	+1.2	+2.0
Very low fire	—	—	—	—	+0.4	+1.0	—
Refuel	—	—	+1.5	—	—	—	—
Rising fire	+1.0	+1.2	+1.7	+1.3	—	—	+0.5
Approaching peak	—	—	+1.9	+1.7	-0.8	+0.6	+0.6
Just past peak	+1.0	+2.6	+0.6	+1.1	+1.4	+0.9	-1.6
Falling fire	+1.0	+1.4	+0.7	+1.7	+1.4	+0.8	—
Low fire	+1.2	+1.2	—	+1.3	—	—	-0.1
Very low fire	—	—	+1.3	—	+1.0	+1.4	—
Refuel	+1.3	—	—	+1.3	—	—	—
Rising fire	+1.2	+1.3	+1.0	+1.0	+1.2	+1.2	-0.1
Approaching peak	+1.3	+1.2	+1.2	+1.0	+1.1	+1.3	-0.2
Just past peak	—	—	+1.6	+0.8	—	—	—
Falling fire	—	+0.9	—	—	—	—	+0.2
Low fire	—	—	+1.1	+1.1	—	—	+0.3
Average of the percentage difference values	+1.1	+1.4	+1.1	+1.5	+1.1	+0.9	+0.4

The second sampling arrangement investigated was that of 5 Tchebycheff (special case) latitudes-5 Tchebycheff (usual form) longitudes, and from the summarized results given in Table 4 it will be seen that the total radiation measured by this sampling arrangement is about 3% greater than that measured by the (21-9) sub-standard arrangement.

Table 4. Effect on measured total radiation of using the (5-5) Russell and the (5-5) Tchebycheff sampling arrangements  
[Fuel: Low-temperature coke (16.12.49)]

State of fire	Percentage difference in measured total radiation compared with the (21-9) Russell arrangement	
	(5-5) Russell sampling arrangement	(5-5) Tchebycheff sampling arrangement
Rising fire	+1.7	+2.8
Approaching peak	—	+6.5
At peak	+1.7	+4.4
Falling fire	+1.6	+3.3
Low fire	+0.6	+1.8
Very low fire	+0.5	-0.1
Refuel	—	—
Rising fire	+0.9	+2.8
Approaching peak	+0.5	+3.5
At peak	-0.1	+3.6
Falling fire	+0.5	+1.8
Low fire	+0.9	+1.9
Average of the percentage difference values	+0.9	+2.9

## 10. CONCLUSIONS

Throughout this investigation it has been assumed that the (21-27) Russell sampling arrangement gives a "perfect" sample of the radiation from an open fire. On this basis the following conclusions concerning the sampling of radiation from an open fire may be drawn from the investigation:

1. For longitude sampling, the use of 9, 7 or 5 Russell positions gives equally accurate results within 0.5% of the true value; the use of 3 Russell longitudes gives an overestimation of 5%. The sampling positions chosen according to a special case of Tchebycheff's quadrature rule give accurate results (less than 0.5% error) when 9 and 7 positions are used, but the errors are 1.5% when 5 or 3 positions are used.

2. For latitude sampling, the use of 7, 5 or 3 Russell positions each results in an overestimation of the radiation by about 1.3%. Sampling at 5 latitude positions calculated according to a special case of Tchebycheff's rule results in an overestimation of less than 1%.

3. The sampling arrangement which provides the most accurate sampling, while requiring the smallest number of thermopiles (latitude positions) and the smallest number of longitude sampling positions, is that of (5 Russell latitudes-5 Russell longitudes). The overestimation with this arrangement is a little over 1%, compared with an overestimation of 1.5% when using the (7-9) Russell sampling arrangement.

4. There was no significant difference between results obtained using either of the fuels—gas coke or low-temperature coke.

## 11. ACKNOWLEDGEMENTS

The work described in this paper formed part of the Fuel Research programme of the Department of Scientific and



Industrial Research and the paper is published by permission of the Director of Fuel Research. The illustrations are Crown copyright and are published by permission of the Controller of H.M. Stationery Office.

## REFERENCES

- (1) SHAW, W. F. B. *J. Roy. Sanit. Inst.*, **73**, p. 1 (1953).
- (2) RUSSELL, A. *J. Instn Elect. Engrs*, **32**, p. 631 (1903).
- (3) BUCKLEY, H. *Illum. Engr, Lond.*, **18**, pp. 69, 70, 93 (1925).
- (4) BENNETT, A. R., and HARTLEY, H. *Instn Gas Engrs, Publ. No. 149/46*, 46 pp. (1936).
- (5) MORPURGO, P. W. R., and SILVER, R. S. *Gas Res. Bd., Communication GRB 35*, p. 8 (Nov. 1947).
- (6) FOX, L. L. *Coke*, **12**, p. 324 (1950).
- (7) MILNE-THOMSON, L. M. *Calculus of Finite Differences* (London: Macmillan and Co. Ltd., 1933).
- (8) KRILOFF, M. A. *Bull. Assoc. Tech. Marit.*, **4**, p. 97 (1893).

## APPENDIX I

## Russell angles

In measuring the total flux of radiation through a hemisphere it is possible to take only a limited number of experimental observations and some method of numerical integration must be employed. The method used to determine the Russell angles is the mid-ordinate or trapezoidal rule and this is applied in turn to two variables to give the required double integral over the surface. The variables taken to define position on the hemisphere are latitude, ( $\theta$ ), and longitude, ( $\phi$ ) (zero longitude in the present case being in the vertical plane through the centre of the fire and normal to the fire surround). An elementary area of the hemisphere is then proportional to  $\cos \theta d\theta d\phi$  or to  $h d\theta d\phi$ , where  $h$  is the height of the element above the equatorial plane. The mid-ordinate rule must therefore be applied, not to the variables  $\theta$  and  $\phi$  but to  $h$  and  $\phi$  in order to determine the sampling positions.

The  $n$  Russell latitudes and the  $m$  Russell longitudes required to give  $nm$  sampling positions are given by:

$$\theta_r = \sin^{-1} \left( \frac{n+1-2r}{n} \right) \quad (r = 1, 2 \dots n)$$

and

$$\phi_r = \frac{\pi}{2} \left( \frac{m+1-2r}{m} \right) \quad (r = 1, 2 \dots m)$$

It has become customary to take odd numbers for  $n$  and  $m$ .

## APPENDIX II

## The use of the (21-27) Russell sampling arrangement to give a standard of measured total radiation

It was desired to obtain a reliable standard of measurement of total radiant flux over the hemisphere against which to compare measurements made using sampling positions determined according to various schemes of numerical integration. First it may be noted that if an infinite number of radiation measurements distributed uniformly over the surface could be taken with an ideal receiver, then there would be no errors, whatever the size and shape of the source or its location inside the hemisphere. It would seem therefore that, in practice, the greater the number of properly distributed measuring positions used, the greater should be the accuracy. It was therefore decided to place on the arc the maximum number of thermopiles that could be accommodated according to the chosen arrangement, and, in addition, to make with them as many observations as practicable in the horizontal traverse across the hemisphere.

It was decided to choose the positions of the thermopiles on the arc, and of the arc in its traverse, according to the mid-ordinate rule because this rule is a simple one, widely used, and involves no other assumptions than that the average value of a smooth function in an interval may be taken, approximately, to be its value at the mid-ordinate position. It is nearly true that the radiant intensity from a solid-fuel fire may be represented by a smooth function of position, although small discontinuities in the functional derivatives may occur due, for example, to the occulting of a straight edge of burning fuel by another parallel edge in the fire or the appliance.

The actual sampling arrangement used as standard was that of 21 Russell latitudes (i.e. 21 thermopiles on the arc)—27 Russell longitudes (i.e. 27 positions of the arc). The error using this arrangement is likely to be quite small, as can be shown by considering the radiation from a small plane source. The distribution of this radiation will follow a cosine law for both variables and the sampling error may thus be easily computed. For this source, the (21-27) Russell arrangement gives a calculated sampling error of 0.35%.

## APPENDIX III

## The use of Tchebycheff's method of numerical integration

This is a method of numerical integration which, like the mid-ordinate rule, enables equal weight to be given to all the experimental observations used in the calculation. The interval of integration is considered as a whole and the measuring positions are so chosen that an exact integral would be given, if the unknown functional relationship between radiation and position could be represented by a polynomial of degree no greater than the number of the measuring positions used.

Tchebycheff's method expressed in its most general form<sup>(7)</sup> gives rules for determining points  $x_1, x_2 \dots x_n$  such that, if  $F(x)$  is a known function and  $f(x)$  an unknown function which it is desired to integrate then:

$$\int_{-1}^{+1} F(x)f(x)dx = k[f(x_1) + f(x_2) + \dots + f(x_n)] + R_n \quad (1)$$

where  $k$  and the points  $x_1 \dots x_n$  are independent of the function  $f(x)$  and where the remainder  $R_n$  depends only on  $f^{(n+1)}(x)$ .

Tchebycheff's method is almost always met with as a special case in which  $F(x)$  is put equal to unity.<sup>(7,8)</sup> In the present paper this special case has been referred to as the usual form of Tchebycheff's method or rule. This usual form has been applied to calculate longitude sampling positions. The usual form could also have been applied to the division of the vertical height above the equatorial plane to determine suitable latitude sampling positions, in a similar way to that in which the mid-ordinate rule has been applied to give Russell angles. However, it is more logical and rigorous to regard the radiation as a smooth function of latitude rather than of vertical height. Thus, if in equation (1)  $x$  is put equal to  $\theta$ , the latitude, and  $F(x)$  is put equal to  $\cos \theta$ , then the unknown radiation function  $f(\theta)$  becomes a function of latitude, while  $\cos \theta d\theta$  represents the required zonal increment. Only two cases yield real solutions. These are:

$$\text{for } n = 3; \theta_1 = -\theta_3 = 47^\circ 58'; \theta_2 = 0.$$

$$\text{for } n = 5; \theta_1 = -\theta_5 = 59^\circ 52'; \theta_2 = -\theta_4 = 15^\circ 52'; \theta_3 = 0.$$

The 5-fold latitudes calculated according to this special case of Tchebycheff's method were used in the experiments referred to in Sections 8 and 9.

# A method of examining the transverse vibrations of rods and reeds

By P. L. KIRBY, M.Sc., A.Inst.P., Research Laboratories, J. A. Jobling and Co. Ltd., Sunderland

[Paper first received 21 October, 1952, and in final form 31 May, 1953]

Apparatus is described with which the vibrations of a thin rod or reed are transformed by means of a capacitance-type electromechanical transducer and a capacity-sensitive circuit into varying electrical potentials. The latter are displayed on a voltmeter and oscillograph, and techniques are described for measuring the internal friction or damping capacity at frequencies of vibration from ten to several hundred cycles per second.

During an investigation of internal friction effects in thin glass rods, apparatus was required to study the damping of free transverse vibrations of an unloaded specimen, clamped at one end, at frequencies above the range in which simple visual methods are possible.<sup>(1)</sup> The internal friction is commonly denoted<sup>(2)</sup> by the term  $\tan \delta$  which is related to the logarithmic decrement  $\lambda$  (the logarithm of the ratio of successive amplitudes on one side of the rest position) by the equation

$$\lambda = \pi \tan \delta \quad (1)$$

It follows that if the amplitude falls from  $a_1$  to  $a_2$  in  $t$  seconds

$$\tan \delta = (\pi \nu t)^{-1} \ln a_1/a_2 \quad (2)$$

where  $\nu$  is the frequency of vibration. At low frequencies it is possible to measure the amplitude at known time intervals visually,<sup>(1)</sup> but such methods are not generally satisfactory at frequencies greater than 10 c/s or when the half-value period of the amplitude decay is less than about 5 sec. The apparatus to be described has been used with glass rods of diameter 0.5 to 2.0 mm and lengths less than 10 cm, which vibrate at frequencies much higher, and decay more rapidly, than the practical limit for visual measurement.

A photographic record of the decay is obtained by surrounding the free end of the vibrating rod with an electrode system whose capacitance varies with the movement of the rod from its rest position. This capacitance is incorporated in a balancing network so that the deflexion of the rod is measured by the out-of-balance voltage. After suitable amplification this voltage is displayed on an oscillograph and a photograph of a typical trace illustrating the damped vibrations is shown in Fig. 1. The electrode assembly and vibrating rod are easily contained in an evacuated vessel when additional damping due to air resistance may be completely eliminated. The apparatus has the further advantage that, unlike methods using electromagnetic pick-ups, measurements can be made on unloaded specimens of non-magnetic materials.

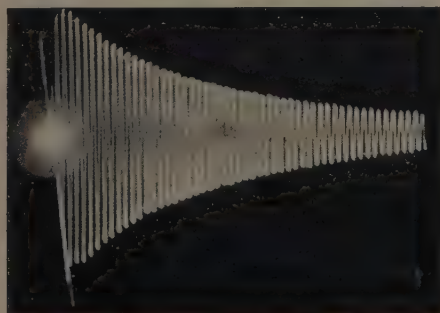


Fig. 1. Damped vibrations of a metallized glass rod surrounded by a push-push electrode system

## TRANSDUCER CIRCUIT

Frommer<sup>(3)</sup> has described a circuit of the type required in which an electrode system is incorporated in a balanced radio-frequency circuit and changes in the capacitance of the system give rise to proportional out-of-balance voltages. This initial linearity between capacitance changes in the electrode system and the resulting signal is maintained during amplification, and the output from the circuit is fed to a voltmeter or an oscillograph. A commercially available instrument (e.g. Proximity meter, Type PM2, by Fielden (Electronics) Ltd.) possessing greater stability and higher sensitivity than the circuit referred to is available and has been used successfully in this work. The output voltage is displayed on a meter on the front panel and auxiliary outputs are available for connexion to other meters or oscillographs.

The metal or glass rod to be examined is placed in the transducer as the movable member of a variable capacitor. In the case of glass, the specimens are first coated with a thin electrically-conducting layer of gold or silver and the rod is then earthed at its fixed end by means of the metal clamp.

In view of the linear response of the capacitance-sensitive circuit it would be preferable to use an electrode system in which a deflexion of the rod produced a proportional capacitance change. The rate of decay of the output voltage amplitude would then equal the rate of decay of transverse oscillations of the rod and damping capacity measurements could be made directly from the former. Such an ideal electrode system is not easily obtained.

When the vibrating element is a flat reed or beam a simple parallel plate capacitor is easily formed and this possesses a  $1/d$  response law. An improvement results from the addition of a second fixed plate connected electrically to the first and at the opposite side of the reed. This symmetrical double-plate system (or push-push system by reason of the capacitance increase when the movable element is deflected in either direction) may be analysed if edge effects are neglected.

Assuming the reed to vibrate about the centre of the electrode system with damped harmonic motion (displacement  $x = x_0 e^{-kt} \sin \omega t$ , where  $k$  is the damping factor) it may be shown that when the amplitude is small compared with the distance between the plates, the output from the electrical circuit  $E$  is given by

$$E \propto (x_0^2 e^{-2kt} \sin^2 \omega t)/d^2 \quad (3)$$

thus the system is governed by a square-law response.

The waveform of this voltage output is characterized by a repetition which, due to the  $\sin^2 \omega t$  term, occurs at twice the frequency of vibration of the bar. It also follows from the occurrence of the factor 2 in the exponent, that measurements made on this waveform will give values for an apparent damping factor equal to twice the actual factor governing the decay of vibrations in the reed.

It can further be shown that the damping factor of the vibrating system ( $k$ ) and the quantity measured from the diminishing output of the capacity-responsive circuit (in the

case cited 2k) are related by a factor equal to the power of the response law of the electrode system.

When measurements are to be made on the damping of transverse vibrations of rods (where the basic capacitance of the system is that of a cylinder lying parallel to a flat plate), there is no simple power law governing the relationship between the deflexion of the rod and the electrical signal. In place of the foregoing analysis a series of values for the deflexion ( $x$ ) of the rod may be taken and the corresponding capacitances ( $C$ ) calculated, as was done for the system shown in Fig. 2(a). It is then necessary to plot  $\log(c - c_0)/c_0$  versus  $\log x$  when the slope of the graph represents the power of the response law of the system at that particular amplitude.

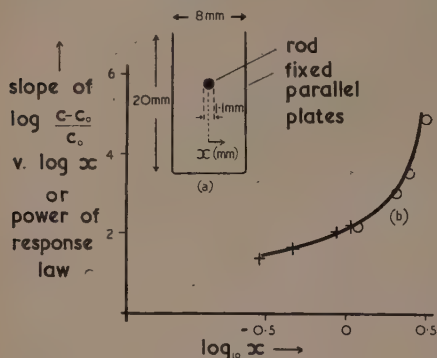


Fig. 2. An electrode assembly (a), for which the conversion factor relating apparent to real damping factor is given by the power of the response law at the appropriate amplitude (b)

Values for this slope are given with varying amplitude in Fig. 2(b). An experimental verification was then carried out by making capacitance measurements while the rod was deflected by means of a micrometer screw gauge. The slope of the logarithmic graph then plotted is given at four points by the circles in Fig. 2(b).

A further check on the calibration of the system was made by measuring a series of apparent damping capacities with the same fibre at different amplitudes. The measured quantities decreased with diminishing amplitude due to a decrease in the power of the appropriate response law. The four crosses on the graph in Fig. 2(b) represent values for apparent damping capacity plotted on an arbitrary linear vertical scale at given mean amplitudes. The close agreement with the theoretical and static measurements justifies the use of this graph to ascertain the value of the conversion factor relating the apparent with the true damping factor.

#### MEASURING TECHNIQUES

When a cylindrical rod of metal or glass is clamped at one end and the free end is deflected to initiate a transverse vibration, in general the latter will continue in one plane only if the cross-section of the rod is perfectly circular. Frequently, however, there is an ellipticity of cross-section in which case the vibrations take the form of a series of Lissajous figures due to there being two perpendicular planes (those containing the major and minor axes of the cross-sectional ellipse) in which free vibrations occur at different frequencies. This may be avoided by initiating the vibration in the plane of either the major or minor axes in which case the vibration proceeds

only in this initial plane. The most stable vibration occurs in the plane of the minor axis.

In its undeflected position, the rod must lie equidistant from the two plates of the electrode assembly. This is achieved by a transverse racking of the assembly until the system possesses minimum capacity as indicated by the capacitance-sensitive circuit.

Alternatively, the rod may be set into vibration and the assembly adjusted until the amplitudes of successive maxima from the amplifying circuit lie between the adjacent maxima. Fig. 3 shows the trace obtained from a slightly off-balance

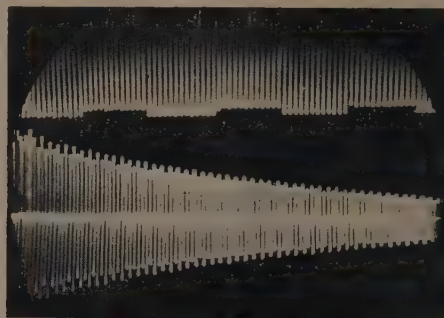


Fig. 3. Damped wave-train from an imperfectly-balanced electrode system with time marker pulses on the Y2 trace

electrode system due to the approach of the vibrating rod nearer to one fixed plate than to the other.

Three methods have been used to measure the apparent damping factors.

(1) When the half-value decay period is less than 0.5 sec, measurements are made from a photographic record of an oscillograph trace. A Cossor model 1049 was used and time intervals are added on the Y2 trace (Fig. 3).

(2) For half-value periods between 0.5 and 5 sec, measurements are made on the output voltmeter by obtaining a multiple-exposure photographic record of the fall of the meter pointer during the decay of a vibration (Fig. 4). It was found convenient to use the camera (Cossor type 1428) from the oscillograph to obtain these records, a high-speed electronic flash-lamp, firing at 0.5 sec intervals, illuminating the meter scale via the trap-door on the top of the camera shield.



Fig. 4. Four consecutive readings of the output voltmeter photographed at half-second time intervals. The final rest position is also shown and the readings illustrate the exponential nature of the decay



It was necessary to paint the meter pointer white (involving a subsequent re-balancing of the pointer) and to insert a black background behind the lower section of the pointer.



Fig. 5. Modulated output from the capacitance sensitive circuit. The period of vibration is given by  $\tau$  and is measured by comparison with the 50 c/s trace on Y2

(3) For half-value periods greater than 5 sec measurement are made from the fall of the pointer of the output voltmeter by visual observation and stopwatch timing.

The half-value period thus obtained is inserted, together with a value for the frequency of vibration, in equation (2), and this apparent damping capacity is converted into the true value by dividing by the factor obtained from Fig. 2(b) at the appropriate amplitude level. Frequency measurements are obtained by examination of the output from the capacity-sensitive circuit on the oscillograph. Fig. 5 shows a trace in which a 3 kc/s carrier wave is modulated by the capacitance changes and compared with a 50 c/s signal. The period of vibration of the rod is equal to the time interval between alternate peaks (the waveform being that of a  $\sin^2 \omega t$  function).

The results of this investigation, which are to be published shortly, show that the values obtained for damping capacity at higher frequencies join smoothly on to the lower frequency results which may be obtained by direct visual observation.

#### ACKNOWLEDGEMENTS

The apparatus described is being used in the Research Laboratories of J. A. Jobling and Co. Ltd., and thanks are due to the Research Director, Dr. S. M. Cox, for permission to publish this paper.

#### REFERENCES

- (1) KIRBY, P. L. *J. Sci. Instrum.*, **30**, p. 339 (1953).
- (2) KIRBY, P. L. *J. Soc. Glass Technol.*, **37**, p. 7 (1953).
- (3) FROMMER, J. C. *Electronics*, p. 104 (July 1943).

## A method of correcting for initial stresses in frozen-stress observations

By H. T. JESSOP, M.Sc., F.Inst.P., and W. H. STABLEFORD, B.Sc., University College, London

[Paper received 4 March, 1953]

Formulae are derived by the use of which it is possible to correct observations on a slice of a "frozen" model for such initial stresses as cannot be removed by annealing. It is demonstrated also that mottle in Marco resin produces an optical effect similar to that of a stress-difference, and that this method of correction may be applied to mottle effects when these are sensibly uniform through the thickness of a slice of the material.

One of the most serious difficulties in the frozen-stress method of investigation of three-dimensional stress-distributions is the practical problem of producing stress-free blocks of photoelastic material. The casting stresses in the material may be attributed to the temperature gradient which develops during polymerization, and this leads to two different types of stress—one due to thermal expansion, the other to a variation in the rate of hardening of the material in different regions. Stresses of the first type may be released by careful annealing, but those of the second type appear to be fixed in the material by chemical action and cannot be removed by subsequent treatment.

Thus it is found that while some reduction in the initial stresses may be produced by a process of annealing, a point is reached after which no further change occurs with further annealing cycles. The stresses which then remain may be called "permanent" initial stresses and these are unaffected by the temperature reached in the freezing process, this temperature being lower than the maximum annealing temperature.

At any point in a model in which stresses have been frozen under load we shall therefore have, in general, two superimposed three-dimensional sets of stresses, which combine to form a single set. The three-dimensional character of the stress systems, however, does not affect the possibility of separating the compound system into its two components by

photoelastic methods, for in each photoelastic observation made we are concerned only with the stresses in one particular plane—the plane of the wave-front of the light passing through the model. Thus in an observation with the light passing in any chosen direction through a thin slice of the frozen model we measure the difference,  $P_1 - Q_1$ , and the inclination  $\alpha_1$  of the secondary principal stresses in the plane of the wave-front at certain points, and these measurements refer to the combined loading and initial stresses. If we now anneal the load stresses from the slice by raising again to the critical "freezing" temperature, and then repeat the observations with the light in the same direction as before, we can measure the difference  $P_0 - Q_0$  and the inclination  $\alpha_0$  of the secondary principal stresses in the same plane due to the initial stress-system only. From these two sets of observations we can deduce the corresponding quantities due to the loading system only.

#### THEORY

It is well known that the distribution at any point of the stresses in any chosen plane is completely defined by the magnitudes and directions of the secondary principal stresses in the plane. Thus if the secondary principal stresses are  $P$  and  $Q$  (Fig. 1), the normal stress  $N$  in a direction  $On$ , inclined at an angle  $\alpha$  to  $Op$ , is given by

$$N = P \cos^2 \alpha + Q \sin^2 \alpha \quad (1)$$

Similarly, the normal stress  $T$ , perpendicular to  $On$  is

$$T = P \sin^2 \alpha + Q \cos^2 \alpha \quad (2)$$

while the shear-stress,

$$S_{nt} = \frac{1}{2}(P - Q) \sin 2\alpha \quad (3)$$

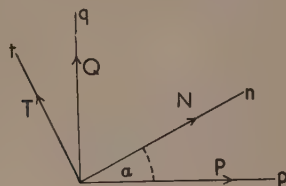


Fig. 1

These relations may be applied to each of the component systems and to the compound system at any point of a slice from a "frozen" model.

Let  $P_1$  and  $Q_1$  (Fig. 2), be the secondary principal stresses in the plane of the wave-front resulting from the combined loading and initial stresses, and let  $P_1$  make an angle  $\alpha_1$ , with a fixed direction  $Ox$  in the plane. Let  $P_0$ ,  $Q_0$  and  $\alpha_0$  be the corresponding quantities for the initial stresses only.

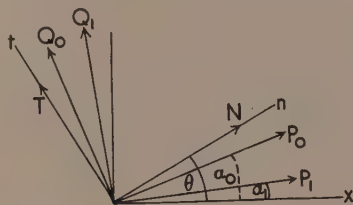


Fig. 2

The stress in any direction due to loading only will be given by the difference of the stresses in that direction due to the two systems.

We first have to find the directions of the principal axes of

Table 1. Sénarmont readings of relative retardation (to nearest 0.005 wavelength)

1st annealing	-0.07	-0.17	-0.155	-0.13	-0.13	-0.13	+0.18	-0.185
2nd annealing	-0.06	-0.175	-0.16	-0.14	-0.135	-0.135	+0.195	-0.185
Change	0.01	0.005	0.005	0.01	0.005	0.005	0.015	0.0

the load system. Consider the stresses in a direction  $On$ , inclined at an angle  $\theta$  to  $Ox$ .

The shear-stress in this direction due to the first system will be

$$S_1 = \frac{1}{2}(P_1 - Q_1) \sin 2(\theta - \alpha_1)$$

That due to the second system will be

$$S_2 = \frac{1}{2}(P_0 - Q_0) \sin 2(\theta - \alpha_0)$$

The shear stress in direction  $n$  due to loading only will thus be

$$S_{nt} = \frac{1}{2}(P_1 - Q_1) \sin 2(\theta - \alpha_1) - \frac{1}{2}(P_0 - Q_0) \sin 2(\theta - \alpha_0)$$

This will be zero when

$$\tan 2\theta = \frac{(P_1 - Q_1) \sin 2\alpha_1 - (P_0 - Q_0) \sin 2\alpha_0}{(P_1 - Q_1) \cos 2\alpha_1 - (P_0 - Q_0) \cos 2\alpha_0} \quad (4)$$

This gives the direction  $\theta$  of one principal axis.

The normal stresses in directions  $n$  and  $t$  due to loading only will then be

$$N = P_1 \cos^2 (\theta - \alpha_1) + Q_1 \sin^2 (\theta - \alpha_1) - [P_0 \cos^2 (\theta - \alpha_0) + Q_0 \sin^2 (\theta - \alpha_0)] \quad (5)$$

$$T = P_1 \sin^2 (\theta - \alpha_1) + Q_1 \cos^2 (\theta - \alpha_1) - [P_0 \sin^2 (\theta - \alpha_0) + Q_0 \cos^2 (\theta - \alpha_0)] \quad (6)$$

These will be the secondary principal stresses when  $\theta$  has the value given by equation (4). The secondary principal stress difference will then be

$$(N - T) = (P_1 - Q_1) \cos 2(\theta - \alpha_1) - (P_0 - Q_0) \cos 2(\theta - \alpha_0) \quad (7)$$

Equations (4) and (7) involve only the directions of the principal stresses and the magnitudes of the stress-differences in the two systems, and these quantities are given directly by the photoelastic observations.

#### USE OF THE METHOD

The successful application of this method depends upon two factors. In the first place the directions of the initial stresses must be sensibly constant at all points on the path of the light ray, and secondly, the initial stresses must remain sensibly unaltered by the annealing out of the load stresses. In most cases the rates of change of the initial stresses from point to point of a model are of a lower order than those of the loading stresses, so that the first condition is likely to be satisfied in any observation for which a similar condition is satisfied by the load stresses. The test of this, in any case, is the distinctness of the isoclinic fringes. If these are sensibly black for both sets of observations, then the directions of both sets of stresses are approximately constant. It is a matter of experience that the second condition is approximately satisfied, but to assess the degree of accuracy likely to be attained, a test was made to verify the persistence of the initial stresses when subjected to several annealing cycles (up to the "freezing" temperature). Eight points were chosen on four different slices of material which had been well annealed (see Table 1).

The greatest change observed was 0.015 wavelength, so that correction for such initial stresses might be expected to have a maximum error of approximately this amount.

The greatest error resulting from such a change in the value of the initial stresses would, of course, occur when the initial and load secondary principal stresses were in parallel directions. The error would be of the second order and negligible when the two sets of axes were at  $45^\circ$  to each other.

#### CORRECTIONS FOR MOTTLE ERRORS

The exact nature of the physical or chemical conditions which produce mottle is still a matter for speculation, but in view of the frequent appearance of the defect in castings of Marco and Fosterite it seemed desirable to make some exploration of the photoelastic effects which it produced. A

point of particular importance was the question whether the fringe-value of the material would vary from point to point of a model containing mottle. Accordingly, a series of tests was carried out on a Marco specimen which contained a large amount of very marked mottle.

Whilst in unpolarized light traces of the mottle could be seen by reflexion and also by oblique transmission, the pattern was practically invisible by normal transmission. This suggests that the Marco in the streaks of mottle has a different refractive index from the rest of the specimen. On the other hand, when rotated between crossed Nicols, isoclinic directions could be found in the mottle streaks in many regions. With a thick slice it was impossible to obtain a proper extinction at some points, and this was found to occur where the mottle streak was far from uniform through the thickness of the slice.

Further observations were now made on a slice 0.1 in. thick; this was found to be sufficiently thin to ensure sensible uniformity of the mottle through the thickness in most places. Stresses were "frozen" into this slice under load, and measurement by the Sénarmont method showed conclusively that at any point of the slice, the optical effect was consistent with

which can be measured in the annealed slice, provided that the mottle is sufficiently uniform through the thickness of the slice to enable clear isoclinic extinctions to be obtained.

The correction method was applied to two regions in a slice taken from a "frozen" model where distinct streaks of mottle crossed one of the isochromatic fringes. The two photographs, taken in circularly polarized light, and the diagram of Fig. 3 show these regions. In each of the regions *A* and *B*, three near points were chosen so that the middle point was at the centre of the mottle streak, and the other points were on either side of it in areas unaffected, or nearly so, by the mottle. In each region the points were chosen in line with the undisturbed isochromatic fringe, so that the final relative retardation figures obtained for the points should be practically the same. The relative retardation at each point was measured by the Sénarmont method, the isoclinic inclination for each point being noted. The slice was then annealed by taking it through the "freezing" cycle—whilst immersed in a suitable fluid to reduce the edge-effect ( $1\frac{1}{2}\%$  water/glycerine mixture\*) and the above measurements repeated. The readings for each point were corrected by applying equations (4) and (7).

## RESULTS

The notation used in Table 2 is the same as used in the first part of the paper, the relative retardations being given in wavelengths of mercury green light.

Table 2. Relative retardations and isoclinic directions at points in "mottled" slice of Marco resin

	Loading plus mottle			Mottle only		Corrected reading	
	$P_1 - Q_1$	$\alpha_1$	$P_0 - Q_0$	$\alpha_0$	$N - T$	$\delta$	
Region A	1	1.09	8°	-0.06	43°	1.11	9.5°
	2	1.28	9°	+0.20	2°	1.10	10.2°
	3	1.10	10°	-0.06	46°	1.12	11.5°
Region B	1	1.06	7°	-0.03	25°	1.08	5.5°
	2	1.17	7°	+0.10	5°	1.07	5.5°
	3	1.02	6°	-0.05	0°	1.06	4.5°

The values for the corrected relative retardation ( $N - T$ ) in each region now agree to within 0.02 fringe, compared with the initial maximum variations of 0.19 fringe and 0.15 fringe in the two regions. There is therefore no indication that the fringe-value of the material is appreciably affected by the mottle.

It thus appears that while complete elimination of the effects of initial stresses and mottle in frozen stress slices cannot be expected, corrections may be made which very substantially reduce the errors due to these effects.

\* SUGARMAN, B., MOXLEY, G. O., and MARSHALL, I. A. *Brit. J. Appl. Phys.*, 3, p. 233 (1952).

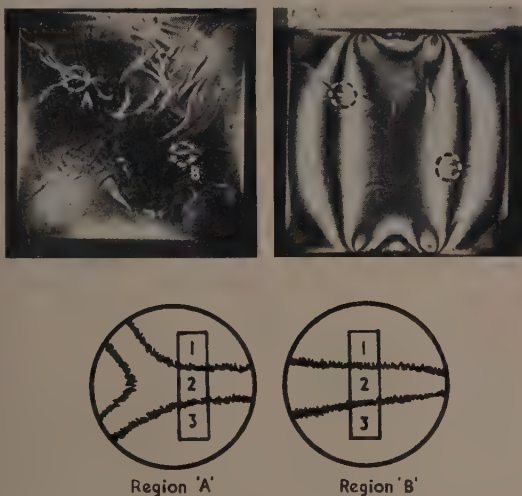


Fig. 3. Effect of mottle in unstressed and stressed slice of Marco resin, showing regions and points at which measurements were made

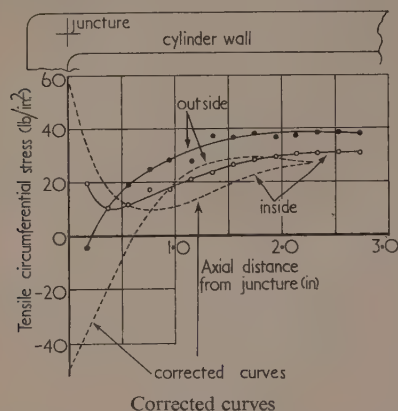
the existence of a relative retardation of two oppositely polarized rays passing through the slice. This was also found to be sensibly true of the optical effects observed in the slice when the load stresses were annealed out; i.e. those due to the mottle alone. Thus we may treat the mottle at any point as an initial stress, the direction and magnitude of



## Correspondence

## Photoelastic determination of stresses in a cylindrical shell

In our recent paper published in this *Journal*\* an error has unfortunately been discovered. Dr. A. A. Wells of the British Welding Research Association has drawn our attention to the fact that the calculated tensile circumferential stresses



in the cylinder as shown in Fig. 7 were inconsistent with the deflexions. On re-checking the calculations one error was found which completely altered the shape of these curves. These corrected curves are plotted in the revised figure.

University of Nottingham.

H. FESSLER  
R. T. ROSE

\* FESSLER, H., and ROSE, R. T. *Brit. J. Appl. Phys.*, **4**, p. 76 (1953).

## Refractive index determination for anisotropic crystals

A. L. Mackay<sup>(1)</sup> has suggested a procedure in the use of the method of measuring the refractive indices of anisotropic crystals described by Ambronn<sup>(2)</sup> and given in Johannsen's text-book.<sup>(3)</sup> But Ambronn's "method" is no method but a fallacy; it is based on a misunderstanding of the fundamentals of crystal optics. If a birefringent crystal is immersed in a liquid having a refractive index which lies between the two indices of the crystal, it is not possible, by rotating the plane of polarization of the incident light, to find any position in which index of the liquid matches that of the crystal. The crystal resolves the light into two components polarized at right angles, and thus "shows" two refractive indices simultaneously. If the polarizer is rotated to a position between the two extinction positions, and the Becke line test is applied, two Becke lines will be seen moving in opposite directions as the objective is raised. It is easy to confirm this with any anisotropic crystal. As the polarizer is rotated, the relative intensities of the two Becke lines change; in no position will the outline of the crystal disappear. The reason why the "method," after being mentioned by Johannsen, disappeared from current text-books, is that it has been found to be a fallacy.

The nomogram suggested by Mackay can be used, and in fact has already been used, in dealing with the changes of

refractive indices which occur on rotating a crystal about a direction at right angles to the line of vision, as in the method of Wood and Ayliffe<sup>(4,5)</sup> for the indirect determination of very high  $\gamma$  indices.

I.C.I. Ltd.,  
Plastics Division,  
Welwyn Garden City, Herts.

C. W. BUNN

## REFERENCES

- (1) MACKAY, A. L. *Brit. J. Appl. Phys.*, **4**, p. 185 (1953).
- (2) AMBRONN, H. *Ber. Sächs. Akad. Wiss. Leipzig*, **45**, p. 316 (1893).
- (3) JOHANNSEN, A. *Manual of Petrographic Methods*, p. 253 (New York: McGraw-Hill Book Co., Inc., 1914).
- (4) WOOD, R. G., and AYLIFFE, S. H. *Phil. Mag.* (7), **21**, p. 324 (1936).
- (5) HARTSHORNE, N. H., and STUART, A. *Crystals and the Polarizing Microscope*, 2nd Ed., p. 319 (London: Edward Arnold and Co., 1950).

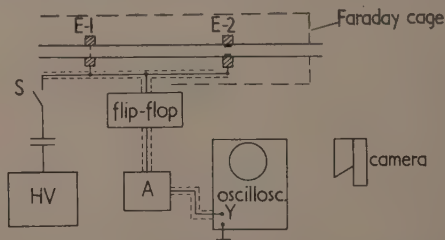
Mr. Bunn is substantially correct and the incident is an example of how a fallacy is propagated in cycles of error and correction. The double Becke lines were found in the experimental test and they were thought to be the true and false Becke lines sometimes observed. The matching point with the liquid was taken to be when they were of equal intensity. In this position the intensities  $B_1$  and  $B_2$  of the two lines corresponding to the indices  $n_1$  and  $n_2$  can be estimated at  $(n_1 - n)^p \cos^2 \theta$  and  $(n - n_2)^p \sin^2 \theta$ , assuming the Becke effect is proportional to some unspecified power,  $p$ , of the difference of refractive indices concerned. When  $B_1 = B_2$ ,  $\tan^2 \theta = (n_1 - n)^p / (n - n_2)^p$ . Calculating from the formula  $\cos^2 \theta / n_1^2 + \sin^2 \theta / n_2^2 = 1/n^2$  gives  $\tan^2 \theta = (n_2/n_1)^2 \cdot (n^2 - n_1^2)/(n_2^2 - n^2)$  and hence, if  $n$  is near to  $n_1$  or  $n_2$  a rough estimate of the correction is still obtained from the wrong formula. This fortuitous similarity tended to supply confirmation of a mistaken theory.

Birkbeck College,  
University of London.

A. L. MACKAY

## Measurements of the speed of little particles in air current

It is important for many problems of dust research to be able to measure the speed of particles in an air current. Since aerodynamical methods are indirect, as they primarily measure the air speed from which the actual speed of the particles is calculated, a method has been developed by means



Apparatus for measurement of speed of particles

of which it is possible to measure the speed of the particles directly.

At one point the particles are charged so that their "run-time" in the air current be measured. By means of the high voltage apparatus *HV* (see figure) a condenser is charged. Charges are sprayed over the injection electrode *E-1* by closing switch *S*. The first impulse of charge is registered on the oscilloscope over a flip-flop-switch and a pre-amplifier *A*. When the charges pass electrode *E-2* a second impulse is registered on the oscilloscope. By means of the time-base of the oscilloscope, the "run-time" can be measured. To obtain exact results, however, only the Y-deflexion of the oscilloscope is used and the deflexion photographed by a camera having a very constant film speed. It should be noted that the particles may be charged electrostatically by friction effects. With the

equipment described, the amplitude of the impulse of measurement was nine times higher than the maximum amplitude of the background.

To make sure that particle speed is measured, and not the speed of ionized air molecules, completely dust-free air was used. The amplitude obtained with this on the oscillograph is approximately half that of the background coming from the electrostatic loadings produced by friction. With a special electrode *E-2* which is adjustable over the cross-section it was also possible to prove that particle speed is not evenly distributed.

Applied Research Laboratories,  
European Office,  
1, Rue du Tunnel,  
Lausanne, Switzerland.

EDGAR LUSCHER

## New books

**The elements of nuclear reactor theory.** By S. GLASSSTONE and M. C. EDLUND. (London: Macmillan and Co. Limited.) Pp. vii + 416. Price 35s.

This is an excellent book on the subject of thermal neutron reactor theory. It covers all aspects of reactor operation, describes methods of calculation and gives declassified values for all the important nuclear constants.

It should be noted that it has never been possible to calculate at all accurately the critical size or other nuclear data for an atomic energy reactor starting from the basic nuclear constants and many simplifying assumptions must be made in order to make the subsequent mathematical computation tractable. These introduce important sources of error when seeking an absolute result. In consequence, empirical methods have been developed. The general principles of these are described, though exact data are omitted. This in no way detracts from the value of the book. In fact, there is no one empirical method of procedure or set of data. Each laboratory both in the U.S.A. and elsewhere undoubtedly has its own recipes.

The book is written in a comprehensive way and is provided with such auxiliary data as to make it easily readable by engineers and physicists with no previous knowledge of the subject. It will form a valuable basis for university and industrial courses on atomic energy as well as being useful to persons working in an atomic energy project.

J. V. DUNWORTH

**The theory of homogeneous turbulence.** By G. K. BATCHELOR, Ph.D. (London: Cambridge University Press.) Pp. xi + 197. Price 25s.

If a uniform mesh of wires is drawn through still air a wake of decaying turbulence is left which is approximately homogeneous and isotropic. The theoretical importance of the study of this decay dates from the introduction by G. I. Taylor in 1935 of the statistical theory of turbulence. For although turbulent flow may be regarded as governed by the Navier-Stokes equation, the three-dimensional nature of the motion, the non-linearity of the equation and difficulty of dealing with boundary conditions involving the statistical specification of random fluctuations of the velocity prevent direct solution, and theory has proceeded by the introduction of simplifying assumptions. In the earlier treatments turbulence was regarded as analogous to the kinetic theory of gases with an "eddy" taking the place of a molecule. This conception was subject to the obvious weakness that an eddy could not preserve its identity after a collision although it

provided a useful pictorial explanation of the enormous increase in transport rates (momentum, heat and matter) caused by turbulence. Taylor considered the fluid as a continuum with a velocity which is a random continuous function of position and time and has a definite correlation between this function at two points. In this treatment the assumption of homogeneous turbulence provides great simplification but is still realizable experimentally. The problem of homogeneous turbulence is then to determine the probability laws that describe the motion at a later time if the initial velocity probability function is given. There is thus defined a branch of fluid dynamics which has all the fascination of simultaneous development of theory based on various simplifying assumptions and of experimental observation for testing the theory. It is true that homogeneous turbulence does not correspond to the character of turbulence in practical systems such as jets and flow round aerofoils, but when more progress has been made with the science of homogeneous turbulence it may assist the understanding of these more complex systems.

In this book Batchelor, who has himself been very active in the development of this subject and can speak with authority, presents a clear survey of material most of which is only available in original papers. He uses either mathematical or verbal argument as seems most appropriate—usually the former! At every stage the theoretical results are compared with experimental ones based on hot-wire anemometer measurements in wind tunnels where the turbulence produced by a grid is decaying with distance from the grid. The author justifies his contention that the problem of turbulence belongs to the field of theoretical physics, which is a science in its own right, but it is clear from the book that the subject is by no means complete and tidy as yet.

M. W. THRING

**Physical similarity and dimensional analysis.** By W. J. DUNCAN, D.Sc., F.R.S. (London: Edward Arnold and Co.) Pp. vii + 156. Price 30s.

This book discusses the conditions under which systems of the same kind are dynamically or physically similar and the use of dimensional analysis to determine the conditions and consequences of similarity in a given phenomenon. A general conclusion is that if two systems are similar then one or more of certain numbers, such as the Froude number, or the Reynolds number, must be the same for both systems. The formula for the period of a simple pendulum, and that for the velocity of deep-water waves, for example, are only special cases of the Froude number. A pleasing result of this synthesis of argument by similarity and dimensional

analysis, which can, after all, be regarded, at least formally, as two aspects of a single subject, is that the dimensional arguments lose some of their customary aura of mathematical prestidigitation. As with most books dealing with dimensions the discussion of fundamentals is none too satisfying—this criticism does not apply to the discussion of similarity. The examples are excellent. E. W. H. SELWYN

**Micrometeorology.** By O. G. SUTTON, C.B.E., D.Sc., F.R.S. (London: McGraw-Hill Publishing Co. Ltd.) Pp. xii + 333. Price 61s.

The sub-title of this book is *A study of physical processes in the lowest layers of the earth's atmosphere*, a subject which here receives its first textual treatment in the English language. A translation of Geiger's well-known book *Das Klima der bodennahen Luftschicht* appeared, it is true, a few years ago, but Geiger's book is essentially descriptive whereas Sutton aims to present "an integrated course of reading . . . in which I have stressed the continuity of atmospheric physics with more familiar studies, as well as the inter-relationships of the topics themselves." There are seven chapters dealing serially with the atmosphere at rest and in motion, heat transfer and diffusion, radiation, the temperature field, wind structure, and diffusion and evaporation. A bibliography attends each chapter.

Given the weather in the broad sense, a subject involving the larger scale physical processes of the atmosphere, those smaller scale processes with which the author deals touch life, both animal and plant, at many points and much of the book is concerned, directly or indirectly, with such matters. The author believes too that micrometeorological processes have proved less stubborn of physical treatment than weather generally and so are good material for the meteorological novice to address himself to. However this may be, and the evidence within these covers cannot be conclusive, the author has done a very professional job within his aims. These do not include the reaction of the micro- on the macro-physical. A reader with sound physics and some mathematical facility will not have difficulty in following the treatment though if he is inquisitive and critical he will find much waiting for explanation—this is the state of the subject. The book is well produced and few misprints have been detected. But the author should revise his remarks about the origin and presence of vorticity in the atmosphere (pp. 18 and 26). The publishers are not encouraging the study or their sales at the price quoted. P. A. SHEPPARD

**Progress in metal physics. Vol. 4.** By B. CHALMERS. (London: Pergamon Press Ltd.) Pp. viii + 403. Price 60s.

This series of reviews is now well established, and Volume 4 contains the following articles; in each case the numerals indicate the number of pages occupied by the review, and of references quoted. 1. Internal friction in metals. A. S. Nowick (66, 149). 2. The mechanism of oxidation of metals and alloys at high temperatures. K. Hauffe (30, 90). 3. Gases in metals. C. R. Cupp (62, 191). 4. The theory of sintering. G. A. Geach (20, 80). 5. Theory of dislocations. A. H. Cottrell (56, 160). 6. Diffusion in metals. A. Le Claire (65, 131). 7. Nucleation. J. H. Hollomon and D. Turnbull (56, 92).

When compared with last year's volume, the present articles are more authoritative and thorough. They will be of great use to those who are working on the subjects concerned, and who wish to ensure that recent work has not escaped them. They will also be valuable to those who

wish to obtain a general knowledge of a subject before starting work on it or on some closely allied branch of science. This improvement in quality has, however, been achieved at the expense of an almost complete loss of sight of the original purpose of the series as stated in the Foreword to Volume I (which is still reprinted), namely to help research workers in one part of the field to remain up to date in other branches. Apart from its length, Professor Cottrell's article is the best for this purpose, but in general the authors show an astonishing lack of power to select what is essential, and to present it clearly and unobscured by minor details. The result is that, in many cases, the main shape of the wood is lost among the individual trees. Many of the contributors appear to regard it as a duty to refer to every published paper on their subject, and fail to realize that if this is done, most readers will be compelled to prepare their own summaries or written reports before they grasp the real progress which has been made. Even the expert on a subject may object to a sentence such as "A mechanism suggested by Mott,<sup>106</sup> and discussed at length in the earlier article,<sup>100</sup> is disputed on the basis of evidence presented by the writer.<sup>101</sup>"

The reviewer would suggest that the Publisher and Editor should reconsider the whole position of this series. If the present type of volume is preferred, it will be most valuable, but should not be sold as a series intended to keep people in touch with branches of metal physics other than their own. If the original purpose of the series is to be resumed, intending authors may well be asked to study some of the outstanding reviews, such as those of Blackman on Specific heats, *Rep. Progr. Phys.*, 8, p. 8 (1941), Stoner on Ferromagnetism, *Rep. Progr. Phys.*, 13, p. 83 (1950), or Lipson on Superlattices, *Progress in Metal Physics*, Vol. 2. A careful study of these will at once reveal the weaknesses of the present volume. With the increasing output of scientific work, there is an ever-increasing need for reports to keep the scientist up to date in subjects which are not his own, and it is to be hoped that the Publisher and Editor of this series will return to their original purpose. W. HUME-ROTHERY

**The comets and their origin.** By R. A. LYTTLETON. (London: Cambridge University Press.) Pp. x + 173. Price 25s.

This book can claim to describe the first theory of the origin and constitution of comets to be worked out with any degree of completeness, and in which all the consequences of the theory are examined in full detail. Its basic assumption is that the sun has moved slowly through a cloud of dust particles, many of which are well known to exist in the galaxy. The particles of the cloud, under the sun's gravitation, then move in hyperbolic orbits about the sun's centre, the initial motion of a particle defining an asymptote of its orbit. As a result, pairs of particles travelling on opposite sides of the sun will collide at some point on the "accretion axis"—a line through the sun's centre, behind the sun and parallel to the original direction of motion of the particles. It is shown how these may form into aggregations, some of which will move outwards and escape from the sun's attraction, and others will be drawn inwards.

These latter aggregations are, however, not drawn directly to the sun's centre, but to the mass-centre of the solar system, which at certain periods is outside the sun's surface. In this way angular momentum about the sun's centre may be obtained by at least some of these aggregates, and orbits about the sun as centre become possible.

The author identifies these successful aggregates as comets. A study of the motions and collisions of the particles within the aggregates produces explanations of the occurrence of the



coma, the envelopes and the tails of comets. Very interesting is the emergence of the reason for the asymmetry of tail formation on the two sides of the perihelion passage. The author even finds a simple explanation of the "string of pearls" feature of the great comet of 1882.

It is noteworthy that this theory derives comets from outside the solar system whereas another recent theory (Oort, 1950) regards them as "born among the planets." This book deals shortly and decisively with the latter.

The first chapters deal extensively with the observational data of comets; and throughout the book, constant comparison is made between these observational facts and the results of the theory, as assessed in orders of magnitude. The clarity of exposition and the rigorous examination of every aspect of the theory make the book of the greatest interest and value.

G. R. GOLDSBROUGH

**Spectrographic analysis of low-alloy steels.** (London: Iron and Steel Institute.) Pp. 83. Price 15s.

Published by the Iron and Steel Institute as Special Report No. 47, this booklet was prepared by the Spectrographic Analysis Sub-Committee of the Methods of Analysis Committee of the British Iron and Steel Research Association.

The comprehensive treatment of the subject is shown by the section headings: the spectrograph, electrodes, excitation sources, photographic plates and processing, plate calibration, photometry, spectral line pairs and direct reading. A recommended method (using the flat sparking surface technique) based on extensive trials in the co-operating laboratories, forms the last section. One minor slip has been noticed: "clear-glass" on page 71 (instead of "clear-plate" as correctly given on pages 43 and 46). Each section is concisely and expertly written and much of the information will be useful to workers in other fields. The present reviewer, for example, found the section on photographic plate calibration particularly interesting.

The booklet concludes with an excellent bibliography from the world's literature. (A further reference—Terms used in spectrographic analysis, B.S. 1636: Part 1, 1950—might well have been included.) It is attractively produced and, at the price, it is remarkably good value.

D. M. SMITH

**Grundlagen der elektronenoptik.** By W. GLASER. (Vienna: Springer-Verlag.) Pp. x + 699. Price DM.120; £10 4s. 6d.

If such a young subject as electron optics can claim a doyen, then he must be Professor Glaser. Since 1933 he has applied himself to the theory of electron lenses and related systems of electromagnetic fields, using especially the method of Hamiltonian eiconals, in which imaging properties are specified in terms of the co-ordinates of the object and image points and the refractive index along paths joining them. By these means it has been possible to treat in a most elegant manner, the conditions of continuous variation in refractive index which are rare in light optics, but inseparable from electron optics. His numerous papers have been of central importance in building up both the general theory and the study of the focusing properties of particular systems. He has now written a systematic treatment of the whole subject, which appears in a volume that is in every way up to the pre-war standard of German scholarship and technical production. No more than a brief indication of the contents of the 32 chapters can be given here. They cover the imaging properties of all types of electron lenses, with detailed treatment of aberrations, which are presented both as mathematical functions and as evaluated for particular field distributions. Practical methods of measuring fields and of investigating

aberrations are also included, as are deflecting systems and directional focusing of the type used in mass- and  $\beta$ -spectrometry. The work is more than a collection of separate papers, being systematically planned and with "bridge passages" that always keep the physical significance of the treatment well in sight. The last section of eight chapters devoted to wave mechanical methods of handling electron optical problems especially contains a great deal of new material. With these rather refined theoretical tools a much more logically satisfying approach to the optics of electrons is presented, although for all practical purposes the end results differ only by a small numerical factor from those obtained with geometrical concepts. Here is indeed the complete handbook of electron optics, which will be the standard work of reference for long to come. The price is high, but one cannot expect a volume with 445 figures and a great deal of mathematics to be produced cheaply.

V. E. COSSLETT

**Electrical measurements and the calculation of errors involved.**

**Part II.** By D. KARO. (London: Macdonald and Co. (Publishers) Ltd.) Pp. xiii + 343. Price 30s.

Part I of this work, dealing with d.c. measurements, was reviewed in this *Journal* in May 1950. The present, and more important, volume deals with a.c. measurements. In the earlier chapters some of the general theory of electrical filters is derived and this is then applied to the derivation of the errors of electrical standards, which are regarded as 4-terminal networks. Information about the practical construction of standards supplements this discussion. Succeeding chapters deal with the vibration galvanometer, the telephone and the cathode-ray oscillograph as a.c. detectors. The last five chapters deal with a.c. bridges, Tuttle's T-circuits and a.c. potentiometers.

The book is intended primarily for a B.Sc. degree course in electrical engineering, but includes not only a.c. measurements beyond the normal scope of such a course but also a very full account of the sources of error in such measurements and the nature of the residuals of a.c. standards. It is very difficult to combine in a single easy text the requirements of the undergraduate and advanced worker. The latter will find much useful information in the present book, but will want to omit a very great deal. The former will find the text difficult, but with perseverance will receive a thorough grounding in a.c. measurements.

T. B. RYMER

**The measurement of particle size in very fine powders.** By H. E. ROSE, Ph.D., M.Sc.(Eng.), A.C.G.I., M.I.Mech.E., A.M.I.C.E. (London: Constable and Co. Ltd.) Pp. 127. Price 9s.

This pleasant little book is based on four public lectures and no doubt this accounts for the somewhat discursive style of writing, which renders it difficult to use as a reference book. It is emphasized in the first lecture that particle size analysis is undertaken as an aid to the control of a process or a product and that, in view of the variety of methods of measurement that are available, a method based on a phenomenon akin to the industrial problem should be chosen whenever possible. This is an important premiss, but many readers would have wished that its consequences had been developed more fully. The discussion of the principles of measurement is followed in the later lectures by accounts of the elutriation, sedimentation, photo-extinction, permeability, adsorption and other methods. Useful material is given on experimental procedure and the precautions necessary to obtain satisfactory results.

Students and newcomers to particle size analysis will find the book a useful introduction.

R. L. BROWN

## Notes and comments

### Conference on applied mass spectrometry

A conference on applied mass spectrometry organized by the Mass Spectrometry Panel of the Institute of Petroleum Hydrocarbon Research Group is to be held in London on Thursday and Friday, 29 and 30 October, 1953, at the Institution of Electrical Engineers, Savoy Place, London. In all there will be eighteen papers, the subjects of which will cover quantitative analysis of gases, liquids and solids, including the continuous monitoring and control of product composition by mass spectrometry; applications to the study of molecular structure, free radicals, and electron/molecule collision processes; and recent developments in instrumentation and computing techniques.

The registration fee is £2 2s. 0d. Applications for further particulars and for registration forms should be made as soon as possible to Mr. W. J. Brown, c/o Metropolitan-Vickers Electrical Co. Ltd., Trafford Park, Manchester 17.

### The chemistry and physics of synthetic fibres

The Plastics and Polymer Group of the Society of Chemical Industry has decided to hold a symposium on the chemistry and physics of synthetic fibres. Papers will be presented and discussed on the chemical and physical basis of fibre formation and the properties of fibres in relation to the molecular structure and conditions of formation. The phrase "synthetic fibres" is to be interpreted in the broader sense, meaning material brought into a fibrous structure by a manufacturing process, irrespective of the source of the raw materials. In order to limit the scope of the symposium, the process of dyeing, the properties of textiles, the economics of the industry and historical surveys will not be included as major items, although reference may be made to such topics if they have an important bearing on the basic theme of the symposium. The symposium will be held on Wednesday, Thursday and Friday, 24, 25 and 26 March, 1954, in the lecture theatre of the Institution of Electrical Engineers, Savoy Place, London, W.C.2. Papers will be presented in full but will not usually take more than 30-40 minutes each. Preprints will be available and authors are asked to submit their manuscripts before 1 November, 1953 to Mr. A. R. Burgess, Plastics and Polymer Group, Society of Chemical Industry, 56 Victoria Street, London, S.W.1.

### The Journal of Photographic Science

To coincide with the centenary of The Royal Photographic Society which falls this year the society has commenced publication of *The Journal of Photographic Science*, being Section B of *The Photographic Journal*. The journal is devoted to the science and applications of photography and appears bi-monthly on the first day of February, April, June, August, October and December. The first issue contains the following contributions: Photographic sensitivity and chemical sensitization of emulsions, by W. F. Berg; Direct observation of solid surfaces at high resolution by reflexion electron

microscopy, by J. W. Menter; Fast multiple frame photography, by J. S. Courtney-Pratt, in addition to some book reviews. The second issue contains the following reviews of progress: Nuclear emulsion technique, by C. Waller; Stereoscopic projection, by H. Dewhurst; Physics of the developed image, by E. W. H. Selwyn; Electron microscopy, by V. E. Cosslett; Medical radiography, by W. Watson; Document copying, by H. Baines. The subscription rate is £1 5s. 0d. per annum, post free, and separate parts are available at 5s. each. Further particulars may be obtained from the Publications Manager, The Royal Photographic Society, 16 Princes Gate, London, S.W.7.

### Erratum

In the article *Information theory* by P. M. Woodward, published in the May issue, equation (12) should read:  $C = I$ .

## Journal of Scientific Instruments

### Contents of the September issue

#### ORIGINAL CONTRIBUTIONS

##### Papers

- A spectrograph unit for use with the N.P.L. gauge interferometer. By C. F. Bruce and V. R. Findlay.  
A controlled-frequency oscillator with frequency "memory." By J. Van Bladel.  
An adjustable direct voltage source for meter calibration. By B. V. Hamon.  
A pressurized  $\gamma$ -radiation monitor for use in inflammable atmospheres. By J. B. Marsh, J. F. Hogg and R. S. Cambray.  
A simple micromanometer. By E. Kovačić.  
A simple electrical method of recording small volume changes. By J. G. Davies.  
Apparatus for automatically recording the absorption of oxygen. By J. C. E. Button and A. J. Davies.  
A wave-height analyser. By M. J. Wilkie and R. F. King.  
A mass spectrometer ion source for solid material. By G. H. Palmer and K. L. Aitken.  
Elimination of dead-time corrections in monitored Geiger-counter X-ray measurements. By J. N. Eastbrook and J. W. Hughes.  
Gas-discharge tubes for control of microwave attenuation. By D. H. Pringle and E. J. Whitmore.  
An electro-mechanical programme controller. By A. F. Watson and P. K. C. Wiggs.  
An omnidirectional photometer of small dimensions. By R. G. Giovanelli.  
A symmetrical cathode follower bridge circuit for direct spectrochemical analysis. By W. G. Walker and S. C. Baker.  
Apparatus for low temperature calorimetry. By R. W. Hill.  
A variable temperature and humidity oven. By J. N. Burcham.
- Laboratory and workshop notes  
A micro-reference flat for multiple beam interferometry. By S. Tolansky and M. Omar.  
A simple apparatus for the calibration of hygrometers. By C. L. Cutting and A. C. Jason.  
A variable temperature vapour-jacket for fractionating columns. By J. F. A. Williams.  
Damping measurements on low frequency transverse vibrations of fibres. By P. L. Kirby.  
Preparation of thin tungsten fibres and their use in place of quartz. By J. O'M. Bockris and D. F. Parsons.

#### NOTES AND NEWS

##### Correspondence

- Some observations on the use of precision X-ray Geiger-counter spectrometers. From G. K. Williamson and R. E. Snallman.  
A mould for pressing plastic disks. From K. H. Stark.  
A contribution to the theory of the Langmuir film balance. From H. Zierfuss, E. Eisma and P. C. Blokker.

##### New instruments, materials and tools

##### Notes and comments

THIS JOURNAL is produced monthly by The Institute of Physics, in London. It deals with all branches of applied physics (including theory and technique). All rights reserved. Responsibility for the statements contained herein attaches only to the writers.

EDITORIAL MATTER. Communications concerning editorial matter should be addressed to the Editor, The Institute of Physics, 47 Belgrave Square, London, S.W.1. (Telephone: Sloane 9806.) Prospective authors are invited to prepare their scripts in accordance with the *Notes on the preparation of contributions*. (Price 2s. 6d. including postage.)

REPRODUCTION. The Institute of Physics is a signatory to The Royal Society's Fair Copying Declaration. Details may be obtained upon application from The Royal Society, London, W.1.

ADVERTISEMENTS. Communications concerning advertisements should be addressed to the agents, Messrs. Walter Judd Ltd., 47 Gresham Street, London, E.C.2. (Telephone: Monarch 7644.)

SUBSCRIPTION RATES. A new volume commences each January. The charge is £4 per volume (\$11.50 U.S.A.), including index (post paid), payable in advance. Single parts, so far as available, may be purchased at 8s. each (\$1.15 U.S.A.), post paid, cash with order. Orders should be sent to The Institute of Physics, 47 Belgrave Square, London, S.W.1, or to any bookseller.



## Recent advances in nuclear physics\*

By SIR JOHN COCKCROFT, K.C.B., C.B.E., Ph.D., M.I.E.E., F.Inst.P., F.R.S., Atomic Energy Research Establishment, Harwell

The lecture on which this article is based was mainly concerned with recent advances in high energy nuclear physics. The synchro-cyclotrons built since the war are enabling studies to be made on the interaction of high-speed nucleons with nuclear matter and on the interaction of individual nucleons. This interaction is related to nuclear forces and in a way not yet understood. The interaction of nucleons produces  $\pi$ -mesons in large quantities and the interaction of these mesons and their decay product the  $\mu$ -meson with nuclei is now producing important new information. The production of  $\pi$ -mesons by the photonuclear effect has now been studied at energies up to about 350 MeV. The frontiers of nuclear physics now merge with cosmic ray physics. Cosmic ray workers have discovered heavier mesons,  $\tau$ ,  $\lambda$ ,  $\kappa$  and  $V$ , and some of these are produced by nucleons of energies of the order of 5 BeV. The Brookhaven proton synchrotron now produces protons of 2.3 BeV energy and a new strong focusing principle seems to make feasible machines for energies up to 100 BeV. Cosmic ray studies extend, however, out to energies of the order of  $10^{17}$  eV.

An account is given of some new phenomena discovered at Harwell which are believed to be due to such high energy events.

Whilst this work in the high energy field continues, experiments with lower energy nucleons are continuing to add to our knowledge of nuclear structure and the evidence for the shell model continues to accumulate.

The study of nuclear physics continues to be one of the most fascinating fields of science. Before the war we were concerned very largely with the transmutations of atomic nuclei by the rapidly increasing number of atomic projectiles which became available. Since the war nuclear physics has divided into two main branches.

The first branch of nuclear physics is concerned with the structure of the nucleus. It proceeds by study of the interaction of nucleons with nuclei, with the measurement of the excitation levels of neighbouring nuclei and the rules which determine changes from one state to another. By these and other methods it is becoming clear that the old model of a nucleus as a "drop" of nuclear fluid needs severe modifications when dealing with states of low excitation, and such modifications are being successfully sought in terms of a shell-model.

The second branch, which may be termed high energy nuclear physics, is concerned mainly with the nature of nuclear forces. It studies the interaction between high-speed nuclei having energies from 10 to at least 10000 million electron volts. Many different varieties of mesons are found to be produced in these interactions; these mesons are short-lived and often decay into lower mass mesons and finally into electrons and neutrinos. Their relation to the nuclear forces in close collision of nucleons and to the quantum field is one of the central problems of physics today. Beyond this region of high energy physics which is now accessible to particle accelerating machines we have the cosmological region of nuclear physics—the particles of energies up to  $10^{18}$  eV which come from outer space and generate enormous particle showers in the earth's atmosphere. We are interested to know where these particles come from and how their enormous energies are generated.

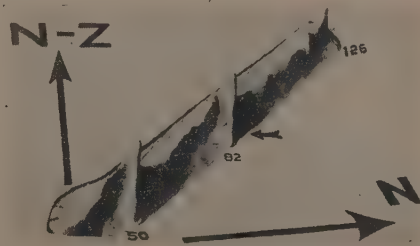
## THE STRUCTURE OF THE ATOMIC NUCLEUS

Our present ideas on the structure of the atomic nucleus derive from Chadwick's discovery of the neutron, since we could then think of nuclei as being built up in a regular way from the two fundamental bricks, protons and neutrons.

\* Based on a lecture delivered on 29 May, 1953, before The Institute of Physics Convention in Bournemouth.

The helium nucleus, or  $\alpha$ -particle, is made up of two protons and two neutrons; heavier stable nuclei up to oxygen are obtained by adding a neutron and then a proton and repeating the sequence—thus we form  ${}^3\text{He}$ ,  ${}^6\text{Li}$ ,  ${}^7\text{Li}$ ,  ${}^8\text{Be}$ ,  ${}^9\text{Be}$  and so on. From oxygen we add two neutrons and then two protons— ${}^{17}\text{O}$ ,  ${}^{18}\text{O}$ ,  ${}^{19}\text{F}$ ,  ${}^{20}\text{Ne}$  and so on, up to  ${}^{36}\text{Ar}$ .  ${}^5\text{He}$  and  ${}^8\text{Be}$  are exceptional in being unstable nuclei.

If we next look at the properties of members of the nuclear species we find evidence for the existence of closed shells of neutrons and protons at the so-called magic numbers of 2, 8, 20, 28, 50, 82 and 126. If the relative abundances of nuclei are plotted against  $Z$  or  $N$ , the protons and neutron numbers, peaks are found at  ${}^{16}\text{O}$  ( $Z = N = 8$ );  ${}^{118}\text{Sn}$  ( $Z = 50$ ),  ${}^{89}\text{Sr}$ ,  ${}^{89}\text{Y}$ ,  ${}^{90}\text{Zr}$  ( $N = 50$ ), and so on. The three-dimensional illustration (Fig. 1) shows this.<sup>(1)</sup>

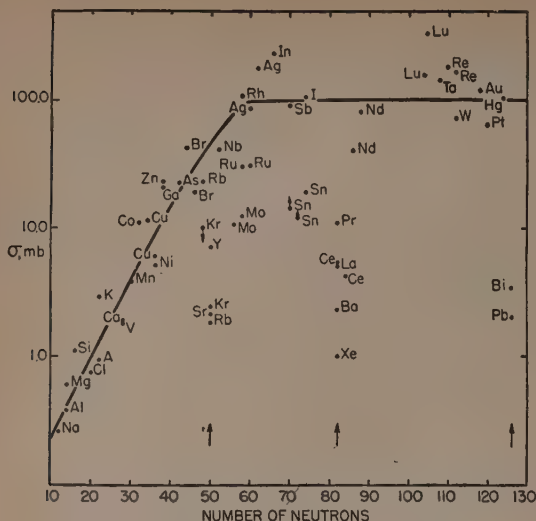


(Reproduced by courtesy of The Clarendon Press)

Fig. 1. A plot of the percentage abundance of isotopes in ( $N$ ,  $N-Z$ ) plane showing the distinct maxima at  $N = 50$  and  $N = 82$ , and the rise towards the maximum at  $N = 126$  [Gamow]

Then, the absorption of fast neutrons by nuclei is in general proportional to the geometrical area of the nucleus, but there are pronounced dips (10–30 times smaller than average) for  $N = 50, 82, 126$ . Fig. 2 shows that the density of energy levels producing the capture is lower near the magic numbers.<sup>(2)</sup>



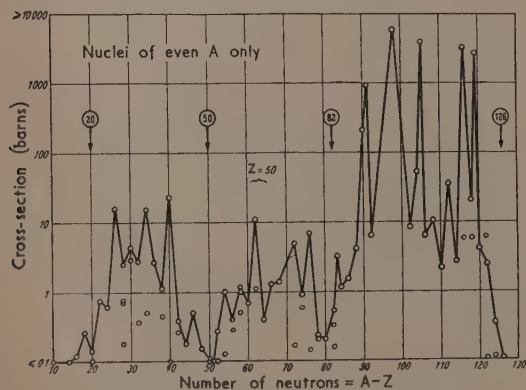


(Reproduced by courtesy of Addison-Wesley Press Inc.)

Fig. 2. Capture cross-sections at 1 MeV as a function of neutron number  $N$ . The isotopes containing magic numbers of neutrons 50, 82 or 126 show extremely low cross-sections [Hughes]

The absorption of thermal or low energy neutrons exhibits similar anomalies (Fig. 3). Several more examples of these discontinuities could be quoted.<sup>(3)</sup>

It has been known for a long time that nuclear volumes are approximately proportional to the atomic weight—the density of nuclear matter is constant. The binding energy per nucleon is also approximately constant, showing that forces between nucleons exhibit strong saturation properties.



(Reproduced by courtesy of Pergamon Press Ltd.)

Fig. 3. Thermal neutron cross-sections

The theory of nuclear structure begins by observing that the enormous electrostatic repulsive forces between protons would blow the nucleus apart unless this was counterbalanced by attractive forces between nucleons—attractive forces which must act between pairs of neutrons, pairs of protons, protons and neutrons. These forces must have a very short range—

of the order of  $2 \times 10^{-13}$  cm—smaller than the nuclear diameter. There must also be still shorter range repulsive forces between nucleons—otherwise the nucleus would collapse. As a result of the short range of nuclear forces the resultant force on a nucleon in the central part of the nucleus will be small but will be large at the outside—the individual nucleon can therefore be thought of to a first approximation as moving in a rectangular potential well of depth about 30 MeV and of width equal to the nuclear diameter (Fig. 4).

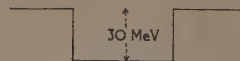


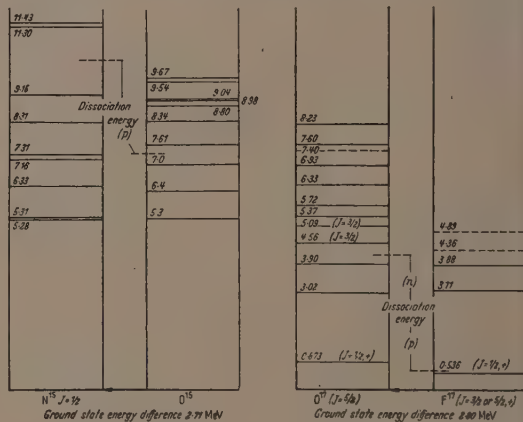
Fig. 4. Potential well in nucleus

The strong local short-range forces might perhaps have been expected to disturb this simple picture, but empirically it proves to be justified.

The theory then calculates the different levels of excitation in increasing order and how many nucleons can be added in the different quantum states,  $s$ ,  $p$ ,  $d$ , in a rather similar way to the study of build-up of electron shells, but making the assumption of strong forces of interaction between spin and orbital motion of the nucleons. It is then found that closed shells of nucleons are formed at the numbers 20, 28, 50, 82, 126. We have long been familiar with the stability of the  $\alpha$ -particle and of the oxygen 16 nucleus. The higher numbers have come to be called the magic numbers.

The next class of evidence on nuclear structure results from a study of energy levels or excited states of nuclei. This is provided by experiments on transmutation leading to transitions between nuclei.

Fig. 5(4) shows the energy levels of some so-called mirror nuclei,  $^{15}\text{N}$ ,  $^{15}\text{O}$ ;  $^{17}\text{O}$ ,  $^{17}\text{F}$ . The nuclei are similar except



(Reproduced by courtesy of Pergamon Press Ltd.)

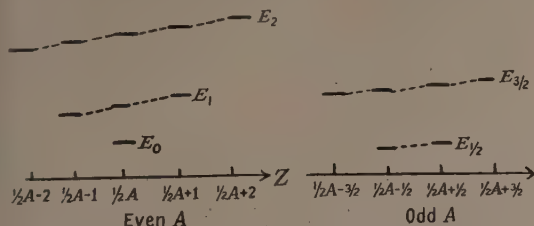
Fig. 5. Energy levels of mirror nuclei  $^{15}\text{N}$ ,  $^{15}\text{O}$ ,  $^{17}\text{O}$ ,  $^{17}\text{F}$

that a neutron is changed into a proton. It will be seen that the level structure is remarkably similar. This must mean that true nuclear forces between two protons and two neutrons are the same in corresponding states. This is the principle of charge independence. The small difference in the energy levels are due to the comparatively weak electric forces, the levels of nuclei with greater charge being somewhat higher. The similarity of levels of triplets of nuclei such as  $^{10}\text{Be}$ ,

$^{10}\text{B}$ ,  $^{10}\text{C}$ , show that neutron-proton forces are the same as  $p$ - $p$  and  $n$ - $n$  forces.

If we look at the energy levels of isobars of the light elements—elements with the same number of nucleons—we find the general pattern shown in Fig. 6.<sup>(5)</sup> Thus the levels of

proton entering nuclear matter can transfer almost the whole of its energy to a single nucleon. In doing so it transfers its charge to a neutron and continues its way as a neutron. This is an example of the charge exchange phenomenon. It also demonstrates directly the short-range character of nuclear



(Reproduced from Proceedings of the Physical Society)

Fig. 6. Energy levels of isobars of light elements [Peierls]

increasing excitation in nuclei of even atomic weight show a singlet, triplet, and quadruplet structure rather like the pattern of Zeeman splitting. A new term, isotopic spin,  $T$ , has therefore been invented to describe the splitting, just as the well-known total angular momentum quantum number  $J$  leads to  $2J + 1$  multiplets corresponding to  $J$ ,  $J - 1$ , etc. The importance of this is that transitions between levels have been found to depend on selection rules in  $T$ , which are just like the selection rules in  $J$ . This has made it possible to explain the occurrences and non-occurrences of transitions in a much more satisfactory way.

This picture of nuclear structure has therefore been built up from very general ideas of the nature of the nuclear forces acting between nucleons. In order to probe more deeply into the nature of the nuclear forces we have to study the interaction between nucleons at high energies.

#### THE INTERACTION OF HIGH-SPEED NUCLEONS

The interaction of high-speed nucleons is studied by using protons from the post-war generation of synchrocyclotrons which produce protons of energies up to 450 MeV. A typical experimental arrangement used at Harwell is shown in Fig. 7.

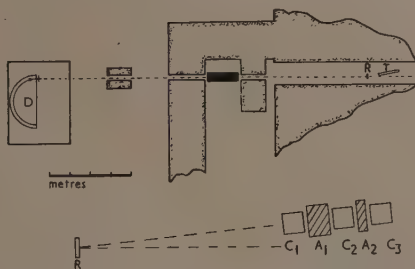


Fig. 7. Experimental arrangement in which protons from the cyclotron knock-out high-speed neutrons from a beryllium target

The protons from the cyclotron knock out high-speed neutrons from a beryllium target and these are then used for experimental purposes.<sup>(6)</sup> The neutrons projected in the forward direction have a very pronounced peak in their energy distribution which is only a little less than the energy of the impinging proton (Fig. 8).<sup>(7)</sup> This shows that a high-speed

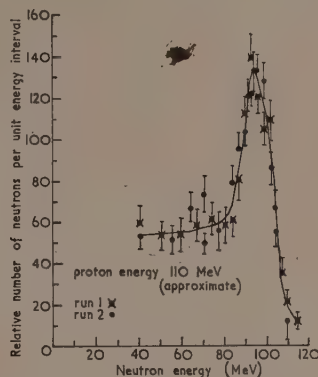


Fig. 8. Neutron energy distribution for beryllium

forces, otherwise the incoming nucleon would react with more nucleons.

If we now measure the total proportion of neutrons removed from the beam by nuclei of increasing complexity, interesting new features are revealed as is shown in Fig. 9,

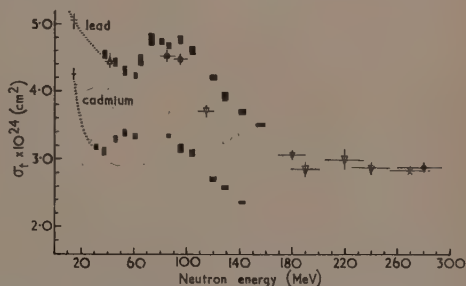


Fig. 9. Neutron total cross-section for lead and cadmium. Vertical extent of point indicates statistical accuracy. Horizontal extent indicates estimated error in energy

- + Amaldi (Camb. Conf.).
- △ Hildebrand and Leith (*P.R.*, 80, p. 842).
- Cook and others (*P.R.*, 75, p. 7).
- ▽ DeJuren and Moyer (*P.R.*, 81, p. 919).
- ◇ DeJuren and Knable (*P.R.*, 77, p. 606).
- × DeJuren (*P.R.*, 80, p. 27).
- Fox and others (*P.R.*, 80, p. 23).
- Harwell.

The interaction with lead nuclei shows that the total cross-section for 20–30 MeV neutrons is twice the geometrical cross-section of the nucleus— $2\pi R^2$ —where  $R$  is  $1.37 \times 10^{-13} A^{1/3}$ . Half of the cross-section is due to absorption and half to diffraction scattering in a manner analogous to Babinet's principle in optics. This result holds for the interaction of low energy neutrons with most nuclei. With increasing neutron energy, the cross-section drops—the nuclear matter becomes more transparent and its interaction can be characterized by a mean free path of the neutrons in

the nuclear matter. For still higher energies the interaction rises again to a maximum and then falls.<sup>(8)</sup> If we measure the position of this maximum in lighter nuclei we find it moves towards lower energies. Now, Lawson has suggested that the peak occurs when the neutron waves are retarded by  $\pi$  in phase traversing the nuclear matter. For then there will be a large amount of interference between the waves which pass through the nucleus and those which pass outside, and the cross-section will reach a maximum. The neutron waves are retarded because the neutron drops into the potential well of about 30 MeV depth in entering the nucleus and so the effective wavelength and refractive index of the neutron wave changes. On fairly plausible assumptions—that the phase retardation is proportionate to the nuclear diameter and inversely proportional to the half power of the neutron energy, the maximum is expected for 100 MeV neutrons in lead, 60 MeV neutrons in cadmium and 14 MeV neutrons in carbon. This agrees with experiment.

In addition to the high energy type of interaction a nucleon can transfer its energy to the nucleus as a whole and in this case low energy neutrons are evaporated. Fig. 10 shows the

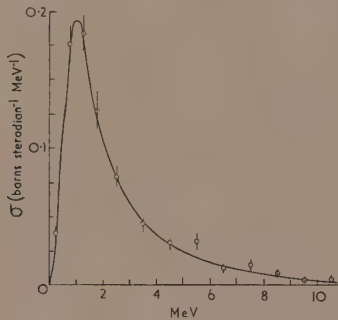


Fig. 10. Spectrum of low-energy neutrons evaporated from carbon

spectrum of these evaporation neutrons from carbon as measured by Mrs. Skyrme with the photographic plate technique.<sup>(9)</sup> If we now increase the energy of the impinging proton the energy carried off by evaporation neutrons increases at first proportionally with the energy put into the nucleus, but at higher energies the extra energy goes into ejection of high-speed particles. We find also that the number of evaporation neutrons increases rapidly with increasing complexity of the struck nucleus—from less than one in the case of carbon to about five in the case of tungsten and more in the case of uranium.

The next type of experiment studies the dynamics of nucleon-nuclear collisions, because of the light they may throw on nuclear forces. When proton-proton collisions are investigated for 146 MeV protons the scattering cross-sections in centre of gravity co-ordinates are shown in Fig. 11.<sup>(10)</sup>

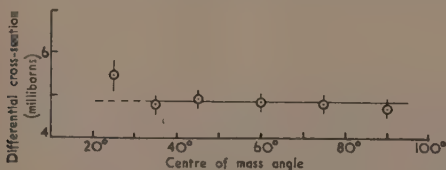


Fig. 11. Scattering cross-sections in centre of gravity co-ordinates for 146 MeV protons in proton-proton collisions

From this can be seen that the cross-section at high energies is independent of angle—as though we were dealing with elastic sphere collisions. But if we study the dynamics of neutron-proton collision we obtain quite different results as shown in Fig. 12. We now have a maximum at zero and

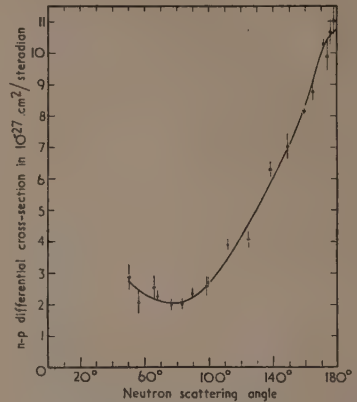


Fig. 12. Scattering cross-sections in neutron-proton collisions

another at 180°. In laboratory co-ordinates there are a maximum of neutrons in the forward direction—we might expect this since the transfer of momenta at these high energies is likely to be small. We should also expect the struck proton to be approximately at right angles. But, if the forces are of the exchange type, protons and neutrons will interchange identities and we should now expect to find neutrons at right angles and this corresponds to our 180° peak in centre of gravity co-ordinates. The results thus show that exchange forces are important. This is illustrated in Fig. 13.

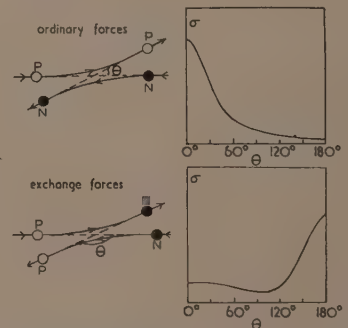


Fig. 13. Illustrating importance of exchange forces. 90 MeV.  $\sigma$  is neutron-proton cross-section

If we now call on the theoretical physicist to provide a quantitative explanation of the  $p$ - $p$  and  $p$ - $n$  scattering, matters become more difficult. He starts by writing down the equation of nuclear forces by analogy with the electrodynamic equation as

$$\nabla^2 u - \kappa^2 u = \frac{1}{c^2} \frac{\partial^2 u}{\partial t^2}$$

This equation is the only variant on the electrodynamic



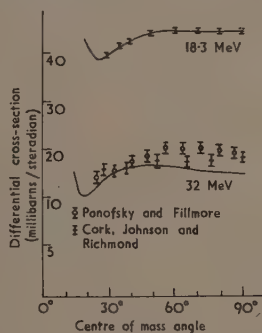
equations consistent with relativity and it leads to short range forces.<sup>(11)</sup> The static solution is

$$u = g \frac{e^{-\kappa r}}{r}$$

where  $1/\kappa$  determines the range of nuclear forces. If in addition we insert the quantum condition of the discreteness of energy units, a particle of meson mass appears, where  $m = \hbar\kappa/c$  is about 300 times the electron mass. In this way Yukawa predicted the existence of mesons related to the nuclear forces.

The constant  $g$ , on the other hand, is analogous to the charge strength in electrodynamics and defines the strength of the nuclear forces. Strong nuclear forces require a high value of  $g$ . Levy has recently produced theoretical reasons for believing that under these conditions we might expect the forces between nucleons to be repulsive at very close distances and outside this attractive.

By an arbitrary choice of the radius of the repulsive core and the magnitude of the coupling constant  $g$  a reasonable fit was obtained for proton-proton scattering at 18 and 32 MeV, as is shown in Fig. 14. We are not yet sure how the results fit at higher energies.



(Reproduced by courtesy of Interscience Publishers Inc.)

Fig. 14. Proton-proton scattering from Levy potential as calculated by Martin and Verlet

○ Panofsky and Fillmore; × Cork, Johnson and Richmond.

#### MESONS

Now if we study the interaction of nucleons at increasing energies we find that  $\pi$ -mesons are materialized in the intense field of the collisions, beginning at about 200 MeV proton energy. The mesons may be visualized as connected with intense fluctuations of the quantum field just as photons are connected with the electrodynamic field.

Fermi has given an interesting picture of the relation of mesons to nuclear forces.<sup>(12)</sup> When a proton approaches a neutron, the proton may be considered as surrounded by a virtual positive meson cloud. At close distance, the proton emits a  $\pi^+$  meson; this is reabsorbed by the neutron which now becomes a proton. This process results in a transfer of momenta and the nucleons change their direction. During the emission of the meson the system "borrows" an energy  $\delta E = mc^2$  to create the mass. Now by the uncertainty principle

$$\delta E \cdot \delta t = \hbar$$

so that

$$\delta t = \frac{\hbar}{\delta E} = \frac{\hbar}{mc^2}$$

During this time the proton cannot travel a greater distance than  $\hbar/mc = 1.4 \times 10^{-13}$  cm which is the range of the nuclear forces.

Now that a large supply of mesons is available, new types of experiments have become possible. A particularly interesting reaction is the production of  $\pi^+$  mesons when protons strike protons in a liquid hydrogen target. The reaction is



The angular distribution of the mesons in centre of gravity co-ordinates is  $0.2 + \cos^2 \theta$  (Fig. 15).<sup>(13)</sup>

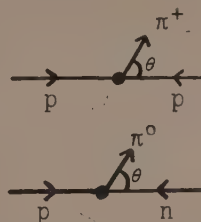


Fig. 15. (a) Illustrating the production of  $\pi^+$  mesons when proton-proton collisions take place in a liquid hydrogen target. (b) Illustrating the production of  $\pi^0$  mesons when neutron-proton collisions take place

A rather similar reaction between neutrons and protons produces uncharged  $\pi^0$  mesons by the reaction



and again we get a distribution of mesons  $0.2 + \cos^2 \theta$ .

The similar nature of these distributions is strong evidence that elementary nucleon-nucleon reactions are independent of charge—i.e. the nuclear forces between protons, and between proton and neutron are the same in corresponding states.

The next class of experiment is to study the interaction of  $\pi$ -mesons with nuclei. A high energy synchrocyclotron such as the 450 MeV Chicago machine can now produce a beam of about 1000  $\pi^+$  mesons per second of 135 MeV energy passing through a tube outside the cyclotron shield. This allows scattering experiments on 135 MeV  $\pi$ -mesons to be carried out just as easily—probably more easily—than Rutherford and Marsden did  $\alpha$ -particle scattering experiments to determine the nature of the external field of the nucleus.

One important experiment carried out at Columbia University was to study the reverse reactions to the production of mesons by proton-proton collisions. The  $\pi$ -mesons from the Columbia cyclotron were used to disintegrate deuterium, producing protons and the frequency of the reverse reaction to equation (1) was compared with the forward reaction. The principle of detailed balancing was now applied to interpret the results which showed unambiguously that the  $\pi$ -meson has spin zero. This is very important in our classification of the elementary particles. The  $\pi$ -meson of spin zero decays into the  $\mu$ -meson of spin  $\frac{1}{2}$  and neutrino of spin  $\frac{1}{2}$ .

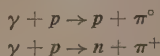
Recent experiments at Chicago have studied the angular distribution of  $\pi^+$  and  $\pi^-$  mesons scattered by protons.

The results show that the elastic scattering of the  $\pi^+$  mesons is very strong in the *backward* direction. The elastic scattering of the  $\pi^-$  mesons is on the contrary roughly isotropic. Another type of scattering takes place when  $\pi^-$  mesons are

turned into  $\pi^0$  mesons. These also have a maximum scattering in the backward direction.<sup>(14)</sup>

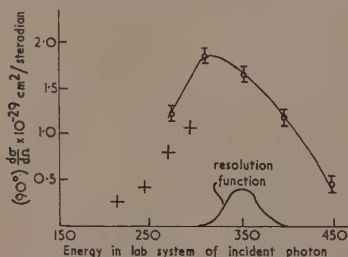
No very simple explanation of these phenomena is possible. If the meson waves are considered to be described by  $S$  and  $p$  wave functions and if suitable isotopic spins are assigned a plausible explanation is obtained.

Charged and uncharged  $\pi$ -mesons can also be created by high energy X-rays from electron synchrotrons by processes such as<sup>(15)</sup>



We can visualize the mesons being knocked out of the meson cloud surrounding the nucleus by the photons. The threshold energy is determined by the energy required to create a  $\pi$ -meson and is about 140 MeV. The cross-section then increases near the threshold as the cube of the  $\pi$ -meson momentum in the centre of mass system.

Experiments with the California Institute of Technology 500 MeV electron synchrotron have demonstrated that the production of  $\pi^0$  mesons at  $90^\circ$  goes through a relatively sharp maximum at 320 MeV and falls to 25% of the peak value at 450 MeV (Fig. 16).

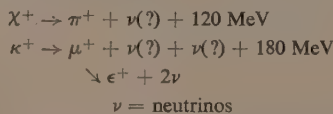


(Reproduced by courtesy of Interscience Publishers Inc.)

Fig. 16. Differential cross-sections at  $90^\circ$  for photo-production of  $\pi^0$  mesons in hydrogen

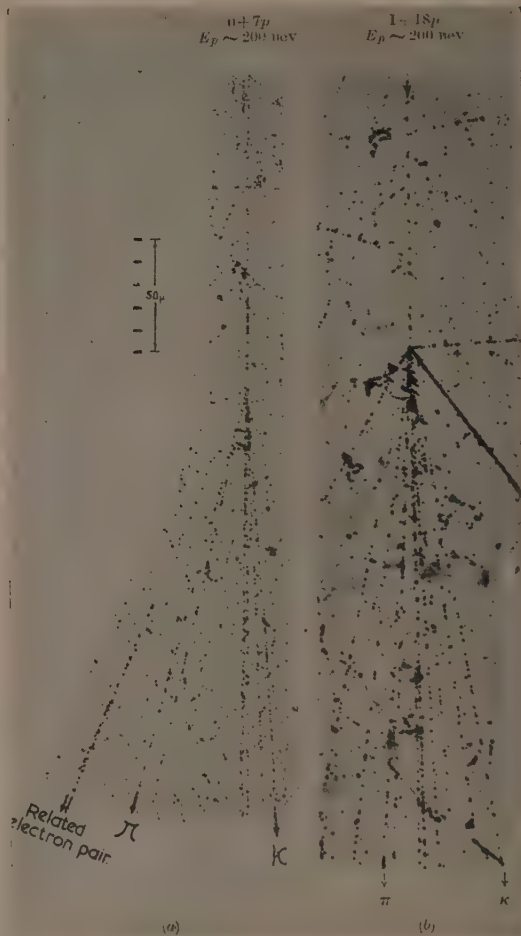
#### PRODUCTION OF HEAVY MESONS

As nucleon energies increase still further, heavier mesons are created in close collisions. Daniel and Perkins have shown that mesons of mass about  $1200 \pm 200 m_e$  are frequently emitted from nuclear disintegrations produced by very high energy protons (say 200 BeV energy) and less frequently by protons with energies as small as 5 BeV. Fig. 17 shows a photograph of one of these events. The heavy mesons are often emitted with high velocity and are identified by a mass determination based on the characteristics of the tracks in the photographic emulsion. The mesons created are either  $\chi$ - or  $\kappa$ -mesons which decay in the manner shown below (Menon and O'Ceallagain):



The energy released in these transformations seems to be divided between  $\pi$ -mesons and  $\chi$ - or  $\kappa$ -mesons in about equal parts, if the energy of the primary particle is of the order of 50 BeV.  $\tau$ -mesons which have been identified in the cosmic rays and which decay into three  $\pi$ -mesons have not yet been identified amongst the high energy disintegration products of nucleon collision.

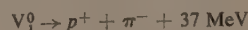
In the recent Royal Society colloquium<sup>(16)</sup> on mesons, Professor Powell suggested that it was reasonable to suppose that the  $\kappa$ - and perhaps the  $\chi$ -mesons might be identical with the charged heavy meson  $V_\pi^\pm$  discovered by Rochester and Butler at Manchester in 1947, which decays into a single charged particle. Over sixty examples of its appearance have so far been found.



(Reproduced from The Philosophical Magazine)

Fig. 17. Particle tracks [Daniel]

Still heavier mesons have been discovered by the cloud chamber technique of the Manchester workers, but in this case the particle is neutral and decays into a proton and  $\pi^-$ -meson according to the scheme



This particle may well be a proton in an excited state and a good deal of energy is being devoted to trying to produce it by accelerated particles. The table gives most known members of the meson family with their masses and half-lives.<sup>(17)</sup>

Name	Symbol	Charge	Mass	Spin	Statistics	Lifetime (seconds)	Decay scheme
Photon	$\gamma$	0	0	1	Bose-Einstein	Stable	
Graviton	G	0	0	2	Bose-Einstein	Stable	
Neutrino	$\nu$	0	0	$\frac{1}{2}$	Fermi-Dirac	Stable	
Electron	$e$	-	1	$\frac{1}{2}$	Fermi-Dirac	Stable	
Positron	$p$	+	1	$\frac{1}{2}$	Fermi-Dirac	Stable	
Positive $\mu$ -meson	$\mu^+$	+	210	$\frac{1}{2}$	Fermi-Dirac	$2.1 \times 10^{-6}$	$\mu^+ \rightarrow p + 2\nu$
Negative $\mu$ -meson	$\mu^-$	-	210	$\frac{1}{2}$	Fermi-Dirac	$2.1 \times 10^{-6}$	$\mu^- \rightarrow e + 2\nu$
Neutral $\pi$ -meson	$\pi^0$	0	265	0	Bose-Einstein	$10^{-15}$	$\pi^0 \rightarrow 2\gamma$
Positive $\pi$ -meson	$\pi^+$	+	276	0	Bose-Einstein	$2.6 \times 10^{-8}$	$\pi^+ \rightarrow \mu^+ + \nu$
Negative $\pi$ -meson	$\pi^-$	-	276	0	Bose-Einstein	$2.6 \times 10^{-8}$	$\pi^- \rightarrow \mu^- + \nu$
$\zeta$ -meson?	$\zeta$	$\pm$	550	?	?	$10^{-12}$	$\zeta \rightarrow \pi + ?$
Neutral V-particle	$V_2^0$	0	850	?	?	$10^{-10}$	$V_2^0 \rightarrow \pi^+ + \pi^- + ?$
$\tau$ -meson	$\tau$	$\pm$	975	?	Bose-Einstein	$10^{-8}$	$\tau \rightarrow 3\pi$
$\kappa$ -meson	$\kappa$	$\pm$	1100	?	?	?	$\kappa \rightarrow \mu + ?$
Positive X-meson	$X^+$	+	1400	?	?	$10^{-9}$	$X^+ \rightarrow \pi^+ + ?$
Negative X-meson	$X^-$	-	1400	?	?	$10^{-9}$	$X^- \rightarrow \pi^- + ?$
Proton	$P$	+	1836	$\frac{1}{2}$	Fermi-Dirac	Stable	
Neutron	$N$	0	1838.5	$\frac{1}{2}$	Fermi-Dirac	750	$N \rightarrow P + e + \nu$
Neutral V-particle	$V_0^0$	0	2190	?	Fermi-Dirac	$3 \times 10^{-10}$	$V_0^0 \rightarrow P + \pi^-$
Positive V-particle?	$V^+$	+	2200	?	?	$10^{-9}$	$V^+ \rightarrow P + ?$

(Reproduced from Scientific American)

## INTERACTION OF MESONS WITH NUCLEI

We have seen previously that the  $\pi$ -mesons which interact strongly with nuclei might be considered as quanta of the nuclear field with a Compton wavelength  $\hbar/mc = 1.4 \times 10^{-13}$ —the range of the nuclear forces. The experiments show that the  $X$ -,  $\kappa$ - and  $\tau$ -mesons interact strongly with nucleons. They might also therefore be considered as heavy quanta each associated with their own quantum field and each giving rise to short range components of the nuclear forces.<sup>(17)</sup>

The negative  $\mu$ -mesons, on the other hand, interact very weakly with atomic nuclei. It has been known for some time that they can be captured by atom  $c$  nuclei, but they first enter Bohr orbits of radii less by a factor 210 than the electron orbits. Transitions between orbits such as  $2P - 1S$  take the short time of the order of  $10^{-16}$  sec, but nuclear capture from a  $k$  orbit varies as  $Z^4$  and is about  $2 \mu\text{sec}$  for  $Z = 10$ . Since they are then very close to the nucleus this shows directly the weak nature of the interaction. In a light element the meson in a  $k$  orbit usually decays into an electron before it is captured.

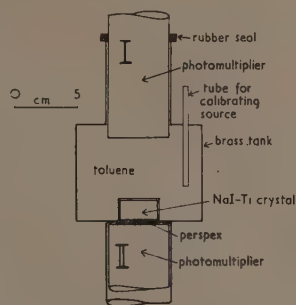


Fig. 18. Arrangement of scintillation counters in measurement of X-radiation emitted in the transition between two mesonic Bohr orbits round carbon nuclei

Recently Butement, at Harwell, has carried out an elegant experiment to measure the X-radiation emitted in the transition between two mesonic Bohr orbits round carbon nuclei.<sup>(18)</sup>

Fig. 18 shows the apparatus of the experiment. A cylinder is filled with toluene to which is added  $p$ -terphenyl so that it is on the one hand a liquid scintillator and on the other a medium for slowing down and capturing mesons in from the cosmic radiation. The liquid scintillator records about 140 pulses per minute, but very few of these are due to a meson which stops in the toluene. The pulse due to a stopping meson is distinguished by a delayed coincidence circuit which responds only if a pulse is followed, within an interval of 0.5 to  $6.0 \mu\text{sec}$ , by a second pulse due to the electron from the decay of the meson. The rate for these events was 7 per hour for the negative mesons.

Below the toluene is a second scintillation counter, with a sodium iodide-thallium crystal, which detects the mesonic X-rays from the toluene and displays the pulses on an oscilloscope. A second coincidence circuit ensures that only radiation due to orbital transitions is recorded.

The histogram for the spectrum of the meson capture radiation given in Fig. 19 shows a single peak with a maximum

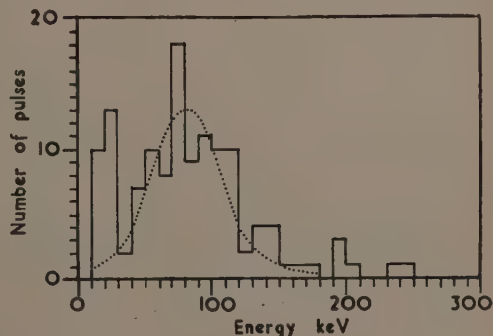
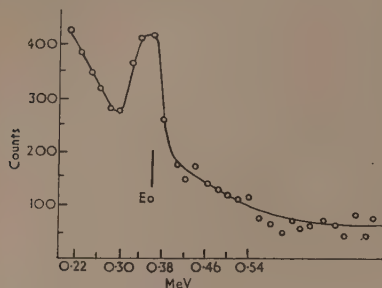


Fig. 19. Histogram for the spectrum of meson capture radiation



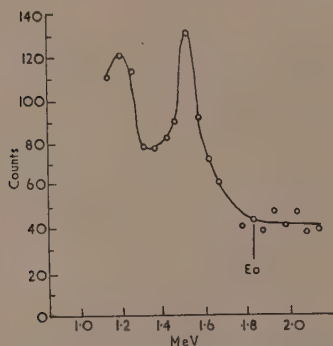
at 80 keV. The calculated energy for a transition between the  $2p$  and  $1s$  orbits of a  $\mu$ -meson in carbon is 77 keV.

The Columbia University group (L. J. Rainwater) have also reported mesonic X-rays from aluminium, copper, lead and other elements. The energy should vary as  $Z^2$ . Figs. 20 and 21 show the results.<sup>(13)</sup>



(Reproduced by courtesy of Interscience Publishers Inc.)

Fig. 20. Aluminium mesonic X-ray spectrum



(Reproduced by courtesy of Interscience Publishers Inc.)

Fig. 21. Copper mesonic X-ray spectrum

#### HIGH ENERGY PARTICLE ACCELERATION

Now that we know that mesons heavier than  $\pi$ -mesons can be produced by protons of less than 6 BeV energy, we are looking forward to their study by proton accelerators



Fig. 22. The Brookhaven proton-synchrotron capable of producing 2.3 BeV protons

working in the Bevatron range. Fig. 22 shows the Brookhaven proton-synchrotron which has produced 2.3 BeV protons. So far no experimental results have been reported.

Fig. 23 shows the still larger Berkeley machine which is being built to produce protons of at least 6 BeV. Emboldened by the success of the Brookhaven machine, the machine



Fig. 23. The Berkeley proton-synchrotron which is designed to produce protons having energies at least 6 BeV

builders are now considering the possibility of building a machine for 100 BeV ( $10^{11}$  eV) energy. They have been encouraged to do this by a new strong focusing principle which promises to reduce the amplitude of oscillation of the protons in their million-fold orbit. This may enable quite small vacuum tube sections to be used—of the order of  $5 \times 5$  cm. This will enable much smaller magnets to be used and for a given expenditure, the final particle energy may be increased by a factor of up to 10.

A machine of this type for a target particle energy of about 30 BeV is being considered for the European Nuclear Research Centre at Geneva. At present, computation of the particle orbits in the presence of perturbations due to magnet imperfections are being carried out by a Harwell group using the A.C.E. computer at the National Physical Laboratory. These perturbations may well increase the necessary section of the orbit tube and the size of the magnets required.

#### VERY HIGH ENERGY PARTICLES

Even if machines can be built to produce  $10^{11}$  eV particles there will still be a particle range of up to  $10^{18}$  eV which can only be studied by use of the cosmic rays. Fig. 24, obtained by the Bristol group, is reproduced here; it records an interaction of a  $10^{13}$  eV proton with another nucleus. It will be noted that the interaction produces a jet of high energy particles—which are largely mesons.

Evidence for the highest energy particles is obtained by studying the very large and extensive cosmic ray showers which result from an entry of such particles into the earth's atmosphere. At Harwell, Cranshaw has an array of 16 counters each of area  $200 \text{ cm}^2$  on a square lattice of 180 m side. A triple coincidence results from a shower of  $10^{16}$  eV energy. An 8-fold coincidence corresponds to  $10^{17}$  eV.

Jelley has recorded very short pulses of light from the night sky which are coincident with these very large showers and may be due to the Cerekov radiation of the particles. A 10 in. mirror focuses the light on to a photomultiplier and the pulse



Fig. 24. Disintegration produced by a proton of energy  $2 \times 10^{13}$  eV. More than 60 charged mesons are created, 38 of them in the central core of which the angular divergence is about  $0.5^\circ$ . There are, in addition, about 30 neutral mesons which lead to the production of "soft cascades" of electrons and photons. The main jet of mesons can be followed through the emulsion of 20 plates, and five disintegrations due to the secondary particles can be distinguished, one of energy greater than  $10^{12}$  eV

triggers off the time base of a cathode-ray oscillograph (Fig. 25). Discharges of the Geiger counter are shown as pulses on the oscillograph. Out of fifty light pulses recorded on one run, eighteen show single Geiger counter pulses, two show double events, one a triple event and one a quadruple event.<sup>(19)</sup>



Fig. 25. Apparatus used in recording very short pulses of light from the night sky which are coincident with very large showers of particles having the highest energies

These extremely energetic particles may be produced by e.m.f.'s generated by variations of very extensive cosmological magnetic fields.<sup>(20)</sup> Another point of interest is whether they come predominantly from particular points in space. All this is for the future to decide.

#### REFERENCES

- (1) GAMOW and CRITCHFIELD. *Theory of the atomic nucleus and large nuclear energy sources* (Oxford: Clarendon Press, 1949).
- (2) HUGHES. *Pile Neutron Research* (Cambridge, Mass.: Addison Wesley Publishing Co., 1953).
- (3) FLOWERS. *Progress in Nuclear Physics*, Vol 2, p. 235 (London: Pergamon Press Ltd., 1952).
- (4) BURCHAM. *Progress in Nuclear Physics*, Vol. 2, p. 218 (London: Pergamon Press Ltd., 1952).
- (5) PEIERLS. *Proc. Phys. Soc. [London]*, **66**, p. 313 (1953).
- (6) TAYLOR, PICKAVANCE, CASSELS and RANDLE. *Phil. Mag.*, **42**, p. 215 (1951).
- (7) BODANSKY. *Phys. Rev.*, **80**, p. 481 (1953).
- (8) TAYLOR and WOOD. *Phil. Mag.*, **44**, p. 95 (1953).
- (9) SKYRME. *Phil. Mag.*, **42**, p. 1187 (1951).
- (10) CASSELS, PICKAVANCE and STAFFORD. *Proc. Roy. Soc. A*, **214**, p. 262 (1952) *proton-proton collisions*. RANDLE, TAYLOR and WOOD. *Proc. Roy. Soc. A*, **213**, p. 392 (1952) *neutron-proton collisions*.
- (11) PEIERLS. *Proc. Phys. Soc. [London]*, **66**, p. 313 (1953).
- (12) FERMI. *Elementary Particles* (Oxford: Clarendon Press, 1951).
- (13, 14, 15) Proceedings of 3rd Conference on High Energy Nuclear Physics, University of Rochester (December 1952).
- (16) Royal Society Conference on V-particles and heavy mesons (January 1953).
- (17) DYSON. *Phys. Today* (April 1953).
- (18) BUTEMENT. *Phil. Mag.*, **44**, p. 206 (1953).
- (19) JELLEY. *Nature [London]*, **171**, p. 349 (1953).
- (20) FERMI. *Nuovo Cimento*, **6**, p. 317 (1949).

## Recent developments in electron diffraction

By T. B. RYMER, Ph.D., F.Inst.P., The University, Reading

An account is given of the electron-optical principles of simple and high-resolution electron diffraction cameras, and of the combined electron microscope and diffraction camera. Electron diffraction patterns can be used to identify materials, to determine the size, shape and orientation of crystals and to determine the orientation of large molecular groups in crystals. The patterns can also be used to study the stresses which occur naturally in many materials when the crystallites are very small. Some results of the dynamical theory of electron diffraction are stated and future applications are outlined.

### 1. GENERAL APPLICATIONS OF ELECTRON DIFFRACTION

The standard English book on electron diffraction is still that of Thomson and Cochrane<sup>(1)</sup> published in 1939. In

this article some of the developments of the subject since that time are reviewed. It is obviously impossible in a few pages to describe the contribution which electron diffraction has made to such subjects as (to name but a few) wear and

lubrication, the adhesion and texture of electroplating, and the corrosion and protection of metals. It must suffice to describe in general terms the kind of information which electron diffraction can provide so that a potential user can judge of its suitability for his purpose. This outline of the field of application of electron diffraction is followed by a consideration of the developments which have occurred in the theory and technique of the subject, together with indications of their future application.

The three commonest types of electron diffraction pattern are transmission, reflexion and Kikuchi patterns. Transmission patterns, consisting of spots or concentric rings, are formed by passing a fine beam of electrons of energy 40 to 100 keV through a specimen on to a photographic plate situated some 50 cm beyond. Fig. 1 shows a typical

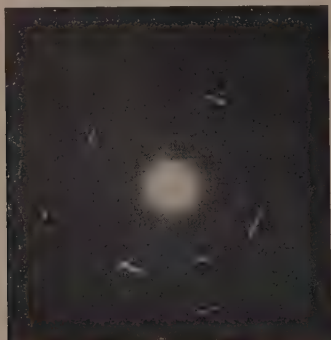


Fig. 1. Transmission pattern of nickel single crystal showing rotational slip. (L. E. Collins)

spot pattern. Reflexion patterns closely resemble transmission patterns except that a segment of less than  $180^\circ$  is visible. Such patterns are formed when a beam of electrons grazes the flat surface of a specimen on its way to the photographic plate; they are often a form of transmission pattern, with the electron beam passing through sub-microscopic projections of the specimen (Fig. 2). Kikuchi patterns are formed when a beam strikes at grazing incidence the flat



Fig. 2. Formation of a "reflexion" pattern by diffraction from sub-microscopic projections from the specimen surface. The specimen itself obscures all but a small segment of the diffraction ring, and the rougher its surface the less of the diffraction ring is visible

surface of a single crystal of a high degree of perfection. Such patterns arise from the diffraction of electrons which have been diffusely scattered in the crystal. They consist of a continuous distribution of intensity crossed by bright and dark lines and bands. The occurrence of Kikuchi patterns is often used as a sensitive test that the outer few atom layers of a crystal have the full degree of order of the bulk of the crystal. Damage and recovery of the crystal lattice by cold work and annealing can be followed by the disappearance and reappearance of Kikuchi patterns. Wilman<sup>(2)</sup> has developed geometrical methods for the determination of

crystal structure from Kikuchi patterns, though there is as yet no record of a new crystal structure having been determined in this way.

Transmission and reflexion patterns may conveniently be considered together. The following information can usually be derived from them. First, by measuring the radii of the diffraction rings, the spacing of atomic planes in the specimen, and hence its crystal structure, can be determined. Thin layers of material can be identified in this way. Thus, by taking reflexion patterns of the surfaces of metal bearings it has been shown that layers of oxide or sulphide are formed by the action of lubricant, and the efficiency of the bearing is closely related to the properties of these layers. By very precise measurement of diffraction rings in transmission patterns it is possible to detect the small change of lattice constant arising from stresses in the specimen (see Section 3). Such stresses occur spontaneously in many very small crystals and appear to be intimately related to crystal growth.

Secondly, if the crystals forming the specimen are not oriented at random, the pattern consists not of rings but of short arcs or spots. It is then possible to deduce the orientation of the crystals in the specimen. A particularly interesting example is Wilman's<sup>(3)</sup> work on rotational slip. It was at one time believed that when crystalline materials were stressed beyond the elastic limit they could only yield by certain atom layers of the crystal sliding over one another like the cards in a pack. Diffraction patterns such as Fig. 1 show that in some instances the atom layers can rotate over each other instead of sliding laterally. Fig. 1 may be regarded as the superposition of several spot patterns rotated through small angles with respect to each other. Wilman has shown that rotation through certain angles will result in a fairly good fit of the atoms of one plane on those of the adjacent one. A new mechanism of plastic deformation has therefore been revealed by electron diffraction.

Thirdly, the size and shape of crystals (provided they are smaller than a few hundred ångströms) can often be determined from the width of diffraction rings, this being roughly inversely proportional to the linear extent of the crystals perpendicular to the reflecting atom planes. In the case of spot patterns, the spots are elongated into lines perpendicular to crystal facets. An example of this use of electron diffraction is the work of Rees and Spink<sup>(4)</sup> on zinc oxide. This substance crystallizes in the hexagonal system, and electron micrographs of smoke particles show that the crystals occur as long needles with a diameter of a few hundred ångströms. It may be assumed that the needle axis is the 0001 crystal axis, but owing to low contrast it is not possible to tell whether the needle is of circular or hexagonal cross-section. If it were of circular cross-section, the thickness in directions  $1\bar{1}00$  and  $11\bar{2}0$  would be the same and the corresponding diffraction spots would be of equal extent. If the needles were bounded by hexagonal prism sides, the mean thickness in the direction  $1\bar{1}00$ , perpendicular to opposite sides of the prism, would be less than that in the direction  $11\bar{2}0$ , the diagonal of the prism. The diffraction spot  $1\bar{1}00$  would therefore be larger than the  $11\bar{2}0$  spot. Diffraction patterns show that this is the case and thus establish the hexagonal shape of the crystals.

Fourthly, suppose the specimen consists of a thin film in the form of a single crystal composed of large molecules arranged parallel to each other (this occurs with many organic compounds). The diffraction pattern then consists of a regular array of spots on which is superposed a number of large diffuse areas of intensity. The latter are due to diffraction by the individual molecules, and from their shape and



position the orientation of the molecules in the crystal can be deduced. This information is valuable in determining the crystal structure of complex substances. Fisher<sup>(5)</sup> has applied this technique to the study of the structure of stretched rubber.

The fundamental character of the electron beam is that it is able to penetrate only about 3000 Å into most materials; on the other hand, intense diffraction patterns can be obtained with short exposures from the thinnest solid specimens or even from gases. These properties of the beam determine both the limitations and the virtues of electron diffraction. The low penetrating power means that in the case of transmission specimens we are restricted to the examination of thin films or powders with a particle size less than  $10^{-5}$  cm. This limit will probably be raised a little with the development of higher voltage cameras. The limitation of the electron beam to thin layers of material has some consequences which are not immediately apparent. For example, the discovery of rotational slip, to which reference has already been made, was helped by the fact that the specimens were necessarily thin and therefore slip could have occurred on only a few planes. An X-ray examination on the other hand, would have required enormously thicker specimens which would have slipped on many planes and given a more diffuse pattern. In general, it is to be expected that the minute crystals effective in electron diffraction will have fewer faults and will be freer from contamination than the far larger crystals needed for X-ray examination. It is probably for this reason that it was possible to identify by electron diffraction three forms of gutta percha<sup>(6)</sup> although X-ray studies had identified only one with certainty. The examples given suggest that as a rule, when a material is available as a powder of particle size  $< 10^{-5}$  cm or as a film of the same thickness, electron diffraction is likely to produce as much or more information than X-ray diffraction.

In the case of reflexion specimens the pattern commonly arises from transmission through sub-microscopic projections, and therefore the determining factor is the roughness of the surface (Fig. 2).

## 2. THE ELECTRON DIFFRACTION CAMERA

Improvements in electron diffraction cameras during the last decade have been largely due to the increased knowledge of electron optics resulting from the development of the electron microscope. The simplest form of electron diffraction camera (Fig. 3a) now consists of an electron gun *G*, a

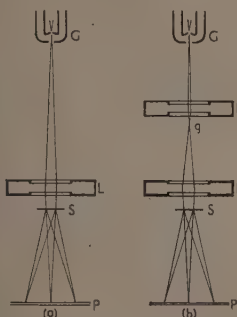


Fig. 3(a). Ray diagram of simple electron diffraction camera

Fig. 3(b). Ray diagram of high resolution electron diffraction camera

magnetic lens *L*, the specimen *S* and the photographic plate or viewing screen *P*. The gun and magnetic lens closely resemble those used in electron microscopes. The lens *L*

is very weak compared with those used in electron microscopes and therefore little difficulty is experienced in designing it so that the aberrations are completely negligible.

A good measure of the performance of a diffraction camera is the ratio of the radius of a certain diffraction ring to the diameter of the main electron beam where it is focused on the photographic plate. It can be shown that this ratio is a maximum when the lens is near to the specimen. Using a specimen-to-plate distance of 50 cm, which gives diffraction rings of convenient (1–6 cm) diameter with a h.t. voltage of 70 kV, there is no difficulty in obtaining a spot size of  $40 \mu$  or less. Since the breadth of almost all diffraction rings is at least  $100 \mu$ , and must therefore be determined largely by the structure of the specimen itself, it would appear that there is little to be gained by further diminishing the spot size. This is indeed true provided it is desired to measure only lattice spacings and orientation. If, however, it is required to investigate the shape of the sub-microscopic crystals in the specimen, refraction effects (see Section 4) or internal stresses, it is necessary to employ a smaller spot size. This can be done by the use of two lenses<sup>(7)</sup> as in Fig. 3(b). The first lens *L*<sub>1</sub>, which should be situated mid-way between the gun and the second lens *L*<sub>2</sub>, is a fairly short focus lens and produces a greatly diminished image of the source at *g*. This is the effective source for the remainder of the instrument, which acts like the simpler instrument of Fig. 3(a). A two-lens camera is capable of producing a spot size of less than  $20 \mu$ .

The close resemblance between an electron diffraction camera and an electron microscope has led to the construction of several instruments which can serve either purpose. The best of these are arranged so that by merely adjusting the current through a magnetic lens either a diffraction pattern or an electron microscope image can be obtained from a selected area of the specimen. Fig. 4(a) shows how this is

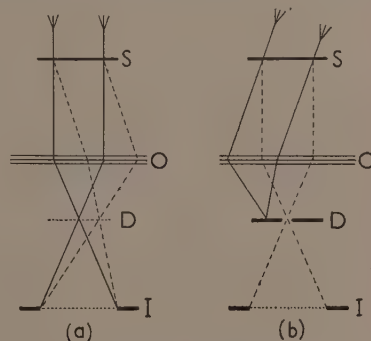


Fig. 4(a). Ray diagram of combined electron diffraction camera and microscope

Fig. 4(b). Ray diagram of electron microscope for study of preferred orientation

done.<sup>(8)</sup> *S* is the specimen and *O* an electron microscope objective lens of wide aperture. Using a gun and condenser lens, the specimen is illuminated by a nearly parallel beam. The full lines represent the path of electrons which pass through the specimen without being diffracted and the dashed lines represent a typical diffracted beam. The objective *O* focuses the main and diffracted rays from any point of the specimen in the intermediate image *I*, which, in the normal use of the electron microscope, is in turn imaged

by a projection lens system on to the photographic plate. A diaphragm is mounted at *I* in order to define the portion of the specimen which is imaged on to the plate. It will be seen that the objective lens forms not only an image of the specimen at *I*, but also a diffraction pattern at *D*. Obviously, it is possible by adjustment of the focal length of the projection lens system to image on to the photographic plate either *I*, the electron microscope picture, or *D*, the diffraction pattern. In the latter case, the diffraction pattern must be that of the part of the specimen whose image falls on the diaphragm at *I*, i.e. the same part which is imaged in the normal electron micrograph. Single crystal diffraction patterns of sub-microscopic crystals have been obtained in this way.

If a diaphragm is placed at the position of *D* so as to pass only one diffracted beam, then the electron microscope image can be formed only from those crystals which are oriented so as to diffract in the appropriate direction. These crystals show up as bright images on a dark background. This technique appears to offer considerable possibilities for the study of preferred orientation. The best arrangement is to place a *central* diaphragm at *D* and to tilt the upper part of the instrument, consisting of the gun and condenser, so that the main beam is intercepted and only the diffracted beam passes (Fig. 4*b*). Instead of tilting the upper part of the apparatus, the same effect can be obtained by the use of a magnet between the condenser and the specimen to bend the electron beam through the appropriate angle. This technique can be used with either reflexion or transmission specimens.

An important future line of development is the production of cameras operating at higher voltages than those hitherto employed. Such cameras<sup>(9)</sup> involve no new principles, but have the following advantages:

(i) The intensity of the diffusely-scattered radiation relative to that in the diffraction rings diminishes as the voltage is increased. Hence for a given amount of background it is possible to use thicker specimens. This is useful when examining powders.

(ii) A higher energy electron beam is less likely to charge up an insulating "reflexion" specimen. This means that reflexion specimens can be examined at appreciably smaller glancing angles. The increased obliquity more than compensates the increased penetration along the line of the beam, so that the actual penetration in depth is reduced. This makes the high-voltage camera suitable for examining monomolecular layers on surfaces.

(iii) Broadening of rings by refraction effects is reduced so that the high-voltage camera should be capable of higher resolution.

### 3. STRESSES; AND RELATIONSHIP OF LATTICE CONSTANT AND CRYSTAL SIZE

Electron-diffraction transmission patterns are obtained from specimens whose crystallites are commonly only a few hundred ångströms in extent and often much less; the usual crystallite size for X-ray diffraction specimens is at least a hundred times greater. Now a two-dimensional sheet of atoms has a different lattice constant from a similar atom plane in a crystal. It is therefore to be expected that the surface layer of a crystal will be stressed, and that lattice constants of the very small crystals effective in electron diffraction will differ from those of the larger crystals used for X-ray diffraction. Such differences between the X-ray and electron-diffraction measurements of lattice constants have been reported by many workers who in general have found that, as would be expected, the difference is greatest

for the smallest crystals. However, although there is no doubt of the reality of this phenomenon, much of the early work must be treated with reserve because the difficulties of exact measurement were not appreciated at the time. The chief of these is that wavelengths of electrons, unlike X-ray wavelengths, are not natural constants but depend on the voltage applied to the electron gun. Most workers have used a comparison method in which patterns of a standard substance (usually gold) and the specimen under examination are superposed on the same photographic plate. The general choice of gold as a standard has been particularly unfortunate because the lattice constant of this is now known to vary with the crystal size. Absolute measurements have recently been made by Rymer and Wright<sup>(10)</sup> who examined the diffraction patterns of specimens of evaporated aluminium, potassium and sodium chlorides and caesium iodide, and at the same time measured the electron gun voltage with a special potentiometer. Their results show that the lattice constants of these substances are within 0.01% of the X-ray lattice constants, at any rate provided the crystal size exceeds about 100 Å. On the other hand, the lattice constants of gold and lithium fluoride depend on crystal size.

The existence of homogeneous stresses in specimens due to the abnormal lattice constant of surface layers of atoms may be studied by a method which does not require a knowledge of the electron wavelength or the use of a standard substance.<sup>(11,12)</sup> Most crystals are elastically anisotropic and therefore a crystallite oriented to give, for example, a 111 reflexion will, for the same stress, be strained differently from one oriented to give some other reflexion. The *relative* radii of the diffraction rings will therefore be abnormal if stresses exist. Such abnormalities in the diffraction patterns of lithium fluoride have been studied by Rymer, Halliday and Wright in a paper now in preparation. They are found to be due to a two-dimensional compression in the specimen plane, together with a compression of about double this magnitude perpendicular to the specimen plane. The magnitude of the stress is independent of the specimen thickness and inversely proportional to the linear dimensions of the crystallites in the specimen plane. It is supposed that the crystallites are in the form of cylinders or prisms perpendicular to the plane of the specimen and that the stresses arise from forces analogous to surface-tension forces arising from the abnormal lattice constant of the surface layers of atoms.

An abnormal spacing of the surface layers has been suggested<sup>(13)</sup> to explain a completely different kind of electron-diffraction observation. Reference has been made to the fact that under suitable conditions a diffraction spot may be elongated into spikes which are perpendicular to important facets of the diffracting crystal. The theory of diffraction by a perfect crystal requires that these spikes always be symmetrical about the main diffraction spot. If, however, the lattice constant of the crystal varies progressively from the surface into the interior, it can be shown that these spikes will be more pronounced towards the centre of the diffraction pattern. Such asymmetrical spikes have been observed in the diffraction pattern of silver and agree in considerable detail with this interpretation. It seems very probable that many crystals are permanently in a state of stress due to the surface atoms having a different equilibrium spacing from those in the interior.

We have so far considered the effect on the diffraction pattern of a stress which is homogeneous throughout the specimen or, what is indistinguishable from this, surface forces acting on each crystallite, such forces being the same in magnitude and direction for all crystallites. It may happen,



however, that the crystallites react on each other, so that tensile stresses in some crystallites are balanced by compressive stresses in surrounding crystallites. This is the state of affairs familiar to workers in X-ray diffraction. Its effect is to produce a broadening of the diffraction rings, for different crystallites in the specimen now have slightly different lattice constants depending on whether they are subject to a compressive or tensile stress. Such broadened diffraction rings are superficially similar to those produced by small crystal size, but by a careful examination of their contours it is possible to distinguish between the two effects. In this way Halteman<sup>(14)</sup> has found internal stresses in specimens of nickel evaporated on to a silicon monoxide substrate. Such studies of the contours of diffraction rings obviously need a high resolution camera. The results tend to be obscured by broadening due to refraction or dynamical effects (see Section 4). Since the magnitude of such effects is inversely proportional to the electron energy, the study of internal stresses would be greatly helped by the development of a high voltage camera of high resolution.

It is obvious that the complete elucidation of stresses in specimens will need a combination of precise measurements of diffraction ring radii to give the homogeneous component of the stress and measurements of the contour of the diffraction rings to give the balanced internal stresses. By such means, electron diffraction should be able to make a useful contribution to our knowledge of crystal texture and growth.

#### 4. REFRACTION AND DYNAMICAL INTERFERENCE

The electrostatic potential inside a crystal differs from that of the surrounding space by a quantity  $\phi_0 (\approx 10 \text{ V})$  known as the "inner potential." The effect of this is that the crystal behaves towards electrons as if it had a refractive index  $n$  given by

$$n^2 = 1 + (1 + eV/2mc^2)\phi_0/V \quad (1)$$

where  $V$  is the potential applied to the electron gun. The approximate form of this equation

$$n = 1 + \phi_0/2V \quad (2)$$

suffices for most purposes.

Refraction causes a beam entering a crystal at an angle of incidence  $\alpha$  to be deflected towards the normal through an angle  $\delta\alpha = (\phi_0/2V)\tan\alpha$ . With the usual camera, the effect of refraction is to shift the position of the spot on the photographic plate by less than  $1/10 \text{ mm}$  unless  $\alpha$  is nearly  $90^\circ$ , i.e. unless the beam enters at almost grazing incidence. The earlier measurements of inner potential were therefore made on reflexion patterns obtained from very smooth surfaces of crystals so that the beam entered and left the crystal by the same surface at almost grazing incidence. The diffracted spot was then displaced several mm by refraction.

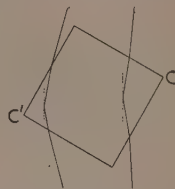
The recent development of the high-resolution camera has made possible the measurement of inner potential from transmission patterns of submicroscopic crystals such as occur in the smokes of magnesium oxide, zinc oxide and similar materials.<sup>(15)</sup> In the usual case where a crystal is bounded by parallel faces (Fig. 5), it is possible for the deviation produced from a set of atom planes to be either increased or decreased by refraction at the entrance and exit surfaces. The effect of refraction at any pair of faces is therefore to split each diffraction spot on the photographic plate into two components. These are displaced in a direction perpendicular to the refracting edge ( $C$  or  $C'$ ) of the crystal by amounts

$$\pm L(\phi_0/2V)(\tan\alpha - \tan\beta) \quad (3)$$

where  $L$  is the specimen-to-plate distance and  $\alpha, \beta$  are the angles between the incident and emergent rays and the inward normals to the corresponding crystal surfaces.

Closely related to the effect of refraction is that of "dynamical interference." The simple "kinematical" theory of diffraction by a crystal assumes that each atom scatters a spherical wavelet of amplitude small compared with that of

Fig. 5. Effect of refraction. The dotted lines represent reflexion planes in the crystal. The refracting edge  $C$  diminishes the total deviation; the edge  $C'$  increases it.



the primary wave. These scattered wavelets combine to give the diffracted wave. This is of appreciable intensity only when the glancing angles  $\theta$  between the incident and diffracted waves and the crystal planes satisfy the Bragg relation  $2d\sin\theta = \lambda$  connecting  $\theta$  with the interplanar spacing  $d$  and the wavelength  $\lambda$ . The kinematical theory assumes that the effect of the scattered wavelets in the direction of the primary wave is negligible compared with the primary wave itself. This is not strictly true. The effect of the scattered wavelets is in some respects analogous to the phenomenon of refraction in optics. It is well known that the reason why the wavelength of light is smaller in glass than in vacuum is that in the former we have not only the primary wave but also the wavelets scattered by each atom, and the superposition of these gives a wave of shorter length than the incident wave. Similarly, when an electron wave passes through a crystal not only the primary wave but also the scattered waves have to be considered, and these combine to give a wave of different length from the incident primary wave. The difference between the transmission of light through glass and the transmission of electron waves through a crystal is that in the latter case the scattering centres are regularly spaced at distances large compared with the wavelength, whereas in the former example the spacing of the scattering centres is so small compared with the wavelength that they may be considered as a continuous distribution. The consequence of this is that the refractive index of a crystal for electron waves depends on the direction in which the beam is travelling, whereas the refractive index of glass for light is independent of direction.

The result of applying the dynamical theory to the problem of refraction in a transmission specimen can now be stated.<sup>(16)</sup> The electrostatic potential in the crystal must vary with position with the periodicity of the crystal lattice, and we may therefore express it in the form of a Fourier series

$$\phi = \phi_0 + \sum \phi_{hkl} \cos 2\pi \left( \frac{lx + my + nz}{d_{hkl}} + \alpha_{hkl} \right) \quad (4)$$

where  $xyz$  are the co-ordinates of a point in the crystal referred to axes parallel to the crystallographic axes,  $lmn$  are the direction cosines of the normal to the atom planes of indices  $hkl$  and spacing  $d_{hkl}$ .  $\alpha_{hkl}$  is a phase factor. Then the diffracted spot  $hkl$  on the photographic plate is displaced in a direction perpendicular to the refracting edge of the crystal by amounts

$$\pm L \left\{ (\phi_0/2V)(\tan\alpha - \tan\beta) + \mu \sin\theta(\tan\alpha + \tan\beta) \right. \\ \left. \pm [\mu^2 \sin^2\theta + (\phi_{hkl}/2V)^2]^{1/2}(\tan\alpha - \tan\beta) \right\} \quad (5)$$



The first term is that due to ordinary refraction (equation 3).  $\theta$  is the Bragg angle and  $\mu$  is the angle by which the incident ray deviates from the direction satisfying the Bragg relation. Dynamical interference has the effect of double refraction, each of the two spots which could arise on a simple theory of refraction being split into two components. It can be shown that the intensity of each of these components is equal and proportional to

$$1/[1 + (2\mu V \sin \theta / \phi_{hkl})^2] \quad (6)$$

The crystal is consequently able to diffract with considerable intensity over a range of angles of incidence of the same order as the Bragg angle  $\theta$ . In a transmission pattern, the most intense spots will be from those crystals oriented so that  $\mu = 0$ , and these will give rise to groups of spots displaced by amounts

$$L(\tan \alpha - \tan \beta)(\pm \phi_0 \pm \phi_{hkl})/2V.$$

Such quartets of spots have been observed in the diffraction patterns of magnesium oxide smoke.

If the specimen is not a powder but a parallel-sided flake of a single crystal such as mica or graphite,  $\alpha - \beta = 180^\circ$  and no splitting of the spots by refraction can occur. Nevertheless double refraction still exists and within the crystal there are two waves in the direction of the primary beam and two in the direction of the diffracted beam. The members of each pair of waves have slightly different wavelength and therefore combine to form "beats." At certain places in the crystal the primary beam is strong and the diffracted beam is weak, while elsewhere the reverse is the case. The relative strength of the two beams on leaving the crystal therefore depends on its thickness, the intensity of the diffracted beam being proportional to

$$\sin^2 \left[ \pi \left( 4\mu^2 \sin^2 \theta + \frac{\phi_{hkl}^2}{V^2} \right)^{\frac{1}{2}} \frac{D}{\lambda \cos \alpha} \right] / \left[ 1 + \left( \frac{2\mu V \sin \theta}{\phi_{hkl}} \right)^2 \right] \quad (7)$$

where  $D$  is the thickness of the crystal.

The dependence of intensity on the angle  $\mu$  has been studied by convergent beam diffraction patterns. In its simplest form this technique consists in focusing the electrons on to the specimen (Fig. 6). After passing the specimen they proceed

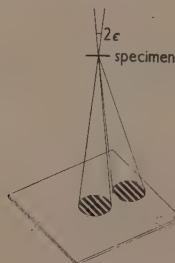


Fig. 6. Formation of convergent beam pattern

in straight lines to the photographic plate. The spots on the plate are thus enlarged to disks of radius  $L\epsilon$  where  $\epsilon$  is the semi-angle of convergence of the electron beam on to the specimen. The disks are crossed by parallel interference fringes corresponding to the values of  $\mu$  which make the expression (7) vanish. From the position of these, it is possible to determine both the thickness of the crystal and the potential  $\phi_{hkl}$ .<sup>(17)</sup>

The interference fringes referred to above are fringes of

equal inclination. If the crystal is illuminated by a parallel beam ( $\mu = \text{const.}$ ) we shall obtain fringes of constant thickness from a non-uniform crystal. To see these it is obviously necessary to image the crystal on to the photographic plate. Such fringes are to be observed in some electron microscope pictures of crystals<sup>(18)</sup> taken with an objective lens aperture so small that it cannot pass both the primary and the diffracted beams from the crystal.

The results of the dynamical theory which have been quoted are incomplete because they assume that a single crystal can produce only one diffracted beam. Since, as we have seen, the tolerance in the angle of incidence is of the order of the Bragg angle, there will usually be several diffracted beams of appreciable intensity. The theory for this case has not yet been stated in a compact form, but its development is being helped by a study of convergent beam patterns. The interference fringes show deviations from the positions predicted by expression (7) and these can be related to the existence of several diffracted beams.

The chief practical application which is likely to be made of either convergent beam patterns or the refraction effects observed in transmission patterns is the determination of the potential coefficients  $\phi_0$  and  $\phi_{hkl}$ . The latter are of particular importance since they are very closely related to the structure factors which determine the intensities of X-ray reflexions. The possibility is therefore opened up of determining these factors, and hence the structure of crystals, by measurement of the position of diffraction spots and fringes on a photographic plate instead of by the more difficult measurement of the intensity of X-rays.

#### REFERENCES

- (1) THOMSON, G. P., and COCHRANE, W. *Theory and Practice of Electron Diffraction* (London: Macmillan and Co. Ltd., 1939).
- (2) WILMAN, H. *Proc. Phys. Soc. [London]*, **60**, p. 341, (1948); **61**, p. 416 (1948).
- (3) WILMAN, H. *Proc. Phys. Soc. [London]*, **A**, **64**, p. 329 (1951).
- (4) REES, A. L. G., and SPINK, J. A. *Acta Cryst.*, **3**, p. 316 (1950).
- (5) FISHER, D. G. *Proc. Phys. Soc. [London]*, **60**, p. 99 (1948).
- (6) FISHER, D. G. *Proc. Phys. Soc. [London]*, **B**, **66**, p. 7 (1953).
- (7) COWLEY, J. M., and REES, A. L. G. *J. Sci. Instrum.*, **30**, p. 33 (1953).
- (8) CHALLICE, C. E. *Proc. Phys. Soc. [London]*, **B**, **63**, p. 59 (1950).
- (9) FINCH, G. I., LEWIS, H. C., and WEBB, D. P. D. *Proc. Phys. Soc. [London]* (in press).
- (10) RYMER, T. B., and WRIGHT, K. H. R. *Proc. Roy. Soc., A*, **215**, p. 550 (1952).
- (11) RYMER, T. B., and BUTLER, C. C. *Proc. Phys. Soc. [London]*, **59**, p. 541 (1947).
- (12) WILLIAMS, E. C. *Research*, **5**, p. 392 (1952).
- (13) PASHLEY, D. W. *Proc. Phys. Soc. [London]*, **A**, **64**, p. 1113 (1951).
- (14) HALTEMAN, E. K. *J. Appl. Phys.*, **23**, p. 150 (1952).
- (15) COWLEY, J. M., and REES, A. L. G. *Proc. Phys. Soc. [London]*, **59**, p. 287 (1947).
- (16) KATO, N. *Proc. Japan Acad.*, **25**, p. 41 (1949).
- (17) HOERNI, J. *Helv. Phys. Acta*, **23**, p. 587 (1950).
- (18) HEIDENREICH, R. D., and STURKEY, L. *J. Appl. Phys.*, **16**, p. 97 (1945).

## Some relative fluorescence efficiencies in the Schumann region

By V. W. MASLEN, B.Sc., Grad.Inst.P., N. E. WHITE, B.Sc., and S. E. WILLIAMS, M.Sc., Ph.D., A.Inst.P.,  
Physics Department, University of Western Australia

[Paper first received 12 March, and in final form 18 May, 1953]

A vacuum grating monochromator, with photomultiplier detector, and slits about  $1.5 \text{ \AA}$  wide has been used to measure the fluorescence quantum efficiency of three (ZnCd)S phosphors, calcium and magnesium tungstates,  $\text{ZnSiO}_4$ , Mn, Apiezon A and B oils and Apiezon L grease, relative to sodium salicylate in the 1000–2000  $\text{\AA}$  region. The efficiency varies from 10 to 50% of that of sodium salicylate, decreasing toward shorter wavelengths. Evidence for the rapid variation of efficiency in bands of the order of  $5 \text{ \AA}$  wide was found for Apiezon grease in the 1300–1600  $\text{\AA}$  region.

The successful use of fluorescence sensitized photomultipliers to measure radiation intensities in the region below 2000  $\text{\AA}$ , makes necessary the determination of the most efficient fluorescing medium at any particular wavelength and the variation of fluorescence quantum efficiencies with wavelength. Constant quantum efficiency, which makes heterochromatic photometry comparatively simple, is desirable. Examination of the characteristics of the fluorescence efficiency curves of similar substances also reveals common features which can be traced to a particular ion or related to the absorption spectra.

Some measurements of this kind have been made by Johnson, Watanabe, and Tousey,<sup>(1)</sup> and by Inn and Watanabe,<sup>(2)</sup> the efficiency being estimated by comparison with an energy distribution curve for the hydrogen arc obtained with a thermocouple. Their results for sodium salicylate in particular indicate a nearly constant efficiency in this wavelength range, and a response several times higher than other substances examined. Some preliminary observations by Bolton and Williams<sup>(3)</sup> showed the need for careful control of the deposition of the fluorescing layer, and for the provision of means for changing the layer covering the photomultiplier cathode without breaking the vacuum or otherwise disturbing the conditions of test.

The experiments described here involved comparing in one test the relative response of four different materials, one of which was usually sodium salicylate. A constant relative efficiency shown by two or more different materials, especially complex organic materials such as vacuum grease or oils, should indicate a constant, or slowly changing, individual efficiency of the substances concerned. A common feature, such as a more or less sudden change in relative efficiency, of a number of different substances, each being compared with a given substance, indicates a characteristic change in the efficiency of the given substance.

## EXPERIMENTAL

The apparatus has already been described.<sup>(3)</sup> The chief modification was the insertion, between exit slit and photomultiplier cathode, about 3 mm in front of the cathode, of a disk carrying four glass windows (Fig. 1). A similar device was used by Johnson.<sup>(4)</sup> The orientation of the disk and the selection of the window to be placed in front of the cathode could be controlled by an external dial. The positioning of each window was controlled by a spring-loaded ball falling into one of four holes. This precaution ensured that the same part of a window was exposed to light each time and avoided inconsistencies arising from uneven coating of the fluorescing substance.

VOL. 4, OCTOBER 1953

A considerable part of the fluorescent light produced in this arrangement was not collected by the photomultiplier cathode, resulting in a much reduced sensitivity of the apparatus compared with that obtained when the cathode surface itself was coated. For example, the response (anode

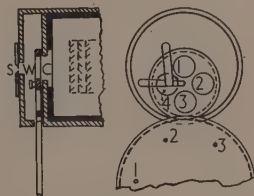


Fig. 1. Detail of photomultiplier window

S, slit; W, window; C, cathode.

current of photomultiplier) to  $\lambda 1215 \text{ \AA}$  was  $2 \mu\text{A}$ , compared with  $20 \mu\text{A}$ , for an equal slit width, when the cathode itself is coated.

Intensities received at the photomultiplier were measured with a reflecting galvanometer of period 5 sec and sensitivity 220 mm per  $\mu\text{A}$ . Since the available intensity from the source, a d.c. hydrogen arc run at current density 5 A per  $\text{cm}^2$ , is low below 1050  $\text{\AA}$  and between 1300  $\text{\AA}$  and 1500  $\text{\AA}$ , resolution was sacrificed in favour of increased intensity by widening both spectrograph and photomultiplier slits. The spectrum below 1600  $\text{\AA}$  is a line spectrum, so that little is to be gained by making the photomultiplier slit wider than the spectrograph slit even though their widths may produce some overlapping of lines. As the slits are widened scattered light is increased, but this can be measured and a correction made—only the error in measuring it being important. The errors resulting from instability in the measuring apparatus, fluctuations in the photomultiplier dark current, and accuracy in reading the galvanometer spot must be kept small compared with the photomultiplier response current.

Scattered light can be estimated in two ways. First, since the hydrogen line spectrum ends at about 850  $\text{\AA}$ , any response below this wavelength will be due to scattered light. Since this should be mainly general scatter from dust on the grating and reflexion from the mount, its contribution should not change greatly in absolute amount as the grating rotates the  $2^\circ$  covering the spectrum range. Second, if the slits are sufficiently narrow, there will be places where the gaps between lines can be examined for minima in illumination. Observations by the second method agree with the first

within the limits of error. The deflexion due to scattered light was found to be proportional to the exit slit width. Its amount varied with the transparency of the coating, being greatest for oil or grease and least for crystalline powders, with the exception of sodium salicylate, which was higher because of its greater fluorescence efficiency. The effect of scatter was reduced by a factor of five by inserting an additional mask about 25 cm in front of the photomultiplier slit, which allowed the slit to "see" only the ruled area of the grating. This was an indication that the scatter from grating mount, spectrograph tube and masks, which it eliminated, is considerably more than anticipated. Table 1 shows observations at 800 Å for three different materials.

Table 1. *Scattered light deflexion at 800 Å*  
1 cm =  $5 \times 10^{-8}$  A anode current

Width of photomultiplier slit (0.001 in. per div.) (0.0254 mm per div.)	1 div.	5 div.	10 div.
L Grease (double layer)	0.07 cm	0.38 cm	0.75 cm
L Grease (single layer)	0.095 cm	0.43 cm	0.91 cm
Sodium salicylate	0.11 cm	0.52 cm	1.03 cm
ZnSiO <sub>4</sub> : Mn	0.06 cm	0.29 cm	0.52 cm

An additional source of inaccuracy is the variation in intensity of the arc source during the taking of a set of observations at a given wavelength. Maximum steadiness of the arc current can be obtained by keeping the interior of the discharge scrupulously clean and avoiding the exposure of wax or other volatile material. The variation, with a 5 sec period galvanometer, then appears to be less than 1%. Manual control of the current by means of a Variac in the supply to the rectifier high tension is sufficient to overcome slow variations.

The conditions finally adopted were:

Spectrograph slit width:	0.096 mm or 1.65 Å equivalent
Exit (photomultiplier) slit width:	0.075 mm or 1.3 Å equivalent
Photomultiplier dark current variation peak to peak:	0.5 mm or $2.5 \times 10^{-9}$ A at 160 V/stage
Error in estimating scattered light: depending on the fluorescing medium involved:	0.2 to 0.4 mm
Galvanometer reading error plus instability:	0.5 mm

A series of observations was made, usually at wavelength intervals of 10 to 30 Å, depending on the location of convenient intensity maxima in the hydrogen spectrum. Wavelengths were read directly from a Veeder counter, checked at 1215 Å and sometimes at 1606 Å; they are accurate to 2 or 3 Å. At a given wavelength the order of observations was: deflexion for no light, for fluorescence from windows one, two, three, four, no light, windows four, three, two, one, no light. Agreement within 0.1 cm between the two deflexions for each window could usually be obtained. The variation in the zero (no-light) deflexion, which is determined by the leakage plus the photomultiplier dark current, was less than the inaccuracy in reading. After the scattered light contribution has been deducted from the response for each substance, ratios indicating the relative fluorescing efficiencies can be obtained.

It is possible, given the errors listed above and the observed consistency of successive deflexions for a given window, to estimate a probable error which depends on the magnitude of the deflexions. This then can be expressed as a probable error in a given ratio. Examples for different deflexions and ratios are given in Table 2.

Table 2. *Net deflexion in mm at 1 m (1 mm =  $5 \times 10^{-9}$  A anode current) after correction for scattered light*

Numerator:	1	2	5	5	10	10	20
Denominator:	2	4	5	10	10	20	40
Probable % error in ratio:	50	30	20	12	10	7	4

The net deflexion =  $(x \pm \Delta x) - (y \pm \Delta y) - (s \pm \Delta s) = (x - y - s) \pm \Delta$ , where  $x$  = indicated current;  $y$  = galvanometer zero;  $s$  = deflexion due to scattered light;  $\Delta y$  and  $\Delta s$  are the estimated errors quoted above;  $\Delta x$  is the estimated error in the mean of two readings of  $x$ , namely, for  $x$  less than 10 mm,  $\Delta x = 0.2$  mm, and for  $x$  greater than 10 mm,  $\Delta x = 0.4$  mm;  $\Delta^2 = \Delta x^2 + \Delta y^2 + \Delta s^2$ .

The corresponding approximate limits have been indicated by the broken lines for the curves shown in Fig. 2.

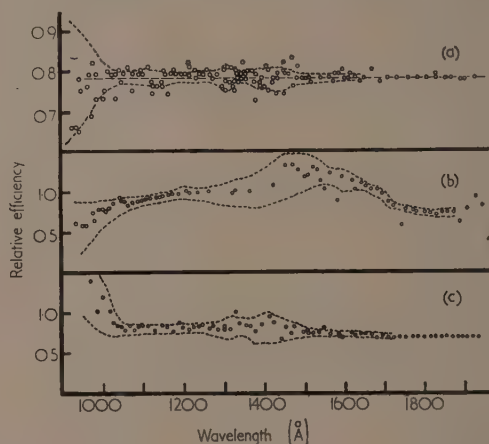


Fig. 2. (a) Apiezon L grease. Double layer versus single layer. (b) Apiezon A oil versus Apiezon B oil. (c) (ZnCd)S: Cu-PLO5 versus (ZnCd)S: Cu+Ag-163E

Apiezon grease films were deposited by dissolving the grease in petrol ether and allowing one or more drops to spread and evaporate. Sodium salicylate was dissolved in methyl alcohol and a drop allowed to spread on a previously warmed window. A more even crystalline layer could be obtained in this way than by applying a warm air blast to a drop on a cold window. Powdered crystalline materials were distributed on to a film of grease by sieving through a fine brass gauze as evenly as possible and removing the excess with a dental blower. Acceptably uniform films could be deposited in this way. The crystals appeared to cover the grease completely so that its fluorescing properties did not affect the results. After some days the loss of whiteness of the crystal layers appeared to indicate that the grease was migrating over the crystals. No success was achieved in depositing on to cellulose cement or from water solutions, the films being too uneven.



## OBSERVATIONS

Fig. 2 shows intercomparison of three pairs of similar substances. The broken lines indicate the probable errors estimated according to Table 2, and can be applied approximately to the curves in the remaining figures. In the case of the Apiezon grease, a layer formed from the evaporation of one drop of solution was compared with a layer formed from two drops. The efficiency of the double layer is 78% of that of the single layer. Comparison of the transmission of the two films with a photoelectric photometer showed 80%. Evidently, the single layer absorbs and converts all incident radiation, but the double layer transmits less to the photo-multiplier cathode. The Apiezon oils, which fluoresce very differently when exposed to a mercury ultra-violet lamp, the B oil being brighter, do not have the same characteristics in the range covered here. Differences in composition must be responsible for the variations in the conversion efficiency. In the third case, the visible glow of the two (ZnCd)S phosphors is different, namely, orange for PLO5 and green for 163E, but the process of absorption is apparently not dissimilar, for the relative efficiency is almost constant for radiation quanta from 6 to 12 V energy. This indicates that absorption by the host crystal governs the change in efficiency with wavelength.

In Fig. 3 are shown comparisons of three (ZnCd)S long afterglow phosphors with sodium salicylate. Again the

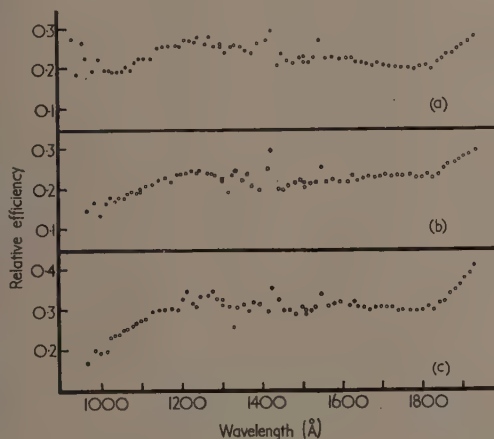


Fig. 3. (a) (ZnCd)S : Cu — PL05 versus sodium salicylate. (b) (ZnCd)S : Cu — P111 versus sodium salicylate. (c) (ZnCd)S : Cu + Ag — 163E versus sodium salicylate

similar behaviour of the three phosphors is marked, a change of slope at 1830 Å occurring in each case. Assuming that increased absorption causes reduced efficiency of conversion, this wavelength should then correspond to the long wave limit of the continuous absorption band.

In Fig. 4, three short persistence phosphors are compared with sodium salicylate. The  $\text{ZnSiO}_4$ : Mn shows changes of slope at 1610 Å and 1835 Å. The tungstates each show a change of slope at 1630 Å, beyond which their efficiency rises rapidly. If these changes of slope are associated with the absorption bands of the host crystals, the  $\text{ZnSiO}_4$ : Mn absorption band appears to have a plateau from 1830 to 1620 Å, and then to reach a further maximum at about 1480 Å.

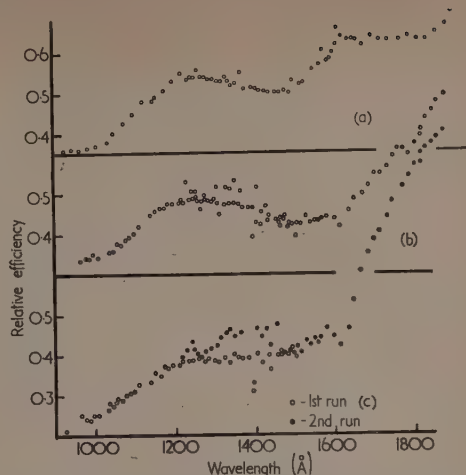


Fig. 4. (a)  $\text{ZnSiO}_4$ : Mn versus sodium salicylate. (b) Magnesium  $\alpha$ -tungstate versus sodium salicylate. (c) Calcium tungstate versus sodium salicylate

Fig. 5 shows the comparison of Apiezon A and B oils with sodium salicylate. Neither curve shows any prominent features. As the high reading which occurs for both oils at 1550 Å, did not appear to occur for the (ZnCd)S—163E phosphor, which was coated on the fourth window in this set of comparisons, it appears possible that it may be a characteristic of the organic materials. It is evident that the B oil drains too easily from the window, reducing the response

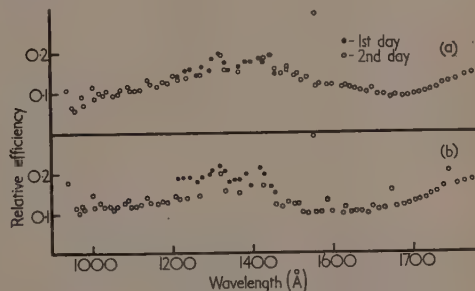


Fig. 5. Apiezon oils versus sodium salicylate  
(a) A oil; (b) B oil.

considerably within twenty-four hours and making the coating useless in a few days. The A oil is less troublesome in this respect.

Fig. 6 shows the comparison of Apiezon L grease with sodium salicylate. The upper curve shows the general trend, with a change of slope at  $1865 \pm 5$  Å. This wavelength seems definitely distinct from that occurring in the case of the crystals containing zinc. If it were not, the change in conversion efficiency to the red side of this wavelength would be attributable to a sudden decrease in the sodium salicylate, rather than a rise in the others. The lower curve shows part of the range on a larger scale. Considerable difficulty was experienced in reconciling the scatter of efficiency values in the 1300–1500 Å region with the estimated accuracy. It was not until observations had been taken on

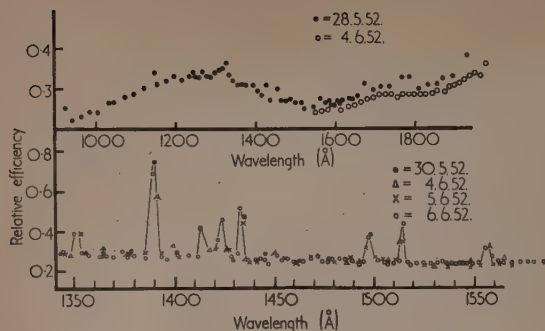


Fig. 6. Apiezon L grease versus sodium salicylate

three separate occasions, each of which included, at nearly identical wavelengths, similar values differing considerably from the mean, that the large apparent variation was believed to be real. A range of 300 Å was then surveyed at intervals of 3 Å, in order to confirm the existence of what appear to be very narrow bands of greatly increased conversion efficiency in the Apiezon grease. The combined results of four runs are plotted on the one graph, the estimated wavelengths of the readings for each of the first three sets having been adjusted by constant amounts of 1 Å to 3 Å to obtain the best fit with the fourth. This adjustment is within the error of reading the wavelength on a long traverse. As the peaks at 1390 Å, 1434 Å, 1498 Å and 1514 Å have been observed in each of three separate runs they are assumed to be real. Their width, about 5 Å, is much less than that usually shown for the absorption bands of organic substances in this region. The wide slits, 17 Å, used in other investigations,<sup>(1,2)</sup> would

make these narrow bands unobservable even if they were present in the organic materials which were tested.

## CONCLUSIONS

Sodium salicylate, apart from its constant efficiency, is better by a factor of three or more, compared with the materials tested in this work. In the case of the crystalline phosphors, the absorption bands of the host crystal affect the fluorescence efficiency markedly. The effect of varying film thickness is demonstrated in the comparison of the two grease films, and the loss of efficiency of the B oil as it drained off the window. The need for caution in using organic materials is shown by the observations on grease. Although these narrow bands of greatly increased efficiency make the grease unsuitable as a fluorescing agent in this region, a careful examination of their structure and distribution over the spectral region should yield information about the absorption spectrum.

## ACKNOWLEDGEMENTS

We are indebted to the Neon Electric Co., Perth, for the  $\text{ZnSiO}_4$ : Mn and tungstates and to Dr. A. L. G. Rees of the Commonwealth Scientific and Industrial Research Organization, Division of Industrial Chemistry for the (ZnCd)S phosphors. Two of us (V. W. M. and N. E. W.) received assistance from the Hackett Scholarship fund.

## REFERENCES

- (1) JOHNSON, WATANABE and TOUSEY. *J. Opt. Soc. Amer.*, **41**, p. 702 (1951).
- (2) INN and WATANABE. *J. Opt. Soc. Amer.*, **42**, p. 869 (1952).
- (3) BOLTON and WILLIAMS. *Brit. J. Appl. Phys.*, **4**, p. 6 (1953).
- (4) JOHNSON. *J. Opt. Soc. Amer.*, **42**, p. 278 (1952).

## Fundamental relations in photoplasticity\*

By S. E. A. BAYOUMI, Ph.D.,† and E. K. FRANKL, M.A., Engineering Laboratory, University of Cambridge

[Paper received 24 April, 1953]

Photoelastic methods of stress analysis have so far been limited to the study of problems of elasticity. The usefulness of such methods has been extended to cover inelastic behaviour by showing that the relative retardation due to loading is determined by the stress and strain components independently of the history of loading. A relation expressing relative retardation as a linear function of stress and strain differences has been derived. This fundamental relation has been verified experimentally for a wide variety of model materials.

A fundamental procedure for photoplastic investigations is proposed. This consists of taking two fringe photographs of the same model, one under load, the second immediately after removal of the load. The difference between the fringe counts at corresponding points gives the stress difference which in elastic problems is derived from a single photograph.

A birefringent body must be optically anisotropic; this means that the velocity of propagation of light through the body is not the same for all planes. The state of optical anisotropy at any point is usually assumed to be homogeneous and hence may be completely defined by  $n_1, n_2, n_3$  ( $n_1 > n_2 > n_3$ ) together with their directions, where  $n_1, n_2, n_3$  are the principal semi-axes of Fresnel's ellipsoid. For a beam of light travelling through such a body the light vector, at any point, has mutually perpendicular components which are

parallel to the axes of the section of Fresnel's ellipsoid cut by a plane parallel to the wave front; the wave velocities are the reciprocals of the semi-axes of this section.

When birefringence is exhibited by an initially optically isotropic body, then, for a particular condition of loading, the resulting state of optical anisotropy at any point corresponds to a state of mechanical anisotropy resulting from loading. The formulation of the existing stress-optic law relies on the hypothesis that the mechanical state is uniquely defined by the stress at that point. This is, in fact, a characteristic of elastic behaviour. Accordingly, an anisotropic mechanical state is defined by  $\sigma_1, \sigma_2, \sigma_3$  ( $\sigma_1 > \sigma_2 > \sigma_3$ ) together with their directions where  $\sigma_1, \sigma_2, \sigma_3$  are the principal stresses.

\* This paper is in part based on a paper read on 26 March, 1953, at the Seventh Annual Conference of the Stress Analysis Group of The Institute of Physics.

† Now Assistant Lecturer in Mechanical Engineering, Fouad I University, Cairo.

If optical and mechanical anisotropy are related in this way, it follows from considerations of symmetry that Fresnel's ellipsoid must have the same axes as the stress quadric. Also, since for any wave-front the directions of polarization are the principal axes of the parallel section of Fresnel's ellipsoid it can be further stipulated that all central sections of Fresnel's ellipsoid and the stress quadric must have the same axes. From these considerations Coker and Filon<sup>(1)</sup> derived the stress-optic relations mathematically. Mindlin and Goodman<sup>(2)</sup> have discussed the nature and order of magnitude of the approximations made in arriving at expressions for the relative retardation.

#### THEORETICAL CONSIDERATIONS

In the case of general inelastic behaviour the stress does not define a unique mechanical state and hence a stress-optic law, as discussed above, cannot be derived. A given mechanical state will depend not only on the existing stress system but also on the previous history of loading; changes of temperature have merely isotropic effects (volumetric dilatation) which cannot affect the anisotropy of the mechanical state.

Consider, for example, a tensile test specimen subjected to a programme of uniaxial loading as shown in Fig. 1. Any

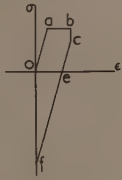


Fig. 1. Programme of loading

point on the path of loading corresponds to a certain observed birefringence. Along *oa*, where Hooke's law holds, any point is defined by the stress alone since for any one value of the stress there is only one definite state of loading. Along *ab*, *bc* or *ce* the stress alone is not sufficient to define the state of loading.

Experiments have been carried out to investigate the effect of the history of loading, including temperature changes, on birefringence (see Figs. 2 and 3). The conclusion drawn from these experiments is that a given state of birefringence is completely defined by the stress and the strain independently from the path of loading employed to arrive at these values of stress and strain, and is unaffected by the temperature at which the test has been carried out. This conclusion is also supported by the repeatedly observed fact that in the "freezing" process, using a material which does not creep at high temperatures, the fringe-pattern observed during cooling to room temperature is seen to remain unaltered throughout, as long as the load is still in position, i.e. as long as the stress and strain at any point are maintained constant. It is therefore on the basis of such experimental evidence that a mechanical state, related to a given birefringence, is uniquely defined by the stress and strain. In this respect the stress and the strain are independent parameters.

If the principal axes of stress coincide with the principal axes of strain, then it follows from considerations of symmetry that these directions are also the principal directions of Fresnel's ellipsoid. Now, in order to identify the axes of polarization for any wave normal with a set of mutually perpendicular directions it is necessary that the principal axes of stress and strain for any central section of the two quadrics coincide. Coker and Filon<sup>(1)</sup> have derived the necessary condition which must hold if this coincidence is to

take place. This condition is that the stress-strain relation must be of the form

$$\sigma_i = H + Q\epsilon_i \quad (i = 1, 2, 3)$$

where *H* and *Q* are symmetric functions of the stress and strain components. This condition, in fact, stipulates that the stress and the strain have to be dependent parameters. This is not necessarily required to define a certain mechanical state (refer to Fig. 1, where along *ab* and *bc* the stress and strain are entirely independent). However, even when inelastic behaviour can be described by a stress-strain relation, the above relation would not be accepted since it provides a unique stress-strain relationship which would break down upon unloading or reloading. The argument used above to relate a state of optical anisotropy to the corresponding state of mechanical anisotropy lacks generality. Furthermore, it cannot be applied if the principal axes of stress do not coincide with the principal axes of strain (which is not excluded in general inelastic behaviour), since then there is no *a priori* indication of the directions of the principal axes of Fresnel's ellipsoid.

The restrictions imposed on the generality of the argument used above may be overcome by considering the stress ( $\sigma$ ) and the strain ( $\epsilon$ ) to be independent parameters which define a mechanical state ( $\lambda$ ).

For any direction *i* defined by *l*, *m*, *n*, where *l*, *m*, *n* are the direction cosines

$$\begin{aligned} \lambda_i &= \lambda_x l^2 + \lambda_y m^2 + \lambda_z n^2 + 2\lambda_{xy} lm + 2\lambda_{yz} mn + 2\lambda_{zx} nl \\ \sigma_i &= \sigma_x l^2 + \sigma_y m^2 + \sigma_z n^2 + 2\sigma_{xy} lm + 2\sigma_{yz} mn + 2\sigma_{zx} nl \\ \epsilon_i &= \epsilon_x l^2 + \epsilon_y m^2 + \epsilon_z n^2 + 2\epsilon_{xy} lm + 2\epsilon_{yz} mn + 2\epsilon_{zx} nl \end{aligned}$$

By comparing the terms in  $l^2$ ,  $m^2$ ,  $n^2$ ,  $lm$ ,  $mn$  and  $nl$  in the above three equations, the relation between  $\lambda_i$  and  $\sigma_i$ ,  $\epsilon_i$  must take the form

$$\lambda_i = a\sigma_i + b\epsilon_i$$

where *a* and *b* are arbitrary constants independent of *l*, *m* and *n*.

$\lambda$  will have principal components  $\lambda_1$ ,  $\lambda_2$ ,  $\lambda_3$  which can be identified with the principal directions of Fresnel's ellipsoid.

Following the procedure of Coker and Filon, the relative phase retardation per unit thickness will then be

$$n/t = C(\lambda'_1 - \lambda'_2)$$

where  $\lambda'_1$  and  $\lambda'_2$  are the secondary principal components for the wave normal, and *C* is a constant. Values of  $\lambda$  can now be calculated as follows:

(i) *Principal directions of stress coincident with the principal directions of strain:*

For the stress the secondary principal components are  $\sigma'_1$  and  $\sigma'_2$ .

For the strain the secondary principal components are  $\epsilon'_1$  and  $\epsilon'_2$ .

Therefore  $\lambda'_1 = a\sigma'_1 + b\epsilon'_1$  and  $\lambda'_2 = a\sigma'_2 + b\epsilon'_2$

$$\begin{aligned} n/t &= C[(a\sigma'_1 + b\epsilon'_1) - (a\sigma'_2 + b\epsilon'_2)] \\ &= A(\sigma'_1 - \sigma'_2) + B(\epsilon'_1 - \epsilon'_2) \end{aligned}$$

where *A* and *B* are constants.

(ii) *Principal directions of stress and strain not coincident:*

For the stress the secondary principal components are  $\sigma'_1$  and  $\sigma'_2$ .

For the strain, the secondary principal components are



$\epsilon'_1$  and  $\epsilon'_2$ , their directions making an angle  $\alpha$  with the directions of  $\sigma'_1$  and  $\sigma'_2$ .

Taking a direction making an angle  $\theta$  with the direction of  $\sigma'_1$

$$\lambda_{\theta} = a\sigma_{\theta} + b\epsilon_{\theta}$$

$$= a\left(\frac{\sigma'_1 + \sigma'_2}{2} + \frac{\sigma'_1 - \sigma'_2}{2} \cos 2\theta\right) +$$

$$b\left(\frac{\epsilon'_1 + \epsilon'_2}{2} + \frac{\epsilon'_1 - \epsilon'_2}{2} \cos 2\theta \cos 2\alpha + \frac{\epsilon'_1 - \epsilon'_2}{2} \sin 2\theta \sin 2\alpha\right)$$

For maximum and minimum then

$$\tan 2\theta = \frac{b(\epsilon'_1 - \epsilon'_2) \sin 2\alpha}{a(\sigma'_1 - \sigma'_2) + b(\epsilon'_1 - \epsilon'_2) \cos 2\alpha}$$

and  $\lambda'_1 - \lambda'_2 =$

$$\sqrt{[a(\sigma'_1 - \sigma'_2) + b(\epsilon'_1 - \epsilon'_2) \cos 2\alpha]^2 + [b(\epsilon'_1 - \epsilon'_2) \sin 2\alpha]^2}$$

and  $n/t =$

$$\sqrt{[A(\sigma'_1 - \sigma'_2) + B(\epsilon'_1 - \epsilon'_2) \cos 2\alpha]^2 + [B(\epsilon'_1 - \epsilon'_2) \sin 2\alpha]^2}$$

(iii) *Special case of non-coincidence:*

(This case corresponds to the experiments described in the next section which gave the results illustrated in Figs. 6 and 7).

Here  $\sigma_x = \sigma$   $\epsilon_0$  is the "frozen-in" strain.

$$\sigma_y = 0$$

$$\tau_{xy} = 0$$

$$\text{Strain } \epsilon_x = \frac{\epsilon_0 - \nu_0 \epsilon_0}{2} + \frac{\epsilon_0 + \nu_0 \epsilon_0}{2} \cos 2\beta + \frac{\sigma}{E}$$

$$\epsilon_y = \frac{\epsilon_0 - \nu_0 \epsilon_0}{2} - \frac{\epsilon_0 + \nu_0 \epsilon_0}{2} \cos 2\beta - \frac{\nu \sigma}{E}$$

$$\gamma_{xy} = (\epsilon_0 + \nu_0 \epsilon_0) \sin 2\beta$$

Therefore

$$\tan 2\theta_{\max} = \frac{\sin 2\beta}{\cos 2\beta + \frac{1}{(1 + \nu_0)\epsilon_0} \left( \frac{1 + \nu}{E} + \frac{a}{b} \right) \sigma}$$

and since for elastic conditions at room temperature

$$\frac{1}{f_{\text{room}}} = a + \frac{1 + \nu}{E} b$$

$$\text{Therefore } \left( \frac{1 + \nu}{E} + \frac{a}{b} \right) = \frac{1}{bf_{\text{room}}}$$

Also after freezing  $\sigma = 0$

Therefore  $n_0/t = b(1 + \nu_0)\epsilon_0$

Then substituting in the equation of  $\tan 2\theta$

$$\tan 2\theta = \frac{\sin 2\beta}{\cos 2\alpha + \frac{1}{(n_0/t)f_{\text{room}}} \sigma}$$

$$\text{and } n/t = (n_0/t) \sqrt{\left[ \sin^2 2\beta + \left( \cos 2\beta + \frac{1}{(n_0/t)f_{\text{room}}} \sigma \right)^2 \right]}$$

#### EXPERIMENTAL EVIDENCE

The experimental evidence in favour of a relation of the form  $n/t = C(\lambda'_1 - \lambda'_2)$  holding for photoelastic materials under a wide variety of conditions may now be examined.

Fig. 2 shows the programme of loading carried out in a uniaxial tensile test at three different temperatures to show

the independence of birefringence from the path of loading history. In Fig. 3 such independence can be seen at  $F$  where the same relative retardation was obtained from three paths of loading. The fact that the points lie closely on a straight line confirms the existence of a linear relation between relative retardation and stress and strain difference.

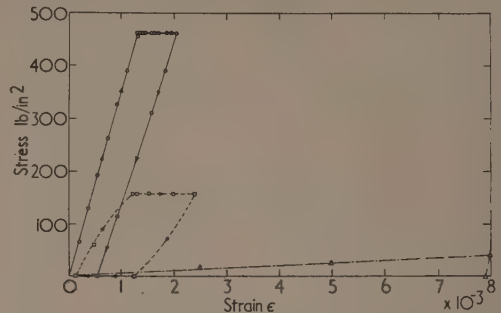


Fig. 2. Catalin 800. Programme of loading in a uniaxial tensile test at different temperatures

—○— = room temperature loading;  
—□— = 55°C loading; —△— = 85°C loading

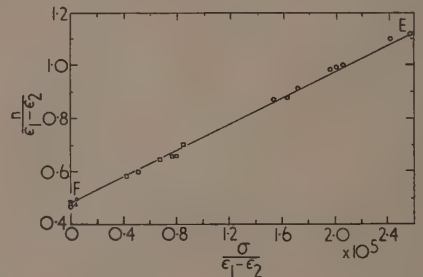


Fig. 3. Catalin 800.  $t = \frac{1}{4}$  in. Fringe order as a function of stress and strain in a uniaxial tensile test for an arbitrary programme of loading at different temperatures

○ = room temperature loading.  $\epsilon_1 - \epsilon_2 = \epsilon_e \times 1.39 + \epsilon_p \times 1.5$  ( $\nu_e = 0.39$ ,  $\nu_p = 0.5$ ).  
□ = 55°C loading.  $\epsilon_1 - \epsilon_2 = \epsilon \times 1.5$ .  
△ = 85°C loading.  $\epsilon_1 - \epsilon_2 = \epsilon \times 1.5$ .  
 $E$  = elastic behaviour at room temperature;  $F$  = elastic behaviour at freezing temperature.

A series of tests was carried out to deal with the case of the coincidence of the principal directions of stress and strain. In Fig. 4 relative retardation is plotted against strain difference for tensile specimens of C.R.39 undergoing creep tests. Points have been selected at three arbitrary levels of stress and it was found that they lie on three reasonably parallel straight lines. Fig. 5 shows similar results relating to Catalin. The data for the lines in Fig. 5 is taken from creep curves in a paper by Mylonas.<sup>(3)</sup>

The results from a further series of tests dealing with the case of the non-coincidence of the principal directions of stress and strain are illustrated in Fig. 6 and Fig. 7. A tensile specimen was subjected to uniaxial loading in a longitudinal direction at 85°C,  $n_0$  fringes being retained after cooling to room temperature and final removal of the load. A specimen having a longitudinal axis inclined at  $\beta$  to the original longitudinal axis was then cut from the specimen. The new model was then subjected to varying tensile loads. The curves in

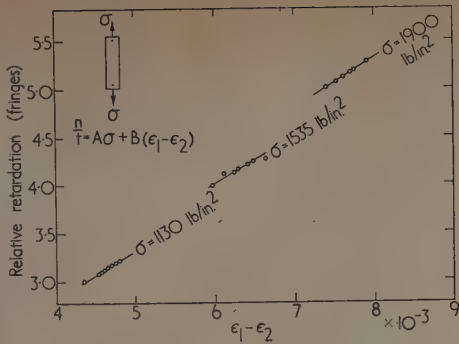


Fig. 4. C.R.39. Creep at room temperature.  $t = \frac{1}{4}$  in.

$\epsilon_1 - \epsilon_2 = \epsilon_e \times 1.37 + \epsilon_p \times 1.5$  ( $\nu_e = 0.37, \nu_p = 0.5$ ).  
From the straight lines  $A = 0.00365, B = 2000$ .

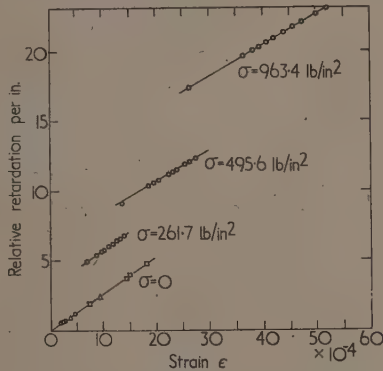


Fig. 5. Catalin 800. Creep at room temperature [Data from Mylonas (1948)]

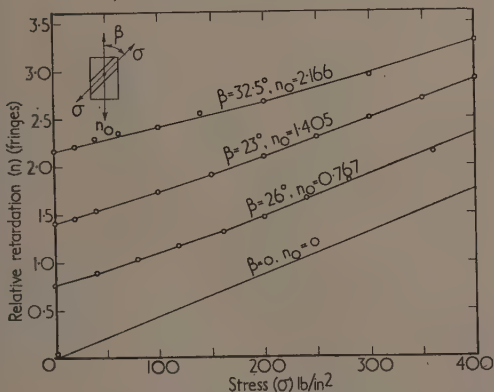


Fig. 6. Catalin 800.  $t = \frac{1}{4}$  in. Relative retardation as a function of stress at room temperature

$$n = n_0 \sqrt{\left[ \left( \cos 2\beta + \frac{1}{(n_0/t) \times f_{room}} \sigma \right)^2 + \sin^2 2\beta \right]}$$

Fig. 6 show the connexion between the applied stress  $\sigma$  and the relative retardation due to the combined system of stress and strains as predicted from the theoretical expressions given

in the previous section. The points marked are the observed experimental points which are seen to be in good agreement. Figs. 7 and 8 show the variation of the direction of polarization with increase of  $\sigma$  both for Catalin and C.R.39 specimens. Again the curves show the connexion between the direction of polarization and  $\sigma$  as derived from the theory, while the points shown have been obtained experimentally.

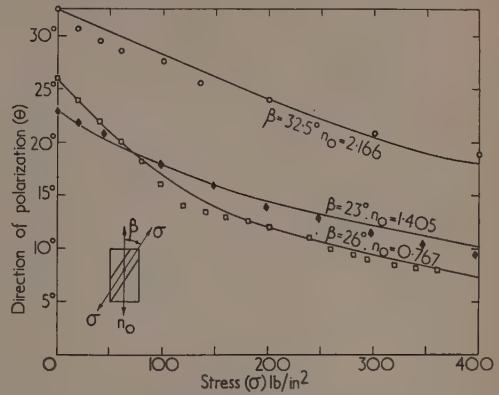


Fig. 7. Catalin 800.  $t = \frac{1}{4}$  in. Direction of polarization as a function of stress at room temperature

$$\tan 2\theta = \frac{\sin 2\beta}{\cos 2\beta + \sigma(n_0 \times f_{room}/t)^{-1}}$$

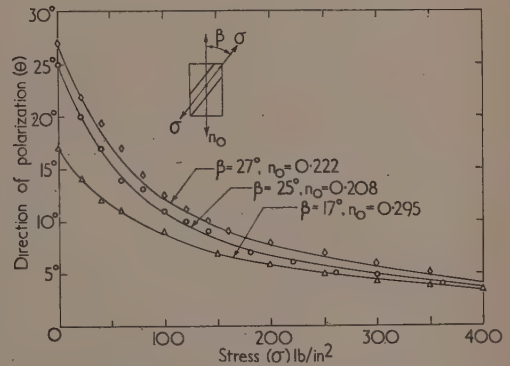


Fig. 8. C.R.39.  $t = \frac{1}{4}$  in. Direction of polarization as a function of stress at room temperature

$$\tan 2\theta = \frac{\sin 2\beta}{\cos 2\beta + \sigma(n_0 \times f_{room}/t)^{-1}}$$

In the experiments discussed above a standard transmission polariscope with a 6 in. diameter field was used. Loads were measured by means of a proving ring, changes of diameter of the proving ring being read directly off a dial gauge. Elongations were measured with mirror extensometers of  $\frac{1}{2}$  in. or 2 in. gauge length. Changes of length between lines scribed on the "frozen" specimens were measured with a special micrometer microscope. Relative retardations were measured by the Tardy method of compensation. Both the measurements by the Tardy method and the measurements of the direction of polarization were made to the nearest  $\frac{1}{2}^\circ$  with the aid of a photomultiplier cell to locate the position of extinction of light.

In 1938 Lee and Armstrong<sup>(4)</sup> published the results of tests made on different types of Bakelite resins and two samples of Marblette, giving the variation of the physical and optical properties of these materials with change of temperature. Their results included curves showing the variation of both the strain-optical coefficients and the stress-optical coefficients of these materials with temperature. If expressions for the strain-optical coefficient ( $C$ ) and the stress-optical coefficient ( $C_1$ ) are substituted in the above relation the resulting equation connecting these two equations is seen to be linear. Fig. 9 shows Lee and Armstrong's data re-plotted to check this predicted linearity.

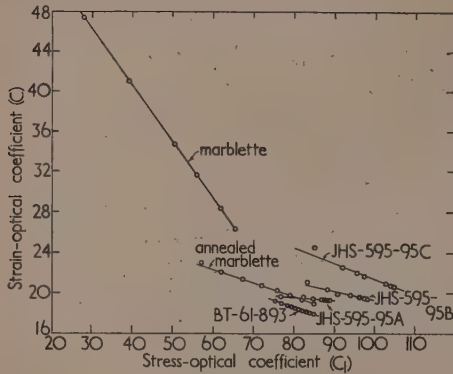


Fig. 9

$$C_1 = \frac{p-q}{n/t} \text{ and } C = \frac{\epsilon_1 - \epsilon_2}{n/t}$$

and since  $n/t = A(p-q) + B(\epsilon_1 - \epsilon_2)$ .  
Therefore  $AC_1 + BC = 1$ .

[Data from Lee and Armstrong (1938)]

#### PRACTICAL PROCEDURE FOR PHOTOPLASTIC INVESTIGATIONS

It is clear that the relations so far derived, although of considerable fundamental interest, cannot, as they stand, be used for the solution of many problems involving inelastic behaviour. The relative retardation which can be measured has been shown to be a function of the stress difference and the strain difference. The need to know the strain difference before the stress difference can be evaluated severely restricts the practical usefulness of these relations.

However, where an inelastic state has been reached after continuously increasing the boundary forces from zero, the total strain consists of the sum of two parts, a plastic strain  $\epsilon_p$  and a recoverable elastic strain  $\epsilon_e$ , as shown diagrammatically in Fig. 10.

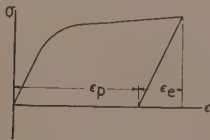


Fig. 10. Plastic and elastic strain

The relation connecting relative retardation and stress difference and strain difference for a two-dimensional problem now becomes

$$n/t = A(\sigma_1 - \sigma_2) + B(\epsilon_{p1} - \epsilon_{p2}) + B(\epsilon_{e1} - \epsilon_{e2})$$

This relation, though strictly applicable only to problems

where the principal directions of stress and strain coincide, will give a good approximation to a solution where this condition does not hold. The graphs shown in Figs. 7 and 8 show that the deviation from a straight line relation caused by values of  $\beta$ , the angle between the principal directions, larger than one would expect in most practical problems, is comparatively slight.

Now  $(\sigma_1 - \sigma_2)/2G = \epsilon_{e1} - \epsilon_{e2}$ , when  $G$  is the modulus of rigidity of the model material. Therefore

$$n/t = (A + B/2G)(\sigma_1 - \sigma_2) + B(\epsilon_{p1} - \epsilon_{p2})$$

A photograph taken with the load in position gives the fringe count  $n$  at a specific point where  $n$  is defined by the above equation.

A second photograph taken immediately after the load has been removed shows  $n'$  fringes at the point under consideration, where  $n'$  is given by

$$n'/t = B(\epsilon_{p1} - \epsilon_{p2})$$

Taking the photograph immediately avoids complications due to further time-dependent elastic recovery.

The algebraic difference between these two expressions is

$$(n - n')/t = (A + B/2G)(\sigma_1 - \sigma_2)$$

which gives the stress difference. The constant  $(A + B/2G)$  is identical with  $1/f$ , where  $f$  is the room temperature fringe value for the elastic condition of the model material.

If  $N$  is the difference between the two observed fringe counts the stress-optic law for inelastic behaviour may be written as

$$N/t = (1/f)(\sigma_1 - \sigma_2)$$

#### CONCLUSIONS

A general relation connecting relative retardation with stress difference and strain difference has been derived. The well-known stress-optic law for elastic behaviour is seen to be a particular case of this general relation. It should be pointed out here that it has been assumed throughout this paper that no chemical changes take place in the material, and that all strains are sufficiently small for the model material to remain physically isotropic.

The procedure for investigations beyond the elastic limit eventually leads to a stress-optic law which is closely analogous to the stress-optic law for elastic behaviour. But just as the mechanical state of material within the elastic range can be specified by one parameter, while two parameters are required to specify the mechanical state of material beyond the elastic limit, so it is found that while one stress pattern suffices for the solution of elastic problems, the difference between two stress patterns has to be taken for the solution of inelastic problems.

The theoretical foundation for stress analysis beyond the elastic limit by stress-optical means has thus been established. For the solution of particular problems, model materials will have to be found which exhibit the appropriate mechanical behaviour and the conditions of similarity which must hold between model and prototype will have to be examined.

#### REFERENCES

- (1) COKER, E. G., and FILON, L. N. G. *A Treatise on Photoelasticity*, Chapter III (London: Cambridge University Press, 1937).
- (2) MINDLIN and GOODMAN. *J. Appl. Phys.*, **20**, p. 89 (1949).
- (3) MYLONAS, C. *Proc. Instn Mech. Engrs*, **158**, p. 244 (1948).
- (4) LEE, G. H., and ARMSTRONG, C. W. *J. Appl. Mech.*, **5**, p. A11 (1938).



# Gold as a grid emission inhibitor in the presence of an oxide-coated cathode\*

By B. O. BAKER, B.Sc.(Eng.), A.C.G.I., A.M.I.E.E., The M.-O. Valve Co. Ltd., at the G.E.C. Research Laboratories, Wembley, Middlesex

[Paper first received 16 January, and in final form 29 April, 1953]

Emission measurements have been made on gold-plated molybdenum and gold-plated manganese-nickel grids in the presence of an oxide-coated cathode. For grids which cannot be designed to operate below  $350^{\circ}\text{C}$ , a minimum thickness of  $1\ \mu$  of gold will suppress grid emission. Silver is not so reliable, but is effective in some cases.

The use of gold plating for the suppression of grid emission in valves with oxide-coated cathodes has been known since 1930,<sup>(1)</sup> but very little quantitative information has been published. Primary grid emission takes place when a sufficiently hot grid becomes thermionically activated by emissive material evaporated from the cathode. This is undesirable, as in many uses the bias potential on the control grid is applied through a high resistance, and a small amount of grid emission is sufficient to reduce this bias and cause the valve to be over-run. The purpose of this paper is to present the results of experiments to find the primary grid emission properties of 5% manganese-nickel, molybdenum, and the corresponding gold-plated wires.

Grid emission is dependent upon many factors, including temperature, vacuum conditions and cathode processing, and it is convenient to use a valve in which the properties of two different materials can be compared under the same condition of vacuum and cathode treatment. A test valve has therefore been designed, Fig. 1, in which the grid consists of two

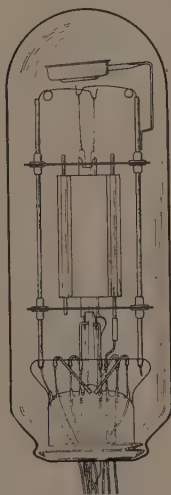


Fig. 1. Sketch of filamentary valve

filaments situated between the cathode and anode, one on either side of the cathode. The filaments are activated as a normal grid by material evaporated from the cathode, but grid emission measurements can be made with the cathode cold, heating the grid directly by passing a current through it.

The temperature of the grid can be determined in terms of the heating current by separate experiments.

Further measurements have been made using a triode of more conventional design, in which the grid is kept at a reasonably uniform temperature by minimizing the heat conducted into the pinch. Finally, larger scale factory trials have been made on the KT81 valve, an output tetrode, to assess the performance of gold-plated molybdenum under factory conditions.

## METHOD OF GRID EMISSION MEASUREMENT

After normal pumping and cathode activation, grid emission measurements were made with the anode and cathode connected together. Fig. 2 shows a typical grid current-voltage curve, the saturated grid emission being determined

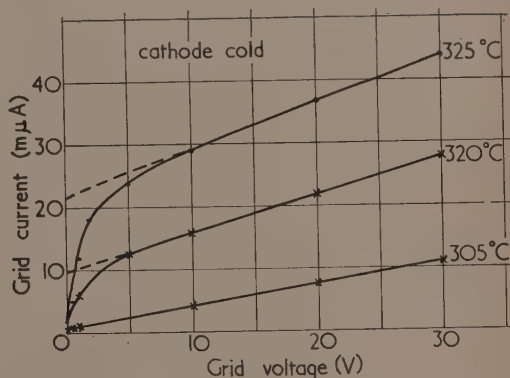


Fig. 2. Typical current-voltage curve. Filamentary "grid"

by extrapolating back to the current axis, to eliminate electrical leak. It was possible to detect grid currents of the order of 1 millimicroampere.

In the valve with filamentary grids, measurements were made with the cathode cold, varying the grid temperature and plotting Richardson lines, Fig. 3. From these the temperature at which the emission reached a rejection limit of  $0.2\ \mu\text{A}/\text{cm}^2$ , which is a fairly severe test for most purposes, could be determined. Life tests were conducted by heating the grid by radiation from the cathode.

## METHOD OF TEMPERATURE MEASUREMENT

Since the temperature range covered by these experiments is below the range of the optical pyrometer, and the temperature of the filamentary grids could not be determined

\* Communication No. 532.

satisfactorily with thermocouples, the method employed for these grids was based on resistance measurements. Assuming the temperature of the filament to be uniform over the centre portion of its length, dropping to a lower value at each end

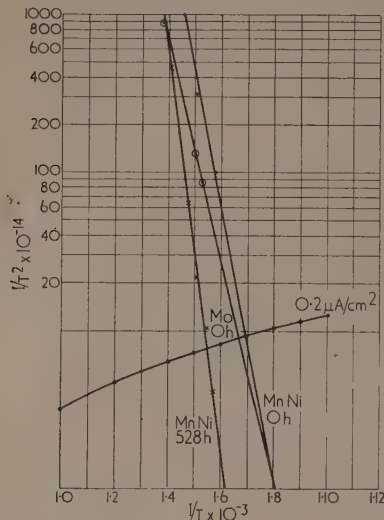


Fig. 3. Typical Richardson lines (filamentary grid)

due to heat conduction into the pinch, it is possible to determine the uniform temperature from the current flowing through the wire providing a correction can be made for the end cooling.

The variation of resistance of manganese-nickel and gold-plated manganese-nickel with change of temperature was determined experimentally in a uniform temperature quartz

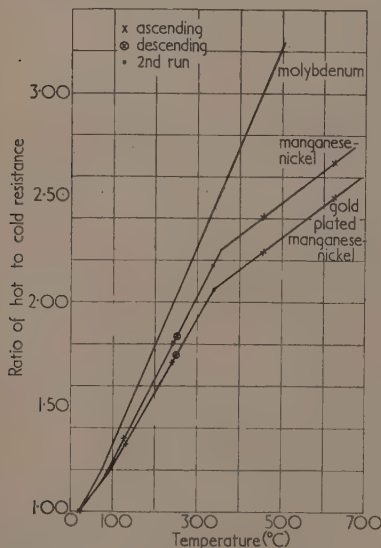


Fig. 4. Temperature coefficient of resistance

furnace in vacuum, three thermocouples being used to check the temperature distribution along the length of the specimen, which was 0.075 mm diameter wire as used in the other experiments. By careful annealing of the wire beforehand, a considerable degree of repeatability was achieved in these measurements (see Fig. 4). For molybdenum, published data<sup>(2)</sup> were used, and it was calculated that gold-plated molybdenum has approximately the same temperature coefficient of resistance, the resistance of the molybdenum being low compared with that of the gold layer.

A separate experiment was carried out to determine the end correction for each of the four materials used. For each material, two filaments of lengths approximately 14 cm and 24 cm were mounted in exactly the same manner as the filaments in the test valves. The filaments were connected in series, and current-voltage readings were taken for each filament in turn using a potentiometer.

It can be shown that for two filaments of the same diameter but different lengths, whose end cooling is assumed to be the same,

$$R_{H1} - R_{H2} = R_{T1}(l_1 - l_2)$$

Where  $R_{H1}$ ,  $R_{H2}$  are the hot resistances of the filaments,  $R_{T1}$  the hot resistance of the wire per unit length at uniform temperature  $T_1$ , and  $l_1$ ,  $l_2$  lengths of filaments at this temperature.

$$\text{Also } R_{H1} - R_{H2} = (V_1 - V_2)/I$$

where  $V_1$ ,  $V_2$  are the volts dropped across the filaments with a current  $I$  passing through. Dividing  $R_{H1} - R_{H2}$  by the difference in cold resistance of the two filaments enables the temperature for the current  $I$  to be deduced from the temperature coefficient curve. This was done for a series of values of current.

The Stefan-Boltzmann law for free radiation provides a convenient means of plotting these results. The energy in a filament of resistance  $R$  is given by  $I^2R = K(T^4 - t^4)$ , where  $T$  = absolute temperature,  $t$  = absolute room temperature.

Neglecting  $t^4$  compared with  $T^4$ , and assuming  $R \propto T$ ,

$$I^2 = \frac{KT^4}{T} = KT^3$$

Therefore  $I \propto T^{3/2}$  (approximately).

The temperature-current relationship is plotted (Fig. 5) on this basis for each of the grid materials, and was checked at the higher temperatures by means of an optical pyrometer. In each case the pyrometer readings were lower than the corresponding temperature obtained by the resistance method, due to glass absorption and low thermal radiation efficiency. The difference was about 55° C for manganese-nickel, 45° C for molybdenum, and 30° C for gold-plated manganese-nickel at 750° C.

The temperature of the filamentary grid when heated by radiation from the cathode, as under the life test running condition, had to be determined separately, since the temperature distribution along the wire was different. An approximation to the grid temperature was made by comparing the grid emission under the two running conditions. This could only be done for manganese-nickel and molybdenum, as no emission could be detected from the gold-plated wires. Since the thermal emissivity of gold is low, it is probable that the gold-plated wires were running at a somewhat lower temperature than the unplated wires,

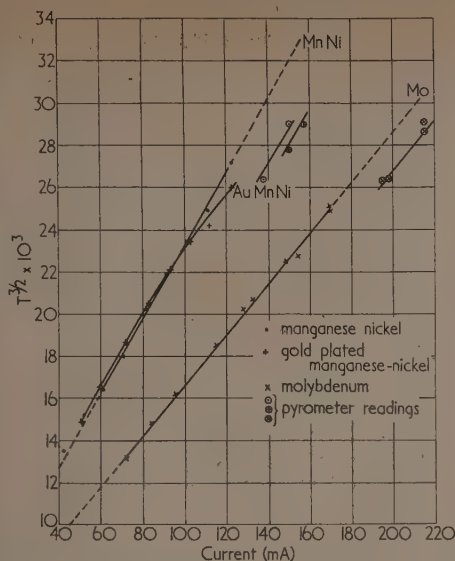


Fig. 5. Temperature-current relations; corrected for end effects (wire diameter 0.075 mm)

the temperatures of which were 420° C (brightness) for manganese-nickel and 440° C (brightness) for molybdenum.

The grid temperature of the triode was determined by means of a thermocouple welded to the grid side rod, the cold junction being outside the valve in a water bath. It was found experimentally that the temperature gradient down the

Table 1. Temperature gradient along grid wires

Material	$\delta T$
5% Mn-Ni	30° C
Mo	10° C
Au Mn-Ni	35° C
Au Mo	10° C

grid support wire was very small (10° C) for grid temperatures ranging between 300–500° C. Also the difference of temperature between the centres of the grid support wires, due to asymmetry of construction, was only 10° C. The temperature gradient along the grid wires was calculated approximately for the thermal conductivities of the various materials, and the temperature difference  $\delta T$  between the centre and the support wire is tabulated in Table 1.

On life test the grid temperature was raised both by radiation from the cathode and from the anode.

## EXPERIMENTAL RESULTS

1. Grid emission measurements on valves with filamentary grids are shown in Table 2.

In no case was any emission detected from either of the gold-plated wires, even up to temperatures as high as 600° C. An examination of the Richardson lines indicated that the emission constants of different samples of the same material varied between wide limits. It is probable that this is more apparent than real, since the deposits on the wire are unlikely to be uniform over the surface.

2. Table 3 shows grid emission measurements made on the test triodes before life test, the batches consisting of 4 to 6 valves.

Table 3. Initial results on test triodes

Material	Batch No.	Maximum grid emission in $m\mu A$		Mean grid emission in $m\mu A$	
		470° C	590° C	470° C	590° C
Manganese-nickel	1	1	102	1	76
	2	4	720	1	270
Molybdenum	1	250	43 000	68	9050
	2	4500	70 000	2330	43 330
Gold-plated	1	0	0	0	0
Manganese-nickel	2	0	0	0	0
	1	0	8	0	1
Molybdenum	2	0	0	0	0

These valves were then life tested, as shown in Table 4, under four different conditions, A, B, C, and D. For example,

Table 2. Comparison between the grid emission of materials A and B in the same valve

Valve	Hours on life test	Material A	Temperature of material A for 0.2 $\mu A/cm^2$	Material B	Temperature of material B for 0.2 $\mu A/cm^2$
1	0	Manganese-nickel	415° C	Gold-plated manganese-nickel	No emission up to 600° C
	296		425° C		
	528		425° C		
2	0	Manganese-nickel	310° C	Gold-plated manganese-nickel	No emission up to 600° C
	296		365° C		
	528		365° C		
3	0	Manganese-nickel	315° C	Gold-plated manganese-nickel	No emission up to 600° C
	296		360° C		
	528		375° C		
4	0	Manganese-nickel	290° C	Gold-plated manganese-nickel	No emission up to 600° C
	0		325° C		
5	0	Molybdenum	405° C	Gold-plated molybdenum	No emission up to 600° C
	216		400° C		
	556		400° C		
6	0	Molybdenum	325° C	Gold-plated molybdenum	No emission up to 600° C
	216		405° C		
	556		400° C		
7	0	Manganese-nickel	315° C	Molybdenum	370° C
	0		315° C		



Table 4. Life test results on test triodes

Material	Batch No.	Test temperature, °C	Maximum grid emission in mA under life test running conditions			
			A	B	C	D
			Cathode 760° B Anode 4.2 W Grid 520° C Time 500 h	760° B 0 W 470° C + 170 h	700° B 4.2 W 465° C + 140 h	920° B 0 W 590° C + 26 h
Manganese-nickel	1	470	50	0		0
		590	7800	15 600		6000
	2	470			0	10 000
		590			410	17 000
Molybdenum	1	470	3600			16 500
		590	100 000			140 000
	2	470			140	
		590			6400	
Gold-plated manganese-nickel	1	470	0			0
		590	0			0
	2	470				0
		590				0
Gold-plated molybdenum	1	470	0			0
		590	1260			0
	2	470				0
		590				0

the first batch of manganese-nickel was life tested for 500 h under condition A, for a further 170 h under condition B, and finally a further 26 h under condition D.

3. A factory trial was conducted on the KT81 valve with a molybdenum grid coated with  $1\mu$  thickness of gold. To achieve the most stringent conditions, the grid radiators were omitted in order to run the grid at maximum temperature. Sample batches of four valves spread over a period of six months production were life tested, a total of five batches in all, and in no case was grid emission experienced. In the first batch the grid side rod temperature was  $480^\circ\text{C}$ , nickel being used, while the remaining batches with copper side rods ran at  $450^\circ\text{C}$ . An attempt to increase the grid temperature by raising the cathode temperature was unsuccessful due to gas evolved from the mica spacers between electrodes. While most of the life tests covered periods of 500 to 600 h, one batch was run satisfactorily for 2600 h without giving grid emission.

A section of one of the grid wires after this period at  $450^\circ\text{C}$  showed that there was no reduction in the thickness of the gold layer. No cracking of the core was observed as reported by Gorham.<sup>(3)</sup>

#### MINIMUM THICKNESS OF GOLD

For economy it is necessary to know the minimum thickness of gold which will inhibit grid emission, and a trial was made in the test triode. Attempts to gold plate molybdenum wire to a thickness less than  $1\mu$  resulted in inadequate coverage, and for the same reason it was not found possible to draw down plated wire. A very thin uniform layer of gold was achieved, however, by coating the wire with gold resinate by a continuous process, subsequent heating in air to  $500^\circ\text{C}$  giving a thin layer of gold. Three batches of wire were tested with gold thicknesses of 1,  $1/3$  and  $1/10\mu$  respectively. The first batch was comparable with previous trials of gold-plated molybdenum having the same thickness of gold, showing no grid emission over a period of 500 h. The other two batches, however, both developed grid emission after 200 h, the  $1/10\mu$  to a greater extent than the  $1/3\mu$  gold layer. It was therefore concluded that  $1\mu$  is the minimum effective layer of gold.

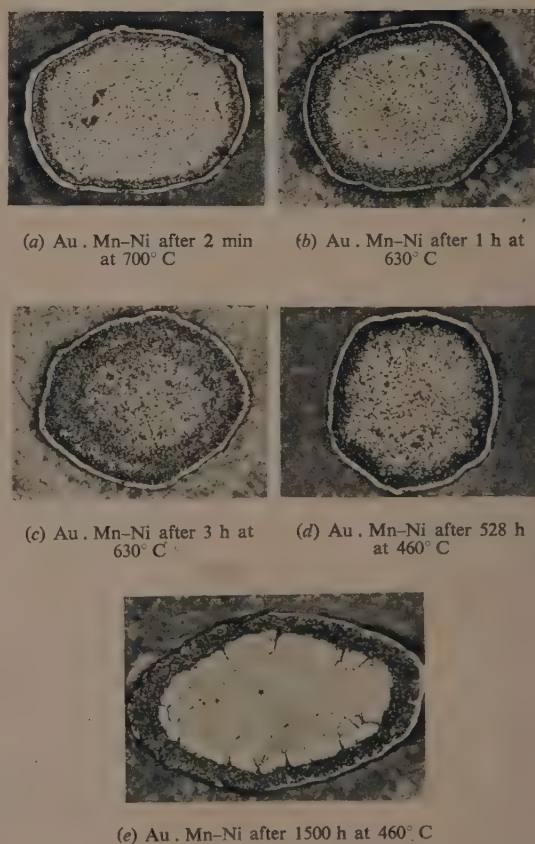


Fig. 6. Heat treatment of plated wires. The gold plating appears as a bright annular surround, inside which intergranular penetration can be seen ( $\times 350$ )

## HEAT TREATMENT OF PLATED WIRES

A study of the diffusion of the gold layer into the core during heat treatment was carried out, as this might materially effect the inhibition of grid emission during life. Micro-sections of gold-plated manganese-nickel and molybdenum wires were examined after various treatments. In view of the small diameter of the wire, the specimens were silver-plated to avoid rounding of the edges during polishing. They were then etched to show up any boundaries which might be present. As the wires had been fully annealed before plating, the possibility of enhancement of the diffusion rate by recrystallization of the drawn wire was eliminated.

Fig. 6 shows typical results of the heat treatment of gold-plated manganese-nickel, in which diffusion has clearly taken place. Wires treated for 1 h at 400° C showed no evidence of diffusion. It is interesting to note that after 1500 h at 460° C, intergranular penetration has taken place beyond the main diffusion zone, and in places the gold layer has completely disappeared. The wire in this state still did not develop emission, so the solid solution of gold and manganese-nickel must be as effective as gold in the suppression of grid emission. In the case of gold-plated molybdenum wires, no diffusion was observed in any specimen.

## DISCUSSION

It is not possible to lay down definite temperature limits for grid materials to avoid grid emission, because grid emission is dependent upon so many factors in the manufacturing process. Nevertheless, it is useful to know the limits under conditions which are ideal for the production of grid emission, and the present evidence on the test valves with filamentary grids is that for molybdenum the maximum safe temperature is 325° C, for manganese-nickel 310° C. In commercial valves, however, the conditions are not necessarily ideal for developing grid emission, and manganese-nickel is usually quite safe up to 380° C.

Above this temperature, gold plating either molybdenum or manganese-nickel is effective in suppressing grid emission up to temperatures in the region of 550–600° C. Experience on screen grid valves with gold-plated grids shows that if the grids are misaligned so that individual turns run hot, gold is evaporated which poisons the primary emission. Thus, although 600° C is satisfactory from the point of view of grid emission, the safe temperature from the point of view of evaporation is probably 500–550° C. The most likely mechanism of grid emission is that barium evaporated from the cathode condenses on the grid, and is partially oxidized by the very small quantity of oxygen being evolved from the cathode. This partial oxidation gives an

emissive layer of barium on barium oxide. Presumably if the grid is gold-plated the barium diffuses into the gold before it can form an emissive layer. This mechanism is supported by some unpublished work of R. W. Taylor of these Laboratories, who showed that barium evaporated on to a gold-plated tungsten wire decreased its resistance, but when the wire was subsequently heated the resistance increased above its original value as the barium alloyed with the gold. With gold-plated molybdenum, a danger region exists between 350° C and 400° C, where grid emission can be developed during pumping and activation which will only disappear slowly during life. The magnitude of this emission is not likely to exceed 0.5  $\mu\text{A}/\text{cm}^2$  on the present evidence. In this temperature range the rate of diffusion of barium into gold is not sufficiently rapid to prevent oxidation of some of the barium, resulting in the formation of an emissive layer. No such danger region exists with gold-plated manganese-nickel, and this may be associated with an initial interdiffusion of gold and manganese-nickel during treatment on the pump, the resulting surface alloy perhaps being more effective than gold in dissolving barium.

While gold plating has been shown to be effective for suppressing grid emission, its use must be considered in every case from the point of view of economics. Silver-plated molybdenum is a cheaper alternative, and two batches of test triodes using this wire were completely free from grid emission. A similar factory trial, however, on the KT81 valve, led to a number of rejects for grid emission although some other trials have given satisfactory results. The unreliability of silver may be associated with the fact that it is readily oxidizable, so that under adverse pumping conditions an emitting barium oxide layer may be formed on the grid. An alloy of 80% silver and 20% gold, plated on molybdenum was considered as a possible alternative, but grid emission was observed in the test triode.

In conclusion it may be said that if a grid cannot be designed to run below 350° C, gold plating to a thickness of at least 1  $\mu$  is the most reliable method of inhibiting grid emission, but in some cases silver is also effective.

## ACKNOWLEDGEMENT

The author desires to tender his acknowledgement to the M.-O. Valve Co. Ltd., on whose behalf the work described in this publication was carried out.

## REFERENCES

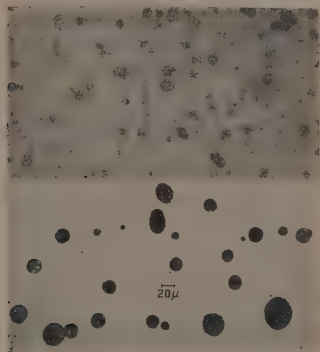
- (1) British Patent No. 350938, 15 March, 1930.
- (2) WORTHING, A. G. *Phys. Rev.*, **28**, p. 191 (1926).
- (3) GORHAM, J. E. *Proc. Inst. Radio Engrs*, **35**, p. 295 (1947).

## Correspondence

## A photographic method of observing the approximate size of liquid droplets produced by an atomizer

A problem in the testing of experimental atomizers (used in this laboratory in electron microscope specimen preparation) is the measurement of the size of the droplets produced. Initially a solution of methylene blue in water was sprayed from the atomizer on to a microscope slide, which was viewed under an optical microscope. A droplet of methylene blue solution  $10\ \mu$  in diameter is, however, not very dense, notwithstanding the intense colour of the dye, and photomicrographic reproduction of the droplet pattern proved difficult due to the low contrast of the image; a typical result of this method is shown in the upper part of the figure.

A great improvement has been obtained by spraying developer on to a previously fogged photographic plate. Kodak Maximum Resolution plates are used in view of the high resolution required, and a high-contrast developer (Kodak formula D-8) is employed to give the highest blackening density in the second or so before the droplets dry.



Photomicrographs of droplet patterns produced by an atomizer

Upper: spray of methylene blue solution on to microscope slide;

Lower: spray of Kodak developer D-8 on to Maximum Resolution plate.

A plate is fogged by the simple expedient of carrying out the work in daylight. The developer is sprayed on to it to give a satisfactorily dense deposit, after which the plate is fixed in the normal manner, care being taken to avoid reticulation (although the very thin emulsion of the Maximum Resolution plate renders this unlikely).

A typical result of this method appears in the lower part of the figure. (The magnifications of both parts of the figure are the same.) The blackened areas obtained for droplets of diameter about  $10\ \mu$  show only slight traces of graininess. The variation in density over a single droplet-area is small.

It is not claimed that this method of observing the droplet pattern is necessarily more accurate than the older methylene blue method. In both cases allowance should ideally be made for the spreading of the droplets on impact, which we have not investigated in detail. It will be seen, however, that the pattern is considerably more distinct in the photographic

method. It should be added that the two patterns were not produced by the same spray nozzle, so that the difference in apparent droplet size is not necessarily a function of the method.

We wish to acknowledge the permission of the Director of the Safety in Mines Research Establishment and of the Ministry of Fuel and Power to publish this note.

Safety in Mines Research  
Establishment,  
Portobello Street, Sheffield, 1.

R. A. BENTLEY  
J. CARTWRIGHT  
R. L. GORDON

## The reduction in apparent particle concentration with multiple strokes of the Owens jet dust counter

Where particle concentrations are low it is often the custom to take several strokes before counting the particles, and it has hitherto been assumed that multiple strokes do not affect the efficiency of the Owens counter.<sup>(1)</sup> However, in an investigation of dust in the cardroom of cotton spinning mills we noted that the apparent concentration of dust particles decreased with increase in the number of strokes of the Owens counter.

Our experimental results are summarized in the following table in which  $C_n$  means the observed average number of particles per c.c. of the particular size concerned for a count of  $n$  strokes. The particles are graded according to the diameter  $D$  of the circle of equal area. Four slides were counted at each stroke number and the strip on each slide counted by noting the number of particles in narrow traverses at intervals along the strip.

Apparent concentration  $C_n$

$D/\mu$	0.46-0.72	0.72-0.90	0.90-1.26	1.26-1.82	1.82-2.53	2.53-3.55	3.55-5.00	>5.00
$n$	0.72	0.90	1.26	1.82	2.53	3.55	5.00	
1	74.8	29.5	26.6	32.1	19.5	7.3	1.3	0.0
2	61.3	23.8	21.3	20.5	14.0	4.3	1.3	0.8
3	54.5	25.3	21.6	20.5	12.1	2.9	1.1	0.5
4	48.2	21.8	23.2	20.0	14.8	4.4	1.4	1.0
5	42.5	22.3	22.6	24.6	10.6	3.0	0.9	0.5
6	42.5	20.5	20.8	20.1	10.3	4.0	1.3	0.5
7	38.1	18.5	19.0	19.2	10.7	4.2	1.3	1.7
8	44.7	21.5	18.7	21.9	11.4	4.1	1.1	0.3
12	34.6	17.6	12.8	18.7	10.8	2.6	0.7	0.4
16	33.8	17.1	15.7	16.1	8.6	3.2	1.0	0.8
20	27.0	15.5	14.8	14.4	7.7	2.2	0.8	0.4

The decrease of  $C_n$  with  $n$  is statistically significant<sup>(2)</sup> on or above the 5% level for all grades of particle size except the largest where there are too few particles to lead to a conclusion. Corrections for overlapping<sup>(3)</sup> were calculated but proved too small to account for the observed effects. These are probably due to the blowing-off noted by Davies, Aylward and Leacey, pp. 368, 391,<sup>(4)</sup> since some particles deposited in the later part of a stroke when the air velocity is low [Ref. (4), p. 397] might well be blown off by the high velocities in the early part of the succeeding stroke.

A correction curve could be obtained by taking counts with different numbers of strokes on samples of air containing the type of dust under investigation, plotting concentration  $C_n$



against stroke-number  $n$  and drawing an empirical curve through these points. The very considerable scatter present in such counts means that a large number of results would be required to obtain a reasonably accurate curve. If some relation between  $C_n$  and  $n$  is known to exist then the fitting of a curve is facilitated and the resulting accuracy greatly improved. A development of the above blowing-off theory suggests that  $C_n$  is linearly related to  $1/n$  to a first approximation and statistical tests on our results showed that they could be explained on this hypothesis. Drawing the regression line for  $C_n$  on  $1/n$  [Ref. (2), p. 230] (or, more simply, just grouping the points into two sets and joining the two centres of gravity) gives a straightforward correction "curve" which is easy to determine, avoids the difficulty of fitting an empirical curve

to points having considerable scatter, and appears to be sufficiently accurate for practical purposes.

Shirley Institute,  
Manchester, 20.

J. K. DONOGHUE  
C. MACK

## REFERENCES

- (1) DRINKER, P., and HATCH, T. *Industrial Dust*, p. 106 (New York: McGraw-Hill Book Co. Inc., 1936).
- (2) TIPPETT, L. H. C. *The Methods of Statistics*, p. 152 (London: Williams and Norgate, Ltd., 4th edition, 1952).
- (3) ARMITAGE, P. *Biometrika*, 36, p. 257 (1949).
- (4) DAVIES, C. N., AYLWARD, M., and LEACEY, D., A.M.A. *Archives of Industrial Hygiene*, 4, p. 354 (1951).

## New books

**Radioisotopes in industry.** Edited by J. R. BRADFORD. (London: Chapman and Hall Ltd.) Pp. 309. Price 64s.

This book consists of a number of separate lectures given at a conference two years ago and it is rare that such an account makes a good book. The fault lies not in the lack of information but in the haphazard way in which it is presented, which makes the location of facts difficult. There is also much duplication. Thus, Chapter 2 gives a general account of the applications of radioisotopes but much of this information is given again in Chapters 5 and 6. The reader is told in four places that Cobalt 60 may be used for taking radiographs, but the relative merits of  $\gamma$ - versus X-radiography are not discussed, nor is the range of materials and thicknesses explorable by the former method. Similar remarks apply to the description of the thickness gauge. Chapter 4 on radiation protection is good as far as it goes, but one looks in vain here for practical guidance, as to the screenage necessary in a given case. This occurs unexpectedly in Chapter 8 on the design of laboratories, in Chapter 10 on tracer experiments, in Chapter 11 on instrumentation in the laboratory and in Chapter 13 on fission products. This information gathered together would be valuable, but scattered it is almost useless. Much duplication also occurs between Chapter 7 and 8, both of which deal with laboratory designs, though the reader will be left in doubt whether to site his laboratory on the top floor or the basement.

Some of the information in the latter chapter, such as that on isotope shipping containers, and on the handling of sealed sources, would have been better placed in the chapter on protection. Readers in this country would also find alternative suggestions to stainless steel useful.

The book makes little reference to countries other than U.S.A. and the accounts of government policy (Chapter 1), the distribution of radioisotopes (Chapter 14) as well as the detailed description of the Reactor Laboratories at Brookhaven National Laboratory are rather superfluous.

Chapter 11 on instrumentation is disappointing, as it deals only with instrumentation for chemical processes. Measuring instruments are not covered adequately anywhere.

Many of the diagrams are too simple for the text. Surely if the reader is familiar with nuclear binding energy (Fig. 3.2) he does not need to be told how to tell the time! (Fig. 3.3). Again, the decay curve in Fig. 10.2 is very similar to that given in Chapter 3.

A number of misprints were noted. The negative signs in the exponential have been omitted on pp. 57 and 173, and the units on the former page should read microcuries. On p. 124 the air velocity at a fume hood would surely not be as

great as 100 ft per second. The figure of 100 ft per minute given on p. 128 appears more reasonable. In Table 10.1, the symbols for Sr and Au are printed incorrectly.

The Editor, in his preface, appears to realize the deficiencies of the book. It is a pity that more thought was not given to its general form before it was undertaken. B. N. CLACK

**Permanent Magnets.** Pp. 58. Price 10s. (Sheffield: The Permanent Magnet Association.)

**Permanent Magnets.** Pp. 64. Gratis; **Ferroxcube.** Pp. iii + 46. Gratis; **N.T.C. Varite resistors.** Pp. 7. Gratis. (London: Mullard Limited.)

The Permanent Magnet Association's attractively produced and beautifully illustrated little book contains an interesting, if rather oddly assorted, collection of information about permanent magnets. Magnet design is treated only briefly although there is a useful collection of recoil loops (published for the first time) for many magnet materials, and a transparent chart, showing permeance lines and lines of constant  $BH$ , for use on demagnetization curves. Data are given, in C.G.S. and M.K.S. units, for those permanent magnet materials produced by members of the Permanent Magnet Association and including the recently developed Columax for which  $BH_{max} = 8.63 \times 10^6$  in C.G.S. units. Finally there are brief accounts of the magnetizing, demagnetizing and testing of magnetic materials, and a useful discussion of their handling and storage. Easy to look at and to read, this book is presumably produced primarily as a publicity venture, but will be a useful addition to the bookshelf of anyone interested in permanent magnets.

Mullard's handbook on permanent magnets contains introductory accounts of magnet design and manufacture, scientific and technical data on magnetic materials (British and American) and details of available standard magnets. And all this is presented in an elegant, copiously illustrated—photographs and diagrams—and beautifully produced handbook complete with thumb index. As the preface points out, the information is presented in a condensed form but it is nevertheless readily intelligible to the engineers and designers for whom it is prepared.

The booklet on Ferroxcube contains a brief account of the development of ferrites and also a very comprehensive collection of graphs and tables giving details of the electrical, magnetic and mechanical properties of Ferroxcube. There are also data on the application of these materials and particulars of standard core shapes and dimensions. In addition there are introductory accounts of the materials and their uses which will be of interest to all users of magnetic materials.

N.T.C. Varite is a ceramic-based semiconductor with a large negative temperature coefficient of resistance and a negligible voltage coefficient of resistance. It is intended for use in surge protection circuits or for temperature control or compensation. This leaflet gives, for the various types, curves showing the variation of resistance with current and with time—warming-up and cooling.

A. E. DE BARR

**Servomechanism analysis.** By GEORGE J. THALER, B.E., Dr.Eng., and ROBERT G. BROWN, B.S., M.S. (London: McGraw-Hill Publishing Co. Ltd.) Pp. xii + 414. Price 64s.

Publication of a new subject takes three forms. Initially come the pioneering papers in technical journals. These are followed by a book, perhaps several, recording the experience of applying the new art. Finally come the text-books; an outcome of teaching the subject. In the United States the subject of servomechanisms is well into the third stage. The present volume falls into the text-book class. The authors have given thought to the order and method of presenting their material. The first quarter of the volume is devoted to the analysis of linear systems in general and the introduction of the Laplace transform method of solving linear differential equations. The main topic is a discussion of the frequency response methods of design either by Nyquist diagram or attenuation-phase analysis. The catalogue of simple stabilizing methods (cascade networks and feedback methods) is dealt with by example. In appendices are some useful descriptions of the physical apparatus of various types of control systems; electrical, mechanical, and hydraulic. One feels it would have strengthened the work if these could have been integrated in with the main material. The treatment of theory is not expected to be very penetrating in this type of book and the authors frequently excuse themselves from detailed proof, but they might usefully have included in a lengthy list of over 200 very practical references some which would help the more discerning reader in this matter.

The authors include final chapters on two quite recent developments in methods of analysis; recommended as a special attraction on the dust cover. The result is not happy in either of these cases for they are clearly inexperienced in applying the methods. In the chapter on relay servomechanisms the sign of an important phase angle is wrong at the outset so that the "stability locus" in Figs. 13-17 and 13-18 should be mirror imaged in the real axis. The chapter on the root locus method concludes with an absurd example (see the transients in Figs. 14-15) which arises from selecting the wrong roots. The authors would have been well advised to omit these chapters which do not fit in with their main purposes of collecting the established prior art. In the previous 12 chapters they do this in a way which is thoughtful with a result that is to be welcomed.

J. H. WESTCOTT

**Progress in biophysics and biophysical chemistry: Vol. 3.** Edited by J. A. V. BUTLER and J. T. RANDALL. (London: Pergamon Press Ltd.) Pp. viii + 386. Price 63s.

Workers in the rapidly growing fields of science which may be included under the headings of biophysics and biophysical chemistry will welcome the appearance of this third volume of nine review articles on certain aspects of work in these fields. Autoradiography is reviewed by I. Doniach, Alma Howard and S. R. Pelc; Polarized ultra-violet microspectrography and molecular structure by W. E. Seeds; The infra-red spectra of biologically important molecules by R. D. B. Fraser. Roy Markham describes some Physico-chemical studies on viruses and Maurice Errera discusses Mechanisms of biological action of ultra-violet and visible radiations. Recent work on

the application of the theory of the ionic double layer to colloidal systems is reviewed by F. Booth. H. G. Davies and P. M. G. Walker review Microspectrometry of living and fixed cells. The other two reviews are by C. Sadron who discusses Methods of determining the form and dimensions of particles in solution in a critical survey and by T. Teorell, who writes on Transport processes and electrical phenomena in ionic membranes.

Each article is well written and carries a good up-to-date bibliography which will be very valuable to the research worker. In every case the important progress that has been made is set out clearly, but not at the cost of avoiding to point out the present limitations of the methods used and the low order of accuracy of quantitative information which the methods often provide. Taken together the articles show what marked progress has been made in recent years towards a better understanding of certain biological entities and phenomena as a result of very varied and ingenious applications of physical and physico-chemical methods of investigation. Still more do they make clear to the scientific novice and younger research worker that nuclear physics is not the only exciting field of investigation which waits to be ploughed.

As were the first two volumes of this series, the book is well produced and it contains some very fine illustrations of biological material. In these difficult times, it is a pity that it could not have been a little cheaper. It is possible that its price will prevent the purchase by many who would like a copy on their bookshelves.

C. W. WILSON

**Fatigue of metals.** By R. CAZAUD; translated by A. J. FENNER, B.Sc., A.M.I.Mech.E. (London: Chapman and Hall Ltd.) Pp. xiv + 334. Price 60s.

In considering a translation it is necessary first to feel that the need for the book is particularly well established and furthermore that nothing is lost in the translation. The two most extensive volumes in English on the subject of fatigue in metals, the Battelle Memorial Institute volume and the report of the Australian symposium, are the handiwork of groups of authors and are not in the form of a text-book, and in this they differ from Cazaud's book. In this work the continuous story follows from chapter to chapter in a way that is impossible in the other volumes. There is therefore every justification for a translation.

The book begins with a brief historical note introducing the subject matter and the following two chapters discuss the mechanism of fatigue failure. A full description is then given of fatigue testing methods and machines, both past and present. The remaining two-thirds of the book may conveniently be regarded as consisting of two parts. The first, comprising five chapters, summarizes many investigations which have been made to evaluate the influence of such factors as testing speed, internal stress, size, shape, temperature, corrosion and fabrication methods on the fatigue strength of metals and alloys, generally on the laboratory scale. The final chapter describes the methods which can and should be employed to reduce the wastage which occurs in industry from fatigue failures.

This summary of the contents will show that practical aspects are emphasized. The specialist in the metallurgy or physics of the subject will be disappointed to find so little attention to this most interesting field of work and even that which is included is over-simplified to an undesirable extent. However, this is not a serious criticism since the book is best regarded as suitable for the beginner in the subject or the practical engineer who wishes to have a useful work of reference.

There is much new data included in the tables, and the



style of writing is pleasing throughout as also is the make-up of the volume. The translator must no doubt receive much credit for the writing. Certainly nothing has been lost in translation, and in fact one can notice a number of small additions which could not have been present in the original French edition. Dr. Gough sums up Fenner's work in his very pleasant Foreword when he declares, "... I was never conscious that the book is a translation." Most readers will agree with this.

L. ROTHERHAM

**Methoden und anwendungen der massenspektroskopie.** By H. EWALD and H. HINTENBERGER. (Weinheim/Bergstrasse: Verlag Chemie.) Pp. 288. Price 43s. 6d.

An attempt is made in this work to survey for the first time the whole field of mass spectroscopy. It includes work on the measurement of isotopic mass in that branch of the subject known as mass spectrography, and work on abundance measurement in mass spectrometry. Some comments are made also on isotope electromagnetic separators. On the whole, it may be said that the attempt has been fairly successful, and the book is likely to prove useful to all workers in these allied fields.

As one might expect from papers previously published by these authors, mass spectrography has priority in treatment, and in consequence the book gives the reviewer the impression that it is directed mainly to workers with mass spectrographs. It is fair to add that most of the main features of work in mass spectrometry receive at least a mention; but the treatment is not so authoritative, and the inclusion of this work has at times something of a make-weight appearance.

The treatment of applications suggests occasionally that mass spectrographs and mass spectrometers are on an equal footing; whereas, in fact, mass spectrographs are restricted in use mainly to determinations of isotopic mass for nuclear research, and mass spectrometers are applied to a wide variety of problems in research and industry.

Although there are a number of features of interest, this book will be valued chiefly, in the reviewer's opinion, for the detailed theoretical analysis given in chapter 4, where the ion optics of magnetic fields, of electric fields and of both in combination are considered for the direction focusing and velocity focusing of ion beams.

A good bibliography is appended to each chapter, and the quality of the production is satisfactory.

G. P. BARNARD

**Modulators and frequency changers.** By D. G. TUCKER, D.Sc., M.I.E.E. [London: Macdonald and Co. (Publishers), Ltd.] Pp. 232. Price 28s.

Dr. Tucker is a recognized authority on modulators and a book from him on this subject is very welcome. Into it he has compressed much valuable information whilst, at the same time, retaining a very readable style; this latter, in fact, is one of the good features of this book. The author sets out in the introduction the aims and limitations of his material with the result that no valuable space is occupied on elementary matter which can be derived from other, more generalized, text-books. He states that it is not a book on modulation theory but is solely concerned with modulators and he also, wisely, does not include high-power transmitting modulators; furthermore, treatment of practical results is confined to frequencies less than 10 Mc/s. By remaining within the framework thus set out the author undoubtedly strengthens the value of the material presented.

The book is aimed at research, development and maintenance engineers who are concerned with modulators and the author hopes that it will be understood and used by them; the reviewer has every confidence that the book will achieve

this end and can recommend it to every telecommunications engineer.

A. J. MADDOCK

**Stress waves in solids.** By H. KOLSKY. (London: Oxford University Press.) Pp. x + 211. Price 25s.

The theoretical sections of this monograph discuss the classical treatment of stress waves in elastic media and the conditions to be satisfied when waves of dilatation and of distortion arrive at the boundaries between a medium and its surroundings. More recent investigations on waves of large amplitude and on the propagation of stress in plastic media are also included. A careful review follows of practical methods for determining elastic pulses in cylindrical rods, including means for studying their attenuation due to internal friction. The last chapters contain first-hand accounts of experiments on the elastic properties of plastics under high frequency stress conditions and the effects of shock waves on plastics of various shapes.

The treatment given has the virtue of leading the reader logically from well-known elementary propositions in the theory of elasticity to the mathematical results required for the subsequent analysis of experimental data.

This first edition is exceptionally free from printers' errors. Two oversights have been noticed: on p. 200 partial differential signs have been omitted in the expansion (A.9) of  $\text{grad } V$  in generalized co-ordinates; in the table of numerical values,  $C_L$  not being listed in the table of principal symbols used, it requires some search to discover its definition on p. 81 as the velocity of plane longitudinal waves in an infinite plate. These are very minor points which will no doubt be corrected in a second edition.

The book is warmly recommended as instructive and authoritative.

I. I. BERENBLUT

**Mathematical structure of the theories of viscoelasticity.** By B. GRÖSS. (Paris: Hermann and Co.) Pp. 74. Price fr. 600.

The physicist encounters linear phenomena throughout his work. The best known examples are the theories of electrical networks, servo-mechanisms, dielectrics, optical spectra and the mechanical properties of solids, which mathematically are concerned with functions which arise from the solution of a series of linear differential equations with constant coefficients. The author has particularly in mind mechanical properties such as after-effect, creep, relaxation and plastic effects, so he mainly limits himself to systems with only relaxation elements, not oscillators, although he gives fundamental relations which are quite general. These fundamental relations are those between the response to a suddenly applied constant force as a function of time, the response to a sinusoidal force as a function of frequency in phase and amplitude, the response to forces varying with time, the relaxation spectrum or distribution. From any one quantity the remainder can be deduced, so that the Monograph contains a number of important basic equations and methods for their solution. In particular the author deals with the rather difficult problem of deducing the relaxation distribution from an observable response. One might criticize the author for wrongly ascribing certain main relations which were discovered by Maxwell, Hopkinson and early workers on network theory before the dates he gives and for not emphasizing their dependence on the physical, not mathematical, hypothesis of the absence of response in negative time. These are, however, academic points and do not detract from the great value of a short work which includes so much important and useful analysis, to which the author has substantially contributed and which ought to be studied with care and interest.

S. WHITEHEAD



## Notes and comments

### Papers on thermal conductivity problems

We have received a copy of a supplement to the *Bulletin de l'Institut International du Froid* containing a résumé of the 14 papers presented at meetings of Commissions 1 and 2 of the Institut in Louvain in June 1952. These papers are all concerned with problems relating to thermal conductivity particularly at low temperatures.

The *Bulletin* itself which appears six times a year summarizes in French and English the many papers on refrigeration and cognate subjects which appear in journals all over the world. Copies of the *Bulletin* may be obtained from J. Raymond, Esq., Refrigeration House, Victoria Road, Woking, Surrey. The annual subscription is £1 17s. 6d.

### Conferences on nuclear physics and on the solid state—July 1954

The following conferences on physics have been arranged in the week following the meeting in London during 8–9 July, 1954 of the General Assembly of the International Union of Pure and Applied Physics: a conference on experimental and theoretical nuclear physics during 13–17 July, 1954 in the University of Glasgow; a conference on the physics of the solid state, with special reference to defects in solids, during 13–17 July, 1954 in the University of Bristol. Both conferences are arranged in co-operation with the International Union. Further information will be published in due course.

### Journal of the Audio Engineering Society

We have received a copy of the first issue of a new American journal entitled *Journal of the Audio Engineering Society*. This consists of 169 pages measuring  $8\frac{1}{2} \times 11$  in. and contains the 30 papers presented at the Audio Fair held in conjunction with the Fourth Annual Convention of the Audio Engineering Society in New York in the autumn of

1952. A wide range of subjects is covered including tape and wire recorders, musical therapy, choice of electron tubes for audio circuits, resistance-capacitance networks in amplifier design, binaural sound reproduction at home, and network transformations. The journal is produced quarterly under the editorship of Lewis S. Goodfriend. The subscription price is \$8 p.a. and the publication office is 104 Liberty Street, Utica, N.Y.

### Mechanical effects of dislocations in crystals

A conference on the mechanical effects of dislocations in crystals has been arranged by the Department of Metallurgy, University of Birmingham, and will be held on 19 and 20 July, 1954.

### List of preferred valves

The second edition of a list of preferred valves has been compiled by the electrical and electronics section of The Scientific Instrument Manufacturers' Association of Great Britain Ltd. The first edition of this booklet was issued in September 1949 and this revised form is now issued to take into account additions to the range of miniature valves and to delete certain standard-sized valves which are classed by the manufacturers only as maintenance types. Electrometer valves have now been added in both standard and miniature sizes.

The list is divided into two categories, namely, standard-sized valves and miniature valves. In general, the aim in the former has been to concentrate on those types employing the international octal type of base, though this cannot be done for all types that it is necessary to include in the range. For the miniature types those valves without cemented caps on the B7G and B9A bases have been adopted.

Copies can be obtained from the Secretary, The Scientific Instrument Manufacturers' Association, 20 Queen Anne Street, London, W.1, price 3s. 6d. post free.

## Journal of Scientific Instruments

### Contents of the October issue

#### ORIGINAL CONTRIBUTIONS

##### Papers

- A simple direct-reading friction meter. By V. E. Gough.
- An electronic temperature controller. By B. E. Nolting and M. A. Snelling.
- Magnetic electron lens aberrations due to mechanical defects. By G. D. Archard.
- A differential capacitance manometer. By I. G. Baxter.
- A modified Michelson refractometer. By P. G. Guest and W. M. Simmons.
- An improved Rankine magnetic susceptibility balance for use in free radical determinations. By J. O'M. Bockris and D. F. Parsons.
- An instrument for measuring speed fluctuations and a method of calibrating such instruments. By A. Swindells.
- A projector-comparator for examining spectrographic plates. By J. C. North.
- A recording fluxmeter. By R. S. Tebble.
- The design of constant stress cantilevers. By A. J. Kennedy.
- A phase-sequence indicator using back-to-back rectifiers. By J. E. Parton.
- A stable source of high voltage. By L. U. Hibbard and D. E. Caro.
- A modification of the Smith bridge, Type III. By M. Gautier.
- A robust air-flow meter for field use. By D. S. M. Phillips.

##### Laboratory and workshop notes

- An improved form of hysteresis loop plotter for magnetic materials. By A. D. Booth.
- A method of measuring the temperature at the surface of a metal tube. By A. G. Monroe and H. A. S. Bristow.
- A simple method of leak finding using a Pirani gauge. By R. N. Bloomer and M. E. Haime.
- An electro-erosion method of strain-free cutting. By J. A. James and C. J. Milner.
- A tritium monitor. By T. O. Jeffries and M. E. Owen.
- A laboratory stirrer for viscous liquids. By M. D. Ashton.
- Glass to metal seal through aluminium using the Al-Fin bond. By R. Aves.

##### NOTES AND NEWS

##### Correspondence

- An error in the correction formula for the dead time of a Geiger-Müller counter. From S. J. Wyard.
- Note on pen friction with vertical drum recording instruments. From R. H. Eldridge.
- An apparatus for recording surface friction and irregularity. From P. F. D. Naylor.

New instruments, materials and tools

## British Journal of Applied Physics

### Original contributions accepted for publication in future issues of this Journal

- The growth of the liquid bridge in an electrical contact. By P. M. Davidson.
- The preparation and use of cells for the realization of the triple point of water. By C. R. Barber, R. Handley and E. F. G. Herington.
- The theoretical characteristics of bichromatic pyrometers. By H. Herne.
- Characteristics of radioluminescence in crystals. By G. T. Wright and G. F. J. Garlick.
- A photometric method of determining configuration factors. By D. I. Lawson and D. Hind.
- The influence of barometric pressure on watch and chronometer rates. By N. W. B. Stone, K. W. T. Elliott and P. H. Bigg.
- The evaluation of interferograms by displacement and stereoscopic methods. By J. W. Gates.
- Some measurements of the relative dielectric strengths of gases. By N. R. McCormick and J. D. Craggs.
- The high-pressure glow discharge in air. By W. A. Gambling and H. Edels.

THIS JOURNAL is produced monthly by The Institute of Physics, in London, and deals with all branches of applied physics (including theory and technique). All rights reserved. Responsibility for the statements contained herein attaches only to the writers.

**EDITORIAL MATTER.** Communications concerning editorial matter should be addressed to the Editor, The Institute of Physics, 47 Belgrave Square, London, S.W.1. (Telephone: Sloane 9806.) Prospective authors are invited to prepare their scripts in accordance with the *Notes on the preparation of contributions*. (Price 2s. 6d. including postage.)

**REPRODUCTION.** The Institute of Physics is a signatory to The Royal Society's Fair Copying Declaration. Details may be obtained upon application from The Royal Society, London, W.1.

**ADVERTISEMENTS.** Communications concerning advertisements should be addressed to the agents, Messrs. Walter Judd Ltd., 47 Gresham Street, London, E.C.2. (Telephone: Monarch 7644.)

**SUBSCRIPTION RATES.** A new volume commences each January. The charge is 4 per volume (\$11.50 U.S.A.), including index (post paid), payable in advance. Single parts, so far as available, may be purchased at 8s. each (\$1.15 U.S.A.), post paid, cash with order. Orders should be sent to The Institute of Physics, 47 Belgrave Square, London, S.W.1, or to any Bookseller.

# Application of digital computing techniques to physics

By R. A. BROOKER, M.A., B.Sc., Computing Machine Laboratory, University of Manchester

Some computations likely to occur in connexion with physical problems are discussed in relation to electronic computers. General discussion is reinforced by examples taken from the literature, for which figures about programming time, machine running time, etc., are given. Some aspects of machine design are discussed. The article concludes with a note on the training of personnel in the use of electronic computers.

Since the war several large scale electronic computers have been completed in this country and elsewhere, and several more are nearing completion.<sup>(1)</sup> It is therefore an appropriate opportunity to describe some of the ways in which these machines can be of help to physicists.

Before any problem, physical or otherwise, can be "run" on a machine it must first be formulated mathematically and then a method for obtaining numerical results must be found. Only when this has been done can one think about translating the problem into machine terms—*programming*. For this reason it is more convenient to classify problems from the mathematical and numerical point of view than by their physical origin. Thus instead of attempting to enumerate the number of physical systems whose behaviour can be described by Laplace's equation it will be assumed that the reader will be more interested to know how such equations are handled on existing electronic computers.

These machines can be of most value with problems which are amenable to routine treatment. Broadly speaking, this is also the distinction between linear and non-linear problems. This does not mean that the machine is not useful where non-linear problems are concerned, but rather that such problems have to be treated individually; in other words they have to be specially programmed and in practice this may have to be done by the physicist himself. Thus linear problems will be discussed first.

## MATRIX ALGEBRA

The most important linear problems are those involving matrix arithmetic. They include the solution of a set of simultaneous equations, inversion of a matrix and determination of the eigenvalues and vectors of a matrix pencil. Most physical problems are self-adjoint and in this case the matrices are symmetric or Hermitian.

For desk machine purposes the most convenient method of dealing with the first two problems is the method of triangular resolution. It is excellently described in two papers by Fox<sup>(2,3)</sup>. To the writer's knowledge this method has not been used on an electronic computer in England. Instead the method of pivotal condensation is preferred. The reason for this is that the size of the numbers arising in the calculation can be more easily controlled, a matter of importance with fixed binary point machines. However, the former method preserves the symmetry of the matrix and hence needs only the distinct elements of the matrix to be recorded in the store of the machine. In the case of floating binary point machines this method may ultimately be preferable. Whatever method is used, however, matrices of size up to  $20 \times 20$  can usually be handled directly by a machine equipped only with a primary store (see final section). To deal with larger matrices it is usually necessary to make use of some form of secondary storage. With most machines the solution is so rapid—a matter of minutes, or even seconds—that the preparation of the data for the machine is the

most time-consuming part of the business. For this reason unless the data are actual experimental results it may pay to mechanize also the original calculations which give rise to the matrix data.

The eigenvalue problem is the determination of scalars  $\lambda_i$  and vectors  $x_i$  satisfying

$$Ax_i = \lambda_i Bx_i \quad (i = 1, 2, \dots, n) \\ (n \text{ being the size of the matrices}).$$

If  $A$  and  $B$  are real symmetric, then this equation can be transformed<sup>(4)</sup> to the more convenient form

$$Cy_i = \lambda_i y_i \quad \text{where } B = LL' \\ y_i = Lx_i \\ C = L^{-1}A(L^{-1})'$$

For this form an elegant method of solution suitable either for desk or electronic application has been given by Lanczos<sup>(5)</sup> who says "The eigenvalue problem of linear operators is of central importance for all vibration problems of physics and engineering. The vibrations of elastic structures, the flutter problems of aerodynamics, the stability problem of electric networks, the atomic and molecular vibrations of particle physics, are all diverse aspects of the same fundamental problem, *viz.*, the principle-axis problem of quadratic forms."

His method, which is based on the Cayley-Hamilton theorem, determines the characteristic equation as the relation between the  $n + 1$  linearly dependent vectors

$$u, Cu, C^2u, \dots, C^{n-1}u, C^nu, u \text{ being an arbitrary vector.}$$

Instead of constructing this sequence however (which would in general demand an impracticable degree of accuracy), the method uses linear combinations of these vectors to construct an orthogonal sequence

$$b_0 \equiv u_0, b_1, b_2, \dots, b_{n-1}, b_n \equiv 0.$$

The recurrence relations connecting successive members of this sequence provide a means for constructing the characteristic equation. It is necessary to store all the members of this orthogonal sequence and, moreover, to associate scale factors with each vector and carry out part of the calculation with a floating binary point. For this reason the storage requirements both for instructions and numbers are considerable and it is impossible to programme this method unless a secondary store is available. Nevertheless, when these demands are satisfied the method gives excellent results, specially in the difficult case of equal or nearly equal roots.<sup>(6)</sup>

## PARTIAL DIFFERENTIAL EQUATIONS

Since starting to write this article the writer's attention has been drawn to an article by Sheldon and Thomas<sup>(7)</sup> entitled "Applications of Large Scale Computing in Physics." This

latter article deals almost entirely with the partial differential equations of mathematical physics and for this reason attention here will be confined to one small aspect of this subject, namely, linear elliptic equations.

The usual technique is to replace derivatives by finite differences yielding a set of linear simultaneous equations to be satisfied at the mesh points of the region. Fox<sup>(8)</sup> has shown that by taking careful account of the truncation error and using a large interval the number of equations to be solved can be considerably reduced. This is particularly important when the equations tend to be ill-conditioned. The equations can be solved by the methods described above.<sup>(9)</sup> Very often, however, the equations take a particularly simple form, reflected by the presence of a large number of zeros in the matrix of coefficients. For this reason other methods may be more efficient.

Fox developed the aforementioned technique in connexion with relaxation methods which, in these circumstances, are particularly suited to desk machine work. Whether they are to be preferred for machine solution is not yet clear—they are certainly not straightforward to programme. Yet simplicity of coding is becoming less important and emphasis will ultimately be placed on the accuracy and efficiency of numerical methods. For this reason the writer would hesitate to say that relaxation is of no importance with electronic computers. Nevertheless, many of the devices used in relaxation can be regarded as means for reducing the contribution of the dominant eigenvectors to the residual error, and for this reason the writer prefers to recommend the formal treatment on these lines given by Lanczos.<sup>(10)</sup> Lanczos describes a method for the solution of  $Kx = b$ , where  $K$  is a given matrix and  $b$  a given vector. The particular merit of this method is that it is not necessary to know  $K$  explicitly, but only its effect on an arbitrary vector  $u$ . That is, given any  $u$  it is necessary only to have rules for forming  $Ku$ . The method requires only  $n$  applications of the matrix operator  $K$  and  $3n$  working locations,  $n$  being the size of the system.

#### CRYSTALLOGRAPHIC APPLICATIONS

The earliest account of the use of an electronic computer in this field is by Bennett and Kendrew.<sup>(11)</sup> They describe an application of the EDSAC\* to the evaluation of expressions like

$$\phi(x, y) = \sum_0^{h_{\max}} \sum_0^{k_{\max}} F_{hk} \exp \left[ 2\pi i \left( \frac{hx}{a} + \frac{ky}{b} \right) \right]$$

where  $h, k$  take positive integral values, at the lattice points of a rectangular net covering the region  $0 \leq x < a, 0 \leq y < b$ . They also consider the more general three-dimensional case, where

$$\phi(x, y, z) = \sum_0^{h_{\max}} \sum_0^{k_{\max}} \sum_0^{l_{\max}} F_{hkl} \exp \left[ 2\pi i \left( \frac{hx}{a} + \frac{ky}{b} + \frac{lz}{c} \right) \right]$$

They use the method based on the addition law satisfied by the circular functions to express  $\phi(x, y)$  as the sum of terms like

$$\sum_0^{h_{\max}} \sum_0^{k_{\max}} F_{hk} \cos 2\pi(hx/a) \cos 2\pi(ky/b)$$

which are evaluated in two stages. In stage 1 a set of  $(k_{\max} + 1)$  terms:

$$A(k, x) = \sum_0^{h_{\max}} F_{hk} \cos \frac{2\pi hx}{a}$$

\* The Electronic Delay Storage Automatic Calculator is in operation at the University Mathematical Laboratory, Cambridge. See Ref. (12).

for a particular value of  $x$  is computed and stored. These are used in stage 2 to compute values of:

$$\sum_0^{k_{\max}} A(k, x) \cos \frac{2\pi ky}{b}$$

for a whole row of points having the same  $x$  co-ordinate. After stage 2 is completed results are printed and stage 1 recommenced with a value of  $x$  corresponding to a new row.

Because of the limited storage capacity of the EDSAC it is necessary to employ certain tricks in order to accommodate all the terms of a typical two-dimensional synthesis. These devices take advantage of the limited accuracy to which the  $F$ 's are normally represented by "packing" two or three terms in a single number location. Sequences of zeros which often occur in crystallographic data (in which the  $F$ 's are greater than or equal to 0) are indicated in a special way. A row of terms such as

$$+5 \ +16 \ 0 \ 0 \ 0 \ +4 \text{ appear in the machine}$$

$$\text{as} \quad +5 \ +16 \ -3 \ +4.$$

This interpretation of the numerical data involves only a trivial extension of instructional data.

For time economy reasons the values of the cosines are selected from a table held in the store. The tabular data is not large because there are only a limited number of values of the argument  $hx/a \pmod{\pi/2}$ . Thirty-three entries are used. The extension of the programme to deal with signs corresponding to arguments in other quadrants is small.

The authors give times of operation for an example involving the evaluation of a single expression of the factored form (Whale myoglobin, c projection of  $P2_12_12_1$ ).

Number of terms ( $F_{hk}$ ) = 260

Size of net =  $17 \times 33 = 561$  points

Computing time 16 min

Printing time 14 min

The loss of time incurred by the operations necessary for unpacking the data is negligible.

The three-dimensional case. In this case there are now three stages in the computation. The first stage is, for a given  $z$  layer, to reduce the synthesis to a two-dimensional synthesis. The terms of this synthesis will be quantities like

$$A(h, k, z) = \sum_0^{l_{\max}} F_{hkl} \cos 2\pi \left( \frac{lz}{c} \right)$$

As it is barely possible to accommodate in the store all the terms of a typical two-dimensional synthesis it is out of the question to store the original  $F$ 's which may number up to 3000. Instead it is necessary to feed in the  $F$  values anew for each  $z$  layer of the synthesis. The authors give an example:

Number of terms  $F_{hkl} = 1288$  ( $h_{\max} = 16, k_{\max} = 10, l_{\max} = 8$ );

Size of net =  $33 \times 33 \times 17 = 18\ 513$  points.

The computing times were as follows:

For each  $z$ , time to take in terms and carry out stage 1, 5 min; time to carry out stages 2 and 3, 15 min; time to print results, 12 min. Total time for whole computation =  $17(5 + 15 + 12) = 9\ h\ 4\ min$  (of which about 50 min is spent in packing and unpacking data).

These results serve to illustrate the general rule that convenience, equipment and time are interchangeable quantities. Thus in the above example time can be saved by: (a) having sufficient storage capacity so that the need to pack data is avoided; (b) having more elaborate output facilities;



(c) economizing on the information printed by, e.g., printing only a single character to describe the magnitude of the  $\phi$  function at each point. On the other hand, the advantage of storing all the original  $F$ 's is less marked. In the above example improved access to the  $F$ 's could at the best only affect a fraction  $5/(5 + 15 + 12)$  of the total time. It only begins to be advantageous when used in connexion with other time economy devices.

# DIFFERENTIAL SYNTHESSES

Another aspect of the three-dimensional case has been developed by Ahmed and Cruickshank<sup>(13)</sup> using the MUEC MK II.\* This involves the evaluation of differential syntheses, i.e. expressions of the form

$$\phi, \frac{\partial \phi}{\partial x}, \frac{\partial^2 \phi}{\partial x^2}, \frac{\partial^2 \phi}{\partial x \partial y}, \text{ etc.}$$

A further difference is that these quantities are needed not at the lattice points of a net, but at a limited number of spot values of  $x, y, z$ . For this reason it is convenient to adopt an alternative computing scheme. The values of the expressions are built up for all the points of the set simultaneously. The values of the  $F$ 's are punched on the input tape in an ordered sequence (with respect to their  $h, k, l$  indices) and read into the store one at a time. As each term is read from the tape its contributions

$$F_{hk} \cos 2\pi \left( \frac{hx_i}{a} + \frac{ky_i}{b} + \frac{lz_i}{c} \right) - \frac{h}{a} F_{hk} \sin 2\pi \left( \frac{hx_i}{a} + \frac{ky_i}{b} + \frac{lz_i}{c} \right)$$

to the values of  $\phi, \partial\phi/\partial x$ , etc., at the points  $x_i, y_i, z_i$  are evaluated and accumulated with the corresponding partial sums. After the final  $F$  is read from the tape and treated the sums are all completed and are then printed. With this method it is not necessary to store the  $F$ 's inside the machine. It was not chosen for this reason, however—the MUEC MK II is not restricted in storage capacity—but because it was also the simplest in other respects.

This example illustrates how "large" problems could be run on machines with limited storage capacity.

# ORDINARY DIFFERENTIAL EQUATIONS

Many physical laws and descriptions of physical systems take the form of differential equations. In many cases their numerical integration is very suitable for machines equipped only with a primary store. The earliest account of a general method, suitable for use with an electronic computer, for treating sets of first order simultaneous equations with given initial conditions is due to Gill<sup>(15)</sup> who developed a modification of the Runge-Kutta method. The convenience of this method is that the storage requirements are kept to a minimum and no special method is needed for starting the solution. This has now become a standard process on most machines. It requires the user to draw up a programme which, given the values of the dependent variables, will compute and place suitably scaled values of the derivatives in pre-assigned storage locations. There are several published accounts of applications of this and other methods. One of these<sup>(16)</sup> will be described here.

*Example 1.* Naur describes an application of the

EDSAC to integrating step-by-step the equations of motion for the minor planets taking into account the attraction of all the major planets. The equations of motion are the Newtonian laws formulated with respect to Cartesian co-ordinates with origin at the sun. These are characterized by the absence of first time derivatives and it is possible to use the well-known central difference method described by Hartree.<sup>(17)</sup> The details of the method will not be discussed further. The main point of interest lies in the means adopted for calculating the perturbation terms. The equations of motion are

$$x'' = -\frac{w^2 k^2 x}{r^3} + \sum_{\text{Major planets}} w^2 k^2 m_{pl} [-(x - x_{pl})\rho^{-3} - x_{pl}r_{pl}^{-3}]$$

with similar expressions for  $y$  and  $z$ , and where

$$\rho^2 = (x - x_{pl})^2 + (y - y_{pl})^2 + (z - z_{pl})^2$$

At each step it is necessary to know the values of the co-ordinates of the seven major planets—21 quantities. Because of the restricted storage capacity it is not possible to retain in the machine the values for every step of the integration. Instead the planetary data is recorded (i.e. punched) on the input data tape in an order corresponding to the consecutive steps of the integration. The programme, which is held in the primary store, is arranged to read each set at the beginning of the corresponding integration step, each set being recorded in place of the previous set which is no longer required.

It may be of interest to reproduce Naur's figures for the times of operation of this programme and the comparison with desk machine methods.

Preparation of planetary data tape	4 h
Integration over 20 steps (this is repeated once as a check so that the total time for this part is 30 min)	15 min
Sundry fiddling	13 min
Total time for 20 steps	4½ h
Average time for one step	14 min

The final figure is 10% of the time required for a desk calculation. The actual running time on the machine is only 2½% of the time for a desk calculation. This latter figure may be taken as fairly typical of the performance of these machines on this sort of problem—it may actually vary between ½% and 3% but improvement of the lower figure is possible only in very favourable circumstances. In this particular problem the overall saving of time is reduced because there is the additional work of punching the data tape. Similar items in other applications should not be overlooked. This example is a further illustration of how a problem which at first sight appears to involve a large amount of data can nevertheless be handled by machines with restricted storage capacity.

# SAMPLING METHODS

The next example illustrates an approach which can sometimes be used when the mathematical formulation of the problem leads to intractable equations. The idea is to set up a mathematical model of the physical system to be studied. Its behaviour in a very large number of different circumstances is assessed by studying its behaviour in a small proportion of the circumstances. As the accuracy of this approach is related to the square root of the sample size so it only becomes feasible with an electronic computer. In the U.S.A. they are called Monte Carlo Methods and an account of some

\* The Manchester University Electronic Computer MK II. See Ref. (14).

applications can be found in an N.B.S. report (Ref. (18), p. 19) from which the following example is taken.

**Example 2.** The problem relates to the behaviour of neutrons diffusing in a medium in which collisions take place. The medium consisted of eight zones of different materials each with different mean free paths and different probabilities of the events occurring in a collision. In each zone a collision can lead to any one of four events; absorption, elastic or inelastic scattering, fission. The relative probabilities of these events in each zone depend on the collision velocity and are given by tabular data. By computing the life history of a sufficiently large sample of neutrons an estimate can be made of, e.g., the shielding properties of the material with respect to neutrons originating from some definite region of phase-space. The position and velocity of a neutron are described by spherical polar co-ordinates, and the logarithm of a random number  $j$  (equi-distributed between 0 and 1) gives the distance to the next collision by  $d = -\lambda \log j$ , where  $\lambda$  is the mean free path. Normally  $d$  gives the actual place of the collision, but it is necessary to compute whether this has brought the neutron into a new zone. If so, then the procedure is repeated with the mean free path of the new zone. If crossing the zonal boundary amounted to escape from the entire assembly, a record is printed and the next neutron processed. A random number selects the type of collision from the probability data corresponding to the collision velocity. In the case of absorption a record or "tombstone" with the vital statistics is printed. In case of scattering a new random velocity direction is chosen. If the scattering was elastic the velocity magnitude is considered unchanged; otherwise it is degraded by an amount selected from the probability data by a random digit. In the case of fission the multiplicity is determined by a single random digit. The details of the fission neutrons are recorded as they have to be processed again. For these neutrons random numbers determine a direction, and select a velocity magnitude from the fission spectrum.

It follows that the task of following the fortunes of a particular neutron is partly arithmetical and partly of a book-keeping nature. Both kinds of operations are well suited to electronic computers. The computer needs to have random numbers available and a great deal of attention has been given to generating pseudo-random numbers of definite arithmetical processes [Ref. (18) pp. 31–38]. The MUEC MK II incorporates a physical random number generator (based on the thermal noise in a resistor) which, in response to a single instruction, places a random number in the accumulator of the arithmetical unit. The advantage of pseudo-random numbers lies in the possibility of repeating results. This is important because it is sometimes necessary to know if the machine is behaving consistently.

#### A FINAL EXAMPLE

**Example 3.** The last example taken from the literature is an application to radio physics.<sup>(19)</sup>

The author treats the propagation of an atmospheric by considering the space between the earth and the ionosphere as a wave-guide. The EDSAC is used to obtain numerical results for the particular case where the surface of the earth is assumed to be perfectly conducting and the ionosphere to be a homogeneous ionized medium with the steady magnetic field of the earth superimposed. The numerical work amounts to finding two roots of the following transcendental equations:

$$\alpha = hkC(C = \cos) \quad (1)$$

$$\sin i = \mu_0 \sin \theta_0 = \mu_e \sin \theta_e \quad (2)$$

$$\mu_0 \mu_e \tan^2 \alpha - j \tan \alpha (\mu_0 + \mu_e) \frac{(C^2 + \cos \theta_0 \cos \theta_e)}{C(\cos \theta_0 + \cos \theta_e)} - 1 = 0. \quad (3)$$

The method of solution was as follows. A trial value of  $C$  was assumed and from it the values of  $\cos \theta_0$  and  $\cos \theta_e$  were calculated using equation (2). The quadratic was then solved for  $\tan \alpha$  from which  $\alpha$  was calculated giving a revised value for  $\tan \alpha$  by equation (1). The process was repeated until a self-consistent solution was obtained. Solutions were required for various values of the parameters  $\mu_0$  and  $\mu_e$ .

In the above reference no details are given about the machine aspect of the solution, but the present writer was closely associated with the actual programming work. The entire calculation was carried out with a floating binary point with complex numbers represented in the form  $a2^p + ib2^q$ . Apart from a floating-point routine little previous programming experience was available in the form of ready-made library routines and most of the programme was original. The amount of numerical data stored was negligible compared with the volume of instructions and this was so large that it was necessary to store the instructions of the master routine on tape and read them one by one—repetitive sequences being multiply punched. Use was made of *interpretive techniques*,<sup>(20)</sup> each "instruction" of the master routine initiating a considerable amount of computing. Thus the loss of time incurred by storing the master routine on tape is not as great as might otherwise be supposed. For each set of values of the parameters the solution required approximately 15 min of machine time. The biggest obstacle, however, was the time spent in drawing up the programme—approximately 3 man-weeks.

#### SOME ASPECTS OF MACHINE DESIGN

It may be of interest to examine, in the light of the foregoing examples, what desirable features an electronic computer should embody. Some aspects of two features, namely the store and the arithmetical unit, will be discussed.

**The store.** The storage requirements for an ideal machine, namely, indefinitely large capacity with immediate\* access to any item of information, can only be economically achieved by making use of a two-level storage system. In this scheme a *primary* store, in which a restricted amount of information is immediately accessible, is backed by a *secondary* store with restricted access to a much larger amount of information. Facilities are provided for transferring blocks of information in either direction between the two stores. If this operation is relatively infrequent, then it need not be very fast. To elaborate, if  $T$  is the average period between references to the secondary store, then there is at most a factor of 2 between the ultimate efficiencies in the extreme cases where the transfer operation takes time  $T$  and where it takes zero time. The less frequently recourse to the secondary store is necessary, then the less stringent need be the access facilities at this level. It is important to realize that the relation between size of primary store and frequency of reference to the secondary store is essentially a non-linear one: if the primary store is doubled, then references are cut by more than half and, in general, by very much more than half. Ultimately there comes a point where the input and output facilities will suffice and it becomes possible to telescope these functions with those of secondary storage. With this in mind the possible alternatives for secondary storage and input-output

\* By "immediate" is meant "in a time comparable to that of an arithmetic operation."



media are: punched paper tape (*A*); punched cards (*B*); magnetic tape (*C*); and magnetic drum (*D*). It is difficult to assess the relative costs of these items but the first is definitely the cheapest and the last the most expensive.

The term output is used here in a general sense. The form of output ultimately required is a printed sheet, but on most machines punched tape or punched cards provide the only form of output directly connected to the machine. The tape or cards are then printed by means of a separate unit removed from the machine.

The important features of these items are as follows. With *A*, *B*, and *C* the access time for all blocks of information is not the same, e.g., in the case of *B* cards far removed from the card feed will take a correspondingly long time to find. On a magnetic drum, however, the blocks are arranged in parallel and immediate access is possible to any block. With *B* and *D* each block is (in the most convenient arrangement) of the same size, but with *A* and *C* the size of the blocks which can be transferred is at the users' discretion. This is important because numerical data and instructional information does not naturally divide itself into groups of a particular size. Moreover, the use of partially filled blocks of information leads to wastage in the primary store. A restrictive feature of punched cards is that it is not possible to read and punch cards in the same deck. Similar considerations apply to punched tape.

What conclusions can be drawn about the storage requirements for the type of problem discussed in the first part of this article? Many of these problems involve large amounts of numerical data which can almost always be ordered in some way. For example, when dealing with a matrix one selects the rows or columns not at random but in a definite sequence. It is this property which enables them to be handled by a machine equipped only with a primary store and using tape as a form of secondary storage. It seems reasonable to suppose that this is a characteristic feature of all large-scale calculations and to conclude that a secondary store with the accessibility characteristics of magnetic tape will suffice in general. This conclusion must be qualified, however, because the examples selected above relate to machines where the instructions are selected at approximately 600 per second from a primary store of capacity  $2^9$  words (1 word  $\equiv$  1 instruction, 2 words  $\equiv$  1 number).

If the accessibility characteristics of the primary store were improved by a factor of 10 then magnetic tape would play the same role as paper tape plays with current primary storage systems. In such a case it would be necessary to either increase the size of the primary store—thus reducing the number of references to the secondary store—or to speed up the passage of the magnetic medium in some way. This can only be achieved by using the higher peripheral speed of a magnetic wheel. This virtually amounts to using a magnetic drum.

There may exist problems for which the basic cycle is too large to be contained in the primary store; in such cases no advantage can be taken of the repetitive nature of the calculation and it becomes necessary to refer to the secondary store at least once during every cycle. The consequences of this may be disastrous with a tape-controlled machine. A parallel-track magnetic drum however provides large secondary storage capacity with reasonable access (50 instr. time units) to any item. Thus with the MUEC MK II virtually any problem can be handled with reasonable efficiency. If magnetic tape is used as a secondary store, then it may be necessary to increase the capacity of the primary store to  $2^{10}$  or even  $2^{11}$  words as a safeguard.

*The arithmetical unit.* All existing electronic machines make use of fixed-binary point arithmetical units. It is likely that some future machines will handle numbers expressed in the floating binary form  $a2^p$ , where  $a$  is expressed to a given number of significant digits. The necessity or otherwise from the programmer's point of view is a controversial topic, but a consequence of such a facility would be to increase the effective capacity of the store. The reason for this is two-fold. In the first place since each instruction initiates more real work less of them are required for a given task. Secondly a floating representation is the most economical way of representing numbers within a given range to a given accuracy. In the case of Example 3 a floating point arithmetical unit would have greatly economized both programming time and machine running time.

#### TRAINING OF PERSONNEL

This section is concerned with the human aspect of programming. Everything depends on the organization surrounding the computer. The machine may be the nucleus of a large permanent staff of skilled programmers by whom all problems for the machine are prepared. If a physicist is fortunate enough to be able to avail himself of such a service then the human aspect will not worry him. It is likely, however, that some machines will be located in places where the permanent staff will not be sufficient to keep the machine fully occupied. In these circumstances the machine may be made available to representatives of other organizations. Such persons, after some initial instruction from the resident staff, will be able to programme their own problems. It is in this way that many skilled programmers have obtained their experience. It may be of interest to conclude with some remarks on the training of personnel for this task. It is convenient to distinguish three stages in "running" a problem on an automatic digital computer, namely, finding a numerical method, translating this into machine terms, and finally running off results. The relative importance of these stages may vary considerably. In many cases all three stages can be and are carried out by a single research worker. This was particularly the case in the earlier history of these machines.

The first stage is, properly, the province of the (pure) mathematician and the last can often be done by unskilled assistants. It is the middle step that is the task of the programmer. If the problem is to be arranged in the most efficient way then the numerical method chosen should take into account any special features of the machine, such as, e.g., a fast multiplier or a very slow divider. For this reason the tasks of the numerical analyst and the programmer cannot be entirely separated.

The programmer is concerned with translating the necessary numerical processes into sequences of the basic operations which the machine performs. He or she must therefore be familiar both with the numerical analysis and the logical organization of the machine. The programmer's task can be alleviated to a certain extent by the existence of prefabricated complexes of instructions called *routines* which effect the more common numerical processes, such as, for example, the calculation of trigonometric functions.<sup>(21)</sup> Nevertheless, a programme of average complexity may involve the writing down of over 1000 original instructions. The task of drawing up the final programme with as few mistakes as possible and the subsequent elimination of those remaining calls for a painstaking regard for a wide variety of detail in addition to the creative ability needed to build the programme. More-



over, the programmer should be prepared to improvise rapidly in certain circumstances. For example, when the machine is only partially serviceable the programmer may be called upon to make some alteration to his programme so as to avoid using the particular unit which is malfunctioning.

The time taken for a person to become usefully familiar with an electronic computer varies from 1 to 3 months, depending on the person's ability, previous training and the logical complexity of the machine. An honours degree, not necessarily in mathematics, is a prerequisite. As the programmer becomes more experienced the time taken to make and perfect a programme for a given calculation will decrease until, after several months, his or her optimum is achieved. This naturally depends on the complexity of the calculation, but any period from 1 week to 6 weeks is reasonable.

Because of the high cost of maintaining an electronic computer it does not pay to assign any but the highest grade personnel to the task of programming. Otherwise the figures given above may be exceeded and final programmes may be inefficient and awkward to use, an important matter if they are to be handed over to unskilled assistants to "run."

## REFERENCES

- (1) See *Mathematical Tables and Other Aids to Computation* (Washington: National Research Council) which is published quarterly.
- (2) FOX, L. *J. Roy. Stat. Soc. (B)*, **12**, p. 120 (1950).
- (3) FOX, L. *J. Roy. Stat. Soc. (B)*, **13**, p. 83 (1951).

- (4) FOX, L. *Quart. J. Mech. Appl. Math.*, **5**, p. 178 (1952).
- (5) LANCZOS, C. *J. Res. Nat. Bur. Stand.*, **45**, p. 255 (1950).
- (6) LANCZOS, C., and others. *J. Res. Nat. Bur. Stand.*, **47**, p. 291 (1951).
- (7) SHELDON, J., and THOMAS, L. H. *J. Appl. Phys.*, **24**, p. 235 (1953).
- (8) FOX, L. *Proc. Roy. Soc., A*, **190**, p. 31 (1947).
- (9) KARLQUIST, O. *Tellus*, **4**, p. 374 (1952).
- (10) LANCZOS, C. *J. Res. Nat. Bur. Stand.*, **49**, No. 1 (1952).
- (11) BENNETT, J. M., and KENDREW, J. C. *Acta Cryst.*, **5**, p. 109 (1952).
- (12) WILKES, M. V., and RENWICK, W. *J. Sci. Instrum.*, **26**, p. 385 (1949).
- (13) AHMED and CRUICKSHANK. *Acta Cryst.* (In press) (1953).
- (14) KILBURN, T. *Nature [London]*, **168**, p. 95 (1951).
- (15) GILL, S. *Proc. Cambridge Phil. Soc.*, **47**, p. 96 (1951).
- (16) NAUR, P. *Monthly Not. Roy. Astron. Soc.*, **111**, p. 609 (1951).
- (17) HARTREE, D. R. *Numerical Analysis*, p. 126 (London: Oxford University Press, 1952).
- (18) *Monte Carlo Method, Applied Math. Series*, 12 (Washington: National Bureau of Standards, June 1952).
- (19) BUDDEN, K. G. *Phil. Mag.*, **53**, p. 1179 (1952).
- (20) BROOKER, R. A., and WHEELER, D. J. *Math. Tables Aids Comput.*, **7**, p. 37 (1953).
- (21) WILKES, M. V., WHEELER, D. J., and GILL, S. *The Preparation of Programs for an Electronic Digital Computer* (Cambridge, Mass.: Addison-Wesley Press Inc., 1951).

## The use of radioactive isotopes in metallurgy

By R. SHUTTLEWORTH, B.Sc., Ph.D., Metallurgy Department, University of Leeds

The  $\gamma$ -radiation from radioactive isotopes is used for radiography, and the  $\beta$ -radiation for gauging the thickness of foils or, by back-scattering, the thickness of a coating on a base metal. The high sensitivity and ease with which isotopes can be detected and measured provides an easy method of estimating minute amounts of metal that have been labelled by pile irradiation. The most important metallurgical use of isotopes is in the measurement of self-diffusion coefficients, and a technique is described by which the two self-diffusion coefficients of copper and zinc in brass have been determined simultaneously. A number of methods of estimating activity are briefly described (Geiger-, proportional- and scintillation-counters, and microautoradiography).

It has been commented<sup>(1)</sup> that during the ten years' operation of nuclear piles the abundant supply of radioactive isotopes has not yet made possible a single great discovery. In metallurgy this is no less true than in biology; indeed, the important advances in the understanding of diffusion<sup>(2)</sup> have arisen, not from self-diffusion experiments, but from the measurement of Kirkendall displacements, and from the mechanical damping due to the movement of interstitial atoms. However, the availability of radioactive cobalt now enables even the smallest foundry to radiograph prototype castings; and increasingly in experimental work radioactive isotopes are being used, sometimes because they are essential but more often because they provide the easiest method of doing a particular piece of work. This casual use of isotopes will increase because there are becoming available<sup>(3)</sup> low-voltage halogen-quenched Geiger counters, high-tension units stabilized by corona discharge tubes, and cold cathode scaling units, which will make the electronic apparatus needed for measuring activity cheaper and more reliable. Furthermore, there are an increasing number of young

graduates who have used isotopes in exercises and research problems and who naturally turn to these methods.

In metallurgy, isotopes are used as convenient sources of  $\beta$ - and  $\gamma$ -radiation for radiography and for thickness gauging. A second class of use arises since after irradiation in a pile, or now less usually by a cyclotron, metals become radioactive and can be readily detected with a sensitivity greater than that provided by a spectrograph. A very real advantage of using radioactive isotopes is that since one is dealing with elementary nuclear phenomena the sensitivity of the measurement can be accurately predicted; indeed, the measurement of activity is usually the least difficult part of an experimental investigation.

### $\gamma$ -RAY RADIOGRAPHY AND THICKNESS GAUGES

Radioactive isotopes decay with the emission of  $\beta$ - and  $\gamma$ -rays.  $\gamma$ -rays will penetrate up to several inches of steel and so are used for radiography and the measurement of the thickness of steel strip.  $\beta$ -rays, depending on their energy, are absorbed by about  $10^{-2}$  in. of metal and are used for

gauging the thickness of thin foils or, by back-scattering, the thickness of coating on a base metal.

The isotopes used in industrial radiography<sup>(4)</sup> are  $^{170}\text{Tm}$ ,  $^{192}\text{Ir}$ ,  $^{182}\text{Ta}$  and  $^{60}\text{Co}$ , and their properties are summarized in Table 1.

$^{60}\text{Co}$  is used for making radiographs of 2-6 in. of steel,  $^{192}\text{Ir}$  for  $\frac{1}{2}$ -1 in. steel, and the 0.084 MeV  $\gamma$ -rays from  $^{170}\text{Tm}$  are used for the radiography of light alloys. The advantages of these isotopes over an X-ray apparatus are their smaller cost, their independence of power supplies and their small size. They are used in small foundries whose output would not be sufficient to occupy fully an X-ray set, to examine welds on sites without a power supply, and for insertion into inaccessible places such as the interior of pipes. However, longer exposures are required than with an X-ray set.

An important problem is the continuous measurement of the thickness of hot steel strip as it is rolled. Fearnside<sup>(5)</sup> has described an instrument that measures the thickness of strip up to 0.15 in., by the  $\gamma$ -radiation emitted by  $^{60}\text{Co}$  and back-

material occurs. Indeed, after irradiation, chemical manipulation is often simplified by the addition of inactive carrier.

Table 2. Sensitivity of detection after pile irradiation

Element	Half-life	Sensitivity
Calcium	152 d	4 $\mu\text{g}$
Copper	12.8 h	0.004
Iron	47 d	24
Manganese	2.6 h	0.003
Phosphorus	14.3 d	1.0
Silver	7.5 and 225 d	0.2
Sulphur	87.1 d	252.0

A classic use of isotopes is the measurement of the small amount of metal that is transferred when two pieces of metal are rubbed together; this is an important problem in the study of friction,<sup>(8)</sup> the wear of tool tips in machining, and the wear of dies in wire-drawing.<sup>(9)</sup> The usual technique is to irradiate one piece of metal, and then measure by means of a Geiger counter or by autoradiography the amount of activity transferred to the second piece after rubbing. An advantage of autoradiography is that it enables an estimate to be made of the size and distribution of the particles that are transferred.

A method of estimating the vapour pressure of a metal is to measure the amount of metallic vapour that in a vacuum effuses from a small hole in a furnace. Schadel and Birchenall<sup>(10)</sup> used activated silver and condensed the vapour which effused from the furnace on a cold target, the weight was found by comparing the activity to that of 20  $\mu\text{g}$  of the same silver. Philbrook, Goldman and Helzel<sup>(11)</sup> used active calcium in an attempt to measure the small amount of calcium that may dissolve in molten steel from calcium slag. They were not able to detect any calcium in the steel and concluded that if any were present the amount was less than 6.0 p.p.m.

Brown and Goldberg<sup>(7)</sup> used pile irradiation and activity measurement as a method of estimating trace elements in meteoric iron. Their procedure was: (1) A portion of the substance to be analysed is irradiated in the pile, together with a standard consisting of a known weight of the element being determined. (2) The unknown is dissolved and a known weight of the element being determined is added to the solution. (3) The element added is chemically processed in order to free it from the activities associated with other elements present in the unknown. (4) The chemical yield of the procedure is determined. (5) The activity of the element in the unknown is compared with that of the standards. (6) The purity of each activity is checked by measurements of half-lives and absorption spectra. By this method Brown and Goldberg found that they could estimate gallium and palladium contents of 50 p.p.m. and 2 p.p.m. in iron meteorites to within an accuracy of a few per cent. This method of analysis provides an accurate method for estimating sodium in aluminium.<sup>(12)</sup>

In industry, the rate of flow of material through reaction vessels is checked by including a tally with the charge. The ease and sensitivity with which a small amount of a  $\gamma$ -emitter, such as  $^{60}\text{Co}$ , can be detected often makes a radioactive tally more convenient than a coloured tally. Radioactive tallies are particularly useful at high temperatures and in chemically reactive atmospheres such as occur in blast furnaces. Voice<sup>(13)</sup> has measured the transit times of solids through a blast furnace by including a small pellet of  $^{60}\text{Co}$  in a lump of ore and measuring the activity of the pig iron with a scintillation counter. He measured the rate at which gases pass through the furnace by instantaneously injecting a small amount of

Table 1. Isotopes used in radiography

Isotope	Half-life	$\gamma$ -energy	Saturation activity at pile factor 1
Thulium 170	127 d	0.084, 0.20, 0.3 MeV	1.03 counts/
Iridium 192	70 d	0.19-0.615	3.4 gm
Tantalum 182	120 d	1.13, 1.22	0.19
Cobalt 60	5.3 y	1.17, 1.33	0.83

scattered from the strip into a scintillation counter. The accuracy of the gauge is  $\pm 1\%$ . An advantage of a back-scattering gauge over a transmission gauge is that the counts depend linearly (up to 0.15 in.) and not exponentially on the thickness. To measure the thickness of thin foils the pure  $\beta$ -emission from  $^{14}\text{C}$ ,  $^{204}\text{Tl}$ , or  $^{90}\text{Sr}$  ( $E_{\text{max}}$  respectively 0.16, 0.78, 1.46 MeV) is used either for transmission or back-scattering gauges.

The absorption of  $\beta$ -rays is essentially independent of the atomic number of the absorber, whilst the amount of back-scattering of  $\beta$ -rays increases with increasing atomic number. So that when the plating and the base metal are of different atomic numbers, e.g. Sn(50) and Fe(26), the amount of  $\beta$ -ray back-scattering will depend upon the thickness of the plating. Seligman<sup>(6)</sup> has shown that by this method the thickness of tin-plate on iron can be estimated to within  $10^{-4}$  in.

#### APPLICATIONS DEPENDING ON EASE AND SENSITIVITY OF DETECTION

When an element is irradiated with neutrons in a pile, radioactive isotopes of the same element are formed by a ( $n, \gamma$ ) reaction (although  $^{14}\text{C}$  is produced by a ( $n, p$ ) reaction from  $^{14}\text{N}$ ). These isotopes, whose half-lives are usually of the order of days, decay with the emission of  $\beta$ - and  $\gamma$ -radiation which can readily be detected and measured by Geiger counters. The sensitivity of detection varies widely from element to element, but it is usually high; in Table 2, due to Brown and Goldberg,<sup>(7)</sup> are indicated the minimum quantities of the elements that can be detected after irradiation in a pile for one week at pile factor 10 ( $10^{12}$  neutrons per  $\text{cm}^2$  per sec), but of course the precise sensitivity of detection will depend upon the counting technique that is used. The activity increases with the time of irradiation, but saturation occurs after about two half-lives. Perhaps the most important advantage of using radioactive isotopes to detect and measure small quantities of elements is that the measurement is not affected if, after irradiation, contamination by inactive



radon in the tuyeres and measuring the activity of the gas samples extracted at the top of the furnace. In order to measure the rate of wear of the refractory lining of the furnace, which is about 2 ft thick, Voice placed pellets containing  $^{60}\text{Co}$  at various depths in the lining and detected when they fell into the furnace by means of a portable Geiger counter on the outside of the furnace. These problems could probably have been solved by other methods, but the use of isotopes was quick and did not involve meticulous experiment or delicate apparatus.

#### SELF-DIFFUSION IN METALS AND ALLOYS

The first use of radioactive isotopes in metallurgy was that of Hevesy and Obtrutsheva<sup>(14)</sup> who in 1925 measured the rate of self-diffusion in lead by means of the natural isotope  $^{212}\text{Pb}$  (Th B), and it is in the study of diffusion that radioactive isotopes make their most unique contribution to metallurgy.

Diffusion arises because of the movement of atoms in a metal and, usually, this movement occurs by the interchange of an atom with a neighbouring vacancy. If a metal or alloy is chemically homogeneous the movement of all the atoms and vacancies will be at random. Because of this random motion the displacement of any particular atom (labelled by being a radioactive isotope) is proportional to the square root of the time; and if at time  $t = 0$  there is a point, line, or area source of labelled atoms then after a time  $t$  the ratio of the concentration at a distance  $r$  to that at the origin is  $c/C_0 = \exp[-(r^2/4D_A^*t)]$ , where  $D_A^*$  is defined as the self-diffusion coefficient of the component  $A$ .  $D_A^*$  is simply related to the jump frequency  $\nu_A$  with which an atom moves to neighbouring lattice points,  $D_A^* = \alpha \nu_A a^2$ , where  $\alpha$  is  $\frac{1}{6}$  and  $\frac{1}{12}$  respectively for body- and face-centred cubic structures of lattice constant  $a$ . There is thus a different self-diffusion coefficient and atomic jump frequency for each of the components of an alloy. The thermodynamic driving force that causes the reduction of the gradient of labelled atoms arises, of course, from the entropy of mixing.

The chemical interdiffusion of two different metals, although the practically important phenomenon, is far more complicated than self-diffusion. During chemical interdiffusion there is a chemical gradient, so that the driving force for interdiffusion arises not only from the entropy of mixing, but also from the different potential energies of atoms at different chemical compositions. Thus, superimposed upon the random motion of atoms and vacancies there is a drift velocity up or down the chemical gradient. If, as usually occurs, the chemical gradient is not constant in place and time, this drift of vacancies will produce excess vacancy concentration in some places and a deficit in others. The equilibrium vacancy concentration is maintained by the creation and annihilation of vacancies at pores and dislocations, producing changes in the external dimensions and displacement of markers (Kirken-dall effect). From a chemical interdiffusion experiment it is possible to obtain a chemical diffusion coefficient for each of the components of a binary alloy *only* if the marker displacement can be measured as well as the concentration-distance curve.

The single self-diffusion coefficients of many pure metals have been measured. The method used is to plate a thin layer of radioactive metal on to the specimen and to measure how far it diffuses into the interior after annealing for a known time. For values of  $\sqrt{(4D^*t)}$  greater than  $\frac{1}{2}$  mm the most accurate method is to cut off sections in a lathe and from the measurement of the activities obtain the activity-distance curve. It should be noted that the value of  $D^*$  depends only

on the ratio  $c/C_0$  so that it is necessary only to measure relative activities. The accuracy with which  $D^*$  can be estimated depends upon how far from the origin measurements can be made so that the sensitivity of activity measurements is invaluable. When an isotope emits mostly radiation that is absorbed by a thickness of metal comparable to the diffusion distance (e.g.  $^{55}\text{Fe}$  decays by K-capture and emission of a readily absorbed X-ray) then it is sufficient to measure the decrease of activity due to the increased absorption as the isotope diffuses into the interior. By this method, Frauenfelder<sup>(15)</sup> determined very small penetration distances since he measured the recoil atoms which are absorbed by a much smaller thickness of metal than are electrons or X-rays. Hoffman<sup>(16)</sup> has reviewed the experimental methods used to determine the self-diffusion coefficients of pure metals.

In the study of diffusion in binary solid solutions the fundamental problem is understanding the different interaction of vacancies with the two kinds of atoms: it is important to know the different activation energies needed for the two kinds of atom to interchange with a vacancy, and how the energy to form vacancy depends upon the numbers of atoms of each kind that surround it. This understanding is best obtained from a knowledge of the jump frequencies of the two kinds of atom as a function of temperature and composition; and perhaps the most important result is the ratio of these jump frequencies.

Johnson<sup>(17)</sup> has measured separately the two self-diffusion coefficients in 50/50 Ag/Au alloys and finds that the ratio of jump frequencies  $\nu_{\text{Ag}}/\nu_{\text{Au}} = 2.5$ . Inman<sup>(18)</sup> and Johnston<sup>(19)</sup> have measured the self-diffusion coefficients of copper and zinc in  $\alpha$  and  $\beta$  brass. Inman finds that for 55/45  $\beta$ -brass  $\nu_{\text{Zn}}/\nu_{\text{Cu}} = 1.9$ , whilst Johnston finds that for 70/30  $\alpha$ -brass  $\nu_{\text{Zn}}/\nu_{\text{Cu}} = 3.2$ . The technique of Inman and Johnston is to irradiate a brass foil so as to produce radioactive copper and zinc, weld this foil between two disks of the same chemical composition, and after a diffusion anneal cut off sections in a lathe parallel to the weld. They find the separate concentration-distance curves for copper and zinc without the trouble of a chemical separation. Since copper has high activity and short life (12.9 h), whilst zinc has lower activity and a long half-life (250 d), an initial count gives the activity due to copper and a count after 10 d the activity due to zinc. This simultaneous measurement of  $D_{\text{Zn}}^*$  and  $D_{\text{Cu}}^*$  avoids systematic errors affecting the value of the ratio  $D_{\text{Zn}}^*/D_{\text{Cu}}^*$ .

Hoffman and Turnbull<sup>(20)</sup> have shown that the rate of diffusion is greater at crystal boundaries than in the interior of the crystal. They allowed radioactive silver from a plating to diffuse into a block of silver, and after milling off a taper section placed the block in contact with a photographic plate. The autoradiograph showed greater blackening at the crystal boundaries because of the greater depth of penetration.

#### THE MEASUREMENT OF RADIOACTIVE ISOTOPES

Activity is detected and measured by photographic films or by counters. Geiger, proportional, and scintillation counters are used, and they can be obtained commercially together with the associated electronic equipment; Taylor<sup>(21)</sup> has given a simple and practical account of the use of these instruments.

The particular counting device to be preferred depends upon the amount, energy and kind ( $\beta$  or  $\gamma$ ) of radiation being measured. A Geiger counter is the most common of the counting devices and it detects all  $\beta$ -rays that enter the active region, but less than 1% of the  $\gamma$ -rays. Geiger counters can



be obtained with thin mica windows that transmit more than half of the low-energy  $\beta$ -rays emitted from  $^{14}\text{C}$  (0.16 MeV), and for  $\beta$ -rays of greater energy Geiger counters are eminently suitable. Veall and Vetter<sup>(22)</sup> have shown that the low efficiency of Geiger tubes for  $\gamma$ -counting can be mitigated if the sample be placed in the centre of a ring of six Geiger tubes connected in parallel to a common scaler; this ensures that almost all the  $\gamma$ -rays emitted pass through a counter. This arrangement was used by Inman<sup>(18)</sup> and Johnston<sup>(19)</sup> to measure the  $\gamma$ -radiation emitted from  $^{64}\text{Cu}$  and  $^{65}\text{Zn}$ ; using six G4Pb miniature Geiger tubes by Twentieth Century Electronics Ltd. they found that zinc irradiated for 1 week at a pile factor 10.5 gave a count of 10 counts/min/ $\mu\text{g}$  (i.e. 1 count per 200 disintegrations), for a background at 30 c/m.

When measuring low energy  $\beta$ -radiation, four or five times greater sensitivity can be obtained if the sample be placed inside a continuous flow proportional counter instead of outside the thin mica window of a Geiger counter (a flow of methane through the counter enables samples to be quickly changed). A factor 2 in sensitivity arises from the absence of absorption in the mica window, and another factor 2 because all the electrons emitted enter the active region.

Scintillation counters<sup>(23)</sup> are most useful for measuring  $\gamma$ -activity. The  $\gamma$ -rays produce scintillations in a phosphor and these are detected and amplified by a photomultiplier. The efficiency for  $\gamma$ -ray counting is about 10%; it is higher than that of a Geiger tube because the phosphor is a solid or liquid and absorbs most of the  $\gamma$ -rays that enter it.

Scarcely ever is it necessary to measure activity absolutely, so that the main experimental problem is to prepare samples in a reproducible manner in order to estimate relative activities.  $\beta$ -rays are easily absorbed, and so if it is necessary to count all the activity in a sample it must be prepared in thin layers.<sup>(24)</sup> If a thick sample be measured the counts will be due only to the activity in the topmost layer, and so the counts will be proportional not to the total activity of the sample but to the activity per unit volume. If, however,  $\gamma$ -rays are measured the count will be proportional to the total activity of the sample, even when it is thick, because of the greater penetration of  $\gamma$ -rays. The counting of  $\gamma$ -rays through glass of a substance in solution is more convenient than the preparation of solid samples for  $\beta$ -counting, and it is to be expected that this method will become more popular especially if a scintillation counter be used.

Autoradiography is more useful than counting if it is required to find the spatial distribution of active material rather than to measure the total activity. Michael and others<sup>(25)</sup> have developed a method for making micro-autoradiographs of metallic surfaces that can be examined at a useful magnification of up to  $\times 100$ . The photographic film is sensitive to  $\beta$ - rather than to  $\gamma$ -radiation, and has greater sensitivity the lower the energy of the  $\beta$ -rays. For high resolution it is necessary to hold specimens, whose thickness is comparable to the resolutions required, close to a photographic film (there must be an inert layer between specimen and the film or artefacts will be produced by chemical action). Michael and others machined specimens in a lathe to 70  $\mu$  thick and then ground them on emery papers to 20  $\mu$ ; they used a commercial fine-grain stripable film

which has an inert layer of cellulose 10  $\mu$  thick to separate it from the metal surface. The autoradiograph and the micro-structure could be compared since it was possible to examine the surface by focusing the microscope through the radiograph and the cellulose layer.

Active components can be introduced into the micro-structure either during casting, which is complicated because of health hazards, or by irradiation of the alloy (after irradiation of a Cu/Al alloy all the activity is due to the  $^{64}\text{Cu}$ ) or, for  $^{14}\text{C}$ , from the gas.

#### REFERENCES

- (1) Bull. Atomic Scientists, **8**, p. 294 (1952).
- (2) LeCLAIRE, A. D. *Progr. Met. Phys.*, **1**, p. 306 (1949); **4**, p. 265 (1953).
- (3) TAYLOR, D. *Engineering [London]*, **175**, p. 449 (1953).
- (4) Memorandum on  $\gamma$ -ray sources for radiography (London: The Institute of Physics, 1952).
- (5) FEARNSIDE, K. *Radioisotope Techniques*, **2**, p. 138 (London: H.M.S.O., 1952).
- (6) SELIGMAN, H. *Radioisotope Techniques*, **2**, p. 1 (London: H.M.S.O., 1952).
- (7) BROWN, H., and GOLDBERG, H. *Science*, **109**, p. 347 (1949).
- (8) SAKMANN, B. W., BURWELL, J. T., and IRVINE, J. W. *J. Appl. Phys.*, **15**, p. 459 (1944).
- (9) BUTTON, J. C. E., DAVIES, A. J., and TOURET, R. *Radioisotope Techniques*, **2**, p. 34 (London: H.M.S.O., 1952).
- (10) SCHADEL, H. M., and BIRCHENALL, C. E. *Metals Transactions*, **188**, p. 1134 (1950).
- (11) PHILBROOK, W. O., GOLDMAN, K. O., and HELZEL, M. M. *Metals Transactions*, **188**, p. 361.
- (12) ALBERT, P., CARON, M., and CHAUDRON, G. *Radioisotope Techniques*, **2**, p. 171 (London: H.M.S.O., 1952).
- (13) VOICE, E. W. *Radioisotope Techniques*, **2**, p. 23 (London: H.M.S.O., 1952).
- (14) HEVESEY, G., and OBRUTSHEVA, A. *Nature [London]*, **115**, p. 674 (1925).
- (15) FRAUENFELDER, H. *Acta Helv. Phys.*, **23**, p. 347 (1950).
- (16) HOFFMAN, R. E. *Atom Movements*, p. 69 (A.S.M., 1951).
- (17) JOHNSON, W. A. *Trans. Amer. Inst. Min. Metall. Engrs*, **147**, p. 331 (1942).
- (18) INMAN, M. C. Unpublished work.
- (19) JOHNSTON, D. Unpublished work.
- (20) HOFFMAN, R. E., and TURNBULL, D. J. *J. Appl. Phys.*, **22**, p. 634 (1951).
- (21) TAYLOR, D. *The Measurement of Radio Isotopes* (London: Methuen and Co., Ltd., 1951).
- (22) VEALL, N., and VETTER, H. *Brit. J. Radiol.*, **25**, p. 85 (1952).
- (23) CURRAN, S. C. *Luminescence and the Scintillation Counter* (London: Butterworths' Scientific Publications Ltd., 1953).
- (24) WRIGHT, M. L. *Nature [London]*, **168**, p. 289 (1951).
- (25) MICHAEL, A. B., LEAVITT, W. Z., BEVER, M. B., and SPEDDON, H. R. *J. Appl. Phys.*, **22**, p. 1403 (1951).

## The sinkage of tracked vehicles on soft ground

By I. EVANS, M.Sc., F.Inst.P.,\* Army Operational Research Group, West Byfleet, Surrey

[Paper received 18 March, 1953]

The depth of the rut made by a tracked vehicle when crossing soft ground (the "sinkage") is an index of the difficulty experienced by the vehicle. Sinkage is due to plastic flow of the soil under the imposed stresses and can be related to the shear strength of the soil and the characteristics of the vehicle. Two distinct theories are given, one by Micklethwait and Sherratt based on deductive reasoning, and a simpler inductive method by the author.

When a tracked vehicle moves over soft ground it may carve a rut, and the depth of the rut is referred to as the sinkage of the vehicle. The greater the sinkage the greater the external resistance to motion. This resistance may increase to such an extent as to cause the engine to stall, or it may become greater than the maximum grip that the track can obtain from the soil so that track slip takes place; in either eventuality the vehicle becomes bogged. It is therefore of importance to know how sinkage is related to the characteristics of soil and vehicle.

The starting point for theoretical investigation is a body of data obtained on field trials for various vehicles. The tests were carried out on level salt-marsh pasture, underlain by soft clay.<sup>(1)</sup> The soil parameter of importance is the shear strength or cohesion, and this was measured by the vane.<sup>(2)</sup> This instrument, now widely used in civil engineering, was developed and constructed for these trials. It was later shown to be capable of yielding reliable absolute values of cohesion,<sup>(3)</sup> but at the time it was regarded as a handy empirical tool which gave a reading directly proportional to the unconfined compressive strength of the soil.

Fig. 1 shows a graph of sinkage against cohesion for four tracked vehicles. Each curve represents the mean of a scatter of experimental points. Such a scatter is inevitable in field

curves is, however, quite well defined. The values of cohesion are the mean values over the top two feet of soil.

### BASIC ASSUMPTIONS

The sinking of a tracked vehicle is an indication of the development of plastic conditions in the soil. It will be assumed that to a first approximation the problem is one in quasi-statics, and analogous to the failure of a foundation in soil mechanics. The justification for this assumption will be discussed later in the light of calculations based on it. It is further assumed that the horizontal stresses exerted on the soil by the projections from the track ("spuds") do not have any effect on sinkage. Laboratory experiments on model tracks have shown that the latter assumption is justified where spud depth is small compared with track width, which is usually the case.

We shall employ the concept of the bearing capacity of clay. This is a somewhat ill-defined quantity, but it is usually taken to mean the vertical stress at which the clay in the vicinity of the footing has been brought entirely into a plastic state. Until this state is reached the vertical movement of the load is small, and determined essentially by the elastic properties of the clay, but thereafter considerable penetration takes place. For a uniform load in the form of an infinitely long strip the slip line field in the clay at the plastic state is taken to be identical with that proposed by Prandtl for the penetration of a rigid punch into metal (Fig. 2).

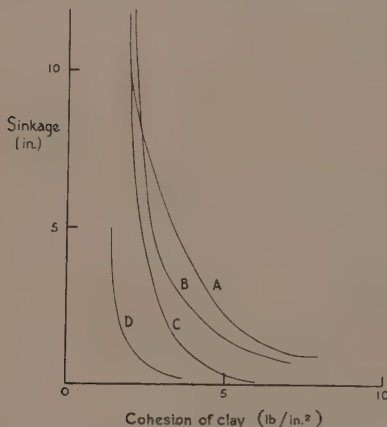


Fig. 1. Sinkage curves from field data

work on soils, owing to the considerable variation in properties over quite short distances. The main trend of the



Fig. 2. Slip line pattern in an ideally plastic metal deformed by rigid punch (plane strain)

This "surface" bearing capacity is not the maximum resistance that can be mobilized by the clay. As the load penetrates further the resistance increases slightly (though at a much smaller rate than during the primarily elastic regime in the soil) until it reaches a steady value at a depth of about twice the width of the strip. Thereafter resistance is constant, independent of depth. It has been suggested by Jaky<sup>(4)</sup> that at the ultimate bearing state the slip line field is that of Fig. 3. In the zones of "radial shear" the circular slip lines now turn through an angle of  $\pi$  radians, as against  $\pi/2$  in the Prandtl system. The bearing capacity calculated from Prandtl's theory is  $(\pi + 2)c$ , where  $c$  is the cohesion of the clay. A simple application by Meyerhof<sup>(5)</sup> of Hencky's theorem<sup>(5)</sup> to Jaky's system shows the ultimate bearing capacity to be  $(2\pi + 2)c$ .

From the point of view of the plastic behaviour of the clay, therefore, the bearing capacity relative to a strip load

\* Now at Fighting Vehicles Research and Development Establishment, Ministry of Supply.

increases from  $5.14c$  at the surface to  $8.28c$  at a penetration of  $2b$ ,  $b$  being the breadth (Fig. 4). The exact mode of growth of bearing capacity between these two points is not certain; a tentative theory by Meyerhof<sup>(6)</sup> for an ideally plastic material indicates that it is probably not very different from the straight line of Fig. 4.

In practice the load-penetration graph is a smooth curve, rising steeply during the elastic regime in the soil and rounding

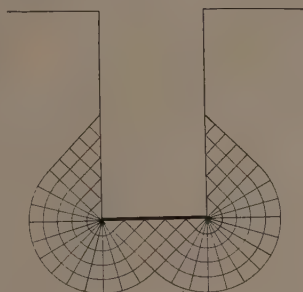
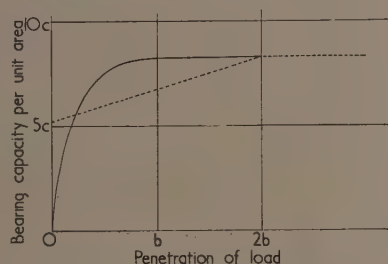


Fig. 3. Slip line pattern in an ideally plastic clay at large penetrations of load (plane strain)





The increase in sinkage after the passage of the  $m$ th wheel is (Fig. 6)

$$p_m - p_{m-1} = (r + \rho)(1 - \cos \zeta_m) \approx \frac{1}{2}(r + \rho)\zeta_m^2 \quad (5)$$

The application of elementary statics to the simple system of Fig. 6 yields the following equations

$$\rho = T/bq \quad (6)$$

$$F_m = (T + brq)\zeta_m \quad (7)$$

where  $b$  = breadth of track  
 $q$  = bearing capacity of soil.

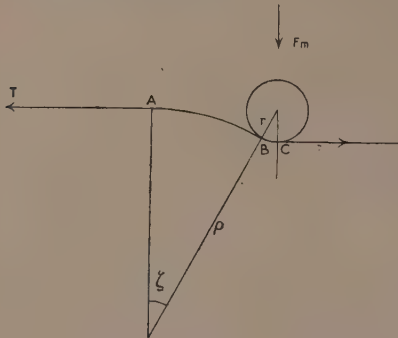


Fig. 6. Equilibrium of a single bogie wheel

From the four equations (3), (5), (6) and (7)  $F_m$ ,  $\rho$ , and  $\zeta_m$  can be eliminated, giving  $(p_m - p_{m-1})$  in terms of the remaining quantities. Equations (5) and (7) must be modified at the first wheel, giving

$$p_1 = \frac{1}{2}r\zeta_1^2 \quad (8)$$

$$F_1 = bq r \zeta_1 \quad (9)$$

from which, in conjunction with equation (4),  $p_1$  can be found. The sinkage of the last wheel is found from equations (4), (5), (6) and (7).

There are  $(n - 2)$  intermediate bogie wheels, so the total sinkage is given by

$$p = p_1 + (n - 2)(p_m - p_{m-1}) + (p_n - p_{n-1}) \\ = \frac{1}{2n^2 bq} \left\{ \left[ \frac{W}{2} - (n - 2)T \sin \omega \right]^2 \left( \frac{1}{brq} + \frac{1}{T + brq} \right) \right. \\ \left. + \frac{(n - 2) \left( \frac{W}{2} + 2T \sin \omega \right)^2}{T + brq} \right\} \quad (10)$$

Sherratt relates  $q$  to  $c$  by the following equation:

$$q = 4c \left( 1 + \frac{p}{b} \right) \quad (11)$$

This is obtained by modifying a formula for surface bearing capacity due to Terzaghi which is now considered to be conservative.

Sherratt makes a semi-empirical correction to equation (10) in order to account for the fact that the track is not continuously flexible, but consists of a number of rigid links pinned together. Further, he relates  $T$ , the track tension when the vehicle is driving to  $T_0$ , the value when the vehicle

is at rest, which can be estimated simply from the sag in the top run of the track. Accordingly, Sherratt's final expression is complicated, and calculation from it is difficult and tiresome. A graver objection is that although the solution is ingenious its accuracy is not high. It places vehicles A, B and C in their correct order of sinkage performance but their relative merit is considerably exaggerated; thus at low values of bearing capacity Sherratt's theory indicates that the sinkage of vehicle C is much less relative to that of vehicle A than is borne out by the experimental curves of Fig. 1. The error in Sherratt's approach appears to lie in his tacit assumption that the suspension springs are infinite in length, thus allowing a continuous reserve of track length needed to take up the assumed convolution of Fig. 6. In practice, the compression is limited in extent and as a result track tension increases more rapidly, and the track on the ground becomes stressed more uniformly, than Sherratt supposes.

#### A SIMPLE THEORY

The disadvantages of Sherratt's theory prompted the author to investigate whether a simpler and more accurate approach could be made by induction. The solution finally arrived at is now given.

*Conditions at deep sinkage.* The striking feature of Fig. 1 is that as the cohesion of the soil decreases, the sinkage curves for vehicles A, B and C tend to run together until ultimately they degenerate into a common vertical straight line. Now these vehicles are very different in weight and in design of suspension, but one thing they have in common, and that is that they have about the same nominal ground pressure (nominal ground pressure is vehicle weight divided by the area of track in contact with the ground on hard ground). The conjunction of these facts suggests, very strongly that at deep sinkage each track has mobilized almost the maximum possible bearing capacity and is behaving in effect as a strip with uniform loading along its length. As we have seen, maximum bearing capacity is theoretically achieved when the penetration is twice the breadth of the load, but the slope of the load-penetration curve is such that a high proportion of the maximum is achieved for smaller penetrations. Of course, the track is not a plane surface, and between two consecutive bogie wheels it is forced into an arc, but its high initial tension and the restricted maximum compression of the suspension springs means that the arc is a fairly flat one.

We have, therefore, one point on the sinkage curve,  $p = 2bq$ , when the mean bearing capacity of the soil under the track  $q$  is equal to  $q_m$ , the nominal ground pressure. We can evaluate  $q$ , for if  $L$  is the length of track on the ground and  $b$  is its breadth, then

$$\bar{q} = \frac{1}{L} \int_0^L q dL$$

If the sinkage at any point of the track is  $p$ , and the complete sinkage  $2b$ , then

$$dp/dL \approx 2b/L$$

and

$$\bar{q} = \frac{q_u}{2b} \int_0^{2b} (1 - \exp(-\alpha p/2b)) dp \\ \approx q_u \left( 1 - \frac{1}{\alpha} \right) \\ \approx 7.4c \quad (12)$$

**Conditions at shallow sinkage.** At the other end of the curve, sinkage will be small when the strain in the soil is governed primarily by the elastic properties. An attempt to designate the lowest value of bearing capacity at which linkage can be regarded to be zero is made as follows:

It is known from the classical theory of elasticity<sup>(9)</sup> that when parallel smooth elastic cylinders are in contact the width of the zone of contact  $B$  is given by

$$B = 2 \left[ \frac{4FR}{\pi} \left( \frac{1 - \sigma_1^2}{E_1} + \frac{1 - \sigma_2^2}{E_2} \right) \right]^{\frac{1}{2}} \quad (13)$$

where  $F$  = load per unit length of surface of contact  
 $E_1$  = Young's modulus for upper cylinder  
 $\sigma_1$  = Poisson's ratio for upper cylinder  
 $r_1$  = radius of upper cylinder.

The same letters with the suffix "2" are used for the properties of the lower cylinder.

$$\text{Also } R = (r_1 r_2) / (r_1 + r_2) \quad (14)$$

We consider a wheel of the vehicle to represent the upper cylinder, and the soil to represent the lower (by making  $r_2$  tend to  $\infty$  the lower cylinder becomes a plane surface). It is assumed that the track is perfectly flexible and that its properties do not enter into the interaction between wheel and soil. Taking into account also that  $E_1$  (steel) is much greater than  $E_2$  (soil), we obtain

$$B = 2 \left[ \frac{4Fr_1}{\pi} \cdot \frac{(1 - \sigma_2^2)}{E_2} \right]^{\frac{1}{2}} \quad (15)$$

Applying equation (15) to the equilibrium of the vehicle, if  $W$  is its weight and  $b$  its track breadth,  $F = W/Nb$ ,  $N$  being the number of bogie wheels. Poisson's ratio for soils may be taken to be  $\frac{1}{2}$ , hence

$$B \simeq 2(Wr/NbE)^{\frac{1}{2}} \quad (16)$$

The suffixes of  $r$  and  $E$  have been dropped in this equation as no ambiguity now exists.

On this soil the vehicle is supported over a total area  $NbB$ , and therefore the bearing capacity at zero sinkage is

$$q = \frac{1}{2}(WE/Nbr)^{\frac{1}{2}} \quad (17)$$

It is difficult to assign a specific value to  $E$ , owing to the variability of soils, but the results of triaxial compression tests suggest that a value of 1000 lb/in.<sup>2</sup> would be fairly appropriate to the soils in which vehicles  $A$ ,  $B$  and  $C$  have barely perceptible sinkage. For the lighter vehicle  $D$  a value of about half this amount is reasonable.

Equation (17) has been obtained on the assumption that the track is continuously flexible. This is not true, in practice it consists of a series of finite links. If the pitch (width) of each is  $d$ , then the weight of the vehicle can never be borne on an area smaller than  $Nbd$ . This corresponds to a bearing capacity

$$q = W/Nbd \quad (18)$$

A simple way of making correction for the finite pitch of the track is therefore as follows: the bearing capacity for zero sinkage is taken from equation (17) except where equation (18) gives a lower value, in which case equation (18) is preferred.

**The sinkage curve.** We now have two points on the sinkage curve,

$$p = 2b \text{ when } q = q_n$$

$$p = 0 \text{ when } q = q_1 = \frac{1}{2} \left( \frac{WE}{Nbr} \right)^{\frac{1}{2}} \text{ or } \frac{W}{Nbd}$$

whichever is the less.

We assume that the form of the curve joining the two points is the same as the load penetration curve of equation (2). The equation of the sinkage curve is then

$$\frac{q_1 - q}{q_1 - q_n} = 1 - \exp(-\alpha p/2b) \quad (19)$$

#### COMPARISON OF THEORETICAL CURVE WITH EXPERIMENT

The form of the curve given by equation (19) is very close to that obtained from field trials, as can be seen from comparisons of Figs. 1 and 7. In order to obtain the best fit with field results, however, it has been necessary to assume that  $q = 8c$ , which is somewhat greater than the theoretical expectation of  $q = 7.4c$  deduced in equation (12). It is quite possible that a cumulative error of this amount may be implicit in the numerous approximations and assumptions made in this paper. There is one further reason for error

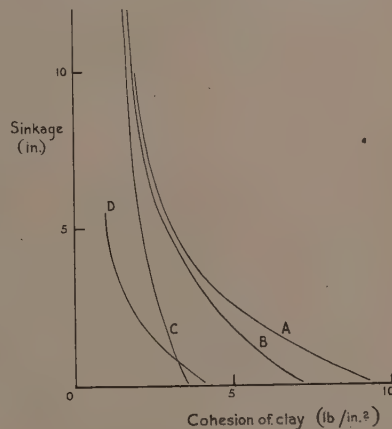


Fig. 7. Theoretical sinkage curves

in the simple theoretical approach, that is that the crossing of soft ground is a problem in dynamics, and not one in statics. It is known that as the rate of strain is increased in a shear test on clay so the shearing resistance increases, and in a dynamic loading test this has the effect of increasing the bearing capacity. The increase of  $q$  from  $7.4c$  to  $8c$  may be partly due to this phenomenon.

This simple theory gives the best agreement with observation at deep sinkage, as intended. The agreement at shallow sinkage is less good, but this is unimportant from the point of view of practical application of the curves. Sherratt's theory has the virtue of showing good agreement at shallow sinkage, but as noted it becomes progressively less good as soil bearing capacity decreases.

#### ACKNOWLEDGEMENT

This paper is published by permission of the Scientific Adviser to the Army Council.

## REFERENCES

- (1) PARKINSON, D. H., and SMITH, A. H. V. *Army Operational Research Group Memorandum No. 540* (1945).
- (2) EVANS, I. *Geotechnique*, **2**, p. 46 (1950).
- (3) EVANS, I., and SHERRATT, G. G. *J. Sci. Instrum.*, **25**, p. 411 (1948).
- (4) JAKY, J. *Proc. 2nd. Int. Conf. Soil Mech.*, **1**, p. 100 (Rotterdam, 1948).
- (5) HENCKY, H. *Z. Angew. Math. Mech.*, **3**, p. 250 (1923).
- (6) MEYERHOF, G. G. *Geotechnique*, **2**, p. 301 (1951).
- (7) MICKLETHWAIT, E. W. E. *Tracks for Fighting Vehicles*, Chapter 25 (Chertsey: Military College of Science, 1944).
- (8) SHERRATT, G. G. *Army Operational Research Group Report No. 253* (1945).
- (9) TIMOSHENKO, S. *Theory of Elasticity*, p. 349. (New York: McGraw-Hill Book Co. Inc., 1934).
- (10) UFFELMANN, F. L. Paper 10, *Ministry of Supply Soil Mechanics Symposium* (1948).

## The colouring of diamonds by neutron and electron bombardment

By R. A. DUGDALE, B.Sc., Atomic Energy Research Establishment, Harwell, Berks.

[Paper received 10 April, 1953]

The colouring of diamonds by neutron and electron bombardment and some effects of subsequent heating are described. The colouring is associated with the introduction of Frenkel defects by bombardment. Evidence for the natural occurrence of radiation coloured diamonds is presented.

The majority of diamonds, in their natural state, have at least some colour, while in many it is quite marked.<sup>(1,2,3)</sup> Apart from grey stones (which are most common and for which the colour is attributed to small inclusions near the surface), yellow, olive green or yellow-green, and brown seem to be the most common colours. The origin of these colours is not clear. It is not even clear whether the colour is generally confined to the surfaces, or distributed through the body of the stones. Certainly, in some cases (yellows and yellow-greens), the colour may become paler on polishing and can often be removed by grinding and therefore appears to be connected with the surface. In such cases the colour has been attributed to the effect of natural radioactivity. There is little evidence for the colouring of diamonds by impurities. Chesley,<sup>(4)</sup> who by spectroscopic examination searched for the presence of thirty elements, found only a minor correlation between colour and minor element content (Fe and Ti). However, his method would not detect the presence of H, B, N, O, P, S, or the halogens.

The change in colour of diamond induced by radium radiation was noticed at the beginning of the century by Sir William Crookes<sup>(5)</sup> and others. These early reports are not very consistent, probably because the irradiations were weak and the colour changes slight. However, it was established in 1923 by Lind and Bardwell<sup>(6)</sup> that diamonds are coloured green by the  $\alpha$ -particles from radium. More than thirty specimens ranging in initial colour from colourless to yellow and brown were treated. Prolonged heating at 500°C restored the original colour. It was not determined whether the colour was confined to a surface layer of thickness 0.001 in. (the range of such  $\alpha$ -particles in diamond), as might be expected, or spread through the body of the stone. In some irradiations in radium emanation black spots were produced well beyond the range of the  $\alpha$ -particles (1 or 2 mm below the surfaces). The nature of these spots, which could be removed by prolonged heating at red heat, was not determined.

There have been several reports, in the last decade, of diamonds coloured by proton, deuteron, and  $\alpha$ -particle bombardment.<sup>(7,8,9)</sup> Various colours from light green to dark brown, depending on the length of exposure and the intensity

of the beam, were obtained. It seems probable that the brown colours were due to a combination of heating and bombardment. In some instances minute black pin points distributed throughout the stones were noticed, but it is not clear whether these have the same origin as the black spots reported by Lind and Bardwell. Cork has shown that, in the case of deuteron bombardment at least, the colour is probably confined to the range of the particles.  $\beta$ ,  $\gamma$ , and X-rays appear to have little effect on the colour of diamonds,<sup>(2,6,10)</sup> although there are somewhat inconsistent reports by early workers<sup>(11)</sup> that cathode rays had an effect in some instances.

The evidence therefore suggests that diamonds are more readily coloured by energetic heavy particles and this supports the idea that the colour centres are connected with the vacant lattice sites and interstitial atoms formed when the particles collide with the carbon atoms. With the advent of the atomic pile it was realized, primarily by Wigner,<sup>(12)</sup> that the high densities of energetic neutrons would be likely to produce physical changes in solids exposed to them, due to just this very mechanism, i.e. the displacing of atoms from their lattice sites. One may expect that the post-irradiation heat treatment may tend to reverse the effect of the pile by annealing at least some of the damage. A study along these lines has been applied to diamonds irradiated in the Harwell pile BEPO and, although mainly qualitative, it leads to some interesting effects and speculations. In addition, colouring by high energy electron bombardment has been studied: the explanation again being consistent with the displaced atom theory.

### THE EFFECT OF PILE IRRADIATIONS

Many more or less colourless diamonds have now been irradiated, both for our own purposes and for others taking an interest in this subject, and it can be said that a green colour is induced which deepens as the irradiation proceeds until the diamonds actually become opaque. The time required to reach the opaque stage depends, of course, on the thickness of the diamond but, for diamonds about 2 mm thick, is about 1 week in an ordinary isotope facility. Any fluorescence and phos-



phorescence the diamonds may have (excited by wavelength 3650 Å) is rapidly extinguished, being quite unnoticeable after a week's irradiation. In general, induced radioactivity is weak and of short half lives of the order of 10 hours. A week after irradiation it was not usually detectable with an ordinary Geiger counter. In some cases it was particularly weak, but no correlation with other features about to be described was found. The appearance of black spots was not noticed.

#### THE EFFECTS OF POST-IRRADIATION HEAT TREATMENT

The changes in the absorption and fluorescence spectra, which occurred on heating, were studied visually and in some detail for twenty-one diamonds. Lonsdale<sup>(1)</sup> has pointed out that one of the main features of diamond is its individuality and that is unwise to base conclusions on a study of only a few. Five of the diamonds had been classified as type II on the basis of their infra-red and ultra-violet absorption spectra by G. B. B. M. Sutherland and D. E. Blackwell. Of the rest only two were known definitely to fall into the type I class (on this basis).<sup>\*</sup> All were colourless, or nearly so, and the majority showed a blue fluorescence. The relevance of these initial properties will be brought out in the following description. The spectrometer used was a simple table type with a 4 cm glass prism and was calibrated against the Fraunhofer lines and the lines of a helium lamp. The accuracy in the region of 5000 Å was  $\pm 10$  Å although at longer wavelengths it was not so good, falling off to about  $\pm 30$  Å at 7000 Å.

The diamonds had been irradiated in three groups for, respectively, 10 h (medium green), 100 h (dense green or opaque), and 1200 h (opaque). All were heated in a vacuum for  $\frac{1}{2}$  h periods at a series of temperatures up to 1000° C. The colour, and absorption and fluorescence spectra were studied at room temperature after each heating. The following summary of the effects of heating (none of which occurred in two unirradiated diamonds) is based on the observations made in this way.

Heating at temperatures up to about 600° C reduced the intensity of the green colour, the higher temperatures being the more effective (a temperature of 500° C caused a 1200 h opaque diamond to transmit in the green). At 650° C the colour changed rather abruptly to a brown shade which was only slightly altered by temperatures up to 1000° C. The ultimate colour after heating at this temperature ranged from pale yellow, brown, or brown-green for the 10 h irradiations to brown-red, brown, or brown-green for the 1200 h irradiations. It was possible to see the absorption at the blue end of the spectrum (which was strong after only 10 h irradiation) decreasing as the temperature was raised. In addition to the colour change various absorption lines and bands appeared and disappeared and these, with comments, are listed in the following:

**5040 Å line.** Observed very faintly near the opaque stage; became strongly visible after heating to temperatures near to 400° C; after heating at 400° C the strength was greater the longer the irradiation; apparent width 10 to 30 Å, increasing with the strength; an accurate measurement in one case (Gillieson) gave the peak at wavelength 5044 Å; vanished abruptly on heating at 425° C; was seen in all but two cases which showed an anomalous behaviour with temperature; when very strong, a faint band at wavelength 4920 Å (width about 50 Å) was also visible.

**6630 Å to 7380 Å band.** Evident after heating in the range 300 to 800° C; this band showed a structure consisting of a line at wavelength 7350 Å and faint diffuse bands with peaks at wavelengths 7230, 7000, and 6700 Å. The whole band was not strong, reaching its maximum intensity after heating at 600° C; not noticed in any of the 10 h irradiations, being presumably too faint.

**5920 Å line.** Evident after heating in the range 600 to 1000° C; not seen in all cases; tended to be stronger in the longer irradiations.

**5040 Å line.** Evident after heating in the range 700 to 1000° C; the wavelength was perhaps 5 Å less than the low temperature line; strength varied considerably from specimen to specimen; absent altogether in a few of the 10 and 100 h irradiations; sometimes accompanied by a band at wavelength 4970 Å.

**Other lines and bands.** These appeared after heating in different temperature ranges. In some cases, a particular line or band was seen in more than one specimen. Usually faint, the tendency was for more to be seen the longer the irradiation.

All except the two showing the anomalous temperature behaviour with the 5040 Å line developed a green fluorescence system after heating at 650 to 700° C which was strengthened somewhat by heating at higher temperatures. In addition, the original fluorescence system was revived, particularly if originally orange or yellow, the blue fluorescence reappearing for the short irradiations only. Thus, after heating, the colour of the fluorescence was either green, or a colour resulting from the combination of the green and the original. The fluorescence was most intense on and near the surface upon which the exciting ultra-violet light (wavelength 3650 Å) was incident: this being particularly marked in the case of the long irradiations where the depth of fluorescence was only 0.2 mm. This seems to indicate that the absorption was high at wavelength 3650 Å even after heating at 1000° C. In some cases geometrical patterns were seen in the green fluorescence.

Particular interest is attached to the green fluorescence because its spectrum has a strong resemblance to the 5032 Å system discovered by Mani<sup>(14)</sup> in diamonds in their natural state. Both consist of a continuous spectrum headed by a band system in the neighbourhood of wavelength 5000 Å. In one case (a 100 hour specimen) the fluorescence was studied at -196° C, where it was found that the intensity increased and the bands became sharper and more discernible. The main bands of Mani's system are compared with those of the pile induced fluorescence in the following table.

#### Green fluorescence spectra

Pile irradiated diamonds, 18° C		Mani's diamonds, 18° C		
Wavelength (Å)	Width	Band	Wavelength (Å)	Width
4960	sharp		4959	sharp
5040	20 Å	I	5038	15 Å
5120	diffuse	III	5123	diffuse
5200	diffuse	IV	5204	diffuse
Continuous to 6300		Continuous to 6500 (other bands being faint)		
—196° C		—189° C		
4950	sharp		4959	sharp
5030	sharp	I	5032	sharp
5130	diffuse	III	5115	diffuse
5200	diffuse	IV	5198	diffuse
5300	diffuse (faint)	V	5286	diffuse
5400	diffuse (faint)	VI	5359	diffuse
Continuous to 6350		Continuous to 6500		

\* Type II: B.P.6, I.44, I.28, B.P.1, I.21. Type I: V.M.91, B.1.  
VOL. 4, NOVEMBER 1953

The 4960 Å line is included because it seems to be a part of the irradiation induced system. Miss Mani found it to be strong in one case only and so excluded it. It is interesting to note that Miss Mani also found the 5032 Å system to co-exist with the 4152 Å system (the system for blue fluorescence). This corresponds to the case of the initially blue fluorescing diamonds irradiated for 10 h and subsequently heated. In absorption at  $-187^{\circ}\text{C}$ , Miss Mani found a sharp line at wavelength 5032 Å with diffuse bands at wavelengths 4950, 4870 and 4790 Å (approximately), which she associated with the 5032 Å fluorescence system. Similar features were observed in the pile irradiated diamond at  $-196^{\circ}\text{C}$ , an accurate measurement (Gillieson) giving the peak of the main line at wavelength 5029 Å. (At low temperatures one sees much more detail in the absorption spectrum and several other lines and bands besides these were found.)

Further evidence that diamonds occur naturally showing some of the effects obtained when pile irradiated diamonds are heated is contained in a paper by Anderson.<sup>(13)</sup> In this is described a class of brown diamonds with which is associated a pale green fluorescence, similar to that described here, together with a main absorption line at wavelength 5040 Å.

As mentioned above, there were two diamonds (B.P.6 and B.P.1) which showed an anomalous temperature behaviour with respect to the low temperature 5040 Å absorption line. These were initially non-fluorescing type II diamonds, and it was found that heating at  $300^{\circ}\text{C}$  caused the line to disappear (in contrast to the rest, for which it was necessary to heat at more than  $400^{\circ}\text{C}$ ). These were also the only diamonds which did not acquire the green fluorescence on heating at high temperatures. The other initially fluorescing type II diamonds behaved in the normal manner, both as regards the low temperature 5040 Å line and the green fluorescence.

#### SOME OBSERVATIONS ON NATURAL GREENS

The effect of heating five natural green diamonds was studied. On one of these, J. F. Custers, who lent it, had ground off two opposite corners to show that the interior was colourless. The stone showed an absorption line at wavelength 5040 Å and, when heated, behaved like the irradiated diamonds, although the green fluorescence which was induced was too dull for its spectrum to be observed. It seems almost certain that the green surfaces, which were covered in darker spots of about  $50\ \mu$  diameter, were coloured by  $\alpha$ -particle bombardment from a naturally active substance in close proximity. The other four were a very pale green and at no time during the heat treatment were any absorption lines seen. However, all turned a very pale brown and acquired the green fluorescence system in addition to their already existing blue fluorescence.

#### COLOURING BY ELECTRON BOMBARDMENT

Some twenty small blue fluorescing colourless diamonds have been coloured by bombarding them with electrons of energies 3, 1 and 0.5 MeV. To obtain a strong colour, exposures of 1 h at 50 to  $100\ \mu\text{A}/\text{cm}^2$  were necessary, i.e. an integrated flux of  $1$  to  $2 \times 10^{18}$  electrons/ $\text{cm}^2$ . To dissipate the heat the diamonds were mounted in Woods metal on a water-cooled pipe. The colours obtained were: blue-green (3 MeV), blue with a slight green tint (1 MeV), blue (0.5 MeV). In the last case, the colour was much weaker, perhaps because the thickness of the window of the Van der Graaf machine amounted to an appreciable part of the electron range. The penetration of the colour induced by the 1 MeV bombardment

was about 0.5 mm although this depended, as might be expected, upon the intensity of the colour.

On subsequent heating, the diamonds coloured by the 3 MeV bombardment behaved in much the same way as those coloured in the pile. The colour, however, remained more blue until they were heated at about  $700^{\circ}\text{C}$  when a yellow-green shade was obtained. Both the low and high temperature lines at 5040 Å, the 4970 Å band and the 5920 Å line were found, and the green fluorescence system appeared in considerable strength. The 1 MeV diamonds showed some further differences. The colour lost its green tint after heating at  $500^{\circ}\text{C}$ , although it was turned to a yellow-green shade by heating at  $700^{\circ}\text{C}$ . The relatively strong low temperature absorption line at wavelength 5040 Å was not found although repeatedly searched for. The green fluorescence system was developed very strongly and, with it, absorption lines were seen faintly at wavelengths 5040 Å and 4970 Å, the latter being the stronger. The 0.5 MeV diamonds were not heated.

#### DISCUSSION

According to Seitz,<sup>(14)</sup> about 25 eV recoil energy is needed for a carbon atom in diamond to be displaced, by bombardment, from its normal lattice site to an interstitial site. In the pile, neutrons of all energies up to 1 or 2 MeV are present and these can give the atoms of a crystal lattice recoil energies up to:

$$W_m = 4ME/(M+1)^2$$

where  $E$  is the neutron energy and  $M$  is the atomic mass in mass units. The average is just half this and the cross-section for the collisions is about 3 barns. In general, the recoiling atom will have sufficient energy to produce, in turn, further displacements. Thus, one fast neutron collision will give rise to many Frenkel defects conglomerated in a small volume of the lattice (this topic is discussed by Seitz<sup>(14)</sup>). The author estimated, on the basis of Seitz's theory, that 0.001% of the atoms in diamond became Frenkel defects in a 10 h irradiation in BEPO. It seems to be a plausible explanation that the green colour is to be associated with these lattice defects. On subsequent heating some mobility of the defects may be expected, enabling some of them to recombine. In this way the reduction in the intensity of the colour may be explained. Heating may also have an effect on the electronic structure of the defects and it is not known how much of the colour change is due to this cause. Quantitative studies of the effect of heat on the neutron induced absorption spectrum, such as those made by Pringsheim and Voreck,<sup>(15)</sup> may perhaps distinguish the different mechanisms.

The electron bombardments described were also able to introduce appreciable numbers of lattice defects; for, the maximum recoil energy which may be given to a nucleus in an elastic collision is, very approximately:

$$W_m = 2E(E + 2m_0c^2)/Mc^2$$

where  $E$  is the electron energy and  $m_0c^2$  and  $Mc^2$  are the rest energies of electron and nucleus respectively. Also, the cross-section for the recoil energy to lie between  $W$  and  $W_m$  is, approximately:

$$\sigma_W^m = 2.5 \cdot 10^{-25} \cdot Z^2 \cdot \frac{(1-\beta^2)}{\beta^4} \cdot \left( \frac{W_m}{W} - 1 - \beta^2 \log \frac{W_m}{W} \right)$$

where  $Z$  is the nuclear charge and  $\beta = v/c$ . (This formula was obtained from the differential scattering cross-section



given by Mott and Massey.<sup>(16)</sup> The values of  $W_m$  and  $\sigma_{25}^{Wm}$  for the three electron energies used are listed in the following table:

$E$ (MeV)	3	1	0.5
$W_m$ (eV)	2150	360	140
$\sigma_{25}^{Wm}$ (barns)	15	14	13

Thus, for an integrated flux of  $2 \times 10^{18}$  electrons/cm<sup>2</sup> the concentration of primary displaced atoms, at the surface upon which the beam was incident, would be about  $3 \times 10^{-5}$ . This would fall off as the beam penetrated due to the decrease, firstly, in flux and secondly, in energy. Due to the dependence of  $\sigma_{25}^{Wm}$  on  $W$  one would expect that the majority of the primary displaced atoms would have received recoil energies very much less than  $W_m$ . The electron bombardment, therefore, would be expected to have produced mainly single Frenkel defects, although an appreciable multiplication—leading to secondary displaced atoms—might have occurred at the higher electron energies (3 MeV). It seems very likely that the blue colour is to be associated with the singly produced Frenkel defects. The blue-green colour induced by the 3 MeV bombardment would then be due to the presence of groups of Frenkel defects; this bombardment having an effect more like the neutron bombardment in the pile.

If the lattice defect theory is correct there should be a threshold energy for colouring by electron bombardment which would be 125 keV, assuming that 25 eV is needed for an atom to be displaced. Moreover, by suitably choosing the mass and energy of other bombarding particles (and  $\gamma$ -rays) effects similar to those of electron bombardment should be obtained.

The absorption lines in the region of wavelengths 5040 Å to 5030 Å and the green fluorescence system seem to be most important. Their correlation with other properties and their accurate wavelength measurements at 18° C and -196° C after different heat treatments seems to be desirable. The non-appearance of the 5040 Å line after the 1 MeV electron bombardment suggests that a certain configuration of defects is responsible for it and that these cannot be achieved in sufficient numbers by the low energy recoils. The various other lines and bands found in the heated pile irradiated diamonds may be connected with impurities.

Of some interest perhaps is the demonstration that diamonds occur naturally which show some of the effects of irradiation plus heat-treatment. Green, yellow and brown diamonds, and those showing the green fluorescence system are to be suspected of such a history. As well as  $\alpha$ -particles,  $\beta$ - and even  $\gamma$ -rays (which would colour the diamond more or less uniformly throughout its body) could have been responsible for these colours. It is also a possibility that the first quality blue-white gem stone owes its value to a natural bombardment.

It is now evident that diamond is a most mysterious sub-

stance (a recent survey of the diamond problem has been given by Grenville-Wells<sup>(17)</sup>), and it may be that a study of the change in properties which occur when lattice defects are introduced artificially will help to achieve a better understanding of it.

#### ACKNOWLEDGEMENTS

The following persons kindly supplied the diamonds for these experiments: Mr. B. W. Anderson, Mr. J. S. Scanlan, Mr. W. F. Cotty, Dr. J. F. Custers, Dr. R. S. Young, Dr. G. B. B. M. Sutherland and Dr. D. E. Blackwell. The author's thanks are due to the following members of the A.E.R.E.: The staff of the BEPO pile for neutron irradiations, Mr. E. R. Wiblin and the linear accelerator section and Mr. J. D. Milne and Van der Graaf section for electron irradiations, Dr. A. H. Gillieson for spectrometric assistance, Mr. T. M. Fry for valued suggestions, and Sir John Cockcroft, Director, for permission to publish this article.

#### REFERENCES

- (1) LONSDALE, K. *Nature, Lond.*, **153**, p. 669 (1944).
- (2) FRISTCH, O. *Gemmologist*, **17**, p. 328 (1948).
- (3) SUTTON, J. R. *Diamond. A Descriptive Treatise*. (London: T. Murby and Co., 1928).
- (4) CHESLEY, F. G. *Amer. Min.*, **27**, p. 20 (1942).
- (5) CROOKES, W. *Diamonds*, pp. 108–110 (London: Harper, 1909).
- (6) LIND, S. C., and BARDWELL, D. C. *Amer. Min.*, **8**, p. 171 (1923).
- (7) HARDY, J. A. *Gems and Gemology*, **6**, p. 167 (1949).
- (8) EHRLMANN, M. L. *Gems and Gemology*, **6**, pp. 295, 318 (1950).
- (9) CORK, J. M. *Phys. Rev.*, **62**, pp. 80 and 494 (1942).
- (10) POUGH, F. H., and ROGERS, T. H. *Amer. Min.*, **32**, p. 31 (1947).
- (11) MELLOR, J. W. *A Comprehensive Treatise on Inorganic and Theoretical Chemistry*, Vol. 5, p. 769 (London: Longmans, Green and Co. Ltd., 1940).
- (12) WIGNER, E. P. *The Science and Engineering of Nuclear Power*, **1**, p. 107 (1947); **2**, p. 209 (New York: Addison-Wesley Co. Inc., 1949).
- (13) ANDERSON, B. W. *Gemmologist*, **12**, p. 33 (1943).
- (14) SEITZ, F. *Crystal Growth. A General Discussion of the Faraday Society*, p. 271 (London: Gurney and Jackson Ltd., 1949).
- (15) PRINGSHEIM, P., and VORECK, R. C. *Z. Phys.*, **133**, p. 2 (1952).
- (16) MOTT, N. F., and MASSEY, H. F. W. *The Theory of Atomic Collisions*, 2nd Ed., p. 80 (London: Oxford University Press, 1949).
- (17) GRENVILLE-WELLS, H. J. *Atomic Scientists News*, **1**, p. 86 (1952).



# Solid bodies appearing in electron microscope specimens

By G. YASUZUMI, M.D., T. MORIOKA and A. TANAKA, Department of Anatomy, Faculty of Medicine, University of Osaka, Japan, and K. KOBAYASHI, M.S., Institute for Chemical Research, University of Kyoto, Japan

[Paper received 8 April, 1953]

This paper deals with the artifacts which may be introduced into the electron microscope specimen in a vacuum and hence into the micrograph. Solid bodies appearing in electron microscope specimens have been examined by means of the electron microscope and electron diffraction. It has been determined that the solid body is of carbon black which has been produced as a result of the combustion of vaporized oil or grease by electron bombardment or radiation of a burnt tungsten filament in a vacuum. The necessity of minute care when examining specimens and interpreting their images in the biological area is emphasized.

It is an established fact that any organic substance which is dried in the air must lie flat on the supporting membrane. Nevertheless, we have often observed interesting images which are rather solid, reminding us of bridges or towers by means of shadow casting (Fig. 1). Some electron micrographs of the residual chicken chromosomes published by Denues<sup>(1)</sup> seem to be the same images as the above mentioned.

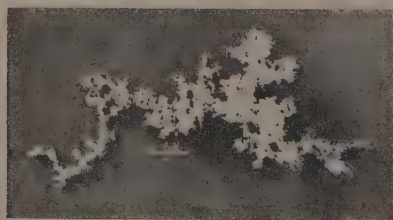


Fig. 1. Electron micrographs of solid bodies appearing in biological electron microscope specimens

Yasuzumi and co-workers<sup>(2,3)</sup> have already made detailed discussions of the microstructure of metabolic chromosomes isolated from erythrocyte nuclei of various animals.

In the first series of experiments we attempted to clarify the origin of the solid bodies appearing in electron microscope specimens. The supporting membranes without materials were placed in the shadow-casting apparatus. Then the



Fig. 2. Electron micrograph of solid body produced in a shadow-casting apparatus

tungsten filament was heated at about 2000° C in a vacuum. Fig. 2 shows the appearance of an artifact which has been produced in the above-mentioned procedure. Fig. 3 is the same image as Fig. 2, but it illustrates a chrome-shadowed

image which has been transformed by repeated electron bombardment. The frequency of appearance of the solid body is about 5% in the shadow-casting apparatus. In the electron microscope body, its frequency is smaller than in the

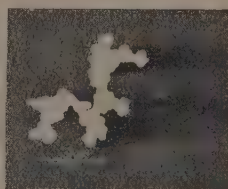


Fig. 3. Chrome shadowed, partially shrunken electron micrograph of the same image as Fig. 2

shadow-casting apparatus. However, the frequency seems to increase in proportion to the greasy contamination within the electron microscopy body. Many of our electron micrographs made so far have disclosed solid bodies which are nothing but artifacts produced in a vacuum through the process.

In the second series of experiments, by making use of an intermediate lens fitted in our electron microscope (type SMK by Shimadzu Manufacturing Co. Ltd.) and a small diaphragm, electron diffraction patterns were taken from the localized area of a specimen and simultaneously an electron micrograph of the corresponding field was obtained, without changing the position of specimen or removing any lenses, or breaking the vacuum or otherwise altering the alignment of the instrument. With this apparatus, electron diffraction patterns have been obtained from the solid bodies.

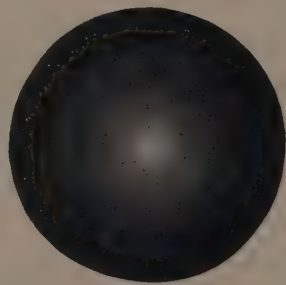


Fig. 4. Electron diffraction pattern obtained from the field ( $8\mu^2$ ) shown in Fig. 2

Electron diffraction pattern of the solid body demonstrated in Fig. 4 shows an amorphous pattern which seems to be a series of carbon black particles (partially graphitized). We know, of course, that the diffraction of the carbon black shows the same amorphous pattern as the collodion film, and that

the pattern in the former is sharper than in the latter. Therefore Fig. 4 is clearly a pattern of a carbon black which has been produced as a result of the combustion of vaporized oil or grease by electron bombardment or radiation of a burnt tungsten filament in a vacuum.

Since the technique of shadow casting was introduced its excellent effects on certain biological specimens have been studied. On the other hand, if employed indiscriminately and without precaution, it may introduce artifacts into the image.

Electron microscopists should be careful not to take the artifacts thus produced for genuine chromosomes.

## REFERENCES

- (1) DENUES, A. R. T. *Science*, **113**, p. 713 (1951).
- (2) YASUZUMI, G. *Chromosoma*, **4**, p. 222 (1951).
- (3) YASUZUMI, G., MIYAO, G., YAMAMOTO, Y., and YOKOYAMA. *Chromosoma*, **4**, p. 359 (1951).

## The field along the axes of symmetry of equal semi-infinite rectangular magnetic pole-pieces

By W. SNOWDON, M.Sc., and N. DAVY, D.Sc., The University, Nottingham

[Paper received 23 April, 1953]

The method of conformal representation is applied to a two-dimensional figure representing the cross-section of rectangular pole-pieces having two axes of symmetry. The field at intervals along these axes is calculated accurately for a number of different values of the ratio of width of pole-pieces to distance separating them. The number and range of values of this ratio for which the calculations are made is sufficient to allow of interpolation for any ratio likely to be met with in practice. Expressions are derived for the values of the potential function along the principal axes.

A common, useful type of magnetic field is that between a pair of rectangular pole-pieces, possibly because of the ease with which they can be made. The field between pole-pieces of this shape has already been described in a general way.<sup>(1)</sup> In the present paper the field is worked out in detail along two important axes of symmetry. Accurate information about the field-strengths along these lines should prove useful not only in connexion with the theory of electromagnets having this particular profile, but also in such work as the testing of steel wire ropes for broken strands. A method of testing ropes by passing them through magnetic fields of this type is already in practical use.

## SPACE TRANSFORMATION

In the following, the usual notation of the Jacobian elliptic functions is used.

Suppose in Fig. 1  $P$  and  $Q$  represent the rectangular cross-sections of two cylindrical pole-pieces of width  $2b$ , whose distance apart is  $2a$ . The transformation from the  $z$ -plane to

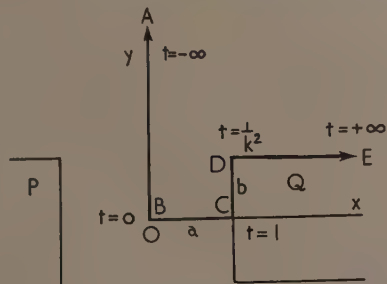


Fig. 1. Pole-pieces in  $z$ -plane showing values of parameter  $t$

the  $t$ -plane which transforms the region to the left of the boundary  $ABCDE$  into the upper half of the  $t$ -plane is given by

$$dz/dt = A'(t - 1/k^2)^{1/2}(t - 1)^{-1/2}$$

where  $A'$  is a constant,  $t$  having the values at the vertices

shown in the figure. The substitution of the Jacobian elliptic function  $t = \text{sn}^2(w, k)$ ,  $0 \leq t \leq 1$ , gives

$$dz/dw = 2A' \text{dn}^2 w/k$$

Therefore

$$z = 2A'E(w)/k + B'$$

where  $B'$  is a constant. When  $t = 0$ ,  $z = 0$  and we may take  $w = 0$ , so that  $B' = 0$ . When  $t = 1$ ,  $z = a$  and  $w = K$ , giving  $A' = ak/2E$ . The final result is

$$z = aE(w)/E \quad (1)$$

$$= a[Z(w) + wE/K]/E \quad (2)$$

This formula is valid along  $BC$  and by a suitable choice of values of  $w$  may be applied to the whole of the region  $ABCDE$ . Substituting  $w = ip$ , (1) becomes

$$z = ia[\text{sn}' p \cdot \text{dn}' p/\text{cn}' p + p - E'(p)]/E$$

where the dashes denote elliptic functions to the complementary modulus. Thus along  $BA$ ,  $p$  takes the values 0 to  $K'$ , making  $z$  purely imaginary and equal  $iy$ , where

$$y = a[\text{sn}' p \cdot \text{dn}' p/\text{cn}' p + p - E'(p)]/E \quad (3)$$

The values of  $w$  for the whole boundary are shown in Fig. 2.

When  $z = a + ib$ ,  $w = K + iK'$  and this gives, on substitution in equation (1),

$$a + ib = a[E + i(K' - E')]/E$$

$$\text{or} \quad b/a = (K' - E')/E \quad (4)$$

This relation connects the ratio of  $b$  to  $a$  with the modulus  $k$  of the elliptic functions.

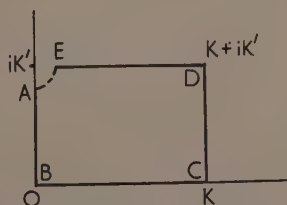


Fig. 2. Transformation of  $ABCDE$  on  $w$ -plane

## FORMULAE FOR FIELD STRENGTH

If  $2V_0$  is the difference in magnetic potential between the pole-pieces in Fig. 1, the complex potential function  $W = U + iV$  is connected with the parameter  $t$  by the relation

$$dW/dt = V_0 t^{-1/2}(t-1)^{-1/2}/\pi \quad (5)$$

The field strength at any point of the domain  $ABCDE$  of the  $z$ -plane is

$$\begin{aligned} |dW/dz| &= |dW/dt| |dt/dz| \\ &= |2V_0 E(t-1/k^2)^{-1/2}/\pi a k| \\ &= |2V_0 E \operatorname{nd} w/\pi a| \end{aligned} \quad (6)$$

The field strength along  $AB$  is therefore

$$2V_0 E \operatorname{cn}' p/\pi a \operatorname{dn}' p \quad (7)$$

$p$  having the same meaning as in equation (3).

## LIMITING CASES

It is of some value as a check on the reasoning to consider the two limiting cases in which  $k \rightarrow 0$  and  $k \rightarrow 1$ .

The first case,  $k \rightarrow 0$ , corresponds to  $b/a \rightarrow \infty$ , i.e. to the case of parallel plates. Along  $BC$ , equations (1) and (6) become

$$x = 2aw/\pi \text{ and field strength} = V_0/a$$

and along  $AB$ , equations (3) and (7) become

$$y = 2ap/\pi \text{ and field strength} = V_0/a$$

The second limiting case,  $k \rightarrow 1$ , corresponds to  $b/a \rightarrow 0$ , i.e. to the case of plates in line. Along  $BC$ , equations (1) and (6) become

$$x = a \tanh w$$

and field strength  $= 2V_0 \cosh w/\pi a = 2V_0/\pi(a^2 - x^2)^{1/2}$  while along  $AB$  equations (3) and (7) become

$$y = a \tan p$$

and field strength  $= 2V_0 \cos p/\pi a = 2V_0/\pi(a^2 + y^2)^{1/2}$

These results agree with the formulae obtained by considering each case directly.

## CALCULATIONS

The procedure in applying the above conclusions has been first to choose a value for  $k$ , the modulus of the elliptic

functions. This fixes a value for the ratio  $b/a$  from equation (4). By giving  $w$  a range of values between zero and  $K$ , the values of  $x/a$  and the field strength along  $BC$ , expressed as multiples of  $2V_0/\pi a$ , have been calculated from equations (2) and (6). The results are given in Table 1. Similarly, by giving  $p$  a range of values between zero and  $K'$ , the values of  $y/a$  and the field strength along  $AB$ , also expressed as multiples of  $2V_0/\pi a$ , have been calculated from equations (3) and (7). These values are assembled in Table 2. Figs. 3 and 4 represent graphs of the results.

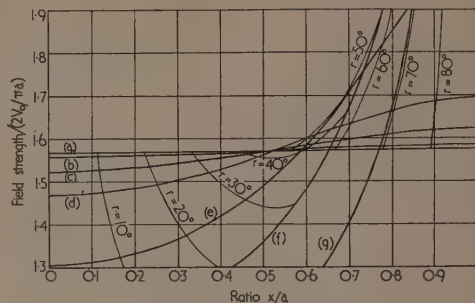


Fig. 3. Curves of field strength along  $BC$  for the following values of  $b/a$ :

(a) 1.7981; (b) 1.3556; (c) 0.9097; (d) 0.6443; (e) 0.3015; (f) 0.1296; (g) 0.

The elliptic functions have been evaluated from the Smithsonian tables.<sup>(2)</sup> In terms of the symbols used on p. 248 of these tables, along  $BC$ ,

$$x/a = [Z(r) + rE/90]/E$$

where  $w = rK/90$

and field strength  $= (2V_0/\pi a)[ED/C(1 - k^2)^{1/2}]$ ,

and along  $AB$ ,

$$y/a = [A'C'/D'B' + r(K' - E)/90 - Z(r)]/E$$

where  $p = rK'/90$

and field strength  $= (2V_0/\pi a)EB'/C'k^{1/2}$ .

Table 1. Field strength  $F$  at points along  $BC$  for different values of  $b/a$

	$k$	$\sin 5^\circ$	$\sin 10^\circ$	$\sin 20^\circ$	$\sin 30^\circ$	$\sin 50^\circ$	$\sin 65^\circ$
	$b/a$	1.7981	1.3556	0.9097	0.6443	0.3015	0.1296
$r = 0^\circ$	$x/a$	0	0	0	0	0	0
	$F/(2V_0/\pi a)$	1.5678	1.5589	1.5238	1.4675	1.3055	1.1638
$r = 10^\circ$	$x/a$	0.1115	0.1128	0.1180	0.1273	0.1633	0.2165
	$F/(2V_0/\pi a)$	1.5680	1.5596	1.5267	1.4738	1.3232	1.1953
$r = 20^\circ$	$x/a$	0.2230	0.2254	0.2351	0.2524	0.3182	0.4118
	$F/(2V_0/\pi a)$	1.5685	1.5617	1.5349	1.4924	1.3752	1.2898
$r = 30^\circ$	$x/a$	0.3344	0.3376	0.3506	0.3736	0.4587	0.5730
	$F/(2V_0/\pi a)$	1.5693	1.5649	1.5477	1.5212	1.4585	1.4469
$r = 40^\circ$	$x/a$	0.4456	0.4492	0.4640	0.4897	0.5818	0.6979
	$F/(2V_0/\pi a)$	1.5703	1.5688	1.5635	1.5573	1.5673	1.6630
$r = 50^\circ$	$x/a$	0.5568	0.5604	0.5750	0.6002	0.6878	0.7914
	$F/(2V_0/\pi a)$	1.5713	1.5730	1.5805	1.5967	1.6918	1.9272
$r = 60^\circ$	$x/a$	0.6677	0.6709	0.6837	0.7055	0.7790	0.8613
	$F/(2V_0/\pi a)$	1.5723	1.5769	1.5966	1.6346	1.8180	2.2151
$r = 70^\circ$	$x/a$	0.7786	0.7809	0.7903	0.8063	0.8589	0.9154
	$F/(2V_0/\pi a)$	1.5731	1.5801	1.6098	1.6662	1.9282	2.4849
$r = 80^\circ$	$x/a$	0.8893	0.8906	0.8956	0.9040	0.9313	0.9599
	$F/(2V_0/\pi a)$	1.5736	1.5822	1.6186	1.6871	2.0040	2.6813
$r = 90^\circ$	$x/a$	1	1	1	1	1	1
	$F/(2V_0/\pi a)$	1.5738	1.5829	1.6216	1.6945	2.0311	2.7539



Table 2. Field strength  $F$  at points along  $AB$  for different values of  $b/a$

	$k$	$\sin 1^\circ$	$\sin 5^\circ$	$\sin 10^\circ$	$\sin 20^\circ$	$\sin 30^\circ$	$\sin 50^\circ$	$\sin 90^\circ$
	$b/a$	2.8231	1.7981	1.3556	0.9097	0.6443	0.3015	0
$r = 0^\circ$	$y/a$	0	0	0	0	0	0	0
	$F/(2V_0/\pi a)$	1.5707	1.5678	1.5589	1.5238	1.4675	1.3055	1
$r = 10^\circ$	$y/a$	0.3845	0.2717	0.2250	0.1832	0.1641	0.1533	0.1763
	$F/(2V_0/\pi a)$	1.5706	1.5667	1.5559	1.5167	1.4568	1.2904	0.9848
$r = 20^\circ$	$y/a$	0.7691	0.5443	0.4520	0.3700	0.3332	0.3140	0.3640
	$F/(2V_0/\pi a)$	1.5701	1.5624	1.5454	1.4937	1.4231	1.2443	0.9397
$r = 30^\circ$	$y/a$	1.1541	0.8193	0.6837	0.5654	0.5140	0.4919	0.5774
	$F/(2V_0/\pi a)$	1.5686	1.5516	1.5225	1.4487	1.3615	1.1657	0.8660
$r = 40^\circ$	$y/a$	1.5407	1.1005	0.9259	0.7778	0.7173	0.7020	0.8391
	$F/(2V_0/\pi a)$	1.5633	1.5265	1.4764	1.3712	1.2637	1.0525	0.7660
$r = 50^\circ$	$y/a$	1.9323	1.3966	1.1908	1.0244	0.9640	0.9730	1.1918
	$F/(2V_0/\pi a)$	1.5459	1.4693	1.3875	1.2451	1.1197	0.9031	0.6428
$r = 60^\circ$	$y/a$	2.3414	1.7310	1.5086	1.3447	1.3021	1.3699	1.7321
	$F/(2V_0/\pi a)$	1.4891	1.3432	1.2238	1.0514	0.9198	0.7178	0.5000
$r = 65^\circ$	$y/a$	2.5641	1.9312	1.7103	1.5622	1.5412	1.6641	2.1445
	$F/(2V_0/\pi a)$	1.4245	1.2355	1.1011	0.9238	0.7972	0.6125	0.4226
$r = 70^\circ$	$y/a$	2.8158	2.1783	1.9713	1.8573	1.8744	2.0865	2.7475
	$F/(2V_0/\pi a)$	1.3132	1.0854	0.9448	0.7742	0.6596	0.4998	0.3420
$r = 75^\circ$	$y/a$	3.1318	2.5228	2.3529	2.3090	2.3968	2.7658	3.7321
	$F/(2V_0/\pi a)$	1.1295	0.8846	0.7523	0.6034	0.5084	0.3808	0.2588
$r = 78^\circ$	$y/a$	3.3890	2.8283	2.7032	2.7368	2.8997	3.4306	4.7046
	$F/(2V_0/\pi a)$	0.9735	0.7381	0.6199	0.4918	0.4121	0.3069	0.2079
$r = 80^\circ$	$y/a$	3.6181	3.1148	3.0383	3.1530	3.3928	4.0880	5.6713
	$F/(2V_0/\pi a)$	0.8479	0.6300	0.5252	0.4140	0.3458	0.2568	0.1736
$r = 83^\circ$	$y/a$	4.1488	3.8117	3.8676	4.1983	4.6403	5.7630	8.1444
	$F/(2V_0/\pi a)$	0.6270	0.4539	0.3750	0.2933	0.2441	0.1806	0.1219
$r = 85^\circ$	$y/a$	4.8032	4.7041	4.9434	5.5688	6.2846	9.9196	11.4301
	$F/(2V_0/\pi a)$	0.4603	0.3288	0.2704	0.2107	0.1751	0.1293	0.0872

The dashes denote functions having the complementary modulus, as before. The calculations have been carried out using six-figure tables.<sup>(3)</sup>

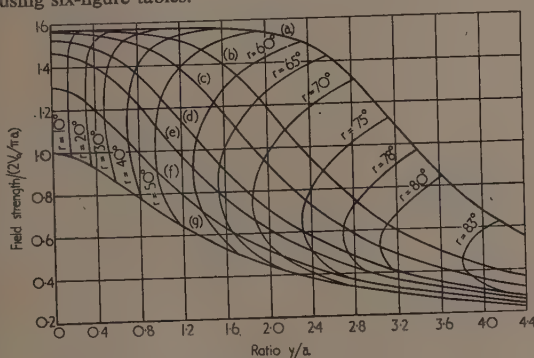


Fig. 4. Curves of field strength along  $AB$  for the following values of  $b/a$ :

(a) 2.8231; (b) 1.7981; (c) 1.3556; (d) 0.9097; (e) 0.6443; (f) 0.3015; (g) 0.

#### FORMULAE FOR THE POTENTIAL FUNCTION

Integration of equation (5) gives the value of the potential function  $W$  at any point. Taking  $W$  zero at the point  $B$  and  $-iV_0$  at the point  $C$ , the result is

$$W = -i(2V_0/\pi) \sin^{-1}(\sin w)$$

Thus along  $Ox$ ,

$$V = -(2V_0/\pi) \sin^{-1}(\sin w) \quad (8)$$

and along  $Oy$ ,

$$U = (2V_0/\pi) \sinh^{-1}(\sin' p/\operatorname{cn}' p) \quad (9)$$

The heavier work of calculating the abscissae and ordinates of points corresponding to values of  $w$  and  $p$  has already been carried out, and the values may be read directly from Tables 1 and 2. To obtain the values of the potential function along the principal axes therefore, it remains only to evaluate the comparatively simple expressions in (8) and (9).

An application of this may be pointed out in the electrodynamic analogy. The above procedure can be applied to the determination of the position on  $BC$  of the end of any equipotential line  $V = \text{a stated value}$ , and on  $AB$  of the end of any line of force  $U = \text{a stated value}$ . This enables lines of force and equipotential lines at defined intervals of the potential function to be plotted experimentally by the use of a Peierls' tank or by some similar method.

#### REFERENCES

- (1) DAVY, N. *Phil. Mag.*, 7, 35, p. 819 (1944).
- (2) ADAMS, E. P., and HIPPLESLEY, R. L. *Smithsonian mathematical formulae and tables of elliptic functions* (Washington: Smithsonian Institution, 1922).
- (3) COMRIE, L. J. *Chambers's six-figure mathematical tables* (London: W. and R. Chambers Ltd., 1948).



bring the furnace above the melting point of nickel ( $1455^{\circ}\text{C}$ ). At the melting point there was an estimated average temperature gradient of about  $12^{\circ}\text{C}$  per in. along the length of the ingot, sufficient to promote crystal growth. The nickel was kept molten for two hours while the furnace attained an equilibrium temperature and the voltage applied to the furnace (approximately 140 V) was then reduced slowly over a period of ten hours, by 0.5 V every hour, resulting in a  $5^{\circ}\text{C}$  drop in temperature per hour until the melt solidified. The voltage was then reduced by 1 V every hour, giving a temperature fall of 15 to  $20^{\circ}\text{C}$  per hour, down to  $1200^{\circ}\text{C}$  and finally the furnace was cooled fairly rapidly to room temperature.

#### EXTRACTION AND PREPARATION OF THE CRYSTAL

The sheath was broken and the ingot removed; grain boundaries between crystals in the specimen could be plainly seen. Traces of dissolved alumina were removed by polishing with coarse emery paper; finer papers were then used and the specimen was deeply etched in hot nitric acid, revealing the grain boundaries more clearly, after which the largest crystal (1 in. by  $\frac{3}{8}$  in. diameter) was carefully cut from the ingot with a jeweller's saw. Any strained material on the surface of the crystal was removed by electrolytic polishing. (Originally etching with hot nitric acid was used but this tended to pit the specimen severely.) The electrolyte, 100 ml orthophosphoric acid, 25 ml sulphuric acid and 75 ml distilled water, was placed in a stainless steel dish which served as the cathode and a current, density of  $1\text{ A/cm}^2$ , was passed through the cell.<sup>(2)</sup>

In order that faces could be cut in a given crystallographic direction in the crystal it was necessary to find the orientation of the crystal with respect to certain reference marks on the specimen; X-ray methods were used in preference to optical methods as greater accuracy can be obtained. The crystal was mounted on the goniometer arcs of a Unicam Universal X-ray camera and back reflexion Laue photographs were taken. The character of the X-ray reflexions, after electrolytic polishing, changed from streaks to clearly defined spots, showing that work-hardened material had been removed and also indicating whether the crystal was deformed in any way. Confirmation of the fact that the specimen was a single crystal was made by taking back reflexion photographs on opposite faces by rotating the crystal through  $180^{\circ}$  in position in the camera. The orientations of the specimen as worked out separately from the two photographs were identical, verifying that the specimen was in fact a complete single crystal.

In subsequently cutting the specimen to the desired shape, it was necessary to avoid introducing any undue strain; the specimen was therefore mounted in a mould by means of which the specimen was gripped while being machined. This procedure also facilitated a more accurate X-ray examination as reference marks could be made on the mould itself. Kallodoc liquid, supplied by I.C.I. Ltd., was found to possess suitable moulding characteristics as it polymerizes at  $45^{\circ}\text{C}$  after removal of the stabilizer with sodium hydroxide solution, the specimen being subjected to neither extreme pressure nor temperature. The resultant polymer, methyl methacrylate (Perspex), is easily machined, is transparent and can be dissolved with amyl acetate. The specimen was mounted in the mould which was then machined in the form of a rectangular block with one face close to, and approximately parallel to, a prominent crystal surface. The thin layer of Perspex above this was removed by polishing, and the crystal surface so exposed was polished as described above and a

back reflexion Laue photograph taken with the X-ray beam normal to the face. From an analysis of the resultant photograph, the positions of the crystal zone axes were plotted on a stereographic projection and indexed, thus enabling the angles which any required crystal planes made with the sides of the mould to be measured directly from the projection.<sup>(3)</sup>

A horizontal milling machine was used to cut the desired plane on the specimen, the cutting tool moving slowly across the crystal. The development of heat was reduced by the use of a large cutting tool and by continuous lubrication of the surface being cut. In order to avoid producing undue strain layers of one half-thousandth of an inch only were removed at a time. The photograph (Fig. 3) of the milling machine in operation shows the cutting tool set so that it made the required angles with the crystal thus enabling the

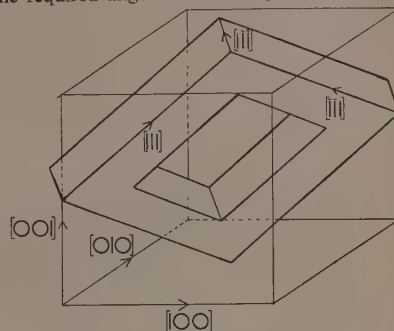


Fig. 2. Orientation of the "picture frame" with respect to the crystallographic axes

crystal plane to be cut in one operation. The specimen was remounted (after cutting one face), to enable a parallel opposite face to be cut, so that at no stage was the crystal subjected to any undue strain.

In shaping the crystal into the form of a picture frame it was necessary to remove the central portion of the specimen. Instead of drilling, a small hole was milled in the centre of the crystal, as less heat was developed and the cutting tool showed no tendency to slip despite the fact that it entered the crystal at an angle to the surface; the hole was then filed to the shape shown in the diagram (Fig. 2), and the "picture



Fig. 3. Photograph of milling machine and specimen in position



frame" crystal removed from the methyl methacrylate. After mechanical and electrolytic polishing, and reannealing, the crystal was in a suitable form for the investigation of its magnetic properties.

## ACKNOWLEDGEMENTS

The author wishes to thank Professor Roberts of the Department of Coal, Gas and Fuel Industries with Metallurgy, for the loan of the furnace; Mr. C. Bastow for assistance in its use; the Mond Nickel Co. for the supply of the nickel; Mr. J. W. Spark who machined the crystal; Dr. R. S. Tebble whose guidance and advice at all stages of the work has been very greatly appreciated, and finally, Professor

E. C. Stoner, under whose direction this work has been carried out. The author is also indebted to the Department of Scientific and Industrial Research and the University of Leeds for a maintenance grant.

## REFERENCES

- (1) BOZORTH, R. M., WILLIAMS, H. J., and WALKER, J. C. *Rev. Sci. Instrum.*, **20**, p. 947 (1949).
- (2) BATES, L. F., and WILSON, G. W. *Proc. Phys. Soc., Lond. A*, **64**, p. 691 (1951).
- (3) BARRETT, C. S. *Structure of Metals*, 2nd ed., p. 185 (New York: McGraw Hill Book Co. Inc., 1952).

## Some aspects of light scattering from polydisperse systems of spherical particles

By E. ATHERTON, B.Sc., A.Inst.P., and R. H. PETERS, B.Sc., Ph.D., Imperial Chemical Industries Ltd., Hexagon House, Manchester, 9

[Paper first received 11 February, and in final form 21 April, 1953]

The simple theory of light scattering, as developed by Debye, is discussed and its application to polydisperse systems of spherical particles examined. Three measurements are possible, namely, dissymmetry, turbidity and the relation of the latter with wavelength. By employing model distributions these three parameters of the scattering may be calculated and the average values for the diameter given by them studied. The dissymmetry ratio, whilst giving an indeterminate average, leads to values of the diameters which approximate to the weight average given by the turbidity technique. The wavelength dependence of turbidity gives a diameter which approximates to the mean of the distribution.

The light scattering properties of colloidal systems have been studied in detail during the last few decades, but it is only recently with the advent of sensitive photo-detectors and a simple theory developed by Debye<sup>(1)</sup> that methods have been developed for the absolute determination of particle size in the submicroscopic range. Debye's treatment falls into two parts: (a) the light scattered from a small solute particle situated in a solvent medium is related to the random fluctuations which occur in the concentration of the solute. This in turn is connected thermodynamically with the molecular weight of the solute particle; (b) particles whose size is large compared with the wavelength of light are treated as though their presence does not perturb the exciting wave. Because of its simplicity and ready interpretation, Debye's theory stimulated many workers, whose results provided experimental justification for his treatment. Notwithstanding its potential value to the technologist working with colloidal dispersions, the majority of investigators have used carefully prepared and highly purified materials. Studies of this type are of value in determining molecular size and configuration as a function of temperature and solution properties, but the results are restricted since the samples employed corresponded to an assembly of identical molecules. Indeed, when the aim of the work is to elucidate the physico-chemical properties of some substance, the removal of homologues and foreign impurities is essential.

However, the technologist must usually confine his attention to systems which are impure and non-homogeneous in respect of size. For such materials the light scattering methods, as at present constituted, lose their precise significance since they only apply rigidly to the pure system outlined above. None the less, it is desirable to develop the present techniques

for application to practical systems, modifying and extending the theory where possible.

The present paper is an attempt to carry out this extension and to review the potential utility of the light scattering methods when applied to relatively impure polydisperse systems.

## THEORETICAL CONSIDERATIONS

The first part of Debye's theory is concerned with small particles whose size is less than  $\lambda/20$ , where  $\lambda$  is the wavelength of light. This restriction enables the particle to be treated as a simple dipole oscillating in phase with the exciting wave. The strength of the dipole is determined by the amplitude of the primary wave and the polarizability of the particle or molecule, and its radiation may be readily calculated in these terms as shown by Lord Rayleigh.<sup>(2)</sup> A solution corresponds to an assembly of particles in an isotropic solvent medium and the scattering of such a system is governed by two factors. Firstly, the intrinsic scattering power of the individual particles, which has already been discussed, and secondly the way in which the scattered light waves are combined at the point of observation.

Scattering from a solution arises from inhomogeneities in the system due to the random motion of the particles and is dependent upon small scale concentration fluctuations. The problem has been solved by Debye<sup>(1)</sup> and an equation (1) derived relating the amount of light scattered to the colligative properties of the system.

$$\frac{32\pi^3 n^2 (\delta n / \delta c)^2}{3N_0 \lambda^4} \left( \frac{c}{\tau} \right) = \frac{1}{M} + \frac{2B}{RT} c \quad (1)$$

where  $n$  is the refractive index of the solvent,  $\delta n/\delta c$  is the change of refractive index with concentration.

$N_0$  = Avogadro's number,

$\lambda$  = the wavelength of light,

$M$  = the molecular weight of the solute,

$R$  = the gas constant,

$T$  = the absolute temperature,

$B$  = the constant allowing for non-ideal behaviour in the osmotic pressure relation of Van't Hoff,

$c$  = the concentration of the solution,

$\tau$  = the turbidity of the solution and is defined as  $-\ln$  (transmission of the solution for unit length of path).

If the particle has a size of the order of  $\lambda/20$  the treatment must be modified by replacing the particle by a set of dipoles each of which is oscillating in phase with the incident light but which, because of their separation, are not in phase with each other. When the light scattered from each of these dipoles is observed at an external point the phase differences cause destructive interference. The extent of the resulting intensity reduction depends on the position of the point of observation relative to the incident beam.

Debye's second calculation deals with larger particles and leads to an angular scattering function,  $f(D, \theta)$ . This function represents the reduced intensity of light scattered from a particle which is characterized by a linear dimension,  $D$ , at a point whose radius vector to the particle makes an angle  $\theta$  with the incident beam. For a sphere,  $D$  is the diameter and the equation for  $f(D, \theta)$  may be written as

$$f(D, \theta) = f(q) = [3q^{-3}(\sin q - q \cos q)]^2 \quad (2)$$

where  $q = 2\pi(D/\lambda) \sin \frac{1}{2}\theta$ .

In Fig. 1  $[f(D, \theta)(1 + \cos^2 \theta)]$  is plotted in polar coordinates for a value of  $D$  of  $0.4\lambda$  and the graph clearly shows the dissymmetrical nature of such an envelope when compared with that of  $(1 + \cos^2 \theta)$  which represents scattering by

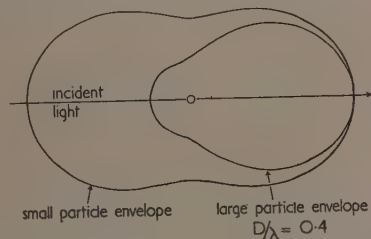


Fig. 1. Scattering by large and small spheres

a small particle (plotted on a comparable scale). The dissymmetry arises from the interference previously mentioned being more destructive in the backward than in the forward direction. Debye has characterized this property by the ratio of the intensities of light scattered at two values of  $\theta$ , one in the forward and the other in the backward direction. This dissymmetry ratio may be written,

$$S = f(D, 45^\circ)/f(D, 135^\circ) \quad (3)$$

For the particles of diameter up to  $\lambda$ , this ratio bears a unique relation with  $D$  and hence a curve relating  $S$  to  $D/\lambda$  may be drawn.

**Derivation of the function  $f(D, \theta)$ .** This may be determined simply by evaluating the Hertzian potential,  $\Pi$ , at a point  $P$  whose position in spherical polar co-ordinates is given by  $(r, \theta, \phi)$  arising from an isotropic sphere of radius,  $a$ , placed at the origin  $O$  and subjected to a parallel beam of light

(Fig. 2). Consider a plane wave whose field vector is  $E$  travelling along  $OZ$  referred to axes  $OXYZ$  and let  $\Sigma$  be a reference plane normal to  $OZ$ . For simplicity,  $E$  may be resolved into components  $E_x$  and  $E_y$ , and the Hertzian

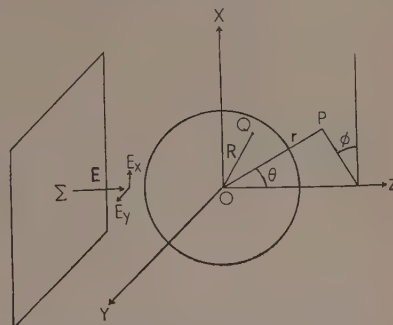


Fig. 2. Interaction of plane wave with sphere

potentials arising from the interactions of each of these with the sphere calculated and superimposed to obtain the resultant potential at  $P$ .  $E = (0, E_y, 0)$  is considered first and gives rise to a dipole  $p \, dv$  at a point  $Q$  in the sphere (Fig. 2).  $p$  has components  $(0, p_y, 0)$  and if the sphere has a polarizability,  $\alpha$ ,  $p$  will be of magnitude  $\alpha E_y$ . Furthermore, since  $E$  is a harmonic function of time

$$E = E_0 \exp [-2\pi(i/\lambda)(ct - d)] \quad (4)$$

where  $E_0$  = the amplitude,

$c$  = the velocity of light,

$d$  = the distance from the reference plane  $\Sigma$  to  $Q$ .

The Hertzian potential  $\Pi$  for the volume  $dv$  will be  $(p/PQ)dv$  and hence the total potential will be the integral of this, i.e.

$$\Pi = \int_{\text{Sphere}} \frac{p}{PQ} dv \quad (5)$$

If  $P$  is assumed to be a long way from  $Q$  and  $E$  is assumed to be undistorted, the integral may be evaluated to give

$$\Pi_y = V\alpha E_0 r^{-1} [f(q)]^{1/2} \exp [-2\pi i/\lambda(ct - d)] \quad (6)$$

where  $V$  is the volume of the particle and is equal to  $4\pi a^3/3$  and  $d$  is the distance from  $\Sigma$  to  $Q$  and  $Q$  to  $P$ .

A similar equation may be found for  $\Pi_x$ ,  $\Pi_z$  being taken to be zero.

The fields  $E_s$  and  $H_s$  associated with the Hertzian potential at the point of observation may be derived from equations

$$\left. \begin{aligned} E_s &= \nabla \nabla \cdot \Pi - \frac{1}{c} \frac{\partial^2 \Pi}{\partial t^2} \\ H_s &= \frac{1}{c} (\nabla \times \frac{\partial \Pi}{\partial t}) = \frac{1}{c} \frac{\partial}{\partial t} (\nabla \times \Pi) \end{aligned} \right\} \quad (7)$$

The fields arising from  $E_s$  and  $H_s$  may be calculated separately, ignoring terms of order  $r^{-2}$  which do not contribute to the radiation field. From these the rate of energy flow per unit area at  $P$  arising from  $\Pi_x$  may be calculated as the time average of the Poynting vector, i.e.

$$I(D, \theta) = (c/8\pi) [\overline{E_s \times H_s}]^t = (c/8\pi) 8\pi^4 \alpha^2 V^2 E_0^2 \lambda^{-4} r^{-2} f(q) \cos^2 \theta \quad (8)$$

If the same calculation is carried out for  $\Pi_y$ , the resultant intensity at  $P$  is

$$I(D, \theta) = (c/8\pi) 8\pi^4 \alpha^2 V^2 E_0^2 \lambda^{-4} r^{-2} f(q) \quad (9)$$

and the intensity for unpolarized light is the sum of these two intensities. Writing it as a fraction of the incident intensity we obtain

$$I(D, \theta)/I_0 = 16\pi^4\alpha^2 V^2 \lambda^{-4} r^{-2} f(q)(1 + \cos^2 \theta) \quad (10)$$

The total scattered intensity expressed as a fraction of the incident intensity, or the turbidity,  $\tau$  as it is called, may be derived by integrating the above equation over the surface of a sphere, radius  $r$ , with its centre at the particle. For a suspension containing  $N$  such particles per unit volume which is sufficiently dilute for the scattering from the particles to be incoherent, the scattering will be  $N$  times that from a single particle. If  $-\delta I_0$  is the loss in intensity when the beam passes through a unit layer of solution, then the turbidity is given by

$$-\delta I_0/I_0 = 16\pi^4\alpha^2 V^2 \lambda^{-4} N \int_{\text{Sphere}} r^{-2} f(q)(1 + \cos^2 \theta) dS \quad (11)$$

#### EXTENSION OF THE THEORY TO POLYDISPERSE SYSTEMS

**Turbidity.** It has been shown experimentally that equation (1) is valid for many types of polymer in solution. As presented the equation only applies to solutions containing one size of molecule or particle, but Zimm and Doty<sup>(4)</sup> have shown that when a range of sizes is present the turbidity method gives the weight average molecular weight of the polymer sample. In the case of a dispersion the value of  $M$  obtained from equation (1) when multiplied by the mass of hydrogen atom gives the weight average weight of the dispersed particles. Measurements of the density enable this value to be converted to an average diameter. Since the weight average molecular weight  $M_W$  is given by

$$M_W = \sum_i n_i M_i^2 / \sum_i n_i M_i$$

it follows that the average diameter obtained in this way, denoted by  $D_r$  is given by

$$D_r = \left[ \sum_i n_i D_i^6 / \sum_i n_i D_i^3 \right]^{1/3} \quad (12)$$

where  $M_i$  and  $D_i$  are the "molecular weight" and diameter of the  $i$ th particle species whose number fraction is  $n_i$ .

In practice, of course, equation (1) may not be used for large particles without modification to allow for reduction of turbidity due to interference effects. The necessary adjustment may be made by determining graphically, for each particle size, the decrease in the scattering envelope from the corresponding "small particle" envelope. This reduction, corresponding to the solid of rotation about the incident light axis of the area between the two envelopes (Fig. 1) is related uniquely to the dissymmetry ratio and if a curve is drawn relating these two quantities, a single measurement of the dissymmetry ratio gives the turbidity correction factor. This method, which has been described in detail by Doty,<sup>(3)</sup> has been used to correct turbidities measured by a spectrophotometer for the calculation of particle size of polymers<sup>(5)</sup> and is used in the present work.

**Dissymmetry.** Many examples have been reported of particle size determinations based on measurements of the dissymmetry ratio and in all cases care was taken to ensure that the systems studied were monodisperse. A good example of this type of study is that by Doty, Oster and Zimm<sup>(6)</sup> of the rod-shaped particles of tobacco mosaic virus. Turbidities were corrected by the method outlined above and excellent agreement was obtained with the electron microscopic method.

These authors measured solutions of the virus at several concentrations and employed the dissymmetry ratio obtained by extrapolation to infinite dilution for their calculations. In this way the optical effects of particle interaction were minimized. This work verifies the accuracy of the dissymmetry method for monodisperse systems and in order to extend its usefulness in practice an attempt has been made to calculate the effect of polydispersity on the dissymmetry ratio, as follows:

For a system containing  $n_i$  particles of linear dimensions  $D_i$ , the total amount of light scattered at an angle  $\theta$  to the incident light is given by

$$\sum_i n_i I(D_i, \theta)$$

and the corresponding dissymmetry ratio  $S$  is given by

$$S = \sum_i n_i I(D_i, 45^\circ) / \sum_i n_i I(D_i, 135^\circ) \quad (13)$$

This is not related in any simple manner to the dissymmetry ratios of the individual species, i.e. to

$$S_i = I(D_i, 45^\circ) / I(D_i, 135^\circ) \quad (14)$$

In measurements of polydisperse samples the diameter is determined from the dissymmetry ratio as defined in equation (3), treating the sample as if it were monodisperse. Such a treatment gives an average diameter,  $D_{DIS}$ , defined by the equation,

$$S = I(D_{DIS}, 45^\circ) / I(D_{DIS}, 135^\circ) \\ = \sum_i n_i I(D_i, 45^\circ) / \sum_i n_i I(D_i, 135^\circ) \quad (15)$$

From equation (10) this reduces to

$$S = \left[ \sum_i n_i D_i^6 f(q_i) \right]_{\theta=45^\circ} / \left[ \sum_i n_i D_i^6 f(q_i) \right]_{\theta=135^\circ} \quad (16)$$

where

$$q_i = 2\pi(D_i/\lambda) \sin \frac{1}{2}\theta$$

If  $n_i$  is a known function of  $D_i$ ,  $S$  may be evaluated and  $D_{DIS}$  found from the graph of  $S$  versus  $D/\lambda$  mentioned above. In order to investigate the nature of  $D_{DIS}$  for different types of polydisperse system equation (15) was evaluated for a number of hypothetical size distributions. Since many practical distributions approximate to it, the Gaussian form was chosen

$$dn = [N/\sigma(2\pi)^{1/2}] \exp [-(D - \bar{D})^2/\sigma^2] dD \quad (17)$$

where  $N$  is the total number of particles,  $\sigma$  the standard deviation,  $\bar{D}$  the mean and  $dn$  refers to the number of particles whose diameters lie between  $D$  and  $D + dD$ . Substituting for  $n_i$  in equation (15) and replacing the sums by integrals gives

$$S = \frac{\left\{ \int_0^\infty D^6 f(q) \exp [-(D - \bar{D})^2/\sigma^2] dD \right\}_{\theta=45^\circ}}{\left\{ \int_0^\infty D^6 f(q) \exp [-(D - \bar{D})^2/\sigma^2] dD \right\}_{\theta=135^\circ}} \quad (18)$$

The distributions examined covered a range of values of  $\bar{D}$  between 0.05  $\mu$  and 0.25  $\mu$  and of  $\sigma$  between 0.1  $\bar{D}$  and 0.3  $\bar{D}$ . For each distribution, the function

$$D^6 f(q) \exp [-(D - \bar{D})^2/\sigma^2]$$

was calculated for various values of  $D$  at  $\theta = 45^\circ$  and  $\theta = 135^\circ$  and plotted against  $D$ . The integrals in equation (18) were determined graphically and the dissymmetry ratios



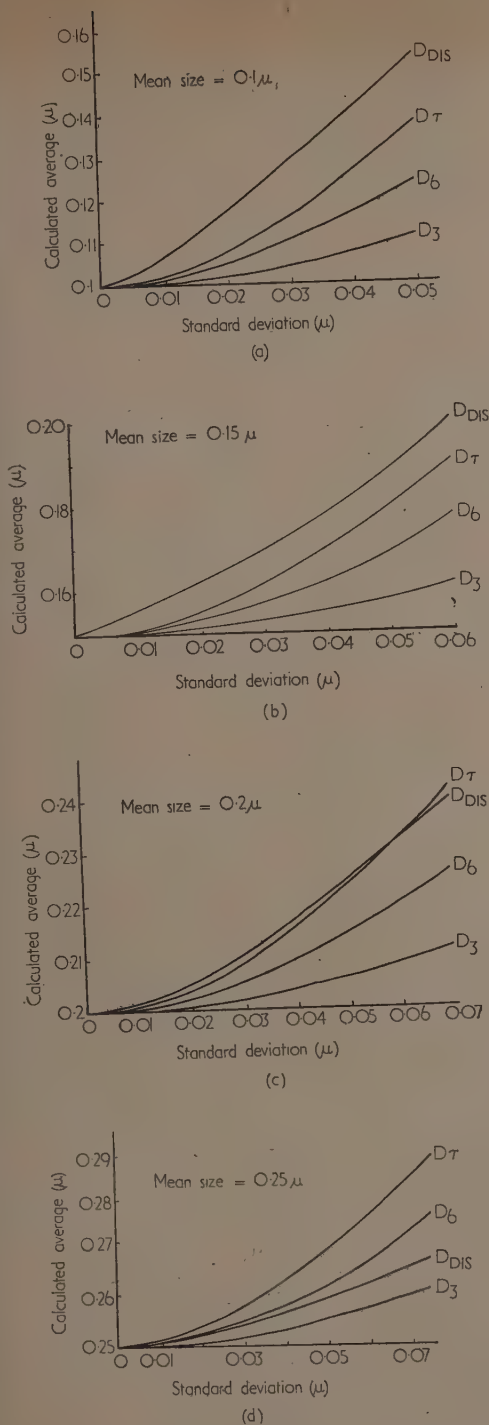


Fig. 3. Average diameters of Gaussian distributions  
VOL. 4, NOVEMBER 1953

calculated from the ratio of the two integrals, the average diameter  $D_{DIS}$  being found from the curve of  $S$  versus  $D/\lambda$ . In order to locate  $D_{DIS}$  relative to other parameters, the moments about the origin were calculated for each distribution studied. The moments were defined by

$$\mu_n = \int_0^{\infty} D^n \exp[-(D - \bar{D})^2/\sigma^2] dD / \int_0^{\infty} \exp[-(D - \bar{D})^2/\sigma^2] dD \quad (19)$$

and the various average diameters calculated by the relation  $D_n = (\mu_n)^{1/n}$ . The turbidity average diameter was calculated as

$$D_{\tau} = (\mu_6/\mu_3)^{1/3} \quad (20)$$

Fig. 3 gives the values of  $D_{DIS}$  plotted as a function of  $\sigma$  for fixed values of  $\bar{D}$ , and the other averages  $D_n$  are included for comparison. It is apparent that the dissymmetry average is not of the same type as any of the others—its position relative to them depending on the values of  $\bar{D}$  and  $\sigma$ . Since dissymmetry measurements can be obtained easily and rapidly in practice it is of interest to know the deviation between the dissymmetry average and any other determinable average, such as that obtained by turbidity. In Fig. 4, the ratio  $D_{DIS}/D_{\tau}$  has been plotted against  $\bar{D}$  for fixed values of  $\bar{D}/\sigma$  and it can be seen that nowhere in the range of sizes studied is the deviation greater than  $\pm 12\%$ . Thus dissymmetry

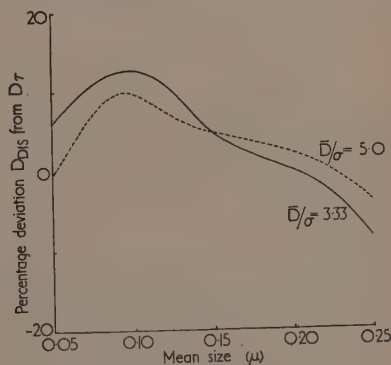


Fig. 4. Divergence of dissymmetry and turbidity average diameters

measurements may be used in practice for rapid size characterization with relatively little ambiguity as to the significance of the result.

**Turbidity—wavelength dependence.** Using equation (1) for small particles at low concentrations, if  $\log \tau$  is plotted against  $\log \lambda$ , a straight line of gradient  $-4$  is obtained. This simple relation is only true for particles whose sizes are small, say less than  $\lambda/20$ , the gradients decreasing in numerical value as the particles increase in size. The deviations of gradient from the value of  $-4$  have been experimentally related to particle size by Heller<sup>(7)</sup>, who worked with aqueous dispersions of polystyrene, polyisoprene and styrene/isoprene co-polymers. The samples studied were monodisperse and varied in size between 0.1  $\mu$  and 0.25  $\mu$  (distribution width  $< 0.02 \mu$ ). Heller obtained straight line plots the gradients of which he related to particle size as determined with the electron microscope. The resulting curve is shown in Fig. 5 and serves as a

calibration for the method if unknown sizes are to be determined by optical measurements. The linearity of the  $\log \tau / \log \lambda$  plots is surprising in view of equation (11), which indicates that  $\tau$  is a power series in  $\lambda$  and not a single term of the form  $\lambda^m$ . The explanation is that over the spectral ranges in which measurements are carried out, the curvature of the plot is not apparent due to the neglect in the Debye treatment of the refractive index and its change with wavelength.

In order to investigate Heller's curve in greater detail, equation (11) was evaluated as

$$Q = \int_{\text{Sphere}} f(q)r^{-2}(1 + \cos^2 \theta)dS = 2\pi \int_{-\pi/2}^{\pi/2} f(q)(1 + \cos^2 \theta) \sin \theta d\theta \quad (21)$$

the other terms being ignored since only the dependence of  $\log \tau$  on  $\log \lambda$ , and not the actual value of  $\tau$ , was required.

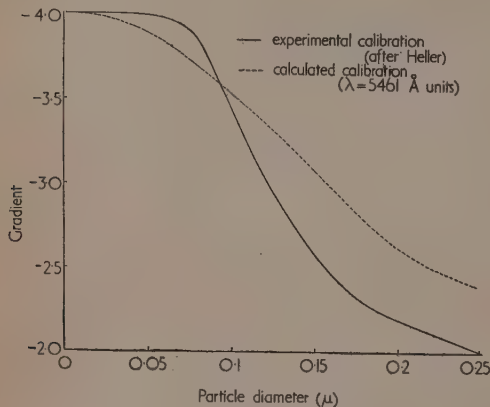


Fig. 5. Relation between gradient of  $\log \tau / \log \lambda$  plot and size

The function  $(\log Q - 4 \log \lambda)$  was plotted against  $\log \lambda$  for a series of values of  $D$  and the plots have a slight curvature (Fig. 6).

It is therefore necessary, in order to characterize the curves by Heller's method, to determine the slope at one particular wavelength, either by calculation or by drawing tangents.

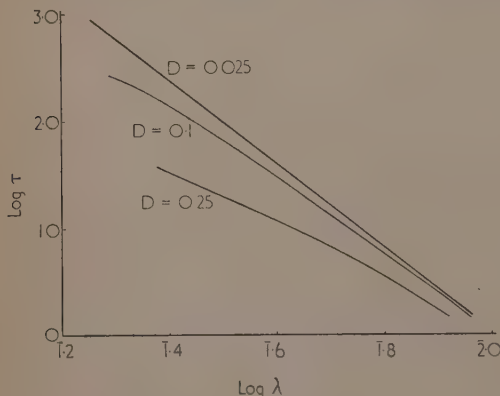


Fig. 6. Plots of  $\log \tau / \log \lambda$

Both these procedures involve the use of graphical methods, and it is important to select the one involving the smaller errors. This is because particle size as determined by this method is sensitive to small differences of gradient. The drawing of tangents may be subject to uncertainty and should be avoided where possible.

In this case the difficulty can be avoided as the following analysis shows.

$$\text{Slope of tangent to } \log \tau / \log \lambda \text{ graph} = \partial \log \tau / \partial \log \lambda = \lambda \tau^{-1} \partial \tau / \partial \lambda$$

$$\begin{aligned} \text{But } \partial \tau / \partial \lambda &= 16\pi^4 \alpha^2 V^2 N [(\partial/\partial \lambda) \lambda^{-4} \int f(q)r^{-2}(1 + \cos^2 \theta)dS] \\ &= 16\pi^4 \alpha^2 V^2 N [-4\lambda^{-5} \int f(q)r^{-2}(1 + \cos^2 \theta)dS + \\ &\quad \lambda^{-4} \int (\partial/\partial \lambda) f(q)r^{-2}(1 + \cos^2 \theta)dS] \end{aligned}$$

(Assuming that the integral is uniformly convergent.)

$$\begin{aligned} \lambda \tau^{-1} (\partial \tau / \partial \lambda) &= -4 + \frac{\lambda \int f'(q)(\partial/\partial \lambda) r^{-2}(1 + \cos^2 \theta)dS}{\int f(q)r^{-2}(1 + \cos^2 \theta)dS} \\ &= -4 - \frac{\int q f'(q) r^{-2}(1 + \cos^2 \theta)dS}{\int f(q)r^{-2}(1 + \cos^2 \theta)dS} \quad (22) \end{aligned}$$

This function involves two integrals which may be evaluated graphically with a planimeter to a high degree of accuracy, and because this method was more reliable than that involving tangent drawing it has been employed in this work.

The functions in equation (22) are dependent only on  $D/\lambda$  and hence the gradients were calculated for a range of values of this variable. The final graph relating the gradient to particle size is given in Fig. 5 for a wavelength of 4097 Å which is equivalent to 5461 Å in air. The calibration curve so obtained is similar in shape to that of Heller but differs in detail. For small particle sizes the gradients are larger, whereas for large sizes they are smaller. The wavelength used for this work was chosen for its central position in the visible region of the spectrum, thereby giving an average value for the gradient. This choice has been justified by its subsequent use in measurements of the particle size of lattices. Furthermore, this wavelength corresponds to the green line in the mercury spectrum and is a convenient one to use in practical work. The difference between the two calibration curves is apparent for the range of sizes studied and may be accounted for by the manner in which Heller measured his turbidities or by the breakdown of the Debye theory. The latter seems unlikely since accurate results may be obtained by the turbidity and dissymmetry techniques for sizes as large as 0.25  $\mu$  with polyvinyl chloride and polycellosolve methacrylate lattices.

These considerations have been extended to polydisperse systems in order to investigate the degree of curvature of the  $\log \tau / \log \lambda$  plot to be expected for such systems and to obtain some knowledge as to the type of average diameter obtained by this method. The gradients for a known polydisperse system of the type studied earlier may be calculated by slightly modifying the previous theory as follows. The turbidity of a sample will be given by:

$$\tau = 16/9 \pi^4 \alpha^2 N \lambda^{-4} \int_{\text{Sphere}} \int_0^\infty D^6 / \sigma(2\pi) \exp [-(D - \bar{D})^2/2] \sigma f(q)r^{-2}(1 + \cos^2 \theta) dD dS$$

this may be differentiated logarithmically to give

$$\log \tau / \log \lambda = -4 -$$

$$\frac{\int_{\text{Sphere}} \int_0^{\infty} D^6 \exp[-(D - \bar{D})^2 / \sigma^2] f'(q) r^{-2} (1 + \cos^2 \theta) dD dS}{\int_{\text{Sphere}} \int_0^{\infty} D^6 \exp[-(D - \bar{D})^2 / \sigma^2] f(q) r^{-2} (1 + \cos^2 \theta) dD dS} = -4 -$$

$$\frac{\int_0^{\infty} D^6 \exp[-(D - \bar{D})^2 / \sigma^2] \int_{\text{Sphere}} q f'(q) r^{-2} (1 + \cos^2 \theta) dS dD}{\int_0^{\infty} D^6 \exp[-(D - \bar{D})^2 / \sigma^2] \int_{\text{Sphere}} f(q) r^{-2} (1 + \cos^2 \theta) dS dD}$$

The integrations employed in equation (22) have been used for this purpose. For a fixed value of  $\lambda$  the inner integrals are known and the total integrands were plotted against  $D$  and graphically integrated. This process was carried out for two model distributions of mean diameters 0.1 and 0.2  $\mu$  and standard deviations of 0.025 and 0.05  $\mu$  respectively.

The average particle diameters corresponding to the calculated gradients are compared with the values of  $\bar{D}$  for the two systems in the table. It is apparent that they do not differ greatly from the means of the distributions, indicating that the  $\log \tau / \log \lambda$  method gives a particle size which approximates to the number average of the system studied.

Effect of polydispersity on  $\log \tau / \log \lambda$  gradients

Mean particle diameter in $\mu$	Standard deviation in $\mu$	Gradient of $\log \tau / \log \lambda$ plot	Predicted particle diameter in $\mu$
0.1	0.025	-3.48	0.11
0.1	—	-3.58	0.10
0.2	0.05	-2.60	0.21
0.2	—	-2.63	0.20

In so far as the  $\log \tau / \log \lambda$  method may be considered to give the mean size there is a possibility of combining this method with the turbidity method (which gives a known weighted average) in order to obtain a picture of the distribution. This can be done only if a known form of distribution be assumed. For a normal distribution as discussed previously, the standard deviation may be calculated by successive approximation using the equation for the turbidity average diameter in terms of  $\bar{D}$  and  $\sigma$  (equation 20).

$$D_{\tau} = \frac{\frac{\sqrt{\pi}}{2} [1 + \operatorname{erf}(\bar{D}/\sigma)] \left( \frac{15}{8} \sigma^7 + \frac{45}{4} \sigma^5 \bar{D}^2 + \frac{15}{2} \sigma^3 \bar{D}^4 + \sigma \bar{D}^6 \right)}{\frac{\sqrt{\pi}}{2} [1 + \operatorname{erf}(\bar{D}/\sigma)] \left( \frac{3}{2} \sigma^3 \bar{D} + \sigma \bar{D}^3 \right)}$$

In this way, a picture of the article size distribution may be derived.

These conclusions apply with a fair degree of accuracy to distributions which have  $\sigma < 0.25 \bar{D}$ , a type which is found in practice among textile bonding and leather finishing agents and will be reported in a subsequent communication.

## CONCLUSIONS

The investigations reported have been directed towards extending the practical utility of the light scattering methods of particle size determination based on Debye's equation. Theoretical analysis of the angular distribution of light scattered from model systems of spherical particles indicates that if measurements are made and Debye's relation is applied, the value of particle diameter obtained is an indeterminate average of the size distribution. The practical value of such measurements, however, is that they provide a rapid means of characterizing a commercial dispersion in terms of particle size by a simple determination of the ratio of two light intensities. The differences which can occur ( $\pm 12\%$  approximately) between the dissymmetry average diameter and a known average of the distribution (the turbidity average) are sufficiently small to make the method of value in many practical cases, as, for instance, in checking the reproducibility of a production process from batch to batch.

The two other optical methods which have been discussed are the determination of turbidity and the wavelength dependence of turbidity. The turbidity method gives an average of the type

$$D_{\tau} = \left[ \frac{\sum n_i D_i^6}{\sum n_i D_i^3} \right]^{1/3}$$

and is of use if more definite information on the material is required, while the  $\log \tau / \log \lambda$  method determines a quantity which approximates to the number average size of the distribution. Most of the results have been obtained from Debye's theory because of its simplicity and ease of manipulation for graphical methods of integration. Since the theory is only approximate, it is to be expected that deviation from the calculated averages will occur in practice. As will be shown in a subsequent paper, these are not sufficiently serious to impair the usefulness of the methods for the particle size characterization of industrial dispersions.

## REFERENCES

- (1) DEBYE, P. *J. App. Phys.*, **15**, p. 338 (1944); *J. Phys. Chem.*, **51**, p. 18 (1947).
- (2) RAYLEIGH, LORD. *Phil. Mag.*, **41**, p. 447 (1871).
- (3) DOTY, P. M. *J. Chim. Phys.*, **44**, p. 242 (1947).
- (4) ZIMM, B. H., and DOTY, P. M. *J. Chem. Phys.*, **12**, p. 203 (1944).
- (5) ATHERTON, E., and PETERS, R. H. *J. Text. Inst. [Manchester]*, **43**, T179 (1952).
- (6) DOTY, P. M., OSTER, G., and ZIMM, B. H. *J. Amer. Chem. Soc.*, **69**, p. 1193 (1947).
- (7) HELLER, W. *J. Chem. Phys.*, **14**, p. 566 (1946).



# Correspondence

## Further applications of the electrical analogue to vacuum systems

The analogous aspects of vacuum systems and certain electrical circuits have long been recognized, but apparently like the application of analogue techniques to heat and mass flow problems, the practical usefulness has taken some time to be appreciated. The letter from M. J. Aitken,<sup>(1)</sup> has indicated that the electrical analogue may play an increasingly important part in the study and design of large vacuum systems, and to these ends, a transient response type would often prove useful.

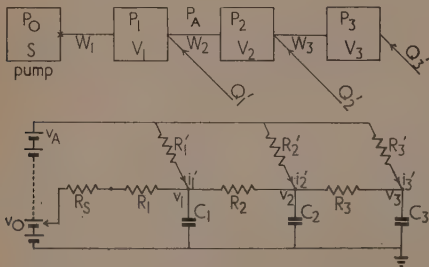
Elementary considerations show that the ordinary type of vacuum system operating under free molecular gas flow conditions may be represented by an  $R$ - $C$  electrical circuit with various sources of e.m.f.'s or currents. The related equations are:

$$Q = \delta P/W = V dP/dt \text{ at constant volume.}$$

$$i = \delta v/R = C dv/dt \text{ at constant capacity.}$$

The analogous quantities are apparent from comparison of these two sets of equations.

A simple vacuum system, shown diagrammatically by the upper part of the figure, has a pump of speed  $S$ , lumped elements of volume  $V$  and tubulation resistances  $W$  with leaks  $Q'$  at various points. These leaks may be viscous in



Analogous vacuum and electrical systems

character and therefore not satisfy the linear pressure relation, but the changes in the gas pressure in the system will usually be so small relative to the external pressure  $P_A$ , that there will be little error in writing,

$$Q_1 = (P_A - P_1)/W'_1, \text{ etc.,}$$

with  $W'_1$  as the effective resistance of the leak.

The lower part of the figure shows the analogous electrical circuit, with resistors  $R$  replacing the tubes, condensers  $C$  replacing the volumes and voltages  $v$  corresponding to the pressures. Measurements of voltages with time will give the corresponding variations of pressures with time, and likewise the various currents  $i$  will give the appropriate values of throughputs  $Q$ .

The scaling factors introduced into the values of the parameters will determine the relative time scales, which in turn will usually decide the mode of presentation of the information provided by the analogue. This subject has been discussed at length by Pashkis and Baker,<sup>(2)</sup> Lawson and McGuire<sup>(3)</sup> and others. Lawson and McGuire have also examined mathematically the accuracy attainable with a lumped element analogue of a continuously distributed

system, which will be relevant in the vacuum case when the system tubulation is also the main volume.

With the analogue envisaged, the effects of inserting pumps or pumping devices at various points in a vacuum line may be easily determined. By switching a metered quantity of charge into a point, the sudden evolution of known quantities of gas or vapour, may be simulated. Similarly, the response of a system to mixtures of gas and/or vapours may be found by varying the values of the parameters appropriate to each component.

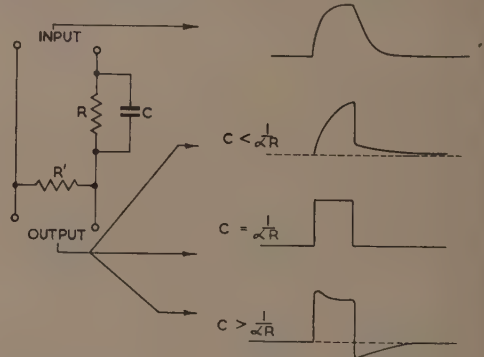
Applied Physics Department,  
Northampton Polytechnic.

D. W. STOPS

- (1) AITKEN, M. J. *Brit. J. Appl. Phys.*, **4**, p. 188, 1953.
- (2) PASHKIS, V., and BAKER, H. O. *Trans. Amer. Soc. Mech. Engrs*, **64**, p. 105, 1942.
- (3) LAWSON, D. I., and MCGUIRE, J. H. Private communication.

## A simple bridge method of measurement of the time constant of exponential decays

The bridge circuit described below was devised for the measurement of the decrement of a high  $Q$ -factor cavity resonator at about 3000 Mc/s. It is assumed that the resonator is excited by a relatively long pulse, at its resonant frequency. When the input pulse ceases, the field in the resonator decays as, say  $\exp(-\alpha t)$ . If the resonator output be rectified, amplified, and applied to the circuit shown in the figure, then the output from the circuit will be zero during



the whole of the decay of the free oscillations in the resonator, if  $CR = 1/\alpha$ .

This is easily shown to be the case. Suppose  $R'$  is short-circuited, then if the pulse amplitude be  $V_0$ , the currents through  $R$  and  $C$  during the decay are

$$I_R = \frac{V_0}{R} \exp(-\alpha t)$$

$$I_C = -\alpha C V_0 \exp(-\alpha t)$$

If  $CR = 1/\alpha$ , then  $I_C + I_R = 0$ , and at balance  $R'$  may be reintroduced without disturbing the circuit, since no current flows in  $R'$ .

The note is published by permission of the Chief Scientist, Ministry of Supply.

Radar Research and  
Development Establishment,  
Malvern.

C. M. BURRELL

## New books

**Radio engineering, Vol. 2.** 2nd edition. By E. K. SANDEMAN, Ph.D., B.Sc., A.C.G.I., M.I.E.E. (London: Chapman and Hall Ltd.) Pp. xxi + 613. Price 55s.

In the second edition of Volume 2, the opportunity has been taken to make a number of minor alterations in the text, to insert a short section on the calculation of the noise factor of a receiver and a longer section of 30 pages on transmission line filters. In the latter section, the author considers the properties of lengths of transmission line shunt- or series-loaded with stubs and filters constituted by two unequal lengths of similar transmission line in parallel. Some unusual properties of such filters are noted, such as their use as quarter-wave transformers of infinitely variable impedance.

T. B. RYMER

**Ferroelectricity.** By E. T. JAYNES. (Princeton: University Press; London: Oxford University Press) Pp. viii + 137. Price 12s. 6d.

This book might more appropriately have been called "Theories of ferroelectricity in barium titanate and rochelle salt." Its main contents are a critical review of current theories of ferroelectricity and an account of further original work by the authors along similar lines. Both of these are interesting and valuable. On the other hand, the introductory outline of experimental facts is sketchy, the facts being selected—perhaps justifiably—for their relevance to the theoretical treatment. Little is said, for example, about  $\text{KH}_2\text{PO}_4$ , and nothing about the occurrence of ferroelectricity in perovskite-type structures in general. There is no clear appreciation of the chemical implications, and the relation of spontaneous polarization to crystal structure is left unexamined. Thus the book is not to be recommended as a comprehensive introduction to the subject, which its title might imply. For those working in the field, with some previous knowledge of the literature, it is an important and useful contribution. There are fairly complete references to work published up to the end of 1951.

The book has been reproduced photographically from typescript, and has a paper cover; it is well produced. This method of making available in semi-permanent form the results of work in a rapidly-advancing subject has much to recommend it.

HELEN D. MEGAW

**Luminescence and the scintillation counter.** By S. C. CURRAN, F.R.S. (London: Butterworths Scientific Publications, Ltd.) Pp. x + 219. Price 32s. 6d.

This book is a valuable compendium of information for those concerned with the use of scintillation counters. It includes chapters on the interaction of radiations with matter, secondary emission, the photomultiplier, luminescence, the preparation and properties of scintillation crystals and liquids, applications, and circuits. The depth of treatment naturally varies over this wide range. It is too detailed in some cases where recourse to original papers by the reader might be presumed, as in the purification and crystallization of organic substances; on the other hand, sulphide phosphors are dealt with very briefly. Some of the sections are very useful as reviews of recent literature, but the chapter on luminescence does not present a very convincing account of a difficult and controversial subject. The emphasis on luminescence in the book's title is perhaps hardly justified.

S. T. HENDERSON

**Wave propagation in periodic structures.** By LEON BRILLOUIN. (New York: Dover Publications, Inc.) Pp. xii + 255. Price \$1.75 paper bound; \$3.50 cloth bound.

In these days of rapid progress in physics, it becomes increasingly more difficult to keep established "classics" up-to-date. Professor Brillouin has solved this problem, at least temporarily, by adding to this fascinating book an appendix, which contains useful references to more recent applications of his general theory. A short discussion on the relation between zone theory and group theory has also been included. The low price of the new paper-bound edition will make this book even more attractive to the young research student, who will benefit greatly by a careful reading of the theory. This book remains a "must" for all those physicists who like to be stimulated by brilliance in thought and elegance in treatment.

P. B. HIRSCH

**Data for X-ray analysis: Vol. 1.** Charts for the solution of Bragg's equation ( $d$  versus  $\theta$  and  $2\theta$ ). By W. PARRISH and B. W. IRWIN. **Vol. 2.** Tables for computing the lattice constant of cubic crystals. By W. PARRISH, M. G. EKSTEIN and B. W. IRWIN. (Netherlands: Philips Technical Library; London: Cleaver-Hume Press Ltd.) Vol. 1: pp. 108; Vol. 2: pp. 90. Price (per volume) 15s.

These volumes are intended to supplement the *International tables for X-ray crystallography*, Vol. 1 of which has already been published for the International Union of Crystallography; and the charts for X-ray crystallography obtainable from The Institute of Physics, London. They will be useful in the many industrial research laboratories where workers are interested in routine analysis of powders or alloys. Vol. 2, which gives values to six decimal places of  $(h^2 + k^2 + l^2)^{1/2} \lambda/2$  for  $K\alpha_1$ ,  $K\alpha_2$  and  $K\beta$  radiations of Cu, Ni, Co, Fe and Cr, is intended for precision work. It is a pity that the authors do not use the wavelength values published in the *Acta Crystallographica*, 3, p. 400 (1950) as being those agreed upon for use in the *International Tables*, but use instead earlier values published in the *J. Sci. Instrum.*, 24, p. 27 (1947). The difference is not large, but it does affect the fifth place of decimals. It is very much to be hoped that the internationally agreed wavelengths will be used in Vol. 3, now in preparation, which is to be entitled *X-ray reflection angles for several standard substances*.

K. LONSDALE

**Introduction to elliptic functions.** By F. BOWMAN. (London: English Universities Press Ltd.) Pp. 115. Price 12s. 6d.

This monograph, the first of a series, gives a condensed but readable account of the Jacobian elliptic functions. After a simple and lucid introduction, with a derivation of the usual formulae, elliptic integrals are discussed followed by the solution of some simple geometrical and dynamical problems in which elliptic functions and integrals arise. This leads to the main part of the book which is concerned with conformal representation and particularly with transformations involving elliptic functions. The Schwarz–Christoffel transformation is explained and applied to certain two-dimensional problems in electrostatics and the analogous problems of steady current flow in uniform conductors. Each chapter includes a collection of useful examples, and there is a good bibliography.

Physicists and engineers, for whom the book is designed, will find it a helpful guide. It is clearly the fruit of many years' teaching experience and of original work in this field.

J. TOPPING

## Notes and comments

### Elections to The Institute of Physics

The following elections have been made by the Board of The Institute of Physics:

*Fellow:* C. C. Evans.

*Associates:* E. E. Adderley, I. G. Austin, R. G. Birch, R. A. G. Carrington, O. H. Critchley, R. Dehn, J. Deller, H. A. Doyle, P. B. F. Evans, J. E. Geake, L. J. Griffiths, A. Harrison, J. Hart, D. C. Hartman, B. Hogley, A. E. Horsfield, D. John, K. H. Jolliffe, K. Landecker, P. E. Lane, R. Lawrance, M. Pickering, D. W. Posener, R. F. Privett, J. Pyddoke, B. Roberts, H. Rose, T. D. Smith, H. C. Tresise, G. S. Walker.

Thirty-one Graduates, five Students and five Subscribers were also elected.

### International Union of Crystallography

The Third General Assembly and International Congress of the International Union of Crystallography will be held in Paris from 21 to 28 July, 1954. Full details of the meeting are now available and details may be obtained from the General Secretary of the Union (R. C. Evans, Crystallographic Laboratory, Cavendish Laboratory, Cambridge, England), from the Secretary of the Programme Committee (A. J. Rose, Laboratoire de Minéralogie, 1 rue Victor Cousin, Paris 5, France), or from any of the following regional representatives of the Programme Committee: G. Menzer (Universitätsinstitut für Kristallographie und Mineralogie, Luisenstrasse 37/II, München 2, Germany), W. H. Taylor (Crystallographic Laboratory, Cavendish Laboratory, Cambridge, England), J. D. H. Donnay (The Johns Hopkins University, Baltimore, Maryland, U.S.A.).

At the congress papers will be presented on all aspects of crystallographic research; there will also be an exhibition of crystallographic apparatus and books. After the congress two specialized symposia will be held on The location and function of hydrogen and The mechanism of phase transitions in crystals, and there will be visits to localities of mineralogical interest. Offers of papers for the congress and symposia and notice of enrolment must reach the Secretary of the Programme Committee by 15 February, 1954.

### Conference on Defects in Crystalline Solids

The H. H. Wills Physical Laboratory of the University of Bristol, in co-operation with the International Union of Pure and Applied Physics (particularly its Commission for the Physics of the Solid State) and with The Institute of Physics, is organizing a conference on Defects in crystalline solids which will be held from 13-17 July, 1954, in Bristol. While not excluding other subjects in the field the organizers propose to give particular attention to defects such as dissolved atoms, vacancies and F-centres, to microwave resonance methods of investigating the properties of defects, and to the way in which defects react with dislocations.

Thus dislocations will be discussed in their chemical aspects, as influencing diffusion and precipitation in the solid state, rather than in relation to plastic flow.

It is hoped that a number of authors from overseas will personally present their papers, and with this in mind the Conference has been arranged to follow immediately after the General Assembly of the International Union of Pure and Applied Physics. Board and lodging will be provided in Wills Hall, a student hall of residence, on special terms, or at hotels. The Conference is open to any scientist interested in this field, subject to the limitations of seating accommodation. Further particulars may be obtained from the Secretary, H. H. Wills Physical Laboratory, Royal Fort, Bristol 8, or from the Secretary, The Institute of Physics, 47 Belgrave Square, London, S.W.1. Those wishing to attend the Conference are asked to apply to the former, marking the envelope "1954 Conference," stating whether they wish to be accommodated at Wills Hall or at an hotel and for what nights accommodation is required.

## Journal of Scientific Instruments

### Contents of the November issue

#### ORIGINAL CONTRIBUTIONS

- A rotating anode gas X-ray tube. By E. A. Owen.  
A mass spectrometer for high precision isotope ratio determinations. By R. K. Wanless and H. G. Thode.  
The use of thermocouples for measuring temperatures below 70° K. A new type of low temperature thermocouple. By T. M. Dauphinee, D. K. C. MacDonald and W. B. Pearson.  
A monochromator system with constant energy output in the 0.7-7  $\mu$  spectral region. By D. G. Avery and P. H. Hammond.  
Design for an auto-focus range finder. By H. Asher.  
An electromagnetic viscometer for molten silicates at temperatures up to 1800° C. By J. O'M. Bockris and D. C. Lowe.  
Creep tests in inert atmospheres. By A. J. Fenner and G. Willoughby.  
A simple recording differential refractometer. By G. H. F. Seiflow.  
A sensitive photometer using modulated light and its application in a uranium fluorimeter. By C. E. Florida and C. N. Davey.  
An apparatus for measuring the dynamic shear elasticity and viscosity of solids at high audio frequencies. By J. J. Benbow.  
The performance of thermistor hygrometers under tropical conditions. By G. W. Smith.  
A compression testing instrument for use with pastes. By P. Mason.  
The effect of humidity variation on the operation of an electronic proximity switch. By R. A. K. Long.  
A frequency response analyser for pneumatic process control systems. By C. R. Webb and D. J. Ozanne.  
A novel X-ray heating camera. By S. S. Marsden and N. R. Sanjana.  
On monitoring a Geiger-counter spectrometer beam. By E. Cillam and D. G. Cole.  
Laboratory and workshop notes  
The use of self-balancing pen recorders as ratimeters. By R. L. Gordon.  
A rotary vacuum seal. By J. Sikorski and H. J. Woods.  
A high temperature furnace. By A. E. De Barr and B. Roberts.  
Equipment for simulating spherical surfaces with constant brightness. By F. Schubert.  
A glass solenoid pump. By L. E. Leake.  
A protective time delay circuit for a thyatron relay. By S. H. Cross.  
Construction of 1 mm and 0.2 mm absorption cells for use in an ultra-violet spectrophotometer. By J. H. Linford.  
A source of slow reciprocating motion. By G. C. Ware.  
A means of referring to the International Resistance Colour Code. By W. Riddle and M. Venner.

#### NOTES AND NEWS

- Correspondence  
Radiac instrumentation. From D. Taylor.  
Left-handed instruments. From G. L. Rogers.  
New books  
New instruments, materials and tools  
Notes and comments

THIS JOURNAL is produced monthly by The Institute of Physics, in London. It deals with all branches of applied physics (including theory and technique). All rights reserved. Responsibility for the statements contained therein attaches only to the writers.

EDITORIAL MATTER. Communications concerning editorial matter should be addressed to the Editor, The Institution of Physics, 47 Belgrave Square, London, S.W.1. (Telephone: Sloane 9806.) Prospective authors are invited to prepare their scripts in accordance with the *Notes on the preparation of contributions*. Price 2s. 6d. including postage.)

REPRODUCTION. The Institute of Physics is a signatory to The Royal Society's Fair Copying Declaration. Details may be obtained upon application from The Royal Society, London, W.1.

ADVERTISEMENTS. Communications concerning advertisements should be addressed to the agents, Messrs. Walter Judd Ltd., 47 Gresham Street, London, E.C.2. (Telephone: Monarch 7644.)

SUBSCRIPTION RATES. A new volume commences each January. The charge is £4 per volume (\$11.50 U.S.A.), including index (post paid), payable in advance. Single parts, so far as available, may be purchased at 8s. each (\$11.5 U.S.A.), post paid, cash with order. Orders should be sent to The Institute of Physics, 47 Belgrave Square, London, S.W.1, or to any bookseller.



# Scintillation counting and its medical applications\*

By PROF. W. V. MAYNEORD, D.Sc., F.Inst.P., Physics Department, Royal Cancer Hospital, London, S.W.3

The development of scintillation counting in the last few years has depended upon the substitution of a photomultiplier tube for the human eye in the detection of small flashes of light by luminescent materials traversed by radiations. A general description is given of the main types of photomultipliers and luminescent materials suitable for such work. The crystals most used in practice are thallium-activated halides or organic crystals such as anthracene or naphthalene. To a first approximation the amplitude of the light pulse produced by the absorption of high energy particles is proportional to the energy absorbed, so that a scintillation detector is, in essence, a proportional counter. Deviations from this linearity, however, occur particularly with organic luminophors.

A short outline is given of the application of scintillation counting techniques to medical problems, to which they are particularly applicable owing to the very high sensitivity and small physical size of the detector. A description is given of needle scintillation counters for the study of the radioactivity of biopsy specimens; of  $4\pi$  counters using a liquid scintillating medium for the study of the radioactivity of samples of blood; and of the application of scintillation counters in the study of the radioactivity of normal and pathological brain tissue. The paper next describes new dosimeters developed by Dr. E. H. Belcher depending upon the measurement of total luminosity of the crystals exposed to ionizing radiations. They are shown to be sensitive, stable, reasonably independent of wavelength errors, and are an important development in clinical radiation dosimetry.

The paper ends with a description of a scanning technique by which it has been possible to form photographic and visual images of the distribution of radioactive materials. In particular, an equipment is described embodying a "storage tube" used in conjunction with television scanning techniques.

The development of scintillation counting constitutes one of the major achievements of the last few years in relation to the detection and measurement of nuclear radiations. These techniques have an elegance and power which make them attractive subjects for study on their own account. They have, moreover, application to a wide range of problems, as for example in the detection of radioactive isotopes within the human body.

The method is about fifty years old this year, and derives from the Crookes' "spinthariscopes," which consists of a speck of radioactive material (in the early days usually radium or polonium) emitting  $\alpha$ -particles which strike a fluorescent screen (perhaps of zinc sulphide) with a resulting shimmering luminescence. It later appeared that each individual flash of light corresponded to the impact of a single particle and that the method could therefore be used in studies of the number and distribution of such ionizing particles. With such simple tools, Rutherford and his school laid much of the experimental foundations for the concept of the nuclear atom, and made such fundamental measurements as indicated that the charge on the atomic nucleus was equal to its atomic number. The technique was then tedious, tiring and restricted to low counting rates. Moreover, it did not appear to be applicable to the counting of fast electrons, though Becquerel had shown very early in the history of radioactivity that such electrons could cause luminescence.

## PHOTOELECTRIC MULTIPLIERS

The present-day development is dependent on the substitution of a photomultiplier tube for the human eye, thus making available the whole gamut of pulse-counting techniques. The multiplier consists essentially of a light sensitive

cathode in a vacuum envelope also containing a series of electrodes. A group of electrons from the cathode is so guided and accelerated by fields between the electrodes as to strike the electrodes in succession, at each impact the electrons being multiplied by secondary emission. A variety of geometrical arrangements of electrodes have been employed, and the number of "stages" has grown until commonly ten or eleven. Even fourteen stage tubes are now available. The practical multiplication factor under normal operating conditions may be of the order of four to five per stage, so that the total gain is frequently of the order of  $10^6$ – $10^7$ . The multiplier therefore constitutes a high gain amplifier of high speed, since in the limit the latter is limited only by electron transit times between the electrodes.

Two main arrangements of electrodes have emerged in practice, namely (1) that adopted by the Radio Corporation of America and (2) the "Venetian blind" design developed with such success by Electric and Musical Industries Ltd. in this country.

One of the main difficulties in the use of photomultipliers arises from thermionic emission from the photocathode, this emission consisting often of single, relatively low energy electrons. The thermionic current may be lowered by suitable choice of cathode material and by using a small area of cathode. In addition, the emission may be greatly reduced by cooling to low temperature (as, for example, in liquid nitrogen) a technique we have employed a good deal; by the use of coincidence counting methods; or by pulse discrimination. The photomultiplier may be used in two ways, first by counting individual pulses at the collector electrode or secondly by measuring the d.c. current, that is, integration of the pulses. The latter, although not strictly scintillation counting, is included here because the two methods are closely related and we may conveniently make use of both of them in medical research and practice.

\* Based on a discourse delivered on 16 April, 1953, at the 37th Physical Society Exhibition.

## LUMINESCENT MATERIALS

In practice the performance of a given instrument will depend upon:

- (a) the luminescent material;
- (b) the photomultiplier;
- (c) the effective coupling of the two

as well as the associated electronics.

Initially the luminescent materials were such well-known polycrystalline luminophors as zinc sulphide, calcium tungstate or naphthalene. A great improvement is, however, obtained by the use of single large transparent crystals since such crystals are optically more efficient in transmitting their luminescent flashes, the optimum size of crystal being often determined by its transparency to visible or near visible radiation. A great many considerations enter into the choice of luminophor.

Let us suppose we wish to measure a feeble beam of  $\gamma$ -rays of high energy. First, the substance must absorb as large a fraction as possible of the incident beam. This calls in the main for high density and large atomic number. We also require a large light yield per unit absorbed energy. As much as possible of the emitted light must be concentrated on the cathode of the multiplier, calling for transparency of crystal and perhaps embedding the crystal in a medium of approximately the same refractive index as the crystal, to reduce the large light losses by internal reflection. Also the crystal must be effectively coupled to the photocathode so as to cause the emission of the maximum number of electrons per light flash from the photocathode, thus ensuring the maximum pulse size. This consideration is of importance in reducing the statistical fluctuation of pulse size arising in the multiplier itself if the number of electrons per flash is small, thus ensuring maximum resolution in spectrometers depending on pulse discrimination. To make use of the high speed of the multiplier, the light pulses must be of short duration, preferably fractions of a microsecond, while naturally the associated electronics must be appropriately designed.

The crystals most used in practice are thallium activated halides, particularly sodium and potassium iodides, or alternatively organic crystals such as anthracene and naphthalene. Pure anthracene is found to give pulses three times the size of those from naphthalene. The *inorganic* luminophors normally have the advantage of high atomic number and therefore high absorption of  $\gamma$ -radiation, as well as yielding large pulses. On the other hand, their decay times are relatively long, of the order often of hundreds of microseconds, and the maximum speed of counting thereby limited. The organic luminophors decay rapidly, having decay times of the order of tenths or hundredths of microseconds, giving short resolving times and therefore high speed counting. Crystalline calcium tungstate was much used in the early days and has the advantages for  $\gamma$ -rays of very high density and atomic number.

It is important to realize that to a first approximation the amplitude of the light pulse produced by the absorption of a high energy quantum or particle is proportional to the energy absorbed, so that the scintillation detector is in essence a proportional counter. This relationship is true over a wide range for thallium activated sodium iodide, but for organic luminophors it no longer holds at low energies below about 100 keV.

$\gamma$ -rays, for example, absorbed photoelectrically in a crystal, cause the emission of a homogeneous group of electrons having nearly the energy of the quantum. These electrons produce a set of light pulses of the same size, which in

turn liberate in fixed geometrical conditions the same number of electrons from the photocathode and therefore a homogeneous group of electrical pulses from the amplifier. By Compton absorption a heterogeneous group of particles and therefore pulses arises. We thus have the possibility of a "scintillation spectrometer," for by simple voltage discrimination we may study the distribution of pulse size from the multiplier and thus deduce the distribution of energy among the particles or quanta causing the luminescence.

In view of the cost and difficulty in obtaining large single crystals of, for example, sodium iodide, considerable practical importance attaches to the discovery that a number of liquid luminophors exist. Normally their pulses are smaller than from crystals, but amply large enough to be useful. Practical examples of such luminophors are  $\alpha\alpha'$  dinaphthyl in benzene and *p*-terphenyl in xylene. We have found<sup>(1)</sup> these liquid systems to be efficient and useful in the design of  $4\pi$  scintillation counters of high sensitivity and convenience.

We cannot here discuss the physics of scintillation counting in detail, but reference may be made to such useful articles as those by Garlick<sup>(2)</sup> on luminescent materials for scintillation counters or the recent book by Rodda<sup>(3)</sup> on photoelectric multipliers.

## MEDICAL APPLICATIONS

With this sketch of the fundamental physics as a background, we now ask why should scintillation counting methods be of particular interest in medicine? We shall confine our discussion to the problems arising in the use of radioactive isotopes. Here, the fundamental physical problem is in essence always the same, namely the study of the distribution of radioactive materials in the body preferably by observations made outside the body.

It is true that the deduction of the distribution of a radioactive material inside a mass of tissues (which scatter the  $\gamma$ -radiation) from observations of the  $\gamma$ -rays emerging from the body is difficult. Suffice it, that the "resolution" which is possible depends upon the geometry of highly directional detectors. In practice we must use very small detectors surrounded by protective material through which run only fine apertures. Here, scintillation counting comes into its own, for the crystal itself is a detector of relatively high efficiency in a small space. For example, a normal Geiger counter may have an efficiency of only 1% for  $\gamma$ -rays of the order of 1 MeV. It is also relatively bulky and, of course, requires high tension supplies. Even a small crystal of sodium iodide with linear dimensions of a few millimetres easily gives an efficiency of 15 to 20%. It is always of importance to reduce to the minimum the amount of radioactive material administered to a patient so that this high sensitivity is of great practical value.

With the possible exception of tritium, the metabolism of the radioactive materials, if administered in small amounts, is exactly the same as that of their non-active counterparts. Radioactive materials emit  $\alpha$ -,  $\beta$ - or  $\gamma$ -rays over a wide range of energies and therefore penetrations, each material emitting a characteristic radiation and decaying exponentially at an equally characteristic rate. The  $\alpha$ -ray emitters are few and of little interest so that we have in practice to deal with materials such as  $^{32}\text{P}$ , emitting pure  $\beta$ -radiation travelling only a few millimetres in soft tissues, or  $^{24}\text{Na}$  emitting both penetrating  $\gamma$ -rays and  $\beta$ -rays;  $^{131}\text{I}$  again emits a mixture, but  $\gamma$ -rays of much less penetration. Recently we have found much interest in such materials as  $^{170}\text{Tm}$  or  $^{133}\text{Xe}$  which emit  $\gamma$ -rays of so low an energy as to simulate the low-voltage X-rays used in diagnosis.<sup>(4)</sup> With suitable detectors we may



therefore study the metabolism of particular elements (or stable compounds containing them) in the body, and use such studies to scrutinize and compare normal and pathological processes.

By introducing much larger amounts of the same materials we may hope to influence metabolism, as for instance the growth of malignant cells, and thus make use of the radioactive substances therapeutically. In the first instance the amount of material administered to the animal or patient will be as small as possible and limited by the sensitivity of the means of detection. In the second, the amount may be thousands of times larger and often limited to our estimate of the maximum amount we dare to give, since, in general, the concentration of radioactive material in the tissue to be treated may be barely sufficient for our purpose. We have, therefore, need of detectors of a very wide range of sensitivity and here again the scintillation method has great advantages.

#### CLINICAL INVESTIGATIONS

In metabolic studies we may proceed in two main ways. In the first, a small quantity of a suitably chosen radioactive isotope may be administered to a patient and subsequently, either during a major surgical operation or at a small operation performed specially for the purpose, a small piece of tissue may be taken for examination microscopically and for its radioactive content. The tissue may be treated chemically so as to yield a solution of radioactive material. This liquid may surround a thin wall Geiger counter and its specific activity may thus be determined. In the second method the radioactivity is studied in the body by counters outside the body, the method of "external counting."

An interesting alternative to the Geiger counter in the first method has been developed by my colleague, Dr. Belcher,<sup>(5)</sup> and consists of a  $4\pi$  counter using a liquid scintillating medium surrounding the specimen contained in a small glass tube. This method has the advantage of requiring no chemical treatment and is particularly useful, for example, for small samples of blood. It has been used with success in studies of iron metabolism after X-radiation. By deposition of the source on a very thin foil which may be dipped into the scintillating medium, useful absolute standardization is possible. The scintillating medium ( $\alpha\alpha'$  terphenyl in xylene, for example) is in optical contact with the photocathode of an electron multiplier so that the efficiency is high.

#### EXTERNAL COUNTING

We now turn to the other important type of technique for the study of the radioactivity of living tissues, namely so-called "external counting." The problems are now quite different but perhaps more fascinating to the physicist.

Much work has been done with Geiger counters placed near to the body containing radioactive materials, and attempts made to deduce therefrom the distribution of radioactive material in the body. From theoretical consideration of the problem we have, however, come to the conclusion that it is much more difficult than usually realized to deduce the distribution of radioactive isotopes, and have therefore attempted to design and construct equipment with high resolving power and precision.

Here the scintillation system comes into its own, for the efficiency of  $\gamma$ -ray detection by a Geiger system is often only of the order of 1%, and a gain of some 10 to 50 times may be obtained with the scintillation system under at least as good geometrical conditions. This gain makes possible reasonable

times of counting to obtain statistically significant results even with low levels of activity.

We may first describe equipment used by us in an attempt to use radioactive iodine (incorporated into diiodofluorescein) as a tracer for brain tumours.<sup>(6,7)</sup> The crystal of sodium iodide is situated at the end of a light-guide of perspex which, again, conveys the light flashes to the multiplier. It was necessary at the high sensitivity requisite to cool the multiplier in liquid nitrogen. The equipment is fitted with an arm and pointer which may be adjusted to a plaster skull cap worn by the patient so that the positioning may be very exact, the problem being the inverse of that met in radiation therapy of accurately directing a beam of radiation into the body. By suitable lead stops the crystal may be allowed to "see" varying volumes or alternatively the resolution studied experimentally under known conditions. We have studied both theoretically and experimentally the behaviour of the apparatus using as a "phantom" a skull containing a gelatine solution whose activity ( $0.033 \mu\text{C/ml}$ ) corresponded to the order observed in the normal brain, experimental "tumours" of varying size, position, and radioactive content being inserted for study. In this way the limits of detection may be defined and measured.<sup>(6,8)</sup>

It was shown to be possible to detect lesions concentrating  $^{131}\text{I}$  provided that the concentration of activity in the brain was 10 times that of the normal brain, and that the size of lesion was greater than a certain minimum depending on the depth. If the depth is 5 cm the limiting volume was 14 ml. At the centre of the brain the limiting volume was 36 ml. These results arise from careful geometrical and statistical studies. A Geiger counter gives such low counting rates as to require prohibitively long examinations to obtain statistically significant numbers of counts.

We have recently also used equipment which uses improved E.M.I. multipliers and a crystal close to the photocathode. It has therefore better optical efficiency and does not require cooling.

Unfortunately, in our two sets of investigations we have been unable to confirm the work of Moore and others<sup>(9)</sup> and Ashkenazy and others<sup>(10)</sup> in the use of diiodofluorescein containing  $^{131}\text{I}$  in the localization of brain tumours. Results of our first series have been published by Belcher, Evans and de Winter.<sup>(8)</sup> Briefly, with the scintillation counter system described, measurements were made on thirty-four patients, taking great care in the application of the detector, statistical analysis of the results and development of suitable methods of display.

In our hands the method has so far failed to give any definite information as to size and position of cerebral tumours in the great majority of cases investigated. The effect of vascular activity seems much greater than of the activity absorbed in the tissues. Four hours after a dose of 1 mc only  $20 \mu\text{C}$  (2%) can be observed in the brain. This makes the influence of the rest of the body and particularly activity in the liver, of great importance. Here, indeed, we meet the main experimental difficulty in this external counting method. If the position of a radioactive mass is to be accurately located, a detector "seeing" only through a small aperture is required. Moreover, at a given moment the detector "sees" only a very small fraction of the total activity of the body, and if the substance used emits penetrating  $\gamma$ -rays it is very difficult to provide satisfactory shielding from this stray radiation. The detection of a small increase in concentration in a given area is then fraught with great difficulty and we are at the moment setting up an "observation post" in which we hope to solve this problem more satisfactorily, but it means heavy equipment and elaborate layout.



In similar experiments  $^{42}\text{K}$  has been administered to eight patients and studies made of activity in liver, muscle, and over the skull. This investigation seems more promising and will be continued with new equipment in the near future.

It is sometimes an advantage to have a small detector which can be inserted into the tissues and we have spent considerable effort in an attempt to develop scintillation needle counters,<sup>(11)</sup> with limited success. A very fine slip of crystal (sodium iodide) is mounted and inserted into a hollow needle (diameter 2 mm) which is filled with a "light-guide" of perspex, the light being thus conveyed to the electron-multiplier. It is, however, difficult to maintain good optical contact between crystal and perspex, while the small size of the crystal and the low optical efficiency make for very small light pulses with consequent complexity of subsequent amplification. The multiplier must be cooled with liquid nitrogen to obtain maximum sensitivity, and the flexibility of the light guide system is consequently small and the equipment not very suitable to use in the operating theatre. The sensitivity for  $\beta$ -rays can hardly be higher (and is sometimes lower) than that of a corresponding Geiger system since the efficiency for either system is often close to 100%. Recently we have (as below) developed methods of moulding crystals into transparent media which may improve the situation. We have made studies of the efficiency of bent light-guides and find that they must be very carefully designed.

Such needles may be used in clinical investigations as, for example, in the study of the uptake of  $^{32}\text{P}$  in a surgically removed breast carcinoma. The sensitivity of the scintillation counters made by us is of the order of 0.3 counters/sec per  $\mu\text{Ci/ml}$ .

#### SCINTILLATION DOSIMETRY

These examples may illustrate how the scintillation counting method may be used medically and we now turn to the application of the principle of light integration.

We realized early in our experiments that we had in the scintillation method the possibility of highly stable and yet sensitive "dosemeters" which might be useful for measuring the amount of radiation received from radioactive isotopes or from beams of X-rays. Usually we shall require less sensitivity than in circumstances for which counting is appropriate, but the apparatus may well have to be used in operating theatres in "tropical" conditions, yet high stability, robustness and small physical dimensions of detector are required since the equipment may have to be inserted into either natural or artificial body cavities. The most useful form of apparatus<sup>(12)</sup> would appear to consist of a small, highly sensitive crystal (say 2 or 3 mm linear dimensions) on the end of a light guide leading to a multiplier. The apparatus must be light, mechanically very strong and capable of being sterilized. It must, of course, be easily portable.

It was found that considerable improvement in sensitivity could be obtained by embedding the crystals in a transparent medium of approximately their own refractive index, preserving some crystals of low stability in air, and surrounding them with an "air wall" material. A technique using Marco resin (by Scott, Bader and Co.) has proved very simple and effective for anthracene and calcium tungstate. The embedding material is "tacky" on the surface as the oxygen of the air inhibits polymerization, but this surface would in any case be machined off so as to form lenticular surfaces on the embedded crystal and resin. Thallium activated sodium and potassium iodides must be embedded in "acrylic granules" (I.C.I. Ltd.) as oxidizing agents liberate free iodine and discolour the crystals. If radioactive sources are

used near such detectors it is found that "light-guides" of materials such as perspex themselves emit light (Čerenkov effect) under the action of ionizing radiations of sufficient energy. Moreover, owing to the large volume of such light-guides compared to that of the crystal this light may constitute a serious problem. There is also a small direct effect of  $\gamma$ - or X-rays on the photocathode of the multiplier itself. It was, however, found that a polished metal tube is itself a very efficient guide, particularly if made of polished Dural.<sup>(12)</sup> We have recently commenced a systematic study of the subject and are making a series of experiments using various metal tubes of different dimensions. Dural appears, however, to be the most efficient material yet tried.<sup>(13)</sup>

As explained above, the thermal pulses from the multiplier are small, corresponding to single electronic emission from the cathode whereas most of the light pulses from the crystal cause the emission of a number of electrons proportional to the energy. It is possible to back off the dark current at room temperature without loss of sensitivity, and using a valve voltmeter circuit a simple robust detector of small dimensions and high sensitivity is attained. With a crystal of sodium iodide of the order of 5 mm linear dimensions it is possible to measure even "tolerance" dosage-rates of 12 mR/h. There are, however, still several outstanding difficulties, a serious one being the energy dependence of such a "dosemeter" with quantum energy. Elaborate studies of these effects have been made by my colleague Dr. Belcher,<sup>(12)</sup> and it is found that by suitable choice of materials, as, for example, embedded anthracene crystals in a thin polished "elektron" shell, the effective atomic number of the detector system may be made equal to that of air or surrounding tissues, in which case the detector will measure directly the energy absorption in tissues. Tests of the apparatus have been made with X-rays produced at voltages from 20 kV up to 24 MeV obtained from our 30 MeV synchrotron. These experiments have also proved the response to be linear with intensity of radiation over a very wide range of intensities and possess surprising freedom from directional effects. The full scale deflection on the most sensitive range and a crystal of 3 mm linear dimensions corresponds in the case of radium  $\gamma$ -radiation to a dosage rate of 3.5 r/h for calcium tungstate and 10.5 r/h for anthracene. Fatigue in the multiplier is negligible as are temperature effects on dark current except in extreme conditions. Some luminophors, particularly calcium tungstate, show variations in sensitivity with temperature, but anthracene shows only a very small effect.

These detectors have already proved very useful in practice. As an example of the kind of measurement which can be made we might quote the exploration of the radiation received in the rectum when radium is placed in the cervix uteri. This is an important matter as over-dosage can easily occur with grave consequences, but the "probe" may be inserted into the rectum or vagina and the distribution of radiation throughout much of the pelvis can be explored and accidents thus avoided. The instrument can also be made sufficiently small and robust to be sterilized and used in other body orifices.

As yet another example of the use of such equipment we may quote the use of a double probe, the multiplier "seeing" two crystals. If, now, these two crystals be placed during surgical operation on a large vein and a small quantity of, for example, radioactive sodium (say 5 to 10  $\mu\text{Ci}$ ) injected a few centimetres "upstream," then as the radioactive material passes near the crystals two deflections are observed. Using a high-speed recorder the time interval between the two pulses corresponding to the passage of the radioactive

material can be measured and hence the blood velocity deduced. Pulses separated by 0.1 sec can be resolved. Studies of this kind are being made in collaboration with my colleagues Dr. Belcher and Mr. Hunt.<sup>(14)</sup>

#### SCANNING TECHNIQUES

We turn finally to a quite fascinating technique which scintillation counting detectors have made possible. It arose in our own instance from one of the most important problems in medical practice, namely the determination of radioactivity in the thyroid after administration of radioactive iodine, either in small quantities diagnostically, or large quantities therapeutically. It is very important indeed to know the extent and speed at which the iodine is taken up and released by the thyroid, and generally to investigate its distribution in the body. Again, some secondary tumours are known themselves to take up radioactive iodine and so may be detected or even treated in this way. The usual method of procedure is to take either a directional Geiger counter or scintillation counter and make observations of counting rate in the vicinity of the thyroid at a number of places, perhaps on a grid pattern. From the distribution of these counting rates diagrams are constructed by joining places, having the same counting rates, and the distribution of radioactive material can thus be roughly deduced. The method in practice has been found laborious and clumsy and it is not at all easy to obtain satisfactory results. With such difficulties in mind it occurred to the writer that it would be worth while to attempt to produce visual or photographic images of the distribution of radioactive material. First experiments<sup>(15)</sup> were made in July 1951 using letters of the alphabet in radioactive gold and tantalum wire as sources. At this stage the detector was in fact a Geiger counter, but the principle is of course the same. A more recent form of the apparatus embodies a scintillation counter.<sup>(16)</sup>

The crystal is situated at the centre of a block of lead and connected by a short light-guide to the photocathode of an E.M.I. photomultiplier. A cylinder of heavy tungsten alloy and lead (with extra "mushroom" protection) and a fine aperture some 3-5 mm in diameter oscillates so as to scan repetitively the area of the body of interest, for example the thyroid. The pulses from the multiplier are amplified, "tailored" and used to modulate the brightness of a cathode-ray spot, arranged by mechanical switch gear to scan in synchronism with the detector head. Two screens are used, one blue and the other green; one for photographic recording and the other for visual observation. It has been shown<sup>(15, 16)</sup> that simple outlines of radioactive sources could easily be obtained, and indeed the apparatus was surprisingly successful. The resolution was low as the picture contained only four hundred picture elements, but much was learned, particularly that the limits of resolution and contrast were largely determined by the statistical fluctuations of the number of quanta per picture point. This number was often, even in a total scan of a quarter of an hour, as low as ten, yet reasonable outlines were obtained. Since these experiments were performed, fairly elaborate theoretical studies of ultimate sensitivity and other details have been made. It soon emerged that although reasonable photographic images could be obtained the production of visual images was much more difficult. As an example of the photographic records we may quote the results of scanning a model thyroid consisting of a glass tube containing 2 mc of  $^{198}\text{Au}$ .<sup>(16)</sup> It is important to be able to relate this image to that of the patient and after much experimental work we found that a very simple pinhole

camera, placed so that the pinhole was in the same position relative to the patient as the recording crystal, produced satisfactory images with exposures of only a few seconds in normal lighting. It is, therefore, possible to superimpose optical and radioactive images. In other experiments we have in fact superimposed an X-ray picture of the part of the body involved on these two records. Records have been obtained of the changes in the shape and size of the thyroid of a patient after the administration of 100 mc of radioactive iodine, a severe therapeutic dose.

As mentioned above, owing to the short persistence time of even the longest fluorescent screens it was found difficult to form satisfactory visual images and we have, therefore, during the last twelve months developed a much more elaborate scanning system, both in its mechanical and electronic aspects (Fig. 1).<sup>(17)</sup> Space is not available to discuss this

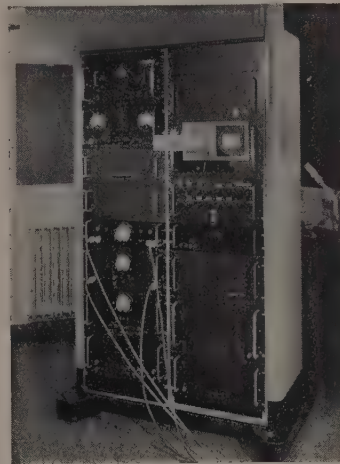


Fig. 1. Electronic equipment including display unit of the scanner

equipment in detail\* but its action depends essentially upon the use of a "storage tube." The scanning head is now mounted on a large mechanical pantograph (Fig. 2), and consists of a crystal of sodium iodide embedded in transparent

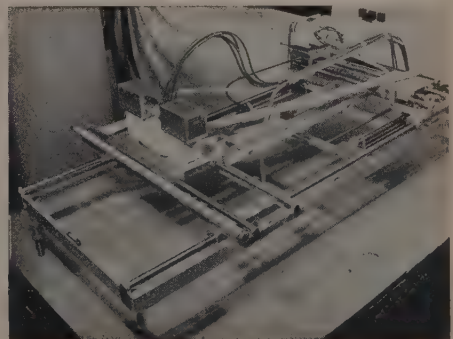


Fig. 2. Mechanical pantograph and coincidence scintillation detector of the scanner

\* The apparatus was demonstrated in action at the lecture.

resin and "seen" simultaneously by two E.M.I. electron multipliers. By the use of coincidence counting techniques the random thermal emission of the multipliers is greatly reduced so that no liquid nitrogen cooling is now required, yet the sensitivity is high. The apparatus is designed so as to scan a large fraction of the body at one time, various sizes and shapes of scanned area being available. The pulses from the coincidence circuits, suitably treated, modulate the writing beam of an E.M.I. VCRX 350 storage tube, so that a distribution of charge on the storage grid corresponds to the distribution of pulses from the material which has been scanned. The image may now be "read" over periods of many minutes up to an hour without much deterioration. We can, therefore, see an image of the distribution of radioactive material as it is built up and the scanning proceeds even though that scanning takes minutes or even days. We may, of course, photograph the black and white image in the usual way. The equipment is complex and will be described elsewhere, but has been designed with a possible view to application in a large number of other fields such as X-ray spectroscopy, ultra-violet microscopy, or indeed any field in which a pattern of stored charges may be obtained by pulse modulation. It is only just coming into commission and we have as yet had little experience with it, but it does seem to be a powerful method of great promise.

There can be no doubt that the highly sensitive and compact scintillation detectors have already proved of use to us. Our first patients were investigated by this method in January 1949, and four years of experience has convinced me that the method represents a major advance in the techniques of pure and applied nuclear physics.

#### ACKNOWLEDGEMENTS \*

I wish to acknowledge my indebtedness to my colleagues who have done so much of the work described, particularly Dr. Belcher, Dr. Evans and Mr. Newbery; I am grateful to Mr. H. Hodt for the design and construction of the mechanical scanning unit.

It is a pleasure to record the great help received from

Dr. McGee, Dr. Broadway, and their staffs at Electric and Musical Industries Ltd., whose storage tube made the latest type of scanning instrument possible. I would like to acknowledge my indebtedness to the Admiralty for allowing us to use this tube.

The research described was supported by the Medical Research Council and later by the Nuffield Foundation which came to our help most promptly and generously.

#### REFERENCES

- (1) BELCHER, E. H. *Nature [London]*, **167**, p. 314 (1951).
- (2) GARLICK, G. F. J. *Progress in Nuclear Physics*, p. 51 (London: Pergamon Press Ltd., 1952).
- (3) RODDA, S. *Photoelectric Multipliers* [London: Macdonald and Co. (Publishers) Ltd., 1953].
- (4) MAYNEORD, W. V. *Brit. J. Radiol.*, **25**, p. 517 (1952).
- (5) BELCHER, E. H. *J. Sci. Instrum.*, **30**, p. 286 (1953).
- (6) BELCHER, E. H., and EVANS, H. D. *Brit. J. Radiol.*, **24**, p. 272 (1951).
- (7) DE WINTER, J. G. *Brit. J. Radiol.*, **24**, p. 280 (1951).
- (8) BELCHER, E. H., EVANS, H. D., and DE WINTER, J. G. *Brit. Med. Bull.*, **8**, p. 172 (1952).
- (9) MOORE, G. E., KOHL, D. A., MARVIN, J. F., WANG, J. C., and CAUDILL, C. M. *Radiology*, **55**, p. 344 (1950).
- (10) ASHKENAZY, M., LEROY, G. V., FIELDS, T., and DAVIS, L. *J. Lab. Clin. Med.*, **34**, p. 1580 (1949).
- (11) MAYNEORD, W. V., and EVANS, H. D. (unpublished).
- (12) BELCHER, E. H. *Brit. J. Radiol.*, **26**, p. 455 (1953).
- (13) MAYNEORD, W. V., and DE VALENCÉ, L. P. (unpublished).
- (14) MAYNEORD, W. V., BELCHER, E. H., and HUNT, A. H. (unpublished).
- (15) MAYNEORD, W. V., TURNER, R. C., NEWBERY, S. P., and HODT, H. J. *Nature [London]*, **168**, p. 762 (1951).
- (16) MAYNEORD, W. V., and NEWBERY, S. P. *Brit. J. Radiol.*, **25**, p. 589 (1952).
- (17) MAYNEORD, W. V., EVANS, H. D., and NEWBERY, S. P. (unpublished).



## Pressure fluctuations in a jet engine

By H. M. NICHOLSON, Ph.D.,\* and A. RADCLIFFE, B.Sc., A.Inst.P., National Gas Turbine Establishment, Farnborough, Hants.

[Paper first received 31 March, and in final form 27 April, 1953]

Pressure fluctuations have been recorded at various points in the ducting of a jet engine. The recordings were made under a variety of steady running and accelerating conditions with a standard engine and with engines adapted for two different after-burning systems. This report includes a brief description of the recording equipment and its method of use, a summary of the test conditions, a description and analysis of the pressure records obtained and a discussion of the test results. In the discussion an attempt is made to explain the observed pressure fluctuations, and their significance in relation to practical engine operation and combustion system design is stressed.

It is generally agreed that one of the more obvious gaps in our knowledge of the operation of jet engines is their behaviour under non-steady running conditions. In particular, within this general category the cause and nature of transient pressure and velocity fluctuations, variously described as "rumbling," and "howling" and "rough" and "noisy" running in gas turbines and ram jets are very imperfectly understood. These phenomena have been observed and reported many times in the course of development work and by "cut and try" methods have been eliminated when troublesome, but only little work is known which describes an investigation of these instabilities in any detail. The reasons for the absence of systematic investigations are not far to seek. In the first place (except in the pulse jet engine), such instabilities must be avoided in a satisfactory engine and the tendency has been to eliminate them by trial and error rather than to invest the considerable effort required for an understanding of their basic causes. Secondly, the equipment needed for experimental observation of these transients is complex and expensive, and finally, it is only in recent years that the mathematical methods for the treatment of transient gas flows have become widely known. The method of characteristics has been applied to the transient flow of gases by German scientists during the war and since 1945 has been exploited in Britain and the U.S.A. The essential of this method as applied to simple isentropic cases have been described in a paper by Kestin and Glass.<sup>(1)</sup> In view of this unsatisfactory state of affairs an investigation has been initiated at N.G.T.E. and this report describes the results obtained in the part of the programme dealing with jet engine pressure fluctuations. The measurements, which were made on a Derwent V engine, were undertaken with the threefold purpose of: (a) securing for reference purposes a comprehensive record of the pressure fluctuations which may be encountered under various running conditions; (b) determining the magnitude and character of fluctuations arising in jet pipe reheat systems; (c) obtaining an insight into the cause of engine flow instabilities particularly that one commonly described as "rumbling."

between the compressor outlet and propelling nozzle. Fig. 2 illustrates the method of mounting the capacity pickups on the combustion chamber air casing. The rubber water cooling pipes, the coaxial cable and a calibrating air line, which is connected to a three-way tap between the boss and pickup are visible. The three-way tap was used for calibrating the recording system before and after each test and

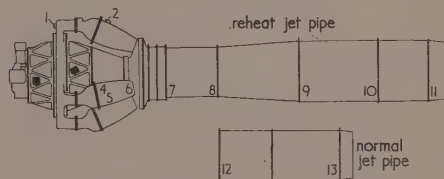


Fig. 1. Positions of recording stations

for isolating the pickup so that the effects of engine vibration and noise on the recording system could be demonstrated to be negligible.

Resonances of the air in the boss, tap and pickup limited the useful upper frequency range of the equipment. The electronics were arranged so that the equipment could be calibrated statically or so that frequencies below 2 c/s were attenuated. As used for the recordings described in this report the frequency response of the system was flat from 2 to 500 c/s. The cathode-ray-tube defectors were recorded on 70 mm paper. The maximum possible deflexion of each



Fig. 2. Mounting of pressure pickups

#### DESCRIPTION OF RECORDING EQUIPMENT AND TECHNIQUE

The main tool of the investigation was a four-channel recording unit. The only modification to the engine was the fitting of bosses as mountings for the pressure pickups. Fig. 1 shows the recording points along the engine duct

trace was 0.40 in. As deflexions could be measured to about 0.01 in. the accuracy of amplitude measurement was not better than  $\pm 5\%$ . The 50 c/s tuning-fork time marking system permitted time intervals to be measured to 2 msec.

\* Now at Johns Hopkins University, Maryland, U.S.A.

## TEST CONDITIONS

Recordings of pressure fluctuations were made under the following conditions:

(a) *Standard engine.*

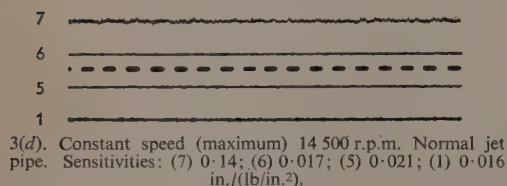
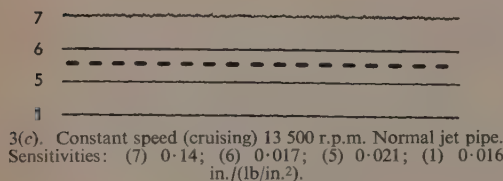
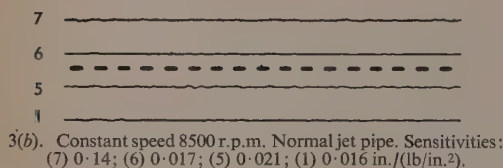
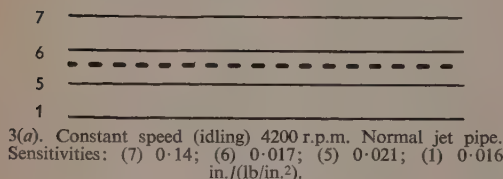
- (i) At various constant engine speeds from idling to maximum r.p.m.
- (ii) During acceleration from start to idling.
- (iii) During acceleration from idling to maximum r.p.m. (Acceleration rates were varied.)

(b) *Fitted with N.G.T.E. (Pyestock) reheat system.*

- (i) At various constant engine speeds from idling to maximum r.p.m. the reheat pipe was fitted but reheat was not in operation. Nozzle diameters of 17 and 20 in. were used.
- (ii) During accelerations from idling to maximum r.p.m. the reheat pipe was fitted but reheat was not in operation. A 17-in. exit nozzle was used.
- (iii) At maximum r.p.m. with various reheat fuel flows and fixed 20-in. exit nozzle.

(c) *Fitted with N.G.T.E. (Whetstone) reheat system.*

- (i) At various constant engine speeds from idling to maximum r.p.m. with the reheat jet pipe fitted but no reheat burning. The variable nozzle was at the minimum setting (i.e., 17 in.).



- (ii) During acceleration from idling to maximum r.p.m. with the reheat jet pipe fitted but no reheat burning. The variable nozzle was at the minimum setting.
- (iii) At maximum r.p.m. with various reheat fuel flows and with the variable nozzle at constant maximum setting (equivalent to 20-in. nozzle).
- (iv) At maximum r.p.m. with various reheat fuel flows and corresponding nozzle sizes.

## TEST RESULTS

Although a wide variety of tests is listed in the preceding section it will be seen that the engine running conditions can be conveniently divided into three main groups: (a) constant speed conditions; (b) accelerations; (c) running with reheat. The nature of the pressure fluctuations in each group is described below and illustrated by Fig. 3. The method of presenting the records is best described by reference to Fig. 3(g). This section of record shows four traces marked (1), (7), (5) and (T). On the pressure traces an upward deflexion is positive. The numbers refer to the pickup points as indicated in Fig. 1 and (T) indicates this channel was connected to the tachometer. The broken line down the centre of the record is the time base and the interval between corresponding points on adjacent marks is 1/50 sec. The text under the figure indicates that this record was made during an acceleration from idling to maximum r.p.m., the

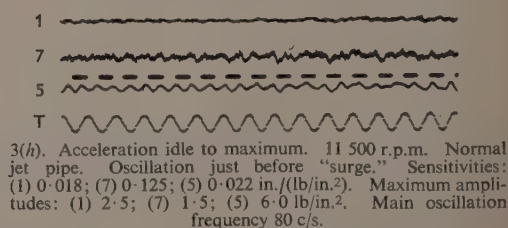
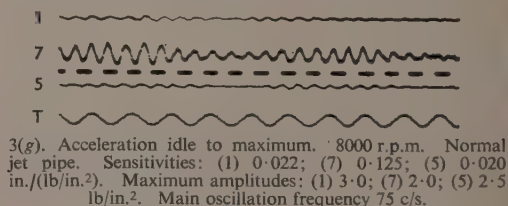
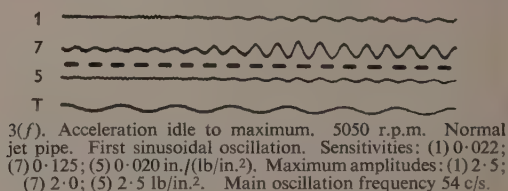
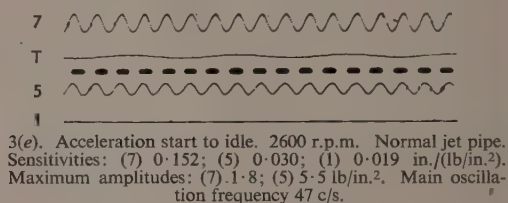
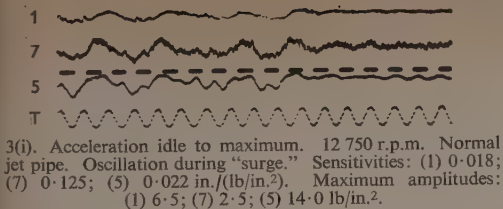
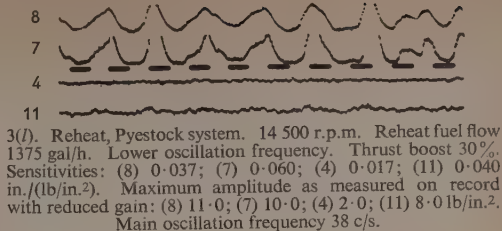
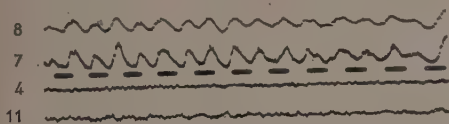


Fig. 3. Pressure records



3(j). Acceleration idle to maximum. 12 500 r.p.m. Normal jet pipe. Oscillation during "surge" at lower rate of acceleration. Sensitivities: (1) 0.018; (7) 0.125; (5) 0.022 in./lb/in.<sup>2</sup>. Maximum amplitudes: (1) 3.0; (7) 1.0; (5) 5.0 lb/in.<sup>2</sup>.



3(m). Reheat, Pyestock system. 14 500 r.p.m. Ignition of reheat. Fuel flow 500 gal/h. Sensitivities: (1) 0.013; (9) 0.045; (7) 0.070; (5) 0.018 in./lb/in.<sup>2</sup>. Maximum amplitude: (9) > 6.0; (7) > 4.0 lb/in.<sup>2</sup>.



3(o). Reheat, Whetstone system. 14 500 r.p.m. Reheat fuel flow 1000 gal/h. Thrust boost 25%. Variable nozzle set at 20 in. Sensitivities: (1) 0.028; (4) 0.015; (7) 0.035; (9) 0.060 in./lb/in.<sup>2</sup>. Maximum amplitudes: (1) 3.0; (7) 10.0; (9) 3.0 lb/in.<sup>2</sup>. Approximate frequency 42 c/s.



Fig. 3—continued. Pressure records

mean engine speed for this section being 8000 r.p.m. The engine was fitted with a standard jet pipe and the feature illustrated in this section is a modulated sinusoidal oscillation described more fully in the text. The sensitivity of each channel in inches deflexion per pound per square inch pressure change is given; for example (1) 0.022 indicates that for channel (1) a change of pressure of 1 lb/in.<sup>2</sup> gives a deflexion of 0.022 in. The next line indicates that the maximum peak to peak pressure variation along this section of record was 3 lb/in.<sup>2</sup> on channel (1), etc. Finally, where the fluctuations are cyclic a frequency is indicated (in this case, 75 c/s).

(a) *Constant speed conditions.* The variables in this group were engine speed, type of tailpipe, and propelling nozzle size. Of these only engine speed appeared to be important. Fig. 3(a), (b), (c) and (d) are sections of typical records at engine speeds of 4200, 8500, 13 500 and 14 500 r.p.m. The most striking feature of these records is the absence of low-frequency fluctuations of appreciable magnitude, at any engine speed. There is some indication that high-frequency oscillations are present and increase in amplitude with engine speed, but the frequency range was such that indicated amplitudes are unreliable. It is usually observed that channels (1) and (7), which are just downstream of the

compressor and turbine respectively, show the greatest high-frequency amplitudes.

(b) *Acceleration.* Fig. 3(e) illustrates an oscillation which may occur during acceleration from start to idling. The very uniform sinusoidal oscillation on channels (5) and (7) is in fact modulated, but at such a low frequency that the amplitude appears uniform over this section of the record. The oscillation on channel (5) has a peak-to-peak amplitude of 5.5 lb/in.<sup>2</sup>. As the mean pressure at station (5) is only of the order of 15 lb/in.<sup>2</sup>, this oscillation is very severe being of the order of  $\pm 15\%$  of the mean pressure level. It is believed that this oscillation is responsible for the audible "rumbling" and "shuddering" which often occurs during the starting sequence. It should be noted that this oscillation is not always set up during starting and it may be that if a slightly reduced acceleration rate was incorporated in the automatic starting sequence it might be eliminated completely. Figs. 3(f), (g), (h), (i) and (j) illustrate various phases during a rapid acceleration from idling to maximum r.p.m. As engine speed increases, an oscillation appears at all recording stations at approximately 5000 r.p.m. This oscillation is a reasonably undistorted sine wave of frequency approximately 50 c/s. It is modulated at a much lower frequency (of the order of 10 c/s) and has the appearance of being generated by a "beat"



mechanism. Fig. 3(f) shows the onset of this oscillation with a frequency of 54 c/s and a maximum amplitude of the order of 2.5 lb/in.<sup>2</sup>. This sinusoidal oscillation increases in frequency as engine speed increases, though not proportionately. Fig. 3(g), a later stage in the acceleration, shows a frequency of 75 c/s at an engine speed of 8000 r.p.m. It also illustrates the continued modulation of the sine wave.

At a still later stage in the acceleration the character of the oscillation changes slightly. Fig. 3(h) shows that the modulation of the sine wave on channel (5) has apparently disappeared and the oscillation on channel (7) has ceased to be sinusoidal. A still more striking change is that which has occurred in the ratio amplitude of channel (7)/amplitude of channel (5) between 8000 and 11 500 r.p.m. The frequency of oscillation has now increased to 80 c/s. Fig. 3(i) is a continuation of Fig. 3(h). It will be seen that the cyclic oscillation suddenly degenerates into a violent irregular pulsation. This is evident on all channels and its peak to peak amplitude varies from 14.0 lb/in.<sup>2</sup> at station (5) to 2.5 lb/in.<sup>2</sup> at station (7). This pulsation has marked low frequency components (20–30 c/s) and persists for approximately a quarter of a second. When this pulsation subsides all major low-frequency oscillations disappear and the record is similar to the constant speed record of Fig. 3(d). Although Fig. 3(f) to 3(i) are typical of the general behaviour during rapid acceleration it was observed that as the acceleration rate was reduced the amplitude of the pulsations decreased until first the irregular pulsation and then the sinusoidal oscillation disappeared completely leaving a clean record without fluctuations. As an example of the effect of reducing the acceleration rate Fig. 3(j) shows that the amplitude of the violent pulsation is reduced from 14.0 lb/in.<sup>2</sup> to 5.0 lb/in.<sup>2</sup> when the maximum acceleration rate is reduced from 3700 r.p.m./sec to 2700 r.p.m./sec.

(c) *Reheat.* Fig. 3(k) to 3(o) illustrate the nature of the pressure fluctuations which occur in the jet pipe when the reheat system is in operation. Figs. 3(k) and 3(l) are consecutive sections of a record chosen to illustrate the occurrence of two main frequencies 75 c/s and 38 c/s when the Pyestock reheat system was used. Fig. 3(m) shows the pressure fluctuations at the instant of ignition and Figs. 3(n) and 3(o) show pulsations which occurred with the Whetstone reheat system at two different fuel flows. It will be seen that although the pulsations do not have a regular sinusoidal form they are undoubtedly cyclic and an approximate frequency can be determined. It is often possible to observe more than one frequency and it is suggested that the behaviour in Figs. 3(k) and 3(l) is the result of two pulsations going in and out of phase. The magnitude, and to a lesser extent the frequency of these reheat pulsations, is dependent on the reheat fuel flow. Both these effects are well illustrated in Figs. 3(n) and 3(o) where the amplitude on channel (7) changes from 5 to 10 lb/in.<sup>2</sup> and the frequency from 50 to 42 c/s as the fuel flow increased from 700 to 1000 gal/h. Since the static pressure in the reheat jet pipe will usually be less than two atmospheres absolute it will be seen that these oscillations of peak to peak amplitude 10 lb/in.<sup>2</sup> are very severe. In isolated instances single oscillations giving a pressure swing of as much as 16–18 lb/in.<sup>2</sup> have been recorded. The records show that these fluctuations do not penetrate upstream into the combustion chamber and so represent variations in drop across the turbine. It is to be expected that such variation in the turbine conditions would cause severe stresses in the rotor shaft and stress measurements at Rolls Royce Ltd. have indeed shown this effect. At station (11) near the open end of the jet pipe the pressure fluctuations are about

one-quarter of those near the turbine. This is shown in Fig. 3(k) and 3(l).

It has been suggested that the nature of the fluctuations in the reheat system might be used as an additional measure of its merit. Fig. 4 shows how the amplitude of pulsation varies

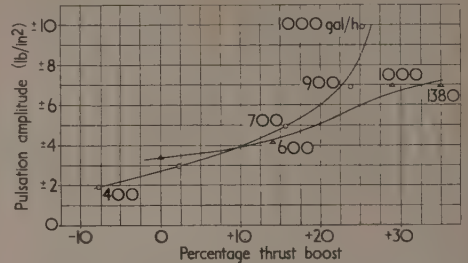


Fig. 4. Pulsation amplitude *versus* thrust boost

Δ = Pyestock system.

○ = Whetstone system.

with percentage thrust boost for the two reheat systems tested. Values of reheat fuel flow are marked beside the individual points. In general these two systems give quite similar results though the divergence at the higher fuel flow may be significant.

#### DISCUSSION OF RESULTS

The absence of low-frequency pressure fluctuations at constant speed conditions calls for no special comment. It is emphasized again, however, that the negligible amplitude of high-frequency components as determined from our records is probably unreal since at frequencies above 500 c/s the attenuation may be severe. Two main types of fluctuations have been detected during accelerations, (a) modulated sinusoidal oscillations and (b) "surge" oscillations. These will be discussed separately.

The modulated sinusoidal oscillations are at the same time most readily explained qualitatively yet the most difficult to pin down quantitatively. It is believed that these oscillations are "organ pipe" vibrations of the whole or part of the air column within the engine. Although no rigorous proof can be offered to support this belief the following points can be cited:

- (i) The oscillations are of undistorted sinusoidal shape.
- (ii) The frequencies are consistent with the leading duct dimensions.
- (iii) During an oscillation all points within the duct are "in phase."

Assuming, then, that we are dealing with "organ pipe" oscillations an attempt will be made to describe in detail the behaviour during an acceleration from idling to maximum r.p.m. It is first necessary to decide which gas column is the main resonator. The records show that between 5000 and 8000 r.p.m. the resonator frequency changes from 50 to 75 c/s. Ignoring Mach number effects, which in any case would tend to reduce frequency, this change corresponds to more than a doubling of the absolute temperature. It appears that for such a temperature change to occur the gas column concerned must be entirely after the combustion chamber. The gas column from the turbine disk to the propelling nozzle fills this requirement. The length of this column is 7 ft 8½ in. and at standard atmospheric conditions if it acted as a quarter wave resonator the frequency would be approximately 37 c/s. Since the maximum frequency is 75 c/s this indicates that the absolute temperature changes by a factor

of four, i.e. increases to approximately 1150° K. Since considerable overfueiling, as evidenced by flames in the jet pipe, occurs during an acceleration, this jet pipe temperature is not unreasonable. It is now necessary to identify the resonator which will produce a frequency near this and so give rise to the beat phenomenon. Examining the total gas column from compressor intake to propelling nozzle we see that it has a total length of 13 ft, and if it acted as a half-wave resonator the frequency would be 42 c/s. If half of this column is heated to 600° C the frequency becomes approximately 55 c/s and it is clear that the possibility of beating exists between the two oscillations described. It is to be expected that as the r.p.m. increase and the nozzle guide vanes choke, the jet pipe oscillation will cease to make itself felt at stations upstream of the turbine. Such an effect appears to take place and produce the change in character of the oscillations observed between Fig. 3(g) and 3(h). It is believed that the nozzle guide vanes begin to choke at about 10 000 r.p.m. when the pressure ratio is approximately 2 to 1.

The oscillation observed on channel (5) of Fig. 3(h) is believed to be a further mode associated perhaps with quarter-wave oscillation of the air column between the head of the combustion chamber and the compressor inlet. This air column is approximately 4 ft long and at the relevant temperature will resonate at approximately 80 c/s which agrees with the observed value.

The explanation given above of the sinusoidal oscillations is in agreement with the observations but a more important point than the detailed explanation of the observed frequencies is to decide why the gas columns are set in vibration at all. It is believed that in essentials the system of air column and combustion chamber is no more than the well-known "singing flame" or perhaps more accurately the "gauze tone" system. It will be recalled that in the latter system a heated gauze placed at the lower end of a vertical cylindrical tube induces resonant vibrations in the air column. The essential feature of this mechanism is the dependence on the air velocity of the rate of heat transfer from the gauze to the air column. When the combined effects of convective and fluctuating velocities are considered it will be seen that a cyclic heat input results, and if this is correctly phased the possibility of amplification of any random fluctuation exists. Following up this analogy it is necessary to see if the heat input in the engine case is in any way velocity dependent. Making the assumption that fuel flow is constant (i.e., that a high-pressure fuel system, virtually independent of the slight pressure oscillations, is used) we can look for cyclic changes in heat input only from cyclic changes in efficiency. These can in fact arise in two ways, (a) by direct effect of velocity on efficiency at constant air/fuel ratio or (b) by variation of efficiency with variation of air/fuel ratio. (A cyclic variation of air/fuel ratio occurs because of the air mass flow pulsation.) We have therefore all the essentials for a heat-maintained oscillation. The phasing of the cyclic heat input is of course important. It is clear that combustion of the injected fuel is not instantaneous, so that a phase displacement between the velocity fluctuation and the resulting cyclic heat input will be present in all practical cases. It is worth noting that this phase lag is likely to be a function of the running conditions (e.g., pressure, temperature) as well as chamber geometry.

It may be felt that the effects of velocity fluctuations will be small and that the above hypothesis is being stressed too hard. In case this is so it will be useful to see what velocity fluctuations can be involved. The section of record shown in Fig. 3(e) shows a peak to peak amplitude of 5.5 lb/in.<sup>2</sup> when the mean pressure level is still approximately atmospheric

(2500 r.p.m.). If this pressure oscillation of  $\pm 2.75$  lb/in.<sup>2</sup> be considered as occurring at the node of an open pipe the corresponding velocity variation at the open ends of the pipe would be approximately  $\pm 130$  ft/sec. It is clear from this calculation that the velocity oscillations in the combustion chamber need not be small and the possibility of complete reversal cannot be excluded. Such reversals would explain the "carbon shadows" sometimes observed on the inside of air casings opposite holes in the flame tube as well as the occurrence of carbon upstream of the swirler and in the dome cavities. Before leaving this point it is worth mentioning that efficiency could also be affected by pressure though it is believed that this effect would be slight over the pressure range due to oscillation.

If the explanation suggested above is correct it has some interesting practical consequences. Firstly, since "rumbling" in engines in flight has been associated with resonant oscillation it is suggested that a cure might be effected by the use of a chamber designed to minimize the rates of change of efficiency with velocity and air/fuel ratio. This argument furnishes an additional reason for striving towards high absolute efficiency as the permissible efficiency variations are thereby reduced. It is also in accord with the fact that "rumbling" of flight engines occurs at high altitudes when (a) absolute efficiency tends to fall, and (b) efficiency losses off design point become more severe. Secondly, where some choice of positioning of a combustion chamber in an engine is allowed it might be advantageous to install it at a pressure rather than a velocity node. This should be especially applicable to the lay-out of industrial sets and may lead to smoother starting and more stable operation.

"Surge" pulsation. This pulsation interrupts the 80 c/s oscillation of Fig. 3(h) and, as implied by the title of this section, appears to be associated with a partial surge of the compressor. Figs. 3(i) and 3(j) are examples of this phenomenon at different rates of acceleration. When this pulsation was first observed it was immediately suspected that surging might be responsible and a quantitative analysis of the records was made to check this possibility. Fortunately during many of the acceleration tests the engine tachometer output had been recorded so that in these cases we had precise knowledge of engine speed and acceleration at any instant. Curves (A) and (B) of Fig. 5 show engine speed and acceleration, respectively, during an acceleration in which the throttle lever was opened fully at 6 sec. Since the tachometer and pressure gauges are recorded simultaneously we are able to show on Fig. 5 the time at which the violent pulsation occurred. This is indicated by the short hatched intervals and it is significant that they occur almost at the time of maximum acceleration.

It is clear that extra work is done to accelerate the rotor.

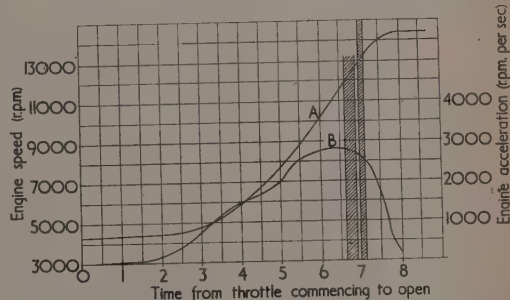


Fig. 5. Variation with time in seconds of engine speed and acceleration



When the moment of inertia and angular acceleration is known the extra work is readily calculated. The providing of this extra work by the engine results in the movement of the compressor operating conditions away from normal equilibrium running line towards the surge line. Fig. 6 shows the running line and surge line typical of a Derwent V compressor. Fig. 6 also includes calculated running lines for (a) constant acceleration of 2000 r.p.m./sec, (b) constant acceleration of 4000 r.p.m./sec, and (c) acceleration varying

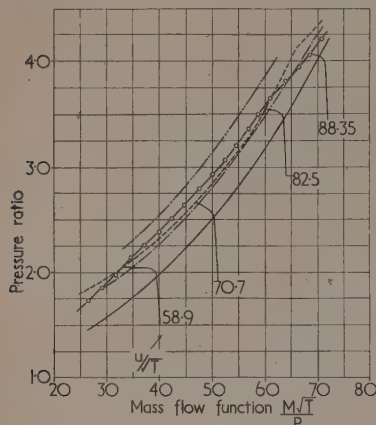


Fig. 6. Operating lines for a Derwent V compressor

- = equilibrium running line; - - - = surge line;
- = actual operating line during acceleration as shown on Fig. 5.
- ... = theoretical operating line for constant acceleration of 2000 r.p.m./sec at sea level.
- ... = theoretical operating line for constant acceleration of 4000 r.p.m./sec at sea level.

with engine speed as indicated in Fig. 5. It is seen on inspection that the operating line as calculated for (c) crosses the surge line to the greatest extent when the engine speed is about 11500 r.p.m. which is the engine speed when the pressure pulsations associated with surging occurred. The fact that, as shown in Fig. 6, the operating line for accelerations of 2000 r.p.m./sec lies just to the right of the surge line and that accelerations of more than 2000 r.p.m./sec were required to cause the pressure fluctuations associated with surging is further and virtually conclusive evidence that compressor surges contribute to the pressure fluctuations of the type shown in Fig. 3(i) and 3(j).

**Reheat running.** Figs. 3(k) to 3(o) show that the violent pressure fluctuations occurring during reheat exhibit a marked periodicity with frequencies lying in the range 75–38 c/s. When a periodic oscillation is observed within a duct the first mechanism to be suspected is a simple "organ pipe" resonance. It is believed in this case, however, that such a mechanism is ruled out since the pressure fluctuations at different stations are not in phase. Similar oscillations have been recorded in a ram jet and it has been suggested that the mechanism involved is an interaction between the fuel injection and pressure pulsations originating in the combustion zone. It has been suggested that a pressure pulse moving upstream from the combustion zone reduced the fuel flow as it passes over the injector since the differential across the injector is transiently reduced. A zone of weak mixture is thus established in the flow and is carried downstream at the mean flow velocity. It was further suggested that when this

weak mixture arrives at the combustion zone a rarefaction pulse occurs which travels upstream and produces a zone of rich mixture on reaching the fuel injector. This is then carried downstream and in turn produces a pressure pulse at the combustion zone which completes the cycle. The period for this cycle is evidently the time required for two passages upstream with sonic velocity plus two passages downstream with flow velocity. Although for a low fuel pressure the explanation above could be substantially correct it is believed that this is a trivial case, which is readily cured by the use of high injection pressures.

Consideration of the interaction of pressure pulses and fuel injection has led us during the present work to suggest quite a different mechanism which unfortunately looks much more intractable, in that it applies when the fuel flow is constant. This mechanism is described briefly below with the help of Fig. 7 which is a space-time or position diagram. In this diagram position along the duct is the abscissa and the ordinate is time shown increasing from top to bottom of

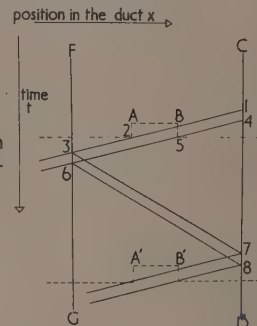


Fig. 7. Position diagram for suggested reheat pulsation mechanism

the figure. The fuel injector and the combustion zone are represented by the vertical lines  $FG$  and  $CD$  respectively. To simplify the argument combustion is supposed to occur in a narrow zone, approximating a plane at  $CD$ .  $AB$  is a pressure pulse, shown rectangular for simplicity, which is advancing upstream against the flow. The lines 1, 2, 3 and 4, 5, 6 which represent the paths of  $A$  and  $B$  respectively show the pressure pulse proceeding upstream at steady velocity and crossing the fuel injector. For the time interval between points 3 and 6 the air flow conditions at the fuel injector are those between  $A$  and  $B$ . It can be shown that the state and velocity of the gas between  $A$  and  $B$  are related to those outside the pulse by the equation

$$5a_0 + V_0 = 5a_1 + V_1 \quad (\gamma = 1.4)$$

where  $a$  represents sound velocity and fixes the state, provided the processes are isentropic and  $V$  represents flow velocity. Suffixes 0 and 1 refer to the undisturbed conditions and the conditions between  $A$  and  $B$  respectively. It is at once evident that within the pressure pulse velocity is reduced and we can look for a change in air/fuel ratio if the fuel flow is assumed constant. A simple calculation shows that mass flow as well as velocity is reduced between  $A$  and  $B$  so that air/fuel ratio is decreased, i.e. a richer bank of mixture is carried downstream with the flow. On Fig. 7 this rich region is bounded by the lines 37 and 68. Between the points 7 and 8 the richer mixture is being burned and we will suppose that this gives rise to a pressure pulse  $A'B'$  which travels forward to start the cycle again. It will be noted that this mechanism gives a period which is half that which results from the hypothesis outlined in the previous paragraph. It is believed



that the simplified hypothesis outlined above is applicable in principle to our case of reheat combustion since we have the necessary elements of a high-pressure fuel injection system upstream of a combustion zone. Fig. 3(m) showing the pressure variations which occur on ignition of the reheat system gives some ground for this belief. Station (9) is approximately 4 ft downstream of (7) and the time between the passage of the initial pulse over these two stations can be seen very clearly. The first few cycles of the process can be easily distinguished but the regularity is soon lost since apparently under these conditions the cycle is attenuating. It will be instructive first to calculate the change of conditions which a pressure pulse can bring about. Suppose that the flow conditions before the pulse are as follows:

$$\begin{aligned} a_0 &= 2000 \text{ ft/sec} \\ V_0 &= 500 \text{ ft/sec} \end{aligned}$$

If now the pulse raises the pressure by 14% corresponding to an increase in  $a$ , the velocity of sound, of 2%, it will be found that the flow velocity is reduced to 300 ft/sec. The corresponding density increase is only 10% so that the actual mass flow rate is reduced by 54%. It can be shown similarly that starting from these same conditions a pulse raising the pressure 40.7% will stop the flow completely. The significance of this mechanism now becomes obvious as it is evident that quite modest pressure pulsations can carry the system outside its stability range and so extinguish the burner.

A further interesting quantitative check is to determine if the actual recorded frequencies are compatible with this proposed mechanism. Ignoring for the moment the apparent 75 c/s of Fig. 3(k), which is believed to be the sum of two independent low-frequency oscillations, it appears that a typical frequency is 40 c/s. Assuming again a sound velocity of 2000 ft/sec and flow velocity of 500 ft/sec we have

$$\frac{1}{40} = \frac{X}{2000 - 500} + \frac{X}{500}$$

where  $X$  is the effective distance between fuel injection and combustion zone, i.e.,  $FC$  on Fig. 7. The terms on the right are the times for the passage of the pulse upstream and the passage of the enriched zone downstream. This equation gives  $X = 9$  ft. In so far as a point 9 ft downstream of the fuel injectors is still within the pipe the recorded frequencies are compatible with the mechanism proposed. Further refinement of the assumptions cannot be justified since the tacit assumption of one dimensional flow is far from the truth. It is clear that one of the most important phases of the cycle of events suggested occurs when the enriched region in the flow enters the combustion zone. Referring to Fig. 7 the interest lies in determining how the "output" pulse  $A'B'$  compares with the assumed "input" pulse  $AB$  in both shape and amplitude as this comparison is likely to determine whether the cycle will build up or attenuate. While it is believed that with sufficient simplifying assumptions it may be possible to solve this problem using the graphical method of characteristics outlined in reference (2) it is felt that such idealized results would have to be interpreted very cautiously.

Finally, since, in general, fluctuating conditions are not desirable it will be useful to see what methods might be adopted to avoid the particular type of oscillation described above. In the matter of fuel injection it would appear that concentration in one plane would be dangerous since in such an arrangement all injectors are affected simultaneously by a forward moving pressure pulse. Similarly there should be gains in stability from distributing the flame holding

elements as far as possible in different planes. The limited evidence from the two reheat systems studied agrees with this suggestion regarding fuel injection in that the Pyestock system with primary and secondary fuel injection separated by approximately 2 ft has the better rich limit and accordingly is capable of higher thrust boost. A second point which suggests itself is that by suitably choosing the fuel injection pressure it may be possible to produce some measure of insensitivity to pressure pulses, i.e. to make the pressure pulse reduce the fuel and air flow simultaneously and so maintain roughly constant air/fuel ratio.

## CONCLUSIONS

This investigation indicates that the engine does not develop any low-frequency pressure fluctuations of appreciable magnitude during constant speed running. It appears that high-frequency oscillations are present under these conditions but limitation in the frequency response of the recording equipment prevented a quantitative examination.

Two types of fluctuation have been identified during rapid accelerations: (a) sinusoidal oscillations of the gas column and (b) irregular pulsations occurring at maximum acceleration rates.

It is concluded that the former are "organ pipe" vibrations maintained by cyclic heat input in the manner of the "singing flame" and sufficient evidence has been secured to warrant the conclusion that the latter are due to partial surge of the compressor.

"Rumbling" is considered to be the audible manifestation of the "organ pipe" oscillations mentioned above. It is concluded that this instability might be eliminated by the use of a chamber in which combustion efficiency is relatively insensitive to variation of velocity and air/fuel ratio.

Cyclic pulsations of large amplitude have been recorded in the jet pipe with reheat in operation. It is suggested that these pulsations are primarily due to pressure pulses travelling forward from the combustion zone and interacting with the fuel injection process. It is pointed out that this interaction can take place even when the fuel flow is unaffected by transient changes in chamber pressure since the pressure pulses give rise to an air mass flow fluctuation.

The explanation proposed to account for reheat pulsation leads to the suggestion that this instability will be discouraged by avoiding the concentration of fuel injectors and flame stabilizers in single planes.

## ACKNOWLEDGEMENT

This paper describes part of a programme of work at the National Gas Turbine Establishment and acknowledgement is made to the Chief Scientist, Ministry of Supply, for permission to publish. Acknowledgements are also due to members of the staff of the National Gas Turbine Establishment, particularly to Mr. T. K. Williams for his share in recording the pressure fluctuations and to Mr. H. G. Waldock for calculating the curves of Fig. 6 from data kindly supplied by Messrs. Rolls Royce Ltd.

Crown copyright reserved. This paper is reproduced with the permission of the Controller of H.M. Stationery Office.

## REFERENCES

- (1) KESTIN, J., and GLASS, J. S. *Proc. Instn Mech. Engrs*, **161**, pp. 250-257 (1949).
- (2) KAHANE, A., and LEES, L. *Third Symposium on Combustion, Flame and Explosion Phenomena*, pp. 222-229 (Baltimore: The Williams and Wilkins Co., 1949).

# Light scattering measurements on polydisperse systems of spherical particles

By E. ATHERTON, B.Sc., A.Inst.P., and R. H. PETERS, B.Sc., Ph.D., Imperial Chemical Industries, Hexagon House, Manchester, 9

[Paper first received 11 February, and in final form 21 April, 1953]

The application of Debye's theory to polydisperse systems of spherical particles is discussed and light scattering measurements have been made using some commercial dispersions. Three methods have been employed, namely, measurement of the dissymmetry, the turbidity and the dependence of the latter on wavelength. The first two give a weighted average whilst the latter gives an approximation to the mean. From these averages the particle size distributions of two dispersions have been determined assuming them to be normal. The distribution curves compare favourably with those obtained by direct means employing the electron microscope.

In a previous paper<sup>(1)</sup> several optical methods of determining the size of spherical particles were discussed and their theoretical significance was indicated for polydisperse systems. The mathematical treatment was based on Debye's equation. The aim of the present paper is to report some applications of the theory to colloidal systems of polymer particles and to indicate the range of applicability of Debye's equation to such systems.

The conditions assumed in the theoretical treatment may be attained practically by irradiating a suitably diluted dispersion with a narrow collimated beam of monochromatic light and by measuring:

- (a) The total amount of light scattered (i.e. turbidity).
- (b) The way in which this light is distributed in space.
- (c) The way in which the scattering varies with wavelength.

The interpretation of these measured quantities in terms of particle size has already been indicated for monodisperse systems by several authors.<sup>(2, 3)</sup> In the previous paper,<sup>(1)</sup> an extension of Debye's theory was proposed and the types of average value obtained by the different methods were evaluated. It was indicated that of the three methods, only the turbidity method gave a rational average, but that for systems in which the range of particle size was not excessive, the arithmetic mean size could be estimated by measuring the rate of change of log. (turbidity) with log. (wavelength). It was also shown by studying hypothetical systems having normal (Gaussian) size distribution that the "dissymmetry average" diameter  $D_{Dis}$  lay within approximately 12% of  $D_\tau$ , the "turbidity average" diameter.

In order to test this prediction, a series of measurements of turbidity and dissymmetry were made on several polymer dispersions of types encountered in practice (vinyl and methacrylate types). Since the ultimate aim of the work was to determine the value of light scattering methods for practical assessment, no attempt was made to work with specially pure or clean materials. The average diameters obtained by the various methods are discussed at length later with special reference to predicting the width of particle size distributions from light scattering properties.

In order to obtain an independent check on the results, the dispersions studied were photographed by the electron microscope at known magnification and the size distributions determined by direct measurements. A critical discussion of the electron microscope method is presented.

## EXPERIMENTAL

The measurements were carried out on aqueous dispersions of polycellosolve methacrylate and polyvinyl chloride selected, with one exception, from commercial materials. This was a polyvinyl chloride dispersion prepared so as to have uniform

particle size. The conditions of cleanliness observed in this work were no more than normally employed for routine chemical investigations, distilled water and glassware cleaned with chromic acid being used.

The dissymmetry ratios were measured with a photoelectric apparatus described elsewhere.<sup>(4)</sup> In this instrument a parallel beam of monochromatic light is passed through the dispersion under investigation, and the scattered light, after collection by a lens/slit system, falls upon a photomultiplier of the 931A type. The latter may be rotated so as to collect light at any angle to the incident light beam, between 40° and 150°.

The turbidities and their wavelength dependence were measured directly by means of Hilger Uvispek and Cary recording spectrophotometers. For systems such as those considered here in which the scattering is sufficiently strong to be measured directly,<sup>(5)</sup> such measurements are more convenient than the usual method involving determination of the scattering at 90°, since it is not necessary to establish and maintain a turbidity standard. The various measurements will now be considered in greater detail.

(a) *Measurements of the dissymmetry ratio.* This is defined as the ratio of the intensities scattered at 45° and 135° to the direction of the incident beam and was measured for each dispersion studied at four concentrations, the material being diluted with distilled water. To avoid complications arising from particle-particle interactions, the results were extrapolated to zero concentration and the dissymmetry ratio  $S$  under these conditions was used in subsequent calculations. From  $S$  the average particle diameter was obtained using the relation between  $S$  and  $D/\lambda$ , given by the equation

$$S = \frac{[3q^{-3}(\sin q - q \cos q)]_{\theta=45^\circ}^2}{[3q^{-3}(\sin q - q \cos q)]_{\theta=135^\circ}^2} \quad (1)$$

where  $q = 2\pi(D/\lambda)(\sin \frac{1}{2}\theta)$ ,

$D$  = the particle diameter,

$\lambda$  = the wavelength of light,

$\theta$  = the angle between the direction of observation and the propagation direction of the incident light beam.

In all the measurements the 5461 Å mercury green line was used.

(b) *Measurements of turbidity.* In using the direct method of measurement it is important that the scattered light should be excluded from the photo-detector of the spectrophotometer. If suitable precautions are not taken to ensure these conditions the measured turbidity will be lower than the true value. This point was checked in the present work by measuring turbidities with the specimen firstly in front of the inlet slit to the instrument and secondly in the normal position behind the outlet slit. The fact that readings obtained in this way



were in good agreement using both the Hilger and Cary instruments indicated that the desired conditions were fulfilled and the results reported were obtained with both instruments.

Turbidities were measured at any desired wavelength in the visible spectrum at several values of  $c$ , the concentration of dispersed polymer. The data was plotted in the conventional way ( $c/\tau$  versus  $c$ ) and the ordinate intercept at zero concentration,  $(c/\tau)_{c=0}$ , was determined. This was corrected for dissymmetry using a method described previously.<sup>(5)</sup> Refractive index increments,  $(\delta n/\delta c)$  of the dispersions were determined with a split cell refractometer and a Rayleigh interferometer. The results by the two methods, whenever they were checked, were in excellent agreement and the values quoted were obtained with the interferometer.

The disperse phase "molecular weight,"  $M$ , was determined from this data using Debye's equation:

$$H\left(\frac{c}{\tau}\right) = \frac{1}{M} + \frac{2B}{RT} \quad (2)$$

where

$$H = \left[ \frac{32\pi^3 n^2 (\delta n)^2}{3N_0 \lambda^4 (\delta c)} \right]$$

The value of  $M$  thus obtained was transformed to a true weight by multiplication by the mass of the hydrogen atom. This weight was converted to a volume, using values of the polymer density as measured with a pycnometer, after correcting for the solids content of the dispersion. Assuming the particles to be spherical, a diameter was computed from the calculated volume.

As an exercise in the use of the technique and to check the method, diameters were calculated from turbidities measured at three different wavelengths. The results are shown in Table 1.

Table 1. Particle diameters determined at three different wavelengths

Sample	Particle diameter ( $\mu$ )		
	$\lambda = 0.578 \mu$	$\lambda = 0.546 \mu$	$\lambda = 0.436 \mu$
Polyvinyl chloride dispersion	0.14(0)	0.13(2)	0.13(5)
Polycellosolve methacrylate dispersion	0.19(5)	0.18(9)	0.18(5)

(c) Measurements of turbidity dependence of wavelength. From the turbidity wavelength plots at various concentrations obtained with the Cary instrument, plots of  $\log \tau$  versus  $\log \lambda$  were constructed in the neighbourhood of  $\lambda = 546 \mu$ , and values of  $d(\log \tau)/d(\log \lambda)$  were obtained.

These values were used to determine an average size using the calibration curve calculated in the previous paper. The exact determination of the  $\log \tau/\log \lambda$  slope, however, is difficult because slight errors in the translation of data from the spectral turbidity to the logarithmic plot can cause differences in the estimated slope, particularly in the size range  $0.1-0.2 \mu$ .

There is no easy way of overcoming these difficulties other than by careful reading and computation. One way of improving the method, which is at present being developed, is the inclusion of two logarithmic cams in a recording spectrophotometer so that the  $\log \tau/\log \lambda$  plots may be obtained directly.

Complete  $\log \tau/\log \lambda$  curves were prepared for one of the dispersions to investigate the magnitude of the curvature present in a practical sample. The result is shown in Fig. 1

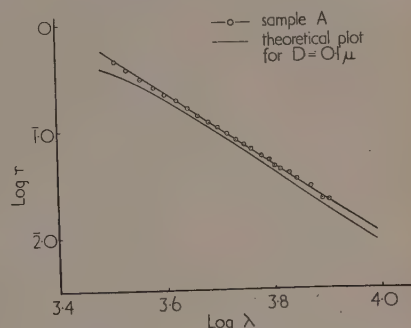


Fig. 1.  $\log \tau/\log \lambda$  curves for polycellosolve methacrylate dispersion

and the theoretical curve from the previous paper is reproduced for comparison. It can be seen that the theoretical plot is more curved, particularly in the region of shorter wavelengths. This is probably caused by the increase of the polymer refractive index with decreasing wavelength, which is not allowed for in the theory, and causes an increased scattering.

The theoretical calibration curve relating the slope of  $\log \tau/\log \lambda$  graph to particle size has been employed in preference to that of Heller since it seemed reasonable to use the same theory throughout and Heller's curve gave obviously erroneous results for the monodisperse sample studied.

**Comparison of the methods.** The results obtained by the different methods on three typical industrial dispersions and one monodisperse sample are shown in Table 2.

It can be seen that in the case of the monodisperse sample the different methods give approximately the same value, whilst for the commercial, polydisperse samples, the  $\log \tau/\log \lambda$  method gives values which are considerably smaller than those obtained by the dissymmetry or turbidity methods. This of course is to be expected from the significance previously attributed to the different averages.

Since the  $\log \tau/\log \lambda$  and turbidity averages can be approximated as

$$D_{\log \tau} = (\sum n_i D_i) / (\sum n_i)$$

$$D_{\tau} = [(\sum n_i D_i^2) / (\sum n_i D_i^3)]^{1/2}$$

Table 2. Measurement of particle size by different methods

(All dimensions in microns)

Polymer dispersion	Dissymmetry method	Turbidity method	$\log \tau/\log \lambda$ method		From electron on microscopic data	
			Theoretical calibration	Heller's calibration	Turbidity average	Mean of distribution
Polycellosolve methacrylate A	0.18(4)	0.17(4)	0.14(3)	0.11(9)	0.17(2)	0.14(7)
Polycellosolve methacrylate B	0.13(3)	0.12(2)	0.10(9)	0.10(5)	0.17(5)	0.10(8)
Polyvinyl chloride A	0.13(9)	0.12(2)	0.09(2)	0.09(7)	0.10(1)	0.05(5)
Polyvinyl chloride B (Monodisperse)	0.25(7)	0.26(9)	0.23(6)	0.14(6)	0.23(1)	0.22(3)



the observed differences should be attributable directly to the distribution of particle diameters in the sample considered.

Using equation (23) in the previous paper,<sup>(1)</sup> connecting  $D_\tau$ ,  $D_{\log \tau}$  and  $\sigma$ , the standard deviation of the normal distribution assumed to represent the size distribution of the sample, it is possible to calculate  $\sigma$  for measured values of  $D_\tau$  and  $D_{\log \tau}$ , by a method of successive approximation. To simplify the process, when carrying out several determinations of this kind, a series of curves relating the three variables have been constructed, Fig. 2. ( $D_\tau/D_{\log \tau}$ ) and  $D_{\log \tau}$  were taken for convenience as the variables and curves were drawn

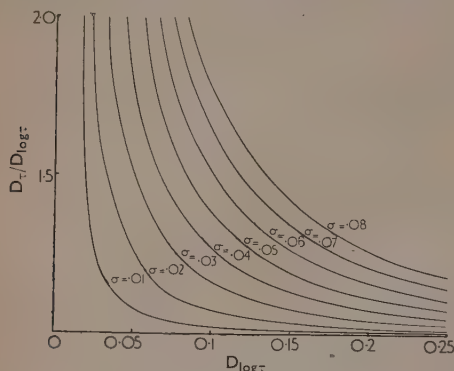


Fig. 2. Curves relating light scattering averages and distribution width.

for various  $\sigma$  values. Using these curves it is possible to calculate  $\sigma$  by interpolation from the two optically determined average diameters in a very short time. The distribution curves obtained in this way for two polycellosolve methacrylate samples are shown in Fig. 3, and the data obtained by the electron microscopic method are included for comparison. The agreement is quite satisfactory in view of the limitation of the electron microscope technique discussed in the next section.

**Electron microscopic determinations.** The following procedure was adopted in preparing specimens for the microscope:

The samples were well mixed by stirring and a glass capillary of about 0.5 mm bore was used to draw up about 2 cm length of the liquid. This was discharged into 150 c.c. of distilled water and stirred. A fresh capillary was then used to deposit one drop of the diluted latex on a clean microscope grid filmed with cellulose nitrate. The grids were dried in a vacuum and gold shadow case at an angle of  $\tan^{-1} 0.2$ , the resulting preparations being of a suitable concentration for counting.

Photographs were taken at  $10^4$  diameters magnification and the prints enlarged twice. Observation of shadow length in comparison with observed particle diameter indicated that, as might be expected, the particles showed marked flattening. In order to calculate the particle size in dispersion it was assumed that on the microscope film the particles were segments of a sphere and from the measured dimensions, equivalent spherical diameters were calculated.

#### DISCUSSION OF THE ELECTRON MICROSCOPIC DATA

In appraising the electron microscope data, several facts should be noted. The specimen examined on the grid of the microscope may not correspond to the same polymer when dispersed in bulk, because plastic particles of the type considered can be modified in several ways during preparation of

the grid. Firstly the particles in the microscope will not, in general, be spherical because of distortion by gravity and by "wetting" of the supporting membrane by the particles. Secondly, the physical nature of the particle may be modified by electron bombardment in the microscope. Extreme effects are shown with the vinyl polymers studied, in which there is

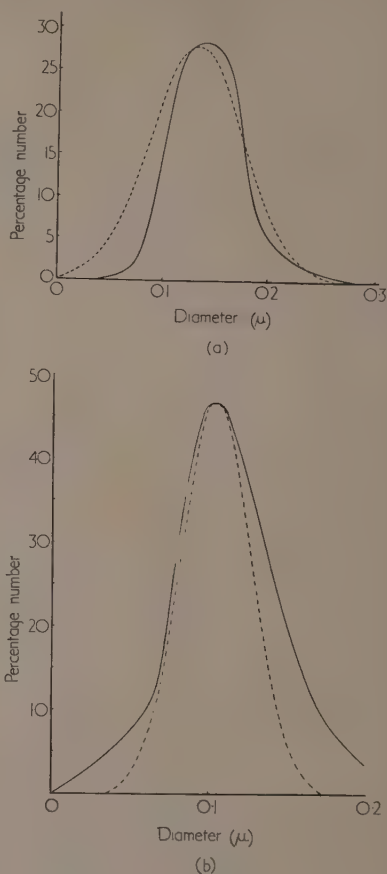


Fig. 3. Particle size distribution. (a) Sample A. (b) Sample B

— — — Theoretical distribution from light scattering.  
— Distribution from electron microscopic data.

a shrinkage of the particles resulting in a diameter reduction of up to 20%. There is also the possibility of error due to faulty calibration of the microscope, a point which was stressed recently by Heller.<sup>(6)</sup>

As evidence of the shrinkage, the size of the monodisperse sample was measured by means of the electron microscope and found to give a value of  $0.22 \mu$ – $0.23 \mu$  as compared with  $0.23 \mu$ – $0.25 \mu$  obtained by light scattering. This higher value has been independently confirmed by Tough<sup>(7)</sup> who obtained a particle size of approx.  $0.25 \mu$  by means of the Sharples centrifuge.

Under these circumstances it is gratifying that one can still obtain reasonable agreement with the light scattering method after correcting for distortion of the particles in the microscope. Even in the case of the methacrylate polymers,

which do not apparently suffer permanent modification in the microscope, it is apparent that, light scattering methods can give results much more quickly, when the lengthy process of measuring up particles on the microscope plates is remembered.

Another source of uncertainty in the microscope method is the possibility of aggregation when the sample droplet is dried down. This tendency has been dealt with in detail elsewhere<sup>(5)</sup> and need only be mentioned here.

#### CONCLUSIONS

Light scattering measurements on polydisperse systems have been shown to give particle size values which may be predicted by Debye's theory. The differences between the various types of size average involved have been explained, and used to predict approximate size distribution curves. It is clear that the techniques and methods of interpretation employed would be useful for plant control purposes in which specifications and tolerances as to size and distribution width could be set up initially. It is also likely that results of sufficient precision could be obtained on less expensive apparatus than has been used in these investigations. In any

event, it is felt that they indicate a useful, if approximate, extension of Debye's theory, to polydisperse materials of the type encountered in industry.

#### ACKNOWLEDGEMENTS

The authors' thanks are due to Dr. I. Harris, I.C.I. Plastics Division, who prepared the polyvinyl chloride sample.

#### REFERENCES

- (1) ATHERTON, E., and PETERS, R. H. *Brit. J. Appl. Phys.*, **4**, p. 344 (1953).
- (2) DOTY, P. M., OSTER, G., and ZIMM, B. H. *J. Amer. Chem. Soc.*, **69**, p. 1193 (1947).
- (3) HELLER, W. *J. Chem. Phys.*, **14**, p. 566 (1946).
- (4) ATHERTON, E. *J. Textile Inst. [Manchester]*, **43**, T173 (1952).
- (5) ATHERTON, E., and PETERS, R. H. *J. Textile Inst. [Manchester]*, **43**, T179 (1952).
- (6) HELLER, W. Symposium on Radiation and Macromolecules, Strasbourg (1952) (In press).
- (7) TOUGH, D. Unpublished work.

## Measurements of orientation in cotton fibres using polarized light\*

By R. MEREDITH, M.Sc., F.Inst.P.,† British Cotton Industry Research Association, Manchester

[Paper first received 12 March, and in final form 28 April, 1953]

The Becke line method of measuring refractive index was used on account of the irregular form of the cotton fibre. The variation in the calculated spiral angle of the fibrils is closely related to the variation in convolution angle and the data suggest that the average spiral angle in the original unconvoluted fibres may be the same for all varieties. A relation between cell length and spiral angle which holds for wood tracheids and bamboo fibres, also applies to cotton fibres if the "cell length" is taken as the average distance between reversals in spiral direction. Strength and initial Young's modulus are shown to be correlated with the degree of orientation calculated from the observed double refraction.

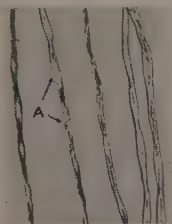
The polarizing microscope is a most useful instrument for obtaining information on the fine structure of fibrous materials, and this is especially so when dealing with the complex structure of the cotton fibre.

Examination of a cotton fibre will show that its shape is extremely variable; it approximates to a collapsed hollow tube which is twisted by varying amounts along its length. Fig. 1 shows the general appearance under the microscope. The fibre consists of a thin outer wall, the primary wall, containing among other constituents strands of cellulose criss-crossed and making an angle of about 70° with the fibre axis, with a secondary wall deposited inside it about 3  $\mu$  thick in a normally developed fibre. The latter consists of fibrils spiralling round the fibre axis at an angle of about 30° with sudden reversals in the direction of the spiral about 20 times per cm. This spiral structure is closely associated with the convolutions or twists developed when the fibre dries.

Fig. 2 shows how the shape of cross-section varies; it ranges from circular to that of a collapsed thin-walled tube. A fair approximation to the average shape is a rectangle capped by semicircular ends, the ratio of length to width of the rectangle ranging from, say, 5 to 0. This variable shape makes it

necessary to measure separately the refractive indices for light vibrating parallel ( $n_{\parallel}$ ) and perpendicular ( $n_{\perp}$ ) to the fibre axis and to take the difference to give the double refraction.

The irregularity and presence of a lumen in cotton fibres makes the method of measurement devised by Freeman and Preston<sup>(1)</sup> difficult, if not impossible. Consequently we are



\* (Reproduced from *Journal of the Textile Institute*)

Fig. 1. Cotton fibres showing convolutions ( $\times 70$ )

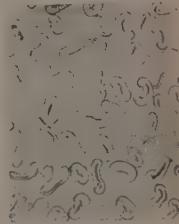


Fig. 2. Cross-sections of cotton fibres ( $\times 200$ )

reduced to using the Becke line method of measuring refractive index. In this method the movement of the bright line which appears at the edge of a fibre when the microscope is slightly raised or lowered from sharp focus is used to indicate whether

\* Based on a lecture given at The Institute of Physics' Conference on "Optical and Electron Microscopical Properties of Textile Fibres," 29 October, 1952.

† Now at the College of Technology, Manchester, 1.

the fibre is of higher or lower refractive index than the liquid in which it is immersed. The refractive index of the liquid is changed until no Becke line can be observed and the edge of the fibre disappears. The refractive index of the fibre then equals that of the liquid, for which the refractive index can easily be measured by means of a refractometer.

The central illumination method of observing the Becke line was used; for details of the method, reference may be made to a paper by Saylor,<sup>(2)</sup> and for general information on the measurement of refractive indices, Preston's book (p. 54)<sup>(3)</sup> may be consulted.

In this paper, it will be shown how the measured double refraction depends on the convolutions in the fibre and that the relation of the distance between reversals to the spiral angle of the fibrils is similar to that of cell length to spiral angle in other fibres. Finally, the relations between orientation, as calculated from double refraction, and the initial Young's modulus and strength of a wide range of varieties of cotton are presented.

#### THE REFRACTIVE INDICES OF DIFFERENT VARIETIES OF COTTON.

A series of liquids with refractive indices increasing in steps of 0.001 was prepared by mixing different volumes of  $\alpha$ -monobromonaphthalene ( $n_D = 1.658$  at  $20^\circ\text{C}$ ) and liquid paraffin ( $n_D = 1.481$  at  $20^\circ\text{C}$ ). For a mixture of two liquids the refractive index of the mixture is  $n = (n_1v_1 + n_2v_2)/(v_1 + v_2)$  where  $n_1$  and  $n_2$  are the refractive indices and  $v_1$  and  $v_2$  are the volumes of liquids 1 and 2. These liquids are miscible, inert to each other and to the fibre, and reasonably stable, although over a period of years it was found that the refractive index of a given mixture changed by a small amount. The refractive indices of the liquid mixtures for the sodium D line were measured at  $20^\circ\text{C}$  with an Abbé refractometer, calibrated with several liquids of known refractive index. Repeated settings with this instrument showed that refractive indices could be measured to  $\pm 0.0002$ . The mixtures have a relatively high temperature coefficient of about  $-0.0004$  per  $^\circ\text{C}$  so that it is important to control or measure their temperature during a determination of refractive index.

In order to keep a close check on the temperature of the immersion liquid, a water cell containing a short thermometer was made from two  $3 \times 1$  in. glass slides and placed on the rotating stage of the microscope. The slide carrying the fibres

was placed on top of this cell and thermal contact assured by a drop of water placed between them. A second thermometer was located just above the slide and below the objective holder to measure the air temperature. The room in which measurements were made was air-conditioned to  $65 \pm 2\%$  R.H. and  $20 \pm 1^\circ\text{C}$ .

To measure the mean values of the higher and lower refractive indices of a sample, nine fibres were selected having values of fibre weight per cm and maturity which were near the average for the sample. The maturity of a fibre was assessed by the polarized light technique described by Schwartz and Shapiro.<sup>(4)</sup> Three groups of three fibres, each having a length of 2 cm, were mounted parallel on a glass slide and arranged so that the average fibre-weight per cm and maturity were about the same for each group. One half of each fibre was used for the measurement of the higher refractive index and the other half for the measurement of the lower refractive index.

A drop of liquid of approximately the same refractive index as the fibre was placed on a group of three fibres and from the observed degree of matching at the outer edge of the fibres, e.g. at the point A in Fig. 1, a second liquid was chosen with higher or lower refractive index as required; similarly for the third group of fibres. The average refractive index of the group of nine fibres was judged from these observations and duplicate tests showed that the accuracy was about  $\pm 0.0005$ .

The results of measurements of the refractive indices of fourteen samples of cotton are given in the table. The cottons are grouped according to their species: thus, the first six are *G. barbadense* followed by four of *G. hirsutum* and then by four of *G. arboreum*. In each group the cottons with highest average length come first: the average length used here is termed the "effective" length. The fineness of the cottons is expressed as the mean mass per unit length. This quantity depends on both the perimeter of the fibres, and on the maturity or thickness of the cell wall, so that to complete the description of the different varieties, the degree of thickening ( $\delta$ ) has been given.  $\delta$  is defined as the ratio of the area of cross-section of the cell wall to that of a circle with the same perimeter as the fibre; it has been obtained from the relation  $\delta = 0.289(N - D)/100 + 0.404$  given by Peirce and Lord,<sup>(5)</sup> the value of  $(N - D)$  being obtained from the "immaturity" count described by Clegg.<sup>(6)</sup>

It will be observed that the longest cottons, which are usually also the finest, have higher refractive indices than the

Mean values for fourteen samples of cotton

Cotton	Symbol	Effective length (cm)	Fineness (μg/cm)	Degree of thickening (δ)	Refractive index for sodium D line (n <sub>D</sub> )	Spiral angle (θ°)	Convolution angle (θ'°)	Distance between reversals (mm)	Optical orientation factor (f <sub>o</sub> )	Initial Young's modulus (10 <sup>10</sup> dyn/cm <sup>2</sup> )	Breaking stress (10 <sup>6</sup> dyn/cm <sup>2</sup> )	
St. Vincent	V	5.1	1.00	0.52	1.581 <sub>0</sub>	1.530 <sub>8</sub>	27.6	4.7	0.40	0.76 <sub>1</sub>	12.8	8.9
St. Vincent	v	5.1	1.04	0.51	1.580 <sub>7</sub>	1.531 <sub>0</sub>	27.9	5.2	0.39	0.74 <sub>7</sub>	12.4	9.0
Maarad	R	4.1	1.44	0.57	1.577 <sub>4</sub>	1.531 <sub>3</sub>	31.5	6.5	0.42	0.69 <sub>0</sub>	9.8	7.3
Sakel	S	3.7	1.42	0.57	1.579 <sub>8</sub>	1.530 <sub>6</sub>	28.9	5.8	0.45	0.72 <sub>9</sub>	10.0	8.5
Giza 12	g	3.6	1.63	0.55	1.577 <sub>6</sub>	1.530 <sub>8</sub>	31.1	7.2	0.50	0.70 <sub>8</sub>	8.6	7.2
Ishan	I	3.1	2.72	0.55	1.576 <sub>2</sub>	1.531 <sub>0</sub>	32.3	7.3	0.59	0.68 <sub>5</sub>	6.0	6.8
Memphis	m	3.4	1.86	0.52	1.574 <sub>0</sub>	1.531 <sub>5</sub>	34.4	9.3	0.50	0.64 <sub>4</sub>	6.3	6.3
Memphis	M	2.9	2.00	0.50	1.575 <sub>4</sub>	1.531 <sub>5</sub>	33.1	8.8	0.48	0.66 <sub>6</sub>	7.3	6.1
Texas	T	2.6	2.03	0.48	1.575 <sub>3</sub>	1.531 <sub>7</sub>	33.1	8.2	0.50	0.66 <sub>1</sub>	6.6	6.2
Texas	t	2.5	2.37	0.53	1.575 <sub>0</sub>	1.531 <sub>8</sub>	33.4	10.0	0.57	0.65 <sub>5</sub>	6.0	5.9
Oomras	O	2.4	2.78	0.54	1.574 <sub>0</sub>	1.531 <sub>5</sub>	34.4	7.9	0.63	0.64 <sub>4</sub>	5.5	6.0
Mollisoni	L	2.2	3.29	0.59	1.573 <sub>5</sub>	1.531 <sub>7</sub>	35.2	9.3	0.58	0.63 <sub>3</sub>	4.2	5.2
Bengals	B	2.0	3.31	0.59	1.574 <sub>0</sub>	1.530 <sub>7</sub>	34.4	7.4	0.61	0.65 <sub>6</sub>	4.4	6.2
Bengals	b	1.8	3.19	0.59	1.574 <sub>7</sub>	1.530 <sub>4</sub>	33.6	7.4	0.58	0.67 <sub>6</sub>	5.0	5.7



shorter cottons for light polarized parallel to the fibre axis; they range from 1.573 to 1.581. For light polarized perpendicular to the fibre axis, the refractive indices show no systematic variation with fibre length and are fairly constant at  $1.531 \pm 0.001$ . The explanation of this constancy is as follows. Consider the index ellipsoid shown in section in Fig. 3, and remember that the Becke line method gives the refractive index near the outer boundary of the fibre. If the

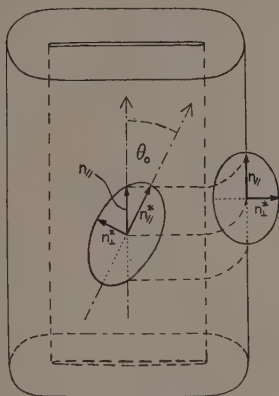


Fig. 3. Diagram of cell wall showing section of the index ellipsoid

chain molecules follow a spiral path making an average angle to the fibre axis at the surface of  $\theta_0$ , then as  $\theta_0$  increases, the index ellipsoid will tilt forward about an axis perpendicular to the fibre axis and the length of the vector which represents  $n_1$  will remain constant, as observed. Any dispersion about the direction of the spiral must be fairly constant between varieties, otherwise there would be a greater variation in  $n_1$  than is observed.

The spiral angle ( $\theta_0$ ) of the chain molecules can be calculated (p. 58)<sup>(3)</sup> from the formula

$$\cos^2 \theta_0 = \frac{(n_{||}^*)^2(n_{||} - n_{\perp}^*)(n_{||} + n_{\perp}^*)}{n_{||}^2(n_{||}^* - n_{\perp}^*)(n_{||} + n_{\perp}^*)} \quad (1)$$

which is deduced from the geometry of the index ellipsoid of the cellulose crystallite (shown in section in Fig. 3). Assuming the values  $n_{||}^* = 1.596$  and  $n_{\perp}^* = 1.530$  at 65% R.H., i.e. the values for ramie in which the orientation is nearly perfect, the spiral angle of the chain molecules or fibrils was calculated to be from about  $28^\circ$  for the long, fine cottons to  $35^\circ$  for the short, coarse varieties.

#### DOUBLE REFRACTION AND CONVOLUTIONS

The average inclination of the chain molecules to the fibre axis will depend on two factors: the spiral angle of the fibrils in the originally unconvoluted fibre and the added twist imparted to the fibrils when the fibre dries out and develops convolutions. It is possible that the variation in average convolution angle may account for the observed variation in double refraction.

An estimate of the average convolution angle ( $\theta_c$ ) was obtained by measuring the pitch of the convolutions ( $c$ ) and the ribbon width of the fibre ( $R$ ), then using the formula

$$\tan \theta_c = (\pi/2)(\overline{R/c}) \quad (2)$$

where  $(\overline{R/c})$  is the average value of  $R/c$  from 150 measurements per sample.

The relation between the mean convolution angles of different samples of cotton and their spiral angles is shown in Fig. 4: as the mean convolution angle increases, the spiral angle increases. Since the range of mean convolution angles

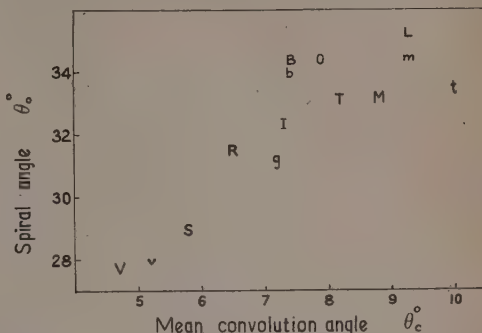


Fig. 4. Relation between spiral angle and convolution angle. (For meaning of symbols, see the table.)

is less than that of spiral angles, only part of the difference in inclination of the chain molecules to the fibre axis appears to be due to differences in the amount of convolution. However, the estimates of convolution angle calculated from equation (2) are probably rather low, owing to a tendency of the more ribbon-like fibres to curl.

Now the refractive index was measured at the edge of fibres which were not curled. An estimate of the average ribbon width of such fibres can be made from the average perimeter ( $P$ ) and degree of thickening ( $\delta$ ) given in the table by assuming the cross-sectional shape is a rectangle capped by semi-circular ends. Let the wall thickness be  $t$  and the length of the rectangular portion be  $x$ , then the area of cross-section, which is also the mass per unit length divided by the density ( $\rho$ ), is given by

$$w/\rho = \pi t^2 + 2xt \quad (3)$$

$$\text{Also, } P = 2\pi t + 2x \quad (4)$$

$$\text{and } R = 2t + x \quad (5)$$

The degree of thickening ( $\delta$ ), defined as the ratio of the area of cross-section of the cell wall to that of a circle with the same perimeter, is

$$\delta = 4\pi w/\rho P^2 \quad (6)$$

Eliminating  $t$  and  $x$  from these equations it can be shown that

$$R = \sqrt{\left(\frac{\pi w}{\rho \delta}\right)} \left\{ 1 - \left(1 - \frac{2}{\pi}\right) [1 - \sqrt{1 - \delta}] \right\} \quad (7)$$

The values of  $R$  thus calculated are, on the average,  $1.40 \pm 0.017$  times greater than the directly measured mean values of  $R$ . Substituting the higher values of  $R$  in equation (2) gives convolution angles ranging from  $7^\circ$  to  $14^\circ$ . If these convolution angles are subtracted from the corresponding spiral angles, the difference is approximately constant at  $21.7 \pm 0.25^\circ$ . This suggests that the spiral angle of the fibrils in the original unconvoluted fibres may be about the same for all varieties of cotton.

It is interesting to inquire to what extent the convolution angle influences the spiral angle within a sample of fibres from

a single variety. A simple way of checking this is to measure the higher refractive index ( $n_{||}$ ) and the associated convolution angle.

Several groups of fibres of average maturity and average fibre weight per cm were mounted on a slide and successive groups were immersed in liquids with refractive indices rising in steps of about 0.002. At the place along any given fibre where its refractive index was judged to match that of the immersion liquid, the ribbon width  $R$  and pitch of the convolutions  $c$  were measured and the convolution angle ( $\theta_c$ ) calculated from equation (2). There were very few places where the convolution was sufficiently well formed and the Becke line completely absent, so that the number of results from the examination of a large number was small.

The refractive indices, corrected for the temperature at which the observation was made, and corresponding convolution angles are plotted in Fig. 5 for fibres from a sample of Giza 12 cotton. Although there is some scatter, the general

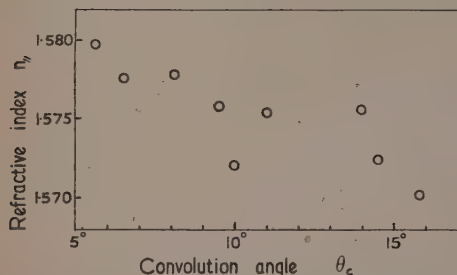


Fig. 5. Refractive index and convolution angle for Giza 12 cotton

trend is towards a decrease in refractive index with increase in convolution angle. From the formula relating spiral angle to  $n_{||}$ , and assuming  $n_{\perp}$  remains constant, it can be shown that the spiral angle increases by about the same amount as the convolution angle. Thus, as  $n_{||}$  ranges from 1.57 to 1.58, the spiral angle decreases from  $38^\circ$  to  $29^\circ$  whilst the convolution angle decreases from  $16^\circ$  to  $6^\circ$ .

#### CELL LENGTH AND SPIRAL ANGLE

It has been shown by Preston (p. 162)<sup>(3)</sup> that the following relation between cell length and spiral angle holds for wood tracheids and bamboo fibres:

$$L = A + B \cot \theta_1 \quad (8)$$

where  $A$  and  $B$  are constants and  $\theta_1$  is the standard angle calculated for a cell breadth of  $24 \mu$ . To obtain this standard angle from the observed spiral angle ( $\theta$ ), use was made of the observation that the breadth of the cell at any point is roughly proportional to  $\sin \theta$ . This relation would be obtained if the length of the fibril in one turn of the spiral remained constant as the breadth of the cell changed.

Assuming that the perimeter is proportional to  $\sin \theta_0$  for cotton fibres, the standard angle can be calculated and compared with the effective length of different varieties; it is found that equation (8) is not obeyed. However, in cotton fibres the direction of the spiral reverses frequently and Preston has suggested that the cotton fibre may be considered as a series of comparatively short cells arranged end to end, the distance between two reversals presumably corresponding to the length of the cell.

The average distance between reversals ( $L$ ) has been

measured for different cottons, using crossed Nicols and a first order red selenite plate with its slow vibration direction at  $45^\circ$  to the plane of polarization to facilitate observation of the reversals; from the table it can be seen that this length is greater in the finer cottons. If values of  $\theta_1$  are calculated from the equation  $\sin \theta_1 = (24\pi/P) \cdot \sin 21.7^\circ$ , where  $P$  is the perimeter in microns calculated from equation (6) and  $21.7^\circ$  is the spiral angle of the unconvoluted fibre, then the relation between  $L$  and  $\cot \theta_1$  shown in Fig. 6 is obtained. It is of the form given by equation (8). An alternative way of expressing

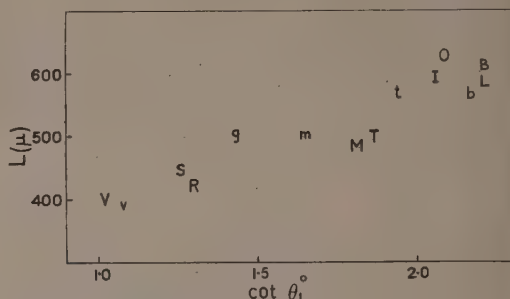


Fig. 6. Distance between reversals in relation to spiral angle

the result is to say that the ratio of the distance between reversals to the perimeter is roughly constant, the average ratio being  $9.2 \pm 0.17$ .

#### YOUNG'S MODULUS, STRENGTH AND ORIENTATION

Sisson and Clark<sup>(7)</sup> first showed that the orientation as measured by X-rays differed between varieties of cotton, and that it was correlated with the fibre tensile strength. About the same time, Morey<sup>(8)</sup> confirmed this correlation, using an optical measure of orientation, depending on the polarization of the fluorescent light from dyed cotton fibres when irradiated with ultra-violet light. The measurements of double refraction recorded in the table were made to investigate the relation between molecular orientation and the mechanical properties such as Young's modulus and tensile strength.

Young's modulus for the initial linear part of the stress-strain curve increases with the optical orientation factor, as shown in Fig. 7. The optical orientation factor takes into account the small variation in the observed values of  $n_{\perp}$ , since it is defined as the observed double refraction divided by

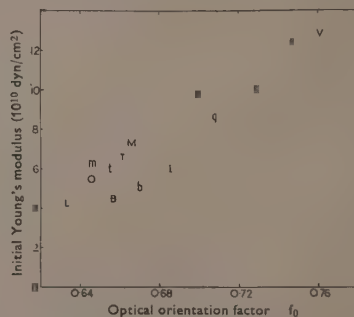


Fig. 7. Correlation of Young's modulus with molecular orientation

that of a perfectly orientated fibre of the same material and the same density,<sup>(9)</sup> i.e.

$$f_0 = (n_{||} - n_{\perp}) / (n_{||}^* - n_{\perp}^*) \quad (9)$$

where  $(n_{||}^* - n_{\perp}^*)$  is taken here as 0.066 at 65% R.H., the double refraction of ramie in which the orientation is nearly perfect.

In Fig. 8 the tensile strengths of forty samples of cotton are

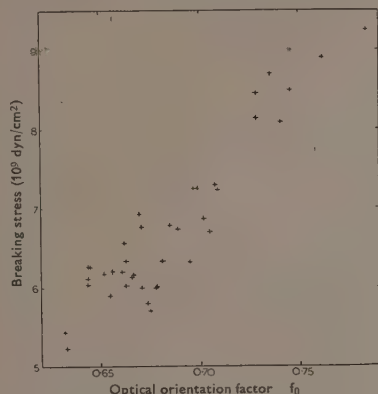


Fig. 8. Correlation of breaking stress with molecular orientation

plotted against the optical orientation factor and a fairly high degree of correlation is found. A test-length of 1 mm was used to eliminate as far as possible the effect of local irregularities which occur along the fibres.

There is a close geometrical similarity between the fibrils in a cotton fibre and the fibres in a twisted yarn. Sullivan<sup>(10)</sup> has evaluated the tension per unit area of cross-section of a bundle of fibres containing twist as  $S = s \cos^2 \theta$ , where  $s$  is the average force per unit area of cross-section of the fibre and acts along the fibre axis which makes an angle  $\theta$  with the bundle axis. Assuming a relation of this kind applies to the fibrils in a cotton fibre, it can be seen that if the breaking stress of the fibrils is constant then the breaking stress of the fibre would decrease as the spiral angle increased.

On this basis, the ratio of the average breaking stresses of two kinds of cotton with average spiral angles of 28° and 35°, representing the extreme values observed, would be 1.16 : 1. An effect of this magnitude is insufficient to account for the observed variation in strength for long and short cottons.

The average chain length, determined from viscosity measurements, varied little with variety of cotton and the high value (about 60000 Å) would suggest that small variations about this value would not affect the strength. However, the regularity of the fibres affects the mean fibre strength. Thus, the ratio of extreme average breaking stresses for fibres

with a test-length of 1 cm is about 2.1 : 1 and that for corresponding cottons with a test-length of 1 mm is about 1.7 : 1. It is possible that with shorter test-lengths the range of breaking stress will be further reduced and approach the ratio 1.16 : 1, which would be expected to apply only to the strengths of short lengths of fibre from which the effect of irregularities along the length of the fibres has been eliminated.

#### SUMMARY

On account of the irregular structure of the cotton fibre, the Becke line method of measuring refractive index was found to be the most suitable. The longer and finer varieties show greater double refraction and lower spiral angles. The average convolution angle is also lower and the data suggest that the original unconvoluted fibres of all varieties may have about the same spiral angle.

Assuming the cotton fibre to be effectively a series of cells of length equal to the average distance between reversals, then the relation between cell length and the cotangent of the "standard angle" at constant breadth is of the same form as that found for wood tracheids and bamboo fibres.

The strength and initial Young's modulus of the various cottons, measured at 65% R.H., are correlated with the degree of orientation calculated from the double refraction measured at 65% R.H., the correlation coefficients being 0.89 and 0.87 respectively.

#### ACKNOWLEDGEMENTS

The writer's thanks are due to Mr. E. Lord for the measurements of the fibre characteristics of length, fineness and maturity given in the table, and to Dr. F. C. Toy, Director of the British Cotton Industry Research Association for permission to publish this paper.

#### REFERENCES

- (1) FREEMAN, K., and PRESTON, J. M. *J. Text. Inst., Manchr*, **34**, p. T19 (1943).
- (2) SAYLOR, C. P. *J. Res. Nat. Bur. Stand.*, **15**, p. 277 (1935).
- (3) PRESTON, R. D. *Molecular Architecture of Plant Cell Walls*, p. 54 (London: Chapman and Hall Ltd., 1952).
- (4) SCHWARTZ, E. R., and SHAPIRO, L. *Rayon Text. Mthly*, **19**, pp. 371, 421 (1938).
- (5) PEIRCE, F. T., and LORD, E. *J. Text. Inst., Manchr*, **30**, p. T173 (1939).
- (6) CLEGG, G. G. *J. Text. Inst., Manchr*, **23**, p. T35 (1932).
- (7) SISSON, W. A., and CLARK, C. H. *Industr. Engng Chem.*, **5**, p. 296 (1933).
- (8) MOREY, D. R. *Textile Research*, **5**, p. 483 (1935).
- (9) HERMANS, P. H. *Physics and Chemistry of Cellulose Fibres*, p. 230 (Amsterdam: Elsevier Publishing Co., 1949).
- (10) SULLIVAN, H. *J. Appl. Phys.*, **13**, p. 159 (1942).



# The theoretical characteristics of bichromatic pyrometers

By H. HERNE,\* Physics Department, British Iron and Steel Research Association, London, S.W.11

[Paper first received 18 March, and in final form 18 May, 1953]

The theory of the bichromatic pyrometer is outlined and its response is calculated for different filter pass bands of different band widths. The ratio of the response at one colour to the response at the other is calculated as a function of the temperature of the source and the results are presented graphically. A range of pass bands in the visible spectrum, having sharply defined cut-off frequencies and uniform transmission in the pass frequencies, is considered and the effect of the width of the pass bands is estimated in each case. One result is given for an infra-red pyrometer with both pass bands wide and accommodated in the sensitive region of typical lead sulphide photoconductive cells.

From these results it is clear that the two pass bands may be close to each other in frequency and that their band widths may be large, without an appreciable loss in sensitivity of the pyrometer. Positive recommendations may then be made that the design of a bichromatic pyrometer should concentrate on energy collection and should therefore adopt two wide pass bands both situated in the red part of the spectrum.

The fundamental idea of two-colour temperature measurement is to use the frequency distribution of the radiant energy from a hot body in order to measure its temperature. In other methods of measuring temperature, such as by total radiation or by optical pyrometers, the quantity actually measured is directly dependent on energy and thus on the appropriate emissivity of the hot body; if this emissivity changes with the temperature of the body a corresponding error is introduced when the measured energy is interpreted as temperature. In two-colour pyrometry what is measured is the ratio of two energies to each other, not their absolute values, and thus a change of emissivity with temperature is unimportant if the proportional change is the same in both colour ranges. What does cause an error when this ratio of energies is calibrated as temperature is a proportional change of colour emissivity which is not the same in both colour ranges. Usually the pyrometer is calibrated for a "grey" body the emissivity of which is, by definition, independent of wavelength. Errors in reading, due to departure from "greyiness," can be due both to the intrinsic emissivity characteristic of the body measured and to its temperature, which has been shown experimentally to affect its "greyiness." For many materials the assumption of greyiness is a useful approximation to the truth. In addition, for most materials the change of emissivity with colour does not vary with temperature so much as the change of a single emissivity with temperature. This implies that bichromatic pyrometry is more generally applicable to different materials than is monochromatic pyrometry.

Although bichromatic pyrometry has been used frequently in the past, no particular effort appears to have been made to estimate the optimum choice of colours, probably because the technique has worked adequately in almost all reported cases without such an investigation. It appears, further, that no attempt has been made to estimate either the importance of the band width of the colour filters or whether there can be ambiguity of reading if the peak radiation frequency of the hot body passes through one or both of the colour bands. The calculation below has been made to deal with these problems and to provide a firm basis for designing future bichromatic pyrometers.

## THEORY OF THE BICHROMATIC PYROMETER

A simple bichromatic pyrometer consists of an optical system,  $P$ , which defines an accepted solid angle of radiation of  $\theta$  steradians from an area  $A$  of the hot body with a transmission  $P_\lambda$  at a wavelength  $\lambda$ .  $M$  is a partially reflecting surface such that  $r_\lambda$  is the reflexion factor at wavelength  $\lambda$

and  $t_\lambda$  the corresponding transmission factor.  $F_1$  is a filter with transmission  $F_{1\lambda}$  at wavelength  $\lambda$  whilst  $F_2$  is a different filter with a corresponding transmission  $F_{2\lambda}$ .  $S_1$  is a detector giving a signal, usually an electric current, proportional at any particular wavelength to the incident energy falling on it; let  $S_{1\lambda}$  be the response of the detector  $S_1$  in coulombs per erg at the wavelength  $\lambda$ . Similarly  $S_2$  is a different detector with a corresponding sensitivity  $S_{2\lambda}$ .

The energy radiated by the hot body at a temperature  $T^\circ \text{K}$  in the waveband  $\lambda$  to  $\lambda + \delta\lambda$  is

$$(e_\lambda c_1 \lambda^{-5} / [\exp(c_2/\lambda T) - 1]) \delta\lambda$$

per unit area per unit time over a solid angle of  $2\pi$  steradians where  $e_\lambda$  is the spectral emissivity at wavelength  $\lambda$ ,  $c_1 = 3.732 \times 10^{-5}$  erg cm<sup>2</sup>/sec and  $c_2 = 1.438$  cm<sup>2</sup>/K. The energy transmitted by the optical system to the partially reflecting surface  $M$  is therefore

$$\{A\theta P_\lambda e_\lambda c_1 \lambda^{-5} / 2\pi [\exp(c_2/\lambda T) - 1]\} \delta\lambda$$

The energy reaching the detector  $S_1$  is then

$$\{A\theta P_\lambda r_\lambda F_{1\lambda} e_\lambda c_1 \lambda^{-5} / 2\pi [\exp(c_2/\lambda T) - 1]\} \delta\lambda$$

in the waveband  $\lambda$  to  $\lambda + \delta\lambda$ . Therefore the total response of the detector  $S_1$  is given by

$$R_1 = \int_0^\infty \{A\theta P_\lambda r_\lambda F_{1\lambda} e_\lambda c_1 \lambda^{-5} / 2\pi [\exp(c_2/\lambda T) - 1]\} d\lambda$$

whilst that of detector  $S_2$  is given by

$$R_2 = \int_0^\infty \{A\theta P_\lambda t_\lambda F_{2\lambda} e_\lambda c_1 \lambda^{-5} / 2\pi [\exp(c_2/\lambda T) - 1]\} d\lambda$$

$R_1$  and  $R_2$  are given in amperes in this form. The problem then becomes that of the relationship between  $R_2/R_1$  and  $T$  for various values of the parameters  $e_\lambda$ ,  $r_\lambda$ ,  $F_{1\lambda}$ ,  $S_{1\lambda}$ , etc.

**General characteristics.** Usually the amount of energy available from the hot body is limited by experimentally possible values of  $\theta$ , the angular acceptance of the optical systems, and  $A$ , the area of body viewed. Often, therefore, it is necessary to accept energy over a wide wavelength range to obtain a useful signal from each detector. In this case it is not possible to deduce a simple relationship between  $R_2/R_1$  and  $T$ .

The general relationship has been computed numerically on the assumption that both detectors respond to no radiation outside a defined pass band and respond with a constant attenuation in that pass band. This is equivalent to a sharp-cut, flat-topped system. The two systems are assumed to have wavelengths  $\lambda_1$  and  $\lambda_2$  for the mid-values of the pass bands

\* Now at C.R.E. II National Coal Board, Isleworth.

and to have equal pass band-widths,  $L$ . This is expressed rigorously as

$$\begin{aligned} P_{\lambda} r_{\lambda} F_{1\lambda} S_{1\lambda} e_{\lambda} &= 0 \text{ for } \lambda < \lambda_1 - \frac{1}{2}L \\ &= 0 \text{ for } \lambda > \lambda_1 + \frac{1}{2}L \\ &= a \text{ for } \lambda_1 - \frac{1}{2}L < \lambda < \lambda_1 + \frac{1}{2}L \\ \text{and } P_{\lambda} r_{\lambda} F_{2\lambda} S_{2\lambda} e_{\lambda} &= 0 \text{ for } \lambda < \lambda_2 - \frac{1}{2}L \\ &= 0 \text{ for } \lambda > \lambda_2 + \frac{1}{2}L \\ &= b \text{ for } \lambda_2 - \frac{1}{2}L < \lambda < \lambda_2 + \frac{1}{2}L \end{aligned}$$

Then

$$\begin{aligned} \frac{R_2}{R_1} &= \frac{b \int_{\lambda_1 - \frac{1}{2}L}^{\lambda_2 + \frac{1}{2}L} \{c_1 \lambda^{-5} / [\exp(c_2/\lambda T) - 1]\} d\lambda}{a \int_{\lambda_1 - \frac{1}{2}L}^{\lambda_1 + \frac{1}{2}L} \{c_1 \lambda^{-5} / [\exp(c_2/\lambda T) - 1]\} d\lambda} \\ &= \frac{b}{a} f(\lambda_1, \lambda_2, L, T) \end{aligned}$$

#### COMPUTATION OF GENERAL CHARACTERISTICS

The function written as  $f(\lambda_1, \lambda_2, L, T)$  above can be computed directly from published tables by A. N. Lowan and G. Blanch\* of the function

$$\int_0^{\lambda T} [c_1(\lambda T)^{-5} [\exp(c_2/\lambda T) - 1] d(\lambda T)]$$

The later set of tables has been used and interpolated as its

\* LOWAN, A. N. *J. Opt. Soc. Amer.*, **30**, p. 70 (1940). Republished in *Miscellaneous Physical Tables* (New York: New York Works Project Administration, 1941).

introduction outlines, and the older value of  $c_2$ , 1.436, which was used in preparing these tables has been adopted. This small inaccuracy facilitates the computing without being appreciable in the graphical representation of the results.

The function  $f(\lambda_1, \lambda_2, L, T)$  is evaluated as a function of  $T$  for a range of fixed values of  $\lambda_1$ ,  $\lambda_2$ , and  $L$ , and the results are presented graphically in Figs. 1 to 15, using a Celsius temperature scale; the function  $f(\lambda_1, \lambda_2, L, T)$  is called the "Response ratio" in these figures. Each figure is a series of results for one value of  $\lambda_1$  and one value of  $\lambda_2$ . An approximate colour scale for these wavelengths is given in the table.

#### Wavelength-colour conversion

Wavelength (Å)	Colour
4500	Blue
5000	Blue-green
5500	Yellow-green
6000	Orange
6500	Red
7000	Deep red
8000	Near infra-red

The different curves on each figure are for the different values of  $L$ , the pass band-width, and values of 100, 1000 and 3000 Å are chosen in each case except Fig. 16 as representative. Usually the 100 Å curve is indistinguishable from that for still smaller values of band-width and it is therefore equivalent to the well-known narrow cut filter case when  $\ln(R_2/R_1) = \text{constant} + \text{constant}/T$ .

#### AN INFRA-RED SYSTEM

The example given in Fig. 16 represents a possible system designed around two lead sulphide photoconductive cells.

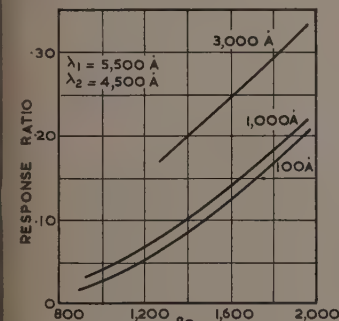


Fig. 1

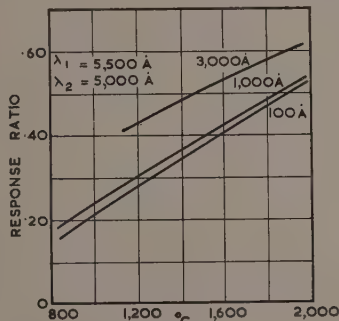


Fig. 2

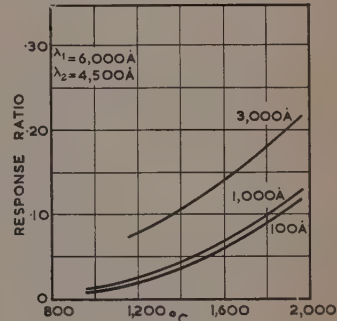


Fig. 3

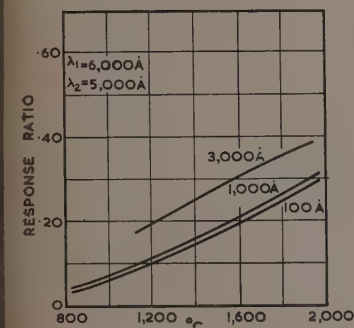


Fig. 4

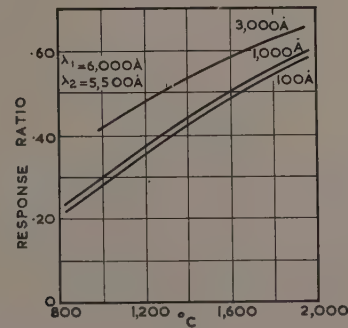


Fig. 5

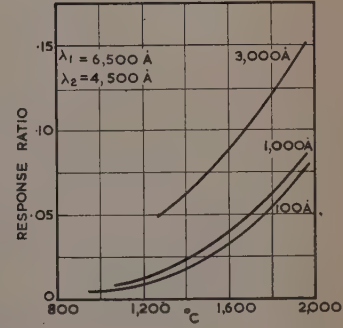


Fig. 6

Figs. 1-6. Response of bichromatic pyrometers as a function of temperature for various values of  $\lambda_1$  and  $\lambda_2$

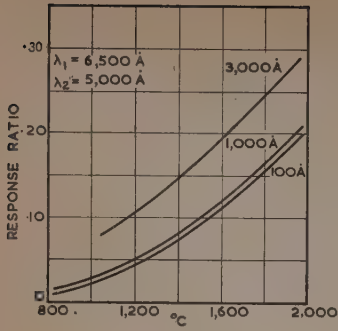


Fig. 7

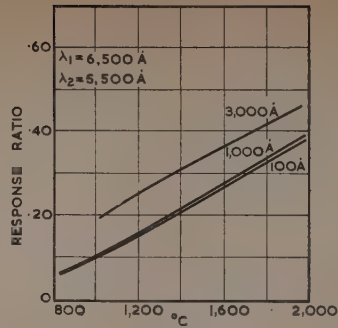


Fig. 8

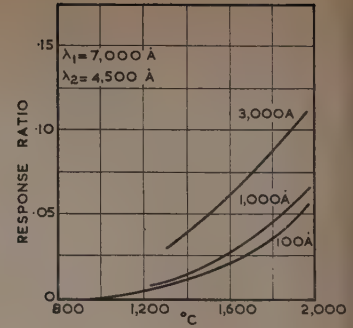


Fig. 9

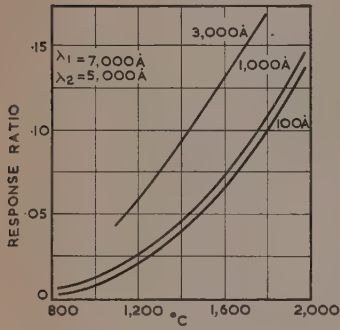


Fig. 10

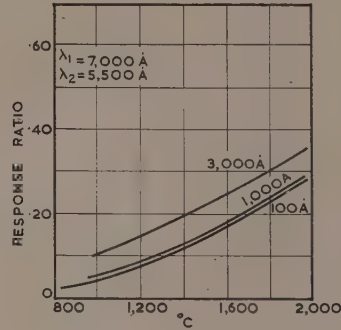


Fig. 11

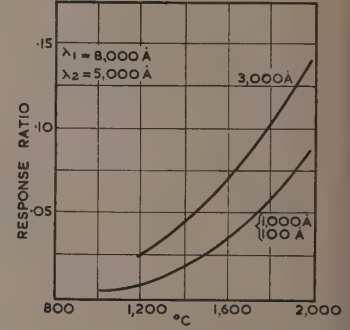


Fig. 12

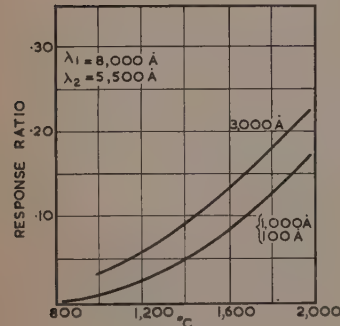


Fig. 13

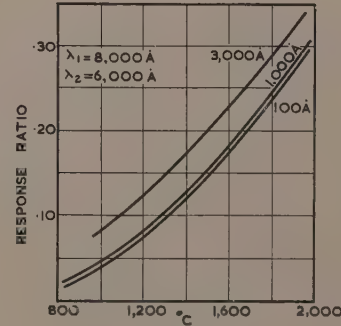


Fig. 14

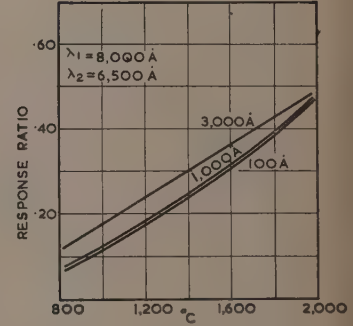


Fig. 15

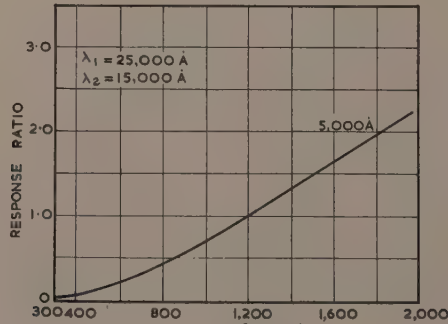


Fig. 16

Figs. 7-16. Response of bi-chromatic pyrometers as a function of temperature for various values of  $\lambda_1$  and  $\lambda_2$



The centres of the two acceptance bands are taken to be 25 000 and 15 000 Å, both band-widths being 5000 Å. Both of these bands are in the infra-red and both are wide enough to ensure a favourable signal to noise ratio in both detectors when the source temperature is too low to stimulate a conventional photosensitive device. Fig. 16 is drawn down to a temperature of 300° C and there seems no obvious reason why such a bichromatic pyrometer might not read down to about 400° C; to reach the lower temperatures the pass bands could easily be widened. However, this Fig. 16 is of further interest in that it shows the smooth curve obtained even though the peak of the radiation curve falls in, and passes through, the acceptance bands of the detectors.

#### CONCLUSIONS

A study of Figs. 1 to 16 leads to clear conclusions. When all the curves of Figs. 1 to 15 are viewed collectively the 3000 Å band-width ones are seen to compare favourably with the narrower band-width ones in each figure. The slope of the curve of the response ratio against temperature is a convenient measure of the sensitivity of the pyrometer, and it is immediately apparent from the figures that this sensitivity is not noticeably reduced by the relatively large band-width of 3000 Å. In order to obtain a large signal, and to ensure a large signal to noise ratio, the large band-width should be adopted, particularly if one pass band is chosen in the blue end of the spectrum. For the higher temperatures the curves for the large band-width are more nearly linear than the corresponding narrow band-width ones, but this factor is of no great importance in practice. There is, however, a marked gain in linearity between response ratio and temperature if the two pass bands are close together. Figs. 6, 7 and 8

illustrate this and show that the gain in linearity when the pass bands approach each other is more marked when both bands are narrow. The two pass bands may indeed overlap each other without detriment to the response ratio.

Fig. 16 covers a temperature range such that the peak value of the Planck radiation curve passes through both pass bands. The curve is, nevertheless, smooth and useful over the range of 400–2000° C at least. This choice would have obvious application to the measurement of low temperatures, but it indicates that the same instrument may readily measure high temperatures too.

If an instrument to read down to about 900° C were to be designed around conventional photoemissive cells, Fig. 15 might well prove a sound compromise. One system would pass energy from 9500 to 6500 Å, the near infra-red and the deep red, and the other from 8000 to 5000 Å, the red to greenish-yellow; the visual appearance of the two systems would be deep red and orange. This would be markedly superior to the conventional red and green combination.

#### RECOMMENDATIONS

In designing a bichromatic pyrometer the following rules should be adopted:

- (i) Choose large band-widths for both colours.
- (ii) Choose pass bands near to each other and permit the pass bands to overlap if necessary.
- (iii) Choose pass bands to give a large signal and a large signal to noise ratio. This usually implies working at the red end of the spectrum or at even longer wavelengths.

#### ACKNOWLEDGEMENT

Miss P. Arnold computed and prepared Figs. 1 to 16.

## On growing single crystals of thallium activated alkali halides

By J. FRANKS, M.Sc., Ph.D.,\* A.Inst.P., Birkbeck College, University of London

[Paper received 17 April, 1953]

A description is given of a furnace for producing single crystals of thallium activated alkali halides according to a modified Stöber method. Some results are given of luminescence measurements on activated alkali iodides, which have an intense emission in the visual range.

Several techniques for growing clear single crystals of the alkali halides for use as optical elements, have for many years been applied with success. The basic procedure for alkali halides or other substances grown from the melt consists of slowly solidifying the molten substance in a furnace under such conditions that only one seed or a small number of seeds are produced, and no further spontaneous nucleation takes place. These conditions may be achieved (1) by maintaining the furnace and crucible with the melt stationary, and varying the thermal fields in a suitable way by continuous control of the current through the heaters<sup>(1, 2, 3)</sup>; (2) by lowering the crucible and melt through a stationary thermal field and temperature gradient<sup>(4–8)</sup>; or (3) by gradually withdrawing a cooled seed with a growing crystal from the melt.<sup>(9–12)</sup>

A modification of Stöber's method was used to grow single crystals of the thallium activated alkali halides, the furnace design being simple, requiring no moving parts, and the absence of convection currents in the melt promoting uniform inclusion of activator in the lattice; a concentration gradient of the impurity cannot, however, entirely be avoided. To

ensure that nucleation commenced at a single point, Stöber's crystallizing dish was hemispherical in shape, resting on a water-cooled plate. A heater element above the dish set up a vertical temperature gradient in the melt, freezing thus commencing at the bottom. In the modified furnace described here, a flat bottom crucible of 0.001 in. platinum foil was used, measuring 2 in. diameter and 1 in. high, the side wall being shaped like the teeth of a cogwheel for flexibility, the foil thus contracted with the cooling crystal introducing little strain. These crucibles were made by pressing flat foil on to a jig. Crystallization from a single point or small region was ensured by arranging the furnace heaters in such a way that the centre of the bottom surface of the crucible was at the lowest temperature. In addition, the temperature and vertical temperature gradient could be varied almost independently of each other; in Stöber's design, the temperature gradient was determined by the temperature at which the heater was run.

The furnace is shown in Fig. 1. An outer lagging enclosure, built of Economite bricks, surrounded the main heater of Kanthal strip which was wound round the inner furnace enclosure of cast Ciment Fondu. A flat disk heater wound of Kanthal strip embedded in Morgan FM42 alumina cement formed the top of the inner enclosure. The crucible, situated immediately below this heater, rested on a silver cooling plate

\* Now at Associated Electrical Industries, Aldermaston, Berkshire.

and rod (to enhance the gradient) from which it was separated by a sheet of 0.001 in. mica. The vertical cylindrical heater was run at about 300 W, giving rise to a radial gradient such that the temperature was lowest along the vertical axis of the furnace. The flat heater run at, for example, 20 W gave rise to a vertical gradient of about  $10^{\circ}\text{C}/\text{cm}$ . The combined

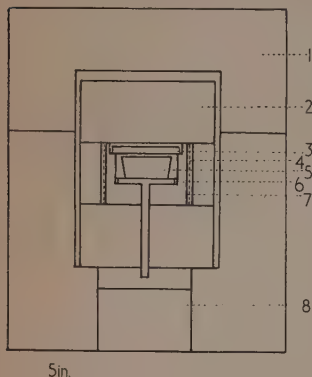


Diagram of furnace

1, Economite brick outer wall; 2, triangle V brick inner wall; 3, flat disk heater; 4, cylindrical heater; 5, platinum crucible; 6, silver plate and rod; 7, Ciment Fondu enclosure; 8, removable brick (for increasing the gradient).

effect of the heaters was to produce thermal fields such that the temperature decreased towards the centre region of the bottom surface of the crucible. The melt thus first solidified in that region, and as the temperature dropped the crystal grew in a roughly hemispherical shape corresponding to the melting point isothermal. The temperature was controlled by varying the current through the cylindrical heater only.

Temperatures were measured with Pt/Pt-Rh (13%) thermocouples placed in the salt. A set of three junctions enabled vertical and lateral gradient measurements and temperature readings to be made in the melt and solidifying crystal, the thermocouple wire (0.008 in. thick) did not disturb crystal growth. The advancing crystal front could be detected by a drop in the temperature gradient caused by the liberation of latent heat. The gradient conditions outside the crucible remained almost constant throughout the growth process. To prevent random nucleation, the temperature gradient must increase steadily across the crystal-melt interface into the melt; a fairly high external gradient therefore promotes the growth of single crystals.

The general procedure was as follows: the crucible was filled to the top with the salt after the thermocouples had been placed in position inside the crucible, and located by means of small ceramic supports above the crucible. Next the heater elements were switched on and temperature readings were taken every 15 min until the salt began to melt, after which the temperature was observed continuously. When the bottom junction again indicated a rise in temperature the current through the vertical heater was reduced and the required temperature gradient (e.g.  $10^{\circ}\text{C}/\text{cm}$ ) was established by controlling the current through the flat heater. No provision was made for visual observation of the liquid melt interface, the position of the advancing crystal front being deduced from the behaviour of the temperature gradient measured between a junction near the bottom of the crucible and one near the top surface of the melt (vertical gradient measurement). As the furnace cooled and the interface approached the lower junction, the gradient decreased; the lower junction cooling at a slower rate than the upper junction because of liberation of latent heat. As solidification progressed, the gradient passed through a minimum and then

increased as the crystal front approached the upper junction. Finally the gradient decreased again and tended to a constant value close to the original setting; the whole melt had then solidified. The growth rate was controlled by the current through the vertical heater, the crystals usually being grown at a rate of about 4 mm per hour.

Crystals were grown of the halides of Na and K (except the fluorides) and of RbI and CsI, activated with about 1% of TI halide. The phosphor slabs, 2 in. diameter and  $\frac{1}{2}$  in. high, were generally either completely single or consisted of a small number of single crystals. The crystals were always clear except for a small region at the top which often contained Pt and TI impurity.

The emission of the activated iodides under electron bombardment is very intense in the visible range, extending from 4000 to 4800 Å for KI(Tl) and RbI(Tl) with a peak at about 4400 Å. The luminescence of CsI(Tl), pale green yellow in colour, appears visually to be the brightest, its emission range commences at 4800 Å and continues throughout the red end of the spectrum (measured up to 6600 Å). Luminescence measurements of these phosphors bombarded with  $\alpha$ -particles indicated that the total light output of CsI(Tl) was 1.15 times that of KI(Tl) and 1.7 times that of RbI(Tl) for a clipping time of 150  $\mu\text{sec}$  or more, but for a clipping time of 10  $\mu\text{sec}$  the ratios were 1.5 and 2.3, indicating that the main light emission from KI(Tl) and RbI(Tl) took place over a fairly long period compared with that of CsI(Tl); in addition the CsI(Tl) sample was found to exhibit phosphorescence. The measurements were made with a 5060 phototube by Electric and Musical Industries Ltd. which cut off in the orange part of the spectrum, full advantage of the emission of CsI(Tl) could therefore not be taken.

The high luminous intensity of the activated alkali iodides, and their ready availability as large crystals, makes these materials suitable for high resolution screens. The luminous images produced by electron or X-ray beams on the crystals remain sharp when observed under high magnification; the images on fluorescent powder screens appear diffuse under microscopic observation because of the scattering of light by the grains. CsI(Tl) screens, apart from giving visually the brightest emission, also appeared more resistant to electron burn than the other alkali halides tested.

#### ACKNOWLEDGEMENTS

I thank Dr. W. Ehrenberg for many helpful and encouraging discussions and I am indebted to Dr. D. K. Butt for the data obtained from photomultiplier measurements.

#### REFERENCES

- STÖBER, F. Z. *Krist.*, **61**, p. 299 (1924).
- RAMSPERGER, H. C., and MELVIN, E. H. *J. Opt. Soc. Amer. and Rev. Sci. Instrum.*, **15**, p. 359 (1927).
- STRONG, J. *Phys. Rev.*, **37**, p. 1663 (1930).
- BRIDGMAN, P. W. *Proc. Amer. Acad. Arts Sci.*, **60**, p. 306 (1925); *Proc. Amer. Acad. Arts Sci.*, **63**, p. 351 (1929).
- STOCKBARGER, D. C. *Rev. Sci. Instrum.*, **7**, p. 133 (1936); *J. Opt. Soc. Amer.*, **27**, p. 416 (1937); *Rev. Sci. Instrum.*, **10**, p. 205 (1939); *Disc. Faraday Soc.* (No. 5), p. 299 (1949).
- KREMERS, H. C. *Industr. Engng Chem.*, **32**, p. 1478 (1940).
- TUTTLE, O. F., and EGLI, P. H. *J. Chem. Phys.*, **14**, p. 571 (1946).
- ZERFOSS, S., JOHNSON, L. R., and EGLI, P. H. *Disc. Faraday Soc.* (No. 5), p. 166 (1949).
- KYROPOULOS, S. *Anorg. Chemie*, **154**, p. 308 (1926).
- KORTH, K. Z. *Phys.*, **84**, p. 677 (1933).
- WYART, J., and KURYLENKO, C. *Cahiers de Phys.*, **27**, p. 50 (1945).
- MENZIES, A. C., and SKINNER, J. *Disc. Faraday Soc.* (No. 5), p. 306 (1949).



# The influence of barometric pressure on watch and chronometer rates

By N. W. B. STONE, M.Sc., A.Inst.P., K. W. T. ELLIOTT and P. H. BIGG, B.Sc., National Physical Laboratory, Teddington, Middlesex

[Paper first received 6 March, and in final form 23 June, 1953]

Experiments are described in which the rate and arc of a high quality watch and a marine chronometer were observed at a number of pressures from zero to 760 mm of mercury. Lack of isochronism can cause pressure variations to affect watch rates differently at different states of winding or in different positions, but fairly consistent values for the pressure coefficients can be derived if allowance is made for change of arc using the rate/arc relationship observed at normal pressures. The observed pressure variations with constant arc are briefly discussed.

In assessing the performance of high quality timepieces as, for example, in the Craftsmanship watch test at the N.P.L., the effects of variations of atmospheric pressure should not be overlooked. The change in rate of a watch is seldom less than 0.007 sec/day per millimetre of mercury, and may be as high as 0.020 sec/day per mm of mercury, the watch gaining at reduced pressure. Changes in atmospheric pressure occasionally exceed 10 mm of mercury in 24 hours, and a change of this magnitude may cause a change in rate of 0.2 sec/day. This is comparable, for the best watches, with day-to-day variations arising from other causes, and with variations due to position and temperature.

It was, accordingly, desirable to obtain some practical experience at the National Physical Laboratory of the effects of pressure upon the rates of watches and chronometers so as to assist in gaining a general appreciation of this phenomenon, to explore the feasibility of making pressure allowances in precision tests, and to gauge their reliability. The results obtained confirm work by Jaquerod,<sup>(1)</sup> Attinger,<sup>(2)</sup> and Guyot,<sup>(3)</sup> and support the view that it is preferable to avoid pressure variations than to attempt to correct for their effect.

As pointed out by Jaquerod, changes in the pressure of a gas surrounding an oscillating balance wheel will have a dual effect. Firstly, the mass of air carried round with the balance will vary and might be expected to be roughly proportional to the pressure. Increase in pressure would thus cause an increase in the moment of inertia of the whole system giving rise to corresponding increase in the period of oscillation. And, secondly, increase in pressure will cause a fall in the amplitude of the swing. Such a change of arc will be accompanied by a change of period unless the oscillator is truly isochronous. (In this paper the term "isochronism" is used with its strict meaning of the independence of amplitude and period.) The influence of arc upon the period of an oscillating balance can be attributed to the combined effect of a multiplicity of mechanical causes of which the escapement error, the centrifugal effect, the poise of the balance, the radial thrust of the balance spring upon the balance staff and the rest position of the balance spring in relation to the curb-pins all play their part. These effects have been freely debated, but the overall dependence of rate on arc can only be found reliably by practical observation.

## METHOD, TECHNIQUE AND PROCEDURE

A Kullberg marine chronometer and a Ditisheim deck watch were selected for study. The rate-pressure relationships were determined with the instruments enclosed in a pressure chamber provided with a horizontal armour-plate glass window. The rates were observed at a number of points as the pressure was first reduced to zero and then returned to

atmospheric pressure. All the work was carried out at about 20° C.

The marine chronometer was placed in the dial down position to facilitate observation of the amplitude of the balance arc, and the deck watch was studied in the dial down position and also in two of the vertical positions. (The general behaviour of the chronometer was found to be similar in the dial down and dial up positions.) In each instance the balance was observed (using a mirror where necessary) through a microscope incorporating a rotating head carrying a pair of cross-wires and a graduated circular scale. By suitably illuminating the oscillating balance the two rest positions of the balance arm were located visually, and by setting the cross-wires of the microscope head on the balance arm in these two extreme positions the mean arc was measured to approximately  $\pm 2^\circ$ .

The ticks, picked up by a crystal microphone, were amplified and limited and a sharp pulse was derived from each, corresponding with the initial sound of the escapement action. These signals were compared with signals from one of the N.P.L. standard quartz oscillator clocks by means of a decimal counter chronometer, and thus, over a period of fifteen minutes, the mean rate was determined to about  $\pm 0.05$  sec/day.

The rate/arc relationships were next determined at a pressure of approximately 760 mm of mercury. The required amplitude variation was obtained in the watch by progressive winding, and in the chronometer by removing the barrel and applying tangentially to the edge of the fusee various loads of from 500 to 4000 g.wt. On the assumption that the relationships do not depend significantly on pressure, the original rate/pressure curves were modified to allow for variation of rate due to change of arc and rate/pressure curves at constant arc were thus derived. It was convenient to apply this modification in a manner which brought the derived rates at atmospheric pressure near to zero.

## THE BEHAVIOUR OF THE MARINE CHRONOMETER

Figs. 1 to 3 represent the behaviour of the marine chronometer, which had a Kullberg auxiliary compensation balance with a mean diameter of approximately 30 mm.

It is seen from Fig. 1 that as the pressure was reduced from atmospheric, the rate of the chronometer at first became less negative (+ = gaining, - = losing). The slope of the curve diminishes progressively, however, until at a pressure of about 350 mm it becomes zero and small pressure changes have little effect. Further pressure reduction results in more negative rates and at the lowest pressures employed the curve is falling away very rapidly. Fig. 1 also shows the corresponding changes in arc.

Fig. 2 shows the variation of rate with arc at constant



pressure. As the arc increases, the rate becomes more negative and this is attributed largely to the expansion of the balance due to centrifugal action. Fig. 3, derived from Fig. 1 by applying corrections for arc on the basis of Fig. 2, shows

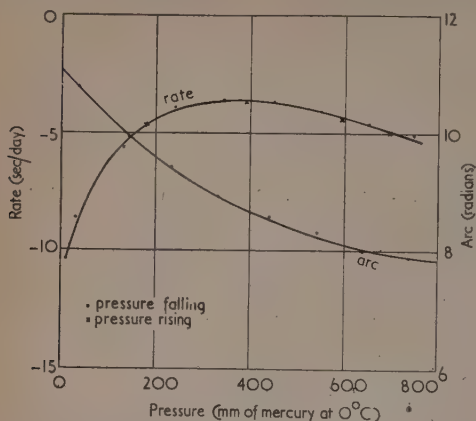


Fig. 1. Rate/pressure and arc/pressure curves obtained with marine chronometer

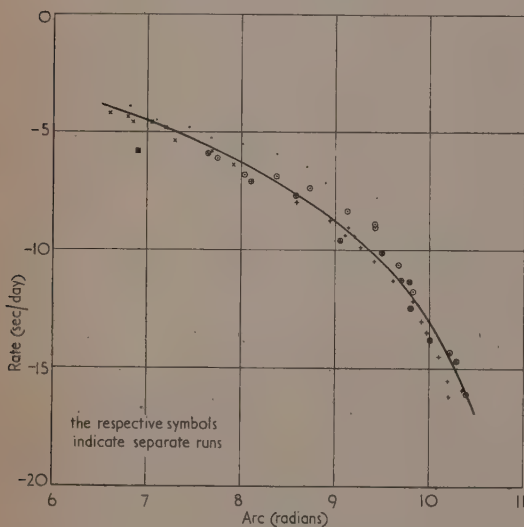


Fig. 2. Rate/arc curve at atmospheric pressure obtained with marine chronometer

that if the arc were constant the rate of the chronometer would become more positive as the pressure is reduced, and that the pressure coefficient increases with decrease of pressure. These results may be expressed in terms of deviations ( $\delta S$  sec) from the nominal half-period (0.25 sec) of swing, thus:

$$\delta S \times 10^5 = -2.85 + 0.0410\sqrt{p} + 0.00204p \\ (+0.01) (+0.011) (\pm 0.0003)$$

(where  $p$  is the pressure in mm of mercury at 0°C). The figures in parenthesis beneath the equation, which has been calculated by the method of least squares, are the respective

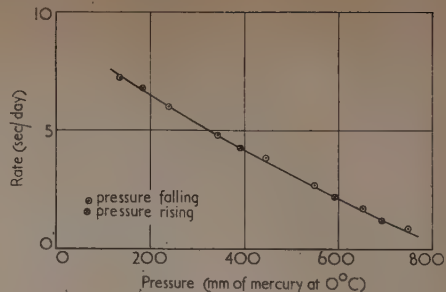


Fig. 3. Rate/pressure curve at constant arc obtained with marine chronometer

$$\text{Coefficient} \begin{cases} 100-200 \text{ mm of mercury} = 0.013 \text{ sec/day per mm of mercury} \\ 600-700 \text{ mm of mercury} = 0.009 \text{ sec/day per mm of mercury} \end{cases}$$

standard errors. Reference will be made to this relationship in the general discussion of the results.

#### THE BEHAVIOUR OF THE DECK WATCH

The watch examined had a Guillaume compensated balance of 19 mm diameter with the usual screws around the rim. Fig. 4 shows its behaviour under pressure variation when in the dial down position, both before and after adjustment for

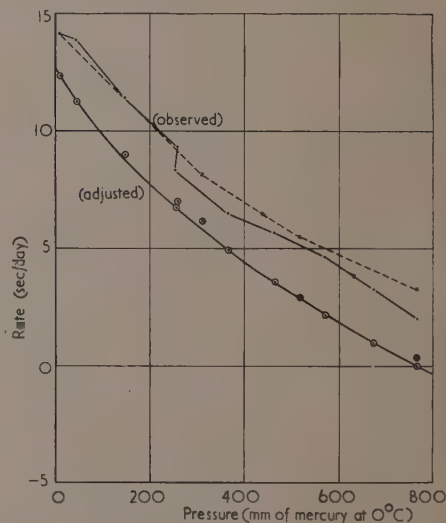


Fig. 4. Rate/pressure curves obtained with watch in dial down position

$$\text{Coefficient} \begin{cases} 100-200 \text{ mm of mercury} = 0.021 \text{ sec/day per mm of mercury} \\ 600-700 \text{ mm of mercury} = 0.012 \text{ sec/day per mm of mercury} \end{cases}$$

arc variation. The changes of arc were very much smaller than those of the marine chronometer and the adjustments are less significant, though they smooth out a number of irregularities in the original curve, for example, where observations were made a second time at about 250 mm of mercury

after a discontinuity of about 1 hour. Very similar results were obtained for the pendant up and pendant down positions.

The corresponding pressure coefficients for the other two positions were as follows:

#### Pendant up

00–200 mm of mercury—0.020 sec/day per mm of mercury  
00–700 mm of mercury—0.013 sec/day per mm of mercury

#### Pendant down

00–200 mm of mercury—0.021 sec/day per mm of mercury  
00–700 mm of mercury—0.011 sec/day per mm of mercury

As with the marine chronometer, after allowing for arc, the pressure coefficients increase progressively as the pressure is reduced. Expressing the results in terms of deviations from the nominal half-period (0.2 sec) of swing and applying the method of calculation by least squares, the following relationships were derived:

#### Dial down

$$\delta S \times 10^5 = -3.14 + 0.0748\sqrt{p} + 0.00141p$$

$$(\pm 0.02) (\pm 0.010) (\pm 0.0003)$$

#### Pendant up

$$\delta S \times 10^5 = -3.28 + 0.0864\sqrt{p} + 0.00130p$$

$$(\pm 0.02) (\pm 0.012) (\pm 0.0004)$$

#### Pendant down

$$\delta S \times 10^5 = -3.10 + 0.0728\sqrt{p} + 0.00145p$$

$$(\pm 0.01) (\pm 0.006) (\pm 0.0002)$$

The standard errors are again bracketed below the figures to which they relate. The relationships are discussed in the following section.

Returning to the influence of arc, unless a watch is truly isochronous the observed pressure coefficient may be expected to depend not only on the position of the watch, but on the state of winding also. To illustrate this, the poise of the balance was modified and the following results were then obtained over the pressure range 540 to 760 mm of mercury:

	Pressure coefficient (sec/day per mm of mercury)	
	Observed	Adjusted
Pendant up, fully wound	0.015	0.011
Pendant up, 21 hours after winding	0.019	0.010
Pendant down, fully wound	0.007	0.014
Pendant down, 21 hours after winding	0.013	0.011

The variations of the observed coefficients with both position and state of winding were very large. The allowances for arc bring the adjusted coefficients into fair agreement, showing that the lack of isochronism was mostly responsible.

#### DISCUSSION OF VARIATION OF RATE WITH PRESSURE

It can be seen from Figs. 3 and 4 that after adjusting for arc variation the effect of pressure change on both the marine chronometer and the deck watch increases considerably as the pressure is reduced.

Attinger<sup>(2)</sup> examined over a wide pressure range the behaviour of an ordinary 17 mm uncut balance wheel with the normal adjusting screws. This balance was fitted on an extension of the balance staff so that the position of the adjacent walls could be varied. His results, which he supports

on theoretical grounds, were in accordance with the relationships

$$\frac{\delta T}{T} \propto p \text{ (balance closely confined)}$$

$$\frac{\delta T}{T} \propto \sqrt{p} \text{ (balance free)}$$

where  $T$  is the period at zero pressure and  $\delta T$  is the change of period due to increase of pressure to  $p$ .

In normal circumstances, a balance wheel is neither very closely confined nor entirely removed from local boundaries, so at constant arc the following relationship might be expected to hold:

$$\frac{\delta T}{T} = a\sqrt{p} + bp$$

where  $a$  and  $b$  are constants dependent partly on the balance and partly on its degree of confinement. The parallel expression

$$\delta S = C + A\sqrt{p} + Bp,$$

(where  $\delta S$  is the deviation of the half-period from nominal,  $C$ ,  $A$  and  $B$  are constants and  $p$  is the pressure as before), has the form of the equations given above as representing the performance of the watch and marine chronometer studied at the N.P.L.

It might have been expected that for the different positions of the watch the coefficients in those equations would have varied very little. On a statistical basis it is unlikely that there is in fact any significant difference between the three equations. Such divergences as do occur may be attributed at least in part to short-period variations of the arc associated with the engagement and disengagement of the teeth of the train wheels (particularly of the barrel and centre pinion), to local conditions at the surface of the mainspring, and to the condition of the mainspring lubricant. Further, the use of rate/arc corrections determined at atmospheric pressure only could give rise to discrepancies, but the slightly better agreement between the adjusted pressure coefficients for the three positions at low pressure suggests that any such effects are small.

A direct comparison of the coefficients for the watch and the marine chronometer would not be valid because the respective balances and their surroundings are not geometrically similar. Therefore no physical significance should be attached to the agreement, judged by statistical tests, of the  $p$  coefficients for the two movements. But since the expressions for  $\delta S$  have been compounded from contributions from a "free" term and a "confined" term there is point in considering the relative contributions of these terms in regard to the two balances. It may be noted that the  $p$  ("confined") term is relatively more effective for the chronometer than for the watch, in accordance with the straighter nature of the chronometer rate/pressure curve (Fig. 3) in comparison with the watch curve (Fig. 4). Though at first sight this was surprising, it was found to accord with the surface areas and clearances concerned.

As one would expect, the "confined" ( $p$ ) effect tends to predominate at the higher pressures, while the "free" ( $\sqrt{p}$ ) effect becomes dominant as the pressure approaches zero.

Over any specified pressure range the adjusted pressure coefficient is greater for the watch than for the chronometer. This is in accordance with the general experience<sup>(1,4,5)</sup> that the smaller the balance, the larger the effect of ambient pressure upon it.



## CONCLUSION

The hydrodynamical conditions prevailing in the air surrounding an oscillating body with such irregular features as a compensated watch balance are too complex to offer hope of an adequate mathematical solution. Besides the movement of air carried round with the balance due to the viscous drag, there will be outward radial flow due to centrifugal action. Additional disturbances due to the displacement of air by the arm of the balance and the projecting balance screws further complicate the problem and the air entrained in the coils of the balance spring and the viscous damping due to the presence of neighbouring walls, etc., introduce other uncertain factors.

The complexity of the pressure relationships makes it impracticable to introduce pressure allowances in precision watch and chronometer tests. Even if a continuous record of the arc were available, allowances on the basis of the adjusted coefficients would not be sufficiently reliable in comparison with the performance of high grade watches. Accordingly, if it is desired to obtain an accurate assessment of the performance of a watch unaffected by pressure varia-

tions it should be isolated from the free atmosphere during test.

The results reported for a high quality watch are in general agreement with work carried out by Attinger. Corresponding work on a marine chronometer has also been reported. The results are valuable for purposes of illustration, and will contribute to the information at the disposal of those who may wish to pursue the subject.

## ACKNOWLEDGEMENT

The work described above has been carried out as part of the research programme of the National Physical Laboratory and this paper is published by permission of the Director of the Laboratory.

## REFERENCES

- (1) JAQUEROD, A. *J. Suisse Horlog.*, 7, p. 149 (1926).
- (2) ATTINGER, C. *Bull. Soc. Suisse Chronom.*, 2, p. 406 (1947).
- (3) GUYOT, E. *Bull. Soc. Suisse Chronom.*, 1, p. 37 (1939).
- (4) DITTSHEIM, P. *C.R. Acad. Sci. [Paris]*, 137, p. 700 (1903).
- (5) GUYOT, E. *Bull. Soc. Suisse Chronom.*, 1, p. 37 (1938).

## NOTES AND NEWS

## Correspondence

## Ratio of convection to conduction loss from a hot wire stretched along the axis of a vertical cylindrical tube

The contribution by Professor Fairbrother to the July issue of your *Journal*\* appears to us unsatisfactory for two reasons. First because it appears to pretend to give a general treatment of the problem of convection in a vertical tube and secondly because the assumptions seem self-contradictory.

In a problem such as that of the wire and open tube the division between heat loss by conduction and convection is not so much a question of geometry but a matter of the actual dimensions. At one extreme is the case of the capillary tube, where surface tension may preclude natural convection. At the other extreme is the wide cylindrical pipe, where the heat loss is almost wholly by natural convection. Between these two extremes lies an infinite variety of problems, each with its own share of conduction and convection. Similarly for the closed tube analysis, the exact mechanism of flow must be the basis of the equations and this is shelved in the article for a mechanism which is contrary to experimental evidence.

One of the inherent assumptions Professor Fairbrother makes is that there is no vertical temperature gradient. Thus apart from the end effects, which he considers negligible, in flowing past the wire every "unit" ring of liquid at whatever vertical height has a constant temperature and velocity, and its heat content is constant over the whole length of the tube. It follows that for each unit length of wire the heat dissipated is conducted from the wire to the outer wall in a horizontal direction, apart from two very short lengths of wire  $\delta l$ , one at each end of the tube, which are responsible for the end effects. It is the entrance end effect, or rather a portion of it, which Prof. Fairbrother calculates. For he infers that the

fluid's heat transport content is  $\int_S^R \rho C_p \theta_0 v 2\pi r dr$  at the entrance

(where  $\theta_0$  is the ambient temperature) and that it changes to

$\int_S^R \rho C_p (\theta + \theta_0) v 2\pi r dr$  after absorbing some or all of the heat

dissipated from the length  $\delta l$  of the wire. The difference between the two integrals is the axial heat loss  $Q_a$ . It is clear therefore, that to omit the vertical temperature gradient whilst retaining the horizontal conduction temperature distribution, does not, by the simple expedient of substituting a fluid for a solid, alter the heat transfer problem.

If the expressions for the ratio of  $Q_a/Q$ , have any meaning they may represent the evaluation of an end effect, but they hardly represent any relationship involving convection transfer. This seems to be borne out by evaluating equation (7) for air and mercury; the results show that the ratio of axial loss to radial loss is of the order of 40 times greater for mercury than for air!

Electrical Research Laboratories,  
C. A. Parsons and Co. Ltd.,  
Newcastle upon Tyne, 6.

E. D. TAYLOR  
B. BERGER  
B. E. WESTERN

My article applies to laminar flow conditions (capillary tubes), and then only to the case when the axial loss is sufficiently small for the temperature drop along the wire to be considered small compared to the radial drop, and as a result of some experiments I made some time ago to measure the thermal conductivity of a liquid. In these experiments a wire was mounted on the axis of a small-bore copper tube and the whole immersed in a bath of the liquid to be studied. There was no free liquid surface and hence no capillary action and the wire temperature was only a degree or so above that of the bath liquid.

University of Natal,  
Pietermaritzburg,  
South Africa.

J. A. V. FAIRBROTHER

\* FAIRBROTHER, J. A. V. *Brit. J. Appl. Phys.*, 4, p. 204 (1953).



## New books

**Physical formulae.** By T. S. E. THOMAS, B.Sc., Ph.D. (London: Methuen and Co. Ltd.) Pp. vii + 118. Price 8s. 6d.

In his preface to this new Methuen Monograph, Dr. Thomas states that his aim is to provide "a reference book for students and workers in physics and engineering, containing a selection of the principal mathematical laws and formulae in the various subdivisions of classical physics." The book is certainly very different from the well-known engineers' pocket books, and the emphasis is definitely on the more mathematical branches of physics. The chapter headings are: I, Mathematics and Statistics; II, Mechanics; III, Hydraulics; IV, Elasticity, V, General Physics; VI, Acoustics and Fourier Series; VII, Heat; VIII, Light; IX, Electricity and Magnetism; X, Electronic Physics.

The first chapter contains formulae for perimeters, areas and volumes, some trigonometrical and hyperbolic functions, Bessel Functions, some vector formulae, a table of Laplace Transforms and a brief section on statistical formulae. Any such selection of mathematical formulae is bound to be somewhat arbitrary and it is unlikely that the user of this book will be able to do without appropriate mathematical reference books. It might have been more useful to the physicist, therefore, to replace the areas and volumes, for example, by formulae not so easily found in the standard reference books, such as Stirling's approximation for the factorial of a large number, and the exponential integrals so often used in kinetic theory. There are a number of errors and misprints in the chapters which follow. The section on kinetic theory could, with advantage, be expanded considerably to include, e.g. formulae for the conductance of a tube, in view of the many applications of vacuum techniques. Less than a page is devoted to radiation.

Dr. Thomas states that the last chapter, on Electronic Physics, is not intended to cover all branches of the subject, but even so it is most disappointing. Some of the information given is out of date or not clearly expressed, and the "electronics" man needing fundamental information is given very little help.

I am sure that a book of this kind is worth compiling and that Dr. Thomas's labour will save time for some physicists, but his book would be much more valuable to more people if his interpretation of "classical" could be made more "modern," if more references were given, where appropriate, to sources of information, and a good index added.

F. A. VICK

**Signal, noise and resolution in nuclear counter amplifiers.** By A. B. GILLESPIE, B.Sc.(Eng.). (London: Pergamon Press Ltd.) Pp. xii + 155. Price 21s.

Several recent books have dealt with various aspects of nuclear counters. The monograph under review is concerned less with the original detecting device than with using its signals to the greatest advantage. The detector provides a pulse of current and one wishes to record, as accurately as possible, both the magnitude of this pulse and the instant at which it commences to flow, while ensuring that the whole apparatus is ready to attend to a further pulse after a short and well-defined "dead time." Mr. Gillespie takes the ionization chamber as the typical detector and analyses clearly and thoroughly the design of the early stages of suitable pulse amplifiers. Effective compromises are established between sensitivity, temporal resolution and rapid

recovery. The various sources of background noise are ably discussed.

Studies of amplifiers responding to transient signals are apt to lead to exercises in differentiation and integration. Mr. Gillespie meets this situation by giving the results in the text and justifying them in eighteen mathematical appendices which are probably the most costly and certainly the least rewarding part of the book. The great merit of the monograph lies in the practical experience that it embodies; choices of circuits and components are backed up by experimental tests.

P. B. MOON

**Television receiver design. Vol. I. I.F. stages.** By A. G. W. UJTJENS. (London: Cleaver Hume Press Ltd.) Pp. x + 177. Price 21s.

This book is excellently written and produced, and aimed at meeting the theoretical requirements of valve and circuit engineers who are concerned with fundamental aspects of design for television receivers. Much of the material, such as that dealing with noise and feedback, is equally relevant to design work for R.F. stages. Tables of modern valve characteristics are included, and the book is unique in providing useful diagrams to illustrate the relative merits of various R.F. valves. Some questions involved in I.F. stage design, for example choice of the I.F., I.F. circuits for the sound channel, A.G.C., signal handling capacity, sound rejection, are left to be dealt with in other books of the same series. At many places in the text, references are given for further elucidation, but it would be useful in a reference book of this type to have a bibliography to articles related to the matter in hand, such as to methods of making the electrical measurements involved. The application of the theory to practical problems is left to the reader, but he is assisted by the fact that the author has included simple examples in most chapters showing how the expressions derived may be used. This book can be recommended as a valuable addition to the library of anyone closely concerned with wide bandwidth high-gain amplifiers.

A. J. BIGGS

**Collected works of Bernhard Riemann.** Edited by HEINRICH WEBER. (New York: Dover Publications Inc.) Pp. x + 558 + supplement (Pp. viii + 116). Price \$2.55 paper bound; \$4.95 cloth bound.

The work of Bernhard Riemann (1826-1866) is remarkable for its penetrating studies of those branches of mathematics which have later formed the bases of many physical theories. As examples, we have the idea of the Riemann multi-leaved surface used in conformal transformations, the researches on minimal surfaces, non-Euclidean geometry and on the propagation of waves of finite amplitude in compressible media. The Cauchy-Riemann equations are well known to all who have encountered harmonic functions.

The book under review is the full collection of Riemann's papers as written, that is, in German, except for one or two in Latin and Italian. This edition is an unabridged reprint of the Second Edition (1892) and contains the supplement added in 1902. There is also an instructive introduction in English by Prof. Hans Lewy. Only a specialist in mathematics will immediately appreciate the contents of these papers. For practical purposes it is sufficient to note that this book has been republished and that it affords the double opportunity of brushing up German with the sampling of the original thinking of an important natural philosopher.

I. I. BERENBLUT



## Notes and comments

### Elections to The Institute of Physics

The following elections have been made by the Board of The Institute of Physics:

*Fellows:* K. M. Greenland, G. F. Hodsmen, R. S. Krishnan, W. Needham, W. Saraga, R. E. Wood.

*Associates:* M. C. S. Archer, U. W. Arndt, E. J. Axton, R. S. Caddy, E. Cohen, J. K. Crawshaw, A. G. Day, M. K. B. Day, R. F. Farr, J. E. Gibbs, G. M. Johnston, H. J. Lowe, D. L. Mawson, G. M. Owen, A. S. Robinson, D. C. Roy, D. R. Scott, W. R. Shackcloth, E. T. Smith.

Forty-seven Graduates, twenty-four Students and eight Subscribers were also elected.

### Protection from ionizing radiations

Attention is called to a new pamphlet entitled *Precautions in the use of ionizing radiations in industry* which has just been published for the Factory Department of the Ministry of Labour and National Service by Her Majesty's Stationery Office at 2s. net. It serves as a companion to two other official publications: *Recommendations of the British X-ray and Radium Protection Committee* and the Medical Research Council's *Introductory Manual on the Control of Health Hazards from Radioactive Materials*, dealing with precautions necessary in hospitals and in university and research laboratories; it also deals with the properties of the various radiations emitted and their effects upon tissues and blood cells.

The main body of the document is taken up with the precautions which should be adopted by all industrial workers liable to be exposed to ionizing radiations; the aim being to suggest, in effect, a code of good practice. Certain general precautions which apply to all such workers are dealt with under the headings of: Planning and equipment, Inhalation and ingestion precautions, Supervision, Training and monitoring, Film or dosimeter tests of workers' radiation exposures, and Medical supervision.

Although blood changes usually give the earliest detectable indication of damage to health from radiation absorption, much more emphasis in planning the protective measures should be placed on the instrumental, film badge, and dosimeter monitoring of radiation exposures than on blood counts.

Suggested special precautions are outlined for the main categories of use of the radiations under the headings: X-radiography of castings and other articles and of welds, X-ray fluoroscopy, X-ray crystallography,  $\gamma$ -radiography of castings and other articles and of welds, Use of radioactive static eliminators, Use of  $\beta$ - (and  $\gamma$ -) ray thickness gauges, Radioactive tracer work and Handling of unsealed radioactive materials.

The pamphlet concludes with a list of references dealing with radiological hazards and protection which has been compiled for those seeking fuller details and factual data on individual aspects of protection problems.

### Award of the Duddell Medal

At a meeting of The Physical Society held in London on 20 November last, the 30th (1953) Duddell Medal was presented to Prof. W. Sucksmith of the University of Sheffield.

The medal is awarded by the Society to "persons who have contributed to the advancement of knowledge by the invention or design of scientific instruments, or by the discovery of materials used in their construction."

The ring balance, invented by Prof. Sucksmith, is admirable in its simplicity and has been widely used in research work on magnetism; it is this instrument, coupled with his contributions to the development of modern magnetic materials, which has won him the award of the Duddell Medal.

Prof. Sucksmith graduated in the University of Leeds in 1921 and was then appointed an assistant lecturer in physics in the University of Bristol, later becoming a Reader. He was appointed Professor of Physics in the University of Sheffield in 1940.

### Essay competition

We are asked to call attention to an essay competition which has been arranged jointly by the publishers of *Research* and *Sunday Times* to encourage young scientists to express clearly and logically the results of scientific investigations and their implications in industry in a manner which would enable a board of directors to make an accurate assessment of their value and a wise decision on future policy. Full details of the competition may be obtained from the Editor of *Research* at 88 Kingsway, London, W.C.2.

## Journal of Scientific Instruments

### Contents of the December issue

#### SPECIAL ARTICLE

Recent developments in applied optics. By A. C. Menzies.

#### ORIGINAL CONTRIBUTIONS

##### Papers

A graphite tube resistance furnace and voltage regulator for equilibrium studies in the temperature range 1500-1800° C. By W. E. Dennis, F. D. Richardson and J. H. Westcott.

A capacitance manometer of low thermal sensitivity. By I. G. Baxter.

A variable phase contact breaker for stroboscopic determination of waveform. By V. R. Peterson.

The production of fine wires by electrolytic polishing. By H. R. Haines and B. W. Mott.

An apparatus for the measurement of the thermal conductivity of biological

Rotary vacuum reaction chambers. By J. F. Duncan and D. T. Warren.

A microphotometer for microradiography. By S. Bourghardt, S.-O. Brattgård,

H. Hyden, B. Jiewertz and S. Larsson.

The background and <sup>14</sup>C detection efficiency of a liquid scintillation counter.

By B. N. Audric and J. V. P. Long.

A portable high-speed cathode-ray oscillograph. By S. Waring and B. Murphy.

Constancy of photomultiplier gain. By R. Wilson.

A simple mass spectrometer for analysis of stable tracer elements. By E. H.

Cooke-Yarborough and M. C. B. Russell.

An automatic micromanometer for the measurement of low air speeds. By

R. A. K. Long.

#### Laboratory and workshop notes

A high-pressure gas valve for use up to 3000 atmospheres. By D. W. Robinson.

Simple apparatus for demonstrating distortion due to non-uniform temperature

changes. By P. M. Gilet.

A slow motion adjustment for horizontal interferometer mirrors. By J. W. Gates.

Glass-refractory seals. By P. J. C. Kent.

A novel type of gauge for the measurement of internal stresses in a soil mass.

By A. Brebner and W. Wright.

An efficient Geiger counter for use with molybdenum K $\alpha$  X-rays. By G. K.

Williamson and R. E. Smallman.

#### NOTES AND NEWS

##### Correspondence

A meniscus thermometer for the measurement of small temperature differentials.

From S. J. Borgars.

Potentiometer operated by atmospheric pressure. From D. R. Grant.

##### New books

New instruments, materials and tools

Notes and comments

THIS JOURNAL is produced monthly by The Institute of Physics, in London. It deals with all branches of applied physics (including theory and technique). All rights reserved. Responsibility for the statements contained herein attaches only to the writers.

EDITORIAL MATTER. Communications concerning editorial matter should be addressed to the Editor, The Institute of Physics, 47 Belgrave Square, London, S.W.1. (Telephone: Sloane 9806.) Prospective authors are invited to prepare their scripts in accordance with the *Notes on the preparation of contributions*. (Price 2s. 6d. including postage.)

REPRODUCTION. The Institute of Physics is a signatory to The Royal Society's Fair Copying Declaration. Details may be obtained upon application from The Royal Society, London, W.1.

ADVERTISEMENTS. Communications concerning advertisements should be addressed to the agents, Messrs. Walter Judd Ltd., 47 Gresham Street, London, E.C.2. (Telephone: Monarch 7644.)

SUBSCRIPTION RATES. A new volume commences each January. The charge is £4 per volume (\$11.50 U.S.A.), including index (post paid), payable in advance. Single parts, so far as available, may be purchased at 8s. each (\$1.15 U.S.A.), post paid, cash with order. Orders should be sent to The Institute of Physics, 47 Belgrave Square, London, S.W.1, or to any bookseller.